

GLOBAL  
EDITION



# Feedback Control of Dynamic Systems

EIGHTH EDITION

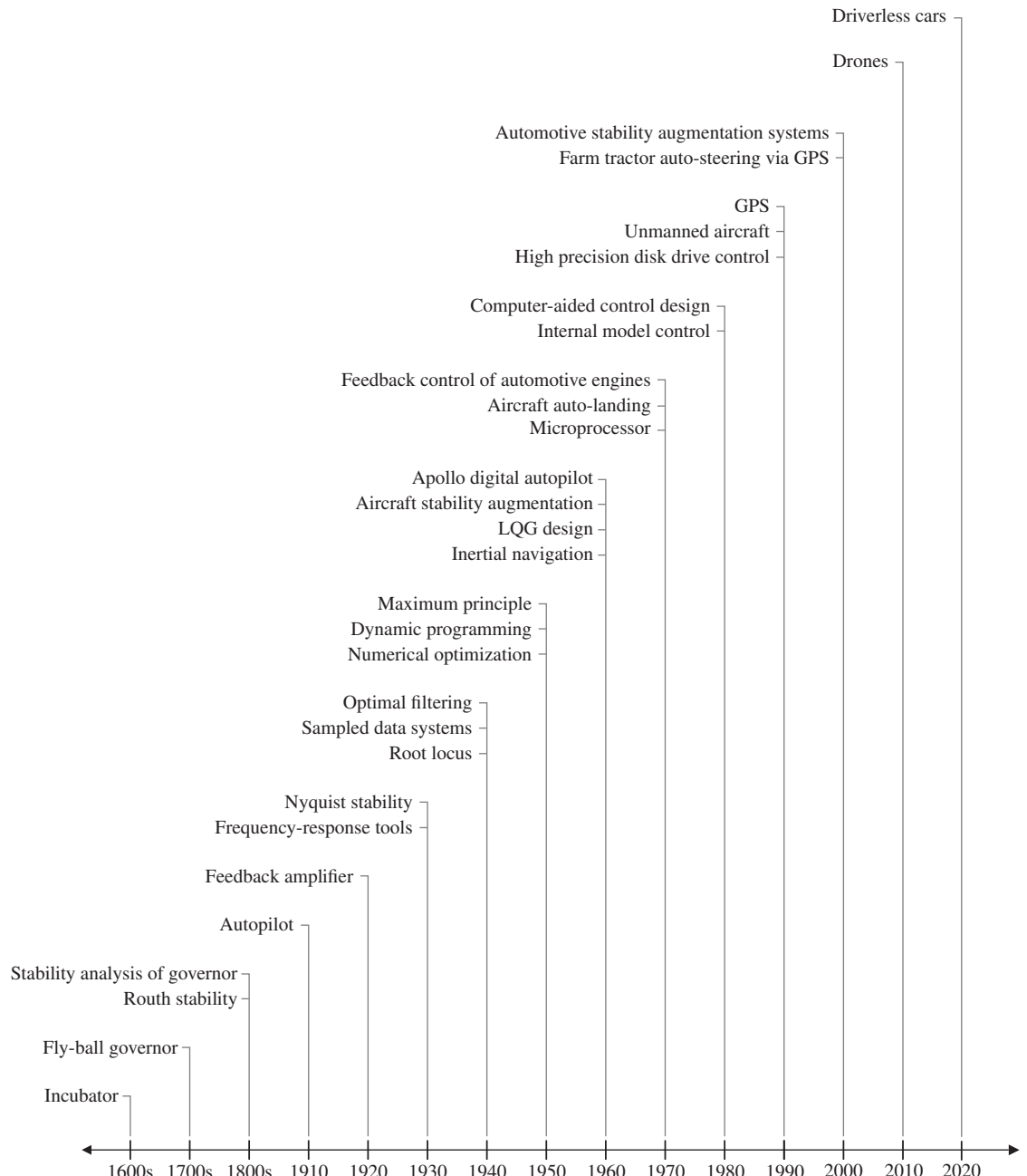
Franklin • Powell • Emami-Naeini



**Table of Laplace Transforms**

Number	$F(s)$	$f(t), t \geq 0$
1	1	$\delta(t)$
2	$\frac{1}{s}$	$1(t)$
3	$\frac{1}{s^2}$	$t$
4	$\frac{2!}{s^3}$	$t^2$
5	$\frac{3!}{s^4}$	$t^3$
6	$\frac{m!}{s^{m+1}}$	$t^m$
7	$\frac{1}{(s+a)}$	$e^{-at}$
8	$\frac{1}{(s+a)^2}$	$te^{-at}$
9	$\frac{1}{(s+a)^3}$	$\frac{1}{2!}t^2e^{-at}$
10	$\frac{1}{(s+a)^m}$	$\frac{1}{(m-1)!}t^{m-1}e^{-at}$
11	$\frac{a}{s(s+a)}$	$1 - e^{-at}$
12	$\frac{a}{s^2(s+a)}$	$\frac{1}{a}(at - 1 + e^{-at})$
13	$\frac{b-a}{(s+a)(s+b)}$	$e^{-at} - e^{-bt}$
14	$\frac{s}{(s+a)^2}$	$(1-at)e^{-at}$
15	$\frac{a^2}{s(s+a)^2}$	$1 - e^{-at}(1+at)$
16	$\frac{(b-a)s}{(s+a)(s+b)}$	$be^{-bt} - ae^{-at}$
17	$\frac{a}{(s^2+a^2)}$	$\sin at$
18	$\frac{s}{(s^2+a^2)}$	$\cos at$
19	$\frac{s+a}{(s+a)^2+b^2}$	$e^{-at}\cos bt$
20	$\frac{b}{(s+a)^2+b^2}$	$e^{-at}\sin bt$
21	$\frac{a^2+b^2}{s[(s+a)^2+b^2]}$	$1 - e^{-at} \left( \cos bt + \frac{a}{b} \sin bt \right)$

# Chronological History of Feedback Control



*This page intentionally left blank*

# **Feedback Control of Dynamic Systems**

---

**Eighth Edition**

**Global Edition**

**Gene F. Franklin**

Stanford University

**J. David Powell**

Stanford University

**Abbas Emami-Naeini**

SC Solutions, Inc.



**Pearson**

330 Hudson Street, NY, NY 10013

Director, Portfolio Management: Engineering, Computer Science & Global Editions: *Julian Partridge*  
Specialist, Higher Ed Portfolio Management: *Norrin Dias*  
Portfolio Management Assistant: *Emily Egan*  
Acquisitions Editor, Global Edition: *Moasenla Jamir*  
Managing Content Producer: *Scott Disanno*  
Content Producer: *Carole Snyder*  
Senior Project Editor, Global Edition: *K.K. Neelakantan*  
Web Developer: *Steve Wright*  
Manager, Media Production, Global Edition:  
*Vikram Kumar*  
Rights and Permissions Manager: *Ben Ferrini*

Manufacturing Buyer, Higher Ed, Lake Side  
Communications Inc (LSC): *Maura Zaldivar-Garcia*  
Senior Manufacturing Controller, Global  
Edition: *Kay Holman*  
Inventory Manager: *Ann Lam*  
Product Marketing Manager: *Yvonne Vannatta*  
Field Marketing Manager: *Demetrius Hall*  
Marketing Assistant: *Jon Bryant*  
Cover Designer: *Lumina Datamatrics, Inc.*  
Cover Art (or Cover Photo): *Dima Zel / Shutterstock*  
Full-Service Project Manager: *George Jacob and Philip Alexander, Integra Software Services Pvt. Ltd.*

Credits and acknowledgments borrowed from other sources and reproduced, with permission, in this textbook appear on appropriate page within text.

Matlab® and Simulink® are registered trademarks of The MathWorks, Inc., 3 Apple Hill Drive, Natick, MA.

Pearson Education Limited  
KAO Two  
KAO Park  
Harlow  
CM17 9NA  
United Kingdom

and Associated Companies throughout the world

Visit us on the World Wide Web at: [www.pearsonglobaleditions.com](http://www.pearsonglobaleditions.com)

© Pearson Education Limited, 2020

The rights of Gene F. Franklin, J. David Powell, and Abbas Emami-Naeini to be identified as the authors of this work have been asserted by them in accordance with the Copyright, Designs and Patents Act 1988.

Authorized adaptation from the United States edition, entitled Feedback Control of Dynamic Systems, 8<sup>th</sup> Edition, ISBN 978-0-13-468571-7 by Gene F. Franklin, J. David Powell, and Abbas Emami-Naeini, published by Pearson Education © 2019.

All rights reserved. No part of this publication may be reproduced, stored in a retrieval system, or transmitted in any form or by any means, electronic, mechanical, photocopying, recording or otherwise, without either the prior written permission of the publisher or a license permitting restricted copying in the United Kingdom issued by the Copyright Licensing Agency Ltd, Saffron House, 6-10 Kirby Street, London EC1N 8TS.

All trademarks used herein are the property of their respective owners. The use of any trademark in this text does not vest in the author or publisher any trademark ownership rights in such trademarks, nor does the use of such trademarks imply any affiliation with or endorsement of this book by such owners. For information regarding permissions, request forms, and the appropriate contacts within the Pearson Education Global Rights and Permissions department, please visit [www.pearsoned.com/permissions](http://www.pearsoned.com/permissions).

This eBook is a standalone product and may or may not include all assets that were part of the print version. It also does not provide access to other Pearson digital products like MyLab and Mastering. The publisher reserves the right to remove any material in this eBook at any time.

British Library Cataloguing-in-Publication Data

A catalogue record for this book is available from the British Library

**ISBN 10:** 1-292-27452-2

**ISBN 13:** 978-1-292-27452-2

**eBook ISBN 13:** 978-1-292-27454-6

*To Valerie, Daisy, Annika, Davenport, Malahat, Sheila, Nima, and to  
the memory of Gene*

*This page intentionally left blank*

# Contents

## Preface 15

### 1

## An Overview and Brief History of Feedback Control 23

A Perspective on Feedback Control	23
Chapter Overview	24
1.1 A Simple Feedback System	25
1.2 A First Analysis of Feedback	28
1.3 Feedback System Fundamentals	32
1.4 A Brief History	33
1.5 An Overview of the Book	40
Summary	41
Review Questions	42
Problems	42

### 2

## Dynamic Models 46

A Perspective on Dynamic Models	46
Chapter Overview	47
2.1 Dynamics of Mechanical Systems	47
2.1.1 Translational Motion	47
2.1.2 Rotational Motion	54
2.1.3 Combined Rotation and Translation	65
2.1.4 Complex Mechanical Systems (W)**	68
2.1.5 Distributed Parameter Systems	68
2.1.6 Summary: Developing Equations of Motion for Rigid Bodies	70
2.2 Models of Electric Circuits	71
2.3 Models of Electromechanical Systems	76
2.3.1 Loudspeakers	76
2.3.2 Motors	78
2.3.3 Gears	82
△ 2.4 Heat and Fluid-Flow Models	83
2.4.1 Heat Flow	84
2.4.2 Incompressible Fluid Flow	88
2.5 Historical Perspective	95
Summary	98
Review Questions	98
Problems	99

\*\*Sections with (W) indicates that additional material is located on the web at [www.pearsonglobaleditions.com](http://www.pearsonglobaleditions.com).

<b>3</b>	<b>Dynamic Response 111</b>
	A Perspective on System Response 111
	Chapter Overview 112
3.1	Review of Laplace Transforms 112
3.1.1	Response by Convolution 113
3.1.2	Transfer Functions and Frequency Response 118
3.1.3	The $\mathcal{L}_-$ Laplace Transform 128
3.1.4	Properties of Laplace Transforms 130
3.1.5	Inverse Laplace Transform by Partial-Fraction Expansion 132
3.1.6	The Final Value Theorem 134
3.1.7	Using Laplace Transforms to Solve Differential Equations 136
3.1.8	Poles and Zeros 138
3.1.9	Linear System Analysis Using Matlab 139
3.2	System Modeling Diagrams 145
3.2.1	The Block Diagram 145
3.2.2	Block-Diagram Reduction Using Matlab 149
3.2.3	Mason's Rule and the Signal Flow Graph (W) 150
3.3	Effect of Pole Locations 150
3.4	Time-Domain Specifications 159
3.4.1	Rise Time 159
3.4.2	Overshoot and Peak Time 160
3.4.3	Settling Time 161
3.5	Effects of Zeros and Additional Poles 164
3.6	Stability 174
3.6.1	Bounded Input–Bounded Output Stability 174
3.6.2	Stability of LTI Systems 176
3.6.3	Routh's Stability Criterion 177
△ 3.7	Obtaining Models from Experimental Data: System Identification (W) 184
△ 3.8	Amplitude and Time Scaling (W) 184
3.9	Historical Perspective 184
	Summary 185
	Review Questions 187
	Problems 187

## 4 A First Analysis of Feedback 208

	A Perspective on the Analysis of Feedback 208
	Chapter Overview 209
4.1	The Basic Equations of Control 210
4.1.1	Stability 211
4.1.2	Tracking 212
4.1.3	Regulation 213
4.1.4	Sensitivity 214

4.2	Control of Steady-State Error to Polynomial Inputs: System Type	216
4.2.1	System Type for Tracking	217
4.2.2	System Type for Regulation and Disturbance Rejection	222
4.3	The Three-Term Controller: PID Control	224
4.3.1	Proportional Control (P)	224
4.3.2	Integral Control (I)	226
4.3.3	Derivative Control (D)	229
4.3.4	Proportional Plus Integral Control (PI)	229
4.3.5	PID Control	233
4.3.6	Ziegler–Nichols Tuning of the PID Controller	238
4.4	Feedforward Control by Plant Model Inversion	244
△ 4.5	Introduction to Digital Control (W)	246
△ 4.6	Sensitivity of Time Response to Parameter Change (W)	247
4.7	Historical Perspective	247
	Summary	249
	Review Questions	250
	Problems	251

## 5 The Root-Locus Design Method 270

	A Perspective on the Root-Locus Design Method	270
	Chapter Overview	271
5.1	Root Locus of a Basic Feedback System	271
5.2	Guidelines for Determining a Root Locus	276
5.2.1	Rules for Determining a Positive ( $180^\circ$ ) Root Locus	278
5.2.2	Summary of the Rules for Determining a Root Locus	284
5.2.3	Selecting the Parameter Value	285
5.3	Selected Illustrative Root Loci	288
5.4	Design Using Dynamic Compensation	301
5.4.1	Design Using Lead Compensation	302
5.4.2	Design Using Lag Compensation	307
5.4.3	Design Using Notch Compensation	310
△ 5.4.4	Analog and Digital Implementations (W)	312
5.5	Design Examples Using the Root Locus	312
5.6	Extensions of the Root-Locus Method	323
5.6.1	Rules for Plotting a Negative ( $0^\circ$ ) Root Locus	323
5.6.2	Successive Loop Closure	326
△ 5.6.3	Time Delay (W)	331
5.7	Historical Perspective	331

Summary	333
Review Questions	335
Problems	335

## 6

### The Frequency-Response Design Method 353

A Perspective on the Frequency-Response Design Method	353
Chapter Overview	354
6.1 Frequency Response	354
6.1.1 Bode Plot Techniques	362
6.1.2 Steady-State Errors	374
6.2 Neutral Stability	376
6.3 The Nyquist Stability Criterion	379
6.3.1 The Argument Principle	379
6.3.2 Application of The Argument Principle to Control Design	380
6.4 Stability Margins	393
6.5 Bode's Gain-Phase Relationship	402
6.6 Closed-Loop Frequency Response	407
6.7 Compensation	408
6.7.1 PD Compensation	409
6.7.2 Lead Compensation (W)	410
6.7.3 PI Compensation	420
6.7.4 Lag Compensation	420
6.7.5 PID Compensation	426
6.7.6 Design Considerations	433
△ 6.7.7 Specifications in Terms of the Sensitivity Function	435
△ 6.7.8 Limitations on Design in Terms of the Sensitivity Function	440
△ 6.8 Time Delay	443
6.8.1 Time Delay via the Nyquist Diagram (W)	445
△ 6.9 Alternative Presentation of Data	445
6.9.1 Nichols Chart	445
6.9.2 The Inverse Nyquist Diagram (W)	450
6.10 Historical Perspective	450
Summary	451
Review Questions	453
Problems	454

## 7

### State-Space Design 479

A Perspective on State-Space Design	479
Chapter Overview	480
7.1 Advantages of State-Space	480
7.2 System Description in State-Space	482
7.3 Block Diagrams and State-Space	488
7.4 Analysis of the State Equations	491

7.4.1	Block Diagrams and Canonical Forms	491
7.4.2	Dynamic Response from the State Equations	503
7.5	Control-Law Design for Full-State Feedback	508
7.5.1	Finding the Control Law	509
7.5.2	Introducing the Reference Input with Full-State Feedback	518
7.6	Selection of Pole Locations for Good Design	522
7.6.1	Dominant Second-Order Poles	522
7.6.2	Symmetric Root Locus (SRL)	524
7.6.3	Comments on the Methods	533
7.7	Estimator Design	534
7.7.1	Full-Order Estimators	534
7.7.2	Reduced-Order Estimators	540
7.7.3	Estimator Pole Selection	544
7.8	Compensator Design: Combined Control Law and Estimator ( $W$ )	547
7.9	Introduction of the Reference Input with the Estimator ( $W$ )	559
7.9.1	General Structure for the Reference Input	561
7.9.2	Selecting the Gain	570
7.10	Integral Control and Robust Tracking	571
7.10.1	Integral Control	571
△	7.10.2 Robust Tracking Control: The Error-Space Approach	573
△	7.10.3 Model-Following Design	585
△	7.10.4 The Extended Estimator	589
△	7.11 Loop Transfer Recovery	592
△	7.12 Direct Design with Rational Transfer Functions	598
△	7.13 Design for Systems with Pure Time Delay	602
7.14	Solution of State Equations ( $W$ )	605
7.15	Historical Perspective	607
	Summary	608
	Review Questions	611
	Problems	612

## 8

## Digital Control 636

A Perspective on Digital Control	636	
Chapter Overview	636	
8.1	Digitization	637
8.2	Dynamic Analysis of Discrete Systems	640
8.2.1	$z$ -Transform	640
8.2.2	$z$ -Transform Inversion	641

8.2.3	Relationship Between $s$ and $z$	643
8.2.4	Final Value Theorem	645
8.3	Design Using Discrete Equivalents	647
8.3.1	Tustin's Method	647
8.3.2	Zero-Order Hold (ZOH) Method	651
8.3.3	Matched Pole-Zero (MPZ) Method	653
8.3.4	Modified Matched Pole-Zero (MMPZ) Method	657
8.3.5	Comparison of Digital Approximation Methods	658
8.3.6	Applicability Limits of the Discrete Equivalent Design Method	659
8.4	Hardware Characteristics	659
8.4.1	Analog-to-Digital (A/D) Converters	660
8.4.2	Digital-to-Analog Converters	660
8.4.3	Anti-Alias Prefilters	661
8.4.4	The Computer	662
8.5	Sample-Rate Selection	663
8.5.1	Tracking Effectiveness	664
8.5.2	Disturbance Rejection	665
8.5.3	Effect of Anti-Alias Prefilter	665
8.5.4	Asynchronous Sampling	666
△ 8.6	Discrete Design	666
8.6.1	Analysis Tools	667
8.6.2	Feedback Properties	668
8.6.3	Discrete Design Example	670
8.6.4	Discrete Analysis of Designs	672
8.7	Discrete State-Space Design Methods (W)	674
8.8	Historical Perspective	674
	Summary	675
	Review Questions	677
	Problems	677

## 9

### Nonlinear Systems 683

A Perspective on Nonlinear Systems	683	
Chapter Overview	684	
9.1	Introduction and Motivation: Why Study Nonlinear Systems?	685
9.2	Analysis by Linearization	687
9.2.1	Linearization by Small-Signal Analysis	687
9.2.2	Linearization by Nonlinear Feedback	692
9.2.3	Linearization by Inverse Nonlinearity	693
9.3	Equivalent Gain Analysis Using the Root Locus	694
9.3.1	Integrator Antiwindup	701

9.4	Equivalent Gain Analysis Using Frequency Response: Describing Functions	706
9.4.1	Stability Analysis Using Describing Functions	712
△ 9.5	Analysis and Design Based on Stability	716
9.5.1	The Phase Plane	717
9.5.2	Lyapunov Stability Analysis	723
9.5.3	The Circle Criterion	731
9.6	Historical Perspective	737
	Summary	738
	Review Questions	739
	Problems	739

# 10

## Control System Design: Principles and Case Studies 751

A Perspective on Design Principles	751	
Chapter Overview	751	
10.1	An Outline of Control Systems Design	753
10.2	Design of a Satellite's Attitude Control	759
10.3	Lateral and Longitudinal Control of a Boeing 747	777
10.3.1	Yaw Damper	782
10.3.2	Altitude-Hold Autopilot	789
10.4	Control of the Fuel–Air Ratio in an Automotive Engine	795
10.5	Control of a Quadrotor Drone	803
10.6	Control of RTP Systems in Semiconductor Wafer Manufacturing	819
10.7	Chemotaxis, or How <i>E. Coli</i> Swims Away from Trouble	833
10.8	Historical Perspective	843
	Summary	845
	Review Questions	847
	Problems	847

## Appendix A Laplace Transforms 865

A.1	The $\mathcal{L}_-$ Laplace Transform	865
A.1.1	Properties of Laplace Transforms	866
A.1.2	Inverse Laplace Transform by Partial-Fraction Expansion	874
A.1.3	The Initial Value Theorem	877
A.1.4	Final Value Theorem	878

**Appendix B Solutions to the Review Questions 880**

**Appendix C Matlab Commands 897**

**Bibliography 903**

**Index 912**

**List of Appendices on the web at [www.pearsonglobaleditions.com](http://www.pearsonglobaleditions.com)**

**Appendix WA: A Review of Complex Variables**

**Appendix WB: Summary of Matrix Theory**

**Appendix WC: Controllability and Observability**

**Appendix WD: Ackermann's Formula for Pole Placement**

**Appendix W2.1.4: Complex Mechanical Systems**

**Appendix W3.2.3: Mason's Rule and the Signal-Flow Graph**

**Appendix W3.6.3.1: Routh Special Cases**

**Appendix W3.7: System Identification**

**Appendix W3.8: Amplitude and Time Scaling**

**Appendix W4.1.4.1: The Filtered Case**

**Appendix W4.2.2.1: Truxal's Formula for the Error Constants**

**Appendix W4.5: Introduction to Digital Control**

**Appendix W4.6: Sensitivity of Time Response to Parameter Change**

**Appendix W5.4.4: Analog and Digital Implementations**

**Appendix W5.6.3: Root Locus with Time Delay**

**Appendix W6.7.2: Digital Implementation of Example 6.15**

**Appendix W6.8.1: Time Delay via the Nyquist Diagram**

**Appendix W6.9.2: The Inverse Nyquist Diagram**

**Appendix W7.8: Digital Implementation of Example 7.31**

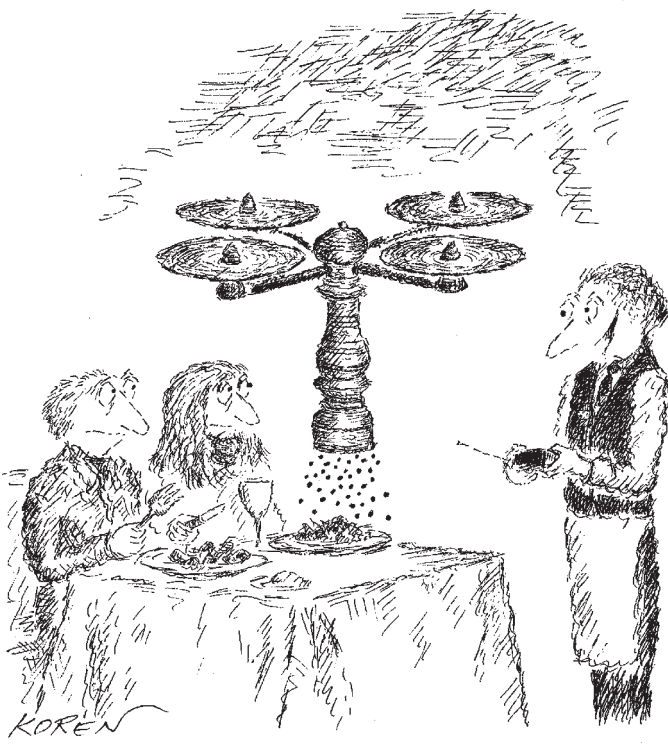
**Appendix W7.9: Digital Implementation of Example 7.33**

**Appendix W7.14: Solution of State Equations**

**Appendix W8.7: Discrete State-Space Design Methods**

# Preface

In this Eighth Edition we again present a text in support of a first course in control and have retained the best features of our earlier editions. For this edition, we have responded to a survey of users by adding some new material (for example, drone dynamics and control) and deleted other little-used material from the book. We have also updated the text throughout so that it uses the improved features of MATLAB®. Drones have been discussed extensively in the controls literature as well as the common press. They are being used in mining, construction, aerial photography, search and rescue, movie industry, package delivery, mapping, surveying, farming, animal research, hurricane hunting, and defense. Since feedback control is a necessary component of all the drones, we develop the equations of motion in Chapter 2, and follow that with control design examples in the chapters 5, 6, 7, and 10. They have great potential for many tasks and could speed up and lessen the cost of these activities. The figure below symbolizes the widespread interest in this exciting new field.



Source: Edward Koren / The New Yorker © Conde Nast

The basic structure of the book is unchanged and we continue to combine analysis with design using the three approaches of the root locus, frequency response, and state-variable equations. The text continues to include many carefully worked out examples to illustrate the material. As before, we provide a set of review questions at the end of each chapter with answers in the back of the book to assist the students in verifying that they have learned the material.

In the three central chapters on design methods we continue to expect the students to learn how to perform the very basic calculations by hand and make a rough sketch of a root locus or Bode plot as a sanity check on the computer results and as an aid to design. However, we introduce the use of Matlab early on in recognition of the universal use of software tools in control analysis and design. As before, we have prepared a collection of all the Matlab files (both “m”files and SIMULINK® “slx” files) used to produce the figures in the book. These are available along with the advanced material described above at our website at [www.pearsonglobaleditions.com](http://www.pearsonglobaleditions.com).

## New to this Edition

We feel that this Eighth Edition presents the material with good pedagogical support, provides strong motivation for the study of control, and represents a solid foundation for meeting the educational challenges. We introduce the study of feedback control, both as a specialty of itself and as support for many other fields.

A more detailed list of the changes is:

- Deleted the disk drive and tape drive examples from Chapters 2, 7, and 10
- Added drone examples and/or problems in Chapters 2, 5, 6, 7, and 10
- Added a thermal system control example to Chapters 2 and 4
- Added a section on anti-windup for integral control in Chapter 9
- Added Cramer’s Rule to chapter 2 and Appendix WB
- Updated Matlab commands throughout the book and in Appendix C
- Updated the section on PID tuning in chapter 4
- Updated the engine control and chemotaxis case studies in Chapter 10
- Over 60 of the problems in this edition are either new or revised from the 7th edition

## Addressing the Educational Challenges

Some of the educational challenges facing students of feedback control are long-standing; others have emerged in recent years. Some of the challenges remain for students across their entire engineering education; others are unique to this relatively sophisticated course. Whether they

are old or new, general or particular, the educational challenges we perceived were critical to the evolution of this text. Here, we will state several educational challenges and describe our approaches to each of them.

- **CHALLENGE** *Students must master design as well as analysis techniques.*

Design is central to all of engineering and especially so to control systems. Students find that design issues, with their corresponding opportunities to tackle practical applications, are particularly motivating. But students also find design problems difficult because design problem statements are usually poorly posed and lack unique solutions. Because of both its inherent importance and its motivational effect on students, design is emphasized throughout this text so confidence in solving design problems is developed from the start.

The emphasis on design begins in Chapter 4 following the development of modeling and dynamic response. The basic idea of feedback is introduced first, showing its influence on disturbance rejection, tracking accuracy, and robustness to parameter changes. The design orientation continues with uniform treatments of the root locus, frequency response, and state variable feedback techniques. All the treatments are aimed at providing the knowledge necessary to find a good feedback control design with no more complex mathematical development than is essential to clear understanding.

Throughout the text, examples are used to compare and contrast the design techniques afforded by the different design methods and, in the capstone case studies of Chapter 10, complex real-world design problems are attacked using all the methods in a unified way.

- **CHALLENGE** *New ideas continue to be introduced into control.*

Control is an active field of research and hence there is a steady influx of new concepts, ideas, and techniques. In time, some of these elements develop to the point where they join the list of things every control engineer must know. This text is devoted to supporting students equally in their need to grasp both traditional and more modern topics.

In each of our editions, we have tried to give equal importance to root locus, frequency response, and state-variable methods for design. In this edition, we continue to emphasize solid mastery of the underlying techniques, coupled with computer-based methods for detailed calculation. We also provide an early introduction to data sampling and discrete controllers in recognition of the major role played by digital controllers in our field. While this material can be skipped to save time without harm to the flow of the text, we feel that it is very important for students to understand that computer control is widely used and that the most basic techniques of computer control are easily mastered.

- **CHALLENGE** *Students need to manage a great deal of information.*

The vast array of systems to which feedback control is applied and the growing variety of techniques available for the solution of control problems means that today's student of feedback control must learn many new ideas. How do students keep their perspective as they plow through lengthy and complex textual passages? How do they identify highlights and draw appropriate conclusions? How do they review for exams? Helping students with these tasks was a criterion for the Fourth, Fifth, Sixth, and Seventh Editions and continues to be addressed in this Eighth Edition. We outline these features below.

## FEATURE

1. *Chapter openers* offer perspective and overview. They place the specific chapter topic in the context of the discipline as a whole, and they briefly overview the chapter sections.
  2. *Margin notes* help students scan for chapter highlights. They point to important definitions, equations, and concepts.
  3. *Shaded highlights* identify key concepts within the running text. They also function to summarize important design procedures.
  4. *Bulleted chapter summaries* help with student review and prioritization. These summaries briefly reiterate the key concepts and conclusions of the chapter.
  5. *Synopsis of design aids*. Relationships used in design and throughout the book are collected inside the back cover for easy reference.
  6. *The color blue* is used (1) to highlight useful pedagogical features, (2) to highlight components under particular scrutiny within block diagrams, (3) to distinguish curves on graphs, and (4) to lend a more realistic look to figures of physical systems.
  7. *Review questions* at the end of each chapter with solutions in the back to guide the student in self-study
  8. *Historical perspectives* at the end of each chapter provide some background and color on how or why the material in that particular chapter evolved.
- **CHALLENGE** *Students of feedback control come from a wide range of disciplines.*

Feedback control is an interdisciplinary field in that control is applied to systems in every conceivable area of engineering. Consequently, some schools have separate introductory courses for control within the standard disciplines and some, such as Stanford, have a single set of courses taken by students from many disciplines. However, to restrict the examples to one field is to miss much of the range and power of feedback but to cover the whole range of applications is overwhelming. In this book, we develop the interdisciplinary nature of the field and

provide review material for several of the most common technologies so that students from many disciplines will be comfortable with the presentation. For Electrical Engineering students who typically have a good background in transform analysis, we include in Chapter 2 an introduction to writing equations of motion for mechanical mechanisms. For mechanical engineers, we include in Chapter 3 a review of the Laplace transform and dynamic response as needed in control. In addition, we introduce other technologies briefly and, from time to time, we present the equations of motion of a physical system without derivation but with enough physical description to be understood from a response point of view. Examples of some of the physical systems represented in the text include a quadrotor drone, a satellite tracking system, the fuel-air ratio in an automobile engine, and an airplane automatic pilot system.

## Outline of the Book

The contents of the printed book are organized into ten chapters and three appendices. Optional sections of advanced or enrichment material marked with a triangle ( $\Delta$ ) are included at the end of some chapters. Examples and problems based on this material are also marked with a triangle ( $\Delta$ ). There are also four full appendices on the website plus numerous appendices that supplement the material in most of the chapters. The appendices in the printed book include Laplace transform tables, answers to the end-of-chapter review questions, and a list of Matlab commands. The appendices on the website include a review of complex variables, a review of matrix theory, some important results related to state-space design, and optional material supporting or extending several of the chapters.

In Chapter 1, the essential ideas of feedback and some of the key design issues are introduced. This chapter also contains a brief history of control, from the ancient beginnings of process control to flight control and electronic feedback amplifiers. It is hoped that this brief history will give a context for the field, introduce some of the key people who contributed to its development, and provide motivation to the student for the studies to come.

Chapter 2 is a short presentation of dynamic modeling and includes mechanical, electrical, electromechanical, fluid, and thermodynamic devices. This material can be omitted, used as the basis of review homework to smooth out the usual nonuniform preparation of students, or covered in-depth depending on the needs of the students.

Chapter 3 covers dynamic response as used in control. Again, much of this material may have been covered previously, especially by electrical engineering students. For many students, the correlation between pole locations and transient response and the effects of extra zeros and poles on dynamic response represent new material. Stability of dynamic

systems is also introduced in this chapter. This material needs to be covered carefully.

Chapter 4 presents the basic equations and transfer functions of feedback along with the definitions of the sensitivity function. With these tools, open-loop and closed-loop control are compared with respect to disturbance rejection, tracking accuracy, and sensitivity to model errors. Classification of systems according to their ability to track polynomial reference signals or to reject polynomial disturbances is described with the concept of system type. Finally, the classical proportional, integral, and derivative (PID) control structure is introduced and the influence of the controller parameters on a system's characteristic equation is explored along with PID tuning methods.

Following the overview of feedback in Chapter 4, the core of the book presents the design methods based on root locus, frequency response, and state-variable feedback in Chapters 5, 6, and 7, respectively.

Chapter 8 develops the tools needed to design feedback control for implementation in a digital computer. However, for a complete treatment of feedback control using digital computers, the reader is referred to the companion text, *Digital Control of Dynamic Systems*, by Franklin, Powell, and Workman; Ellis-Kagle Press, 1998.

In Chapter 9, the nonlinear material includes techniques for the linearization of equations of motion, analysis of zero memory nonlinearity as a variable gain, frequency response as a describing function, the phase plane, Lyapunov stability theory, and the circle stability criterion.

In Chapter 10, the three primary approaches are integrated in several case studies, and a framework for design is described that includes a touch of the real-world context of practical control design.

## Course Configurations

The material in this text can be covered flexibly. Most first-course students in controls will have some dynamics and Laplace transforms. Therefore, Chapter 2 and most of Chapter 3 would be a review for those students. In a ten-week quarter, it is possible to review Chapter 3, and cover all of Chapters 1, 4, 5, and 6. Most optional sections should be omitted. In the second quarter, Chapters 7 and 9 can be covered comfortably including the optional sections. Alternatively, some optional sections could be omitted and selected portions of Chapter 8 included. A semester course should comfortably accommodate Chapters 1–7, including the review materials of Chapters 2 and 3, if needed. If time remains after this core coverage, some introduction of digital control from Chapter 8, selected nonlinear issues from Chapter 9, and some of the case studies from Chapter 10 may be added.

The entire book can also be used for a three-quarter sequence of courses consisting of modeling and dynamic response (Chapters 2

and 3), classical control (Chapters 4–6), and modern control (Chapters 7–10).

Two basic 10-week courses are offered at Stanford and are taken by seniors and first-year graduate students who have not had a course in control, mostly in the departments of Aeronautics and Astronautics, Mechanical Engineering, and Electrical Engineering. The first course reviews Chapters 2 and 3 and covers Chapters 4–6. The more advanced course is intended for graduate students and reviews Chapters 4–6 and covers Chapters 7–10. This sequence complements a graduate course in linear systems and is the prerequisite to courses in digital control, nonlinear control, optimal control, flight control, and smart product design. Some of the subsequent courses include extensive laboratory experiments. Prerequisites for the course sequence include dynamics or circuit analysis and Laplace transforms.

## Prerequisites to This Feedback Control Course

This book is for a first course at the senior level for all engineering majors. For the core topics in Chapters 4–7, prerequisite understanding of modeling and dynamic response is necessary. Many students will come into the course with sufficient background in those concepts from previous courses in physics, circuits, and dynamic response. For those needing review, Chapters 2 and 3 should fill in the gaps.

An elementary understanding of matrix algebra is necessary to understand the state-space material. While all students will have much of this in prerequisite math courses, a review of the basic relations is given in online Appendix WB and a brief treatment of particular material needed in control is given at the start of Chapter 7. The emphasis is on the relations between linear dynamic systems and linear algebra.

## Supplements

The website [www.pearsonglobaleditions.com](http://www.pearsonglobaleditions.com) includes the dot-m and dot-slx files used to generate all the Matlab figures in the book, and these may be copied and distributed to the students as desired. The websites also contain some more advanced material and appendices which are outlined in the Table of Contents. A Solutions Manual with complete solutions to all homework problems is available to instructors only.

## Acknowledgments

Finally, we wish to acknowledge our great debt to all those who have contributed to the development of feedback control into the exciting field it is today and specifically to the considerable help and education we have received from our students and our colleagues. In particular, we have benefited in this effort by many discussions with the following

who taught introductory control at Stanford: A. E. Bryson, Jr., R. H. Cannon, Jr., D. B. DeBra, S. Rock, S. Boyd, C. Tomlin, P. Enge, A. Okamura, and C. Gerdes. Other colleagues who have helped us include D. Fraser, N. C. Emami, B. Silver, M. Dorfman, K. Rudie, L. Pao, F. Khorrami, K. Lorell, M. Tischler, D. de Roover, R. Patrick, M. Berrios, J. K. Lee, J. L. Ebert, I. Kroo, K. Leung, and M. Schwager. Special thanks go to the many students who have provided almost all the solutions to the problems in the book.

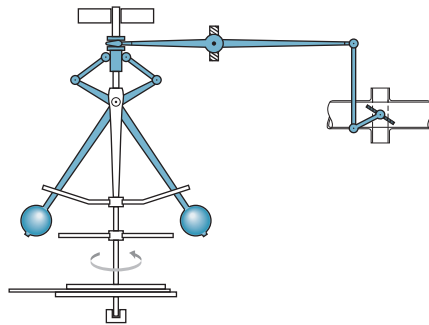
We especially want to express our great appreciation for the contributions to the book by Gene Franklin. Gene was a mentor, teacher, advisor, and good friend to us both. We had many meetings as we collaborated on earlier editions of the book over the last 28 years of his life, and every single one of those meetings has been friendly and enjoyable as we meshed our views on how to present the material. We learned control along with humor from Gene in grad school classes, and we benefitted from his mentoring: in one case as a new assistant professor, and in the other as a Ph.D. advisee. Collectively, we collaborated on research, created new courses and laboratories, and written two textbooks over a period of 40 years. Gene always had a smile with a twinkle in his eye, and was a pleasure to work with; he was a true gentleman.

J.D.P.  
A.E.-N.  
Stanford, California

## Acknowledgments for the Global Edition

Pearson would like to thank and acknowledge Benjamin Chong, University of Leeds, Mehmet Canevi, Istanbul Technical University, and Turan Söylemez, Istanbul Technical University, for contributing to the Global Edition, and Murat Dogruel, Marmara University, Ivo Grondman, Quang Ha, University of Technology Sydney, Philippe Mullhaupt, Ecole Polytechnique Fédérale de Lausanne, and Rahul Sharma, The University of Queensland for reviewing the Global Edition. We would also like to thank Benjamin Chong, Li Li, University of Technology Sydney, Rahul Sharma, Turan Söylemez, and Mark Vanpaemel, Universiteit Antwerpen, for their valuable feedback on the Global Edition.

# An Overview and Brief History of Feedback Control



## A Perspective on Feedback Control

Feedback control of dynamic systems is a very old concept with many characteristics that have evolved over time. The central idea is that a dynamic system's output can be measured and fed back to a controller of some kind then used to affect the system. There are several variations on this theme.

A system that involves a person controlling a machine, as in driving an automobile, is called **manual** control. A system that involves machines only, as when room temperature can be set by a thermostat, is called **automatic** control. Systems designed to hold an output steady against unknown disturbances are called **regulators**, while systems designed to track a reference signal are called **tracking** or **servo** systems. Control systems are also classified according to the information used to compute the controlling action. If the controller does *not* use a measure of the system output being controlled in computing the control action to take, the system is called **open-loop** control. If the controlled output signal is measured and fed back for use in the control computation, the system is called **closed-loop** or **feedback** control. There are many other important properties of control systems in addition to these most basic characteristics. For example, we will mainly consider feedback of current measurements

as opposed to predictions of the future; however, a very familiar example illustrates the limitation imposed by that assumption. When driving a car, the use of simple feedback corresponds to driving in a thick fog where one can *only see the road immediately at the front of the car* and is unable to see the future required position! Looking at the road ahead is a form of predictive control and this information, which has obvious advantages, would always be used where it is available. In most automatic control situations studied in this book, observation of the future track or disturbance is not possible. In any case, the control designer should study the process to see if any information could anticipate either a track to be followed or a disturbance to be rejected. If such a possibility is feasible, the control designer should use it to **feedforward** an early warning to the control system. An example of this is in the control of steam pressure in the boiler of an electric power generation plant. The electricity demand cycle over a day is well known; therefore, when it is known that there will soon be an increased need for electrical power, that information can be fed forward to the boiler controller in anticipation of a soon-to-be-demanded increase in steam flow.

The applications of feedback control have never been more exciting than they are today. Feedback control is an essential element in aircraft of all types: most manned aircraft, and all unmanned aircraft from large military aircraft to small drones. The FAA has predicted that the number of drones registered in the U.S. will reach 7 million by 2020! Automatic landing and collision avoidance systems in airliners are now being used routinely, and the use of satellite navigation in future designs promises a revolution in our ability to navigate aircraft in an ever more crowded airspace. The use of feedback control in driverless cars is an essential element to their success. They are now under extensive development, and predictions have been made that driverless cars will ultimately reduce the number of cars on the road by a very large percentage. The use of feedback control in surgical robotic systems is also emerging. Control is essential to the operation of systems from cell phones to jumbo jets and from washing machines to oil refineries as large as a small city. The list goes on and on. In fact, many engineers refer to control as a *hidden technology* because of its essential importance to so many devices and systems while being mainly out of sight. The future will no doubt see engineers create even more imaginative applications of feedback control.

## Chapter Overview

In this chapter, we begin our exploration of feedback control using a simple familiar example: a household furnace controlled by a thermostat. The generic components of a control system are identified within the context of this example. In another example in Section 1.2—an automobile cruise control—we will develop the

elementary static equations and assign numerical values to elements of the system model in order to compare the performance of open-loop control to that of feedback control when dynamics are ignored. Section 1.3 then introduces the key elements in control system design. In order to provide a context for our studies, and to give you a glimpse of how the field has evolved, Section 1.4 provides a brief history of control theory and design. In addition, later chapters have brief sections of additional historical notes on the topics covered there. Finally, Section 1.5 provides a brief overview of the contents and organization of the entire book.

## 1.1 A Simple Feedback System

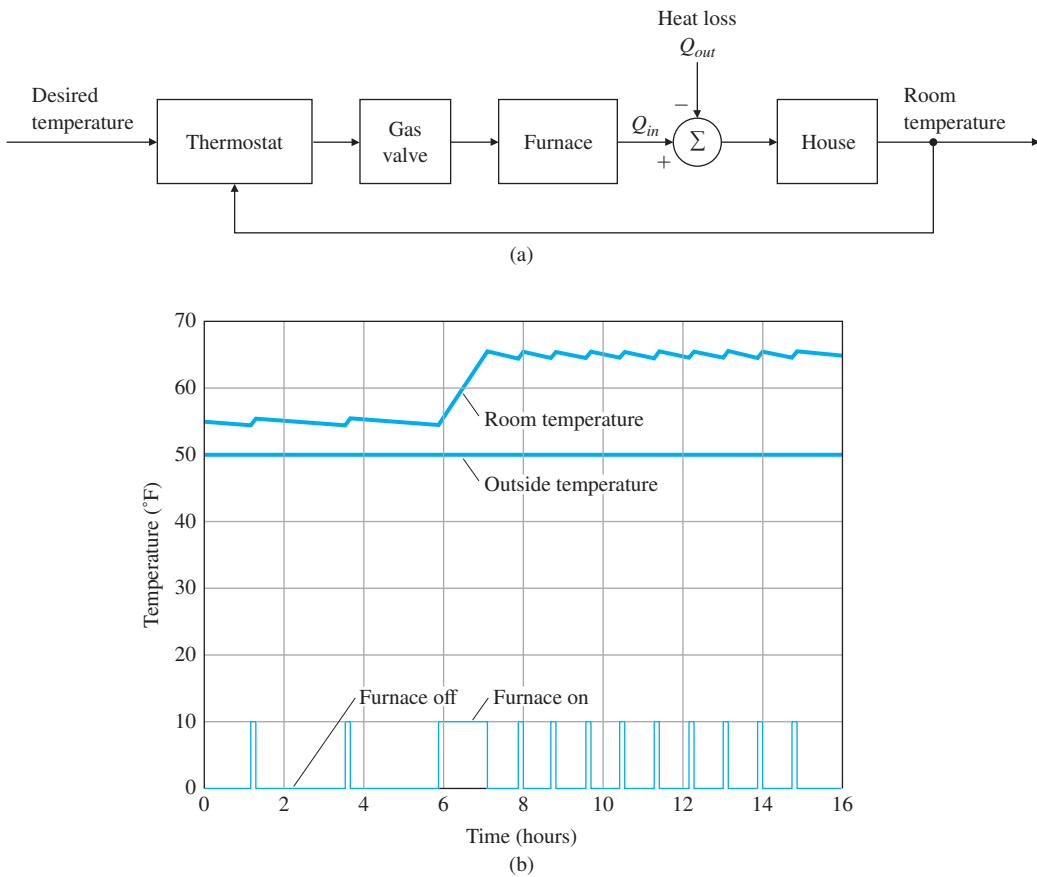
In feedback systems, the variable being controlled—such as temperature or speed—is measured by a sensor and the measured information is fed back to the controller to influence the controlled variable. The principle is readily illustrated by a very common system, the household furnace controlled by a thermostat. The components of this system and their interconnections are shown in Fig. 1.1. Such an illustration identifies the major parts of the system and shows the directions of information flow from one component to another.

We can easily analyze the operation of this system qualitatively from the graph. Suppose both the temperature in the room where the thermostat is located and the outside temperature are significantly below the reference temperature (also called the setpoint) when power is applied. The thermostat will be *on* and the control logic will open the furnace gas valve and light the fire box. This will cause heat  $Q_{in}$  to be supplied to the house at a rate that will be significantly larger than the heat loss  $Q_{out}$ . As a result, the room temperature will rise until it exceeds the thermostat reference setting by a small amount. At this time, the furnace will be turned off and the room temperature will start to fall toward the outside value. When it falls a small amount below the setpoint,<sup>1</sup> the thermostat will come on again and the cycle will repeat. Typical plots of room temperature along with the furnace cycles of on and off are shown in Fig. 1.1. The outside temperature remains at 50°F and the thermostat is initially set at 55°F. At 6 a.m., the thermostat is stepped to 65°F and the furnace brings it to that level and cycles the temperature around that value thereafter. Notice the house is well insulated, so the fall of temperature with the furnace off is significantly slower than the rise with the furnace on. From this example, we can identify the generic components of the elementary feedback control system, as shown in Fig. 1.2.

The central component of this feedback system is the **process** whose output is to be controlled. In our example the process would be the house whose output is the room temperature and the **disturbance** to

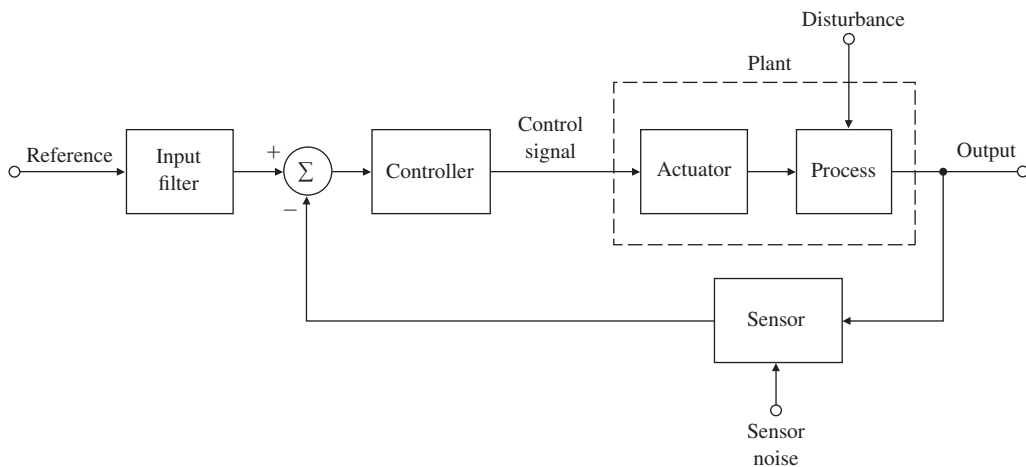
---

<sup>1</sup>The **setpoint**, **reference**, and **desired input** are all the same thing and shown in Figs. 1.1–1.3.

**Figure 1.1**

Feedback control: (a) component block diagram of a room temperature control system; (b) plot of room temperature and furnace action

the process is the flow of heat from the house,  $Q_{out}$ , due to conduction through the walls and roof to the lower outside temperature. (The outward flow of heat also depends on other factors such as wind, open doors, and so on.) The design of the process can obviously have a major impact on the effectiveness of the controls. The temperature of a well-insulated house with thermopane windows is clearly easier to control than otherwise. Similarly, the design of aircraft with control in mind makes a world of difference to the final performance. In every case, the earlier the concepts of control are introduced into the process design, the better. The **actuator** is the device that can influence the controlled variable of the process. In our case, the actuator is a gas furnace. Actually, the furnace usually has a pilot light or striking mechanism, a gas valve, and a blower fan, which turns on or off depending on the air temperature in the furnace. These details illustrate the fact that many feedback systems contain components that themselves

**Figure 1.2**

Component block diagram of an elementary feedback control

form other feedback systems.<sup>2</sup> The central issue with the actuator is its ability to move the process output with adequate speed and range. The furnace must produce more heat than the house loses on the worst day, and must distribute it quickly if the house temperature is to be kept in a narrow range. Power, speed, and reliability are usually more important than accuracy. Generally, the process and the actuator are intimately connected and the control design centers on finding a suitable input or control signal to send to the actuator. The combination of process and actuator is called the **plant**, and the component that actually computes the desired control signal is the **controller**. Because of the flexibility of electrical signal processing, the controller typically works on electrical signals, although the use of pneumatic controllers based on compressed air has a long and important place in process control. With the development of digital technology, cost-effectiveness and flexibility have led to the use of digital signal processors as the controller in an increasing number of cases. The component labeled **thermostat** in Fig. 1.1 measures the room temperature and is called the **sensor** in Fig. 1.2, a device whose output inevitably contains sensor noise. Sensor selection and placement are very important in control design, for it is sometimes not possible for the true controlled variable and the sensed variable to be the same. For example, although we may really wish to control the house temperature as a whole, the thermostat is in one particular room, which may or may not be at the same temperature as the rest of the house. For instance, if the thermostat is set to 68°F but is placed in the living room near a roaring fireplace, a person working in

<sup>2</sup>Jonathan Swift (1733) said it this way: “So, Naturalists observe, a flea Hath smaller fleas that on him prey; And these have smaller still to bite ‘em; And so proceed, *ad infinitum.*” Swift, J., *On Poetry: A Rhapsody*, 1733, J. Bartlett, ed., *Familiar Quotations*, 15th ed., Boston: Little Brown, 1980.

the study could still feel uncomfortably cold.<sup>3,4</sup> As we will see, in addition to placement, important properties of a sensor are the accuracy of the measurements as well as low noise, reliability, and linearity. The sensor will typically convert the physical variable into an electrical signal for use by the controller. Our general system also includes an **input filter** whose role is to convert the reference signal to electrical form for later manipulation by the controller. In some cases, the input filter can modify the reference command input in ways that improve the system response. Finally, there is a **controller** to compute the difference between the reference signal and the sensor output to give the controller a measure of the system error. The thermostat on the wall includes the sensor, input filter, and the controller. A few decades ago, the user simply set the thermostat manually to achieve the desired room temperature at the thermostat location. Over the last few decades, the addition of a small computer in the thermostat has enabled storing the desired temperature over the day and week and more recently, thermostats have gained the ability to learn what the desired temperature should be and to base that value, in part, on whether anybody will be home soon! A thermostat system that includes a motion detector can determine whether anybody is home and learns from the patterns observed what the desired temperature profile should be. The process of learning the desired setpoint is an example of artificial intelligence (AI) or machine learning, which is gaining acceptance in many fields as the power and affordability of computers improve. The combination of feedback control, AI, sensor fusion, and logic to tie it all together will become an essential feature in many future devices such as drones, driverless cars, and many others.

This text will present methods for analyzing feedback control systems and will describe the most important design techniques engineers can use in applying feedback to solve control problems. We will also study the specific advantages of feedback that compensate for the additional complexity it demands.

## 1.2 A First Analysis of Feedback

The value of feedback can be readily demonstrated by quantitative analysis of a simplified model of a familiar system, the cruise control of an automobile (see Fig. 1.3). To study this situation analytically, we

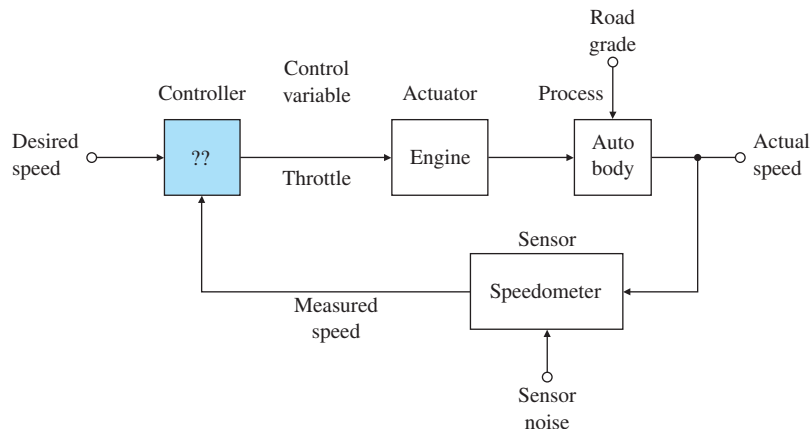
---

<sup>3</sup>In the renovations of the kitchen in the house of one of the authors, the new ovens were placed against the wall where the thermostat was mounted on the other side. Now when dinner is baked in the kitchen on a cold day, the author freezes in his study unless the thermostat is reset.

<sup>4</sup>The story is told of the new employee at the nitroglycerin factory who was to control the temperature of a critical part of the process manually. He was told to “keep that reading below 300°.” On a routine inspection tour, the supervisor realized that the batch was dangerously hot and found the worker holding the thermometer under cold water tap to bring it down to 300°. They got out just before the explosion. Moral: sometimes automatic control is better than manual.

**Figure 1.3**

Component block diagram of automobile cruise control



need a mathematical **model** of our system in the form of a set of quantitative relationships among the variables. For this example, we ignore the dynamic response of the car and consider only the steady behavior. (Dynamics will, of course, play a major role in later chapters.) Furthermore, we assume that for the range of speeds to be used by the system, we can approximate the relations as linear. After measuring the speed of the vehicle on a level road at 65 mph, we find that a  $1^\circ$  change in the throttle angle (our control variable,  $u$ ) causes a 10 mph change in speed (the output variable,  $y$ ), hence the value 10 in the box between  $u$  and  $y$  in Fig. 1.4, which is a **block diagram** of the plant. Generally, the block diagram shows the mathematical relationships of a system in graphical form. From observations while driving up and down hills, it is found that when the grade changes by 1%, we measure a speed change of 5 mph, hence the value 0.5 in the upper box in Fig. 1.4, which reflects that a 1% grade change has half the effect of a  $1^\circ$  change in the throttle angle. The speedometer is found to be accurate to a fraction of 1 mph and will be considered exact. In the block diagram, the connecting lines carry signals and a block is like an ideal amplifier which multiplies the signal at its input by the value marked in the block to give the output signal. To sum two or more signals, we show lines for the signals coming into a **summer**, a circle with the summation sign  $\Sigma$  inside. An algebraic sign (plus or minus) beside each arrow head indicates whether the input

**Figure 1.4**

Block diagram of the cruise control plant

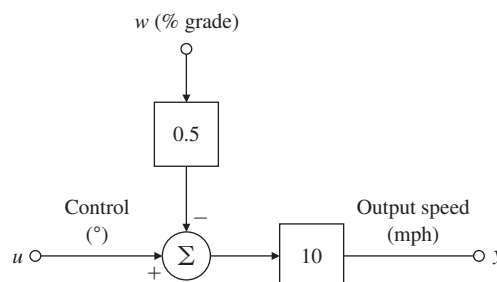
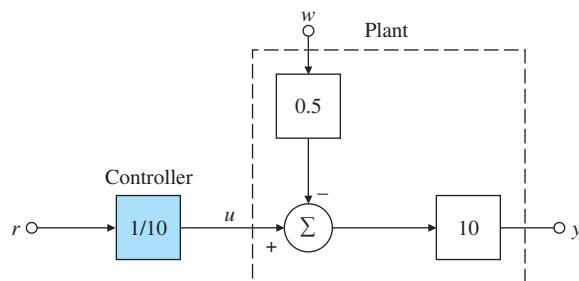


**Figure 1.5**

Open-loop cruise control



adds to or subtracts from the total output of the summer. For this analysis, we wish to compare the effects of a 1% grade on the output speed when the reference speed is set for 65 with and without feedback to the controller.

In the first case, shown in Fig. 1.5, the controller does not use the speedometer reading but sets  $u = r/10$ , where  $r$  is the reference speed, which is, 65 mph. This is an example of an **open-loop control system**. The term *open-loop* refers to the fact that there is no closed path or loop around which the signals go in the block diagram; that is, the control variable  $u$  is independent of the output variable,  $y$ . In our simple example, the open-loop output speed,  $y_{ol}$ , is given by the equations

$$\begin{aligned} y_{ol} &= 10(u - 0.5w) \\ &= 10\left(\frac{r}{10} - 0.5w\right) \\ &= r - 5w. \end{aligned}$$

The error in output speed is

$$e_{ol} = r - y_{ol} \quad (1.1)$$

$$= 5w, \quad (1.2)$$

and the percent error is

$$\% \text{error} = 500 \frac{w}{r}. \quad (1.3)$$

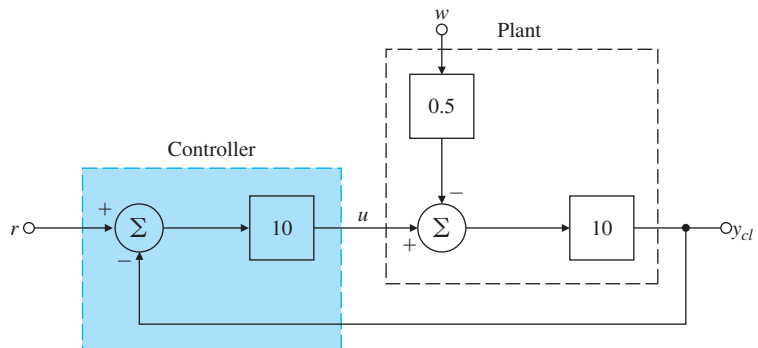
If  $r = 65$  and the road is level, then  $w = 0$  and the speed will be 65 with no error. However, if  $w = 1$  corresponding to a 1% grade, then the speed will be 60 and we have a 5-mph error, which is a 7.69% error in the speed. For a grade of 2%, the speed error would be 10 mph, which is an error of 15.38%, and so on. The example shows that there would be no error when  $w = 0$ , but this result depends on the controller gain being the exact inverse of the plant gain of 10. In practice, the plant gain is subject to change and if it does, errors are introduced by this means also. If there is an error in the plant gain in open-loop control, the percent speed error would be the same as the percent plant-gain error.

The block diagram of a feedback scheme is shown in Fig. 1.6, where the controller gain has been set to 10. In this simple example, we have assumed that we have an ideal sensor providing a measurement of  $y_{cl}$ . In this case, the equations are

### Open-loop control

**Figure 1.6**

Closed-loop cruise control



$$y_{cl} = 10u - 5w,$$

$$u = 10(r - y_{cl}).$$

Combining them yields

$$y_{cl} = 100r - 100y_{cl} - 5w,$$

$$101y_{cl} = 100r - 5w,$$

$$y_{cl} = \frac{100}{101}r - \frac{5}{101}w,$$

$$e_{cl} = \frac{r}{101} + \frac{5w}{101}.$$

Thus, the feedback has reduced the sensitivity of the speed error to the grade by a factor of 101 when compared with the open-loop system. Note, however, that there is now a small speed error on level ground because even when  $w = 0$ ,

$$y_{cl} = \frac{100}{101}r = 0.99r \text{ mph.}$$

This error will be small as long as the loop gain (product of plant and controller gains) is large.<sup>5</sup> If we again consider a reference speed of 65 mph and compare speeds with a 1% grade, the percent error in the output speed is

$$\% \text{ error} = 100 \frac{\frac{65 \times 100}{101} - \left( \frac{65 \times 100}{101} - \frac{5}{101} \right)}{\frac{65 \times 100}{101}} \quad (1.4)$$

$$= 100 \frac{5 \times 101}{101 \times 65 \times 100} \quad (1.5)$$

$$= 0.0769\%. \quad (1.6)$$

---

<sup>5</sup>In case the error is too large, it is common practice to *reset* the reference, in this case to  $\frac{101}{100}r$ , so the output reaches the true desired value.

### The design trade-off

The reduction of the speed sensitivity to grade disturbances and plant gain in our example is due to the loop gain of 100 in the feedback case. Unfortunately, there are limits to how high this gain can be made; when dynamics are introduced, the feedback can make the response worse than before, or even cause the system to become unstable. The dilemma is illustrated by another familiar situation where it is easy to change a feedback gain. If one tries to raise the gain of a public-address amplifier too much, the sound system will squeal in a most unpleasant way. This is a situation where the gain in the feedback loop—from the speakers to the microphone through the amplifier back to the speakers—is too much. The issue of how to get the gain as large as possible to reduce the errors without making the system become unstable is called the design trade-off and is what much of feedback control design is all about.

## 1.3 Feedback System Fundamentals

To achieve good control there are typical goals:

- **Stability.** The system must be stable at all times. This is an absolute requirement.
- **Tracking.** The system output must track the command reference signal as closely as possible.
- **Disturbance rejection.** The system output must be as insensitive as possible to disturbance inputs.
- **Robustness.** The aforementioned goals must be met even if the model used in the design is not completely accurate or if the dynamics of the physical system change over time.

The requirement of **stability** is basic and instability may have two causes. In the first place, the system being controlled may be unstable. This is illustrated by the Segway vehicle, which will simply fall over if the control is turned off. A second cause of instability may be the addition of feedback! Such an instability is called a “vicious circle,” where the feedback signal that is circled back makes the situation worse rather than better. Stability will be discussed in much more detail in Chapters 3 and 4.

There are many examples of the requirement of having the system’s output track a command signal. For example, driving a car so the vehicle stays in its lane is **command tracking**. Today, this is done by the driver; however, there are schemes now under development where the car’s “autodriver” will carry out this task using feedback control while the driver does other things, for example, surfing the Internet. Similarly, flying an airplane on the approach to landing requires that a glide path be accurately tracked by the pilot or an autopilot. It is routine for today’s aircraft autopilots to carry this out including the flare to the actual touchdown. The autopilot accepts inputs from the Instrument Landing System (ILS) that provides an electronic signal showing the

desired landing trajectory, then commands the aircraft control surfaces so it follows the desired trajectory as closely as possible.

**Disturbance rejection** is one of the very oldest applications of feedback control. In this case, the “command” is simply a constant setpoint to which the output is to be held as the environment changes. A very common example of this is the room thermostat whose job it is to hold the room temperature close to the setpoint as outside temperature and wind change, and as doors and windows are opened and closed.

Finally, to design a controller for a dynamic system, it is necessary to have a **mathematical model** of the dynamic response of the system being controlled in all but the simplest cases. Unfortunately, almost all physical systems are very complex and often nonlinear. As a result, the design will usually be based on a simplified model and must be **robust** enough that the system meets its performance requirements when applied to the real device. Furthermore, as time and the environment change, even the best of models will be in error because the system dynamics have changed. Again, the design must not be too **sensitive** to these inevitable changes and it must work well enough regardless.

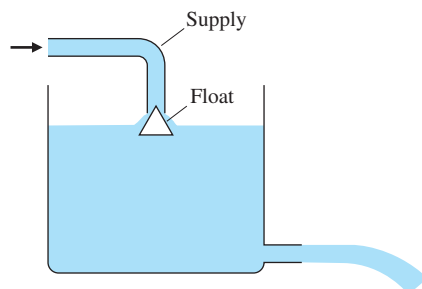
The **tools** available to control engineers to design and build feedback control systems have evolved over time. The development of digital computers has been especially important both as computation aids and as embedded control devices. As computation devices, computers have permitted identification of increasingly complex models and the application of very sophisticated control design methods. Also, as embedded devices, digital controllers have permitted the implementation of very complex control laws. Control engineers must not only be skilled in using these design tools, but also need to understand the concepts behind these tools to be able to make the best use of them. Also important is that the control engineer understands both the capabilities and the limitations of the controller devices available.

## 1.4 A Brief History

Interesting histories of early work on feedback control have been written by Mayr (1970) and Åström (2014), who trace the control of mechanisms to antiquity. Two of the earliest examples are the control of flow rate to regulate a water clock and the control of liquid level in a wine vessel, which is thereby kept full regardless of how many cups are dipped from it. The control of fluid flow rate is reduced to the control of fluid level, since a small orifice will produce constant flow if the pressure is constant, which is the case if the level of the liquid above the orifice is constant. The mechanism of the liquid-level control invented in antiquity and still used today (for example, in the water tank of the ordinary flush toilet) is the **float valve**. As the liquid level falls, so does the float, allowing the flow into the tank to increase; as the level rises, the flow is reduced and if necessary cut off. Figure 1.7 shows how a float valve operates. Notice here the sensor and actuator are not separate

**Figure 1.7**

Early historical control of liquid level and flow

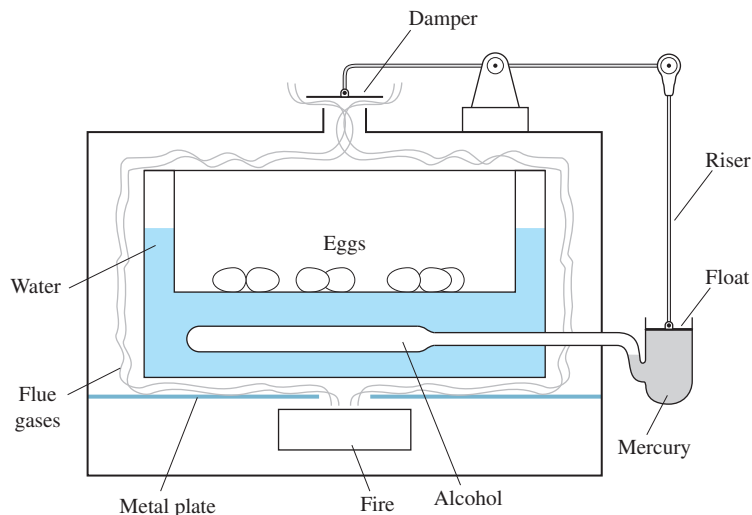
**Drebble's incubator**

devices but are contained in the carefully shaped float-and-supply-tube combination.

A more recent invention described by Mayr (1970) is a system, designed by Cornelis Drebble in about 1620, to control the temperature of a furnace used to heat an incubator<sup>6</sup> (see Fig. 1.8). The furnace consists of a box to contain the fire, with a flue at the top fitted with a damper. Inside the fire box is the double-walled incubator box, the hollow walls of which are filled with water to transfer the heat evenly to the incubator. The temperature sensor is a glass vessel filled with alcohol and mercury and placed in the water jacket around the incubator box. As the fire heats the box and water, the alcohol expands and the riser floats up, lowering the damper on the flue. If the box is too cold, the alcohol contracts, the damper is opened, and the fire burns hotter.

**Figure 1.8**

Drebble's incubator for hatching chicken eggs




---

<sup>6</sup>French doctors introduced incubators into the care of premature babies over 100 years ago.

The desired temperature is set by the length of the riser, which sets the opening of the damper for a given expansion of the alcohol.

A famous problem in the chronicles of control systems was the search for a means to control the rotation speed of a shaft. Much early work (Fuller, 1976) seems to have been motivated by the desire to automatically control the speed of the grinding stone in a wind-driven flour mill. Of various methods attempted, the one with the most promise used a conical pendulum, or **fly-ball governor**, to measure the speed of the mill. The sails of the driving windmill were rolled up or let out with ropes and pulleys, much like a window shade, to maintain fixed speed. However, it was adaptation of these principles to the steam engine in the laboratories of James Watt around 1788 that made the fly-ball governor famous. An early version is shown in Fig. 1.9, while Figs. 1.10 and 1.11 show a close-up of a fly-ball governor and a sketch of its components.

The action of the fly-ball governor (also called a centrifugal governor) is simple to describe. Suppose the engine is operating in equilibrium. Two weighted balls spinning around a central shaft can be seen to describe a cone of a given angle with the shaft. When a load is suddenly applied to the engine, its speed will slow, and the balls of the governor will drop to a smaller cone. Thus the ball angle is used to sense the output speed. This action, through the levers, will open the main valve to the steam chest (which is the actuator) and admit more steam to the engine, restoring most of the lost speed. To hold the steam valve at a new position, it is necessary for the fly balls to rotate at a different angle, implying that the speed under load is not exactly the same as before. We saw this effect earlier with cruise control, where feedback control gave a very small error. To recover the exact same speed in the system, it would require resetting the desired speed setting by changing the length of the rod from the lever to the valve. Subsequent inventors

### Fly-ball governor

**Figure 1.9**

Photograph of an early Watt steam engine

*Source: Chronicle/Alamy Stock Photo*



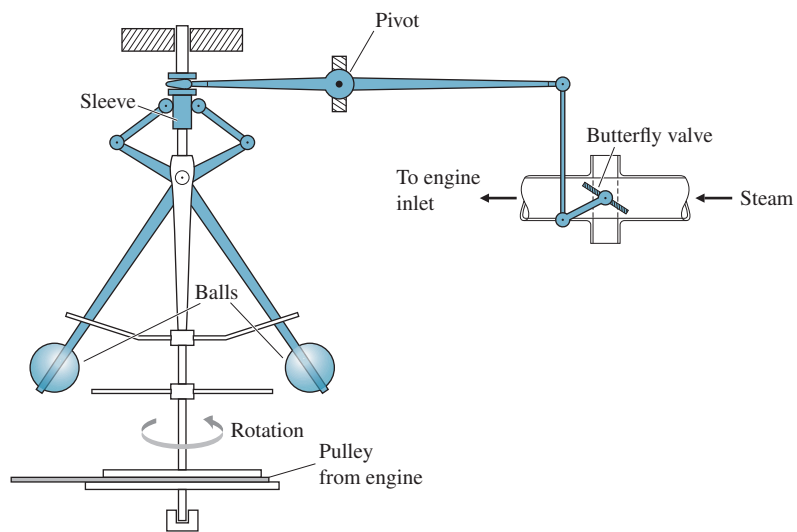
**Figure 1.10**

Close-up of the fly-ball governor

*Source: Washington Imaging/Alamy Stock Photo*

**Figure 1.11**

Operating parts of a fly-ball governor



introduced mechanisms that integrated the speed error to provide automatic reset. In Chapter 4, we will analyze these systems to show that such integration can result in feedback systems with zero steady-state error to constant disturbances.

Because Watt was a practical man, he did not engage in theoretical analysis of the governor, similar to the millwrights earlier. Fuller (1976) has traced the early development of control theory to a period of studies from Christiaan Huygens in 1673 to James Clerk Maxwell in 1868. Fuller gives particular credit to the contributions of G. B. Airy,

professor of mathematics and astronomy at Cambridge University from 1826 to 1835 and Astronomer Royal at Greenwich Observatory from 1835 to 1881. Airy was concerned with speed control; if his telescopes could be rotated counter to the rotation of the earth, a fixed star could be observed for extended periods. Using the centrifugal-pendulum governor he discovered that it was capable of unstable motion—"and the machine (if I may so express myself) became perfectly wild" (Airy, 1840; quoted in Fuller, 1976). According to Fuller, Airy was the first worker to discuss instability in a feedback control system and the first to analyze such a system using differential equations. These attributes signal the beginnings of the study of feedback control dynamics.

The first systematic study of the stability of feedback control was apparently given in the paper "On Governors" by Maxwell (1868).<sup>7</sup> In this paper, Maxwell developed the differential equations of the governor, linearized them about equilibrium, and stated that stability depends on the roots of a certain (characteristic) equation having negative real parts. Maxwell attempted to derive conditions on the coefficients of a polynomial that would hold if all the roots had negative real parts. He was successful only for second- and third-order cases. Determining criteria for stability was the problem for the Adams Prize of 1877, which was won by E. J. Routh.<sup>8</sup> His criterion, developed in his essay, remains of sufficient interest that control engineers are still learning how to apply his simple technique. Analysis of the characteristic equation remained the foundation of control theory until the invention of the electronic feedback amplifier by H. S. Black in 1927 at Bell Telephone Laboratories.

Shortly after publication of Routh's work, the Russian mathematician Lyapunov (1892) began studying the question of stability of motion. His studies were based on the nonlinear differential equations of motion, and also included results for linear equations that are equivalent to Routh's criterion. His work was fundamental to what is now called the state-variable approach to control theory, but was not introduced into the control literature until about 1958.

The development of the feedback amplifier is briefly described in an interesting article based on a talk by Bode (1960) reproduced in Bellman and Kalaba (1964). With the introduction of electronic amplifiers, long-distance telephoning became possible in the decades following World War I. However, as distances increased, so did the loss of electrical energy; in spite of using larger-diameter wires, increasing numbers of amplifiers were needed to replace the lost energy. Unfortunately, large numbers of amplifiers resulted in much distortion since the small non-linearity of the vacuum tubes then used in electronic amplifiers were

---

<sup>7</sup>An exposition of Maxwell's contribution is given in Fuller (1976).

<sup>8</sup>E. J. Routh was first academically in his class at Cambridge University in 1854, while J. C. Maxwell was second. In 1877, Maxwell was on the Adams Prize Committee that chose the problem of stability as the topic for the year.

### Stability analysis

### Frequency response

multiplied many times. To solve the problem of reducing distortion, Black proposed the feedback amplifier. As mentioned earlier in connection with the automobile cruise control, the more we wish to reduce errors (or distortion), the more feedback we need to apply. The loop gain from actuator to plant to sensor to actuator must be made very large. With high gain the feedback loop begins to squeal and is unstable. Here was Maxwell's and Routh's stability problem again, except that in this technology, the dynamics were so complex (with differential equations of order 50 being common) that Routh's criterion was not very helpful. So the communications engineers at Bell Telephone Laboratories, familiar with the concept of frequency response and the mathematics of complex variables, turned to complex analysis. In 1932, H. Nyquist published a paper describing how to determine stability from a graphical plot of the loop frequency response. From this theory developed an extensive methodology of feedback-amplifier design described by Bode (1945) and still extensively used in the design of feedback controls. Nyquist and Bode plots will be discussed in more detail in Chapter 6.

Simultaneous with the development of the feedback amplifier, feedback control of industrial processes was becoming standard. This field, characterized by processes that are not only highly complex but also nonlinear and subject to relatively long time delays between actuator and sensor, developed the concept of **proportional-integral-derivative (PID) control**. The PID controller was first described by Callender et al. (1936). This technology was based on extensive experimental work and simple linearized approximations to the system dynamics. It led to standard experiments suitable to application in the field and eventually to satisfactory “tuning” of the coefficients of the PID controller. (PID controllers will be covered in Chapter 4.) Also under development at this time were devices for guiding and controlling aircraft; especially important was the development of sensors for measuring aircraft altitude and speed. An interesting account of this branch of control theory is given in McRuer (1973).

An enormous impulse was given to the field of feedback control during World War II. In the United States, engineers and mathematicians at the MIT Radiation Laboratory combined their knowledge to bring together not only Bode's feedback amplifier theory and the PID control of processes, but also the theory of stochastic processes developed by Wiener (1930). The result was the development of a comprehensive set of techniques for the design of **servomechanisms**, as control mechanisms came to be called. Much of this work was collected and published in the records of the Radiation Laboratory by James et al. (1947).

Another approach to control systems design was introduced in 1948 by W. R. Evans, who was working in the field of guidance and control of aircraft. Many of his problems involved unstable or neutrally stable dynamics, which made the frequency methods difficult, so he

#### PID control

## Root locus

suggested returning to the study of the characteristic equation that had been the basis of the work of Maxwell and Routh nearly 70 years earlier. However, Evans developed techniques and rules allowing one to follow graphically the paths of the roots of the characteristic equation as a parameter was changed. His method, the **root locus**, is suitable for design as well as for stability analysis and remains an important technique today. The root-locus method developed by Evans will be covered in Chapter 5.

## State-variable design

During the 1950s, several authors, including R. Bellman and R. E. Kalman in the United States and L. S. Pontryagin in the U.S.S.R., began again to consider the ordinary differential equation (ODE) as a model for control systems. Much of this work was stimulated by the new field of control of artificial earth satellites, in which the ODE is a natural form for writing the model. Supporting this endeavor were digital computers, which could be used to carry out calculations unthinkable 10 years before. (Now, of course, these calculations can be done by any engineering student with a laptop computer.) The work of Lyapunov was translated into the language of control at about this time, and the study of optimal controls, begun by Wiener and Phillips during World War II, was extended to optimizing trajectories of nonlinear systems based on the calculus of variations. Much of this work was presented at the first conference of the newly formed International Federation of Automatic Control held in Moscow in 1960.<sup>9</sup> This work did not use the frequency response or the characteristic equation but worked directly with the ODE in “normal” or “state” form and typically called for extensive use of computers. Even though the foundations of the study of ODEs were laid in the late 19th century, this approach is now often called **modern control** to distinguish it from **classical control**, which uses Laplace transforms and complex variable methods of Bode and others. In the period from the 1970s continuing through the present, we find a growing body of work that seeks to use the best features of each technique.

Thus, we come to the current state of affairs where the principles of control are applied in a wide range of disciplines, including every branch of engineering. The well-prepared control engineer needs to understand the basic mathematical theory that underlies the field and must be able to select the best design technique suited to the problem at hand. With the ubiquitous use of computers, it is especially important that the engineer is able to use his or her knowledge to guide and verify calculations done on the computer.<sup>10</sup>

---

<sup>9</sup>Optimal control gained a large boost when Bryson and Denham (1962) showed that the path of a supersonic aircraft should actually dive at one point in order to reach a given altitude in minimum time. This nonintuitive result was later demonstrated to skeptical fighter pilots in flight tests.

<sup>10</sup>For more background on the history of control, see the survey papers appearing in the *IEEE Control Systems Magazine* of November 1984 and June 1996.

## 1.5 An Overview of the Book

The central purpose of this book is to introduce the most important techniques for single-input–single-output control systems design. **Chapter 2** will review the techniques necessary to obtain physical models of the dynamic systems that we wish to control. These include model making for mechanical, electric, electromechanical, and a few other physical systems, including a simple model for a quadrotor drone, which will be used in subsequent chapters. Chapter 2 will also briefly describe the linearization of nonlinear models, although this will be discussed more thoroughly in **Chapter 9**.

In **Chapter 3** and **Appendix A**, we will discuss the analysis of dynamic response using Laplace transforms along with the relationship between time response and the poles and zeros of a transfer function. The chapter also includes a discussion of the critical issue of system stability, including the Routh test.

In **Chapter 4**, we will cover the basic equations and features of feedback. An analysis of the effects of feedback on disturbance rejection, tracking accuracy, sensitivity to parameter changes, and dynamic response will be given. The idea of elementary PID control is discussed.

In **Chapters 5, 6, and 7**, we introduce the techniques for realizing the control objectives first identified in Chapter 4 in more complex dynamic systems. These include the root locus, frequency response, and state variable techniques. These are alternative means to the same end and have different advantages and disadvantages as guides to design of controls. The methods are fundamentally complementary, and each needs to be understood to achieve the most effective control systems design.

In **Chapter 8**, we will develop the ideas of implementing controllers in a digital computer. The chapter addresses how one “digitizes” the control equations developed in Chapters 4 through 7, how the sampling introduces a delay that tends to destabilize the system, and how the sample rate needs to be a certain multiple of the system frequencies for good performance. Just as the Laplace transform does for nonsampled signals, the analysis of sampled systems requires another analysis tool—the  $z$ -transform—and that tool is described and its use is illustrated.

Most real systems are nonlinear to some extent. However, the analyses and design methods in most of the book up to here are for linear systems. In **Chapter 9**, we will explain why the study of linear systems is pertinent, why it is useful for design even though most systems are nonlinear, and how designs for linear systems can be modified to handle many common nonlinearities in the systems being controlled. The chapter will cover saturation, describing functions, adaptive control and the anti-windup controller, and contains a brief introduction to Lyapunov stability theory.

Application of all the techniques to problems of substantial complexity will be discussed in **Chapter 10**. The design methods discussed in Chapters 4–7 are all brought to bear simultaneously on specific case

studies which are representative of real world problems. These cases are somewhat simplified versions of control systems that are in use today in satellites on orbit, in most commercial aircraft, in all automobiles sold in the Western world today, in semiconductor manufacturing throughout the world, and in the drones being used in many fields.

#### Computer aids

Control designers today make extensive use of computer-aided control systems design software that is commercially available. Furthermore, most instructional programs in control systems design make software tools available to the students. The most widely used software for the purpose are Matlab® and Simulink® from The MathWorks. Matlab routines have been included throughout the text to help illustrate this method of solution and many problems require computer aids for solution. Many of the figures in the book were created using Matlab and the files for their creation are available free of charge on the web at [www.pearsonglobaleditions.com](http://www.pearsonglobaleditions.com). Students and instructors are invited to use these files as it is believed that they should be helpful in learning how to use computer methods to solve control problems.

Needless to say, many topics are not treated in the book. We do not extend the methods to multivariable controls, which are systems with more than one input and/or output, except as part of the case study of the rapid thermal process in Chapter 10. Nor is optimal control treated in more than a very introductory manner in Chapter 7.

Also beyond the scope of this text is a detailed treatment of the experimental testing and modeling of real hardware, which is the ultimate test of whether any design really works. The book concentrates on analysis and design of linear controllers for linear plant models—not because we think that is the final test of a design, but because that is the best way to grasp the basic ideas of feedback and is usually the first step in arriving at a satisfactory design. We believe that mastery of the material here will provide a foundation of understanding on which to build knowledge of the actual physical behavior of control systems—a foundation strong enough to allow one to build a personal design method in the tradition of all those who worked to give us the knowledge we present here.

## SUMMARY

- **Control** is the process of making a system variable adhere to a particular value, called the **reference value**. A system designed to follow a changing reference is called **tracking control** or a **servo**. A system designed to maintain an output fixed regardless of the disturbances present is called a **regulating control** or a **regulator**.
- Two kinds of control were defined and illustrated based on the information used in control and named by the resulting structure. In **open-loop control**, the system does *not* measure the output and there is no correction of the actuating signal to make that output conform to the reference signal. In **closed-loop control**, the system

includes a sensor to measure the output and uses **feedback** of the sensed value to influence the control variable.

- A simple feedback system consists of the **process** (or **plant**) whose output is to be controlled, the **actuator** whose output causes the process output to change, a **reference command signal**, and **output sensors** that measure these signals, and the **controller** that implements the logic by which the control signal that commands the actuator is calculated.
- **Block diagrams** are helpful for visualizing system structure and the flow of information in control systems. The most common block diagrams represent the mathematical relationships among the signals in a control system.
- A well-designed feedback control system will be **stable**, **track a desired input** or setpoint, **reject disturbances**, and be insensitive (or **robust**) to changes in the **math model** used for design.
- The theory and design techniques of control have come to be divided into two categories: **classical control** methods use Laplace transforms (or  $z$ -transform) and were the dominant methods for control design until **modern control** methods based on ODEs in state form were introduced into the field starting in the 1960s. Many connections have been discovered between the two categories and well-prepared engineers must be familiar with both techniques.

## REVIEW QUESTIONS

- 1.1 What are the main components of a feedback control system?
- 1.2 What is the purpose of the sensor?
- 1.3 Give three important properties of a good sensor.
- 1.4 What is the purpose of the actuator?
- 1.5 Give three important properties of a good actuator.
- 1.6 What is the purpose of the controller? Give the input(s) and output(s) of the controller.
- 1.7 What physical variable is measured by a tachometer?
- 1.8 Describe three different techniques for measuring temperature.
- 1.9 Why do most sensors have an electrical output, regardless of the physical nature of the variable being measured?

## PROBLEMS

- 1.1 Draw a component block diagram for each of the following feedback control systems:
  - (a) The manual steering system of an automobile
  - (b) Drebbel's incubator

(c) The water level controlled by a float and valve

(d) Watt's steam engine with fly-ball governor

In each case, indicate the location of the elements listed below and give the units associated with each signal:

- The process
- The process desired output signal
- The sensor
- The actuator
- The actuator output signal
- The controller
- The controller output signal
- The reference signal
- The error signal

Notice that in a number of cases the same physical device may perform more than one of these functions.

**1.2** Identify the physical principles and describe the operation of the thermostat in your home or office.

**1.3** A machine for making paper is diagrammed in Fig. 1.12. There are two main parameters under feedback control: the density of fibers as controlled by the consistency of the thick stock that flows from the headbox onto the wire, and the moisture content of the final product that comes out of the dryers. Stock from the machine chest is diluted by white water returning from under the wire as controlled by a control valve (CV). A meter supplies a reading of the consistency. At the "dry end" of the machine, there is a moisture sensor. Draw a block diagram and identify the nine components listed in Problem 1.1 part (d) for the following:

- (a) Control of consistency
- (b) Control of moisture

**1.4** Many variables in the human body are under feedback control. For each of the following controlled variables, draw a block diagram showing the process being controlled, the sensor that measures the variable, the actuator that causes it to increase and/or decrease, the information path that completes the feedback path, and the disturbances that upset the variable. You may need to consult an encyclopedia or textbook on human physiology for information on this problem.

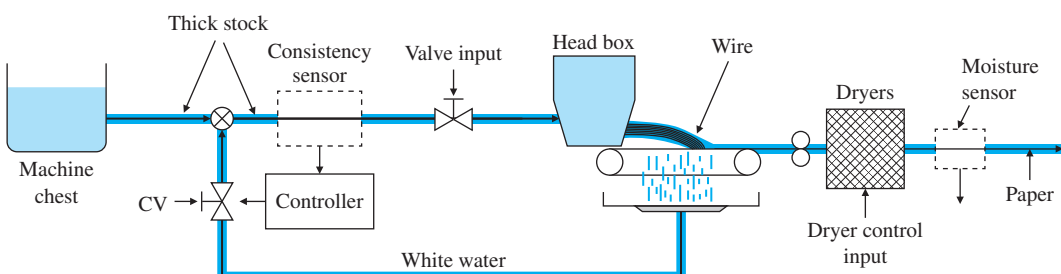


**Figure 1.12**

A papermaking machine

- (a) Blood pressure
- (b) Blood sugar concentration
- (c) Heart rate
- (d) Eye-pointing angle
- (e) Eye-pupil diameter

**1.5** Draw a block diagram of the components for an elevator-position control.

Indicate how you would measure the position of the elevator car. Consider a combined coarse and fine measurement system. What accuracies do you suggest for each sensor? Your system should be able to correct for the fact that in elevators for tall buildings there is significant cable stretch as a function of cab load.

**1.6** Feedback control requires being able to sense the variable being controlled.

Because electrical signals can be transmitted, amplified, and processed easily, often we want to have a sensor whose output is a voltage or current proportional to the variable being measured. Describe a sensor that would give an electrical output proportional to the following:

- (a) Temperature
- (b) Pressure
- (c) Liquid level
- (d) Flow of liquid along a pipe (or blood along an artery)
- (e) Linear position
- (f) Rotational position
- (g) Linear velocity
- (h) Rotational speed
- (i) Translational acceleration
- (j) Torque

**1.7** Each of the variables listed in Problem 1.6 can be brought under feedback control. Describe an actuator that could accept an electrical input and be used to control the variables listed. Give the units of the actuator output signal.

#### **1.8 Feedback in Biology**

**(a) Negative Feedback in Biology:** When a person is under long-term stress (say, a couple of weeks before an exam!), hypothalamus (in the brain) secretes a hormone called Corticotropin Releasing Factor (CRF) which binds to a receptor in the pituitary gland stimulating it to produce Adrenocorticotrophic hormone (ACTH), which in turn stimulates the adrenal cortex (outer part of the adrenal glands) to release the stress hormone Glucocorticoid (GC). This in turn shuts down (turns off the stress response) for both CRF and ACTH production by negative feedback via the bloodstream until GC returns to its normal level. Draw a block diagram of this closed-loop system.

**(b) Positive Feedback in Biology:** This happens in some unique circumstances. Consider the birth process of a baby. Pressure from the head of

the baby going through the birth canal causes contractions via secretion of a hormone called oxytocin which causes more pressure which in turn intensifies contractions. Once the baby is born, the system goes back to normal (negative feedback). Draw a block diagram of this closed-loop system.

# Dynamic Models



## A Perspective on Dynamic Models

The overall goal of feedback control is to use feedback to cause the output variable of a dynamic process to follow a desired reference variable accurately, regardless of the reference variable's path and regardless of any external disturbances or any changes in the dynamics of the process. This complex design goal is met by a number of simple, distinct steps. The first of these is to develop a mathematical description (called a **dynamic model** or **mathematical model**) of the process to be controlled. The term **model**, as it is used and understood by control engineers, means a set of differential equations that describe the dynamic behavior of the process. A model can be obtained using principles of the underlying physics or by testing a prototype of the device, measuring its response to inputs, and using the data to construct an analytical model. We will focus only on using physics in this chapter. There are entire books written on experimentally determining models, sometimes called **system identification**, and these techniques will be described very briefly in Chapter 3. A careful control system designer will typically rely on at least some experiments to verify the accuracy of the model when it is derived from physical principles.

In many cases, the modeling of complex processes is difficult and expensive, especially when the important steps of building and testing prototypes are included. However, in this introductory text, we will focus on the most basic principles of modeling for the most common physical systems. More comprehensive sources and specialized texts will be referenced throughout where appropriate for those wishing more detail.

---

*Source:* burnel1/123RF

In later chapters, we will explore a variety of analysis methods for dealing with the dynamic equations and their solution for purposes of designing feedback control systems.

## Chapter Overview

The fundamental step in building a dynamic model is writing the dynamic equations for the system. Through discussion and a variety of examples, Section 2.1 demonstrates how to write the dynamic equations for a variety of mechanical systems. In addition, the section demonstrates the use of Matlab to find the time response of a simple system to a step input. Furthermore, the ideas of transfer functions and block diagrams are introduced, along with the idea that problems can also be solved via Simulink.

Electric circuits and electromechanical systems will be modeled in Sections 2.2 and 2.3, respectively.

For those wanting modeling examples for more diverse dynamic systems, Section 2.4, which is optional, will extend the discussion to heat- and fluid-flow systems.

The chapter then concludes with Section 2.5, a discussion of the history behind the discoveries that led to the knowledge that we take for granted today.

The differential equations developed in modeling are often nonlinear. Because nonlinear systems are significantly more challenging to solve than linear ones, and because linear models are usually adequate for purposes of control design, the emphasis in the early chapters is primarily on linear systems. However, we do show how to linearize simple nonlinearities in this chapter and show how to use Simulink to numerically solve for the motion of a nonlinear system. A much more extensive discussion of linearization and analysis of nonlinear systems is contained in Chapter 9.

In order to focus on the important first step of developing mathematical models, we will defer explanation of the computational methods used to solve the dynamic equations developed in this chapter until Chapter 3.

## 2.1 Dynamics of Mechanical Systems

### 2.1.1 Translational Motion

Newton's law for translational motion

The cornerstone for obtaining a mathematical model, or the **dynamic equations**,<sup>1</sup> for any mechanical system is Newton's law,

$$\mathbf{F} = m\mathbf{a}, \quad (2.1)$$

---

<sup>1</sup>For systems with moving parts, these equations are typically referred to as the “**equations of motion**.”

where

$\mathbf{F}$  = the vector sum of all forces applied to each body in a system, newtons (N),

$\mathbf{a}$  = the vector acceleration of each body with respect to an **inertial reference frame** (that is, one that is neither accelerating nor rotating with respect to the stars); often called **inertial acceleration**, m/sec<sup>2</sup>,

$m$  = mass of the body, kg.

Note that here in Eq. (2.1), as throughout the text, we use the convention of boldfacing the type to indicate that the quantity is a matrix or vector, possibly a vector function.

A force of 1 N will impart an acceleration of 1 m/sec<sup>2</sup> to a mass of 1 kg. The “weight” of an object is  $mg$ , where  $g$  is the acceleration of gravity (= 9.81 m/sec<sup>2</sup>), which is the quantity measured on scales. Scales are typically calibrated in kilograms, which is used as a direct measure of mass assuming the standard value for  $g$ .

#### Use of free-body diagram in applying Newton's law

Application of this law typically involves defining convenient coordinates to account for the body's motion (position, velocity, and acceleration), determining the forces on the body using a free-body diagram, then writing the equations of motion from Eq. (2.1). The procedure is simplest when the coordinates chosen express the position with respect to an inertial reference frame because, in this case, the accelerations needed for Newton's law are simply the second derivatives of the position coordinates.

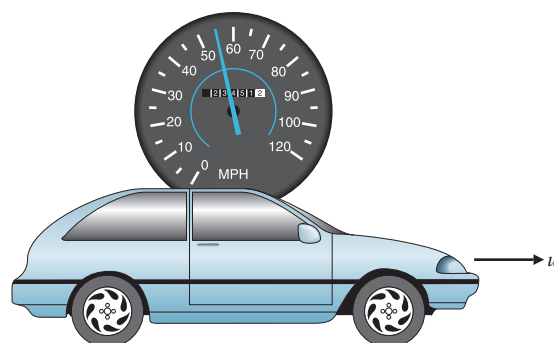
### EXAMPLE 2.1

#### *A Simple System; Cruise Control Model*

1. Write the equations of motion for the speed and forward motion of the car shown in Fig. 2.1, assuming the engine imparts a force  $u$  as shown. Take the Laplace transform of the resulting differential equation and find the transfer function between the input  $u$  and the output  $v$ .

**Figure 2.1**

Cruise control model



2. Use Matlab to find the response of the velocity of the car for the case in which the input jumps from being  $u = 0$  at time  $t = 0$  to a constant  $u = 500$  N thereafter. Assume the car mass  $m$  is 1000 kg and viscous drag coefficient,  $b = 50$  N·sec/m.

### Solution

- Equations of motion:** For simplicity, we assume the rotational inertia of the wheels is negligible, and that there is friction retarding the motion of the car that is proportional to the car's speed with a proportionality constant,  $b$ .<sup>2</sup> The car can then be approximated for modeling purposes using the free-body diagram seen in Fig. 2.2, which defines coordinates, shows all forces acting on the body (heavy lines), and indicates the acceleration (dashed line). The coordinate of the car's position,  $x$ , is the distance from the reference line shown and is chosen so positive is to the right. Note in this case, the inertial acceleration is simply the second derivative of  $x$  (that is,  $\mathbf{a} = \ddot{\mathbf{x}}$ ) because the car position is measured with respect to an inertial reference frame. The equation of motion is found using Eq. (2.1). The friction force acts opposite to the direction of motion; therefore it is drawn opposite to the direction of positive motion and entered as a negative force in Eq. (2.1). The result is

$$u - b\dot{x} = m\ddot{x}, \quad (2.2)$$

or

$$\ddot{x} + \frac{b}{m}\dot{x} = \frac{u}{m}. \quad (2.3)$$

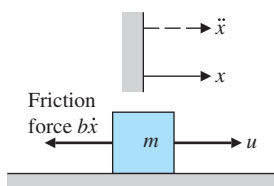
For the case of the automotive cruise control where the variable of interest is the speed,  $v$  ( $=\dot{x}$ ), the equation of motion becomes

$$\dot{v} + \frac{b}{m}v = \frac{u}{m}. \quad (2.4)$$

The solution of such an equation will be covered in detail in Chapter 3; however, the essence is that you assume a solution of

**Figure 2.2**

Free-body diagram for cruise control




---

<sup>2</sup>If the speed is  $v$ , the aerodynamic portion of the friction force is actually proportional to  $v^2$ . We have assumed it to be linear here for simplicity.

the form  $v = V_o e^{st}$  given an input of the form  $u = U_o e^{st}$ . Then, since  $\dot{v} = sV_o e^{st}$ , the differential equation can be written as<sup>3</sup>

$$\left(s + \frac{b}{m}\right) V_o e^{st} = \frac{1}{m} U_o e^{st}. \quad (2.5)$$

The  $e^{st}$  term cancels out, and we find that

$$\frac{V_o}{U_o} = \frac{\frac{1}{m}}{s + \frac{b}{m}}. \quad (2.6)$$

For reasons that will become clear in Chapter 3, this is often written using capital letters to signify that it is the “transform” of the solution, or

$$\frac{V(s)}{U(s)} = \frac{\frac{1}{m}}{s + \frac{b}{m}}. \quad (2.7)$$

### Transfer function

This expression of the differential equation (2.4) is called the **transfer function** and will be used extensively in later chapters. Note that, in essence, we have substituted  $s$  for  $d/dt$  in Eq. (2.4). This transfer function serves as a math model that relates the car’s velocity to the forces propelling the car, that is, inputs from the accelerator pedal. Transfer functions of a system will be used in later chapters to design feedback controllers such as a cruise control device found in many modern cars.

2. **Time response:** The dynamics of a system can be prescribed to Matlab in terms of its transfer function as can be seen in the Matlab statements below that implements Eq. (2.7). The step function in Matlab calculates the time response of a linear system to a unit step input. Because the system is linear, the output for this case can be multiplied by the magnitude of the input step to derive a step response of any amplitude. Equivalently, sys can be multiplied by the magnitude of the input step.

The statements

```
s=tf('s'); % sets up the mode to define the
            % transfer function
sys = (1/1000)/(s + 50/1000); % defines the transfer function from
                                % Eq. (2.7) with the numbers filled in.
step(500*sys); % plots the step response for u = 500.
```

calculate and plot the time response of velocity for an input step with a 500-N magnitude. The step response is shown in Fig. 2.3.

Newton’s law also can be applied to systems with more than one mass. In this case, it is particularly important to draw the free-body

<sup>3</sup>The use of an operator for differentiation was developed by Cauchy in about 1820 based on the Laplace transform, which was developed in about 1780. In Chapter 3, we will show how to derive transfer functions using the Laplace transform (refer to Gardner and Barnes, 1942).

**Figure 2.3**

Response of the car velocity to a step in  $u$

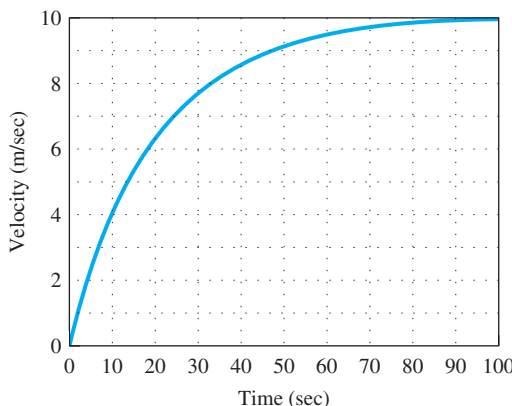


diagram of each mass, showing the applied external forces as well as the equal and opposite internal forces that act from each mass on the other.

### EXAMPLE 2.2

#### *A Two-Mass System: Suspension Model*

Figure 2.4 shows an automobile suspension system. Write the equations of motion for the automobile and wheel motion assuming one-dimensional vertical motion of one quarter of the car mass above one wheel. A system consisting of one of the four-wheel suspensions is usually referred to as a **quarter-car model**. The system can be approximated by the simplified system shown in Fig. 2.5 where two spring constants and a damping coefficient are defined. Assume the model is for a car with a mass of 1580 kg, including the four wheels, which have a mass of 20 kg each. By placing a known weight (an author) directly over a wheel and measuring the car's deflection, we find that  $k_s = 130,000 \text{ N/m}$ . Measuring the wheel's deflection for the same applied weight, we find that  $k_w \approx 1,000,000 \text{ N/m}$ . By using the step response data in Fig. 3.19(b) and qualitatively observing that the car's response to a step change matches the damping coefficient curve for  $\zeta = 0.7$  in the figure, we conclude that  $b = 9800 \text{ N}\cdot\text{sec}/\text{m}$ .

**Figure 2.4**

Automobile suspension

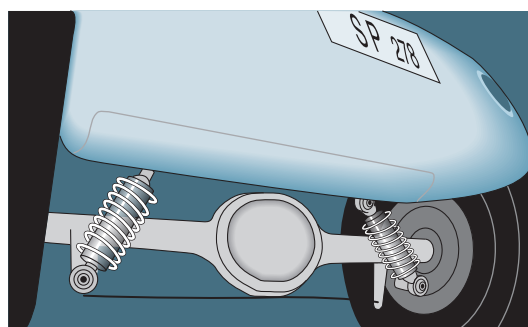
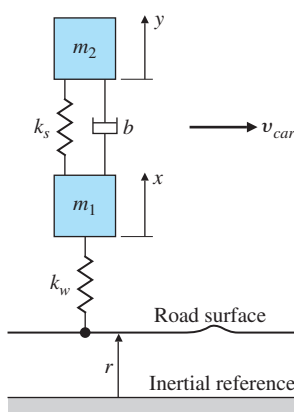


**Figure 2.5**

The quarter-car model

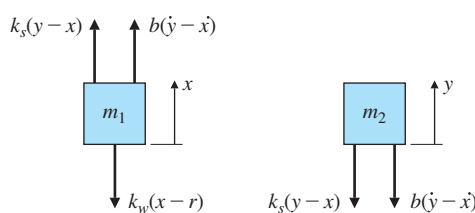


**Solution.** The system can be approximated by the simplified system shown in Fig. 2.5. The coordinates of the two masses,  $x$  and  $y$ , with the reference directions as shown, are the displacements of the masses from their equilibrium positions because of the force of gravity. The equilibrium positions are offset from the springs' unstretched positions because of the force of gravity. The shock absorber is represented in the schematic diagram by a dashpot symbol with friction constant  $b$ . The magnitude of the force from the shock absorber is assumed to be proportional to the rate of change of the relative displacement of the two masses—that is, the force =  $b(\dot{y} - \dot{x})$ . The force of gravity could be included in the free-body diagram; however, its effect is to produce a constant offset of  $x$  and  $y$ . By defining  $x$  and  $y$  to be the distance from the equilibrium position, the need to include the gravity forces is eliminated.

The force from the car suspension acts on both masses in proportion to their relative displacement with spring constant  $k_s$ . Figure 2.6 shows the free-body diagram of each mass. Note the forces from the spring on the two masses are equal in magnitude but act in opposite directions, which is also the case for the damper. A positive displacement  $y$  of mass  $m_2$  will result in a force from the spring on  $m_2$  in the direction shown and a force from the spring on  $m_1$  in the direction shown. However, a positive displacement  $x$  of mass  $m_1$  will result in a force from the spring  $k_s$  on  $m_1$  in the opposite direction to that drawn in Fig. 2.6, as indicated by the *minus*  $x$  term for the spring force.

**Figure 2.6**

Free-body diagrams for suspension system



The lower spring  $k_w$  represents the tire compressibility, for which there is insufficient damping (velocity-dependent force) to warrant including a dashpot in the model. The force from this spring is proportional to the distance the tire is compressed and the nominal equilibrium force would be that required to support  $m_1$  and  $m_2$  against gravity. By defining  $x$  to be the distance from equilibrium, a force will result if either the road surface has a bump ( $r$  changes from its equilibrium value of zero) or the wheel bounces ( $x$  changes). The motion of the simplified car over a bumpy road will result in a value of  $r(t)$  that is not constant.

As previously noted, there is a constant force of gravity acting on each mass; however, this force has been omitted, as have been the equal and opposite forces from the springs. Gravitational forces can always be omitted from vertical-spring mass systems (1) if the position coordinates are defined from the equilibrium position that results when gravity is acting, and (2) if the spring forces used in the analysis are actually the perturbation in spring forces from those forces acting at equilibrium.

Applying Eq. (2.1) to each mass, and noting that some forces on each mass are in the negative (down) direction, yields the system of equations

$$\begin{aligned} b(\dot{y} - \dot{x}) + k_s(y - x) - k_w(x - r) &= m_1\ddot{x}, \\ -k_s(y - x) - b(\dot{y} - \dot{x}) &= m_2\ddot{y}. \end{aligned}$$

Some rearranging results in

$$\ddot{x} + \frac{b}{m_1}(\dot{x} - \dot{y}) + \frac{k_s}{m_1}(x - y) + \frac{k_w}{m_1}x = \frac{k_w}{m_1}r, \quad (2.8)$$

$$\ddot{y} + \frac{b}{m_2}(\dot{y} - \dot{x}) + \frac{k_s}{m_2}(y - x) = 0. \quad (2.9)$$

The most common source of error in writing equations for systems such as these are sign errors. The method for keeping the signs straight in the preceding development entailed mentally picturing the displacement of the masses and drawing the resulting force in the direction that the displacement would produce. Once you have obtained the equations for a system, a check on the signs for systems that are obviously stable from physical reasoning can be quickly carried out. As we will see when we study stability in Section 3.6 of Chapter 3, a stable system always has the same signs on similar variables. For this system, Eq. (2.8) shows that the signs on the  $\ddot{x}$ ,  $\dot{x}$ , and  $x$  terms are all positive, as they must be for stability. Likewise, the signs on the  $\ddot{y}$ ,  $\dot{y}$ , and  $y$  terms are all positive in Eq. (2.9).

The transfer function is obtained in a similar manner as before for zero initial conditions. Substituting  $s$  for  $d/dt$  in the differential equations yields

[Check for sign errors](#)

$$s^2 X(s) + s \frac{b}{m_1} (X(s) - Y(s)) + \frac{k_s}{m_1} (X(s) - Y(s)) + \frac{k_w}{m_1} X(s) = \frac{k_w}{m_1} R(s),$$

$$s^2 Y(s) + s \frac{b}{m_2} (Y(s) - X(s)) + \frac{k_s}{m_2} (Y(s) - X(s)) = 0,$$

which can also be written in matrix form as

$$\begin{bmatrix} s^2 + s \frac{b}{m_1} + \frac{k_s}{m_1} + \frac{k_w}{m_1} & -s \frac{b}{m_1} - \frac{k_s}{m_1} \\ -s \frac{b}{m_2} - \frac{k_s}{m_2} & s^2 + s \frac{b}{m_2} + \frac{k_s}{m_2} \end{bmatrix} \begin{bmatrix} X(s) \\ Y(s) \end{bmatrix} + \begin{bmatrix} \frac{k_w}{m_1} \\ 0 \end{bmatrix} R(s).$$

for which Cramer's Rule (see Appendix WB) can be used to find the transfer function

$$\frac{Y(s)}{R(s)} = \frac{\frac{k_w b}{m_1 m_2} \left( s + \frac{k_s}{b} \right)}{s^4 + \left( \frac{b}{m_1} + \frac{b}{m_2} \right) s^3 + \left( \frac{k_s}{m_1} + \frac{k_s}{m_2} + \frac{k_w}{m_1} \right) s^2 + \left( \frac{k_w b}{m_1 m_2} \right) s + \frac{k_w k_s}{m_1 m_2}}.$$

To determine numerical values, we subtract the mass of the four wheels from the total car mass of 1580 kg and divide it by 4 to find that  $m_2 = 375$  kg. The wheel mass was measured directly to be  $m_1 = 20$  kg. Therefore, the transfer function with the numerical values is

$$\frac{Y(s)}{R(s)} = \frac{1.31e06(s + 13.3)}{s^4 + (516.1)s^3 + (5.685e04)s^2 + (1.307e06)s + 1.733e07}.$$

We will see in Chapter 3 (and later chapters) how this sort of transfer function will allow us to find the response of the car body to inputs resulting from the car motion over a bumpy road.

### 2.1.2 Rotational Motion

[Newton's law for rotational motion](#)

Application of Newton's law to one-dimensional rotational systems requires that Eq. (2.1) be modified to

$$M = I\alpha, \quad (2.10)$$

where

$M$  = the sum of all external moments about the center of mass of a body,  $\text{N} \cdot \text{m}$ ,

$I$  = the body's mass moment of inertia about its center of mass,  $\text{kg} \cdot \text{m}^2$ ,

$\alpha$  = the angular acceleration of the body,  $\text{rad/sec}^2$ .

### EXAMPLE 2.3

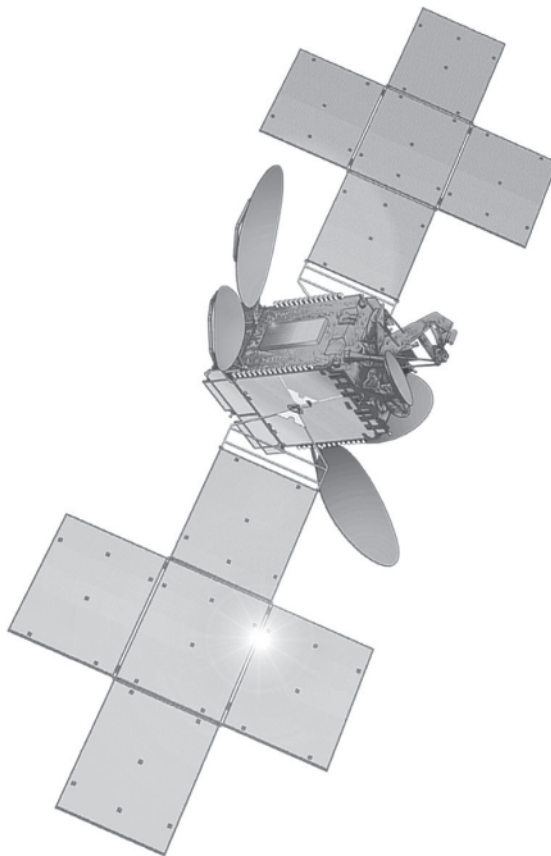
#### *Rotational Motion: Satellite Attitude Control Model*

Satellites, as shown in Fig. 2.7, usually require attitude control so antennas, sensors, and solar panels are properly oriented. Antennas are usually pointed toward a particular location on earth, while solar panels need to be oriented toward the sun for maximum power generation. To

**Figure 2.7**

Communications  
satellite

*Source: Courtesy Thaicom PLC  
and Space Systems/Loral*



gain insight into the full three-axis attitude control system, it is helpful to consider one axis at a time. Write the equations of motion for one axis of this system then show how they would be depicted in a block diagram. In addition, determine the transfer function of this system and construct the system as if it were to be evaluated via Matlab's Simulink.

**Solution.** Figure 2.8 depicts this case, where motion is allowed only about the axis perpendicular to the page. The angle  $\theta$  that describes the satellite orientation must be measured with respect to an inertial reference—that is, a reference that has no angular acceleration. The control force comes from reaction jets that produce a moment of  $F_c d$  about the mass center. There may also be small disturbance moments  $M_D$  on the satellite, which arise primarily from solar pressure acting on any asymmetry in the solar panels. Applying Eq. (2.10) yields the equation of motion

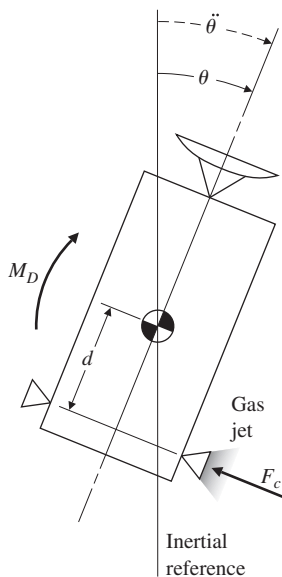
$$F_c d + M_D = I \ddot{\theta}. \quad (2.11)$$

**Double-integrator  
plant**

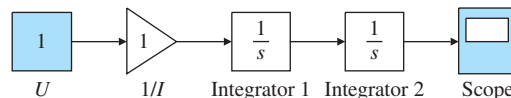
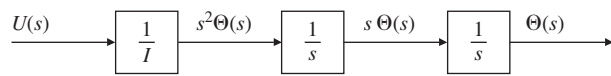
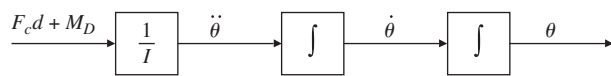
The output of this system,  $\theta$ , results from integrating the sum of the input torques twice; hence, this type of system is often referred to as

**Figure 2.8**

Satellite control schematic

**Figure 2.9**

Block diagrams representing Eq. (2.11) in the upper half and Eq. (2.12) in the lower half

**Figure 2.10**

Simulink block diagram of the double-integrator plant

the **double-integrator plant**. The transfer function can be obtained as described for Eq. (2.7) and is

$$\frac{\Theta(s)}{U(s)} = \frac{1}{I} \frac{1}{s^2}, \quad (2.12)$$

where  $U = F_c d + M_D$ . In this form, the system is often referred to as the  **$1/s^2$  plant**.

Figure 2.9 shows a block diagram representing Eq. (2.11) in the upper half, and a block diagram representing Eq. (2.12) in the lower half. This simple system can be analyzed using the linear analysis techniques that will be described in later chapters, or via Matlab as we saw in Example 2.1. It can also be numerically evaluated for an arbitrary input time history using Simulink, which is a sister software package to Matlab for interactive, nonlinear simulation and has a graphical user interface with drag and drop properties. Figure 2.10 shows a block diagram of the system as depicted by Simulink.

In many cases a system, such as the satellite shown in Fig. 2.7, has some flexibility in the structure. Depending on the nature of the flexibility, it can cause challenges in the design of a control system. Particular difficulty arises when there is flexibility between the sensor and actuator locations. Therefore, it is often important to include this flexibility in the model even when the system seems to be quite rigid.

## EXAMPLE 2.4

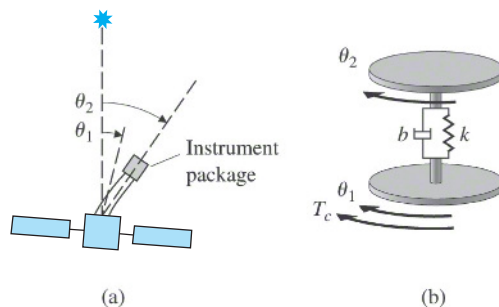
### Flexibility: Flexible Satellite Attitude Control

Figure 2.11(a) shows the situation where there is some flexibility between the satellite attitude sensor ( $\theta_2$ ) and the body of the satellite ( $\theta_1$ ) where the actuators are placed. Find the equations of motion and transfer function relating the motion of the instrument package to a control torque applied to the body of the satellite. For comparison, also determine the transfer function between the control torque to the attitude of the body of the satellite as if the sensors were located there. Retain the flexible model of the overall satellite for this second case, however.

**Solution.** The dynamic model for this situation is shown schematically in Fig. 2.11(b). This model is dynamically similar to the resonant system shown in Fig. 2.5, and results in equations of motion that are similar in form to Eqs. (2.8) and (2.9). The moments on each body are shown in the free-body diagrams in Fig. 2.12. The discussion of the moments on each body is essentially the same as the discussion for Example 2.2,

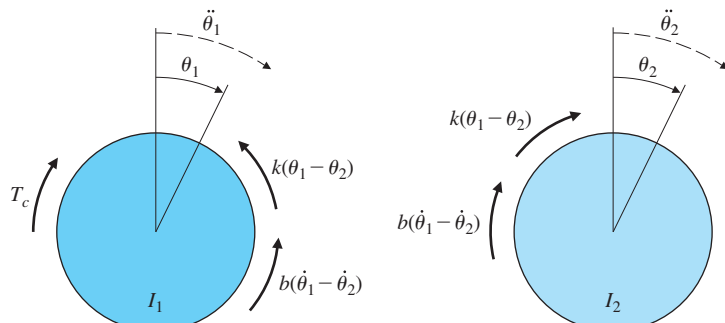
**Figure 2.11**

Model of the flexible satellite



**Figure 2.12**

Free-body diagrams of the flexible satellite



except the springs and damper in that case produced forces, instead of moments that act on each inertia, as in this case. When the moments are summed, equated to the accelerations according to Eq. (2.10), and rearranged, the result is

$$\begin{aligned} I_1 \ddot{\theta}_1 + b(\dot{\theta}_1 - \dot{\theta}_2) + k(\theta_1 - \theta_2) &= T_c \\ I_2 \ddot{\theta}_2 + b(\dot{\theta}_2 - \dot{\theta}_1) + k(\theta_2 - \theta_1) &= 0. \end{aligned}$$

Ignoring the damping  $b$  for simplicity, and substituting  $s$  for  $d/dt$  in the differential equations as we did for Example 2.2 yields

$$\begin{aligned} (I_1 s^2 + k)\Theta_1(s) - k\Theta_2(s) &= T_c \\ -k\Theta_1(s) + (I_2 s^2 + k)\Theta_2(s) &= 0. \end{aligned}$$

**Non-collocated sensor and actuator**

Using Cramer's Rule as we did for Example 2.2, we find the transfer function between the control torque,  $T_c$ , and the sensor angle,  $\theta_2$ , to be

$$\frac{\Theta_2(s)}{T_c(s)} = \frac{k}{I_1 I_2 s^2 \left( s^2 + \frac{k}{I_1} + \frac{k}{I_2} \right)}. \quad (2.13)$$

For the second case, where we assume the attitude sensor is on the main body of the satellite, we want the transfer function between the control torque,  $T_c$ , and the satellite body angle,  $\theta_1$ . Using Cramer's Rule again, we find that

$$\frac{\Theta_1(s)}{T_c(s)} = \frac{I_2 s^2 + k}{I_1 I_2 s^2 \left( s^2 + \frac{k}{I_1} + \frac{k}{I_2} \right)}. \quad (2.14)$$

**Collocated sensor and actuator**

These two cases are typical of many situations in which the sensor and actuator may or may not be placed in the same location in a flexible body. We refer to the situation between sensor and actuator in Eq. (2.13) as the "noncollocated" case, whereas Eq. (2.14) describes the "collocated" case. You will see in Chapter 5 that it is far more difficult to control a system when there is flexibility between the sensor and actuator (noncollocated case) than when the sensor and actuator are rigidly attached to one another (the collocated case).

## EXAMPLE 2.5

### *Rotational Motion: Quadrotor Drone*

Figure 2.13 shows a small drone with four rotors. Find the equations of motion between an appropriate command to the individual motors and the three degrees of freedom; that is, pitch, roll, and yaw as defined by Fig. 2.14. The  $x$  and  $y$  axes are in the horizontal plane, while the  $z$ -axis is straight down. For this example, we only wish to describe the situation for very small motion about the initially level position of the coordinate system shown in Fig. 2.14. Note rotors 1 and 3 are rotating clockwise (CW) and rotors 2 and 4 are rotating counter clockwise (CCW); therefore, rotors 1 and 3 have an angular momentum in the

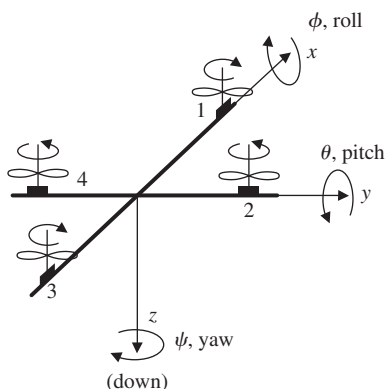
**Figure 2.13**

Quadcopter with a camera

*Source: narongpon chaibot/Shutterstock*

**Figure 2.14**

Orientation of the four rotors and definition of the attitude angles



$+z$  direction, while rotors 2 and 4 have an angular velocity in the  $-z$  direction. Also, define what the “appropriate” commands would be in order to only produce the desired angular motion of pitch, roll, or yaw, without disturbing the other axes. The equations of motion for larger motions are complex and involve coupling between the axes as well as nonlinear terms due to angular motion, inertia asymmetry, and aerodynamics. These terms will be discussed in Chapter 10.

**Solution.** First, we need to establish what the commands should be to the motors attached to each of the four rotor blades in order to produce the desired motion without producing any undesired motion in another axis. Let’s define the torque to each rotor as  $T_1, T_2, T_3, T_4$ . In steady hovering flight, there will be a torque applied to each rotor that maintains a steady rotor speed and thus a constant lift. The rotor speed stays constant because the torque from the motor just balances the aerodynamic drag on the rotor. If we were to add a perturbation that increased the torque magnitude applied to a rotor, the angular speed

would increase until it reached a new equilibrium with the drag, and the rotor would produce an increased amount of lift. Likewise, for a negative perturbation in the torque magnitude on a rotor, the speed of the rotor and the lift would decrease. Note rotors 1 and 3 are rotating in a positive (CW) direction, hence there will be positive torques ( $T_1$  and  $T_3$ ) applied to those rotors, and negative torques ( $T_2$  and  $T_4$ ) applied to rotors 2 and 4 to maintain their negative (CCW) rotation. Another important aspect of this arrangement results from Newton's Third Law, that is: **For every action, there is an equal and opposite reaction.** This law tells us there are equal and opposite torques applied on the motors. Thus there are negative torques being applied to the 1 and 3 motors, while there are positive torques being applied to the 2 and 4 motors. In steady hovering flight, the torques being applied to the motors are all of equal magnitude and the two positive torques cancel out the two negative torques, hence the body of the quadrotor has no net torque applied about the  $z$ -axis and there is no yaw motion produced. (This is not the case for a single rotor helicopter where there is a large reaction torque applied to the engine, and that torque must be balanced by the tail rotor mounted perpendicular to the large lift rotor on top.)

To produce a control action to increase pitch,  $\theta$ , without producing a torque about the other two axes, it makes sense to apply a small increase to the torque on rotor 1 with an equally small decrease to the torque on rotor 3. Thus, there is no net increase in the overall lift on the drone, and there is no change in the balance of the torques on the rotors nor their reaction torques on the drone itself. However, the positive change in lift from rotor 1 coupled with the negative change in lift from rotor 3 will produce a positive torque about the  $y$ -axis which will act to increase  $\theta$ . Therefore, we produce the control torque for positive  $\theta$  motion,  $T_\theta$ , by setting  $\delta T_1 = +T_\theta$  and  $\delta T_3 = -T_\theta$ . Following Example 2.3, the transfer function for pitch is

$$\frac{\Theta(s)}{T_\theta(s)} = \frac{1}{I_y} \frac{1}{s^2}. \quad (2.15)$$

Similarly, for roll control, we produce a positive roll torque,  $T_\phi$ , by setting  $\delta T_4 = -T_\phi$ , thus increasing the negative rotation rate for rotor 4 and increasing its resulting lift. Furthermore, we set  $\delta T_2 = +T_\phi$ , which reduces the lift from rotor 2, thus keeping the overall lift constant and contributing to the desired roll torque. The resulting transfer function for roll is

$$\frac{\Phi(s)}{T_\phi(s)} = \frac{1}{I_x} \frac{1}{s^2}. \quad (2.16)$$

Positive yaw control is accomplished by increasing the torque magnitude on rotors 2 and 4, while decreasing the torque magnitude on rotors 1 and 3 an equal amount. This will increase the lift from rotors 2 and 4 while decreasing the lift on rotors 1 and 3, thus producing no net change in the lift nor a torque that would influence  $\theta$  or  $\phi$ . But,

the reaction torques will be in the positive direction for all four motors! This comes about because rotors 1 and 3 are rotating in a CW (positive direction) so a decrease in the torque applied to their rotors is a negative perturbation, thus resulting in positive reaction torques on the motors. Rotors 2 and 4 are rotating in a CCW (negative direction) so an increase in the torque magnitude applied to their rotors is also a negative perturbation, thus adding to the positive reaction torque applied to the motors. Therefore, the control torque for positive  $\psi$  motion,  $T_\psi$ , is produced by setting  $\delta T_1 = \delta T_2 = \delta T_3 = \delta T_4 = -T_\psi$ . The resulting transfer function is

$$\frac{\Psi(s)}{T_\psi(s)} = \frac{1}{I_z} \frac{1}{s^2}. \quad (2.17)$$

These three equations assume there is small motion from the horizontal orientation and thus any damping from aerodynamic forces are assumed negligible and the equations remain linear.

This example shows why quadrotors have become so popular for small drones; it is a well-balanced simple arrangement and does not require any complex mechanical arrangements to balance the torques. All the control can be accomplished by simply controlling the torque to the four rotors. Furthermore, with the definitions developed above for the motor commands and repeated here,

$$\text{For pitch; } \delta T_1 = +T_\theta; \quad \delta T_3 = -T_\theta, \quad (2.18)$$

$$\text{For roll; } \delta T_2 = +T_\phi; \quad \delta T_4 = -T_\phi, \quad (2.19)$$

$$\text{For yaw; } \delta T_1 = \delta T_2 = \delta T_3 = \delta T_4 = -T_\psi, \quad (2.20)$$

the dynamics for each degree of attitude motion is uncoupled from the motion in the other axes.

In the special case in which a point in a rotating body is fixed with respect to an inertial reference frame, as is the case with a pendulum, Eq. (2.10) can be applied such that  $M$  is the sum of all moments about the *fixed* point, and  $I$  is the moment of inertia about the fixed point.

## EXAMPLE 2.6

### *Rotational Motion: Pendulum*

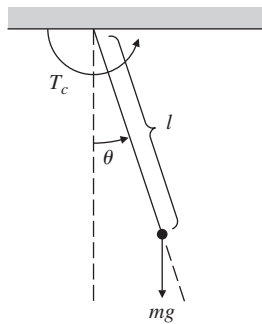
1. Write the equations of motion for the simple pendulum shown in Fig. 2.15, where all the mass is concentrated at the end point and there is a torque,  $T_c$ , applied at the pivot.
2. Use Matlab to determine the time history of  $\theta$  to a step input in  $T_c$  of 1 N·m. Assume  $l = 1$  m,  $m = 1$  kg, and  $g = 9.81$  m/sec<sup>2</sup>.

### Solution

1. **Equations of motion:** The moment of inertia about the pivot point is  $I = ml^2$ . The sum of moments about the pivot point contains a

**Figure 2.15**

Pendulum



term from gravity as well as the applied torque  $T_c$ . The equation of motion, obtained from Eq. (2.10), is

$$T_c - mgl \sin \theta = I\ddot{\theta}, \quad (2.21)$$

which is usually written in the form

$$\ddot{\theta} + \frac{g}{l} \sin \theta = \frac{T_c}{ml^2}. \quad (2.22)$$

This equation is nonlinear due to the  $\sin \theta$  term. A general discussion of nonlinear equations will be contained in Chapter 9; however, we can proceed with a linearization of this case by assuming the motion is small enough that  $\sin \theta \cong \theta$ . Then, Eq. (2.22) becomes the linear equation

$$\ddot{\theta} + \frac{g}{l}\theta = \frac{T_c}{ml^2}. \quad (2.23)$$

With no applied torque, the natural motion is that of a harmonic oscillator with a natural frequency of<sup>4</sup>

$$\omega_n = \sqrt{\frac{g}{l}}. \quad (2.24)$$

The transfer function can be obtained as described for Eq. (2.7), yielding

$$\frac{\Theta(s)}{T_c(s)} = \frac{\frac{1}{ml^2}}{s^2 + \frac{g}{l}}. \quad (2.25)$$

2. **Time history:** The dynamics of a system can be prescribed to Matlab in terms of its transfer function and the step response via the step function. The Matlab statements

---

<sup>4</sup>In a grandfather clock, it is desired to have a pendulum period of exactly 2 sec. Show that the pendulum should be approximately 1 m in length.

```

t = 0:0.02:10; % vector of times for output, 0 to 10 at 0.02
% increments
m = 1; % value of mass (Kg)
L = 1; % value of length (m)
g = 9.81; % value of gravity, g (m/sec2)
s = tf('s'); % sets up transfer function input mode
sys = (1/(m*L^2))/ % computes step responses at times given
(s^2 + g/L) by t for step at t = 0
y = step(sys,t); % converts radians to degrees
Rad2Deg = 57.3; % converts output from radians to degrees
plot(t, Rad2Deg*y) % plots step response

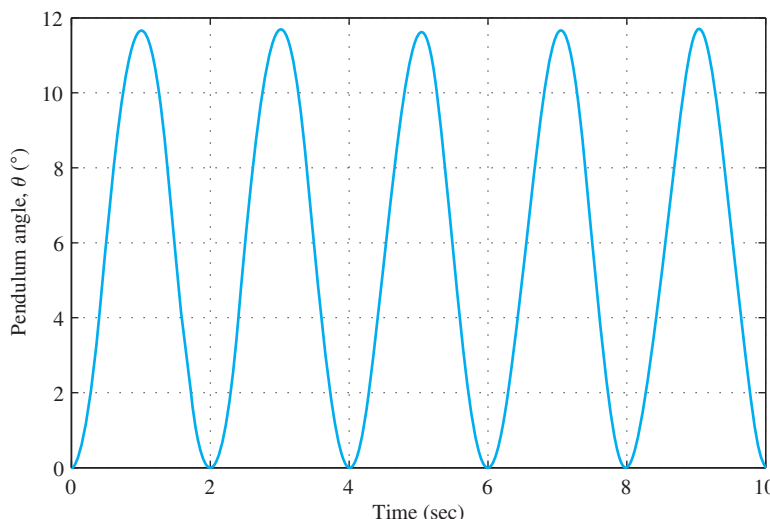
```

will produce the desired time history shown in Fig. 2.16.

As we saw in this example, the resulting equations of motion are often nonlinear. Such equations are much more difficult to solve than linear ones, and the kinds of possible motions resulting from a nonlinear model are much more difficult to categorize than those resulting from a linear model. It is therefore useful to linearize models in order to gain access to linear analysis methods. It may be that the linear models and linear analysis are used only for the design of the control system (whose function may be to maintain the system in the linear region). Once a control system is synthesized and shown to have desirable performance based on linear analysis, it is then prudent to carry out further analysis or an accurate numerical simulation of the system with the significant nonlinearities in order to validate that performance. **Simulink** is an expedient way to carry out these simulations and can handle most

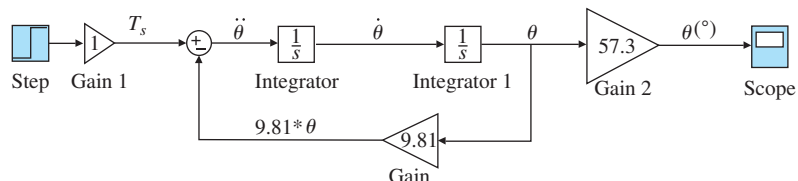
### Simulink

**Figure 2.16**  
Response of the pendulum to a step input of 1 N·m in the applied torque

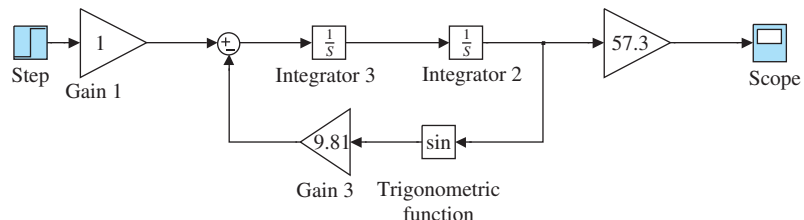


**Figure 2.17**

The Simulink block diagram representing the linear equation (2.26)

**Figure 2.18**

The Simulink block diagram representing the nonlinear equation (2.27)



nonlinearities. Use of this simulation tool is carried out by constructing a block diagram<sup>5</sup> that represents the equations of motion. The linear equation of motion for the pendulum with the parameters as specified in Example 2.6 can be seen from Eq. (2.23) to be

$$\ddot{\theta} = -9.81 * \theta + 1, \quad (2.26)$$

and this is represented in Simulink by the block diagram in Fig. 2.17. Note the circle on the left side of the figure with the + and – signs indicating addition and subtraction, implements Eq. (2.26).

The result of running this numerical simulation will be essentially identical to the linear solution shown in Fig. 2.16 because the solution is for relatively small angles where  $\sin \theta \cong \theta$ . However, using Simulink to solve for the response enables us to simulate the nonlinear equation so we could analyze the system for larger motions. In this case, Eq. (2.26) becomes

$$\ddot{\theta} = -9.81 * \sin \theta + 1, \quad (2.27)$$

and the Simulink block diagram shown in Fig. 2.18 implements this nonlinear equation.

Simulink is capable of simulating all commonly encountered nonlinearities, including deadzones, on-off functions, stiction, hysteresis, aerodynamic drag (a function of  $v^2$ ), and trigonometric functions. All real systems have one or more of these characteristics in varying degrees. These nonlinearities will be expanded upon in detail in Chapter 9.

## EXAMPLE 2.7

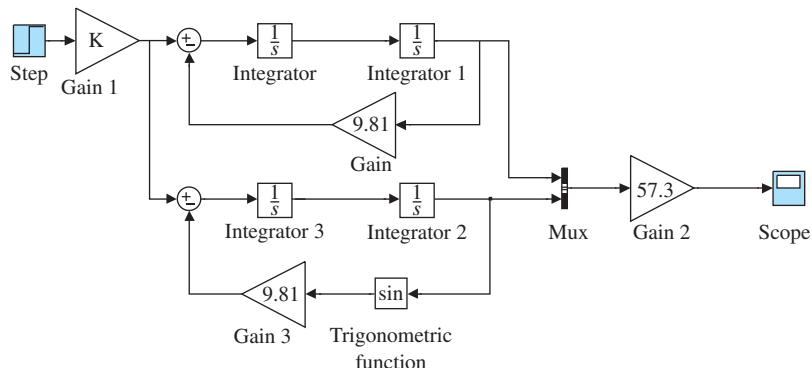
### *Use of Simulink for Nonlinear Motion: Pendulum*

Use Simulink to determine the time history of  $\theta$  for the pendulum in Example 2.6. Compare it against the linear solution for  $T_c$  values of 1 N·m and 4 N·m.

<sup>5</sup>A more extensive discussion of block diagrams is contained in Section 3.2.1 of Chapter 3

**Figure 2.19**

Block diagram of the pendulum for both the linear and nonlinear models



**Solution.** Time history: The Simulink block diagrams for the two cases discussed above are combined and both outputs in Figs. 2.17 and 2.18 are sent via a “multiplexer block (Mux)” to the “scope” so they can be plotted on the same graph. Figure 2.19 shows the combined block diagram where the gain,  $K$ , represents the values of  $T_c$ . The outputs of this system for  $T_c$  values of 1 N·m and 4 N·m are shown in Fig. 2.20. Note for  $T_c = 1$  N·m, the outputs at the top of the figure remain at 12° or less, and the linear approximation is extremely close to the nonlinear output. For  $T_c = 4$  N·m, the output angle grows near to 50° and a substantial difference in the response magnitude and frequency is apparent due to  $\theta$  being a poor approximation to  $\sin \theta$  at these magnitudes. In fact, since  $\sin \theta$  compared to  $\theta$  signifies a reduced gravitational restoring force at the higher angles, we see an increased amplitude and slower frequency.

Chapter 9 will be devoted to the analysis of nonlinear systems and greatly expands on these ideas.

### 2.1.3 Combined Rotation and Translation

In some cases, mechanical systems contain both translational and rotational portions. The procedure is the same as that described in Sections 2.1.1 and 2.1.2: sketch the free-body diagrams, define coordinates and positive directions, determine all forces and moments acting, and apply Eqs. (2.1) and/or (2.10). An exact derivation of the equations for these systems can become quite involved; therefore, the complete analysis for the following example is contained in Appendix W2.1.4 located at [www.pearsonglobaleditions.com](http://www.pearsonglobaleditions.com), and only the linearized equations of motion and their transfer functions are given here.

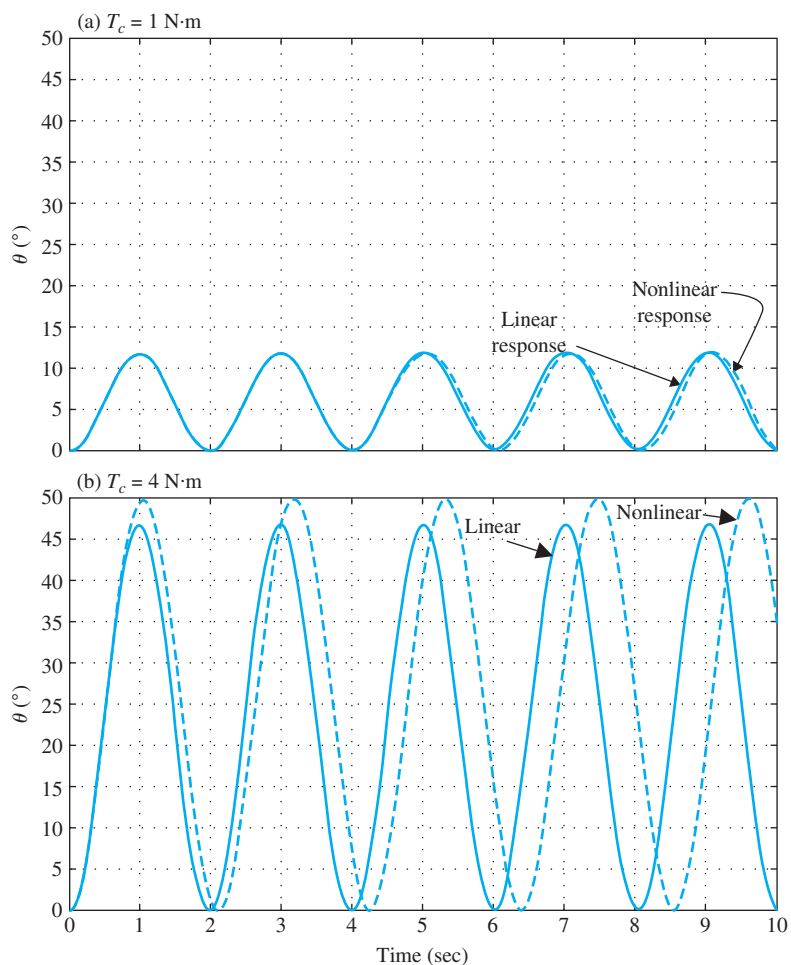
## EXAMPLE 2.8

### *Rotational and Translational Motion: Hanging Crane*

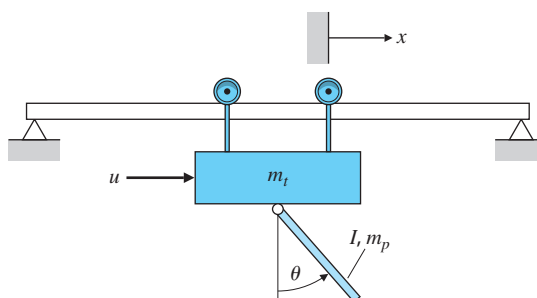
Write the equations of motion for the hanging crane shown schematically in Fig. 2.21. Linearize the equations about  $\theta = 0$ , which would typically be valid for the hanging crane. Also, linearize the equations for

**Figure 2.20**

Response of the pendulum Simulink numerical simulation for the linear and nonlinear models:  
 (a) for  $T_c = 1 \text{ N}\cdot\text{m}$ ;  
 (b)  $T_c = 4 \text{ N}\cdot\text{m}$

**Figure 2.21**

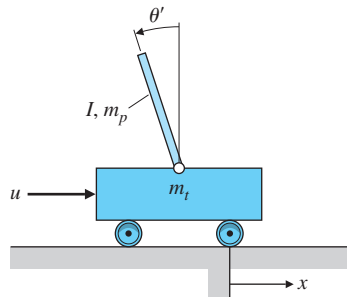
Schematic of the crane with hanging load



$\theta = \pi$ , which represents the situation for the inverted pendulum shown in Fig. 2.22. The trolley has mass  $m_t$  and the hanging crane (or pendulum) has mass  $m_p$  and inertia about its mass center of  $I$ . The distance from the pivot to the mass center of the pendulum is  $l$ ; therefore, the moment of inertia of the pendulum about the pivot point is  $(I + m_p l^2)$ .

**Figure 2.22**

Inverted pendulum



**Solution.** Free-body diagrams need to be drawn for the trolley and the pendulum and the reaction forces considered where the two attach to one another. We carry out this process in Appendix W2.1.3. After Newton's laws are applied for the translational motion of the trolley and the rotational motion of the pendulum, it will be found that the reaction forces between the two bodies can be eliminated, and the only unknowns will be  $\theta$  and  $x$ . The results are two coupled second-order nonlinear differential equations in  $\theta$  and  $x$  with the input being the force applied to the trolley,  $u$ . They can be linearized in a manner similar to that done for the simple pendulum by assuming small angles. For small motions about  $\theta = 0$ , we let  $\cos \theta \cong 1$ ,  $\sin \theta \cong \theta$ , and  $\dot{\theta}^2 \cong 0$ ; thus the equations are approximated by

$$(I + m_p l^2) \ddot{\theta} + m_p g l \theta = -m_p l \ddot{x}, \\ (m_t + m_p) \ddot{x} + b \dot{x} + m_p l \ddot{\theta} = u. \quad (2.28)$$

Note the first equation is very similar to the simple pendulum, Eq. (2.21), where the applied torque arises from the trolley accelerations. Likewise, the second equation representing the trolley motion,  $x$ , is very similar to the car translation in Eq. (2.3), where the forcing term arises from the angular acceleration of the pendulum. Eliminating  $x$  in these two coupled equations leads to the desired transfer function. Neglecting the friction term,  $b$ , simplifies the algebra and leads to an approximate transfer function from the control input  $u$  to hanging crane angle  $\theta$ :

$$\frac{\Theta(s)}{U(s)} = \frac{-m_p l}{((I + m_p l^2)(m_t + m_p) - m_p^2 l^2)s^2 + m_p g l(m_t + m_p)}. \quad (2.29)$$

Inverted pendulum  
equations

For the inverted pendulum in Fig. 2.22, where  $\theta \cong \pi$ , assume  $\theta = \pi + \theta'$ , where  $\theta'$  represents motion from the vertical *upward* direction. In this case,  $\sin \theta \cong -\theta'$ ,  $\cos \theta \cong -1$ , and the nonlinear equations become<sup>6</sup>

<sup>6</sup>The inverted pendulum is often described with the angle of the pendulum being positive for *clockwise* motion. If defined that way, then the sign reverses on all terms in Eqs. (2.30) in  $\theta'$  or  $\dot{\theta}'$ .

$$(I + m_p l^2) \ddot{\theta}' - m_p g l \dot{\theta}' = m_p l \ddot{x}, \\ (m_t + m_p) \ddot{x} + b \dot{x} - m_p l \ddot{\theta}' = u. \quad (2.30)$$

As noted in Example 2.2, a stable system will always have the same signs on each variable, which is the case for the stable hanging crane modeled by Eqs. (2.28). However, the signs on  $\theta$  and  $\ddot{\theta}$  in the first equation in Eq. (2.30) are opposite, thus indicating instability, which is the characteristic of the inverted pendulum.

The transfer function, again without friction, is

$$\frac{\Theta'(s)}{U(s)} = \frac{m_p l}{((I + m_p l^2)(m_t + m_p) - m_p^2 l^2)s^2 - m_p g l(m_t + m_p)}. \quad (2.31)$$

Evaluation of this transfer function for an infinitesimal step in  $u$  will result in a diverging value of  $\theta'$  thus requiring feedback to remain upright, a subject for Chapter 5.

In Chapter 5, you will learn how to stabilize systems using feedback and will see that even unstable systems like an inverted pendulum can be stabilized provided there is a sensor that measures the output quantity and a control input. For the case of the inverted pendulum perched on a trolley, it would be required to measure the pendulum angle,  $\theta'$ , and provide a control input,  $u$ , that accelerated the trolley in such a way that the pendulum remained pointing straight up. In years past, this system existed primarily in university control system laboratories as an educational tool. However, more recently, there is a practical device in production and being sold that employs essentially this same dynamic system: the Segway. It uses a gyroscope so the angle of the device is known with respect to vertical, and electric motors provide a torque on the wheels so it balances the device and provides the desired forward or backward motion. It is shown in Fig. 2.23.

### 2.1.4 Complex Mechanical Systems

This section contains the derivation of the equations of motion for mechanical systems. In particular, it contains the full derivation of the equations of motion for the hanging crane in Example 2.8 and the inverted pendulum on a cart. See Appendix W2.1.4 at [www.pearsonglobaleditions.com](http://www.pearsonglobaleditions.com).

### 2.1.5 Distributed Parameter Systems

All the preceding examples contained one or more rigid bodies, although some were connected to others by springs. Actual structures—for example, satellite solar panels, airplane wings, or robot arms—usually bend, as shown by the flexible beam in Fig. 2.24(a). The equation describing its motion is a fourth-order *partial* differential equation that arises because the mass elements are continuously distributed along the beam with a small amount of flexibility between

**Figure 2.23**

The Segway, which is similar to the inverted pendulum and is kept upright by a feedback control system

*Source: Photo courtesy of David Powell*



elements. This type of system is called a **distributed parameter system**. The dynamic analysis methods presented in this section are not sufficient to analyze this case; however, more advanced texts (Thomson and Dahleh, 1998) show the result is

$$EI \frac{\partial^4 w}{\partial x^4} + \rho \frac{\partial^2 w}{\partial t^2} = 0, \quad (2.32)$$

where

$E$  = Young's modulus,

$I$  = beam area moment of inertia,

$\rho$  = beam density,

$w$  = beam deflection at length  $x$  along the beam.

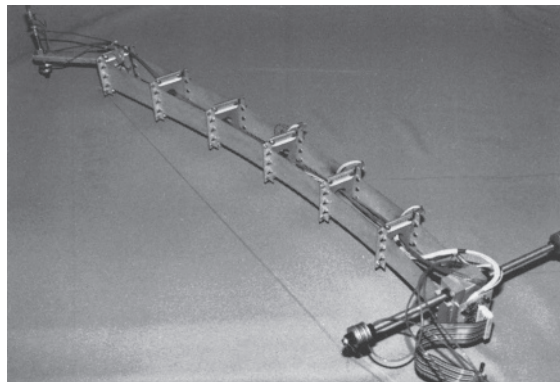
The exact solution to Eq. (2.32) is too cumbersome to use in designing control systems, but it is often important to account for the gross effects of bending in control systems design.

The continuous beam in Fig. 2.24(b) has an infinite number of vibration-mode shapes, all with different frequencies. Typically, the lowest-frequency modes have the largest amplitude and are the most

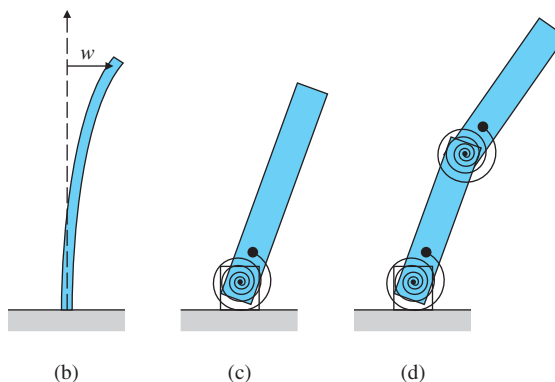
**Figure 2.24**

- (a) Flexible robot arm used for research at Stanford University;
- (b) model for continuous flexible beam;
- (c) simplified model for the first bending mode;
- (d) model for the first and second bending modes

*Source: Photo courtesy of E. Schmitz*



(a)



(b)

(c)

(d)

A flexible structure can be approximated by a lumped parameter model

important to approximate well. The simplified model in Fig. 2.24(c) can be made to duplicate the essential behavior of the first bending mode shape and frequency, and would usually be adequate for controller design. If frequencies higher than the first bending mode are anticipated in the control system operation, it may be necessary to model the beam as shown in Fig. 2.24(d), which can be made to approximate the first two bending modes and frequencies. Likewise, higher-order models can be used if such accuracy and complexity are deemed necessary (Schmitz, 1985; Thomson and Dahleh, 1998). When a continuously bending object is approximated as two or more rigid bodies connected by springs, the resulting model is sometimes referred to as a **lumped parameter model**.

### 2.1.6 Summary: Developing Equations of Motion for Rigid Bodies

The physics necessary to write the equations of motion of a rigid body is entirely given by Newton's laws of motion. The method is as follows:

1. Assign variables such as  $x$  and  $\theta$  that are both necessary and sufficient to describe an *arbitrary* position of the object.
2. Draw a free-body diagram of each component. Indicate *all* forces acting on each body and their reference directions. Also indicate the accelerations of the center of mass with respect to an inertial reference for each body.
3. Apply Newton's law in translation [Eq. (2.1)] and/or rotation [Eq. (2.10)] form.
4. Combine the equations to eliminate internal forces.
5. The number of independent equations should equal the number of unknowns.

## 2.2 Models of Electric Circuits

Electric circuits are frequently used in control systems largely because of the ease of manipulation and processing of electric signals. Although controllers are increasingly implemented with digital logic, many functions are still performed with analog circuits. Analog circuits are faster than digital and, for very simple controllers, an analog circuit would be less expensive than a digital implementation. Furthermore, the power amplifier for electromechanical control and the anti-alias prefilters for digital control must be analog circuits.

Electric circuits consist of interconnections of sources of electric voltage and current, and other electronic elements such as resistors, capacitors, and transistors. An important building block for circuits is an operational amplifier (or op-amp),<sup>7</sup> which is also an example of a complex feedback system. Some of the most important methods of feedback system design were developed by the designers of high-gain, wide-bandwidth feedback amplifiers, mainly at the Bell Telephone Laboratories between 1925 and 1940. Electric and electronic components also play a central role in electromechanical energy conversion devices such as electric motors, generators, and electrical sensors. In this brief survey, we cannot derive the physics of electricity or give a comprehensive review of all the important analysis techniques. We will define the variables, describe the relations imposed on them by typical elements and circuits, and describe a few of the most effective methods available for solving the resulting equations.

Symbols for some linear circuit elements and their current–voltage relations are given in Fig. 2.25. Passive circuits consist of interconnections of resistors, capacitors, and inductors. With electronics, we increase the set of electrical elements by adding active devices, including diodes, transistors, and amplifiers.

---

<sup>7</sup>Oliver Heaviside introduced the mathematical operation  $p$  to signify differentiation so that  $pv = dv/dt$ . The Laplace transform incorporates this idea, using the complex variable  $s$ . Ragazzini et al. (1947) demonstrated that an ideal, high-gain electronic amplifier permitted one to realize arbitrary “operations” in the Laplace transform variable  $s$ , so they named it the operational amplifier, commonly abbreviated to op-amp.

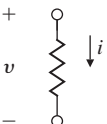
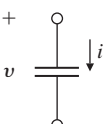
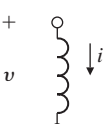
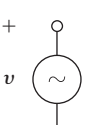
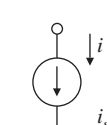
[Kirchhoff's laws](#)

The basic equations of electric circuits, called Kirchhoff's laws, are as follows:

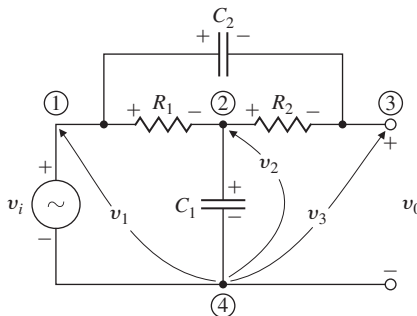
- Kirchhoff's current law (KCL).** The algebraic sum of currents leaving a junction or node equals the algebraic sum of currents entering that node.
- Kirchhoff's voltage law (KVL).** The algebraic sum of all voltages taken around a closed path in a circuit is zero.

With complex circuits of many elements, it is essential to write the equations in a careful, well-organized way. Of the numerous methods for doing this, we choose for description and illustration the popular and powerful scheme known as **node analysis**. One node is selected as a reference and we assume the voltages of all other nodes to be unknowns. The choice of reference is arbitrary in theory, but in actual electronic circuits the common, or ground, terminal is the obvious and standard choice. Next, we write equations for the selected unknowns using the current law (KCL) at each node. We express these currents in terms of the selected unknowns by using the element equations in Fig. 2.25. If the circuit contains voltage sources, we must substitute a voltage law (KVL) for such sources. Example 2.9 illustrates how node analysis works.

**Figure 2.25**  
Elements of electric circuits

	Symbol	Equation
Resistor		$v = Ri$
Capacitor		$i = C \frac{dv}{dt}$
Inductor		$v = L \frac{di}{dt}$
Voltage source		$v = v_s$
Current source		$i = i_s$

**Figure 2.26**  
Bridged tee circuit



### EXAMPLE 2.9 Equations for the Bridged Tee Circuit

Determine the differential equations for the circuit shown in Fig. 2.26.

**Solution.** We select node 4 as the reference and the voltages  $v_1$ ,  $v_2$ , and  $v_3$  at nodes 1, 2, and 3 as the unknowns. We start with the degenerate KVL relationship

$$v_1 = v_i. \quad (2.33)$$

At node 2, the KCL is

$$-\frac{v_1 - v_2}{R_1} + \frac{v_2 - v_3}{R_2} + C_1 \frac{dv_2}{dt} = 0, \quad (2.34)$$

and at node 3, the KCL is

$$\frac{v_3 - v_2}{R_2} + C_2 \frac{d(v_3 - v_1)}{dt} = 0. \quad (2.35)$$

These three equations describe the circuit. If desired, one could eliminate  $v_2$  from the above equations, thus obtaining a second-order differential equation that describes the dynamic relationship between the input,  $v_i (= v_1)$ , and output,  $v_3 (= v_o)$ .

### EXAMPLE 2.10 Equations for a Circuit with a Current Source

Determine the differential equations for the circuit shown in Fig. 2.27. Choose the capacitor voltages and the inductor current as the unknowns.

**Solution.** We select node 3 as the reference and the voltages  $v_1$  and  $v_2$ , and the current through the inductor,  $i_L$ , as unknowns. We start the KCL relationships: relationships:

At node 1, the KCL is

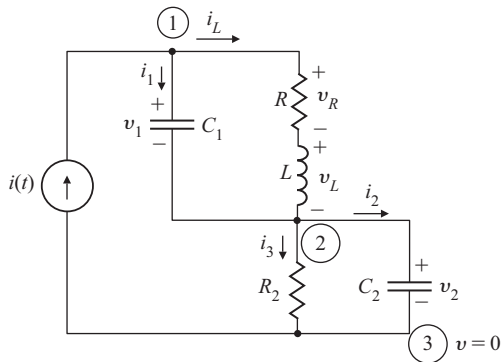
$$i(t) = i_L + i_1, \quad (2.36)$$

and at node 2, the KCL is

$$i_L + i_1 = i_2 + i_3. \quad (2.37)$$

**Figure 2.27**

Circuit for Example 2.10



Furthermore, from Fig. 2.27, we see that

$$i_3 = \frac{v_2}{R_2}, \quad (2.38)$$

$$i_1 = C_1 \frac{dv_1}{dt}, \quad (2.39)$$

$$i_2 = C_2 \frac{dv_2}{dt}, \quad (2.40)$$

$$v_R = i_L R, \quad (2.41)$$

$$L \frac{di_L}{dt} = v_1 - v_R. \quad (2.42)$$

These reduce to three differential equations in the three unknowns,

$$L \frac{di_L}{dt} = v_1 - i_L R, \quad (2.43)$$

$$C_1 \frac{dv_1}{dt} = i(t) - i_L, \quad (2.44)$$

$$C_2 \frac{dv_2}{dt} = i(t) - \frac{v_2}{R_2}. \quad (2.45)$$

### Operational amplifier

Kirchhoff's laws can also be applied to circuits that contain an **operational amplifier**. The simplified circuit of the op-amp is shown in Fig. 2.28(a) and the schematic symbol is drawn in Fig. 2.28(b). If the positive terminal is not shown, it is assumed to be connected to ground,  $v_+ = 0$ , and the reduced symbol of Fig. 2.28(c) is used. For use in control circuits, it is usually assumed that the op-amp is *ideal* with the values  $R_1 = \infty$ ,  $R_0 = 0$ , and  $A = \infty$ . The equations of the ideal op-amp are extremely simple, being

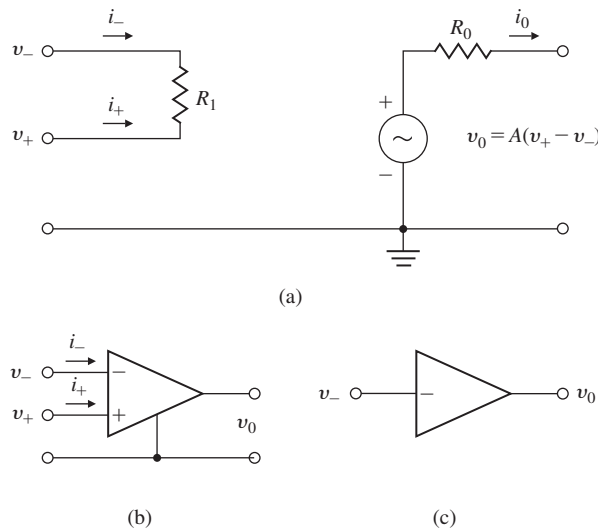
$$i_+ = i_- = 0, \quad (2.46)$$

$$v_+ - v_- = 0. \quad (2.47)$$

The gain of the amplifier is assumed to be so high that the output voltage becomes  $v_{out} = \text{whatever it takes}$  to satisfy these equations. Of

**Figure 2.28**

(a) Op-amp simplified circuit; (b) op-amp schematic symbol; (c) reduced symbol for  $v_+ = 0$



course, a real amplifier only approximates these equations, but unless they are specifically described, we will assume all op-amps are ideal. More realistic models are the subject of several problems given at the end of the chapter.

### EXAMPLE 2.11

#### *Op-Amp Summer*

Find the equations and transfer functions of the circuit shown in Fig. 2.29.

**Solution.** Equation (2.47) requires that  $v_- = 0$ , and thus the currents are  $i_1 = v_1/R_1$ ,  $i_2 = v_2/R_2$ , and  $i_{out} = v_{out}/R_f$ . To satisfy Eq. (2.46),  $i_1 + i_2 + i_{out} = 0$ , from which it follows that  $v_1/R_1 + v_2/R_2 + v_{out}/R_f = 0$ , and we have

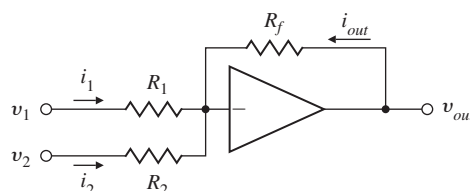
$$v_{out} = - \left[ \frac{R_f}{R_1} v_1 + \frac{R_f}{R_2} v_2 \right]. \quad (2.48)$$

From this equation, we see the circuit output is a weighted sum of the input voltages with a sign change. The circuit is called a **summer**.

A second important example for control is given by the op-amp integrator.

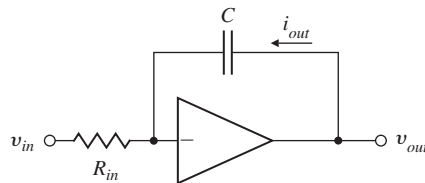
**Figure 2.29**

The op-amp summer



**Figure 2.30**

The op-amp integrator

**EXAMPLE 2.12***Integrator*

Op-amp as integrator

Find the transfer function for the circuit shown in Fig. 2.30.

**Solution.** In this case, the equations are differential and Eqs. (2.46) and (2.47) require

$$i_{in} + i_{out} = 0, \quad (2.49)$$

so

$$\frac{v_{in}}{R_{in}} + C \frac{dv_{out}}{dt} = 0. \quad (2.50)$$

Equation (2.50) can be written in integral form as

$$v_{out} = -\frac{1}{R_{in}C} \int_0^t v_{in}(\tau) d\tau + v_{out}(0). \quad (2.51)$$

Using the operational notation that  $d/dt = s$  in Eq. (2.50), the transfer function (which assumes zero initial conditions) can be written as

$$V_{out}(s) = -\frac{1}{s} \frac{V_{in}(s)}{R_{in}C}. \quad (2.52)$$

Thus the ideal op-amp in this circuit performs the operation of integration and the circuit is simply referred to as an **integrator**.

## 2.3 Models of Electromechanical Systems

Electric current and magnetic fields interact in two ways that are particularly important to an understanding of the operation of most electromechanical actuators and sensors. If a current of  $i$  amp in a conductor of length  $l$  m is arranged at right angles in a magnetic field of  $B$  teslas, then there is a force on the conductor at right angles to the plane of  $i$  and  $B$ , with magnitude

$$F = Bli \text{ N.} \quad (2.53)$$

Law of motors

This equation is the basis of conversion of electric energy to mechanical work and is called the **law of motors**.

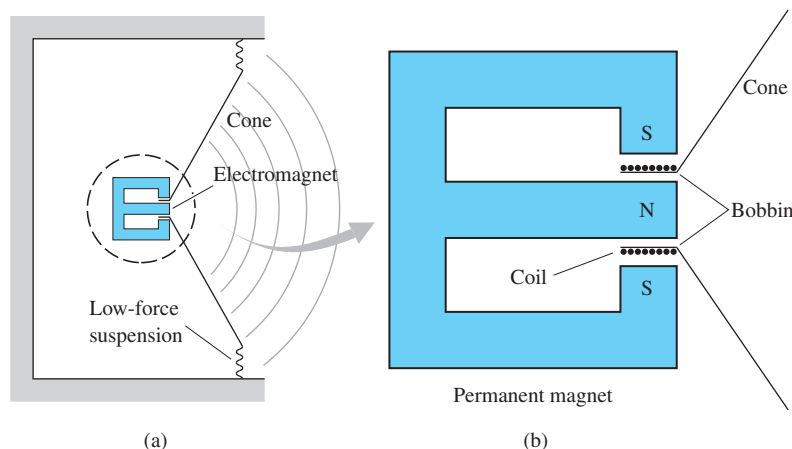
### 2.3.1 Loudspeakers

*Modeling a Loudspeaker***EXAMPLE 2.13**

A typical geometry for a loudspeaker for producing sound is sketched in Fig. 2.31. The permanent magnet establishes a radial field in the cylindrical gap between the poles of the magnet. The force on the conductor

**Figure 2.31**

Geometry of a loudspeaker: (a) overall configuration; (b) the electromagnet and voice coil



wound on the bobbin causes the voice coil to move, producing sound. The effects of the air can be modeled as if the cone had equivalent mass  $M$  and viscous friction coefficient  $b$ . Assume the magnet establishes a uniform field  $B$  of 0.4 tesla and the bobbin has 18 turns at a 1.9-cm diameter. Write the equations of motion of the device.

**Solution.** The current is at right angles to the field, and the force of interest is at right angles to the plane of  $i$  and  $B$ , so Eq. (2.53) applies. In this case the field strength is  $B = 0.4$  tesla and the conductor length is

$$l = 18 \times 2\pi \frac{0.95}{100} = 1.074 \text{ m.}$$

Thus, the force is

$$F = 0.4 \times 1.074 \times i = 0.43i \text{ N.}$$

The mechanical equation follows from Newton's laws, and for a mass  $M$  and friction coefficient  $b$ , the equation is

$$M\ddot{x} + b\dot{x} = 0.43i. \quad (2.54)$$

This second-order differential equation describes the motion of the loudspeaker cone as a function of the input current  $i$  driving the system. Substituting  $s$  for  $d/dt$  in Eq. (2.54) as before, the transfer function is easily found to be

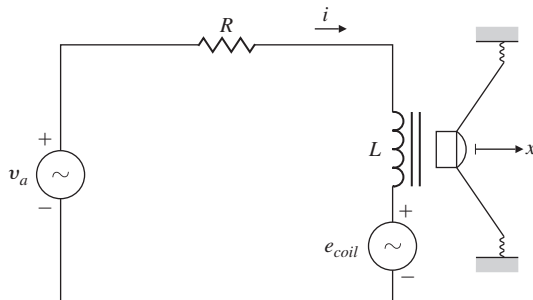
$$\frac{X(s)}{I(s)} = \frac{\frac{0.43}{M}}{s\left(s + \frac{b}{M}\right)}. \quad (2.55)$$

The second important electromechanical relationship is the effect of mechanical motion on electric voltage. If a conductor of length  $l$  m is moving in a magnetic field of  $B$  teslas at a velocity of  $v$  m/sec at mutually right angles, an electric voltage is established across the conductor with magnitude

$$e = Blv \text{ V.} \quad (2.56)$$

**Figure 2.32**

A loudspeaker showing the electric circuit



### Law of generators

### EXAMPLE 2.14

This expression is called the **law of generators**.

#### Loudspeaker with Circuit

For the loudspeaker in Fig. 2.31 and the circuit driving it in Fig. 2.32, find the differential equations relating the input voltage  $v_a$  to the output cone displacement  $x$ . Assume the effective circuit resistance is  $R$  and the inductance is  $L$ .

**Solution.** The loudspeaker motion satisfies Eq. (2.54), and the motion results in a voltage across the coil as given by Eq. (2.56), with the velocity  $\dot{x}$ . The resulting voltage is

$$e_{coil} = Bl\dot{x} = 0.43\dot{x}. \quad (2.57)$$

This induced voltage effect needs to be added to the analysis of the circuit. The equation of motion for the electric circuit is

$$L \frac{di}{dt} + Ri = v_a - 0.43\dot{x}. \quad (2.58)$$

These two coupled equations, (2.54) and (2.58), constitute the dynamic model for the loudspeaker.

Again, substituting  $s$  for  $d/dt$  in these equations and replacing all the parameters with the given numerical values, the transfer function between the applied voltage and the loudspeaker displacement is found to be

$$\frac{X(s)}{V_a(s)} = \frac{0.43}{s[(Ms + b)(Ls + R) + (0.43)^2]}. \quad (2.59)$$

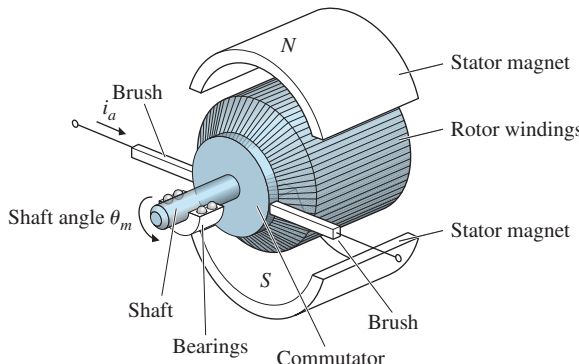
### 2.3.2 Motors

#### DC motor actuators

A common actuator based on the laws of motors and generators and used in control systems is the direct current (DC) motor to provide rotary motion. A sketch of the basic components of a DC motor is given in Fig. 2.33. In addition to housing and bearings, the nonturning part (stator) has magnets, which establish a field across the rotor. The magnets may be electromagnets or, for small motors, permanent magnets. The brushes contact the rotating commutator, which causes the current

**Figure 2.33**

Sketch of a DC motor



always to be in the proper conductor windings so as to produce maximum torque. If the direction of the current is reversed, the direction of the torque is reversed.

The motor equations give the torque  $T$  on the rotor in terms of the armature current  $i_a$  and express the back emf voltage in terms of the shaft's rotational velocity  $\dot{\theta}_m$ .<sup>8</sup>

Thus,

$$T = K_t i_a, \quad (2.60)$$

$$e = K_e \dot{\theta}_m. \quad (2.61)$$

In consistent units, the torque constant  $K_t$  equals the electric constant  $K_e$ , but in some cases, the torque constant will be given in other units, such as ounce-inches per ampere, and the electric constant may be expressed in units of volts per 1000 rpm. In such cases, the engineer must make the necessary translations to be certain the equations are correct.

### EXAMPLE 2.15

#### *Modeling a DC Motor*

Find the equations for a DC motor with the equivalent electric circuit shown in Fig. 2.34(a). Assume the rotor has inertia  $J_m$  and viscous friction coefficient  $b$ .

**Solution.** The free-body diagram for the rotor, shown in Fig. 2.34(b), defines the positive direction and shows the two applied torques,  $T$  and  $b\dot{\theta}_m$ . Application of Newton's laws yields

$$J_m \ddot{\theta}_m + b\dot{\theta}_m = K_t i_a. \quad (2.62)$$

Analysis of the electric circuit, including the back emf voltage, shows the electrical equation to be

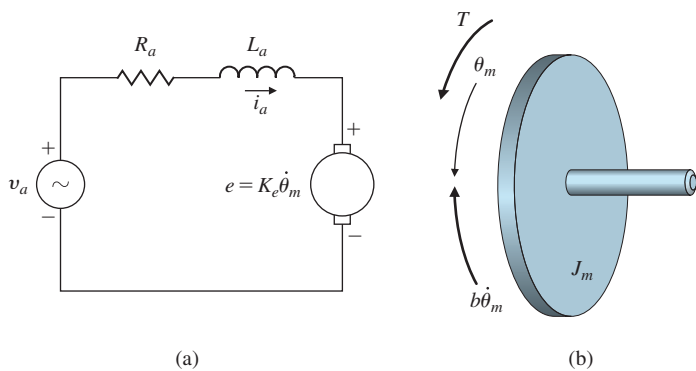
$$L_a \frac{di_a}{dt} + R_a i_a = v_a - K_e \dot{\theta}_m. \quad (2.63)$$

---

<sup>8</sup>Because the generated electromotive force (emf) works against the applied armature voltage, it is called the **back emf**.

**Figure 2.34**

DC motor: (a) electric circuit of the armature; (b) free-body diagram of the rotor



With  $s$  substituted for  $d/dt$  in Eqs. (2.62) and (2.63), the transfer function for the motor is readily found to be

$$\frac{\Theta_m(s)}{V_a(s)} = \frac{K_t}{s[(J_ms + b)(L_as + R_a) + K_t K_e]}. \quad (2.64)$$

In many cases the relative effect of the inductance is negligible compared with the mechanical motion and can be neglected in Eq. (2.63). If so, we can combine Eqs. (2.62) and (2.63) into one equation to get

$$J_m \ddot{\theta}_m + \left( b + \frac{K_t K_e}{R_a} \right) \dot{\theta}_m = \frac{K_t}{R_a} v_a. \quad (2.65)$$

From Eq. (2.65) it is clear that in this case the effect of the back emf is indistinguishable from the friction, and the transfer function is

$$\frac{\Theta_m(s)}{V_a(s)} = \frac{\frac{K_t}{R_a}}{J_ms^2 + \left( b + \frac{K_t K_e}{R_a} \right) s} \quad (2.66)$$

$$= \frac{K}{s(\tau s + 1)}, \quad (2.67)$$

where

$$K = \frac{K_t}{bR_a + K_t K_e}, \quad (2.68)$$

$$\tau = \frac{R_a J_m}{bR_a + K_t K_e}. \quad (2.69)$$

In many cases, a transfer function between the motor input and the output speed ( $\omega = \dot{\theta}_m$ ) is required. In such cases, the transfer function would be

$$\frac{\Omega(s)}{V_a(s)} = s \frac{\Theta_m(s)}{V_a(s)} = \frac{K}{\tau s + 1}. \quad (2.70)$$

---

Another device used for electromechanical energy conversion is the alternating current (AC) induction motor invented by N. Tesla. Elementary analysis of the AC motor is more complex than that of the DC motor. A typical experimental set of curves of torque versus speed for

fixed frequency and varying amplitude of applied (sinusoidal) voltage is given in Fig. 2.35. Although the data in the figure are for a constant engine speed, they can be used to extract the motor constants that will provide a dynamic model for the motor. For analysis of a control problem involving an AC motor such as that described by Fig. 2.35, we make a linear approximation to the curves for speed near zero and at a midrange voltage to obtain the expression

$$T = K_1 v_a - K_2 \dot{\theta}_m. \quad (2.71)$$

The constant  $K_1$  represents the ratio of a change in torque to a change in voltage at zero speed, and is proportional to the distance between the curves at zero speed. The constant  $K_2$  represents the ratio of a change in torque to a change in speed at zero speed and a midrange voltage; therefore, it is the slope of a curve at zero speed as shown by the line at  $V_2$ . For the electrical portion, values for the armature resistance  $R_a$  and inductance  $L_a$  are also determined by experiment. Once we have values for  $K_1$ ,  $K_2$ ,  $R_a$ , and  $L_a$ , the analysis proceeds as the analysis in Example 2.15 for the DC motor. For the case in which the inductor can be neglected, we can substitute  $K_1$  and  $K_2$  into Eq. (2.65) in place of  $K_t/R_a$  and  $K_t K_e/R_a$ , respectively.

In addition to the DC and AC motors mentioned here, control systems use brushless DC motors (Reliance Motion Control Corp., 1980) and stepping motors (Kuo, 1980). Models for these machines, developed in the works just cited, do not differ in principle from the motors considered in this section. In general, the analysis, supported by experiment, develops the torque as a function of voltage and speed similar to the AC motor torque-speed curves given in Fig. 2.35. From such curves, one can obtain a linearized formula such as Eq. (2.71) to use in

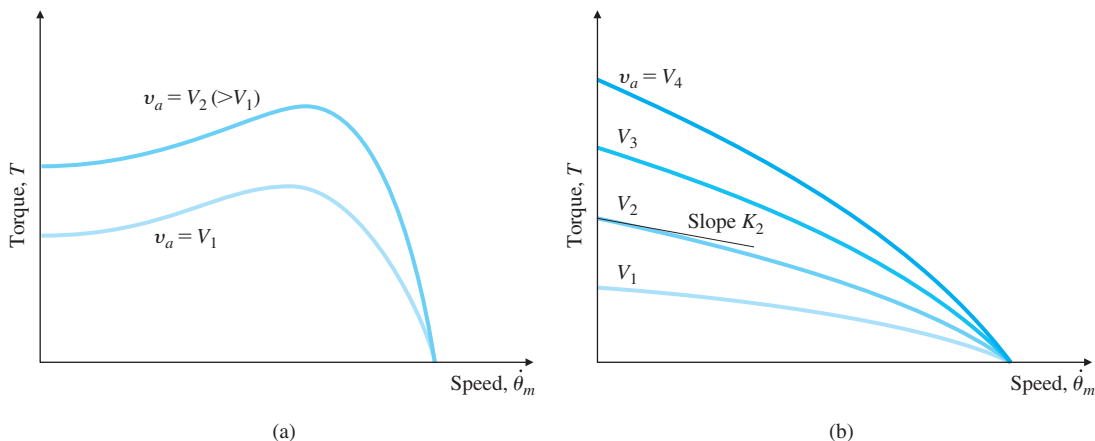


**Figure 2.35**

Torque-speed curves for a servo motor showing four amplitudes of armature voltage: (a) low-rotor-resistance machine; (b) high-rotor-resistance machine showing four values of armature voltage,  $v_a$

the mechanical part of the system and an equivalent circuit consisting of a resistance and an inductance to use in the electrical part.

### △ 2.3.3 Gears

The motors used for control purposes are often used in conjunction with gears as shown in Fig. 2.36 in order to multiply the torque. The force transmitted by the teeth of one gear is equal and opposite to the force applied to the other gear as shown in Fig. 2.36(a); therefore, since torque = force  $\times$  distance, the torques applied to and from each shaft by the teeth obeys

$$\frac{T_1}{r_1} = \frac{T_2}{r_2} = f, \text{ force applied by teeth} \quad (2.72)$$

and thus, we see that the torque multiplication is proportional to the radius of the gears,  $r$ , or equivalently, the number of teeth,  $N$ , in each gear,

$$\frac{T_2}{T_1} = \frac{r_2}{r_1} = \frac{N_2}{N_1} = n, \quad (2.73)$$

where we have defined the quantity,  $n$ , to be the gear ratio.

Similarly, the velocity of the contact tooth of one gear is the same as the velocity of the tooth on the opposite gear, and since velocity =  $\omega r$ , where  $\omega$  is the angular velocity,

$$\omega_1 r_1 = \omega_2 r_2 = v.$$

Thus,

$$\frac{\omega_1}{\omega_2} = \frac{r_2}{r_1} = \frac{N_2}{N_1} = n. \quad (2.74)$$

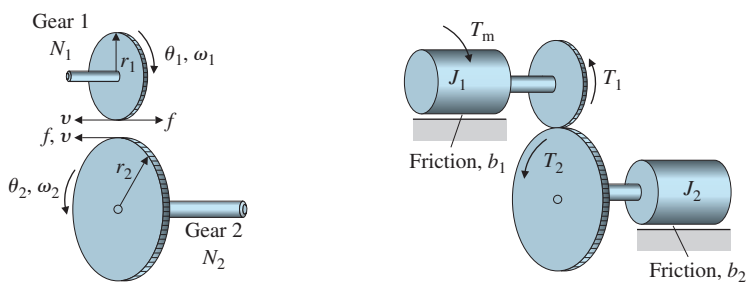
Furthermore, the angles will change in proportion to the angular velocities, so

$$\frac{\theta_1}{\theta_2} = \frac{\omega_1}{\omega_2} = \frac{N_2}{N_1} = n. \quad (2.75)$$

Note these are all geometric relationships in the sense that we have not considered any inertias or accelerations of the gear train. These relationships simply change the scale factor on the torque and speed from a motor. There is also another effect that must be considered: the

**Figure 2.36**

(a) Geometry definitions and forces on teeth; (b) definitions for the dynamic analysis



effective rotational inertia and damping of the system when considering the dynamics. Suppose the servo motor whose output torque is  $T_m$  is attached to gear 1. Also suppose the servo's gear 1 is meshed with gear 2, and the angle  $\theta_2$  describes its position (body 2). Furthermore, the inertia of gear 1 and all that is attached to it (body 1) is  $J_1$ , while the inertia of the second gear and all the attached load (body 2) is  $J_2$ , similarly for the friction  $b_1$  and  $b_2$ . We wish to determine the transfer function between the applied torque,  $T_m$ , and the output  $\theta_2$ , that is,  $\Theta_2(s)/T_m(s)$ . The equation of motion for body 1 is

$$J_1\ddot{\theta}_1 + b_1\dot{\theta}_1 = T_m - T_1, \quad (2.76)$$

where  $T_1$  is the reaction torque from gear 2 acting back on gear 1. For body 2, the equation of motion is

$$J_2\ddot{\theta}_2 + b_2\dot{\theta}_2 = T_2, \quad (2.77)$$

where  $T_2$  is the torque applied on gear 2 by gear 1. Note that these are not independent systems because the motion is tied together by the gears. Substituting  $\theta_2$  for  $\theta_1$  in Eq. (2.76) using the relationship from Eq. (2.75), replacing  $T_2$  with  $T_1$  in Eq. (2.77) using the relationship in Eq. (2.73), and eliminating  $T_1$  between the two equations results in

$$(J_2 + J_1n^2)\ddot{\theta}_2 + (b_2 + b_1n^2)\dot{\theta}_2 = nT_m. \quad (2.78)$$

So the transfer function is

$$\frac{\Theta_2(s)}{T_m(s)} = \frac{n}{J_{eq}s^2 + b_{eq}s}, \quad (2.79)$$

where

$$J_{eq} = J_2 + J_1n^2, \text{ and } b_{eq} = b_2 + b_1n^2. \quad (2.80)$$

These quantities are referred to as the “equivalent” inertias and damping coefficients.<sup>9</sup> If the transfer function had been desired between the applied torque,  $T_m$ , and  $\theta_1$ , a similar analysis would be required to arrive at the equivalent inertias and damping, which would be different from those above.

## △ 2.4 Heat and Fluid-Flow Models

Thermodynamics, heat transfer, and fluid dynamics are each the subject of complete textbooks. For purposes of generating dynamic models for use in control systems, the most important aspect of the physics is to represent the dynamic interaction between the variables. Experiments are usually required to determine the actual values of the parameters, and thus to complete the dynamic model for purposes of control systems design.

---

<sup>9</sup>The equivalent inertia is sometimes referred to as “reflected impedance”; however, this term is more typically applied to electronic circuits.

### 2.4.1 Heat Flow

Some control systems involve regulation of temperature for portions of the system. The dynamic models of temperature control systems involve the flow and storage of heat energy. Heat energy flows through substances at a rate proportional to the temperature difference across the substance; that is,

$$q = \frac{1}{R}(T_1 - T_2), \quad (2.81)$$

where

$q$  = heat-energy flow, joules per second (J/sec),

$R$  = thermal resistance,  $^{\circ}\text{C}/\text{J} \cdot \text{sec}$ ,

$T$  = temperature,  $^{\circ}\text{C}$ .

The net heat-energy flow into a substance affects the temperature of the substance according to the relation

$$\dot{T} = \frac{1}{C}q, \quad (2.82)$$

where  $C$  is the thermal capacity. Typically, there are several paths for heat to flow into or out of a substance, and  $q$  in Eq. (2.82) is the sum of heat flows obeying Eq. (2.81).

#### EXAMPLE 2.16

##### Heat Flow from a Room

A room with all but two sides insulated ( $1/R = 0$ ) is shown in Fig. 2.37. Find the differential equations that determine the temperature in the room.

**Solution.** Application of Eqs. (2.81) and (2.82) yields

$$\dot{T}_I = \frac{1}{C_I} \left( \frac{1}{R_1} + \frac{1}{R_2} \right) (T_O - T_I),$$

where

$C_I$  = thermal capacity of air within the room,

$T_O$  = temperature outside,

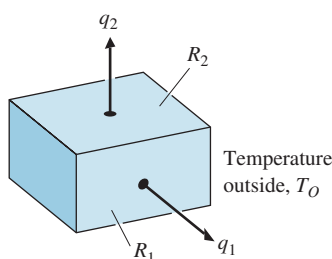
$T_I$  = temperature inside,

$R_2$  = thermal resistance of the room ceiling,

$R_1$  = thermal resistance of the room wall.

**Figure 2.37**

Dynamic model for room temperature



Normally the material properties are given in tables as follows:

**Specific heat**

1. The specific heat at constant volume  $c_v$ , which is converted to heat capacity by

$$C = mc_v, \quad (2.83)$$

where  $m$  is the mass of the substance;

**Thermal conductivity**

2. The thermal conductivity<sup>10</sup>  $k$ , which is related to thermal resistance  $R$  by

$$\frac{1}{R} = \frac{kA}{l},$$

where  $A$  is the cross-sectional area and  $l$  is the length of the heat-flow path.

## EXAMPLE 2.17

### A Thermal Control System

The system consists of two thermal masses in contact with one another where heat is being applied to the mass on the left, as shown in Fig. 2.38. There is also heat transferred directly to the second mass in contact with it, and heat is lost to the environment from both masses. Find the relevant dynamic equations and the transfer function between the heat input,  $u$ , and the temperature of the mass on the right.

**Solution.** Applying Eqs. (2.81) and (2.82) yields

$$C_1 \dot{T}_1 = u - H_1 T_1 - H_x(T_1 - T_2), \quad (2.84)$$

$$C_2 \dot{T}_2 = H_x(T_1 - T_2) - H_2 T_2, \quad (2.85)$$

where

$C_1$  = thermal capacity of mass 1,

$C_2$  = thermal capacity of mass 2,

$T_o$  = temperature outside the masses,

$T_1 = T_1^* - T_o$  temperature difference of mass 1,

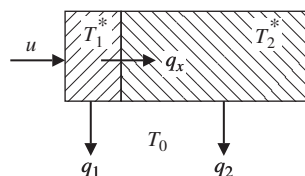
$T_2 = T_2^* - T_o$  temperature difference of mass 2,

$H_1 = 1/R_1$  = thermal resistance from mass 1,

$H_2 = 1/R_2$  = thermal resistance from mass 2,

$H_x = 1/R_x$  = thermal resistance from mass 1 to mass 2.

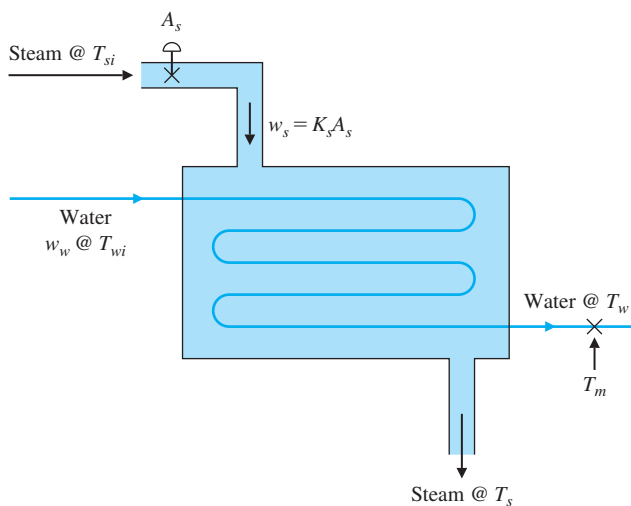
**Figure 2.38**  
A Thermal Control System



<sup>10</sup>In the case of insulation for houses, resistance is quoted as  $R$ -values; for example,  $R-11$  refers to a substance that has a resistance to heat-flow equivalent to that given by 11 in. of solid wood.

**Figure 2.39**

Heat exchanger



Using Cramer's Rule with Eqs. (2.84) and (2.85) yields the desired transfer function

$$\frac{T_2(s)}{U(s)} = \frac{H_x}{(C_1s + H_x + H_1)(C_2s + H_x + H_2)}. \quad (2.86)$$

In addition to flow due to transfer, as expressed by Eq. (2.81), heat can also flow when a warmer mass flows into a cooler mass, or vice versa. In this case,

$$q = wc_v(T_1 - T_2), \quad (2.87)$$

where  $w$  is the mass flow rate of the fluid at  $T_1$  flowing into the reservoir at  $T_2$ . For a more complete discussion of dynamic models for temperature control systems, see Cannon (1967) or textbooks on heat transfer.

### EXAMPLE 2.18

#### *Equations for Modeling a Heat Exchanger*

A heat exchanger is shown in Fig. 2.39. Steam enters the chamber through the controllable valve at the top, and cooler steam leaves at the bottom. There is a constant flow of water through the pipe that winds through the middle of the chamber so it picks up heat from the steam. Find the differential equations that describe the dynamics of the measured water outflow temperature as a function of the area  $A_s$  of the steam-inlet control valve when open. The sensor that measures the water outflow temperature, being downstream from the exit temperature in the pipe, lags the temperature by  $t_d$  sec.

**Solution.** The temperature of the water in the pipe will vary continuously along the pipe as the heat flows from the steam to the water. The temperature of the steam will also reduce in the chamber as it passes

over the maze of pipes. An accurate thermal model of this process is therefore quite involved because the actual heat transfer from the steam to the water will be proportional to the local temperatures of each fluid. For many control applications, it is not necessary to have great accuracy because the feedback will correct for a considerable amount of error in the model. Therefore, it makes sense to combine the spatially varying temperatures into single temperatures  $T_s$  and  $T_w$  for the outflow steam and water temperatures, respectively. We then assume the heat transfer from steam to water is proportional to the difference in these temperatures, as given by Eq. (2.81). There is also a flow of heat into the chamber from the inlet steam that depends on the steam flow rate and its temperature according to Eq. (2.87),

$$q_{in} = w_s c_{vs} (T_{si} - T_s),$$

where

$w_s = K_s A_s$ , mass flow rate of the steam,

$A_s$  = area of the steam inlet valve,

$K_s$  = flow coefficient of the inlet valve,

$c_{vs}$  = specific heat of the steam,

$T_{si}$  = temperature of the inflow steam,

$T_s$  = temperature of the outflow steam.

The net heat flow into the chamber is the difference between the heat from the hot incoming steam and the heat flowing out to the water. This net flow determines the rate of temperature change of the steam according to Eq. (2.82),

$$C_s \dot{T}_s = A_s K_s c_{vs} (T_{si} - T_s) - \frac{1}{R} (T_s - T_w), \quad (2.88)$$

where

$C_s = m_s c_{vs}$  is the thermal capacity of the steam in the chamber with mass  $m_s$ ,

$R$  = the thermal resistance of the heat flow averaged over the entire exchanger.

Likewise, the differential equation describing the water temperature is

$$C_w \dot{T}_w = w_w c_{cw} (T_{wi} - T_w) + \frac{1}{R} (T_s - T_w), \quad (2.89)$$

where

$w_w$  = mass flow rate of the water,

$c_{cw}$  = specific heat of the water,

$T_{wi}$  = temperature of the incoming water,

$T_w$  = temperature of the outflowing water.

To complete the dynamics, the time delay between the measurement and the exit flow is described by the relation

$$T_m(t) = T_w(t - t_d),$$

where  $T_m$  is the measured downstream temperature of the water and  $t_d$  is the time delay. There may also be a delay in the measurement of the steam temperature  $T_s$ , which would be modeled in the same manner.

Equation (2.88) is nonlinear because the quantity  $T_s$  is multiplied by the control input  $A_s$ . The equation can be linearized about  $T_{so}$  (a specific value of  $T_s$ ) so  $T_{si} - T_s$  is assumed constant for purposes of approximating the nonlinear term, which we will define as  $\Delta T_s$ . In order to eliminate the  $T_{wi}$  term in Eq. (2.89), it is convenient to measure all temperatures in terms of deviation in degrees from  $T_{wi}$ . The resulting equations are then

$$\begin{aligned} C_s \dot{T}_s &= -\frac{1}{R} T_s + \frac{1}{R} T_w + K_s c_{vs} \Delta T_s A_s, \\ C_w \dot{T}_w &= -\left(\frac{1}{R} + w_w c_{vw}\right) T_w + \frac{1}{R} T_s, \\ T_m &= T_w(t - t_d). \end{aligned}$$

Although the time delay is not a nonlinearity, we will see in Chapter 3 that operationally,  $T_m = e^{-t_d s} T_w$ . Therefore, the transfer function of the heat exchanger has the form

$$\frac{T_m(s)}{A_s(s)} = \frac{K e^{-t_d s}}{(\tau_1 s + 1)(\tau_2 s + 1)}. \quad (2.90)$$


---

## 2.4.2 Incompressible Fluid Flow

[Hydraulic actuator](#)

Fluid flows are common in many control system components. One example is the hydraulic actuator, which is used extensively in control systems because it can supply a large force with low inertia and low weight. They are often used to move the aerodynamic control surfaces of airplanes; to gimbal rocket nozzles; to move the linkages in earth-moving equipment, farm tractor implements, snow-grooming machines; and to move robot arms.

[The continuity relation](#)

The physical relations governing fluid flow are continuity, force equilibrium, and resistance. The continuity relation is simply a statement of the conservation of matter; that is,

$$\dot{m} = w_{in} - w_{out}, \quad (2.91)$$

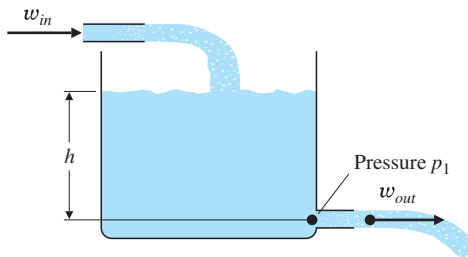
where

$m$  = fluid mass within a prescribed portion of the system,

$w_{in}$  = mass flow rate into the prescribed portion of the system,

$w_{out}$  = mass flow rate out of the prescribed portion of the system.

**Figure 2.40**  
Water tank example



### EXAMPLE 2.19

#### Equations for Describing Water Tank Height

Determine the differential equation describing the height of the water in the tank in Fig. 2.40.

**Solution.** Application of Eq. (2.91) yields

$$\dot{h} = \frac{1}{A\rho} (w_{in} - w_{out}), \quad (2.92)$$

where

$A$  = area of the tank,

$\rho$  = density of water,

$h = m/A\rho$  = height of water,

$m$  = mass of water in the tank.

Force equilibrium must apply exactly as described by Eq. (2.1) for mechanical systems. Sometimes in fluid-flow systems, some forces result from fluid pressure acting on a piston. In this case, the force from the fluid is

$$f = pA, \quad (2.93)$$

where

$f$  = force,

$p$  = pressure in the fluid,

$A$  = area on which the fluid acts.

### EXAMPLE 2.20

#### Modeling a Hydraulic Piston

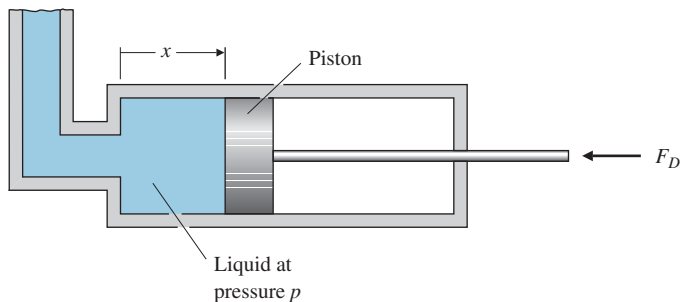
Determine the differential equation describing the motion of the piston actuator shown in Fig. 2.41, given that there is a force  $F_D$  acting on it and a pressure  $p$  in the chamber.

**Solution.** Equations (2.1) and (2.93) apply directly, where the forces include the fluid pressure as well as the applied force. The result is

$$M\ddot{x} = Ap - F_D,$$

**Figure 2.41**

Hydraulic piston actuator



where

$A$  = area of the piston,

$p$  = pressure in the chamber,

$M$  = mass of the piston,

$x$  = position of the piston.

In many cases of fluid-flow problems, the flow is resisted either by a constriction in the path or by friction. The general form of the effect of resistance is given by

$$w = \frac{1}{R}(p_1 - p_2)^{1/\alpha}, \quad (2.94)$$

where

$w$  = mass flow rate,

$p_1, p_2$  = pressures at ends of the path through which flow is occurring,

$R, \alpha$  = constants whose values depend on the type of restriction.

Or, as is more commonly used in hydraulics,

$$Q = \frac{1}{\rho R}(p_1 - p_2)^{1/\alpha}, \quad (2.95)$$

where

$Q$  = volume flow rate, where  $Q = w/\rho$ ,

$\rho$  = fluid density.

The constant  $\alpha$  takes on values between 1 and 2. The most common value is approximately 2 for high flow rates (those having a Reynolds number  $Re > 10^5$ ) through pipes or through short constrictions or nozzles. For very slow flows through long pipes or porous plugs wherein the flow remains laminar ( $Re \lesssim 1000$ ),  $\alpha = 1$ . Flow rates between these extremes can yield intermediate values of  $\alpha$ . The Reynolds number indicates the relative importance of inertial forces and viscous forces in the flow. It is proportional to a material's velocity and density and to

the size of the restriction, and it is inversely proportional to the viscosity. When  $\text{Re}$  is small, the viscous forces predominate and the flow is laminar. When  $\text{Re}$  is large, the inertial forces predominate and the flow is turbulent.

Note a value of  $\alpha = 2$  indicates that the flow is proportional to the square root of the pressure difference and therefore will produce a nonlinear differential equation. For the initial stages of control systems analysis and design, it is typically very useful to linearize these equations so the design techniques described in this book can be applied. Linearization involves selecting an operating point and expanding the nonlinear term to be a small perturbation from that point.

### EXAMPLE 2.21

#### *Linearization of Water Tank Height and Outflow*

Find the nonlinear differential equation describing the height of the water in the tank in Fig. 2.40. Assume there is a relatively short restriction at the outlet and that  $\alpha = 2$ . Also linearize your equation about the operating point  $h_o$ .

**Solution.** Applying Eq. (2.94) yields the flow out of the tank as a function of the height of the water in the tank:

$$w_{out} = \frac{1}{R}(p_1 - p_a)^{1/2}. \quad (2.96)$$

Here,

$p_1 = \rho gh + p_a$ , the hydrostatic pressure,

$p_a$  = ambient pressure outside the restriction.

Substituting Eq. (2.96) into Eq. (2.92) yields the nonlinear differential equation for the height:

$$\dot{h} = \frac{1}{A\rho} \left( w_{in} - \frac{1}{R} \sqrt{p_1 - p_a} \right). \quad (2.97)$$

Linearization involves selecting the operating point  $p_o = \rho g h_o + p_a$  and substituting  $p_1 = p_o + \Delta p$  into Eq. (2.96). Then, we expand the nonlinear term according to the relation

$$(1 + \varepsilon)^\beta \cong 1 + \beta\varepsilon, \quad (2.98)$$

where  $\varepsilon \ll 1$ . Equation (2.96) can thus be written as

$$\begin{aligned} w_{out} &= \frac{\sqrt{p_o - p_a}}{R} \left( 1 + \frac{\Delta p}{p_o - p_a} \right)^{1/2} \\ &\cong \frac{\sqrt{p_o - p_a}}{R} \left( 1 + \frac{1}{2} \frac{\Delta p}{p_o - p_a} \right). \end{aligned} \quad (2.99)$$

The linearizing approximation made in Eq. (2.99) is valid as long as  $\Delta p \ll p_o - p_a$ ; that is, as long as the deviations of the system pressure from the chosen operating point are relatively small.

Combining Eqs. (2.92) and (2.99) yields the following linearized equation of motion for the water tank level:

$$\Delta\dot{h} = \frac{1}{A\rho} \left[ w_{in} - \frac{\sqrt{p_o - p_a}}{R} \left( 1 + \frac{1}{2} \frac{\Delta p}{p_o - p_a} \right) \right].$$

Because  $\Delta p = \rho g \Delta h$ , this equation reduces to

$$\Delta\dot{h} = -\frac{g}{2AR\sqrt{p_o - p_a}} \Delta h + \frac{w_{in}}{A\rho} - \frac{\sqrt{p_o - p_a}}{\rho AR}, \quad (2.100)$$

which is a linear differential equation for  $\Delta\dot{h}$ . The operating point is not an equilibrium point because some control input is required to maintain it. In other words, when the system is at the operating point ( $\Delta h = 0$ ) with no input ( $w_{in} = 0$ ), it will move from that point because  $\Delta\dot{h} \neq 0$ . So, if no water is flowing into the tank, the tank will drain, thus moving it from the reference point. To define an operating point that is also an equilibrium point, we need to require that there be a nominal flow rate,

$$\frac{w_{in_0}}{A\rho} = \frac{\sqrt{p_o - p_a}}{\rho AR},$$

and define the linearized input flow to be a perturbation from that value.

### Hydraulic actuators

Hydraulic actuators obey the same fundamental relationships we saw in the water tank: continuity [Eq. (2.91)], force balance [Eq. (2.93)], and flow resistance [Eq. (2.94)]. Although the development here assumes the fluid to be perfectly incompressible, in fact, hydraulic fluid has some compressibility due primarily to entrained air. This feature causes hydraulic actuators to have some resonance because the compressibility of the fluid acts like a stiff spring. This resonance limits their speed of response.

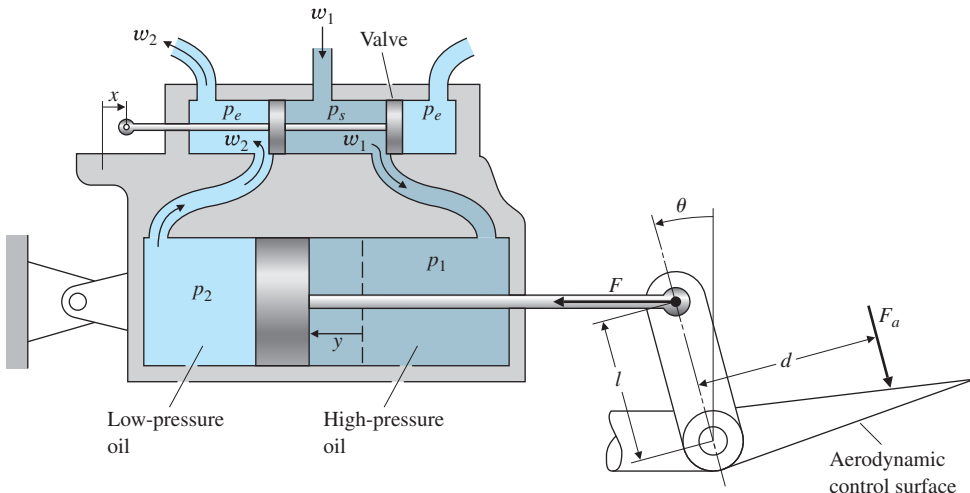
## EXAMPLE 2.22

### *Modeling a Hydraulic Actuator*

- Find the nonlinear differential equations relating the movement  $\theta$  of the control surface to the input displacement  $x$  of the valve for the hydraulic actuator shown in Fig. 2.42.
- Find the linear approximation to the equations of motion when  $\dot{y} = \text{constant}$ , with and without an applied load—that is, when  $F \neq 0$  and when  $F = 0$ . Assume  $\theta$  motion is small.

### Solution

- Equations of motion:** When the valve is at  $x = 0$ , both passages are closed and no motion results. When  $x > 0$ , as shown in Fig. 2.42, the oil flows clockwise as shown and the piston is forced to the left. When  $x < 0$ , the fluid flows counterclockwise. The oil supply at high pressure  $p_s$  enters the *left* side of the large piston chamber, forcing the piston to the right. This causes the oil to flow out of the valve chamber from the rightmost channel instead of the left.

**Figure 2.42**

Hydraulic actuator with valve

We assume the flow through the orifice formed by the valve is proportional to  $x$ ; that is,

$$Q_1 = \frac{1}{\rho R_1} (p_s - p_1)^{1/2} x. \quad (2.101)$$

Similarly,

$$Q_2 = \frac{1}{\rho R_2} (p_2 - p_e)^{1/2} x. \quad (2.102)$$

The continuity relation yields

$$A\dot{y} = Q_1 = Q_2, \quad (2.103)$$

where

$$A = \text{piston area.}$$

The force balance on the piston yields

$$A(p_1 - p_2) - F = m\ddot{y}, \quad (2.104)$$

where

$m$  = mass of the piston and the attached rod,

$F$  = force applied by the piston rod to the control surface attachment point.

Furthermore, the moment balance of the control surface using Eq. (2.10) yields

$$I\ddot{\theta} = Fl \cos \theta - F_a d, \quad (2.105)$$

where

$I$  = moment of inertia of the control surface and attachment about the hinge,

$F_a$  = applied aerodynamic load.

To solve this set of five equations, we require the following additional kinematic relationship between  $\theta$  and  $y$ :

$$y = l \sin \theta. \quad (2.106)$$

The actuator is usually constructed so the valve exposes the two passages equally; therefore,  $R_1 = R_2$ , and we can infer from Eqs. (2.101) to (2.103) that

$$p_s - p_1 = p_2 - p_e. \quad (2.107)$$

These relations complete the nonlinear differential equations of motion; they are formidable and difficult to solve.

2. **Linearization and simplification:** For the case in which  $\dot{y} = 0$  and there is no applied load ( $F = 0$ ), Eqs. (2.104) and (2.107) indicate that

$$p_1 = p_2 = \frac{p_s + p_e}{2}. \quad (2.108)$$

Therefore, using Eq. (2.103) and letting  $\sin \theta = \theta$  (since  $\theta$  is assumed to be small), we get

$$\dot{\theta} = \frac{\sqrt{p_s - p_e}}{\sqrt{2}A\rho Rl}x. \quad (2.109)$$

This represents a single integration between the input  $x$  and the output  $\theta$ , where the proportionality constant is a function only of the supply pressure and the fixed parameters of the actuator. For the case  $\dot{y} = \text{constant}$  but  $F \neq 0$ , Eqs. (2.104) and (2.107) indicate that

$$p_1 = \frac{p_s + p_e + F/A}{2}$$

and

$$\dot{\theta} = \frac{\sqrt{p_s - p_e - F/A}}{\sqrt{2}A\rho Rl}x. \quad (2.110)$$

This result is also a single integration between the input  $x$  and the output  $\theta$ , but the proportionality constant now depends on the applied load  $F$ .

As long as the commanded values of  $x$  produce  $\theta$  motion that has a sufficiently small value of  $\ddot{\theta}$ , the approximation given by Eq. (2.109) or (2.110) is valid and no other linearized dynamic relationships are necessary. However, as soon as the commanded values of  $x$  produce accelerations in which the inertial forces ( $m\ddot{y}$  and the reaction to  $I\ddot{\theta}$ ) are a significant fraction of  $p_s - p_e$ , the approximations are no longer valid. We must then incorporate these forces into the equations, thus obtaining a dynamic relationship between  $x$  and  $\theta$  that is much more involved than the pure integration implied by Eq. (2.109) or (2.110). Typically, for initial control system designs, hydraulic actuators are assumed to obey the simple relationship of Eq. (2.109) or (2.110). When hydraulic

actuators are used in feedback control systems, resonances have been encountered that are not explained by using the approximation that the device is a simple integrator as in Eq. (2.109) or (2.110). The source of the resonance is the neglected accelerations discussed above along with the additional feature that the oil is slightly compressible due to small quantities of entrained air. This phenomenon is called the “oil-mass resonance.”

---

## 2.5 Historical Perspective

Newton's second law of motion (Eq. 2.1) was first published in his *Philosophiae Naturalis Principia Mathematica* in 1686 along with his two other famous laws of motion. The first: A body will continue with the same uniform motion unless acted on by an external unbalanced force, and the third: To every action, there is an equal and opposite reaction. Isaac Newton also published his law of gravitation in this same publication, which stated that every mass particle attracts all other particles by a force proportional to the inverse of the square of the distance between them and the product of their two masses. His basis for developing these laws was the work of several other early scientists, combined with his own development of the calculus in order to reconcile all the observations. It is amazing that these laws still stand today as the basis for almost all dynamic analysis with the exception of Einstein's additions in the early 1900s for relativistic effects. It is also amazing that Newton's development of calculus formed the foundation of our mathematics that enable dynamic modeling. In addition to being brilliant, he was also very eccentric. As Brennan writes in *Heisenberg Probably Slept Here*, “He was seen about campus in his disheveled clothes, his wig askew, wearing run-down shoes and a soiled neckpiece. He seemed to care about nothing but his work. He was so absorbed in his studies that he forgot to eat.” Another interesting aspect of Newton is that he initially developed the calculus and the now famous laws of physics about 20 years prior to publishing them! The incentive to publish them arose from a bet between three men having lunch at a pub in 1684: Edmond Halley, Christopher Wren, and Robert Hooke. They all had the opinion that Kepler's elliptical characterization of planetary motion could be explained by the inverse square law, but nobody had ever proved it, so they “placed a bet as to who could first prove the conjecture.”<sup>11</sup> Halley went to Newton for help due to his fame as a mathematician, who responded he had already done it many years ago and would forward the papers to him. He not only did that shortly afterward, but followed it up with the *Principia* with all the details two years later.

---

<sup>11</sup>Much of the background on Newton was taken from *Heisenberg Probably Slept Here*, by Richard P. Brennan, 1997. The book discusses his work and the other early scientists that laid the groundwork for Newton.

The basis for Newton's work started with the astronomer Nicholas Copernicus more than a hundred years before the *Principia* was published. He was the first to speculate that the planets revolved around the sun, rather than everything in the skies revolving around the earth. But Copernicus' heretical notion was largely ignored at the time, except by the church who banned his publication. However, two scientists did take note of his work: Galileo Galilei in Italy and Johannes Kepler in Austria. Kepler relied on a large collection of astronomical data taken by a Danish astronomer, Tycho Brahe, and concluded that the planetary orbits were ellipses rather than the circles that Copernicus had postulated. Galileo was an expert telescope builder and was able to clearly establish that the earth was not the center of all motion, partly because he was able to see moons revolving around other planets. He also did experiments with rolling balls down inclined planes that strongly suggested that  $F = ma$  (alas, it's a myth that he did his experiments by dropping objects out of the Leaning Tower of Pisa). Galileo published his work in 1632, which raised the ire of the church who then later banned him to house arrest until he died.<sup>12</sup> It was not until 1985 that the church recognized the important contributions of Galileo! These men laid the groundwork for Newton to put it all together with his laws of motion and the inverse square gravitational law. With these two physical principles, all the observations fit together with a theoretical framework that today forms the basis for the modeling of dynamic systems.

The sequence of discoveries that ultimately led to the laws of dynamics that we take for granted today were especially remarkable when we stop to think that they were all carried out without a computer, a calculator, or even a slide rule. On top of that, Newton had to invent calculus in order to reconcile the data.

After publishing the *Principia*, Newton went on to be elected to Parliament and was given high honors, including being the first man of science to be knighted by the Queen. He also got into fights with other scientists fairly regularly and used his powerful positions to get what he wanted. In one instance, he wanted data from the Royal Observatory that was not forthcoming fast enough. So he created a new board with authority over the Observatory and had the Astronomer Royal expelled from the Royal Society. Newton also had other less scientific interests. Many years after his death, John Maynard Keynes found that Newton had been spending as much of his time on metaphysical occult, alchemy, and biblical works as he had been on physics.

More than a hundred years after Newton's *Principia*, Michael Faraday performed a multitude of experiments and postulated the notion of electromagnetic lines of force in free space. He also discovered induction (Faraday's Law), which led to the electric motor and the laws of electrolysis. Faraday was born into a poor family, had virtually no schooling, and became an apprentice to a bookbinder at age 14. There

---

<sup>12</sup>Galileo's life, accomplishments, and house arrest are very well described in Dava Sobel's book, *Galileo's Daughter*.

he read many of the books being bound and became fascinated by science articles. Enthralled by these, he maneuvered to get a job as a bottle washer for a famous scientist, eventually learned enough to be a competitor to him, and ultimately became a professor at the Royal Institution in London. But lacking a formal education, he had no mathematical skills, and lacked the ability to create a theoretical framework for his discoveries. Faraday became a famous scientist in spite of his humble origins. After he had achieved fame for his discoveries and was made a Fellow of the Royal Society, the prime minister asked him what good his inventions could be.<sup>13</sup> Faraday's answer was, "Why Prime Minister, someday you can tax it." But in those days, scientists were almost exclusively men born into privilege; so Faraday had been treated like a second-class citizen by some of the other scientists. As a result, he rejected knighthood as well as burial at Westminster Abbey. Faraday's observations, along with those by Coulomb and Ampere, led James Clerk Maxwell to integrate all their knowledge on magnetism and electricity into Maxwell's equations. Against the beliefs of most prominent scientists of the day (Faraday being an exception), Maxwell invented the concepts of fields and waves that explained magnetic and electrostatic forces and was the key to creating the unifying theory. Although Newton had discovered the spectrum of light, Maxwell was also the first to realize that light was one type of the same electromagnetic waves, and its behavior was explained as well by Maxwell's equations. In fact, the only constants in his equations are  $\mu$  and  $\epsilon$ . The constant speed of light is  $c = 1/\sqrt{\mu\epsilon}$ .

Maxwell was a Scottish mathematician and theoretical physicist. His work has been called the second great unification in physics, the first being that due to Newton. Maxwell was born into the privileged class and was given the benefits of an excellent education and excelled at it. In fact, he was an extremely gifted theoretical and experimental scientist as well as a very generous and kind man with many friends and little vanity. In addition to unifying the observations of electromagnetism into a theory that still governs our engineering analyses today, he was the first to present an explanation of how light travels, the primary colors, the kinetic theory of gases, the stability of Saturn's rings, and the stability of feedback control systems! His discovery of the three primary colors (red, green, and blue) forms the basis of our color television to this day. His theory showing the speed of light is a constant was difficult to reconcile with Newton's laws and led Albert Einstein to create the special theory of relativity in the early 1900s. This led Einstein to say, "One scientific epoch ended and another began with James Clerk Maxwell."<sup>14</sup>

---

<sup>13</sup>*E = MC<sup>2</sup>, A Biography of the World's Most Famous Equation*, by David Bodanis, Walker and Co., New York, 2000.

<sup>14</sup>*The Man Who Changed Everything: The Life of James Clerk Maxwell*, Basil Mahon, Wiley, Chichester, UK, 2003.

## SUMMARY

Mathematical modeling of the system to be controlled is the first step in analyzing and designing the required system controls. In this chapter we developed analytical models for representative systems. Important equations for each category of system are summarized in Table 2.1. It is also possible to obtain a mathematical model using experimental data exclusively. This approach will be discussed briefly in Chapter 3 and more extensively in Chapter 12 of Franklin, Powell, and Workman (1998).

**TABLE 2.1****Key Equations for Dynamic Models**

System	Important Laws or Relationships	Associated Equations	Equation Number(s)
Mechanical	Translational motion (Newton's law)	$F = ma$	(2.1)
	Rotational motion	$M = I\alpha$	(2.10)
Electrical	Operational amplifier		(2.46), (2.47)
	Law of motors	$F = Blv$	(2.53)
Electromechanical	Law of generators	$e = Blv$	(2.56)
	Torque developed in a rotor	$T = K_t i_a$	(2.60)
Back emf	Voltage generated as a result of rotation of a rotor	$e = K_e \dot{\theta}_m$	(2.61)
	Effective inertia	$J_{eq} = J_2 + J_1 n^2$	(2.80)
Gears	Heat-energy flow	$q = 1/R(T_1 - T_2)$	(2.81)
	Temperature as a function of heat-energy flow	$\dot{T} = \frac{1}{C} q$	(2.82)
Heat flow	Specific heat	$C = mc_V$	(2.83)
	Continuity relation (conservation of matter)	$\dot{m} = w_{in} - w_{out}$	(2.91)
Fluid flow	Force of a fluid acting on a piston	$f = pA$	(2.93)
	Effect of resistance to fluid flow	$w = 1/R(p_1 - p_2)^{1/\alpha}$	(2.94)

## REVIEW QUESTIONS

- 2.1 What is a “free-body diagram”?
- 2.2 What are the two forms of Newton’s law?
- 2.3 For a structural process to be controlled, such as a robot arm, what is the meaning of “collocated control”? “Noncollocated control”?
- 2.4 State Kirchhoff’s current law.
- 2.5 State Kirchhoff’s voltage law.
- 2.6 When, why, and by whom was the device named an “operational amplifier”?

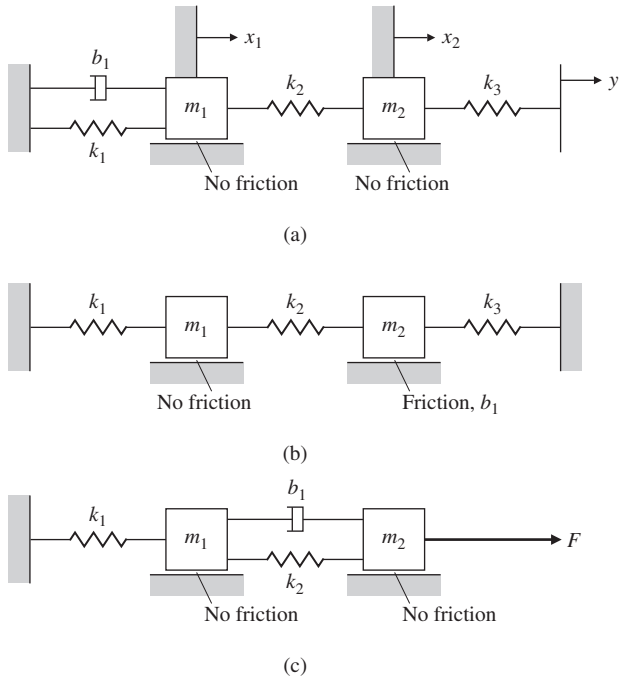
- 2.7** What is the major benefit of having zero input current to an operational amplifier?
- 2.8** Why is it important to have a small value for the armature resistance  $R_a$  of an electric motor?
- 2.9** What are the definition and units of the electric constant of a motor?
- 2.10** What are the definition and units of the torque constant of an electric motor?
- 2.11** Why do we approximate a physical model of the plant (which is *always* nonlinear) with a linear model?
- △ **2.12** Give the relationships for the following:
- Heat flow across a substance
  - Heat storage in a substance
- △ **2.13** Name and give the equations for the three relationships governing fluid flow.

## PROBLEMS

### Problems for Section 2.1: Dynamics of Mechanical Systems

- 2.1** Write the differential equations for the mechanical systems shown in Fig. 2.43. For Fig. 2.43(a) and (b), state whether you think the system will eventually decay so it has no motion at all, given that there are nonzero

**Figure 2.43**  
Mechanical systems

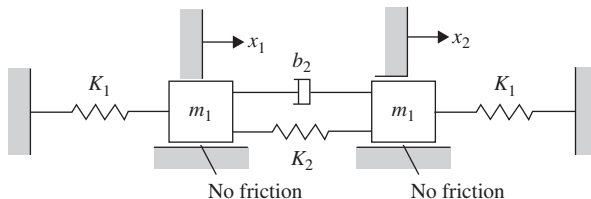


initial conditions for both masses and there is no input; give a reason for your answer. Also, for part (c), answer the question for  $F = 0$ .

- 2.2** Write the differential equation for the mechanical system shown in Fig. 2.44. State whether you think the system will eventually decay so it has no motion at all, given that there are nonzero initial conditions for both masses, and give a reason for your answer.

**Figure 2.44**

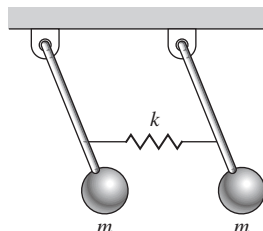
Mechanical system for Problem 2.2



- 2.3** Write the equations of motion for the double-pendulum system shown in Fig. 2.45. Assume the displacement angles of the pendulums are small enough to ensure the spring is always horizontal. The pendulum rods are taken to be massless, of length  $l$ , and the springs are attached three-fourths of the way down.

**Figure 2.45**

Double pendulum



- 2.4** Write the equations of motion of a pendulum consisting of a thin, 2 kg stick of length  $l$  suspended from a pivot. How long should the rod be in order for the period to be exactly 1 sec? (The inertia  $I$  of a thin stick about an end point is  $\frac{1}{3}ml^2$ . Assume  $\theta$  is small enough that  $\sin\theta \cong \theta$ .) Why do you think grandfather clocks are typically about 6 ft high?

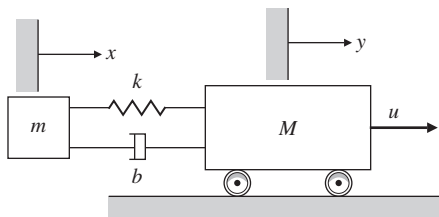
- 2.5** For the car suspension discussed in Example 2.2, plot the position of the car and the wheel after the car hits a “unit bump”(that is,  $r$  is a unit step) using Matlab. Assume  $m_1 = 10$  kg,  $m_2 = 350$  kg,  $K_w = 500,000$  N/m, and  $K_s = 10,000$  N/m. Find the value of  $b$  that you would prefer if you were a passenger in the car.

- 2.6** For the quadcopter shown in Figs. 2.13 and 2.14:

- Determine the appropriate commands to rotor #s 1, 2, 3, & 4 so a pure vertical force will be applied to the quadcopter, that is, a force that will have no effect on pitch, roll, or yaw.
- Determine the transfer function between  $F_h$ , and altitude,  $h$ . That is, find  $h(s)/F_h(s)$ .

- 2.7** Automobile manufacturers are contemplating building active suspension systems. The simplest change is to make shock absorbers with a changeable damping,  $b(u_1)$ . It is also possible to make a device to be placed in parallel with the springs that has the ability to supply an equal force,  $u_2$ , in opposite directions on the wheel axle and the car body.
- Modify the equations of motion in Example 2.2 to include such control inputs.
  - Is the resulting system linear?
  - Is it possible to use the force  $u_2$  to completely replace the springs and shock absorber? Is this a good idea?
- 2.8** In many mechanical positioning systems, there is flexibility between one part of the system and another. An example is shown in Fig. 2.7 where there is flexibility of the solar panels. Figure 2.46 depicts such a situation, where a force  $u$  is applied to the mass  $M$  and another mass  $m$  is connected to it. The coupling between the objects is often modeled by a spring constant  $k$  with a damping coefficient  $b$ , although the actual situation is usually much more complicated than this.
- Write the equations of motion governing this system.
  - Find the transfer function between the control input  $u$  and the output  $y$ .

**Figure 2.46**  
Schematic of a system with flexibility



- 2.9** Modify the equation of motion for the cruise control in Example 2.1, Eq. (2.4), so it has a control law; that is, let

$$u = K(v_r - v), \quad (2.111)$$

where

$$v_r = \text{reference speed}, \quad (2.112)$$

$$K = \text{constant}. \quad (2.113)$$

This is a “proportional” control law in which the difference between  $v_r$  and the actual speed is used as a signal to speed the engine up or slow it down. Revise the equations of motion with  $v_r$  as the input and  $v$  as the output and find the transfer function. Assume  $m = 1500 \text{ kg}$  and  $b = 70 \text{ N}\cdot\text{sec}/\text{m}$ , and find the response for a unit step in  $v_r$  using Matlab. Using trial and error, find a value of  $K$  that you think would result in a control system in which the actual speed converges as quickly as possible to the reference speed with no objectionable behavior.

- 2.10** Determine the dynamic equations for lateral motion of the robot in Fig. 2.47. Assume it has three wheels with a single, steerable wheel in the front where the controller has direct control of the rate of change of the steering angle,  $U_{steer}$ , with geometry as shown in Fig. 2.48. Assume the robot is going in approximately a straight line and its angular deviation from that straight line is very small. Also assume the robot is traveling at a constant speed,  $V_o$ . The dynamic equations relating the lateral velocity of the center of the robot as a result of commands in  $U_{steer}$  are desired.

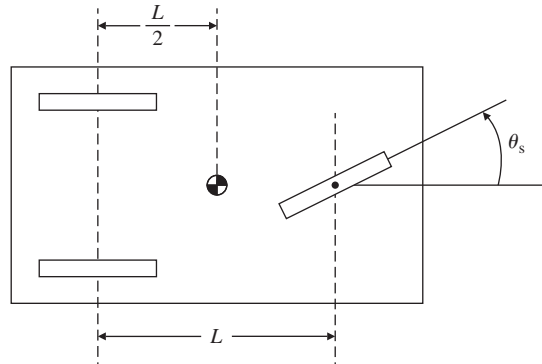
**Figure 2.47**

Robot for delivery of hospital supplies

Source: Bill Clark/Daily Progress/AP Images

**Figure 2.48**

Model for robot motion



- 2.11** Determine the pitch, yaw, and roll control equations for the hexacopter shown in Fig. 2.49 that are similar to those for the quadcopter given in Eqs. (2.18) to (2.20).

Assume rotor #1 is in the direction of flight, and the remaining rotors are numbered CW from that rotor. In other words, rotors #1 and #4 will determine the pitch motion. Rotor #s 2, 3, 5, & 6 will determine roll motion. Pitch, roll and yaw motions are defined by the coordinate system shown in Fig. 2.14 in Example 2.5. In addition to developing the equations for the 3 degrees of freedom in terms of how the six rotor motors should be commanded (similar to those for the quadrotor in Eqs. (2.18)–(2.20)), it will also be necessary to decide which rotors are

**Figure 2.49**

Hexacopter



turning CW and which ones are turning CCW. The direction of rotation for the rotors needs to be selected so there is no net torque about the vertical axis; that is, the hexicpter will have no tendency for yaw rotation in steady-state. Furthermore, a control action to affect pitch should have no effect on yaw or roll. Likewise, a control action for roll should have no effect on pitch or yaw, and a control action for yaw should have no effect on pitch or roll. In other words, the control actions should produce no cross-coupling between pitch, roll, and yaw just as was the case for the quadcopter in Example 2.5.

- 2.12** In most cases, quadcopters have a camera mounted that does not swivel in the  $x$ - $y$  plane and its direction of view is oriented at  $45^\circ$  to the arms supporting the rotors. Therefore, these drones typically fly in a direction that is aligned with the camera rather than along an axis containing two of the rotors. To simplify the flight dynamics, the  $x$ -direction of the coordinate system is aligned with the camera direction. Based on the coordinate definitions for the axes in Fig. 2.14, assume the  $x$ -axis lies half way between rotors # 1 and 2 and determine the rotor commands for the four rotors that would accomplish independent motion for pitch, roll, and yaw.

### Problems for Section 2.2: Models of Electric Circuits

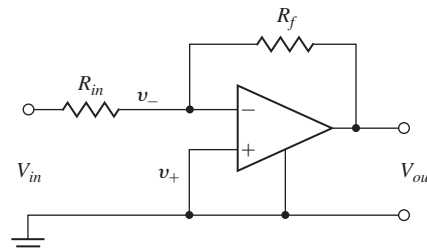
- 2.13** A first step toward a realistic model of an op-amp is given by the following equations and is shown in Fig. 2.50:

$$V_{out} = \frac{10^7}{s+1} [v_+ - v_-], \\ i_+ = i_- = 0.$$

Find the transfer function of the simple amplification circuit shown using this model.

**Figure 2.50**

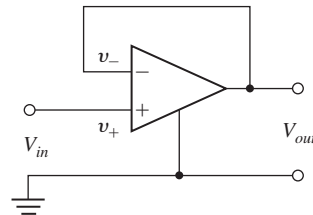
Circuit for Problem 2.13



- 2.14** Show the op-amp connection shown in Fig. 2.51 results in  $V_{out} = V_{in}$  if the op-amp is ideal. Give the transfer function if the op-amp has the nonideal transfer function of Problem 2.13.

**Figure 2.51**

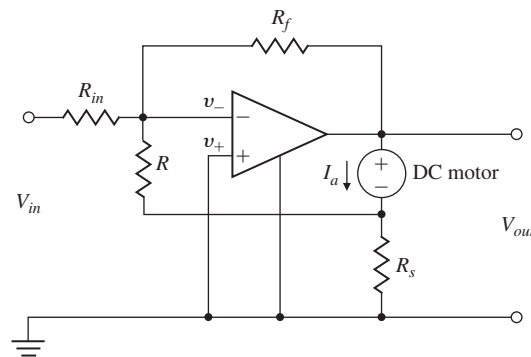
Circuit for Problem 2.14



- 2.15** A common connection for a motor power amplifier is shown in Fig. 2.52. The idea is to have the motor current follow the input voltage, and the connection is called a current amplifier. Assume the sense resistor  $r_s$  is very small compared with the feedback resistor  $R$ , and find the transfer function from  $V_{in}$  to  $I_a$ . Also show the transfer function when  $R_f = \infty$ .

**Figure 2.52**

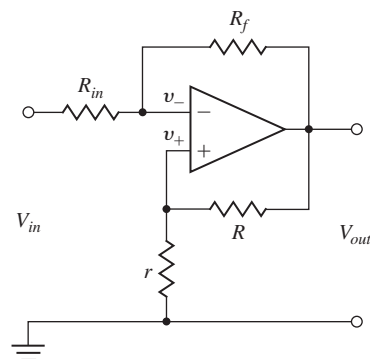
Op-amp circuit for Problem 2.15



- 2.16** An op-amp connection with feedback to both the negative and the positive terminals is shown in Fig. 2.53. If the op-amp has the nonideal transfer function given in Problem 2.13, give the maximum value possible for the positive feedback ratio,  $P = \frac{r}{r+R}$ , in terms of the negative feedback ratio,  $N = \frac{R_{in}}{R_{in}+R_f}$ , for the circuit to remain stable.

**Figure 2.53**

Op-amp circuit for Problem 2.16

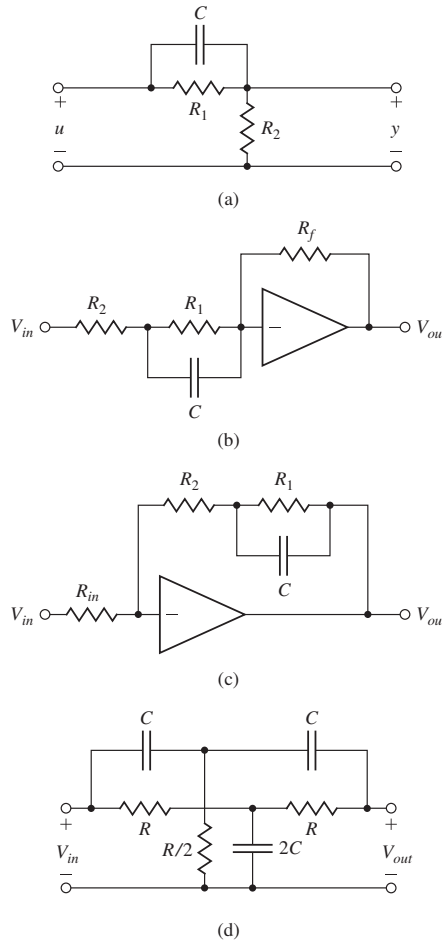


**2.17** Write the dynamic equations and find the transfer functions for the circuits shown in Fig. 2.54.

- (a) Passive lead circuit
- (b) Active lead circuit
- (c) Active lag circuit
- (d) Passive notch circuit

**Figure 2.54**

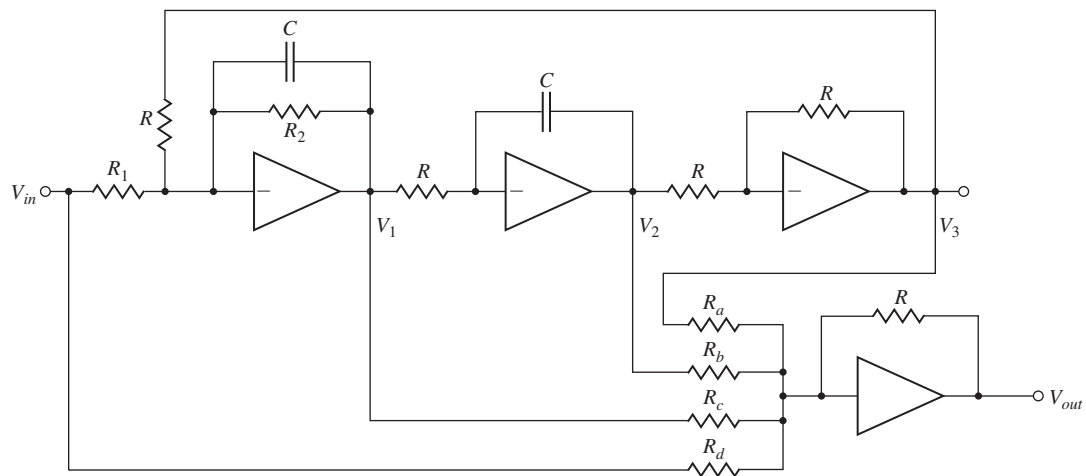
- (a) Passive lead;
  - (b) active lead;
  - (c) active lag; and
  - (d) passive notch
- circuits



**2.18** The very flexible circuit shown in Fig. 2.55 is called a biquad because its transfer function can be made to be the ratio of two second-order or quadratic polynomials. By selecting different values for  $R_a$ ,  $R_b$ ,  $R_c$ , and  $R_d$ , the circuit can realize a low-pass, band-pass, high-pass, or band-reject (notch) filter.

- (a) Show that if  $R_a = R$  and  $R_b = R_c = R_d = \infty$ , the transfer function from  $V_{in}$  to  $V_{out}$  can be written as the low-pass filter

$$\frac{V_{out}}{V_{in}} = \frac{A}{\frac{s^2}{\omega_n^2} + 2\zeta \frac{s}{\omega_n} + 1}, \quad (2.114)$$

**Figure 2.55**

Op-amp biquad

where

$$A = \frac{R}{R_1},$$

$$\omega_n = \frac{1}{RC},$$

$$\zeta = \frac{R}{2R_2}.$$

- (b)** Using the Matlab command *step*, compute and plot on the same graph the step responses for the biquad of Fig. 2.55 for  $A = 2$ ,  $\omega_n = 3$ , and  $\zeta = 0.1, 0.5$ , and  $1.0$ .

- 2.19** Find the equations and transfer function for the biquad circuit of Fig. 2.55 if  $R_a = R$ ,  $R_d = R_1$ , and  $R_b = R_c = \infty$ .

### Problems for Section 2.3: Models of Electromechanical Systems

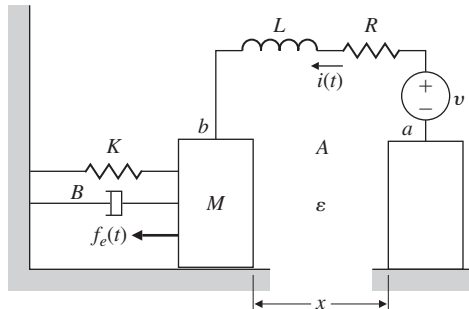
- 2.20** The torque constant of a motor is the ratio of torque to current and is often given in ounce-inches per ampere. (Ounce-inches have dimension force  $\times$  distance, where an ounce is  $1/16$  of a pound.) The electric constant of a motor is the ratio of back emf to speed and is often given in volts per 1000 rpm. In consistent units, the two constants are the same for a given motor.
- (a)** Show that the units ounce-inches per ampere are proportional to volts per 1000 rpm by reducing both to MKS (SI) units.
- (b)** A certain motor has a back emf of 30 V at 1000 rpm. What is its torque constant in ounce-inches per ampere?
- (c)** What is the torque constant of the motor of part (b) in newton-meters per ampere?

- 2.21** The electromechanical system shown in Fig. 2.56 represents a simplified model of a capacitor microphone. The system consists in part of a parallel plate capacitor connected into an electric circuit. Capacitor plate  $a$  is rigidly fastened to the microphone frame. Sound waves pass through the mouthpiece and exert a force  $f_e(t)$  on plate  $b$ , which has mass  $M$  and is connected to the frame by a set of springs and dampers. The capacitance  $C$  is a function of the distance  $x$  between the plates, as follows:

$$C(x) = \frac{\epsilon A}{x},$$

**Figure 2.56**

Simplified model for capacitor microphone



where

$\epsilon$  = dielectric constant of the material between the plates,

$A$  = surface area of the plates.

The charge  $q$  and the voltage  $e$  across the plates are related by

$$q = C(x)e.$$

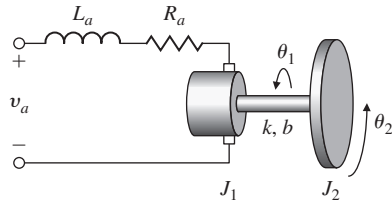
The electric field in turn produces the following force  $f_e$  on the movable plate that opposes its motion:

$$f_e = \frac{q^2}{2\epsilon A}.$$

- (a) Write differential equations that describe the operation of this system. (It is acceptable to leave in nonlinear form.)
- (b) Can one get a linear model?
- (c) What is the output of the system?
- 2.22** A very typical problem of electromechanical position control is an electric motor driving a load that has one dominant vibration mode. The problem arises in computer-disk-head control, reel-to-reel tape drives, and many other applications. A schematic diagram is sketched in Fig. 2.57. The motor has an electrical constant  $K_e$ , a torque constant  $K_t$ , an armature inductance  $L_a$ , and a resistance  $R_a$ . The rotor has an inertia  $J_1$  and a viscous friction  $B$ . The load has an inertia  $J_2$ . The two inertias are connected by a shaft with a spring constant  $k$  and an equivalent viscous damping  $b$ . Write the equations of motion.

**Figure 2.57**

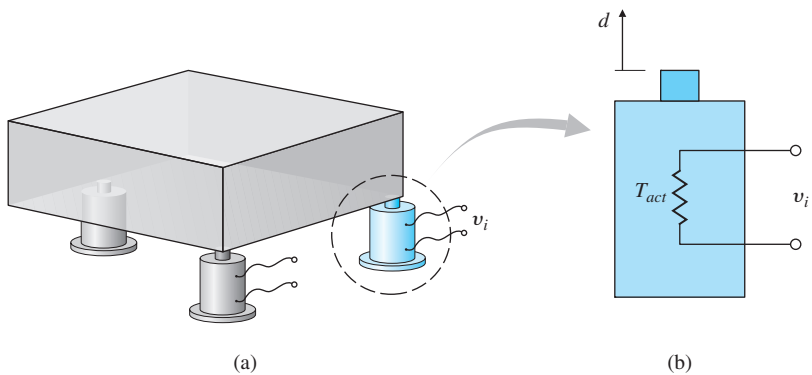
Motor with a flexible load



- △ **2.23** For the robot in Fig. 2.47, assume you have command of the torque on a servo motor that is connected to the drive wheels with gears that have a 2:1 ratio, so the torque on the wheels is increased by a factor of 2 over that delivered by the servo. Determine the dynamic equations relating the speed of the robot with respect to the torque command of the servo. Your equations will require certain quantities, for example, mass of vehicle, inertia, and radius of the wheels. Assume you have access to whatever you need.
- △ **2.24** Using Fig. 2.36, derive the transfer function between the applied torque,  $T_m$ , and the output,  $\theta_2$ , for the case when there is a spring attached to the output load. That is, there is a torque applied to the output load,  $T_s$ , where  $T_s = -K_s\theta_2$ .

**Figure 2.58**

(a) Precision table kept level by actuators;  
(b) side view of one actuator



### △ *Problems for Section 2.4: Heat and Fluid-Flow Models*

- 2.25** A precision table-leveling scheme shown in Fig. 2.58 relies on thermal expansion of actuators under two corners to level the table by raising or lowering their respective corners. The parameters are as follows:

$T_{act}$  = actuator temperature,

$T_{amb}$  = ambient air temperature,

$R_f$  = heat-flow coefficient between the actuator and the air,

$C$  = thermal capacity of the actuator,

$R$  = resistance of the heater.

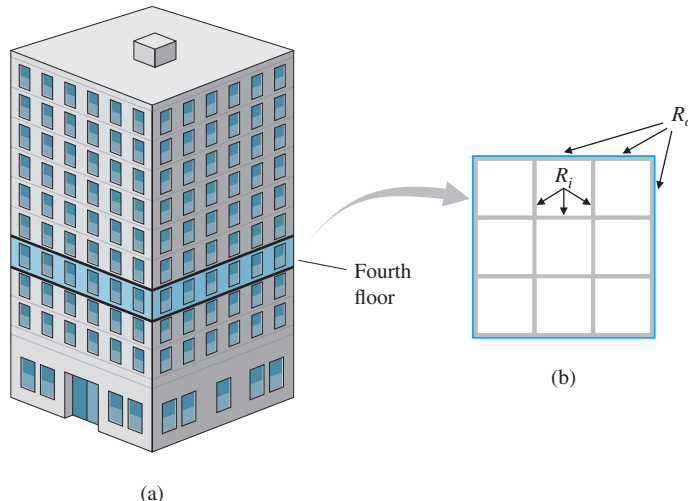
Assume (1) the actuator acts as a pure electric resistance, (2) the heat flow into the actuator is proportional to the electric power input, and (3) the

motion  $d$  is proportional to the difference between  $T_{act}$  and  $T_{amb}$  due to thermal expansion. Find the differential equations relating the height of the actuator  $d$  versus the applied voltage  $v_i$ .

- 2.26** An air conditioner supplies cold air at the same temperature to each room on the fourth floor of the high-rise building shown in Fig. 2.59(a). The floor plan is shown in Fig. 2.59(b). The cold airflow produces an equal amount of heat flow  $q$  out of each room. Write a set of differential equations governing the temperature in each room, where

**Figure 2.59**

Building air-conditioning:  
(a) high-rise building;  
(b) floor plan of the fourth floor



(a)

(b)

$T_o$  = temperature outside the building,

$R_o$  = resistance to heat flow through the outer walls,

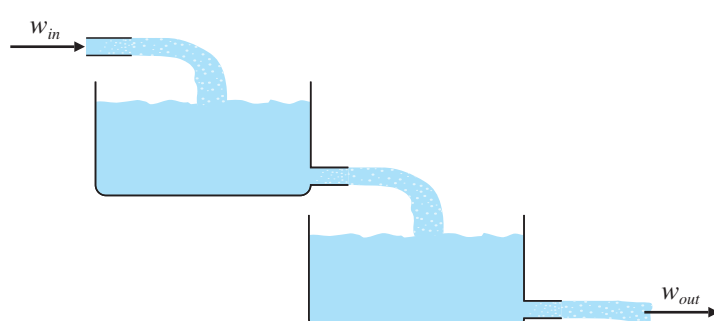
$R_i$  = resistance to heat flow through the inner walls.

Assume (1) all rooms are perfect squares, (2) there is no heat flow through the floors or ceilings, and (3) the temperature in each room is uniform throughout the room. Take advantage of symmetry to reduce the number of differential equations to three.

- 2.27** For the two-tank fluid-flow system shown in Fig. 2.60, find the differential equations relating the flow into the first tank to the flow out of the second tank.

**Figure 2.60**

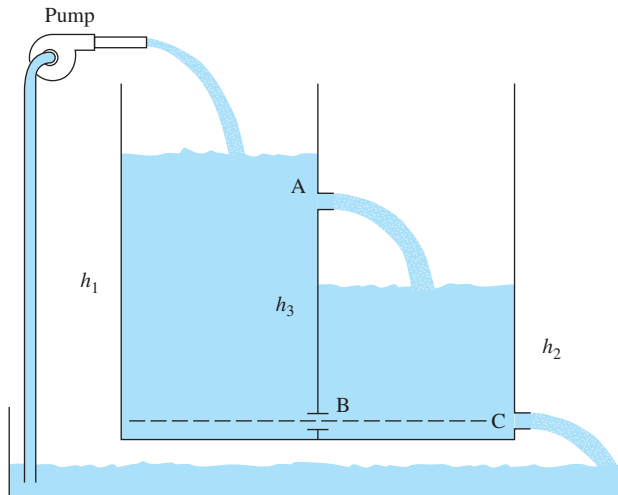
Two-tank fluid-flow system for Problem 2.27



- 2.28** A laboratory experiment in the flow of water through two tanks is sketched in Fig. 2.61. Assume Eq. (2.96) describes flow through the equal-sized holes at points A, B, or C.

**Figure 2.61**

Two-tank fluid-flow system for Problem 2.28



- (a) With holes at B and C, but none at A, write the equations of motion for this system in terms of  $h_1$  and  $h_2$ . Assume when  $h_2 = 15$  cm, the outflow is 200 g/min.
- (b) At  $h_1 = 30$  cm and  $h_2 = 10$  cm, compute a linearized model and the transfer function from pump flow (in cubic-centimeters per minute) to  $h_2$ .
- (c) Repeat parts (a) and (b) assuming hole B is closed and hole A is open. Assume  $h_3 = 20$  cm,  $h_1 > 20$  cm, and  $h_2 < 20$  cm.
- 2.29** The equations for heating a house are given by Eqs. (2.81) and (2.82), and in a particular case can be written with time in hours as

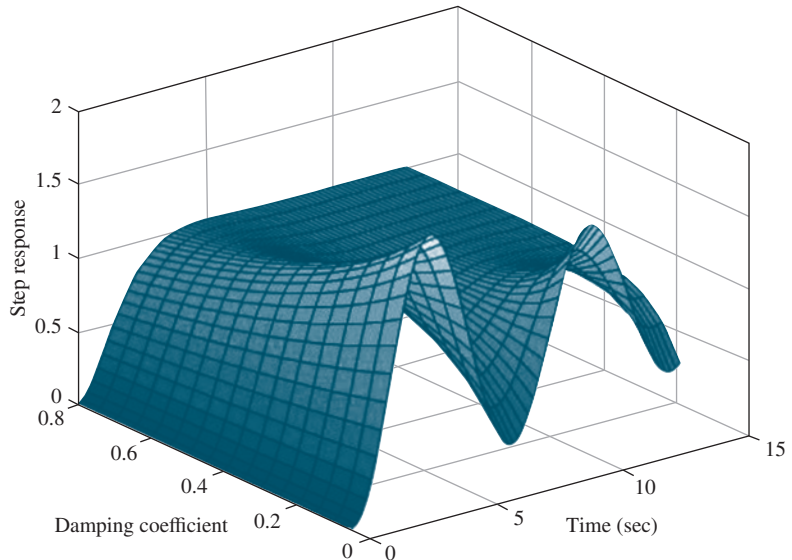
$$C \frac{dT_h}{dt} = Ku - \frac{T_h - T_o}{R},$$

where

- (a)  $C$  is the thermal capacity of the house, BTU/ $^{\circ}$ F,
- (b)  $T_h$  is the temperature in the house,  $^{\circ}$ F,
- (c)  $T_o$  is the temperature outside the house,  $^{\circ}$ F,
- (d)  $K$  is the heat rating of the furnace, = 90,000 BTU/h,
- (e)  $R$  is the thermal resistance,  $^{\circ}$ F per BTU/h,
- (f)  $u$  is the furnace switch, = 1 if the furnace is on and = 0 if the furnace is off.

It is measured that, with the outside temperature at  $32^{\circ}$ F and the house at  $60^{\circ}$ F, the furnace raises the temperature  $2^{\circ}$ F in six min (0.1 h). With the furnace off, the house temperature falls  $2^{\circ}$ F in 40 min. What are the values of  $C$  and  $R$  for the house?

# Dynamic Response



## A Perspective on System Response

We discussed in Chapter 2 how to obtain the dynamic model of a system. In designing a control system, it is important to see how well a trial design matches the desired performance. We do this by solving the equations of the system model.

There are two ways to approach solving the dynamic equations. For a quick, *approximate* analysis, we use linear analysis techniques. The resulting approximations of system response provide insight into why the solution has certain features and how the system might be changed to modify the response in a desired direction. In contrast, a *precise* picture of the system response typically calls for numerical simulation of nonlinear equations of motion using computer aids. This chapter focuses on linear analysis and computer tools that can be used to solve for the time response of linear systems.

There are three domains within which to study dynamic response: the **Laplace transform (s-plane)**, the **frequency response**, and the **state space** (analysis using the state-variable description). The

well-prepared control engineer needs to be fluent in all of them, so they will be treated in depth in Chapters 5, 6, and 7, respectively. The purpose of this chapter is to discuss some of the fundamental mathematical tools needed before studying analysis in the  $s$ -plane, frequency response, and state space.

## Chapter Overview

The Laplace transform, reviewed in Section 3.1 (and Appendix A), is the mathematical tool for transforming differential equations into an easier-to-manipulate algebraic form. In addition to the mathematical tools at our disposal, there are graphical tools that can help us to visualize the model of a system and evaluate the pertinent mathematical relationships between elements of the system. One approach is the block diagram, which was introduced in Chapter 1. Block-diagram manipulation will be discussed in Section 3.2 and allows the manipulation of transfer functions.

Once the transfer function has been determined, we can identify its poles and zeros, which tell us a great deal about the system characteristics, including its frequency response introduced in Section 3.1. Sections 3.3 to 3.5 will focus on poles and zeros and some of the ways for manipulating them to steer system characteristics in a desired way. When feedback is introduced, the possibility that the system may become *unstable* is introduced. To study this effect, in Section 3.6 we consider the definition of stability and Routh's test, which can determine stability by examining the coefficients of the system's characteristic equation. Finally, Section 3.7 will provide a historical perspective for the material in this chapter. An alternative representation of a system in graphical form is the signal-flow graph and flow graphs that allow the determination of complicated transfer functions, which are discussed in Appendix W3.2.3 online at [www.pearsonglobaleditions.com](http://www.pearsonglobaleditions.com).

### 3.1 Review of Laplace Transforms

Two attributes of linear time-invariant systems (LTIs) form the basis for almost all analytical techniques applied to these systems:

1. A linear system response obeys the principle of superposition.
2. The response of an LTI system can be expressed as the convolution of the input with the unit impulse response of the system.

The concepts of superposition, convolution, and impulse response will be defined shortly.

From the second property (as we will show), it follows immediately that the response of an LTI system to an exponential input is also exponential. This result is the principal reason for the usefulness of Fourier and Laplace transforms in the study of LTI systems.

### Superposition principle

#### 3.1.1 Response by Convolution

The **principle of superposition** states that if the system has an input that can be expressed as a sum of signals, then the response of the system can be expressed as the sum of the individual responses to the respective signals. We can express superposition mathematically. Consider the system to have input  $u$  and output  $y$ . Suppose further that, with the system at rest, we apply the input  $u_1(t)$  and observe the output  $y_1(t)$ . After restoring the system to rest, we apply a second input  $u_2(t)$  and again observe the output, which we call  $y_2(t)$ . Then, we form the composite input  $u(t) = \alpha_1 u_1(t) + \alpha_2 u_2(t)$ . Finally, if superposition applies, then the response will be  $y(t) = \alpha_1 y_1(t) + \alpha_2 y_2(t)$ . Superposition will apply if and only if the system is linear.

#### EXAMPLE 3.1

##### *Superposition*

Show that superposition holds for the system modeled by the first-order linear differential equation

$$\dot{y} + ky = u.$$

**Solution.** We let  $u = \alpha_1 u_1 + \alpha_2 u_2$  and assume  $y = \alpha_1 y_1 + \alpha_2 y_2$ . Then  $\dot{y} = \alpha_1 \dot{y}_1 + \alpha_2 \dot{y}_2$ . If we substitute these expressions into the system equation, we get

$$\alpha_1 \dot{y}_1 + \alpha_2 \dot{y}_2 + k(\alpha_1 y_1 + \alpha_2 y_2) = \alpha_1 u_1 + \alpha_2 u_2.$$

From this, it follows that

$$\alpha_1(\dot{y}_1 + ky_1 - u_1) + \alpha_2(\dot{y}_2 + ky_2 - u_2) = 0. \quad (3.1)$$

If  $y_1$  is the solution with input  $u_1$  and  $y_2$  is the solution with input  $u_2$ , then Eq. (3.1) is satisfied, the response is the sum of the individual responses, and superposition holds.

Notice the superposition result of Eq. (3.1) would also hold if  $k$  were a function of time. If  $k$  were constant, we call the system *time invariant*. In that case, it follows that if the input is delayed or shifted in time, then the output is unchanged except also being shifted by exactly the same amount. Mathematically, this is expressed by saying that, if  $y_1(t)$  is the output caused by  $u_1(t)$  then  $y_1(t - \tau)$  will be the response to  $u_1(t - \tau)$ .

#### EXAMPLE 3.2

##### *Time Invariance*

Consider

$$\dot{y}_1(t) + k(t)y_1(t) = u_1(t), \quad (3.2)$$

and

$$\dot{y}_2(t) + k(t)y_2(t) = u_1(t - \tau),$$

where  $\tau$  is a constant shift. Assume that  $y_2(t) = y_1(t - \tau)$ ; then

$$\frac{dy_1(t - \tau)}{dt} + k(t)y_1(t - \tau) = u_1(t - \tau).$$

Let us make the change of variable  $t - \tau = \eta$ , then

$$\frac{dy_1(\eta)}{d\eta} + k(\eta + \tau)y_1(\eta) = u_1(\eta). \quad (3.3)$$

Eq. (3.3) can satisfy Eq. (3.2) only if  $\tau = 0$ , or if  $k(\eta + \tau) = k$  = constant, in which case

$$\frac{dy_1(\eta)}{d\eta} + ky_1(\eta) = u(\eta),$$

which is Eq. (3.1). Therefore, we conclude that if the system is time invariant,  $y(t - \tau)$  will be the response to  $u(t - \tau)$ ; that is, if the input is delayed by  $\tau$  sec, then the output is also delayed by  $\tau$  sec.

We are able to solve for the response of a linear system to a general signal simply by decomposing the given signal into a sum of the elementary components and, by superposition, concluding that the response to the general signal is the sum of the responses to the elementary signals. In order for this process to work, the elementary signals need to be sufficiently “rich” that any reasonable signal can be expressed as a sum of them, and their responses have to be easy to find. The most common candidates for elementary signals for use in linear systems are the impulse and the exponential.

Suppose the input signal to an LTI system is a short pulse as  $u_1(t) = p(t)$ , and the corresponding output signal is  $y_1(t) = h(t)$ , as shown in Fig. 3.1(a). Now if the input is scaled to  $u_1(t) = u(0)p(t)$ , then by the scaling property of superposition, the output response will be  $y_1(t) = u(0)h(t)$ . We showed that an LTI system obeys time invariance. If we delay the short pulse signal in time by  $\tau$ , then the input is of the form  $u_2(t) = p(t - \tau)$  and the output response will also be delayed by the same amount  $y_2(t) = h(t - \tau)$  as shown in Fig. 3.1(b). Now, by superposition, the response to the two short pulses will be the sum of their individual outputs as shown in Fig. 3.1(c). If we have four pulses as the input, then the output will be the sum of the four individual responses as shown in Fig. 3.1(d). Any arbitrary input signal  $u(t)$  may be approximated by a series of pulses as shown in Fig. 3.2. We define a short pulse  $p_\Delta(t)$  as a rectangular pulse having *unit area* such that

$$p_\Delta(t) = \begin{cases} \frac{1}{\Delta}, & 0 \leq t \leq \Delta \\ 0, & \text{elsewhere} \end{cases} \quad (3.4)$$

as shown in Fig. 3.1(a). Suppose the response of the system to  $p_\Delta(t)$  is defined as  $h_\Delta(t)$ . The response at time  $n\Delta$  to  $\Delta u(k\Delta)p_\Delta(k\Delta)$  is

$$\Delta u(k\Delta) h_\Delta(n\Delta - k\Delta).$$

By superposition, the total response to the series of the short pulses at time  $t$  is given by

$$y(t) = \sum_{k=0}^{k=\infty} \Delta u(k\Delta) h_\Delta(t - k\Delta). \quad (3.5)$$

**Short pulse**

**Figure 3.1**

Illustration of convolution as the response of a system to a series of short pulse (impulse) input signals

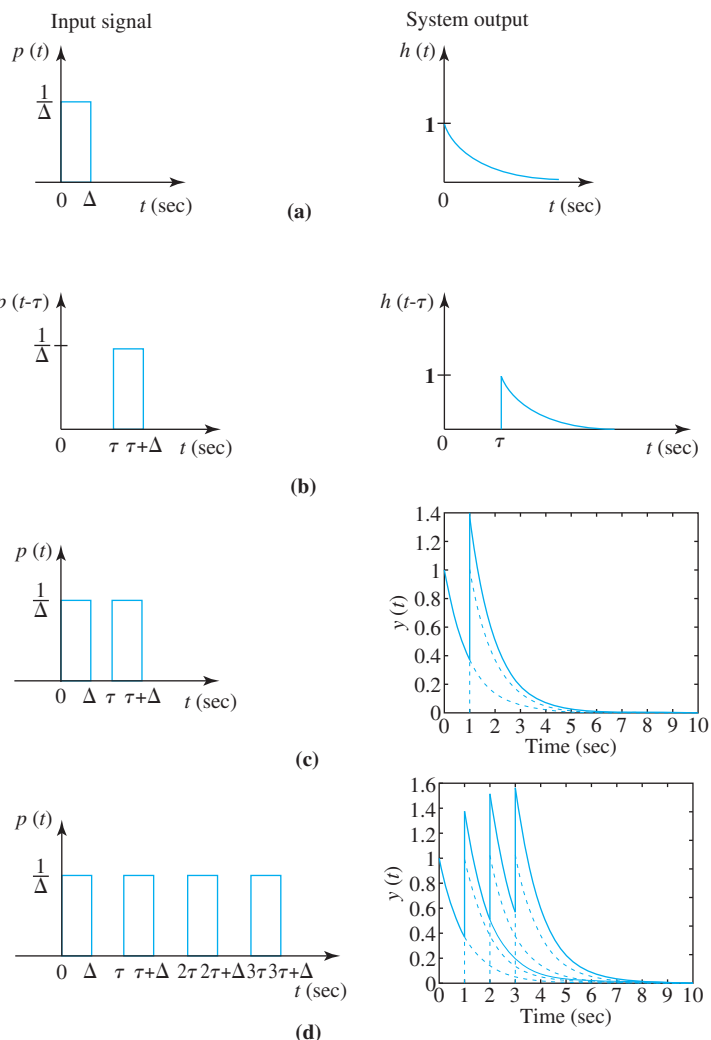
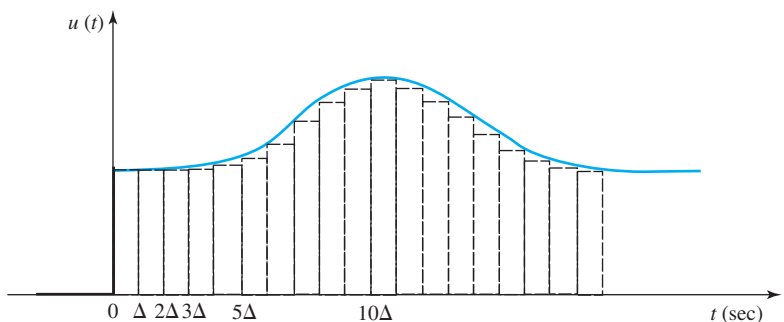
**Figure 3.2**

Illustration of the representation of a general input signal as the sum of short pulses



If we take the limit as  $\Delta \rightarrow 0$ , the basic pulse gets more and more narrow and taller while holding a *constant area*. We then have the concept of an **impulse signal**,  $\delta(t)$ , and that will allow us to treat continuous signals. In that case, we have

$$\lim_{\Delta \rightarrow 0} p_\Delta(t) = \delta(t), \quad (3.6)$$

$$\lim_{\Delta \rightarrow 0} h_\Delta(t) = h(t) = \text{the impulse response.} \quad (3.7)$$

Moreover, in the limit as  $\Delta \rightarrow 0$ , the summation in Eq. (3.5) is replaced by the integral

$$y(t) = \int_0^\infty u(\tau)h(t - \tau) d\tau, \quad (3.8)$$

which is the convolution integral.

The idea for the impulse comes from dynamics. Suppose we wish to study the motion of a baseball hit by a bat. The details of the collision between the bat and ball can be very complex as the ball deforms and the bat bends; however, for purposes of computing the path of the ball, we can summarize the effect of the collision as the net velocity change of the ball over a very short time period. We assume the ball is subjected to an **impulse**, a very intense force for a very short time. The physicist Paul Dirac suggested that such forces could be represented by the mathematical concept of an impulse  $\delta(t)$ , which has the property that

$$\delta(t) = 0 \quad t \neq 0, \quad (3.9)$$

$$\int_{-\infty}^{\infty} \delta(t) dt = 1. \quad (3.10)$$

[Impulse response](#)

[Definition of impulse](#)

[Sifting property of impulse](#)

If  $f(t)$  is continuous at  $t = \tau$ , then it has the “sifting property.”

$$\int_{-\infty}^{\infty} f(\tau)\delta(t - \tau) d\tau = f(t). \quad (3.11)$$

In other words, the impulse is so short and so intense that no value of  $f$  matters except over the short range where the  $\delta$  occurs. Since integration is a limit of a summation process, Eq. (3.11) can be viewed as representing the function  $f$  as a sum of impulses. If we replace  $f$  by  $u$ , then Eq. (3.11) represents an input  $u(t)$  as a sum of impulses of intensity  $u(t - \tau)$ . To find the response to an arbitrary input, the principle of superposition tells us that we need only find the response to a unit impulse.

If the system is not only linear but also time invariant (LTI), then the impulse response is given by  $h(t - \tau)$  because the response at  $t$  to an input applied at  $\tau$  depends only on the difference between the time the impulse is applied and the time we are observing the response, that is, the *elapsed time*. Time-invariant systems are called shift invariant for this reason. For time-invariant systems, the output for a general input is given by the integral

$$y(t) = \int_{-\infty}^{\infty} u(\tau)h(t - \tau) d\tau, \quad (3.12)$$

or by changing of variables as  $\tau_1 = t - \tau$

$$y(t) = \int_{-\infty}^{-\infty} u(t - \tau_1)h(\tau_1) (-d\tau_1) = \int_{-\infty}^{\infty} h(\tau)u(t - \tau) d\tau. \quad (3.13)$$

The convolution integral

### EXAMPLE 3.3

#### *Convolution*

We can illustrate convolution with a simple system. Determine the impulse response for the system described by the differential equation

$$\dot{y} + ky = u = \delta(t),$$

with an initial condition of  $y(0) = 0$  before the impulse.

**Solution.** Because  $\delta(t)$  has an effect only near  $t = 0$ , we can integrate this equation from just before zero to just after zero with the result that

$$\int_{0^-}^{0^+} \dot{y} dt + k \int_{0^-}^{0^+} y dt = \int_{0^-}^{0^+} \delta(t) dt.$$

The integral of  $\dot{y}$  is simply  $y$ , the integral of  $y$  over so small a range is zero, and the integral of the impulse over the same range is unity. Therefore,

$$y(0^+) - y(0^-) = 1.$$

Because the system was at rest before application of the impulse,  $y(0^-) = 0$ . Thus the effect of the impulse is that  $y(0^+) = 1$ . For positive time, we have the differential equation

$$\dot{y} + ky = 0, \quad y(0^+) = 1.$$

If we assume a solution  $y = Ae^{st}$ , then  $\dot{y} = Ase^{st}$ . The preceding equation then becomes

$$\begin{aligned} Ase^{st} + kAe^{st} &= 0, \\ s + k &= 0, \\ s &= -k. \end{aligned}$$

Because  $y(0^+) = 1$ , it is necessary that  $A = 1$ . Thus the solution for the impulse response is  $y(t) = h(t) = e^{-kt}$  for  $t > 0$ . To take care of the fact that  $h(t) = 0$  for negative time, we define the **unit-step function**

$$1(t) = \begin{cases} 0, & t < 0, \\ 1, & t \geq 0. \end{cases}$$

Unit step

With this definition, the impulse response of the first-order system becomes

$$h(t) = e^{-kt}1(t).$$

The response of this system to a general input is given by the convolution of this impulse response with the input

$$\begin{aligned}
 y(t) &= \int_{-\infty}^{\infty} h(\tau)u(t - \tau) d\tau \\
 &= \int_{-\infty}^{\infty} e^{-k\tau} 1(\tau)u(t - \tau) d\tau \\
 &= \int_0^{\infty} e^{-k\tau} u(t - \tau) d\tau.
 \end{aligned}$$

For time-invariant systems, the output for a general input is given by the integral

$$y(t) = \int_{-\infty}^{\infty} u(\tau)h(t - \tau)d\tau. \quad (3.14)$$

Notice the limits on the integral are at infinity. Thus, either or both  $h$  and  $u$  may be nonzero for negative time. If  $h$  has values for negative time, it means that the system response starts *before the input is applied!* Systems which do this are called non-causal because they do not obey the usual law of cause and effect.<sup>1</sup> Of course, all physical systems are causal. Furthermore, in most cases of interest we take  $t = 0$  as the time when the input starts. In this case, with causal systems, the integral may be written as

$$y(t) = \int_0^t u(\tau)h(t - \tau)d\tau. \quad (3.15)$$

### 3.1.2 Transfer Functions and Frequency Response

A simple version of the transfer function concept was developed in Chapter 2. A more rigorous treatment of this concept using the convolution integral follows. The evaluation of the convolution integral Eq. (3.14) can be difficult and an indirect approach has been developed using the Laplace transform<sup>2</sup> defined as

$$Y(s) = \int_{-\infty}^{\infty} y(t)e^{-st}dt.$$

Applying this transform to the convolution,

$$Y(s) = \int_{-\infty}^{\infty} \left[ \int_{-\infty}^{\infty} h(\tau)u(t - \tau)d\tau \right] e^{-st}dt.$$

Next, we exchange the order of integration such that we integrate with respect to  $t$  first

<sup>1</sup>A system is said to be causal if the output is not dependent on future inputs, that is, “the system does not laugh before it is tickled.”

<sup>2</sup>Many properties of the Laplace transform are given in Appendix A.

Non-causal system

$$Y(s) = \int_{-\infty}^{\infty} \left[ \int_{-\infty}^{\infty} u(t-\tau) e^{-st} dt \right] h(\tau) d\tau.$$

Changing variables of the inner integral by defining  $t - \tau = \eta$ , we get

$$Y(s) = \int_{-\infty}^{\infty} \left[ \int_{-\infty}^{\infty} u(\eta) e^{-s(\eta+\tau)} d\eta \right] h(\tau) d\tau, \quad (3.16)$$

$$Y(s) = \left[ \int_{-\infty}^{\infty} u(\eta) e^{-s\eta} d\eta \right] \int_{-\infty}^{\infty} h(\tau) e^{-s\tau} d\tau,$$

$$Y(s) = U(s)H(s).$$

In this solution,  $U(s)$  is the Laplace transform of the input time function and  $H(s)$ , the Laplace transform of the impulse response, is defined as the **transfer function**. By this operation, the complicated convolution integral is replaced by a simple multiplication of the transforms. What remains is to interpret the transforms and the transfer function. In the first instance, the integrals of the transforms usually do not converge for all values of the variable  $s$ , and they are only defined for a finite region in the  $s$ -plane.

An immediate consequence of convolution is that an input of the form  $e^{st}$  results in an output  $H(s)e^{st}$ . Note that both the input and output are exponential time functions, and that the output differs from the input only in the amplitude  $H(s)$ .  $H(s)$  is defined as the transfer function of the system. The specific constant  $s$  may be complex, expressed as  $s = \sigma_1 + j\omega$ . Thus, both the input and the output may be complex. If we let  $u(t) = e^{st}$  in Eq. (3.13), then

$$\begin{aligned} y(t) &= \int_{-\infty}^{\infty} h(\tau)u(t-\tau) d\tau, \\ y(t) &= \int_{-\infty}^{\infty} h(\tau)e^{s(t-\tau)} d\tau, \\ y(t) &= \int_{-\infty}^{\infty} h(\tau)e^{st}e^{-s\tau} d\tau, \\ y(t) &= \int_{-\infty}^{\infty} h(\tau)e^{-s\tau} d\tau e^{st}, \\ y(t) &= H(s)e^{st}, \end{aligned} \quad (3.17)$$

where

$$H(s) = \int_{-\infty}^{\infty} h(\tau)e^{-s\tau} d\tau. \quad (3.18)$$

---

<sup>3</sup>The integral does not converge for every value of  $s$  and care must be taken to be sure that the result is not used where it does not exist. Refer to Appendix A for details.

Laplace defined this integral and it is called the Laplace transform. Notice the limits on the integral are  $-\infty$  to  $+\infty$ , implying that  $h(t)$  may have values at any time. Equation (3.18) needs to be interpreted carefully.<sup>4</sup> Notice this input is exponential for *all time* ( $-\infty < t < \infty$ ) and Eq. (3.18) represents the response for all time and hence there are no initial conditions, and Eq. (3.17) gives the steady-state behavior of the system. Therefore, if the input is an exponential for all time, and if we know the transfer function  $H(s)$ , the output is readily computed by multiplication and the need for convolution goes away! The important conclusion is that if the input is an exponential time function so is the output and the scaling term is the transfer function. For any real, causal system,  $h(t) = 0$  for  $t < 0$ , and the limits on the integral can be set from 0 to  $\infty$

$$H(s) = \int_0^{\infty} h(\tau) e^{-s\tau} d\tau.$$

For a causal system, Eq. (3.13) simplifies to

$$y(t) = \int_0^{\infty} h(\tau) u(t - \tau) d\tau. \quad (3.19)$$

## EXAMPLE 3.4

### Transfer Function

Compute the transfer function for the system of Example 3.1, and find the output  $y$  for all time ( $-\infty < t < \infty$ ) when the input  $u = e^{st}$  for all time and  $s$  is a given complex number.

**Solution.** The system equation from Example 3.3 is

$$\dot{y}(t) + ky(t) = u(t) = e^{st}. \quad (3.20)$$

We assume we can express  $y(t)$  as  $H(s)e^{st}$ . With this form, we have  $\dot{y} = sH(s)e^{st}$ , and Eq. (3.20) reduces to

$$sH(s)e^{st} + kH(s)e^{st} = e^{st}. \quad (3.21)$$

Solving for the transfer function  $H(s)$ , we get

$$H(s) = \frac{1}{s + k}.$$

Substituting this back into Eq. (3.17) yields the output for all time

$$y(t) = \frac{e^{st}}{s + k}.$$

The integral in Eq. (3.18) does not need to be computed to find the transfer function of a system. Instead, one can assume a solution of the form of Eq. (3.17), substitute that into the differential equation of the system, then solve for the transfer function  $H(s)$ .

The transfer function can be formally defined as follows: The function  $H(s)$ , which is the transfer gain from  $U(s)$  to  $Y(s)$ —input to output—is called the **transfer function** of the system. It is the ratio of the

### Transfer function

<sup>4</sup>The corresponding output for the system is the particular solution from the well-known result for solving linear ordinary differential equations.

Laplace transform of the output of the system to the Laplace transform of the input. We can derive the transfer function explicitly. If we take the Laplace transform of both sides of Eq. (3.19), we have  $Y(s) = H(s)U(s)$  and

$$\frac{Y(s)}{U(s)} = H(s), \quad (3.22)$$

with the *key assumption* that all of the initial conditions on the system are zero.

### Transfer function

The transfer function  $H(s)$  is the ratio of the Laplace transform of the output of the system to its input assuming all zero initial conditions.

If the input  $u(t)$  is the unit impulse  $\delta(t)$ , then  $y(t)$  is the unit impulse response. The Laplace transform of  $u(t)$  is 1 and the transform of  $y(t)$  is  $H(s)$  because

$$Y(s) = H(s). \quad (3.23)$$

In words, this is to say

### Transfer function

The transfer function  $H(s)$  is the Laplace transform of the unit impulse response  $h(t)$ .

Thus, one way to characterize an LTI system is by applying a unit impulse and measuring the resulting response, which is a description (the inverse Laplace transform) of the transfer function.

For example, given the ordinary differential equation describing a third-order system with the output  $y(t)$  and input  $u(t)$

$$\ddot{y} + a_1\dot{y} + a_2y + a_3y = b_1\ddot{u} + b_2\dot{u} + b_3u, \quad (3.24)$$

we take the Laplace transform of both sides of the equation, *assuming zero initial conditions* ( $y(0^-) = \dot{y}(0^-) = \ddot{y}(0^-) = u(0^-) = \dot{u}(0^-) = 0$ ), to obtain

$$s^3 Y(s) + a_1 s^2 Y(s) + a_2 s Y(s) + a_3 Y(s) = b_1 s^2 U(s) + b_2 s U(s) + b_3 U(s), \quad (3.25)$$

$$(s^3 + a_1 s^2 + a_2 s + a_3) Y(s) = (b_1 s^2 + b_2 s + b_3) U(s),$$

which leads to the transfer function  $H(s)$ ,

$$H(s) = \frac{Y(s)}{U(s)} = \frac{b_1 s^2 + b_2 s + b_3}{s^3 + a_1 s^2 + a_2 s + a_3} = \frac{b(s)}{a(s)}. \quad (3.26)$$

This idea can then be easily extended to a system of any order  $n$ .

**EXAMPLE 3.5***Transfer Function for an RC Circuit*

Compute the transfer function for the RC circuit driven by a voltage source as shown in Fig. 3.3.

**Solution.** The system equation from Kirchhoff's voltage law is

$$Ri(t) + y(t) = u(t),$$

$$i(t) = C \frac{dy(t)}{dt},$$

or

$$RC\dot{y} + y = u(t).$$

If the input voltage is a unit impulse signal

$$RC\dot{y} + y = \delta(t),$$

and we take the Laplace transform of both sides of the above equation (see Appendix A)

$$RC(sY(s) - y(0^-)) + Y(s) = U(s) = 1.$$

Then assuming zero initial condition ( $y(0^-) = 0$ ) we find

$$H(s) = \frac{Y(s)}{U(s)} = Y(s) = \frac{1}{RCs + 1}.$$

The output, that is, the inverse Laplace transform of  $Y(s)$ , is the impulse response

$$y(t) = h(t) = \frac{1}{RC} e^{-\frac{t}{RC}} 1(t).$$

Therefore, the transfer function for this system is

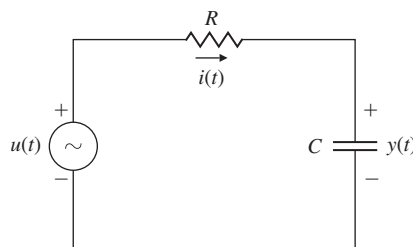
$$H(s) = \mathcal{L}\{h(t)\} = \frac{1}{RCs + 1}.$$

**Frequency response**

A very common way to use the exponential response of LTIs is in finding the **frequency response**, or response to a sinusoid. First, we express the sinusoid as a sum of two exponential expressions (Euler's relation):

$$A \cos(\omega t) = \frac{A}{2} (e^{j\omega t} + e^{-j\omega t}).$$

**Figure 3.3**  
RC circuit diagram



If we let  $s = j\omega$  in the basic response formula Eq. (3.17), then the response to  $u(t) = e^{j\omega t}$  is  $y(t) = H(j\omega)e^{j\omega t}$ ; similarly, the response to  $u(t) = e^{-j\omega t}$  is  $H(-j\omega)e^{-j\omega t}$ . By superposition, the response to the sum of these two exponentials, which make up the cosine signal, is the sum of the responses:

$$y(t) = \frac{A}{2} [H(j\omega)e^{j\omega t} + H(-j\omega)e^{-j\omega t}]. \quad (3.27)$$

The transfer function  $H(j\omega)$  is a complex number that can be represented in polar form or in magnitude-and-phase form as  $H(j\omega) = M(\omega)e^{j\varphi(\omega)}$ , or simply  $H = Me^{j\varphi}$ . With this substitution, Eq. (3.27) becomes

$$\begin{aligned} y(t) &= \frac{A}{2} M \left( e^{j(\omega t + \varphi)} + e^{-j(\omega t + \varphi)} \right), \\ &= AM \cos(\omega t + \varphi), \end{aligned} \quad (3.28)$$

where

$$M = |H(j\omega)|, \varphi = \angle H(j\omega).$$

This means if a system represented by the transfer function  $H(s)$  has a sinusoidal input with magnitude  $A$ , the output will be sinusoidal at the same frequency with magnitude  $AM$  and will be shifted in phase by the angle  $\varphi$ .

## EXAMPLE 3.6

### Frequency Response

For the system in Example 3.1, find the response to the sinusoidal input  $u = A \cos(\omega t)$ . That is, find the frequency response and plot the response for  $k = 1$ .

**Solution.** In Example 3.4, we found the transfer function of the system in Example 3.1. To find the frequency response, we let  $s = j\omega$  so

$$H(s) = \frac{1}{s+k} \implies H(j\omega) = \frac{1}{j\omega+k}.$$

From this, we get

$$M = \left| \frac{1}{j\omega+k} \right| = \frac{1}{\sqrt{\omega^2+k^2}} \quad \text{and} \quad \varphi = -\tan^{-1}\left(\frac{\omega}{k}\right).$$

According to Eq. (3.28), the response of this system to a sinusoid will be

$$y(t) = AM \cos(\omega t + \varphi). \quad (3.29)$$

$M$  is usually referred to as the **amplitude ratio** and  $\varphi$  is referred to as the **phase**, and they are both functions of the input frequency,  $\omega$ . The Matlab program that follows is used to compute the amplitude ratio and phase for  $k = 1$ , as shown in Fig. 3.4. The `logspace` command is used to set the frequency range (on a logarithmic scale) and the `bode` command is used to compute the frequency response in Matlab. Presenting frequency response in this manner (that is, on a log-log scale)

was originated by H. W. Bode; thus, these plots are referred to as “Bode plots.”<sup>5</sup> (See Chapter 6, Section 6.1.)

```
k = 1;
tf = ('s');
sysH = 1/(s+k);
w = logspace(-2,2);
[mag,phase] = bode(sysH,w);
loglog(w,squeeze(mag));
semilogx(w,squeeze(phase));
```

% define Laplace variable  
 % define system by its transfer function  
 % set frequency w to 50 values from  
 %  $10^{-2}$  to  $10^{+2}$   
 % compute frequency response  
 % log-log plot of magnitude  
 % semi-log plot of phase

We can generalize the frequency response by study of the **Laplace transform** of a signal  $f(t)$  as a generalization of Eq. (3.18),

$$F(s) = \int_{-\infty}^{\infty} f(t)e^{-st} dt. \quad (3.30)$$

The key property of Laplace transforms

If we apply this definition to both  $u(t)$  and  $y(t)$  and use the convolution integral Eq. (3.13), we find that

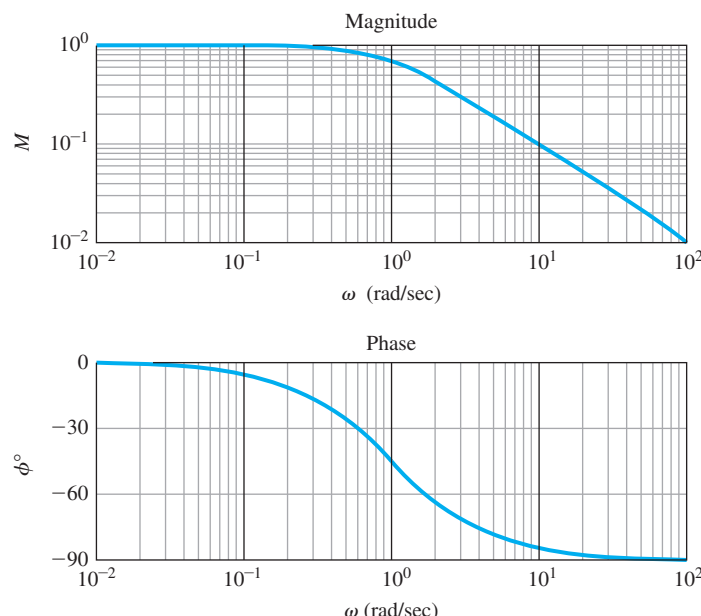
$$Y(s) = H(s)U(s), \quad (3.31)$$

where  $Y(s)$  and  $U(s)$  are the Laplace transforms of  $y(t)$  and  $u(t)$ , respectively.

**Figure 3.4**

Frequency-response plot for  $k = 1$

Source: Reprinted with permission of The MathWorks, Inc.



<sup>5</sup>Note % is used in Matlab to denote comments.

### Transient response

Laplace transforms such as Eq. (3.30) can be used to study the complete response characteristics of feedback systems, including the **transient response**—that is, the time response to an initial condition or suddenly applied signal. This is in contrast to the use of Fourier transforms, which only take into account the steady-state response. A standard problem in control is to find the response  $y(t)$  of a system given the input  $u(t)$  and a model of the system. With Eq. (3.30), we have a means for computing the response of LTI systems to quite general inputs. Given any input into a system, we compute the transform of the input and the transfer function for the system. The transform of the output is then given by Eq. (3.31) as the product of these two. If we wanted the time function of the output, we would need to “invert”  $Y(s)$  to get what is called the **inverse transform**; this step is typically not carried out explicitly. Nevertheless, understanding the process necessary for deriving  $y(t)$  from  $Y(s)$  is important because it leads to insight into the behavior of linear systems. Hence, given a general linear system with transfer function  $H(s)$  and an input signal  $u(t)$ , the procedure for determining  $y(t)$  using the Laplace transform is given by the following steps:

STEP 1. Determine the transfer function:  $H(s) = \mathcal{L}\{\text{impulse response of the system}\}$ . Compute  $H(s)$  by the following steps:

(a) Take the Laplace transform of the equations of motion. A table of transform properties is frequently useful in this process.

(b) Solve the resulting algebraic equations. Often this step is greatly helped by drawing the corresponding block diagram and solving the equations by graphical manipulation of the blocks or using Matlab.

STEP 2. Determine the Laplace transform of the input signal:  $U(s) = \mathcal{L}\{u(t)\}$ .

STEP 3. Compute the Laplace transform of the output:  $Y(s) = H(s) U(s)$ .

STEP 4. Break up  $Y(s)$  by partial-fraction expansion.

STEP 5. Find the output of the system by computing the inverse Laplace transform of  $Y(s)$  in Step 4,  $y(t) = \mathcal{L}^{-1}\{Y(s)\}$  [that is, invert  $Y(s)$  to get  $y(t)$ ]:

(a) Look up the components of  $y(t)$  in a table of transform–time function pairs.

(b) Combine the components to give the total solution in the desired form.

As mentioned above, Steps 4 and 5 are almost never carried out in practice, and a modified solution for a *qualitative* rather than a quantitative solution is often adequate and *almost always used for control design*

*purposes.* The process begins with the first three steps as before. However, rather than inverting  $Y(s)$ , one can use prior knowledge and intuition about the effects of pole and zero locations in  $Y(s)$  on the response  $y(t)$  to estimate key features of  $y(t)$ . That is, we get information about  $y(t)$  from the pole-zero constellation of  $Y(s)$  without actually inverting it, as discussed in the rest of this chapter. We can also obtain equivalent information from the Bode plot if that is available (see Chapter 6).

While it is possible to determine the transient response properties of the system using Eq. (3.30), it is generally more useful to use a simpler version of the Laplace transform based on the input beginning at time zero.

## EXAMPLE 3.7

### Frequency Response (Example 3.6 continued)

To continue with the system in Example 3.6, determine the response to an input that begins at  $t = 0$  as  $u(t) = \sin(10t)U(t)$ , notice from Laplace transform tables (see Appendix A, Table A.2), we have

$$\mathcal{L}\{u(t)\} = \mathcal{L}\{\sin(10t)\} = \frac{10}{s^2 + 100},$$

where  $\mathcal{L}$  denotes the Laplace transform, and the output of the system using partial fraction expansion (see Section 3.1.5) is given by

$$\begin{aligned} Y(s) &= H(s)U(s) \\ &= \frac{1}{s+1} \frac{10}{s^2 + 100}, \\ &= \frac{\alpha_1}{s+1} + \frac{\alpha_0}{s+j10} + \frac{\alpha_0^*}{s-j10}, \\ &= \frac{\frac{10}{101}}{s+1} + \frac{\frac{j}{2(1-j10)}}{s+j10} + \frac{\frac{-j}{2(1+j10)}}{s-j10}. \end{aligned}$$

The inverse Laplace transform of the output is given by (see Appendix A)

$$\begin{aligned} y(t) &= \frac{10}{101}e^{-t} + \frac{1}{\sqrt{101}} \sin(10t + \varphi) \\ &= y_1(t) + y_2(t), \end{aligned}$$

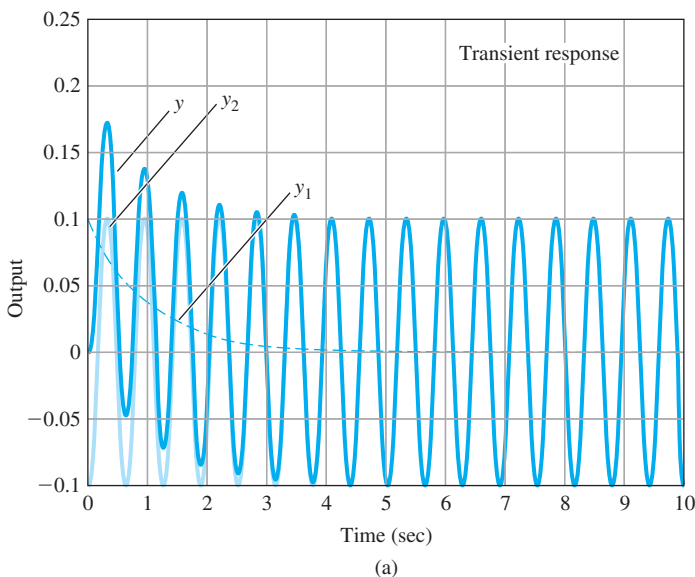
where

$$\varphi = \tan^{-1}(-10) = -84.2^\circ.$$

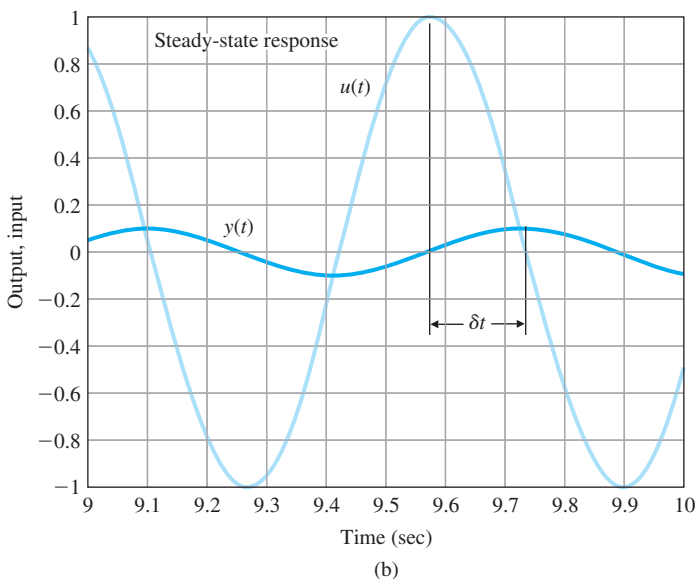
The component  $y_1(t)$  is called the *transient* response as it decays to zero as time goes on, and the component  $y_2(t)$  is called the *steady state* and equals the response given by Eq. (3.29). Fig. 3.5(a) is a plot of the time history of the output showing the different components ( $y_1$ ,  $y_2$ ) and the composite ( $y$ ) output response. The output frequency is 10 rad/sec and the steady-state phase difference measured from Fig. 3.5(b)

**Figure 3.5**

(a) Complete transient response; (b) phase lag between output and input



(a)



(b)

is approximately  $10^* \delta t = 1.47$  rad =  $84.2^\circ$ .<sup>6</sup> Figure 3.5(b) shows the output lags the input by  $84.2^\circ$ . It also shows that the steady-state amplitude of the output is the amplitude ratio  $\frac{1}{\sqrt{101}} = 0.0995$  (that is, the amplitude of the input signal times the magnitude of the transfer function evaluated at  $\omega = 10$  rad/sec).

This example illustrates that the response of an LTI system to a sinusoid of frequency  $\omega$  is a sinusoid with the *same* frequency and with an amplitude ratio equal to the magnitude of the transfer function

<sup>6</sup>The phase difference may also be determined by a Lissajous pattern.

evaluated at the input frequency. Furthermore, the phase difference between input and output signals is given by the phase of the transfer function evaluated at the input frequency. The magnitude ratio and phase difference can be computed from the transfer function as just discussed; they can also be measured experimentally quite easily in the laboratory by driving the system with a known sinusoidal input and measuring the steady-state amplitude and phase of the system's output. The input frequency is set to sufficiently many values so curves such as the one in Fig. 3.4 are obtained.

### 3.1.3 The $\mathcal{L}_-$ Laplace Transform

[Definition of Laplace transform](#)

In this book, it is useful to define a **one-sided (or unilateral) Laplace transform**, which uses  $0^-$  (that is, a value just before  $t = 0$ ) as the lower limit of integration in Eq. (3.30). The  $\mathcal{L}_-$  Laplace transform of  $f(t)$ , denoted by  $\mathcal{L}_-\{f(t)\} = F(s)$ , is a function of the complex variable  $s = \sigma_1 + j\omega$ , where

$$F(s) \triangleq \int_{0^-}^{\infty} f(t)e^{-st} dt. \quad (3.32)$$

The decaying exponential term in the integrand in effect provides a built-in convergence factor if  $\sigma_1 > 0$ . This means that even if  $f(t)$  does not vanish as  $t \rightarrow \infty$ , the integrand will vanish for sufficiently large values of  $\sigma$  if  $f$  does not grow at a faster-than-exponential rate. The fact that the lower limit of integration is at  $0^-$  allows the use of an impulse function at  $t = 0$ , as illustrated in Example 3.3; however, this distinction between  $t = 0^-$  and  $t = 0$  does not usually come up in practice. We will therefore, for the most part, drop the minus superscript on  $t = 0$ ; however, we will return to using the notation  $t = 0^-$  when an impulse at  $t = 0$  is involved and the distinction is of practical value.

If Eq. (3.32) is a one-sided transform, then by extension, Eq. (3.30) is a **two-sided Laplace transform**.<sup>7</sup> We will use the  $\mathcal{L}$  symbol from here on to mean  $\mathcal{L}_-$ .

On the basis of the formal definition in Eq. (3.32), we can ascertain the properties of Laplace transforms and compute the transforms of common time functions. The analysis of linear systems by means of Laplace transforms usually involves using tables of common properties and time functions, so we have provided this information in Appendix A. The tables of time functions and their Laplace transforms, together with the table of properties, permit us to find transforms of complex signals from simpler ones. For a thorough study of Laplace transforms and extensive tables, see Churchill (1972) and Campbell and Foster (1948). For more study of the two-sided transform, see Van der Pol and Bremmer (1955). These authors show that the time function can be obtained from the Laplace transform by the inverse relation

---

<sup>7</sup>The other possible one-sided transform is, of course,  $\mathcal{L}_+$ , in which the lower limit of the integral is  $0^+$ . This is sometimes used in other applications.

$$f(t) = \frac{1}{2\pi j} \int_{\sigma_c-j\infty}^{\sigma_c+j\infty} F(s)e^{st} ds, \quad (3.33)$$

where  $\sigma_c$  is a selected value to the right of all the singularities of  $F(s)$  in the  $s$ -plane. In practice, this relation is seldom used. Instead, complex Laplace transforms are broken down into simpler ones that are listed in the tables along with their corresponding time responses.

Let us compute a few Laplace transforms of some typical time functions.

### EXAMPLE 3.8

#### *Step and Ramp Transforms*

Find the Laplace transform of the step  $a1(t)$  and ramp  $bt1(t)$  functions.

**Solution.** For a step of size  $a$ ,  $f(t) = a1(t)$ , and from Eq. (3.32), we have

$$F(s) = \int_0^\infty ae^{-st} dt = \left[ -\frac{ae^{-st}}{s} \right]_0^\infty = 0 - \left( -\frac{a}{s} \right) = \frac{a}{s}, \quad \text{Re}(s) > 0.$$

For the ramp signal  $f(t) = bt1(t)$ , again from Eq. (3.32), we have

$$F(s) = \int_0^\infty bte^{-st} dt = \left[ -\frac{bte^{-st}}{s} - \frac{be^{-st}}{s^2} \right]_0^\infty = \frac{b}{s^2}, \quad \text{Re}(s) > 0,$$

where we employed the technique of integration by parts,

$$\int u dv = uv - \int v du,$$

with  $u = bt$  and  $dv = e^{-st} dt$ . We can then extend the domain of the validity of  $F(s)$  to the entire  $s$ -plane except at the pole location namely the origin (see Appendix A).

A more subtle example is that of the impulse function.

### EXAMPLE 3.9

#### *Impulse Function Transform*

Find the Laplace transform of the unit-impulse function.

**Solution.** From Eq. (3.32), we get

$$F(s) = \int_{0^-}^\infty \delta(t)e^{-st} dt = \int_{0^-}^{0^+} \delta(t) dt = 1. \quad (3.34)$$

It is the transform of the unit-impulse function that led us to choose the  $\mathcal{L}_-$  transform rather than the  $\mathcal{L}_+$  transform.

### EXAMPLE 3.10

#### *Sinusoid Transform*

Find the Laplace transform of the sinusoid function.

**Solution.** Again, we use Eq. (3.32) to get

$$\mathcal{L}\{\sin \omega t\} = \int_0^\infty (\sin \omega t)e^{-st} dt. \quad (3.35)$$

If we substitute the relation from Eq. (WA.34) in Appendix WA (available online at [www.pearsonglobaleditions.com](http://www.pearsonglobaleditions.com)),

$$\sin \omega t = \frac{e^{j\omega t} - e^{-j\omega t}}{2j}$$

into Eq. (3.35), we find that

$$\begin{aligned}\mathcal{L}\{\sin \omega t\} &= \int_0^\infty \left( \frac{e^{j\omega t} - e^{-j\omega t}}{2j} \right) e^{-st} dt \\ &= \frac{1}{2j} \int_0^\infty (e^{(j\omega-s)t} - e^{-(j\omega+s)t}) dt, \\ &= \frac{1}{2j} \left[ \frac{1}{j\omega - s} e^{(j\omega-s)t} - \frac{1}{j\omega + s} e^{-(j\omega+s)t} \right]_0^\infty, \\ &= \frac{\omega}{s^2 + \omega^2}, \quad \operatorname{Re}(s) > 0.\end{aligned}$$

We can then extend the domain of the validity of computed Laplace transform to the entire  $s$ -plane except at the pole locations  $s = \pm j\omega$  (see Appendix A).

Table A.2 in Appendix A lists Laplace transforms for elementary time functions. Each entry in the table follows from direct application of the transform definition of Eq. (3.32), as demonstrated by Examples 3.8 through 3.10.

### 3.1.4 Properties of Laplace Transforms

In this section, we will address each of the significant properties of the Laplace transform listed in Table A.1. For the proofs of these properties and related examples as well as the Initial Value Theorem, the reader is referred to Appendix A.

#### 1. Superposition

One of the most important properties of the Laplace transform is that it is linear, which means that the principle of superposition applies:

$$\mathcal{L}\{\alpha f_1(t) + \beta f_2(t)\} = \alpha F_1(s) + \beta F_2(s). \quad (3.36)$$

The amplitude scaling property is a special case of this; that is,

$$\mathcal{L}\{\alpha f(t)\} = \alpha F(s). \quad (3.37)$$

#### 2. Time Delay

Suppose a function  $f(t)$  is delayed by  $\lambda > 0$  units of time,  $f_1(t) = f(t - \lambda)$ . Its Laplace transform is

$$F_1(s) = \int_0^\infty f(t - \lambda) e^{-st} dt = e^{-s\lambda} F(s). \quad (3.38)$$

From this result, we see that a time delay of  $\lambda$  corresponds to multiplication of the transform by  $e^{-s\lambda}$ .

### 3. Time Scaling

It is sometimes useful to time-scale equations of motion. For example, in the control system of a disk drive, it is meaningful to measure time in milliseconds (see also Chapter 10). If the time  $t$  is scaled by a factor  $a$ ,  $f_1(t) = f(at)$ , then the Laplace transform of the time-scaled signal is

$$F_1(s) = \int_0^\infty f(at)e^{-st} dt = \frac{1}{|a|} F\left(\frac{s}{a}\right). \quad (3.39)$$

### 4. Shift in Frequency

Multiplication (modulation) of  $f(t)$  by an exponential expression in the time domain,  $f_1(t) = e^{-at}f(t)$ , corresponds to a shift in the frequency domain:

$$F_1(s) = \int_0^\infty e^{-at}f(t)e^{-st} dt = F(s+a). \quad (3.40)$$

### 5. Differentiation

The transform of the derivative of a signal is related to its Laplace transform and its initial condition as follows:

$$\mathcal{L}\left\{\frac{df}{dt}\right\} = \int_{0^-}^\infty \left(\frac{df}{dt}\right) e^{-st} dt = -f(0^-) + sF(s). \quad (3.41)$$

Another application of Eq. (3.41) leads to

$$\mathcal{L}\{\ddot{f}\} = s^2 F(s) - sf(0^-) - \dot{f}(0^-). \quad (3.42)$$

Repeated application of Eq. (3.41) leads to

$$\mathcal{L}\{f^m(t)\} = s^m F(s) - s^{m-1}f(0^-) - s^{m-2}\dot{f}(0^-) - \dots - f^{(m-1)}(0^-), \quad (3.43)$$

where  $f^m(t)$  denotes the  $m$ th derivative of  $f(t)$  with respect to time.

### 6. Integration

The Laplace transform of the integral of a time function  $f(t)$ ;  $f_1(t) = \int_0^t f(\xi) d\xi$ , is given by,

$$F_1(s) = \mathcal{L}\left\{\int_0^t f(\xi) d\xi\right\} = \frac{1}{s} F(s), \quad (3.44)$$

which means that we simply multiply the function's Laplace transform by  $\frac{1}{s}$ .

### 7. Convolution

We have seen previously that the response of a system is determined by convolving the input with the impulse response of the system, or by forming the product of the transfer function and the Laplace transform of the input. The discussion that follows extends this concept to various time functions.

Convolution in the time domain corresponds to multiplication in the frequency domain. Assume  $\mathcal{L}\{f_1(t)\} = F_1(s)$  and  $\mathcal{L}\{f_2(t)\} = F_2(s)$ . Then,

$$\mathcal{L}\{f_1(t) * f_2(t)\} = \int_0^\infty f_1(t) * f_2(t) e^{-st} dt = F_1(s)F_2(s). \quad (3.45)$$

where  $*$  is the convolution operator. This implies that

$$\mathcal{L}^{-1}\{F_1(s)F_2(s)\} = f_1(t) * f_2(t). \quad (3.46)$$

A similar, or dual, of this result is discussed next.

### 8. Time Product

Multiplication in the time domain corresponds to convolution in the frequency domain:

$$\mathcal{L}\{f_1(t)f_2(t)\} = \frac{1}{2\pi j} F_1(s) * F_2(s). \quad (3.47)$$

### 9. Multiplication by Time

Multiplication by time  $f_1(t) = tf(t)$  corresponds to differentiation in the frequency domain:

$$F_1(s) = \mathcal{L}\{tf(t)\} = -\frac{d}{ds}F(s). \quad (3.48)$$

### 3.1.5 Inverse Laplace Transform by Partial-Fraction Expansion

The easiest way to find  $f(t)$  from its Laplace transform  $F(s)$ , if  $F(s)$  is rational, is to expand  $F(s)$  as a sum of simpler terms that can be found in the tables. The basic tool for performing this operation is called **partial-fraction expansion**. Consider the general form for the rational function  $F(s)$  consisting of the ratio of two polynomials:

$$F(s) = \frac{b_1 s^m + b_2 s^{m-1} + \cdots + b_{m+1}}{s^n + a_1 s^{n-1} + \cdots + a_n}. \quad (3.49)$$

By factoring the polynomials, this same function could also be expressed in terms of the product of factors as

$$F(s) = K \frac{\prod_{i=1}^m (s - z_i)}{\prod_{i=1}^n (s - p_i)}. \quad (3.50)$$

We will discuss the simple case of distinct poles here. For a transform  $F(s)$  representing the response of any physical system,  $m \leq n$ . When  $s = z_i$ ,  $s$  is referred to as a **zero** of the function, and when  $s = p_i$ ,  $s$  is referred to as a **pole** of the function. Assuming for now the poles  $\{p_i\}$  are real or complex but distinct, we rewrite  $F(s)$  as the partial fraction

$$F(s) = \frac{C_1}{s - p_1} + \frac{C_2}{s - p_2} + \cdots + \frac{C_n}{s - p_n}. \quad (3.51)$$

Next, we determine the set of constants  $\{C_i\}$ . We multiply both sides of Eq. (3.51) by the factor  $s - p_1$  to get

$$(s - p_1)F(s) = C_1 + \frac{s - p_1}{s - p_2}C_2 + \cdots + \frac{(s - p_1)}{s - p_n}C_n. \quad (3.52)$$

If we let  $s = p_1$  on both sides of Eq. (3.52), then all the  $C_i$  terms will equal zero except for the first one. For this term,

$$C_1 = (s - p_1)F(s)|_{s=p_1}. \quad (3.53)$$

The other coefficients can be expressed in a similar form:

$$C_i = (s - p_i)F(s)|_{s=p_i}.$$

**The cover-up method of determining coefficients**

This process is called the **cover-up method** because, in the factored form of  $F(s)$  [Eq. (3.50)], we can cover up the individual denominator terms, evaluate the rest of the expression with  $s = p_i$ , and determine the coefficients  $C_i$ . Once this has been completed, the time function becomes

$$f(t) = \sum_{i=1}^n C_i e^{p_i t} 1(t),$$

because, as entry 7 in Table A.2 shows, if

$$F(s) = \frac{1}{s - p_i},$$

then

$$f(t) = e^{p_i t} 1(t).$$

For the cases of quadratic factors or repeated roots in the denominator, see Appendix A.

### EXAMPLE 3.11

#### Partial-Fraction Expansion: Distinct Real Roots

Suppose you have computed  $Y(s)$  and found that

$$Y(s) = \frac{(s+4)(s+3)}{s(s+9)(s+2)}.$$

Find  $y(t)$ .

**Solution.** We may write  $Y(s)$  in terms of its partial-fraction expansion:

$$Y(s) = \frac{C_1}{s} + \frac{C_2}{s+9} + \frac{C_3}{s+2}.$$

Using the cover-up method, we get

$$C_1 = \left. \frac{(s+4)(s+3)}{(s+9)(s+2)} \right|_{s=0} = \frac{2}{3}.$$

In a similar fashion,

$$C_2 = \frac{(s+4)(s+3)}{s(s+2)} \Big|_{s=-9} = \frac{10}{21},$$

and

$$C_3 = \frac{(s+4)(s+3)}{s(s+9)} \Big|_{s=-2} = -\frac{1}{7}.$$

We can check the correctness of the result by adding the components again to verify that the original function has been recovered. With the partial fraction the solution can be looked up in the tables at once to be

$$y(t) = \frac{2}{3}1(t) + \frac{10}{21}e^{-9t}1(t) - \frac{1}{7}e^{-2t}1(t).$$

The partial fraction expansion may be computed using the residue function in Matlab:

```
num = conv([1 4],[1 3]); % form numerator polynomial
den = conv([1 9 0],[1 2]); % form denominator polynomial
[r,p,k] = residue(num,den); % compute the residues
```

which yields the result

```
r = [0.4762 -0.1429 0.6667]'; p = [-9 -2 0]'; k = [];
```

and agrees with the hand calculations. Note the conv function in Matlab is used to multiply two polynomials. (The arguments of the functions are the polynomials coefficients.)

---

### 3.1.6 The Final Value Theorem

An especially useful property of the Laplace transform in control known as the **Final Value Theorem** allows us to compute the constant steady-state value of a time function given its Laplace transform. The theorem follows from the development of partial-fraction expansion. Suppose we have a transform  $Y(s)$  of a signal  $y(t)$  and wish to know the final value  $y(t)$  from  $Y(s)$ . There are three possibilities for the limit. It can be constant, undefined, or unbounded. If  $Y(s)$  has any poles (that is, denominator roots, as described in Section 3.1.5) in the right half of the  $s$ -plane—that is, if the real part of any  $p_i > 0$ —then  $y(t)$  will grow and the limit will be unbounded. If  $Y(s)$  has a pair of poles on the imaginary axis of the  $s$ -plane (that is,  $p_i = \pm j\omega$ ), then  $y(t)$  will contain a sinusoid that persists forever, and the final value will not be defined. Only one case can provide a nonzero constant final value: If all poles of  $Y(s)$  are in the left half of the  $s$ -plane, except for one at  $s = 0$ , then all terms of  $y(t)$  will decay to zero except the term corresponding to the pole at  $s = 0$ , and that term corresponds to a constant in time. Thus, the

final value is given by the coefficient associated with the pole at  $s = 0$ . Therefore, the Final Value Theorem is as follows:

### The Final Value Theorem

If all poles of  $sY(s)$  are in the left half of the  $s$ -plane, then

$$\lim_{t \rightarrow \infty} y(t) = \lim_{s \rightarrow 0} sY(s). \quad (3.54)$$

This relationship is proved in Appendix A.

### EXAMPLE 3.12

#### *Final Value Theorem*

Find the final value of the system corresponding to

$$Y(s) = \frac{7(s+5)}{2s(s^2 + 2s + 3)}.$$

**Solution.** Applying the Final Value Theorem, we obtain

$$y(\infty) = sY(s)|_{s=0} = \frac{7 \cdot 5}{2 \cdot 3} = 5.83.$$

Thus, after the transients have decayed to zero,  $y(t)$  will settle to a constant value of 5.83.

### Use the Final Value Theorem on stable systems only

Care must be taken to apply the Final Value Theorem only to stable systems (see Section 3.6). While one could use Eq. (3.54) on any  $Y(s)$ , doing so could result in erroneous results, as shown in the next example.

### EXAMPLE 3.13

#### *Incorrect Use of the Final Value Theorem*

Find the final value of the signal corresponding to

$$Y(s) = \frac{4}{s(s^2 - 5s + 6)}.$$

**Solution.** If we blindly apply Eq. (3.54), we obtain

$$y(\infty) = sY(s)|_{s=0} = \frac{2}{3}.$$

However,

$$y(t) = \frac{2}{3} - 2e^{2t} + \frac{4}{3}e^{3t}$$

which leads to an unbounded final value when  $t$  is equal to  $\infty$ . This is due to the presence of the unstable poles at  $s = 2$  and  $s = 3$ .

### Computing DC gain by the Final Value Theorem

The theorem can also be used to find the DC gain of a system. The **DC gain** is the ratio of the output of a system to its input (presumed constant) after all transients have decayed. To find the DC gain, we assume there is a unit-step input [ $U(s) = 1/s$ ] and we use the Final Value

Theorem to compute the steady-state value of the output. Therefore, for a system transfer function  $G(s)$ ,

$$\text{DC gain} = \lim_{s \rightarrow 0} sG(s) \frac{1}{s} = \lim_{s \rightarrow 0} G(s). \quad (3.55)$$

**EXAMPLE 3.14***DC Gain*

A system whose transfer function is

$$G(s) = \frac{4(s + A)}{s^2 + 7s + 5}$$

has a DC gain of 2.5. Find the value of  $A$ .

**Solution.** Applying Eq. (3.55) we get

$$\text{DC gain} = G(s)|_{s=0} = \frac{4A}{5} = 2.5.$$

Therefore,  $A = 3.125$ .

---

### 3.1.7 Using Laplace Transforms to Solve Differential Equations

Laplace transforms can be used to solve differential equations using the properties described in Appendix A. First, we find the Laplace transform of the differential equation using the differentiation properties in Eqs. (A.12) and (A.13) in Appendix A. Then we find the Laplace transform of the output; using partial-fraction expansion and Table A.2, this can be converted to a time response function. We will illustrate this with three examples.

**EXAMPLE 3.15***Homogeneous Differential Equation*

Find the solution to the differential equation

$$\ddot{y}(t) + y(t) = 0, \quad \text{where } y(0) = \alpha, \dot{y}(0) = \beta.$$

**Solution.** Using Eq. (3.42), the Laplace transform of the differential equation is

$$s^2 Y(s) - \alpha s - \beta + Y(s) = 0,$$

$$(s^2 + 1) Y(s) = \alpha s + \beta,$$

$$Y(s) = \frac{\alpha s}{s^2 + 1} + \frac{\beta}{s^2 + 1}.$$

After looking up in the transform tables (see Appendix A, Table A.2) the two terms on the right side of the preceding equation, we get

$$y(t) = [\alpha \cos t + \beta \sin t] 1(t),$$

where  $1(t)$  denotes a unit-step function. We can verify this solution is correct by substituting it back into the differential equation.

---

Another example will illustrate the solution when the equations are not homogeneous—that is, when the system is forced.

### EXAMPLE 3.16

#### *Forced Differential Equation*

Find the solution to the differential equation  $\ddot{y}(t) + 5\dot{y}(t) + 4y(t) = 3$ , where  $y(0) = \alpha$ ,  $\dot{y}(0) = \beta$ .

**Solution.** Taking the Laplace transform of both sides using Eqs. (3.41) and (3.42), we get

$$s^2 Y(s) - s\alpha - \beta + 5[sY(s) - \alpha] + 4Y(s) = \frac{3}{s}.$$

Solving for  $Y(s)$  yields

$$Y(s) = \frac{s(s\alpha + \beta + 5\alpha) + 3}{s(s+1)(s+4)}.$$

The partial-fraction expansion using the cover-up method is

$$Y(s) = \frac{\frac{3}{s}}{\frac{3}{s+1}} - \frac{\frac{3-\beta-4\alpha}{s+1}}{\frac{3}{s+1}} + \frac{\frac{3-4\alpha-4\beta}{s+4}}{\frac{12}{s+4}}.$$

Therefore, the time function is given by

$$y(t) = \left( \frac{3}{4} + \frac{-3 + \beta + 4\alpha}{3} e^{-t} + \frac{3 - 4\alpha - 4\beta}{12} e^{-4t} \right) 1(t).$$

By differentiating this solution twice and substituting the result in the original differential equation, we can verify this solution satisfies the differential equation.

The solution is especially simple if the initial conditions are all zero.

### EXAMPLE 3.17

#### *Forced Equation Solution with Zero Initial Conditions*

Find the solution to  $\dot{y}(t) + 6y(t) = u(t)$ ,  $y(0) = 0$ ,  $u(t) = 1 - 0.3e^{-3t}$ ,

1. using partial-fraction expansion,
2. using Matlab.

#### **Solution**

1. Taking the Laplace transform of both sides, we get

$$sY(s) + 6Y(s) = \frac{1}{s} - \frac{0.3}{s+3}$$

Solving for  $Y(s)$  yields

$$Y(s) = \frac{0.7s + 3}{s(s+3)(s+6)}$$

The partial-fraction expansion using the cover-up method is

$$Y(s) = \frac{\frac{1}{6}}{s} + \frac{\frac{10}{30}}{s+3} + \frac{\frac{2}{30}}{s+6}.$$

Therefore, the time function is given by

$$y(t) = \left( \frac{1}{6} - \frac{1}{10}e^{-3t} - \frac{2}{30}e^{-6t} \right) 1(t).$$

2. The partial-fraction expansion may also be computed using the Matlab residue function,

```
num = [0.7 3]; % form numerator
den = poly([0;-3;-6]); % form denominator polynomial
% from its roots
[r,p,k] = residue(num,den); % compute the residues
```

which results in the desired answer

$$r = [-0.0667 -0.1000 0.1667]'; p = [-6 -3 0]'; k = [];$$

and agrees with the hand calculations.

Poles indicate response character.

The primary value of using the Laplace transform method of solving differential equations is that it provides information concerning the qualitative characteristic behavior of the response. Once we know the values of the poles of  $Y(s)$ , we know what kind of characteristic terms will appear in the response. In the last example, the pole at  $s = -1$  produced a decaying  $y = Ce^{-t}$  term in the response. The pole at  $s = -4$  produced a  $y = Ce^{-4t}$  term in the response, which decays faster. If there had been a pole at  $s = +1$ , there would have been a growing  $y = Ce^{+t}$  term in the response. Using the pole locations to understand in essence how the system will respond is a powerful tool, and will be developed further in Section 3.3. Control systems designers often manipulate design parameters so that the poles have values that would give acceptable responses, and they skip the steps associated with converting those poles to actual time responses until the final stages of the design. They use trial-and-error design methods (as will be described in Chapter 5) that graphically present how changes in design parameters affect the pole locations. Once a design has been obtained, with pole locations predicted to give acceptable responses, the control designer determines a time response to verify that the design is satisfactory. This is typically done by computer, which solves the differential equations directly by using numerical computer methods.

### 3.1.8 Poles and Zeros

A rational transfer function can be described either as a ratio of two polynomials in  $s$ ,

$$H(s) = \frac{b_1 s^m + b_2 s^{m-1} + \cdots + b_{m+1}}{s^n + a_1 s^{n-1} + \cdots + a_n} = \frac{N(s)}{D(s)}, \quad (3.56)$$

or as a ratio in factored zero pole form

$$H(s) = K \frac{\prod_{i=1}^m (s - z_i)}{\prod_{i=1}^n (s - p_i)}. \quad (3.57)$$

**Zeros**

$K$  is called the transfer function gain. The roots of the numerator  $z_1, z_2, \dots, z_m$  are called the finite **zeros** of the system. The zeros are locations in the  $s$ -plane where the transfer function is zero. If  $s = z_i$ , then

$$H(s)|_{s=z_i} = 0.$$

The zeros also correspond to the signal transmission-blocking properties of the system and are also called the transmission zeros of the system. The system has the inherent capability to block frequencies coinciding with its zero locations. If we excite the system with the nonzero input,  $u = u_0 e^{s_0 t}$ , where  $s_0$  is not a pole of the system, then the output is identically zero,<sup>8</sup>  $y \equiv 0$ , for frequencies where  $s_0 = z_i$ . The zeros also have a significant effect on the transient properties of the system (see Section 3.5).

**Poles**

The roots of the denominator,  $p_1, p_2, \dots, p_n$ , are called the **poles**<sup>9</sup> of the system. The poles are locations in the  $s$ -plane where the magnitude of the transfer function becomes infinite. If  $s = p_i$ , then

$$|H(s)|_{s=p_i} = \infty.$$

The poles of the system determine its stability properties, as we shall see in Section 3.6. The poles of the system also determine the natural or unforced behavior of the system, referred to as the **modes** of the system. The zeros and poles may be complex quantities, and we may display their locations in a complex plane, which we refer to as the  $s$ -plane. The locations of the poles and zeros lie at the heart of feedback control design and have significant practical implications for control system design. The system is said to have  $n-m$  zeros at infinity if  $m < n$  because the transfer function approaches zero as  $s$  approaches infinity. If the zeros at infinity are also counted, the system will have the same number of poles and zeros. No physical system can have  $n < m$ ; otherwise, it would have an infinite response at  $\omega = \infty$ . If  $z_i = p_j$ , then there are *cancellations* in the transfer function, which may lead to undesirable system properties as will be discussed in Chapter 7.

### 3.1.9 Linear System Analysis Using Matlab

The first step in analyzing a system is to write down (or generate) the set of time-domain differential equations representing the dynamic behavior of the physical system. These equations are generated from the physical laws governing the system behavior—for example, rigid body dynamics, thermo-fluid mechanics, and electromechanics, as described in Chapter 2. The next step in system analysis is to determine and designate inputs and outputs of the system then to compute the transfer function characterizing the input–output behavior of the dynamic

---

<sup>8</sup>Identically zero means that the output and all of its derivatives are zero for  $t > 0$ .

<sup>9</sup>The meaning of the pole can also be appreciated by visualizing a 3-D plot of the transfer function, where the real and imaginary parts of  $s$  are plotted on the  $x$  and  $y$  axes, and the magnitude of the transfer function is plotted on the vertical  $z$  axis. For a single pole, the resulting 3-D plot will look like a tent with the “tent-pole” being located at the pole of the transfer function!

system. Earlier in this chapter, we discussed that a linear dynamic system may also be represented by the Laplace transform of its differential equation—that is, its transfer function. The transfer function may be expressed as a ratio of two polynomials as in Eq. (3.56) or in factored zero–pole form as in Eq. (3.57). By analyzing the transfer function, we can determine the dynamic properties of the system, both in a qualitative and quantitative manner. One way of extracting useful system information is simply to determine the pole–zero locations and deduce the essential characteristics of the dynamic properties of the system. Another way is to determine the time-domain properties of the system by determining the response of the system to typical excitation signals such as impulses, steps, ramps, and sinusoids. Yet another way is to determine the time response analytically by computing the inverse Laplace transform using partial-fraction expansions and Tables A.1 and A.2 in Appendix A. Of course, it is also possible to determine the system response to an arbitrary input.

We will now illustrate this type of analysis by carrying out the preceding calculations for some of the physical systems addressed in the examples in Chapter 2 in order of increasing degree of difficulty. We will go back and forth between the different representations of the system, transfer function, pole–zero, and so on, using Matlab as our computational engine. Matlab typically accepts the specification of a system in several forms, including transfer function and zero–pole, and refers to these two descriptions as `tf` and `zp`, respectively. Furthermore, it can transform the system description from any one form to another.

### EXAMPLE 3.18

#### *Cruise Control Transfer Function Using Matlab*

Find the transfer function between the input  $u$  and the position of the car  $x$  in the cruise control system in Example 2.1 of Chapter 2.

**Solution.** From Example 2.1 of Chapter 2, we find the transfer function of the system is

$$H(s) = \frac{0.001}{s^2 + 0.05s} = \frac{0.001}{s(s + 0.05)}.$$

In Matlab, the transfer function is specified as follows:

```
s=tf('s'); % define Laplace variable
sysH=0.001/(s^2+0.05*s); % form transfer function
```

The pole–zero description is computed using the following Matlab commands:

```
p=pole(sysH); % compute poles
[z,k]=zero(sysH); % compute zeros and transfer function gain
```

and would result in the transfer function in factored form, where  $z = [ ]$ ,  $p = [0 \quad -0.05]'$ , and  $k = 0.001$ .

**EXAMPLE 3.19***DC Motor Transfer Function Using Matlab*

In Example 2.15 of Chapter 2, assume that  $J_m = 0.02 \text{ kg} \cdot \text{m}^2$ ,  $b = 0.005 \text{ N} \cdot \text{m} \cdot \text{sec}$ ,  $K_t = K_e = 0.5$ ,  $R_a = 2.5 \Omega$ , and  $L_a = 0.1 \text{ H}$ . Find the transfer function between the input  $v_a$  and

1. the output  $\theta_m$ ,
2. the output  $\omega = \dot{\theta}_m$ .

**Solution.**

1. Substituting the preceding parameters into Example 2.15 of Chapter 2, we find that the transfer function of the system is

$$H(s) = \frac{250}{s^3 + 25.25s^2 + 131.25s} = \frac{250}{s(s^2 + 25.25s + 131.25)}.$$

In Matlab, the transfer function is specified as

```
s = tf('s'); % define Laplace variable
sysH = 250/(s^3+25.25*s^2+131.25*s); % form transfer function
```

Again, the pole-zero description is computed using the Matlab commands

```
p = pole(sysH); % compute poles
[z,k] = zero(sysH); % compute zeros and transfer function gain
```

which results in

$$z = [], \quad p = [0 \quad -17.9298 \quad -7.3202]', \quad k = 250,$$

and yields the transfer function in factored form:

$$H(s) = \frac{250}{s(s + 17.9298)(s + 7.3202)}.$$

2. If we consider the velocity  $\dot{\theta}_m$  as the output, the transfer function is

$$G(s) = \frac{250s}{s^3 + 25.25s^2 + 131.25s} = \frac{250}{s^2 + 25.25s + 131.25}.$$

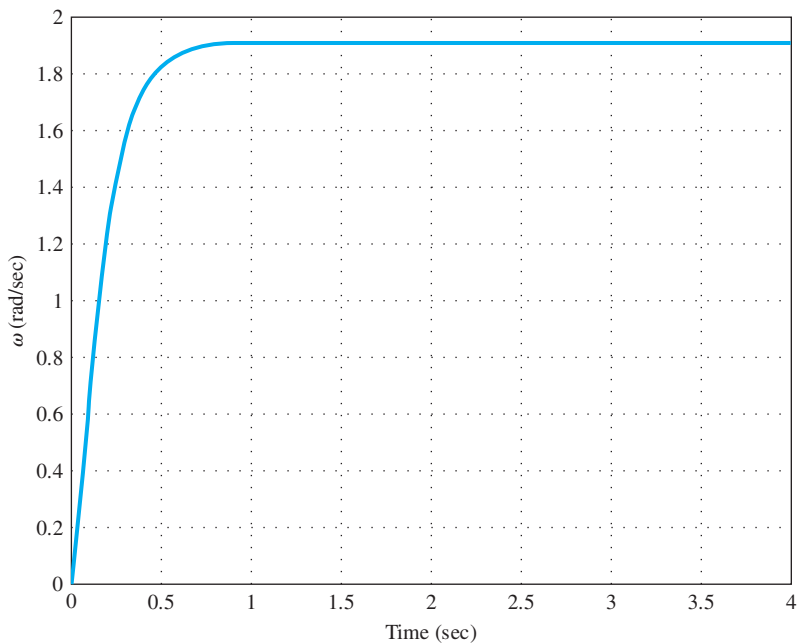
This is as expected, because  $\dot{\theta}_m$  is simply the derivative of  $\theta_m$ ; thus  $\mathcal{L}\{\dot{\theta}_m\} = s\mathcal{L}\{\theta_m\}$ . For a unit-step command in  $v_a$ , we can compute the step response in Matlab as follows (recall Example 2.1 of Chapter 2):

```
s = tf('s'); % define Laplace variable
sysG = 250/(s^2+25.25*s+131.25); % form transfer function
t = 0:0.01:4; % form time vector
y = step(sysG,t); % compute step response;
plot(t,y); % plot step response
```

The system yields a steady-state constant angular velocity as shown in Fig.3.6. Since the system does not have unity DC gain, this is not unity.

**Figure 3.6**

Transient response for  
DC motor



When a dynamic system is represented by a single differential equation of any order, finding the polynomial form of the transfer function from that differential equation is usually easy. Therefore, you will find it best in these cases to specify a system directly in terms of its transfer function.

### EXAMPLE 3.20

#### *Transformations Using Matlab*

Find the transfer function of the system whose differential equation is

$$2\ddot{y} + 5\dot{y} + 6 = 7u + 3\dot{u}.$$

**Solution.** Using the differentiation rules given by Eqs. (3.41) and (3.42), and considering zero initial conditions, we see by inspection that

$$G(s) = \frac{Y(s)}{U(s)} = \frac{3s + 7}{2s^2 + 5s + 6}.$$

The Matlab statements are as follows:

```
s = tf('s'); % define Laplace variable
sysG = (3*s+7)/(2*s^2+5*s+6); % form transfer function
```

If the transfer function poles and zeros and transfer function gain are desired they can be obtained by the following Matlab statements:

```
% compute poles, zeros, and transfer function gain
p= pole(sysG); % compute poles
[z,k]=zero(sysG); % compute zeros and transfer function gain
```

would result in  $z = -2.333$ ,  $p = [-1.25 + j1.199 \quad -1.25 - j1.199]'$ ,  $k = 15$ . This means that the transfer function could also be written as

$$G(s) = \frac{Y(s)}{U(s)} = \frac{1.5(s + 2.333)}{(s + 1.25 + j1.199)(s + 1.25 - j1.199)}.$$

### EXAMPLE 3.21

#### Satellite Transfer Function Using Matlab

- Find the transfer function between the input  $F_c$  and the satellite attitude  $\theta$  in Example 2.3, and;
- Determine the response of the system to a 25-N pulse of 0.1-sec duration, starting at  $t = 5$  sec. Let  $d = 1$  m and  $I = 5000 \text{ kg}\cdot\text{m}^2$ .

#### Solution

- From Example 2.3,  $\frac{d}{I} = \frac{1}{5000} = 0.0002 \left[ \frac{\text{m}}{\text{kg}\cdot\text{m}^2} \right]$  and this means that the transfer function of the system is

$$H(s) = \frac{0.0002}{s^2},$$

which can also be determined by inspection for this particular case. We may display the coefficients of the numerator polynomial as the row vector num and the denominator as the row vector den. The results for this example are

$$\text{numG} = [0 \quad 0 \quad 0.0002] \quad \text{and} \quad \text{denG} = [1 \quad 0 \quad 0].$$

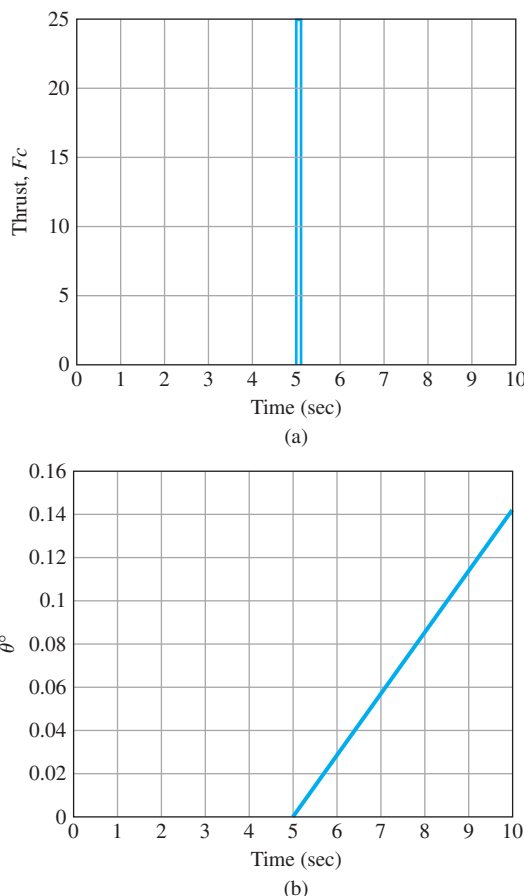
- The following Matlab statements compute the response of the system to a 25-N, 0.1-sec duration thrust pulse input:

```
s=tf('s'); % define Laplace variable
sysG=0.0002/s.^2; % define system by its transfer function
t=0:0.01:10; % set up time vector with dt = 0.01 sec
% pulse of 25N, at 5 sec, for 0.1 sec duration
u1=[zeros(1,500)
    25*ones(1,10)
    zeros(1,491)]; % pulse input
[y1]=lsim(sysG,u1,t); % linear simulation
ff=180/pi; % conversion factor from radians to degrees
y1=ff*y1; % output in degrees
plot(t,u1); % plot input signal
plot(t,y1); % plot output response
```

The system is excited with a short pulse (an impulse input) that has the effect of imparting a nonzero angle  $\theta_0$  at time  $t = 5$  sec on the system. Because the system is undamped, in the absence of any control it drifts with constant angular velocity with a value imparted by the impulse at  $t = 5$  sec. The time response of the input is shown in Fig. 3.7(a), along with the drift in angle  $\theta$  in Fig. 3.7(b).

**Figure 3.7**

Transient response for satellite: (a) thrust input; (b) satellite attitude

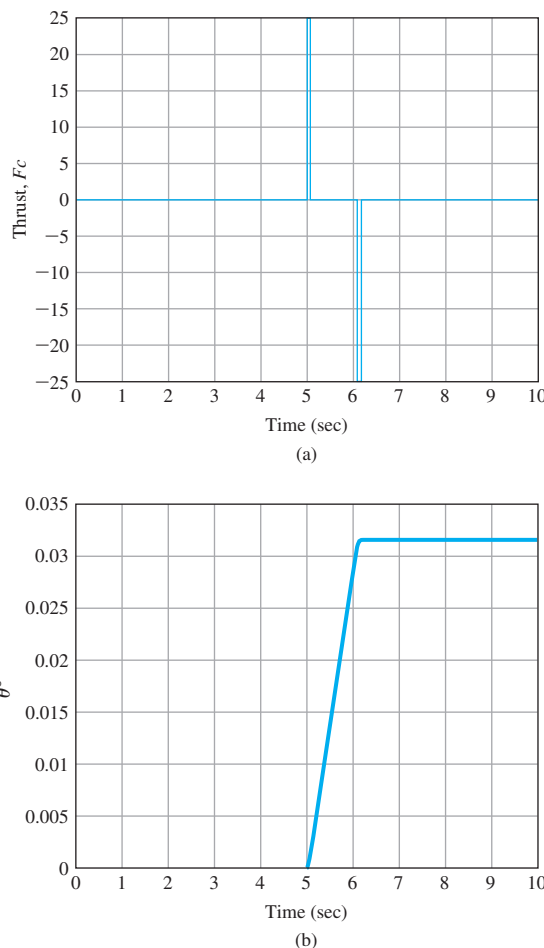


We now excite the system with the same positive-magnitude thrust pulse at time  $t = 5$  sec, but follow that with a negative pulse with the same magnitude and duration at time  $t = 6.1$  sec. (See Fig. 3.8(a) for the input thrust.) Then the attitude response of the system is as shown in Fig. 3.8(b). This is actually how the satellite attitude angle is controlled in practice. The additional relevant Matlab statements are as follows:

```
% double pulse input
u2=[zeros(1,500) 25*ones(1,10) zeros(1,100) -25*ones(1,10)
    zeros(1,381)];
[y2]=lsim(sysG,u2,t); % linear simulation
plot(t,u2); % plot input signal
ff=180/pi; % conversion factor from radians to degrees
y2=ff*y2; % output in degrees
plot(t,y2); % plot output response
```

**Figure 3.8**

Transient response for satellite (double pulse):  
 (a) thrust input;  
 (b) satellite attitude



## 3.2 System Modeling Diagrams

### 3.2.1 The Block Diagram

To obtain the transfer function, we need to find the Laplace transform of the equations of motion and solve the resulting algebraic equations for the relationship between the input and the output. In many control systems, the system equations can be written so their components do not interact except by having the input of one part be the output of another part. In these cases, it is easy to draw a block diagram that represents the mathematical relationships in a manner similar to that used for the component block diagram in Fig. 1.2. The transfer function of each component is placed in a box, and the input–output relationships between components are indicated by lines and arrows. We can then

solve the equations by graphical simplification, which is often easier and more informative than algebraic manipulation, even though the methods are in every way equivalent. Drawings of three elementary block diagrams are shown in Fig. 3.9. It is convenient to think of each block as representing an electronic amplifier with the transfer function printed inside. The interconnections of blocks include summing points, where any number of signals may be added together. These are represented by a circle with the symbol  $\Sigma$  inside. In Fig. 3.9(a), the block with transfer function  $G_1(s)$  is in series with the block with transfer function  $G_2(s)$ , and the overall transfer function is given by the product  $G_2G_1$ . In Fig. 3.9(b) two systems are in parallel with their outputs added, and the overall transfer function is given by the sum  $G_1 + G_2$ . These diagrams derive simply from the equations that describe them.

Figure 3.9(c) shows a more complicated case. Here the two blocks are connected in a feedback arrangement so each feeds into the other. When the feedback  $Y_2(s)$  is *subtracted*, as shown in the figure, we call it **negative feedback**. As you will see, negative feedback is usually required for system stability. For now, we will simply solve the equations then relate them back to the diagram. The equations are

$$U_1(s) = R(s) - Y_2(s),$$

$$Y_2(s) = G_2(s)G_1(s)U_1(s),$$

$$Y_1(s) = G_1(s)U_1(s),$$

and their solution is

$$Y_1(s) = \frac{G_1(s)}{1 + G_1(s)G_2(s)}R(s). \quad (3.58)$$

We can express the solution by the following rule:

The gain of a single-loop negative feedback system is given by the forward gain divided by the sum of 1 plus the loop gain.

### Positive feedback

When the feedback is added instead of subtracted, we call it **positive feedback**. In this case, the gain is given by the forward gain divided by the sum of 1 minus the loop gain.

The three elementary cases given in Fig. 3.9 can be used in combination to solve, by repeated reduction, any transfer function defined by a block diagram. However, the manipulations can be tedious and subject to error when the topology of the diagram is complicated. Fig. 3.10 shows examples of block-diagram algebra that complement those shown in Fig. 3.9. Figures 3.10(a) and (b) show how the interconnections of a block diagram can be manipulated without affecting the mathematical relationships. Figure 3.10(c) shows how the manipulations can be used to convert a general system (on the left) to a system without a component in the feedback path, usually referred to as a **unity feedback system**.

### Unity feedback system

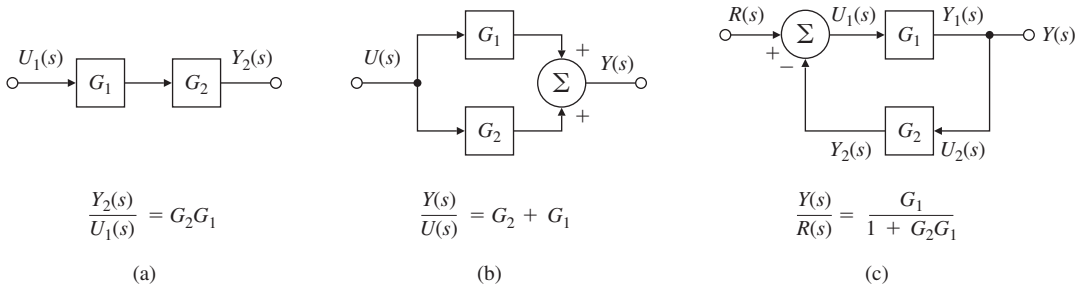
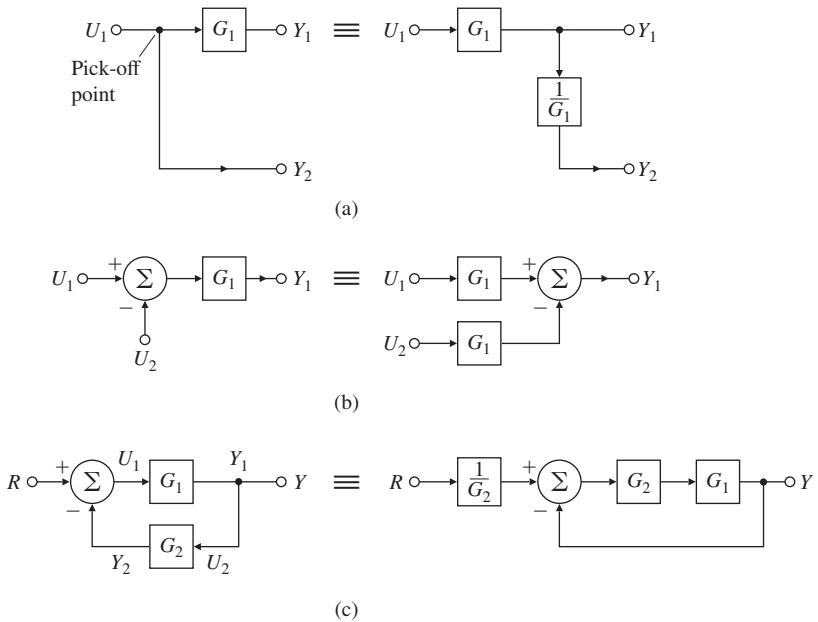


## Figure 3.9

Three examples of elementary block diagrams: (a) series; (b) parallel; (c) feedback

## Figure 3.10

Examples of  
block-diagram algebra:  
(a) moving a pickoff  
point; (b) moving a  
summer; (c) conversion  
to unity feedback



In all cases, the basic principle is to simplify the topology while maintaining exactly the same relationships among the remaining variables of the block diagram. In relation to the algebra of the underlying linear equations, block-diagram reduction is a pictorial way to solve equations by eliminating variables.

### EXAMPLE 3.22

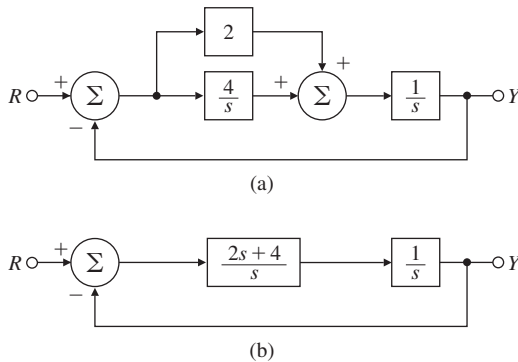
## *Transfer Function from a Simple Block Diagram*

Find the transfer function of the system shown in Fig. 3.11(a).

**Solution.** First we simplify the block diagram by reducing the parallel combination of the controller path. This results in the diagram of Fig. 3.11(b), and we use the feedback rule to obtain the closed-loop transfer function:

**Figure 3.11**

Block diagram of a second-order system



$$T(s) = \frac{Y(s)}{R(s)} = \frac{\frac{2s+4}{s^2}}{1 + \frac{2s+4}{s^2}} = \frac{2s+4}{s^2 + 2s + 4}.$$

### EXAMPLE 3.23

#### *Transfer Function from the Block Diagram*

Find the transfer function of the system shown in Fig. 3.12(a).

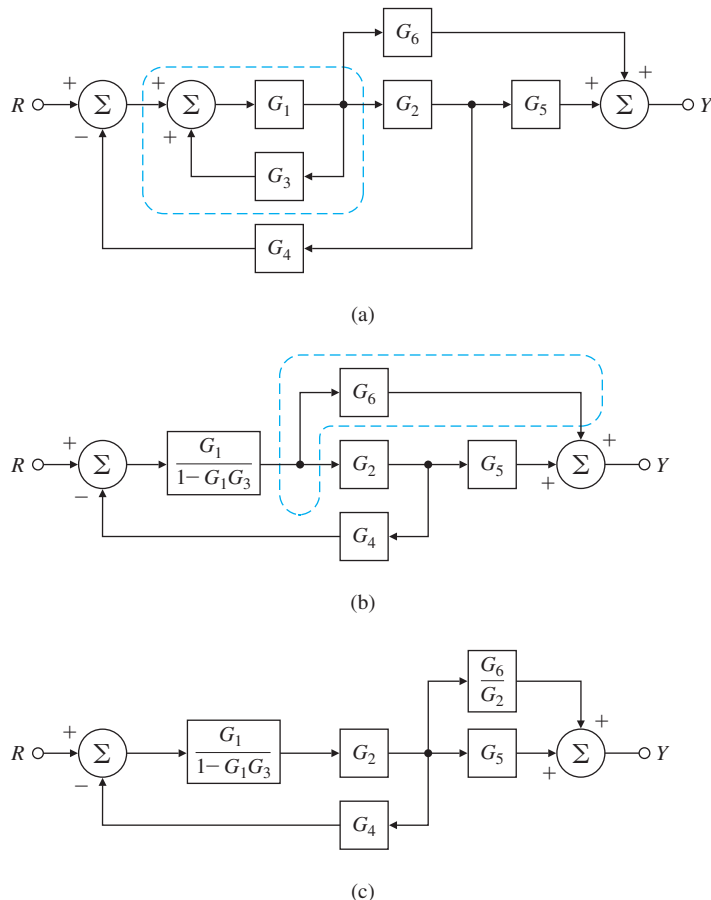
**Solution.** First, we simplify the block diagram. Using the principles of Eq. (3.58), we replace the feedback loop involving  $G_1$  and  $G_3$  by its equivalent transfer function, noting that it is a positive feedback loop. The result is Fig. 3.12(b). The next step is to move the pick off point preceding  $G_2$  to its output [see Fig. 3.12(a)], as shown in Fig. 3.12(c). The negative feedback loop on the left is in series with the subsystem on the right, which is composed of the two parallel blocks  $G_5$  and  $G_6/G_2$ . The overall transfer function can be written using all three rules for reduction given by Fig. 3.9:

$$\begin{aligned} T(s) &= \frac{Y(s)}{R(s)} = \frac{\frac{G_1 G_2}{1 - G_1 G_3}}{1 + \frac{G_1 G_2 G_4}{1 - G_1 G_3}} \left( G_5 + \frac{G_6}{G_2} \right), \\ &= \frac{G_1 G_2 G_5 + G_1 G_6}{1 - G_1 G_3 + G_1 G_2 G_4}. \end{aligned}$$

As we have seen, a system of algebraic equations may be represented by a block diagram that represents individual transfer functions by blocks, and has interconnections that correspond to the system equations. A block diagram is a convenient tool to visualize the system as a collection of interrelated subsystems that emphasize the relationships among the system variables.

**Figure 3.12**

Example for block-diagram simplification



### 3.2.2 Block-Diagram Reduction Using Matlab

If the individual transfer functions are available for components in a control system, it is possible to use Matlab commands to compute the transfer functions of interconnected systems. The three commands `series`, `parallel`, and `feedback` can be used for this purpose. They compute the transfer functions of two component block transfer functions in series, parallel, and feedback configurations, respectively. The next simple example illustrates their use.

#### EXAMPLE 3.24

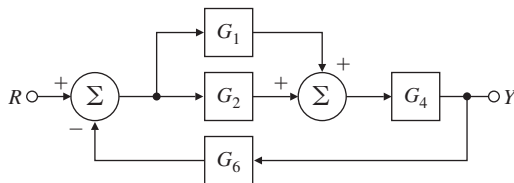
#### *Transfer Function of a Simple System Using Matlab*

Repeat the computation of the transfer function for the block diagram in Fig. 3.11(a) using Matlab.

**Solution.** We label the transfer function of the separate blocks shown in Fig. 3.11(a) as illustrated in Fig. 3.13. Then we combine the two parallel blocks  $G_1$  and  $G_2$  by

**Figure 3.13**

Example for  
block-diagram  
simplification



```

s=tf('s');
% specify a transfer function using
% a rational function in the Laplace
% variable s

sysG1=2;
% define subsystem G1

sysG2=4/s;
% define subsystem G2

sysG3=parallel(sysG1,sysG2);
% parallel combination of G1 and G2

sysG4=1/s;
% define subsystem G4

sysG5=series(sysG3,sysG4);
% series combination of G3 and G4

sysG6=1;
% define subsystem G6

sysCL=feedback(sysG5,sysG6,-1); % feedback combination of G5 and G6
  
```

The Matlab results are sysCL of the form

$$\frac{Y(s)}{R(s)} = \frac{2s + 4}{s^2 + 2s + 4},$$

and this is the same result as the one obtained by block-diagram reduction.

### 3.2.3 Mason's Rule and the Signal Flow Graph

An alternative to block-diagram reduction is the Mason's rule that is a useful technique for determining transfer functions of complicated interconnected systems. See Appendix W3.2.3 online at [www.pearsonglobaleditions.com](http://www.pearsonglobaleditions.com).

## 3.3 Effect of Pole Locations

Once the transfer function has been determined by any of the available methods, we can start to analyze the response of the system it represents. When the system equations are simultaneous ordinary differential equations (ODEs), the transfer function that results will be a ratio of polynomials; that is,

$$H(s) = b(s)/a(s).$$

If we assume  $b$  and  $a$  have no common factors (as is usually the case), then values of  $s$  such that  $a(s) = 0$  will represent points where  $H(s)$  is infinity. As discussed in Section 3.1.5, these  $s$ -values are called poles of  $H(s)$ . Values of  $s$  such that  $b(s) = 0$  are points where  $H(s) = 0$  and the corresponding  $s$ -locations are called zeros. The effect of zeros on the transient response will be discussed in Section 3.5. These poles and

Poles

Zeros

The impulse response is the natural response.

First-order system impulse response

Stability

Time constant  $\tau$

zeros completely describe  $H(s)$  except for a constant multiplier. Because the impulse response is given by the time function corresponding to the transfer function, we call the impulse response the **natural response** of the system. We can use the poles and zeros to compute the corresponding time response and thus identify time histories with pole locations in the  $s$ -plane. For example, the poles identify the classes of signals contained in the impulse response, as may be seen by a partial-fraction expansion of  $H(s)$ . For a first-order pole,

$$H(s) = \frac{1}{s + \sigma}.$$

Table A.2, Appendix A entry 7 indicates that the impulse response will be an exponential function; that is,

$$h(t) = e^{-\sigma t} 1(t).$$

When  $\sigma > 0$ , the pole is located at  $s < 0$ , the exponential expression decays, and we say the impulse response is **stable**. If  $\sigma < 0$ , the pole is to the right of the origin. Because the exponential expression here grows with time, the impulse response is referred to as **unstable** (see Section 3.6). Fig. 3.14(a) shows a typical stable response and defines the **time constant**

$$\tau = 1/\sigma, \quad (3.59)$$

as the time when the response is  $1/e$  times the initial value. Hence, it is a measure of the rate of decay. The straight line is tangent to the exponential curve at  $t = 0$  and terminates at  $t = \tau$ . This characteristic of an exponential expression is useful in sketching a time plot or checking computer results.

Figure 3.14 (b) shows the impulse and step responses for a first-order system computed using Matlab. It also shows the percentage rise in the step response for integral multiples of the time constant,  $\tau$ , which is a metric for the **speed of response** of the system. In particular, we observe that after one time constant ( $\tau$  seconds), the system reaches 63% of its steady-state value, and after about 5 time constants ( $5\tau$  seconds), the system is at steady-state.

## EXAMPLE 3.25

### *Response versus Pole Locations, Real Roots*

Compare the time response with the pole locations for the system with a transfer function between input and output given by

$$H(s) = \frac{2s + 1}{s^2 + 3s + 2}. \quad (3.60)$$

**Solution.** The numerator is

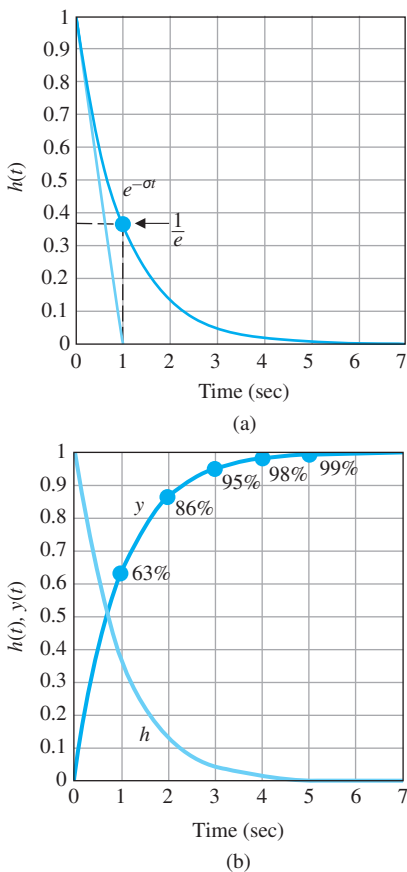
$$b(s) = 2 \left( s + \frac{1}{2} \right),$$

and the denominator is

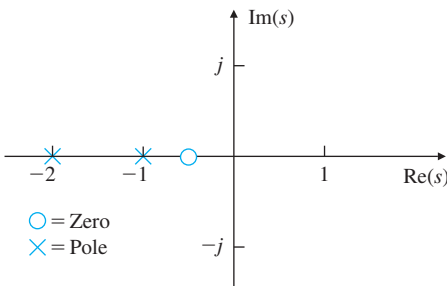
$$a(s) = s^2 + 3s + 2 = (s + 1)(s + 2).$$

**Figure 3.14**

First-order system response: (a) impulse response; (b) impulse response and step response using Matlab

**Figure 3.15**

Sketch of  $s$ -plane showing poles as crosses and zeros as circles



The poles of  $H(s)$  are therefore at  $s = -1$  and  $s = -2$  and the one (finite) zero is at  $s = -\frac{1}{2}$ . A complete description of this transfer function is shown by the plot of the locations of the poles and the zeros in the  $s$ -plane (see Fig. 3.15) using the Matlab `pzmap(num,den)` function with

```
num=[2 1];
den=[1 3 2];
```

A partial-fraction expansion of  $H(s)$  results in

$$H(s) = -\frac{1}{s+1} + \frac{3}{s+2}.$$

From Table A.2, in Appendix A, we can look up the inverse of each term in  $H(s)$ , which will give us the time function  $h(t)$  that would result if the system input were an impulse. In this case,

$$h(t) = \begin{cases} -e^{-t} + 3e^{-2t} & t \geq 0, \\ 0 & t < 0. \end{cases} \quad (3.61)$$

We see that the shape of the component parts of  $h(t)$ , which are  $e^{-t}$  and  $e^{-2t}$ , are determined by the poles at  $s = -1$  and  $-2$ . This is true of more complicated cases as well: In general, the shapes of the components of the natural response are determined by the locations of the poles of the transfer function.

"Fast poles" and "slow poles" refer to relative rate of signal decay

A sketch of these pole locations and corresponding natural responses is given in Fig. 3.16, along with other pole locations including complex ones, which will be discussed shortly.

The role of the numerator in the process of partial-fraction expansion is to influence the size of the coefficient that multiplies each component. Because  $e^{-2t}$  decays faster than  $e^{-t}$ , the signal corresponding to the pole at  $-2$  decays faster than the signal corresponding to the pole at  $-1$ . For brevity, we simply say that the pole at  $-2$  is faster than the pole at  $-1$ . In general, poles farther to the left in the  $s$ -plane are associated with natural signals that decay faster than those associated with poles closer to the imaginary axis. If the poles had been located with positive values of  $s$  (in the right half of the  $s$ -plane), the response would have been a growing exponential function and thus unstable. Figure 3.17 shows that the fast  $3e^{-2t}$  term dominates the early part of the time history, and that the  $-e^{-t}$  term is the primary contributor later on.

**Figure 3.16**

Time functions associated with points in the  $s$ -plane (LHP, left half-plane; RHP, right half-plane)

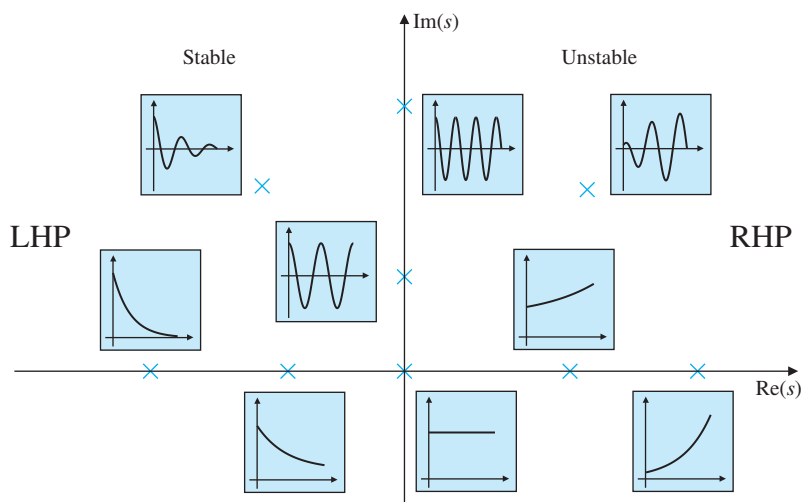
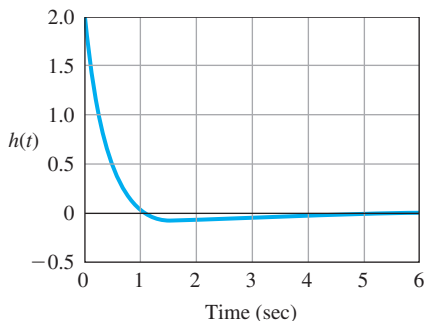


**Figure 3.17**

Impulse response  
of Example 3.25  
[Eq. (3.60)]



Impulse response using  
Matlab

The purpose of this example is to illustrate the relationship between the poles and the character of the response, which can be done exactly only by finding the inverse Laplace transform and examining each term as before. However, if we simply wanted to plot the impulse response for this example, the expedient way would be to use the following Matlab sequence:

```
s=tf('s'); % define Laplace variable
sysH=(2*s+1)/(s^2+3*s+2); % define system from its numerator
                             and denominator
impulse(sysH); % compute impulse response
```

The result is shown in Fig. 3.17.

Complex poles can be defined in terms of their real and imaginary parts, traditionally referred to as

$$s = -\sigma \pm j\omega_d.$$

This means a pole has a negative real part if  $\sigma$  is positive. Since complex poles always come in complex conjugate pairs, the denominator corresponding to a complex pair will be

$$a(s) = (s + \sigma - j\omega_d)(s + \sigma + j\omega_d) = (s + \sigma)^2 + \omega_d^2. \quad (3.62)$$

When finding the transfer function from second-order differential equations, we typically write the result in the polynomial form

$$H(s) = \frac{\omega_n^2}{s^2 + 2\xi\omega_n s + \omega_n^2}. \quad (3.63)$$

By multiplying out the form given by Eq. (3.62) and comparing it with the coefficients of the denominator of  $H(s)$  in Eq. (3.63), we find the correspondence between the parameters to be

$$\sigma = \xi\omega_n \quad \text{and} \quad \omega_d = \omega_n\sqrt{1 - \xi^2}, \quad (3.64)$$

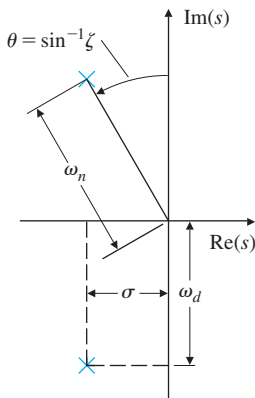
where the parameter  $\xi$  is the **damping ratio**<sup>10</sup> and  $\omega_n$  is the **undamped natural frequency**. The poles of this transfer function are located at

Damping ratio; damped  
and undamped natural  
frequency

<sup>10</sup>In communications and filter engineering, the standard second-order transfer function is written as  $H = 1/[1 + Q(s/\omega_n + \omega_n/s)]$ . Here,  $\omega_n$  is called the **band center** and  $Q$  is the **quality factor**. Comparison with Eq. (3.63) shows that  $Q = 1/2\xi$ .

**Figure 3.18**

s-plane plot for a pair of complex poles



a radius  $\omega_n$  in the s-plane and at an angle  $\theta = \sin^{-1} \zeta$ , as shown in Fig. 3.18. Therefore, the damping ratio reflects the level of damping as a fraction of the critical damping value where the poles become real. In rectangular coordinates, the poles are at  $s = -\sigma \pm j\omega_d$ . When  $\zeta = 0$ , we have no damping,  $\theta = 0$ , and the damped natural frequency  $\omega_d = \omega_n$ , the undamped natural frequency.

For purposes of finding the time response from Table A.2 in Appendix A, corresponding to a complex transfer function, it is easiest to manipulate the  $H(s)$  so the complex poles fit the form of Eq. (3.62), because then the time response can be found directly from the table. Equation (3.63) can be rewritten as

$$H(s) = \frac{\omega_n^2}{(s + \zeta\omega_n)^2 + \omega_n^2(1 - \zeta^2)}. \quad (3.65)$$

Therefore, from entry number 20 in Table A.2 and the definitions in Eq. (3.64), we see that the impulse response is

$$h(t) = \frac{\omega_n}{\sqrt{1 - \zeta^2}} e^{-\sigma t} (\sin \omega_d t) 1(t). \quad (3.66)$$

Fig. 3.19(a) plots  $h(t)$  for several values of  $\zeta$  such that time has been normalized to the undamped natural frequency  $\omega_n$ . Note the actual frequency  $\omega_d$  decreases slightly as the damping ratio increases. Note also for very low damping the response is oscillatory, while for large damping ( $\zeta$  near 1) the response shows no oscillation. A few of these responses are sketched in Fig. 3.16 to show qualitatively how changing pole locations in the s-plane affect impulse responses. You will find it useful as a control designer to commit the image of Fig. 3.16 to memory so you can understand instantly how changes in pole locations influence the time response.

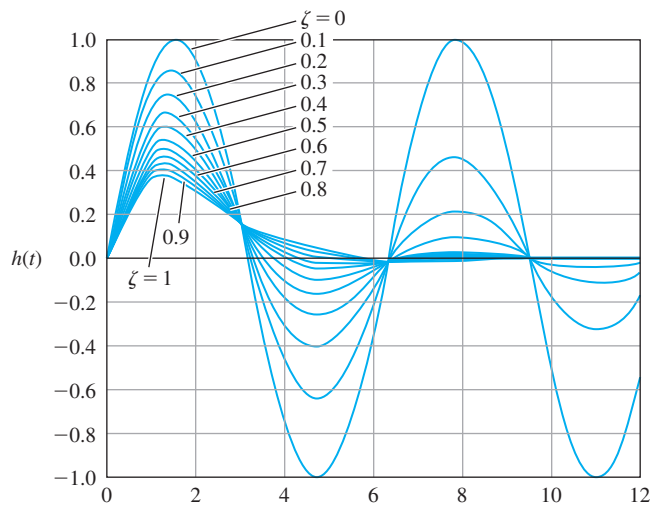
Three pole locations are shown in Fig. 3.20 for comparison with the corresponding impulse responses in Fig. 3.19(a). The negative real part of the pole,  $\sigma$ , determines the decay rate of an exponential envelope

### Standard second-order system impulse response

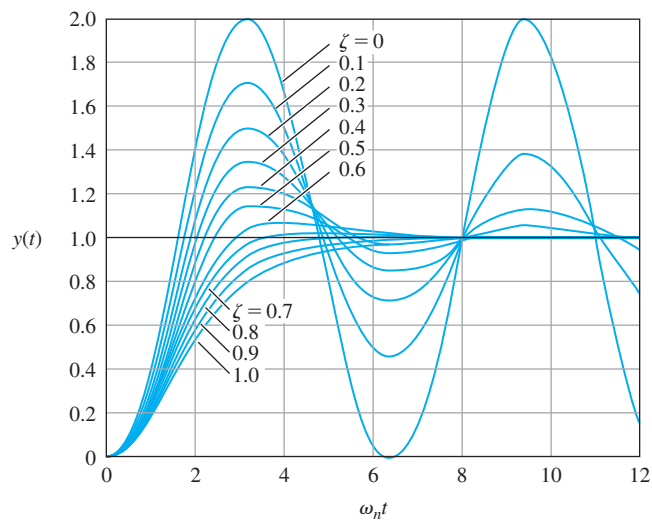
Stability depends on whether natural response grows or decays

**Figure 3.19**

Responses of second-order systems versus  $\zeta$  : (a) impulse responses; (b) step responses



(a)



(b)

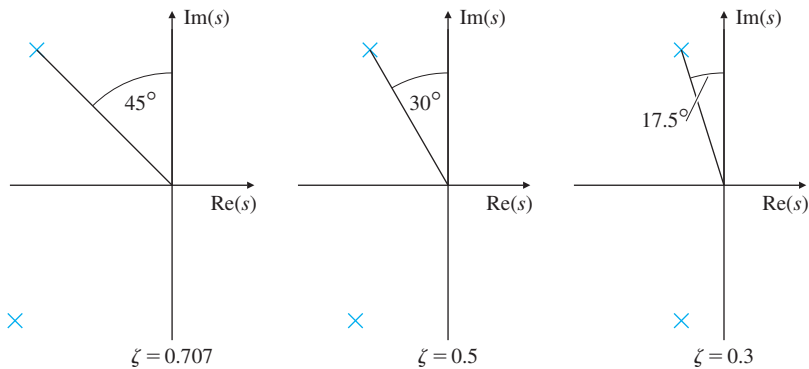
that multiplies the sinusoid, as shown in Fig. 3.21. Note if  $\sigma < 0$  (and the pole is in the RHP), then the natural response will grow with time, so, as defined earlier, the system is said to be unstable. If  $\sigma = 0$ , the natural response neither grows nor decays, so stability is open to debate. If  $\sigma > 0$ , the natural response decays, so the system is stable.

#### Step response

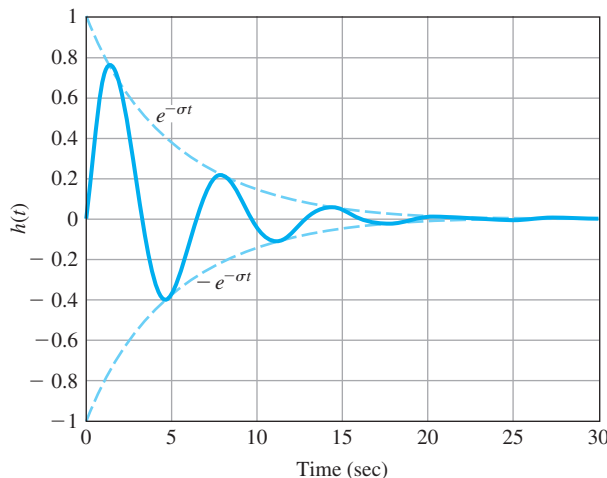
It is also interesting to examine the step response of  $H(s)$ —that is, the response of the system  $H(s)$  to a unit-step input  $u = 1(t)$ , where  $U(s) = 1/s$ . The step-response transform is given by  $Y(s) = H(s)U(s)$ , which is found in Appendix A, Table A.2, entry 21. Figure 3.19(b),

**Figure 3.20**

Pole locations corresponding to three values of  $\zeta$

**Figure 3.21**

Second-order system response with an exponential envelope bound



which plots  $y(t)$  for several values of  $\zeta$ , shows the basic transient response characteristics from the impulse response carry over quite well to the step response; the difference between the two responses is that the step response's final value is the commanded unit step.

### EXAMPLE 3.26

#### Oscillatory Time Response

Discuss the correlation between the poles of

$$H(s) = \frac{2s + 1}{s^2 + 2s + 5}, \quad (3.67)$$

and the impulse response of the system, then find the exact impulse response.

**Solution.** From the form of  $H(s)$  given by Eq. (3.63), we see that

$$\omega_n^2 = 5 \Rightarrow \omega_n = \sqrt{5} = 2.24 \text{ rad/sec}$$

and

$$2\xi\omega_n = 2 \Rightarrow \xi = \frac{1}{\sqrt{5}} = 0.447.$$

This indicates that we should expect a frequency of around 2 rad/sec with very little oscillatory motion. In order to obtain the exact response, we manipulate  $H(s)$  until the denominator is in the form of Eq. (3.62):

$$H(s) = \frac{2s + 1}{s^2 + 2s + 5} = \frac{2s + 1}{(s + 1)^2 + 2^2}.$$

From this equation, we see the poles of the transfer function are complex, with real part  $-1$  and imaginary parts  $\pm 2j$ . Table A.2 in Appendix A has two entries, numbers 19 and 20, that match the denominator. The right side of the preceding equation needs to be broken into two parts so they match the numerators of the entries in the table:

$$H(s) = \frac{2s + 1}{(s + 1)^2 + 2^2} = 2 \frac{s + 1}{(s + 1)^2 + 2^2} - \frac{1}{2} \frac{2}{(s + 1)^2 + 2^2}.$$

Thus, the impulse response is

$$h(t) = \left( 2e^{-t} \cos 2t - \frac{1}{2}e^{-t} \sin 2t \right) 1(t).$$

Fig. 3.22 is a plot of the response and shows how the envelope attenuates the sinusoid, the domination of the  $2 \cos 2t$  term, and the small phase shift caused by the  $-\frac{1}{2} \sin 2t$  term.

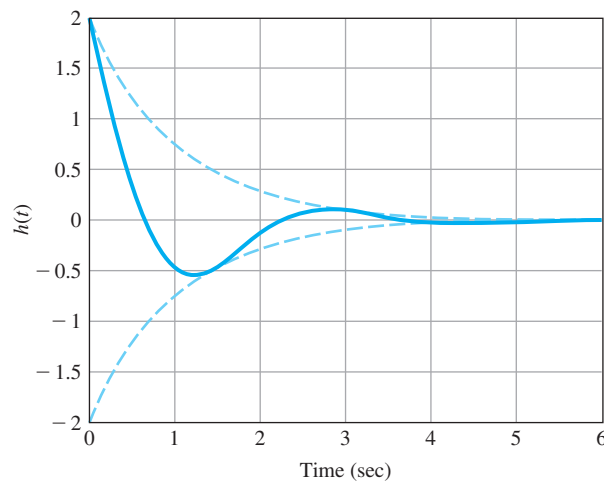
As in the previous example, the expedient way of determining the impulse response would be to use the following Matlab sequence:

```
s=tf('s'); % define Laplace variable
sysH=(2*s+1)/(s^2+2*s+5); % define system by its numerator
                             and denominator
t=0:0.1:6; % form time vector
y=impulse(sysH,t); % compute impulse response
plot(t,y); % plot impulse response
```

as shown in Fig. 3.22.

[Impulse response by Matlab](#)

**Figure 3.22**  
System response for Example 3.26



## 3.4 Time-Domain Specifications

Definitions of rise time, settling time, overshoot, and peak time

Performance specifications for a control system design often involve certain requirements associated with the time response of the system. The requirements for a step response are expressed in terms of the standard quantities illustrated in Fig. 3.23:

1. The **rise time**  $t_r$  is the time it takes the system to reach the vicinity of its new set point.
2. The **settling time**  $t_s$  is the time it takes the system transients to decay.
3. The **overshoot**  $M_p$  is the maximum amount the system overshoots its final value divided by its final value (and is often expressed as a percentage).
4. The **peak time**  $t_p$  is the time it takes the system to reach the maximum overshoot point.

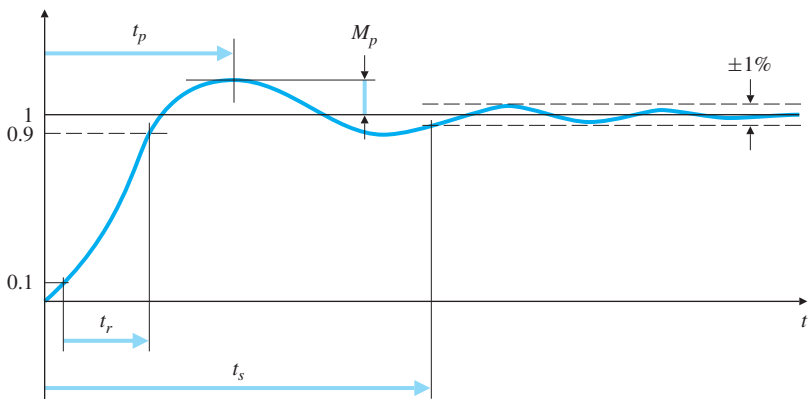
### 3.4.1 Rise Time

For a second-order system, the time responses shown in Fig. 3.19(b) yield information about the specifications that is too complex to be remembered unless converted to a simpler form. By examining these curves in light of the definitions given in Fig. 3.23, we can relate the curves to the pole-location parameters  $\zeta$  and  $\omega_n$ . For example, all the curves rise in roughly the same time. If we consider the curve for  $\zeta = 0.5$  to be an average, the rise time<sup>11</sup> from  $y = 0.1$  to  $y = 0.9$  is approximately  $\omega_n t_r = 1.8$ . Thus, we can say

$$t_r \cong \frac{1.8}{\omega_n}. \quad (3.68)$$

Although this relationship could be embellished by including the effect of the damping ratio, it is important to keep in mind how Eq. (3.68) is typically used. It is accurate only for a second-order system with no zeros; for all other systems, it is a rough approximation to the

**Figure 3.23**  
Definition of rise time  $t_r$ , settling time  $t_s$ , and overshoot  $M_p$



<sup>11</sup>Rise time  $t_r$ .

relationship between  $t_r$  and  $\omega_n$ . Most systems being analyzed for control systems design are more complicated than the pure second-order system, so designers use Eq. (3.68) with the knowledge that it is only a rough approximation.

### 3.4.2 Overshoot and Peak Time

For the overshoot  $M_p$ , we can be more analytical. This value occurs when the derivative is zero, which can be found from calculus. The time history of the curves in Fig. 3.19(b), found from the inverse Laplace transform of  $H(s)/s$ , is

$$y(t) = 1 - e^{-\sigma t} \left( \cos \omega_d t + \frac{\sigma}{\omega_d} \sin \omega_d t \right), \quad (3.69)$$

where  $\omega_d = \omega_n \sqrt{1 - \zeta^2}$  and  $\sigma = \zeta \omega_n$ . We may rewrite the preceding equation using the trigonometric identity

$$A \sin(\alpha) + B \cos(\alpha) = C \cos(\alpha - \beta),$$

or

$$C = \sqrt{A^2 + B^2} = \frac{1}{\sqrt{1 - \zeta^2}},$$

$$\beta = \tan^{-1} \left( \frac{A}{B} \right) = \tan^{-1} \left( \frac{\zeta}{\sqrt{1 - \zeta^2}} \right) = \sin^{-1}(\zeta),$$

with  $A = \frac{\sigma}{\omega_d}$ ,  $B = 1$ , and  $\alpha = \omega_d t$ , in a more compact form as

$$y(t) = 1 - \frac{e^{-\sigma t}}{\sqrt{1 - \zeta^2}} \cos(\omega_d t - \beta). \quad (3.70)$$

**Standard second-order system step response**

When  $y(t)$  reaches its maximum value, its derivative will be zero:

$$\begin{aligned} \dot{y}(t) &= \sigma e^{-\sigma t} \left( \cos \omega_d t + \frac{\sigma}{\omega_d} \sin \omega_d t \right) - e^{-\sigma t} (-\omega_d \sin \omega_d t + \sigma \cos \omega_d t) = 0, \\ &= e^{-\sigma t} \left( \frac{\sigma^2}{\omega_d} + \omega_d \right) \sin \omega_d t = 0. \end{aligned}$$

This occurs when  $\sin \omega_d t = 0$ , so

$$\omega_d t_p = \pi$$

and thus,

$$t_p = \frac{\pi}{\omega_d}. \quad (3.71)$$

**Peak time  $t_p$**

Substituting Eq. (3.71) into the expression for  $y(t)$ , we compute

$$\begin{aligned} y(t_p) &\stackrel{\Delta}{=} 1 + M_p = 1 - e^{-\sigma \pi / \omega_d} \left( \cos \pi + \frac{\sigma}{\omega_d} \sin \pi \right), \\ &= 1 + e^{-\sigma \pi / \omega_d}. \end{aligned}$$

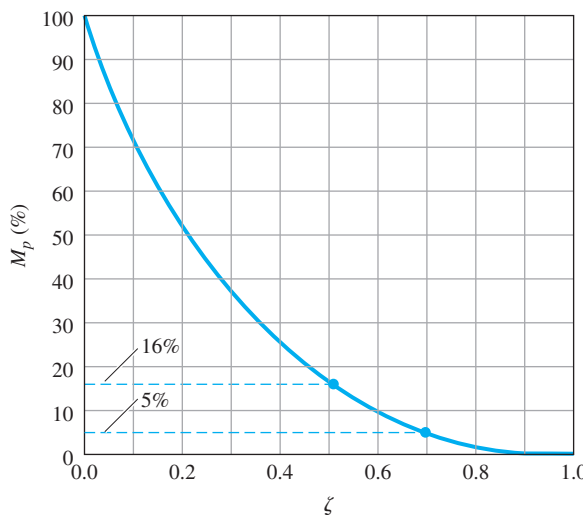
**Overshoot  $M_p$**

Thus, we have the formula

$$M_p = e^{-\pi \zeta / \sqrt{1 - \zeta^2}}, \quad 0 \leq \zeta < 1, \quad (3.72)$$

**Figure 3.24**

Overshoot versus damping ratio for the second-order system



which is plotted in Fig. 3.24. Two frequently used values from this curve are  $M_p = 0.16$  for  $\zeta = 0.5$  and  $M_p = 0.05$  for  $\zeta = 0.7$ , that is, 16% and 5% overshoot, respectively.

### 3.4.3 Settling Time

The final parameter of interest from the transient response is the settling time  $t_s$ . This is the time required for the transient to decay to a small value so that  $y(t)$  is almost in the steady state. Various measures of smallness are possible. For illustration, we will use 1% as a reasonable measure; in other cases, 2% or 5% are used. As an analytic computation, we notice that the deviation of  $y$  from 1 is the product of the decaying exponential  $e^{-\sigma t}$  and the circular functions sine and cosine. The duration of this error is essentially decided by the transient exponential, so we can define the settling time as that value of  $t_s$  when the decaying exponential reaches 1%:

$$e^{-\zeta \omega_n t_s} = 0.01.$$

Therefore,

$$\zeta \omega_n t_s = 4.6,$$

or

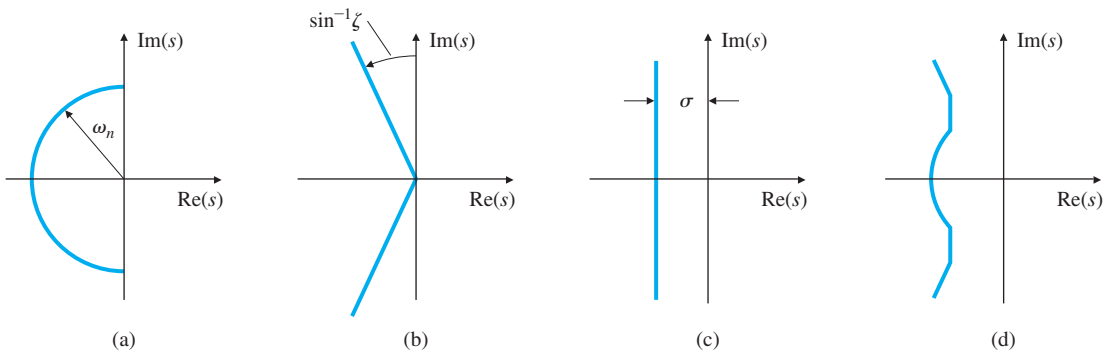
$$t_s = \frac{4.6}{\zeta \omega_n} = \frac{4.6}{\sigma}, \quad (3.73)$$

where  $\sigma$  is the negative real part of the pole, as may be seen in Fig. 3.18.

Equations (3.68), (3.72), and (3.73) characterize the transient response of a system having no finite zeros and two complex poles and with undamped natural frequency  $\omega_n$ , damping ratio  $\zeta$ , and negative real part  $\sigma$ . In analysis and design, they are used to estimate rise time, overshoot, and settling time, respectively, for just about any system. In design synthesis, we wish to specify  $t_r$ ,  $M_p$ , and  $t_s$  and to ask where the

Settling time  $t_s$

Design synthesis

**Figure 3.25**

Graphs of regions in the  $s$ -plane delineated by certain transient requirements: (a) rise time; (b) overshoot; (c) settling time; (d) composite of all three requirements

poles need to be so that the actual responses are less than or equal to these specifications. For specified values of  $t_r$ ,  $M_p$ , and  $t_s$ , the synthesis form of the equation is then

$$\omega_n \geq \frac{1.8}{t_r}, \quad (3.74)$$

$$\zeta \geq \zeta(M_p) \quad (\text{from Fig. 3.24}), \quad (3.75)$$

$$\sigma \geq \frac{4.6}{t_s}. \quad (3.76)$$

These equations, which can be graphed in the  $s$ -plane as shown in Fig. 3.25(a–c), will be used in later chapters to guide the selection of pole and zero locations to meet control system specifications for dynamic response.

It is important to keep in mind that Eqs. (3.74)–(3.76) are qualitative guides and not precise design formulas. They are meant to provide only a starting point for the design iteration. After the control design is complete, the time response should always be checked by an exact calculation, usually by numerical simulation, to verify whether the time specifications have actually been met. If not, another iteration of the design is required.

#### First-order system step response

For a first-order system,

$$H(s) = \frac{\sigma}{s + \sigma},$$

and the transform of the step response is

$$Y(s) = \frac{\sigma}{s(s + \sigma)}.$$

We see from entry 11 in Table A.2 (see Appendix A) that  $Y(s)$  corresponds to

$$y(t) = (1 - e^{-\sigma t})1(t). \quad (3.77)$$

Comparison with the development for Eq. (3.73) shows the value of  $t_s$  for a first-order system is the same:

$$t_s = \frac{4.6}{\sigma}.$$

No overshoot is possible, so  $M_p = 0$ . The rise time from  $y = 0.1$  to  $y = 0.9$  can be seen from Fig. 3.14 to

$$t_r = \frac{\ln 0.9 - \ln 0.1}{\sigma} = \frac{2.2}{\sigma}.$$

**Time constant  $\tau$**

However, it is more typical to describe a first-order system in terms of its time constant, which was defined in Fig. 3.14 to be  $\tau = 1/\sigma$ .

### EXAMPLE 3.27

#### *Transformation of the Specifications to the s-Plane*

Find the allowable regions in the  $s$ -plane for the poles of the transfer function of the system if the system response requirement is  $t_r \leq 0.6$  sec,  $M_p \leq 10\%$ , and  $t_s \leq 3$  sec.

**Solution.** Without knowing whether or not the system is second order with no zeros, it is impossible to find the allowable region accurately. Regardless of the system, we can obtain a first approximation using the relationships for a second-order system. Equation (3.74) indicates that

$$\omega_n \geq \frac{1.8}{t_r} = 3.0 \text{ rad/sec},$$

Eq. (3.75) and Fig. 3.24 indicate that

$$\zeta \geq 0.6,$$

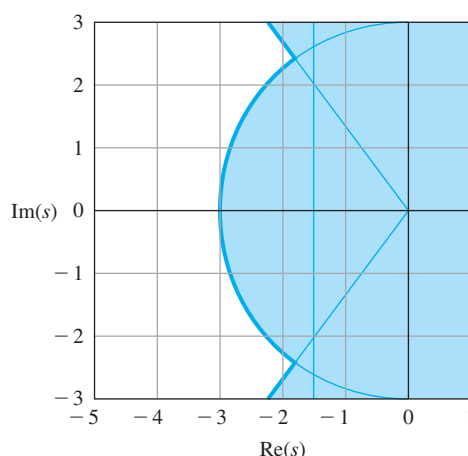
and Eq. (3.76) indicates that

$$\sigma \geq \frac{4.6}{3} = 1.5 \text{ sec.}$$

The allowable region is anywhere to the left of the solid line in Fig. 3.26. Note any pole meeting the  $\zeta$  and  $\omega_n$  restrictions will automatically meet the  $\sigma$  restriction.

**Figure 3.26**

Time domain specifications region in  $s$ -plane for Example 3.27



### 3.5 Effects of Zeros and Additional Poles

Relationships such as those shown in Fig. 3.25 are correct for the simple second-order system; for more complicated systems, they can be used only as guidelines. If a certain design has an inadequate rise time (is too slow), we must raise the natural frequency; if the transient has too much overshoot, then the damping needs to be increased; if the transient persists too long, the poles need to be moved to the left in the  $s$ -plane.

Thus far only the poles of  $H(s)$  have entered into the discussion. There may also be zeros of  $H(s)$ .<sup>12</sup> At the level of transient analysis, the zeros exert their influence by modifying the coefficients of the exponential terms whose shape is decided by the poles, as seen in Example 3.25. To illustrate this further, consider the following two transfer functions, which have the same poles but different zeros:

$$\begin{aligned} H_1(s) &= \frac{2}{(s+1)(s+2)} \\ &= \frac{2}{s+1} - \frac{2}{s+2}, \end{aligned} \quad (3.78)$$

$$\begin{aligned} H_2(s) &= \frac{2(s+1.1)}{1.1(s+1)(s+2)} \\ &= \frac{2}{1.1} \left( \frac{0.1}{s+1} + \frac{0.9}{s+2} \right) \\ &= \frac{0.18}{s+1} + \frac{1.64}{s+2}. \end{aligned} \quad (3.79)$$

They are normalized to have the same DC gain (that is, gain at  $s = 0$ ). Notice the coefficient of the  $(s+1)$  term has been modified from 2 in  $H_1(s)$  to 0.18 in  $H_2(s)$ . This dramatic reduction is brought about by the zero at  $s = -1.1$  in  $H_2(s)$ , which almost cancels the pole at  $s = -1$ . If we put the zero exactly at  $s = -1$ , this term will vanish completely. In general, a zero near a pole reduces the amount of that term in the total response. From the equation for the coefficients in a partial-fraction expansion, Eq. (3.51),

$$C_1 = (s - p_1)F(s)|_{s=p_1},$$

we can see that if  $F(s)$  has a zero near the pole at  $s = p_1$ , the value of  $F(s)$  will be small because the value of  $s$  is near the zero. Therefore, the coefficient  $C_1$ , which reflects how much of that term appears in the response, will be small.

---

<sup>12</sup>We assume  $b(s)$  and  $a(s)$  have no common factors. If this is not so, it is possible for  $b(s)$  and  $a(s)$  to be zero at the same location and for  $H(s)$  to not equal zero there. The implications of this case will be discussed in Chapter 7, when we have a state-space description.

In order to take into account how zeros affect the transient response when designing a control system, we consider transfer functions with two complex poles and one zero. To expedite the plotting for a wide range of cases, we write the transform in a form with normalized time and zero locations:

$$H(s) = \frac{(s/\alpha\zeta\omega_n) + 1}{(s/\omega_n)^2 + 2\zeta(s/\omega_n) + 1}. \quad (3.80)$$

The zero is located at  $s = -\alpha\zeta\omega_n = -\alpha\sigma$ . If  $\alpha$  is large, the zero will be far removed from the poles, and the zero will have little effect on the response. If  $\alpha \approx 1$ , the value of the zero will be close to that of the real part of the poles, and can be expected to have a substantial influence on the response. The step-response curves for  $\zeta = 0.5$  and  $\zeta = 0.707$  for several values of  $\alpha$  are plotted in Figs. 3.27 and 3.28. We see that the major effect of the zero is to increase the overshoot  $M_p$  and reduce rise time,  $t_r$ , whereas it has very little influence on the settling time. A plot of  $M_p$  versus  $\alpha$  is given in Fig. 3.29. The plot shows the zero has very little effect on  $M_p$  if  $\alpha > 3$ , but as  $\alpha$  decreases below 3, it has an increasing effect, especially when  $\alpha = 1$  or less.

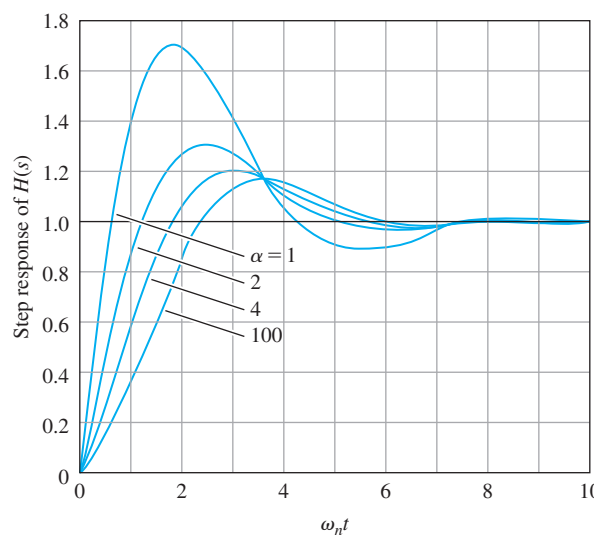
Figure 3.27 can be explained in terms of Laplace-transform analysis. First, we replace  $s/\omega_n$  with  $s$ :

$$H(s) = \frac{s/\alpha\zeta + 1}{s^2 + 2\zeta s + 1}.$$

This has the effect of normalizing frequency in the transfer function and normalizing time in the corresponding step responses; thus  $\tau = \omega_n t$ . We then rewrite the transfer function as the sum of two terms:

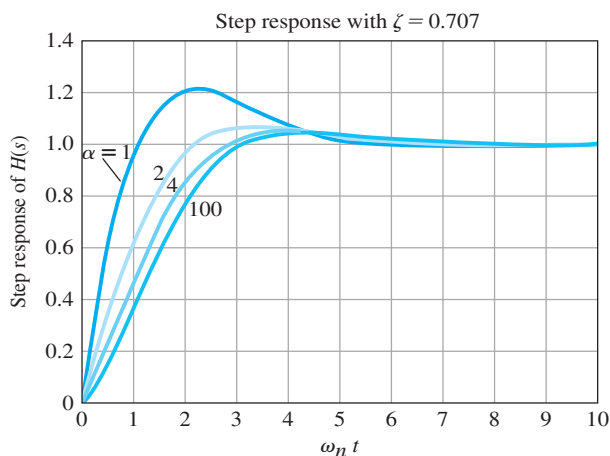
$$H(s) = \frac{1}{s^2 + 2\zeta s + 1} + \frac{1}{\alpha\zeta} \frac{s}{s^2 + 2\zeta s + 1}. \quad (3.81)$$

**Figure 3.27**  
Plots of the step response of a second-order system with a zero ( $\zeta = 0.5$ )

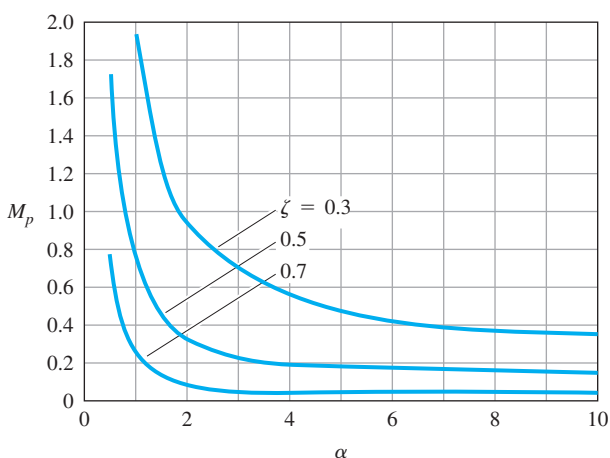


**Figure 3.28**

Plots of the step response of a second-order system with a zero ( $\zeta = 0.707$ )

**Figure 3.29**

Plot of overshoot  $M_p$  as a function of normalized zero location  $\alpha$ . At  $\alpha = 1$ , the real part of the zero equals the real part of the poles



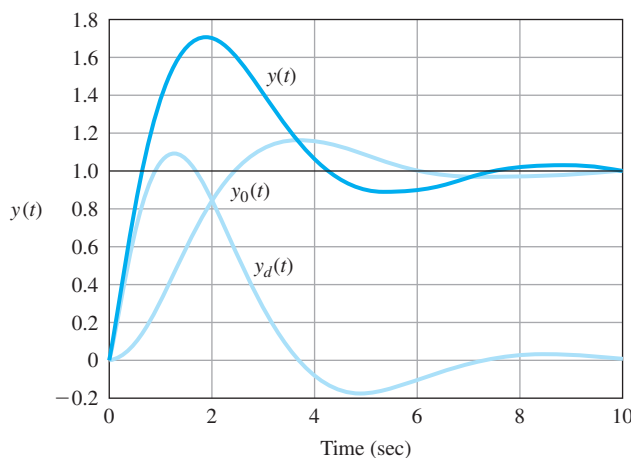
The first term, which we shall call  $H_0(s)$ , is the original term (having no finite zero), and the second term  $H_d(s)$ , which is introduced by the zero, is a product of a constant  $(1/\alpha\zeta)$  times  $s$  times the original term. The Laplace transform of  $df/dt$  is  $sF(s)$ , so  $H_d(s)$  corresponds to a product of a constant times the derivative of the original term, that is,

$$y(t) = y_0(t) + y_d(t) = y_0(t) + \frac{1}{\alpha\zeta} y_0'(t).$$

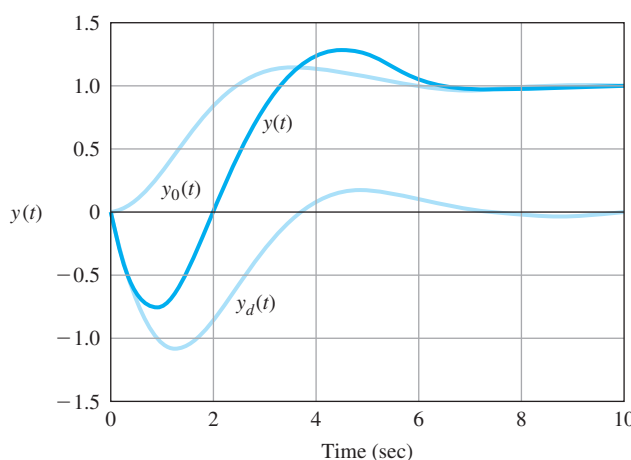
The step responses of  $H_0(s)$  denoted by  $y_0(t)$  and  $H_d(s)$  denoted by  $y_d(t)$  are plotted in Fig. 3.30. Looking at these curves, we can see why the zero increased the overshoot: The derivative has a large hump in the early part of the curve, and adding this to the  $H_0(s)$  response lifts up the total response of  $H(s)$  to produce the overshoot. This analysis is also very informative for the case when  $\alpha < 0$  and the zero is in the RHP where  $s > 0$ . (This is typically called an **RHP zero** and is sometimes referred

**Figure 3.30**

Second-order step responses  $y(t)$  of the transfer functions  $H(s)$ ,  $H_0(s)$ , and  $H_d(s)$

**Figure 3.31**

Step responses  $y(t)$  of a second-order system with a zero in the RHP: a nonminimum-phase system



to as a **nonminimum-phase zero**, a topic to be discussed in more detail in Section 6.1.1.) In this case, the derivative term is subtracted rather than added. A typical case is sketched in Fig. 3.31.

### EXAMPLE 3.28

#### *Effect of the Proximity of the Zero to the Pole Locations on the Transient Response*

Consider the second-order system with a finite zero and unity DC gain,

$$H(s) = \frac{24}{z} \frac{(s+z)}{(s+4)(s+6)}.$$

Determine the effect of the zero location ( $s = -z$ ) on the unit-step response when  $z = \{1, 2, 3, 4, 5, 6\}$ .

**Solution.** The step response is the inverse Laplace transform of

$$H_1(s) = H(s) \frac{1}{s} = \frac{24}{z} \frac{(s+z)}{s(s+4)(s+6)} = \frac{24}{z} \frac{s}{s(s+4)(s+6)} + \frac{24}{s(s+4)(s+6)}$$

and is the sum of the two parts,

$$y(t) = y_1(t) + y_2(t),$$

where

$$y_1(t) = \frac{12}{z} e^{-4t} - \frac{12}{z} e^{-6t},$$

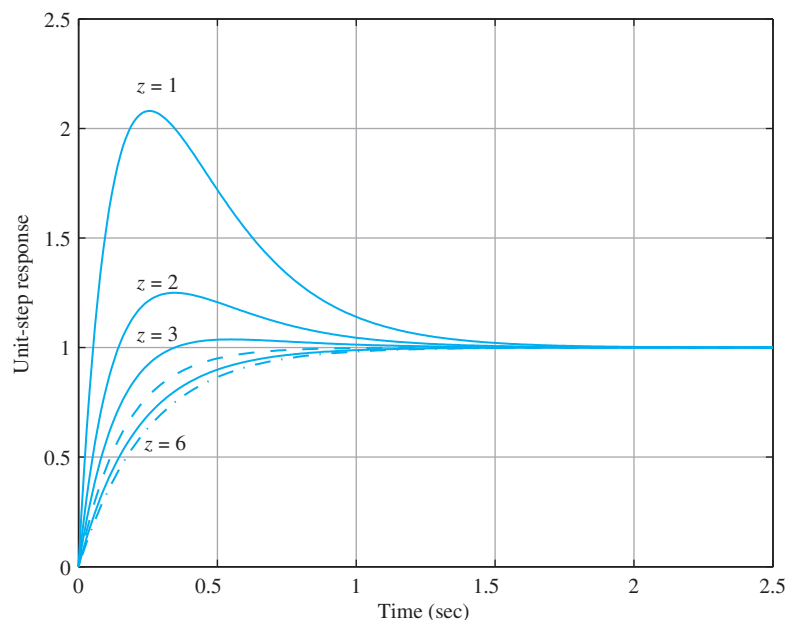
$$y_2(t) = z \int_0^t y_1(\tau) d\tau = -3e^{-4t} + 2e^{-6t} + 1,$$

and

$$y(t) = 1 + \left( \frac{12}{z} - 3 \right) e^{-4t} + \left( 2 - \frac{12}{z} \right) e^{-6t}.$$

If  $z = 4$  or  $z = 6$ , one of the modes of the system is absent from the output, and the response is first order due to the pole-zero cancellations. The step responses of the system is shown in Fig. 3.32 ( $z = 4$ , dashed,  $z = 6$  dot dashed). The effect of the zero is most pronounced in terms of the additional overshoot for  $z = 1$  (zero location closest to the origin). The system also has overshoot for  $z = 2, 3$ . For  $z = 4$  or  $z = 6$  the responses are first order as expected. It is interesting that for  $z = 5$ , where the zero is located between the two poles, there is no overshoot.

**Figure 3.32**  
Effect of zero on  
transient response



This is generally the case because the zero effectively compensates for the effect of the second pole, rendering the system as first order at any given frequency.

### EXAMPLE 3.29

#### *Effect of the Proximity of the Complex Zeros to the Lightly Damped Poles*

Consider the third-order feedback system with a pair of lightly damped poles and a pair of complex zeros with the transfer function,

$$H(s) = \frac{(s + \alpha)^2 + \beta^2}{(s + 1)[(s + 0.1)^2 + 1]}.$$

Determine the effect of the complex zero locations ( $s = -\alpha \pm j\beta$ ) on the unit-step response of the system for the three different zero locations  $(\alpha, \beta) = (0.1, 1.0)$ ,  $(\alpha, \beta) = (0.25, 1.0)$ , and  $(\alpha, \beta) = (0.5, 1.0)$ , as shown in Fig. 3.33.

**Solution.** We plot the three unit-step responses using Matlab as shown in Fig. 3.34. The effect of the lightly damped modes are clearly seen as oscillations in the step responses for the cases where  $(\alpha, \beta) = (0.25, 1.0)$  or  $(\alpha, \beta) = (0.5, 1.0)$ , that is, when the complex zeros are not close to the locations of the lightly damped poles as shown in Fig. 3.33. On the other hand, if the complex zeros cancel the lightly damped poles exactly as is the case for  $(\alpha, \beta) = (0.1, 1.0)$ , the oscillations are completely eliminated in the step response. In practice, the locations of the lightly damped poles are not known precisely, and exact cancellation is

**Figure 3.33**  
Locations of complex  
zeros

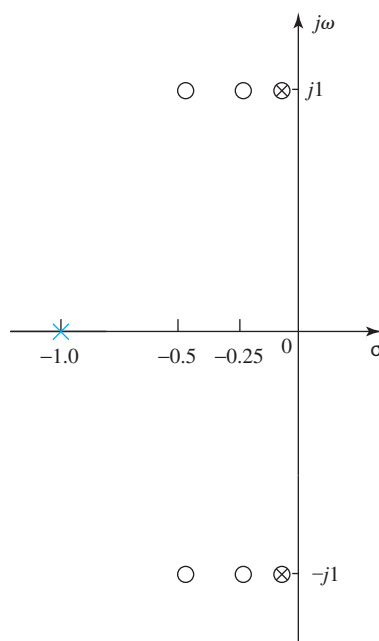
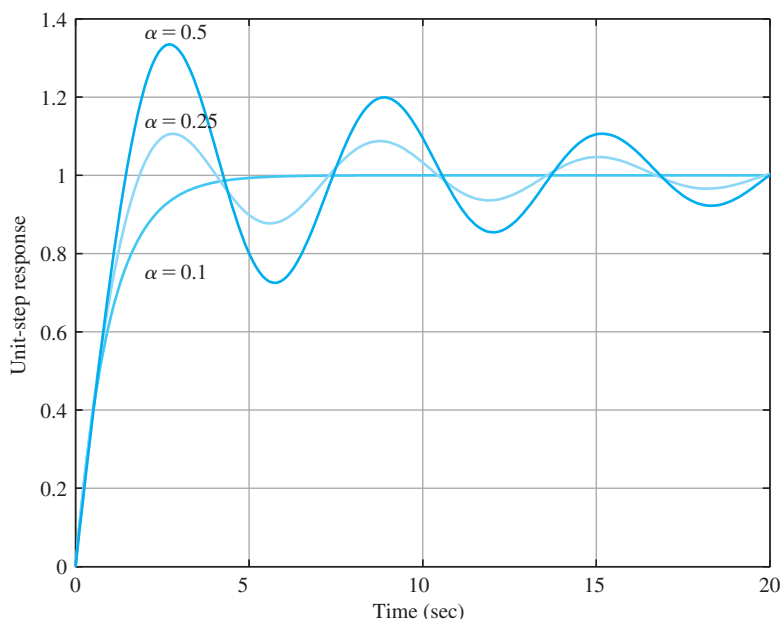


**Figure 3.34**

Effect of complex zeros  
on transient response



not really possible. However, placing the complex zeros near the locations of the lightly damped poles may provide sufficient improvement in step response performance. We will come back to this technique later in Chapters 5, 7, and 10 in the context of dynamic compensator design.

### EXAMPLE 3.30

#### *Aircraft Response Using Matlab*

The transfer function between the elevator and altitude of the Boeing 747 aircraft described in Section 10.3.2 can be approximated as

$$\frac{h(s)}{\delta_e(s)} = \frac{30(s - 6)}{s(s^2 + 4s + 13)}.$$

1. Use Matlab to plot the altitude time history for a  $1^\circ$  impulsive elevator input. Explain the response, noting the physical reasons for the nonminimum-phase nature of the response.
2. Examine the accuracy of the approximations for  $t_r$ ,  $t_s$ , and  $M_p$  [see Eqs. (3.68) and (3.73) and Fig. 3.24].

#### Solution

1. The Matlab statements to create the impulse response for this case are as follows:

```

u = -1; % u = delta e
sysG=u*30*(s-6)/ % define system by its transfer function
(s^3+4*s^2+13*s)
y=impulse(sysG); % compute impulse response; y = h
plot(y); % plot impulse response

```

The result is the plot shown in Fig. 3.35. Notice how the altitude drops initially and then rises to a new final value. The final value is predicted by the Final Value Theorem:

$$h(\infty) = s \frac{30(s - 6)(-1)}{s(s^2 + 4s + 13)} \Big|_{s=0} = \frac{30(-6)(-1)}{13} = +13.8.$$

Response of a nonminimum-phase system

The fact that the response has a finite final value for an impulsive input is due to the  $s$ -term in the denominator. This represents a pure integration, and the integral of an impulse function is a finite value. If the input had been a step, the altitude would have continued to increase with time; in other words the integral of a step function is a ramp function.

The initial drop is predicted by the RHP zero in the transfer function. The negative elevator deflection is defined to be upward by convention (see Fig. 10.30). The upward deflection of the elevators drives the tail down, which rotates the craft nose up and produces the climb. The deflection at the initial instant causes a downward force before the craft has rotated; therefore, the initial altitude response is down. After rotation, the increased lift resulting from the increased angle of attack of the wings causes the airplane to climb.

2. The rise time from Eq. (3.68) is

$$t_r = \frac{1.8}{\omega_n} = \frac{1.8}{\sqrt{13}} = 0.5 \text{ sec.}$$

We find the damping ratio  $\zeta$  from the relation

$$2\zeta\omega_n = 4 \Rightarrow \zeta = \frac{2}{\sqrt{13}} = 0.55.$$

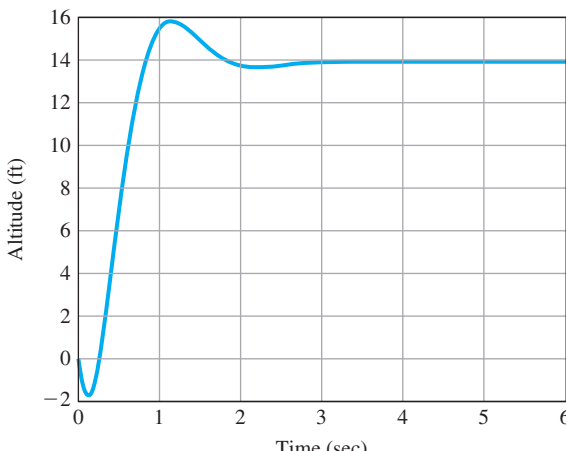
From Fig. 3.24 we find the overshoot  $M_p$  to be 0.14. Because  $2\zeta\omega_n = 2\sigma = 4$ , Eq. (3.73) shows that

$$t_s = \frac{4.6}{\sigma} = \frac{4.6}{2} = 2.3 \text{ sec.}$$

Detailed examination of the time history  $h(t)$  from Matlab output shows that  $t_r \cong 0.43$  sec,  $M_p \cong 0.14$ , and  $t_s \cong 2.6$  sec, which are

Figure 3.35

Response of an airplane's altitude to an impulsive elevator input



reasonably close to the estimates. The only significant effect of the nonminimum-phase zero was to cause the initial response to go in the “wrong direction” and make the response somewhat sluggish.

### Effect of extra pole

In addition to studying the effects of zeros, it is useful to consider the effects of an extra pole on the standard second-order step response. In this case, we take the transfer function to be

$$H(s) = \frac{1}{(s/\alpha\zeta\omega_n + 1)[(s/\omega_n)^2 + 2\zeta(s/\omega_n) + 1]}. \quad (3.82)$$

Plots of the step response for this case are shown in Fig. 3.36 for  $\zeta = 0.5$ , and in Fig. 3.37 for  $\zeta = 0.707$  for several values of  $\alpha$ . In this case, the

**Figure 3.36**

Step responses for several third-order systems with  $\zeta = 0.5$

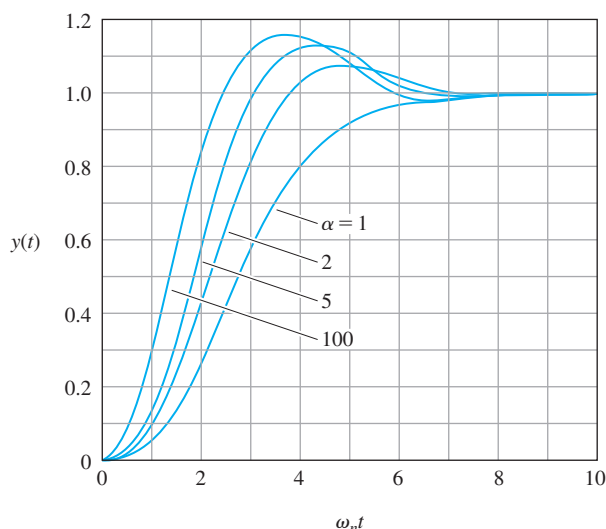


**Figure 3.37**

Step responses for several third-order systems with  $\zeta = 0.707$

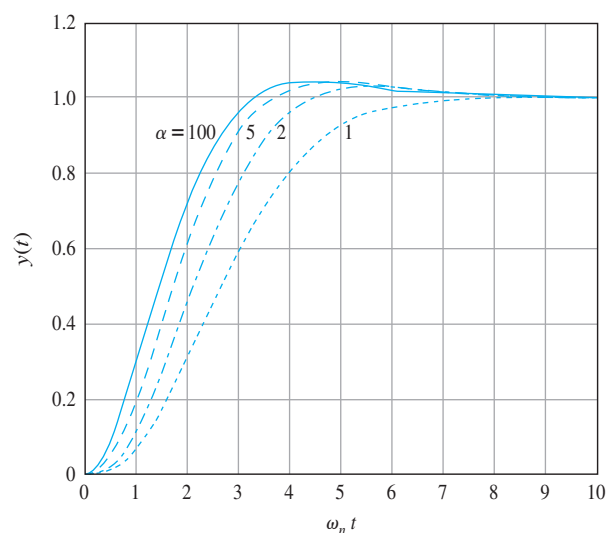
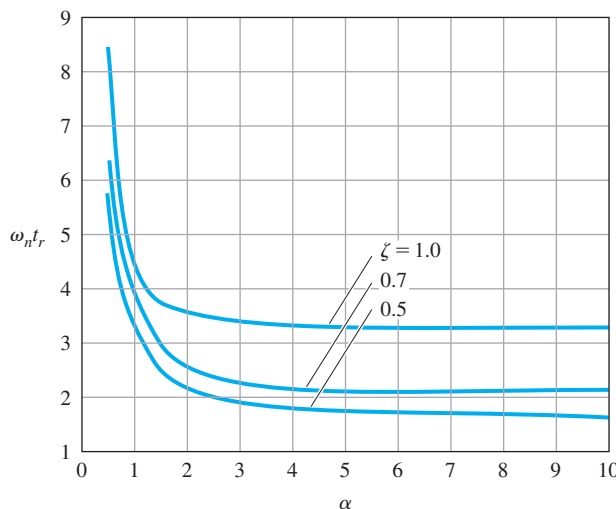


**Figure 3.38**

Normalized rise time for several locations of an additional pole



major effect is to increase the rise time. A plot of the rise time versus  $\alpha$  is shown in Fig. 3.38 for several values of  $\zeta$ .

From this discussion, we can draw several conclusions about the dynamic response of a simple system as revealed by its pole-zero patterns:

#### *Effects of Pole-Zero Patterns on Dynamic Response*

1. For a second-order system with no finite zeros, the transient response parameters are approximated as follows:

$$\text{Rise time: } t_r \cong \frac{1.8}{\omega_n},$$

$$\text{Overshoot: } M_p \cong \begin{cases} 5\%, & \zeta = 0.7, \\ 16\%, & \zeta = 0.5 \\ 35\%, & \zeta = 0.3, \end{cases} \quad (\text{see Fig. 3.24}),$$

$$\text{Settling time: } t_s \cong \frac{4.6}{\sigma}.$$

2. A zero in the left half-plane (LHP) will increase the overshoot if the zero is within a factor of 4 of the real part of the complex poles. A plot is given in Fig. 3.29.
3. A zero in the RHP will depress the overshoot (and may cause the step response to start out in the wrong direction).
4. An additional pole in the LHP will increase the rise time significantly if the extra pole is within a factor of 4 of the real part of the complex poles. A plot is given in Fig. 3.38.

## 3.6 Stability

For nonlinear and time-varying systems, the study of stability is a complex and often difficult subject. In this section, we will consider only LTI systems for which we have the following condition for stability:

An LTI system is said to be stable if all the roots of the transfer function denominator polynomial have negative real parts (that is, they are *all* in the left hand  $s$ -plane), and is unstable otherwise.

**Stable system**

**Unstable system**

A system is stable if its initial conditions decay to zero and is unstable if they diverge. As just stated, an LTI (constant parameter) system is **stable** if *all* the poles of the system are strictly inside the left half  $s$ -plane [that is, all the poles have negative real parts ( $s = -\sigma + j\omega$ ,  $\sigma > 0$ )]. If *any* pole of the system is in the right half  $s$ -plane (that is, has a positive real part,  $s = -\sigma + j\omega$ ,  $\sigma < 0$ ), then the system is **unstable**, as shown in Fig. 3.16. With any simple pole on the  $j\omega$  axis ( $\sigma = 0$ ), small initial conditions will persist. For any other pole with  $\sigma = 0$ , oscillatory motion will persist. Therefore, a system is stable if its transient response decays and unstable if it does not. Figure 3.16 shows the time response of a system due to its pole locations.

In later chapters, we will address more advanced notions of stability, such as Nyquist's frequency-response stability test (see Chapter 6) and Lyapunov stability (see Chapter 9).

### 3.6.1 Bounded Input-Bounded Output Stability

A system is said to have **bounded input–bounded output (BIBO) stability** if every bounded input results in a bounded output (regardless of what goes on inside the system). A test for this property is readily available when the system response is given by convolution. If the system has input  $u(t)$ , output  $y(t)$ , and impulse response  $h(t)$ , then

$$y(t) = \int_{-\infty}^{\infty} h(\tau)u(t-\tau)d\tau. \quad (3.83)$$

If  $u(t)$  is bounded, then there is a constant  $M$  such that  $|u| \leq M < \infty$ , and the output is bounded by

$$\begin{aligned} |y| &= \left| \int hu d\tau \right| \\ &\leq \int |h||u| d\tau \\ &\leq M \int_{-\infty}^{\infty} |h(\tau)| d\tau. \end{aligned}$$

Thus, the output will be bounded if  $\int_{-\infty}^{\infty} |h| d\tau$  is bounded.

On the other hand, suppose the integral is not bounded and the bounded input  $u(t - \tau) = +1$  if  $h(\tau) > 0$  and  $u(t - \tau) = -1$  if  $h(\tau) < 0$ . In this case,

$$y(t) = \int_{-\infty}^{\infty} |h(\tau)| d\tau, \quad (3.84)$$

and the output is not bounded. We conclude that

### Mathematical definition of BIBO stability

The system with impulse response  $h(t)$  is BIBO-stable if and only if the integral

$$\int_{-\infty}^{\infty} |h(\tau)| d\tau < \infty.$$

### EXAMPLE 3.31

#### BIBO Stability for a Capacitor

As an example, determine the capacitor driven by a current source sketched in Fig. 3.39. The capacitor voltage is the output and the current is the input.

**Solution.** The impulse response of this setup is  $h(t) = 1(t)$ , the unit step. Now for this response,

$$\int_{-\infty}^{\infty} |h(\tau)| d\tau = \int_0^{\infty} d\tau \quad (3.85)$$

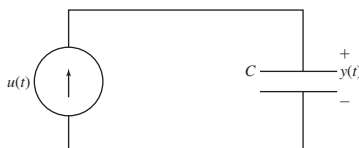
is not bounded. The capacitor is not BIBO-stable. Notice the transfer function of the system is  $1/s$  and has a pole on the imaginary axis. Physically, we can see that constant input current will cause the voltage to grow, and thus the system response is neither bounded nor stable. In general, if an LTI system has any pole<sup>13</sup> on the imaginary axis or in the RHP, the response will not be BIBO-stable; if every pole is inside the LHP, then the response will be BIBO-stable. Thus for these systems, pole locations of the transfer function can be used to check for stability.

---

An alternative to computing the integral of the impulse response or even to locating the roots of the characteristic equation is given by Routh's stability criterion, which we will discuss in Section 3.6.3.

**Figure 3.39**

Capacitor driven by current source




---

<sup>13</sup>Determination of BIBO stability by pole location.

### 3.6.2 Stability of LTI Systems

Consider the LTI system whose transfer function denominator polynomial leads to the characteristic equation

$$s^n + a_1 s^{n-1} + a_2 s^{n-2} + \cdots + a_n = 0. \quad (3.86)$$

Assume the roots  $\{p_i\}$  of the characteristic equation are real or complex, but are distinct. Note Eq. (3.86) shows up as the denominator in the transfer function for the system as follows *before any cancellation of poles by zeros is made*:

$$\begin{aligned} T(s) &= \frac{Y(s)}{R(s)} = \frac{b_0 s^m + b_1 s^{m-1} + \cdots + b_m}{s^n + a_1 s^{n-1} + \cdots + a_n} \\ &= \frac{K \prod_{i=1}^m (s - z_i)}{\prod_{i=1}^n (s - p_i)}, \quad m \leq n. \end{aligned} \quad (3.87)$$

The solution to the differential equation whose characteristic equation is given by Eq. (3.86) may be written using partial-fraction expansion as

$$y(t) = \sum_{i=1}^n K_i e^{p_i t}, \quad (3.88)$$

where  $\{p_i\}$  are the roots of Eq. (3.86) and  $\{K_i\}$  depend on the initial conditions and zero locations. If a zero were to cancel a pole in the RHP for the transfer function, the corresponding  $K_i$  would equal zero in the output, but the unstable transient would appear in some internal variable.

The system is stable if and only if (necessary and sufficient condition) every term in Eq. (3.88) goes to zero as  $t \rightarrow \infty$ :

$$e^{p_i t} \rightarrow 0 \text{ for all } p_i.$$

This will happen if all the poles of the system are strictly in the LHP, where

$$\operatorname{Re}\{p_i\} < 0. \quad (3.89)$$

**Internal stability occurs when all poles are strictly in the LHP.**

**The  $j\omega$  axis is the stability boundary.**

If any poles are repeated, the response must be changed from that of Eq. (3.88) by including a polynomial in  $t$  in place of  $K_i$ , but the conclusion is the same. This is called **internal stability**. Therefore, the stability of a system can be determined by computing the location of the roots of the characteristic equation and determining whether they are all in the LHP. If the system has any poles in the RHP, it is **unstable**. Hence the  $j\omega$  axis is the stability boundary between asymptotically stable and unstable response. If the system has nonrepeated  $j\omega$  axis poles, then it is said to be **neutrally stable**. For example, a pole at the origin (an integrator) results in a nondecaying transient. A pair of complex  $j\omega$  axis poles results in an oscillating response (with constant amplitude). If the system has repeated poles on the  $j\omega$  axis, then it is **unstable** [as it results in  $te^{\pm j\omega_i t}$  terms in Eq. (3.88)]. For example, a pair of poles at the origin (double integrator) results in an unbounded response. Matlab software

makes the computation of the poles, and therefore determination of the stability of the system, relatively easy.

An alternative to locating the roots of the characteristic equation is given by Routh's stability criterion, which we will discuss next.

### 3.6.3 Routh's Stability Criterion

There are several methods of obtaining information about the locations of the roots of a polynomial without actually solving for the roots. These methods were developed in the 19th century and were especially useful before the availability of Matlab software. They are still useful for determining the ranges of coefficients of polynomials for stability, especially when the coefficients are in symbolic (nonnumerical) form. Consider the characteristic equation of an  $n$ th-order system<sup>14</sup>:

$$a(s) = s^n + a_1 s^{n-1} + a_2 s^{n-2} + \cdots + a_{n-1} s + a_n. \quad (3.90)$$

It is possible to make certain statements about the stability of the system without actually solving for the roots of the polynomial. This is a classical problem, and several methods exist for the solution.

A *necessary condition for stability* of the system is that all of the roots of Eq. (3.90) have negative real parts, which in turn requires that all the  $\{a_i\}$  be positive.<sup>15</sup>

A necessary (but not sufficient) condition for stability is that all the coefficients of the characteristic polynomial be positive.

If any of the coefficients are missing (are zero) or are negative, then the system will have poles located outside the LHP. This condition can be checked by inspection. Once the elementary necessary conditions have been satisfied, we need a more powerful test. Equivalent tests were independently proposed by Routh in 1874 and Hurwitz in 1895; we will discuss the former. Routh's formulation requires the computation of a triangular array that is a function of the  $\{a_i\}$ . He showed that a *necessary and sufficient condition for stability* is that all of the elements in the first column of this array be positive.

A system is stable if and only if *all* the elements in the first column of the Routh array are positive.

To determine the Routh array, we first arrange the coefficients of the characteristic polynomial in two rows, beginning with the first

---

<sup>14</sup>Without loss of generality, we can assume the polynomial to be monic (that is, the coefficient of the highest power of  $s$  is 1).

<sup>15</sup>This is easy to see if we construct the polynomial as a product of first- and second-order factors.

A necessary condition for Routh stability

A necessary and sufficient condition for stability

## Routh array

and second coefficients, then followed by the even-numbered and odd-numbered coefficients:

$$\begin{array}{rccccc} s^n & : & 1 & a_2 & a_4 & \dots \\ s^{n-1} & : & a_1 & a_3 & a_5 & \dots \end{array}$$

We then add subsequent rows to complete the **Routh array**:

Row	$n$	$s^n:$	1	$a_2$	$a_4$	$\dots$
Row	$n - 1$	$s^{n-1}:$	$a_1$	$a_3$	$a_5$	$\dots$
Row	$n - 2$	$s^{n-2}:$	$b_1$	$b_2$	$b_3$	$\dots$
Row	$n - 3$	$s^{n-3}:$	$c_1$	$c_2$	$c_3$	$\dots$
⋮		⋮	⋮	⋮	⋮	
Row	2	$s^2:$	*	*		
Row	1	$s^1:$	*			
Row	0	$s^0:$	*			

We compute the elements from the  $(n-2)^{\text{th}}$  and  $(n-3)^{\text{th}}$  rows as follows:

$$b_1 = -\frac{\det \begin{bmatrix} 1 & a_2 \\ a_1 & a_3 \end{bmatrix}}{a_1} = \frac{a_1 a_2 - a_3}{a_1},$$

$$b_2 = -\frac{\det \begin{bmatrix} 1 & a_4 \\ a_1 & a_5 \end{bmatrix}}{a_1} = \frac{a_1 a_4 - a_5}{a_1},$$

$$b_3 = -\frac{\det \begin{bmatrix} 1 & a_6 \\ a_1 & a_7 \end{bmatrix}}{a_1} = \frac{a_1 a_6 - a_7}{a_1},$$

$$c_1 = -\frac{\det \begin{bmatrix} a_1 & a_3 \\ b_1 & b_2 \end{bmatrix}}{b_1} = \frac{b_1 a_3 - a_1 b_2}{b_1},$$

$$c_2 = -\frac{\det \begin{bmatrix} a_1 & a_5 \\ b_1 & b_3 \end{bmatrix}}{b_1} = \frac{b_1 a_5 - a_1 b_3}{b_1},$$

$$c_3 = -\frac{\det \begin{bmatrix} a_1 & a_7 \\ b_1 & b_4 \end{bmatrix}}{b_1} = \frac{b_1 a_7 - a_1 b_4}{b_1}.$$

Note the elements of the  $(n-2)^{\text{th}}$  row and the rows beneath it are formed from the two previous rows using determinants, with the two elements in the first column and other elements from successive columns. Normally, there are  $n+1$  elements in the first column when the array terminates. If these are all positive, then all the roots of the characteristic polynomial are in the LHP. However, if the elements of the first column are not all positive, then the number of roots in the RHP equals the number of sign changes in the column. A pattern of  $+, -, +$  is counted as *two*

sign changes: one change from + to –, and another from – to +. For a simple proof of the Routh test, the reader is referred to Ho et al. (1998).

### EXAMPLE 3.32

#### Routh's Test

The polynomial

$$a(s) = s^6 + s^5 + s^4 + 2s^3 + 5s^2 + 2s + 3$$

satisfies the necessary condition for stability since all the  $\{a_i\}$  are positive and nonzero. Determine whether any of the roots of the polynomial are in the RHP.

**Solution.** The Routh array for this polynomial is

$$\begin{array}{ccccc} s^6: & 1 & 1 & 5 & 3 \\ s^5: & 1 & 2 & 2 & 0 \\ s^4: & -1 = \frac{1 \cdot 1 - 1 \cdot 2}{4} & 3 = \frac{1 \cdot 5 - 1 \cdot 2}{1} & 3 = \frac{1 \cdot 3 - 1 \cdot 0}{1} \\ s^3: & 5 = \frac{-1 \cdot 2 - 1 \cdot 3}{-1} & 5 = \frac{-1 \cdot 2 - 1 \cdot 3}{-1} & 0 \\ s^2: & 4 = \frac{5 \cdot 3 + 1 \cdot 5}{5} & 3 = \frac{5 \cdot 3 + 1 \cdot 0}{5} \\ s: & \frac{5}{4} = \frac{4 \cdot 5 - 5 \cdot 3}{4} & 0 \\ s^0: & 3 = \frac{\frac{5}{4} \cdot 3 - 4.0}{\frac{5}{4}} \end{array}$$

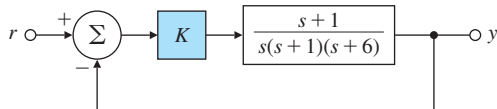
We conclude that the polynomial has RHP roots, since the elements of the first column are not all positive. In fact, there are two poles in the RHP because there are two sign changes.

Note, in computing the Routh array, we can simplify the rest of the calculations by multiplying or dividing a row by a positive constant. Also note the last two rows each have one nonzero element.

Routh's method is also useful in determining the range of parameters for which a feedback system remains stable.

**Figure 3.40**

A feedback system for testing stability

**EXAMPLE 3.33***Stability versus Parameter Range*

Consider the system shown in Fig. 3.40. The stability properties of the system are a function of the proportional feedback gain  $K$ . Determine the range of  $K$  over which the system is stable.

**Solution.** The characteristic equation for the system is given by

$$1 + K \frac{s+1}{s(s-1)(s+6)} = 0,$$

or

$$s^3 + 5s^2 + (K - 6)s + K = 0.$$

The corresponding Routh array is

$$\begin{array}{ccc} s^3 : & 1 & K - 6 \\ s^2 : & 5 & K \\ s : & (4K - 30)/5 & \\ s^0 : & K. & \end{array}$$

For the system to be stable, it is necessary that

$$\frac{4K - 30}{5} > 0 \quad \text{and} \quad K > 0,$$

or

$$K > 7.5 \quad \text{and} \quad K > 0.$$

Thus, Routh's method provides an analytical answer to the stability question. Although any gain satisfying this inequality stabilizes the system, the dynamic response could be quite different depending on the specific value of  $K$ . Given a specific value of the gain, we may compute the closed-loop poles by finding the roots of the characteristic polynomial. The characteristic polynomial has the coefficients represented by the row vector (in descending powers of  $s$ )

$$\text{denT} = [1 \ 5 \ K-6 \ K]$$

**Computing roots by Matlab**

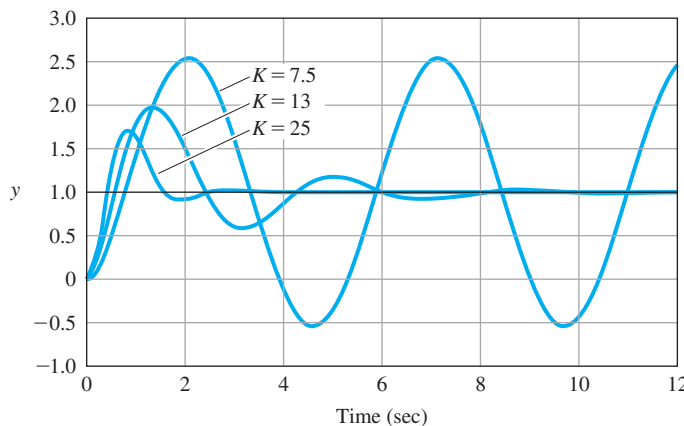
and we may compute the roots using the Matlab function

$$\text{roots}(\text{denT}).$$

For  $K = 7.5$  the roots are at  $-5$  and  $\pm 1.22j$ , and the system is neutrally stable. Note that Routh's method predicts the presence of poles on the  $j\omega$  axis for  $K = 7.5$ . If we set  $K = 13$ , the closed-loop poles are at  $-4.06$  and  $-0.47 \pm 1.7j$ , and for  $K = 25$ , they are at  $-1.90$  and  $-1.54 \pm 3.27j$ . In both these cases, the system is stable as predicted by Routh's method. Fig. 3.41 shows the transient responses for

**Figure 3.41**

Transient responses for the system in Fig. 3.40



the three gain values. To obtain these transient responses, we compute the closed-loop transfer function

$$T(s) = \frac{Y(s)}{R(s)} = \frac{K(s+1)}{s^3 + 5s^2 + (K-6)s + K},$$

```
s=tf('s');
sysT=K*(s+1)/(s^3+5*s^2+(K-6)*s+K); % define the Laplace variable
step(sysT); % define transfer function
% compute the step response
```

produce a plot of the (unit) step response.

### EXAMPLE 3.34

#### *Stability versus Two Parameter Ranges*

Find the range of the controller gains ( $K, K_I$ ) so the PI (proportional–integral; see Chapter 4) feedback system in Fig. 3.42 is stable.

**Solution.** The characteristic equation of the closed-loop system is

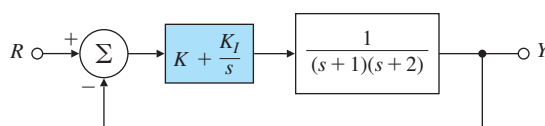
$$1 + \left( K + \frac{K_I}{s} \right) \frac{1}{(s+1)(s+2)} = 0,$$

which we may rewrite as

$$s^3 + 3s^2 + (2 + K)s + K_I = 0.$$

**Figure 3.42**

System with proportional-integral (PI) control



The corresponding Routh array is

$$\begin{array}{lll} s^3 : & 1 & 2 + K \\ s^2 : & 3 & K_I \\ s : & (6 + 3K - K_I)/3 & \\ s^0 : & K_I. \end{array}$$

For internal stability we must have

$$K_I > 0 \quad \text{and} \quad K > \frac{1}{3}K_I - 2.$$

The allowable region can be plotted in Matlab using the following commands

```
fh=@(KI,K) 6+3*K-KI;
ezplot(fh)
hold on;
f=@(KI, K) KI;
ezplot(f);
```

and is the shaded area in the  $(K_I, K)$  plane shown in Fig. 3.43, which represents an analytical solution to the stability question. This example illustrates the real value of Routh's approach and why it is superior to the numerical approaches. It would have been more difficult to arrive at these bounds on the gains using numerical search techniques. The closed-loop transfer function is

$$T(s) = \frac{Y(s)}{R(s)} = \frac{Ks + K_I}{s^3 + 3s^2 + (2 + K)s + K_I}.$$

As in Example 3.33, we may compute the closed-loop poles for different values of the dynamic compensator gains by using the Matlab function `roots` on the denominator polynomial:

[Matlab roots](#)

```
denT = [1 3 2+K KI]; % form denominator
```

**Figure 3.43**

Allowable region for stability

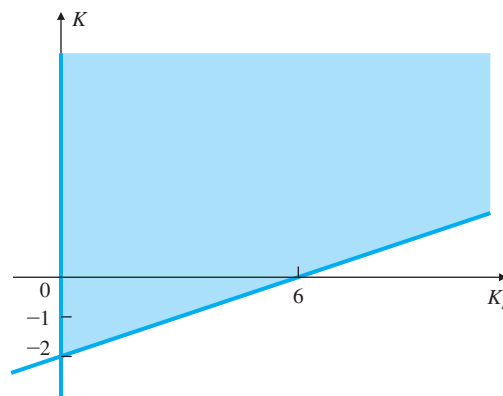
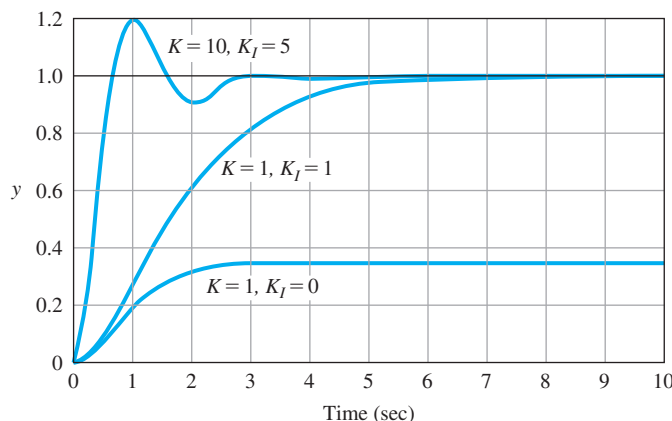


**Figure 3.44**

Transient response for the system in Fig. 3.42



Similarly, we may find the zero by finding the roots of the numerator polynomial

```
numT = [K KI]; % form numerator
```

The closed-loop zero of the system is at  $-K_I/K$ . Fig. 3.44 shows the transient response for three sets of feedback gains. For  $K = 1$  and  $K_I = 0$ , the closed-loop poles are at 0 and  $-1.5 \pm 0.86j$ , and there is a zero at the origin. For  $K = K_I = 1$ , the poles and zeros are all at  $-1$ . For  $K = 10$  and  $K_I = 5$ , the closed-loop poles are at  $-0.46$  and  $-1.26 \pm 3.3j$  and the zero is at  $-0.5$ . The step responses were obtained using the following Matlab function:

```
sysT=tf(numT,denT); % define system by its numerator and denominator
step(sysT) % compute step response
```

There is a large steady-state error in this case when  $K_I = 0$ . (See Chapter 4.)

If the first term in one of the rows is zero or if an entire row is zero, then the standard Routh array cannot be formed, so we have to use one of the special techniques described next.

### Special Cases

If only the first element in one of the rows of the Routh array is zero or an entire row of the Routh array is zero, special modifications to the Routh array computations are necessary. For details, see Appendix W.3.6.3 available online at [www.pearsonglobaleditions.com](http://www.pearsonglobaleditions.com).

The Routh–Hurwitz result assumes the characteristic polynomial coefficients are known precisely. It is well known the roots of a polynomial can be very sensitive to even slight perturbations in the polynomial coefficients. If the range of variation on each one of the polynomial coefficients is known, then a remarkable result called the Kharitonov

Theorem (1978) allows one to test just four so-called Kharitonov polynomials, using the Routh test, to see if the polynomial coefficient variations result in instability.

### △ 3.7 Obtaining Models from Experimental Data: System Identification

There are several reasons for using experimental data to obtain a model of the dynamic system to be controlled. The available information and related techniques in this area are under the banner of system identification. See Appendix W3.7 available online at [www.pearsonglobaleditions.com](http://www.pearsonglobaleditions.com).

### △ 3.8 Amplitude and Time Scaling

In some cases in practice, due to extreme variations in magnitudes of real data, amplitude scaling is necessary. See Appendix W3.8 available online at [www.pearsonglobaleditions.com](http://www.pearsonglobaleditions.com).

## 3.9 Historical Perspective

Oliver Heaviside (1850–1925) was an eccentric English electrical engineer, mathematician, and physicist. He was self-taught and left school at the age of 16 to become a telegraph operator. He worked mostly outside the scientific community that was hostile to him. He reformulated Maxwell's equations into the form that is used today. He also laid down the foundations of telecommunication and hypothesized the existence of the ionosphere. He developed the symbolic procedure known as Heaviside's operational calculus for solving differential equations. The Heaviside calculus was widely popular among electrical engineers in the 1920s and 1930s. This was later shown to be equivalent to the more rigorous Laplace transform named after the French mathematician Pierre-Simon Laplace (1749–1827) who had earlier worked on operational calculus.

Laplace was also an astronomer and a mathematician who is sometimes referred to as the “The Newton of France.” He studied the origin and dynamical stability of the solar system completing Newton's work in his five-volume *Méchanique céleste* (Celestial Mechanics). Laplace invented the general concept of potential as in a gravitational or electric field and described by Laplace's equation. Laplace had a brief political career as Napoleon's Interior Minister. During a famous exchange with Napoleon who asked Laplace why he had not mentioned God in *Méchanique céleste*, Laplace is said to have replied “Sir, there was no need for that hypothesis.” He was an opportunist and changed sides as the political winds shifted. Laplace's operational property transforms a differential equation into an algebraic operation that is much easier to manipulate in engineering applications. It is also applicable to

solutions of partial differential equations, the original problem that Laplace was concerned with while developing the transform. Laplace formulated the Laplace's equation with applications to electromagnetic theory, fluid dynamics, and astronomy. Laplace also made fundamental contributions to probability theory.

Laplace and Fourier transforms are intimately related (see Appendix A). The Fourier series and the Fourier transform, developed in that order, provide methods for representing signals in terms of exponential functions. Fourier series are used to represent a periodic signal with discrete spectra in terms of a series. Fourier transforms are used to represent a non-periodic signal with continuous spectra in terms of an integral. The Fourier transform is named after the French mathematician Jean Batiste Joseph Fourier (1768–1830) who used Fourier series to solve the heat conduction equation expressed in terms of Fourier series. Laplace and Fourier were contemporaries and knew each other very well. In fact, Laplace was one of Fourier's teachers. Fourier accompanied Napoleon on his Egyptian expedition in 1798 as a science advisor, and is also credited with the discovery of the greenhouse effect.

Transform methods provide a unifying method in applications to solving many engineering problems. Linear transforms such as the Laplace transform and Fourier transform are useful for studying linear systems. While Fourier transforms are useful to study the steady-state behavior, Laplace transforms are used for studying the transient and closed-loop behavior of dynamic systems. The book by Gardner and Barnes in 1942 was influential in popularizing the Laplace transform in the United States.

## SUMMARY

- The Laplace transform is the primary tool used to determine the behavior of linear systems. The Laplace transform of a time function ( $t$ ) is given by

$$\mathcal{L}[f(t)] = F(s) = \int_{0^-}^{\infty} f(t)e^{-st} dt. \quad (3.91)$$

- This relationship leads to the key property of Laplace transforms, namely,

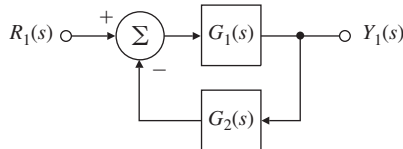
$$\mathcal{L}[\dot{f}(t)] = sF(s) - f(0^-). \quad (3.92)$$

- This property allows us to find the transfer function of a linear ODE. Given the transfer function  $G(s)$  of a system and the input  $u(t)$ , with transform  $U(s)$ , the system output transform is  $Y(s) = G(s)U(s)$ .
- Normally, inverse transforms are found by referring to tables, such as Table A.2 in Appendix A, or by computer. Properties of Laplace transforms and their inverses are summarized in Table A.1 in Appendix A.

- The Final Value Theorem is useful in finding steady-state errors for stable systems: If all the poles of  $s Y(s)$  are in the LHP, then

$$\lim_{t \rightarrow \infty} y(t) = \lim_{s \rightarrow 0} s Y(s). \quad (3.93)$$

- Block diagrams are a convenient way to show the relationships between the components of a system. They can usually be simplified using the relations in Fig. 3.10 and Eq. (3.58); that is, the transfer function of the block diagram



is equivalent to

$$Y_1(s) = \frac{G_1(s)}{1 + G_1(s)G_2(s)} R_1(s). \quad (3.94)$$

- The locations of poles in the  $s$ -plane determine the character of the response, as shown in Fig. 3.16.
- The location of a pole in the  $s$ -plane is defined by the parameters shown in Fig. 3.18. These parameters are related to the time-domain quantities of rise time  $t_r$ , settling time  $t_s$ , and overshoot  $M_p$ , which are defined in Fig. 3.23. The correspondences between them, for a second-order system with no zeros, are given by

$$t_r \cong \frac{1.8}{\omega_n}, \quad (3.95)$$

$$M_p = e^{-\pi\xi/\sqrt{1-\xi^2}}, \quad (3.96)$$

$$t_s = \frac{4.6}{\zeta\omega_n}. \quad (3.97)$$

- When a zero in the LHP is present, the overshoot increases. This effect is summarized in Figs. 3.27, 3.28 and 3.29.
- When a real RHP is present, the step response starts off in the “wrong direction,” and the response is more sluggish. This effect is summarized in Fig. 3.31, and is called the nonminimum phase behavior.
- When an additional stable pole is present, the system response is more sluggish. This effect is summarized in Figs. 3.36, 3.37 and 3.38.
- For a stable system, all the closed-loop poles must be in the LHP.
- A system is stable if and only if all the elements in the first column of the Routh array are positive. To determine the Routh array, refer to the formulas in Section 3.6.3.

## REVIEW QUESTIONS

- 3.1** What is the definition of a “transfer function”?
- 3.2** What are the properties of systems whose responses can be described by transfer functions?
- 3.3** What is the Laplace transform of  $f(t - \lambda)1(t - \lambda)$  if the transform of  $f(t)$  is  $F(s)$ ?
- 3.4** State the Final Value Theorem (FVT).
- 3.5** What is the most common use of the FVT in control?
- 3.6** Given a second-order transfer function with damping ratio  $\zeta$  and natural frequency  $\omega_n$ , what is the estimate of the step response rise time? What is the estimate of the percent overshoot in the step response? What is the estimate of the settling time?
- 3.7** What is the major effect of a zero in the left half-plane on the second-order step response?
- 3.8** What is the most noticeable effect of a zero in the right half-plane on the step response of the second-order system?
- 3.9** What is the main effect of an extra real pole on the second-order step response?
- 3.10** Why is stability an important consideration in control system design?
- 3.11** What is the main use of Routh’s criterion?
- 3.12** Under what conditions might it be important to know how to estimate a transfer function from experimental data?

## PROBLEMS

### *Problems for Section 3.1: Review of Laplace Transforms*

- 3.1** Show that, in a partial-fraction expansion, complex conjugate poles have coefficients that are also complex conjugates. (The result of this relationship is that whenever complex conjugate pairs of poles are present, only one of the coefficients needs to be computed.)
- 3.2** Find the Laplace transform of the following time functions:
  - (a)  $f(t) = 0.5 + 2.5t$
  - (b)  $f(t) = 1.5 + 9t + 0.3t^2 + \delta(t)$ , where  $\delta(t)$  is the unit impulse function
  - (c)  $f(t) = 5.5e^{-t} + 3e^{-2t} + 2.5t^2e^{-3t}$
  - (d)  $f(t) = (2t + 1)^2$
  - (e)  $f(t) = \cosh 0.2t$
- 3.3** Find the Laplace transform of the following time functions:
  - (a)  $f(t) = 8 \sin 0.75t$
  - (b)  $f(t) = \cos 1.5t + 4 \sin 1.5t + 1.7e^{-0.5t} \cos 1.5t$
  - (c)  $f(t) = 0.4t^3 + 1.8e^t \sin 2.2t$
- 3.4** Find the Laplace transform of the following time functions:
  - (a)  $f(t) = t \cos t$
  - (b)  $f(t) = t \sin 0.9t$

- (c)  $f(t) = te^{-0.1t} + 2t \cos 0.6t$   
 (d)  $f(t) = 3t^2 - 2t \sin 1.3t + 5t \cos 7.2t$   
 (e)  $f(t) = t^2 \cos t + t^2 \sin 0.9t$

3.5 Find the Laplace transform of the following time functions (\* denotes convolution):

- (a)  $f(t) = \sin 5t \cos t$   
 (b)  $f(t) = 2 + 3 \sin^2 4t + 5 \cos^2 t$   
 (c)  $f(t) = (\sin t)/t$   
 (d)  $f(t) = \sin t * \cos 2t$   
 (e)  $f(t) = \int_0^t \sin(t-\tau) \sin \tau d\tau$

3.6 Given the Laplace transform of  $f(t)$  is  $F(s)$ , find the Laplace transform of the following:

- (a)  $g(t) = f(t) \cos t$   
 (b)  $g(t) = \int_0^t \int_0^t f(\tau) d\tau dt_1$

3.7 Find the time function corresponding to each of the following Laplace transforms using partial-fraction expansions:

- (a)  $F(s) = \frac{5}{s(s+7)}$   
 (b)  $F(s) = \frac{6}{s(s+1)(s+2)}$   
 (c)  $F(s) = \frac{8s+2}{s^2+s+20}$   
 (d)  $F(s) = \frac{5s+3}{(s+1)(s^2+2s+30)}$   
 (e)  $F(s) = \frac{s+4}{s^2+2}$   
 (f)  $F(s) = \frac{s+1}{s(s^2+4)}$   
 (g)  $F(s) = \frac{s+9}{s^2(s+1)}$   
 (h)  $F(s) = \frac{5}{s^5}$   
 (i)  $F(s) = \frac{18}{s^4+9}$   
 (j)  $F(s) = \frac{e^{-3}}{s^3}$

3.8 Find the time function corresponding to each of the following Laplace transforms:

- (a)  $F(s) = \frac{1}{s(s+2)^2}$   
 (b)  $F(s) = \frac{s^2+s+1}{s^3-1}$   
 (c)  $F(s) = \frac{2(s^2+s+1)}{s(s+1)^2}$   
 (d)  $F(s) = \frac{s^3+2s+4}{s^4-16}$   
 (e)  $F(s) = \frac{2(s+2)(s+5)^2}{(s+1)(s^2+4)^2}$   
 (f)  $F(s) = \frac{s^2-1}{(s^2+1)^2}$   
 (g)  $F(s) = \tan^{-1}\left(\frac{1}{s}\right)$

**3.9** Solve the following ODEs using Laplace transforms:

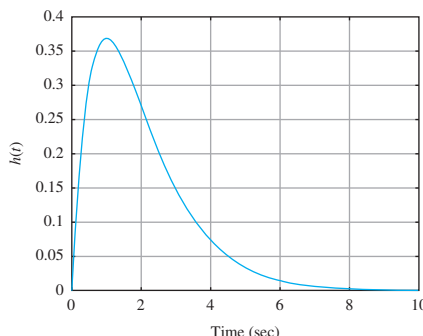
- (a)  $\ddot{y}(t) + \dot{y}(t) + 3y(t) = 0; y(0) = 1, \dot{y}(0) = 2$
- (b)  $\ddot{y}(t) - 2\dot{y}(t) + 4y(t) = 0; y(0) = 1, \dot{y}(0) = 2$
- (c)  $\ddot{y}(t) + \dot{y}(t) = \sin t; y(0) = 1, \dot{y}(0) = 2$
- (d)  $\ddot{y}(t) + 3y(t) = \sin t; y(0) = 1, \dot{y}(0) = 2$
- (e)  $\ddot{y}(t) + 2\dot{y}(t) = e^t; y(0) = 1, \dot{y}(0) = 2$
- (f)  $\ddot{y}(t) + y(t) = t; y(0) = 1, \dot{y}(0) = -1$

**3.10** Using the convolution integral, find the step response of the system whose impulse response is given below and shown in Fig. 3.45:

$$h(t) = \begin{cases} te^{-t} & t \geq 0, \\ 0 & t < 0. \end{cases}$$

**Figure 3.45**

Impulse response for Problem 3.10

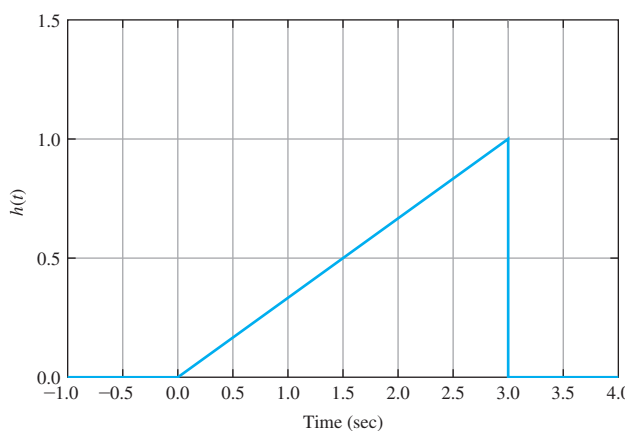


**3.11** Using the convolution integral, find the step response of the system whose impulse response is given below and shown in Fig. 3.46:

$$h(t) = \begin{cases} t/3, & 0 \leq t \leq 3 \\ 0, & t < 0 \text{ and } t > 3. \end{cases}$$

**Figure 3.46**

Impulse response for Problem 3.11



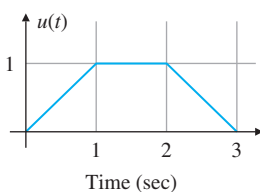
**3.12** Consider the standard second-order system

$$G(s) = \frac{\omega_n^2}{s^2 + 2\xi\omega_n s + \omega_n^2}.$$

- (a) Write the Laplace transform of the signal in Fig. 3.47.
- (b) What is the transform of the output if this signal is applied to  $G(s)$ ?
- (c) Find the output of the system for the input shown in Fig. 3.47.

**Figure 3.47**

Plot of input signal for Problem 3.12



- 3.13** A rotating load is connected to a field-controlled DC motor with negligible field inductance. A test results in the output load reaching a speed of 1 rad/sec within 1/2 sec when a constant input of 100 V is applied to the motor terminals. The output steady-state speed from the same test is found to be 2 rad/sec. Determine the transfer function  $\frac{\Theta(s)}{V_f(s)}$  of the motor.
- 3.14** For the system in Fig. 2.57, compute the transfer function from the motor voltage to position  $\theta_2$ .
- 3.15** Compute the transfer function for the two-tank system in Fig. 2.61 with holes at A and C.
- 3.16** For a second-order system with transfer function

$$G(s) = \frac{5}{s^2 + s + 4},$$

Determine the following:

- (a) The DC gain and whether the system is stable.
  - (b) The final value of the output if the input is applied with a step of 2 units or  $R(s) = \frac{2}{s}$ .
- 3.17** Consider the continuous rolling mill depicted in Fig. 3.48. Suppose the motion of the adjustable roller has a damping coefficient  $b$ , and the force exerted by the rolled material on the adjustable roller is proportional to the material's change in thickness:  $F_s = c(T - x)$ . Suppose further the DC motor has a torque constant  $K_t$  and a back emf constant  $K_e$ , and the rack-and-pinion has effective radius of  $R$ .
- (a) What are the inputs to this system? The output?
  - (b) Without neglecting the effects of gravity on the adjustable roller, draw a block diagram of the system that explicitly shows the following quantities:  $V_s(s)$ ,  $I_0(s)$ ,  $F(s)$  (the force the motor exerts on the adjustable roller), and  $X(s)$ .
  - (c) Simplify your block diagram as much as possible while still identifying each output and input separately.

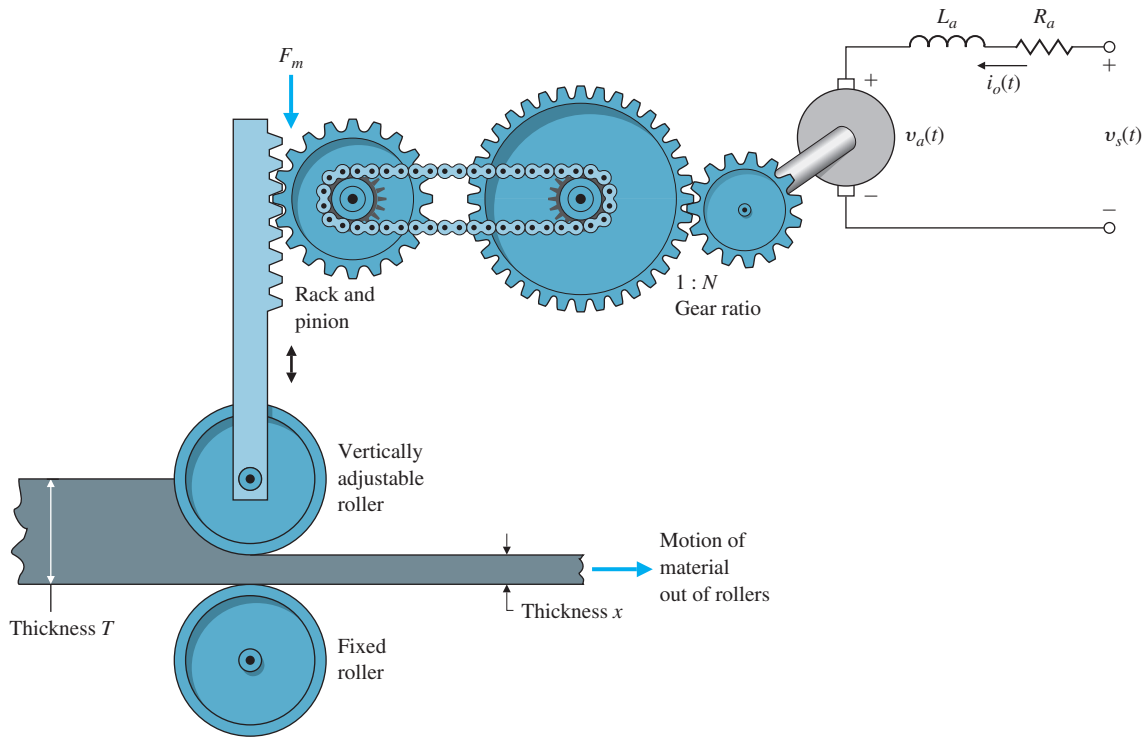
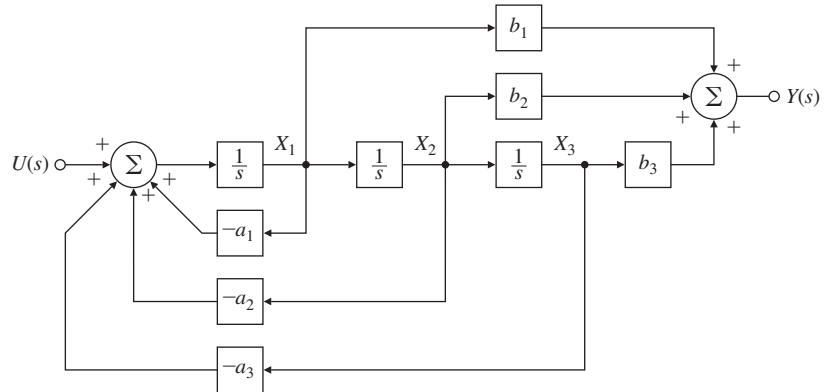


**Figure 3.48**  
Continuous rolling mill

### Problems for Section 3.2: System Modeling Diagrams

- 3.18** Consider the block diagram shown in Fig. 3.49. Note  $a_i$  and  $b_i$  are constants. Compute the transfer function for this system. This special structure is called the “control canonical form”, and will be discussed further in Chapter 7.

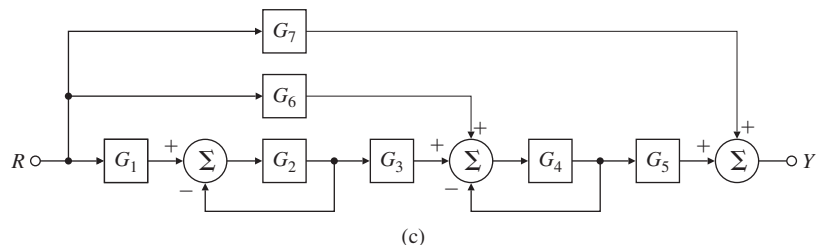
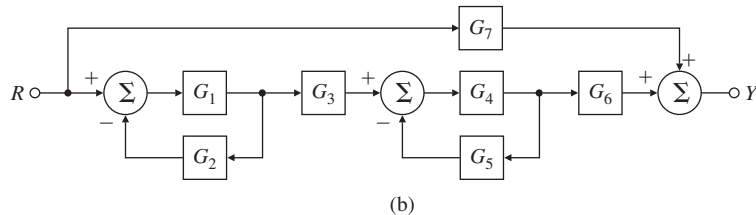
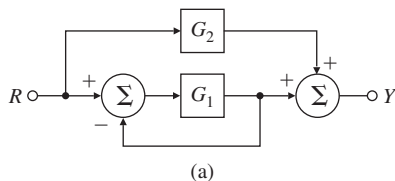
**Figure 3.49**  
Block diagram for  
Problem 3.18



- 3.19** Find the transfer functions for the block diagrams in Fig. 3.50.

**Figure 3.50**

Block diagrams for  
Problem 3.19



- 3.20** Find the transfer functions for the block diagrams in Fig. 3.51, using the ideas of block-diagram simplification. The special structure in Fig. 3.51(b) is called the “observer canonical form”, and will be discussed in Chapter 7.

- 3.21** Use block-diagram algebra to determine the transfer function between  $R(s)$  and  $Y(s)$  in Fig. 3.52.

- △ **3.22** Find the transfer functions for the block diagrams in Fig. 3.51, using Mason’s rule.
- △ **3.23** Use Mason’s rule to determine the transfer function between  $R(s)$  and  $Y(s)$  in Fig. 3.52.

### Problems for Section 3.3: Effect of Pole Locations

- 3.24** For the electric circuit shown in Fig. 3.53, find the following:
- The time-domain equation relating  $i(t)$  and  $v_1(t)$ ;
  - The time-domain equation relating  $i(t)$  and  $v_2(t)$ ;
  - Assuming all initial conditions are zero, the transfer function  $\frac{v_2(s)}{v_1(s)}$  and the damping ratio  $\zeta$  and undamped natural frequency  $\omega_n$  of the system;
  - The range of  $C$  values that will result in  $v_2(t)$  having an overshoot of no more than 20%, assuming  $v_1(t)$  is a unit step,  $L = 1.5 \text{ mH}$ , and  $R = 5\Omega$ .

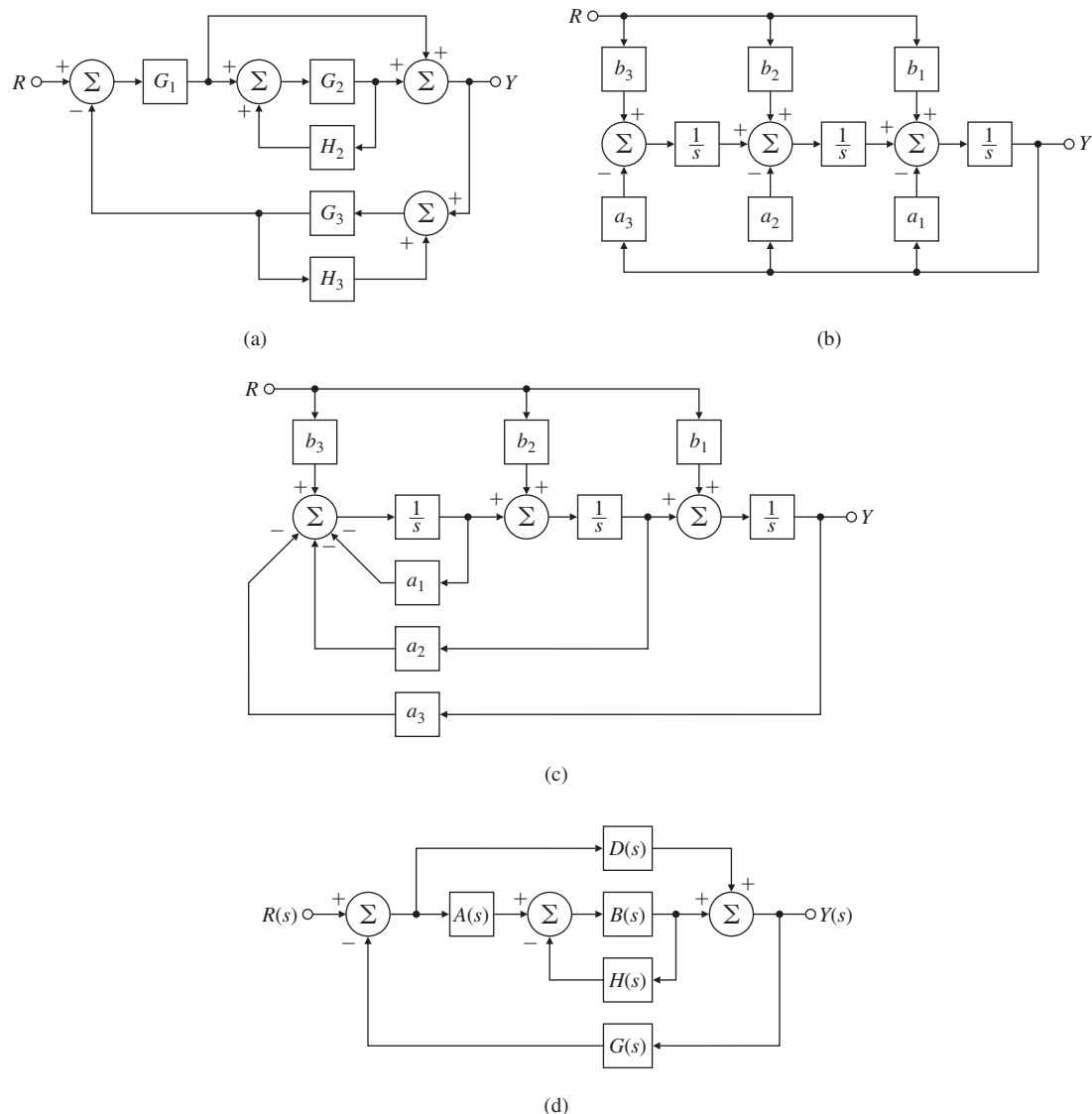


**Figure 3.51**

Block diagrams for Problem 3.20

**Figure 3.52**

Block diagram for  
Problem 3.21

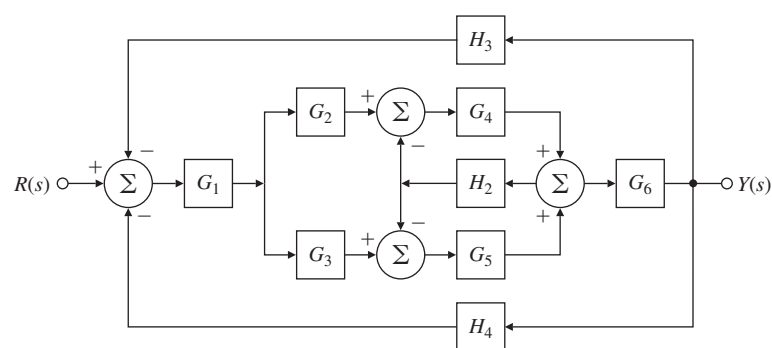
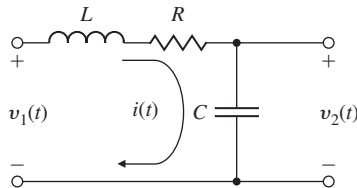


**Figure 3.53**

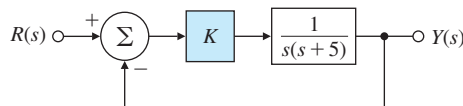
Circuit for Problem 3.24



- 3.25** For the unit feedback system shown in Fig. 3.54, specify the gain  $K$  of the proportional controller so that the output  $y(t)$  has an overshoot of no more than 12% in response to a unit step.

**Figure 3.54**

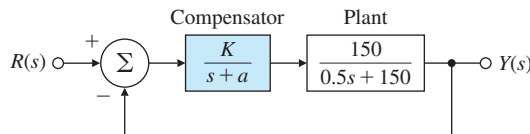
Unity feedback system for Problem 3.25



- 3.26** For the unity feedback system shown in Fig. 3.55, specify the gain and pole location of the compensator so that the overall closed-loop response to a unit-step input has an overshoot of no more than 18% and a 1% settling time of no more than 0.01 sec. Verify your design using Matlab.

**Figure 3.55**

Unity feedback system for Problem 3.26



### Problems for Section 3.4: Time-Domain Specification

- 3.27** Suppose you desire the peak time of a given second-order system to be less than  $t_p'$ . Draw the region in the  $s$ -plane that corresponds to values of the poles that meet the specification  $t_p < t_p'$ .
- 3.28** A certain servomechanism system has dynamics dominated by a pair of complex poles and no finite zeros. The time-domain specifications on the rise time ( $t_r$ ), percent overshoot ( $M_p$ ), and settling time ( $t_s$ ) are given by:

$$t_r \leq 0.6 \text{ sec},$$

$$M_p \leq 17\%,$$

$$t_s \leq 9.2 \text{ sec}.$$

- (a) Sketch the region in the  $s$ -plane where the poles could be placed so that the system will meet *all* three specifications.
- (b) Indicate on your sketch the specific locations (denoted by  $\times$ ) that will have the smallest rise time and also meet the settling time specification *exactly*.

- 3.29** A feedback system has the following response specifications:

- Percent overshoot  $M_p \leq 16\%$
  - Settling time  $t_s \leq 6.9$  sec
  - Rise time  $t_r \leq 1.8$  sec
- (a) Sketch the region of acceptable closed-loop poles in the  $s$ -plane for the system, assuming the transfer function can be approximated as simple second order.
- (b) What is the expected overshoot if the rise time and settling time specifications are met *exactly*?
- 3.30** Suppose you are to design a unity feedback controller for a first-order plant depicted in Fig. 3.56. (As you will learn in Chapter 4, the configuration shown is referred to as a proportional–integral controller.) You are to design the controller so that the closed-loop poles lie within the shaded regions shown in Fig. 3.57.

**Figure 3.56**  
Unity feedback system  
for Problem 3.30

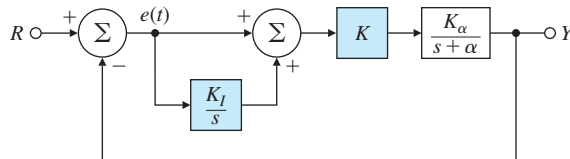
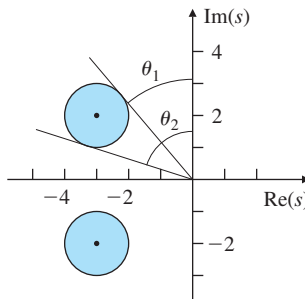


**Figure 3.57**  
Desired closed-loop  
pole locations for  
Problem 3.30



- (a) What values of  $\omega_n$  and  $\zeta$  correspond to the shaded regions in Fig. 3.57? (A simple estimate from the figure is sufficient.)
- (b) Let  $K_\alpha = \alpha = 2$ . Find values for  $K$  and  $K_I$  so the poles of the closed-loop system lie within the shaded regions.
- (c) Prove that no matter what the values of  $K_\alpha$  and  $\alpha$  are, the controller provides enough flexibility to place the poles anywhere in the complex (left-half) plane.

- 3.31** The open-loop transfer function of a unity feedback system is

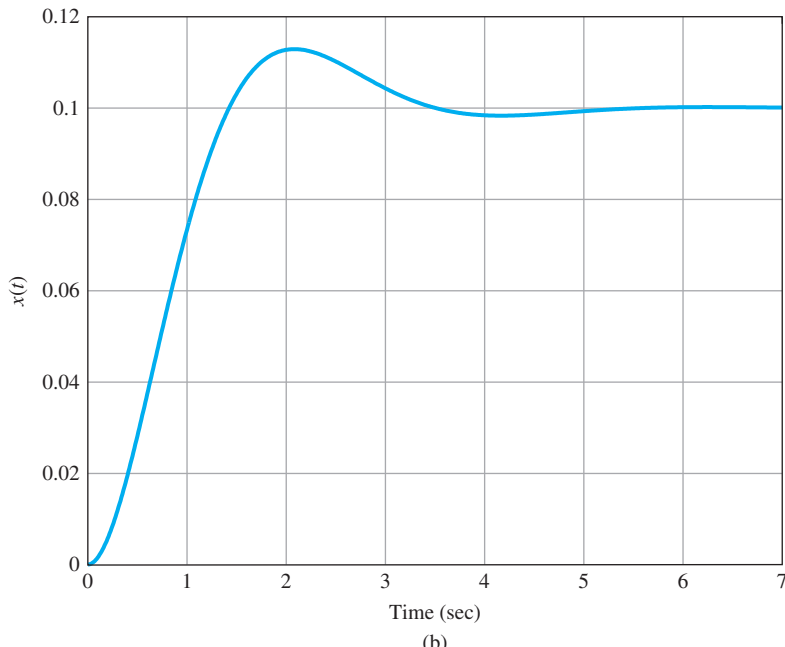
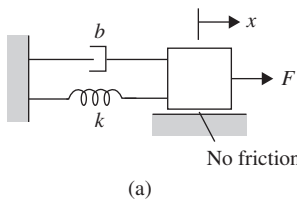
$$G(s) = \frac{K}{s(s+2)}.$$

The desired system response to a step input is specified as peak time  $t_p = 1$  sec and overshoot  $M_p = 5\%$ .

- (a) Determine whether both specifications can be met simultaneously by selecting the right value of  $K$ .
- (b) Sketch the associated region in the  $s$ -plane where both specifications are met, and indicate what root locations are possible for some likely values of  $K$ .
- (c) Relax the specifications in part (a) by the same factor and pick a suitable value for  $K$ , and use Matlab to verify that the new specifications are satisfied.
- 3.32** A simple mechanical system is shown in Fig. 3.58(a). The parameters are  $k$  = spring constant,  $b$  = viscous friction constant,  $m$  = mass. A step of 2 N force is applied as  $F = 2 \times 1(t)$  and the resulting step response is shown in Fig. 3.58(b). What are the values of the system parameters  $k$ ,  $b$ , and  $m$ ?

**Figure 3.58**

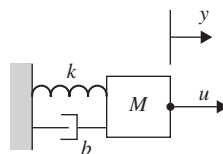
- (a) Mechanical system for Problem 3.32;  
 (b) step response for Problem 3.32



- 3.33** A mechanical system is shown in Fig. 3.59. The mass  $M = 18 \text{ kg}$  and the control force,  $u$ , is proportional to the reference input,  $u = Ar$ .
- (a) Derive the transfer function from  $R$  to  $Y$ .

**Figure 3.59**

Simple mechanical system for Problem 3.33



- (b)** Determine the values of the parameters  $k$ ,  $b$ ,  $A$  such that the system has a rise time of  $t_r = 0.7$  s and overshoot of  $M_p = 14\%$ , and zero steady-state error to a step in  $r$ .

- 3.34** The equations of motion for the DC motor shown in Fig. 2.33 were given in Eqs (2.65) as

$$J_m \ddot{\theta}_m + \left( b + \frac{K_t K_e}{R_a} \right) \dot{\theta}_m = \frac{K_t}{R_a} v_a.$$

Assume that

$$J_m = 0.05 \text{ kg}\cdot\text{m}^2,$$

$$b = 0.009 \text{ N}\cdot\text{m}\cdot\text{sec},$$

$$K_e = 0.07 \text{ V}\cdot\text{sec},$$

$$K_t = 0.07 \text{ N}\cdot\text{m/A},$$

$$R_a = 12 \Omega.$$

- (a)** Find the transfer function between the applied voltage  $v_a$  and the motor speed  $\dot{\theta}_m$ .
- (b)** What is the steady-state speed of the motor after a voltage  $v_a = 15$  V has been applied?
- (c)** Find the transfer function between the applied voltage  $v_a$  and the shaft angle  $\theta_m$ .
- (d)** Suppose feedback is added to the system in part (c) so it becomes a position servo device such that the applied voltage is given by

$$v_a = K(\theta_r - \theta_m)$$

where  $K$  is the feedback gain. Find the transfer function between  $\theta_r$  and  $\theta_m$ .

- (e)** What is the maximum value of  $K$  that can be used if an overshoot  $M < 16\%$  is desired?
- (f)** What values of  $K$  will provide a rise time of less than 5.2 sec? (Ignore the  $M_p$  constraint.)
- (g)** Use Matlab to plot the step response of the position servo system for values of the gain  $K = 0.6, 1$ , and  $2$ . Find the overshoot and rise time for each of the three step responses by examining your plots. Are the plots consistent with your calculations in parts (e) and (f)?

- 3.35** You wish to control the elevation of the satellite-tracking antenna shown in Fig. 3.60 and Fig. 3.61. The antenna and drive parts have a moment of inertia  $J$  and a damping  $B$ ; these arise to some extent from bearing

**Figure 3.60**

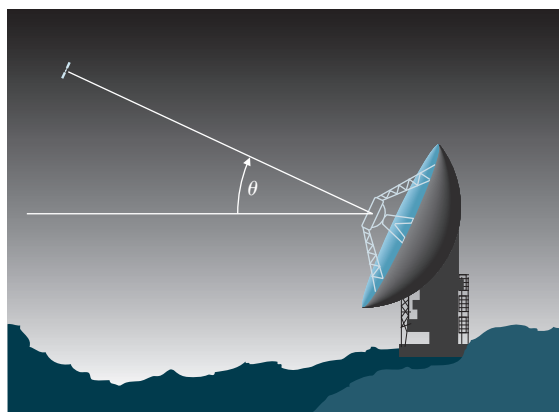
Satellite-tracking antenna

Source:

fstockfoto/Shutterstock

**Figure 3.61**

Schematic of antenna for Problem 3.35



and aerodynamic friction, but mostly from the back emf of the DC drive motor. The equations of motion are

$$J\ddot{\theta} + B\dot{\theta} = T_c,$$

where  $T_c$  is the torque from the drive motor. Assume

$$J = 600,000 \text{ kg}\cdot\text{m}^2 \quad B = 20,000 \text{ N}\cdot\text{m}\cdot\text{sec.}$$

- (a) Find the transfer function between the applied torque  $T_c$  and the antenna angle  $\theta$ .
- (b) Suppose the applied torque is computed so  $\theta$  tracks a reference command  $\theta_r$  according to the feedback law

$$T_c = K(\theta_r - \theta),$$

where  $K$  is the feedback gain. Find the transfer function between  $\theta_r$  and  $\theta$ .

- (c) What is the maximum value of  $K$  that can be used if you wish to have an overshoot  $M_p < 10\%$ ?
- (d) What values of  $K$  will provide a rise time of less than 80 sec? (Ignore the  $M_p$  constraint.)

- (e) Use Matlab to plot the step response of the antenna system for  $K = 200, 400, 1000$ , and  $2000$ . Find the overshoot and rise time of the four step responses by examining your plots. Do the plots to confirm your calculations in parts (c) and (d)?

- 3.36 Show that the second-order system

$$\ddot{y} + 2\zeta\omega_n\dot{y} + \omega_n^2 y = 0, \quad y(0) = y_0, \quad \dot{y}(0) = 0,$$

has the initial condition response

$$y(t) = y_0 \frac{e^{-\sigma t}}{\sqrt{1 - \zeta^2}} \sin(\omega_d t + \cos^{-1} \zeta).$$

Prove that, for the underdamped case ( $\zeta < 1$ ), the response oscillations decay at a predictable rate (see Fig. 3.62) called the **logarithmic decrement**,  $\delta$ .

$$\begin{aligned} \delta &= \ln \frac{y_0}{y_1} = \ln e^{\sigma \tau_d} = \sigma \tau_d = \frac{2\pi\zeta}{\sqrt{1 - \zeta^2}} \\ &\cong \ln \frac{\Delta y_1}{y_1} \cong \ln \frac{\Delta y_i}{y_i}, \end{aligned}$$

where

$$\tau_d = \frac{2\pi}{\omega_d} = \frac{2\pi}{\omega_n \sqrt{1 - \zeta^2}},$$

is the damped natural period of vibration. The damping coefficient in terms of the logarithmic decrement is then

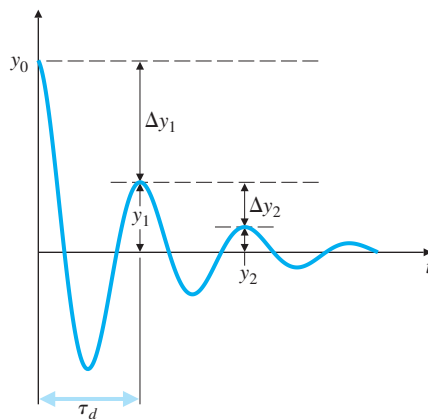
$$\zeta = \frac{\delta}{\sqrt{4\pi^2 + \delta^2}}.$$

### Problems for Section 3.5: Effects of Zeros and Additional Poles

- 3.37 In aircraft control systems, an ideal pitch response ( $q_o$ ) versus a pitch command ( $q_c$ ) is described by the transfer function

$$\frac{Q_o(s)}{Q_c(s)} = \frac{\tau \omega_n^2 (s + \frac{1}{\tau})}{s^2 + 2\zeta\omega_n s + \omega_n^2}.$$

**Figure 3.62**  
Definition of  
logarithmic decrement



The actual aircraft response is more complicated than this ideal transfer function; nevertheless, the ideal model is used as guide for autopilot design. Assume that  $t_r$  is the desired rise time and

$$\omega_n = \frac{1.789}{t_r},$$

$$\frac{1}{\tau} = \frac{2}{t_r},$$

$$\zeta = 0.89.$$

Show that this ideal response possesses fast transient response with minimal overshoot by plotting the step response for  $t_r = 1.0$  and  $1.5$  sec.

- 3.38** Approximate each of the following transfer functions with a second-order transfer function.

$$G_1(s) = \frac{(0.6s + 1)(0.35s + 1)}{(0.38s + 1)(0.55s + 1)(s^2 + 1.1s + 1)},$$

$$G_2(s) = \frac{(0.6s + 1)(0.35s + 1)}{(0.38s + 1)(0.55s + 1)(s^2 + 0.2s + 1)},$$

$$G_3(s) = \frac{(0.6s + 1)(-0.35s + 1)}{(0.08s + 1)(0.55s + 1)(s^2 + 1.1s + 1)},$$

$$G_4(s) = \frac{(0.6s + 1)(0.35s + 1)}{(0.08s + 1)(0.55s + 1)(s^2 + 1.1s + 1)},$$

$$G_5(s) = \frac{(0.01s + 1)(0.35s + 1)}{(0.38s + 1)(0.55s + 1)(s^2 + 1.1s + 1)}.$$

- 3.39** A system has the closed-loop transfer function

$$\frac{Y(s)}{R(s)} = T(s) = \frac{1500(s + 30)}{(s + 1.5)(s + 16)(s + 31)(s + 10s + 50)},$$

where  $R$  is a step of size 5.

- (a) Given an expression for the form of the output time history as a sum of terms showing the shape of each component of the response.

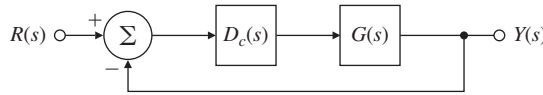
- (b) Given an estimate of the settling time of this step response.

- 3.40** Consider the system shown in Fig. 3.63, where

$$G(s) = \frac{1}{s(s + 3)} \quad \text{and} \quad D_c(s) = \frac{K(s + z)}{s + p}.$$

Find  $K$ ,  $z$ , and  $p$  so the closed-loop system has a 10% overshoot to a step input and a settling time of 1.5 sec (1% criterion).

**Figure 3.63**  
Unity feedback system  
for Problem 3.40



- △ **3.41** Sketch the step response of a system with the transfer function

$$G(s) = \frac{s/2 + 1}{(s/40 + 1)[(s/4)^2 + s/4 + 1]}.$$

Justify your answer on the basis of the locations of the poles and zeros. (Do not find the inverse Laplace transform.) Then compare your answer with the step response computed using Matlab.

- 3.42** A closed-loop transfer function is given:

$$H(s) = \frac{\left[\left(\frac{s}{10}\right)^2 + 0.1\left(\frac{s}{10}\right) + 1\right]\left[\frac{s}{2} + 1\right]\left[\frac{s}{0.1} + 1\right]}{\left[\left(\frac{s}{4}\right)^2 + \left(\frac{s}{4}\right) + 1\right]\left[\left(\frac{s}{10}\right)^2 + 0.09\left(\frac{s}{10}\right) + 1\right]\left[\frac{s}{0.02} + 1\right]}.$$

Estimate the percent overshoot,  $M_p$ , and the transient settling time,  $t_s$ , for this system.

- 3.43** A transfer function,  $G(s)$ , is given:

$$G(s) = \frac{\left[\left(\frac{s}{100}\right)^2 + 0.01\left(\frac{s}{100}\right) + 1\right]}{\left[\left(\frac{s}{10}\right)^2 + \left(\frac{s}{10}\right) + 1\right]\left[\frac{s}{5} + 1\right]\left[\left(\frac{s}{100}\right)^2 + 0.1\left(\frac{s}{100}\right) + 1\right]}.$$

If a step input is applied to this plant, what do you estimate the rise-time, settling time, and overshoot to be? Give a brief statement of your reasons in each case.

- 3.44** Three closed-loop transfer functions are given below.

$$\frac{Y(s)}{R(s)} = T_1(s) = \frac{2.7}{s^2 + 1.64s + 2.7},$$

$$\frac{Y(s)}{R(s)} = T_2(s) = \frac{2(s + 1.5)}{1.11(s^2 + 1.64s + 2.7)},$$

$$\frac{Y(s)}{R(s)} = T_3(s) = \frac{4.1}{(s + 1.5)(s^2 + 1.64s + 2.7)}.$$

In each case, provide estimates of the rise-time, settling time, and percent overshoot to a unit step input in  $r$ .

**3.45** Six transfer functions with unity DC gain are given below.

- (a) Which transfer function(s) will meet an overshoot specification of  $M_p \leq 17\%$ ?
- (b) Which transfer function(s) will meet a rise time specification of  $t_r \leq 0.3$  sec?
- (c) Which transfer function(s) will meet a settling time specification of  $t_s \leq 1.3$  sec?

$$G_1(s) = \frac{53.5}{(s^2 + 7.31s + 53.5)},$$

$$G_2(s) = \frac{313}{(s + 5.85)(s^2 + 7.31s + 53.5)},$$

$$G_3(s) = \frac{313}{0.5319(s + 11)(s^2 + 7.31s + 53.5)},$$

$$G_4(s) = \frac{5.9(s + 9.1)}{(s^2 + 7.31s + 53.5)},$$

$$G_5(s) = \frac{9.8(s^2 + 8s + 60)}{(s + 11)(s^2 + 7.31s + 53.5)},$$

$$G_6(s) = \frac{1.78(s^2 + 8s + 60)}{(s + 2)(s^2 + 7.31s + 53.5)}.$$

**3.46** Consider the following two nonminimum-phase systems:

$$G_1(s) = -\frac{2(s - 1)}{(s + 1)(s + 2)}, \quad (3.98)$$

$$G_2(s) = \frac{3(s - 1)(s - 2)}{(s + 1)(s + 2)(s + 3)}. \quad (3.99)$$

- (a) Sketch the unit-step responses for  $G_1(s)$  and  $G_2(s)$ , paying close attention to the transient part of the response.
- (b) Explain the difference in the behavior of the two responses as it relates to the zero locations.
- (c) Consider a stable, strictly proper system (that is,  $m$  zeros and  $n$  poles, where  $m < n$ ). Let  $y(t)$  denote the step response of the system. The step response is said to have an undershoot if it initially starts off in the “wrong” direction. Prove that a stable, strictly proper system has an undershoot if and only if its transfer function has an *odd* number of *real* RHP zeros.

**3.47** Find the relationships for the impulse response and the step response corresponding to Eq. (3.65) for the cases where

- (a) the roots are repeated.
- (b) the roots are both real. Express your answers in terms of hyperbolic functions ( $\sinh$ ,  $\cosh$ ) to best show the properties of the system response.
- (c) the value of the damping coefficient,  $\zeta$ , is negative.

**3.48** Consider the following second-order system with an extra pole:

$$H(s) = \frac{\omega_n^2 p}{(s + p)(s^2 + 2\zeta\omega_n s + \omega_n^2)}.$$

Show the unit-step response is

$$y(t) = 1 + Ae^{-pt} + Be^{-\sigma t} \sin(\omega_d t - \theta),$$

where

$$\begin{aligned} A &= \frac{-\omega_n^2}{\omega_n^2 - 2\xi\omega_np + p^2}, \\ B &= \frac{p}{\sqrt{(p^2 - 2\xi\omega_np + \omega_n^2)(1 - \xi^2)}}, \\ \theta &= \tan^{-1} \left( \frac{\sqrt{1 - \xi^2}}{-\xi} \right) + \tan^{-1} \left( \frac{\omega_n\sqrt{1 - \xi^2}}{p - \xi\omega_n} \right). \end{aligned}$$

- (a) Which term dominates  $y(t)$  as  $p$  gets large?
- (b) Give approximate values for  $A$  and  $B$  for small values of  $p$ .
- (c) Which term dominates as  $p$  gets small? (Small with respect to what?)
- (d) Using the preceding explicit expression for  $y(t)$  or the step command in Matlab, and assuming  $\omega_n = 1$  and  $\xi = 0.7$ , plot the step response of the preceding system for several values of  $p$  ranging from very small to very large. At what point does the extra pole cease to have much effect on the system response?

- 3.49** Consider the second-order unity DC gain system with an extra zero:

$$H(s) = \frac{\omega_n^2(s+z)}{z(s^2 + 2\xi\omega_ns + \omega_n^2)}.$$

- (a) Show that the unit-step response for the system is given by

$$y(t) = 1 - \frac{\sqrt{1 + \frac{\omega_n^2}{z^2} - \frac{2\xi\omega_n}{z}}}{\sqrt{1 - \xi^2}} e^{-\sigma t} \cos(\omega_d t + \beta_1),$$

where

$$\beta_1 = \tan^{-1} \left( \frac{-\xi + \frac{\omega_n}{z}}{\sqrt{1 - \xi^2}} \right).$$

- (b) Derive an expression for the step response overshoot,  $M_p$ , of this system.
  - (c) For a given value of overshoot,  $M_p$ , how do we solve for  $\xi$  and  $\omega_n$ ?
- 3.50** The block diagram of an autopilot designed to maintain the pitch attitude  $\theta$  of an aircraft is shown in Fig. 3.64. The transfer function relating the elevator angle  $\delta_e$  and the pitch attitude  $\theta$  is

$$\frac{\Theta(s)}{\delta_e(s)} = G(s) = \frac{50(s+1)(s+2)}{(s^2 + 5s + 40)(s^2 + 0.03s + 0.06)},$$

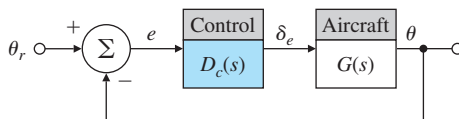
where  $\theta$  is the pitch attitude in degrees and  $\delta_e$  is the elevator angle in degrees. The autopilot controller uses the pitch attitude error  $e$  to adjust the elevator according to the transfer function

$$\frac{\delta_e(s)}{E(s)} = D_c(s) = \frac{K(s+3)}{s+10}.$$

Using Matlab, find a value of  $K$  that will provide an overshoot of less than 10% and a rise time faster than 0.5 sec for a unit-step change in  $\theta_r$ . After examining the step response of the system for various values of  $K$ , comment on the difficulty associated with meeting rise time and overshoot specifications for complicated systems.

**Figure 3.64**

Block diagram of autopilot for Problem 3.50



### Problems for Section 3.6: Stability

- 3.51** A measure of the degree of instability in an unstable aircraft response is the amount of time it takes for the *amplitude* of the time response to double (see Fig. 3.65), given some nonzero initial condition.

- (a) For a first-order system, show that the **time to double** is

$$\tau_2 = \frac{\ln 2}{p}$$

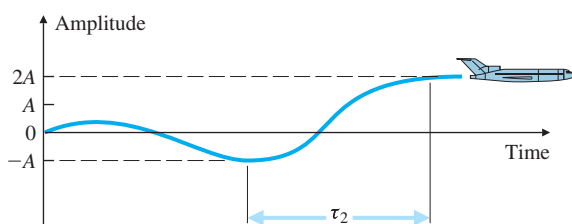
where  $p$  is the pole location in the RHP.

- (b) For a second-order system (with two complex poles in the RHP), show that

$$\tau_2 = \frac{\ln 2}{-\zeta \omega_n}.$$

**Figure 3.65**

Time to double



- 3.52** Suppose that unity feedback is to be applied around the listed open-loop systems. Use Routh's stability criterion to determine whether the resulting closed-loop systems will be stable.

(a)  $K(s)G(s) = \frac{5(s+5)}{(s+1)(s^3+2s+5)}$

(b)  $K(s)G(s) = \frac{0.2(s^2+0.95s+0.11)}{s(s^2+0.36s+0.72)}$

(c)  $K(s)G(s) = \frac{(s^3+15.5s^2+12.2s+100)}{(s+1)^2(47.7s^3+23.4s^2+20.3s+1)}$

- 3.53** Use Routh's stability criterion to determine how many roots with positive real parts the following equations have:

(a)  $s^4 + 5.2s^3 + 18.9s^2 + 43.2s + 45.4$

- (b)  $s^5 + 0.102s^4 + 1.123s^3 + 0.686s^2 + 0.154s + 2$   
 (c)  $s^4 + 152s^3 + 12s^2 - 1932s - 4921$   
 (d)  $99s^3 - s^2 - 6s - 7$   
 (e)  $s^4 + 8s^2 + 36$

- 3.54** Find the range of  $K$  for which all the roots of the following polynomial are in the LHP:

$$s^5 + 5s^4 + 10s^3 + 10s^2 + 5s + K = 0.$$

Use Matlab to verify your answer by plotting the roots of the polynomial in the  $s$ -plane for various values of  $K$ .

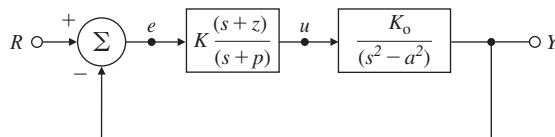
- 3.55** The transfer function of a typical tape-drive system is given by

$$KG(s) = \frac{K(s+6)}{s[(s+0.7)(s+1.2)(s^2+0.8s+6)]},$$

where time is measured in milliseconds. Using Routh's stability criterion, determine the range of  $K$  for which this system is stable when the characteristic equation is  $1 + KG(s) = 0$ .

- 3.56** Consider the closed-loop magnetic levitation system shown in Fig. 3.66. Determine the conditions on the system parameters ( $a$ ,  $K$ ,  $z$ ,  $p$ ,  $K_o$ ) to guarantee closed-loop system stability.

**Figure 3.66**  
Magnetic levitation  
system for Problem 3.56



- 3.57** Consider the system shown in Fig. 3.67.

- (a) Compute the closed-loop characteristic equation.  
 (b) For what values of  $(T, A)$  is the system stable? Hint: An approximate answer may be found using

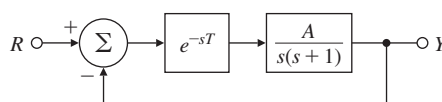
$$e^{-Ts} \cong 1 - Ts,$$

or

$$e^{-Ts} \cong \frac{1 - \frac{T}{2}s}{1 + \frac{T}{2}s},$$

for the pure delay. As an alternative, you could use the computer Matlab (Simulink) to simulate the system or to find the roots of the system's characteristic equation for various values of  $T$  and  $A$ .

**Figure 3.67**  
Control system for  
Problem 3.57



- 3.58** Modify the Routh criterion so that it applies to the case in which all the poles are to be the left  $-\alpha$  when  $\alpha > 0$ . Apply the modified test to the polynomial

$$s^3 + (0.5 + K)s^2 + (1 + 2K)s + 3K = 0,$$

finding those values of  $K$  for which all poles have a real part less than  $-0.7$ .

- 3.59** Suppose the characteristic polynomial of a given closed-loop system is computed to be

$$s^4 + (11 + K_2)s^3 + (121 + K_1)s^2 + (K_1 + K_1 K_2 + 110K_2 + 210)s + 11K_1 + 100 = 0.$$

Find constraints on the two gains  $K_1$  and  $K_2$  that guarantee a stable closed-loop system, and plot the allowable region(s) in the  $(K_1, K_2)$  plane. You may wish to use the computer to help solve this problem.

- 3.60** Overhead electric power lines sometimes experience a low-frequency, high-amplitude vertical oscillation, or **gallop**, during winter storms when the line conductors become covered with ice. In the presence of wind, this ice can assume aerodynamic lift and drag forces that result in a gallop up to several meters in amplitude. Large-amplitude gallop can cause clashing conductors and structural damage to the line support structures caused by the large dynamic loads. These effects in turn can lead to power outages. Assume the line conductor is a rigid rod, constrained to vertical motion only, and suspended by springs and dampers as shown in Fig. 3.68. A simple model of this conductor galloping is

$$m\ddot{y} + \frac{D(\alpha)\dot{y} - L(\alpha)v}{(\dot{y}^2 + v^2)^{1/2}} + T\left(\frac{n\pi}{\ell}\right)y = 0,$$

where

$m$  = mass of conductor,

$y$  = conductor's vertical displacement,

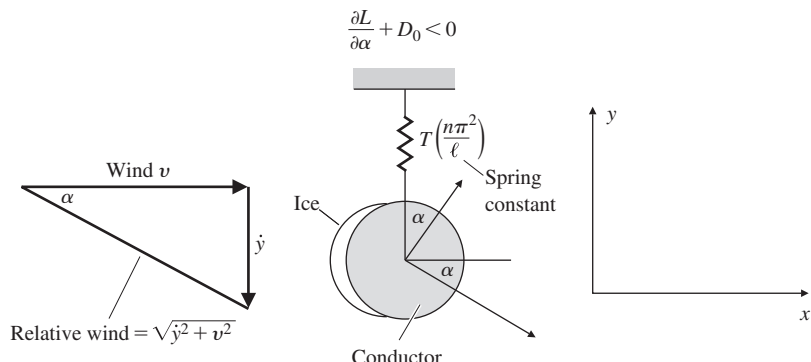
$D$  = aerodynamic drag force,

$L$  = aerodynamic lift force,

$v$  = wind velocity,

$\alpha$  = aerodynamic angle of attack =  $-\tan^{-1}(\dot{y}/v)$ ,

**Figure 3.68**  
Electric power-line conductor



$T$  = conductor tension,

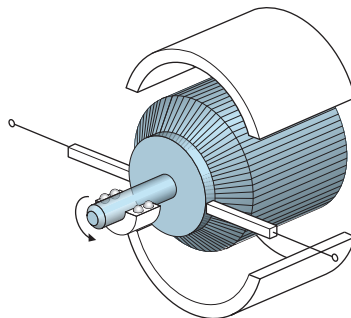
$n$  = number of harmonic frequencies,

$\ell$  = length of conductor.

Assume  $L(0) = 0$  and  $D(0) = D_0$  (a constant), and linearize the equation around the value  $y = \dot{y} = 0$ . Use Routh's stability criterion to show that galloping can occur whenever

$$\frac{\partial L}{\partial \alpha} + D_0 < 0.$$

# A First Analysis of Feedback



## A Perspective on the Analysis of Feedback

In the next three chapters, we will introduce three techniques for the design of controllers. Before doing so, it is useful to develop the assumptions to be used and to derive the equations that are common to each of the design approaches we will describe. As a general observation, the dynamics of systems to which control is applied are nonlinear and very complex. However, in this initial analysis, we assume the plant to be controlled as well as the controller can be represented as dynamic systems which are linear and time invariant (LTI). We also assume they have only single inputs and single outputs, for the most part, and may thus be represented by simple scalar transfer functions. As we mentioned in Chapter 1, our basic concerns for control are **stability**, **tracking**, **regulation**, and **sensitivity**. The goal of the analysis in this chapter is to revisit each of these requirements in a linear dynamic setting, and to develop equations that will expose constraints placed on the controller and identify elementary objectives to be suggested for the controllers.

The two fundamental structures for realizing controls are the open-loop structure, as shown in Fig. 4.1, and the closed-loop structure, also known as feedback control, as shown in Fig. 4.2. The definition of open-loop control is that there is no closed signal path whereby the output influences the control effort. In the structure shown in Fig. 4.1, the controller transfer function modifies the

reference input signal before it is applied to the plant. This controller might cancel the unwanted dynamics of the plant and replace them with the more desirable dynamics of the controller. In other cases, open-loop control actions are taken on the plant as the environment changes, actions that are calibrated to give a good response but are not dependent on measuring the actual response. An example of this would be an aircraft autopilot whose parameters are changed with altitude or speed but not by feedback of the craft's motion. Feedback control, on the other hand, uses a sensor to measure the output and by feedback indirectly modifies the dynamics of the system. Although it is possible that feedback may cause an otherwise stable system to become unstable (a vicious circle), feedback gives the designer more flexibility and a preferable response to each of our objectives when compared to open-loop control.

## Chapter Overview

The chapter begins with consideration of the basic equations of a simple open-loop structure and of an elementary feedback structure. In Section 4.1, the equations for the two structures are presented in general form and compared in turn with respect to **stability**, **tracking**, **regulation**, and **sensitivity**. In Section 4.2, the steady-state errors in response to polynomial inputs will be analyzed in more detail. As part of the language of steady-state performance, control systems are assigned a **type** number according to the maximum degree of the input polynomial for which the steady-state error is a finite constant. For each type, an appropriate error constant is defined, which allows the designer to easily compute the size of this error.

Although Maxwell and Routh developed a mathematical basis for assuring stability of a feedback system, design of controllers from the earliest days was largely trial and error based on experience. From this tradition, there emerged an almost universal controller, the **proportional–integral–derivative (PID)** structure considered in Section 4.3. This device has three elements: a **P**roportional term to close the feedback loop, an **I**ntegral term to assure zero error to constant reference and disturbance inputs, and a **D**erivative term to improve (or realize!) stability and good dynamic response. In this section, these terms will be considered and their respective effects illustrated. As part of the evolution of the PID controller design, a major step was the development of a simple procedure for selecting the three parameters, a process called “tuning the controller.” Ziegler and Nichols developed and published a set of experiments to be run, characteristics to be measured, and tuning values to be recommended as a result. These procedures are discussed in this section. The concept of feedforward control by plant model inversion will be discussed in Section 4.4. In the optional Section 4.5, a brief introduction to

the increasingly common digital implementation of controllers will be given. Sensitivity of time response to parameter changes will be discussed in Section 4.6. Finally, Section 4.7 will provide the historical perspective for the material in this chapter.

## 4.1 The Basic Equations of Control

We begin by collecting a set of equations and transfer functions that will be used throughout the rest of the text. For the open-loop system of Fig. 4.1, if we take the disturbance to be at the input of the plant, the output is given by

$$Y_{ol} = GD_{ol}R + GW, \quad (4.1)$$

and the error, the difference between reference input and system output, is given by

$$E_{ol} = R - Y_{ol}, \quad (4.2)$$

$$= R - [GD_{ol}R + GW], \quad (4.3)$$

$$= [1 - GD_{ol}]R - GW. \quad (4.4)$$

The open-loop transfer function in this case is  $T_{ol}(s) = G(s)D_{ol}(s)$ .

For feedback control, Fig. 4.2 gives the basic unity feedback structure of interest. There are three external inputs: the reference,  $R$ , which the output is expected to track; the plant disturbance,  $W$ , which the control is expected to counteract so it does not disturb the output; and the sensor noise,  $V$ , which the controller is supposed to ignore.

For the feedback block diagram of Fig. 4.2, the equations for the output and the control are given by the superposition of the responses to the three inputs individually, as follows:

$$Y_{cl} = \frac{GD_{cl}}{1 + GD_{cl}}R + \frac{G}{1 + GD_{cl}}W - \frac{GD_{cl}}{1 + GD_{cl}}V, \quad (4.5)$$

$$U = \frac{D_{cl}}{1 + GD_{cl}}R - \frac{GD_{cl}}{1 + GD_{cl}}W - \frac{D_{cl}}{1 + GD_{cl}}V. \quad (4.6)$$

**Figure 4.1**

Open-loop system showing reference,  $R$ , control,  $U$ , disturbance,  $W$ , and output  $Y$

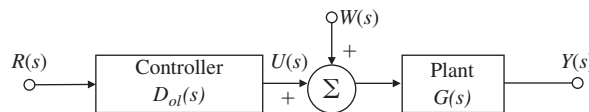
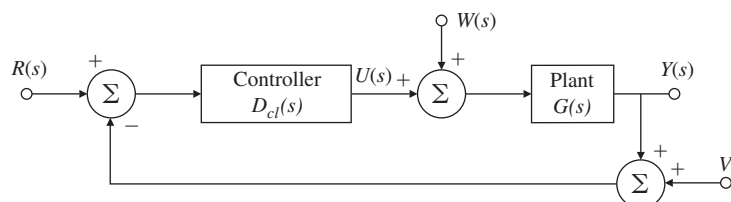


**Figure 4.2**

Closed-loop system showing the reference,  $R$ , control,  $U$ , disturbance,  $W$ , output,  $Y$ , and sensor noise,  $V$



Perhaps more important than these is the equation for the error,  $E_{cl} = R - Y_{cl}$ .

$$E_{cl} = R - \left[ \frac{GD_{cl}}{1 + GD_{cl}} R + \frac{G}{1 + GD_{cl}} W - \frac{GD_{cl}}{1 + GD_{cl}} V \right], \quad (4.7)$$

$$= \frac{1}{1 + GD_{cl}} R - \frac{G}{1 + GD_{cl}} W + \frac{GD_{cl}}{1 + GD_{cl}} V. \quad (4.8)$$

We can rewrite Eqs. (4.5), (4.6) and (4.8) in a nice compact form:

$$Y_{cl} = \mathcal{T}R + GSW - \mathcal{T}V, \quad (4.9)$$

$$U = D_{cl}\mathcal{S}R - \mathcal{T}W - D_{cl}\mathcal{S}V, \quad (4.10)$$

$$E_{cl} = \mathcal{S}R - GSW + \mathcal{T}V, \quad (4.11)$$

where we define the two transfer functions

$$\mathcal{S} = \frac{1}{1 + GD_{cl}}, \quad (4.12)$$

and

$$\mathcal{T} = \frac{GD_{cl}}{1 + GD_{cl}}. \quad (4.13)$$

In this case, the closed-loop transfer function is  $T_{cl} = \mathcal{T} = \frac{GD_{cl}}{1 + GD_{cl}}$ .

The significance of these two transfer functions will become apparent later in this section.

With these equations, we will explore the four basic objectives of **stability**, **tracking**, **regulation**, and **sensitivity** for both the open-loop and the closed-loop cases.

#### 4.1.1 Stability

As we discussed in Chapter 3, the requirement for stability is simply stated: All poles of the transfer function must be in the left half-plane (LHP). In the open-loop case described by Eq. (4.1), these are the poles of  $GD_{ol}$ . To see the restrictions this requirement places on the controller, we define the polynomials  $a(s)$ ,  $b(s)$ ,  $c(s)$ , and  $d(s)$  so  $G(s) = \frac{b(s)}{a(s)}$  and  $D_{ol}(s) = \frac{c(s)}{d(s)}$ . Therefore  $GD_{ol} = \frac{bc}{ad}$ . With these definitions, the stability requirement is that neither  $a(s)$  nor  $d(s)$  may have roots in the right half-plane (RHP). A naive engineer might believe that if the plant is unstable with  $a(s)$  having a root in the RHP, the system might be made stable by canceling this pole with a zero of  $c(s)$ . However, the unstable pole remains and the slightest noise or disturbance will cause the output to grow until stopped by saturation or system failure. Likewise, if the plant shows poor response because of a zero of  $b(s)$  in the RHP, an attempt to fix this by cancellation using a root of  $d(s)$  will similarly result in an unstable system. We conclude that an open-loop structure *cannot* be used to make an unstable plant to be stable, and therefore cannot be used if the plant is already unstable.

For the feedback system, from Eq. (4.8), the system poles are the roots of  $1 + GD_{cl} = 0$ . Again using the polynomials defined above, the system characteristic equation is

$$1 + GD_{cl} = 0, \quad (4.14)$$

$$1 + \frac{b(s)c(s)}{a(s)d(s)} = 0, \quad (4.15)$$

$$a(s)d(s) + b(s)c(s) = 0. \quad (4.16)$$

From this equation, it is clear that the feedback case grants considerably more freedom to the controller design than does the open-loop case. However, one must still avoid unstable cancellations. For example, if the plant is unstable and therefore  $a(s)$  has a root in the RHP, we might cancel this pole by putting a zero of  $c(s)$  at the same place. However, Eq. (4.16) shows that as a result, the unstable pole remains a pole of the system and this method will not work. However, unlike the open-loop case, having a pole of  $a(s)$  in the RHP does NOT prevent the design of a feedback controller that will make the system stable. For example, in Chapter 2, we derived the transfer function for the inverted pendulum, which, for simple values, might be  $G(s) = \frac{1}{s^2 - 1}$  for which we have  $b(s) = 1$  and  $a(s) = s^2 - 1 = (s + 1)(s - 1)$ . Suppose we try  $D_{cl}(s) = \frac{K(s+\gamma)}{s+\delta}$ . The characteristic equation that results for the system is

$$(s + 1)(s - 1)(s + \delta) + K(s + \gamma) = 0. \quad (4.17)$$

This is the problem that Maxwell faced in his study of governors: Under what conditions on the parameters will all the roots of this equation be in the LHP? The problem was solved by Routh. In our case, a simple solution is to take  $\gamma = 1$  and the common (stable) factor cancels. Note the cancellation is fine in this case, because  $(s + 1)$  is a stable pole. The resulting second-order equation can be easily solved to place the remaining two poles at any point desired.

**Exercise.** If we wish to force the characteristic equation to be  $s^2 + 2\zeta\omega_n s + \omega_n^2 = 0$ , solve for  $K$  and  $\delta$  in terms of  $\zeta$  and  $\omega_n$ .

### 4.1.2 Tracking

The tracking problem is to cause the output to follow the reference input as closely as possible. In the open-loop case, if the plant is stable and has neither poles nor zeros in the RHP, then in principle, the controller can be selected to cancel the transfer function of the plant and substitute whatever desired transfer function the engineer wishes. This apparent freedom, however, comes with three caveats. First, in order to physically build it, the controller transfer function must be *proper*, meaning that it cannot be given more zeros than it has poles. Second, the engineer must not get greedy and request an unrealistically fast design. This entire analysis has been based on the assumption that the plant is linear and a demand for a fast response will demand large inputs to the plant,

inputs that will be sure to saturate the system if the demand is too great. Again, it is the responsibility of the engineer to know the limits of the plant and to set the desired overall transfer function to a reasonable value with this knowledge. Third and finally, although one can, in principle, stably cancel *any* pole in the LHP, the next section on sensitivity faces up to the fact that the plant transfer function is subject to change and if one tries to cancel a pole that is barely inside the LHP, there is a good chance of disaster as that pole moves a bit and exposes the system response to unacceptable transients.

**Exercise.** For a plant having the transfer function  $G(s) = \frac{1}{s^2+3s+9}$  it is proposed to use a controller in a unity feedback system and having the transfer function  $D_{cl}(s) = \frac{c_2s^2+c_1s+c_0}{s(s+d_1)}$ . Solve for the parameters of this controller so the closed loop will have the characteristic equation  $(s + 6)(s + 3)(s^2 + 3s + 9) = 0$ .<sup>1</sup>

{Answer:  $c_2 = 18$ ,  $c_1 = 54$ ,  $c_0 = 162$ ,  $d_1 = 9$ }.

**Exercise.** Show that if the reference input to the system of the above exercise is a step of amplitude  $A$ , the steady-state error will be zero.

### 4.1.3 Regulation

The problem of regulation is to keep the error small when the reference is at most a constant setpoint and disturbances are present. A quick look at the open-loop block diagram reveals that the controller has no influence at all on the system response to either of the disturbances,  $w$ , or  $v$ , so this structure is useless for regulation. We turn to the feedback case. From Eq. (4.8), we find a conflict between  $w$  and  $v$  in the search for a good controller. For example, the term giving the contribution of the plant disturbance to the system error is  $\frac{G}{1+GD_{cl}}W$ . To select  $D_{cl}$  to make this term small, we should make  $D_{cl}$  as large as possible and infinite if that is feasible. On the other hand, the error term for the sensor noise is  $\frac{GD_{cl}}{1+GD_{cl}}V$ . In this case, unfortunately, if we select  $D_{cl}$  to be large, the transfer function tends to unity and the sensor noise is not reduced at all! What are we to do? The resolution of the dilemma is to observe that each of these terms is a function of frequency so one of them can be large for some frequencies and small for others. With this in mind, we also note the frequency content of most plant disturbances occurs at very low frequencies and, in fact, the most common case is a bias, which is all at zero frequency! On the other hand, a good sensor will have no bias and can be constructed to have very little noise over the entire range of low frequencies of interest. Thus, using this information, we design the controller transfer function to be large at the low frequencies, where it will reduce the effect of  $w$ , and we make it small at the higher frequencies, where it will reduce the effects of the high frequency sensor noise. The control engineer must determine in each case the best

---

<sup>1</sup>This process is called “pole placement,” a technique to be discussed in Chapter 7.

place on the frequency scale to make the crossover from amplification to attenuation.

**Exercise.** Show that if  $w$  is a constant bias and if  $D_{cl}$  has a pole at  $s = 0$ , then the error due to this bias will be zero. However, show that if  $G$  has a pole at zero, the error due to this bias will not be zero.

#### 4.1.4 Sensitivity

Suppose a plant is designed with gain  $G$  at a particular frequency, but in operation it changes to be  $G + \delta G$ . This represents a fractional or percent change of gain of  $\delta G/G$ . For the purposes of this analysis, we set the frequency at zero and take the open-loop controller gain to be fixed at  $D_{ol}(0)$ . In the open-loop case, the nominal overall gain is thus  $T_{ol} = GD_{ol}$ , and with the perturbed plant gain, the overall gain would be

$$T_{ol} + \delta T_{ol} = D_{ol}(G + \delta G) = D_{ol}G + D_{ol}\delta G = T_{ol} + D_{ol}\delta G.$$

Therefore, the gain change is  $\delta T_{ol} = D_{ol}\delta G$ . The sensitivity,  $S_G^T$ , of a transfer function,  $T_{ol}$ , to a plant gain,  $G$ , is *defined* to be the ratio of the fractional change in  $T_{ol}$  defined as  $\frac{\delta T_{ol}}{T_{ol}}$  to the fractional change in  $G$ . In equation form,

$$S_G^T = \frac{\frac{\delta T_{ol}}{T_{ol}}}{\frac{\delta G}{G}}, \quad (4.18)$$

$$= \frac{G}{T_{ol}} \frac{\delta T_{ol}}{\delta G}. \quad (4.19)$$

Substituting the values, we find that

$$\frac{\delta T_{ol}}{T_{ol}} = \frac{D_{ol}\delta G}{D_{ol}G} = \frac{\delta G}{G}. \quad (4.20)$$

This means that a 10% error in  $G$  would yield a 10% error in  $T_{ol}$ . In the open-loop case, therefore, we have computed that  $S = 1$ .

From Eq. (4.5), the same change in  $G$  in the feedback case yields the new steady-state feedback gain as

$$T_{cl} + \delta T_{cl} = \frac{(G + \delta G)D_{cl}}{1 + (G + \delta G)D_{cl}},$$

where  $T_{cl}$  is the closed-loop gain. We can compute the sensitivity of this closed-loop gain directly using differential calculus. The closed-loop steady-state gain is

$$T_{cl} = \frac{GD_{cl}}{1 + GD_{cl}}.$$

The first-order variation is proportional to the derivative and is given by

$$\delta T_{cl} = \frac{dT_{cl}}{dG}\delta G.$$

The general expression for sensitivity from Eq. (4.18) is given by

$$\begin{aligned}\mathcal{S}_G^{T_{cl}} &\triangleq \text{sensitivity of } T_{cl} \text{ with respect to } G, \\ \mathcal{S}_G^{T_{cl}} &\triangleq \frac{G}{T_{cl}} \frac{dT_{cl}}{dG},\end{aligned}\quad (4.21)$$

so

$$\begin{aligned}\mathcal{S}_G^{T_{cl}} &= \frac{G}{GD_{cl}/(1+GD_{cl})} \frac{(1+GD_{cl})D_{cl} - D_{cl}(GD_{cl})}{(1+GD_{cl})^2}, \\ &= \frac{1}{1+GD_{cl}}.\end{aligned}\quad (4.22)$$

### Advantage of feedback

In feedback control, the error in the overall transfer function gain is less sensitive to variations in the plant gain by a factor of  $\mathcal{S} = \frac{1}{1+GD_{cl}}$  compared to errors in open-loop control gain.

If the gain is such that  $1+GD_{cl} = 100$ , a 10% change in plant gain  $G$  will cause only a 0.1% change in the steady-state gain. The open-loop controller is 100 times more sensitive to gain changes than the closed-loop system with loop gain of 100. The example of the unity feedback case is so common that we will refer to the result of Eq. (4.22) simply as the **sensitivity**,  $\mathcal{S}$ , without subscripts or superscripts. Hence, we define the **sensitivity function** for a feedback system as

$$\mathcal{S} \triangleq \frac{1}{1+GD_{cl}}. \quad (4.23)$$

Its usefulness will be demonstrated for dynamic feedback controller design in Chapter 6. The **complementary sensitivity function** is defined as (a fancy alternative name for the closed-loop transfer function!)

$$\mathcal{T} \triangleq \frac{GD_{cl}}{1+GD_{cl}} = 1 - \mathcal{S}. \quad (4.24)$$

These two transfer functions are very important for feedback control design, and they illustrate the fundamental relationship of feedback systems (that also will be explored further in Chapter 6)

$$\mathcal{S} + \mathcal{T} = 1. \quad (4.25)$$

The results in this section so far have been computed under the assumption of the steady-state error in the presence of constant inputs, either reference or disturbance. Very similar results can be obtained for the steady-state behavior in the presence of a sinusoidal reference or disturbance signal. This is important because there are times when such

### A fundamental relationship of feedback systems

---

<sup>2</sup>Bode, who developed the theory of sensitivity as well as many other properties of feedback, defined sensitivity as  $S = 1 + GD_{cl}$ , the inverse of our choice.

signals naturally occur as, for example, with a disturbance of 60 Hz due to power-line interference in an electronic system. The concept is also important because more complex signals can be described as containing sinusoidal components over a band of frequencies and analyzed using superposition of one frequency at a time. For example, it is well known that human hearing is restricted to signals in the frequency range of about 60 to 15,000 Hz. A feedback amplifier and loudspeaker system designed for high-fidelity sound must accurately track any sinusoidal (pure tone) signal in this range. If we take the controller in the feedback system shown in Fig. 4.2 to have the transfer function  $D_{cl}(s)$ , and we take the process to have the transfer function  $G(s)$ , then the steady-state open-loop gain at the sinusoidal signal of frequency  $\omega_o$  will be  $|G(j\omega_o)D_{cl}(j\omega_o)|$ , and the error of the feedback system will be

$$|E(j\omega_o)| = |R(j\omega_o)| \left| \frac{1}{1 + G(j\omega_o)D_{cl}(j\omega_o)} \right|. \quad (4.26)$$

Thus, to reduce errors to 1% of the input at the frequency  $\omega_o$ , we must make  $|1 + GD_{cl}| \geq 100$  or, effectively,  $|G(j\omega_o)D_{cl}(j\omega_o)| \gtrsim 100$  and a good audio amplifier must have this loop gain over the range  $2\pi 60 \leq \omega \leq 2\pi 15,000$ . We will revisit this concept in Chapter 6 as part of the design based on frequency-response techniques.

### The Filtered Case

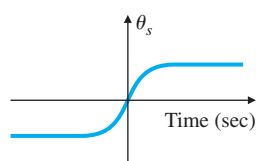
For the case where there is a non-unity pre filter  $F(s)$  following the reference input,  $R(s)$ , and non-unity sensor dynamics  $H(s)$ , the equations for the system output and the various sensitivity functions need to be re-derived. The details are available in Appendix W4.1.4.1 online at [www.pearsonglobaleditions.com](http://www.pearsonglobaleditions.com).

## 4.2 Control of Steady-State Error to Polynomial Inputs: System Type

In studying the regulator problem, the reference input is taken to be a constant. It is also the case that the most common plant disturbance is a constant bias. Even in the general tracking problem, the reference input is often constant for long periods of time or may be adequately approximated as if it were a polynomial in time, usually one of low degree. For example, when an antenna is tracking the elevation angle to a satellite, the time history as the satellite approaches overhead is an S-shaped curve as sketched in Fig. 4.3. This signal may be approximated

**Figure 4.3**

Signal for satellite tracking



by a linear function of time (called a ramp function or velocity input) for a significant time relative to the speed of response of the servomechanism. As another example, the position control of an elevator has a ramp function reference input, which will direct the elevator to move with constant speed until it comes near the next floor. In rare cases, the input can even be approximated over a substantial period as having a constant acceleration. Consideration of these cases leads us to consider steady-state errors in stable systems with polynomial inputs.

As part of the study of steady-state errors to polynomial inputs, a terminology has been developed to express the results. For example, we classify systems as to “**type**” according to the degree of the polynomial that they can reasonably track. For example, a system that can track a polynomial of degree 1 with a constant error is called *Type I*. Also, to quantify the tracking error, several “**error constants**” are defined. In all of the following analysis, it is assumed that the systems are stable, else the analysis makes no sense at all.

### System type

#### 4.2.1 System Type for Tracking

In the unity feedback case shown in Fig. 4.2, the system error is given by Eq. (4.8). If we consider tracking the reference input alone and set  $W = V = 0$ , then the equation for the error is simply

$$E = \frac{1}{1 + GD_{cl}} R = \mathcal{S}R, \quad \text{where } \mathcal{S} = \frac{1}{1 + GD_{cl}}. \quad (4.27)$$

To consider polynomial inputs, we let  $r(t) = t^k/k!1(t)$  for which the transform is  $R = \frac{1}{s^{k+1}}$ . We take a mechanical system as the basis for a generic reference nomenclature, calling step inputs for which  $k = 0$  “position” inputs, ramp inputs for which  $k = 1$  are called “velocity” inputs, and if  $k = 2$ , the inputs are called “acceleration” inputs, regardless of the units of the actual signals. Application of the Final Value Theorem to the error formula gives the result

$$\lim_{t \rightarrow \infty} e(t) = e_{ss} = \lim_{s \rightarrow 0} sE(s), \quad (4.28)$$

$$= \lim_{s \rightarrow 0} \frac{1}{1 + GD_{cl}} R(s), \quad (4.29)$$

$$= \lim_{s \rightarrow 0} \frac{1}{1 + GD_{cl}} \frac{1}{s^{k+1}}. \quad (4.30)$$

We consider first a system for which  $GD_{cl}$  has no pole at the origin, that is, no integrator, and a unit-step input for which  $R(s) = 1/s$ . Thus,  $r(t)$  is a polynomial of degree 0. In this case, Eq. (4.30) reduces to

$$e_{ss} = \lim_{s \rightarrow 0} \frac{1}{1 + GD_{cl}} \frac{1}{s}, \quad (4.31)$$

$$\frac{e_{ss}}{r_{ss}} = \frac{e_{ss}}{1} = e_{ss} = \frac{1}{1 + GD_{cl}(0)}, \quad (4.32)$$

where  $r_{ss} = \lim_{t \rightarrow \infty} r(t) = 1$ . We define this system to be *Type 0* and we define the constant,  $GD_{cl}(0) \triangleq K_p$ , as the “*position error constant*.” Notice the above equation yields the relative error and if the input should be a polynomial of degree higher than 1, the resulting error would grow without bound. A polynomial of degree 0 is the highest degree a system of *Type 0* can track at all. If  $GD_{cl}(s)$  has one pole at the origin, we could continue this line of argument and consider first-degree polynomial inputs but it is quite straightforward to evaluate Eq. (4.30) in a general setting. For this case, it is necessary to describe the behavior of the controller and plant as  $s$  approaches 0. For this purpose, we collect all the terms except the pole ( $s$ ) at the origin into a function  $GD_{clo}(s)$ , which is finite at  $s = 0$  so that we can define the constant  $GD_{clo}(0) = K_n$  and write the loop transfer function as

$$GD_{cl}(s) = \frac{GD_{clo}(s)}{s^n}. \quad (4.33)$$

For example, if  $GD_{cl}$  has no integrator, then  $n = 0$ . If the system has one integrator, then  $n = 1$ , and so forth. Substituting this expression into Eq. (4.30),

$$e_{ss} = \lim_{s \rightarrow 0} s \frac{1}{1 + \frac{GD_{clo}(s)}{s^n}} \frac{1}{s^{k+1}}, \quad (4.34)$$

$$= \lim_{s \rightarrow 0} \frac{s^n}{s^n + K_n} \frac{1}{s^k}. \quad (4.35)$$

From this equation, we can see at once that if  $n > k$  then  $e = 0$  and if  $n < k$  then  $e \rightarrow \infty$ . If  $n = k = 0$ , then  $e_{ss} = \frac{1}{1+K_0}$  and if  $n = k \neq 0$ , then  $e_{ss} = 1/K_n$ . As we discussed above, if  $n = k = 0$ , the input is a zero-degree polynomial otherwise known as a step or position, the constant  $K_0$  is called the “*position constant*” written as  $K_p$ , and the system is classified as “*Type 0*.” If  $n = k = 1$ , the input is a first-degree polynomial otherwise known as a ramp or velocity input and the constant  $K_1$  is called the “*velocity constant*” written as  $K_v$ . This system is classified “*Type 1*” (read “type one”). In a similar way, systems of *Type 2* and higher types may be defined. A clear picture of the situation is given by the plot in Fig. 4.4 for a system of Type 1 having a ramp reference input. The error between input and output of size  $\frac{1}{K_v}$  is clearly marked.

Using Eq. (4.33), these results can be summarized by the following equations:

$$K_p = \lim_{s \rightarrow 0} GD_{cl}(s), \quad n = 0, \quad (4.36)$$

$$K_v = \lim_{s \rightarrow 0} s GD_{cl}(s), \quad n = 1, \quad (4.37)$$

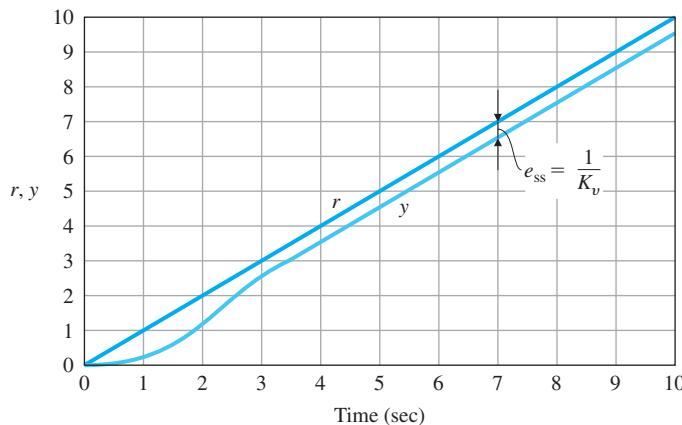
$$K_a = \lim_{s \rightarrow 0} s^2 GD_{cl}(s), \quad n = 2. \quad (4.38)$$

The type information can also be usefully gathered in a table of error values as a function of the degree of the input polynomial and the type of the system, as shown in Table 4.1.

### Error constants

**Figure 4.4**

Relationship between ramp response and  $K_v$

**TABLE 4.1****Errors as a Function of System Type**

Type Input	Step (position)	Ramp (velocity)	Parabola (acceleration)
Type 0	$\frac{1}{1 + K_p}$	$\infty$	$\infty$
Type 1	0	$\frac{1}{K_v}$	$\infty$
Type 2	0	0	$\frac{1}{K_a}$

**EXAMPLE 4.1***System Type for Speed Control*

Determine the system type and the relevant error constant for speed control with proportional feedback given by  $D_{cl}(s) = k_P$ . The plant transfer function is  $G = \frac{A}{\tau s + 1}$ .

**Solution.** In this case,  $GD_{cl} = \frac{k_P A}{\tau s + 1}$  and applying Eq. (4.36), we see  $n = 0$  as there is no pole at  $s = 0$ . Thus, the system is Type 0, and the error constant is a position constant given by  $K_p = k_P A$ .

**EXAMPLE 4.2***System Type Using Integral Control*

Determine the system type and the relevant error constant for the speed-control example with proportional plus integral control having controller given by  $D_{cl} = k_P + k_I/s$ . The plant transfer function is  $G = \frac{A}{\tau s + 1}$ .

**Solution.** In this case, the loop transfer function is  $GD_{cl}(s) = \frac{A(k_P s + k_I)}{s(\tau s + 1)}$  and, as a unity feedback system with a single pole at  $s = 0$ , the system is immediately seen as Type 1. The velocity constant is given by Eq. (4.37) to be  $K_v = \lim_{s \rightarrow 0} sGD_{cl}(s) = Ak_I$ .

**Robustness of system type**

The definition of system type helps us to identify quickly the ability of a system to track polynomials. In the unity feedback structure, if the process parameters change without removing the pole at the origin in a Type 1 system, the velocity constant will change but the system will still have zero steady-state error in response to a constant input and will still be Type 1. Similar statements can be made for systems of Type 2 or higher. Thus, we can say that system type is a **robust property** with respect to parameter changes in the unity feedback structure. Robustness is a major reason for preferring unity feedback over other kinds of control structure.

Another form of the formula for the error constants can be developed directly in terms of the closed-loop transfer function  $\mathcal{T}(s)$ . From Fig. 4.5, the transfer function including a sensor transfer function is

$$\frac{Y(s)}{R(s)} = \mathcal{T}(s) = \frac{GD_c}{1 + GD_c H}, \quad (4.39)$$

and the system error is

$$E(s) = R(s) - Y(s) = R(s) - \mathcal{T}(s)R(s). \quad (4.40)$$

The reference-to-error transfer function is thus

$$\frac{E(s)}{R(s)} = 1 - \mathcal{T}(s), \quad (4.41)$$

and the system error transform is

$$E(s) = [1 - \mathcal{T}(s)] R(s). \quad (4.42)$$

We assume the conditions of the Final Value Theorem are satisfied, namely that all poles of  $sE(s)$  are in the LHP. In that case, the steady-state error is given by applying the Final Value Theorem to get

$$e_{ss} = \lim_{t \rightarrow \infty} e(t) = \lim_{s \rightarrow 0} sE(s) = \lim_{s \rightarrow 0} s[1 - \mathcal{T}(s)]R(s). \quad (4.43)$$

If the reference input is a polynomial of degree  $k$ , the error transform becomes

$$E(s) = \frac{1}{s^{k+1}} [1 - \mathcal{T}(s)], \quad (4.44)$$

and the steady-state error is given again by the Final Value Theorem:

$$e_{ss} = \lim_{s \rightarrow 0} s \frac{1 - \mathcal{T}(s)}{s^{k+1}} = \lim_{s \rightarrow 0} \frac{1 - \mathcal{T}(s)}{s^k}. \quad (4.45)$$

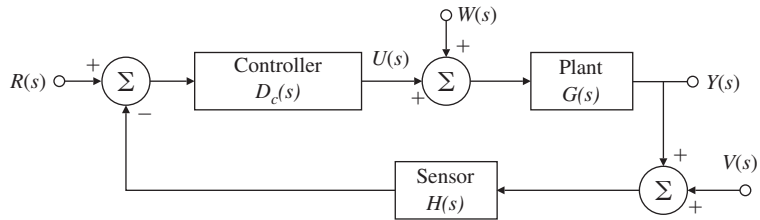
As before, the result of evaluating the limit in Eq. (4.45) can be zero, a nonzero constant, or infinite, and if the solution to Eq. (4.45) is a nonzero constant, the system is referred to as *Type k*. Notice a system of Type 1 or higher has a closed-loop DC gain of 1.0, which means that  $T(0) = 1$  in these cases.

**EXAMPLE 4.3***System Type for a Servo with Tachometer Feedback*

Consider an electric motor position control problem including a non-unity feedback system caused by having a tachometer fixed to the motor

**Figure 4.5**

Closed-loop system with sensor dynamics.  $R$  = reference,  $U$  = control,  $Y$  = output,  $V$  = sensor noise



shaft and its voltage (which is proportional to shaft speed) is fed back as part of the control as shown in Fig. 4.5. The parameters are

$$G(s) = \frac{1}{s(\tau s + 1)},$$

$$D_c(s) = k_P,$$

$$H(s) = 1 + k_t s.$$

Determine the system type and relevant error constant with respect to reference inputs.

**Solution.** The system error is

$$\begin{aligned} E(s) &= R(s) - Y(s), \\ &= R(s) - \mathcal{T}(s)R(s), \\ &= R(s) - \frac{D_c(s)G(s)}{1 + H(s)D_c(s)G(s)}R(s), \\ &= \frac{1 + (H(s) - 1)D_c(s)G(s)}{1 + H(s)D_c(s)G(s)}R(s). \end{aligned}$$

The steady-state system error from Eq. (4.45) is

$$e_{ss} = \lim_{s \rightarrow 0} sR(s) [1 - \mathcal{T}(s)].$$

For a polynomial reference input,  $R(s) = 1/s^{k+1}$  and hence

$$\begin{aligned} e_{ss} &= \lim_{s \rightarrow 0} \frac{[1 - \mathcal{T}(s)]}{s^k} = \lim_{s \rightarrow 0} \frac{1}{s^k} \frac{s(\tau s + 1) + (1 + k_t s - 1)k_P}{s(\tau s + 1) + (1 + k_t s)k_P}, \\ &= 0, \quad k = 0, \\ &= \frac{1 + k_t k_P}{k_P}, \quad k = 1; \end{aligned}$$

therefore the system is Type 1 and the velocity constant is  $K_v = \frac{k_P}{1 + k_t k_P}$ . Notice if  $k_t > 0$ , perhaps to improve stability or dynamic response, the velocity constant is smaller than with simply the unity feedback value of  $k_P$ . The conclusion is that if tachometer feedback is used to improve dynamic response, the steady-state error is usually increased, that is, there is a trade-off between improving stability and reducing steady-state error.

### 4.2.2 System Type for Regulation and Disturbance Rejection

A system can also be classified with respect to its ability to reject polynomial disturbance inputs in a way analogous to the classification scheme based on reference inputs. The transfer function from the disturbance input  $W(s)$  to the error  $E(s)$  is

$$\frac{E(s)}{W(s)} = -\frac{Y(s)}{W(s)} = T_w(s), \quad (4.46)$$

because, if the reference is equal to zero, the output is the error. In a similar way as for reference inputs, the system is Type 0 if a step disturbance input results in a nonzero constant steady-state error, and is Type 1 if a ramp disturbance input results in a steady-state value of the error that is a nonzero constant, and so on. In general, following the same approach used in developing Eq. (4.35), we assume a constant  $n$  and a function  $T_{o,w}(s)$  can be defined with the properties that  $T_{o,w}(0) = 1/K_{n,w}$  and the disturbance-to-error transfer function can be written as

$$T_w(s) = s^n T_{o,w}(s). \quad (4.47)$$

Then, the steady-state error to a disturbance input, which is a polynomial of degree  $k$ , is

$$\begin{aligned} y_{ss} &= \lim_{s \rightarrow 0} \left[ s T_w(s) \frac{1}{s^{k+1}} \right], \\ &= \lim_{s \rightarrow 0} \left[ T_{o,w}(s) \frac{s^n}{s^k} \right]. \end{aligned} \quad (4.48)$$

From Eq. (4.48), if  $n > k$ , then the error is zero and if  $n < k$ , then the error is unbounded. If  $n = k$ , then the system is type  $k$  and the error is given by  $1/K_{n,w}$ .

#### EXAMPLE 4.4

##### *System Type for a DC Motor Position Control*

Consider the simplified model of a DC motor in unity feedback as shown in Fig. 4.6, where the disturbance torque is labeled  $W(s)$ . This case was considered in Example 2.11.

(a) Use the controller

$$D_c(s) = k_P, \quad (4.49)$$

and determine the system type and steady-state error properties with respect to disturbance inputs.

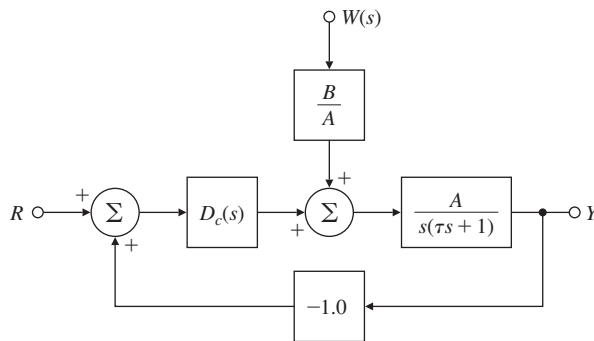
(b) Let the controller transfer function be given by

$$D_c(s) = k_P + \frac{k_I}{s}, \quad (4.50)$$

and determine the system type and the steady-state error properties for disturbance inputs.

**Figure 4.6**

DC motor with unity feedback



**Solution.** (a) The closed-loop transfer function from  $W$  to  $E$  (where  $R = 0$ ) is

$$\begin{aligned} T_w(s) &= -\frac{B}{s(\tau s + 1) + Ak_p}, \\ &= s^0 T_{o,w}, \\ n &= 0, \\ K_{o,w} &= -\frac{Ak_p}{B}. \end{aligned}$$

Applying Eq. (4.48), we see that the system is Type 0 and the steady-state error to a unit-step torque input is  $e_{ss} = -B/Ak_p$ . From the earlier section, this system is seen to be Type 1 for reference inputs, and illustrates that system type can be different for different inputs to the same system.

(b) For this controller the disturbance error transfer function is

$$T_w(s) = -\frac{Bs}{s^2(\tau s + 1) + (k_p s + k_I)A}, \quad (4.51)$$

$$n = 1, \quad (4.52)$$

$$K_{n,w} = -\frac{Ak_I}{B}, \quad (4.53)$$

therefore the system is Type 1, and the error to a unit-ramp disturbance input will be

$$e_{ss} = -\frac{B}{Ak_I}. \quad (4.54)$$

### Truxal's Formula

Truxal (1955) derived a formula for the velocity constant of a Type 1 system in terms of the closed-loop poles and zeros. See Appendix W4.2.2.1 online at [www.pearsonglobaleditions.com](http://www.pearsonglobaleditions.com).

## 4.3 The Three-Term Controller: PID Control

In later chapters, we will study three general analytic and graphical design techniques based on the root locus, the frequency response, and the state-space formulation of the equations. Here, we describe a control method having an older pedigree that was developed through long experience and by trial and error. Starting with simple proportional feedback, engineers early discovered integral control action as a means of eliminating bias offset. Then, finding poor dynamic response in many cases, an “anticipatory” term based on the derivative was added. The result is called the three-term or PID controller, and has the transfer function

$$D_c(s) = k_P + \frac{k_I}{s} + k_D s, \quad (4.55)$$

where  $k_P$  is the proportional term,  $k_I$  is the integral term, and  $k_D$  is the derivative term. We will discuss them in turn.

### 4.3.1 Proportional Control (P)

When the feedback control signal is linearly proportional to the system error

$$u(t) = k_P e(t), \quad (4.56)$$

#### Proportional control

we call the result **proportional feedback**. Hence, the control signal is related to the system error instantaneously. This was the case for the feedback used in the controller of speed in Section 4.1, for which the controller transfer function is

$$\frac{U(s)}{E(s)} = D_{cl}(s) = k_P. \quad (4.57)$$

The controller is purely algebraic with no dynamics and  $k_P$  is called the *proportional gain*. We can view the proportional controller as an amplifier with a “knob” that can be adjusted up or down. If the plant is second order, as, for example, for a motor with non-negligible inductance,<sup>3</sup> then the plant transfer function can be written as

$$G(s) = \frac{A}{s^2 + a_1 s + a_2}. \quad (4.58)$$

In this case, the characteristic equation for the closed-loop system with proportional control is

$$1 + k_P G(s) = 0, \quad (4.59)$$

that results in

$$s^2 + a_1 s + a_2 + k_P A = 0. \quad (4.60)$$

The designer can control the constant term,  $(a_2 + k_P A)$ , in this equation by selecting  $k_P$ , which determines the natural frequency but cannot control the damping term  $a_1$  since it is independent of  $k_P$ . The system is

---

<sup>3</sup>See Section 2.3.

Type 0 and if  $k_P$  is made large to get adequately small steady-state error, the damping may be much too low for satisfactory transient response with proportional control alone. To illustrate these features of proportional control, assume we have the plant  $G(s)$  under proportional control as shown in Fig. 4.2 and assume  $a_1 = 1.4$ ,  $a_2 = 1$ , and  $A = 1$ . The proportional controller is indicated by Eq. (4.57). Figure 4.7 shows the closed-loop response of

$$\frac{Y(s)}{R(s)} = T(s) = \frac{k_P G(s)}{1 + k_P G(s)}, \quad (4.61)$$

for a unit-step command input,  $r = 1(t)$ , with  $k_P = 1.5$  and  $k_P = 6$ . The output,  $y$ , of the system exhibits a steady-state tracking error that decreases as the proportional feedback gain is increased. Furthermore, the response also clearly exhibits a decrease in damping as the gain is increased and an increase in the speed of response. Using the Final Value Theorem would also show that the steady-state error decreases as the gain,  $k_P$ , is increased as well as the fact that the control value,  $u(t)$ , reaches a steady non zero value.

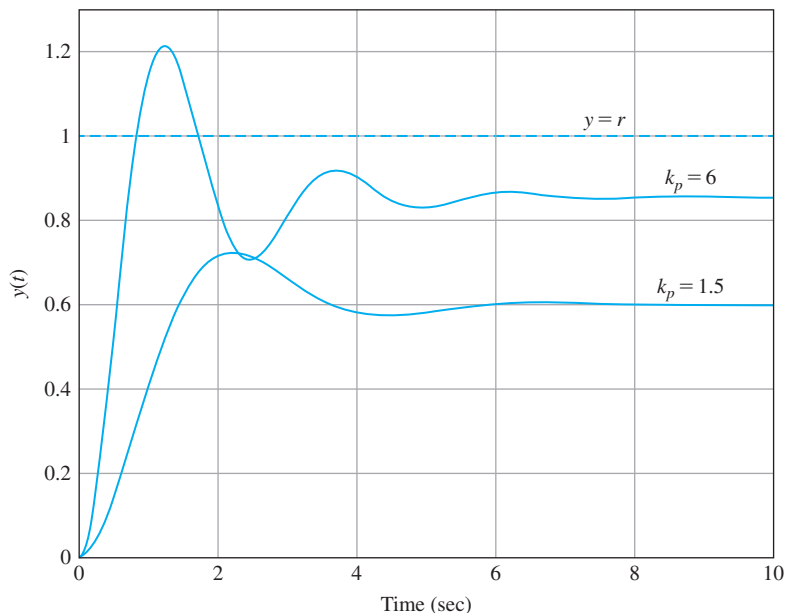
The output and the control signal due to a disturbance are given by

$$\frac{Y(s)}{W(s)} = \frac{G(s)}{1 + k_P G(s)}, \quad \frac{U(s)}{W(s)} = -\frac{k_P G(s)}{1 + k_P G(s)}.$$

By comparing the closed-loop transfer functions between the disturbance response and the command response, it can be seen that a step disturbance,  $w$ , will also yield a steady-state tracking error and control value in a similar manner to the reference input shown in Fig. 4.7.

**Figure 4.7**

Illustration of the steady-state tracking error and the effect of the different proportional feedback gain values on the system damping



The error due to the disturbance will also decrease as the gain,  $k_P$ , is increased and the damping will degrade.

For systems beyond second order, the situation is more complicated than that illustrated above. The damping of some of the poles might increase while decreasing in others as the gain is increased. Also, a higher gain will increase the speed of response but typically at the cost of a larger transient overshoot and less overall damping. For systems of large order, increasing proportional gain will typically lead to instability for a high enough gain. Any Type 0 system with proportional control will have a nonzero steady-state offset in response to a constant reference input, and will not be capable of completely rejecting a constant disturbance input. One way to improve the steady-state accuracy of control without using extremely high proportional gain is to introduce integral control, which we will discuss next.

### 4.3.2 Integral Control (I)

#### Integral control

When a feedback control signal is linearly proportional to the integral of the system error, we call the result **integral feedback**. The goal of integral control is to minimize the steady-state tracking error and the steady-state output response to disturbances. This control law is of the form

$$u(t) = k_I \int_{t_0}^t e(\tau) d\tau, \quad (4.62)$$

and  $k_I$  is called the *integral gain*. This means that the control signal at each instant of time is a summation of all past values of the tracking error; therefore, the control action is based on the “history” of the system error. Figure 4.8 illustrates that the control signal at any instant of time is proportional to the area under the system error curve (shown here for time  $t_1$ ). The controller becomes

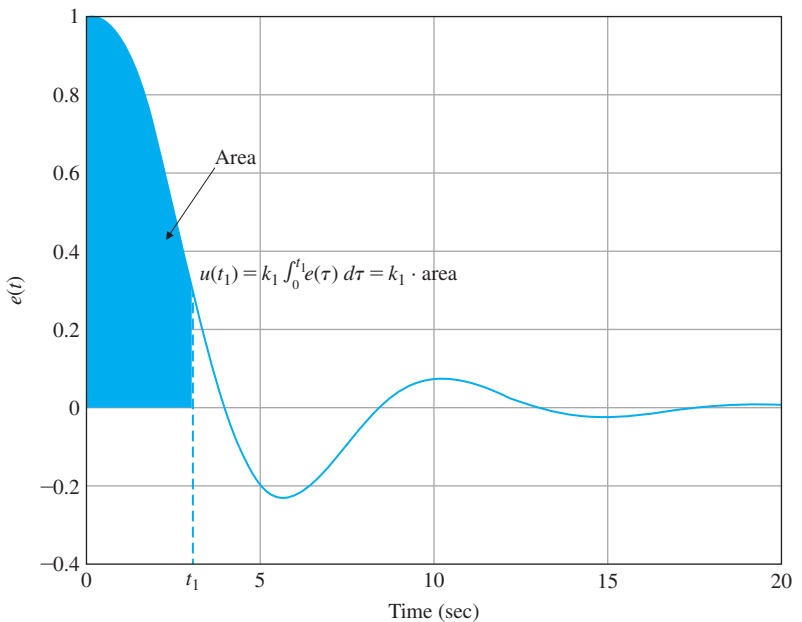
$$\frac{U(s)}{E(s)} = D_{cl}(s) = \frac{k_I}{s}, \quad (4.63)$$

which is *dynamic* and we see it has infinite gain at DC (that is, for  $s = 0$ ). Hence, we would certainly expect superior performance in the steady-state from such a controller. That is indeed the case as illustrated shortly. This feedback has the primary virtue that it can provide a finite value of control with zero system error. This comes about because  $u(t)$  is a function of all past values of  $e(t)$  rather than just the current value, as in the proportional case. This feature means that constant disturbances can be canceled with zero error because  $e(t)$  no longer has to be finite to produce a control signal that will counteract the constant disturbance.

Again, assume we have the plant  $G(s)$  under integral control as shown in Fig. 4.2, and  $G(s)$  is for the same motor that we used in Section 4.3.1. This simple system can be stabilized by integral control alone. From Fig. 4.2 and using the controller in Eq. (4.63), we see the tracking error, the control signal, and the output due to a *reference input* are given by

**Figure 4.8**

Integral control is based on the history of the system error



$$\frac{E(s)}{R(s)} = \frac{1}{1 + \frac{k_I}{s} G(s)} = \frac{s}{s + k_I G(s)}, \quad \frac{U(s)}{R(s)} = \frac{\frac{k_I}{s}}{1 + \frac{k_I}{s} G(s)} = \frac{k_I}{s + k_I G(s)}, \quad (4.64)$$

$$\frac{Y(s)}{R(s)} = T(s) = \frac{\frac{k_I}{s} G(s)}{1 + \frac{k_I}{s} G(s)} = \frac{k_I G(s)}{s + k_I G(s)}. \quad (4.65)$$

Now assume a unit-step reference input  $r(t) = 1(t)$  with  $R(s) = 1/s$ . From Eqs. (4.64) and (4.65) and using the Final Value Theorem (noting  $G(0) = 1$ ), we have

$$y(\infty) = \frac{k_I G(0)}{0 + k_I G(0)} = 1, \quad e(\infty) = \frac{0}{0 + k_I G(0)} = 0, \quad (4.66)$$

$$u(\infty) = \frac{k_I}{0 + k_I G(0)} = G(0)^{-1} = 1. \quad (4.67)$$

Note the steady-state tracking error will be zero no matter what the value of  $k_I$  is, whereas there was always a tracking error with the proportional controller no matter what the value of  $k_P$  was. The integral gain  $k_I$  can be selected purely to provide an acceptable dynamic response; however, typically it will cause instability if raised sufficiently high. Note also the steady-state control is a constant and is equal to the inverse DC gain of the plant, which makes a lot of sense intuitively.

The output and the control signal due to a *disturbance input* are given by

$$\frac{Y(s)}{W(s)} = \frac{sG(s)}{s + k_I G(s)}, \quad \frac{U(s)}{W(s)} = -\frac{k_I G(s)}{s + k_I G(s)}. \quad (4.68)$$

Now assume a unit-step disturbance input  $w(t) = 1(t)$  with  $W(s) = 1/s$ . From Eq. (4.68) and using the Final Value Theorem we have

$$y(\infty) = \frac{0 \cdot G(0)}{0 + k_I G(0)} = 0, \quad u(\infty) = -\frac{k_I G(0)}{0 + k_I G(0)} = -1. \quad (4.69)$$

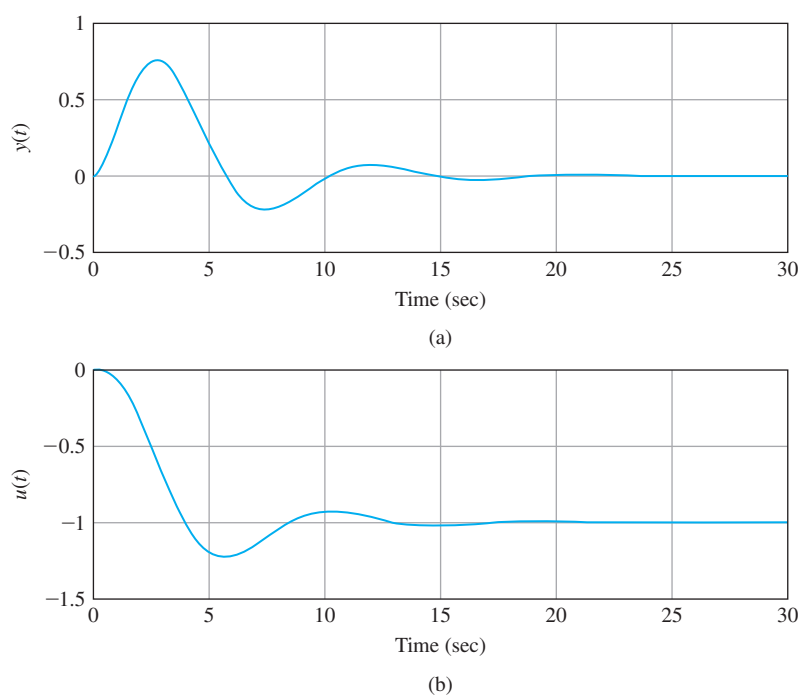
These two equations show a zero steady-state error in the output and a final value of the control signal that cancels the disturbance exactly. Figure 4.9 illustrates the responses for  $k_I = 0.5$ . The conclusion is that in this case, integral feedback results in zero steady-state output error in both tracking and disturbance rejection. Furthermore, plant parameter changes can be tolerated; that is, the results above are independent of the plant parameter values. Also, regardless of the value of the integral gain,  $k_I$ , the asymptotic tracking and disturbance rejection properties are preserved, provided that the closed-loop system remains stable. These properties of integral control are referred to as *robust*. The addition of integral control to the  $G(s)$  above caused the closed-loop system to become Type 1 and those features will occur for any Type 1 system. However, as already discussed in Section 4.2.2, Type 1 systems do have a constant tracking error to a ramp reference input as will this example of integral control.

Given these remarkable properties of integral control, it is certainly worth the additional cost in implementation complexity. Whenever an actuator is used that can saturate (which is almost always the case), extra care is required in implementing integral control. The controller must

### Robustness property of integral control

**Figure 4.9**

Illustration of constant disturbance rejection property of integral control: (a) system output; (b) control effort



be augmented with an anti-windup feature to deal with the actuator saturation (see Chapter 9).

### 4.3.3 Derivative Control (D)

#### Derivative control

The final term in the classical controller is **derivative feedback**, also called *rate feedback*. The goal of derivative feedback is to improve closed-loop system stability as well as speeding up the transient response and reducing overshoot. Therefore, whenever increased stability is desired, the use of derivative feedback is called for. In derivative feedback, the control law is

$$u(t) = k_D \dot{e}(t), \quad (4.70)$$

where  $k_D$  is the *derivative gain* and the control signal is proportional to the rate of change (or derivative) of the system error for which the  $D_{cl}(s)$  in Fig. 4.2 becomes

$$\frac{U(s)}{E(s)} = D_{cl}(s) = k_D s. \quad (4.71)$$

Derivative control is almost never used by itself; it is usually augmented by proportional control. The key reason is that the derivative does not supply information on the desired end state. In addition, if  $e(t)$  were to remain constant, the output of a derivative controller would be zero and a proportional or integral control would be needed to provide a control signal at this time. A key feature of derivative control is that derivative control “knows” the slope of the error signal, so it takes control action based on the trend in the error signal. Hence, it is said to have an “anticipatory” behavior. One disadvantage of derivative control is that it tends to amplify noise, a subject that will be discussed in more depth in Chapter 6.

An important effect of the derivative term is that it gives a sharp response to suddenly changing signals. Because of this, the derivative term is sometimes introduced into the feedback path as shown in Fig. 4.10(a) in order to eliminate an excessive response to a step in the reference input. This could be either a part of the standard controller, or could describe a velocity sensor such as a tachometer on the shaft of a motor. The closed-loop characteristic equation is the same as if the term were in the forward path as given by Eq. (4.55) and drawn in Fig. 4.10(b). It is important to notice the *zeros* from the reference to the output are different in the two cases. With the derivative in the feedback path, the reference is not differentiated, which is how the undesirable response to sudden changes is avoided.

### 4.3.4 Proportional Plus Integral Control (PI)

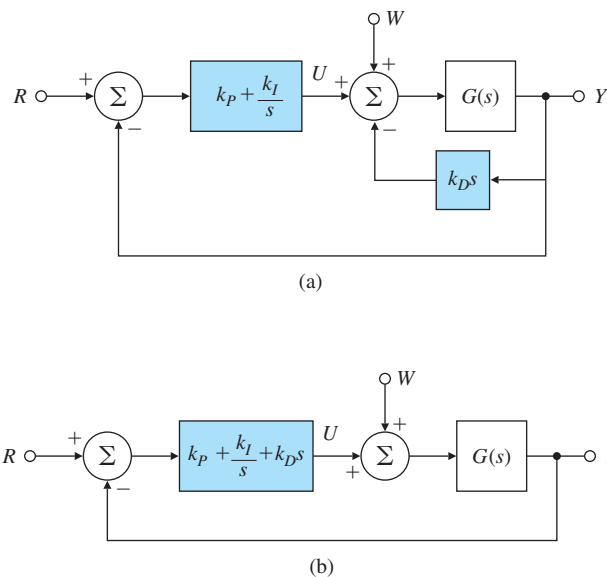
#### Proportional plus integral control

Adding an integral term to the proportional controller to achieve the lower steady-state errors results in the **proportional plus integral (PI)** control equation in the time domain:

$$u(t) = k_P e(t) + k_I \int_{t_0}^t e(\tau) d\tau, \quad (4.72)$$

**Figure 4.10**

Block diagram of the PID controller: (a) with the D-term in the feedback path; (b) with the D-term in the forward path



for which the  $D_{cl}(s)$  in Fig. 4.2 becomes

$$\frac{U(s)}{E(s)} = D_{cl}(s) = k_P + \frac{k_I}{s}. \quad (4.73)$$

Most controllers implemented in practice, if they have an integral term, will also have a proportional term. This combination generally allows for a faster response than a pure integral control alone. Introduction of the integral term raises the type to Type 1, and the system can therefore reject completely constant bias disturbances. If the system is second order or higher the use of PID control is required if we wish to have arbitrary dynamics.

## EXAMPLE 4.5

### *PI Control of a Thermal System<sup>4</sup>*

Consider the thermal system consisting of the lumped second-order model of two thermal masses connected by conduction, as shown in Figure 2.38 of Chapter 2. The transfer function from the heater to the sensed output was derived to be of the form

$$G(s) = \frac{K_o}{(\tau_1 s + 1)(\tau_2 s + 1)}$$

where

$$\tau_1 = \frac{C_1}{H_x + H_1}, \tau_2 = \frac{C_2}{H_x + H_1}, K_o = \frac{H_x}{(H_x + H_1)(H_x + H_2)}$$

---

<sup>4</sup>This Example was suggested by Dr. Jon L. Ebert.

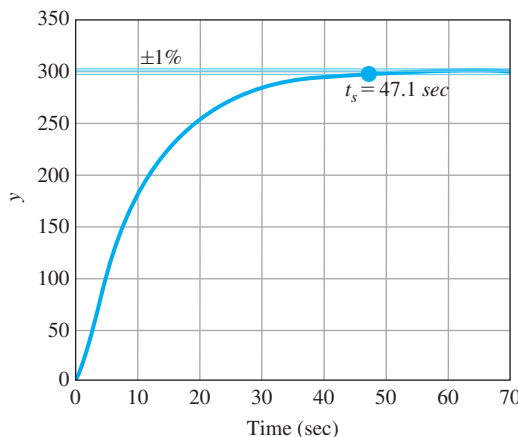
and we select realistic values for the system parameters so  $\tau_1 = 1$ ,  $\tau_2 = 10$ , and  $K_o = 1000$ . The goal is to design a PI controller to track the reference input temperature signal,  $r(t)$ , which is a ramp with a slope of  $30^\circ\text{C/sec}$  and a steady-state value of  $300^\circ\text{C}$  and a duration of 30 seconds as shown in Figure 4.11. It is desired that the system exhibit negligible overshoot. Robustness with respect to perturbations in system parameters  $K_o$ ,  $\tau_1$ , and  $\tau_2$  is also desired as usually the exact values of these parameters are not known. Explore the use of open-loop control, P control, and PI control to achieve the goal of tracking the reference signal accurately.

**Solution.** We will now discuss each controller design case separately.

**Open-loop Control:** One idea that comes to mind is to excite the system with an input step of size 0.3 since the DC gain of the system is 1000. The response of the open-loop system is shown in Figure 4.11 and exhibits a slow response with a settling time of  $t_s = 47.1$  sec and has zero steady-state error. The system could be controlled with an open-loop controller, but such a system is highly sensitive to errors in the plant gain. In this case, a 5% error in plant gain would result in a steady-state error of 5% in the output, which would typically be unacceptable.

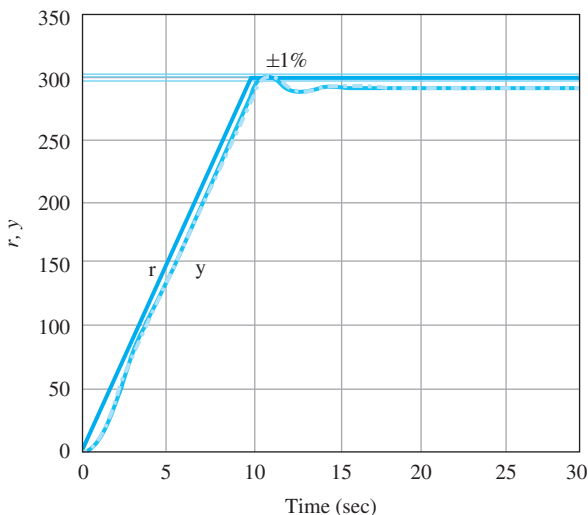
**P Control:** A proportional gain of  $k_P = 0.03$  corresponding to a closed-loop damping ratio of  $\zeta = 0.3$  results in a constant DC offset (bias) of  $10^\circ\text{C}$  as shown in Figure 4.12. Although the response is significantly faster than open-loop control, this level of offset is unacceptable in applications such as Rapid Thermal Processing (see Chapter 10). Fig. 4.12 shows the response for the nominal case as well as  $\pm 10\%$  of the gain value. The fact that the three responses are indistinguishable shows that gain changes for the feedback case have little effect and the system is robust. The associated control effort signals are shown in Figure 4.13.

**Figure 4.11**  
Open-loop step response

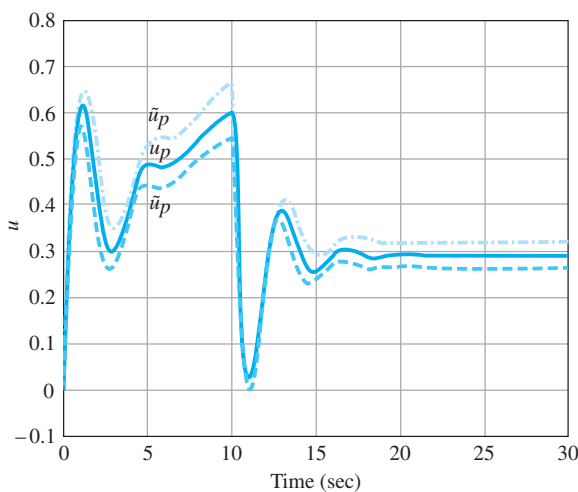


**Figure 4.12**

Closed-loop response  
for the P controller

**Figure 4.13**

Closed-loop control  
signals for the P  
controller



Note the fact that the effect of the gain changes are noticeable in the associated control signals in Fig. 4.13.

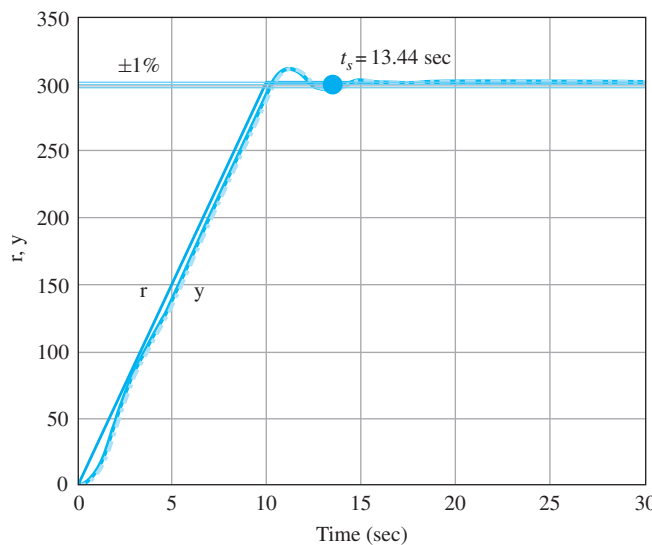
**PI Control:** Let us use the same proportional gain as before,  $k_P = 0.03$ , and choose an integral gain that is an order of magnitude lower,  $k_I = 0.003$  to obtain the PI controller

$$D_c(s) = 0.03 + \frac{0.003}{s}.$$

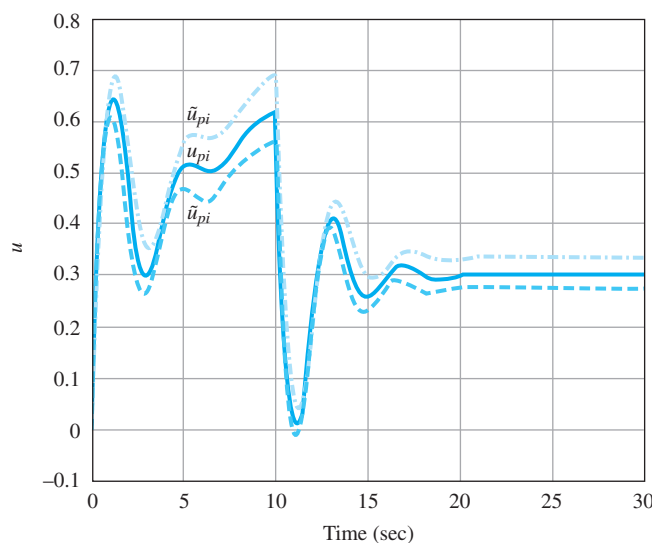
The response of the closed-loop PI-controlled system is shown in Figure 4.14 and the bias is eliminated as expected. The response settles at  $t_s = 13.44$  sec, but there is some overshoot. The system is also robust with respect to a  $\pm 10\%$  change in the gain,  $K_o$ , as shown in Figure 4.14. The associated control effort signals are shown in Figure 4.15. Note in this

**Figure 4.14**

Closed-loop response for the PI controller

**Figure 4.15**

Closed-loop control signals for the PI controller



case, the controller has a zero at -0.1 that cancels the open-loop stable pole of the plant at -0.1, effectively rendering the closed-loop system as second-order.

### 4.3.5 PID Control

Putting all the three terms together results in the **proportional plus integral plus derivative (PID)** control equation in the time domain:

PID control

$$u(t) = k_P e(t) + k_I \int_{t_0}^t e(\tau) d\tau + k_D \dot{e}(t), \quad (4.74)$$

for which the  $D_{cl}(s)$  in Fig. 4.2 becomes

$$\frac{U(s)}{E(s)} = D_{cl}(s) = k_P + \frac{k_I}{s} + k_D s. \quad (4.75)$$

To illustrate the effect of PID control, consider speed control but with the second-order plant as in Eq. (4.58). In that case, the characteristic equation from  $1 + GD_{cl} = 0$  becomes

$$\begin{aligned} s^2 + a_1 s + a_2 + A(k_P + \frac{k_I}{s} + k_D s) &= 0, \\ s^3 + a_1 s^2 + a_2 s + A(k_P s + k_I + k_D s^2) &= 0. \end{aligned} \quad (4.76)$$

Collecting like powers of  $s$  terms results in

$$s^3 + (a_1 + Ak_D)s^2 + (a_2 + Ak_P)s + Ak_I = 0. \quad (4.77)$$

The point here is that this equation, whose three roots determine the nature of the dynamic response of the system, has three free parameters in  $k_P$ ,  $k_I$ , and  $k_D$  and that by selection of these parameters, the roots can be uniquely and, in theory, arbitrarily determined. Without the derivative term, there would be only two free parameters, but with three roots, the choice of roots of the characteristic equation would be restricted. To illustrate the effect more concretely, a numerical example is useful.

## EXAMPLE 4.6

### PID Control of Motor Speed

Consider the DC motor speed control with parameters<sup>5</sup>

$$\begin{aligned} J_m &= 1.13 \times 10^{-2} & b &= 0.028 \text{ N}\cdot\text{m}\cdot\text{sec}/\text{rad}, & L_a &= 10^{-1} \text{ H}, \\ && \text{N}\cdot\text{m}\cdot\text{sec}^2/\text{rad}, && & \\ R_a &= 0.45 \Omega, & K_t &= 0.067 \text{ N}\cdot\text{m}/\text{amp}, & K_e &= 0.067 \text{ V}\cdot\text{sec}/\text{rad}. \end{aligned} \quad (4.78)$$

These parameters were defined in Example 2.15 in Chapter 2. Use the controller parameters

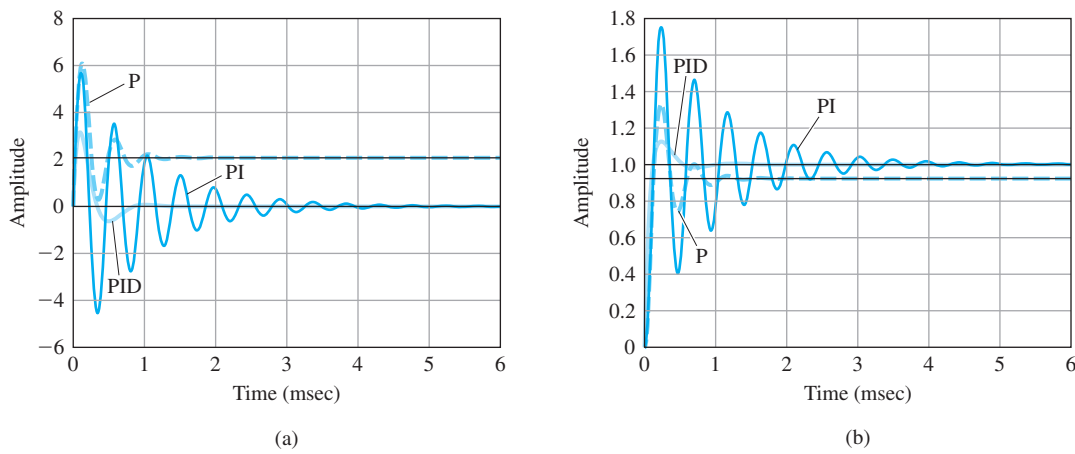
$$k_P = 3, \quad k_I = 15 \text{ sec}, \quad k_D = 0.3 \text{ sec} \quad (4.79)$$

and discuss the responses of this system to steps in a disturbance torque and steps in the reference input using the three different controllers: P, PI, and PID. Let the unused controller parameters be zero.

**Solution.** Figure 4.16(a) illustrates the effects of P, PI, and PID feedback on the step disturbance response of the system. Note adding

---

<sup>5</sup>These values have been scaled to measure time in milliseconds by multiplying the true  $L_a$  and  $J_m$  by 1000 each.

**Figure 4.16**

Responses of P, PI, and PID control to: (a) step disturbance input; (b) step reference input

the integral term increases the oscillatory behavior, but eliminates the steady-state error, and adding the derivative term reduces the oscillation while maintaining zero steady-state error. Figure 4.16(b) illustrates the effects of P, PI, and PID feedback on the step reference response with similar results. The step responses can be computed by forming the numerator and denominator coefficient vectors (in descending powers of  $s$ ) and using the step function in Matlab.

### EXAMPLE 4.7

#### *PI Control for a DC-DC Voltage Converter*

Consider the control of a DC-DC converter using the unity feedback structure as shown in Fig. 4.5 where

$$G(s) = V_{in} \frac{1}{LCs^2 + \frac{L}{R_c}s + 1}, \quad (4.80)$$

$H(s) = 1$  and  $V(s) = 0$ . Assume the inductor  $L$  and capacitor  $C$  constitute the output filter for the converter while the converter input voltage is  $V_{in}$  and the load is  $R_c$ .

(a) Use the proportional controller

$$D_c(s) = k_P, \quad (4.81)$$

and determine the system type and steady-state error properties with respect to disturbance inputs.

(b) Let the control be PI as given by

$$D_c(s) = k_P + \frac{k_I}{s}, \quad (4.82)$$

and determine the system type and steady-state error properties with respect for disturbance inputs.

**Solution.** (a) The closed-loop transfer function from  $W$  to  $E$  (where  $R_c = 0$ ) is

$$\begin{aligned} T_w(s) &= -\frac{V_{in}}{\left(LCs^2 + \frac{L}{R_c}s + 1\right) + V_{in}K_p}, \\ &= s^0 T_{o,w}, \\ n &= 0, \\ K_{o,w} &= -\frac{(1 + V_{in}K_p)}{V_{in}}. \end{aligned}$$

Applying Eq. (4.48) we see the system is Type 0 and the steady-state error to a unit-step disturbance input is

$$e_{ss} = -\frac{V_{in}}{1 + V_{in}k_p}. \quad (4.83)$$

(b) If the controller is PI, the disturbance error transfer function is

$$T_w(s) = -\frac{V_{in}s}{s\left(LCs^2 + \frac{L}{R_c}s + 1\right) + V_{in}(k_ps + k_I)}, \quad (4.84)$$

$$n = 1, \quad (4.85)$$

$$K_{1,w} = -k_I, \quad (4.86)$$

and therefore the system is Type 1. The error to a unit-ramp disturbance input in this case will be

$$e_{ss} = -\frac{1}{k_I}, \quad (4.87)$$

which is independent of  $V_{in}$ .

## EXAMPLE 4.8

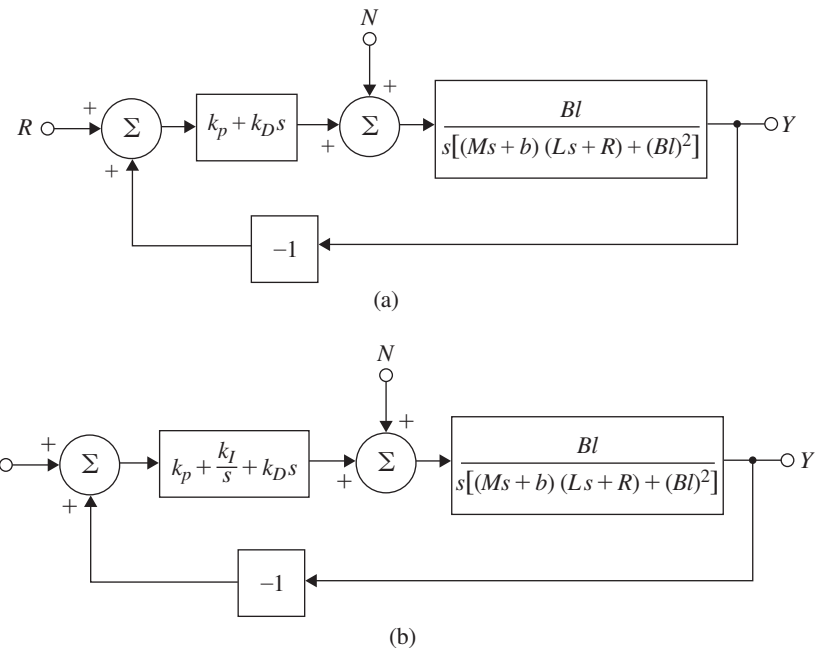
### Cone Displacement Control for a Loudspeaker

Consider the closed-loop control system for regulating the output cone displacement of the loudspeaker discussed in Example 2.14. With a PD controller, the block diagram for the system is shown in Fig. 4.17(a), and with a PID controller, it is re-drawn as Fig. 4.17(b).  $N$  is the noise that affects  $V_a$ , the voltage applied to the loudspeaker, while  $B$ ,  $b$ ,  $L$ ,  $l$ ,  $M$ , and  $R$  were defined in Examples 2.13 and 2.14 in Chapter 2. Assume the control results in a stable system and determine the system types and error responses to disturbances of the control system for

- (a) System Fig. 4.17(a);
- (b) System Fig. 4.17(b).

**Figure 4.17**

Cone displacement control for a loudspeaker: (a) PD control; (b) PID control<sup>6</sup>



**Solution.** (a) We see from inspection of Fig. 4.17(a), that with one pole at the origin in the plant, the system is Type 1 with respect to the reference inputs. The transfer function from disturbance to error is

$$T_w(s) = -\frac{Bl}{s[(Ms + b)(Ls + R) + (Bl)^2] + (k_{Ds} + k_p)Bl}, \quad (4.88)$$

$$= T_{o,w}, \quad (4.89)$$

for which  $n = 0$ ,  $K_{o,w} = k_p$ . The system is Type 0, and the error to a unit disturbance step is  $-1/k_p$ .

(b) With PID control, the forward gain has two poles at the origin, so this system is Type 2 for reference inputs, but the disturbance transfer function is

$$T_w(s) = -\frac{Bl s}{s^2[(Ms + b)(Ls + R) + (Bl)^2] + (k_{Ds}^2 + k_p s + k_I)Bl}, \quad (4.90)$$

$$n = 1, \quad (4.91)$$

$$T_{o,w}(s) = \frac{Bl}{s^2[(Ms + b)(Ls + R) + (Bl)^2] + (k_{Ds}^2 + K_p s + k_I)Bl}, \quad (4.92)$$

---

<sup>6</sup>K. J. Åström and others have pointed out that a time constant,  $\tau$ , can also be estimated from the curve, and claim that a more effective tuning can be done by including that parameter.

from which the system is Type 1 and the error constant is  $k_I$ ; the error to a disturbance ramp of unit slope will be  $-1/k_I$ .

### 4.3.6 Ziegler–Nichols Tuning of the PID Controller

When the PID controller was being developed, selecting values for the several terms (known as “tuning” the controller) was often a hit and miss affair. To bring order to the situation and make life easier for plant operators, control engineers looked for ways to make the tuning more systematic. Callender et al. (1936) proposed a design for PID controllers by specifying satisfactory values for the terms based on estimates of the plant parameters that an operating engineer could make from experiments on the process itself. This approach was extended by Ziegler and Nichols (1942, 1943) who recognized that the step responses of a large number of process control systems exhibit a **process reaction curve** such as that shown in Fig. 4.18, which can be generated from experimental step response data. The S-shape of the curve is characteristic of many systems and can be approximated by the step response of a plant with transfer function

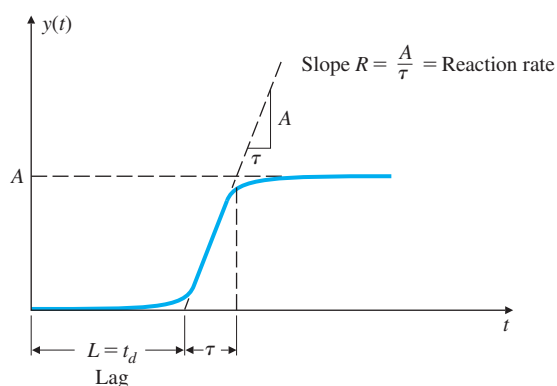
$$\frac{Y(s)}{U(s)} = \frac{Ae^{-st_d}}{\tau s + 1}, \quad (4.93)$$

Transfer function for a high-order system with a characteristic process reaction curve

which is a first-order system with a time delay or “transportation lag” of  $t_d$  sec. The constants in Eq. (4.93) can be determined from the unit-step response of the process. If a tangent is drawn at the inflection point of the reaction curve, then the slope of the line is  $R = A/\tau$ , the intersection of the tangent line with the time axis identifies the time delay  $L = t_d$  and the final value gives the value of  $A$ .

**Figure 4.18**

Process reaction curve



**Tuning by decay ratio of 0.25**

Ziegler and Nichols gave two methods for tuning the PID controller for such a model. In the first method, the choice of controller parameters is designed to result in a closed-loop step response transient with a decay ratio of approximately 0.25. This means that the transient decays to a quarter of its value after one period of oscillation, as shown in Fig. 4.19. A quarter decay corresponds to  $\zeta = 0.21$  and, while low for many applications, was seen as a reasonable compromise between quick response and adequate stability margins for the process controls being considered. The authors simulated the equations for the system on an analog computer and adjusted the controller parameters until the transients showed the decay of 25% in one period. The regulator parameters suggested by Ziegler and Nichols for the controller terms defined by

$$D_c(s) = k_P \left( 1 + \frac{1}{T_{IS}} + T_D s \right), \quad (4.94)$$

are given in Table 4.2.

**Figure 4.19**  
Quarter decay ratio

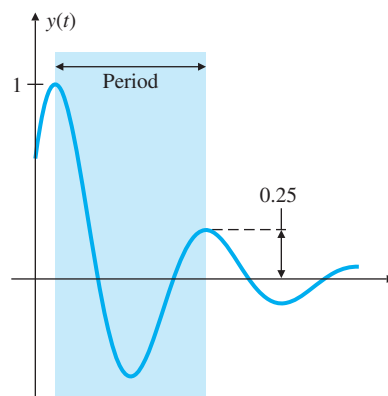


**TABLE 4.2**

**Ziegler–Nichols Tuning for the Regulator**  
 $D_c(s) = k_P(1 + 1/T_{IS} + T_D s)$ , for a Decay Ratio of 0.25

Type of Controller      Optimum Gain

P	$k_P = 1/RL$
PI	$\begin{cases} k_P = 0.9/RL \\ T_I = L/0.3 \end{cases}$
PID	$\begin{cases} k_P = 1.2/RL \\ T_I = 2L \\ T_D = 0.5L \end{cases}$

Tuning by evaluation at limit of stability, (ultimate sensitivity method)

In the **ultimate sensitivity method**, the criteria for adjusting the parameters are based on evaluating the amplitude and frequency of the oscillations of the system at the limit of stability, rather than on taking a step response. To use the method, the proportional gain is increased until the system becomes marginally stable and continuous oscillations just begin with amplitude limited by the saturation of the actuator. The corresponding gain is defined as  $K_u$  (called the **ultimate gain**) and the period of oscillation is  $P_u$  (called the **ultimate period**). These are determined as shown in Figs. 4.20 and 4.21.  $P_u$  should be measured when the amplitude of oscillation is as small as possible. Then, the tuning parameters are selected as shown in Table 4.3.

Experience has shown that the controller settings according to Ziegler–Nichols rules provide acceptable closed-loop response for many

**Figure 4.20**

Determination of ultimate gain and period

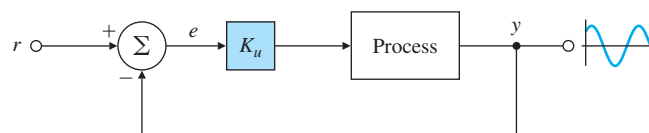


**Figure 4.21**

Neutrally stable system

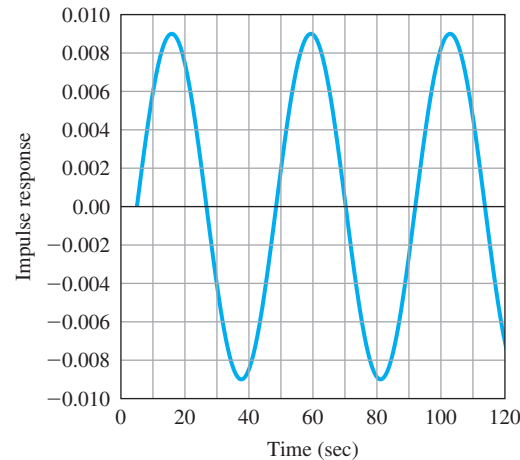


**TABLE 4.3**

#### Ziegler-Nichols Tuning for the Regulator

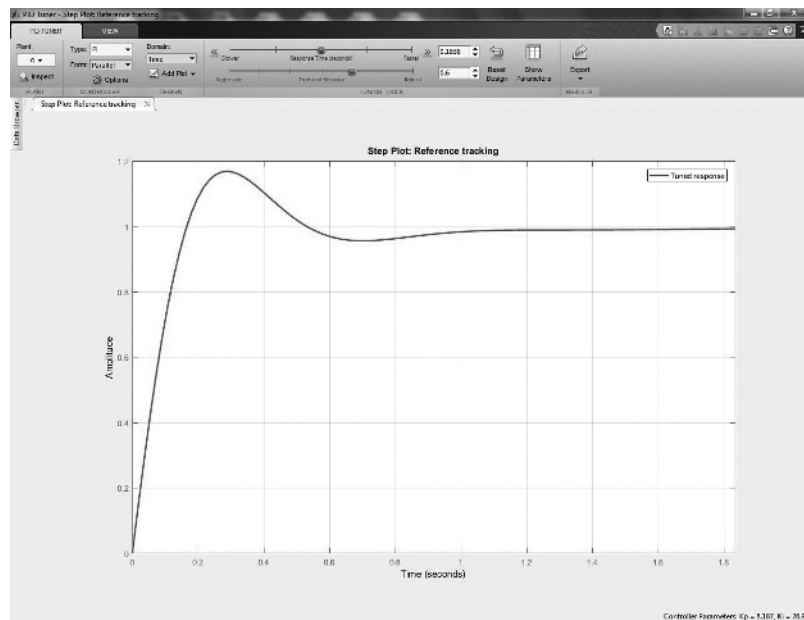
$D_c(s) = k_p(1 + 1/T_I s + T_D s)$ , Based on the Ultimate Sensitivity Method

Type of Controller	Optimum Gain
P	$k_p = 0.5K_u$
PI	$\begin{cases} k_p = 0.45K_u \\ T_I = \frac{P_u}{1.2} \end{cases}$
PID	$\begin{cases} k_p = 1.6K_u \\ T_I = 0.5P_u \\ T_D = 0.125P_u \end{cases}$

**Figure 4.22**

Matlab's pidTuner GUI

Source: Franklin, Gene F. *Feedback Control of Dynamic Systems*, 8E, 2019, Pearson Education, Inc., New York, NY.



systems. As seen from the ensuing examples, the step response method generally suggests gains that are higher than the ultimate sensitivity method. The process operator will often perform final tuning of the controller iteratively on the actual process to yield satisfactory control.

Several variations on Zeigler-Nichols tuning rules and automatic tuning techniques have been developed for industrial applications by several authors.<sup>7</sup>

PID tuning can also be done using Matlab's PID Tuner App. The pidTuner App is an interface that lets the user see how the time response changes as you vary the gains of the PID controller. Matlab's algorithm for PID tuning meets the three-fold objectives of stability, performance, and robustness by tuning the PID gains to achieve a good balance between performance and robustness. Figure 4.22 shows the GUI interface for the Matlab pidTuner App. PID tuning can be done using optimization techniques (Hast et al., 2013).

## EXAMPLE 4.9

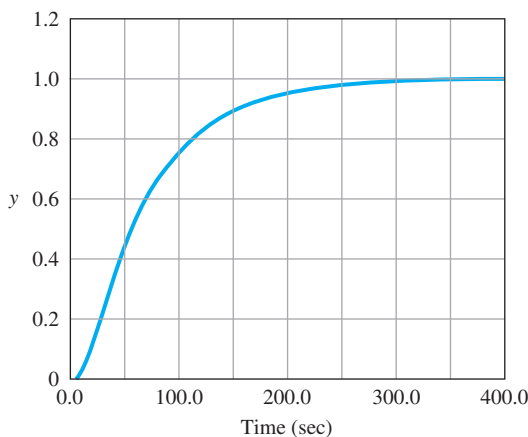
### *Tuning of a Heat Exchanger: Quarter Decay Ratio*

Consider the heat exchanger discussed in Chapter 2. The process reaction curve of this system is shown in Fig. 4.23. Determine proportional and PI regulator gains for the system using the Ziegler–Nichols

<sup>7</sup>Åström and Hägglund (2006), Luyben and Luyben (1997), Cohen-Coon (1953), and Chien, Hrones and Reswick (1952).

**Figure 4.23**

A measured process reaction curve

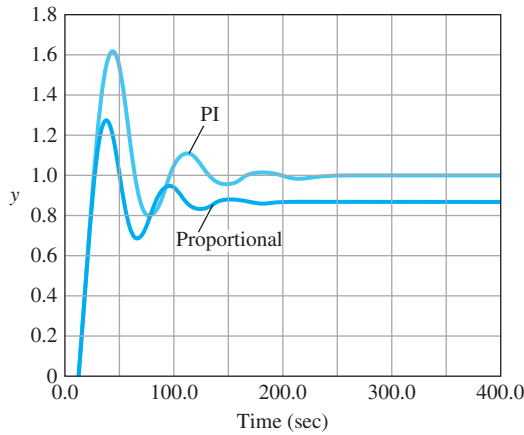


rules to achieve a quarter decay ratio. Plot the corresponding step responses.

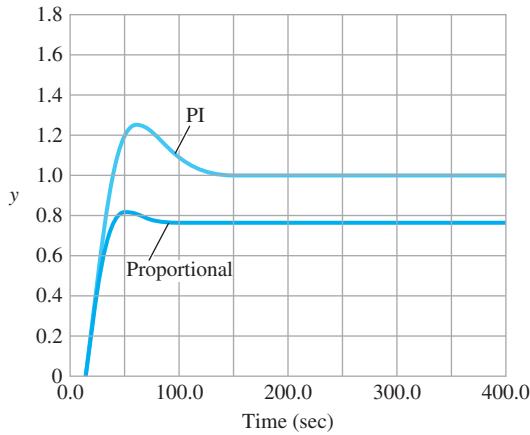
**Solution.** From the process reaction curve, we measure the maximum slope to be  $R \cong \frac{1}{90}$  and the time delay to be  $L \cong 13$  sec. According to the Ziegler–Nichols rules of Table 4.2, the gains are

$$\text{Proportional : } k_P = \frac{1}{RL} = \frac{90}{13} = 6.92,$$

$$\text{PI : } k_P = \frac{0.9}{RL} = 6.22 \quad \text{and} \quad T_I = \frac{L}{0.3} = \frac{13}{0.3} = 43.3.$$



(a)



(b)

**Figure 4.24**

Closed-loop step responses

Figure 4.24(a) shows the step responses of the closed-loop system to these two regulators. Note the proportional regulator results in a steady-state offset, while the PI regulator tracks the step exactly in the steady state. Both regulators are rather oscillatory and have considerable overshoot. If we arbitrarily reduce the gain  $k_P$  by a factor of 2 in each case, the overshoot and oscillatory behaviors are substantially reduced, as shown in Fig. 4.24(b).

## EXAMPLE 4.10

### *Tuning of a Heat Exchanger: Oscillatory Behavior*

Proportional feedback was applied to the heat exchanger in the previous example until the system showed nondecaying oscillations in response to a short pulse (impulse) input, as shown in Fig. 4.25. The ultimate gain is measured to be  $K_u = 15.3$ , and the period was measured at  $P_u = 42$  sec. Determine the proportional and PI regulators according to the Ziegler–Nichols rules based on the ultimate sensitivity method. Plot the corresponding step responses.

**Solution.** The regulators from Table 4.3 are

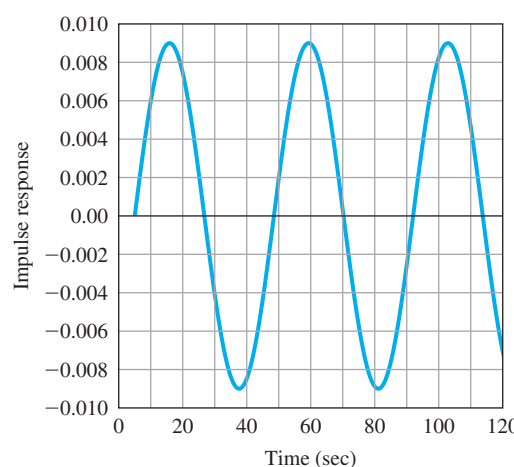
$$\text{Proportional : } k_P = 0.5K_u, \quad k_P = 7.65,$$

$$\text{PI : } k_P = 0.45K_u, \quad k_P = 6.885, \quad \text{and} \quad T_I = \frac{1}{1.2}P_u = 35.$$

The step responses of the closed-loop system are shown in Fig. 4.26(a). Note the responses are similar to those in Example 4.9. If we reduce  $k_P$  by 50%, then the overshoot is substantially reduced, as shown in Fig. 4.26(b). This shows that the tuning rules provide a good starting point, but considerable fine tuning may still be needed.

**Figure 4.25**

Ultimate period of heat exchanger



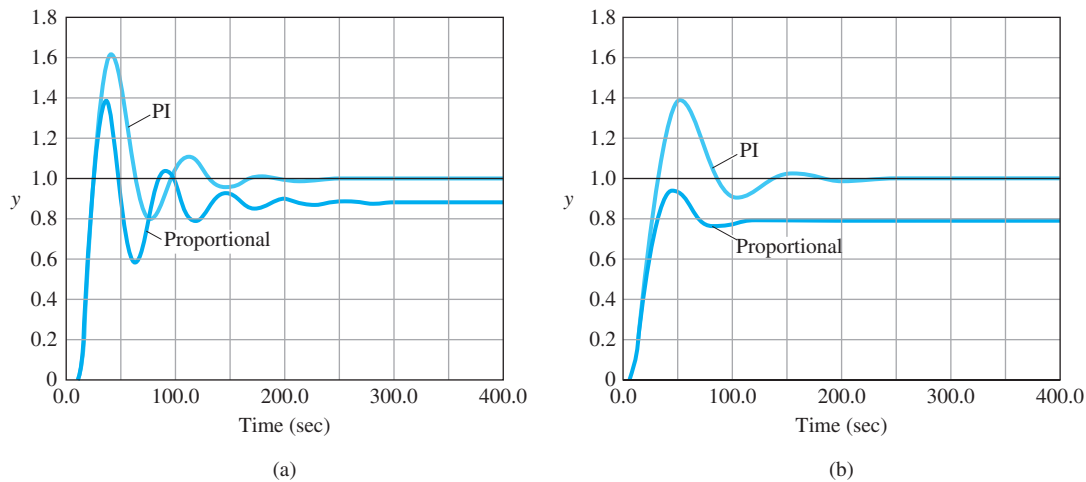


**Figure 4.26**

## Closed-loop step responses

## 4.4 Feedforward Control by Plant Model Inversion

Section 4.3 showed that proportional control typically yields a steady-state error in the output due to disturbances or input commands. Integral control was introduced in order to reduce those errors to zero for steady disturbances or constant reference commands; however, integral control typically decreases the damping or stability of a system. One way to partly resolve this conflict is to provide some **feedforward** of the control that will eliminate the steady-state errors due to command inputs. This is possible because the command inputs are known and can be determined directly by the controller; thus, we should be able to compute the value of the control input that will produce the desired outputs being commanded. Disturbances are not always measurable, but can also be used for feedforward control whenever they are measured. The solution is simply to determine the inverse of the DC gain of the plant transfer function model and incorporate that into the controller as shown in Fig. 4.27. If this is done, the feedforward will provide the control effort required for the desired command input, and the feedback takes care of the differences between the real plant and the plant model plus the effects of any disturbances.

## Feedforward

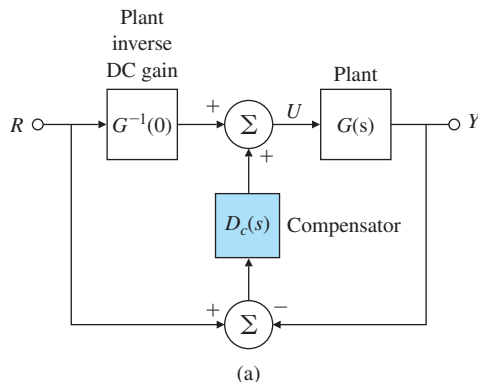
## EXAMPLE 4.11

Feedforward Control for DC Motor

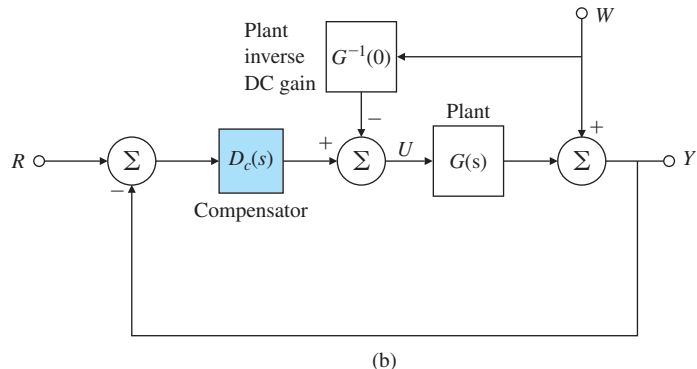
Consider the same DC motor speed-control system (Eq. 4.58) of Section 4.3 with the two different values of proportional controller gain  $k_P = 1.5, 6$ . (a) Use feedforward control to eliminate the steady-state tracking error for a step reference input. (b) Also use feedforward

**Figure 4.27**

Feedforward control structure for:  
 (a) tracking;  
 (b) disturbance rejection



(a)



(b)

control to eliminate the effect of a constant output disturbance signal on the output of the system.

**Solution.** (a) In this case, the plant inverse DC gain is  $G^{-1}(0) = 1$ . We implement the closed-loop system as shown in Fig. 4.27(a) with  $G(s)$  given by Eq. (4.58) and  $D_c(s) = k_P$ . The closed-loop transfer function is

$$Y(s) = G(s)[k_P E(s) + R(s)],$$

$$E(s) = R(s) - Y(s),$$

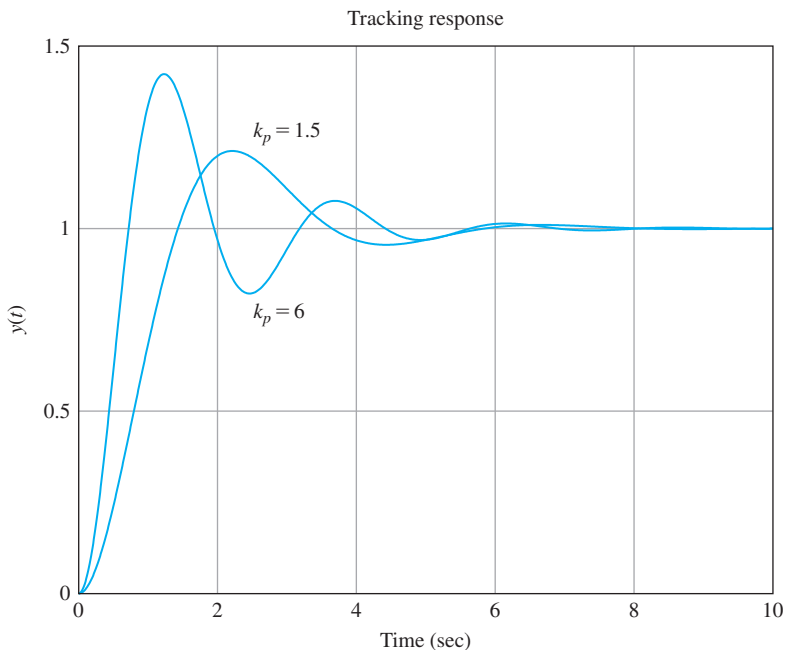
$$\frac{Y(s)}{R(s)} = \mathcal{T}(s) = \frac{(1 + k_P)G(s)}{1 + k_P G(s)}.$$

Note the closed-loop DC gain is unity ( $\mathcal{T}(0) = 1$ ). Figure 4.28 illustrates the effect of feedforward control in eliminating the steady-state tracking error due to a step reference input for the two values of  $k_P$ . Addition of the feedforward control results in zero steady-state tracking error.

(b) Similarly, we implement the closed-loop system as shown in Fig. 4.27(b) with  $G(s)$  given by Eq. (4.58) and  $D_c(s) = k_P$ . The closed-loop transfer function is

**Figure 4.28**

Tracking performance  
with addition of  
feedforward



$$Y(s) = W(s) + G(s)[k_P E(s) - W(s)],$$

$$E(s) = R(s) - Y(s), \text{ with } R(s) = 0,$$

$$\frac{Y(s)}{W(s)} = T_w(s) = \frac{1 - G(s)}{1 + k_P G(s)}.$$

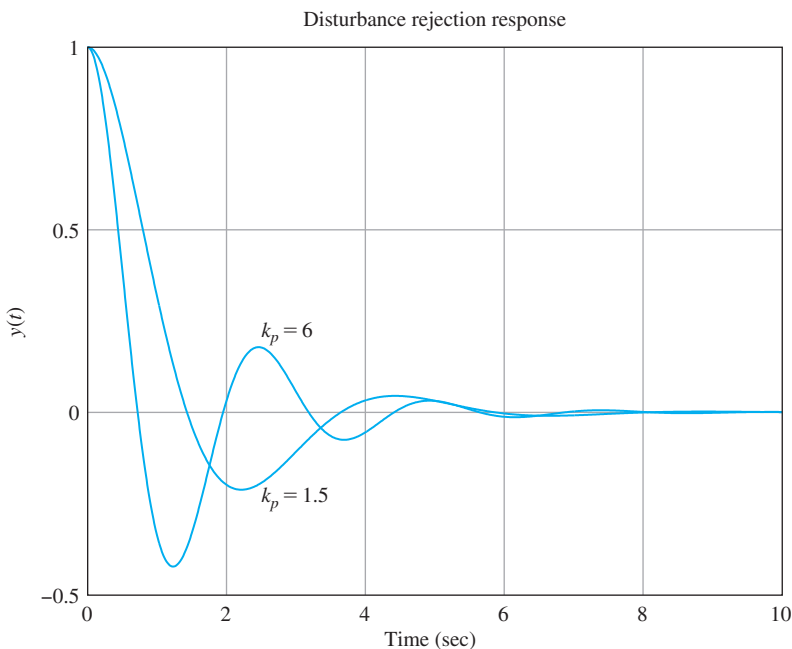
Note the closed-loop DC gain is zero ( $T_w(0) = 0$ ). Figure 4.29 illustrates the effect of feedforward control in eliminating the steady-state error for a constant output disturbance, again for the two values of  $k_P$ . We observe that by using the inverse of the DC gain, this feedforward only controls the steady-state effect of the reference and disturbance inputs. More complex feedforward control can be used by inverting  $G(s)$  over an entire frequency range.

## △ 4.5 Introduction to Digital Control

So far, we have assumed the systems and controllers are all continuous time systems, and they obey differential equations. That implies that the controllers would be implemented using analog circuits such as those discussed in Section 2.2. In fact, most control systems today are implemented in digital computers which are not able to implement the continuous controllers exactly. Instead, they approximate the continuous control by algebraic equations called difference equations. A very short description of how one would convert a continuous  $D_c(s)$  to

**Figure 4.29**

Constant disturbance rejection performance with addition of feedforward



difference equations that can be coded directly into a computer is contained in Appendix W4.5 online at [www.pearsonglobaleditions.com](http://www.pearsonglobaleditions.com). For more details, see Chapter 8 in this text or see *Digital Control of Dynamic Systems*, by Franklin, Powell, and Workman, 3rd ed, 1998, for a complete discussion of the topic.

## △ 4.6 Sensitivity of Time Response to Parameter Change

Since many control specifications are in terms of the step response, the sensitivity of the time response to parameter changes is sometimes very useful to explore. To learn more, see Appendix W4.6 online at [www.pearsonglobaleditions.com](http://www.pearsonglobaleditions.com).

## 4.7 Historical Perspective

The field of control is characterized by two paths: theory and practice. Control theory is basically the application of mathematics to solve control problems, whereas control practice, as used here, is the practical application of feedback in devices where it is found to be useful. Historically, practical applications have come first with control being introduced by trial and error. Although the applicable mathematics is often known, the theory describing how the control works and pointing the way to improvements has typically been applied later. For example, James Watt's company began manufacturing steam engines using

the fly-ball governor in 1788, but it was not until 1840 that G. B. Airy described instability in a similar device, and not until 1868 when J. C. Maxwell published “On Governors” with a theoretical description of the problem. Then it was not until 1877, almost 100 years after the steam engine control was introduced, that E. J. Routh published a solution giving the requirements for stability. This situation has been called the “Gap between Theory and Practice” and continues to this day as a source of creative tension that stimulates both theory and practice.

Regulation is central to the process industries, from making beer to making gasoline. In these industries, there are a host of variables that need to be kept constant. Typical examples are temperature, pressure, volume, flow rates, composition, and chemical properties such as pH level. However, before one can regulate by feedback, one must be able to measure the variable of interest. Before there was control, there were sensors. In 1851, George Taylor and David Kendall founded the company that later became the Taylor Instrument Company in Rochester, NY, to make thermometers and barometers for weather forecasting. In 1855, they were making thermometers for several industries, including the brewing industry where they were used for manual control. Other early entries into the instrument field were the Bristol Company, founded in Naugatuck, CT, in 1889 by William Bristol, and the Foxboro Company, founded in Foxboro, MA, in 1908 by William’s father and two of his brothers. For example, one of Bristol’s instruments was used by Henry Ford to measure (and presumably control) steam pressure while he worked at the Detroit Edison Company. The Bristol Company pioneered in telemetry that permitted instruments to be placed at a distance from the process so a plant manager could monitor several variables at once. As the instruments became more sophisticated, and devices such as motor-driven valves became available, they were used in feedback control often using simple on-off methods, as described in Chapter 1 for the home furnace. An important fact was that the several instrument companies agreed upon standards for the variables used so a plant could mix and match instruments and controllers from different suppliers. In 1920, Foxboro introduced a controller based on compressed air that included reset or integral action. Eventually, each of these companies introduced instruments and controllers that could implement full PID action. A major step was taken for tuning PID controllers in 1942 when Ziegler and Nichols, working for Taylor Instruments, published their method for tuning based on experimental data.

The poster child for the tracking problem was that of the anti-aircraft gun, whether on land or at sea. The idea was to use radar to track the target and to have a controller that would predict the path of the aircraft and aim the gun to a position such that the projectile would hit the target when it got there. The Radiation Laboratory was set up at MIT during World War II to develop such radars, one of which was the SCR-584. Interestingly, one of the major contributors to the control methods developed for this project was none other than Nick Nichols

who had earlier worked on tuning PID controllers. When the record of the Rad Lab was written, Nichols was selected to be one of the editors of volume 25 on control.

H. S. Black joined Bell Laboratories in 1921 and was assigned to find a design for an electronic amplifier suitable for use as a repeater on the long lines of the telephone company. The basic problem was that the gain of the vacuum tube components he had available drifted over time and he needed a design that, over the audio frequency range, maintained a specific gain with great precision in the face of these drifts. Over the next few years he tried many approaches, including a feed forward technique designed to cancel the tube distortion. While this worked in the laboratory, it was much too sensitive to be practical in the field. Finally, in August of 1927,<sup>8</sup> while on the ferry boat from Staten Island to Manhattan, he realized that negative feedback might work and he wrote the equations on the only paper available, a page of the New York Times. He applied for a patent in 1928 but it was not issued until December 1937.<sup>9</sup> The theory of sensitivity and many other theories of feedback were worked out by H. W. Bode.

## SUMMARY

- The most important measure of the performance of a control system is the system error to all inputs.
- Compared to open-loop control, feedback can be used to stabilize an otherwise unstable system, to reduce errors to plant disturbances, to improve the tracking of reference inputs, and to reduce the system's transfer function sensitivity to parameter variations.
- Sensor noise introduces a conflict between efforts to reduce the error caused by plant disturbances and efforts to reduce the errors caused by the sensor noise.
- Classifying a system as Type  $k$  indicates the ability of the system to achieve zero steady-state error to polynomials of degree less than but not equal to  $k$ . A stable *unity* feedback system is Type  $k$  with respect to reference inputs if the loop gain  $G(s)D_c(s)$  has  $k$  poles at the origin in which case we can write

$$G(s)D_c(s) = \frac{A(s + z_1)(s + z_2)\cdots}{s^k(s + p_1)(s + p_2)\cdots},$$

and the error constant is given by

$$K_k = \lim_{s \rightarrow 0} s^k G(s)D_c(s) = \frac{Az_1z_2\cdots}{p_1p_2\cdots}. \quad (4.95)$$

<sup>8</sup>Black was 29 years old at the time.

<sup>9</sup>According to the story, many of Black's colleagues at the Bell laboratories did not believe it was possible to feed back a signal 100 times as large as was the input and still keep the system stable. As will be discussed in Chapter 6, this dilemma was solved by H. Nyquist, also at the labs.

- A table of steady-state errors for unity feedback systems of Types 0, 1, and 2 to reference inputs is given in Table 4.1.
- Systems can be classified as to type for rejecting disturbances by computing the system error to polynomial disturbance inputs. The system is Type  $k$  to disturbances if the error is zero to all disturbance polynomials of degree less than  $k$ , but nonzero for a polynomial of degree  $k$ .
- Increasing the proportional feedback gain reduces steady-state errors but high gain almost always destabilizes the system. Integral control provides robust reduction in steady-state errors, but also may make the system less stable. Derivative control increases damping and improves stability. These three kinds of control combined to form the classical three-term PID controller.
- The standard PID controller is described by the equations

$$U(s) = \left( k_P + \frac{k_I}{s} + k_D s \right) E(s) \quad \text{or}$$

$$U(s) = k_P \left( 1 + \frac{1}{T_I s} + T_D s \right) E(s) = D_c(s)E(s).$$

This latter form is ubiquitous in the process-control industry and describes the basic controller in many control systems.

- Useful guidelines for tuning PID controllers were presented in Tables 4.2 and 4.3.
- Matlab can compute a discrete equivalent with the command c2d.

## REVIEW QUESTIONS

- 4.1** Give three advantages of feedback in control.
- 4.2** Give two disadvantages of feedback in control.
- 4.3** A temperature control system is found to have zero error to a constant tracking input and an error of  $0.5^\circ\text{C}$  to a tracking input that is linear in time, rising at the rate of  $40^\circ\text{C}/\text{sec}$ . What is the system type of this control system and what is the relevant error constant ( $K_p$  or  $K_v$  or  $K_a$ )?
- 4.4** What are the units of  $K_p$ ,  $K_v$ , and  $K_a$ ?
- 4.5** What is the definition of system type with respect to reference inputs?
- 4.6** What is the definition of system type with respect to disturbance inputs?
- 4.7** Why does system type depend on where the external signal enters the system?
- 4.8** What is the main objective of introducing integral control?
- 4.9** What is the major objective of adding derivative control?
- 4.10** Why might a designer wish to put the derivative term in the feedback rather than in the error path?
- 4.11** What is the advantage of having a “tuning rule” for PID controllers?

- 4.12** Give two reasons to use a digital controller rather than an analog controller.
- 4.13** Give two disadvantages to using a digital controller.

## PROBLEMS

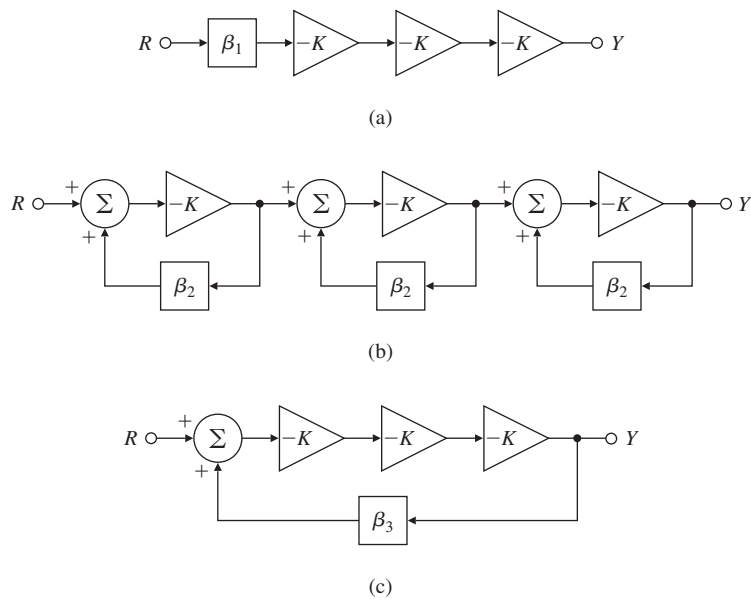
### Problems for Section 4.1: The Basic Equations of Control

- 4.1** If  $S$  is the sensitivity of the unity feedback system to changes in the plant transfer function and  $T$  is the transfer function from reference to output, show that  $S + T = 1$ .
- 4.2** We define the sensitivity of a transfer function  $G$  to one of its parameters  $K$  as the ratio of percent change in  $G$  to percent change in  $K$ .

$$S_K^G = \frac{dG/G}{dK/K} = \frac{d \ln G}{d \ln K} = \frac{K}{G} \frac{dG}{dK}.$$

The purpose of this problem is to examine the effect of feedback on sensitivity. In particular, we would like to compare the topologies shown in Fig. 4.30 for connecting three amplifier stages with a gain of  $-K$  into a single amplifier with a gain of  $-10$ .

**Figure 4.30**  
Three-amplifier topologies for Problem 4.2



- (a) For each topology in Fig. 4.30, compute  $\beta_i$  so if  $K = 10$ ,  $Y = -10R$ .
- (b) For each topology, compute  $S_K^G$  when  $G = \frac{Y}{R}$ . (Use the respective  $\beta_i$  values found in part (a).) Which case is the *least* sensitive?
- (c) Compute the sensitivities of the systems in Fig. 4.30(b,c) to  $\beta_2$  and  $\beta_3$ . Using your results, comment on the relative need for precision in sensors and actuators.

- 4.3** Compare the two structures shown in Fig. 4.31 with respect to sensitivity to changes in the overall gain due to changes in the amplifier gain. Use the relation

$$S = \frac{d \ln F}{d \ln K} = \frac{K}{F} \frac{dF}{dK},$$

as the measure. Select  $H_1$  and  $H_2$  so the nominal system outputs satisfy  $F_1 = F_2$ , and assume  $KH_1 > 0$ .

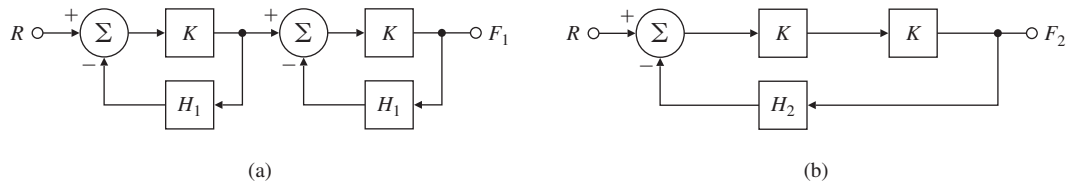


**Figure 4.31**

Block diagrams for Problem 4.3

- 4.4** A unity feedback control system has the open-loop transfer function

$$G(s) = \frac{A}{s(s+a)}.$$

- (a) Compute the sensitivity of the closed-loop transfer function to changes in the parameter  $A$ .
  - (b) Compute the sensitivity of the closed-loop transfer function to changes in the parameter  $a$ .
  - (c) If the unity gain in the feedback changes to a value of  $\beta \neq 1$ , compute the sensitivity of the closed-loop transfer function with respect to  $\beta$ .
- 4.5** Compute the equation for the system error for the feedback system shown in Fig. 4.5.

### Problems for Section 4.2: Control of Steady-State Error

- 4.6** Consider the DC motor control system with rate (tachometer) feedback shown in Fig. 4.32(a).

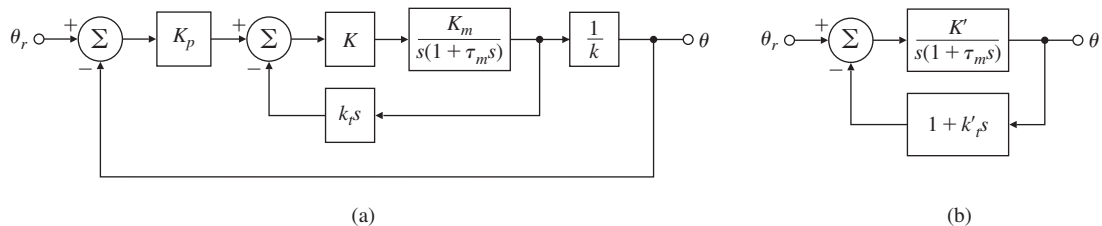
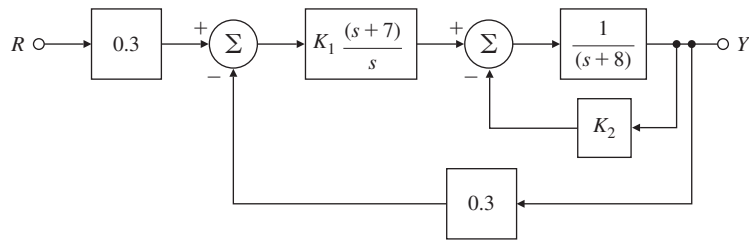


**Figure 4.32**

Control system for Problem 4.6

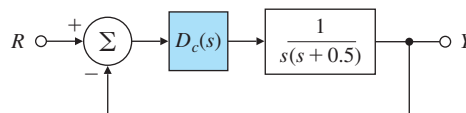
- (a) Find values for  $K'$  and  $k'_t$  so the system of Fig. 4.32(b) has the same transfer function as the system of Fig. 4.32(a).
- (b) Determine the system type with respect to tracking  $\theta_r$  and compute the system  $K_v$  in terms of parameters  $K'$  and  $k'_t$ .
- (c) Does the addition of tachometer feedback with positive  $k_t$  increase or decrease  $K_v$ ?
- 4.7** A block diagram of a control system is shown in Fig. 4.33.
- (a) If  $r$  is a step function and the system is closed-loop stable, what is the steady-state tracking error?
- (b) What is the system type?
- (c) What is the steady-state error to a ramp velocity 2.5 if  $K_2 = 2$  and  $K_1$  is adjusted so that the system step response approximately has a rise time of 0.65 s and a settling time of 0.23 s?

**Figure 4.33**  
Closed-loop system for  
Problem 4.7



- 4.8** A standard feedback control block diagram is shown in Fig. 4.5 with
- $$G(s) = \frac{1.5}{s}; D_c(s) = \frac{(s+9)}{(s+3)}; H(s) = \frac{70}{(s+70)}; V_{(s)} = 0.$$
- (a) Let  $W = 0$  and compute the transfer function from  $R$  to  $Y$ .
- (b) Let  $R = 0$  and compute the transfer function from  $W$  to  $Y$ .
- (c) What is the tracking error if  $R$  a unit-step input and  $W = 0$ ?
- (d) What is the tracking error if  $R$  is a unit-ramp input and  $W = 0$ ?
- (e) What is the system type with respect to the reference inputs and the corresponding error coefficient?

**Figure 4.34**  
Control system for  
Problem 4.10



- 4.9** A generic negative feedback system with non-unity transfer function in the feedback path is shown in Fig. 4.5.
- (a) Suppose,
- $$G(s) = \frac{1}{s(s+1)^2}; D_{cl}(s) = 0.42; H(s) = P \frac{(0.58s+1)}{(0.35s+1)}; V(s) = 0,$$
- showing a lead compensation in the feedback path. What is the requirement on  $P$  such that the system will remain a Type 1 system with respect to the reference input?

- (b) For part (a), find the steady-state tracking error for this system to a unit ramp reference input if  $P = 1$ .

- (c) For part (b), what is the value of the velocity error coefficient,  $K_v$ ?

- 4.10** Consider the system shown in Fig. 4.34 where

$$D_c(s) = K \frac{(s^2 + \alpha s + 1)}{(s^2 + \omega_0^2)}.$$

- (a) Prove that if the system is stable, it is capable of tracking a sinusoidal reference input  $r = \sin \omega_0 t$  with a zero steady-state error. (*Hint:* Look at the transfer function from  $R$  to  $E$  and consider the gain at  $\omega_0$ .)

- (b) Use the Routh's criterion to find the range of  $K$  such that the closed-loop system remains stable if  $\omega_0 = 1$  and  $\alpha = 0.3$ .

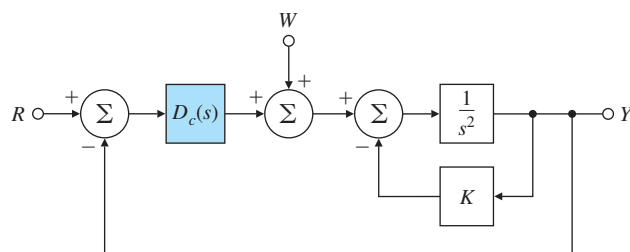
- 4.11** Consider the system shown in Fig. 4.35, which represents control of the angle of a pendulum that has no damping.

- (a) What condition must  $D_c(s)$  satisfy so the system can track a ramp reference input with constant steady-state error?

- (b) For a transfer function  $D_c(s)$  that stabilizes the system and satisfies the condition in part (a), find the class of disturbances  $w(t)$  that the system can reject with zero steady-state error.

**Figure 4.35**

Control system for Problem 4.11



- 4.12** A unity feedback system has the overall transfer function

$$\frac{Y(s)}{R(s)} = T(s) = \frac{6}{(7s+2)(s+3)}.$$

Give the system type and the corresponding error constant for tracking polynomial reference inputs in terms of  $\zeta$  and  $\omega_n$ .

- 4.13** Consider the second-order system

$$G(s) = \frac{2}{s^2 + 4\zeta s + 2}.$$

We would like to add a transfer function of the form  $D_c(s) = K(s+a)/(s+b)$  in cascade with  $G(s)$  in a unity-feedback structure.

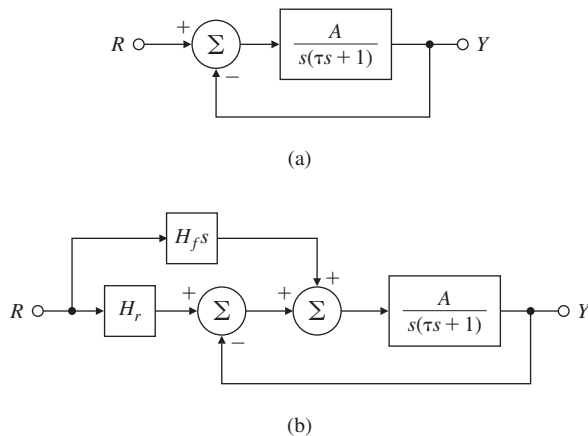
- (a) Ignoring stability for the moment, what are the constraints on  $K$ ,  $a$ , and  $b$  so that the system is Type 1?

- (b) What are the constraints on  $a$ , and  $b$  so that the system is both Type 1 and remains stable for every positive value for  $K$ ?

- (c) When  $a = 5$ ,  $b = 4$ , what is the constraint on  $K$  so that the steady-state tracking error is less than 0.1 unit when the reference input to the feedback system is a unit step?

**4.14** Consider the system shown in Fig. 4.36(a).

**Figure 4.36**  
Control system for  
Problem 4.14



- (a) What is the system type? Compute the steady-state tracking error due to a ramp input  $r(t) = r_o t 1(t)$ .

- (b) For the modified system with a feed forward path shown in Fig. 4.36(b), give the value of  $H_f$  so the system is Type 2 for reference inputs and compute the  $K_a$  in this case.  
(c) Is the resulting Type 2 property of this system robust with respect to changes in  $H_f$ , that is, will the system remain Type 2 if  $H_f$  changes slightly?

**4.15** A controller for a DC servo motor with transfer function  $G(s) = \frac{5}{s(s+10)}$  has been designed with a unity feedback structure and has the transfer function  $D_c(s) = 6 \frac{(s+7)(s+9)}{s(s+12)}$ .

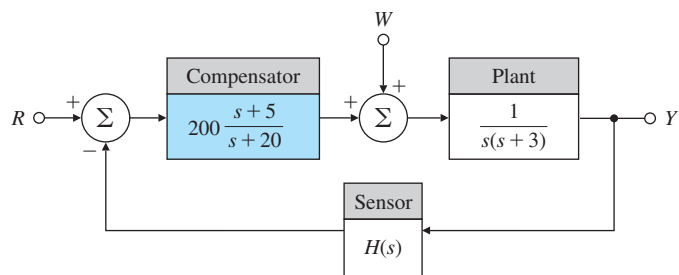
- (a) Find the system type for reference tracking and the corresponding error constant for this system.  
(b) If a disturbance torque  $w$  adds to the control so that the input to the process is  $u + w$ , what is the system type and corresponding error constant with respect to disturbance rejection?

**4.16** A compensated motor position control system is shown in Fig. 4.37. Assume the sensor dynamics are  $H(s) = 1$ .

- (a) Can the system track a step reference input  $r$  with zero steady-state error? If yes, give the value of the velocity constant.  
(b) Can the system reject a step disturbance  $w$  with zero steady-state error? If yes, give the value of the velocity constant.  
(c) Compute the sensitivity of the closed-loop transfer function to changes in the plant pole at  $-3$ .  
(d) In some instances there are dynamics in the sensor. Repeat parts (a) to (c) for  $H(s) = \frac{25}{s+25}$  and compare the corresponding velocity constants.

**Figure 4.37**

Control system for Problem 4.16



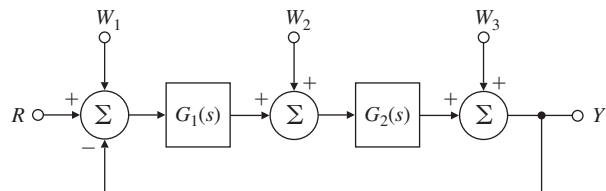
- 4.17** The general unity feedback system shown in Fig. 4.38 has disturbance inputs  $w_1$ ,  $w_2$ , and  $w_3$  and is asymptotically stable. Also,

$$G_1(s) = \frac{K_1 \prod_{i=1}^{m_1} (s + z_{1i})}{s^{l_1} \prod_{i=1}^{m_1} (s + p_{1i})}, \quad G_2(s) = \frac{K_2 \prod_{i=1}^{m_1} (s + z_{2i})}{s^{l_2} \prod_{i=1}^{m_1} (s + p_{2i})}.$$

Show that the system is of Type 0, Type  $l_1$ , and Type  $(l_1 + l_2)$  with respect to disturbance inputs  $w_1$ ,  $w_2$ , and  $w_3$ , respectively.

**Figure 4.38**

Single input-single output unity feedback system with disturbance inputs

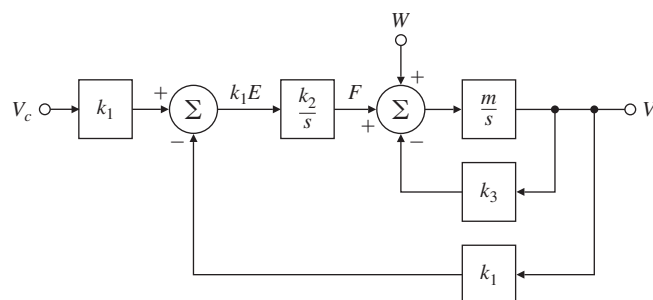


- 4.18** One possible representation of an automobile speed-control system with integral control is shown in Fig. 4.39.

- (a) With a zero reference velocity input  $v_c = 0$ , find the transfer function relating the output speed  $v$  to the wind disturbance  $w$ .
- (b) What is the steady-state response of  $v$  if  $w$  is a unit-ramp function?
- (c) What type is this system in relation to reference inputs? What is the value of the corresponding error constant?
- (d) What is the type and corresponding error constant of this system in relation to tracking the disturbance  $w$ ?

**Figure 4.39**

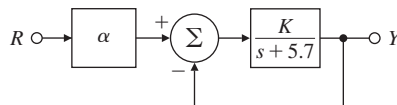
System using integral control



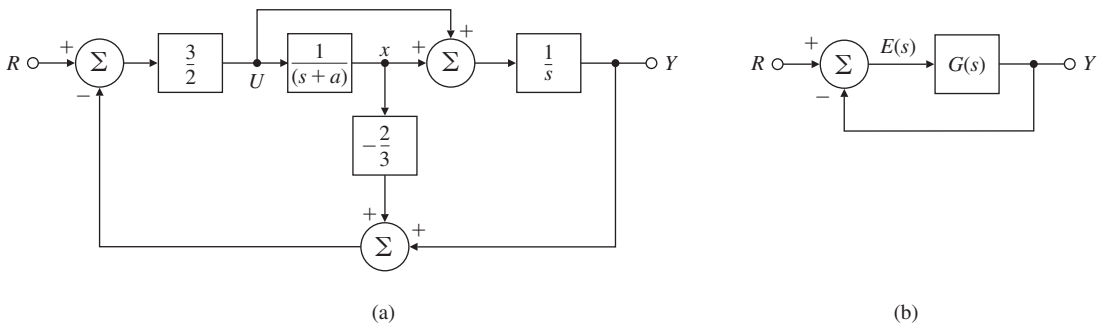
- 4.19** For the feedback system shown in Fig. 4.40, find the value of  $\alpha$  that will make the system Type 1 for  $K = 3$ . Give the corresponding velocity constant. Show that the system is not robust by using this value of  $\alpha$  and computing the tracking error  $e = r - y$  to a step reference for  $K = 4$  and  $K = 6$ .

**Figure 4.40**

Control system for Problem 4.19



- 4.20** Suppose you are given the system depicted in Fig. 4.41(a), where the plant parameter  $a$  is subject to variations.

**Figure 4.41**

Control system for Problem 4.20

- (a) Find  $G(s)$  so that the system shown in Fig. 4.41(b) has the same transfer function from  $r$  to  $y$  as the system in Fig. 4.41(a).
- (b) Assume that  $a = 1$  is the nominal value of the plant parameter. What is the system type and the error constant in this case?
- (c) Now assume that  $a = 1 + \delta a$ , where  $\delta a$  is some perturbation to the plant parameter. What is the system type and the error constant for the perturbed system?
- 4.21** Two feedback systems are shown in Fig. 4.42.
- (a) Determine values for  $K_1$ ,  $K_2$ , and  $K_3$  so that both systems:
- Exhibit zero steady-state error to step inputs (that is, both are Type 1), and
  - whose static velocity error constant  $K_v = 10$  when  $K_0 = 7.5$ .
- (b) Suppose  $K_0$  undergoes a small perturbation:  $K_0 \rightarrow K_0 + \delta K_0$ . What effect does this have on the system type in each case? Which system has a type which is robust? Which system do you think would be preferred?

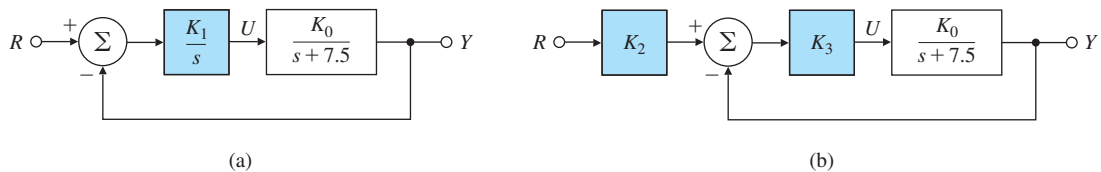


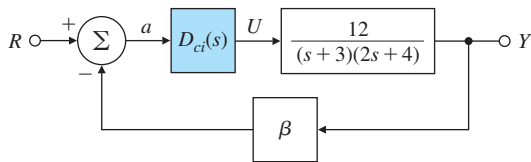
**Figure 4.42**

## Two feedback systems for Problem 4.21

- 4.22** You are given the system shown in Fig. 4.43, where the feedback gain  $\beta$  is subject to variations. You are to design a controller for this system so that the output  $y(t)$  accurately tracks the reference input  $r(t)$ .

**Figure 4.43**

## Control system for Problem 4.22



- (a) Let  $\beta = 1$ . You are given the following three options for the controller  $D_{ci}(s)$ :

$$D_{c1}(s) = k_P, \quad D_{c2}(s) = \frac{k_P s + k_I}{s}, \quad D_{c3}(s) = \frac{k_P s^2 + k_I s + k_2}{s^2}.$$

Choose the controller (including particular values for the controller constants) that will result in a Type 1 system with a steady-state error to a unit reference ramp of less than  $\frac{1}{15}$ .

- (b) Next, suppose there is some attenuation in the feedback path that is modeled by  $\beta = 0.85$ . Find the steady-state error due to a ramp input for your choice of  $D_{ci}(s)$  in part (a).

(c) If  $\beta = 0.85$ , what is the system type for part (b)? What are the values of the appropriate error constant?

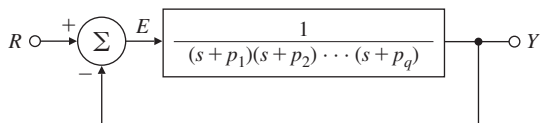
- 4.23** Consider the system shown in Fig. 4.44.

- (a) Find the transfer function from the reference input to the tracking error.

(b) For this system to respond to inputs of the form  $r(t) = t^n l(t)$  (where  $n < q$ ) with zero steady-state error, what constraint is placed on the open-loop poles  $p_1, p_2, \dots, p_q$ ?

**Figure 4.44**

## Control system for Problem 4.23

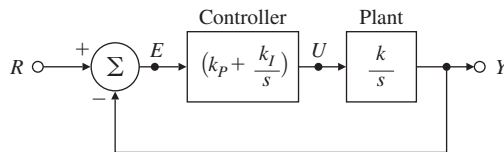


**4.24** Consider the system shown in Fig. 4.45.

- Compute the transfer function from  $R(s)$  to  $E(s)$  and determine the steady-state error ( $e_{ss}$ ) for a unit-step reference input signal, and a unit-ramp reference input signal.
- Determine the locations of the closed-loop poles of the system.
- Select the system parameters ( $k, k_p, k_I$ ) such that the closed-loop system has damping coefficient  $\zeta = 0.707$  and  $\omega_n = 1$ . What percent overshoot would you expect in  $y(t)$  for unit-step reference input?
- Find the tracking error signal as a function of time,  $e(t)$ , if the reference input to the system,  $r(t)$ , is a unit-ramp.
- How can we select the PI controller parameters ( $k_p, k_I$ ) to ensure that the amplitude of the transient tracking error,  $|e(t)|$ , from part (d) is small?
- What is the transient behavior of the tracking error,  $e(t)$ , for a unit-ramp reference input if the magnitude of the integral gain,  $k_I$ , is very large? Does the unit-ramp response have an overshoot in that case?

**Figure 4.45**

Control system diagram for Problem 4.24



**4.25** A linear ODE model of the DC motor with negligible armature inductance ( $L_a = 0$ ) and with a disturbance torque  $w$  was given earlier in the chapter; it is restated here, in slightly different form, as

$$\frac{JR_a}{K_t} \ddot{\theta}_m + K_e \dot{\theta}_m = v_a + \frac{R_a}{K_t} w,$$

where  $\theta_m$  is measured in radians. Dividing through by the coefficient of  $\ddot{\theta}_m$ , we obtain

$$\ddot{\theta}_m + a_1 \dot{\theta}_m = b_0 v_a + c_0 w,$$

where

$$a_1 = \frac{K_e K_t}{J R_a}, \quad b_0 = \frac{K_t}{J R_a}, \quad c_0 = \frac{1}{J}.$$

With rotating potentiometers, it is possible to measure the positioning error between  $\theta$  and the reference angle  $\theta_r$  or  $e = \theta_r - \theta_m$ . With a tachometer, we can measure the motor speed  $\dot{\theta}_m$ . Consider using feedback of the error  $e$  and the motor speed  $\dot{\theta}_m$  in the form

$$v_a = K(e - T_D \dot{\theta}_m),$$

where  $K$  and  $T_D$  are controller gains to be determined.

- Draw a block diagram of the resulting feedback system showing both  $\theta_m$  and  $\dot{\theta}_m$  as variables in the diagram representing the motor.
- Suppose the numbers work out so that  $a_1 = 80$ ,  $b_0 = 320$ , and  $c_0 = 11$ . If there is no load torque ( $w = 0$ ), what speed (in rpm) results from  $v_a = 120$  V?

- (c) Using the parameter values given in part (b), find  $K$  and  $T_D$  so that using the results in Chapter 3, a step change in  $\theta_r$  with zero load torque results in a transient that has an approximately 14% overshoot and that settles to within 4% of steady state in less than 0.03 sec.

- (d) Derive an expression for the steady-state error to a reference angle input, and compute its value for your design in part (c) assuming  $\theta_r = 1$  rad.

- (e) Derive an expression for the steady-state error to a constant disturbance torque when  $\theta_r = 0$  and compute its value for your design in part (c) assuming  $w = 1.2$ .

- 4.26** We wish to design an automatic speed control for an automobile. Assume that (1) the car has a mass  $m$  of 1100 kg, (2) the accelerator is the control  $U$  and supplies a force on the automobile of 12 N per degree of accelerator motion, and (3) air drag provides a friction force proportional to velocity of 11 N · sec/m.

- (a) Assume the velocity changes are given by

$$V(s) = \frac{1}{s + 0.01} U(s) + \frac{0.07}{s + 0.01} W(s),$$

where  $V$  is given in meters per second,  $U$  is in degrees, and  $W$  is the percent grade of the road. Design a proportional control law  $U = -k_P(V - V_d)$  that will maintain a velocity error of less than 1 m/sec in the presence of a constant 1.5% grade.

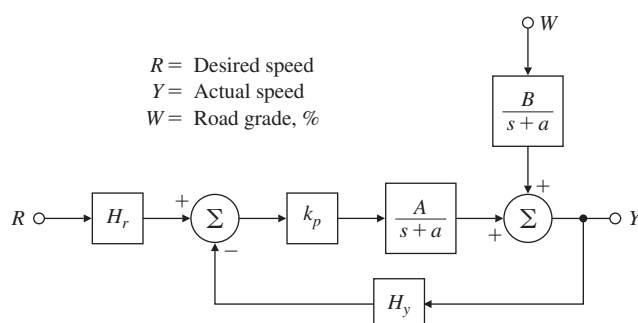
- (b) Discuss what advantage (if any) integral control would have for this problem.

- (c) Assuming that pure integral control (that is, no proportional term) is advantageous, select the feedback gain so that the roots have critical damping ( $\zeta = 1$ ).

- 4.27** Consider the automobile speed control system depicted in Fig. 4.46.

**Figure 4.46**

Automobile speed-control system



- (a) Find the transfer functions from  $W(s)$  and from  $R(s)$  to  $Y(s)$ .

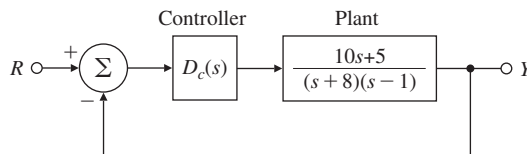
- (b) Assume the desired speed is a constant reference  $r$ , so  $R(s) = \frac{r_o}{s}$ . Assume the road is level, so  $w(t) = 0$ . Compute values of the gains  $k_P$ ,  $H_r$ , and  $H_y$  to guarantee that

$$\lim_{t \rightarrow \infty} y(t) = r_o.$$

Include both the open-loop (assuming  $H_y = 0$ ) and feedback cases ( $H_y \neq 0$ ) in your discussion.

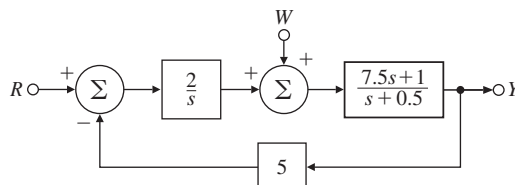
- (c) Repeat part (b) assuming a constant grade disturbance  $W(s) = \frac{w_0}{s}$  is present *in addition to* the reference input. In particular, find the variation in speed due to the grade change for both the feedforward and feedback cases. Use your results to explain (1) why feedback control is necessary and (2) how the gain  $k_P$  should be chosen to reduce steady-state error.
- (d) Assume  $w(t) = 0$  and the gain  $A$  undergoes the perturbation  $A + \delta A$ . Determine the error in speed due to the gain change for both the feedforward and feedback cases. How should the gains be chosen in this case to reduce the effects of  $\delta A$ ?
- 4.28** Prove that the step response of a Type II closed-loop stable system must *always* have a non-zero overshoot.
- 4.29** Consider the feedback control system shown in Figure 4.47.
- (a) Assume  $D_c(s) = K$ . What values of  $K$  would make the closed-loop system stable? Explain all your reasoning.
- (b) Now consider the controller of the form  $D_c(s) = \frac{1}{s^n}$  with  $n$  being a non-negative integer. For what values of  $n$  is the closed-loop system stable? Explain all your reasoning.

**Figure 4.47**  
Unity feedback system



- 4.30** A feedback control system is shown in Fig. 4.48.
- (a) Determine the system type with respect to the reference input.
- (b) Compute the steady-state tracking errors,  $e$ , for unit step and ramp inputs.
- (c) Determine the system type with respect to the disturbance input,  $w$ .
- (d) Compute the steady-state errors,  $e$ , for unit step and ramp disturbance inputs.

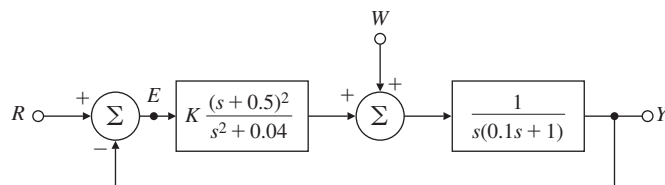
**Figure 4.48**  
Feedback system for  
Problem 4.30



- 4.31** Consider the closed-loop system shown in Fig. 4.49.
- (a) What is the condition on the gain,  $K$ , for the closed-loop system to be stable?
- (b) What is the system type with respect to the reference input,  $r$ ?

**Figure 4.49**

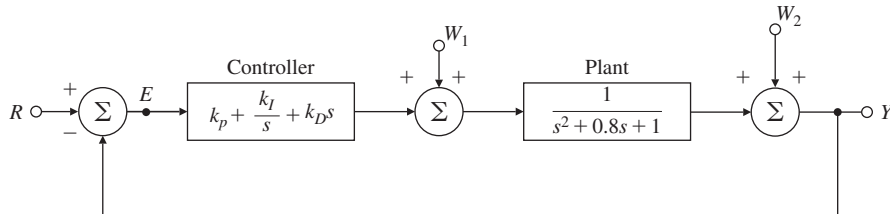
Feedback system for Problem 4.31



- (c) What is the system type with respect to the disturbance input,  $w$ ?
- (d) Prove that the system can track a sinusoidal input,  $r = \sin(0.2t)$ , with zero steady-state error.

**4.32** A servomechanism system is shown in Fig. 4.50.

- (a) Determine the conditions on the PID gain parameters to guarantee closed-loop stability.
- (b) What is the system type with respect to the reference input?
- (c) What is the system type with respect to the disturbance inputs  $w_1$  and  $w_2$ ?

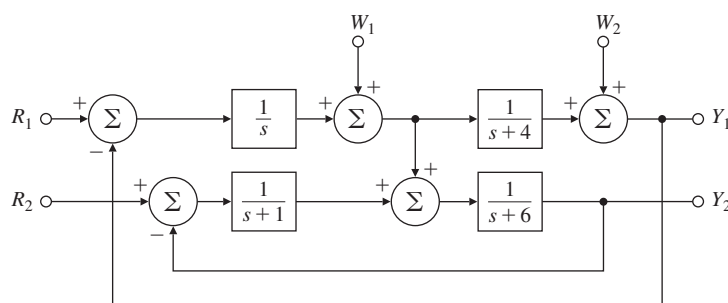
**Figure 4.50**

Feedback system for Problem 4.32

- 4.33** Consider the multivariable system shown in Fig. 4.51. Assume that the system is stable. Find the transfer functions from each disturbance input to each output and determine the steady-state values of  $y_1$  and  $y_2$  for constant disturbances. We define a multivariable system to be Type  $k$  with respect to polynomial inputs at  $w_i$  if the steady-state value of every output is zero for any combination of inputs of degree less than  $k$  and at least one input is a non-zero constant for an input of degree  $k$ . What is the system type with respect to disturbance rejection at  $w_1$ ? At  $w_2$ ?

**Figure 4.51**

Multivariable control system for Problem 4.33

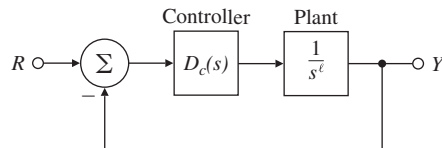


*Problems for Section 4.3: The Three-Term Controller.  
PID Control*

- 4.34** For the system shown in Figure 4.47,
- Design a proportional controller to stabilize the system.
  - Design a PD controller to stabilize the system.
  - Design a PI controller to stabilize the system.
  - What is the velocity error coefficient  $K_v$  for the system in part (c)?
- 4.35** Consider the feedback control system with the plant transfer function  $G(s) = \frac{1}{(s+0.1)(s+0.5)}$ .
- Design a proportional controller so the closed-loop system has damping of  $\zeta = 0.707$ . Under what conditions on  $k_P$  is the closed-loop system stable?
  - Design a PI controller so that the closed-loop system has no overshoot. Under what conditions on  $(k_P, k_I)$  is the closed-loop system is stable?
  - Design a PID controller such that the settling time is less than 1.7 sec.
- 4.36** Consider the liquid level control system with the plant transfer function  $G(s) = \frac{14}{s^2 + 9s + 14}$ .
- Design a proportional controller so that the damping ratio is  $\zeta = 0.6$ .
  - Design a PI controller so that the rise time is less than 1 sec.
  - Design a PD controller so that the rise time is less than 0.7 sec.
  - Design a PID controller so that the settling time is less than 1.8 sec.
- 4.37** Consider the process control system with the plant transfer function  $G(s) = \frac{10}{(8s+1)(7s+1)}$ .
- Design a PI controller such that the rise time is less than 2.5 sec.
  - Design a PID controller so that the system has no overshoot and the settling time is 5 sec.
  - Design a controller such that the peak time is less than 4.5 sec.
- 4.38** Consider the multiple-integrator plant feedback control system shown in Fig. 4.52, where  $\ell$  is an integer.
- Assume  $\ell = 1$  (voltage controlled oscillator used in the phase-locked loop of telecommunication systems). Let  $D_c(s) = \frac{k(s+5)}{s}$ . Prove that it is possible to stabilize the system with this dynamic controller. Use the Routh test to determine the range of the gain  $K$  for the closed-loop stability.
  - Assume  $\ell = 2$  (drone or satellite). Let  $D_c(s) = \frac{K(s+5)^2}{s}$ . Prove that it is possible to stabilize the system with this dynamic controller. Again use the Routh test to determine the range of the gain  $K$  for the closed-loop stability.
  - Assume  $\ell = 3$  (hospital delivery robot or the Apollo Lunar Module). Let  $D_c(s) = \frac{K(s+5)^3}{s}$ . Prove that it is possible to stabilize the system with this dynamic controller. Again use the Routh test to determine the range of the gain  $K$  for the closed-loop stability.
  - Assume  $\ell \geq 4$ . What form of controller will be required to stabilize the system?

**Figure 4.52**

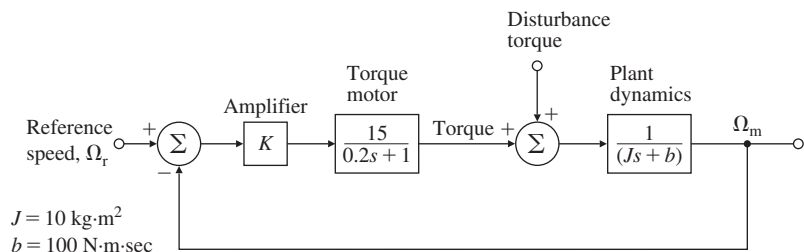
Multiple-integrator plant system



- 4.39** The transfer functions for a generator speed control system are shown in Fig. 4.53. The speed sensor is fast enough that its dynamics can be neglected and the diagram shows the equivalent unity feedback system.

**Figure 4.53**

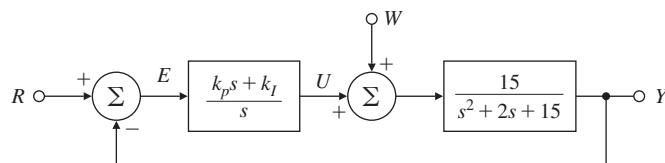
Feedback system for Problem 4.39



- (a) Assuming the reference is zero, what is the steady-state error due to a step disturbance torque of 1 N.m? What must the amplifier gain  $K$  be in order to make the steady-state error to have a magnitude of less than 0.008 rad/sec or  $|e_{ss}| \leq 0.008$  rad/sec?
- (b) Plot the roots of the closed-loop system in the complex plane, and accurately sketch the time response of the output for a step reference input using the gain  $K$  determined in part (a).
- (c) Plot the region in the complex plane of acceptable closed-loop poles corresponding to the specifications of a 1% settling time of  $t_s \leq 0.23$  sec and an overshoot  $M_p \leq 2\%$ .
- (d) A PD controller is added in the feedback loop while using the gain  $K$  determined in part (a). Select the values for  $k_p$  and  $k_d$  for the PD controller which will meet the specifications in part (c).
- (e) How would the disturbance-induced steady-state error change with the new control scheme in part (d)? How could the steady-state error to a disturbance torque be eliminated entirely?
- 4.40** Consider the system shown in Fig. 4.54 with PI control.
- (a) Determine the transfer function from  $R$  to  $Y$ .
- (b) Determine the transfer function from  $W$  to  $Y$ .
- (c) Under what conditions on  $(k_p, k_I)$  is the closed-loop system stable?

**Figure 4.54**

Feedback system for Problem 4.40



- (d) What are the system types and error constants with respect to reference input and with respect to disturbance rejection?

**4.41** Consider the second-order plant with transfer function

$$G(s) = \frac{1}{(s + 4.5)(s + 5.7)}.$$

and in a unity feedback structure.

- (a) Determine the system type and error constant with respect to tracking polynomial reference inputs of the system for P [ $D = k_p$ ], PD [ $D = k_p + k_D s$ ], and PID [ $D = k_p + \frac{k_I}{s} + k_D s$ ] controllers. Let  $k_p = 75$ ,  $k_I = 38$ , and  $k_D = 0.1$ .
- (b) Determine the system type and error constant of the system with respect to disturbance inputs for each of the three regulators in part (a) assuming the disturbance  $w(t)$  is introduced at the *input* to the plant.
- (c) Is this system better at tracking references or rejecting disturbances? Explain your responses briefly.

With PID, verify your results for parts (a) and (b) using Matlab by plotting unit step and ramp responses for both tracking and disturbance rejection.

**4.42** The DC motor speed control shown in Fig. 4.55 is described by the differential equation

$$\dot{y} + 60y = 600v_a - 1500w,$$

where  $y$  is the motor speed,  $v_a$  is the armature voltage, and  $w$  is the load torque. Assume the armature voltage is computed using the PI control law

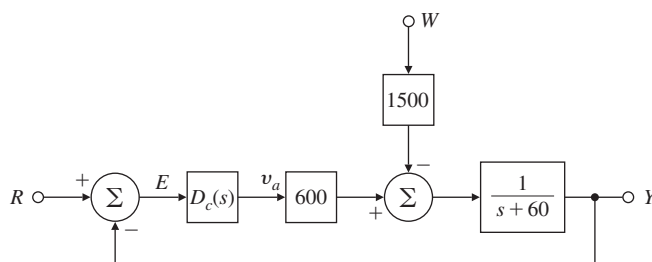
$$v_a = -\left(k_P e + k_I \int_0^t edt\right),$$

where  $e = r - y$ .

- (a) Compute the transfer function from  $W$  to  $Y$  as a function of  $k_P$  and  $k_I$ .
- (b) Compute values for  $k_P$  and  $k_I$  so the characteristic equation of the closed-loop system will have roots at  $-60 \pm 60j$ .
- 4.43** For the system in Fig. 4.55, compute the following steady-state errors:
- (a) to a unit-step reference input;
- (b) to a unit-ramp reference input;

**Figure 4.55**

DC Motor speed-control block diagram for Problems 4.42 and 4.43



- (c) to a unit-step disturbance input;
- (d) for a unit-ramp disturbance input.
- (e) Verify your answers to (a) and (d) using Matlab. Note a ramp response can be generated as a step response of a system modified by an added integrator at the reference input.

- 4.44** Consider the satellite-attitude control problem shown in Fig. 4.56 where the normalized parameters are

$$J = 10 \text{ spacecraft inertia, N}\cdot\text{m}\cdot\text{sec}^2/\text{rad}.$$

$\theta_r$  = reference satellite attitude, rad.

$\theta$  = actual satellite attitude, rad.

$$H_y = 1 \text{ sensor scale factor, V/rad.}$$

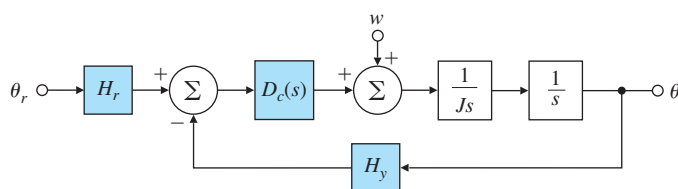
$$H_r = 1 \text{ reference sensor scale factor, V/rad.}$$

$$w = \text{disturbance torque, N}\cdot\text{m}.$$

- (a) Use proportional control, P, with  $D_c(s) = k_P$ , and give the range of values for  $k_P$  for which the system will be stable.
- (b) Use PD control, let  $D_c(s) = (k_P + k_D s)$ , and determine the system type and error constant with respect to reference inputs.
- (c) Use PD control, let  $D_c(s) = (k_P + k_D s)$ , and determine the system type and error constant with respect to disturbance inputs.
- (d) Use PI control, let  $D_c(s) = (k_P + \frac{k_I}{s})$ , and determine the system type and error constant with respect to reference inputs.
- (e) Use PI control, let  $D_c(s) = (k_P + \frac{k_I}{s})$ , and determine the system type and error constant with respect to disturbance inputs.
- (f) Use PID control, let  $D_c(s) = (k_P + \frac{k_I}{s} + k_D s)$ , and determine the system type and error constant with respect to reference inputs.
- (g) Use PID control, let  $D_c(s) = (k_P + \frac{k_I}{s} + k_D s)$ , and determine the system type and error constant with respect to disturbance inputs.

**Figure 4.56**

Satellite attitude control



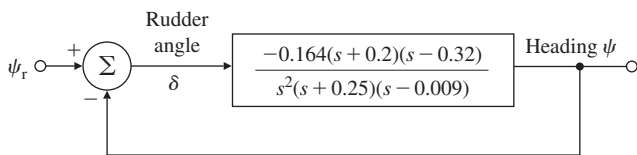
- 4.45** Automatic ship steering is particularly useful in heavy seas when it is important to maintain the ship along an accurate path. Such a control system for a large tanker is shown in Fig. 4.57, with the plant transfer function relating heading changes to rudder deflection in radians.

- (a) Write the differential equation that relates the heading angle to rudder angle for the ship *without* feedback.

- (b) This control system uses simple proportional feedback with the gain of unity. Is the closed-loop system stable as shown? (*Hint:* use Routh's criterion.)
- (c) Is it possible to stabilize this system by changing the proportional gain from unity to a lower value?
- (d) Use Matlab to design a dynamic controller of the form  $D_c(s) = K \left( \frac{s+a}{s+b} \right)^2$  so the closed-loop system is stable and in response to a step heading command it has zero steady-state error and less than 10% overshoot. Are these reasonable values for a large tanker?

**Figure 4.57**

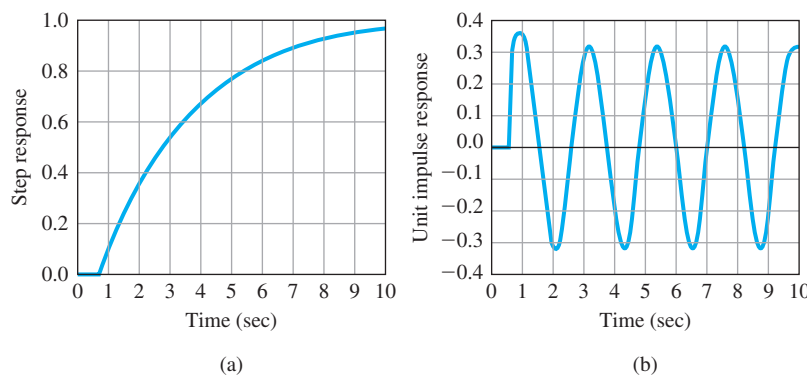
Ship-steering control system for Problem 4.45



- 4.46** The unit-step response of a paper machine is shown in Fig. 4.58(a) where the input into the system is stock flow onto the wire and the output is basis weight (thickness). The time delay and slope of the transient response may be determined from the figure.

**Figure 4.58**

Paper-machine response data for Problem 4.46



- (a) Find the proportional-, PI-, and PID-controller parameters using the Ziegler–Nichols transient-response method.
- (b) Using proportional feedback control, control designers have obtained a closed-loop system with the unit impulse response shown in Fig. 4.58(b). When the gain  $K_u = 8.556$ , the system is on the verge of instability. Determine the proportional-, PI-, and PID-controller parameters according to the Ziegler–Nichols ultimate sensitivity method.

- 4.47** A paper machine has the transfer function

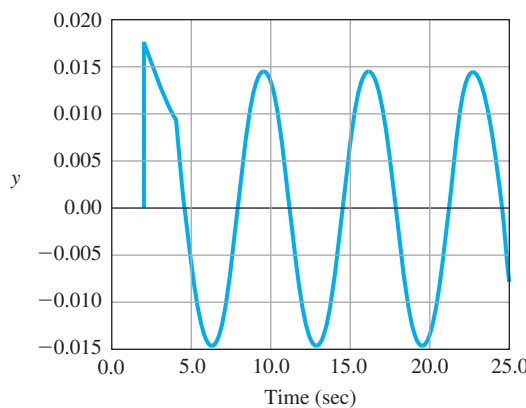
$$G(s) = \frac{e^{-2s}}{3s + 1},$$

where the input is stock flow onto the wire and the output is basis weight or thickness.

- (a) Find the PID-controller parameters using the Ziegler–Nichols tuning rules.
- (b) The system becomes marginally stable for a proportional gain of  $K_u = 3.044$  as shown by the unit impulse response in Fig. 4.59. Find the optimal PID-controller parameters according to the Ziegler–Nichols tuning rules.

**Figure 4.59**

Unit impulse response for the paper machine in Problem 4.47

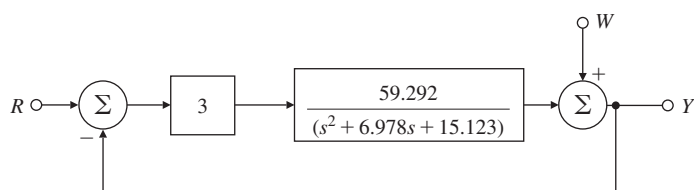


△ *Problems for Section 4.4: Feedforward Control by Plant Model Inversion*

- 4.48** Consider the DC motor speed-control system shown in Fig. 4.60 with proportional control. (a) Add feedforward control to eliminate the steady-state tracking error for a step reference input. (b) Also add feedforward control to eliminate the effect of a constant output disturbance signal,  $w$ , on the output of the system.

**Figure 4.60**

Block diagram for Problem 4.48



△ *Problems for Section 4.5: Introduction to Digital Control*

- 4.49** Compute the discrete equivalents for the following possible controllers using the trapezoid rule (Tustin's method) discussed in Appendix W4.5 available online at [www.pearsonglobaleditions.com](http://www.pearsonglobaleditions.com) and in Section 8.3.1. Let  $T_s = 0.05$  sec in each case.

- (a)  $D_{c1}(s) = (s + 2)/2$ ,
- (b)  $D_{c2}(s) = 2\frac{s+2}{s+4}$ ,

- (c)  $D_{c3}(s) = 5 \frac{s+2}{s+10}$ ,
- (d)  $D_{c4}(s) = 5 \frac{(s+2)(s+0.1)}{(s+10)(s+0.01)}$ .
- 4.50** Give the difference equations corresponding to the discrete controllers found in Problem 4.49, respectively.
- (a) Part 1.
- (b) Part 2.
- (c) Part 3.
- (d) Part 4.

# The Root-Locus Design Method



## A Perspective on the Root-Locus Design Method

In Chapter 3, we related the features of a step response, such as rise time, overshoot, and settling time, to pole locations in the  $s$ -plane of the transform of a second-order system characterized by the natural frequency  $\omega_n$ , the damping ratio  $\zeta$ , and the real part  $\sigma$ . This relationship is shown graphically in Fig. 3.16. We also examined the changes in these transient-response features when a pole or a zero is added to the transfer function. In Chapter 4, we saw how feedback can improve steady-state errors and can also influence dynamic response by changing the system's pole locations. In this chapter, we present a specific technique that shows how changes in one of a system's parameters will modify the *roots of the characteristic equation*, which are the closed-loop poles, and thus change the system's dynamic response. The method was developed by W. R. Evans who gave rules for plotting the paths of the roots, a plot he called the **Root Locus**. With the development of Matlab and similar software, the rules are no longer needed for detailed plotting, but we feel it is essential for a control designer to understand how proposed dynamic controllers will influence a locus as a guide in the design process. We

also feel that it is important to understand the basics of how loci are generated in order to perform sanity checks on the computer results. For these reasons, the study of the Evans rules is important.

The root locus is most commonly used to study the effect of loop gain variations; however, the method is general and can be used to plot the roots of any polynomial with respect to any one real parameter that enters the equation linearly. For example, the root-locus method can be used to plot the roots of a characteristic equation as the gain of a velocity sensor feedback changes, or the parameter can be a physical parameter, such as motor inertia or armature inductance.

## Chapter Overview

We open Section 5.1 by illustrating the root locus for some simple feedback systems for which the equations can be solved directly. In Section 5.2, we will show how to put an equation into the proper form for developing the rules for the root-locus behavior. In Section 5.3, this approach will be applied to determine the locus for a number of typical control problems, which illustrate the factors that influence the final shape. Matlab is used for detailed plotting of specific loci. When adjustment of the selected parameter alone cannot produce a satisfactory design, designs using other parameters can be studied or dynamic elements such as lead, lag, or notch compensations can be introduced, as is described in Section 5.4. In Section 5.5, the uses of the root locus for design will be demonstrated in two examples including a comprehensive design for the attitude control of a small airplane. In Section 5.6, the root-locus method will be extended to guide the design of systems with a negative parameter, systems with more than one variable parameter, and systems with simple time delay. Finally, Section 5.7 will give historical notes on the origin of root-locus design.

### 5.1 Root Locus of a Basic Feedback System

We begin with the basic feedback system shown in Fig. 5.1. For this system, the closed-loop transfer function is

$$\frac{Y(s)}{R(s)} = T(s) = \frac{D_c(s)G(s)}{1 + D_c(s)G(s)H(s)}, \quad (5.1)$$

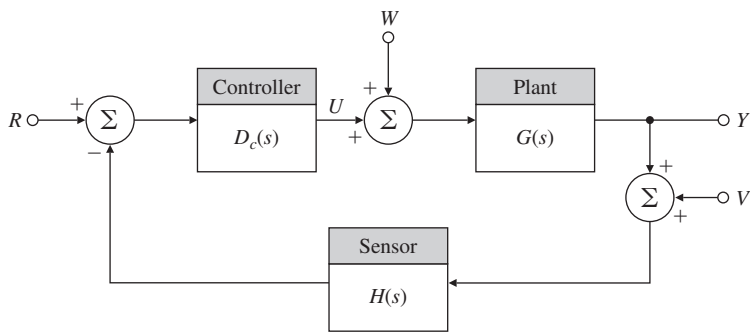
and the characteristic equation, whose roots are the poles of this transfer function, is

$$1 + D_c(s)G(s)H(s) = 0. \quad (5.2)$$

To put the equation in a form suitable for study of the roots as a parameter changes, we first put the equation in polynomial form and select the parameter of interest, which we will call  $K$ . We assume we can define component polynomials  $a(s)$  and  $b(s)$  so the characteristic polynomial is

**Figure 5.1**

Basic closed-loop block diagram



in the form  $a(s) + Kb(s)$ . We then define the transfer function  $L(s) = \frac{b(s)}{a(s)}$  so the characteristic equation can be written as<sup>1</sup>

$$1 + KL(s) = 0 \text{ where } L(s) = \frac{b(s)}{a(s)}. \quad (5.3)$$

If, as is often the case, the parameter is the gain of the controller, then  $L(s)$  is simply proportional to  $D_c(s)G(s)H(s)$ . Evans suggested we plot the locus of *all possible* roots of Eq. (5.3) as  $K$  varies from zero to infinity, and then use the resulting plot to aid us in selecting the best value of  $K$ . Furthermore, by studying the effects of additional poles and zeros on this graph, we can determine the consequences of additional dynamics added to  $D_c(s)$  as compensation in the loop. We thus have a tool not only for selecting the specific parameter value, but for designing the dynamic compensation as well. The graph of all possible roots of Eq. (5.3) relative to parameter  $K$  is called the **root locus**, and the set of rules to construct this graph is called the **root-locus method of Evans**. We begin our discussion of the method with the mechanics of constructing a root locus, using the equation in the form of Eq. (5.3) and  $K$  as the variable parameter.

To set the notation for our study, we assume here the transfer function  $L(s)$  is a rational function whose numerator is a monic<sup>2</sup> polynomial  $b(s)$  of degree  $m$  and whose denominator is a monic polynomial  $a(s)$  of degree  $n$  such that<sup>3</sup>  $n \geq m$ . Therefore,  $m =$  the number of zeros, while  $n =$  the number of poles. We can factor these polynomials as

$$\begin{aligned} b(s) &= s^m + b_1 s^{m-1} + \cdots + b_m \\ &= (s - z_1)(s - z_2) \cdots (s - z_m) \end{aligned}$$

<sup>1</sup>In the most common case,  $L(s)$  is the loop transfer function of the feedback system and  $K$  is the gain of the controller–plant combination. However, the root locus is a general method suitable for the study of any polynomial and any parameter that can be put in the form of Eq. (5.3).

<sup>2</sup>Monic means that the coefficient of the highest power of  $s$  is 1.

<sup>3</sup>If  $L(s)$  is the transfer function of a physical system, it is necessary that  $n \geq m$  or else the system would have an infinite response to a finite input. If the parameter should be chosen so  $n < m$ , then we can consider the equivalent equation  $1 + K^{-1}L(s)^{-1} = 0$ .

### Evans's method

$$\begin{aligned}
 &= \prod_{i=1}^m (s - z_i), \\
 a(s) &= s^n + a_1 s^{n-1} + \cdots + a_n, \\
 &= \prod_{i=1}^n (s - p_i).
 \end{aligned} \tag{5.4}$$

The roots of  $b(s) = 0$  are the zeros of  $L(s)$  and are labeled  $z_i$ , and the roots of  $a(s) = 0$  are the poles of  $L(s)$  and are labeled  $p_i$ . The roots of the characteristic equation itself are  $r_i$  from the factored form ( $n > m$ ),

$$a(s) + Kb(s) = (s - r_1)(s - r_2) \cdots (s - r_n). \tag{5.5}$$

We may now state the root-locus problem expressed in Eq. (5.3) in several equivalent but useful ways. Each of the following equations has the same roots:

$$1 + KL(s) = 0, \tag{5.6}$$

$$1 + K \frac{b(s)}{a(s)} = 0, \tag{5.7}$$

$$a(s) + Kb(s) = 0, \tag{5.8}$$

$$L(s) = -\frac{1}{K}. \tag{5.9}$$

### Root-locus forms

Equations (5.6)–(5.9) are sometimes referred to as the **root-locus form** or Evans form of a characteristic equation. The root locus is the set of values of  $s$  for which Eqs. (5.6)–(5.9) hold for some positive real value<sup>4</sup> of  $K$ . Because the solutions to Eqs. (5.6)–(5.9) are the roots of the closed-loop system characteristic equation and are thus closed-loop poles of the system, the root-locus method can be thought of as a method for inferring dynamic properties of the closed-loop system as the parameter  $K$  changes.

## EXAMPLE 5.1

### *Root Locus of a Motor Position Control*

In Chapter 2, we saw that a normalized transfer function of a DC motor voltage-to-position can be

$$\frac{\Theta_m(s)}{V_a(s)} = \frac{Y(s)}{U(s)} = G(s) = \frac{A}{s(s + c)}.$$

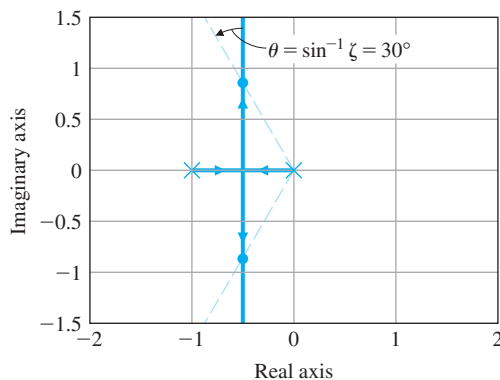
Solve for the root locus of closed-loop poles of the system created by feeding back the output  $\Theta_m$  as shown in Fig. 5.1 with respect to the parameter  $A$  if  $D_c(s) = H(s) = 1$  and also  $c = 1$ .

---

<sup>4</sup>If  $K$  is positive, the locus is called the “positive” locus. We will later consider the simple changes if  $K < 0$ , resulting in a “negative” locus.

**Figure 5.2**

Root locus for  
 $L(s) = \frac{1}{s(s+1)}$



**Solution.** In terms of our notation, the values are

$$L(s) = \frac{1}{s(s+1)}, \quad b(s) = 1, \quad m = 0, \quad z_i = \{\text{empty}\}, \quad (5.10)$$

$$K = A, \quad a(s) = s^2 + s, \quad n = 2, \quad p_i = 0, -1.$$

From Eq. (5.8), the root locus is a graph of the roots of the quadratic equation

$$a(s) + Kb(s) = s^2 + s + K = 0. \quad (5.11)$$

Using the quadratic formula, we can immediately express the roots of Eq. (5.11) as

$$r_1, r_2 = -\frac{1}{2} \pm \frac{\sqrt{1-4K}}{2}. \quad (5.12)$$

A plot of the corresponding root locus is shown in Fig. 5.2. For  $0 \leq K \leq 1/4$ , the roots are real between  $-1$  and  $0$ . At  $K = 1/4$  there are two roots at  $-1/2$ , and for  $K > 1/4$  the roots become complex with real parts constant at  $-1/2$  and imaginary parts that increase essentially in proportion to the square root of  $K$ . The dashed lines in Fig. 5.2 correspond to roots with a damping ratio  $\zeta = 0.5$ . The poles of  $L(s)$  at  $s = 0$  and  $s = -1$  are marked by the symbol  $\times$ , and the points where the locus crosses the lines where the damping ratio equals  $0.5$  are marked with dots ( $\bullet$ ). We can compute  $K$  at the point where the locus crosses  $\zeta = 0.5$  because we know that if  $\zeta = 0.5$ , then  $\theta = 30^\circ$  and the magnitude of the imaginary part of the root is  $\sqrt{3}$  times the magnitude of the real part. Since the size of the real part is  $\frac{1}{2}$ , from Eq. (5.12) we have

$$\frac{\sqrt{4K-1}}{2} = \frac{\sqrt{3}}{2},$$

and, therefore,  $K = 1$ .

We can observe several features of this simple locus by looking at Eqs. (5.11) and (5.12) and Fig. 5.2. First, there are two roots and, thus, two loci which we call branches of the root locus. At  $K = 0$  these branches begin at the poles of  $L(s)$  (which are at  $0$  and  $-1$ ), as they should, since for  $K = 0$  the system is open-loop and the characteristic

**Breakaway points are where roots move away from the real axis**

equation is  $a(s) = 0$ . As  $K$  is increased, the roots move toward each other, coming together at  $s = -\frac{1}{2}$ , and at that point they break away from the real axis. After the **breakaway point**, the roots move off to infinity with equal real parts, so the sum of the two roots is always  $-1$ . From the viewpoint of design, we see that by altering the value of the parameter  $K$ , we can cause the closed-loop poles to be at any point along the locus in Fig. 5.2. If some points along this locus correspond to a satisfactory transient response, then we can complete the design by choosing the corresponding value of  $K$ ; otherwise, we are forced to consider a more complex controller. As we pointed out earlier, the root locus technique is not limited to focusing on the system gain ( $K = A$  in Example 5.1); the same ideas are applicable for finding the locus with respect to *any* parameter that enters linearly in the characteristic equation.

## EXAMPLE 5.2

### *Root Locus with Respect to Plant Open-Loop Pole and Zero*

Consider the characteristic equation as in Example 5.1, again with  $D_c(s) = H(s) = 1$  except now, instead of a constant  $A$ , let there be a zero in the form of  $A = s + 2c$ . Select  $c$  as the parameter of interest in the equation

$$1 + G(s) = 1 + \frac{s + 2c}{s(s + c)}. \quad (5.13)$$

Find the root locus of the characteristic equation with respect to  $c$ .

**Solution.** The corresponding closed-loop characteristic equation in polynomial form is

$$s^2 + s + c(s + 2) = 0. \quad (5.14)$$

Equation (5.6) applies directly if we rearrange Eq. (5.14) with the following definitions:

$$L(s) = \frac{s+2}{s(s+1)}, \quad b(s) = s + 2, \quad m = 1, \quad z_i = -2, \quad (5.15)$$

$$K = c, \quad a(s) = s(s + 1), \quad n = 2, \quad p_i = 0, -1.$$

Thus, the root-locus form of the characteristic equation is

$$1 + \frac{c(s + 2)}{s(s + 1)} = 0.$$

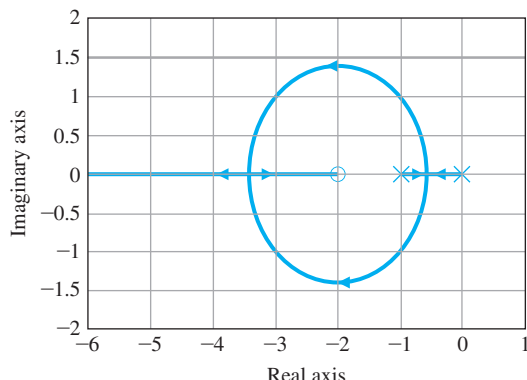
The solutions to Eq. (5.14) are easily computed using the quadratic formula as

$$r_1, r_2 = -\frac{c + 1}{2} \pm \frac{\sqrt{c^2 - 6c + 1}}{2}. \quad (5.16)$$

The locus of solutions is shown in Fig. 5.3, with the poles [roots of  $a(s)$ ] again indicated by  $\times$ 's and the zero [root of  $b(s)$ ] by the circle ( $\circ$ ). Note that when  $c^2 - 6c + 1 < 0$ , the roots become complex. This happens when  $0.172 < c < 5.828$ . When  $c < 0.172$ , the roots are on the real axis between  $s = 0$  and  $-1$  points. There are two roots at  $s = -0.586$ , when  $c = 0.172$  and another two roots at  $s = -3.41$  when  $c = 5.828$ ; these point of multiple roots where two or more roots merge at the real axis is called a **break-in point**. When  $c > 5.828$ , the two locus segments

**Figure 5.3**

Root locus versus parameter  $c$  for  
 $1 + G(s) = 0$   
 $1 + \frac{s+2c}{s(s+c)} = 0$



**Break-in point**

move in opposite along the real axis; one is moving towards the infinite  $s$ -plane and the other towards the location of the zero.

Of course, computing the root locus for a quadratic equation is easy to do since we can solve the characteristic equation for the roots, as was done in Eqs. (5.12) and (5.16), and directly plot these as a function of the parameter  $K$  or  $c$ . To be useful, the method must be suitable for higher-order systems for which explicit solutions are difficult to obtain; therefore, rules for the construction of a general root locus were developed by Evans. With the availability of Matlab, these rules are no longer necessary to plot a specific locus because the command `rlocus(sys)` will do that. However, in control design we are interested not only in a specific locus but also in how to modify the dynamics in such a way as to propose a system that will meet the dynamic response specifications for good control performance. For this purpose, it is very useful to be able to roughly sketch a locus so as to be able to evaluate the consequences of possible compensation alternatives. It is also important to be able to quickly evaluate the correctness of a computer-generated locus to verify that what is plotted by Matlab is in fact what was meant to be plotted. It is easy to get a constant wrong or to leave out a term and GIGO<sup>5</sup> is the well-known first rule of computation.

## 5.2 Guidelines for Determining a Root Locus

We begin with a formal definition of a root locus. From the form of Eq. (5.6), we define the root locus this way:

**Definition I.** The root locus is the set of values of  $s$  for which  $1 + KL(s) = 0$  is satisfied as the real parameter  $K$  varies from 0 to  $+\infty$ . Typically,  $1 + KL(s) = 0$  is the characteristic equation of the system, and in this case the roots on the locus are the closed-loop poles of that system.

---

<sup>5</sup>Garbage in, Garbage out.

Now suppose we look at Eq. (5.9). If  $K$  is to be real and positive,  $L(s)$  must be real and negative. In other words, if we arrange  $L(s)$  in polar form as magnitude and phase, then the phase of  $L(s)$  must be  $180^\circ$  in order to satisfy Eq. (5.9). We can thus define the root locus in terms of this **phase condition** as follows.

The basic root-locus rule;  
the phase of  $L(s) = 180^\circ$

**Definition II.** The root locus of  $L(s)$  is the set of points in the  $s$ -plane where the phase of  $L(s)$  is  $180^\circ$ . To test whether a point in the  $s$ -plane is on the locus, we define the angle to the test point from a zero as  $\psi_i$  and the angle to the test point from a pole as  $\phi_i$  then Definition II is expressed as those points in the  $s$ -plane where, for an integer  $\ell$ ,

$$\sum \psi_i - \sum \phi_i = 180^\circ + 360^\circ(l - 1). \quad (5.17)$$

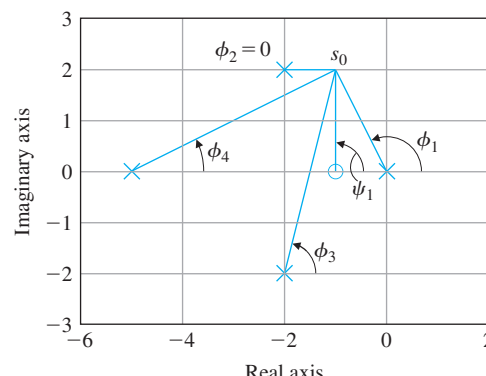
The immense merit of Definition II is that, while it is very difficult to solve a high-order polynomial by hand, computing the phase of a transfer function is relatively easy. The usual case is when  $K$  is real and positive, and we call this case the **positive or  $180^\circ$  locus**. When  $K$  is real and negative,  $L(s)$  must be real and positive with a phase of  $0^\circ$ , and this case is called the **negative or  $0^\circ$  locus**.

From Definition II we can, in principle, determine a positive root locus for a complex transfer function by measuring the phase and marking those places where we find  $180^\circ$ . This direct approach can be illustrated by considering the example

$$L(s) = \frac{s + 1}{s(s + 5)[(s + 2)^2 + 4]}. \quad (5.18)$$

In Fig. 5.4, the poles of this  $L(s)$  are marked  $\times$  and the zero is marked  $\bigcirc$ . Suppose we select the test point  $s_0 = -1 + 2j$ . We would like to test whether or not  $s_0$  lies on the root locus for some value of  $K$ . For

**Figure 5.4**  
Measuring the phase of  
Eq. (5.18)



this point to be on the locus, we must have  $\angle L(s_0) = 180^\circ + 360^\circ(l - 1)$  for some integer  $l$ , or equivalently, from Eq. (5.18),

$$\angle(s_0+1) - \angle s_0 - \angle(s_0+5) - \angle[(s_0+2)^2 + 4] = 180^\circ + 360^\circ(l-1). \quad (5.19)$$

The angle from the zero term  $s_0 + 1$  can be computed<sup>6</sup> by drawing a line from the location of the zero at  $-1$  to the test point  $s_0$ . In this case the line is vertical and has a phase angle marked  $\psi_1 = 90^\circ$  in Fig. 5.4. In a similar fashion, the vector from the pole at  $s = 0$  to the test point  $s_0$  is shown with angle  $\phi_1$ , and the angles of the two vectors from the complex poles at  $-2 \pm 2j$  to  $s_0$  are shown with angles  $\phi_2$  and  $\phi_3$ . The phase of the vector  $s_0 + 5$  is shown with angle  $\phi_4$ . From Eq. (5.19), we find the total phase of  $L(s)$  at  $s = s_0$  to be the sum of the phases of the numerator term corresponding to the zero minus the phases of the denominator terms corresponding to the poles:

$$\begin{aligned} \angle L &= \psi_1 - \phi_1 - \phi_2 - \phi_3 - \phi_4 \\ &= 90^\circ - 116.6^\circ - 0^\circ - 76^\circ - 26.6^\circ \\ &= -129.2^\circ. \end{aligned}$$

Since the phase of  $L(s)$  is not  $180^\circ$ , we conclude that  $s_0$  is *not* on the root locus, so we must select another point and try again. Although measuring phase is not particularly hard, measuring phase at every point in the  $s$ -plane is hardly practical. Therefore, to make the method practical, we need some general guidelines for determining where the root locus is. Evans developed a set of rules for this purpose, which we will illustrate by applying them to the root locus for

$$L(s) = \frac{1}{s[(s+4)^2 + 16]}. \quad (5.20)$$

We begin by considering the positive locus, which is by far the most common case.<sup>7</sup> The first three rules are relatively simple to remember and are essential for any reasonable sketch. The last two are less useful but are used occasionally. As usual, we assume Matlab or its equivalent is always available to make an accurate plot of a promising locus.

### 5.2.1 Rules for Determining a Positive ( $180^\circ$ ) Root Locus

**RULE 1.** The  $n$  branches of the locus start at the poles of  $L(s)$  and  $m$  of these branches end on the zeros of  $L(s)$ . From the equation  $a(s) + Kb(s) = 0$ , if  $K = 0$ , the equation reduces to  $a(s) = 0$ , whose roots are the poles. When  $K$  approaches infinity,  $s$  must be such that either  $b(s) = 0$  or  $s \rightarrow \infty$ . Since there are  $m$  zeros where  $b(s) = 0$ ,  $m$  branches can end in these places. The case for  $s \rightarrow \infty$  is considered in Rule 3.

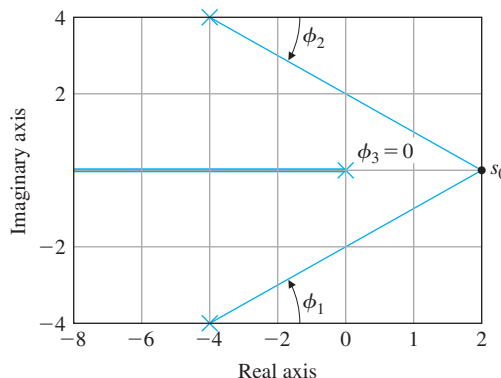
---

<sup>6</sup>The graphical evaluation of the magnitude and phase of a complex number is reviewed in Appendix WA, Section WA.3 online at [www.pearsonglobaleditions.com](http://www.pearsonglobaleditions.com).

<sup>7</sup>The negative locus will be considered in Section 5.6.

**Figure 5.5**

Rule 2. The real-axis parts of the locus are to the left of an odd number of poles and zeros



**RULE 2.** The loci are on the real axis to the left of an odd number of poles and zeros.

If we take a test point on the real axis, such as  $s_0$  in Fig. 5.5, we find that the angles  $\phi_1$  and  $\phi_2$  of the two complex poles cancel each other, as would the angles from complex conjugate zeros. Angles from real poles or zeros are  $0^\circ$  if the test point is to the right and  $180^\circ$  if the test point is to the left of a given pole or zero. Therefore, for the total angle to add to  $180^\circ + 360^\circ(l-1)$ , the test point must be to the left of an odd number of real-axis poles plus zeros as shown in Fig. 5.5.

**RULE 3.** For large  $s$  and  $K$ ,  $n - m$  branches of the loci are asymptotic to lines at angles  $\phi_l$  radiating out from the point  $s = \alpha$  on the real axis, where

$$\phi_l = \frac{180^\circ + 360^\circ(l-1)}{n-m}, \quad l = 1, 2, \dots, n-m, \quad (5.21)$$

$$\alpha = \frac{\sum p_i - \sum z_i}{n-m}.$$

As  $K \rightarrow \infty$ , the equation

$$L(s) = -\frac{1}{K}, \quad (5.22)$$

can be satisfied only if  $L(s) = 0$ . This can occur in two apparently different ways. In the first instance, as discussed in Rule 1,  $m$  roots will be found to approach the zeros of  $L(s)$ . The second manner in which  $L(s)$  may go to zero is if  $s \rightarrow \infty$  since, by assumption,  $n$  is larger than  $m$ . The asymptotes describe how these  $n - m$  roots approach  $s \rightarrow \infty$ . For large  $s$ , the equation

$$1 + K \frac{s^m + b_1 s^{m-1} + \dots + b_m}{s^n + a_1 s^{n-1} + \dots + a_n} = 0, \quad (5.23)$$

can be approximated<sup>8</sup> by

$$1 + K \frac{1}{(s - \alpha)^{n-m}} = 0. \quad (5.24)$$

This is the equation for a system in which there are  $n - m$  poles, all clustered at  $s = \alpha$ . Another way to visualize this same result is to consider the picture we would see if we could observe the locations of poles and zeros from a vantage point of very large  $s$ : They would appear to cluster near the  $s$ -plane origin. Thus,  $m$  zeros would cancel the effects of  $m$  of the poles, and the other  $n - m$  poles would appear to be in the same place. We say the locus of Eq. (5.23) is asymptotic to the locus of Eq. (5.24) for large values of  $K$  and  $s$ . We need to compute  $\alpha$  to find the locus for the resulting asymptotic system. To find the locus, we choose our search point  $s_0$  such that  $s_0 = Re^{j\phi}$  for some large fixed value of  $R$  and variable  $\phi$ . Since all poles of this simple system are in the same place, the angle of its transfer function is  $180^\circ$  if all  $n - m$  angles, each equal to  $\phi_l$ , sum to  $180^\circ$ . Therefore,  $\phi_l$  is given by

$$(n - m)\phi_l = 180^\circ + 360^\circ(l - 1),$$

#### The angles of the asymptotes

for some integer  $l$ . Thus, the asymptotic root locus consists of radial lines at the  $n - m$  distinct angles given by

$$\phi_l = \frac{180^\circ + 360^\circ(l - 1)}{n - m}, \quad l = 1, 2, \dots, n - m. \quad (5.25)$$

For the system described by Eq. (5.20),  $n - m = 3$  and  $\phi_{1,2,3} = 60^\circ, 180^\circ$ , and  $300^\circ$  or  $\pm 60^\circ, 180^\circ$ .

The lines of the asymptotic locus come from  $s_0 = \alpha$  on the real axis. To determine  $\alpha$ , we make use of a simple property of polynomials. Suppose we consider the monic polynomial  $a(s)$  with coefficients  $a_i$  and roots  $p_i$ , as in Eq. (5.4), and we equate the polynomial form with the factored form

$$s^n + a_1 s^{n-1} + a_2 s^{n-2} + \dots + a_n = (s - p_1)(s - p_2) \cdots (s - p_n).$$

If we multiply out the factors on the right side of this equation, we see that the coefficient of  $s^{n-1}$  is  $-p_1 - p_2 - \dots - p_n$ . On the left side of the equation, we see that this term is  $a_1$ . Thus  $a_1 = -\sum p_i$ ; in other words, the coefficient of the *second* highest term in a monic polynomial is the negative sum of its roots—in this case, the poles of  $L(s)$ . Applying this result to the polynomial  $b(s)$ , we find the negative sum of the zeros to be  $b_1$ . These results can be written as

$$\begin{aligned} -b_1 &= \sum z_i, \\ -a_1 &= \sum p_i. \end{aligned} \quad (5.26)$$

Finally, we apply this result to the closed-loop characteristic polynomial obtained from Eq. (5.23):

---

<sup>8</sup>This approximation can be obtained by dividing  $a(s)$  by  $b(s)$  and matching the dominant two terms (highest powers in  $s$ ) to the expansion of  $(s - \alpha)^{n-m}$ .

$$\begin{aligned} s^n + a_1 s^{n-1} + \cdots + a_n + K(s^m + b_1 s^{m-1} + \cdots + b_m) &= (s - r_1)(s - r_2) \cdots (s - r_n) = 0. \end{aligned} \quad (5.27)$$

Note the sum of the roots is the negative of the coefficient of  $s^{n-1}$  and is independent of  $K$  if  $m < n - 1$ . Therefore, if  $L(s)$  has at least two more poles than zeros, we have  $a_1 = -\sum r_i$ . We have thus shown that the center point of the roots does not change with  $K$  if  $m < n - 1$ , and that the open-loop and closed-loop sum is the same and is equal to  $-a_1$ , which can be expressed as

$$-\sum r_i = -\sum p_i. \quad (5.28)$$

For large values of  $K$ , we have seen that  $m$  of the roots  $r_i$  approach the zeros  $z_i$  and  $n - m$  of the roots approach the branches of the asymptotic system  $\frac{1}{(s-\alpha)^{n-m}}$  whose poles add up to  $(n - m)\alpha$ . Combining these results, we conclude that the sum of all the roots equals the sum of those roots that go to infinity plus the sum of those roots that go to the zeros of  $L(s)$ :

$$-\sum r_i = -(n - m)\alpha - \sum z_i = -\sum p_i.$$

Solving for  $\alpha$ , we get

$$\alpha = \frac{\sum p_i - \sum z_i}{n - m}. \quad (5.29)$$

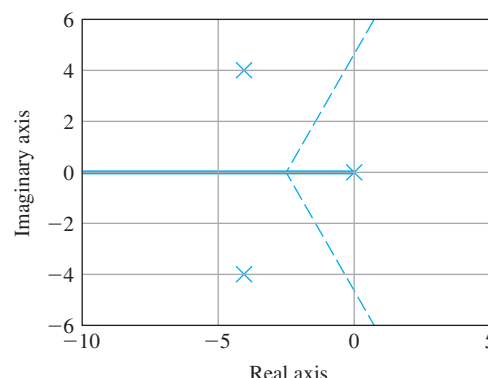
Notice in the sums  $\sum p_i$  and  $\sum z_i$ , the imaginary parts always add to zero, since complex poles and zeros always occur in complex conjugate pairs. Thus, Eq. (5.29) requires information about the real parts only. For Eq. (5.20),

$$\begin{aligned} \alpha &= \frac{-4 - 4 + 0}{3 - 0} \\ &= -\frac{8}{3} = -2.67. \end{aligned}$$

The asymptotes at  $\pm 60^\circ$  are shown dashed in Fig. 5.6. Notice they cross the imaginary axis at  $\pm(2.67)j\sqrt{3} = \pm 4.62j$ . The asymptote at  $180^\circ$  was already found on the real axis by Rule 2.

**Figure 5.6**

The asymptotes are  $n - m$  radial lines from  $\alpha$  at equal angles



**RULE 4.** The angle of departure of a branch of the locus from a single pole is given by

$$\phi_{dep} = \sum \psi_i - \sum_{i \neq dep} \phi_i - 180^\circ, \quad (5.30)$$

where  $\sum \phi_i$  is the sum of the angles to the remaining poles and  $\sum \psi_i$  is the sum of the angles to all the zeros. The angles of departure for repeated poles with multiplicity,  $q$ , is given by

Rule for departure angles

$$q\phi_{l,dep} = \sum \psi_i - \sum_{i \neq l,dep} \phi_i - 180^\circ - 360^\circ(l-1), \quad (5.31)$$

where  $l$  is an integer and takes on the values  $1, 2, \dots, q$ . Note if there are  $q$  repeated poles, there will be  $q$  branches of the locus departing from the poles.

Likewise, the angle(s) of arrival of a branch at a zero with multiplicity  $q$  is given by

Rule for arrival angles

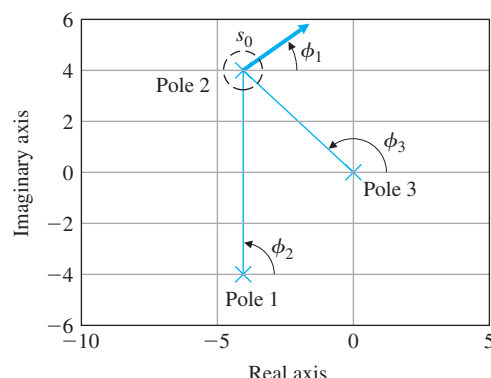
$$q\psi_{l,arr} = \sum \phi_i - \sum_{i \neq l,arr} \psi_i + 180^\circ + 360^\circ(l-1), \quad (5.32)$$

where  $\sum \phi_i$  is the sum of the angles to all the poles,  $\sum \psi_i$  is the sum of the angles to the remaining zeros, and again,  $l$  takes on the values  $1, 2, \dots, q$  so there will be  $q$  branches of the locus arriving at the zeros.

The rules above all arise from the basic root locus phase condition in Eq. (5.17) as we will now demonstrate. To compute the angle by which a branch of the locus departs from one of the poles, we take a test point  $s_0$  very near the pole in question, define the angle from that pole to the test point as  $\phi_1$ , and transpose all other terms of Eq. (5.17) to the right-hand side. We can illustrate the process by taking the test point  $s_0$  to be near the pole at  $-4 + 4j$  of our example and computing the angle of  $L(s_0)$ . The situation is sketched in Fig. 5.7, and the angle from  $-4 + 4j$  to the test point we define as  $\phi_1$ . We select the test point close enough to the pole that the angles  $\phi_2$  and  $\phi_3$  to the test point can be considered the same as those angles to the pole. Thus,  $\phi_2 = 90^\circ$ ,  $\phi_3 = 135^\circ$ , and  $\phi_1$  can be calculated from the angle condition as *whatever it takes* to make the total be  $180^\circ$ . The calculation is

Figure 5.7

The departure and arrival angles are found by looking near a pole or zero



$$\phi_1 = -90^\circ - 135^\circ - 180^\circ \quad (5.33)$$

$$= -405^\circ \quad (5.34)$$

$$= -45^\circ. \quad (5.35)$$

By the complex conjugate symmetry of the plots, the angle of departure of the locus near the pole at  $-4 - 4j$  will be  $+45^\circ$ .

If there had been zeros in  $L(s)$ , the angles from the pole to the zeros would have been added to the right side of Eq. (5.33). For the general case, we can see from Eq. (5.33) that the angle of departure from a single pole is that given by Eq. (5.30). For a multiple pole of order  $q$ , we must count the angle from the pole  $q$  times. This alters Eq. (5.30) to Eq. (5.31) where  $l$  takes on  $q$  values because there are  $q$  branches of the locus that depart from such a multiple pole.

The process of calculating a departure angle for small values of  $K$ , as shown in Fig. 5.7, is also valid for computing the angle by which a root locus arrives at a zero of  $L(s)$  for large values of  $K$ . The general formula that results is that given by Eq. (5.32).

This rule is particularly useful if a system has poles near the imaginary axis, because it will show if the locus branch from the pole starts off toward the stable left half-plane (LHP) or heads toward the unstable right half-plane (RHP).

**RULE 5.** The locus can have multiple roots at points on the locus and the branches will approach a point of  $q$  roots at angles separated by

$$\frac{180^\circ + 360^\circ(l-1)}{q}, \quad (5.36)$$

and will depart at angles with the same separation. As with any polynomial, it is possible for a characteristic polynomial of a degree greater than 1 to have multiple roots. For example, in the second-order locus of Fig. 5.2, there are two roots at  $s = -1/2$  when  $K = 1/4$ . Here the horizontal branches of the locus come together and the vertical branches break away from the real axis, becoming complex for  $K > 1/4$ . The locus arrives at  $0^\circ$  and  $180^\circ$  and departs at  $+90^\circ$  and  $-90^\circ$ .

In order to compute the angles of arrival and departure from a point of multiple roots, it is useful to use a trick we call the **continuation locus**. We can imagine plotting a root locus for an initial range of  $K$ , perhaps for  $0 \leq K \leq K_1$ . If we let  $K = K_1 + K_2$ , we can then plot a new locus with parameter  $K_2$ , a locus which is the *continuation of the original locus*, and whose starting poles are the roots of the original system at  $K = K_1$ . To see how this works, we return to the second-order root locus of Eq. (5.11) and let  $K_1$  be the value corresponding to the breakaway point  $K_1 = 1/4$ . If we let  $K = 1/4 + K_2$ , we have the locus equation  $s^2 + s + 1/4 + K_2 = 0$ , or

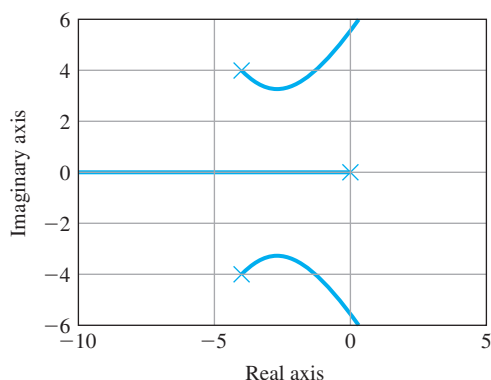
$$\left(s + \frac{1}{2}\right)^2 + K_2 = 0. \quad (5.37)$$

The steps for plotting this locus are, the same as for any other, except that now the initial departure of the locus of Eq. (5.37) corresponds to

### Continuation locus

**Figure 5.8**

Root locus for  
 $L(s) = \frac{1}{s(s^2+8s+32)}$



the breakaway point of the original locus of Eq. (5.11), i.e.,  $s = -1/2$  on Fig. 5.2. Applying the rule for departure angles [Eq. (5.31)] from the double pole at  $s = -1/2$ , we find that

$$2\phi_{dep} = -180^\circ - 360^\circ(l - 1), \quad (5.38)$$

$$\phi_{dep} = -90^\circ - 180^\circ(l - 1), \quad (5.39)$$

$$\phi_{dep} = \pm 90^\circ \text{ (departure angles at breakaway).} \quad (5.40)$$

In this case, the arrival angles at  $s = -1/2$  are, from the original root locus, along the real axis and are clearly  $0^\circ$  and  $180^\circ$ .

The complete locus for our third-order example is drawn in Fig. 5.8. It combines all the results found so far—that is, the real-axis segment, the center of the asymptotes and their angles, and the angles of departure from the poles. It is usually sufficient to draw the locus by using only Rules 1 to 3, which should be memorized. Rule 4 is sometimes useful to understand how locus segments will depart, especially if there is a pole near the  $j\omega$  axis. Rule 5 is sometimes useful to help interpret plots that come from the computer and, as we will see in the next section, to explain qualitative changes in some loci as a pole or zero is moved. The actual locus in Fig. 5.8 was drawn using the Matlab commands

```
s = tf('s');
sysL = 1/(s*(s+4)^2 + 16);
rlocus(sysL)
```

We will next summarize the rules for drawing a root locus.

### 5.2.2 Summary of the Rules for Determining a Root Locus

**RULE 1.** The  $n$  branches of the locus start at the poles of  $L(s)$  and  $m$  branches end on the zeros of  $L(s)$ .

**RULE 2.** The loci are on the real axis to the left of an odd number of poles and zeros.

RULE 3. For large  $s$  and  $K$ ,  $n - m$  branches of the loci are asymptotic to lines at angles  $\phi_l$  radiating out from the center point  $s = \alpha$  on the real axis, where

$$\phi_l = \frac{180^\circ + 360^\circ(l-1)}{n-m}, \quad l = 1, 2, \dots, n-m, \quad (5.41)$$

$$\alpha = \frac{\sum p_i - \sum z_i}{n-m}. \quad (5.42)$$

RULE 4. The angle(s) of departure of a branch of the locus from a pole of multiplicity  $q$  is given by

$$q\phi_{l,dep} = \sum \psi_i - \sum \phi_i - 180^\circ - 360^\circ(l-1), \quad (5.43)$$

where  $l = 1, 2, \dots, q$  and the angle(s) of arrival of a branch at a zero of multiplicity  $q$  is given by

$$q\psi_{l,arr} = \sum \phi_i - \sum \psi_i + 180^\circ + 360^\circ(l-1). \quad (5.44)$$

RULE 5. The locus can have multiple roots at points on the locus of multiplicity  $q$ . The branches will approach a point of  $q$  roots at angles separated by

$$\frac{180^\circ + 360^\circ(l-1)}{q}, \quad (5.45)$$

and will depart at angles with the same separation, forming an array of  $2q$  rays equally spaced. If the point is on the real axis, then the orientation of this array is given by the real-axis rule. If the point is in the complex plane, then the angle of departure rule must be applied.

### 5.2.3 Selecting the Parameter Value

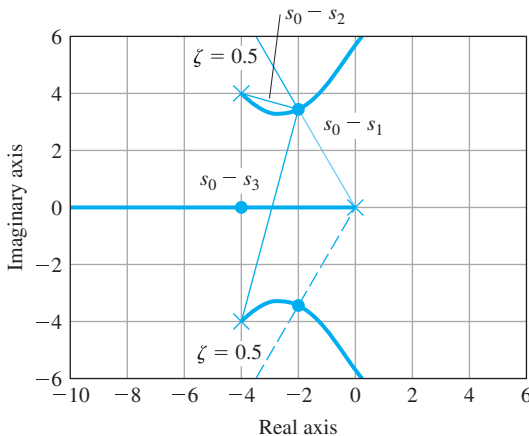
The positive root locus is a plot of *all possible locations* for roots to the equation  $1 + KL(s) = 0$  for some real positive value of  $K$ . The purpose of design is to select a particular value of  $K$  that will meet the specifications for static and dynamic response. We now turn to the issue of selecting  $K$  from a particular locus so the roots are at specific places. Although we shall show how the gain selection can be made by hand calculations from a plot of the locus, this is almost never done by hand because the determination can be accomplished easily by Matlab. It is useful, however, to be able to perform a rough sanity check by hand on the computer-based results.

Using Definition II of the locus, we developed rules to sketch a root locus from the phase of  $L(s)$  alone. If the equation is actually to have a root at a particular place when the phase of  $L(s)$  is  $180^\circ$ , then a **magnitude condition** must also be satisfied. This condition is given by Eq. (5.9), rearranged as

$$K = -\frac{1}{L(s)}. \quad (5.46)$$

**Figure 5.9**

Root locus for  
 $L(s) = \frac{1}{s[(s+4)^2 + 16]}$   
 showing calculations of  
 gain  $K$



For values of  $s$  on the root locus, the phase of  $L(s)$  is  $180^\circ$ , so we can write the magnitude condition as

$$K = \frac{1}{|L|}. \quad (5.47)$$

Equation (5.47) has both an algebraic and a graphical interpretation. To see the latter, consider the locus of  $1 + KL(s)$ , where

$$L(s) = \frac{1}{s[(s+4)^2 + 16]}. \quad (5.48)$$

For this transfer function, the locus is plotted in Fig. 5.9. In Fig. 5.9, the lines corresponding to a damping ratio of  $\zeta = 0.5$  are sketched and the points where the locus crosses these lines are marked with dots (•). Suppose we wish to set the gain so the roots are located at the dots. This corresponds to selecting the gain so that two of the closed-loop system poles have a damping ratio of  $\zeta = 0.5$ . (We will find the third pole shortly.) What is the value of  $K$  when a root is at the dot? From Eq. (5.47), the value of  $K$  is given by 1 over the magnitude of  $L(s_0)$ , where  $s_0$  is the coordinate of the dot. On the figure we have plotted three vectors marked  $s_0 - s_1$ ,  $s_0 - s_2$ , and  $s_0 - s_3$ , which are the vectors from the poles of  $L(s)$  to the point  $s_0$ . (Since  $s_1 = 0$ , the first vector equals  $s_0$ .) Algebraically, we have

$$L(s_0) = \frac{1}{s_0(s_0 - s_2)(s_0 - s_3)}. \quad (5.49)$$

Using Eq. (5.47), this becomes

$$K = \frac{1}{|L(s_0)|} = |s_0||s_0 - s_2||s_0 - s_3|. \quad (5.50)$$

The graphical interpretation of Eq. (5.50) shows that its three magnitudes are the lengths of the corresponding vectors drawn on Fig. 5.9 (see Appendix WD online at [www.pearsonglobaleditions.com](http://www.pearsonglobaleditions.com)). Hence, we can compute the gain to place the roots at the dot ( $s = s_0$ ) by

measuring the lengths of these vectors and multiplying the lengths together, *provided that the scales of the imaginary and real axes are identical*. Using the scale of the figure, we estimate that

$$|s_0| \cong 4.0,$$

$$|s_0 - s_2| \cong 2.1,$$

$$|s_0 - s_3| \cong 7.7.$$

Thus, the gain is estimated to be

$$K = 4.0(2.1)(7.7) \cong 65.$$

We conclude that if  $K$  is set to the value 65, then a root of  $1 + KL$  will be at  $s_0$ , which has the desired damping ratio of 0.5. Another root is at the conjugate of  $s_0$ . Where is the third root? The third branch of the locus lies along the negative real axis. If performing the calculations by hand, we would need to take a test point, compute a trial gain, and repeat this process until we have found the point where  $K = 65$ . However, if performing a check on Matlab's determination, it is sufficient to merely use the procedure above to verify the gain at the root location indicated by the computer.

To use Matlab, plot the locus using the command `rlocus(sysL)`, for example, then the command `[K,p] = rlocfind(sysL)` will produce a crosshair on the plot and, when spotted at the desired location of the root and selected with a mouse click, the value of the gain  $K$  is returned as well as the roots corresponding to that  $K$  in the variable  $p$ . The use of `sisotool` makes this even easier, and will be discussed in more detail in Example 5.7.

Finally, with the gain selected, it is possible to compute the error constant of the control system. A process with the transfer function given by Eq. (5.48) has one integrator and, in a unity feedback configuration, will be a Type 1 control system. In this case, the steady-state error in tracking a ramp input is given by the velocity constant:

$$K_v = \lim_{s \rightarrow 0} sKL(s) \quad (5.51)$$

$$= \lim_{s \rightarrow 0} s \frac{K}{s[(s+4)^2 + 16]} \quad (5.52)$$

$$= \frac{K}{32}. \quad (5.53)$$

With the gain set for complex roots at a damping  $\zeta = 0.5$ , the root-locus gain is  $K = 65$ , so from Eq. (5.53) we get  $K_v = 65/32 \cong 2 \text{ sec}^{-1}$ . If the closed-loop dynamic response, as determined by the root locations, is satisfactory and the steady-state accuracy, as measured by  $K_v$ , is good enough, then the design can be completed by gain selection alone. However, if no value of  $K$  satisfies all of the constraints, as is typically the case, then additional modifications are necessary to meet the system specifications.

### 5.3 Selected Illustrative Root Loci

A number of important control problems are characterized by a process with the simple “double integrator” transfer function

$$G(s) = \frac{1}{s^2}. \quad (5.54)$$

In Chapter 2, Example 2.3 showed that the attitude control of a satellite is described by this equation. Also, Example 2.5 showed that the basic attitude motions of a drone obey this transfer function. Furthermore, it will be shown in Example 5.16 that the translational motion of a drone obeys the same dynamics. The result is a plant described by Eq. (5.54). If we form a unity feedback system with this plant, and a proportional controller, the root locus with respect to controller gain is

$$1 + k_p \frac{1}{s^2} = 0. \quad (5.55)$$

If we apply the rules to this (trivial) case, the results are as follows:

RULE 1. The locus has two branches that start at  $s = 0$ .

RULE 2. There are no parts of the locus on the real axis.

RULE 3. The two asymptotes intersect at  $s = 0$  and are at the angles of  $\pm 90^\circ$ .

RULE 4. The loci depart from  $s = 0$  at the angles of  $\pm 90^\circ$ .

Conclusion: The locus consists of the imaginary axis, and the transient would be oscillatory for any value of  $k_p$ . A more useful design results with the use of proportional plus derivative control.

#### EXAMPLE 5.3

#### *Root Locus for Satellite Attitude Control with PD Control*

The characteristic equation with PD control is

$$1 + [k_p + k_D s] \frac{1}{s^2} = 0. \quad (5.56)$$

To put the equation in root-locus form, we define  $K = k_D$ , and for the moment arbitrarily select the gain ratio<sup>9</sup> as  $k_p/k_D = 1$ , which results in the root-locus form

$$1 + K \frac{s + 1}{s^2} = 0. \quad (5.57)$$

**Solution.** Again we compute the results of the rules:

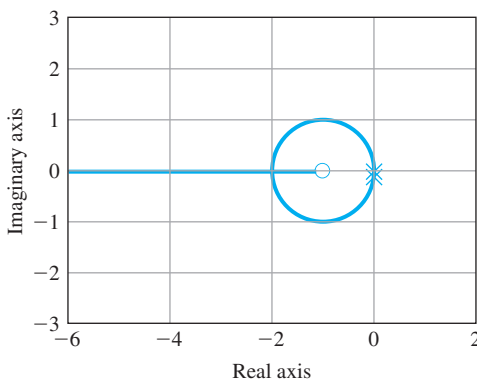
RULE 1. There are two branches that start at  $s = 0$ , one of which terminates on the zero at  $s = -1$  and the other of which approaches infinity.

---

<sup>9</sup>Given a specific physical system, this number would be selected with consideration of the specified rise time of the design or the maximum control signal (control authority) of the actuator.

**Figure 5.10**

Root locus for  
 $L(s) = G(s) = \frac{(s+1)}{s^2}$



RULE 2. The real axis to the left of  $s = -1$  is on the locus.

RULE 3. Since  $n - m = 1$ , there is one asymptote along the negative real axis.

RULE 4. The angles of departure from the double pole at  $s = 0$  are  $\pm 90^\circ$ .

RULE 5. From Rules 1–4, it should be clear that the locus will curl around the zero, rejoin the real axis to the left of the zero, and terminate as indicated by Rule 1. It turns out that the locus segments rejoin the real axis at  $s = -2$ , which creates a point of multiple roots. Evaluation of the angle of arrival at this point will show that the segments arrive at  $\pm 90^\circ$ .

We conclude that two branches of the locus leave the origin going north and south, and that they curve around<sup>10</sup> without passing into the RHP and break into the real axis at  $s = -2$ , from which point one branch goes west toward infinity and the other goes east to rendezvous with the zero at  $s = -1$ . The locus is plotted in Fig. 5.10 with the commands

```
s = tf('s');
sysS = (s + 1)/(s^2);
rlocus(sysS)
```

Comparing this case with that for the simple  $1/s^2$ , we see that

The addition of the zero has pulled the locus into the LHP, a point of general importance in constructing a compensation.

<sup>10</sup> You can prove that the path is a circle by assuming that  $s + 1 = e^{j\theta}$  and showing that the equation has a solution for a range of positive  $K$  and real  $\theta$  under this assumption. (See Problem 5.18.)

In the previous case, we considered pure PD control. However, as we have mentioned earlier, the physical operation of differentiation is not practical and in practice PD control is approximated by

$$D_c(s) = k_p + \frac{k_D s}{s/p + 1}, \quad (5.58)$$

which can be put in root-locus form by defining  $K = k_p + p k_D$  and  $z = p k_p / K$  so that<sup>11</sup>

$$D_c(s) = K \frac{s+z}{s+p}. \quad (5.59)$$

For reasons we will see when we consider design by frequency response, this controller transfer function is called a “lead compensator” provided  $z < p$  or, referring to the frequent implementation by electrical components, a “lead network.” The characteristic equation for the  $1/s^2$  plant with this controller is

$$1 + D_c(s)G(s) = 1 + KL(s) = 0,$$

$$1 + K \frac{s+z}{s^2(s+p)} = 0.$$

## EXAMPLE 5.4

### *Root Locus of the Satellite Control with Modified PD or Lead Compensation*

To evaluate the effect of the added pole, we will again set  $z = 1$  and consider three different values for  $p$ . We begin with a somewhat large value,  $p = 12$ , and consider the root locus for

$$1 + K \frac{s+1}{s^2(s+12)}. \quad (5.60)$$

**Solution.** Again, we apply the rules for plotting a root locus:

RULE 1. There are now three branches to the locus, two starting at  $s = 0$  and one starting at  $s = -12$ .

RULE 2. The real axis segment  $-12 \leq s \leq -1$  is part of the locus.

RULE 3. There are  $n - m = 3 - 1 = 2$  asymptotes centered at  $\alpha = \frac{-12 - (-1)}{2} = -11/2$  and at the angles  $\pm 90^\circ$ .

RULE 4. The angles of departure of the branches at  $s = 0$  are again  $\pm 90^\circ$ . The angle of departure from the pole at  $s = -12$  is at  $0^\circ$ .

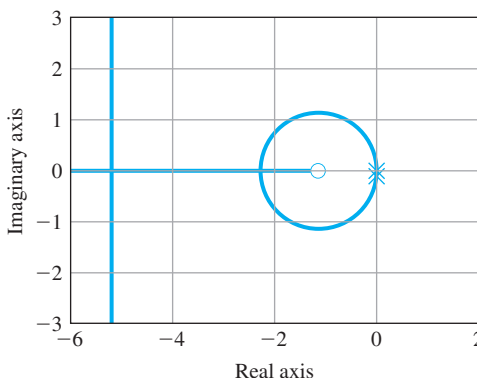
There are several possibilities on how the locus segments behave while still adhering to the guidance above. Matlab is the expedient way to discover the paths. The Matlab commands

---

<sup>11</sup>The use of  $z$  here for zero is not to be confused with the use of the operator  $z$  used in defining the discrete transfer function that will be described in Chapter 8.

**Figure 5.11**

Root locus for  
 $L(s) = \frac{(s+1)}{s^2(s+12)}$



```
s = tf('s');
sysL = (s + 1)/((s^2)*(s + 12));
rlocus(sysL)
```

show that two branches of locus break vertically from the poles at  $s = 0$ , curve around to the left without passing into the RHP, and break in at  $s = -2.3$ , where one branch goes right to meet the zero at  $s = -1$  and the other goes left, where it is met by the root that left the pole at  $s = -12$ . These two form a multiple root at  $s = -5.2$  and break away there and approach the vertical asymptotes located at  $s = -5.5$ . The locus is plotted in Fig. 5.11.

---

Considering this locus, we see that the effect of the added pole has been to distort the simple circle of the PD control but, for points near the origin, the locus is quite similar to the earlier case. The situation changes when the pole is brought closer in.

## EXAMPLE 5.5

### *Root Locus of the Satellite Control with Lead Having a Relatively Small Value for the Pole*

Now consider  $p = 4$  and draw the root locus for

$$1 + K \frac{s + 1}{s^2(s + 4)} = 0. \quad (5.61)$$

**Solution.** Again, by the rules, we have the following:

RULE 1. There are again three branches to the locus, two starting from  $s = 0$  and one from  $s = -4$ .

RULE 2. The segment of the real axis  $-4 \leq s \leq -1$  is part of the locus.

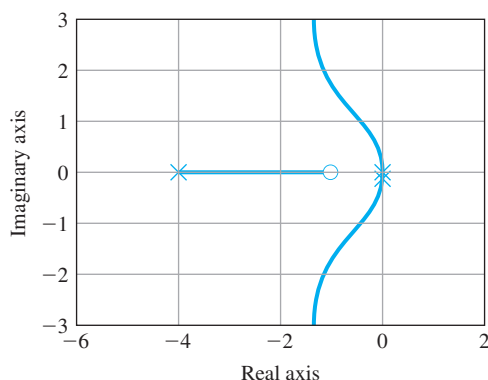
RULE 3. There are two asymptotes centered at  $\alpha = -3/2$  and at the angles  $\pm 90^\circ$ .

RULE 4. The branches again depart from the poles at  $s = 0$  at  $\pm 90^\circ$ .

RULE 5. The Matlab commands

**Figure 5.12**

Root locus for  
 $L(s) = \frac{(s+1)}{s^2(s+4)}$



```
s = tf('s');
sysL = (s + 1)/((s^2)*(s + 4));
rlocus(sysL)
```

show that two branches of this locus break away vertically from the poles at  $s = 0$ , curve slightly to the left and join the asymptotes going north and south. The locus segment from the root at  $s = -4$  goes east and terminates at the zero. In this case, the locus differs from the case when  $s = -12$  in that there are no break-in or breakaway points on the real axis as part of the locus. The Matlab plot is given in Fig. 5.12.

In these two cases we have similar systems, but in one case,  $p = 12$ , there were both break-in and breakaway points on the real axis, whereas for  $p = 4$ , these features have disappeared. A logical question might be to ask at what point they went away. As a matter of fact, it happens at  $p = 9$ , and we'll look at that locus next.

## EXAMPLE 5.6

### *The Root Locus for the Satellite with a Transition Value for the Pole*

Plot the root locus for

$$1 + K \frac{s + 1}{s^2(s + 9)} = 0. \quad (5.62)$$

**Solution.**

RULE 1. The locus has three branches, starting from  $s = 0$  and  $s = -9$ .

RULE 2. The real axis segment  $-9 \leq s \leq -1$  is part of the locus.

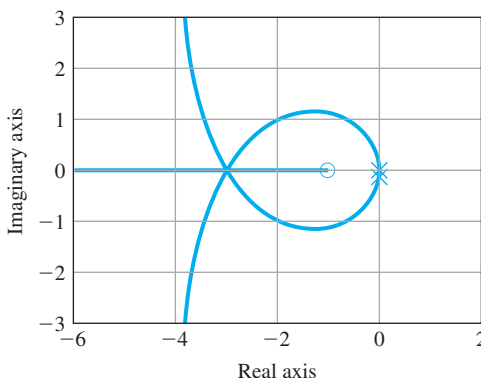
RULE 3. The two asymptotes are centered at  $\alpha = -8/2 = -4$ .

RULE 4. The departures are, as before, at  $\pm 90^\circ$  from  $s = 0$ .

RULE 5. The Matlab commands

**Figure 5.13**

Root locus for  
 $L(s) = \frac{(s+1)}{s^2(s+9)}$



```
s = tf('s')
sysL = (s + 1)/((s^2)*(s+9));
rlocus(sysL)
```

produces the locus in Fig. 5.13. It shows the two branches of this locus break away vertically from the poles at  $s = 0$  and curl around and join the real axis again at  $s = -3$  with an angle of arrival of  $\pm 60^\circ$ , while the branch from the pole at  $s = -9$  heads east and joins the other two poles at  $s = -3$  with an angle of arrival of  $0^\circ$ . These three locus segments continue on by splitting out of  $s = -3$  at the departure angles of  $0^\circ$  and  $\pm 120^\circ$ , with one heading into the zero and the other two heading away to the northwest to join the asymptotes. Using Rule 5 would confirm these angles of arrival and departure.<sup>12</sup>

Note this special locus shape only occurs when the ratio of the pole value to the zero value is exactly 9:1 for this form of  $L(s)$ . It is the transition locus between the two types depicted by Examples 5.4 and 5.5. This transition is discussed in more detail below, and will be demonstrated via Matlab in Example 5.7.

---

From Figs. 5.11 through 5.13, it is evident that when the third pole is near the zero ( $p$  near 1), there is only a modest distortion of the locus that would result for  $D_c(s)G(s) \cong \frac{K}{s^2}$ , which consists of two straight-line locus branches departing at  $\pm 90^\circ$  from the two poles at  $s = 0$ . Then, as we increase  $p$ , the locus changes until at  $p = 9$ ; the locus breaks in at  $-3$  in a triple multiple root. As the pole  $p$  is moved to the left beyond  $-9$ , the locus exhibits distinct break-in and breakaway points, approaching, as  $p$  gets very large, the circular locus of one zero and two poles. Figure 5.13, when  $p = 9$ , is thus a transition locus between the two second-order extremes, which occur at  $p = 1$  (when the zero is canceled) and  $p \rightarrow \infty$  (where the extra pole has no effect).

---

<sup>12</sup>The shape of this special root locus is a trisectrix of Maclaurin, a plane curve that can be used to trisect an angle.

**EXAMPLE 5.7***An Exercise to Repeat the Prior Examples Using sisotool*

Repeat Examples 5.3 through 5.6 using Matlab's sisotool feature.

**Solution.** sisotool is an interactive design tool in Matlab that provides a graphical user interface (GUI) for performing analysis and design. sisotool provides an easy way to design feedback controllers because it allows rapid iterations and quickly shows their effect on the resulting root-locus and the other aspects of the control performance. To illustrate the use of the tool, the Matlab commands

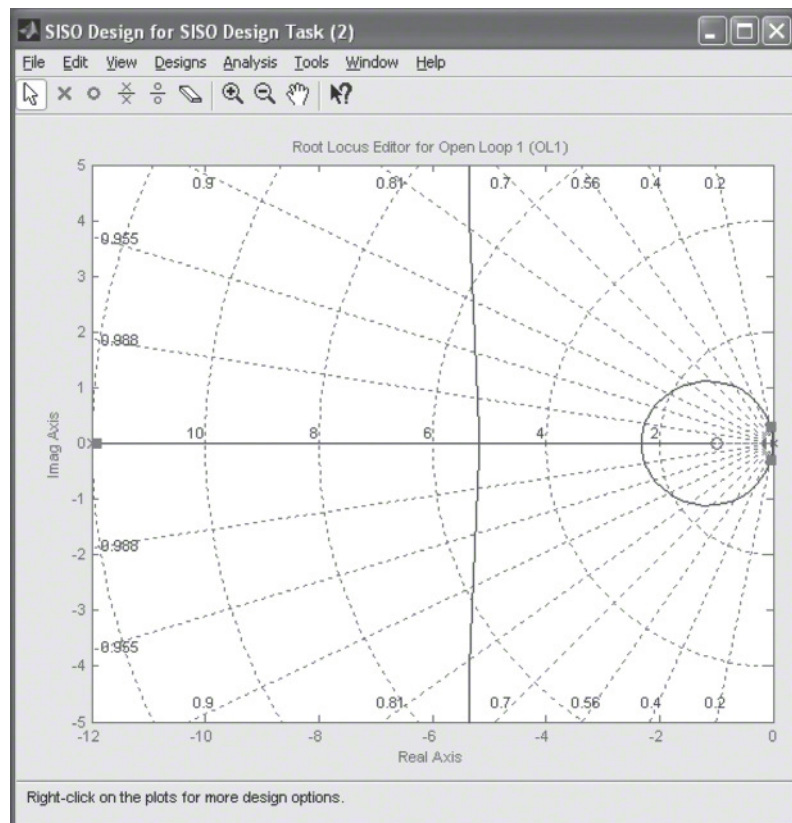
```
s = tf('s');
sysL = (s + 1)/(s^2);
sisotool('rlocus',sysL)
```

will initiate the GUI and produce the root locus shown in Fig. 5.10, which is similar to Examples 5.4 through 5.6, but without the pole on the negative real axis that was moved around for illustration purposes in the three prior examples. By clicking on "Compensator Editor" in the "Control and Estimation Tools Manager" window, right clicking on the "Dynamics" dialog window and selecting "add pole/zero," you can add a pole at the location  $s = -12$ . This will produce the locus that is shown in Figs. 5.11 and 5.14. Now put your mouse on the pole at  $s = -12$ ,

**Figure 5.14**

sisotool graphical user interface

*Source: Reprinted with permission of The MathWorks, Inc.*



hold down the mouse button, and slide it from  $s = -12$  to  $s = -4$  slowly, so you can examine the locus shapes at all intermediate points. Be especially careful (and slow) as you pass through  $s = -9$  because the locus shape changes very quickly with the pole in this region. Note you can also put your mouse on one of the closed-loop poles (squares) and slide that along the locus. It will show you the location of the other roots that correspond to that value of the gain,  $K$ , and the frequency and damping of the closed-loop roots will be shown for when the roots are complex pairs. More detail can be found in the sisotool Tutorial in Appendix WR online at [www.pearsonglobaleditions.com](http://www.pearsonglobaleditions.com).

A useful conclusion drawn from this example is the following:

An additional pole moving in from the far left tends to push the locus branches to the right as it approaches a given locus.

The double integrator is the simplest model of the examples, assuming a rigid body with no friction. A more realistic case would include the effects of flexibility in the satellite attitude control, where at least the solar panels would be flexible. Another possibility is that the sensor is not rigidly attached to the base of the satellite that contains the thrusters, as discussed in Example 2.4 in Chapter 2. So, we see there are two possibilities, depending on whether the sensor is on the same rigid body as the actuator, which is called the collocated case,<sup>13</sup> or is on another body, which is called the noncollocated case.<sup>14</sup> We begin with consideration of the collocated case similar to that given by Eq. (2.14). As we saw in Chapter 2, the transfer function in the collocated case has not only a pair of complex poles but also a pair of nearby complex zeros located at a lower natural frequency than the poles. The numbers in the examples that follow are chosen more to illustrate the root-locus properties than to represent particular physical models.

## EXAMPLE 5.8

### *Root Locus of the Satellite Control with a Collocated Flexibility*

Plot the root locus of the characteristic equation  $1 + G(s)D_c(s) = 0$ , where

$$G(s) = \frac{(s + 0.1)^2 + 6^2}{s^2[(s + 0.1)^2 + 6.6^2]}, \quad (5.63)$$

---

<sup>13</sup>Typical of the satellite attitude control, where the flexibility arises from solar panels and both actuator and sensor act on the main body of the satellite.

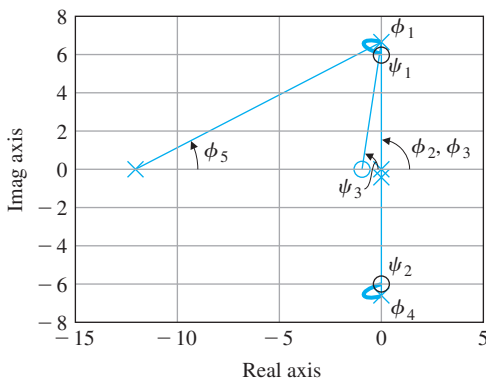
<sup>14</sup>Typical of the satellite, where there is flexibility between an attitude sensor and the controller.

**Figure 5.15**

Figure for computing a departure angle for

$L(s) =$

$$\frac{s+1}{s+12} \frac{(s+0.1)^2 + 6^2}{s^2[(s+0.1)^2 + 6.6^2]}$$



is in a unity feedback structure with the controller transfer function

$$D_c(s) = K \frac{s+1}{s+12}. \quad (5.64)$$

**Solution.** In this case,

$$L(s) = \frac{s+1}{s+12} \frac{(s+0.1)^2 + 6^2}{s^2[(s+0.1)^2 + 6.6^2]}$$

has both poles and zeros near the imaginary axis and we should expect to find the departure angles of particular importance.

### Solution

RULE 1. There are five branches to the locus, three of which approach finite zeros and two of which approach the asymptotes.

RULE 2. The real-axis segment  $-12 \leq s \leq -1$  is part of the locus.

RULE 3. The center of the two asymptotes is at

$$\alpha = \frac{-12 - 0.1 - 0.1 - (-0.1 - 0.1 - 1)}{5 - 3} = -\frac{11}{2}.$$

The angle of the asymptotes is  $\pm 90^\circ$ .

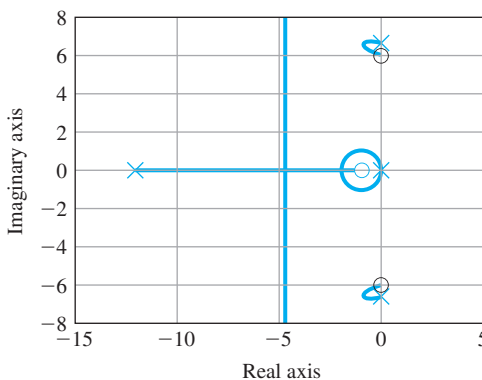
RULE 4. We compute the departure angle from the pole at  $s = -0.1 + j6.6$ . The angle at this pole we will define to be  $\phi_1$ . The other angles are marked on Fig. 5.15. The root-locus condition is

$$\begin{aligned} \phi_1 &= \psi_1 + \psi_2 + \psi_3 - (\phi_2 + \phi_3 + \phi_4 + \phi_5) - 180^\circ, \\ \phi_1 &= 90^\circ + 90^\circ + \tan^{-1}(6.6) - [90^\circ + 90^\circ + 90^\circ \\ &\quad + \tan^{-1}\left(\frac{6.6}{12}\right)] - 180^\circ, \\ \phi_1 &= 81.4^\circ - 90^\circ - 28.8^\circ - 180^\circ, \\ &= -217.4^\circ = 142.6^\circ, \end{aligned} \quad (5.65)$$

so the root leaves this pole up and to the left, into the stable region of the plane. An interesting exercise would be to compute the arrival angle at the zero located at  $s = -0.1 + j6$ .

**Figure 5.16**

Root locus for  $L(s) = \frac{s+1}{s+12} \frac{(s+0.1)^2 + 6^2}{s^2[(s+0.1)^2 + 6.6^2]}$



Using Matlab, the locus is plotted in Fig. 5.16. Note all the attributes that were determined using the simple rules were exhibited by the plot, thus verifying in part that the data were entered correctly.

The previous example showed

In the collocated case, the presence of a single flexible mode introduces a lightly damped root to the characteristic equation but does not cause the system to be unstable.

The departure angle calculation showed the root departs from the pole introduced by the flexible mode toward the LHP. Next, let's consider the noncollocated case, which was also discussed in Example 2.4 and resulted in Eq. (2.13). Using that as a guide, we assume here the plant transfer function is

$$G(s) = \frac{1}{s^2[(s + 0.1)^2 + 6.6^2]}, \quad (5.66)$$

and is compensated again by the lead

$$D_c(s) = K \frac{s + 1}{s + 12}. \quad (5.67)$$

As these equations show, the noncollocated transfer function has the complex poles but does not have the associated complex zeros as in the previous example, and that we also saw for the collocated case of Chapter 2 in Eq. (2.14). This will have a substantial effect, as illustrated by Example 5.9.

## EXAMPLE 5.9

### *Root locus for the Noncollocated Cased*

Apply the rules and draw the root locus for

$$KL(s) = D_c G = \frac{K(s + 3)}{s + 18} \frac{1}{(s + 1)^2[(s + 0.5)^2 + 9^2]}, \quad (5.68)$$

paying special attention to the departure angles from the complex poles.

**Solution**

RULE 1. There are five branches to the root locus, of which one approaches the zero and four approach the asymptotes.

RULE 2. The real-axis segment defined by  $-18 \leq s \leq -3$  is part of the locus.

RULE 3. The center of the asymptotes is located at

$$\alpha = \frac{-18 - (1)(2) - (0.5)(2) - (-3)}{5 - 1} = \frac{-18}{4},$$

and the angles for the four asymptotic branches area at  $\pm 45^\circ, \pm 135^\circ$ .

RULE 4. We again compute the departure angle from the pole at  $s = -0.5 + j9$ . We will define the angle at this pole to be  $\phi_1$ . The other angles are marked on Fig. 5.17. The root locus condition is

$$\phi_1 = \psi_1 - (\phi_2 + \phi_3 + \phi_4 + \phi_5) - 180^\circ,$$

$$\begin{aligned} \phi_1 &= \tan^{-1}\left(\frac{9}{2.5}\right) - \left[2 \times \tan^{-1}\left(\frac{9}{0.5}\right) + \right. \\ &\quad \left. 90^\circ + \tan^{-1}\left(\frac{9}{17.5}\right)\right] - 180^\circ, \end{aligned} \quad (5.69)$$

$$\phi_1 = 74.48^\circ - 173.64^\circ - 90^\circ - 27.22^\circ - 180^\circ,$$

$$\phi_1 = -36.38^\circ.$$

In this case, the root leaves the pole down and to the *right*, toward the unstable region. We would expect the system to become unstable as gain is increased.

RULE 5. The locus is plotted in Fig. 5.18 with the commands

```
s = tf('s');
sysG = 1/((s+1)^2*((s+0.5)^2+9^2));
sysD = (s+3)/(s+18);
sysL = sysG*sysD;
rlocfind(sysL)
```

and is seen to agree with the calculations above. By using sisotool, we see that the locus from the complex poles enter into the RHP almost

**Figure 5.17**

Figure to compute  
departure angle for

$$L(s) = \frac{s+3}{s+18} \frac{1}{(s+1)^2[(s+0.5)^2+9^2]}$$

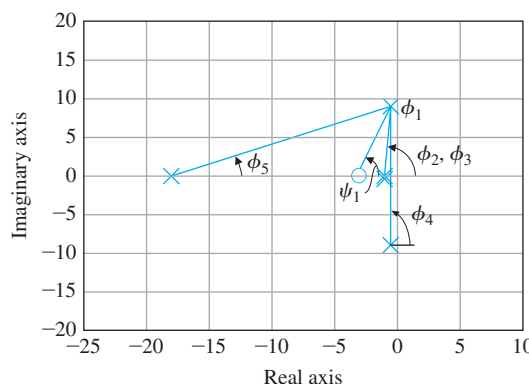
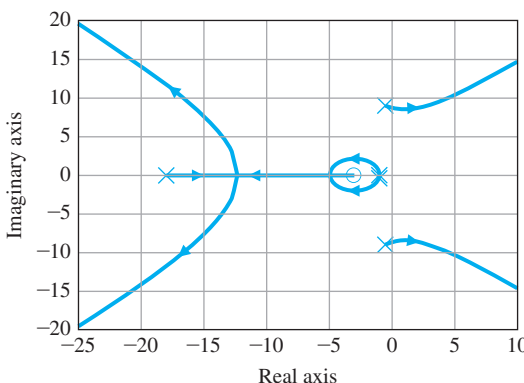


**Figure 5.18**

Root locus for  $L(s) = \frac{s+3}{s+18} \frac{1}{(s+1)^2[(s+0.5)^2+9^2]}$



immediately as the gain is increased. Furthermore, by selecting those roots so that they are just to the left of the imaginary axis, it can be seen that the dominant slow roots down near the origin have extremely low damping. Therefore, this system will have a very lightly damped response with very oscillatory flexible modes. It would not be considered acceptable with the lead compensator as chosen for this example.

### *A Locus with Complex Multiple Roots*

We have seen loci with break-in and breakaway points on the real axis. Of course, an equation of fourth or higher order can have multiple roots that are complex. Although such a feature of a root locus is a rare event, it is an interesting curiosity that is illustrated by the next example.

## EXAMPLE 5.10

### *Root Locus Having Complex Multiple Roots*

Sketch the root locus  $1 + KL(s) = 0$ , where

$$L(s) = \frac{1}{(s+4)(s+1)[(s+2.5)^2 + 16]}.$$

#### Solution

RULE 1. There are four branches of the roots, all of which approach the four asymptotes.

RULE 2. The real-axis segment  $-4 \leq s \leq -1$  is on the locus.

RULE 3. The center of the asymptotes is at

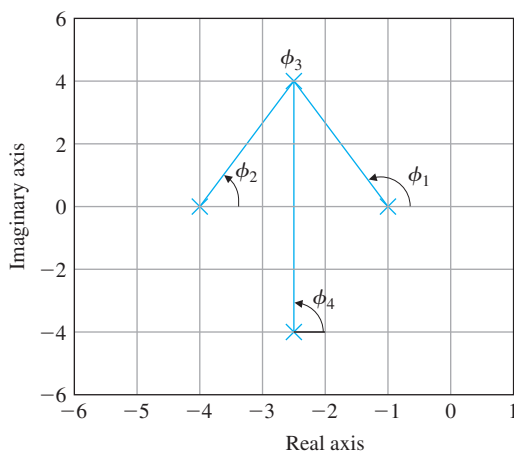
$$\alpha = \frac{-4 - 1 - (2.5)(2)}{4} = -\frac{10}{4} = -2.5,$$

and the angles are  $\phi_l = \pm 45^\circ, \pm 135^\circ$ .

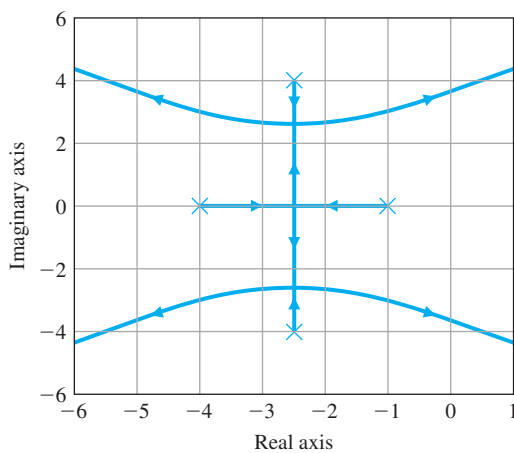
RULE 4. The departure angle  $\phi_{dep}$  from the pole at  $= -2.5 + 4j$ , based on Fig. 5.19, is

**Figure 5.19**

Figure to compute  
departure angle for  
 $L(s) = \frac{1}{(s+4)(s+1)[(s+2.5)^2 + 16]}$

**Figure 5.20**

Root locus for  $L(s) = \frac{1}{(s+4)(s+1)[(s+2.5)^2 + 16]}$



$$\phi_{\text{dep}} = \phi_3 = -\phi_1 - \phi_2 - \phi_4 + 180^\circ$$

$$= -\left(180^\circ - \tan^{-1}\left(\frac{4}{1.5}\right)\right) - \tan^{-1}\left(\frac{4}{1.5}\right) - 90^\circ + 180^\circ \\ = -90^\circ.$$

We can observe at once that, along the line  $s = -2.5 + j\omega$ ,  $\phi_2$  and  $\phi_1$  are angles of an isosceles triangle and always add to  $180^\circ$ . Hence, the entire line from one complex pole to the other is on the locus *in this special case*.

**RULE 5.** Using Matlab, we see there are multiple roots at  $s = -2.5 \pm 2.62j$ , and branches of the locus (Fig. 5.20) come together at  $-2.5 \pm 2.62j$ . Using Rule 5, we can verify that the locus segments break away at  $0^\circ$  and  $180^\circ$ , as shown by Matlab. The codes are given below:

```
s = tf('s');
L = 1/((s+4)*(s+1)*((s + 2.5)^2 + 16));
rlocus(L);
```

The locus in this example is a transition between two types of loci: one where the complex poles are to the left of the example case and approach the asymptotes at  $\pm 135^\circ$ , and another where the complex poles are to the right of their positions in the example and approach the asymptotes at  $\pm 45^\circ$ .

## 5.4 Design Using Dynamic Compensation

Consideration of control design begins with the design of the process itself. The importance of early consideration of potential control problems in the design of the process and selection of the actuator and sensor cannot be overemphasized. It is not uncommon for a first study of the control to suggest that the process itself can be changed by, for example, adding damping or stiffness to a structure to make a flexibility easier to control. Once these factors have been taken into account, the design of the controller begins. If the process dynamics are of such a nature that a satisfactory design cannot be obtained by adjustment of the proportional gain alone, then some modification or compensation of the dynamics is indicated. While the variety of possible compensation schemes is great, three categories have been found to be particularly simple and effective. These are lead, lag, and notch compensations.<sup>15</sup>

**Lead compensation** approximates the function of PD control and acts mainly to speed up a response by lowering rise time and decreasing the transient overshoot. **Lag compensation** approximates the function of PI control, and is usually used to improve the steady-state accuracy of the system. **Notch compensation** will be used to achieve stability for systems with lightly damped flexible modes, as we saw with the satellite attitude control having noncollocated actuator and sensor. In this section, we will examine techniques to select the parameters of these three schemes. Lead, lag, and notch compensations have historically been implemented using analog electronics and, hence were often, referred to as networks. Today, however, most new control system designs use digital computer technology, in which the compensation is implemented in the software. In this case, one needs to compute discrete equivalents to the analog transfer functions, as will be described in Chapter 8, and in Franklin et al. (1998).

Compensation with a transfer function of the form

$$D_c(s) = K \frac{s + z}{s + p} \quad (5.70)$$

is called lead compensation if  $z < p$  and lag compensation if  $z > p$ . Compensation is typically placed in series with the plant, as shown in Fig. 5.21. It can also be placed in the feedback path, and in that location has the same effect on the overall system poles, but results in different

---

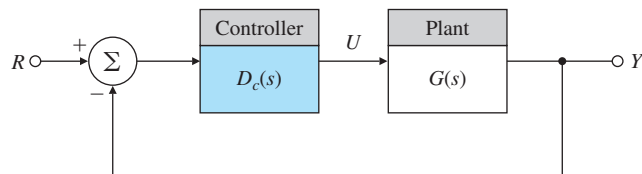
<sup>15</sup>The names of these compensation schemes derive from their frequency (sinusoidal) responses, wherein the output leads the input in one case (a positive phase shift) and lags the input in another (a negative phase shift). The frequency response of the third looks as if a notch had been cut in an otherwise flat frequency response. (See Chapter 6.)

Lead and lag  
compensations

Notch compensation

**Figure 5.21**

Feedback system with compensation



transient responses from reference inputs. The characteristic equation of the system in Fig. 5.21 is

$$1 + D_c(s)G(s) = 0,$$

$$1 + KL(s) = 0,$$

where  $K$  and  $L(s)$  are selected to put the equation in root-locus form as before.

### 5.4.1 Design Using Lead Compensation

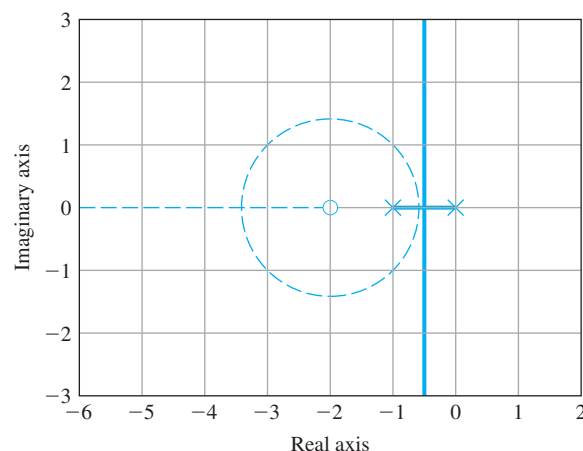
To explain the basic stabilizing effect of lead compensation on a system, we first consider proportional control for which  $D_c(s) = K$ . If we apply this compensation to a second-order position control system with normalized transfer function

$$G(s) = \frac{1}{s(s+1)},$$

the root locus with respect to  $K$  is shown as the solid-line portion of the locus in Fig. 5.22. Also shown in Fig. 5.22 is the locus produced by proportional plus derivative control, where  $D_c(s) = K(s+2)$ . The modified locus is the circle sketched with dashed lines. As we saw in the previous examples, the effect of the zero is to move the locus to the left, toward the more stable part of the  $s$ -plane. Now, if our speed-of-response specification calls for  $\omega_n \cong 2$  rad/sec, then proportional control alone ( $D_c = K$ ) can produce only a very low value of damping ratio  $\zeta$  when the roots are put at the required value of  $\omega_n$ . Hence, at

**Figure 5.22**

Root loci for  
 $1 + D_c(s)G(s) = 0$ ,  
 $G(s) = \frac{1}{s(s+1)}$ : with  
compensation  
 $D_c(s) = K$  (solid lines)  
and with  
 $D_c(s) = K(s+2)$   
(dashed lines)



the required gain, the transient overshoot will be substantial. However, by adding the zero of PD control, we can move the locus to a position having closed-loop roots at  $\omega_n = 2$  rad/sec and damping ratio  $\zeta \geq 0.5$ . We have “compensated” the given dynamics by using  $D_c(s) = K(s + 2)$ .

As we observed earlier, pure derivative control is not normally practical because of the amplification of sensor noise implied by the differentiation and must be approximated. If the pole of the lead compensation is placed well outside the range of the design  $\omega_n$ , then we would not expect it to upset the dynamic response of the design in a serious way. For example, consider the lead compensation

$$D_c(s) = K \frac{s + 2}{s + p}.$$

The root loci for two cases with  $p = 10$  and  $p = 20$  are shown in Fig. 5.23, along with the locus for PD control. The important fact about these loci is that for small gains, before the real root departing from  $-p$  approaches  $-2$ , the loci with lead compensation are almost identical to the locus for which  $D_c(s) = K(s + 2)$ . Note the effect of the pole is to lower the damping, but for the early part of the locus, the effect of the pole is not great if  $p > 10$ .

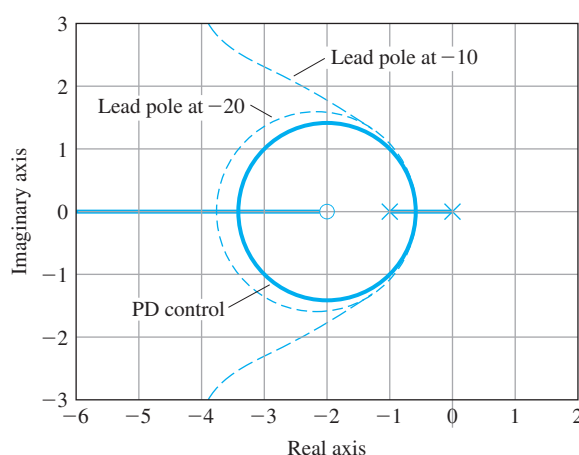
Selecting exact values of  $z$  and  $p$  in Eq. (5.70) for particular cases is often done by trial and error, which can be minimized with experience. In general, the zero is placed in the neighborhood of the closed-loop  $\omega_n$ , as determined by rise-time or settling-time requirements, and the pole is located at a distance 5 to 25 times the value of the zero location. But there are trade-offs to consider. The choice of the exact pole location is a compromise between the conflicting effects of noise suppression, for which one wants a small value for  $p$ , and compensation effectiveness for which one wants a large  $p$ . In general, if the pole is too close to the zero, then, as seen in Fig. 5.23, the root locus does not move as much from its uncompensated shape, and the zero is not as successful in doing its job.

#### Selection of the zero and pole of a lead

**Figure 5.23**

Root loci for three cases with  $G(s) = \frac{1}{s(s+1)}$ :

- (a)  $D_c(s) = \frac{(s+2)}{(s+20)}$ ;
- (b)  $D_c(s) = \frac{(s+2)}{(s+10)}$ ;
- (c)  $D_c(s) = s + 2$  (solid lines)



On the other hand, for reasons that are perhaps easier to understand from the frequency response, when the pole is too far to the left, the magnification of sensor noise appearing at the output of  $D_c(s)$  is too great and the motor or other actuator of the process can be overheated by noise energy in the control signal,  $u(t)$ . With a large value of  $p$ , the lead compensation approaches pure PD control. A simple example will illustrate the approach.

### EXAMPLE 5.11

#### *Design Using Lead Compensation*

Find a compensation for  $G(s) = 1/[s(s+1)]$  that will provide overshoot of no more than 20% and rise time of no more than 0.3 sec.

**Solution.** From Chapter 3, we estimate that a damping ratio of  $\zeta \geq 0.5$  and a natural frequency of  $\omega_n \cong \frac{1.8}{0.3} \cong 6$  rad/sec should satisfy the requirements. To provide some margin, we will shoot for  $\zeta \geq 0.5$  and  $\omega_n \geq 7$  rad/sec. Considering the root loci plotted in Fig. 5.23, we will first try

$$D_c(s) = K \frac{s + 2}{s + 10}.$$

Figure 5.24 shows that  $K = 70$  will yield  $\zeta = 0.56$  and  $\omega_n = 7.7$  rad/sec, which satisfies the goals based on the initial estimates. The third pole will be at  $s = -2.4$  with  $K = 70$ . Because this third pole is so near the lead zero at  $-2$ , the overshoot should not be increased very much from the second-order case. However, Fig. 5.25 shows that the step response of the system exceeds the overshoot specification by a small amount. Typically, lead compensation in the forward path will increase the step-response overshoot because the zero of the compensation has a differentiating effect, as was discussed in Chapter 3. The rise-time specification has been met because the time for the amplitude to go from 0.1 to 0.9 is less than 0.3 sec.

**Figure 5.24**

Root locus for lead design

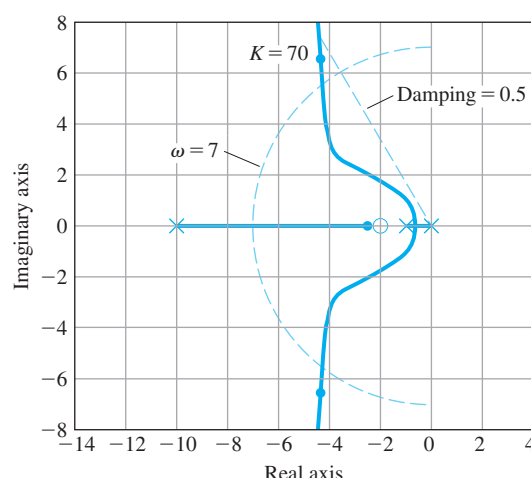
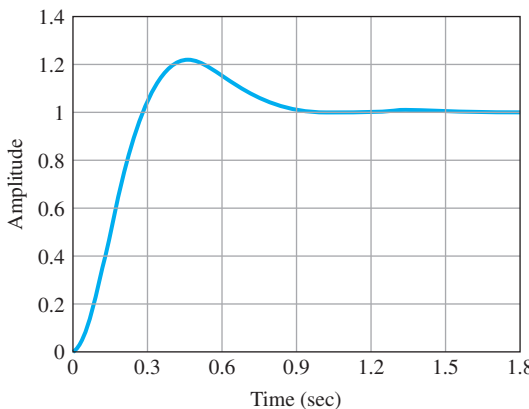


**Figure 5.25**

Step response for Example 5.11



We want to adjust the compensator to achieve better damping in order to reduce the overshoot in the transient response. Generally, it is best to increase  $p$  in order to increase damping, providing the  $p/z$  ratio stays below approximately 25. Clearly, there is not much increase in damping required for this example. So a logical choice would be to increase  $p$  by a modest amount, say, from 10 to 13. This means the lead compensator becomes

$$D_c(s) = K \frac{(s + 2)}{(s + 13)}.$$

The root locus with this change can be created using the Matlab statements:

```
s=tf('s');
sysG=1/(s*(s+1));
sysD=(s+2)/(s+13);
rlocus(sysG*sysD)
grid on
```

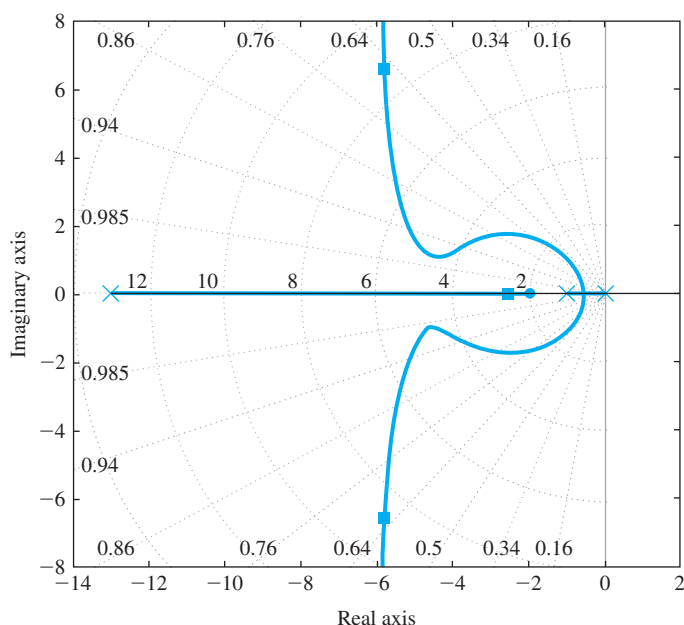
It is shown in Fig. 5.26. It shows that complex roots are possible at a natural frequency greater than 8 rad/sec at a damping greater than 0.64. Placing your cursor on the locus at the point marked in the figure shows that  $K = 91$  at that location and it will produce a damping,  $\zeta = 0.67$  and  $\omega_n = 8.63$  rad/sec. These values appear to be better than the first iteration so that the overshoot and time response should be satisfied. In fact, the additional Matlab statements:

```
sysD=91*(s+2)/(s+13);
sysCL=feedback(sysG*sysD,1);
step(sysCL)
```

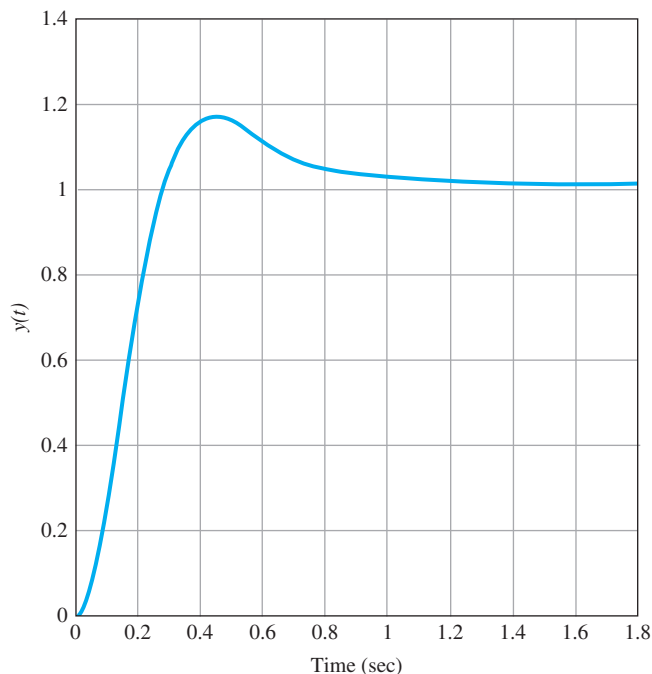
produce the time response shown in Fig. 5.27, which shows that the time domain specifications are met. That is,  $t_r < 0.3$  sec. and  $M_p < 20\%$ .

**Figure 5.26**

Root Locus for  
 $D_c(s) = K \frac{(s+2)}{(s+13)}$  with  
 dotted lines for  
 constant  $\zeta$  and  $\omega_n$

**Figure 5.27**

Time response for  
 $D_c(s) = 91 \frac{(s+2)}{(s+13)}$




---

As stated earlier, the name *lead compensation* is a reflection of the fact that to sinusoidal signals, these transfer functions impart phase lead. For example, the phase of Eq. (5.70) at  $s = j\omega$  is given by

$$\phi = \tan^{-1}\left(\frac{\omega}{z}\right) - \tan^{-1}\left(\frac{\omega}{p}\right). \quad (5.71)$$

If  $z < p$ , then  $\phi$  is positive, which by definition indicates phase lead. The details of design using the phase angle of the lead compensation will be treated in Chapter 6.

### Design Procedure for Lead Compensation

1. Determine where the closed-loop roots need to be in the  $s$ -plane in order to meet the desired specifications on the speed of response and damping (or overshoot).
  - (a) pick the limits for  $\omega_n$  and  $\zeta$ , or
  - (b) pick the limits for  $\sigma$  and  $\omega_d$ .
2. Create the root locus vs.  $K$  with no compensation.
3. If more damping is required, select a value of  $z$  in Eq. (5.70) to be approximately 1/4 to 1 times the value of the desired  $\omega_n$  or  $\omega_d$  and pick  $p$  to be  $10^*z$ .
4. Examine the resulting root locus; and adjust as necessary to meet the required specifications as determined in step 1.
  - (a) decrease  $p$  if less damping is needed,
  - (b) increase  $p$  if more damping is needed, and/or decrease  $z$ ,
  - (c) it is desirable to keep the value of  $p/z$  as low as possible ( $p/z \lesssim 25$ ) in order to minimize the amplification of sensor noise by the compensation.
5. When the values of  $z$  and  $p$  are selected so that the resulting locus passes through an acceptable region of the  $s$ -plane, determine the value of  $K$  to select the closed-loop root locations.
6. Verify that all time domain specifications are met by examining the time response to a unit step input, and adjust the desired  $s$ -plane specifications if needed and go back to step 2.
7. Determine if the resulting value of  $K$  meets the steady-state error requirements, if any. If a value of  $K$  can not be found that meets the requirement, then add Integral Control or a Lag Compensator.

### 5.4.2 Design Using Lag Compensation

Once satisfactory dynamic response has been obtained, perhaps by using one or more lead compensations, we may discover that the low-frequency gain—the value of the relevant steady-state error constant, such as  $K_v$ —is still too low. As we saw in Chapter 4, the system type, which determines the degree of the polynomial the system is capable of following, is determined by the order of the pole of the transfer function  $D_c(s)G(s)$  at  $s = 0$ . If the system is Type 1, the velocity-error constant, which determines the magnitude of the error to a ramp input, is given by  $\lim_{s \rightarrow 0} sD_c(s)G(s)$ . In order to increase this constant, it is necessary to do so in a way that does not upset the already satisfactory dynamic

response. Thus, we want an expression for  $D_c(s)$  that will yield a significant gain at  $s = 0$  to raise  $K_v$  (or some other steady-state error constant) but is nearly unity (no effect) at the higher frequency  $\omega_n$ , where dynamic response is determined. The result is

$$D_c(s) = \frac{s+z}{s+p}, \quad z > p, \quad (5.72)$$

where the values of  $z$  and  $p$  are very small compared with  $\omega_n$ , yet  $D_c(0) = z/p = 3$  to 10 (the value depending on the extent to which the steady-state gain requires boosting). Because  $z > p$ , the phase  $\phi$  given by Eq. (5.71) is negative, corresponding to phase lag. Hence, a device with this transfer function is called lag compensation.

#### An example of lag compensation

The effects of lag compensation on dynamic response can be studied by looking at the corresponding root locus. Again, we take  $G(s) = \frac{1}{s(s+1)}$ , include the lead compensation  $KD_{c1}(s) = \frac{K(s+2)}{(s+13)}$  that produced the locus in Fig. 5.26. With the gain of  $K = 91$  from the previous tuned example, we find that the velocity constant is

$$\begin{aligned} K_v &= \lim_{s \rightarrow 0} sKD_{c1}G \\ &= \lim_{s \rightarrow 0} s(91) \frac{s+2}{s+13} \frac{1}{s(s+1)} \\ &= \frac{91 * 2}{13} = 14. \end{aligned}$$

Suppose we require that  $K_v = 70 \text{ sec}^{-1}$  in order to reduce the velocity error by a factor of 5. To obtain this, we require a lag compensation with  $z/p = 5$  in order to increase the velocity constant by a factor of 5. This can be accomplished with a pole at  $p = -0.01$  and a zero at  $z = -0.05$ , which keeps the values of both  $z$  and  $p$  very small so  $D_{c2}(s)$  would have little effect on the portions of the locus representing the dominant dynamics around  $\omega_n = 7 \text{ rad/sec}$ . The result is a lag compensation with the transfer function of

$$D_{c2}(s) = \frac{(s+0.05)}{(s+0.01)}.$$

The root locus with both lead and lag compensation is plotted in Fig. 5.28 and we see that, for the large scale on the left, the locus is not noticeably different from that in Fig. 5.26. This was the result of selecting very small values for the lag compensator pole and zero. With  $K = 91$ , the dominant roots are at  $-5.8 \pm j6.5$ . The effect of the lag compensation can be seen by expanding the region of the locus around the origin as shown on the right side of Fig. 5.28. Here we can see the circular locus that is a result of the very small lag pole and zero. A closed-loop root remains very near the lag-compensation zero at  $-0.05 + 0j$ ; therefore, the transient response corresponding to this root will be a very slowly decaying term, which will have a small magnitude because the zero will almost cancel the pole in the transfer

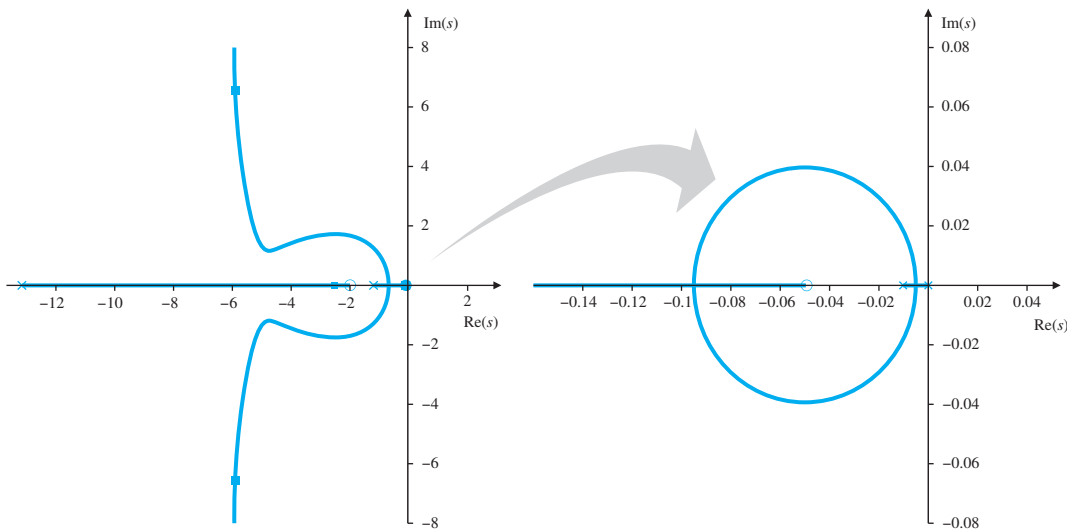


**Figure 5.28**

Root locus with both lead and lag compensation

function. Still, the decay is so slow that this term may seriously influence the settling time. Furthermore, the zero will *not* be present in the step response to a disturbance torque and the slow transient will be much more evident there. Because of this effect, it is important to place the lag pole-zero combination at as high a frequency as possible without causing major shifts in the dominant root locations.

#### Design Procedure for Lag Compensation

1. Determine the amount of gain amplification to be contributed by the lag compensation at low frequencies in order to achieve the desired  $K_p$  or  $K_v$  or  $K_a$  as determined by Eqs. (4.36–4.38).
2. Select the value of  $z$  in Eq. (5.72) so it is approximately a factor of 100 to 200 smaller than the system dominant natural frequency.
3. Select the value of  $p$  in Eq. (5.72) so that  $z/p$  is equal to the desired gain amplification determined in step 1.
4. Examine the resulting root locus to verify that the frequency and damping of the dominant closed-loop roots are still satisfactory. If not, adjust the lead compensation as needed.
5. Verify that all time domain specifications are met by examining the time response to a unit step input. If the slow root introduced by the lag compensation is too slow, increase the values of  $z$  and  $p$  somewhat while keeping  $z/p$  constant, and go back to step 4. However, do so with the understanding that the closer the values of the lag compensator's  $z$  and  $p$  come to the dominant roots of the closed loop system, the more they will affect those dominant root characteristics.

### 5.4.3 Design Using Notch Compensation<sup>16</sup>

Suppose the design has been completed with lead and lag compensation given by

$$KD_c(s) = 91 \left[ \frac{s+2}{s+13} \right] \left[ \frac{s+0.05}{s+0.01} \right], \quad (5.73)$$

but is found to have a substantial oscillation at about 50 rad/sec when tested, because there was an unsuspected flexibility of the noncollocated type at a natural frequency of  $\omega_n = 50$  rad/sec. On reexamination, the plant transfer function, including the effect of the flexibility, is estimated to be

$$G(s) = \frac{2500}{s(s+1)(s^2 + s + 2500)}. \quad (5.74)$$

A mechanical engineer claims that some of the “control energy” has spilled over into the lightly damped flexible mode and caused it to be excited. In other words, as we saw from the similar system whose root locus is shown in Fig. 5.18, the very lightly damped roots at 50 rad/sec have been made even less damped or perhaps unstable by the feedback. The best method to fix this situation is to modify the structure so there is a mechanical increase in damping. Unfortunately, this is often not possible because it is found too late in the design cycle. If it isn’t possible, how else can this oscillation be corrected? There are at least two possibilities. An additional lag compensation might lower the loop gain far enough that there is greatly reduced spillover and the oscillation is eliminated. Reducing the gain at the high frequency is called **gain stabilization**. If the response time resulting from gain stabilization is too long, a second alternative is to add a zero near the resonance so as to shift the departure angles from the resonant poles so as to cause the closed-loop root to move into the LHP, thus causing the associated transient to die out. This approach is called **phase stabilization**, and its action is similar to that of flexibility in the collocated motion control discussed earlier. Gain and phase stabilization will be explained more precisely by their effect on the frequency response in Chapter 6 where these methods of stabilization will be discussed further. For phase stabilization, the result is called a notch compensation, and an example has a transfer function

$$D_{notch}(s) = \frac{s^2 + 2\zeta\omega_0 s + \omega_0^2}{(s + \omega_0)^2}. \quad (5.75)$$

A necessary design decision is whether to place the notch frequency above or below that of the natural resonance of the flexibility in order to get the necessary phase. A check of the angle of departure shows that with the plant as compensated by Eq. (5.73) and the notch as given, it is necessary to place the frequency of the notch *above* that of the resonance to get the departure angle to point toward the LHP. Thus the compensation is added with the transfer function

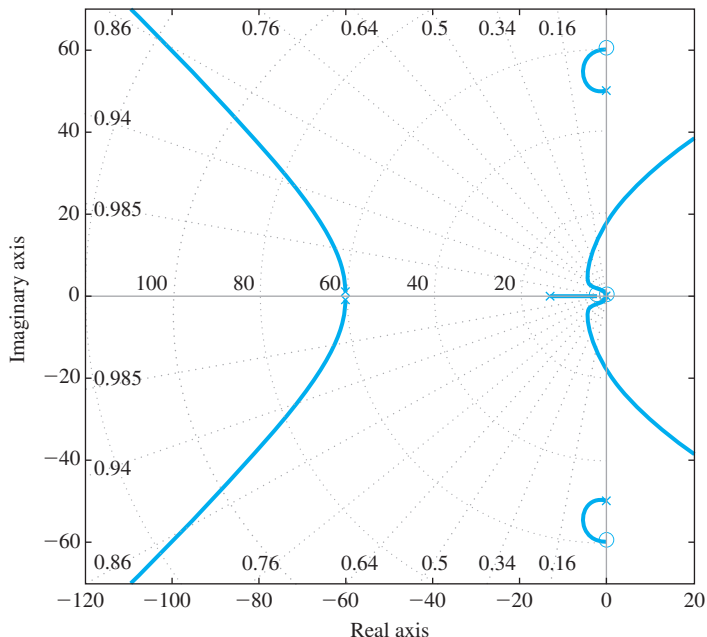
---

<sup>16</sup>This type of compensation is often referred to as a “Notch Filter” because it basically is attenuating the input around the prescribed unwanted frequency.

Gain stabilization

Phase stabilization

**Figure 5.29**  
Root locus with lead,  
lag, and notch



$$D_{notch}(s) = \frac{s^2 + 0.8s + 3600}{(s + 60)^2}. \quad (5.76)$$

The gain of the notch at  $s = 0$  has been kept at 1 so as not to change the  $K_v$ . The new root locus is shown in Fig. 5.29, and the step response is shown in Fig. 5.30 for the system with and without the notch compensation included. Note from the step responses that the notch damps the oscillations well but degrades the overshoot somewhat. The rise time specification was not affected. To rectify the increased overshoot and strictly meet all the specifications, further iteration should be carried out in order to provide more damping of the fast roots in the vicinity of  $\omega_n = 7$  rad/sec.

**Figure 5.30**  
Step response with lead  
and lag, with and  
without the notch filter

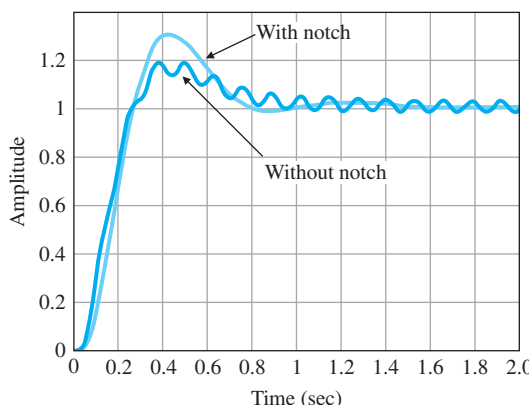
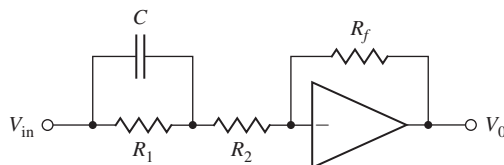


**Figure 5.31**

Possible circuit of a lead compensation



When considering notch or phase stabilization, it is important to understand that its success depends on maintaining the correct phase at the frequency of the resonance. If that frequency is subject to significant change, which is common in many cases, then the notch needs to be removed far enough from the nominal frequency in order to work for all cases. The result may be interference of the notch with the rest of the dynamics and poor performance. As a general rule, gain stabilization is substantially more robust to plant changes than is phase stabilization.

#### △ 5.4.4 Analog and Digital Implementations

Compensation can be physically realized in various ways. Most compensation can be implemented using analog electronics similar to that described in Section 2.2. However, it is very common today to implement compensation using digital devices.

As an example of an analog realization, a circuit diagram for lead compensation using an operational amplifier is shown in Fig. 5.31. The transfer function of the circuit in Fig. 5.31 is readily found by the methods from Chapter 2 to be

$$D_{lead}(s) = -a \frac{s + z}{s + p}, \quad (5.77)$$

where

$$a = \frac{p}{z}, \quad \text{if } R_f = R_1 + R_2,$$

$$z = \frac{1}{R_1 C},$$

$$p = \frac{R_1 + R_2}{R_2} \cdot \frac{1}{R_1 C}.$$

A short section describing the implementation of a lead compensation using a digital device and a comparison of the results with an analog implementation is contained in online Appendix W5.4.4. (See [www.pearsonglobaleditions.com](http://www.pearsonglobaleditions.com))

## 5.5 Design Examples Using the Root Locus

### EXAMPLE 5.12

#### *Control of a Quadrotor Drone Pitch Axis*

For the quadrotor shown in Fig. 2.13, the transfer function between a pitch control input,  $T_{lon}$ , and the pitch angle,  $\theta$ , is

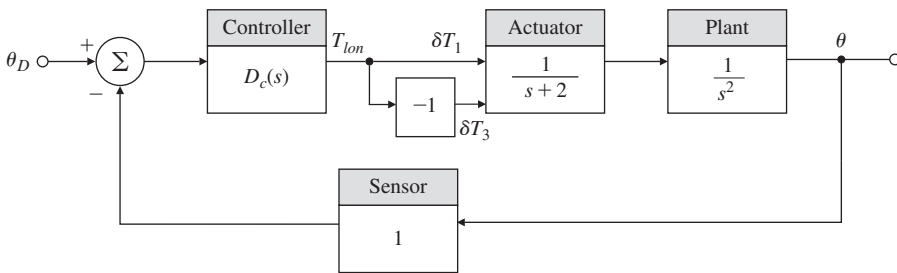


**Figure 5.32**

Block diagram for the quadrotor design Example 5.12

$$\frac{\theta(s)}{T_{lon}(s)} = G_1(s) = \frac{1}{s^2(s+2)}.$$

This is similar to the transfer function obtained in Eq. (2.15) in Chapter 2; however, an extra term has been added to account for the lag associated with the rotor coming up to the newly commanded thrust and speed. The lag term selected,  $(s + 2)$ , is for a fairly large quadrotor of perhaps 2 meters in diameter. The more detailed drone example in Chapter 10 (see Example 10.5) will include this term along with some of the aerodynamic terms. However, for purposes of understanding the essential control features, this simplified example should suffice. The block diagram of the control system is shown in Fig. 5.32. It shows the quadrotor dynamics given by  $\theta(s)/T_{lon}(s)$  and shows the compensator,  $D_c(s)$ , to be designed via the root locus method. The desired specifications for this system are:

$$\omega_n \geq 1 \text{ rad/sec},$$

$$\zeta \geq 0.44.$$

Using lead compensation, find a set of parameters for  $D_c(s)$  that meet the required specifications.

**Solution.** Knowing the desired  $\omega_n$  and  $\zeta$  values is the **first step** in the Lead Compensation Design Procedure. The **second step** in the process is to determine a root locus for the uncompensated system. The ensuing Matlab commands will generate such a locus:

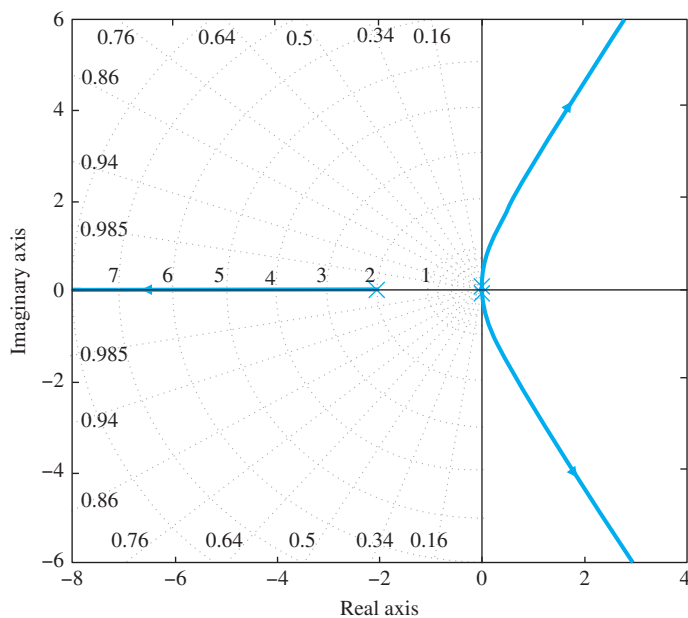
```
s = tf('s');
sysG1=1/((s^2)*(s+2));
rlocus(sysG1)
axis([-8 4 -6 6])
grid on
```

Note use of the grid command places the  $\omega_n$  and  $\zeta$  values on the root locus plot as an aid in the determination of whether the specifications are met. The result is shown in Fig. 5.33.

The uncompensated system exhibits increasing instability as the gain,  $K$ , is increased; therefore, it is likely that significant more lead will be required compared to Example 5.11 where the uncompensated

**Figure 5.33**

Uncompensated system,  
i.e., with  $D_c(s) = K$ .



system was always stable, as was shown in Fig. 5.22. For the **third step** we select  $z = 1$  and  $p = 10$  in Eq. (5.70) so

$$D_c(s) = K \frac{s + 1}{s + 10}.$$

This compensation is implemented into the quadrotor control system by the Matlab commands

```
s = tf('s');
sysG1=1/((s^2)*(s+2));
sysD=(s+1)/(s+10);
rlocus(sysG1*sysD)
axis([-3 1 -2 2])
grid on
```

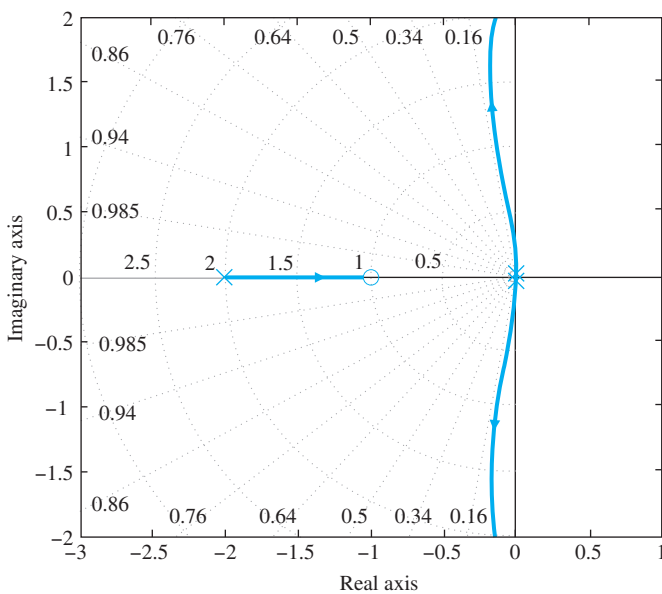
which produce the root locus in Fig. 5.34. It shows that no value of  $K$  will produce the level of damping required, that is,  $\zeta \geq 0.44$ .

Clearly, significantly more damping from the compensator is required so we move on to **step 4** in the procedure. For our next attempt, let's choose a value of  $z = 0.5$  instead of 1. However, it will show that it is still not possible to meet both specifications. Therefore, let's also increase  $p$  to 15 and examine whether that will create a locus with  $\zeta \geq 0.44$ . Therefore the compensation is now

$$D_c(s) = K \frac{s + 0.5}{s + 15}.$$

**Figure 5.34**

Compensated system  
with  $D_c(s) = K \frac{s+1}{s+10}$



A root locus of the system with this compensator is found from the ensuing Matlab statements

```
s = tf('s');
sysG1=1/((s^2)*(s+2));
sysD=(s+0.5)/(s+15);
rlocus(sysG1*sysD)
axis([-3 1 -2 2])
grid on
```

which produces the locus shown in Fig. 5.35.

Comparing the locus with the lines of constant damping shows that it comes very close to the  $\zeta = 0.5$  line, and thus most likely will satisfy the requirement that  $\zeta \geq 0.44$ . Also note that the point on the locus that is closest to the  $\zeta = 0.5$  line is approximately at  $\omega_n = 1$  rad/sec. Thus, **step 5** consists of verifying this result. This can be carried out by placing your cursor on the Matlab generated root locus at the point of best damping. Doing so shows that

$$K = 30,$$

$$\omega_n = 1.03, \text{ and}$$

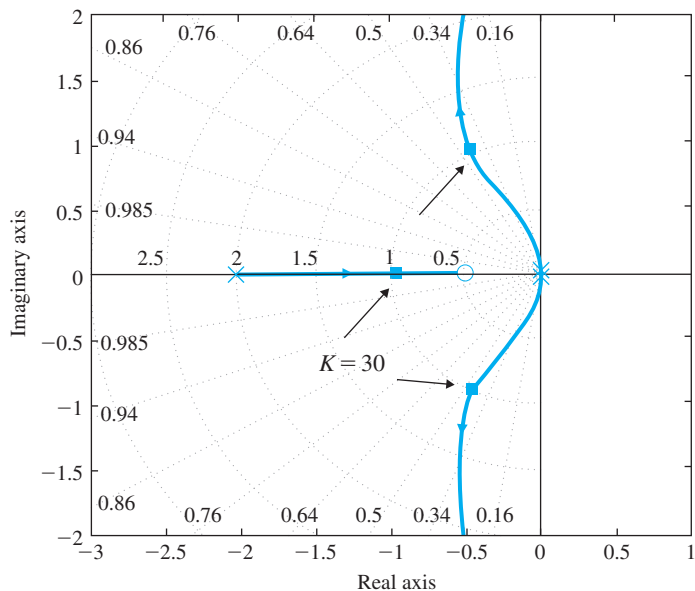
$$\zeta = 0.446,$$

which satisfies **step 5** in the design procedure and yields the value of  $K$  in the lead compensation. Therefore, we now have the complete set of parameters, and the final design is

$$D_c(s) = 30 \frac{s + 0.5}{s + 15}.$$

**Figure 5.35**

Root locus of the quadrotor with  
 $D_c(s) = K \frac{s+0.5}{s+15}$



Thus, all the specifications are now met. Since no time domain or steady-state requirements have been made, **steps 6 and 7** do not apply in this case. Had there been a time response specification that was not met, it would be necessary to return to **step 2** and revise the desired  $\omega_n$  and  $\zeta$  so as to improve the situation. A higher value of  $\omega_n$  would speed up the response time and a higher value of  $\zeta$  would decrease the overshoot. If the steady-state error requirements had not been met, it is sometimes possible to increase  $K$  and still meet the other specifications; however, in this case any increase in  $K$  from the selected value of 30 would decrease the damping,  $\zeta$ , so it would be necessary to add a lag compensator or integral control had a higher value of  $K$  been necessary.

### EXAMPLE 5.13

#### *Control of a Small Airplane*

For the Piper Dakota shown in Fig. 5.36, the transfer function between the elevator input and the pitch attitude is

$$G(s) = \frac{\theta(s)}{\delta_e(s)} = \frac{160(s + 2.5)(s + 0.7)}{(s^2 + 5s + 40)(s^2 + 0.03s + 0.06)}, \quad (5.78)$$

where

$\theta$  = pitch attitude, degrees (see Fig. 10.30),

$\delta_e$  = elevator angle, degrees.

(For a more detailed discussion of longitudinal aircraft motion, refer to Section 10.3.)

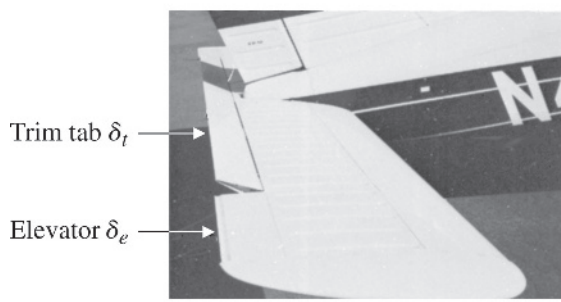
**Figure 5.36**

Autopilot design in the Piper Dakota, showing elevator and trim tab

*Source: Photos courtesy of Denise Freeman*



(a)



(b)

1. Design an autopilot so the response to a step elevator input has a rise time of 1 sec or less and an overshoot less than 10%.
2. When there is a constant disturbing moment acting on the aircraft so the pilot must supply a constant force on the controls for steady flight, it is said to be out of trim. The transfer function between the disturbing moment and the attitude is the same as that due to the elevator; that is,

$$\frac{\theta(s)}{M_d(s)} = \frac{160(s + 2.5)(s + 0.7)}{(s^2 + 5s + 40)(s^2 + 0.03s + 0.06)}, \quad (5.79)$$

where  $M_d$  is the moment acting on the aircraft. There is a separate aerodynamic surface for trimming,  $\delta_t$ , that can be actuated and will change the moment on the aircraft. It is shown in the close-up of the tail in Fig. 5.36(b), and its influence is depicted in the block diagram shown in Fig. 5.37(a). For both manual and autopilot flight, it is desirable to adjust the trim so there is no steady-state control effort required from the elevator (that is, so  $\delta_e = 0$ ). In manual flight, this means no force is required by the pilot to keep the aircraft at a constant altitude, whereas in autopilot control it means reducing the amount of electrical power required and saving

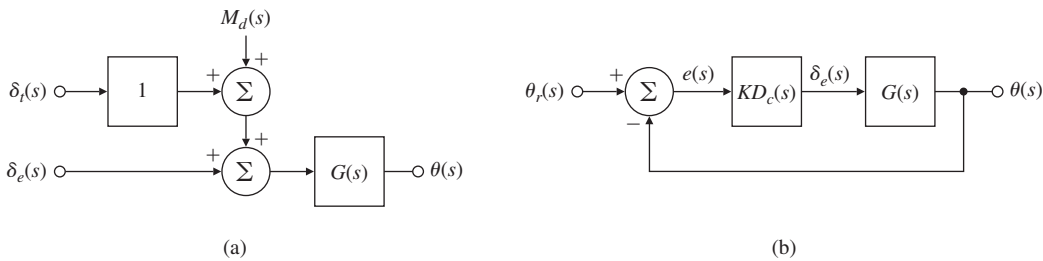


**Figure 5.37**

Block diagrams for autopilot design: (a) open loop; (b) feedback scheme excluding trim

wear and tear on the servomotor that drives the elevator. Design an autopilot that will command the trim  $\delta_t$  so as to drive the steady-state value of  $\delta_e$  to zero for an arbitrary constant moment  $M_d$  as well as meet the specifications in part (a).

## Solution

1. To satisfy the requirement that the rise time  $t_r \leq 1$  sec, Eq. (3.68) indicates that, for the ideal second-order case,  $\omega_n$  must be greater than 1.8 rad/sec. And to provide an overshoot of less than 10%, Fig. 3.24 indicates that  $\zeta$  should be greater than 0.6, again, for the ideal second-order case. In the design process, we can examine a root locus for a candidate for feedback compensation and then look at the resulting time response when the roots appear to satisfy the design guidelines. However, since this is a fourth-order system, the design guidelines might not be sufficient, or they might be overly restrictive.

To initiate the design process, it is often instructive to look at the system characteristics with proportional feedback, that is, where  $D_c(s) = 1$  in Fig. 5.37(b). The statements in Matlab to create a root locus with respect to  $K$  and a time response for the proportional feedback case with  $K = 0.3$  are as follows:

```

s = tf('s');
sysG = (160*(s + 2.5)*(s + 0.7))/((s^2 + 5*s + 40)*(s^2 + 0.03*s +
    0.06));
rlocus(sysG)
K = 0.3;
sysL = K*sysG;
[sysT] = feedback (sysL,1);
step(sysT)

```

The resulting root locus and time response are shown with dashed lines in Figs. 5.38 and 5.39. Notice from Fig. 5.38 that the two faster roots will always have a damping ratio  $\zeta$  that is less than 0.4; therefore, proportional feedback will not be acceptable. Also, the slower roots have some effect on the time response shown

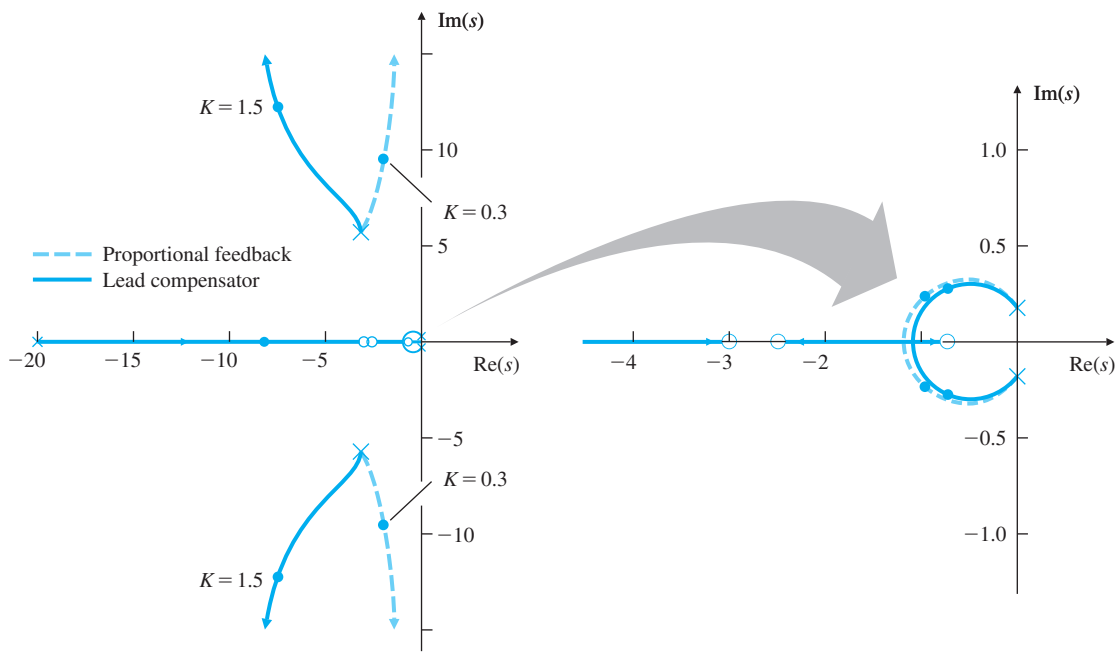
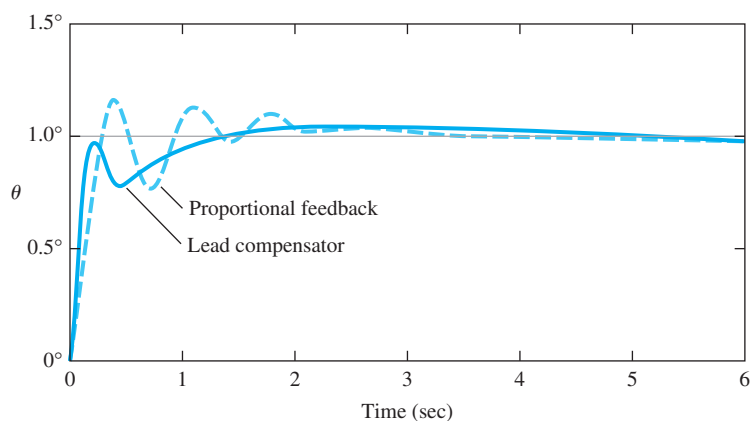


**Figure 5.38**  
Root loci for autopilot design

**Figure 5.39**  
Time-response plots for autopilot design



in Fig. 5.39 (dashed curve) with  $K = 0.3$  in that they cause a long-term settling. However, the dominating characteristic of the response that determines whether or not the compensation meets the specifications is the behavior in the first few seconds, which is dictated by the fast roots. The low damping of the fast roots causes the time response to be oscillatory, which leads to excess overshoot and a longer settling time than desired.

We saw in Section 5.4.1 that lead compensation causes the locus to shift to the left, a change needed here to increase the damping. Some trial and error will be required to arrive at a suitable pole and zero location. Values of  $z = 3$  and  $p = 20$  in Eq. (5.70) have a substantial effect in moving the fast branches of the locus to the left; thus

$$D_c(s) = \frac{s + 3}{s + 20}.$$

Trial and error is also required to arrive at a value of  $K$  that meets the specifications. The statements in Matlab to add this compensation are as follows:

**Lead compensation via Matlab**

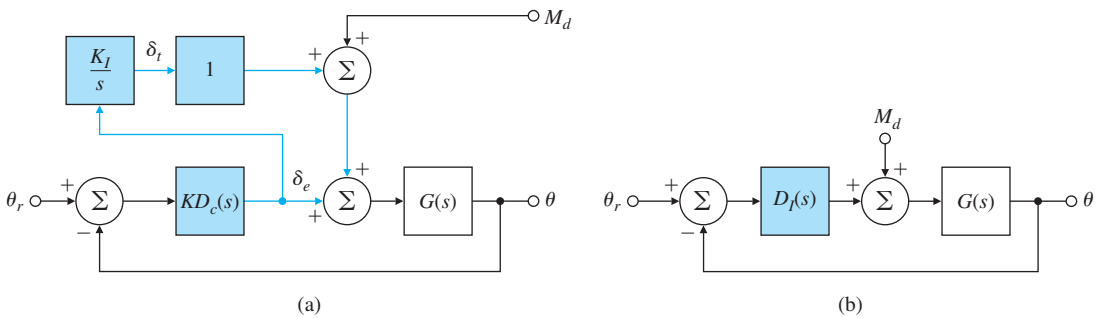
```
sysD = (s + 3)/(s + 20);
sysDG = sysD*sysG;
rlocus(sysDG)
K = 1.5;
sysKDG = K*sysDG;
sysT = feedback(sysKDG,1);
step(sysT)
```

The root locus for this case and the corresponding time response are also shown in Figs. 5.38 and 5.39 by the solid lines. Note the damping of the fast roots that corresponds to  $K = 1.5$  is  $\zeta = 0.52$ , which is slightly lower than we would like; also, the natural frequency is  $\omega_n = 15$  rad/sec, much faster than we need. However, these values are close enough to meeting the guidelines to suggest a look at the time response. In fact, the time response shows that  $t_r \cong 0.9$  sec and  $M_p \cong 8\%$ , both within the specifications, although by a very slim margin.

In summary, the primary design path consisted of adjusting the compensation to influence the fast roots, examining their effect on the time response, and continuing the design iteration until the time specifications were satisfied.

2. The purpose of the trim is to provide a moment that will eliminate a steady-state nonzero value of the elevator. Therefore, if we integrate the elevator command  $\delta_e$  and feed this integral to the trim device, the trim should eventually provide the moment required to hold an arbitrary altitude, thus eliminating the need for a steady-state  $\delta_e$ . This idea is shown in Fig. 5.40(a). If the gain on the integral term  $K_I$  is small enough, the destabilizing effect of adding the integral should be small and the system should behave approximately as before, since that feedback loop has been left intact. The block diagram in Fig. 5.40(a) can be reduced to that in Fig. 5.40(b) for analysis purposes by defining the compensation to include the PI form

$$D_I(s) = KD_c(s) \left( 1 + \frac{K_I}{s} \right).$$

**Figure 5.40**

Block diagram showing the trim-command loop

However, it is important to keep in mind that, physically, there will be two outputs from the compensation:  $\delta_e$  (used by the elevator servomotor) and  $\delta_t$  (used by the trim servomotor).

The characteristic equation of the system with the integral term is

$$1 + KD_c G + \frac{K_I}{s} KD_c G = 0.$$

To aid in the design process, it is desirable to find the locus of roots with respect to  $K_I$ , but the characteristic equation is not in any of the root-locus forms given by Eqs. (5.6)–(5.9). Therefore, dividing by  $1 + KD_c G$  yields

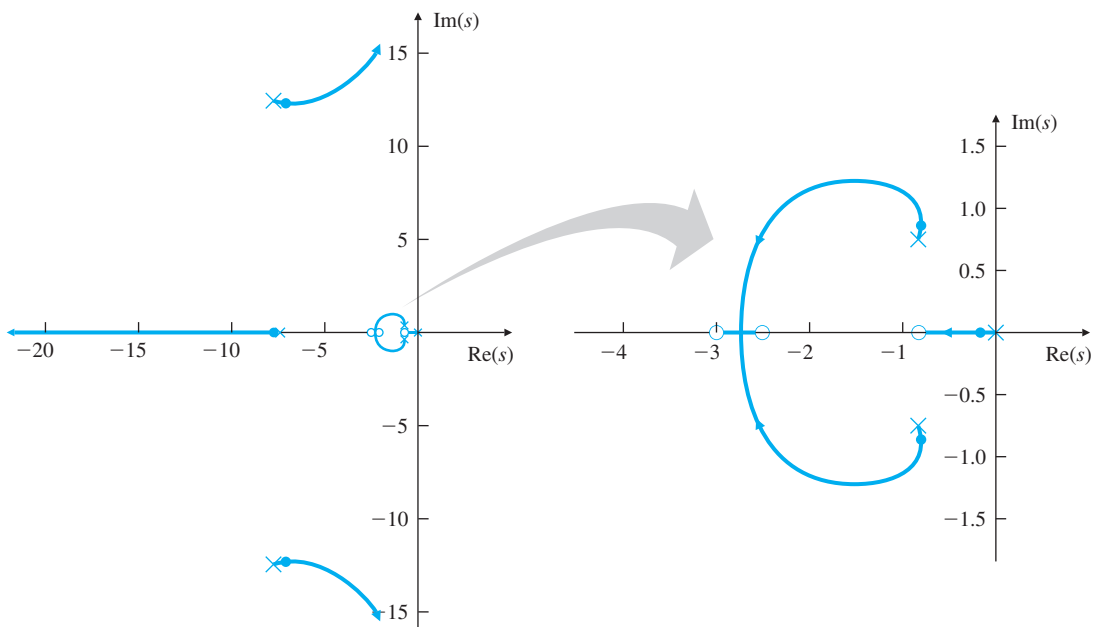
$$1 + \frac{(K_I/s)KD_c G}{1 + KD_c G} = 0.$$

To put this system in root locus form, we define

$$L(s) = \frac{1}{s} \frac{KD_c G}{1 + KD_c G}, \quad (5.80)$$

so  $K_I$  becomes the root locus parameter. In Matlab, with  $\frac{KD_c G}{1+KD_c G}$  already computed as sysT, we construct the integrator as sysIn =  $1/s$ , the loop gain of the system with respect to  $K_I$  as sysL = sysIn\*sysT, and the root locus with respect to  $K_I$  is found with sisotool('rlocus',sysL).

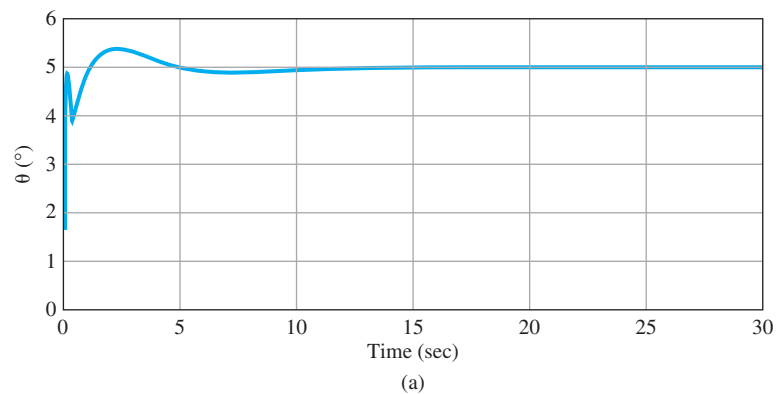
It can be seen from the locus in Fig. 5.41 that the damping of the fast roots decreases as  $K_I$  increases, as is typically the case when integral control is added. This shows the necessity for keeping the value of  $K_I$  as low as possible. After some trial and error, we select  $K_I = 0.15$ . This value has little effect on the roots—note the roots are virtually on top of the previous roots obtained without the integral term—and little effect on the short-term behavior of the step response, as shown in Fig. 5.42(a), so the specifications are still met.  $K_I = 0.15$  does cause the longer-term attitude behavior to approach the commanded value with no error, as we

**Figure 5.41**

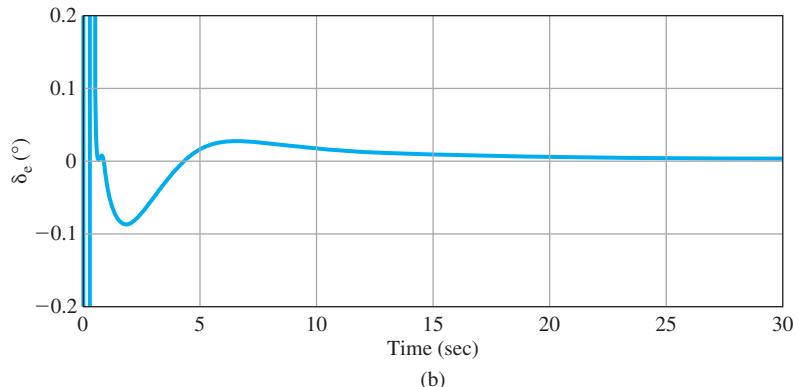
Root locus versus  $K_I$ : assumes an added integral term and lead compensation with a gain  $K = 1.5$ ; roots for  $K_I = 0.15$  marked with ●

**Figure 5.42**

Step response for the case with an integral term and  $5^\circ$  command



(a)



(b)

would expect with integral control. It also causes  $\delta_e$  to approach zero (Fig. 5.42(b) shows it settling in approximately 30 sec) which is good because this is the reason for choosing integral control in the first place. The time for the integral to reach the correct value is predicted by the new, slow real root that is added by the integral term at  $s = -0.14$ . The time constant associated with this root is  $\tau = 1/0.14 \cong 7$  sec. The settling time to 1% for a root with  $\sigma = 0.14$  is shown by Eq. (3.73) to be  $t_s = 33$  sec, which agrees with the behavior in Fig. 5.42(b).

## 5.6 Extensions of the Root-Locus Method

As we have seen in this chapter, the root-locus technique is a graphical scheme to show locations of possible roots of an algebraic equation as a single real parameter varies. The method can be extended to consider negative values of the parameter, a sequential consideration of more than one parameter, and systems with time delay. In this section, we examine these possibilities. Another interesting extension to nonlinear systems will be discussed in Chapter 9.

### 5.6.1 Rules for Plotting a Negative ( $0^\circ$ ) Root Locus

We now consider modifying the root-locus procedure to permit analysis of negative values of the parameter. In a number of important cases, the transfer function of the plant has a zero in the RHP and is said to be nonminimum phase. The result is often a locus of the form  $1 + A(z_i - s)G'(s) = 1 + (-A)(s - z_i)G'(s) = 0$ , and in the standard form the parameter  $K = -A$  must be negative. Another important issue calling for understanding the negative locus arises in building a control system. In any physical implementation of a control system there are inevitably a number of amplifiers and components whose gain sign must be selected. By Murphy's Law,<sup>17</sup> when the loop is first closed, the sign will be wrong and the behavior will be unexpected unless the engineer understands how the response will go if the gain which should be positive is instead negative. So what are the rules for a negative locus (a root locus relative to a negative parameter)? First of all, Eqs. (5.6)–(5.9) must be satisfied for negative values of  $K$ , which implies that  $L(s)$  is real and *positive*. In other words, for the negative locus, the phase condition is

**Definition of a Negative Root Locus**

The angle of  $L(s)$  is  $0^\circ + 360^\circ(l - 1)$  for  $s$  on the negative locus.

The steps for plotting a negative locus are essentially the same as for the positive locus, except that we search for places where the angle

<sup>17</sup>Anything that *can* go wrong, *will* go wrong.

of  $L(s)$  is  $0^\circ + 360^\circ(l - 1)$  instead of  $180^\circ + 360^\circ(l - 1)$ . For this reason, a negative locus is also referred to as a  $0^\circ$  root locus. This time we find that the locus is to the left of an *even* number of real poles plus zeros (the number zero being even). Computation of the center of the asymptotes for large values of  $s$  is, as before, given by

$$\alpha = \frac{\sum p_i - \sum z_i}{n - m}, \quad (5.81)$$

but we modify the angles to be

$$\phi_l = \frac{360^\circ(l - 1)}{n - m}, \quad \text{where } l = 1, 2, 3, \dots, n - m$$

(shifted by  $\frac{180^\circ}{n-m}$  from the  $180^\circ$  locus). Following are the guidelines for plotting a  $0^\circ$  locus:

**RULE 1.** (As before) The  $n$  branches of the locus leave the poles and  $m$  branches approach the zeros and  $n - m$  branches approach the asymptotes.

**RULE 2.** The locus is on the real axis to the left of an *even* number of real poles plus zeros.

**RULE 3.** The asymptotes are described by

$$\begin{aligned} \alpha &= \frac{\sum p_i - \sum z_i}{n - m} = \frac{-a_1 + b_1}{n - m}, \\ \phi_l &= \frac{360^\circ(l - 1)}{n - m}, \quad l = 1, 2, 3, \dots, n - m. \end{aligned}$$

Notice the angle condition here is measured from  $0^\circ$  rather than from  $180^\circ$ , as it was in the positive locus.

**RULE 4.** Departure angles from poles and arrival angles to zeros are found by searching in the near neighborhood of the pole or zero where the phase of  $L(s)$  is  $0^\circ$ , so that

$$q\phi_{\text{dep}} = \sum \psi_i - \sum \phi_i - 360^\circ(l - 1),$$

$$q\psi_{\text{arr}} = \sum \phi_i - \sum \psi_i + 360^\circ(l - 1),$$

where  $q$  is the order of the pole or zero and  $l$  takes on  $q$  integer values such that the angles are between  $\pm 180^\circ$ .

**RULE 5.** The locus can have multiple roots at points on the locus, and the branches will approach a point of  $q$  roots at angles separated by

$$\frac{180^\circ + 360^\circ(l - 1)}{q},$$

and will depart at angles with the same separation.

The result of extending the guidelines for constructing root loci to include negative parameters is that we can visualize the root locus as a set of continuous curves showing the location of possible solutions to

the equation  $1 + KL(s) = 0$  for *all real values of K*, both positive and negative. One branch of the locus departs from every pole in one direction for positive values of  $K$ , and another branch departs from the same pole in another direction for negative  $K$ . Likewise, all zeros will have two branches arriving, one with positive and the other with negative values of  $K$ . For the  $n - m$  excess poles, there will be  $2(n - m)$  branches of the locus asymptotically approaching infinity as  $K$  approaches positive and negative infinity, respectively. For a single pole or zero, the angles of departure or arrival for the two locus branches will be  $180^\circ$  apart. For a double pole or zero, the two positive branches will be  $180^\circ$  apart, and the two negative branches will be at  $90^\circ$  to the positive branches.

The negative locus is often required when studying a nonminimum phase transfer function. A well-known example is that of the control of liquid level in the boiler of a steam power plant. If the level is too low, the actuator valve adds (relatively) cold water to the boiling water in the vessel. As demonstrated in Fig. 3.31, the initial effect of the addition is to slow down the rate of boiling, which reduces the number and size of the bubbles and causes the level to fall momentarily, before the added volume and heat cause it to rise again to the new increased level. This initial underflow is typical of nonminimum phase systems. Another typical nonminimum phase transfer function is that of the altitude control of an airplane. To make the plane climb, the upward deflection of the elevators initially causes the plane to drop before it rotates and climbs. A Boeing 747 in this mode can be described by the scaled and normalized transfer function

$$G(s) = \frac{6 - s}{s(s^2 + 4s + 13)}. \quad (5.82)$$

To put  $1 + KG(s)$  in root-locus form, we need to multiply by  $-1$  to get

$$G(s) = -\frac{s - 6}{s(s^2 + 4s + 13)}. \quad (5.83)$$

## EXAMPLE 5.14

### *Negative Root Locus for an Airplane*

Sketch the negative root locus for the equation

$$1 + \frac{K(s - 3)}{s(s^2 + 5s + 19)} = 0. \quad (5.84)$$

#### Solution

RULE 1. There are three branches and two asymptotes.

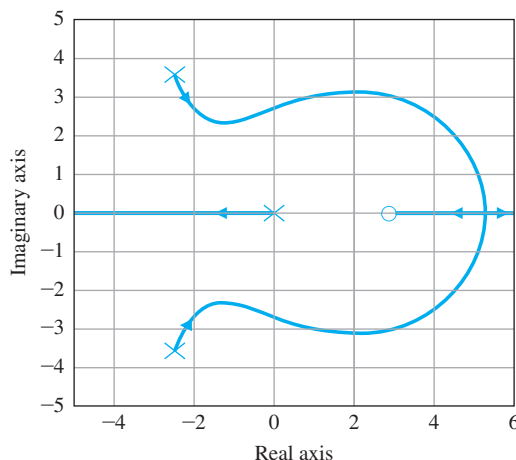
RULE 2. A real-axis segment is to the right of  $s = 3$  and a segment is to the left of  $s = 0$ .

RULE 3. The angles of the asymptotes are  $\phi_1 = \frac{(l-1)360^\circ}{2} = 0^\circ, 180^\circ$ .

RULE 4. The branch departs the pole at  $s = -2.5 + j3.5707$  at the angle

**Figure 5.43**

Negative root locus corresponding to  
 $\frac{K(s-3)}{s(s^2+5s+19)}$



$$\begin{aligned}\phi &= \left(180^\circ - \tan^{-1}\left(\frac{3.5707}{5.5}\right)\right) - \left(180^\circ - \tan^{-1}\left(\frac{3.5707}{2.5}\right)\right) \\ &\quad - 90^\circ + 360(l-1), \\ &= 147^\circ - 125^\circ - 90^\circ + 360(l-1), \\ &= -68^\circ.\end{aligned}$$

The locus is plotted, in Fig. 5.43 by Matlab, which is seen to be consistent with these values.

### △ 5.6.2 Successive Loop Closure

An important technique for practical control is to consider a structure with two loops: an inner loop around an actuator or part of the process dynamics, and an outer loop around the entire plant-plus-inner-controller. The process is called **successive loop closure**. A controller is selected for the inner loop to be robust and give good response alone, and then the outer loop can be designed to be simpler and more effective than if the entire control was done without the aid of the inner loop. The use of the root locus to study such a system with two parameters can be illustrated by a simple example.

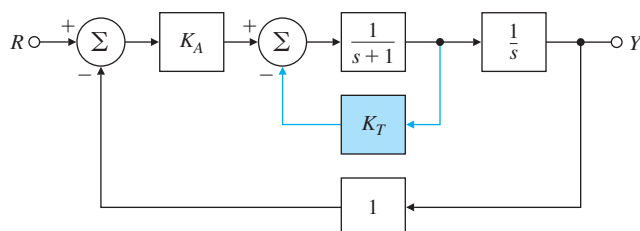
## EXAMPLE 5.15

### *Root Locus Using Two Parameters in Succession*

A block diagram of a relatively common servomechanism structure is shown in Fig. 5.44. Here a speed-measuring device (a tachometer) is

**Figure 5.44**

Block diagram of a servomechanism structure, including tachometer feedback



available and the problem is to use the root locus to guide the selection of the tachometer gain  $K_T$  as well as the amplifier gain  $K_A$ . The characteristic equation of the system in Fig. 5.44 is

$$1 + \frac{K_A}{s(s+1)} + \frac{K_T}{s+1} = 0,$$

which is not in the standard  $1 + KL(s)$  form. After clearing fractions, the characteristic equation becomes

$$s^2 + s + K_A + K_T s = 0, \quad (5.85)$$

which is a function of two parameters, whereas the root locus technique can consider only one parameter at a time. In this case, we set the gain  $K_A$  to a nominal value of 4 and consider first the locus with respect to  $K_T$ . With  $K_A = 4$ , Eq. (5.85) can be put into root-locus form for a root-locus study with respect to  $K_T$  with  $L(s) = \frac{s}{s^2+s+4}$ , or

$$1 + K_T \frac{s}{s^2 + s + 4} = 0. \quad (5.86)$$

For this root locus, the zero is at  $s = 0$  and the poles are at the roots of  $s^2 + s + 4 = 0$ , or  $s = -\frac{1}{2} \pm 1.94j$ . A sketch of the locus using the rules as before is shown in Fig. 5.45.

From this locus, we can select  $K_T$  so the complex roots have a specific damping ratio or take any other value of  $K_T$  that would result in satisfactory roots for the characteristic equation. Consider  $K_T = 1$ . Having selected a trial value of  $K_T$ , we can now re-form the equation to consider the effects of changing from  $K_A = 4$  by taking the new parameter to be  $K_1$  so  $K_A = 4 + K_1$ . The locus with respect to  $K_1$  is governed by Eq. (5.50), now with  $L(s) = \frac{1}{s^2+2s+4}$ , so the locus is for the equation

$$1 + K_1 \frac{1}{s^2 + 2s + 4} = 0. \quad (5.87)$$

Note the *poles* of the new locus corresponding to Eq. (5.87) are the *roots* of the previous locus, which was drawn versus  $K_T$ , and the roots were taken at  $K_T = 1$ . The locus is sketched in Fig. 5.46, with the previous locus versus  $K_T$  left dashed. We could draw a locus with respect to

**Figure 5.45**

Root locus of closed-loop poles of the system in Fig. 5.44 versus  $K_T$

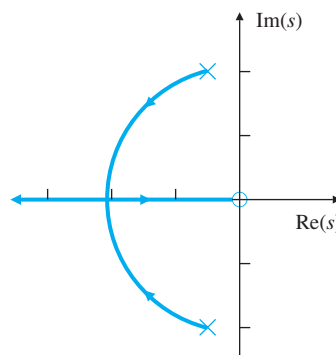
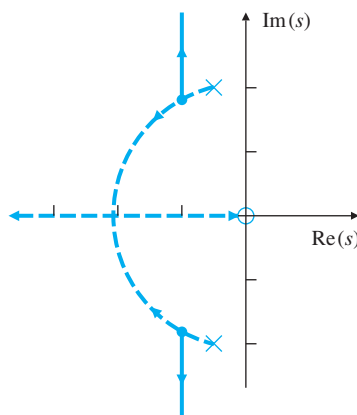


**Figure 5.46**

Root locus versus  
 $K_1 = K_A + 4$  after  
choosing  $K_T = 1$



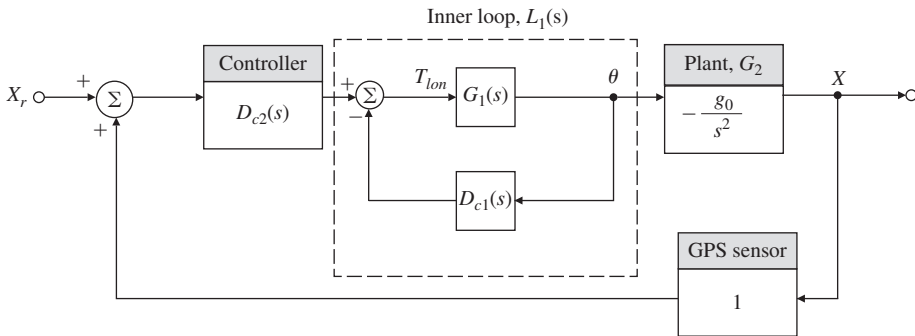
$K_1$  for a while, stop, resolve the equation, and continue the locus with respect to  $K_T$ , in a sort of see-saw between the parameters  $K_A$  and  $K_T$ , and thus use the root locus to study the effects of two parameters on the roots of a characteristic equation. Notice, of course, we can also plot the root locus for negative values of  $K_1$ , and thus consider values of  $K_A$  less than 4.

**EXAMPLE 5.16***Control of a Quadrotor Drone x-Axis Position*

For the quadrotor pitch angle control shown in Fig. 5.32, the transfer function between the pitch control input,  $T_\theta$ , and the pitch angle,  $\theta$ , is  $G_1 = \frac{1}{s^2(s+2)}$ . We found a lead compensator,  $D_{c1}(s) = 30\frac{s+0.5}{s+15}$ , that provided well-damped roots of the closed-loop system based on a measurement of the pitch angle and commands to the two pitch rotors, 1 and 3, shown in Fig. 2.14. We can use the pitch angle to control position along the  $x$ -axis since a small non-zero value of the pitch angle,  $\theta$ , provides a component of thrust along the negative  $x$ -axis  $= -g_o \sin(\theta) \simeq -g_o\theta$ . Integrated twice, this thrust component will produce a change in the  $x$ -position. Thus, we have the additional dynamics,

$$G_2(s) = \frac{x(s)}{\theta(s)} = -\frac{g_o}{s^2}.$$

The block diagram of the complete position control system for the  $x$ -axis control is shown in Fig. 5.47. It includes the inner, pitch attitude loop plus the outer loop that provides the position control that depends on a position measurement, typically obtained for drones using a GPS on board. Note that, due to the negative  $x$ -axis thrust produced by the positive  $\theta$ , the sign on the outer feedback loop has been made positive for proper control action.

**Figure 5.47**

Inner and outer loop of the drone position control system

Design the outer loop compensation,  $D_{c2}(s)$ , so that the natural frequency,  $\omega_n$ , of the complex roots are  $\geq 0.4$  rad/sec and  $\zeta \geq 0.5$ .

**Solution.** The inner loop's dynamics were obtained in Example 5.12 and those need to be included in the analysis of the outer loop. To determine the transfer function of that loop, we can use the Matlab feedback function as follows:

```
s=tf('s');
sysG1=1/((s^2)*(s+2));
sysD1=(s+0.5)/(s+15);
K=30;
sysL1=feedback(sysG1,sysD1*K)
```

The result, which can also be computed by hand, is that the transfer function of the inner pitch control loop is

$$L_1(s) = K \frac{s + 15}{s^4 + 17s^3 + 30s^2 + 30s + 15}.$$

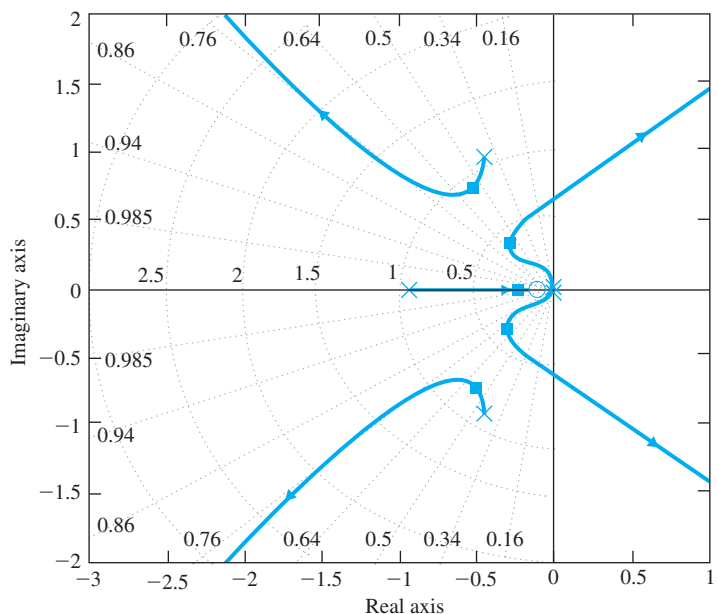
The first step in the design of the outer loop is to take a look at the root locus of the loop with the compensation,  $D_{c2}(s) = K_2$ . The Matlab commands for that step are:

```
sysG2=32.2/s^2;
rlocus(sysL1*sysG2)
```

As you might expect with two poles at the origin, the locus departs north and south from the origin and, because of the poles of  $L_1(s)$  located as shown in Fig. 5.35, the locus quickly departs into the unstable RHP. Therefore, it is clear that some lead compensation [ $D_{c2}(s)$ ] is required for this outer loop to be stable with acceptable characteristics. After some iteration with the pole and zero of  $D_{c2}(s)$ , using

**Figure 5.48**

Root locus of the  $x$ -axis control system showing the location of the closed loop roots with  $D_{c2}(s) = .081 \frac{s+0.1}{s+10}$



```
rlocus(sysD2*sysL1*sysG2),
```

it can be found that

$$D_{c2}(s) = K_2 \frac{s + 0.1}{s + 10},$$

will provide a root locus that allows closed-loop roots with acceptable frequency and damping. In fact, selecting  $K_2 = .081$  yields two sets of complex roots, one set with  $\omega_n = 0.4$  and  $\zeta \approx 0.7$  and another set with  $\omega_n = 0.9$  and  $\zeta \approx 0.6$ . In addition, there are real roots at  $s \cong -0.2$  and  $-10$ . Thus, the design is complete and the closed-loop roots of the entire system meet the desired specifications. The root locus with  $D_{c2}(s)$  showing the location of the closed-loop roots for  $K_2 = .081$  is shown in Fig. 5.48. Although the general rule is that the pole/zero ratio should be less than 25, in this case, it can be violated because the GPS sensor systems generally supply the position and velocity. Hence, pure derivative feedback is practical and the pole in that case would essentially be at negative infinity.

It is theoretically possible to compensate this type of system using only the outer-loop output,  $x$ . However, in practice, when it is possible to use a sensor for an inner loop closure, this approach is universally used in order to obtain a better control design due to its improved robustness and reduced sensitivity to sensor noise. The relationship between lead compensation characteristics and sensitivity to sensor noise will be discussed in more depth in Chapter 6.

### △ 5.6.3 Time Delay

Time delays always reduce the stability of a system

Time delays often arise in control systems, both from delays in the process itself and from delays in the processing of sensed signals. Chemical plants often have processes with a time delay representing the time material takes to be transported via pipes or other conveyer. In measuring the attitude of a spacecraft en route to Mars, there is a significant time delay for the sensed quantity to arrive back on Earth due to the speed of light. Time delay *always* reduces the stability of a system; therefore, it is important to be able to analyze its effect. Use of the **Padé approximant** adds a rational function that approximates the effect of a time delay so one can analyze its effect on the stability of a system. This method is described in Appendix W5.6.3 found online at [www.pearsonglobaleditions.com](http://www.pearsonglobaleditions.com). The effect of time delays will also be covered via frequency response design in Chapter 6. Using frequency response methods, it is possible to show the effect of a time delay exactly and easily. The destabilizing effect is clearly exposed by Fig. 6.80.

## 5.7 Historical Perspective

In Chapter 1, we gave an overview of the early development of feedback control analysis and design including frequency response and root-locus design. Root-locus design was introduced in 1948 by Walter R. Evans, who was working in the field of guidance and control of aircraft and missiles at the Autonetics Division of North American Aviation (now a part of The Boeing Co.). Many of his problems involved unstable or neutrally stable dynamics, which made the frequency methods difficult, so he suggested returning to the study of the characteristic equation that had been the basis of the work of Maxwell and Routh nearly 70 years earlier. However, rather than treat the algebraic problem, Evans posed it as a graphical problem in the complex  $s$ -plane. Evans was also interested in the character of the dynamic response of the aerospace vehicles being controlled; therefore, he wanted to solve for the closed-loop roots in order to understand the dynamic behavior. To facilitate this understanding, Evans developed techniques and rules allowing one to follow graphically the paths of the roots of the characteristic equation as a parameter was changed. His method is suitable for design as well as for stability analysis and remains an important technique today. Originally, it enabled the solutions to be carried out by hand since computers were not readily available to designers; however, root-loci remain an important tool today for aiding the design process. As we learned in this chapter, Evans method involves finding a locus of points where the angles to the other poles and zeros add up to a certain value. To aid in this determination, Evans invented the “Spirule.” It could be used to measure the angles and to perform the addition or subtraction very quickly. A skilled controls engineer could evaluate whether the angle criterion was met for a fairly complex design problem in a few seconds. In

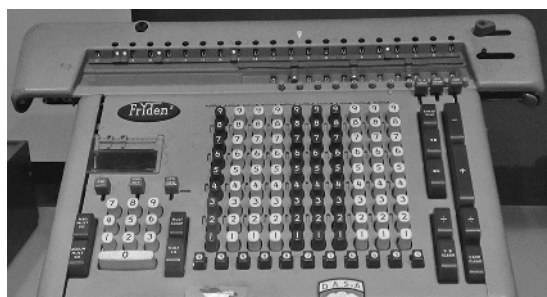
addition, a logarithmic spiral curve on a portion of the device allowed the designer to multiply distances from points on the locus to the poles and zeros, in order to determine the gain at a selected spot on the locus in a manner analogous to a slide rule.

Evans was clearly motivated to aid the engineer in their design and analysis of control systems. Computers were basically not available to designers in the 1940s and 50s. Large mainframe computers started being used, somewhat, for large-scale data processing by corporations in the 1950s, but there were no courses in engineering programs that taught the use of computers for analysis and design until about 1960. Engineering usage became commonplace through the 1960s, but the process involved submitting a job to a mainframe computer via a large deck of punched cards and waiting for the results for hours or overnight, a situation that was not conducive to any kind of design iteration. Mainframe computers in that era were just transitioning from vacuum tubes to transistors, random access memory would be in the neighborhood of 32k(!), and the long-term data storage was by a magnetic tape drive. Random access drums and disks arrived during that decade, thus greatly speeding up the process of retrieving data. A big step forward in computing for engineers occurred when the batch processing based on punched cards was replaced by time share with many users at remote terminals during the late 1960s and early 1970s. Mechanical calculators were also available through the 1940s, 50s, and 60s that could add, subtract, multiply, and divide, and cost about \$1500 in the early 1960s. The very high-end devices (about \$3000) could also do square roots (see Fig. 5.49). These machines were the basis for the complex computations done at Los Alamos and Langley Field during World War II. They were the size of a typewriter, had a large carriage that went back and forth during the calculations, and would occasionally ring a bell at the end of the carriage stroke (see Fig. 5.49). They were accurate to eight or more decimal places and were often used after the advent of computers to perform spot checks of the results, but a square root could take tens of seconds to complete, the machines were noisy, and the process was tedious. Enterprising engineers learned which particular calculations played certain tunes, and it was not unusual to hear favorites such as Jingle Bells.

**Figure 5.49**

The Friden mechanical calculator

*Source: Photo courtesy of David Powell*



The personal computer arrived in the late 1970s, although the ones at that time utilized an audio cassette tape for data storage and had very limited random access memory, usually less than 16k. But as these desktop machines matured over the ensuing decade, the age of the computer for engineering design came into its own. First came the floppy disk for long-term data storage, followed by the hard drive toward the mid- and late-1980s. Initially, the BASIC and APL languages were the primary methods of programming. Matlab was introduced by Cleve Moler in the 1970s. Two events took place in 1984: Apple introduced the point-and-click Macintosh and PC-Matlab was introduced by The MathWorks, which was specifically founded to commercialize Matlab on personal computers. Initially, Matlab was primarily written for control system analysis, but has branched out into many fields since the initial introduction. At that point in the evolution, the engineer could truly perform design iterations with little or no time between trials. Other similar programs were available for mainframe computers before that time; two being CTRL-C and MATRIXx; however, those programs did not adapt to the personal computer revolution, and have faded from general use.

## SUMMARY

- A root locus is a graph of the values of  $s$  that are solutions to the equation

$$1 + KL(s) = 0$$

with respect to a real parameter  $K$ .

1. When  $K > 0$ ,  $s$  is on the locus if  $\angle L(s) = 180^\circ$ , producing a  $180^\circ$  or positive  $K$  locus.
  2. When  $K < 0$ ,  $s$  is on the locus if  $\angle L(s) = 0^\circ$ , producing a  $0^\circ$  or negative  $K$  locus.
- If  $KL(s)$  is the loop transfer function of a system with negative feedback, then the characteristic equation of the closed-loop system is

$$1 + KL(s) = 0,$$

and the root-locus method displays the effect of changing the gain  $K$  on the closed-loop system roots.

- A specific locus for a system  $sysL$  in Matlab notation can be plotted by `rlocus(sysL)` and `sisotool('rlocus',sysL)`.
- A working knowledge of how to determine a root locus is useful for verifying computer results and for suggesting design alternatives.
- The key features for aid in sketching or verifying a computer generated  $180^\circ$  locus are as follows:

1. The locus is on the real axis to the left of an odd number of poles plus zeros.

2. Of the  $n$  branches,  $m$  approach the zeros of  $L(s)$  and  $n - m$  branches approach asymptotes centered at  $\alpha$  and leaving at angles  $\phi_l$ :

$n$  = number of poles,

$m$  = number of zeros,

$n - m$  = number of asymptotes,

$$\alpha = \frac{\sum p_i - \sum z_i}{n - m},$$

$$\phi_l = \frac{180^\circ + 360^\circ(l - 1)}{n - m}, \quad l = 1, 2, \dots, n - m.$$

3. Branches of the locus depart from the poles of order  $q$  and arrive at the zeros of order  $q$  with angles

$$\phi_{l,dep} = \frac{1}{q} \left( \sum \psi_i - \sum_{i \neq dep} \phi_i - 180^\circ - 360^\circ(l - 1) \right),$$

$$\psi_{l,arr} = \frac{1}{q} \left( \sum \phi_i - \sum_{i \neq arr} \psi_i + 180^\circ + 360^\circ(l - 1) \right),$$

where

$q$  = order of the repeated pole or zero,

$\psi_i$  = angles from the zeros,

$\phi_i$  = angles from the poles.

$$l = 1, 2, \dots, q$$

- The parameter  $K$  corresponding to a root at a particular point  $s_0$  on the locus can be found from

$$K = \frac{1}{|L(s_0)|},$$

where  $|L(s_0)|$  can be found graphically by measuring the distances from  $s_0$  to each of the poles and zeros.

- For a locus drawn with `rlocus(sysL)`, the parameter and corresponding roots can be found with `[K,p] = rlocfind(sysL)` or with `sisotool`.
- Lead compensation, given by

$$D_c(s) = \frac{s + z}{s + p}, \quad z < p,$$

approximates proportional-derivative (PD) control. For a fixed error coefficient, it generally moves the locus to the left and improves the system damping.

- Lag compensation, given by

$$D_c(s) = \frac{s + z}{s + p}, \quad z > p,$$

- approximates proportional-integral (PI) control. It generally improves the steady-state error for fixed speed of response by increasing the low-frequency gain and typically degrades stability.
- △ • The root locus can be used to analyze successive loop closures by studying two (or more) parameters in succession.

## REVIEW QUESTIONS

- 5.1** Give two definitions for the root locus.
- 5.2** Define the negative root locus.
- 5.3** Where are the sections of the (positive) root locus on the real axis?
- 5.4** What are the angles of departure from two coincident poles at  $s = -a$  on the real axis? There are no poles or zeros to the right of  $-a$ .
- 5.5** What are the angles of departure from *three* coincident poles at  $s = -a$  on the real axis? There are no poles or zeros to the right of  $-a$ .
- 5.6** What is the principal effect of a lead compensation on a root locus?
- 5.7** What is the principal effect of a lag compensation on a root locus in the vicinity of the dominant closed-loop roots?
- 5.8** What is the principal effect of a lag compensation on the steady-state error to a reference input?
- 5.9** Why is the angle of departure from a pole near the imaginary axis especially important?
- 5.10** Define a conditionally stable system.
- 5.11** Show, with a root-locus argument, that a system having three poles at the origin MUST be either unstable or, at best, conditionally stable.

## PROBLEMS

### Problems for Section 5.1: Root Locus of a Basic Feedback System

- 5.1** Set up the listed characteristic equations in the form suited to Evans's root-locus method. Give  $L(s)$ ,  $a(s)$ , and  $b(s)$  and the parameter  $K$  in terms of the original parameters in each case. Be sure to select  $K$  so  $a(s)$  and  $b(s)$  are monic in each case, and the degree of  $b(s)$  is not greater than that of  $a(s)$ .
  - (a)  $s + (1/\tau) = 0$  versus parameter  $\tau$
  - (b)  $s^2 + cs + c + 1 = 0$  versus parameter  $c$
  - (c)  $(s + c)^3 + A(Ts + 1) = 0$ 
    - (i) versus parameter  $A$ ,
    - (ii) versus parameter  $T$ ,
    - (iii) versus the parameter  $c$ , if possible. Say why you can or cannot. Can a plot of the roots be drawn versus  $c$  for given constant values of  $A$  and  $T$  by any means at all?

(d)  $1 + \left[ k_p + \frac{k_I}{s} + \frac{k_D s}{\tau s + 1} \right] G(s) = 0$ . Assume  $G(s) = A \frac{c(s)}{d(s)}$ , where  $c(s)$  and  $d(s)$  are monic polynomials with the degree of  $d(s)$  greater than that of  $c(s)$ .

- (i) versus  $k_p$
- (ii) versus  $k_I$
- (iii) versus  $k_D$
- (iv) versus  $\tau$

### Problems for Section 5.2: Guidelines for Sketching a Root Locus

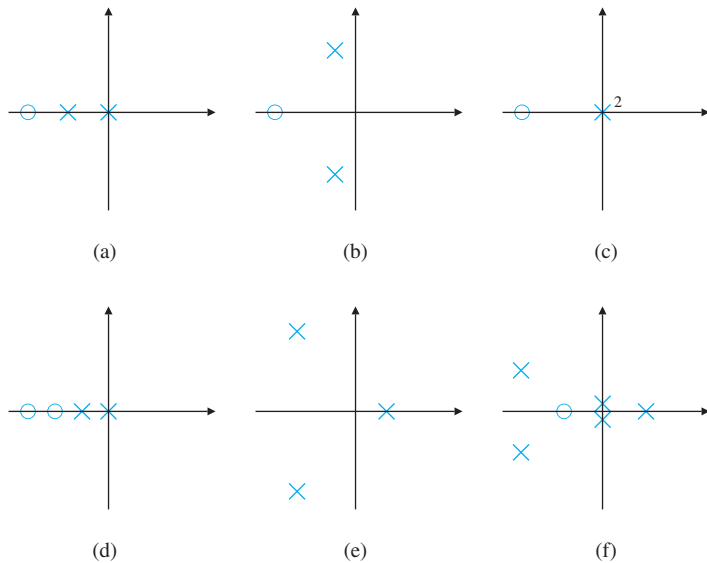
- 5.2 Roughly sketch the root loci for the pole-zero maps as shown in Fig. 5.50 without the aid of a computer. Show your estimates of the center and angles of the asymptotes, a rough evaluation of arrival and departure angles for complex poles and zeros, and the loci for positive values of the parameter  $K$ . Each pole-zero map is from a characteristic equation of the form

$$1 + K \frac{b(s)}{a(s)} = 0,$$

where the roots of the numerator  $b(s)$  are shown as small circles  $\circ$  and the roots of the denominator  $a(s)$  are shown as  $\times$ 's on the  $s$ -plane. Note in Fig. 5.50(c), there are two poles at the origin.

**Figure 5.50**

Pole-zero maps



- 5.3 For the characteristic equation

$$1 + \frac{K}{s^2(s+1)(s+5)} = 0,$$

- (a) Draw the real-axis segments of the corresponding root locus.  
 (b) Sketch the asymptotes of the locus for  $K \rightarrow \infty$ .

- (c) Sketch the locus  
 (d) Verify your sketch with a Matlab plot.
- 5.4** *Real poles and zeros.* Sketch the root locus with respect to  $K$  for the equation  $1 + KL(s) = 0$  and the listed choices for  $L(s)$ . Be sure to give the asymptotes, and the arrival and departure angles at any complex zero or pole. After completing each hand sketch, verify your results using Matlab. Turn in your hand sketches and the Matlab results on the same scales.
- (a)  $L(s) = \frac{2}{s(s+1)(s+5)(s+10)}$   
 (b)  $L(s) = \frac{(s+2)}{s(s+1)(s+5)(s+10)}$   
 (c)  $L(s) = \frac{(s+2)(s+20)}{s(s+1)(s+5)(s+10)}$   
 (d)  $L(s) = \frac{(s+2)(s+6)}{s(s+1)(s+5)(s+10)}$
- 5.5** *Complex poles and zeros.* Sketch the root locus with respect to  $K$  for the equation  $1 + KL(s) = 0$  and the listed choices for  $L(s)$ . Be sure to give the asymptotes and the arrival and departure angles at any complex zero or pole. After completing each hand sketch, verify your results using Matlab. Turn in your hand sketches and the Matlab results on the same scales.
- (a)  $L(s) = \frac{1}{s^2+3s+10}$   
 (b)  $L(s) = \frac{1}{s(s^2+3s+10)}$   
 (c)  $L(s) = \frac{(s^2+2s+8)}{s(s^2+2s+10)}$   
 (d)  $L(s) = \frac{(s^2+2s+12)}{s(s^2+2s+10)}$   
 (e)  $L(s) = \frac{s^2+1}{s(s^2+4)}$   
 (f)  $L(s) = \frac{s^2+4}{s(s^2+1)}$
- 5.6** *Multiple poles at the origin.* Sketch the root locus with respect to  $K$  for the equation  $1 + KL(s) = 0$  and the listed choices for  $L(s)$ . Be sure to give the asymptotes and the arrival and departure angles at any complex zero or pole. After completing each hand sketch, verify your results using Matlab. Turn in your hand sketches and the Matlab results on the same scales.
- (a)  $L(s) = \frac{1}{s^2(s+10)}$   
 (b)  $L(s) = \frac{1}{s^3(s+10)}$   
 (c)  $L(s) = \frac{1}{s^4(s+10)}$   
 (d)  $L(s) = \frac{(s+3)}{s^2(s+10)}$   
 (e)  $L(s) = \frac{(s+3)}{s^3(s+4)}$

(f)  $L(s) = \frac{(s+1)^2}{s^3(s+4)}$

(g)  $L(s) = \frac{(s+1)^2}{s^3(s+10)}$

- 5.7** *Mixed real and complex poles.* Sketch the root locus with respect to  $K$  for the equation  $1 + KL(s) = 0$  and the listed choices for  $L(s)$ . Be sure to give the asymptotes and the arrival and departure angles at any complex zero or pole. After completing each hand sketch, verify your results using Matlab. Turn in your hand sketches and the Matlab results on the same scales.

(a)  $L(s) = \frac{(s+3)}{s(s+10)(s^2+2s+2)}$

(b)  $L(s) = \frac{(s+3)}{s^2(s+10)(s^2+6s+25)}$

(c)  $L(s) = \frac{(s+3)^2}{s^2(s+10)(s^2+6s+25)}$

(d)  $L(s) = \frac{(s+3)(s^2+4s+68)}{s^2(s+10)(s^2+4s+85)}$

(e)  $L(s) = \frac{[(s+1)^2+1]}{s^2(s+2)(s+3)}$

- 5.8** *RHP and zeros.* Sketch the root locus with respect to  $K$  for the equation  $1 + KL(s) = 0$  and the listed choices for  $L(s)$ . Be sure to give the asymptotes and the arrival and departure angles at any complex zero or pole. After completing each hand sketch, verify your results using Matlab. Turn in your hand sketches and the Matlab results on the same scales.

(a)  $L(s) = \frac{s+2}{s+10} \frac{1}{s^2-1}$ ; the model for a case of magnetic levitation with lead compensation.

(b)  $L(s) = \frac{s+2}{s(s+10)} \frac{1}{(s^2-1)}$ ; the magnetic levitation system with integral control and lead compensation.

(c)  $L(s) = \frac{s-1}{s^2}$

(d)  $L(s) = \frac{s^2+2s+1}{s(s+20)^2(s^2-2s+2)}$ . What is the largest value that can be obtained for the damping ratio of the stable complex roots on this locus?

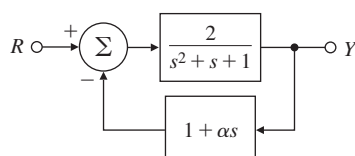
(e)  $L(s) = \frac{(s+2)}{s(s-1)(s+6)^2}$

(f)  $L(s) = \frac{1}{(s-1)[(s+2)^2+3]}$

- 5.9** Put the characteristic equation of the system shown in Fig. 5.51 in root-locus form with respect to the parameter  $\alpha$ , and identify the corresponding  $L(s)$ ,  $a(s)$ , and  $b(s)$ . When  $\alpha = 0.5$ , 1.0, and 1.5, find the

**Figure 5.51**

Control system for Problem 5.9



closed-loop pole locations, verify your results from the root locus with respect to the parameter  $\alpha$  and sketch the corresponding step responses. Use Matlab to check the accuracy of your approximate step responses.

- 5.10** Use the Matlab function `sisotool` to study the behavior of the root locus of  $1 + KL(s)$  for

$$L(s) = \frac{(s+a)}{s(s+1)(s^2 + 8s + 52)}$$

as the parameter  $a$  is varied from 0 to 10, paying particular attention to the region between 2.5 and 3.5. Verify that a multiple root occurs at a complex value of  $s$  for some value of  $a$  in this range.

- 5.11** Use Routh's criterion to find the range of the gain  $K$  for which the systems in Fig. 5.52 are stable, and use the root locus to confirm your calculations.

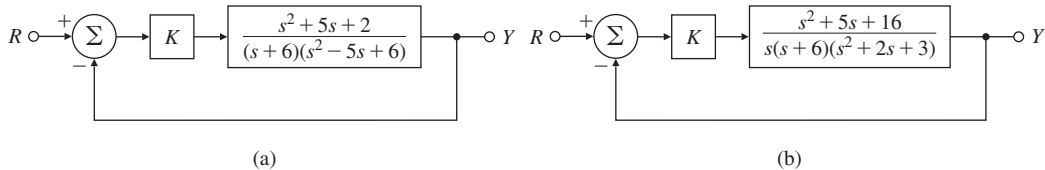


**Figure 5.52**

## Feedback systems for Problem 5.11

- 5.12** Sketch the root locus for the characteristic equation of the system for which

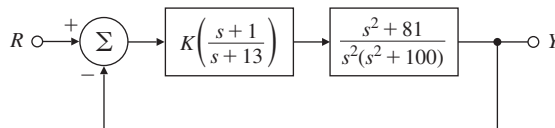
$$L(s) = \frac{(s+2)}{s^2(s+10)},$$

and determine the value of the root-locus gain for which the complex conjugate poles have the maximum damping ratio. What is the approximate value of the damping?

- 5.13** For the system in Fig. 5.53,

  - (a) Find the locus of closed-loop roots with respect to  $K$ .
  - (b) Is there a value of  $K$  that will cause all roots to have a damping ratio greater than 0.5?
  - (c) Find the values of  $K$  that yield closed-loop poles with the damping ratio  $\zeta = 0.707$ .
  - (d) Use Matlab to plot the response of the resulting design to a reference step.

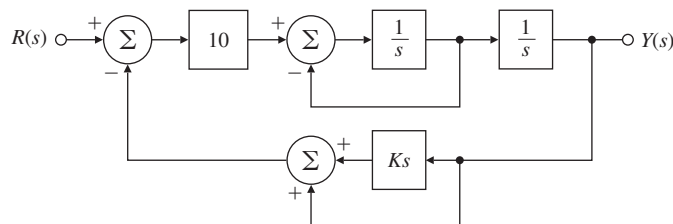
**Figure 5.53**  
Feedback system for  
Problem 5.13



- 5.14** For the feedback system shown in Fig. 5.54, find the value of the gain  $K$  that results in dominant closed-loop poles with a damping ratio  $\zeta = 0.5$ .

**Figure 5.54**

Feedback system for Problem 5.14



### Problems for Section 5.3: Selected Illustrative Root Loci

- 5.15** A simplified model of the longitudinal motion of a certain helicopter near hover has the transfer function

$$G(s) = \frac{8.5(s^2 - 0.7s + 4)}{(s + 0.5)(s^2 - 0.2s + 2)},$$

and the characteristic equation  $1 + D_c(s)G(s) = 0$ . Let  $D_c(s) = k_p$  at first.

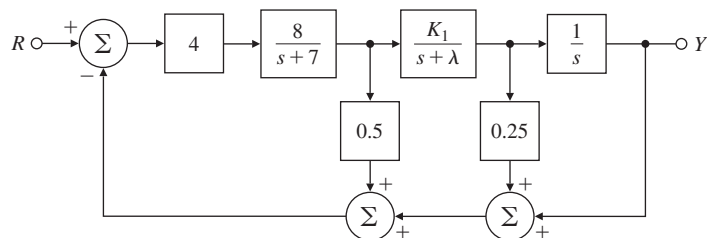
- (a) Compute the departure and arrival angles at the complex poles and zeros.
- (b) Sketch the root locus for this system for parameter  $K = 8.5k_p$ . Use axes  $-1.4 \leq x \leq 0.6; -3 \leq y \leq 3$ .
- (c) Verify your answer using Matlab. Use the command `axis([-1.4 0.6 -3 3])` to get the right scales.
- (d) Suggest a practical (at least as many poles as zeros) alternative compensation  $D_c(s)$  which will at least result in a stable system.

- 5.16** For the system given in Fig. 5.55,

- (a) Plot the root locus of the characteristic equation as the parameter  $K_1$  is varied from 0 to  $\infty$  with  $\lambda = 2$ . Find the corresponding  $L(s)$ ,  $a(s)$ , and  $b(s)$ .
- (b) Repeat part (a) with  $\lambda = 4$ . Is there anything special about this value?
- (c) Repeat part (a) for fixed  $K_1 = 2$ , with the parameter  $K = \lambda$  varying from 0 to  $\infty$ .

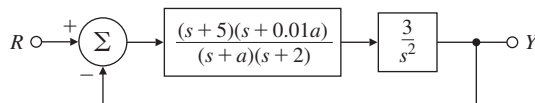
**Figure 5.55**

Control system for Problem 5.16



- 5.17** For the system shown in Fig. 5.56, determine the characteristic equation and sketch the root locus of it with respect to positive values of parameter  $a$ . Give  $L(s)$ ,  $a(s)$ , and  $b(s)$ , and be sure to show with arrows the direction in which  $a$  increases on the locus.

**Figure 5.56**  
Control system for  
Problem 5.17



**5.18** The loop transmission of a system has two poles at  $s = -1$  and a zero at  $s = -2$ . There is a third real-axis pole  $p$  located somewhere to the left of the zero. Several different root loci are possible, depending on the exact location of the third pole. The extreme cases occur when the pole is located at infinity or when it is located at  $s = -2$ . Give values for  $p$  and sketch the three distinct types of loci.

**5.19** For the feedback configuration of Fig. 5.57, use asymptotes, center of asymptotes, angles of departure and arrival, and the Routh array to sketch root loci for the characteristic equations of the listed feedback control systems versus the parameter  $K$ . Use Matlab to verify your results.

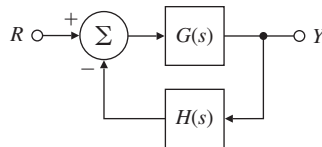
(a)  $G(s) = \frac{K}{s(s+2+8j)(s+2-8j)}$ ,  $H(s) = \frac{s+1}{s+6}$

(b)  $G(s) = \frac{K}{s^2}$ ,  $H(s) = \frac{s+2}{s+5}$

(c)  $G(s) = \frac{K(s+4)}{(s+3)}$ ,  $H(s) = \frac{s+9}{s+2}$

(d)  $G(s) = \frac{K(s+2+1j)(s+2-1j)}{s(s+5-7j)(s+5+7j)}$ ,  $H(s) = \frac{1}{s+3}$

**Figure 5.57**  
Feedback system for  
Problem 5.19

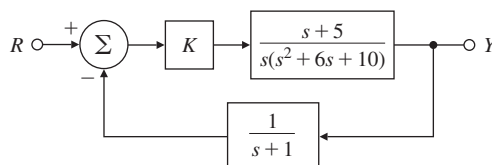


**5.20** Consider the system in Fig. 5.58.

(a) Using Routh's stability criterion, determine all values of  $K$  for which the system is stable.

(b) Use Matlab to draw the root locus versus  $K$  and find the values of  $K$  at the imaginary-axis crossings.

**Figure 5.58**  
Feedback system for  
Problem 5.20



### Problems for Section 5.4: Design Using Dynamic Compensation

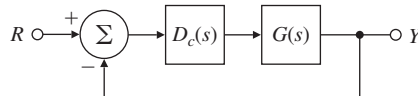
**5.21** Let

$$G(s) = \frac{1}{s^2 + 7s + 12} \quad \text{and} \quad D_c(s) = K \frac{(s+a)}{s+b}.$$

Using root-locus techniques, find the values for the parameters  $a, b$ , and  $K$  of the compensation  $D_c(s)$  that will produce closed-loop poles at  $s = -1.5 \pm 1.5j$  for the system shown in Fig. 5.59.

**Figure 5.59**

Unity feedback system  
for Problems 5.21–5.27,  
and 5.32



**5.22** Suppose in Fig. 5.59

$$G(s) = \frac{1}{s(s^2 + 3s + 7)} \quad \text{and} \quad D(s) = \frac{K}{s + 3}.$$

Without using Matlab, sketch the root locus with respect to  $K$  of the characteristic equation for the closed-loop system, paying particular attention to points that generate multiple roots. Find the value of  $K$  at that point, state what the location of the multiple roots, and how many multiple roots there are.

**5.23** Suppose the unity feedback system of Fig. 5.59 has an open-loop plant given by  $G(s) = \frac{1}{s(s+1)}$ . Design a lead compensation  $D_c(s) = K \frac{s+z}{s+p}$  to be added in cascade with the plant so that the dominant poles of the closed-loop system are located at  $s = -3.2 \pm 3.2j$ .

**5.24** Assume that the unity feedback system of Fig. 5.59 has the open-loop plant

$$G(s) = \frac{s+7}{s(s+9)(s+5)}.$$

Design a lag compensation  $D_c(s) = K \frac{(s-z)}{s-p}$  to meet the following specifications:

- The step response rise time is to be less than 0.45 sec.
- The step response overshoot is to be less than 5%.
- The steady-state error to a unit ramp input must not exceed 10%.

**5.25** A numerically controlled machine tool positioning servomechanism has a normalised and scaled transfer function given by

$$G(s) = \frac{1}{(s + 0.8)(s + 0.5)}.$$

Performance specifications of the system in the unit feedback configuration of Fig. 5.59 are satisfied if the closed-loop poles are located at  $s = -1 \pm j2$ .

- (a) Show that this specification cannot be achieved by choosing proportional control alone,  $D_c(s) = k_p$ .
- (b) Design a lead compensator  $D_c(s) = K \frac{s-z}{s-p}$  that will meet the specification.

**5.26** A servomechanism position control has the plant transfer function

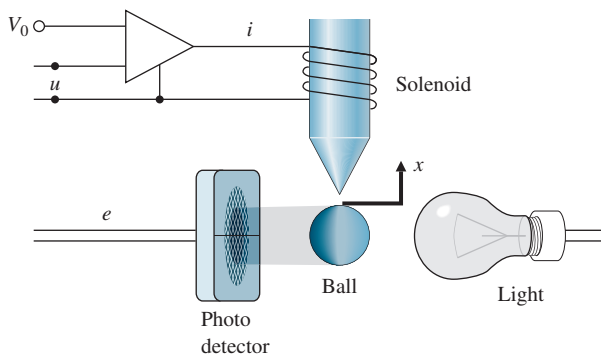
$$G(s) = \frac{10}{s(s+1)(s+10)}.$$

You are to design a series compensation transfer function  $D_c(s)$  in the unity feedback configuration to meet the following closed-loop specifications:

- The response to a reference step input is to have no more than 16% overshoot.

- The response to a reference step input is to have a rise time of no more than 0.4 sec.
  - The steady-state error to a unit ramp at the reference input must be less than 0.05.
- (a) Design a lead compensation that will cause the system to meet the dynamic response specifications, ignoring the error requirement.
- (b) What is the velocity constant  $K_v$  for your design? Does it meet the error specification?
- (c) Design a lag compensation to be used in series with the lead you have designed to cause the system to meet the steady-state error specification.
- (d) Give the Matlab plot of the root locus of your final design.
- (e) Give the Matlab response of your final design to a reference step.
- 5.27** Assume the closed-loop system of Fig. 5.59 has a feed forward transfer function  $G(s)$  given by
- $$G(s) = \frac{1}{(s+1)(s+2)}.$$
- Design a lag compensation so that the dominant poles of the closed-loop system are located at  $s = -1.5 \pm j1.5$  and the steady-state error to a unit step input is less than 0.1.
- 5.28** An elementary magnetic suspension scheme is depicted in Fig. 5.60. For small motions near the reference position, the voltage  $e$  on the photo detector is related to the ball displacement  $x$  (in meters) by  $e = 100x$ . The upward force (in newtons) on the ball caused by the current  $i$  (in amperes) may be approximated by  $f = 0.5i + 20x$ . The mass of the ball is 20 g and the gravitational force is 9.8 N/kg. The power amplifier is a voltage-to-current device with an output (in amperes) of  $i = u + V_0$ .

**Figure 5.60**  
Elementary magnetic suspension



- (a) Write the equations of motion for this set up.
- (b) Give the value of the bias  $V_0$  that results in the ball being in equilibrium at  $x = 0$ .
- (c) What is the transfer function from  $u$  to  $e$ ?
- (d) Suppose that the control input  $u$  is given by  $u = -Ke$ . Sketch the root locus of the closed-loop system as a function of  $K$ .
- (e) Assume a lead compensation is available in the form  $\frac{U}{E} = D_c(s) = K \frac{s+z}{s+p}$ . Give values of  $K$ ,  $z$ , and  $p$  that yield improved performance over the one proposed in part (d).

- 5.29** A certain plant with the non-minimum phase transfer function

$$G(s) = \frac{7 - 3s}{s^2 + s + 5},$$

is in a unity positive feedback system with the controller transfer function  $D_c(s)$ .

- (a) Use Matlab to determine a (negative) value for  $D_c(s) = K$  so that the closed-loop system with negative feedback has a damping ratio  $\zeta = 0.707$ .

- (b) Use Matlab to plot the system's response to a reference step.

- 5.30** Consider the rocket-positioning system shown in Fig. 5.61.

- (a) Show that if the sensor that measures  $x$  has a unity transfer function, the lead compensator

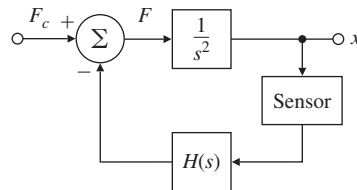
$$H(s) = K \frac{s + 3}{s + 6},$$

stabilizes the system.

- (b) Assume that the sensor transfer function is modelled by a single pole with a 0.1 sec time constant and unit DC gain, and  $H(s)$  is a PD controller having transfer function  $K(s + 1)$ . Using the root-locus procedure, find a value for the gain  $K$  that will provide the maximum damping ratio while its step response has the lowest settling time.

**Figure 5.61**

Block diagram for rocket-positioning control system

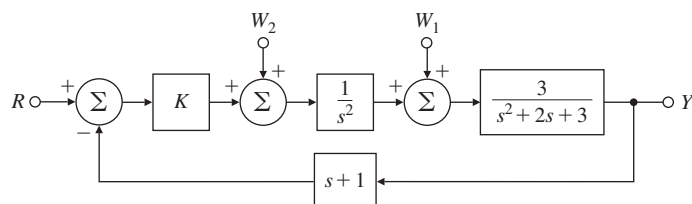


- 5.31** For the system in Fig. 5.62,

- (a) Find the locus of closed-loop roots with respect to  $K$ .  
 (b) Find the maximum value of  $K$  for which the system is stable. Assume  $K = 0.5$  for the remaining parts of this problem.  
 (c) What is the steady-state error ( $e = r - y$ ) for a step change in  $r$ ?  
 (d) What is the steady-state error in  $y$  for a constant disturbance  $w_1$ ?  
 (e) What is the steady-state error in  $y$  for a constant disturbance  $w_2$ ?

**Figure 5.62**

Control system for Problem 5.31



- (f) If you wished to have more damping, what changes would you make to the system?

**5.32** Consider the plant transfer function

$$G(s) = \frac{bs + k}{s^2[mMs^2 + (M+m)bs + (M+m)k]}$$

to be put in the unity feedback loop of Fig. 5.59. This is the transfer function relating the input force  $u(t)$  of mass  $M$  in the non-collocated sensor and actuator problem. In this problem, we will use root-locus techniques to design a controller  $D_c(s)$  so that the closed-loop step response has a rise time of less than 0.5 sec and an overshoot of less than 15%. You may use Matlab for any of the following questions:

- (a) Approximate  $G(s)$  by assuming that  $m \approx 0$ , and let  $M = 1$ ,  $k = 1$ ,  $b = 0.5$ , and  $D_c(s) = K$ . Can  $K$  be chosen to satisfy the performance specifications? Why or why not?
- (b) Repeat part (a) assuming  $D_c(s) = K(s + z)$ , and show that  $K$  and  $z$  can be chosen to meet the specifications.
- (c) Repeat part (b) but with a practical controller given by the transfer function

$$D_c(s) = K \frac{p(s + z)}{s + p}.$$

and using the value for  $z$  in part(b), pick  $p$  and  $K$  so that the step response similar to part (b) is obtained.

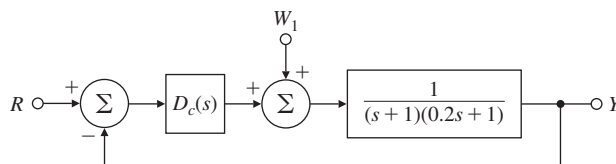
- (d) Now suppose that the small mass  $m$  is not negligible, but is given by  $m = M/10$ . Check to see if the controller you design in part (c) still meets the given specifications. If not, adjust the controller parameters or suggest a new controller so that the specifications are met.

**5.33** Consider the Type 1 system drawn in Fig. 5.63. We would like to design the compensation  $D_c(s)$  to meet the following requirements: (1) The steady-state value of  $y$  due to a constant unit disturbance  $w$  should be less than 0.1, and (2) the damping ratio  $\zeta > 0.7$ . Using root-locus techniques,

- (a) Show that proportional control alone is not adequate.
- (b) Show that proportional-derivative control will work.
- (c) Find values of the gains  $k_p$  and  $k_D$  for  $D_c(s) = k_p + k_D s$  that meet the design specifications with at least 10% margin.

**Figure 5.63**

Control system for Problem 5.33



- △ **5.34** Using a sample rate of 10 Hz, find the  $D_c(z)$  that is the discrete equivalent to your  $D_c(s)$  from Problem 5.7 using the trapezoid rule. Evaluate the time response using Simulink, and determine whether the damping ratio requirement is met with the digital implementation. (Note: The material to do this problem is covered in the online Appendix W4.5 at [www.pearsonglobaleditions.com](http://www.pearsonglobaleditions.com) or in Chapter 8.)

*Problems for Section 5.5: A Design Example Using the Root Locus*

- 5.35** Consider the positioning servomechanism system shown in Fig. 5.64, where

$$e_i = K_o \theta_i, \quad e_o = K_{pot} \theta_o, \quad K_o = 10 \text{ V/rad},$$

$$T = \text{motor torque} = K_t i_a,$$

$$k_m = K_t = \text{torque constant} = 0.1 \text{ N}\cdot\text{m/A},$$

$$K_e = \text{back emf constant} = 0.1 \text{ V}\cdot\text{sec},$$

$$R_a = \text{armature resistance} = 10 \Omega,$$

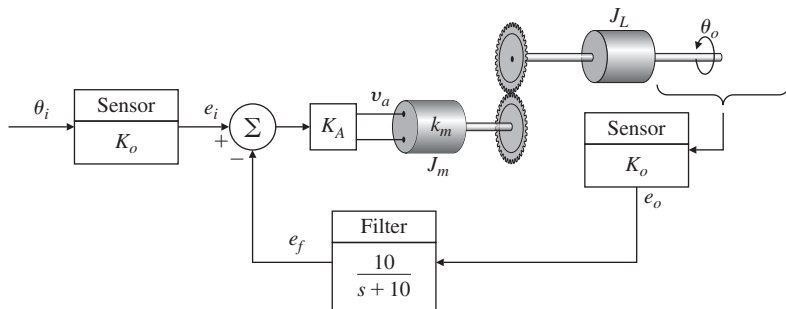
Gear ratio = 1:1,

$$J_L + J_m = \text{total inertia} = 10^{-3} \text{ kg}\cdot\text{m}^2,$$

$$v_a = K_A (e_i - e_f).$$

**Figure 5.64**

Positioning  
servomechanism



- (a) What is the range of the amplifier gain  $K_A$  for which the system is stable? Estimate the upper limit graphically using a root-locus plot.  
 (b) Choose a gain  $K_A$  that gives roots at  $\zeta = 0.7$ . Where are all three closed-loop root locations for this value of  $K_A$ ?

- 5.36** We wish to design a velocity control for a tape-drive servomechanism. The transfer function from current  $I(s)$  to tape velocity  $\Omega(s)$  (in millimeters per millisecond per ampere) is

$$\frac{\Omega(s)}{I(s)} = \frac{23(s^2 + 0.5s + 0.7)}{(s + 1)(s^2 + 0.7s + 1)}.$$

We wish to design a Type 1 feedback system so that the response to a reference step satisfies

$$t_r \leq 6 \text{ msec}, \quad t_s \leq 15 \text{ msec}, \quad M_p \leq 0.15.$$

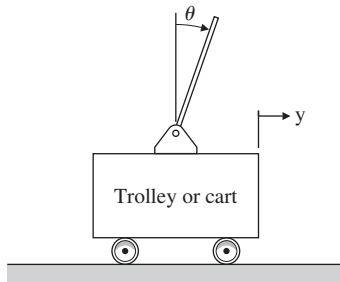
- (a) Use the integral compensator  $k_I/s$  to achieve Type 1 behavior, and sketch the root-locus with respect to  $k_I$ . Show on the same plot the region of acceptable pole locations corresponding to the specifications and is the integral compensator able to help satisfy all the specifications?

- (b) Assume a proportional-integral compensator of the form  $k_p(s+\alpha)/s$ , and select the best possible values of  $k_p$  and  $\alpha$  you can find. Sketch the root-locus plot of your design, giving values for  $k_p$  and  $\alpha$ , and the velocity constant  $K_v$  your design achieves. On your plot, indicate the closed-loop poles with a dot ( $\bullet$ ) and include the boundary of the region of acceptable root locations.
- 5.37** The normalized, scaled equations of a cart as drawn in Fig. 5.65 of mass  $m_c$  holding an inverted uniform pendulum of mass  $m_p$  and length  $\ell$  with no friction are

$$\begin{aligned}\ddot{\theta} - \theta &= -v, \\ \ddot{y} + \beta\theta &= v,\end{aligned}\quad (5.88)$$

**Figure 5.65**

Figure of cart pendulum for Problem 5.37



where  $\beta = \frac{3m_p}{4(m_c+m_p)}$  is a mass ratio bounded by  $0 < \beta < 0.75$ . Time is measured in terms of  $\tau = \omega_0 t$  where  $\omega_0^2 = \frac{3g(m_c+m_p)}{\ell(4m_c+m_p)}$ . The cart motion  $y$  is measured in units of pendulum length as  $y = \frac{3x}{4\ell}$  and the input is force normalized by the system weight  $v = \frac{u}{g(m_c+m_p)}$ . These equations can be used to compute the transfer functions

$$\frac{\Theta}{V} = -\frac{1}{s^2 - 1}, \quad (5.89)$$

$$\frac{Y}{V} = \frac{s^2 - 1 + \beta}{s^2(s^2 - 1)}. \quad (5.90)$$

In this problem, you are to design a control for the system by first closing a loop around the pendulum, Eq. (5.89), then, with this loop closed, closing a second loop around the cart plus pendulum, Eq. (5.90). For this problem, let the mass ratio be  $m_c = 5m_p$ .

- (a) Draw a block diagram for the system with  $V$  input and both  $Y$  and  $\theta$  as outputs.
- (b) Design a lead compensation  $D_c(s) = K \frac{s+z}{s+p}$  for the  $\Theta$  loop to cancel the pole at  $s = -1$  and place the two remaining poles at  $-4 \pm j4$ . The new control is  $U(s)$ , where the force is  $V(s) = U(s) + D_c(s)\Theta(s)$ . Draw the root locus of the angle loop.
- (c) Compute the transfer function of the new plant from  $U$  to  $Y$  with  $D_c(s)$  in place.

- (d) Design a controller  $D_c(s)$  for the cart position with the pendulum loop closed. Draw the root locus with respect to the gain of  $D_c(s)$ .
- (e) Use Matlab to plot the control, cart position, and pendulum position for a unit step change in cart position.
- 5.38** Consider the 270-ft U.S. Coast Guard cutter *Tampa* (902) shown in Fig 5.66(a). Parameter identification based on sea-trials data (Trankle, 1987) was used to estimate the hydrodynamic coefficients in the equations of motion. The result is that the response of the heading angle of the ship  $\psi$  to rudder angle  $\delta$  and wind changes  $w$  can be described by the block diagram in Fig 5.66(b) and the second-order transfer functions

$$G_\delta(s) = \frac{\psi(s)}{\delta(s)} = \frac{-0.0184(s + 0.0068)}{s(s + 0.2647)(s + 0.0063)},$$

$$G_w(s) = \frac{\psi(s)}{w(s)} = \frac{0.0000064}{s(s + 0.2647)(s + 0.0063)},$$

where

- $\psi$  = heading angle, rad,  
 $\psi_r$  = reference heading angle, rad,  
 $r$  = yaw rate,  $\dot{\psi}$ , rad/sec,  
 $\delta$  = rudder angle, rad,  
 $w$  = wind speed, m/sec.

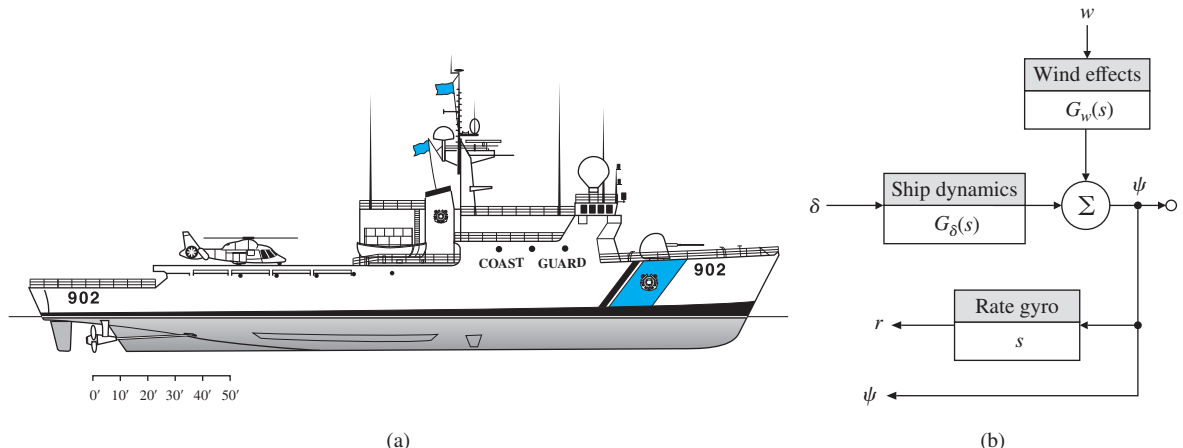


**Figure 5.66**

(a) USCG *Tampa* for Problem 5.38, (b) partial block diagram for the system

- (a) Determine the open-loop settling time of  $r$  for a step change in  $\delta$ .
- (b) In order to regulate the heading angle  $\psi$ , design a compensator that uses  $\psi$  and the measurement provided by a yaw-rate gyroscope (that is, by  $\dot{\psi} = r$ ). The settling time of  $\psi$  to a step change in  $\psi_r$  is specified

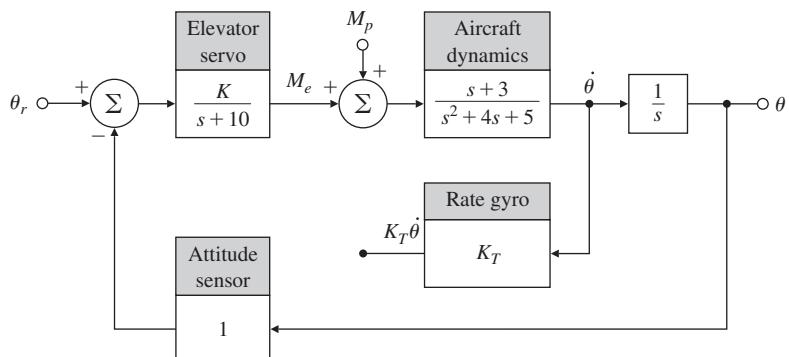
to be less than 50 sec, and for a  $5^\circ$  change in heading, the maximum allowable rudder angle deflection is specified to be less than  $10^\circ$ .

- (c) Check the response of the closed-loop system you designed in part (b) to a wind gust disturbance of 10 m/sec. (Model the disturbance as a step input.) If the *steady-state* value of the heading due to this wind gust is more than  $0.5^\circ$ , modify your design so it meets this specification as well.
- 5.39** Golden Nugget Airlines has opened a free bar in the tail of their airplanes in an attempt to lure customers. In order to automatically adjust for the sudden weight shift due to passengers rushing to the bar when it first opens, the airline is mechanizing a pitch-attitude autopilot. Figure 5.67 shows the block diagram of the proposed arrangement. We will model the passenger moment as a step disturbance  $M_p(s) = M_0/s$ , with a maximum expected value for  $M_0$  of 0.6.
- (a) Assuming the bar has opened, and the passengers have rushed to it, what value of  $K$  is required to keep the steady-state error in  $\theta$  to less than  $0.02 \text{ rad} (\cong 1^\circ)$ ? (Assume the system is stable.)
- (b) Draw a root locus with respect to  $K$ .
- (c) Based on your root locus, what is the value of  $K$  when the system becomes unstable?
- (d) Suppose the value of  $K$  required for acceptable steady-state behavior is 600. Show that this value yields an unstable system with roots at

$$s = -2.9, -13.5, +1.2 \pm 6.6j.$$

- (e) You are given a black box with *rate gyro* written on the side, and told that, when installed, it provides a perfect measure of  $\dot{\theta}$ , with output  $K_T \dot{\theta}$ . Assume  $K = 600$  as in part (d) and draw a block diagram indicating how you would incorporate the rate gyro into the autopilot. (Include transfer functions in boxes.)
- (f) For the rate gyro in part (e), sketch a root locus with respect to  $K_T$ .
- (g) What is the maximum damping factor of the complex roots obtainable with the configuration in part (e)?
- (h) What is the value of  $K_T$  for part (g)?

**Figure 5.67**  
Golden Nugget Airlines autopilot



- (i) Suppose you are not satisfied with the steady-state errors and damping ratio of the system with a rate gyro in parts (e) through (h). Discuss the advantages and disadvantages of adding an integral term and extra lead networks in the control law. Support your comments using Matlab or with rough root-locus sketches.

- 5.40** Consider the instrument servomechanism with the parameters given in Fig. 5.68. For each of the following cases, draw a root locus with respect to the parameter  $K$ , and indicate the location of the roots corresponding to your final design:

- (a) *Lead network:* Let

$$H(s) = 1, \quad D_c(s) = K \frac{s+z}{s+p}, \quad \frac{p}{z} = 6.$$

Select  $z$  and  $K$  so the roots nearest the origin (the dominant roots) yield

$$\zeta \geq 0.4, \quad -\sigma \leq -7, \quad K_v \geq 16 \frac{2}{3} \text{ sec}^{-1}.$$

- (b) *Output-velocity (tachometer) feedback:* Let

$$H(s) = 1 + K_T s \quad \text{and} \quad D_c(s) = K.$$

Select  $K_T$  and  $K$  so the dominant roots are in the same location as those of part (a). Compute  $K_v$ . If you can, give a physical reason explaining the reduction in  $K_v$  when output derivative feedback is used.

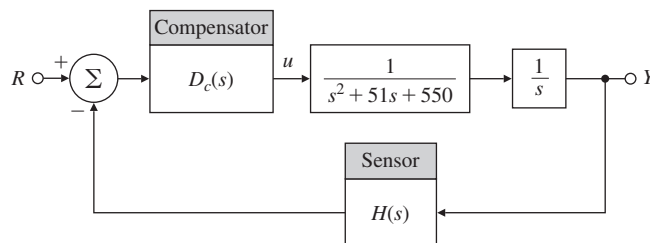
- (c) *Lag network:* Let

$$H(s) = 1 \quad \text{and} \quad D_c(s) = K \frac{s+1}{s+p}.$$

Using proportional control, is it possible to obtain a  $K_v = 12$  at  $\zeta = 0.4$ ? Select  $K$  and  $p$  so the dominant roots correspond to the proportional-control case but with  $K_v = 100$  rather than  $K_v = 12$ .

**Figure 5.68**

Control system for Problem 5.40



- 5.41** For the quadrotor shown in Figs. 2.13 and 2.14 (see Example 2.5),

- (a) Describe what the commands should be to rotors 1, 2, 3, & 4 in order to produce a yaw torque,  $T_\psi$ , that has no effect on pitch or roll, and

will not produce any net vertical thrust of the 4 rotors. In other words, find the relation between  $\delta T_1, \delta T_2, \delta T_3, \delta T_4$  so that  $T_\psi$  produces the desired response.

- (b) The system dynamics for the yaw motion of a quadrotor are given in Eq. (2.17). Assuming the value of  $I_z = 200$ , find a compensation that gives a rise time less 0.2 seconds with an overshoot less than 20%.

### Problems for Section 5.6: Extensions of the Root Locus Method

- 5.42** Plot the loci for the  $0^\circ$  locus or negative  $K$  for each of the following:

- (a) The examples given in Problem 5.3
- (b) The examples given in Problem 5.4
- (c) The examples given in Problem 5.5
- (d) The examples given in Problem 5.6
- (e) The examples given in Problem 5.7
- (f) The examples given in Problem 5.8

- 5.43** Suppose you are given the plant

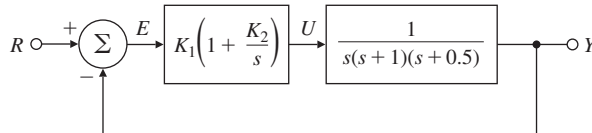
$$L(s) = \frac{1}{s^3 + 5s^2 + (4 + \alpha)s + (1 + 2\alpha)},$$

where  $\alpha$  is a system parameter that is subject to variations. Use both positive and negative root-locus methods to determine what variations in  $\alpha$  can be tolerated before instability occurs.

- △ **5.44** Consider the system in Fig. 5.69.

- (a) Use Routh's criterion to determine the regions in the  $K_1, K_2$  plane for which the system is stable.
- (b) Use sisotool to verify your answer to part (a).

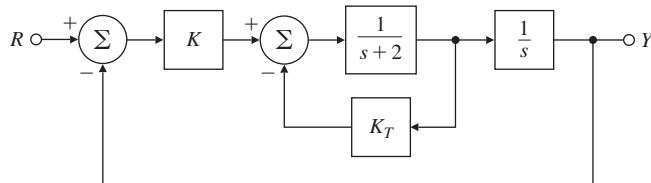
**Figure 5.69**  
Feedback system for  
Problem 5.44



- △ **5.45** The block diagram of a positioning servomechanism is shown in Fig. 5.70.

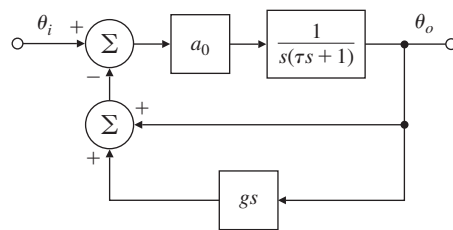
- (a) Sketch the root locus with respect to  $K$  when no tachometer feedback is present  $K_T = 0$ .

**Figure 5.70**  
Control system for  
Problem 5.45



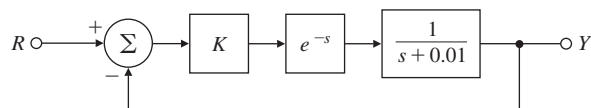
- (b) Indicate the root locations corresponding to  $K = 16$  on the locus of part (a). For these locations, estimate the transient-response parameters  $t_r$ ,  $M_p$ , and  $t_s$ . Compare your estimates to measurements obtained using the step command in Matlab.
- (c) For  $K = 16$ , draw the root locus with respect to  $K_T$ .
- (d) For  $K = 16$  and with  $K_T$  set so  $M_p = 0.05$  ( $\zeta = 0.707$ ), estimate  $t_r$  and  $t_s$ . Compare your estimates to the actual values of  $t_r$  and  $t_s$  obtained using Matlab.
- (e) For the values of  $K$  and  $K_T$  in part (d), what is the velocity constant  $K_v$  of this system?
- $\triangle$  **5.46** Consider the mechanical system shown in Fig. 5.71, where  $g$  and  $a_0$  are gains. The feedback path containing  $gs$  controls the amount of rate feedback. For a fixed value of  $a_0$ , adjusting  $g$  corresponds to varying the location of a zero in the  $s$ -plane.
- (a) With  $g = 0$  and  $\tau = 1$ , find a value for  $a_0$  such that the poles are complex.
- (b) Fix  $a_0$  at this value, and construct a root locus that demonstrates the effect of varying  $g$ .

**Figure 5.71**  
Control system for  
Problem 5.46



- $\triangle$  **5.47** Sketch the root locus with respect to  $K$  for the system in Fig. 5.72 using the Padé(1,1) approximation and the first-order lag approximation. For both approximations, what is the range of values of  $K$  for which the system is unstable? (Note: The material to answer this question is contained in Appendix W5.6.3 at [www.pearsonglobaleditions.com](http://www.pearsonglobaleditions.com).)

**Figure 5.72**  
Control system for  
Problem 5.47



- $\triangle$  **5.48** For the equation  $1 + KG(s)$ , where

$$G(s) = \frac{1}{s(s+p)[(s+1)^2 + 4]},$$

use Matlab to examine the root locus as a function of  $p$  in the range from  $p = 1$  to  $p = 10$ , making sure to include the point  $p = 2$ .

# The Frequency-Response Design Method



## A Perspective on the Frequency-Response Design Method

The design of feedback control systems in industry is probably accomplished using frequency-response methods more often than any other. Frequency-response design is popular primarily because it provides good designs in the face of uncertainty in the plant model. For example, for systems with poorly known or changing high-frequency resonances, we can temper the feedback compensation to alleviate the effects of those uncertainties. Currently, this tempering is carried out more easily using frequency-response design than with any other method.

Another advantage of using frequency response is the ease with which experimental information can be used for design purposes. Raw measurements of the output amplitude and phase of a plant undergoing a sinusoidal input excitation are sufficient to design a suitable feedback control. No intermediate processing of the data (such as finding poles and zeros or determining system matrices) is required to arrive at the system model. The wide availability of computers has

---

IM\_photo/Shutterstock.

rendered this advantage less important now than it was years ago; however, for relatively simple systems, frequency response is often still the most cost-effective design method. Yet another advantage is that specifications for control systems are typically provided in terms of a system's frequency-response characteristics. Therefore, design in the frequency domain directly ensures that the specifications are met rather than having to transform them to other parameters.

The underlying theory for determining stability in all situations is somewhat challenging and requires a rather broad knowledge of complex variables. However, the methodology of frequency-response design does not require that the designer remembers the details of the theory and the stability rules are fairly straightforward.

## Chapter Overview

The chapter opens with a discussion of how to obtain the frequency response of a system by analyzing its poles and zeros. An important extension of this discussion is how to use Bode plots to graphically display the frequency response. In Sections 6.2 and 6.3, we will discuss stability briefly, then in more depth the use of the Nyquist stability criterion. In Sections 6.4 through 6.6, we will introduce the notion of stability margins, discuss Bode's gain-phase relationship, and study the closed-loop frequency response of dynamic systems. The gain-phase relationship suggests a very simple rule for compensation design: Shape the frequency-response magnitude so it crosses magnitude 1 with a slope of  $-1$ . As with our treatment of the root-locus method, we will describe how adding dynamic compensation can adjust the frequency response (see Section 6.7) and improve system stability and/or error characteristics.

In optional Sections 6.7.7 and 6.7.8, we will discuss issues of sensitivity that relate to the frequency response, including material on sensitivity functions and stability robustness. The next two sections on analyzing time delays in the system and Nichols charts will represent additional, somewhat advanced material that may also be considered optional. The final Section 6.10 is a short history of the frequency-response design method.

### 6.1 Frequency Response

The basic concepts of frequency response were discussed in Section 3.1.2. In this section, we will review those ideas and extend the concepts for use in control system design.

A linear system's response to sinusoidal inputs—called the system's **frequency response**—can be obtained from knowledge of its pole and zero locations.

To review the ideas, we consider a system described by

$$\frac{Y(s)}{U(s)} = G(s),$$

where the input  $u(t)$  is a sine wave with an amplitude  $A$ :

$$u(t) = A \sin(\omega_o t) \mathbf{1}(t).$$

This sine wave has a Laplace transform

$$U(s) = \frac{A\omega_o}{s^2 + \omega_o^2}.$$

With zero initial conditions, the Laplace transform of the output is

$$Y(s) = G(s) \frac{A\omega_o}{s^2 + \omega_o^2}. \quad (6.1)$$

### Partial-fraction expansion

A partial-fraction expansion of Eq. (6.1) [assuming that the poles of  $G(s)$  are distinct] will result in an equation of the form

$$Y(s) = \frac{\alpha_1}{s - p_1} + \frac{\alpha_2}{s - p_2} + \cdots + \frac{\alpha_n}{s - p_n} + \frac{\alpha_o}{s + j\omega_o} + \frac{\alpha_o^*}{s - j\omega_o}, \quad (6.2)$$

where  $p_1, p_2, \dots, p_n$  are the poles of  $G(s)$ ,  $\alpha_o$  would be found by performing the partial-fraction expansion, and  $\alpha_o^*$  is the complex conjugate of  $\alpha_o$ . The time response that corresponds to  $Y(s)$  is

$$y(t) = \alpha_1 e^{p_1 t} + \alpha_2 e^{p_2 t} + \cdots + \alpha_n e^{p_n t} + 2|\alpha_o| \cos(\omega_o t + \phi), \quad t \geq 0, \quad (6.3)$$

where

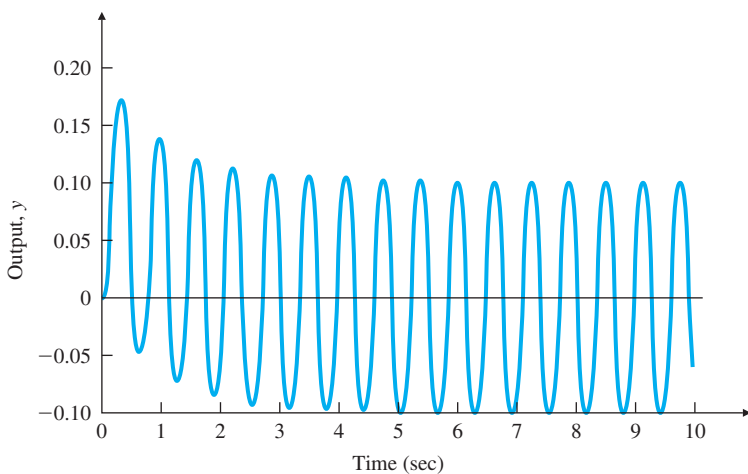
$$\phi = \tan^{-1} \left[ \frac{\text{Im}(\alpha_o)}{\text{Re}(\alpha_o)} \right].$$

If all the poles of the system represent stable behavior (the real parts of  $p_1, p_2, \dots, p_n < 0$ ), the natural unforced response will die out eventually, and therefore the steady-state response of the system will be due solely to the sinusoidal term in Eq. (6.3), which is caused by the sinusoidal excitation. Example 3.7 determined the response of the system  $G(s) = \frac{1}{(s+1)}$  to the input  $u = \sin 10t$  and showed that response in Fig. 3.5, which is repeated here as Fig. 6.1. It shows that  $e^{-t}$ , the natural part of the response associated with  $G(s)$ , disappears after several time constants, and the pure sinusoidal response is essentially all that remains. Example 3.7 showed that the remaining sinusoidal term in Eq. (6.3) can be expressed as

$$y(t) = AM \cos(\omega_o t + \phi), \quad (6.4)$$

**Figure 6.1**

Response of  
 $G(s) = \frac{1}{(s+1)}$  to an input  
of  $\sin 10t$



where

$$\begin{aligned} M &= |G(j\omega_o)| = |G(s)|_{s=j\omega_o} \\ &= \sqrt{\{\text{Re}[G(j\omega_o)]\}^2 + \{\text{Im}[G(j\omega_o)]\}^2}, \end{aligned} \quad (6.5)$$

$$\phi = \tan^{-1} \left[ \frac{\text{Im}[G(j\omega_o)]}{\text{Re}[G(j\omega_o)]} \right] = \angle G(j\omega_o). \quad (6.6)$$

In polar form,

$$G(j\omega_o) = Me^{j\phi}. \quad (6.7)$$

### Frequency-response plot

Equation (6.4) shows that a stable system with transfer function  $G(s)$  excited by a sinusoid with unit amplitude and frequency  $\omega_o$  will, after the response has reached steady-state, exhibit a sinusoidal output with a magnitude  $M(\omega_o)$  and a phase  $\phi(\omega_o)$  at the frequency  $\omega_o$ . The facts that the output  $y$  is a sinusoid with the *same* frequency as the input  $u$ , and that the magnitude ratio  $M$  and phase  $\phi$  of the output are independent of the amplitude  $A$  of the input, are a consequence of  $G(s)$  being a linear constant system. If the system being excited were a nonlinear or time-varying system, the output might contain frequencies other than the input frequency, and the output–input ratio might be dependent on the input magnitude.

### Magnitude and phase

More generally, the **magnitude**  $M$  is given by  $|G(j\omega)|$ , and the **phase**  $\phi$  is given by  $\angle G(j\omega)$ ; that is, the magnitude and angle of the complex quantity  $G(s)$  are evaluated with  $s$  taking on values along the imaginary axis ( $s = j\omega$ ). The frequency response of a system consists of these functions of frequency that tell us how a system will respond to a sinusoidal input of any frequency. We are interested in analyzing the frequency response not only because it will help us understand how a system responds to a sinusoidal input, but also because evaluating  $G(s)$  with  $s$  taking on values along the  $j\omega$  axis will prove to be very useful in determining the stability of a closed-loop system. As we saw in Chapter 3,

the  $j\omega$  axis is the boundary between stability and instability; we will see in Section 6.4 that evaluating  $G(j\omega)$  provides information that allows us to determine closed-loop stability from the open-loop  $G(s)$ .

## EXAMPLE 6.1

### Frequency-Response Characteristics of a Capacitor

Consider the capacitor described by the equation

$$i = C \frac{dv}{dt},$$

where  $v$  is the voltage input and  $i$  is the current output. Determine the sinusoidal steady-state response of the capacitor.

**Solution.** The transfer function of this circuit is

$$\frac{I(s)}{V(s)} = G(s) = Cs,$$

so

$$G(j\omega) = Cj\omega.$$

Computing the magnitude and phase, we find that

$$M = |Cj\omega| = C\omega \quad \text{and} \quad \phi = \angle(Cj\omega) = 90^\circ.$$

For a unit-amplitude sinusoidal input  $v$ , the output  $i$  will be a sinusoid with magnitude  $C\omega$ , and the phase of the output will lead the input by  $90^\circ$ . Note for this example, the magnitude is proportional to the input frequency while the phase is independent of frequency.

## EXAMPLE 6.2

### Frequency-Response Characteristics of a Lead Compensator

Recall from Chapter 5 [see Eq. (5.70)] the transfer function of the lead compensation, which is equivalent to

$$D_c(s) = K \frac{Ts + 1}{\alpha Ts + 1}, \quad \alpha < 1. \quad (6.8)$$

1. Analytically determine its frequency-response characteristics and discuss what you would expect from the result.
2. Use Matlab to plot  $D_c(j\omega)$  with  $K = 1$ ,  $T = 1$ , and  $\alpha = 0.1$  for  $0.1 \leq \omega \leq 100$ , and verify the features predicted from the analysis in 1. above.

#### Solution

1. **Analytical evaluation:** Substituting  $s = j\omega$  into Eq. (6.8), we get

$$D_c(j\omega) = K \frac{Tj\omega + 1}{\alpha Tj\omega + 1}.$$

From Eqs. (6.5) and (6.6) the amplitude is

$$M = |D_c| = |K| \frac{\sqrt{1 + (\omega T)^2}}{\sqrt{1 + (\alpha\omega T)^2}},$$

and the phase is given by

$$\begin{aligned}\phi &= \angle(1 + j\omega T) - \angle(1 + j\alpha\omega T) \\ &= \tan^{-1}(\omega T) - \tan^{-1}(\alpha\omega T).\end{aligned}$$

At very low frequencies, the amplitude is just  $|K|$ , and at very high frequencies, it is  $|K/\alpha|$ . Therefore, the amplitude is higher at very high frequency. The phase is zero at very low frequencies and goes back to zero at very high frequencies. At intermediate frequencies, evaluation of the  $\tan^{-1}(\cdot)$  functions would reveal that  $\phi$  becomes positive. These are the general characteristics of lead compensation.

2. **Computer evaluation:** A Matlab script for frequency-response evaluation was shown for Example 3.6. A similar script for the lead compensation:

```
s = tf('s');
sysD = (s + 1)/ (s/10 + 1);
w=logspace(-1,2); % determines frequencies over
% computes magnitude and phase
range of interest
[mag,phase] = bode(sysD,w); % computes magnitude and phase
loglog(w,squeeze(mag)),grid;
axis([0.1 100 1 10])
semilogx(w,squeeze(phase)),grid;
axis([0.1 100 0 60])
```

produces the frequency-response magnitude and phase plots shown in Fig 6.2.

The analysis indicated that the low-frequency magnitude should be  $K (= 1)$  and the high-frequency magnitude should be  $K/\alpha (= 10)$ , which are both verified by the magnitude plot. The phase plot also verifies that the value approaches zero at high and low frequencies, and that the intermediate values are positive.

---

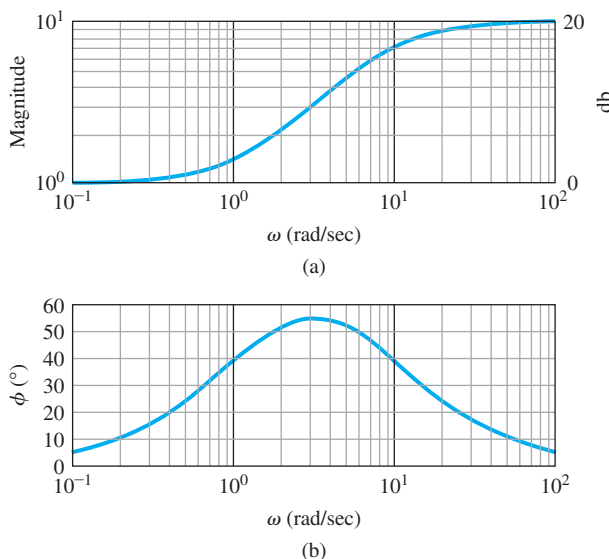
In the cases for which we do not have a good model of the system, and wish to determine the frequency-response magnitude and phase experimentally, we can excite the system with a sinusoid varying in frequency. The magnitude  $M(\omega)$  is obtained by measuring the ratio of the output sinusoid to input sinusoid in the steady-state at each frequency. The phase  $\phi(\omega)$  is the measured difference in phase between input and output signals.<sup>1</sup>

---

<sup>1</sup>Agilent Technologies produces instruments called spectrum analyzers that automate this experimental procedure and greatly speed up the process.

**Figure 6.2**

- (a) Magnitude;  
 (b) phase for the lead compensation in Example 6.2



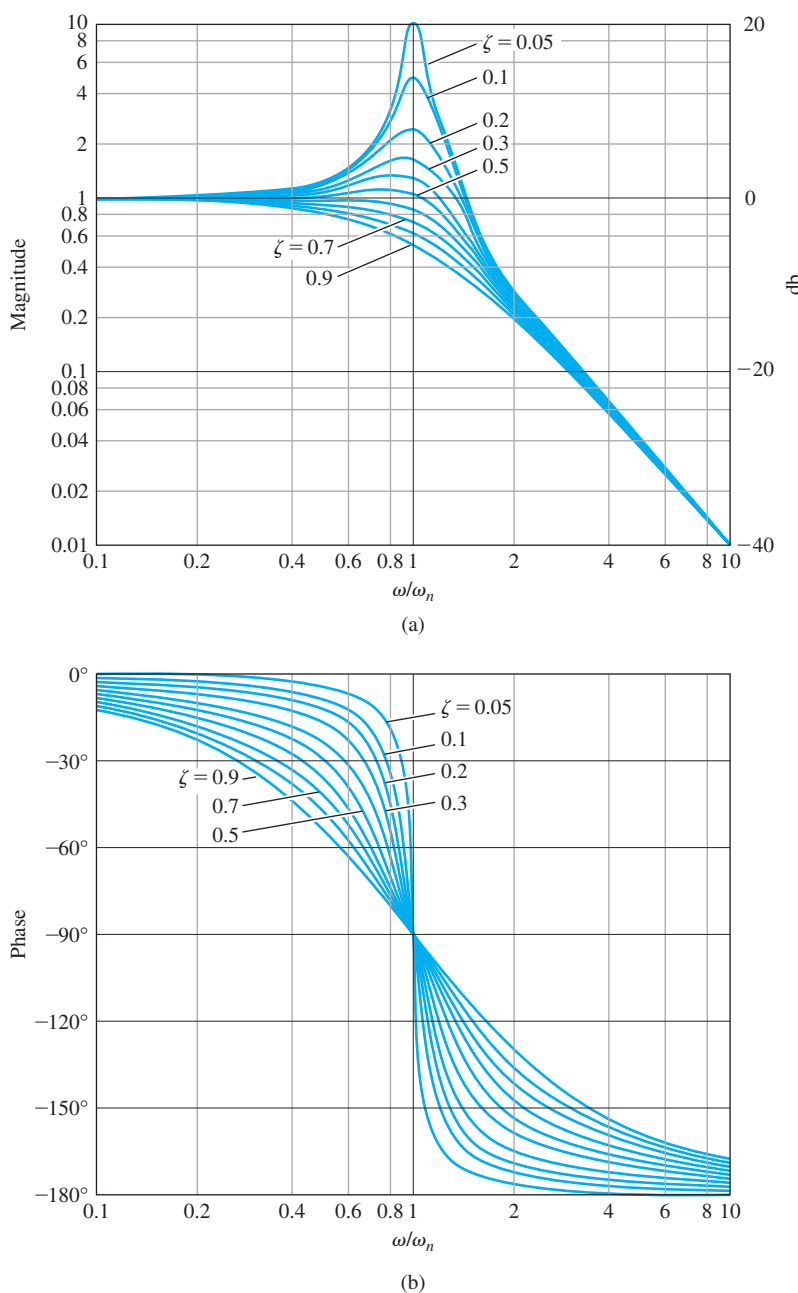
A great deal can be learned about the dynamic response of a system from knowledge of the magnitude  $M(\omega)$  and the phase  $\phi(\omega)$  of its transfer function. In the obvious case, if the signal is a sinusoid, then  $M$  and  $\phi$  completely describe the response. Furthermore, if the input is periodic, then a Fourier series can be constructed to decompose the input into a sum of sinusoids, and again  $M(\omega)$  and  $\phi(\omega)$  can be used with each component to construct the total response. For transient inputs, our best path to understanding the meaning of  $M$  and  $\phi$  is to relate the frequency response  $G(j\omega)$  to the transient responses calculated by the Laplace transform. For example, in Fig. 3.19(b), we plotted the step response of a system having the transfer function

$$G(s) = \frac{1}{(s/\omega_n)^2 + 2\xi(s/\omega_n) + 1}, \quad (6.9)$$

for various values of  $\xi$ . These transient curves were normalized with respect to time as  $\omega_n t$ . In Fig. 6.3, we plot  $M(\omega)$  and  $\phi(\omega)$  for these same values of  $\xi$  to help us see what features of the frequency response correspond to the transient-response characteristics. Specifically, Figs. 3.19(b) and 6.3 indicate the effect of damping on system time response and the corresponding effect on the frequency response. They show that the damping of the system can be determined from the transient-response overshoot or from the peak in the magnitude of the frequency response [Fig. 6.3 (a)]. Furthermore, from the frequency response, we see that  $\omega_n$  is approximately equal to the bandwidth—the frequency where the magnitude starts to fall off from its low-frequency value. (We will define bandwidth more formally in the next paragraph.) Therefore, the rise time can be estimated from the bandwidth. We also see that the magnitude of peak overshoot is approximately  $1/2\xi$  for

**Figure 6.3**

Frequency response  
of Eq. (6.9);  
(a) Magnitude;  
(b) Phase



$\zeta < 0.5$ , so the peak overshoot in the step response can be estimated from the peak overshoot in the frequency response. Thus, we see that essentially the same information is contained in the frequency-response curve as is found in the transient-response curve.

A natural specification for system performance in terms of frequency response is the **bandwidth**, defined to be the maximum frequency

**Figure 6.4**  
Simplified system definition

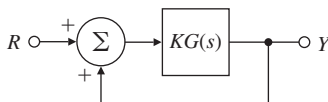
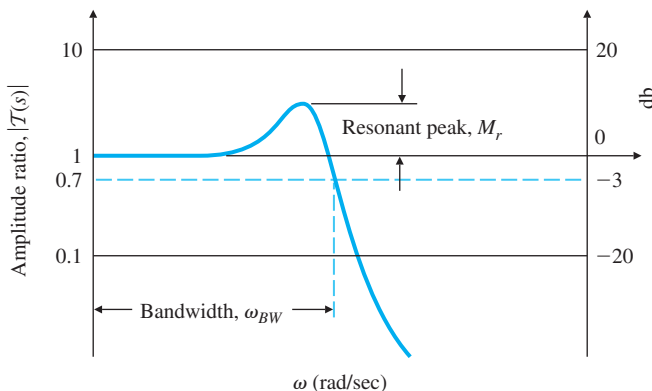


**Figure 6.5**  
Definitions of bandwidth and resonant peak



at which the output of a system will track an input sinusoid in a satisfactory manner. By convention, for the system shown in Fig. 6.4 with a sinusoidal input  $r$ , the bandwidth is the frequency of  $r$  at which the output  $y$  is attenuated to a factor of 0.707 times the input.<sup>2</sup> Figure 6.5 depicts the idea graphically for the frequency response of the *closed-loop* transfer function

$$\frac{Y(s)}{R(s)} \triangleq T(s) = \frac{KG(s)}{1 + KG(s)}.$$

The plot is typical of most closed-loop systems, in that (1) the output follows the input ( $|T| \approx 1$ ) at the lower excitation frequencies, and (2) the output ceases to follow the input ( $|T| < 1$ ) at the higher excitation frequencies. The maximum value of the frequency-response magnitude is referred to as the **resonant peak**  $M_r$ .

Bandwidth is a measure of speed of response, and is therefore similar to time-domain measures such as rise time and peak time or the *s*-plane measure of dominant-root(s) natural frequency. In fact, if the  $KG(s)$  in Fig. 6.4 is such that the closed-loop response is given by Fig. 6.3, we can see that the bandwidth will equal the natural frequency of the closed-loop root (that is,  $\omega_{BW} = \omega_n$  for a closed-loop damping ratio of  $\zeta = 0.7$ ). For other damping ratios, the bandwidth is approximately equal to the natural frequency of the closed-loop roots, with an error typically less than a factor of 2.

The definition of the bandwidth stated here is meaningful for systems that have a low-pass filter behavior, as is the case for most any physical control system. In other applications, the bandwidth may be defined differently. Also, if the ideal model of the system does not have

<sup>2</sup>If the output is a voltage across a 1- $\Omega$  resistor, the power is  $v^2$  and when  $|v| = 0.707$ , the power is reduced by a factor of 2. By convention, this is called the half-power point.

a high-frequency roll-off (e.g., if it has an equal number of poles and zeros), the bandwidth is infinite; however, this does not occur in nature as nothing responds well at infinite frequencies.

In many cases, the designer's primary concern is the error in the system due to disturbances rather than the ability to track an input. For error analysis, we are more interested in one of the sensitivity functions defined in Section 4.1,  $S(s)$ , rather than  $T(s)$ . For most open-loop systems with high gain at low frequencies,  $S(s)$  for a disturbance input will have very low values at low frequencies and grows as the frequency of the input or disturbance approaches the bandwidth. For analysis of either  $T(s)$  or  $S(s)$ , it is typical to plot their response versus the frequency of the input. Either frequency response for control systems design can be evaluated using the computer, or can be quickly sketched for simple systems using the efficient methods described in the following Section 6.1.1. The methods described next are also useful to expedite the design process, as well as to perform sanity checks on the computer output.

### 6.1.1 Bode Plot Techniques

Display of frequency response is a problem that has been studied for a long time. Before computers, this was accomplished by hand; therefore, it was useful to be able to accomplish this quickly. The most useful technique for hand plotting was developed by H. W. Bode at Bell Laboratories between 1932 and 1942. This technique allows plotting that is quick and yet sufficiently accurate for control systems design. Most control systems designers now have access to computer programs that diminish the need for hand plotting; however, it is still important to develop good intuition so you can quickly identify erroneous computer results, and for this, you need the ability to perform a sanity check and in some cases to determine approximate results by hand.

The idea in Bode's method is to plot magnitude curves using a logarithmic scale and phase curves using a linear scale. This strategy allows us to plot a high-order  $G(j\omega)$  by simply adding the separate terms graphically, as discussed in Appendix WB. This addition is possible because a complex expression with zero and pole factors can be written in polar (or phasor) form as

$$G(j\omega) = \frac{\vec{s}_1 \vec{s}_2}{\vec{s}_3 \vec{s}_4 \vec{s}_5} = \frac{r_1 e^{j\theta_1} r_2 e^{j\theta_2}}{r_3 e^{j\theta_3} r_4 e^{j\theta_4} r_5 e^{j\theta_5}} = \left( \frac{r_1 r_2}{r_3 r_4 r_5} \right) e^{j(\theta_1 + \theta_2 - \theta_3 - \theta_4 - \theta_5)}. \quad (6.10)$$

(The overhead arrow indicates a phasor.) Note from Eq. (6.10) the phases of the individual terms are added directly to obtain the phase of the **composite** expression,  $G(j\omega)$ . Furthermore, because

$$|G(j\omega)| = \frac{r_1 r_2}{r_3 r_4 r_5},$$

it follows that

$$\log_{10} |G(j\omega)| = \log_{10} r_1 + \log_{10} r_2 - \log_{10} r_3 - \log_{10} r_4 - \log_{10} r_5. \quad (6.11)$$

**Composite plot from individual terms**

We see that addition of the logarithms of the individual terms provides the logarithm of the magnitude of the composite expression. The frequency response is typically presented as two curves; the logarithm of magnitude versus  $\log \omega$  and the phase versus  $\log \omega$ . Together, these two curves constitute a **Bode plot** of the system. Because

$$\log_{10} M e^{j\phi} = \log_{10} M + j\phi \log_{10} e, \quad (6.12)$$

**Decibel** we see the Bode plot shows the real and imaginary parts of the logarithm of  $G(j\omega)$ . In communications, it is standard to measure the power gain in decibels (db), or “**Power db**”:<sup>3</sup>

$$|G|_{\text{db}} = 10 \log_{10} \frac{P_2}{P_1}. \quad (6.13)$$

Here  $P_1$  and  $P_2$  are the input and output powers. Because power is proportional to the square of the voltage, the power gain is also given by

$$|G|_{\text{db}} = 20 \log_{10} \frac{V_2}{V_1}. \quad (6.14)$$

Hence, we can present a Bode plot as the magnitude in decibels versus  $\log \omega$ , and the phase in degrees versus  $\log \omega$ .<sup>4</sup> In this book, we give Bode plots in the form  $\log |G|$  versus  $\log \omega$ ; also, we mark an axis in decibels on the right-hand side of the magnitude plot to give you the choice of working with the representation you prefer. However, for frequency-response plots, we are not actually plotting power, and use of Eq. (6.14) can be somewhat misleading. If the magnitude data are derived in terms of  $\log |G|$ , it is conventional to plot them on a log scale but identify the scale in terms of  $|G|$  only (without “log”). If the magnitude data are given in decibels, the vertical scale is linear such that each decade of  $|G|$  represents 20 db.

### *Advantages of Working with Frequency Response in Terms of Bode Plots*

#### **Advantages of Bode plots**

1. Dynamic compensator design can be based entirely on Bode plots.
2. Bode plots can be determined experimentally.
3. Bode plots of systems in series (or tandem) simply add, which is quite convenient.
4. The use of a log scale permits a much wider range of frequencies to be displayed on a single plot than is possible with linear scales.

It is important for the control systems engineer to understand the Bode plot techniques for several reasons: This knowledge allows

---

<sup>3</sup>Researchers at Bell Laboratories first defined the unit of power gain as a **bel** (named for Alexander Graham Bell, the founder of the company). However, this unit proved to be too large, and hence a **decibel or db** (1/10 of a bel) was selected as a more useful unit. The abbreviation dB is also used sometimes; however, Bode used db and we choose to follow his lead.

<sup>4</sup>Henceforth, we will drop the base of the logarithm; it is understood to be 10.

the engineer not only to deal with simple problems, but also to perform a sanity check on computer results for more complicated cases. Often approximations can be used to quickly sketch the frequency response and deduce stability, as well as to determine the form of the needed dynamic compensations. Finally, an understanding of the plotting method is useful in interpreting frequency-response data that have been generated experimentally.

In Chapter 5, we wrote the open-loop transfer function in the form

$$KG(s) = K \frac{(s - z_1)(s - z_2) \cdots}{(s - p_1)(s - p_2) \cdots} \quad (6.15)$$

because it was the most convenient form for determining the degree of stability from the root locus with respect to the gain  $K$ . In working with frequency response, we are only interested in evaluating  $G(s)$  along the  $j\omega$  axis, so it is more convenient to replace  $s$  with  $j\omega$  and to write the transfer functions in the **Bode form**

$$KG(j\omega) = K_o(j\omega)^n \frac{(j\omega\tau_1 + 1)(j\omega\tau_2 + 1) \cdots}{(j\omega\tau_a + 1)(j\omega\tau_b + 1) \cdots}. \quad (6.16)$$

This form also causes the gain  $K_o$  to be directly related to the transfer-function magnitude at very low frequencies. In fact, for systems with  $n = 0$ ,  $K_o$  is the gain at  $\omega = 0$  in Eq. (6.16) and is also equal to the DC gain of the system. Although a straightforward calculation will convert a transfer function in the form of Eq. (6.15) to an equivalent transfer function in the form of Eq. (6.16), note  $K$  and  $K_o$  will not usually have the same value in the two expressions.

Transfer functions can also be rewritten according to Eqs. (6.10) and (6.11). As an example, suppose

$$KG(j\omega) = K_o \frac{j\omega\tau_1 + 1}{(j\omega)^2(j\omega\tau_a + 1)}. \quad (6.17)$$

Then

$$\angle KG(j\omega) = \angle K_o + \angle(j\omega\tau_1 + 1) - \angle(j\omega)^2 - \angle(j\omega\tau_a + 1) \quad (6.18)$$

and

$$\begin{aligned} \log |KG(j\omega)| &= \log |K_o| + \log |j\omega\tau_1 + 1| - \log |(j\omega)^2| \\ &\quad - \log |j\omega\tau_a + 1|. \end{aligned} \quad (6.19)$$

In decibels, Eq. (6.19) becomes

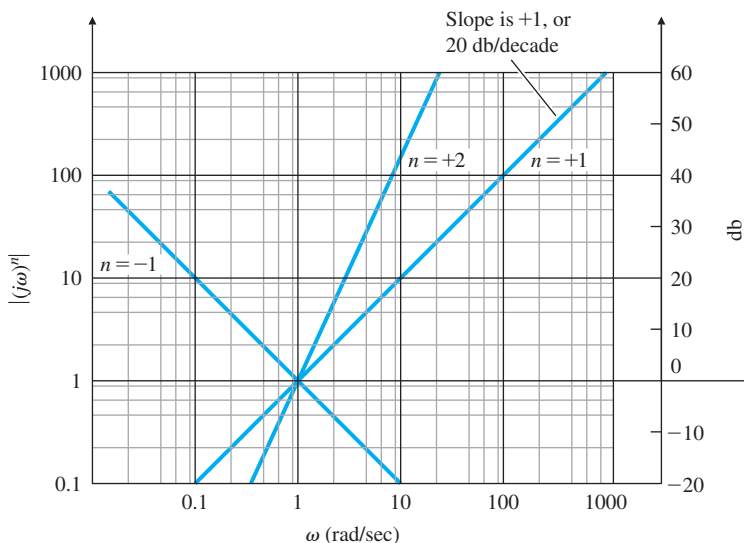
$$\begin{aligned} |KG(j\omega)|_{\text{db}} &= 20 \log |K_o| + 20 \log |j\omega\tau_1 + 1| - 20 \log |(j\omega)^2| \\ &\quad - 20 \log |j\omega\tau_a + 1|. \end{aligned} \quad (6.20)$$

All transfer functions for the kinds of systems we have talked about so far are composed of three classes of terms:

1.  $K_o(j\omega)^n$ .
2.  $(j\omega\tau + 1)^{\pm 1}$ .
3.  $\left[ \left( \frac{j\omega}{\omega_n} \right)^2 + 2\xi \frac{j\omega}{\omega_n} + 1 \right]^{\pm 1}$ .

### Bode form of the transfer function

### Classes of terms of transfer functions

**Figure 6.6**Magnitude of  $(j\omega)^n$ 

First, we will discuss the plotting of each individual term and how the terms affect the composite plot including all the terms; then, we will discuss how to draw the composite curve.

**Class 1: singularities at the origin**

1.  $K_o(j\omega)^n$ : Because

$$\log K_o |(j\omega)^n| = \log K_o + n \log |j\omega|,$$

the magnitude plot of this term is a straight line with a slope  $n \times 20$  db per decade. Examples for different values of  $n$  are shown in Fig. 6.6.  $K_o(j\omega)^n$  is the only class of term that affects the slope at the lowest frequencies, because all other terms are constant in that region. The easiest way to draw the curve is to locate  $\omega = 1$  then plot  $\log K_o$  at that frequency. Then draw the line with slope  $n$  through that point.<sup>5</sup> The phase of  $(j\omega)^n$  is  $\phi = n \times 90^\circ$ ; it is independent of frequency and is thus a horizontal line:  $-90^\circ$  for  $n = -1$ ,  $-180^\circ$  for  $n = -2$ ,  $+90^\circ$  for  $n = +1$ , and so forth.

**Class 2: first-order term**

2.  $(j\omega\tau + 1)$ : The magnitude of this term approaches one asymptote at very low frequencies and another asymptote at very high frequencies:

- (a) For  $\omega\tau \ll 1$ ,  $j\omega\tau + 1 \cong 1$ .
- (b) For  $\omega\tau \gg 1$ ,  $j\omega\tau + 1 \cong j\omega$ .

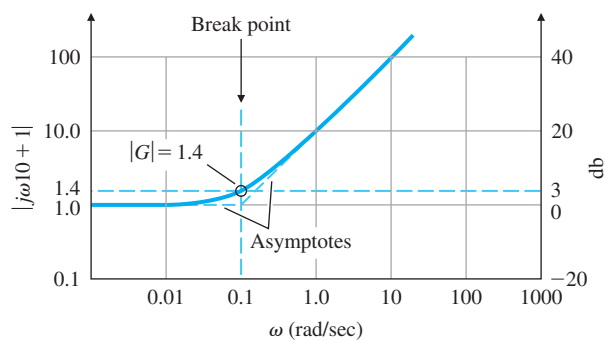
**Break point**

If we call  $\omega = 1/\tau$  the **break point**, then we see that below the break point the magnitude curve is approximately constant ( $= 1$ ), while above the break point the magnitude curve behaves approximately like the class 1 term  $K_o(j\omega)$ . The example plotted in Fig. 6.7,  $G(s) =$

<sup>5</sup>In decibels the slopes are  $n \times 20$  db per decade or  $n \times 6$  db per octave (an octave is a change in frequency by a factor of 2).

**Figure 6.7**

Magnitude plot for  
 $j\omega\tau + 1; \tau = 10$



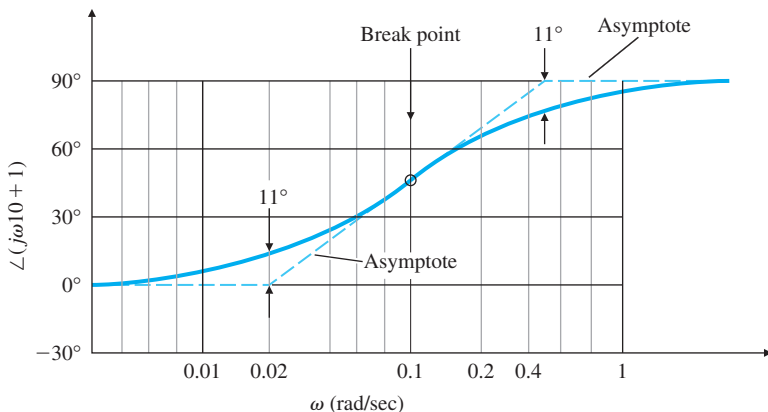
$10s + 1$ , shows how the two asymptotes cross at the break point and how the actual magnitude curve lies above that point by a factor of 1.4 (or +3 db). (If the term were in the denominator, it would be below the break point by a factor of 0.707 or -3 db.) Note this term will have only a small effect on the composite magnitude curve below the break point, because its value is equal to 1 (= 0 db) in this region. The slope at high frequencies is +1 (or +20 db per decade). The phase curve can also be easily drawn by using the following low- and high-frequency asymptotes:

- (a) For  $\omega\tau \ll 1$ ,  $\angle 1 = 0^\circ$ .
- (b) For  $\omega\tau \gg 1$ ,  $\angle(j\omega\tau + 1) = 90^\circ$ .
- (c) For  $\omega\tau \cong 1$ ,  $\angle(j\omega\tau + 1) \cong 45^\circ$ .

For  $\omega\tau \cong 1$ , the  $\angle(j\omega + 1)$  curve is tangent to an asymptote going from  $0^\circ$  at  $\omega\tau = 0.2$  to  $90^\circ$  at  $\omega\tau = 5$ , as shown in Fig. 6.8. The figure also illustrates the three asymptotes (dashed lines) used for the phase plot and how the actual curve deviates from the asymptotes by  $11^\circ$  at their intersections. Both the composite phase and magnitude curves are unaffected by this class of term at frequencies below the break point by more than a factor of 10 because the term's magnitude is 1 (or 0 db) and its phase is less than  $5^\circ$ .

**Figure 6.8**

Phase plot for  $j\omega\tau + 1$ ;  
 $\tau = 10$



## Class 3: second-order term

3.  $[(j\omega/\omega_n)^2 + 2\xi(j\omega/\omega_n) + 1]^{\pm 1}$ : This term behaves in a manner similar to the class 2 term, with differences in detail: The break point is now  $\omega = \omega_n$ . The magnitude changes slope by a factor of +2 (or +40 db per decade) at the break point (and -2, or -40 db per decade, when the term is in the denominator). The phase changes by  $\pm 180^\circ$ , and the transition through the break-point region varies with the damping ratio  $\xi$ . Figure 6.3 shows the magnitude and phase for several different damping ratios when the term is in the denominator. Note the magnitude asymptote for frequencies above the break point has a slope of -2 (or -40 db per decade), and that the transition through the break-point region has a large dependence on the damping ratio. A rough determination of this transition can be made by noting that

$$|G(j\omega)| = \frac{1}{2\xi} \quad \text{at } \omega = \omega_n \quad (6.21)$$

## Peak amplitude

for this class of second-order term in the denominator. If the term was in the numerator, the magnitude would be the reciprocal of the curve plotted in Fig. 6.3(a).

No such handy rule as Eq. (6.21) exists for sketching in the transition for the phase curve; therefore, we would have to resort to Fig. 6.3(b) for an accurate plot of the phase. However, a very rough idea of the transition can be gained by noting that it is a step function for  $\xi = 0$ , while it obeys the rule for two first-order (class 2) terms when  $\xi = 1$  with simultaneous break-point frequencies. All intermediate values of  $\xi$  fall between these two extremes. The phase of a second-order term is always  $\pm 90^\circ$  at  $\omega_n$ .

## Composite curve

When the system has several poles and several zeros, plotting the frequency response requires that the components be combined into a composite curve. To plot the composite magnitude curve, it is useful to note that the slope of the asymptotes is equal to the sum of the slopes of the individual curves. Therefore, the composite asymptote curve has integer slope changes at each break-point frequency: +1 for a first-order term in the numerator, -1 for a first-order term in the denominator, and  $\pm 2$  for second-order terms. Furthermore, the lowest-frequency portion of the asymptote has a slope determined by the value of  $n$  in the  $(j\omega)^n$  term and is located by plotting the point  $K_0\omega^n$  at  $\omega = 1$ . Therefore, the complete procedure consists of plotting the lowest-frequency portion of the asymptote, then sequentially changing the asymptote's slope at each break point in order of ascending frequency, and finally drawing the actual curve by using the transition rules discussed earlier for classes 2 and 3.

The composite phase curve is the sum of the individual curves. Addition of the individual phase curves graphically is made possible by locating the curves so the composite phase approaches the individual curve as closely as possible. A quick but crude sketch of the composite phase can be found by starting the phase curve below the lowest

break point and setting it equal to  $n \times 90^\circ$ . The phase is then stepped at each break point in order of ascending frequency. The amount of the phase step is  $\pm 90^\circ$  for a first-order term and  $\pm 180^\circ$  for a second-order term. Break points in the numerator indicate a positive step in phase, while break points in the denominator indicate a negative phase step.<sup>6</sup> The plotting rules so far have only considered poles and zeros in the left half-plane (LHP). Changes for singularities in the right half-plane (RHP) will be discussed at the end of the section.

### *Summary of Bode Plot Rules*

1. Manipulate the transfer function into the Bode form given by Eq. (6.16).
2. Determine the value of  $n$  for the  $K_o(j\omega)^n$  term (class 1). Plot the low-frequency magnitude asymptote through the point  $K_o$  at  $\omega = 1$  with a slope of  $n$  (or  $n \times 20$  db per decade).
3. Complete the composite magnitude asymptotes: Extend the low-frequency asymptote until the first frequency break point. Then step the slope by  $\pm 1$  or  $\pm 2$ , depending on whether the break point is from a first- or second-order term in the numerator or denominator. Continue through all break points in ascending order.
4. The approximate magnitude curve is increased from the asymptote value by a factor of 1.4 (+3 db) at first-order numerator break points, and decreased by a factor of 0.707 (-3 db) at first-order denominator break points. At second-order break points, the resonant peak (or valley) occurs according to Fig. 6.3(a), using the relation  $|G(j\omega)| = 1/2\xi$  at denominator (or  $|G(j\omega)| = 2\xi$  at numerator) break points.
5. Plot the low-frequency asymptote of the phase curve,  $\phi = n \times 90^\circ$ .
6. As a guide, the approximate phase curve changes by  $\pm 90^\circ$  or  $\pm 180^\circ$  at each break point in ascending order. For first-order terms in the numerator, the change of phase is  $+90^\circ$ ; for those in the denominator the change is  $-90^\circ$ . For second-order terms, the change is  $\pm 180^\circ$ .
7. Locate the asymptotes for each individual phase curve so their phase change corresponds to the steps in the phase toward or away from the approximate curve indicated by Step 6. Each individual phase curve occurs as indicated by Fig. 6.8 or Fig. 6.3(b).
8. Graphically add each phase curve. Use grids if an accuracy of about  $\pm 5^\circ$  is desired. If less accuracy is acceptable, the composite curve can be done by eye. Keep in mind that the curve will start at the lowest-frequency asymptote and end on the highest-frequency asymptote and will approach the intermediate asymptotes to an extent that is determined by how close the break points are to each other.

---

<sup>6</sup>This approximate method was pointed out to us by our Parisian colleagues.

**EXAMPLE 6.3***Bode Plot for Real Poles and Zeros*

Plot the Bode magnitude and phase for the system with the transfer function

$$KG(s) = \frac{2000(s + 0.5)}{s(s + 10)(s + 50)}.$$

**Solution**

1. We convert the function to the Bode form of Eq. (6.16):

$$KG(j\omega) = \frac{2[(j\omega/0.5) + 1]}{j\omega[(j\omega/10) + 1][(j\omega/50) + 1]}.$$

2. We note the term in  $j\omega$  is first order and in the denominator, so  $n = -1$ . Therefore, the low-frequency asymptote is defined by the first term:

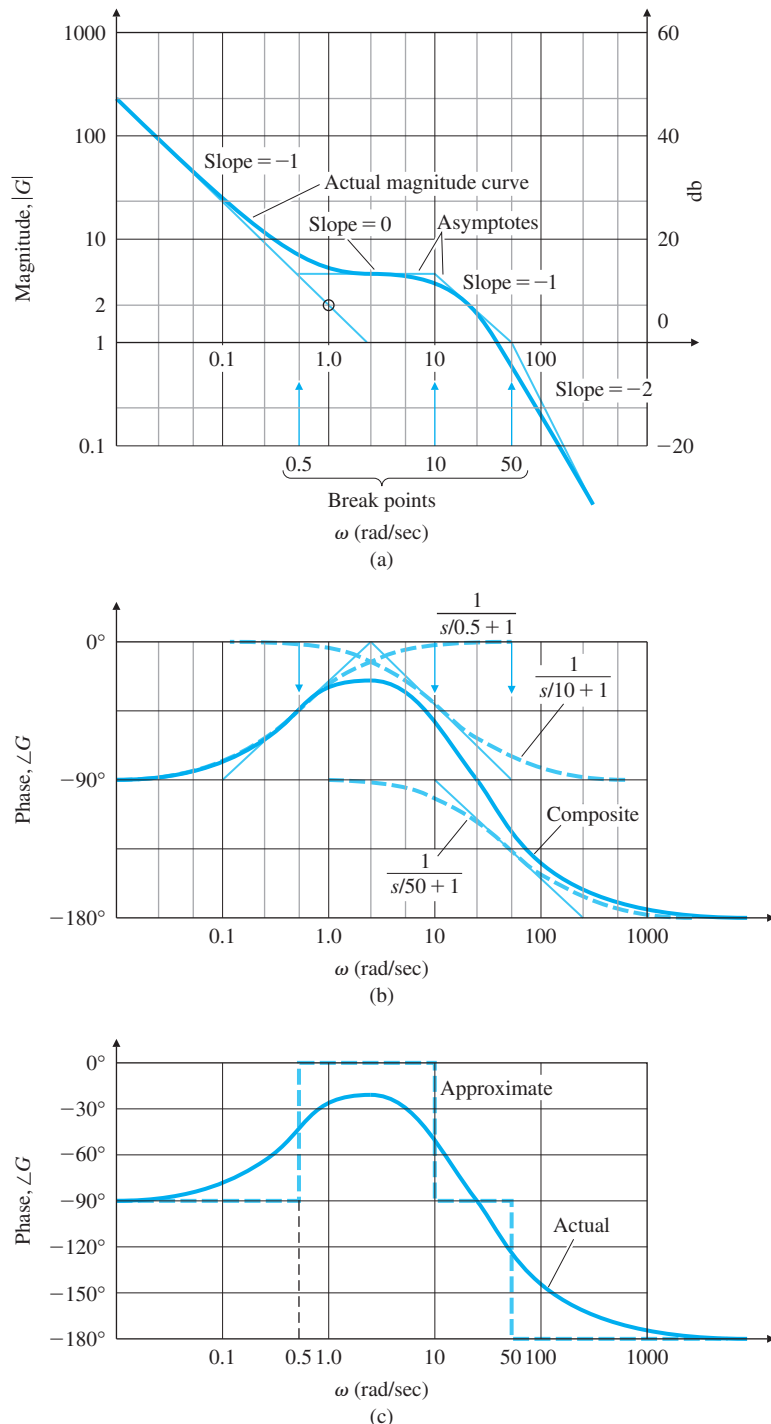
$$KG(j\omega) = \frac{2}{j\omega}.$$

This asymptote is valid for  $\omega < 0.1$ , because the lowest break point is at  $\omega = 0.5$ . The magnitude plot of this term has the slope of  $-1$  (or  $-20$  db per decade). We locate the magnitude by passing through the value 2 at  $\omega = 1$  even though the composite curve will not go through this point because of the break point at  $\omega = 0.5$ . This is shown in Fig. 6.9(a).

3. We obtain the remainder of the asymptotes, also shown in Fig. 6.9(a): The first break point is at  $\omega = 0.5$  and is a first-order term in the numerator, which thus calls for a change in slope of  $+1$ . We therefore draw a line with 0 slope that intersects the original  $-1$  slope. Then, we draw a  $-1$  slope line that intersects the previous one at  $\omega = 10$ . Finally, we draw a  $-2$  slope line that intersects the previous  $-1$  slope at  $\omega = 50$ .
4. The actual curve is approximately tangent to the asymptotes when far away from the break points, a factor of 1.4 ( $+3$  db) above the asymptote at the  $\omega = 0.5$  break point, and a factor of 0.7 ( $-3$  db) below the asymptote at the  $\omega = 10$  and  $\omega = 50$  break points.
5. Because the phase of  $2/j\omega$  is  $-90^\circ$ , the phase curve in Fig. 6.9(b) starts at  $-90^\circ$  at the lowest frequencies.
6. The result is shown in Fig. 6.9(c).
7. The individual phase curves, shown dashed in Fig. 6.9(b), have the correct phase change for each term and are aligned vertically so their phase change corresponds to the steps in the phase from the approximate curve in Fig. 6.9(c). Note the composite curve approaches each individual term.
8. The graphical addition of each dashed curve results in the solid composite curve in Fig. 6.9(b). As can be seen from the figure, the vertical placement of each individual phase curve makes the required graphical addition particularly easy because the composite curve approaches each individual phase curve in turn.

**Figure 6.9**

Composite plots:  
 (a) magnitude;  
 (b) phase;  
 (c) approximate phase



**EXAMPLE 6.4***Bode Plot with Complex Poles*

As a second example, draw the frequency response for the system

$$KG(s) = \frac{10}{s[s^2 + 0.4s + 4]}. \quad (6.22)$$

**Solution.** A system like this is more difficult to plot than the one in the previous example because the transition between asymptotes is dependent on the damping ratio; however, the same basic ideas illustrated in Example 6.3 apply.

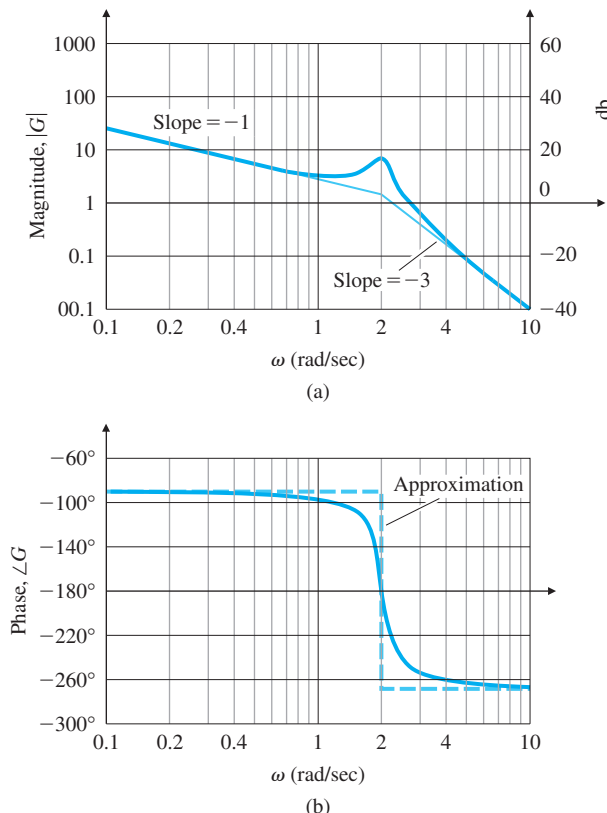
This system contains a second-order term in the denominator. Proceeding through the steps, we convert Eq. (6.22) to the Bode form of Eq. (6.16):

$$KG(s) = \frac{10}{4} \frac{1}{s(s^2/4 + 2(0.1)s/2 + 1)}.$$

Starting with the low-frequency asymptote, we have  $n = -1$  and  $|G(j\omega)| \cong 2.5/\omega$ . The magnitude plot of this term has a slope of  $-1$  ( $-20$  db per decade) and passes through the value of  $2.5$  at  $\omega = 1$ , as shown in Fig. 6.10(a). For the second-order pole, note  $\omega_n = 2$  and

**Figure 6.10**

Bode plot for a transfer function with complex poles: (a) magnitude; (b) phase



$\zeta = 0.1$ . At the break-point frequency of the poles,  $\omega = 2$ , the slope shifts to  $-3$  ( $-60$  db per decade). At the pole break point, the magnitude ratio above the asymptote is  $1/2\zeta = 1/0.2 = 5$ . The phase curve for this case starts at  $\phi = -90^\circ$ , corresponding to the  $1/s$  term, falls to  $\phi = -180^\circ$  at  $\omega = 2$  due to the pole as shown in Fig. 6.10(b), then approaches  $\phi = -270^\circ$  for higher frequencies. Because the damping is small, the stepwise approximation is a very good one. The true composite phase curve is shown in Fig. 6.10(b).

---

## EXAMPLE 6.5

### Bode Plot for Complex Poles and Zeros: Satellite with Flexible Appendages

As a third example, draw the Bode plots for a system with second-order terms. The transfer function represents a mechanical system with two equal masses coupled with a lightly damped spring. The applied force and position measurement are collocated on the same mass. For the transfer function, the time scale has been chosen so the resonant frequency of the complex zeros is equal to 1. The transfer function is

$$KG(s) = \frac{0.01(s^2 + 0.01s + 1)}{s^2[(s^2/4) + 0.02(s/2) + 1]}.$$

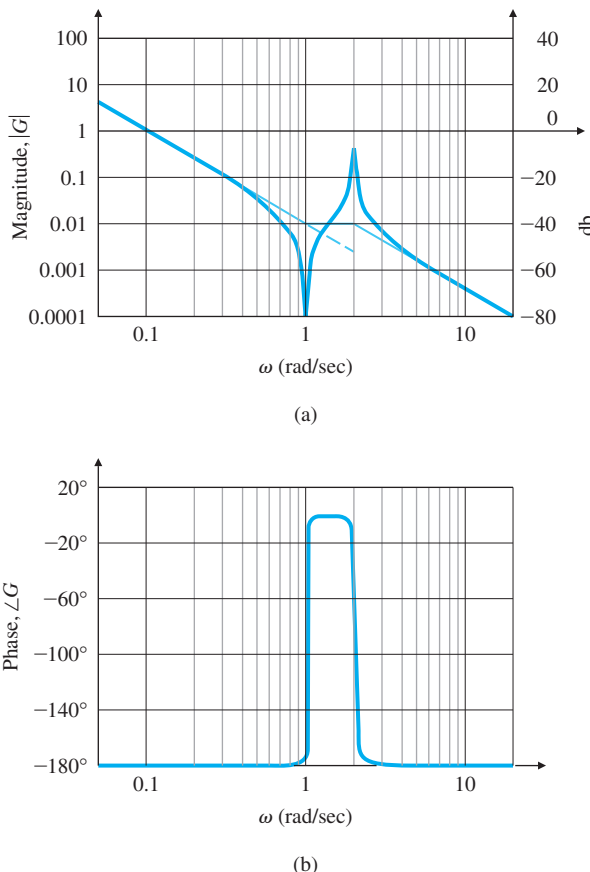
**Solution.** Proceeding through the steps, we start with the low-frequency asymptote,  $0.01/\omega^2$ . It has a slope of  $-2$  ( $-40$  db per decade) and passes through magnitude  $= 0.01$  at  $\omega = 1$ , as shown in Fig. 6.11(a). At the break-point frequency of the zero,  $\omega = 1$ , the slope shifts to zero until the break point of the pole, which is located at  $\omega = 2$ , when the slope returns to a slope of  $-2$ . To interpolate the true curve, we plot the point at the zero break point,  $\omega = 1$ , with a magnitude ratio below the asymptote of  $2\zeta = 0.01$ . At the pole break point, the magnitude ratio above the asymptote is  $1/2\zeta = 1/0.02 = 50$ . The magnitude curve is a “doublet” of a negative pulse followed by a positive pulse. Figure 6.11(b) shows that the phase curve for this system starts at  $-180^\circ$  (corresponding to the  $1/s^2$  term), jumps  $180^\circ$  to  $\phi = 0$  at  $\omega = 1$ , due to the zeros, then falls  $180^\circ$  back to  $\phi = -180^\circ$  at  $\omega = 2$ , due to the pole. With such small damping ratios the stepwise approximation is quite good. (We haven’t drawn this on Fig. 6.11(b), because it would not be easily distinguishable from the true phase curve.) Thus, the true composite phase curve is a nearly square pulse between  $\omega = 1$  and  $\omega = 2$ .

---

In actual designs, Bode plots are made with a computer. However, acquiring the ability to determine how Bode plots should behave is a useful skill, because it gives the designer insight into how changes in the compensation parameters will affect the frequency response. This allows the designer to iterate to the best designs more quickly.

**Figure 6.11**

Bode plot for a transfer function with complex poles and zeros:  
 (a) magnitude;  
 (b) phase



### EXAMPLE 6.6

### Computer-Aided Bode Plot for Complex Poles and Zeros

Repeat Example 6.5 using Matlab.

**Solution.** To obtain Bode plots using Matlab, we call the function bode as follows:

```
s = tf('s');
sysG = 0.01*(s^2 + 0.01*s + 1)/((s^2)*(s^2)/4 + 0.01*s + 1);
[mag, phase, w] = bode(sysG);
loglog(w,squeeze(mag))
semilogx(w,squeeze(phase))
```

These commands will result in a Bode plot which matches that in Fig. 6.11 very closely. To obtain the magnitude plot in decibels, the last three lines can be replaced with

```
bode(sysG).
```

## Nonminimum-Phase Systems

A system with a zero in the RHP undergoes a net change in phase when evaluated for frequency inputs between zero and infinity, which, for an associated magnitude plot, is greater than if all poles and zeros were in the LHP. Such a system is called **nonminimum phase**. As can be deduced from the construction in Fig. WA.3 in online Appendix WA,<sup>7</sup> if the zero is in the RHP, then the phase *decreases* at the zero break point instead of exhibiting the usual phase increase that occurs for an LHP zero. Consider the transfer functions

$$G_1(s) = 10 \frac{s+1}{s+10},$$

$$G_2(s) = 10 \frac{s-1}{s+10}.$$

Both transfer functions have the same magnitude for all frequencies; that is,

$$|G_1(j\omega)| = |G_2(j\omega)|,$$

as shown in Fig. 6.12(a). But the phases of the two transfer functions are drastically different [see Fig. 6.12(b)]. A “minimum-phase” system (i.e., all zeros in the LHP) with a given magnitude curve will produce the smallest *net* change in the associated phase, as shown in  $G_1$ , compared with what the nonminimum-phase system will produce, as shown by the phase of  $G_2$ . The discrepancy between  $G_1$  and  $G_2$  with regard to the phase change would be greater if two or more zeros of the plant were in the RHP.

### 6.1.2 Steady-State Errors

We saw in Section 4.2 that the steady-state error of a feedback system decreases as the gain of the open-loop transfer function increases. In plotting a composite magnitude curve, we saw in Section 6.1.1 that the open-loop transfer function, at very low frequencies, is approximated by

$$KG(j\omega) \cong K_o(j\omega)^n. \quad (6.23)$$

Therefore, we can conclude that the larger the value of the magnitude on the low-frequency asymptote, the lower the steady-state errors will be for the closed-loop system. This relationship is very useful in the design of compensation: Often we want to evaluate several alternate ways to improve stability, and to do so we want to be able to see quickly how changes in the compensation will affect the steady-state errors.

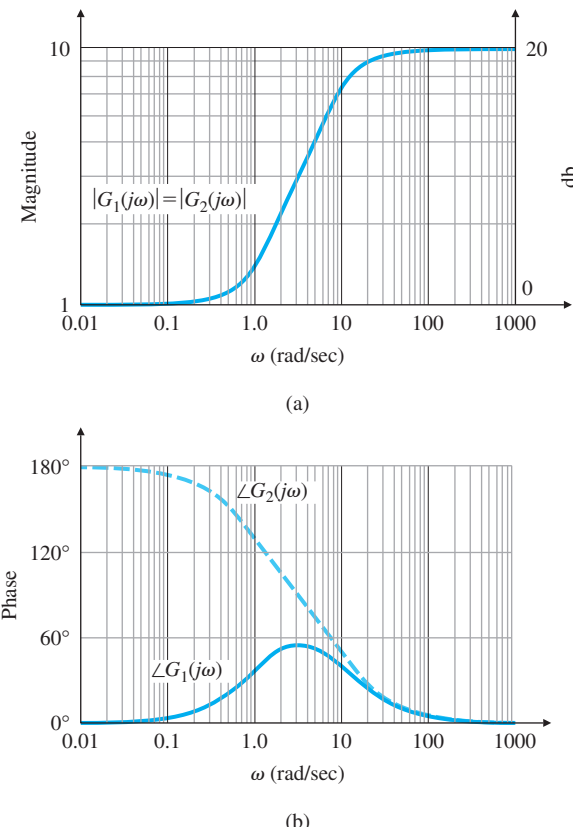
For a system of the form given by Eq. (6.16)—that is, where  $n = 0$  in Eq. (6.23) (a Type 0 system)—the low-frequency asymptote is a constant, and the gain  $K_o$  of the open-loop system is equal to the position-error constant  $K_p$ . For a unity feedback system with a

---

<sup>7</sup>See [www.pearsonglobaleditions.com](http://www.pearsonglobaleditions.com).

**Figure 6.12**

Bode plot of minimum- and nonminimum-phase systems: for  
(a) magnitude;  
(b) phase



unit-step input, the Final Value Theorem (see Section 3.1.6) was used in Section 4.2.1 to show that the steady-state error is given by

$$e_{ss} = \frac{1}{1 + K_p}.$$

#### Velocity error coefficient

For a unity-feedback system in which  $n = -1$  in Eq. (6.23), defined to be a Type 1 system in Section 4.2.1, the low-frequency asymptote has a slope of  $-1$ . The magnitude of the low-frequency asymptote is related to the gain according to Eq. (6.23); therefore, we can again read the gain,  $K_o/\omega$ , directly from the Bode magnitude plot. Equation (4.37) tells us that the velocity-error constant

$$K_v = K_o,$$

where, for a unity-feedback system with a unit-ramp input, the steady-state error is

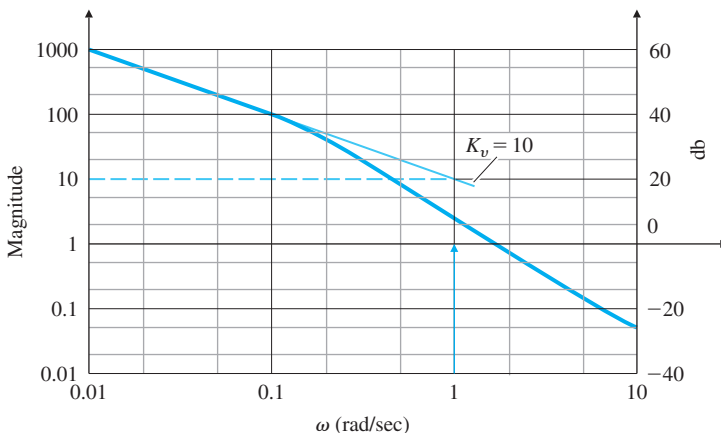
$$e_{ss} = \frac{1}{K_v}.$$

The easiest way of determining the value of  $K_v$  in a Type 1 system is to read the magnitude of the low-frequency asymptote at  $\omega = 1$  rad/sec, because this asymptote is  $A(\omega) = K_v/\omega$ . In some cases, the lowest-frequency break point will be below  $\omega = 1$  rad/sec; therefore, the

**Figure 6.13**

Determination of  $K_v$  from the Bode plot for the system  

$$KG(s) = \frac{10}{s(s+1)}$$



asymptote needs to extend to  $\omega = 1$  rad/sec in order to read  $K_v$  directly. Alternately, we could read the magnitude at any frequency on the low-frequency asymptote and compute it from  $K_v = \omega A(\omega)$ .

### EXAMPLE 6.7

#### *Computation of $K_v$*

As an example of the determination of steady-state errors, a Bode magnitude plot of an open-loop system is shown in Fig. 6.13. Assuming there is unity feedback as in Fig. 6.4, find the velocity-error constant,  $K_v$ .

**Solution.** Because the slope at the low frequencies is  $-1$ , we know the system is Type 1. The extension of the low-frequency asymptote crosses  $\omega = 1$  rad/sec at a magnitude of 10. Therefore,  $K_v = 10$  and the steady-state error to a unit ramp for a unity-feedback system would be 0.1. Alternatively, at  $\omega = 0.01$  we have  $|A(\omega)| = 1000$ ; therefore, from Eq. (6.23) we have

$$K_o = K_v \cong \omega |A(\omega)| = 0.01(1000) = 10.$$

## 6.2 Neutral Stability

In the early days of electronic communications, most instruments were judged in terms of their frequency response. It is therefore natural that when the feedback amplifier was introduced, techniques to determine stability in the presence of feedback were based on this response.

Suppose the closed-loop transfer function of a system is known. We can determine the stability of a system by simply inspecting the denominator in factored form (because the factors give the system roots directly) to observe whether the real parts are positive or negative. However, the closed-loop transfer function is usually not known; in fact, the

whole purpose behind understanding the root-locus technique is to be able to find the factors of the denominator in the closed-loop transfer function, given only the open-loop transfer function. Another way to determine closed-loop stability is to evaluate the frequency response of the *open-loop* transfer function  $KG(j\omega)$ , then perform a test on that response. Note that this method also does not require factoring the denominator of the closed-loop transfer function. In this section, we will explain the principles of this method.

Suppose we have a system defined by Fig. 6.14(a) and whose root locus behaves as shown in Fig. 6.14(b); that is, instability results if  $K$  is larger than 2. The neutrally stable points lie on the imaginary axis—that is, where  $K = 2$  and  $s = j1.0$ . Furthermore, we saw in Section 5.1 that all points on the locus have the property that

$$|KG(s)| = 1 \quad \text{and} \quad \angle G(s) = 180^\circ.$$

At the point of neutral stability, we see that these root-locus conditions hold for  $s = j\omega$ , so

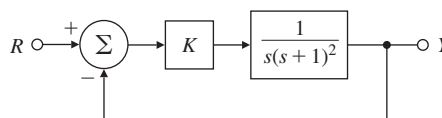
$$|KG(j\omega)| = 1 \quad \text{and} \quad \angle G(j\omega) = 180^\circ. \quad (6.24)$$

Thus, a Bode plot of a system that is neutrally stable (i.e., with  $K$  defined such that a closed-loop root falls on the imaginary axis) will satisfy the conditions of Eq. (6.24). Figure 6.15 shows the frequency response for the system whose root locus is plotted in Fig. 6.14(b) for various values of  $K$ . The magnitude response corresponding to  $K = 2$  passes through 1 at the same frequency ( $\omega = 1$  rad/sec) at which the phase passes through  $180^\circ$ , as predicted by Eq. (6.24).

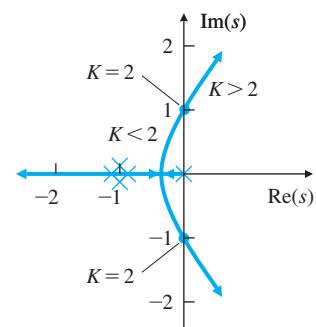
Having determined the point of neutral stability, we turn to a key question: Does increasing the gain increase or decrease the system's stability? We can see from the root locus in Fig. 6.14(b) that any value of  $K$  less than the value at the neutrally stable point will result in a stable system. At the frequency  $\omega$  where the phase  $\angle G(j\omega) = -180^\circ$  ( $\omega = 1$  rad/sec), the magnitude  $|KG(j\omega)| < 1.0$  for stable values of  $K$  and  $> 1$  for unstable values of  $K$ . Therefore, we have the following trial

**Figure 6.14**

Stability example:  
(a) system definition;  
(b) root locus



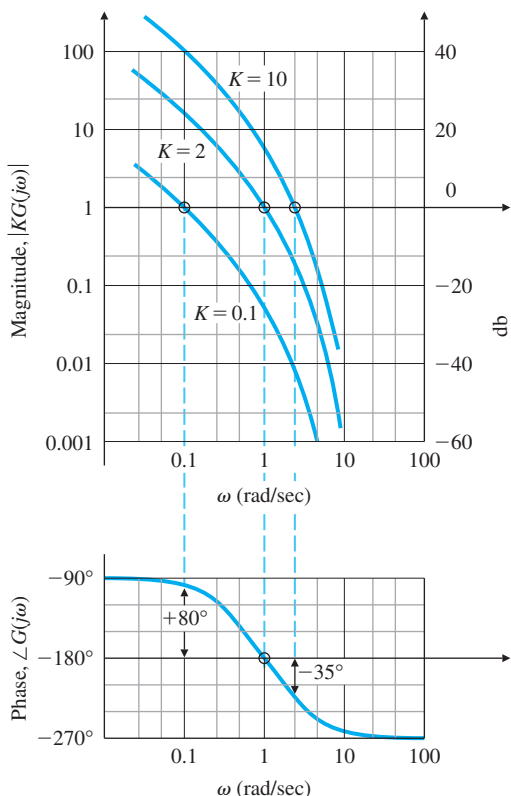
(a)



(b)

**Figure 6.15**

Frequency-response magnitude and phase for the system in Fig. 6.14



stability condition, based on the character of the open-loop frequency response:

#### Stability condition

$$|KG(j\omega)| < 1 \quad \text{at} \quad \angle G(j\omega) = -180^\circ. \quad (6.25)$$

This stability criterion holds for all systems for which increasing gain leads to instability and  $|KG(j\omega)|$  crosses the magnitude (=1) once, the most common situation. However, there are systems for which an increasing gain can lead from instability to stability; in this case, the stability condition is

$$|KG(j\omega)| > 1 \quad \text{at} \quad \angle G(j\omega) = -180^\circ. \quad (6.26)$$

There are also cases when  $|KG(j\omega)|$  crosses magnitude (=1) more than once. One way to resolve the ambiguity that is usually sufficient is to perform a rough sketch of the root locus. Another more rigorous way to resolve the ambiguity is to use the Nyquist stability criterion, the subject of the next section. However, because the Nyquist criterion is fairly complex, it is important while studying it to bear in mind the theme of this section—namely, that for most systems a simple relationship exists between closed-loop stability and the open-loop frequency response.

## 6.3 The Nyquist Stability Criterion

For most systems, as we saw in the previous section, an increasing gain eventually causes instability. In the very early days of feedback control design, this relationship between gain and stability margins was assumed to be universal. However, designers found occasionally that in the laboratory the relationship reversed itself; that is, the amplifier would become unstable when the gain was decreased. The confusion caused by these conflicting observations motivated Harry Nyquist of the Bell Telephone Laboratories to study the problem in 1932. His study explained the occasional reversals, and resulted in a more sophisticated analysis without loopholes. Not surprisingly, his test has come to be called the **Nyquist stability criterion**. It is based on a result from complex variable theory known as the **argument principle**,<sup>8</sup> as we briefly explain in this section. More detail is contained in online Appendix WD.

The Nyquist stability criterion relates the open-loop frequency response to the number of closed-loop poles of the system in the RHP. Study of the Nyquist criterion will allow you to determine stability from the frequency response of a complex system, perhaps with one or more resonances, where the magnitude curve crosses 1 several times and/or the phase crosses  $180^\circ$  several times. It is also very useful in dealing with open-loop unstable systems, nonminimum-phase systems, and systems with pure delays (transportation lags).

### 6.3.1 The Argument Principle

Consider the transfer function  $H_1(s)$  whose poles and zeros are indicated in the  $s$ -plane in Fig. 6.16(a). We wish to evaluate  $H_1$  for values of  $s$  on the clockwise contour  $C_1$ . (Hence this is called a **contour evaluation**.) We choose the test point  $s_o$  for evaluation. The resulting complex quantity has the form  $H_1(s_o) = \vec{v} = |\vec{v}|e^{j\alpha}$ . The value of the argument of  $H_1(s_o)$  is

$$\alpha = \theta_1 + \theta_2 - (\phi_1 + \phi_2).$$

As  $s$  traverses  $C_1$  in the clockwise direction starting at  $s_o$ , the angle  $\alpha$  of  $H_1(s)$  in Fig. 6.16(b) will change (decrease or increase), but it will not undergo a net change of  $360^\circ$  as long as there are no poles or zeros within  $C_1$ . This is because none of the angles that make up  $\alpha$  go through a net revolution. The angles  $\theta_1$ ,  $\theta_2$ ,  $\phi_1$ , and  $\phi_2$  increase or decrease as  $s$  traverses around  $C_1$ , but they return to their original values as  $s$  returns to  $s_o$  without rotating through  $360^\circ$ . This means that the plot of  $H_1(s)$  [see Fig. 6.16(b)] will not encircle the origin. This conclusion follows from the fact that  $\alpha$  is the sum of the angles indicated in Fig. 6.16(a), so the only way that  $\alpha$  can be changed by  $360^\circ$  after  $s$  executes one full traverse of  $C_1$  is for  $C_1$  to contain a pole or zero.

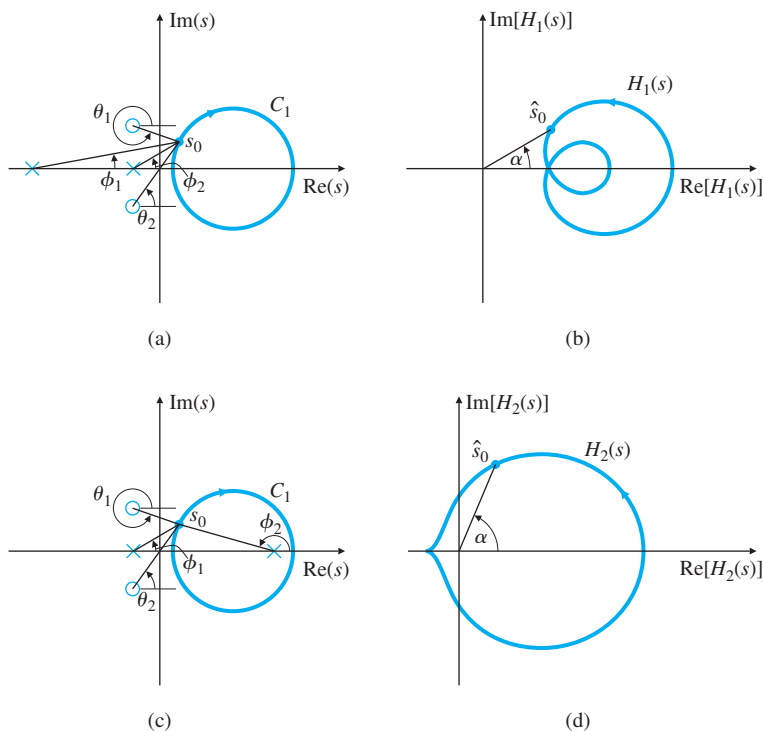
Now consider the function  $H_2(s)$ , whose pole-zero pattern is shown in Fig. 6.16(c). Note it has a singularity (pole) within  $C_1$ . Again, we start

---

<sup>8</sup>Sometimes referred to as “Cauchy’s Principle of the Argument.”

**Figure 6.16**

Contour evaluations:  
 (a)  $s$ -plane plot of poles and zeros of  $H_1(s)$  and the contour  $C_1$ ;  
 (b)  $H_1(s)$  for  $s$  on  $C_1$ ;  
 (c)  $s$ -plane plot of poles and zeros of  $H_2(s)$  and the contour  $C_1$ ;  
 (d)  $H_2(s)$  for  $s$  on  $C_1$



at the test point  $s_o$ . As  $s$  traverses in the clockwise direction around  $C_1$ , the contributions from the angles  $\theta_1$ ,  $\theta_2$ , and  $\phi_1$  change, but they return to their original values as soon as  $s$  returns to  $s_o$ . In contrast,  $\phi_2$ , the angle from the pole within  $C_1$ , undergoes a net change of  $-360^\circ$  after one full traverse of  $C_1$ . Therefore, the argument of  $H_2(s)$  undergoes the same change, causing  $H_2$  to encircle the origin in the counterclockwise direction, as shown in Fig. 6.16(d). The behavior would be similar if the contour  $C_1$  had enclosed a zero instead of a pole. The mapping of  $C_1$  would again enclose the origin once in the  $H_2(s)$ -plane, except it would do so in the clockwise direction.

Thus we have the essence of the argument principle:

A contour map of a complex function will encircle the origin  $Z - P$  times, where  $Z$  is the number of zeros and  $P$  is the number of poles of the function inside the contour.

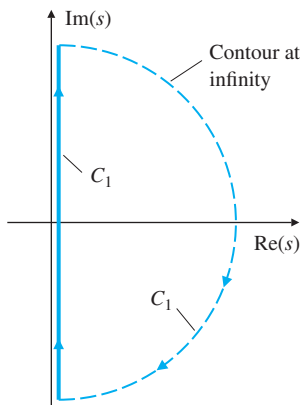
For example, if the number of poles and zeros within  $C_1$  is the same, the net angles cancel and there will be no net encirclement of the origin.

### 6.3.2 Application of The Argument Principle to Control Design

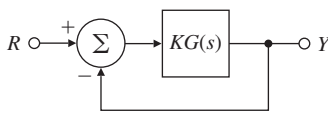
To apply the principle to control design, we let the  $C_1$  contour in the  $s$ -plane encircle the entire RHP, the region in the  $s$ -plane where a pole

**Figure 6.17**

An  $s$ -plane plot of a contour  $C_1$  that encircles the entire RHP

**Figure 6.18**

Block diagram for  
 $Y(s)/R(s) = KG(s)/[1 + KG(s)]$



would cause an unstable system (see Fig. 6.17). The resulting evaluation of  $H(s)$  will encircle the origin only if  $H(s)$  has an RHP pole or zero.

As stated earlier, what makes all this contour behavior useful is that a contour evaluation of an *open-loop*  $KG(s)$  can be used to determine stability of the *closed-loop* system. Specifically, for the system in Fig. 6.18, the closed-loop transfer function is

$$\frac{Y(s)}{R(s)} = T(s) = \frac{KG(s)}{1 + KG(s)}.$$

Therefore, the closed-loop roots are the solutions of

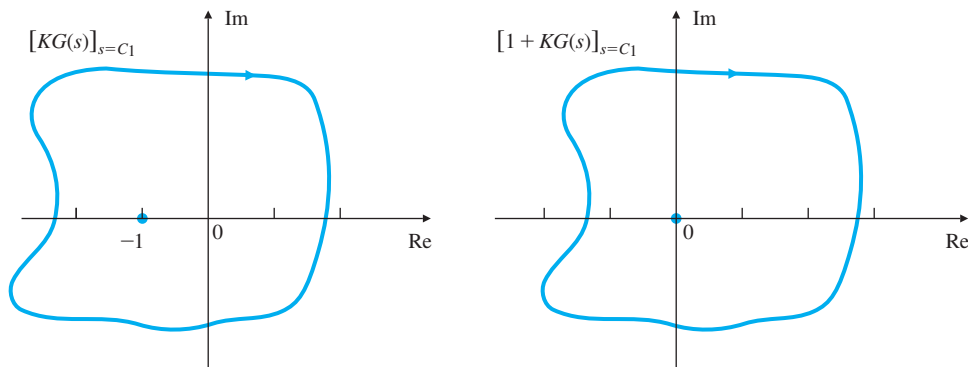
$$1 + KG(s) = 0,$$

and we apply the principle of the argument to the function  $1 + KG(s)$ . If the evaluation contour of this function of  $s$  enclosing the entire RHP contains a zero or pole of  $1 + KG(s)$ , then the evaluated contour of  $1 + KG(s)$  will encircle the origin. Notice  $1 + KG(s)$  is simply  $KG(s)$  shifted to the right 1 unit, as shown in Fig. 6.19. Therefore, if the plot of  $1 + KG(s)$  encircles the origin, the plot of  $KG(s)$  will encircle  $-1$  on the real axis. Therefore, we can plot the contour evaluation of the open-loop  $KG(s)$ , examine its encirclements of  $-1$ , and draw conclusions about the origin encirclements of the closed-loop function  $1 + KG(s)$ . Presentation of the evaluation of  $KG(s)$  in this manner is often referred to as a **Nyquist plot**, or **polar plot**, because we plot the magnitude of  $KG(s)$  versus the angle of  $KG(s)$ .

To determine whether an encirclement is due to a pole or zero, we write  $1 + KG(s)$  in terms of poles and zeros of  $KG(s)$ :

$$1 + KG(s) = 1 + K \frac{b(s)}{a(s)} = \frac{a(s) + Kb(s)}{a(s)}. \quad (6.27)$$

**Nyquist plot; polar plot**

**Figure 6.19**

Evaluations of  $KG(s)$  and  $1 + KG(s)$ : Nyquist plots

Equation (6.27) shows the poles of  $1 + KG(s)$  are also the poles of  $G(s)$ . Because it is safe to assume the poles of  $G(s)$  [or factors of  $a(s)$ ] are known, the (rare) existence of any of these poles in the RHP can be accounted for. Assuming for now there are no poles of  $G(s)$  in the RHP, an encirclement of  $-1$  by  $KG(s)$  indicates a zero of  $1 + KG(s)$  in the RHP, and thus an unstable root of the closed-loop system.

We can generalize this basic idea by noting that a clockwise contour  $C_1$  enclosing a zero of  $1 + KG(s)$ —that is, a closed-loop system root—will result in  $KG(s)$  encircling the  $-1$  point in a clockwise direction. Likewise, if  $C_1$  encloses a pole of  $1 + KG(s)$ —that is, if there is an unstable open-loop pole—there will be a counterclockwise  $KG(s)$  encirclement of  $-1$ . Furthermore, if two poles or two zeros are in the RHP,  $KG(s)$  will encircle  $-1$  twice, and so on. The net number of clockwise encirclements,  $N$ , equals the number of zeros (closed-loop system roots) in the RHP,  $Z$ , minus the number of open-loop poles in the RHP,  $P$ :

$$N = Z - P.$$

This is the key concept of the Nyquist stability criterion.

A simplification in the plotting of  $KG(s)$  results from the fact that any  $KG(s)$  that represents a physical system will have zero response at infinite frequency (i.e., has more poles than zeros). This means that the big arc of  $C_1$  corresponding to  $s$  at infinity (see Fig. 6.17) results in  $KG(s)$  being a point of infinitesimally small value near the origin for that portion of  $C_1$ . Therefore, we accomplish a complete evaluation of a physical system  $KG(s)$  by letting  $s$  traverse the imaginary axis from  $-j\infty$  to  $+j\infty$  (actually, from  $-j\omega_h$  to  $+j\omega_h$ , where  $\omega_h$  is large enough that  $|KG(j\omega)|$  is much less than 1 for all  $\omega > \omega_h$ ). The evaluation of  $KG(s)$  from  $s = 0$  to  $s = j\infty$  has already been discussed in Section 6.1 under the context of finding the frequency response of  $KG(s)$ . Because  $G(-j\omega)$  is the complex conjugate of  $G(j\omega)$ , we can easily obtain the entire plot of  $KG(s)$  by reflecting the  $0 \leq s \leq +j\infty$  portion about the real axis, to get the  $-j\infty \leq s < 0$  portion. Hence, we see that

closed-loop stability can be determined in all cases by examination of the frequency response of the open-loop transfer function on a polar plot. In some applications, models of physical systems are simplified so as to eliminate some high-frequency dynamics. The resulting reduced-order transfer function might have an equal number of poles and zeros. In that case, the big arc of  $C_1$  at infinity needs to be considered.

In practice, many systems behave like those discussed in Section 6.2, so you need not carry out a complete evaluation of  $KG(s)$  with subsequent inspection of the  $-1$  encirclements; a simple look at the frequency response may suffice to determine stability. However, in the case of a complex system for which the simplistic rules given in Section 6.2 become ambiguous, you will want to perform the complete analysis, summarized as follows:

#### *Procedure for Determining Nyquist Stability*

1. Plot  $KG(s)$  for  $-j\infty \leq s \leq +j\infty$ . Do this by first evaluating  $KG(j\omega)$  for  $\omega = 0$  to  $\omega_h$ , where  $\omega_h$  is so large that the magnitude of  $KG(j\omega)$  is negligibly small for  $\omega > \omega_h$ , then reflecting the image about the real axis and adding it to the preceding image. The magnitude of  $KG(j\omega)$  will be small at high frequencies for any physical system. The Nyquist plot will always be symmetric with respect to the real axis. The plot is normally created by the NYQUIST Matlab function.
2. Evaluate the number of clockwise encirclements of  $-1$ , and call that number  $N$ . Do this by drawing a straight line in any direction from  $-1$  to  $\infty$ . Then count the net number of left-to-right crossings of the straight line by  $KG(s)$ . If encirclements are in the counterclockwise direction,  $N$  is negative.
3. Determine the number of unstable (RHP) poles of  $G(s)$ , and call that number  $P$ .
4. Calculate the number of unstable closed-loop roots  $Z$ :

$$Z = N + P. \quad (6.28)$$

For stability, we wish to have  $Z = 0$ ; that is, no characteristic equation roots in the RHP.

Let us now examine a rigorous application of the procedure for determining stability using Nyquist plots for some examples.

### EXAMPLE 6.8

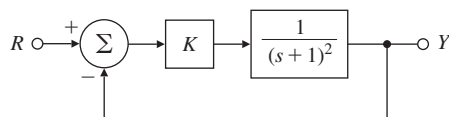
#### *Nyquist Plot for a Second-Order System*

Determine the stability properties of the system defined in Fig. 6.20.

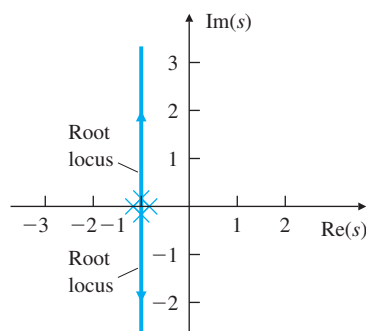
**Solution.** The root locus of the system in Fig. 6.20 is shown in Fig. 6.21. It shows the system is stable for all values of  $K$ . The magnitude of the frequency response of  $KG(s)$  is plotted in Fig. 6.22(a) for  $K = 1$ , and the

**Figure 6.20**

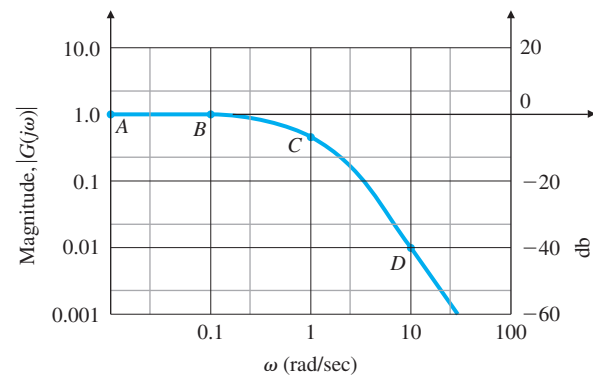
Control system for Example 6.8

**Figure 6.21**

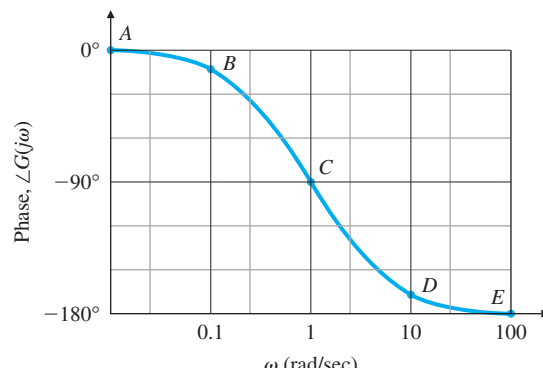
Root locus of  $G(s) = \frac{1}{(s+1)^2}$  with respect to  $K$

**Figure 6.22**

Open-loop Bode plot for  $G(s) = \frac{1}{(s+1)^2}$



(a)

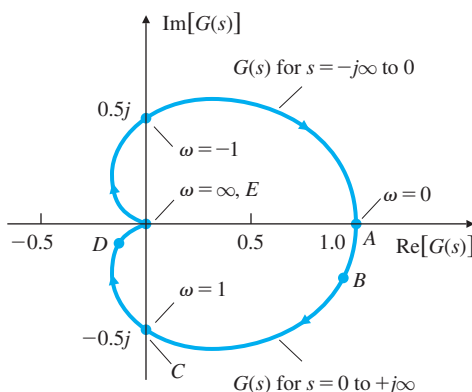


(b)

phase is plotted in Fig. 6.22(b); this is the typical Bode method of presenting frequency response and represents the evaluation of  $G(s)$  over the interesting range of frequencies. The same information is replotted in Fig. 6.23 in the Nyquist (polar) plot form. Note how the points A,

**Figure 6.23**

Nyquist plot<sup>9</sup> of the evaluation of  $KG(s)$  for  $s = C_1$  and  $K = 1$



$B$ ,  $C$ ,  $D$ , and  $E$  are mapped from the Bode plot to the Nyquist plot in Fig. 6.23. The arc from  $G(s) = +1$  ( $\omega = 0$ ) to  $G(s) = 0$  ( $\omega = \infty$ ) that lies below the real axis is derived from Fig. 6.22. The portion of the  $C_1$  arc at infinity from Fig. 6.17 transforms into  $G(s) = 0$  in Fig. 6.23; therefore, a continuous evaluation of  $G(s)$  with  $s$  traversing  $C_1$  is completed by simply reflecting the lower arc about the real axis. This creates the portion of the contour above the real axis and completes the Nyquist (polar) plot. Because the plot does not encircle  $-1$ ,  $N = 0$ . Also, there are no poles of  $G(s)$  in the RHP, so  $P = 0$ . From Eq. (6.28), we conclude that  $Z = 0$ , which indicates there are no unstable roots of the closed-loop system for  $K = 1$ . Furthermore, different values of  $K$  would simply change the magnitude of the polar plot, but no positive value of  $K$  would cause the plot to encircle  $-1$ , because the polar plot will always cross the negative real axis when  $KG(s) = 0$ . Thus the Nyquist stability criterion confirms what the root locus indicated: the closed-loop system is stable for all  $K > 0$ .

The Matlab statements that will produce this Nyquist plot are

```
s = tf('s');
sysG = 1/(s+1)^2;
nyquist(sysG);
```

---

Often the control systems engineer is more interested in determining a range of gains  $K$  for which the system is stable than in testing for stability at a specific value of  $K$ . To accommodate this requirement, but to avoid drawing multiple Nyquist plots for various values of the gain, the test can be modified slightly. To do so, we scale  $KG(s)$  by  $K$  and examine  $G(s)$  to determine stability for a range of gains  $K$ . This is possible because an encirclement of  $-1$  by  $KG(s)$  is equivalent to

---

<sup>9</sup>The shape of this Nyquist plot is a cardioid, meaning “heart-shaped,” plane curve. The name was first used by de Castillon in the *Philosophical Transactions of the Royal Society* in 1741. The cardioid is also used in optics.

an encirclement of  $-1/K$  by  $G(s)$ . Therefore, instead of having to deal with  $KG(s)$ , we need only consider  $G(s)$ , and count the number of the encirclements of the  $-1/K$  point.

Applying this idea to Example 6.8, we see that the Nyquist plot cannot encircle the  $-1/K$  point. For positive  $K$ , the  $-1/K$  point will move along the negative real axis, so there will not be an encirclement of  $G(s)$  for any value of  $K > 0$ .

(There are also values of  $K < 0$  for which the Nyquist plot shows the system to be stable; specifically,  $-1 < K < 0$ . This result may be verified by drawing the  $0^\circ$  locus.)

## EXAMPLE 6.9

### Nyquist Plot for a Third-Order System

As a second example, consider the system  $G(s) = 1/s(s + 1)^2$  for which the closed-loop system is defined in Fig. 6.24. Determine its stability properties using the Nyquist criterion.

**Solution.** This is the same system discussed in Section 6.2. The root locus in Fig. 6.14(b) shows this system is stable for small values of  $K$ , but unstable for large values of  $K$ . The magnitude and phase of  $G(s)$  in Fig. 6.25 are transformed into the Nyquist plot shown in Fig. 6.26. Note how the points  $A, B, C, D$ , and  $E$  on the Bode plot of Fig. 6.25 map into those on the Nyquist plot of Fig. 6.26. Also note the large arc at infinity that arises from the open-loop pole at  $s = 0$ . This pole creates an infinite magnitude of  $G(s)$  at  $\omega = 0$ ; in fact, a pole anywhere on the imaginary axis will create an arc at infinity. To correctly determine the number of  $-1/K$  point encirclements, we must draw this arc in the proper half-plane: Should it cross the positive real axis, as shown in Fig. 6.26, or the negative one? It is also necessary to assess whether the arc should sweep out  $180^\circ$  (as in Fig. 6.26),  $360^\circ$ , or  $540^\circ$ .

A simple artifice suffices to answer these questions. We modify the  $C_1$  contour to take a small detour around the pole either to the right (see Fig. 6.27) or to the left. It makes no difference to the final stability question which way the detour goes around the pole, but it is more convenient to go to the right because then no poles are introduced within the  $C_1$  contour, keeping the value of  $P$  equal to 0. Because the phase of  $G(s)$  is the negative of the sum of the angles from all of the poles, we see that the evaluation results in a Nyquist plot moving from  $+90^\circ$  for  $s$  just below the pole at  $s = 0$ , across the positive real axis to  $-90^\circ$  for

**Figure 6.24**  
Control system for  
Example 6.9

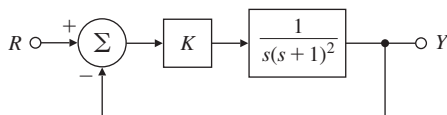


**Figure 6.25**  
Bode plot for  
 $G(s) = 1/s(s + 1)^2$

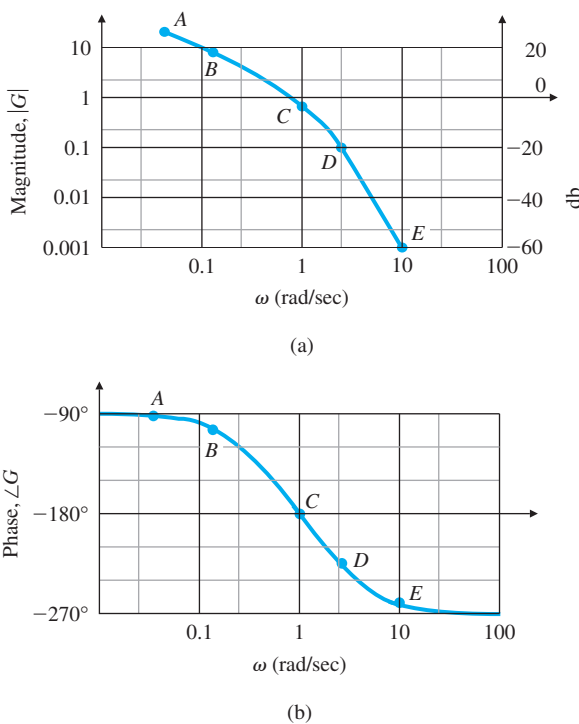
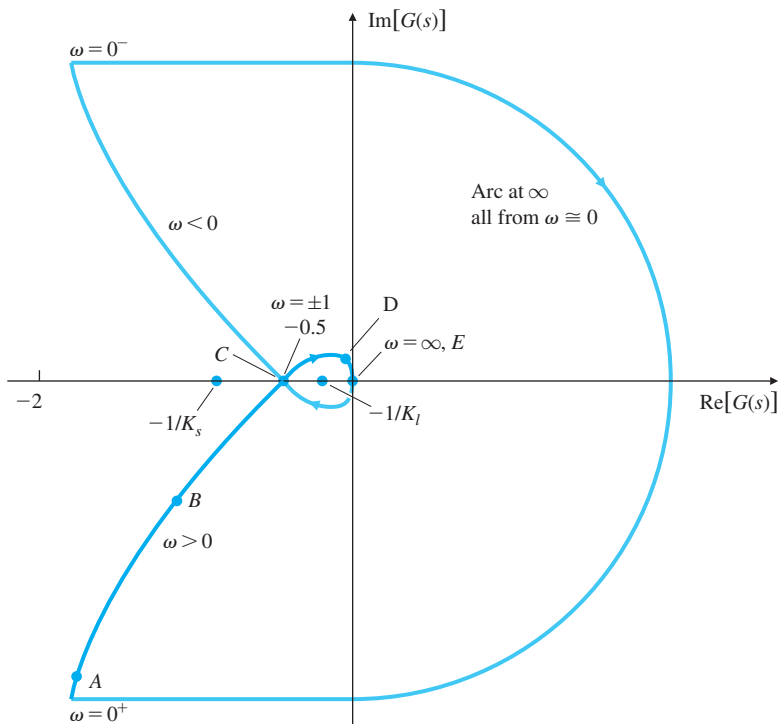


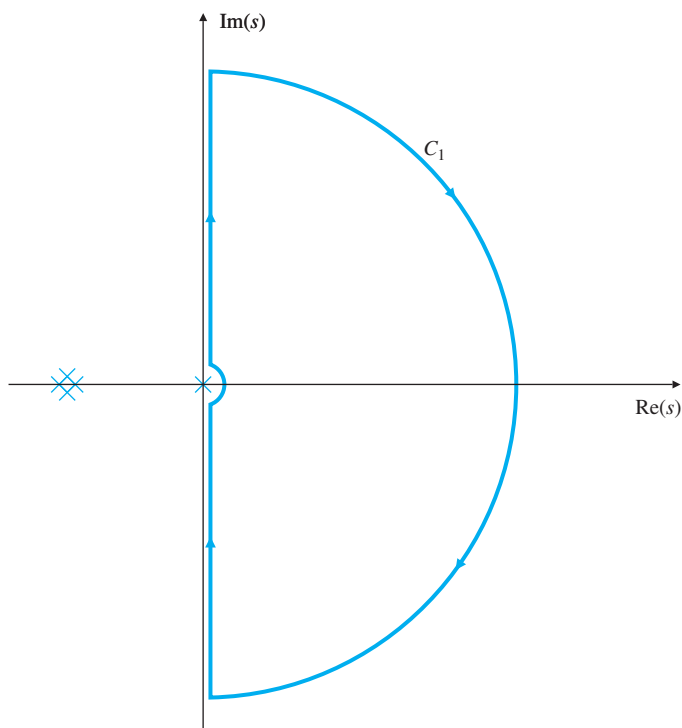
**Figure 6.26**  
Nyquist plot<sup>10</sup> for  
 $G(s) = \frac{1}{s(s+1)^2}$



<sup>10</sup>The shape of this Nyquist plot is a translated strophoid plane curve, meaning “a belt with a twist.” The curve was first studied by Barrow in 1670.

**Figure 6.27**

$C_1$  contour enclosing the RHP for the system in Example 6.9



$s$  just above the pole. Had there been two poles at  $s = 0$ , the Nyquist plot at infinity would have executed a full  $360^\circ$  arc, and so on for three or more poles. Furthermore, for a pole elsewhere on the imaginary axis, a  $180^\circ$  clockwise arc would also result but would be oriented differently than the example shown in Fig. 6.26.

The Nyquist plot crosses the real axis at  $\omega = 1$  with  $|G| = 0.5$ , as indicated by the Bode plot. For  $K > 0$ , there are two possibilities for the location of  $-1/K$ : inside the two loops of the Nyquist plot, or outside the Nyquist contour completely. For large values of  $K$  ( $K_l$  in Fig. 6.26),  $-0.5 < -1/K_l < 0$  will lie inside the two loops; hence  $N = 2$ , and therefore,  $Z = 2$ , indicating that there are two unstable roots. This happens for  $K > 2$ . For small values of  $K$  ( $K_s$  in Fig. 6.26),  $-1/K$  lies outside the loops; thus  $N = 0$ , and all roots are stable. All this information is in agreement with the root locus in Fig. 6.14(b). (When  $K < 0$ ,  $-1/K$  lies on the positive real axis, then  $N = 1$ , which means  $Z = 1$  and the system has one unstable root. The  $0^\circ$  root locus will verify this result.)

For this and many similar systems, we can see that the encirclement criterion reduces to a very simple test for stability based on the open-loop frequency response: The system is stable if  $|KG(j\omega)| < 1$  when the phase of  $G(j\omega)$  is  $180^\circ$ . Note this relation is identical to the stability criterion given in Eq. (6.25); however, by using the Nyquist criterion,

we don't require the root locus to determine whether  $|KG(j\omega)| < 1$  or  $|KG(j\omega)| > 1$ .

We draw the Nyquist plot using Matlab, with

```
s = tf('s');
sysG = 1 / (s*(s+1)^2);
nyquist(sysG)
axis([-3 3 -3 3])
```

The axis command scaled the plot so only points between +3 and -3 on the real and imaginary axes were included. Without manual scaling, the plot would be scaled based on the maximum values computed by Matlab and the essential features in the vicinity of the -1 region would be lost.

For systems that are open-loop unstable, care must be taken because now  $P \neq 0$  in Eq. (6.28). We shall see that the simple rules from Section 6.2 will need to be revised in this case.

## EXAMPLE 6.10

### Nyquist Plot for an Open-Loop Unstable System

The third example is defined in Fig. 6.28. Determine its stability properties using the Nyquist criterion.

**Solution.** The root locus for this system is sketched in Fig. 6.29 for  $K > 1$ . The open-loop system is unstable because it has a pole in the RHP. The open-loop Bode plot is shown in Fig. 6.30. Note in the Bode that  $|KG(j\omega)|$  behaves exactly the same as if the pole had been in the LHP. However,  $\angle G(j\omega)$  increases by  $90^\circ$  instead of the usual decrease

**Figure 6.28**  
Control system for Example 6.10

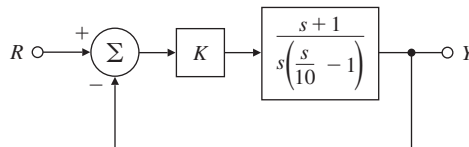


**Figure 6.29**  
Root locus for  
 $G(s) = \frac{(s+1)}{s(s/10-1)}$

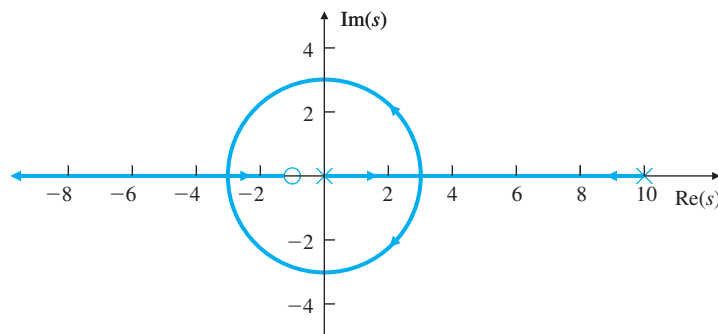
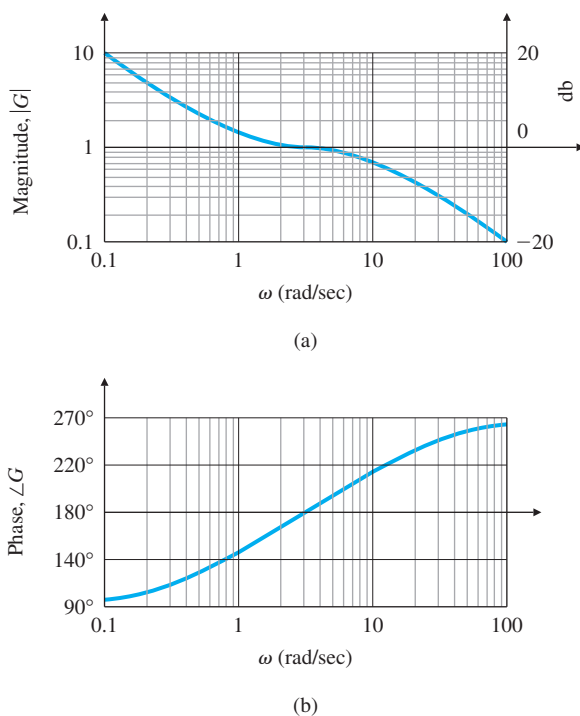


**Figure 6.30**

Bode plot for  
 $G(s) = \frac{(s+1)}{s(s/10-1)}$



at a pole. Any system with a pole in the RHP is unstable; hence, it is difficult<sup>11</sup> to determine its frequency response experimentally because the system never reaches a steady-state sinusoidal response for a sinusoidal input. It is, however, possible to compute the magnitude and phase of the transfer function according to the rules in Section 6.1. The pole in the RHP affects the Nyquist encirclement criterion, because the value of  $P$  in Eq. (6.28) is +1.

We convert the frequency-response information of Fig. 6.30 into the Nyquist plot in Fig. 6.31(a) as in the previous examples. As before, the  $C_1$  detour around the pole at  $s = 0$  in Fig. 6.31(b) creates a large arc at infinity in Fig. 6.31(a). This arc crosses the *negative* real axis because of the  $180^\circ$  phase contribution of the pole in the RHP as shown by Fig. 6.31(b).

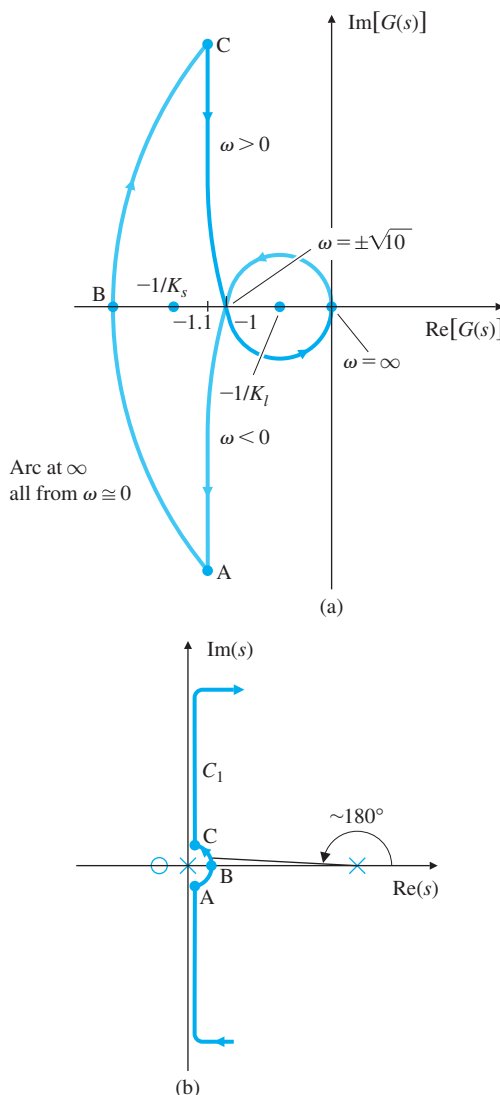
The real-axis crossing occurs at  $|G(s)| = 1$  because in the Bode plot  $|G(s)| = 1$  when  $\angle G(s) = +180^\circ$ , which happens to be at  $\omega \cong 3$  rad/sec.

By expanding  $G(j\omega)$  into its real and imaginary parts, it can be seen that the real part approaches  $-1.1$  as  $\omega \rightarrow \pm\infty$ . This is shown to be the case as the asymptotes approach points A and C in Fig. 6.31(a).

<sup>11</sup>It is possible to determine the frequency response of an unstable plant experimentally by placing a stabilizing feedback around it, then measuring the amplitude and phase of the input and output of the plant while providing input to the entire system through the frequency range of interest.

**Figure 6.31**

Example 6.10, (a)  
 Nyquist plot of  
 $G(s) = \frac{(s+1)}{s(s/10-1)}$ , (b)  $C_1$   
 contour



The contour shows two different behaviors, depending on the values of  $K$  ( $> 0$ ). For large values of  $K$  ( $K_l$  in Fig. 6.31(a)), there is one counterclockwise encirclement of the  $-1$  point ( $-1/K_l$  in the figure); hence,  $N = -1$ . However, because  $P = 1$  from the RHP pole,  $Z = N + P = 0$ , so there are no unstable system roots and the system is stable for  $K > 1$ . For small values of  $K$  [ $K_s$  in Fig. 6.31(a)],  $N = +1$  because of the clockwise encirclement of  $-1$  ( $-1/K_s$  in the figure) and  $Z = 2$ , indicating two unstable roots. These results can be verified qualitatively by the root locus in Fig. 6.29 where we see that low values of  $K$  produce the portions of the loci that are in the RHP (unstable) and that both branches cross into the LHP (stable) for high values of  $K$ .

If  $K < 0$ ,  $-1/K$  is on the positive real axis so  $N = 0$  and  $Z = 1$ , indicating the system will have one unstable closed-loop pole. A  $0^\circ$  root locus will show a branch of the locus emanating from the pole at  $s = +10$  to infinity; thus verifying that there will always be one unstable root.

As with all systems, the stability boundary occurs at  $|KG(j\omega)| = 1$  for the phase of  $\angle G(j\omega) = 180^\circ$ . However, in this case,  $|KG(j\omega)|$  must be greater than 1 to yield the correct number of  $-1$  point encirclements to achieve stability. This polarity reversal of the normal rules can be rigorously determined via the Nyquist plot; however, in practice, it is usually more expedient to sketch the root locus and to determine the correct rules based on its behavior.

To draw the Nyquist plot using Matlab, use the following commands:

```
s = tf('s');
sysG = (s + 1)/(s*(s/10 - 1));
nyquist(sysG)
axis([-3 3 -3 3])
```

The existence of the RHP pole in Example 6.10 affected the Bode plotting rules of the phase curve and affected the relationship between encirclements and unstable closed-loop roots because  $P = 1$  in Eq. (6.28). But we apply the Nyquist stability criterion without any modifications. The same is true for systems with a RHP zero; that is, a nonminimum-phase zero has no effect on the Nyquist stability criterion, but the Bode plotting rules are affected.

## EXAMPLE 6.11

### *Nyquist Plot Characteristics*

Find the Nyquist plot for the second-order system

$$G(s) = \frac{s^2 + 3}{(s + 1)^2}$$

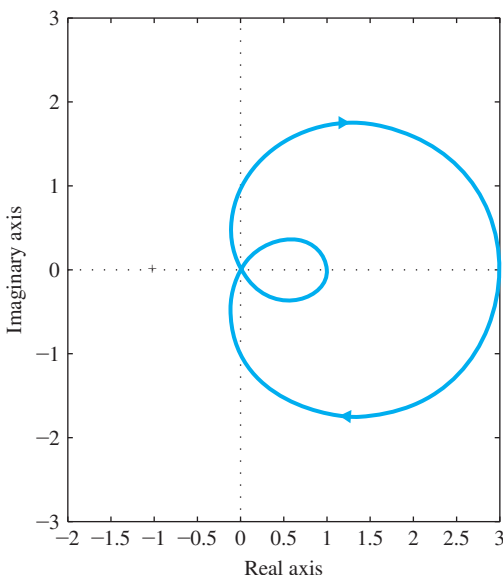
and reconcile the plot with the characteristics of  $G(s)$ . If the  $G(s)$  is to be included in a feedback system as shown in Fig. 6.18, then determine whether the system is stable for all positive values of  $K$ .

**Solution.** To draw the Nyquist plot using Matlab, use the following commands:

```
s = tf('s');
sysG = (s^2 + 3)/(s + 1)^2;
nyquist(sysG)
axis([-2 3 -3 3])
```

The result is shown in Fig. 6.32. Note there are no arcs at infinity for this case due to the lack of any poles at the origin or on the  $j\omega$  axis. Also note the Nyquist curve associated with the Bode plot ( $s = +j\omega$ ) starts

**Figure 6.32**  
Nyquist plot<sup>12</sup> for  
Example 6.11



at  $(3, 0)$ , ends at  $(1, 0)$ , and, therefore, starts and ends with a phase angle of  $0^\circ$ . This is as it should be since the numerator and denominator of  $G(s)$  are equal order and there are no singularities at the origin. So the Bode plot should start and end with a zero phase. Also note the Nyquist plot goes through  $(0, 0)$  as  $s$  goes through  $s = +j\sqrt{3}$ , as it should since the magnitude equals zero when  $s$  is at a zero. Furthermore, note the phase goes from  $-120^\circ$  as  $s$  approaches  $(0, 0)$  to  $+60^\circ$  as  $s$  departs from  $(0, 0)$ . This behavior follows since a Bode plot phase will jump by  $+180^\circ$  instantaneously as  $s$  passes through a zero on the  $j\omega$  axis. The phase initially decreases as the plot leaves the starting point at  $(3, 0)$  because the lowest frequency singularity is the pole at  $s = -1$ .

Changing the gain,  $K$ , will increase or decrease the magnitude of the Nyquist plot but it can never cross the negative-real axis. Therefore, the closed-loop system will always be stable for positive  $K$ . Exercise: Verify this result by making a rough root-locus sketch by hand.

## 6.4 Stability Margins

A large fraction of control system designs behave in a pattern roughly similar to that of the system in Section 6.2 and Example 6.9 in Section 6.3; that is, the system is stable for all small gain values and becomes unstable if the gain increases past a certain critical point. Knowing exactly what the margins are for which a control system remains stable is of critical importance. Two commonly used quantities that measure the stability margin for such systems are directly related

<sup>12</sup>The shape of this Nyquist plot is a limaçon, a fact pointed out by the third author's son, who was in a 10th grade trigonometry class at the time. Limaçon means "snail" in French from the Latin "limax," and was first investigated by Dürer in 1525.

to the stability criterion of Eq. (6.25): gain margin and phase margin. In this section, we will define and use these two concepts to study system design. Another measure of stability, originally defined by Smith (1958), combines these two margins into one called the **vector margin** (sometimes called the **complex margin**) which gives a better indication of stability for complicated cases.

### Gain margin

The **gain margin (GM)** is the factor by which the gain can be increased (or decreased in certain cases) before instability results. For the typical case, it can be read directly from the Bode plot (see Fig. 6.15) by measuring the vertical distance between the  $|KG(j\omega)|$  curve and the magnitude = 1 line at the frequency where  $\angle G(j\omega) = -180^\circ$ . We see from the figure that when  $K = 0.1$ , the  $GM = 20$  (or 26 db) because  $|KG(j\omega)| = 0.05$ . When  $K = 2$ , the system is neutrally stable with  $|KG(j\omega)| = 1$ , thus  $GM = 1$  (0 db). For  $K = 10$ ,  $|KG(j\omega)| = 5$ , the  $GM = 0.2$  (-14 db) and the system is unstable. Note, for this typical system, the GM is the *factor* by which the gain  $K$  can be increased before instability results; therefore,  $|GM| < 1$  (or  $|GM| < 0$  db) indicates an unstable system. The GM can also be determined from a root locus with respect to  $K$  by noting two values of  $K$ : (1) at the point where the locus crosses the  $j\omega$ -axis, and (2) at the nominal closed-loop poles. The GM is the ratio of these two values.

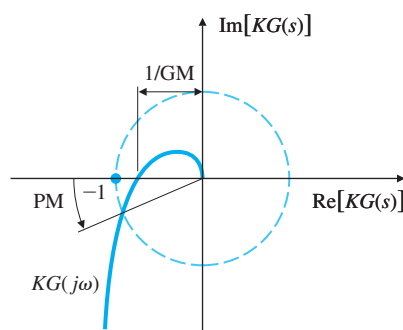
### Phase margin

Another measure that is used to indicate the stability margin in a system is the **phase margin (PM)**. It is the amount by which the phase of  $G(j\omega)$  exceeds  $-180^\circ$  when  $|KG(j\omega)| = 1$ , which is an alternative way of measuring the degree to which the stability conditions of Eq. (6.25) are met. For the case in Fig. 6.15, we see that  $PM \cong 80^\circ$  for  $K = 0.1$ ,  $PM = 0^\circ$  for  $K = 2$ , and  $PM = -35^\circ$  for  $K = 10$ . A positive PM is required for stability.

The stability margins may also be defined in terms of the Nyquist plot. Figure 6.33 shows that GM and PM are measures of how close the complex quantity  $G(j\omega)$  comes to encircling the  $-1$  point, which is another way of stating the neutral-stability point specified by Eq. (6.24). Again we can see that the GM indicates how much the gain can be raised before instability results in a system like the one in Example 6.9. The PM is the difference between the phase of  $G(j\omega)$  and  $180^\circ$  when  $KG(j\omega)$  crosses the circle  $|KG(s)| = 1$ ; the positive value of PM is assigned to

**Figure 6.33**

Nyquist plot for defining GM and PM



the stable case (i.e., with no Nyquist encirclements). So we see that the two margins measure the distance between the Nyquist plot and the  $-1$  point in two dimensions; the GM measures along the horizontal axis, while the PM measures along the unit circle.

It is easier to determine these margins directly from the Bode plot than from the Nyquist plot. The term **crossover frequency**,  $\omega_c$ , is often used to refer to the frequency at which the magnitude is unity, or 0 db. While the crossover frequency is easily determined from the open-loop frequency-response plot, this frequency is highly correlated with the closed-loop system bandwidth and, therefore, the speed of response of the system. The closed-loop system bandwidth was defined in Section 6.1 and its detailed relationship to the crossover frequency will be discussed in Section 6.6.

The open-loop frequency-response data shown in Figure 6.34 is the same data plotted in Fig. 6.25, but for the case with  $K = 1$ . The PM ( $= 22^\circ$ ) and GM ( $= 2$ ) are apparent from Figure 6.34 and match those that could have been obtained (with more difficulty) from the Nyquist plot shown in Fig. 6.26. The real-axis crossing at  $-0.5$  corresponds to a GM

### Crossover frequency

**Figure 6.34**  
GM and PM from the magnitude and phase plot

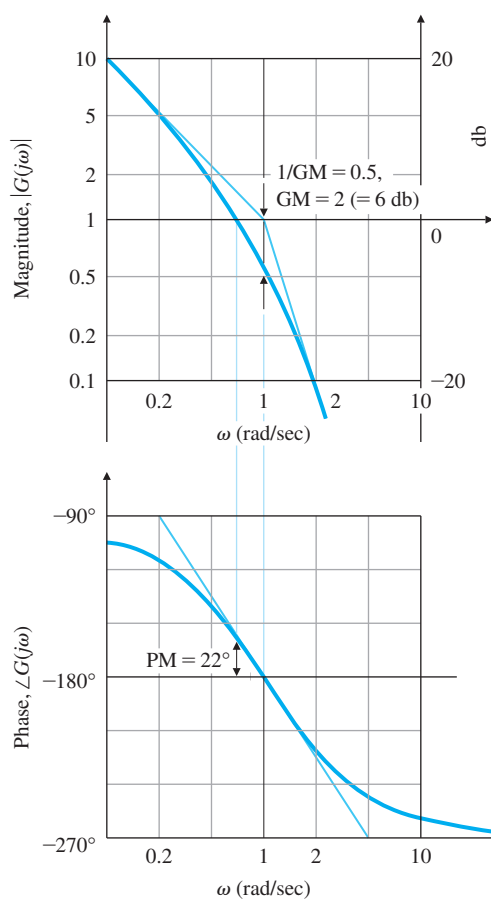
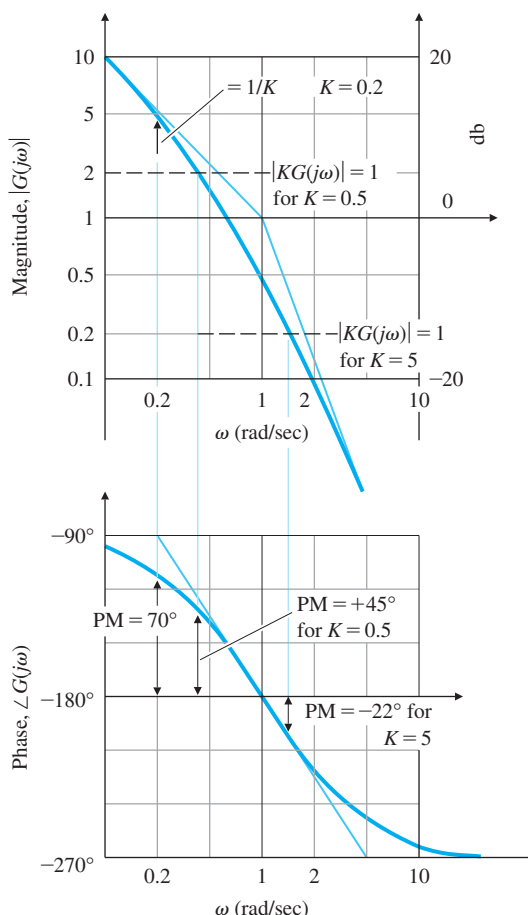


**Figure 6.35**

PM versus  $K$  from the frequency-response data



of  $1/0.5$  or  $2$  and the PM could be computed graphically by measuring the angle of  $G(j\omega)$  as it crosses the magnitude  $= 1$  circle.

One of the useful aspects of frequency-response design is the ease with which we can evaluate the effects of gain changes. In fact, we can determine the PM from Fig. 6.34 for any value of  $K$  without redrawing the magnitude or phase information. We need only indicate on the figure where  $|KG(j\omega)| = 1$  for selected trial values of  $K$ , as has been done with dashed lines in Fig. 6.35. Now we can see that  $K = 5$  yields an unstable PM of  $-22^\circ$ , while a gain of  $K = 0.5$  yields a PM of  $+45^\circ$ . Furthermore, if we wish a certain PM (say  $70^\circ$ ), we simply read the value of  $|G(j\omega)|$  corresponding to the frequency that would create the desired PM (here  $\omega = 0.2$  rad/sec yields  $70^\circ$ , where  $|G(j\omega)| = 5$ ), and note that the magnitude at this frequency is  $1/K$ . Therefore, a PM of  $70^\circ$  will be achieved with  $K = 0.2$ .

The PM is more commonly used to specify control system performance because it is most closely related to the damping ratio of the system. This can be seen for the open-loop second-order system

$$G(s) = \frac{\omega_n^2}{s(s + 2\zeta\omega_n)}, \quad (6.29)$$

which, with unity feedback, produces the closed-loop system

$$\mathcal{T}(s) = \frac{\omega_n^2}{s^2 + 2\zeta\omega_n s + \omega_n^2}. \quad (6.30)$$

It can be shown that the relationship between the PM and  $\zeta$  in this system is

$$\text{PM} = \tan^{-1} \left[ \frac{2\zeta}{\sqrt{\sqrt{1+4\zeta^4}-2\zeta^2}} \right]. \quad (6.31)$$

This function is plotted in Fig. 6.36. Note the function is approximately a straight line up to about  $\text{PM} = 60^\circ$ . The dashed line shows a straight-line approximation to the function, where

$$\zeta \cong \frac{\text{PM}}{100}. \quad (6.32)$$

It is clear that the approximation holds only for PM below about  $70^\circ$ . Furthermore, Eq. (6.31) is only accurate for the second-order system of Eq. (6.30). In spite of these limitations, Eq. (6.32) is often used as a rule of thumb for relating the closed-loop damping ratio to PM. It is useful as a starting point; however, it is always important to check the actual damping of a design, as well as other aspects of the performance, before calling the design complete.

The GM for the second-order system [given by Eq. (6.29)] is infinite ( $\text{GM} = \infty$ ), because the phase curve does not cross  $-180^\circ$  as the frequency increases. This would also be true for any first- or second-order system.

Additional data to aid in evaluating a control system based on its PM can be derived from the relationship between the resonant peak  $M_r$  and  $\zeta$  seen in Fig. 6.3. Note this figure was derived for the same system [Eq. (6.9)] as Eq. (6.30). We can convert the information in Fig. 6.36 into a form relating  $M_r$  to the PM. This is depicted in Fig. 6.37, along with the step-response overshoot  $M_p$ . Therefore, we see that, given the PM, one can determine the overshoot of the closed-loop step response for a

**Figure 6.36**

Damping ratio versus PM

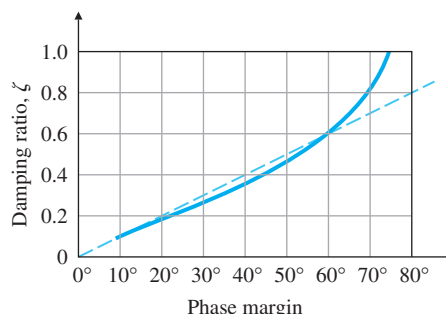
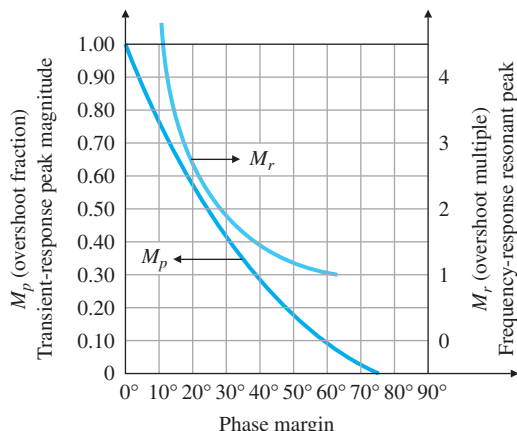


**Figure 6.37**

Transient-response overshoot ( $M_p$ ) and frequency-response resonant peak ( $M_r$ ) versus PM for

$$T(s) = \frac{\omega_n^2}{s^2 + 2\zeta\omega_n s + \omega_n^2}$$



second-order system with no zeros, which serves as a rough estimate for any system.

#### Importance of PM

Many engineers think directly in terms of the PM when judging whether a control system is adequately stabilized. In these terms, a  $PM = 30^\circ$  is often judged to be the lowest adequate value. Furthermore, some value of the PM is often stated specifically as a required specification of the feedback system design. In addition to testing the stability of a system design using the PM, a designer would typically also be concerned with meeting a speed-of-response specification such as bandwidth, as discussed in Section 6.1. In terms of the frequency-response parameters discussed so far, the crossover frequency would best describe a system's speed of response. This idea will be discussed further in Sections 6.6 and 6.7.

In some cases, the PM and GM are not helpful indicators of stability. For first- and second-order systems, the phase never crosses the  $180^\circ$  line; hence, the GM is always  $\infty$  and not a useful design parameter. For higher-order systems, it is possible to have more than one frequency where  $|KG(j\omega)| = 1$  or where  $\angle KG(j\omega) = 180^\circ$ , and the margins as previously defined need clarification. An example of this can be seen in Fig. 10.12, where the magnitude crosses 1 three times. In that case, a decision was made to define PM by the first crossing, because the PM at this crossing was the smallest of the three values and thus the most conservative assessment of stability. A Nyquist plot based on the data in Fig. 10.12 would show that the portion of the Nyquist curve closest to the  $-1$  point was the critical indicator of stability, and therefore use of the crossover frequency yielding the minimum value of PM was the logical choice. Alternatively, the **Nichols plot** discussed in Section 6.9 can be used to resolve any uncertainty in the stability margins. At best, a designer needs to be judicious when applying the margin definitions described in Fig. 6.33. In fact, the actual stability margin of a system can be rigorously assessed only by examining the Nyquist or Nichols plots to determine its closest approach to the  $-1$  point.

#### Nichols Plot

### Vector margin

### Conditionally stable systems

To aid in this analysis, Smith (1958) introduced the **vector margin** (sometimes called the complex margin), which he defined to be the distance to the  $-1$  point from the closest approach of the Nyquist plot.<sup>13</sup> Figure 6.38 illustrates the idea graphically. Because the vector margin is a single margin parameter, it removes all the ambiguities in assessing stability that come with using GM and PM in combination. In the past it has not been used extensively due to difficulties in computing it. However, with the widespread availability of computer aids, the idea of using the vector margin to describe the degree of stability is much more feasible.

There are certain practical examples in which an increase in the gain can make the system stable. As we saw in Chapter W3.8, these systems are called **conditionally stable**. A representative root-locus plot for such systems is shown in Fig. 6.39. For a point on the root locus, such as  $A$ , an increase in the gain would make the system stable by bringing the unstable roots into the LHP. For point  $B$ , either a gain increase or decrease could make the system become unstable. Therefore, several GMs exist that correspond to either gain reduction or gain increase, and the definition of the GM in Fig. 6.33 is not valid.

**Figure 6.38**

Definition of the vector margin on the Nyquist plot

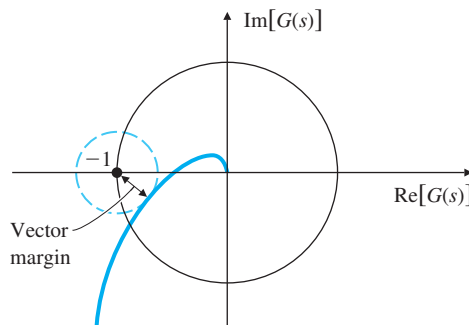
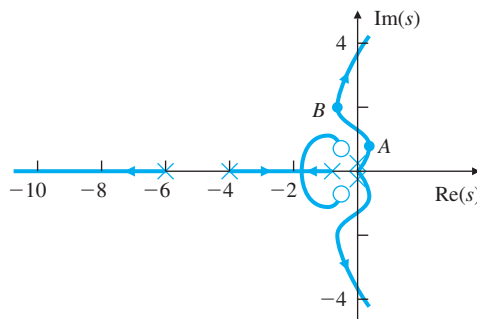


**Figure 6.39**

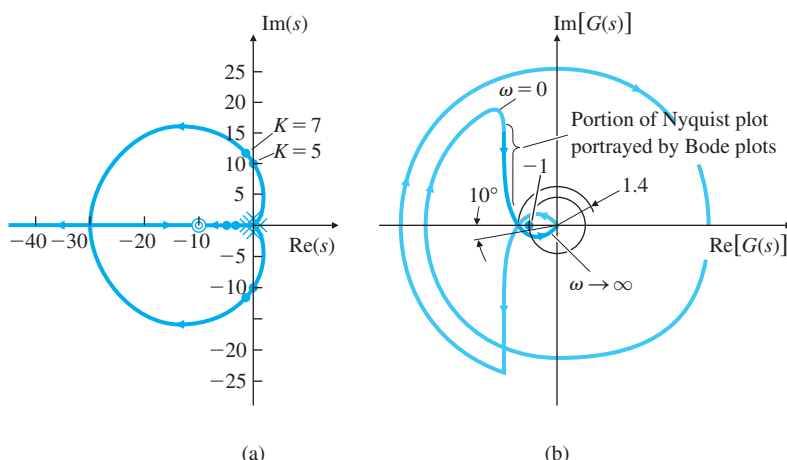
Root locus for a conditionally stable system



<sup>13</sup>This value is closely related to the use of the sensitivity function for design and the concept of stability robustness, to be discussed in optional Section 6.7.8.

**Figure 6.40**

System in which increasing gain leads from instability to stability: (a) root locus; (b) Nyquist plot

**EXAMPLE 6.12***Stability Properties for a Conditionally Stable System*

Determine the stability properties as a function of the gain  $K$  for the system with the open-loop transfer function

$$KG(s) = \frac{K(s+10)^2}{s^3}.$$

**Solution.** This is a system for which increasing gain causes a transition from instability to stability. The root locus in Fig. 6.40(a) shows that the system is unstable for  $K < 5$  and stable for  $K > 5$ . The Nyquist plot in Fig. 6.40(b) was drawn for the stable value  $K = 7$ . Determination of the margins according to Fig. 6.33 yields  $\text{PM} = +10^\circ$  (stable) and  $\text{GM} = 0.7$  (unstable). According to the rules for stability discussed earlier, these two margins yield conflicting signals on the system's stability.

We resolve the conflict by counting the Nyquist encirclements in Fig. 6.40(b). There is one clockwise encirclement and one counterclockwise encirclement of the  $-1$  point. Hence there are no net encirclements, which confirms that the system is stable for  $K = 7$ . For systems such as this, it is best to resort to the root locus and/or Nyquist plot (rather than the Bode plot) to determine stability.

**EXAMPLE 6.13***Nyquist Plot for a System with Multiple Crossover Frequencies*

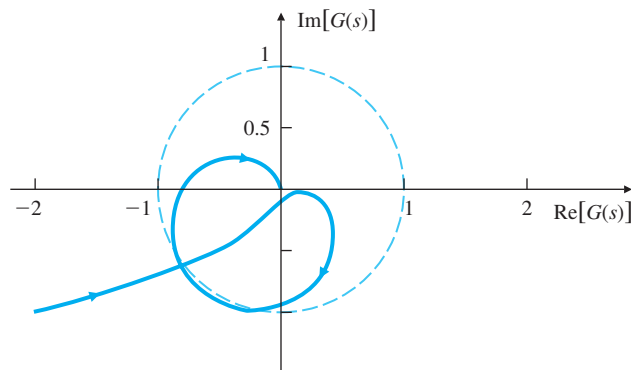
Draw the Nyquist plot for the system

$$\begin{aligned} G(s) &= \frac{85(s+1)(s^2 + 2s + 43.25)}{s^2(s^2 + 2s + 82)(s^2 + 2s + 101)} \\ &= \frac{85(s+1)(s+1 \pm 6.5j)}{s^2(s+1 \pm 9j)(s+1 \pm 10j)}, \end{aligned}$$

and determine the stability margins.

**Figure 6.41**

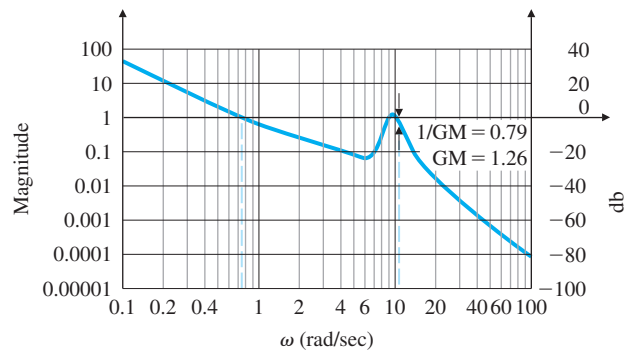
Nyquist plot of the complex system in Example 6.13



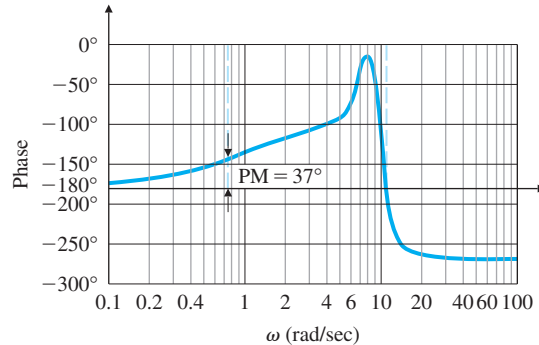
**Solution.** The Nyquist plot (see Fig. 6.41) shows qualitatively that there are three crossover frequencies of the magnitude = 1 circle; therefore, there will be three corresponding PM values. The Bode plot for this system (see Fig. 6.42) shows the three crossings of magnitude = 1 at 0.75, 9.0, and 10.1 rad/sec which indicate PM's of  $37^\circ$ ,  $80^\circ$ , and  $40^\circ$ , respectively. The key indicator of stability in this case is the proximity of the Nyquist plot as it approaches the  $-1$  point while crossing the real axis. Because there is only one crossing of the real axis of the Nyquist plot

**Figure 6.42**

Bode plot of the system in Example 6.13



(a)



(b)

(and, therefore, one crossing of the  $-180^\circ$  line of the Phase plot), there is only one value of the GM. From the Bode plot, we see the phase crosses  $-180^\circ$  at  $\omega = 10.4$  rad/sec where the magnitude = 0.79. Therefore, the  $GM = 1/0.79 = 1.26$  which is the most useful stability margin for this example. Note if there had been multiple crossings of  $-180^\circ$ , the smallest value of the GM determined at the various  $-180^\circ$  crossings would be the correct value of GM because that is where the system would become unstable as the gain is increased. (Tischler, 2012, pg. 226.)

---

In summary, many systems behave roughly like Example 6.9, and for them, the GM and PM are well defined and useful. There are also frequent instances of more complicated systems where the Bode plot has multiple magnitude 1 or  $-180^\circ$  crossovers for which the stability criteria defined by Fig. 6.33 are less clear; therefore, we need to determine possible values of GM and PM, then revert back to the Nyquist stability criterion for an in-depth understanding and determination of the correct stability margins.

## 6.5 Bode's Gain-Phase Relationship

One of Bode's important contributions is the following theorem:

For any stable minimum-phase system (i.e., one with no RHP zeros or poles), the phase of  $G(j\omega)$  is uniquely related to the magnitude of  $G(j\omega)$ .

When the slope of  $|G(j\omega)|$  versus  $\omega$  on a log–log scale persists at a constant value for approximately a decade of frequency, the relationship is particularly simple and is given by

$$\angle G(j\omega) \cong n \times 90^\circ, \quad (6.33)$$

where  $n$  is the slope of  $|G(j\omega)|$  in units of decade of amplitude per decade of frequency. For example, in considering the magnitude curve alone in Fig. 6.43, we see Eq. (6.33) can be applied to the two frequencies  $\omega_1 = 0.1$  (where  $n = -2$ ) and  $\omega_2 = 10$  (where  $n = -1$ ), which are a decade removed from the change in slope, to yield the approximate values of phase,  $-180^\circ$  and  $-90^\circ$ . The exact phase curve shown in the figure verifies that indeed the approximation is quite good. It also shows that the approximation will degrade if the evaluation is performed at frequencies closer to the change in slope.

An exact statement of the Bode gain–phase theorem is

$$\angle G(j\omega_o) = \frac{1}{\pi} \int_{-\infty}^{+\infty} \left( \frac{dM}{du} \right) W(u) du \quad \text{in radians,} \quad (6.34)$$

where

$$M = \log \text{ magnitude} = \ln |G(j\omega)|,$$

$$u = \text{normalized frequency} = \ln(\omega/\omega_0),$$

$$dM/du \cong \text{slope } n, \text{ as defined in Eq. (6.33)},$$

$$W(u) = \text{weighting function} = \ln(\coth|u|/2).$$

Figure 6.44 is a plot of the weighting function  $W(u)$  and shows how the phase is most dependent on the slope at  $\omega_0$ ; it is also dependent, though to a lesser degree, on slopes at neighboring frequencies. The

**Figure 6.43**

An approximate gain-phase relationship demonstration

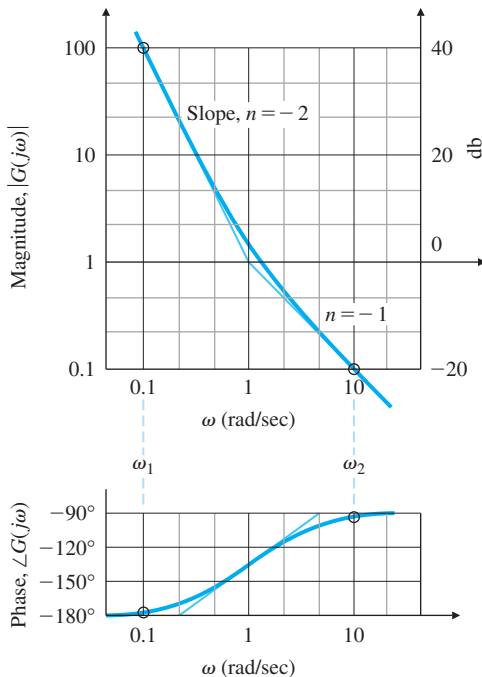


**Figure 6.44**

Weighting function in Bode's gain-phase theorem

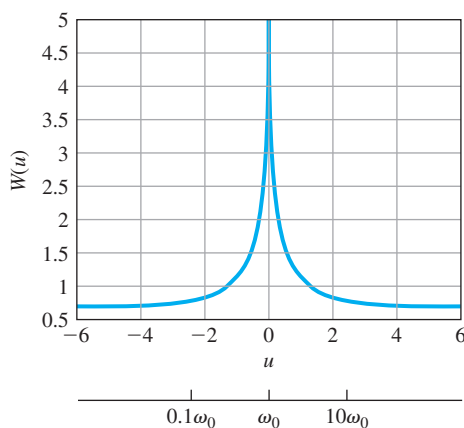


figure also suggests that the weighting could be approximated by an impulse function centered at  $\omega_o$ . We may approximate the weighting function as

$$W(u) \cong \frac{\pi^2}{2} \delta(u),$$

which is precisely the approximation made to arrive at Eq. (6.33) using the “sifting” property of the impulse function (and conversion from radians to degrees).

In practice, Eq. (6.34) is never used, but Eq. (6.33) is used as a guide to infer stability from  $|G(j\omega)|$  alone. When  $|KG(j\omega)| = 1$ ,

$$\begin{aligned}\angle G(j\omega) &\cong -90^\circ \quad \text{if } n = -1, \\ \angle G(j\omega) &\cong -180^\circ \quad \text{if } n = -2.\end{aligned}$$

#### Crossover frequency

For stability, we want  $\angle G(j\omega) > -180^\circ$  for the PM to be  $> 0$ . Therefore, we adjust the  $|KG(j\omega)|$  curve so it has a slope of  $-1$  at the “crossover” frequency,  $\omega_c$  (i.e., where  $|KG(j\omega)| = 1$ ). If the slope is  $-1$  for a decade above and below the crossover frequency, then  $PM \cong 90^\circ$ ; however, to ensure a reasonable PM, it is usually necessary only to insist that a  $-1$  slope ( $-20$  db per decade) persist for a decade in frequency that is centered at the crossover frequency. We therefore see there is a very simple design criterion:

Adjust the slope of the magnitude curve  $|KG(j\omega)|$  so it crosses over magnitude 1 with a slope of  $-1$  for a decade around  $\omega_c$ .

This criterion will usually be sufficient to provide an acceptable PM, and hence provide adequate system damping. To achieve the desired speed of response, the system gain is adjusted so the crossover point is at a frequency that will yield the desired bandwidth or speed of response as determined by Eq. (3.68). Recall that the natural frequency  $\omega_n$ , bandwidth, and crossover frequency are all approximately equal, as will be discussed further in Section 6.6.

### EXAMPLE 6.14

#### *Use of Simple Design Criterion for Spacecraft Attitude Control*

#### Disturbance Rejection Bandwidth, $\omega_{DRB}$

For the spacecraft attitude-control problem defined in Fig. 6.45, find a suitable expression for  $KD_c(s)$  that will provide good damping and a bandwidth of approximately  $0.2$  rad/sec. Also determine the frequency where the sensitivity function  $|S| = 0.7$  ( $= -3$  db). This frequency is often referred to as the “**Disturbance Rejection Bandwidth**,” or  $\omega_{DRB}$ .

**Solution.** The magnitude of the frequency response of the spacecraft (see Fig. 6.46) clearly requires some reshaping, because it has a slope of  $-2$  (or  $-40$  db per decade) everywhere. The simplest compensation

**Figure 6.45**  
Spacecraft  
attitude-control system

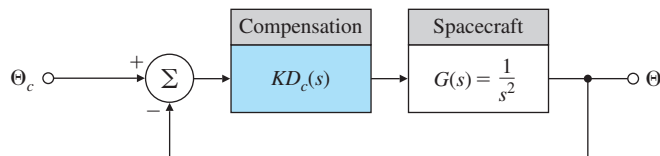
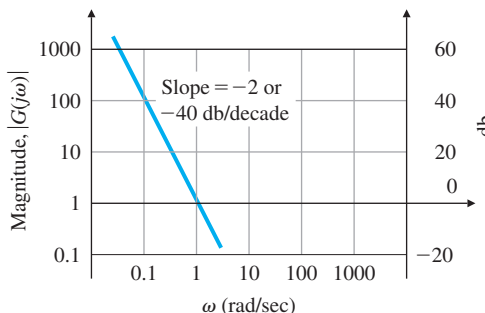


**Figure 6.46**  
Magnitude of the  
spacecraft's frequency  
response

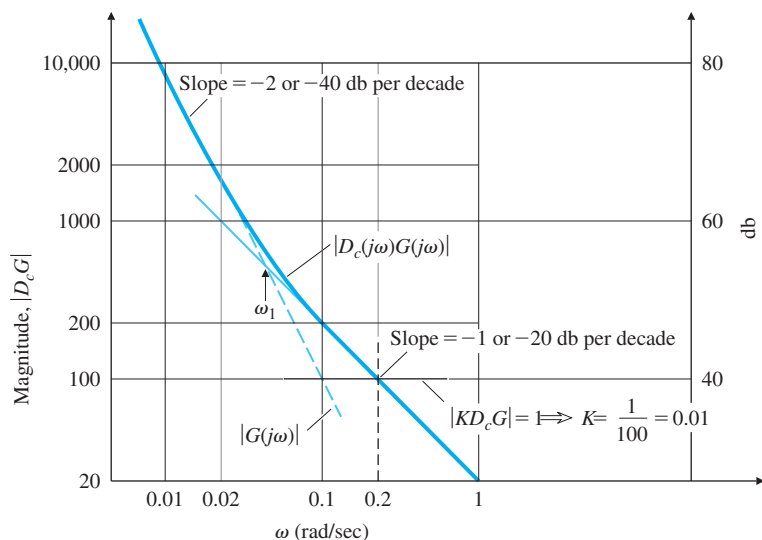


to do the job consists of using proportional and derivative terms (a PD compensator), which produces the relation

$$KD_c(s) = K(T_D s + 1). \quad (6.35)$$

We will adjust the gain  $K$  to produce the desired bandwidth, and adjust break point  $\omega_1 = 1/T_D$  to provide the  $-1$  slope at the crossover frequency. The actual design process to achieve the desired specifications is now very simple: We pick a value of  $K$  to provide a crossover at 0.2 rad/sec, and choose a value of  $\omega_1$  that is about four times lower than the crossover frequency, so the slope will be  $-1$  in the vicinity of the crossover. Figure 6.47 shows the steps we take to arrive at the final compensation:

**Figure 6.47**  
Compensated open-loop  
transfer function



1. Plot  $|G(j\omega)|$ .
2. Modify the plot to include  $|D_c(j\omega)|$ , with  $\omega_1 = 0.05$  rad/sec ( $T_D = 20$ ), so the slope will be  $\cong -1$  at  $\omega = 0.2$  rad/sec.
3. Determine that  $|D_c G| = 100$ , where the  $|D_c G|$  curve crosses the line  $\omega = 0.2$  rad/sec, which is where we want magnitude 1 crossover to be.
4. In order for crossover to be at  $\omega = 0.2$  rad/sec, compute

$$K = \frac{1}{|D_c G|_{\omega=0.2}} = \frac{1}{100} = 0.01.$$

Therefore,

$$KD_c(s) = 0.01(20s + 1)$$

will meet the specifications, thus completing the design.

If we were to draw the phase curve of  $KD_c G$ , we would find that  $PM = 75^\circ$ , which is certainly quite adequate. This result follows because the slope of  $-1$  occurs for a decade centered around the crossover frequency. A plot of the closed-loop frequency-response magnitude,  $\mathcal{T}(s)$ , (see Fig. 6.48) shows that, indeed, the crossover frequency and the bandwidth are almost identical in this case; therefore, the desired bandwidth of 0.2 rad/sec has been met. The sensitivity function was defined by Eq. (4.23) and for this problem is

$$\mathcal{S} = \frac{1}{1 + KD_c G}.$$

$\mathcal{S}(s)$  is also shown on Fig. 6.48, where it can be seen that  $|\mathcal{S}|$  has the value of 0.7 or  $-3\text{db}$  at  $\omega = 0.15$  rad/sec. The concept of a disturbance rejection characteristic at a certain frequency ( $\omega_{DRB}$ ) is often specified as a requirement for an acceptable design of a feedback system.

**Figure 6.48**

Closed-loop frequency response of  $\mathcal{T}(s)$  and  $\mathcal{S}(s)$

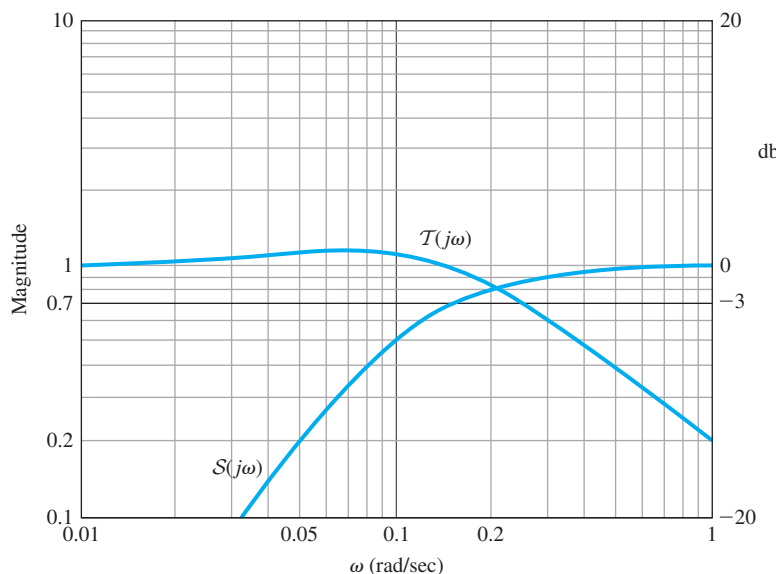
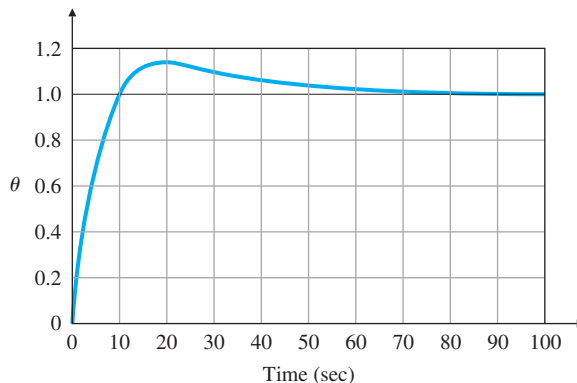


**Figure 6.49**

Step response for PD compensation



Basically,  $\omega_{DRB}$  is the maximum frequency at which the disturbance rejection (i.e., the sensitivity function,  $S$ ) is below a certain amount, in this case  $-3\text{db}$ ; so in this example,  $\omega_{DRB} = 0.15 \text{ rad/sec}$ .

The step response of the closed-loop system is shown in Fig. 6.49, and its 14% overshoot confirms the adequate damping.

## 6.6 Closed-Loop Frequency Response

The closed-loop bandwidth was defined in Section 6.1 and in Fig. 6.5. Figure 6.3 showed that the natural frequency is always within a factor of two of the bandwidth for a second-order system. In Example 6.14, we designed the compensation so the crossover frequency was at the desired bandwidth and verified by computation that the bandwidth was identical to the crossover frequency. Generally, the match between the crossover frequency and the bandwidth is not as good as in Example 6.14. We can help establish a more exact correspondence by making a few observations. Consider a system in which  $|KG(j\omega)|$  shows the typical behavior

$$|KG(j\omega)| \gg 1 \quad \text{for } \omega \ll \omega_c,$$

$$|KG(j\omega)| \ll 1 \quad \text{for } \omega \gg \omega_c,$$

where  $\omega_c$  is the crossover frequency. The closed-loop frequency-response magnitude is approximated by

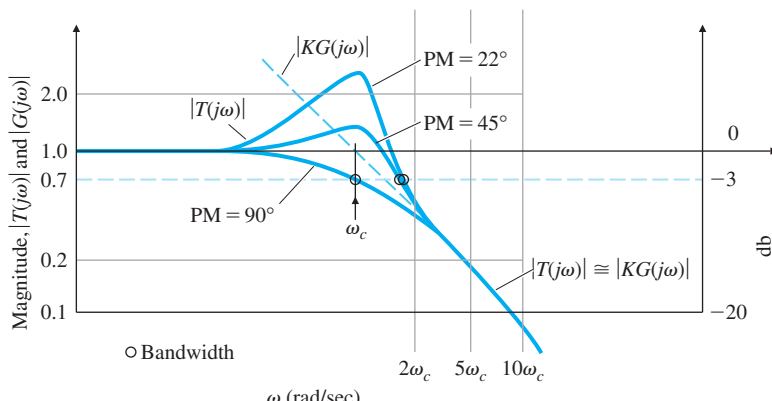
$$|\mathcal{T}(j\omega)| = \left| \frac{KG(j\omega)}{1 + KG(j\omega)} \right| \cong \begin{cases} 1, & \omega \ll \omega_c, \\ |KG|, & \omega \gg \omega_c. \end{cases} \quad (6.36)$$

In the vicinity of crossover, where  $|KG(j\omega)| = 1$ ,  $|\mathcal{T}(j\omega)|$  depends heavily on the PM. A PM of  $90^\circ$  means that  $\angle G(j\omega_c) = -90^\circ$ , and therefore  $|\mathcal{T}(j\omega_c)| = 0.707$ . On the other hand, PM =  $45^\circ$  yields  $|\mathcal{T}(j\omega_c)| = 1.31$ .

The exact evaluation of Eq. (6.36) was used to generate the curves of  $|\mathcal{T}(j\omega)|$  in Fig. 6.50. It shows that the bandwidth for smaller values

**Figure 6.50**

Closed-loop bandwidth with respect to PM



of PM is typically somewhat greater than  $\omega_c$ , though usually it is less than  $2\omega_c$ ; thus

$$\omega_c \leq \omega_{BW} \leq 2\omega_c.$$

Another specification related to the closed-loop frequency response is the resonant-peak magnitude  $M_r$ , defined in Fig. 6.5. Figures 6.3 and 6.37 show that, for linear systems,  $M_r$  is generally related to the damping of the system. In practice,  $M_r$  is rarely used; most designers prefer to use the PM to specify the damping of a system, because the imperfections that make systems nonlinear or cause delays usually erode the phase more significantly than the magnitude.

As demonstrated in the last example, it is also important in the design to achieve certain error characteristics and these are often evaluated as a function of the input or disturbance frequency. In some cases, the primary function of the control system is to regulate the output to a certain constant input in the presence of disturbances. For these situations, the key item of interest for the design would be the closed-loop frequency response of the error with respect to disturbance inputs.

## 6.7 Compensation

As discussed in Chapters 4 and 5, dynamic elements (or compensation) are typically added to feedback controllers to improve the system's stability and error characteristics because the process itself cannot be made to have acceptable characteristics with proportional feedback alone.

Section 4.3 discussed the basic types of feedback: proportional, derivative, and integral. Section 5.4 discussed three kinds of dynamic compensation: lead compensation, which approximates proportional-derivative (PD) feedback, lag compensation, which approximates proportional-integral (PI) control, and notch compensation, which has special characteristics for dealing with resonances. In this section, we discuss these and other kinds of compensation in terms of their frequency-response characteristics.

The frequency-response stability analysis to this point has usually considered the closed-loop system to have the characteristic equation  $1 + KG(s) = 0$ . With the introduction of compensation, the closed-loop characteristic equation becomes  $1 + KD_c(s)G(s) = 0$ , and all the previous discussion in this chapter pertaining to the frequency response of  $KG(s)$  applies directly to the compensated case if we apply it to the frequency response of  $KD_c(s)G(s)$ . We call this quantity  $L(s)$ , the “loop gain,” or open-loop transfer function of the system, where  $L(s) = KD_c(s)G(s)$ .

### 6.7.1 PD Compensation

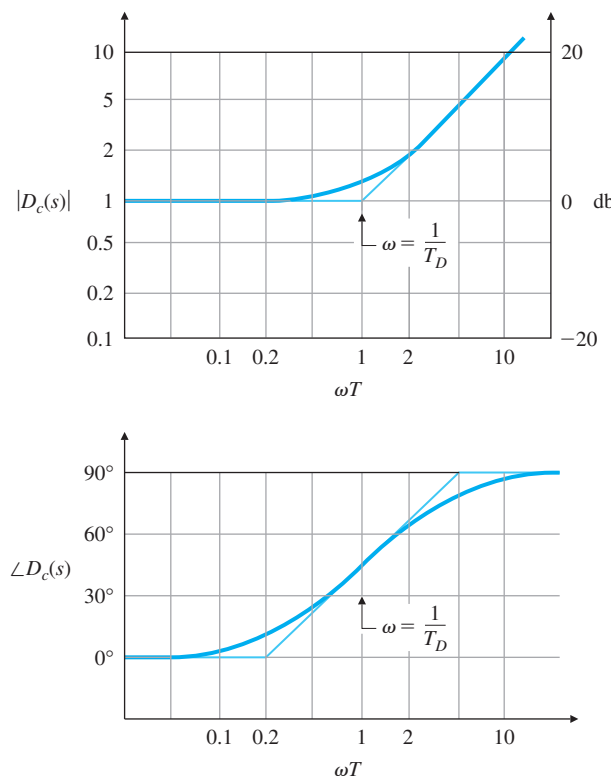
#### PD compensation

We will start the discussion of compensation design by using the frequency response with PD control. The compensator transfer function, given by

$$D_c(s) = (T_D s + 1), \quad (6.37)$$

was shown in Fig. 5.22 to have a stabilizing effect on the root locus of a second-order system. The frequency-response characteristics of Eq. (6.37) are shown in Fig. 6.51. A stabilizing influence is apparent by the increase in phase and the corresponding +1 slope at frequencies above the break point  $1/T_D$ . We use this compensation by locating  $1/T_D$

**Figure 6.51**  
Frequency response of  
PD control



so the increased phase occurs in the vicinity of crossover (that is, where  $|KD_c(s)G(s)| = 1$ ), thus increasing the PM.

Note the magnitude of the compensation continues to grow with increasing frequency. This feature is undesirable because it amplifies the high-frequency noise that is typically present in any real system and, as a continuous transfer function, cannot be realized with physical elements. It is also the reason, as stated in Section 5.4, that pure derivative compensation gives trouble.

### 6.7.2 Lead Compensation

#### Lead compensation

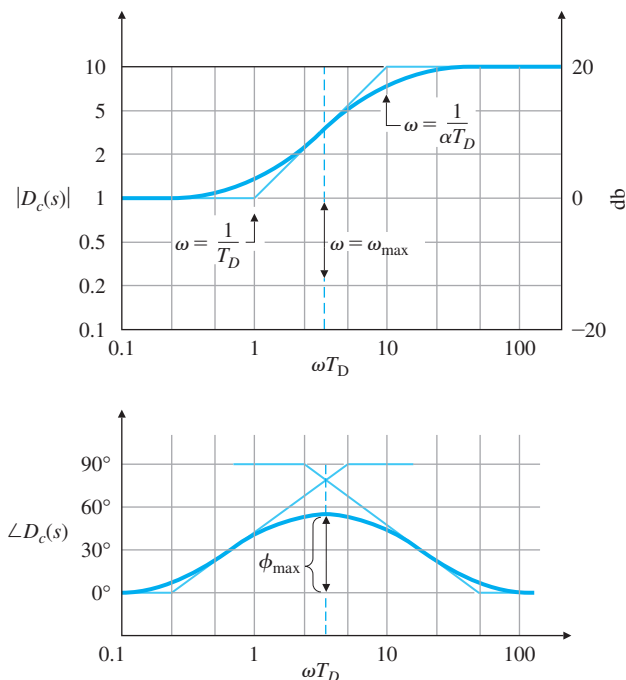
In order to alleviate the high-frequency amplification of the PD compensation, a first-order pole is added in the denominator at frequencies substantially higher than the break point of the PD compensator. Thus the phase increase (or lead) still occurs, but the amplification at high frequencies is limited. The resulting **lead compensation** has a transfer function of

$$D_c(s) = \frac{T_D s + 1}{\alpha T_D s + 1}, \quad \alpha < 1, \quad (6.38)$$

where  $1/\alpha$  is the ratio between the pole/zero break-point frequencies. Figure 6.52 shows the frequency response of this lead compensation. Note a significant amount of phase lead is still provided, but with much less amplification at high frequencies. A lead compensator is generally

**Figure 6.52**

Lead-compensation frequency response with  $1/\alpha = 10$



used whenever a substantial improvement in damping of the system is required.

The phase contributed by the lead compensation in Eq. (6.38) is given by

$$\phi = \tan^{-1}(T_D \omega) - \tan^{-1}(\alpha T_D \omega).$$

It can be shown (see Problem 6.44) that the frequency at which the phase is maximum is given by

$$\omega_{\max} = \frac{1}{T_D \sqrt{\alpha}}. \quad (6.39)$$

The maximum phase contribution—that is, the peak of the  $\angle D_c(s)$  curve in Fig. 6.52—corresponds to

$$\sin \phi_{\max} = \frac{1 - \alpha}{1 + \alpha}, \quad (6.40)$$

or

$$\alpha = \frac{1 - \sin \phi_{\max}}{1 + \sin \phi_{\max}}.$$

Another way to look at this is the following: The maximum phase occurs at a frequency that lies midway between the two break-point frequencies (sometimes called corner frequencies) on a logarithmic scale,

$$\begin{aligned} \log \omega_{\max} &= \log \frac{1/\sqrt{T_D}}{\sqrt{\alpha T_D}} \\ &= \log \frac{1}{\sqrt{T_D}} + \log \frac{1}{\sqrt{\alpha T_D}} \\ &= \frac{1}{2} \left[ \log \left( \frac{1}{T_D} \right) + \log \left( \frac{1}{\alpha T_D} \right) \right], \end{aligned} \quad (6.41)$$

as shown in Fig. 6.52. Alternatively, we may state these results in terms of the pole-zero locations. Rewriting  $D_c(s)$  in the form used for root-locus analysis, we have

$$D_c(s) = \frac{s + z}{s + p}. \quad (6.42)$$

Problem 6.44 shows that

$$\omega_{\max} = \sqrt{|z| |p|} \quad (6.43)$$

and

$$\log \omega_{\max} = \frac{1}{2} (\log |z| + \log |p|). \quad (6.44)$$

These results agree with the previous ones if we choose  $z = -1/T_D$  and  $p = -1/\alpha T_D$  in Eqs. (6.39) and (6.41).

For example, a lead compensator with a zero at  $s = -2$  ( $T_D = 0.5$ ) and a pole at  $s = -10$  ( $\alpha T_D = 0.1$ ) (and thus  $\alpha = \frac{1}{5}$ ) would yield the maximum phase lead at

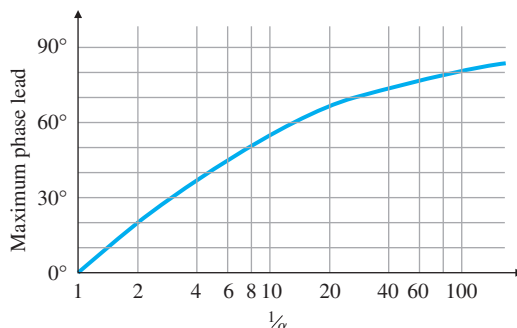
$$\omega_{\max} = \sqrt{2 \cdot 10} = 4.47 \text{ rad/sec.}$$

The amount of phase lead at the midpoint depends only on  $\alpha$  in Eq. (6.40) and is plotted in Fig. 6.53. For  $\alpha = 1/5$ , Fig. 6.53 shows that

**Figure 6.53**

Maximum phase increase for lead compensation

Lead ratio



$\phi_{\max} = 40^{\circ}$ . Note from the figure that we could increase the phase lead up to  $90^{\circ}$  using higher<sup>14</sup> values of the **lead ratio**,  $1/\alpha$ ; however, Fig. 6.52 shows that increasing values of  $1/\alpha$  also produces higher amplifications at higher frequencies. Thus our task is to select a value of  $1/\alpha$  that is a good compromise between an acceptable PM and an acceptable noise sensitivity at high frequencies. Usually the compromise suggests that a lead compensation should contribute a maximum of  $70^{\circ}$  to the phase. If a greater phase lead is needed, then a double-lead compensation would be suggested, where

$$D_c(s) = \left( \frac{T_D s + 1}{\alpha T_D s + 1} \right)^2.$$

Even if a system had negligible amounts of noise present and the pure derivative compensation of Eq. (6.37) were acceptable, a continuous compensation would look more like Eq. (6.38) than Eq. (6.37) because of the impossibility of building a pure differentiator. No physical system—mechanical or electrical—responds with infinite amplitude at infinite frequencies, so there will be a limit in the frequency range (or bandwidth) for which derivative information (or phase lead) can be provided. This is also true with a digital implementation. Here, the sample rate limits the high-frequency amplification and essentially places a pole in the compensation transfer function.

## EXAMPLE 6.15

### Lead Compensation for a DC Motor

As an example of designing a lead compensator, let us repeat the design of compensation for the DC motor with the transfer function

$$G(s) = \frac{1}{s(s+1)},$$

that was carried out in Section 5.4.1. This also represents the model of a satellite tracking antenna (see Fig. 3.60). This time we wish to obtain a steady-state error of less than 0.1 for a unit-ramp input. Furthermore, we desire an overshoot  $M_p < 25\%$ . Determine the lead compensation satisfying the specifications.

---

<sup>14</sup>Lead ratio =  $1/\alpha$ .

**Solution.** The steady-state error is given by

$$e_{ss} = \lim_{s \rightarrow 0} s \left[ \frac{1}{1 + KD_c(s)G(s)} \right] R(s), \quad (6.45)$$

where  $R(s) = 1/s^2$  for a unit ramp, so Eq. (6.45) reduces to

$$e_{ss} = \lim_{s \rightarrow 0} \left\{ \frac{1}{s + KD_c(s)[1/(s+1)]} \right\} = \frac{1}{KD_c(0)}.$$

Therefore, we find that  $KD_c(0)$ , the steady-state gain of the compensation, cannot be less than 10 ( $K_v \geq 10$ ) if it is to meet the error criterion, so we pick  $K = 10$ . To relate the overshoot requirement to PM, Fig. 6.37 shows that a PM of  $45^\circ$  should suffice. The frequency response of  $KG(s)$  in Fig. 6.54 shows that the PM =  $20^\circ$  if no phase lead is added by compensation. If it were possible to simply add phase without affecting the magnitude, we would need an additional phase of only  $25^\circ$  at the  $KG(s)$  crossover frequency of  $\omega = 3$  rad/sec. However, maintaining the same low-frequency gain and adding a compensator zero would increase the

**Figure 6.54**

Frequency response for lead-compensation design

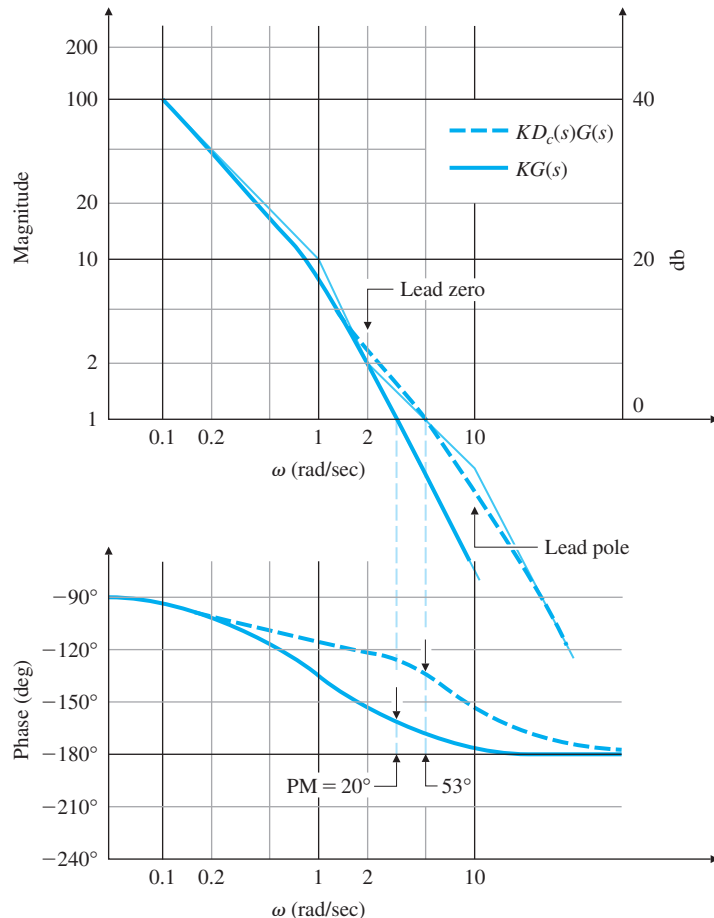
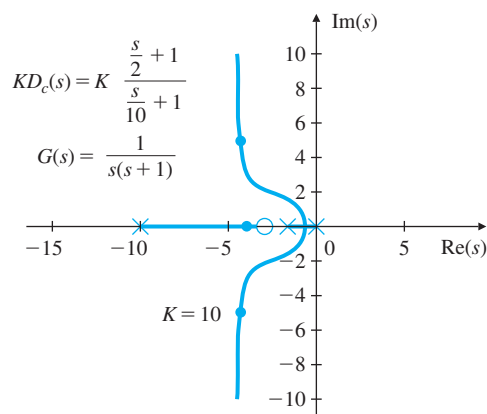


**Figure 6.55**

Root locus for lead compensation design



crossover frequency; hence more than a  $25^\circ$  phase contribution will be required from the lead compensation. To be safe, we will design the lead compensator so it supplies a maximum phase lead of  $40^\circ$ . Fig. 6.53 shows that  $1/\omega_n = 5$  will accomplish that goal. We will derive the greatest benefit from the compensation if the maximum phase lead from the compensator occurs at the crossover frequency. With some trial and error, we determine that placing the zero at  $\omega = 2$  rad/sec and the pole at  $\omega = 10$  rad/sec causes the maximum phase lead to be at the crossover frequency. The compensation, therefore, is

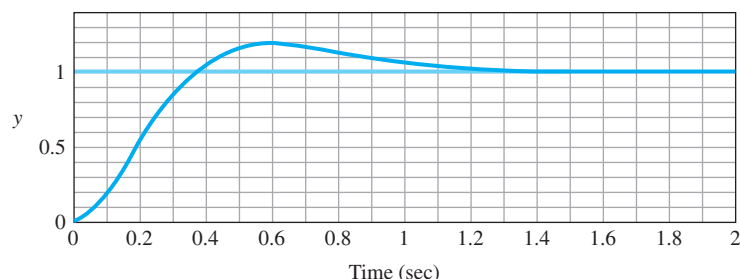
$$KD_c(s) = 10 \frac{s/2 + 1}{s/10 + 1}.$$

The frequency-response characteristics of  $KD_c(s)G(s)$  in Fig. 6.54 can be seen to yield a PM of  $53^\circ$ , which satisfies the design goals.

1. The root locus for this design, originally given as Fig. 5.24, is repeated here as Fig. 6.55, with the root locations marked for  $K = 10$ . The locus is not needed for the frequency-response design procedure; it is presented here only for comparison with the root-locus design method presented in Chapter 5, which had an equivalent gain of  $K = 14$ . For further comparison, Fig. 6.56

**Figure 6.56**

Step response of lead compensator design for Example 6.15



shows the time response of the system to a step command. Comparing it to Fig. 5.25, we see the current design is slightly slower, having a rise time  $t_r = 0.33$  sec compared to the  $t_r = 0.26$  sec for Fig. 5.25.

---

The design procedure used in Example 6.15 can be summarized as follows:

1. Determine the low-frequency gain so the steady-state errors are within specification.
2. Select the combination of lead ratio  $1/\alpha$  and zero values ( $1/T_D$ ) that achieves an acceptable PM at crossover.
3. The pole location is then at  $(1/\alpha T_D)$ .

This design procedure will apply to many cases; however, keep in mind that the specific procedure followed in any particular design may need to be tailored to its particular set of specifications.

In Example 6.15, there were two specifications: peak overshoot and steady-state error. We transformed the overshoot specification into a PM, but the steady-state error specification we used directly. No speed-of-response type of specification was given; however, it would have impacted the design in the same way that the steady-state error specification did. The speed of response or bandwidth of a system is directly related to the crossover frequency, as we pointed out earlier in Section 6.6. Figure W6.1 shows that the crossover frequency was  $\sim 5$  rad/sec. We could have increased it by raising the gain  $K$  and increasing the frequency of the lead compensator pole and zero in order to keep the slope of  $-1$  at the crossover frequency. Raising the gain would also have decreased the steady-state error to be better than the specified limit. The GM was never introduced into the problem because the stability was adequately specified by the PM alone. Furthermore, the GM would not have been useful for this system because the phase never crossed the  $180^\circ$  line, and the GM was always infinite.

In lead-compensation designs, there are three primary design parameters:

1. The crossover frequency  $\omega_c$ , which determines bandwidth  $\omega_{BW}$ , rise time  $t_r$ , and settling time  $t_s$ ;
2. The PM, which determines the damping coefficient  $\zeta$  and the overshoot  $M_p$ ;
3. The low-frequency gain, which determines the steady-state error characteristics.

The design problem is to find the best values for the parameters, given the requirements. In essence, lead compensation increases the value of  $\omega_c/L(0)$  ( $= \omega_c/K_v$  for a Type 1 system). That means that, if the low-frequency gain is kept the same, the crossover frequency

#### Design parameters for lead networks

will increase. Or, if the crossover frequency is kept the same, the low-frequency gain will decrease. Keeping this interaction in mind, the designer can assume a fixed value of one of these three design parameters, then adjust the other two iteratively until the specifications are met. One approach is to set the low-frequency gain to meet the error specifications and add a lead compensator to increase PM at the crossover frequency. An alternative is to pick the crossover frequency to meet a time response specification, then adjust the gain and lead characteristics so the PM specification is met. A step-by-step procedure is outlined next for these two cases. They apply to a sizable class of problems for which a single lead is sufficient. As with all such design procedures, it provides only a starting point; the designer will typically find it necessary to go through several design iterations in order to meet all the specifications.

#### Design Procedure for Lead Compensation

1. Determine the gain  $K$  to satisfy error or bandwidth requirements:
  - (a) to meet error requirements, pick  $K$  to satisfy error constants ( $K_p$ ,  $K_v$ , or  $K_a$ ) so  $e_{ss}$  error specification is met, or alternatively,
  - (b) to meet bandwidth requirements, pick  $K$  so the open-loop crossover frequency is a factor of two below the desired closed-loop bandwidth.
2. Evaluate the PM of the uncompensated system using the value of  $K$  obtained from Step 1.
3. Allow for extra margin (about  $10^\circ$ ), and determine the needed phase lead  $\phi_{\max}$ .
4. Determine  $\alpha$  from Eq. (6.40) or Fig. 6.53.
5. Pick  $\omega_{\max}$  to be at the crossover frequency; thus the zero is at  $1/T_D = \omega_{\max}\sqrt{\alpha}$  and the pole is at  $1/\alpha T_D = \omega_{\max}/\sqrt{\alpha}$ .
6. Draw the compensated frequency response and check the PM.
7. Iterate on the design. Adjust compensator parameters (poles, zeros, and gain) until all specifications are met. Add an additional lead compensator (that is, a double-lead compensation) if necessary.

While these guidelines will not apply to all the systems you will encounter in practice, they do suggest a systematic trial-and-error process to search for a satisfactory compensator that will usually be successful.

#### EXAMPLE 6.16

##### *Lead Compensator for a Temperature Control System*

The third-order system

$$KG(s) = \frac{K}{(s/0.5 + 1)(s + 1)(s/2 + 1)}$$

is representative of a typical temperature control system. Design a lead compensator such that  $K_p = 9$  and the PM is at least  $25^\circ$ .

**Solution.** Let us follow the design procedure:

- Given the specification for  $K_p$ , we solve for  $K$ :

$$K_p = \lim_{s \rightarrow 0} KG(s) = K = 9.$$

- The Bode plot of the uncompensated system,  $KG(s)$ , with  $K = 9$  can be created by the Matlab statements below, and is shown in Fig. 6.57 along with the two compensated cases.

```
s = tf('s');
sysG = 9/((s/0.5 + 1)*(s + 1)*(s/2 + 1));
w=logspace(-1,1);
[mag,phase] = bode(sysG,w);
loglog(w,squeeze(mag)),grid;
semilogx(w,squeeze(phase)),grid;
```

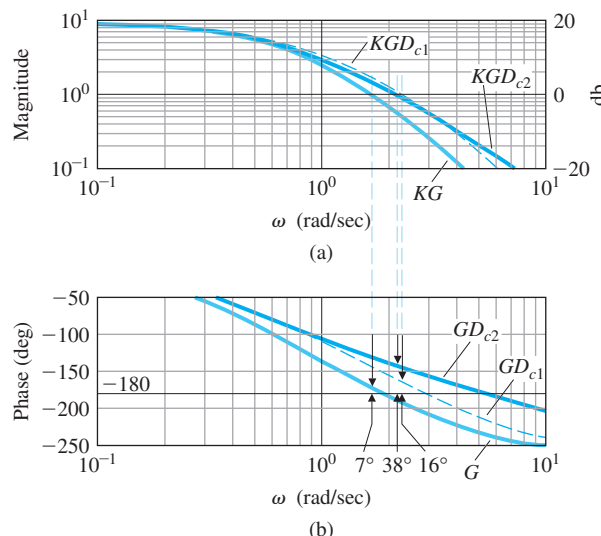
It is difficult to read the PM and crossover frequencies accurately from the Bode plots; therefore, the Matlab command

```
[GM,PM,Wcg,Wcp] = margin(mag,phase,w);
```

can be invoked. The quantity PM is the phase margin and Wcp is the frequency at which the gain crosses magnitude 1. (GM and, Wcg are the GM and the frequency at which the phase crosses  $-180^\circ$  respectively.) For this example, the output is

GM = 1.25, PM = 7.14, Wcg = 1.87, Wcp = 1.68,

**Figure 6.57**  
Bode plot for the lead-compensation design in Example 6.16



which says that the PM of the uncompensated system is  $7^\circ$  and that this occurs at a crossover frequency of 1.7 rad/sec.

3. Allowing for  $10^\circ$  of extra margin, we want the lead compensator to contribute  $25^\circ + 10^\circ - 7^\circ = 28^\circ$  at the crossover frequency. The extra margin is typically required because the lead will increase the crossover frequency from the open-loop case, at which point more phase increase will be required.
4. From Fig. 6.53, we see that  $\alpha = 1/3$  will produce approximately  $30^\circ$  phase increase midway between the zero and pole.
5. As a first cut, let's place the zero at 1 rad/sec ( $T_D = 1$ ) and the pole at 3 rad/sec ( $\alpha T_D = 1/3$ ), thus bracketing the open-loop crossover frequency and preserving the factor of 3 between pole and zero, as indicated by  $\alpha = 1/3$ . The lead compensator is

$$D_{c1}(s) = \frac{s+1}{s/3+1} = \frac{1}{0.333} \left( \frac{s+1}{s+3} \right).$$

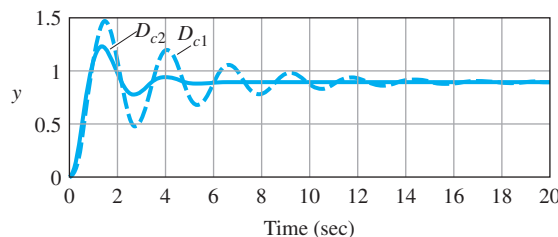
6. The Bode plot of the system with  $D_{c1}(s)$  (see Fig. 6.57, middle curve) has a PM of  $16^\circ$ . We did not achieve the desired PM of  $30^\circ$ , because the lead shifted the crossover frequency from 1.7 rad/sec to 2.3 rad/sec, thus increasing the required phase increase from the lead. The step response of the system with  $D_{c1}(s)$  (see Fig. 6.58) shows a very oscillatory response, as we might expect from the low PM of  $16^\circ$ .
7. We repeat the design with extra phase increase and move the zero location slightly to the right so the crossover frequency won't be shifted so much. We choose  $\alpha = 1/10$  with the zero at  $s = -1.5$ , so

$$D_{c2}(s) = \frac{s/1.5+1}{s/15+1} = \frac{1}{0.1} \left( \frac{s+1.5}{s+15} \right).$$

This compensation produces a PM =  $38^\circ$ , and the crossover frequency lowers slightly to 2.2 rad/sec. Figure 6.57 (upper curve) shows the frequency response of the revised design. Figure 6.58 shows a substantial reduction in the oscillations, which you should expect from the higher PM value.

**Figure 6.58**

Step response for lead-compensation design in Example 6.16



**EXAMPLE 6.17***Lead-Compensator Design for a Type 1 Servomechanism System*

Consider the third-order system

$$KG(s) = K \frac{10}{s(s/2.5 + 1)(s/6 + 1)}.$$

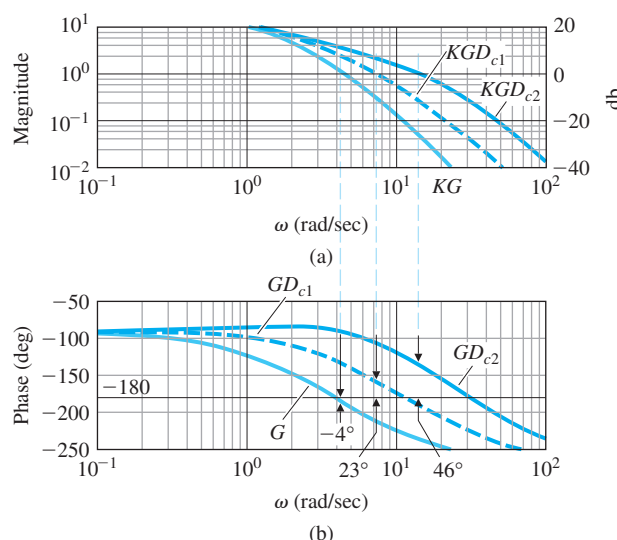
This type of system would result for a DC motor with a lag in the shaft position sensor. Design a lead compensator so that the PM = 45° and  $K_v = 10$ .

**Solution.** Again, we follow the design procedure given earlier:

- As given,  $KG(s)$  will yield  $K_v = 10$  if  $K = 1$ . Therefore, the  $K_v$  requirement is met by  $K = 1$  and the low-frequency gain of the compensation should be 1.
- The Bode plot of the system is shown in Fig. 6.59. The PM of the uncompensated system (lower curve) is approximately  $-4^\circ$ , and the crossover frequency is at  $\omega_c \cong 4$  rad/sec.
- Allowing for 5° of extra PM, we need  $PM = 45^\circ + 5^\circ - (-4^\circ) = 54^\circ$  to be contributed by the lead compensator.
- From Fig. 6.53 we find  $\alpha$  must be 0.1 to achieve a maximum phase lead of 54°.
- The new gain crossover frequency will be higher than the open-loop value of  $\omega_c = 4$  rad/sec, so let's select the pole and zero of the lead compensation to be at 20 and 2 rad/sec, respectively. So the candidate compensator is

$$D_{c1}(s) = \frac{s/2 + 1}{s/20 + 1} = \frac{1}{0.1} \frac{s + 2}{s + 20}.$$

**Figure 6.59**  
Bode plot for the lead-compensation design in Example 6.17



6. The Bode plot of the compensated system (see Fig. 6.59, middle curve) shows a PM of  $23^\circ$ . Further iteration will show that a single-lead compensator cannot meet the specification because of the high-frequency slope of  $-3$ .
7. We need a double-lead compensator in this system. If we try a compensator of the form

$$D_{c2}(s) = \frac{1}{(0.1)^2} \frac{(s+2)(s+4)}{(s+20)(s+40)} = \frac{(s/2+1)(s/4+1)}{(s/20+1)(s/40+1)},$$

we obtain  $\text{PM} = 46^\circ$ . The Bode plot for this case is shown as the upper curve in Fig. 6.59.

Both Examples 6.16 and 6.17 are third order. Example 6.17 was more difficult to design compensation for, because the error requirement,  $K_v$ , forced the crossover frequency,  $\omega_c$ , to be so high that a single lead could not provide enough PM.

### 6.7.3 PI Compensation

In many problems, it is important to keep the bandwidth low and also to reduce the steady-state error. For this purpose, a proportional-integral (PI) or lag compensator is useful. From Eq. (4.73), we see that PI control has the transfer function

$$D_c(s) = \frac{K}{s} \left( s + \frac{1}{T_I} \right), \quad (6.46)$$

which results in the frequency-response characteristics shown in Fig. 6.60. The desirable aspect of this compensation is the infinite gain at zero frequency, which reduces the steady-state errors. This is accomplished, however, at the cost of a phase decrease at frequencies lower than the break point at  $\omega = 1/T_I$ . Therefore,  $1/T_I$  is usually located at a frequency substantially less than the crossover frequency so the system's PM is not affected significantly.

### 6.7.4 Lag Compensation

As we discussed in Section 5.4, **lag compensation** approximates PI control. Its transfer function was given by Eq. (5.72) for root-locus design, but for frequency-response design, it is more convenient to write the transfer function of the lag compensation *alone* in the Bode form

$$D_c(s) = \alpha \frac{T_{IS} + 1}{\alpha T_{IS} + 1}, \quad \alpha > 1, \quad (6.47)$$

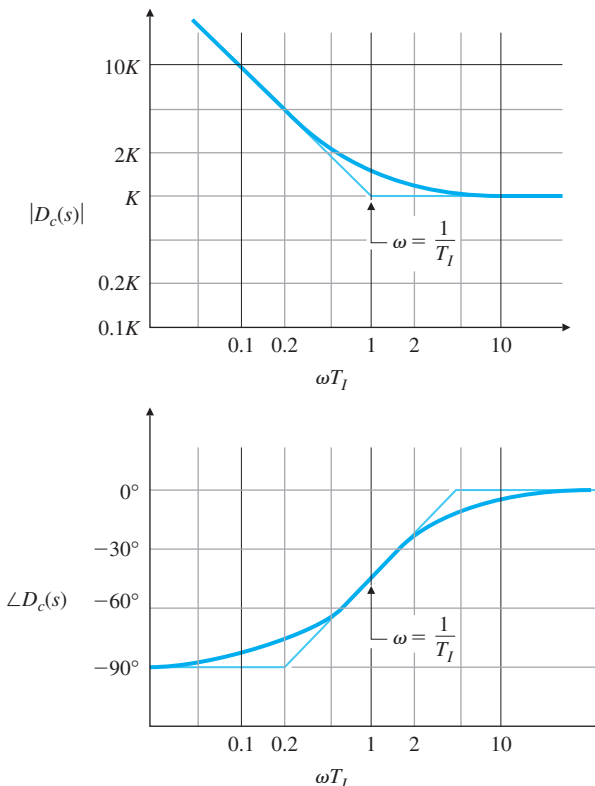
where  $\alpha$  is the ratio between the zero/pole break-point frequencies. The complete controller will almost always include an overall gain  $K$  and perhaps other dynamics in addition to the lag compensation. Although Eq. (6.47) looks very similar to the lead compensation in Eq. (6.38), the

**PI compensation**

**Lag compensation**

**Figure 6.60**

Frequency response of PI control

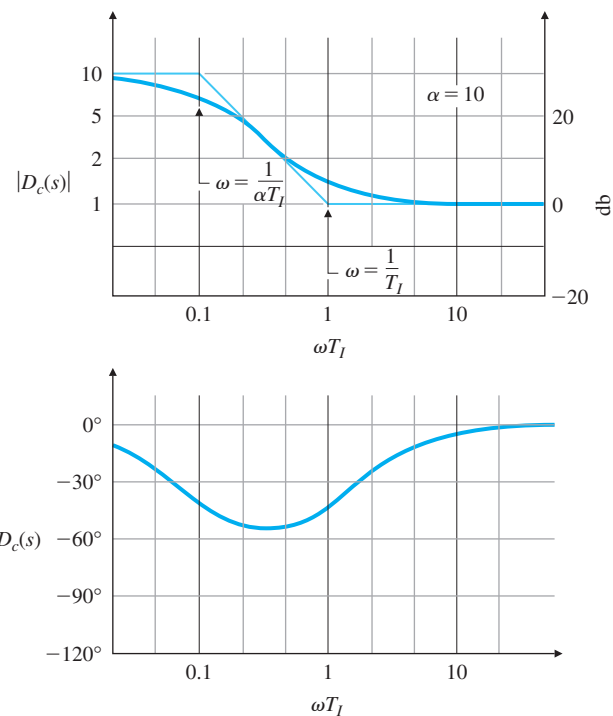


fact is that  $\alpha > 1$  causes the pole to have a lower break-point frequency than the zero. This relationship produces the low-frequency increase in amplitude and phase decrease (lag) apparent in the frequency-response plot in Fig. 6.61 and gives the compensation the essential feature of integral control—an increased low-frequency gain. The typical objective of lag-compensation design is to provide additional gain of  $\alpha$  in the low-frequency range and to leave the system sufficient PM. Of course, phase lag is not a useful effect, and the pole and zero of the lag compensator are selected to be at much lower frequencies than the uncompensated system crossover frequency in order to keep the effect on the PM to a minimum. Thus, the lag compensator increases the open-loop DC gain, thereby improving the steady-state response characteristics, without changing the transient-response characteristics significantly. If the pole and zero are relatively close together and near the origin (that is, if the value of  $T_I$  is large), we can increase the low-frequency gain (and thus  $K_p$ ,  $K_v$ , or  $K_a$ ) by a factor  $\alpha$  without moving the closed-loop poles appreciably. Hence, the transient response remains approximately the same while the steady-state response is improved.

We now summarize a step-by-step procedure for lag-compensator design.

**Figure 6.61**

Frequency response of lag compensation with  $\alpha = 10$



### Design Procedure for Lag Compensation

1. Determine the open-loop gain  $K$  that will meet the PM requirement without compensation.
2. Draw the Bode plot of the uncompensated system with crossover frequency from Step 1, and evaluate the low-frequency gain.
3. Determine  $\alpha$  to meet the low-frequency gain error requirement.
4. Choose the corner frequency  $\omega = 1/T_I$  (the zero of the lag compensator) to be one octave to one decade below the new crossover frequency  $\omega_c$ .
5. The other corner frequency (the pole location of the lag compensator) is then  $\omega = 1/\alpha T_I$ .
6. Iterate on the design. Adjust compensator parameters (poles, zeros, and gain) to meet all the specifications.

### EXAMPLE 6.18

#### Lag-Compensator Design for Temperature Control System

Again consider the third-order system of Example 6.16:

$$KG(s) = \frac{K}{\left(\frac{1}{0.5}s + 1\right)(s + 1)\left(\frac{1}{2}s + 1\right)}.$$

Design a lag compensator so the PM is at least  $40^\circ$  and  $K_p = 9$ .

**Solution.** We follow the design procedure previously enumerated.

- From the open-loop plot of  $KG(s)$ , shown for  $K = 9$  in Fig. 6.57, it can be seen a  $PM > 40^\circ$  will be achieved if the crossover frequency  $\omega_c \lesssim 1$  rad/sec. This will be the case if  $K = 3$ . So we pick  $K = 3$  in order to meet the PM specification.
- The Bode plot of  $KG(s)$  in Fig. 6.62 with  $K = 3$  shows the PM is  $\approx 50^\circ$  and the low-frequency gain is now 3. Exact calculation of the PM using Matlab's margin shows that  $PM = 53^\circ$ .
- The low-frequency gain should be raised by a factor of 3, which means the lag compensation needs to have  $\alpha = 3$ .
- We choose the corner frequency for the zero to be approximately a factor of 5 slower than the expected crossover frequency—that is, at 0.2 rad/sec. So,  $1/T_I = 0.2$ , or  $T_I = 5$ .
- We then have the value for the other corner frequency:  $\omega = 1/\alpha T_I = \frac{1}{(3)(5)} = 1/15$  rad/sec. The compensator is thus

$$D_c(s) = 3 \frac{5s + 1}{15s + 1}.$$

The compensated frequency response is also shown in Fig. 6.62. The low-frequency gain of  $KD_c(0)G(0) = 3K = 9$ , thus  $K_p = 9$  and the PM lowers slightly to  $44^\circ$ , which satisfies the specifications. The step response of the system, shown in Fig. 6.63, illustrates the reasonable damping that we would expect from  $PM = 44^\circ$ .

- No iteration is required in this case.

**Figure 6.62**  
Frequency response of  
lag-compensation  
design in Example 6.18

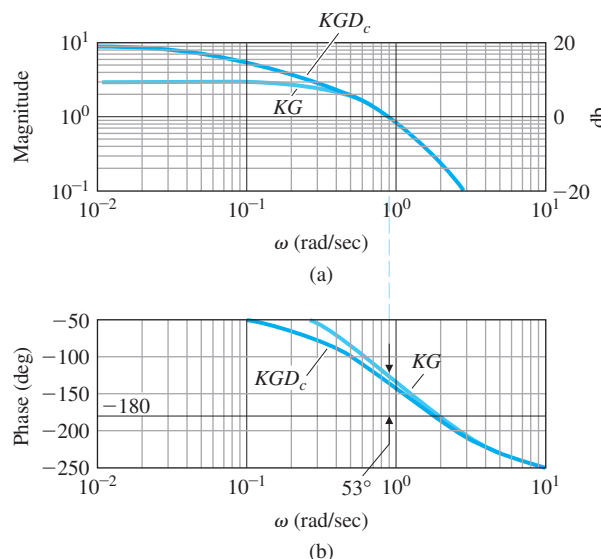
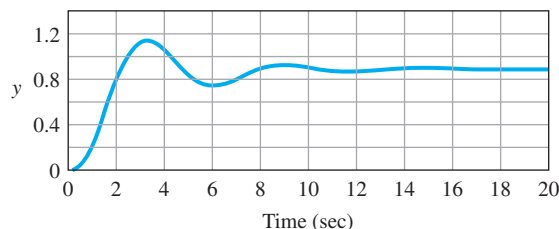


**Figure 6.63**

Step response of lag-compensation design in Example 6.18



Note Examples 6.16 and 6.18 are both for the same plant, and both had the same steady-state error requirement. One was compensated with lead, and one was compensated with lag. The result is the bandwidth of the lead-compensated design is higher than that for the lag-compensated design by approximately a factor of 3. This result can be seen by comparing the crossover frequencies of the two designs.

A beneficial effect of lag compensation, an increase in the low-frequency gain for better error characteristics, was just demonstrated in Example 6.18. However, in essence, lag compensation reduces the value of  $\omega_c/L(0)$  ( $= \omega_c/K_v$  for a Type 1 system). That means that, if the crossover frequency is kept the same, the low-frequency gain will increase. Likewise, if the low-frequency gain is kept the same, the crossover frequency will decrease. Therefore, lag compensation could also be interpreted to reduce the crossover frequency and thus obtain a better PM. The procedure for design in this case is partially modified. First, pick the low-frequency gain to meet error requirements, then locate the lag compensation pole and zero in order to provide a crossover frequency with adequate PM. The next example illustrates this design procedure. The end result of the design will be the same no matter what procedure is followed.

### EXAMPLE 6.19

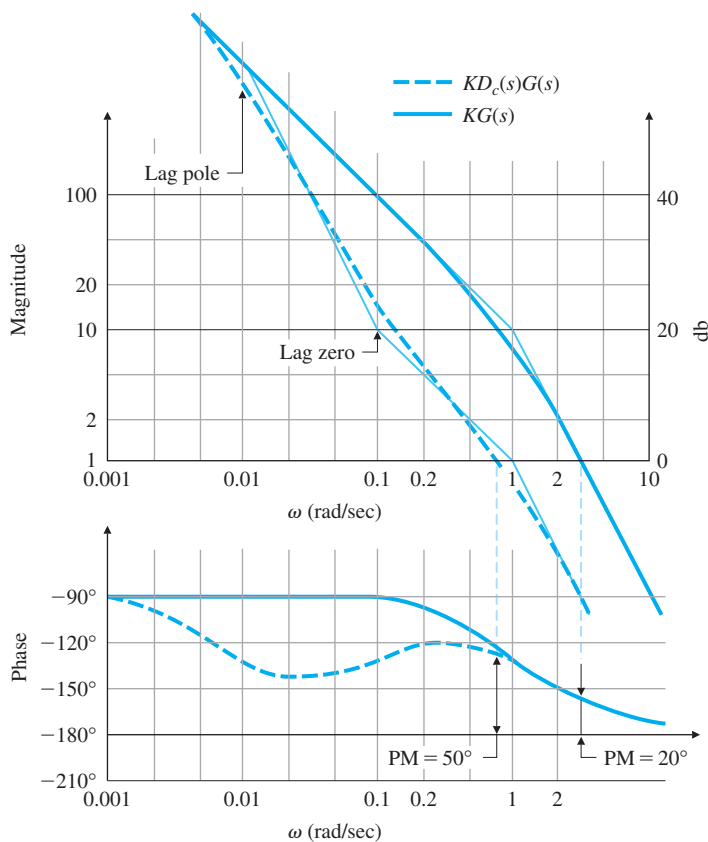
#### Lag Compensation of the DC Motor

Repeat the design of the DC motor control in Example 6.15, this time using lag compensation. Fix the low-frequency gain in order to meet the error requirement of  $K_v = 10$ ; then use the lag compensation to meet the PM requirement of  $45^\circ$ . Compare the open-loop Bode magnitude plots and the time responses for Examples 6.15 and 6.19.

**Solution.** The frequency response of the system  $KG(s)$ , with the required gain of  $K = 10$ , is shown in Fig. 6.64. The uncompensated system has a crossover frequency at approximately 3 rad/sec where the PM =  $20^\circ$ . The designer's task is to select the lag compensation break points so the crossover frequency is lowered and more favorable PM results. To prevent detrimental effects from the compensation phase lag, the pole and zero position values of the compensation need to be substantially lower than the new crossover frequency. One possible choice is shown in Fig. 6.64: The lag zero is at 0.1 rad/sec, and the lag pole is at

**Figure 6.64**

Frequency response of lag-compensation design in Example 6.19

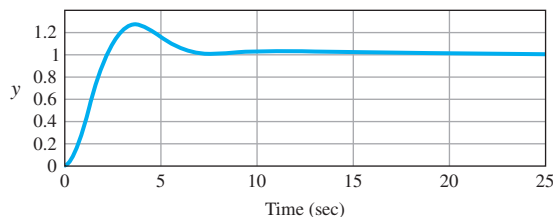


0.01 rad/sec. This selection of parameters produces a PM of  $50^\circ$ , thus satisfying the specifications. Here the stabilization is achieved by keeping the crossover frequency to a region where  $G(s)$  has favorable phase characteristics. However, note  $\omega_c \cong 0.8$  rad/sec for this case compared to the  $\omega_c \cong 5$  rad/sec for the Example 6.15 where lead compensation was used. The criterion for selecting the pole and zero locations  $1/T_I$  is to make them low enough to minimize the effects of the phase lag from the compensation at the crossover frequency. Generally, however, the pole and zero are located no lower than necessary, because the additional system root (compare with the root locus of a similar system design in Fig. 5.28) introduced by the lag will be in the same frequency range as the compensation zero and will have some effect on the output response, especially the response to disturbance inputs.

The response of the system to a step reference input is shown in Fig. 6.65. It shows no steady-state error to a step input, because this is a Type 1 system. However, the introduction of the slow root from the lag compensation has caused the response to require about 25 sec to settle down to the zero steady-state value and the rise time,  $t_r = 2$

**Figure 6.65**

Step response of lag-compensation design in Example 6.19



sec compared to  $t_r = 0.33$  sec for Example 6.15. This difference in rise time is to be expected based on the difference in crossover frequencies. The overshoot  $M_p$  is somewhat larger than you would expect from the guidelines, based on a second-order system shown in Fig. 6.37 for a PM = 50°; however, the performance is adequate.

As we saw previously for a similar situation, Examples 6.15 and 6.19 meet an identical set of specifications for the same plant in very different ways. In the first case, the specifications are met with a lead compensation, and a crossover frequency  $\omega_c = 5$  rad/sec ( $\omega_{BW} \approx 6$  rad/sec) results. In the second case, the same specifications are met with a lag compensation, and  $\omega_c \approx 0.8$  rad/sec ( $\omega_{BW} \approx 0.9$  rad/sec) results. Clearly, had there been specifications for rise time or bandwidth, they would have influenced the choice of compensation (lead or lag). Likewise, if the slow settling to the steady-state value was a problem, it might have suggested the use of lead compensation instead of lag.

In more realistic systems, dynamic elements usually represent the actuator and sensor as well as the process itself, so it is typically impossible to raise the crossover frequency much beyond the value representing the speed of response of the components being used. Although linear analysis seems to suggest that almost any system can be compensated, in fact, if we attempt to drive a set of components much faster than their natural frequencies, the system will saturate, the linearity assumptions will no longer be valid, and the linear design will represent little more than wishful thinking. With this behavior in mind, we see that simply increasing the gain of a system and adding lead compensators to achieve an adequate PM may not always be possible. It may be preferable to satisfy error requirements by adding a lag network so that the closed-loop bandwidth is kept at a more reasonable frequency.

**Important caveat on design strategy**

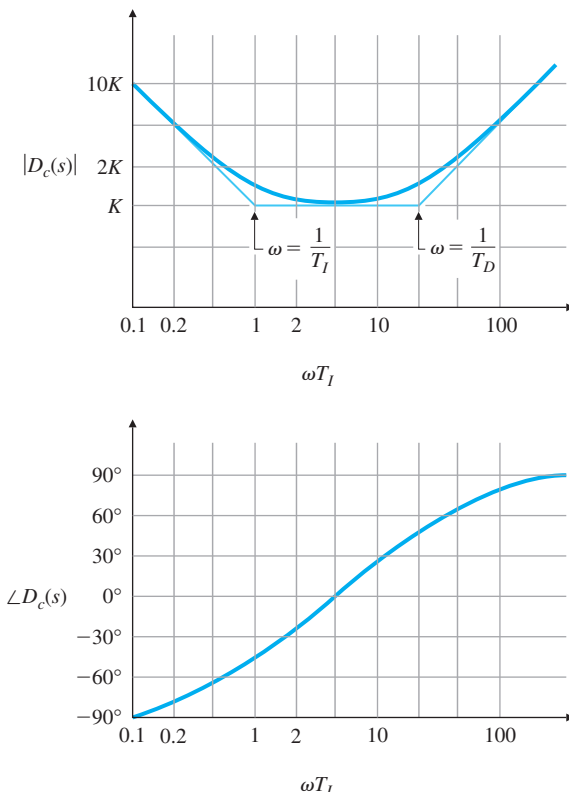
**PID compensation**

### 6.7.5 PID Compensation

For problems that need PM improvement at  $\omega_c$  and low-frequency gain improvement, it is effective to use both derivative and integral control. By combining Eqs. (6.37) and (6.46), we obtain PID control. A common way to write its transfer function is

**Figure 6.66**

Frequency response of PID compensation with  $\frac{T_I}{T_D} = 20$



$$D_c(s) = \frac{K}{s} \left[ (T_D s + 1) \left( s + \frac{1}{T_I} \right) \right], \quad (6.48)$$

and its frequency-response characteristics are shown in Fig. 6.66. This form is slightly different from that given by Eq. (4.75); however, the effect of the difference is inconsequential. This compensation is roughly equivalent to combining lead and lag compensators in the same design, and so is sometimes referred to as a **lead-lag compensator**. Hence, it can provide simultaneous improvement in transient and steady-state responses.

### EXAMPLE 6.20

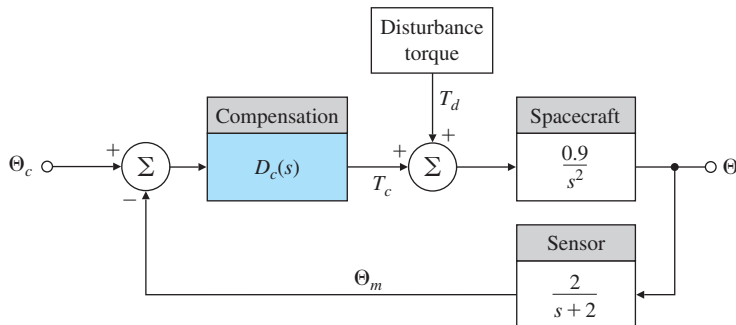
#### *PID Compensation Design for Spacecraft Attitude Control*

A simplified design for spacecraft attitude control was presented in Section 6.5; however, here we have a more realistic situation that includes a sensor lag and a disturbing torque. Figure 6.67 defines the system.

1. Design a PID controller to have zero steady-state error to a constant-disturbance torque, a PM of  $65^\circ$ , and as high a bandwidth as is reasonably possible.

**Figure 6.67**

Block diagram of spacecraft control using PID design in Example 6.20



2. Plot the step response versus a command input and the step response to a constant disturbance torque.
3. Plot the closed-loop frequency response,  $\frac{\Theta}{\Theta_c}$ , and the sensitivity function,  $S$ .
4. Determine  $\omega_{BW}$  and  $\omega_{DRB}$ .
5. For a torque disturbance from solar pressure that acts as a sinusoid at the orbital rate ( $\omega = 0.001 \text{ rad/sec}$  or  $\approx 100\text{-minute period}$ ), comment on the usefulness of this controller to attenuate solar pressure effects.

**Solution.** First, let us take care of the steady-state error. For the spacecraft to be at a steady final value, the total input torque,  $T_d + T_c$ , must equal zero. Therefore, if  $T_d \neq 0$ , then  $T_c = -T_d$ . The only way this can be true with no error ( $e_{ss} = 0$ ) is for  $D_c(s)$  to contain an integral term. Hence, including integral control in the compensation will meet the steady-state requirement. This could also be verified mathematically by use of the Final Value Theorem (see Problem 6.47).

The frequency response of the spacecraft and sensor,  $GH$ , where

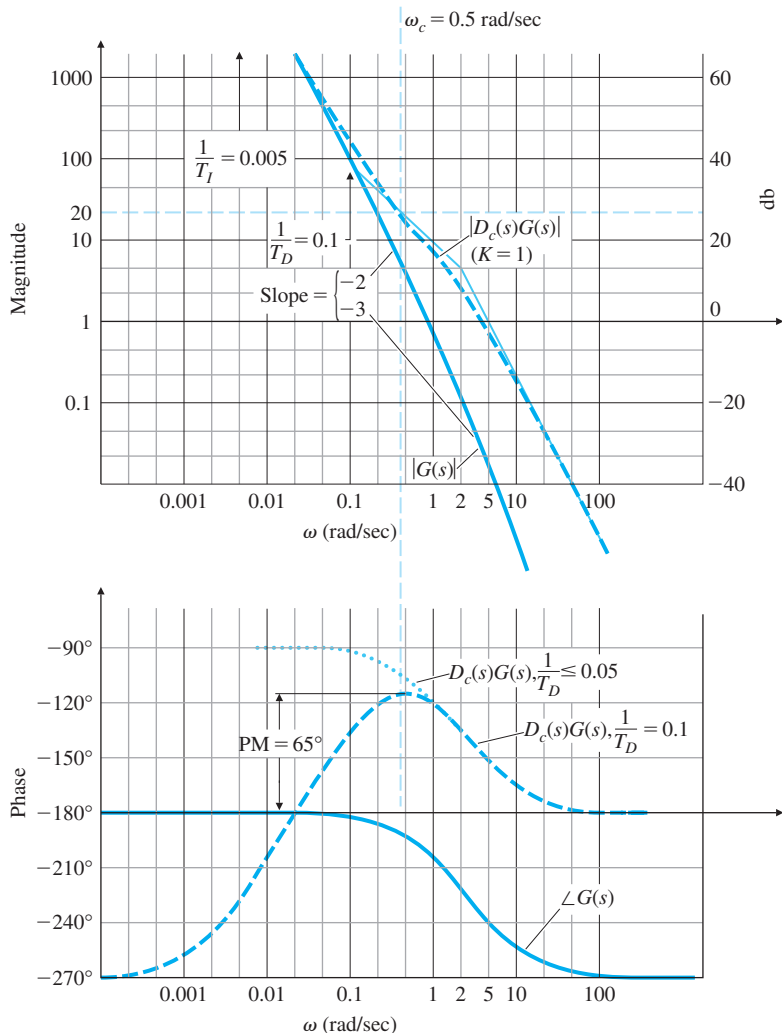
$$G(s) = \frac{0.9}{s^2} \quad \text{and} \quad H(s) = \left( \frac{2}{s+2} \right), \quad (6.49)$$

is shown in Fig. 6.68. The slopes of  $-2$  (that is,  $-40 \text{ db per decade}$ ) and  $-3$  ( $-60 \text{ db per decade}$ ) show that the system would be unstable for any value of  $K$  if no derivative feedback were used. This is clear because of Bode's gain-phase relationship, which shows that the phase would be  $-180^\circ$  for the  $-2$  slope and  $-270^\circ$  for the  $-3$  slope, which would correspond to a PM of  $0^\circ$  or  $-90^\circ$ , respectively. Therefore, derivative control is required to bring the slope to  $-1$  at the crossover frequency that was shown in Section 6.5 to be a requirement for stability. The problem now is to pick values for the three parameters in Eq. (6.48)— $K$ ,  $T_D$ , and  $T_I$ —that will satisfy the specifications.

The easiest approach is to work first on the phase so  $\text{PM} = 65^\circ$  is achieved at a reasonably high frequency. This can be accomplished primarily by adjusting  $T_D$ , noting that  $T_I$  has a minor effect if sufficiently larger than  $T_D$ . Once the phase is adjusted, we establish the crossover frequency; then we can easily determine the gain  $K$ .

**Figure 6.68**

Compensation for PID design in Example 6.20



We examine the phase of the PID controller in Fig. 6.66 to determine what would happen to the compensated spacecraft system,  $D_c(s)G(s)$ , as  $T_D$  is varied. If  $1/T_D \geq 2$  rad/sec, the phase lead from the PID control would simply cancel the sensor phase lag, and the composite phase would never exceed  $-180^\circ$ , an unacceptable situation. If  $1/T_D \leq 0.01$ , the composite phase would approach  $-90^\circ$  for some range of frequencies and would exceed  $-115^\circ$  for an even wider range of frequencies; the latter threshold would provide a PM of  $65^\circ$ . In the compensated phase curve shown in Fig. 6.68,  $1/T_D = 0.1$ , which is the largest value of  $1/T_D$  that could provide the required PM of  $65^\circ$ . The phase would never cross the  $-115^\circ$  ( $65^\circ$  PM) line for any  $1/T_D > 0.1$ . For  $1/T_D = 0.1$ , the crossover frequency  $\omega_c$  that produces the  $65^\circ$  PM is  $0.5$  rad/sec. For a value of  $1/T_D \ll 0.05$ , the phase essentially follows the dotted curve in Fig. 6.68, which indicates that the maximum possible  $\omega_c$

is approximately 1 rad/sec and is provided by  $1/T_D = 0.05$ . Therefore,  $0.05 < 1/T_D < 0.1$  is the only sensible range for  $1/T_D$ ; anything less than 0.05 would provide no significant increase in bandwidth, while anything more than 0.1 could not meet the PM specification. Although the final choice is somewhat arbitrary, we have chosen  $1/T_D = 0.1$  for our final design.

Our choice for  $1/T_I$  is a factor of 20 lower than  $1/T_D$ ; that is,  $1/T_I = 0.005$ . A factor less than 20 would negatively impact the phase at crossover, thus lowering the PM. Furthermore, it is generally desirable to keep the compensated magnitude as large as possible at frequencies below  $\omega_c$  in order to have a faster transient response and smaller errors; maintaining  $1/T_D$  and  $1/T_I$  at the highest possible frequencies will bring this about. An alternate approach for this problem would have been to pick  $1/T_D = 0.05$  in order to have a larger phase increase. This would have allowed a higher value of  $1/T_I$  which would have provided for a faster response of the integral portion of the controller. Note for this system that the sensor break point at 2 rad/sec is limiting how high  $1/T_D$  can be selected. Problem 6.63 examines alternate designs for this system.

The only remaining task is to determine the proportional part of the PID controller, or  $K$ . Unlike the system in Example 6.18, where we selected  $K$  in order to meet a steady-state error specification, here we select a value of  $K$  that will yield a crossover frequency at the point corresponding to the required PM of  $65^\circ$ . The basic procedure for finding  $K$  (discussed in Section 6.6) consists of plotting the compensated system amplitude with  $K = 1$ , finding the amplitude value at crossover, then setting  $1/K$  equal to that value. Figure 6.68 shows that when  $K = 1$ ,  $|D_c(s)G(s)| = 20$  at the desired crossover frequency  $\omega_c = 0.5$  rad/sec. Therefore,

$$\frac{1}{K} = 20, \quad \text{so} \quad K = \frac{1}{20} = 0.05.$$

The compensation equation that satisfies all of the specifications is now complete:

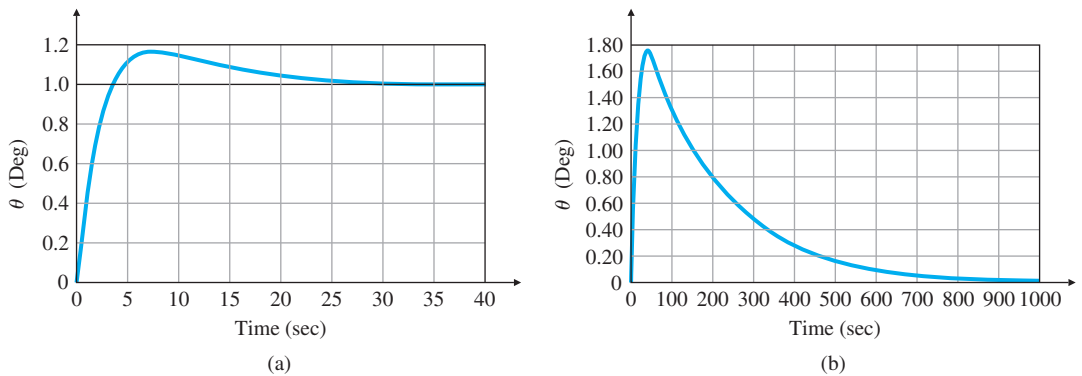
$$D_c(s) = \frac{0.05}{s}[(10s + 1)(s + 0.005)].$$

It is interesting to note this system would become unstable if the gain were lowered so that  $\omega_c \leq 0.02$  rad/sec, the region in Fig. 6.68 where the phase of the compensated system is less than  $-180^\circ$ . As mentioned in Section 6.4, this situation is referred to as a conditionally stable system. A root locus with respect to  $K$  for this and any conditionally stable system would show the portion of the locus corresponding to very low gains in the RHP.

The response of the system for a unit step  $\theta_{com}$  is found from

$$T(s) = \frac{\Theta}{\Theta_c} = \frac{D_c G}{1 + D_c G H},$$

and is shown in Fig. 6.69(a). It exhibits well damped behavior, as should be expected with a  $65^\circ$  PM. The response of the system for a step disturbance torque of  $T_d$  is found from

**Figure 6.69**

Transient response for PID example: (a) unit step command response; (b) step torque disturbance response

$$\frac{\Theta}{T_d} = \frac{G}{1 + D_c GH}.$$

Very low values of disturbance torques exist in space, for example a constant  $T_d = 0.0175$  N-m yields the response shown in Fig. 6.69(b). Note that the integral control term does eventually drive the error to zero; however, it is slow due to the presence of a closed-loop pole and zero both in the vicinity of  $s = -0.005$ . They resulted from the integral term  $1/T_I$  being located slow enough to not impact the PM unduly. If the slow disturbance response is not acceptable, increasing  $1/T_I$  will speed up the response; however, it will also decrease the PM and damping of the system. Alternatively, it would also be possible to select a lower value of  $1/T_D$ , thus giving some extra PM and allowing for a higher value of  $1/T_I$  without sacrificing the desired PM. Problem 6.63 provides the reader with the opportunity to examine other design possibilities for this system.

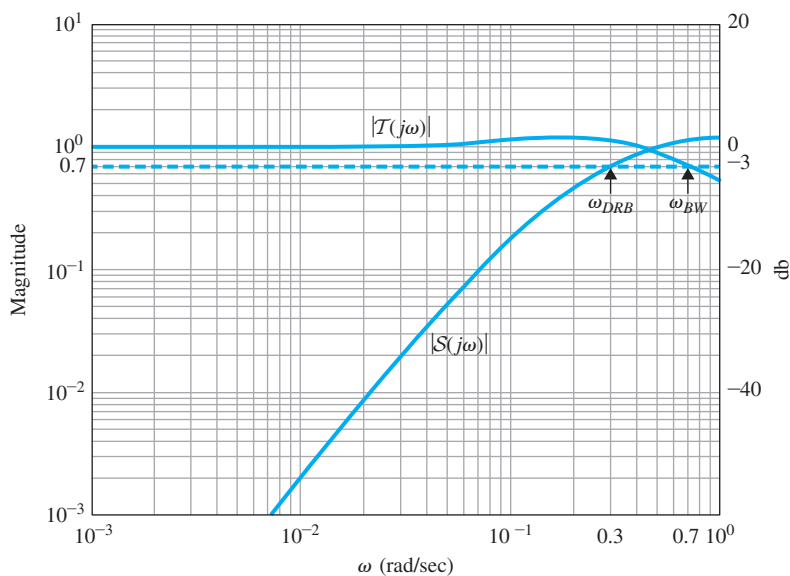
The sensitivity function,  $S$ , represents a general indication of the response of a system to errors and is often plotted along with the closed-loop frequency response. The frequency response of  $\mathcal{T}(s)$  and  $S(s)$  [Eqs. (4.12) and (4.13)] for the system are shown in Fig. 6.70, where

$$S(s) = \frac{1}{1 + D_c GH}.$$

When these two curves cross the magnitude 0.707 ( $-3$  db) line, the values of  $\omega_{BW}$  and  $\omega_{DRB}$  are determined as shown in the figure. The result is that  $\omega_{BW} = 0.7$  rad/sec and  $\omega_{DRB} = 0.3$  rad/sec. Most disturbances on satellites have a periodicity at the orbital rate of 0.001 rad/sec. We see from the figure that the sensitivity function,  $S$ , is approximately  $10^{-5}$  at that frequency, which implies a large attenuation of errors. There is decreasing error attenuation as the disturbance frequency increases, and there is almost no error attenuation at the system bandwidth of  $\approx 0.7$  rad/sec, as you would expect. Another guide to the errors on orbit is

**Figure 6.70**

Frequency responses of the closed-loop transfer function,  $T(j\omega)$ , and the sensitivity function,  $S(j\omega)$



apparent from Fig. 6.69(b). Here we see a step error essentially dies out to zero in approximately 1000 sec due to the integral control feature. This compares with the orbital period of 100 min, or 6000 sec. Therefore, we see orbital disturbances will be heavily attenuated by this controller.

Note from the design process that the bandwidth was limited by the response characteristics of the sensor, which had a bandwidth of 2 rad/sec. Therefore, the only way to improve the error characteristics would be to increase the bandwidth of the sensor. On the other hand, increasing the bandwidth of the sensor may introduce jitter from the high-frequency sensor noise. Thus we see one of the classic trade-off dilemmas: the designer has to make a judgment as to which feature (low errors due to disturbances or low errors due to sensor noise) is the more important to the overall system performance.

### Summary of Compensation Characteristics

1. *PD control* adds phase lead at all frequencies above the break point. If there is no change in gain on the low-frequency asymptote, PD compensation will increase the crossover frequency and the speed of response. The increase in magnitude of the frequency response at the higher frequencies will increase the system's sensitivity to noise.
2. *Lead compensation* adds phase lead at a frequency band between the two break points, which are usually selected to bracket the crossover frequency. If there is no change in gain on the low-frequency asymptote, lead compensation will increase both the crossover frequency and the speed of response over the uncompensated system.

3. *PI control* increases the frequency-response magnitude at frequencies below the break point, thereby decreasing steady-state errors. It also contributes phase lag below the break point, which must be kept at a low enough frequency to avoid degrading the stability excessively.
4. *Lag compensation* increases the frequency-response magnitude at frequencies below the two break points, thereby decreasing steady-state errors. Alternatively, with suitable adjustments in  $K$ , lag compensation can be used to decrease the frequency-response magnitude at frequencies above the two break points, so that  $\omega_c$  yields an acceptable PM. Lag compensation also contributes phase lag between the two break points, which must be kept at frequencies low enough to keep the phase decrease from degrading the PM excessively. This compensation will typically provide a slower response than using lead compensation.

### 6.7.6 Design Considerations

We have seen in the preceding designs that characteristics of the open-loop Bode plot of the loop gain,  $L(s) (= KD_cG)$ , determine performance with respect to steady-state errors, low-frequency errors, and dynamic response including stability margins. Other properties of feedback, developed in Chapter 4, include reducing the effects of sensor noise and parameter changes on the performance of the system.

The consideration of steady-state errors or low-frequency errors due to command inputs and disturbances has been an important design component in the different design methods presented. Design for acceptable errors due to command inputs and disturbances can be thought of as placing a lower bound on the low-frequency gain of the open-loop system. Another aspect of the sensitivity issue concerns the high-frequency portion of the system. So far, Chapter 4 and Sections 5.4 and 6.7 have briefly discussed the idea that, to alleviate the effects of sensor noise, the gain of the system at high frequencies must be kept low. In fact, in the development of lead compensation, we added a pole to pure derivative control specifically to reduce the effects of sensor noise at the higher frequencies. It is not unusual for designers to place an extra pole in the compensation, that is, to use the relation

$$D_c(s) = \frac{T_{DS} + 1}{(\alpha T_{DS} + 1)^2},$$

in order to introduce even more attenuation for noise reduction.

A second consideration affecting high-frequency gains is that many systems have high-frequency dynamic phenomena, such as mechanical resonances, that could have an impact on the stability of a system.

In very-high-performance designs, these high-frequency dynamics are included in the plant model, and a compensator is designed with a specific knowledge of those dynamics. A standard approach to designing for unknown high-frequency dynamics is to keep the high-frequency gain low, just as we did for sensor-noise reduction. The reason for this can be seen from the gain–frequency relationship of a typical system, as shown in Fig. 6.71. The only way instability can result from high-frequency dynamics is if an unknown high-frequency resonance causes the magnitude to rise above 1. Conversely, if all unknown high-frequency phenomena are guaranteed to remain below a magnitude of 1, stability can be guaranteed. The likelihood of an unknown resonance in the plant  $G$  rising above 1 can be reduced if the nominal high-frequency loop gain ( $L$ ) is lowered by the addition of extra poles in  $D_c(s)$ . When the stability of a system with resonances is assured by tailoring the high-frequency magnitude never to exceed 1, we refer to this process as **amplitude** or **gain stabilization**. Of course, if the resonance characteristics are known exactly, a specially tailored compensation, such as one with a notch at the resonant frequency, can be used to change the phase at a specific frequency to avoid encirclements of  $-1$ , thus stabilizing the system even though the amplitude does exceed magnitude 1. This method of stabilization is referred to as **phase stabilization**. A drawback to phase stabilization is that the resonance information is often not available with adequate precision or varies with time; therefore, the method is more susceptible to errors in the plant model used in the design. Thus, we see sensitivity to plant uncertainty and sensor noise are both reduced by sufficiently low loop gain at high-frequency.

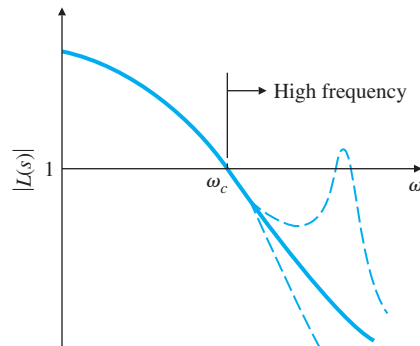
These two aspects of sensitivity—high- and low-frequency behavior—can be depicted graphically, as shown in Fig. 6.72. There is a minimum low-frequency gain allowable for acceptable steady-state and low-frequency error performance, and a maximum high-frequency gain allowable for acceptable noise performance and for low probability of instabilities caused by plant-modeling errors. We define the low-frequency lower bound on the frequency response as  $W_1$  and the upper

### Gain stabilization

### Phase stabilization

**Figure 6.71**

Effect of high-frequency plant uncertainty



bound as  $W_2^{-1}$ , as shown in the figure. Between these two bounds the control engineer must achieve a gain crossover near the required bandwidth; as we have seen, the crossover must occur at a slope of  $-1$  or slightly steeper for good PM and hence damping.

For example, if a control system was required to follow a sinusoidal reference input with frequencies from 0 to  $\omega_1$  with errors no greater than 1%, the function  $W_1$  would be 100 from  $\omega = 0$  to  $\omega_1$ . Similar ideas enter into defining possible values for the  $W_2^{-1}$  function which would constrain the open-loop gain to be below  $W_2^{-1}$  for frequencies above  $\omega_2$ . These ideas will be discussed further in the following subsections.

### △ 6.7.7 Specifications in Terms of the Sensitivity Function

We have seen how the gain and phase margins give useful information about the relative stability of nominal systems and can be used to guide the design of lead and lag compensations. However, the GM and PM are only two numbers and have limitations as guides to the design of realistic control problems. We can express more complete design specifications in the frequency domain if we first give frequency descriptions for the external signals, such as the reference and disturbance, and consider the sensitivity function defined in Section 4.1. For example, we have so far described dynamic performance by the transient response to simple steps and ramps. A more realistic description of the actual complex input signals is to represent them as random processes with corresponding frequency power density spectra. A less sophisticated description, which is adequate for our purposes, is to assume the signals can be represented as a sum of sinusoids with frequencies in a specified range. For example, we can usually describe the frequency content of the reference input as a sum of sinusoids with relative amplitudes given by a magnitude function  $|R|$ , such as that plotted in Fig. 6.73, which represents a signal with sinusoidal components having about the same amplitudes up to some value  $\omega_1$  and very small amplitudes for

**Figure 6.72**

Design criteria for low sensitivity

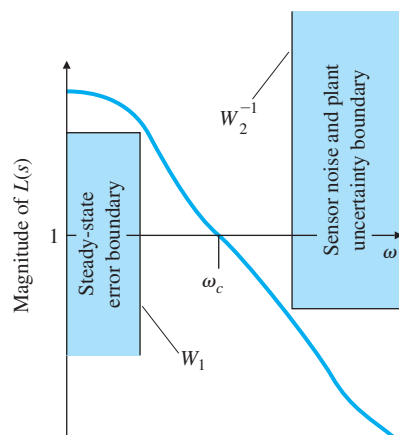
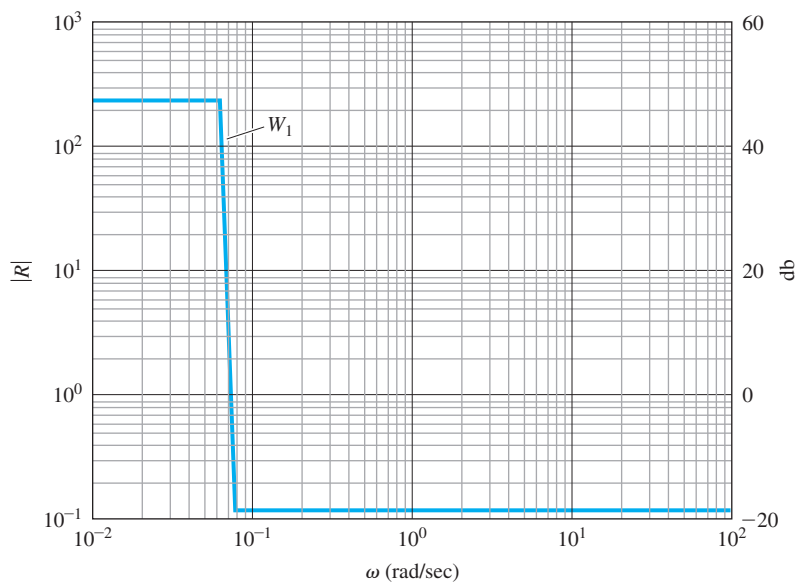


**Figure 6.73**

Plot of typical reference spectrum



frequencies above that. With this assumption, the response tracking specification can be expressed by a statement such as “the magnitude of the system error is to be less than the bound  $e_b$  (a value such as 0.01) for any sinusoid of frequency  $\omega_o$  in the range  $0 \leq \omega_o \leq \omega_1$  with amplitude given by  $|R(j\omega_o)|$ .” To express such a performance requirement in terms that can be used in design, we consider again the unity-feedback system drawn in Fig. 6.74. For this system, the error is given by

$$E(j\omega) = \frac{1}{1 + D_c G} R \triangleq S(j\omega) R, \quad (6.50)$$

**Sensitivity function**

where we have used the **sensitivity function**

$$S \triangleq \frac{1}{1 + D_c G}. \quad (6.51)$$

In addition to being the factor multiplying the system error, the sensitivity function is also the reciprocal of the distance of the Nyquist curve,  $D_c G$ , from the critical point  $-1$ . A large value for  $S$  indicates a Nyquist plot that comes close to the point of instability. The frequency-based error specification based on Eq. (6.50) can be expressed as  $|E| = |S| |R| \leq e_b$ . In order to normalize the problem without needing to

**Figure 6.74**

Closed-loop block diagram

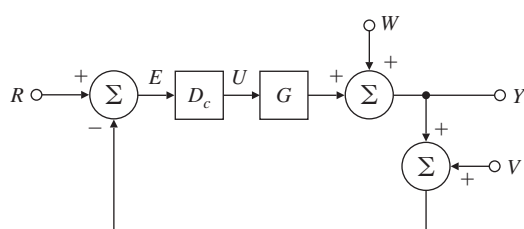
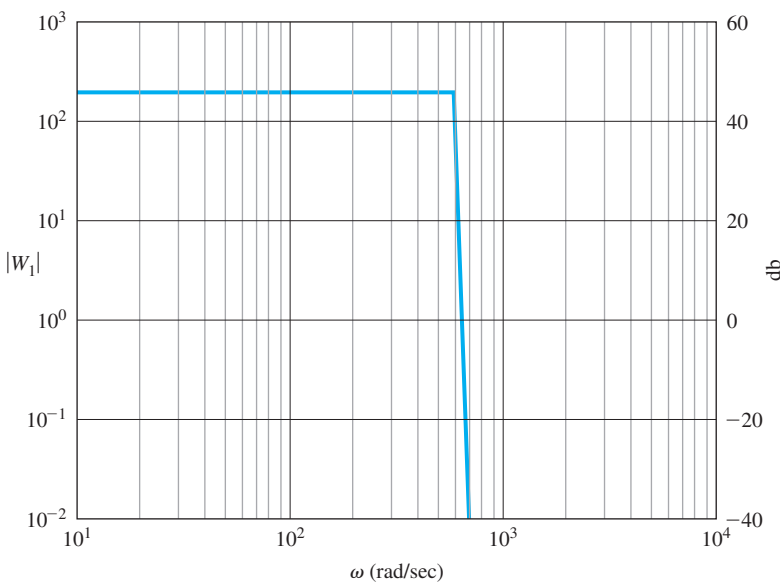


**Figure 6.75**  
Plot of example performance function,  $W_1$



define both the spectrum  $R$  and the error bound each time, we define the real function of frequency  $W_1(\omega) = |R|/e_b$  and the requirement can be written as

$$|\mathcal{S}|W_1 \leq 1. \quad (6.52)$$

### EXAMPLE 6.21

#### Performance Bound Function

A unity-feedback system is to have an error less than 0.005 for all unity amplitude sinusoids below frequency 100 Hertz. Draw the performance function  $W_1(\omega)$  for this design.

**Solution.** The spectrum, from the problem description, is unity for  $0 \leq \omega \leq 200\pi$  rad/sec. Because  $e_b = 0.005$ , the required function is given by a rectangle of amplitude  $1/0.005 = 200$  over the given range. The function is plotted in Fig. 6.75.

---

The expression in Eq. (6.52) can be translated to the more familiar Bode plot coordinates and given as a requirement on loop gain by observing that over the frequency range when errors are small the loop gain is large. In that case  $|\mathcal{S}| \approx 1/|D_c G|$ , and the requirement is approximately

$$\frac{W_1}{|D_c G|} \leq 1, \\ |D_c G| \geq W_1. \quad (6.53)$$

**Stability robustness**

This requirement can be seen as an extension of the steady-state error requirement from just  $\omega = 0$  to the range  $0 \leq \omega_o \leq \omega_1$ .

In addition to the requirement on dynamic performance, the designer is usually required to design for **stability robustness**. By this we mean that, while the design is done for a nominal plant transfer function, the actual system is expected to be stable for an entire class of transfer functions that represents the range of changes that are expected to be faced as temperature, age, and other operational and environmental factors vary the plant dynamics from the nominal case. A realistic way to express this uncertainty is to describe the plant transfer function as having a multiplicative uncertainty:

$$G(j\omega) = G_o(j\omega)[1 + W_2(\omega)\Delta(j\omega)]. \quad (6.54)$$

In Eq. (6.54), the real function  $W_2$  is a magnitude function that expresses the size of changes as a function of frequency that the transfer function is expected to experience. In terms of  $G$  and  $G_o$ , the expression is

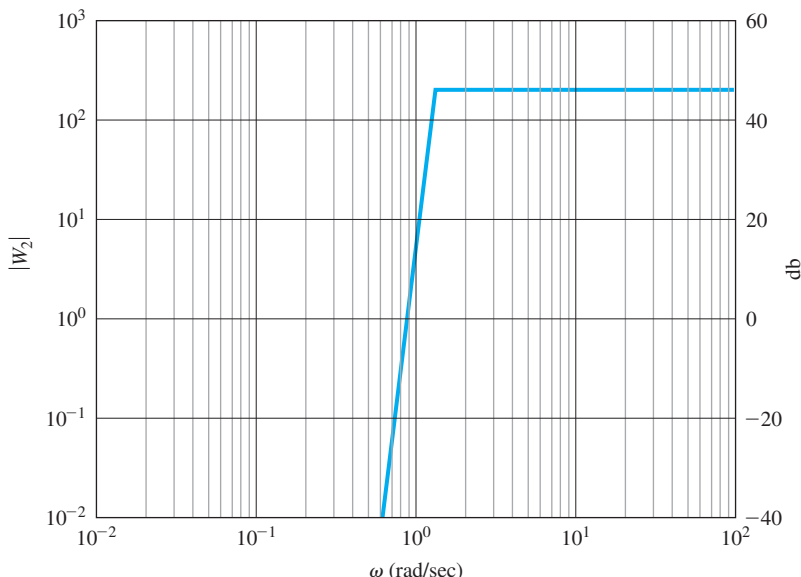
$$W_2 = \left| \frac{G - G_o}{G_o} \right|. \quad (6.55)$$

The shape of  $W_2$  is almost always very small for low frequencies (we know the model very well there) and increases substantially as we go to higher frequencies, where unmodeled system dynamics are common. A typical shape is sketched in Fig. 6.76. The complex function,  $\Delta(j\omega)$ , represents the uncertainty in phase and is restricted only by the constraint

$$0 \leq |\Delta| \leq 1. \quad (6.56)$$

**Figure 6.76**

Plot of typical plant uncertainty,  $W_2$



We assume the nominal design has been done and is stable, so that the Nyquist plot of  $D_c G_o$  satisfies the Nyquist stability criterion. In this case, the nominal characteristic equation  $1 + D_c G_o = 0$  is never satisfied for any real frequency. If the system is to have stability robustness, the characteristic equation using the uncertain plant as described by Eq. (6.54) must not go to zero for any real frequency for any value of  $\Delta$ . The requirement can be written as

$$1 + D_c G \neq 0, \quad (6.57)$$

$$1 + D_c G_o [1 + W_2 \Delta] \neq 0,$$

$$(1 + D_c G_o)(1 + \mathcal{T} W_2 \Delta) \neq 0,$$

where we have defined the **complementary sensitivity function** as

$$\mathcal{T}(j\omega) \triangleq D_c G_o / (1 + D_c G_o) = 1 - \mathcal{S}. \quad (6.58)$$

Because the nominal system is stable, the first term in Eq. (6.57),  $(1 + D_c G_o)$ , is never zero. Thus, if Eq. (6.57) is not to be zero for any frequency and any  $\Delta$ , then it is necessary and sufficient that

$$|\mathcal{T} W_2 \Delta| < 1,$$

which reduces to

$$|\mathcal{T}| W_2 < 1, \quad (6.59)$$

making use of Eq. (6.56). As with the performance specification, for single-input-single-output unity-feedback systems this requirement can be approximated by a more convenient form. Over the range of high frequencies where  $W_2$  is non-negligible because there is significant model uncertainty,  $D_c G_o$  is small. Therefore we can approximate  $\mathcal{T} \approx D_c G_o$ , and the constraint reduces to

$$\begin{aligned} |D_c G_o| W_2 &< 1, \\ |D_c G_o| &< \frac{1}{W_2}. \end{aligned} \quad (6.60)$$

The robustness issue is important to design and can affect the high-frequency open-loop frequency response, as discussed earlier. However, as also discussed earlier, it is important to limit the high-frequency magnitude in order to attenuate noise effects.

## EXAMPLE 6.22

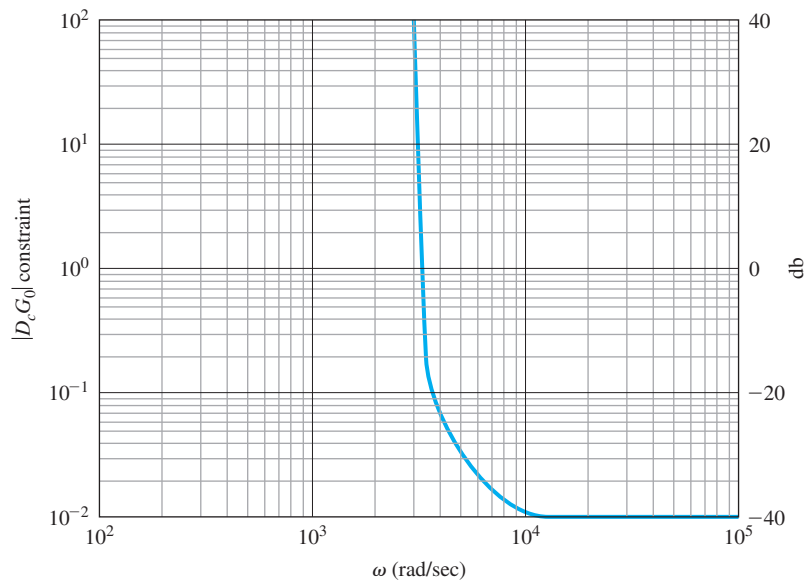
### Typical Plant Uncertainty

The uncertainty in a plant model is described by a function  $W_2$  that is zero until  $\omega = 3000$ , increases linearly from there to a value of 100 at  $\omega = 10,000$ , and remains at 100 for higher frequencies. Plot the constraint on  $D_c G_o$  to meet this requirement.

**Solution.** Where  $W_2 = 0$ , there is no constraint on the magnitude of loop gain; above  $\omega = 3000$ ,  $1/W_2 = D_c G_o$  is a hyperbola from  $\infty$  to 0.01 at  $\omega = 10,000$  and remains at 0.01 for  $\omega > 10,000$ . The bound is sketched in Fig. 6.77.

**Figure 6.77**

Plot of constraint on  
 $|D_c G_o| (= |W_2^{-1}|)$



In practice, the magnitude of the loop gain is plotted on log–log (Bode) coordinates, and the constraints of Eqs. (6.53) and (6.60) are included on the same plot. A typical sketch is drawn in Fig. 6.72. The designer is expected to construct a loop gain that will stay above  $W_1$  for frequencies below  $\omega_1$ , cross over the magnitude 1 line ( $|D_c G| = 0$ ) in the range  $\omega_1 \leq \omega \leq \omega_2$ , and stay below  $1/W_2$  for frequencies above  $\omega_2$ .

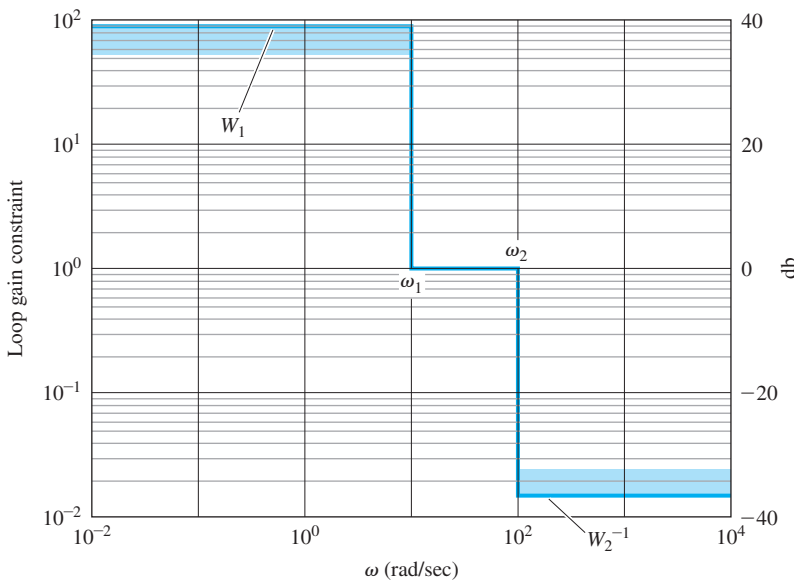
### △ 6.7.8 Limitations on Design in Terms of the Sensitivity Function

One of the major contributions of Bode was to derive important limitations on transfer functions that set limits on achievable design specifications. For example, one would like to have the system error kept small for the widest possible range of frequencies, and yet have a system that is robustly stable for a very uncertain plant. In terms of the plot in Fig. 6.78, we want  $W_1$  and  $W_2$  to be very large in their respective frequency ranges, and for  $\omega_1$  to be pushed up close to  $\omega_2$ . Thus the loop gain is expected to plunge with a large negative slope from being greater than  $W_1$  to being less than  $1/W_2$  in a very short span, while maintaining a good PM to assure stability and good dynamic performance. The Bode gain–phase formula given earlier shows that this is *impossible* with a linear controller, by showing that the minimum possible phase is determined by an integral depending on the slope of the magnitude curve. If the slope is constant for a substantial range around  $\omega_o$ , then Eq. (6.34) can be approximated by

$$\phi(\omega_o) \approx \frac{\pi}{2} \left. \frac{dM}{du} \right|_{u=0}, \quad (6.61)$$

**Figure 6.78**

Tracking and stability robustness constraints on the Bode plot; an example of impossible constraints



where  $M$  is the log magnitude and  $u = \log \omega / \omega_o$ . If, for example, the phase is to be kept above  $-150^\circ$  to maintain a  $30^\circ$  PM, then the magnitude slope near  $\omega_o$  is estimated to be

$$\begin{aligned}\frac{dM}{du} &\approx \frac{2}{\pi} \left( -150 \frac{\pi}{180} \right) \\ &\approx -1.667.\end{aligned}$$

If we try to make the average slope steeper (more negative) than this, we will lose the PM. From this condition, the design rule was developed that the asymptotes of the Bode plot magnitude, which are restricted to be integral values for rational functions, should be made to cross over the zero-db line at a slope of  $-1$  over a frequency range of about one decade around the crossover frequency, as already discussed in Section 6.5. Modifications to this rule need to be made in particular cases, of course, but the limitation implied by Eq. (6.61) is a hard limit that cannot be avoided. Thus, it is clear that it would be impossible to stabilize the system of Fig. 6.78.

### EXAMPLE 6.23

#### *Robustness Constraints*

If  $W_1 = W_2 = 100$ , and we want  $\text{PM} = 30^\circ$ , what is the minimum ratio of  $\omega_2/\omega_1$ ?

**Solution.** The slope is

$$\frac{\log W_1 - \log \frac{1}{W_2}}{\log \omega_1 - \log \omega_2} = \frac{2 + 2}{\log \frac{\omega_1}{\omega_2}} = -1.667.$$

Thus, the log of the ratio is  $\log \omega_1/\omega_2 = -2.40$  and  $\omega_2 = 251\omega_1$ .

An alternative to the standard Bode plot as a design guide can be based on a plot of the sensitivity function as a function of frequency. In this format, Eq. (6.52) requires that  $|\mathcal{S}| < \frac{1}{W_1}$  over the range  $0 \leq \omega \leq \omega_1$  for performance, and Eq. (6.60) requires that  $|\mathcal{S}| \approx 1$  over the range  $\omega_2 \leq \omega$  for stability robustness. It should come as no surprise that Bode found a limitation on the possibilities in this case, too. The constraint, extended by Freudenberg and Looze (1985), shows that an integral of the sensitivity function is determined by the presence of poles in the RHP. Suppose the loop gain  $D_c G_o$  has  $n_p$  poles,  $p_i$ , in the RHP and “rolls off” at high frequencies at a slope faster than  $-1$ . For rational functions, this means that there is an excess of at least two more finite poles than zeros. Then it can be shown that

$$\int_0^\infty \ln(|\mathcal{S}|) d\omega = \pi \sum_{i=1}^{n_p} \operatorname{Re}\{p_i\}. \quad (6.62)$$

If there are no RHP poles, then the integral is zero. This means that if we make the log of the sensitivity function very negative over some frequency band to reduce errors in that band, then, *of necessity*,  $\ln |\mathcal{S}|$  will be positive over another part of the band, and errors will be amplified there. This characteristic is sometimes referred to as the “water bed effect.” If there are unstable poles, the situation is worse, because the positive area where sensitivity magnifies the error must *exceed* the negative area where the error is reduced by the feedback. If the system is minimum phase, then it is, in principle, possible to keep the magnitude of the sensitivity small by spreading the sensitivity increase over all positive frequencies to infinity, but such a design requires an excessive bandwidth and is rarely practical. If a specific bandwidth is imposed, then the sensitivity function is constrained to take on a finite, possibly large, positive value at some point below the bandwidth. As implied by the definition of the vector margin (VM) in Section 6.4 (Fig. 6.38), a large  $\mathcal{S}_{\max}$  corresponds to a Nyquist plot that comes close to the  $-1$  critical point and a system having a small vector margin, because

$$\text{VM} = \frac{1}{\mathcal{S}_{\max}}. \quad (6.63)$$

If the system is not minimum-phase, the situation is worse. An alternative to Eq. (6.62) is true if there is a nonminimum-phase zero of  $D_c G_o$ , a zero in the RHP. Suppose the zero is located at  $z_o = \sigma_o + j\omega_o$ , where  $\sigma_o > 0$ . Again, we assume there are  $n_p$  RHP poles at locations  $p_i$  with conjugate values  $\bar{p}_i$ . Now, the condition can be expressed as a two-sided weighted integral

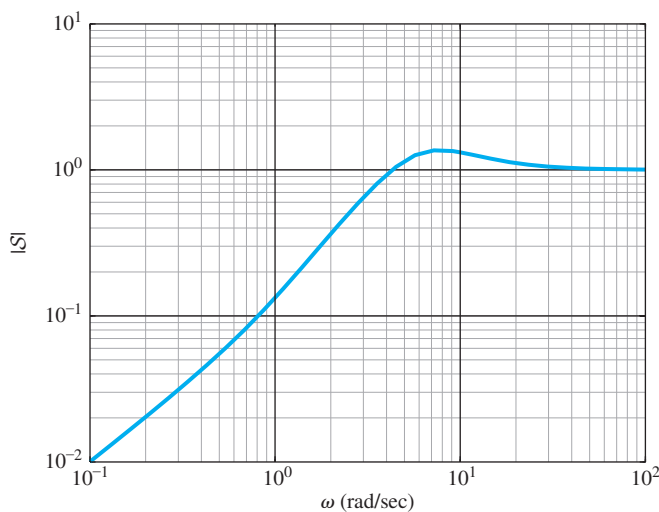
$$\int_{-\infty}^{\infty} \ln(|\mathcal{S}|) \frac{\sigma_o}{\sigma_o^2 + (\omega - \omega_o)^2} d\omega = \pi \sum_{i=1}^{n_p} \ln \left| \frac{\bar{p}_i + z_o}{p_i - z_o} \right|. \quad (6.64)$$

In this case, we do not have the “roll-off” restriction, and there is no possibility of spreading the positive area over high frequencies, because the weighting function goes to zero with frequency. The important point

**Water bed effect**

**Vector margin**

**Figure 6.79**  
Sensitivity function for Example 6.24



about this integral is that if the nonminimum-phase zero is close to a RHP pole, the right side of the integral can be very large, and the excess of positive area is required to be correspondingly large. Based on this result, one expects especially great difficulty meeting both tracking and robustness specifications on sensitivity with a system having RHP poles and zeros close together.

## EXAMPLE 6.24

### Sensitivity Function for Antenna

Compute and plot the sensitivity function for the design of the antenna for which  $G(s) = 1/s(s + 1)$  and  $D_c(s) = 10(0.5s + 1)/(0.1s + 1)$ .

**Solution.** The sensitivity function for this case is

$$S = \frac{s(s + 1)(s + 10)}{s^3 + 11s^2 + 60s + 100}, \quad (6.65)$$

and the plot shown in Fig. 6.79 is given by the Matlab commands

```
s = tf('s');
sysS = s*(s + 1)*(s + 10)/(s^3 + 11*s^2 + 60*s + 100);
[mag,ph,w] = bode(sysS);
loglog(w,squeeze(mag)),grid
```

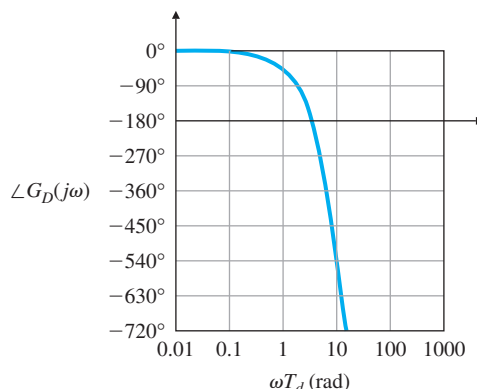
The largest value of  $S$  is given by  $M = \max(\text{mag})$  and is 1.366, from which the vector margin is  $VM = 0.732$ .

## △ 6.8 Time Delay

The Laplace transform of a pure time delay is  $G_D(s) = e^{-sT_d}$ , which can be approximated by a rational function (Padé approximate) as shown in online Appendix W5.6.3. Although this same approximation could be

**Figure 6.80**

Phase lag due to pure time delay



used with frequency-response methods, an exact analysis of the delay is possible.

#### Time-delay magnitude

The frequency response of the delay is given by the magnitude and phase of  $e^{-sT_d}|_{s=j\omega}$ . The magnitude is

$$|G_D(j\omega)| = |e^{-j\omega T_d}| = 1, \quad \text{for all } \omega. \quad (6.66)$$

#### Time-delay phase

This result is expected, because a time delay merely shifts the signal in time and has no effect on its magnitude. The phase is

$$\angle G_D(j\omega) = -\omega T_d \quad (6.67)$$

in radians, and it grows increasingly negative in proportion to the frequency. This, too, is expected, because a fixed time delay  $T_d$  becomes a larger fraction or multiple of a sine wave as the period drops, due to increasing frequency. A plot of  $\angle G_D(j\omega)$  is drawn in Fig. 6.80. Note the phase lag is greater than  $270^\circ$  for values of  $\omega T_d$  greater than about 5 rad. This trend implies it would be virtually impossible to stabilize a system (or to achieve a positive PM) with a crossover frequency greater than  $\omega = 5/T_d$ , and it would be difficult for frequencies greater than  $\omega \approx 3/T_d$ . These characteristics essentially place a constraint on the achievable bandwidth of any system with a time delay. (See Problem 6.64 for an illustration of this constraint.)

The frequency domain concepts such as the Nyquist criterion apply directly to systems with pure time delay. This means that no approximations (Padé type or otherwise) are needed and the exact effect of time delay can be applied to a Bode plot, as shown in the following example.

### EXAMPLE 6.25

#### Effect of Sampling on Stability

When implementing a control system with a digital computer to create compensation, the output of the plant is sampled periodically, used for computer calculations, then output as the control at the same sample rate. The effect of this is to create a delay that, on average, is half the sample period,  $T_s$ . Determine the effect on the PM in Example 6.15 if

it were implemented with a digital controller with a sample period of  $T_s = 0.05$  sec and estimate what that would do to the step response overshoot. How slowly could you sample if it was necessary to limit the decrease in the PM to less than  $20^\circ$ ?

**Solution.** A sample period of  $T_s = 0.05$  sec will inject a time delay of  $T_s/2 = 0.05/2 = 0.025 = T_d$  sec. From Eq. (6.67), we see the phase lag due to this sampling at Example 6.15's crossover frequency of 5 rad/sec, where we measure the PM, is  $\angle G_D = -\omega T_d = -(5)(0.025) = -0.125$  rad =  $-7^\circ$ . Therefore, the PM will decrease from  $53^\circ$  for the continuous implementation to approximately  $46^\circ$  for the digital implementation. Figure 6.37 shows that the overshoot,  $M_p$ , will be degraded from  $\approx 16\%$  to  $\approx 22\%$ . This is a very approximate analysis, but gives a rough idea of what to expect when implementing a controller via sampling and a digital computer.

In order to limit the phase lag to  $20^\circ$  at  $\omega = 5$  rad/sec, we see from Eq.(6.67) that the maximum tolerable  $T_d = 20/(5 * 57.3) = 0.07$  sec, so the slowest sampling acceptable would be  $T_s = 0.14$  sec. Note, however, this large decrease in the PM would result in the overshoot increasing from  $\approx 20\%$  to  $\approx 40\%$ .

The example illustrates that a time delay, whether introduced by digital sampling or by any other source, has a very severe effect on the achievable bandwidth. Evaluation of the effect using Eq. (6.67) or Fig. 6.80 is simple and straightforward, thus giving a quick analysis of the limitations imposed by any delay in the system.

### 6.8.1 Time Delay via the Nyquist Diagram

One can also evaluate the effect of a time delay using a Nyquist diagram, and this is shown in Appendix W6.8.1 available online at [www.pearsonglobaleditions.com](http://www.pearsonglobaleditions.com).

## △ 6.9 Alternative Presentation of Data

Other ways to present frequency-response data have been developed to aid both in understanding design issues and in easing the designer's work load. Their use in easing the work load has largely been eliminated with the common use of computer-aided design; however, one technique that continues to be widely used in the design process is the Nichols chart. For those interested, we also present the inverse Nyquist method in online Appendix W6.9.2 available at [www.pearsonglobaleditions.com](http://www.pearsonglobaleditions.com).

### 6.9.1 Nichols Chart

A rectangular plot of  $\log |G(j\omega)|$  versus  $\angle G(j\omega)$  can be drawn by simply transferring the information directly from the separate magnitude

and phase portions in a Bode plot; one point on the new curve thus results from a given value of the frequency  $\omega$ . This means the new curve is parameterized as a function of frequency. As with the Bode plots, the magnitude information is plotted on a logarithmic scale, while the phase information is plotted on a linear scale. This template was suggested by N. Nichols and is usually referred to as a **Nichols chart**. The idea of plotting the magnitude of  $G(j\omega)$  versus its phase is similar to the concept of plotting the real and imaginary parts of  $G(j\omega)$ , which formed the basis for the Nyquist plots shown in Sections 6.3 and 6.4. However, it is difficult to capture all the pertinent characteristics of  $G(j\omega)$  on the linear scale of the Nyquist plot. The log scale for magnitude in the Nichols chart alleviates this difficulty, allowing this kind of presentation to be useful for design.

For any value of the complex transfer function  $G(j\omega)$ , Section 6.6 showed there is a unique mapping to the unity-feedback closed-loop transfer function

$$T(j\omega) = \frac{G(j\omega)}{1 + G(j\omega)}, \quad (6.68)$$

or in polar form,

$$T(j\omega) = M(\omega)e^{j\alpha(\omega)}, \quad (6.69)$$

where  $M(\omega)$  is the magnitude of the closed-loop transfer function and  $\alpha(\omega)$  is the phase of the closed-loop transfer function. Specifically, let us define  $M$  and  $N$  such that

$$M = \left| \frac{G}{1 + G} \right|, \quad (6.70)$$

$$\alpha = \tan^{-1}(N) = \angle \frac{G}{1 + G}. \quad (6.71)$$

It can be proven that the contours of constant closed-loop magnitude and phase are circles when  $G(j\omega)$  is presented in the *linear* Nyquist plot. These circles are referred to as the **M and N circles**, respectively.

The Nichols chart also contains contours of constant *closed-loop* magnitude and phase based on these relationships, as shown in Fig. 6.81; however, they are no longer circles, because the Nichols charts are semilog plots of magnitude versus linear phase. A designer can therefore graphically determine the bandwidth of a closed-loop system from the plot of the open-loop data on a Nichols chart by noting where the open-loop curve crosses the 0.70 contour of the closed-loop magnitude and determining the frequency of the corresponding data point. Likewise, a designer can determine the resonant-peak amplitude  $M_r$  by noting the value of the magnitude of the highest closed-loop contour tangent to the curve. The frequency associated with the magnitude and phase at the point of tangency is sometimes referred to as the **resonant frequency**  $\omega_r$ . Similarly, a designer can determine the GM by observing the value of the gain where the Nichols plot crosses the  $-180^\circ$  line, and the PM by observing the phase where the plot crosses the amplitude

### M and N circles

### Resonant frequency

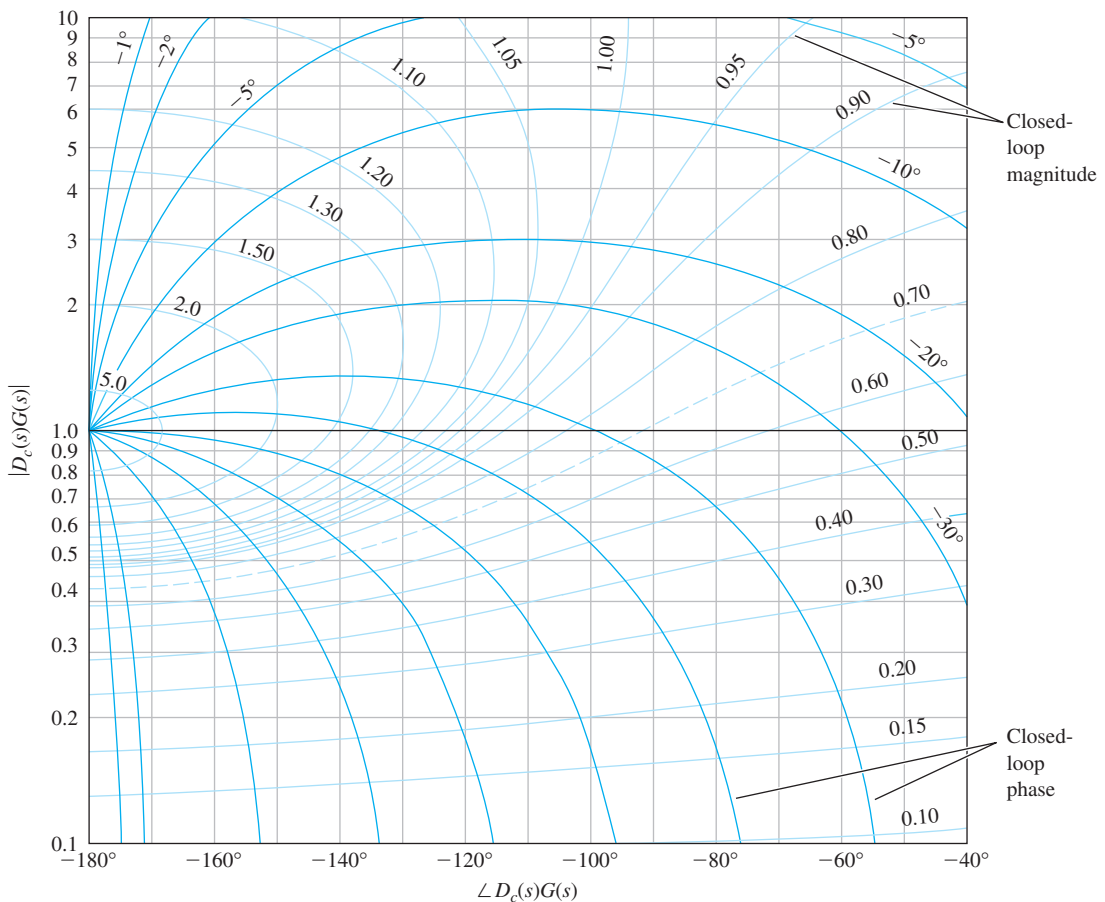


**Figure 6.81**  
Nichols chart

1 line.<sup>15</sup> Matlab provides for easy drawing of a Nichols chart via the nichols command.

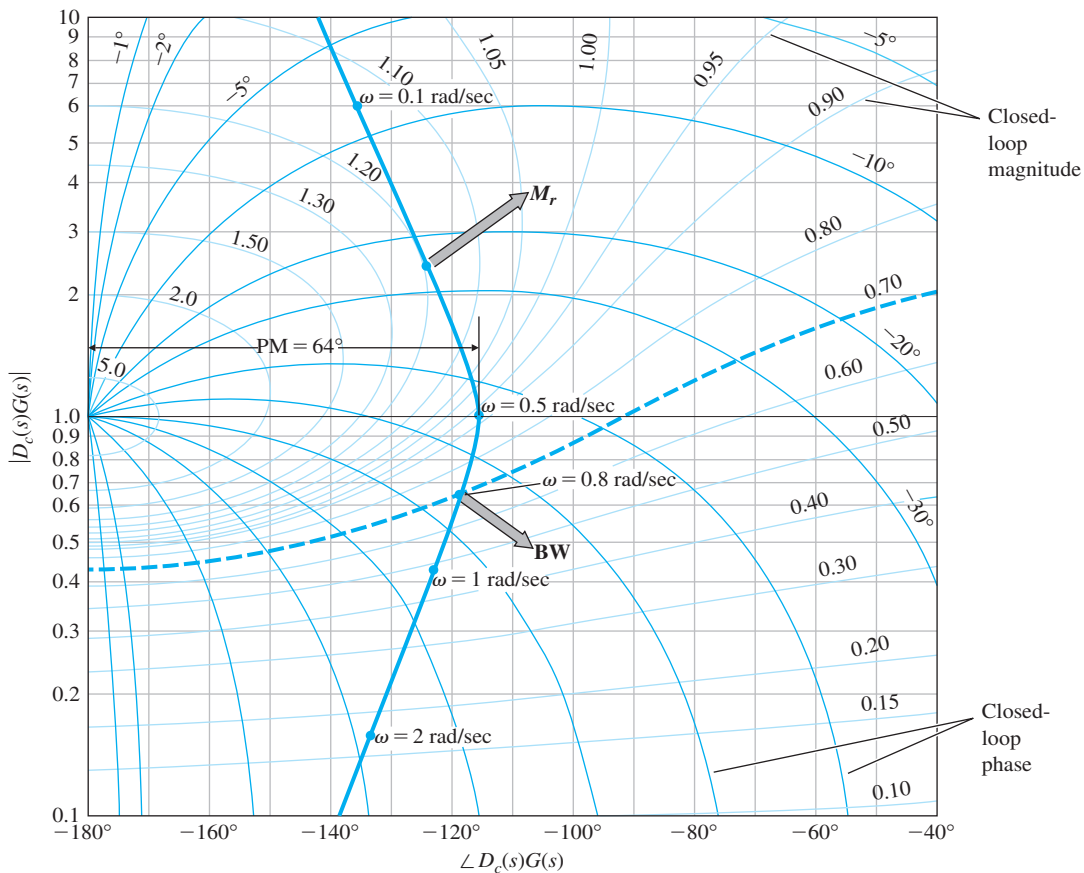
### EXAMPLE 6.26

#### Nichols Chart for PID Example

Determine the a) bandwidth, b) resonant-peak magnitude, and c) PM of the compensated system whose frequency response is shown in Fig. 6.68.

**Solution.** The open-loop magnitude and phase information of the compensated design example seen in Fig. 6.68 is shown on a Nichols chart in Fig. 6.82. When comparing the two figures, it is important to divide the magnitudes in Fig. 6.68 by a factor of 20 in order to obtain  $|D_c(s)G(s)|$  rather than the normalized values used in Fig. 6.68. Because the curve

<sup>15</sup>James, H. M., N. B. Nichols, and R. S. Phillips (1947).

**Figure 6.82**

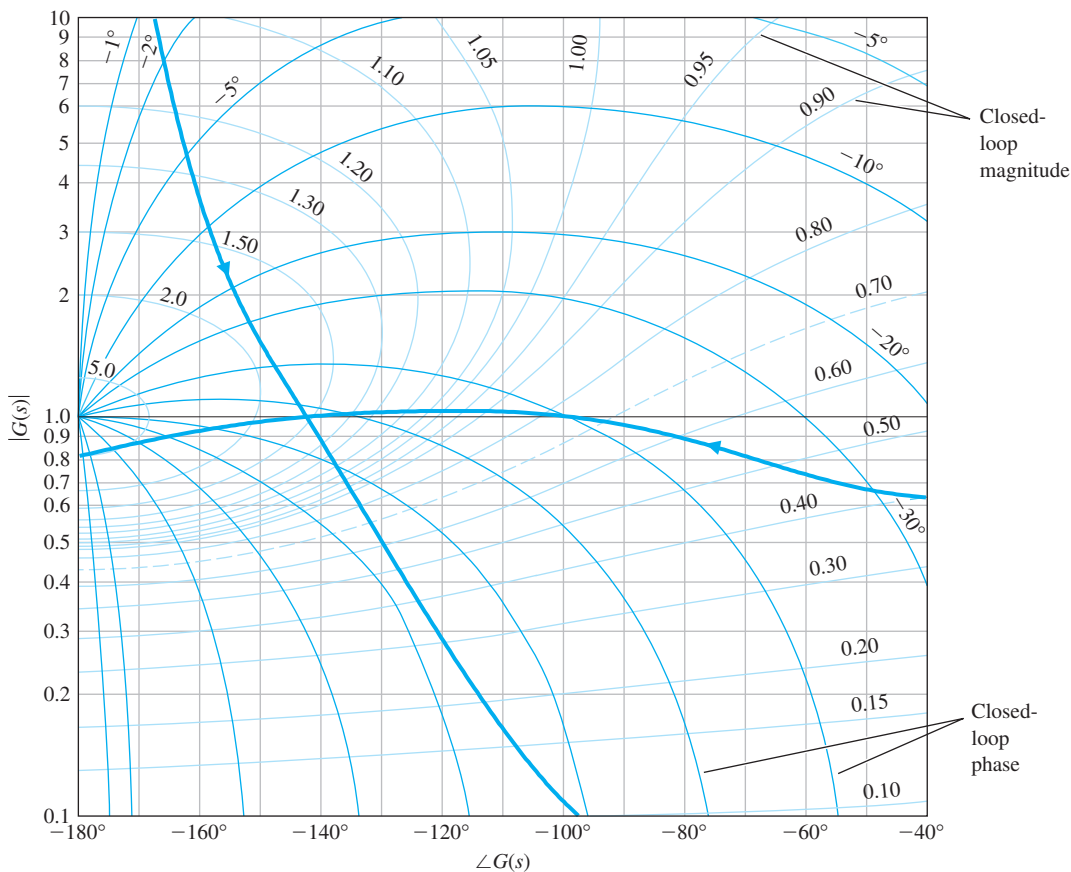
Nichols chart for determining bandwidth,  $M_r$ , and PM for Example 6.26

crosses the closed-loop magnitude 0.70 contour at  $\omega = 0.8$  rad/sec, we see that the bandwidth of this system is 0.8 rad/sec. The PM is determined by the phase when the curve crosses the magnitude = 1 line. Because the largest-magnitude contour touched by the curve is 1.20, we also see that  $M_r = 1.2$ .

**EXAMPLE 6.27***Stability Margins from Nichols Chart for Complex System*

For the system of Example 6.13, whose Nyquist plot is shown in Fig. 6.41, determine the PM and GM using the Nichols plot. Comment on which margin is the more critical.

**Solution.** Figure 6.83 shows a Nichols chart with frequency-response data from Fig. 6.42. Note the PM for the magnitude 1 crossover frequency is  $37^\circ$  and the GM is 1.26 ( $= 1/0.8$ ). It is clear from this

**Figure 6.83**

Nichols chart of the complex system in Examples 6.13 and 6.27

presentation of the data that the most critical portion of the curve is where it crosses the  $-180^\circ$  line; hence, the GM is the most relevant stability margin in this example.

**Exclusion zone for a stability specification**

For complex systems for which the  $-1$  encirclements need to be evaluated, the magnitude log scale of the Nichols chart enables us to examine a wider range of frequencies than a Nyquist plot does, as well as allowing us to read the gain and phase margins directly. Although Matlab will directly compute PM and GM, the algorithm may lead to suspicious results for very complex cases, and the analyst may want to verify the result using the Matlab nichols m-file so the actual encirclements can be examined and the bases for the PM and GM better understood. In some cases, the specifications for the desired margins are stated in terms of an “exclusion zone” around the  $-1$  point on the Nichols chart (magnitude = 1, phase =  $-180^\circ$ ). The zone is typically

an ellipse or similar shape with the vertical and horizontal axes limits given. To satisfy the specification, the frequency-response data on the Nichols chart must not pierce any portion of the ellipse; thus, this sort of stability margin requirement is similar to the vector margin described in Section 6.7.8

Historically, the Nichols chart was used to aid the design process when done without benefit of a computer. A change in gain, for example, can be evaluated by sliding the curve vertically on transparent paper over a standard Nichols chart as shown in Fig. 6.81. The GM, PM, and bandwidth were then easy to read off the chart, thus allowing evaluations of several values of gain with a minimal amount of effort. With access to computer-aided methods, however, we can now calculate the bandwidth and perform many repetitive evaluations of the gain or any other parameter with a few key strokes. Some modern design techniques, such as the Quantitative Feedback Theory (“QFT,” Horowitz and Sidi, 1992), still heavily rely on the Nichols chart as the central tool to guide the feedback design.

### 6.9.2 The Inverse Nyquist Diagram

The inverse Nyquist diagram simplifies a determination of the stability margins and has been used in the past. It is described in more detail in Appendix W6.9.2 available online at [www.pearsonglobaleditions.com](http://www.pearsonglobaleditions.com).

## 6.10 Historical Perspective

As discussed in Chapter 5, engineers before 1960s did not have access to computers to help in their analyses. Therefore, any method that allowed the determination of stability or response characteristics that did not require factoring the characteristic equation was highly useful. The invention of the electronic feedback amplifier by H. S. Black in 1927 at Bell Telephone Laboratories provided extra incentive to develop methods for feedback control design, and the development of the frequency-response method was the first that enabled design iteration for this purpose.

The development of the feedback amplifier is briefly described in an interesting article based on a talk by Hendrik W. Bode (1960) reproduced in Bellman and Kalaba (1964). With the introduction of electronic amplifiers, long-distance telephoning became possible in the decades following World War I. However, as distances increased, so did the loss of electrical energy; in spite of using larger-diameter wire, increasing numbers of amplifiers were needed to replace the lost energy. Unfortunately, large numbers of amplifiers resulted in much distortion since the small nonlinearity of the vacuum tubes then used in electronic amplifiers was multiplied many times. To solve the problem of reducing distortion, Black proposed the feedback amplifier. As discussed in Chapter 4, the more we wish to reduce errors (or distortion), the

higher the feedback needs to be. The loop gain from actuator to plant to sensor to actuator must be made very large. But the designers found that too high a gain produced a squeal and the feedback loop became unstable. In this technology, the dynamics were so complex (with differential equations of order 50 being common) that Routh's criterion, the only way of solving for stability at the time, was not very helpful. So the communications engineers at Bell Telephone Laboratories, familiar with the concept of frequency response and the mathematics of complex variables, turned to complex analysis. In 1932, H. Nyquist published a paper describing how to determine stability from a graphical plot of the open-loop frequency response. Bode then developed his plotting methods in 1938 that made them easy to create without extensive calculations or help from a computer. From the plotting methods and Nyquist's stability theory, an extensive methodology of feedback amplifier design was developed by Bode (1945) and extensively used still in the design of feedback controls. The reasons for using the method today are primarily to allow for a good design no matter what the unmodeled dynamics are, to expedite the design process even when carried out with a computer that is fully capable of solving the characteristic equation, and to provide a visual tool to examine the design. After developing the frequency-response design methods prior to World War II, Bode went on to help in electronic fire control devices during the war. The methods that he had developed for feedback amplifiers proved highly applicable to servomechanisms for the effort. Bode characterized this crossover of control system design methods as being a "sort of shotgun marriage."

## SUMMARY

- The frequency-response **Bode plot** is a graph of the transfer function magnitude in logarithmic scale and the phase in linear scale versus frequency in logarithmic scale. For a transfer function  $G(s)$ ,

$$\begin{aligned} M &= |G(j\omega)| = |G(s)|_{s=j\omega} \\ &= \sqrt{\{\text{Re}[G(j\omega)]\}^2 + \{\text{Im}[G(j\omega)]\}^2} \\ \phi &= \tan^{-1} \left[ \frac{\text{Im}[G(j\omega)]}{\text{Re}[G(j\omega)]} \right] = \angle G(j\omega). \end{aligned}$$

- For a transfer function in Bode form,

$$KG(\omega) = K_0(j\omega)^n \frac{(j\omega\tau_1 + 1)(j\omega\tau_2 + 1)\dots}{(j\omega\tau_a + 1)(j\omega\tau_b + 1)\dots},$$

the Bode frequency response can be easily plotted by hand using the rules described in Section 6.1.1.

- Bode plots can be obtained using computer algorithms (bode in Matlab), but hand-plotting skills are still extremely helpful.

- For a second-order system, the peak magnitude of the Bode plot is related to the damping by

$$|G(j\omega)| = \frac{1}{2\zeta} \quad \text{at } \omega = \omega_n.$$

- A method of determining the stability of a closed-loop system based on the frequency response of the system's open-loop transfer function is the **Nyquist stability criterion**. Rules for plotting the **Nyquist plot** are described in Section 6.3. The number of RHP closed-loop roots is given by

$$Z = N + P,$$

where

$N$  = number of clockwise encirclements of the  $-1$  point,

$P$  = number of open-loop poles in the RHP.

For a stable closed-loop system,  $Z$  must be 0, resulting in  $N = -P$ .

- The Nyquist plot may be obtained using computer algorithms (nyquist in Matlab).
- The **gain margin** (GM) and **phase margin** (PM) can be determined directly by inspecting the open-loop Bode plot or the Nyquist plot. Also, use of Matlab's margin function determines the values directly.
- For a standard second-order system, the PM is related to the closed-loop damping by Eq. (6.32),

$$\zeta \cong \frac{\text{PM}}{100}.$$

- The **bandwidth** of the system is a measure of speed of response. For control systems, it is defined as the frequency corresponding to 0.707 ( $-3$  db) in the closed-loop magnitude Bode plot and is approximately given by the crossover frequency  $\omega_c$ , which is the frequency at which the open-loop gain curve crosses magnitude 1.
- The **vector margin** is a single-parameter stability margin based on the closest point of the Nyquist plot of the open-loop transfer function to the critical point  $-1/K$ .
- For a stable minimum-phase system, Bode's gain–phase relationship uniquely relates the phase to the gain of the system and is approximated by Eq. (6.33),

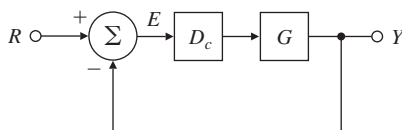
$$\angle G(j\omega) \cong n \times 90^\circ,$$

where  $n$  is the slope of  $|G(j\omega)|$  in units of decade of amplitude per decade of frequency. The relationship shows that, in most cases, stability is ensured if the gain plot crosses the magnitude 1 line with a slope of  $-1$ .

- Experimental frequency-response data of the open-loop system can be used directly for analysis and design of a closed-loop control system with no analytical model.

**Figure 6.84**

Typical unity feedback system



- For the system shown in Fig. 6.84, the open-loop Bode plot is the frequency response of  $GD_c$ , and the closed-loop frequency response is obtained from  $T(s) = GD_c/(1 + GD_c)$ .
- The frequency-response characteristics of several types of compensation have been described, and examples of design using these characteristics have been discussed. Design procedures were given for lead and lag compensators in Section 6.7. The examples in that section show the ease of selecting specific values of design variables, a result of using frequency-response methods. A summary was provided at the end of Section 6.7.5.
- Lead compensation**, given by Eq. (6.38),

$$D_c(s) = \frac{T_{DS} + 1}{\alpha T_{DS} + 1}, \quad \alpha < 1,$$

is a high-pass filter and approximates PD control. It is used whenever substantial improvement in damping of the system is required. It tends to increase the speed of response of a system for a fixed low-frequency gain.

- Lag compensation**, given by Eq. (6.47),

$$D_c(s) = \alpha \frac{T_{IS} + 1}{\alpha T_{IS} + 1}, \quad \alpha > 1, \quad (6.72)$$

is a low-pass filter and approximates PI control. It is usually used to increase the low-frequency gain of the system so as to improve steady-state response for fixed bandwidth. For a fixed low-frequency gain, it will decrease the speed of response of a system.

- PID compensation** can be viewed as a combination of lead and lag compensation.
- Tracking-error reduction and disturbance rejection can be specified in terms of the low-frequency gain of the Bode plot. Sensor-noise rejection can be specified in terms of high-frequency attenuation of the Bode plot (see Fig. 6.72).
- △ The **Nichols plot** is an alternate representation of the frequency response as a plot of gain versus phase and is parameterized as a function of frequency.
- △ Time delay can be analyzed exactly in a Bode plot or a Nyquist plot.

## REVIEW QUESTIONS

- 6.1** Why did Bode suggest plotting the magnitude of a frequency response on log-log coordinates?

- 6.2** Define a decibel.
- 6.3** What is the transfer-function magnitude if the gain is listed as 14 db?
- 6.4** Define gain crossover.
- 6.5** Define phase crossover.
- 6.6** Define phase margin, PM.
- 6.7** Define gain margin, GM.
- 6.8** What Bode plot characteristic is the best indicator of the closed-loop step response overshoot?
- 6.9** What Bode plot characteristic is the best indicator of the closed-loop step response rise time?
- 6.10** What is the principal effect of a lead compensation on Bode plot performance measures?
- 6.11** What is the principal effect of a lag compensation on Bode plot performance measures?
- 6.12** How do you find the  $K_v$  of a Type 1 system from its Bode plot?
- 6.13** Why do we need to know beforehand the number of open-loop unstable poles in order to tell stability from the Nyquist plot?
- 6.14** What is the main advantage in control design of counting the encirclements of  $-1/K$  of  $D_c(j\omega)G(j\omega)$  rather than encirclements of  $-1$  of  $KD_c(j\omega)G(j\omega)$ ?
- 6.15** Define a conditionally stable feedback system. How can you identify one on a Bode plot?
- △ **6.16** A certain control system is required to follow sinusoids, which may be any frequency in the range  $0 \leq \omega_\ell \leq 450$  rad/sec and have amplitudes up to 5 units, with (sinusoidal) steady-state error to be never more than 0.01. Sketch (or describe) the corresponding performance function  $W_1(\omega)$ .

## PROBLEMS

### *Problems for Section 6.1: Frequency Response*

- 6.1 (a)** Show  $\alpha_0$  in Eq. (6.2), with  $A = U_o$  and  $\omega_o = \omega$ , is

$$\alpha_0 = \left[ G(s) \frac{U_0 \omega}{s - j\omega} \right] \Big|_{s=-j\omega} = -U_0 G(-j\omega) \frac{1}{2j},$$

and

$$\alpha_0^* = \left[ G(s) \frac{U_0 \omega}{s + j\omega} \right] \Big|_{s=+j\omega} = U_0 G(j\omega) \frac{1}{2j}.$$

- (b)** By assuming the output can be written as

$$y(t) = \alpha_0 e^{-j\omega t} + \alpha_0^* e^{j\omega t},$$

derive Eqs. (6.4)–(6.6).

- 6.2 (a)** Calculate the magnitude and phase of

$$G(s) = \frac{1}{s + 7}$$

by hand for  $\omega = 1, 2, 7, 10, 20, 50$ , and 100 rad/sec.

- (b) Sketch the asymptotes for  $G(s)$  according to the Bode plot rules, and compare these with your computed results from part (a).

**6.3** Sketch the asymptotes of the Bode plot magnitude and phase for each of the following open loop transfer functions. After completing the hand sketches verify your results using Matlab. Turn in your hand sketches and the Matlab results on the same scales.

(a)  $L(s) = \frac{6000}{s(s+300)}$

(b)  $L(s) = \frac{500}{s(0.2s+1)(0.1s+1)}$

(c)  $L(s) = \frac{1}{s(5s+1)(s+40)}$

(d)  $L(s) = \frac{5000}{(s+7)(s+18)^3}$

(e)  $L(s) = \frac{10(s+2)}{s(s+20)(s+200)}$

(f)  $L(s) = \frac{2(s+0.3)}{s(s+0.1)(s+0.5)^2}$

(g)  $L(s) = \frac{(s+17)(s+13)}{s(s+52)(s+5)}$

(h)  $L(s) = \frac{10s(s+50)}{(s+10)(s+70)}$

(i)  $L(s) = \frac{1000s}{(s+2)(s+60)(s+500)}$

**6.4** *Real poles and zeros.* Sketch the asymptotes of the Bode plot magnitude and phase for each of the following open-loop transfer functions. After completing the hand sketches verify your results using Matlab. Turn in your hand sketches and the Matlab results on the same scales.

(a)  $L(s) = \frac{5}{s(s+4)(s+9)(s+17)}$

(b)  $L(s) = \frac{5(s+12)}{s(s+4)(s+9)(s+17)}$

(c)  $L(s) = \frac{5(s+7)(s+12)}{s(s+4)(s+9)(s+17)}$

(d)  $L(s) = \frac{5(s+7)(s+1)}{s(s+4)(s+9)(s+17)}$

**6.5** *Complex poles and zeros.* Sketch the asymptotes of the Bode plot magnitude and phase for each of the following open-loop transfer functions. After completing the hand sketches verify your results using Matlab. Turn in your hand sketches and the Matlab results on the same scales.

(a)  $L(s) = \frac{1}{s^2 + 4s + 21}$

(b)  $L(s) = \frac{1}{s(s^2 + 2s + 9)}$

(c)  $L(s) = \frac{(s^2 + 5s + 11)}{s(s^2 + 5s + 15)}$

(d)  $L(s) = \frac{(s^2 + 1)}{s(s^2 + 6)}$

(e)  $L(s) = \frac{(s^2 + 6)}{s(s^2 + 1)}$

- 6.6** *Multiple poles at the origin.* Sketch the asymptotes of the Bode plot magnitude and phase for each of the following open-loop transfer functions. After completing the hand sketches, verify your results using Matlab. Turn in your hand sketches and the Matlab results on the same scales.

(a)  $L(s) = \frac{1}{s^2(s+0.7)}$

(b)  $L(s) = \frac{100}{s^3(s+80)}$

(c)  $L(s) = \frac{1}{s^4(2s+5)}$

(d)  $L(s) = \frac{s+7.5}{s^2(s+75)}$

(e)  $L(s) = \frac{1.5s+1}{s^3(s+0.1)}$

(f)  $L(s) = \frac{(s+9)^2}{s^3(s+50)}$

(g)  $L(s) = \frac{(s+0.6)^2}{s^3(s+1.3)^2}$

- 6.7** *Mixed real and complex poles.* Sketch the asymptotes of the Bode plot magnitude and phase for each of the following open-loop transfer functions. After completing the hand sketches verify your results using Matlab. Turn in your hand sketches and the Matlab results on the same scales.

(a)  $L(s) = \frac{(s+0.5)}{s(5s+1)(s^2+0.2s+0.6)}$

(b)  $L(s) = \frac{(2s+4)}{s^2(s+8)(s^2+5s+27)}$

(c)  $L(s) = \frac{(s+0.75)^2}{s^2(1.2s+8.1)(s^2+5s+27)}$

(d)  $L(s) = \frac{(s+50)(2s^2+5s+4)}{s^2(s+5)(s^2+60s+120)}$

(e)  $L(s) = \frac{[(s+2)^2+2]}{s^2(s^2+7s+5)}$

- 6.8** *Right half-plane poles and zeros.* Sketch the asymptotes of the Bode plot magnitude and phase for each of the following open-loop transfer functions. Make sure the phase asymptotes properly take the RHP singularity into account by sketching the complex plane to see how the  $\angle L(s)$  changes as  $s$  goes from 0 to  $+j\infty$ . After completing the hand sketches verify your results using Matlab. Turn in your hand sketches and the Matlab results on the same scales.

(a)  $L(s) = \frac{s+4}{s+12} \frac{1}{s^2-9}$ ; (The model for a case of magnetic levitation with lead compensation.)

(b)  $L(s) = \frac{s+4}{s(s+6)} \frac{1}{s^2-22}$ ; (The magnetic levitation system with integral control and lead compensation.)

(c)  $L(s) = \frac{11s-7}{s^2}$

(d)  $L(s) = \frac{s^2+4s+3}{s(s+2.5)^2(s^2-3s+5)}$

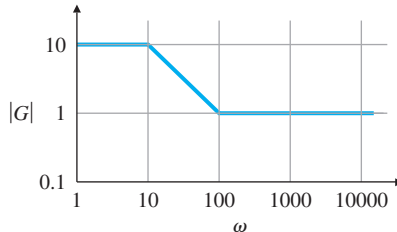
(e)  $L(s) = \frac{(s+7.5)}{s(s-0.5)(s+20)^2}$

(f)  $L(s) = \frac{1}{(s-9)[(s+2)^2 + 5]}$

- 6.9** A certain system is represented by the asymptotic Bode diagram shown in Fig. 6.85. Find and sketch the response of this system to a unit step input (assuming zero initial conditions).

**Figure 6.85**

Magnitude portion of Bode plot for Problem 6.9.



- 6.10** Prove that magnitude slope of  $-2$  in a Bode plot corresponds to  $-40$  db per decade or  $-12$  db per octave.  
**6.11** A second-order system with a damping ratio  $\zeta = 0.6$  and an additional zero is given by

$$G(s) = \frac{\left(\frac{s}{\alpha} + 1\right)}{s^2 + 1.2s + 1}.$$

Use Matlab to compare the  $M_p$  from the step response of the system for  $a = 0.01, 0.1, 1, 10$ , and  $100$  with the  $M_r$  from the frequency response of each case. Is there a correlation between  $M_r$  and  $M_p$ ?

- 6.12** A second order system with  $\zeta = 0.6$  and an additional pole is given by

$$G(s) = \frac{2}{\left[\left(\frac{s}{p}\right) + 1\right](s^2 + 1.2\sqrt{2}s + 2)}$$

Draw Bode plots with  $p = 0.01, 0.1, 1, 10$ , and  $100$ . What conclusions can you draw about the effect of an extra pole on the bandwidth compared to the bandwidth for the second-order system with no extra pole?

- 6.13** For the closed-loop transfer function

$$T(s) = \frac{\omega_n^2}{s^2 + 2\zeta\omega_n s + \omega_n^2},$$

derive the following expression for the bandwidth  $\omega_{BW}$  of  $T(s)$  in terms of  $\omega_n$  and  $\zeta$ :

$$\omega_{BW} = \omega_n \sqrt{1 - 2\zeta^2 + \sqrt{2 + 4\zeta^4 - 4\zeta^2}}.$$

Assuming  $\omega_n = 1$ , plot  $\omega_{BW}$  for  $0 \leq \zeta \leq 1$ .

- 6.14** Consider the system whose transfer function is

$$G(s) = \frac{A_0 \omega_0 s}{s^2 + \frac{\omega_0}{Q} s + \omega_0^2}.$$

This is a model of a tuned circuit with *quality factor*  $Q$ .

- (a) Compute the magnitude and phase of the transfer function analytically, and plot them for  $Q = 0.5, 1, 2$ , and  $5$  as a function of the normalized frequency  $\omega/\omega_0$ .

- (b) Define the bandwidth as the distance between the frequencies on either side of  $\omega_0$  where the magnitude drops to  $3\text{ db}$  below its value at  $\omega_0$ , and show the bandwidth is given by

$$\text{BW} = \frac{1}{2\pi} \left( \frac{\omega_0}{Q} \right).$$

- (c) What is the relation between  $Q$  and  $\zeta$ ?

- 6.15** A DC voltmeter schematic is shown in Fig. 6.86. The pointer is damped so its maximum overshoot to a step input is  $10\%$ .

- (a) What is the undamped natural frequency of the system?

- (b) What is the damped natural frequency of the system?

- (c) Plot the frequency response using Matlab to determine what input frequency will produce the largest magnitude output?

- (d) Suppose this meter is now used to measure a  $1\text{-V AC}$  input with a frequency of  $2\text{ rad/sec}$ . What amplitude will the meter indicate after initial transients have died out? What is the phase lag of the output with respect to the input? Use a Bode plot analysis to answer these questions. Use the `lsim` command in Matlab to verify your answer in part (d).

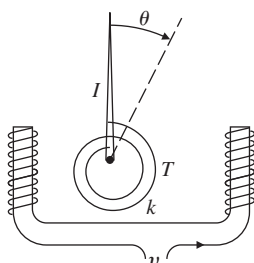
### Problems for Section 6.2: Neutral Stability

- 6.16** Determine the range of  $K$  for which the closed-loop systems (see Fig. 6.18) are stable for each of the cases below by making a Bode plot for  $K = 1$  and imagining the magnitude plot sliding up or down until instability results. Verify your answers by using a very rough sketch of a root-locus plot.

(a)  $KG(s) = \frac{K(s+2)}{s+20}$

**Figure 6.86**

Voltmeter schematic



$$I = 40 \times 10^{-6} \text{ kg} \cdot \text{m}^2$$

$$k = 4 \times 10^{-6} \text{ kg} \cdot \text{m}^2/\text{sec}^2$$

$$T = \text{input torque} = K_m v$$

$$v = \text{input voltage}$$

$$K_m = 4 \times 10^{-6} \text{ N} \cdot \text{m/V}$$

(b)  $KG(s) = \frac{K}{(s+10)(s+1)^2}$

(c)  $KG(s) = \frac{K(s+10)(s+1)}{(s+100)(s+5)^3}$

- 6.17** Determine the range of  $K$  for which each of the listed systems is stable by making a Bode plot for  $K = 1$  and imagining the magnitude plot sliding up or down until instability results. Verify your answers by using Matlab with the marginal stability value of  $K$ .

(a)  $KG(s) = \frac{K(s+1)}{s(s+10)}$

(b)  $KG(s) = \frac{K(s+1)}{s^2(s+10)}$

(c)  $KG(s) = \frac{K}{(s+2)(s^2+9)}$

(d)  $KG(s) = \frac{K(s+1)^2}{s^3(s+10)}$

### Problems for Section 6.3: The Nyquist Stability Criterion

- 6.18** (a) Sketch the Nyquist plot for an open-loop system with transfer function  $1/s^2$ ; that is, sketch

$$\left. \frac{1}{s^2} \right|_{s=C_1},$$

where  $C_1$  is a contour enclosing the entire RHP, as shown in Fig. 6.17. (*Hint:* Assume  $C_1$  takes a small detour around the poles at  $s = 0$ , as shown in Fig. 6.27)

- (b) Repeat part (a) for an open-loop system whose transfer function is  $G(s) = \frac{1}{s^2 + \omega_0^2}$ .

- 6.19** Sketch the Nyquist plot based on the Bode plots for each of the following systems, then compare your result with that obtained by using the Matlab command nyquist: Don't be concerned with the details of exactly where the curve goes, but do make sure it crosses the real axis at the right spot, has the correct number of  $-1$  encirclements and goes off to infinity in the correct direction.

(a)  $KG(s) = \frac{K(s+2)}{s+10}$

(b)  $KG(s) = \frac{K}{(s+10)(s+2)^2}$

(c)  $KG(s) = \frac{K(s+10)(s+1)}{(s+100)(s+2)^3}$

- (d) Using your plots, estimate the range of  $K$  for which each system is stable, and qualitatively verify your result by using a rough sketch of a root-locus plot.

- 6.20** Draw a Nyquist plot for

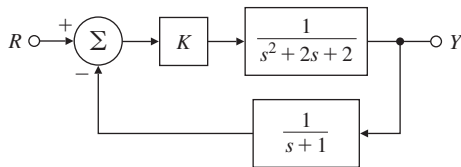
$$KG(s) = \frac{K(s+1)}{s(s+3)}, \quad (6.73)$$

choosing the contour to be to the right of the singularity on the  $j\omega$ -axis. Next, using the Nyquist criterion, determine the range of  $K$  for which the system is stable. Then redo the Nyquist plot, this time choosing the contour to be to the left of the singularity on the imaginary axis. Again,

using the Nyquist criterion, check the range of  $K$  for which the system is stable. Are the answers the same? Should they be?

- 6.21** Draw the Nyquist plot for the system in Fig. 6.87. Using the Nyquist stability criterion, determine the range of  $K$  for which the system is stable. Consider both positive and negative values of  $K$ .

**Figure 6.87**  
Control system for  
Problem 6.21



- 6.22 (a)** For  $\omega = 0.1$  to 100 rad/sec, sketch the phase of the minimum-phase system

$$G(s) = \left. \frac{s+1}{s+10} \right|_{s=j\omega}$$

and the nonminimum-phase system

$$G(s) = -\left. \frac{s-1}{s+10} \right|_{s=j\omega},$$

noting that  $\angle(j\omega - 1)$  decreases with  $\omega$  rather than increasing.

- (b)** Does an RHP zero affect the relationship between the  $-1$  encirclements on a polar plot and the number of unstable closed-loop roots in Eq. (6.28)?
- (c)** Sketch the phase of the following unstable system for  $\omega = 0.1$  to 100 rad/sec:

$$G(s) = \left. \frac{s+1}{s-10} \right|_{s=j\omega}.$$

- (d)** Check the stability of the systems in (a) and (c) using the Nyquist criterion on  $KG(s)$ . Determine the range of  $K$  for which the closed-loop system is stable, and check your results qualitatively by using a rough root-locus sketch.

- 6.23** *Nyquist plots and the classical plane curves:* Determine the Nyquist plot, using Matlab, for the systems given below, with  $K = 1$ , and verify that the beginning point and end point for the  $j\omega > 0$  portion have the correct magnitude and phase:

- (a)** The classical curve called Cayley's Sextic, discovered by Maclaurin in 1718:

$$KG(s) = K \frac{1}{(s+1)^3}.$$

- (b)** The classical curve called the Cissoid, meaning ivy-shaped:

$$KG(s) = K \frac{1}{s(s+1)}.$$

- (c)** The classical curve called the Folium of Kepler, studied by Kepler in 1609:

$$KG(s) = K \frac{1}{(s-1)(s+1)^2}.$$

(d) The classical curve called the Folium (not Kepler's):

$$KG(s) = K \frac{1}{(s-1)(s+2)}.$$

(e) The classical curve called the Nephroid, meaning kidney-shaped:

$$KG(s) = K \frac{2(s+1)(s^2 - 4s + 1)}{(s-1)^3}.$$

(f) The classical curve called Nephroid of Freeth, named after the English mathematician T. J. Freeth:

$$KG(s) = K \frac{(s+1)(s^2 + 3)}{4(s-1)^3}.$$

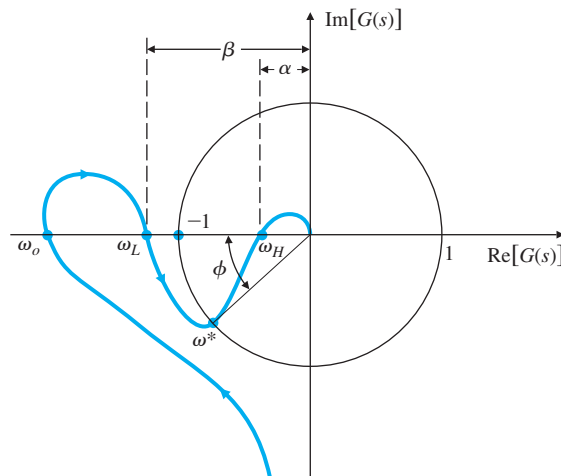
(g) A shifted Nephroid of Freeth:

$$KG(s) = K \frac{(s^2 + 1)}{(s-1)^3}.$$

### Problems for Section 6.4: Stability Margins

- 6.24** The Nyquist plots for some actual control systems resemble the one shown in Fig. 6.88. What are the gain and phase margin(s) for the system of Fig. 6.88, given that  $\alpha = 0.4$ ,  $\beta = 1.3$ , and  $\phi = 40^\circ$ . Describe what happens to the stability of the system as the gain goes from zero to a very large value. Sketch what the corresponding root locus must look like for such a system. Also, sketch what the corresponding Bode plots would look like for the system.

**Figure 6.88**  
Nyquist plot for Problem 6.24



- 6.25** The Bode plot for

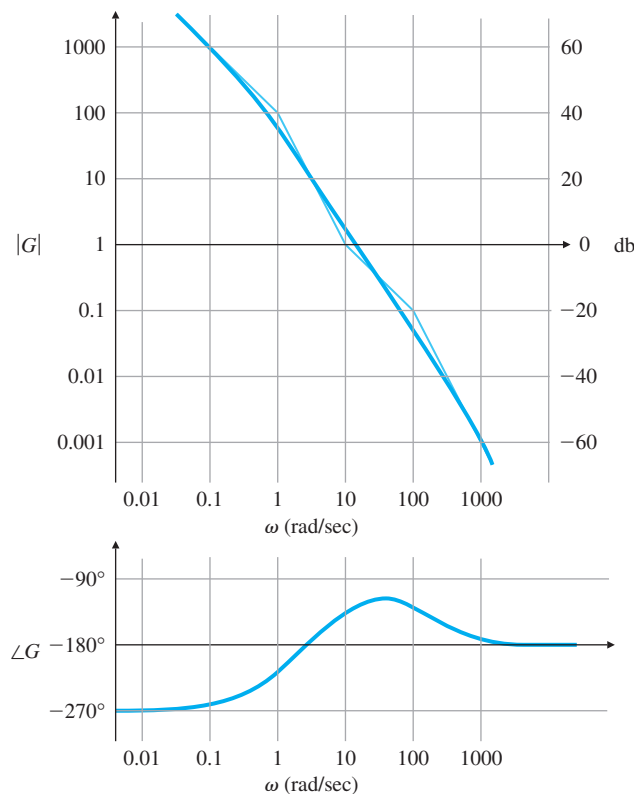
$$G(s) = \frac{100[(s/10) + 1]}{s[(s/1) - 1][(s/100) + 1]}$$

is shown in Fig. 6.89.

- (a) Why does the phase start at  $-270^\circ$  at the low frequencies?
- (b) Sketch the Nyquist plot for  $G(s)$ .
- (c) Is the closed-loop system for the Bode plot shown in Fig. 6.89 stable?
- (d) Will the system be stable if the gain is lowered by a factor of 100? Make a rough sketch of a root locus for the system, and qualitatively confirm your answer.

**Figure 6.89**

Bode plot for Problem 6.25



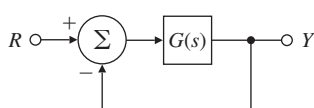
**6.26** Suppose in Fig. 6.90,

$$G(s) = \frac{25(s+1)}{s(s+2)(s^2 + 2s + 16)}.$$

Use Matlab's margin to calculate the PM and GM for  $G(s)$  and, on the basis of the Bode plots, conclude which margin would provide more useful information to the control designer for this system.

**Figure 6.90**

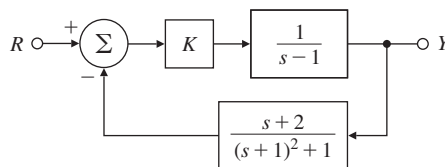
Control system for Problem 6.26



**6.27** Consider the system given in Fig. 6.91.

- Use Matlab to obtain Bode plots for  $K = 1$ , then use the plots to estimate the range of  $K$  for which the system will be stable.
- Verify the stable range of  $K$  by using margin to determine PM for selected values of  $K$ .
- Use rlocus to determine the values of  $K$  at the stability boundaries.
- Sketch the Nyquist plot of the system, and use it to verify the number of unstable roots for the unstable ranges of  $K$ .
- Using Routh's criterion, determine the ranges of  $K$  for closed-loop stability of this system.

**Figure 6.91**  
Control system for  
Problem 6.27



**6.28** Suppose in Fig. 6.90,

$$G(s) = \frac{3.2(s+1)}{s(s+2)(s^2 + 0.2s + 16)}.$$

Use Matlab's margin to calculate the PM and GM for  $G(s)$ , and comment on whether you think this system will have well-damped closed-loop roots.

- 6.29** For a given system, show that the ultimate period  $P_u$  and the corresponding ultimate gain  $K_u$  for the Ziegler–Nichols method can be found by using the following:
- Nyquist diagram
  - Bode plot
  - Root locus
- 6.30** If a system has the open-loop transfer function

$$G(s) = \frac{\omega_n^2}{s(s+2\zeta\omega_n)},$$

with unity feedback, then the closed-loop transfer function is given by

$$T(s) = \frac{\omega_n^2}{s^2 + 2\zeta\omega_n s + \omega_n^2}.$$

Verify the values of the PM shown in Fig. 6.36 for  $\zeta = 0.1, 0.4$ , and  $0.7$ .

- 6.31** Consider the unity feedback system with the open-loop transfer function

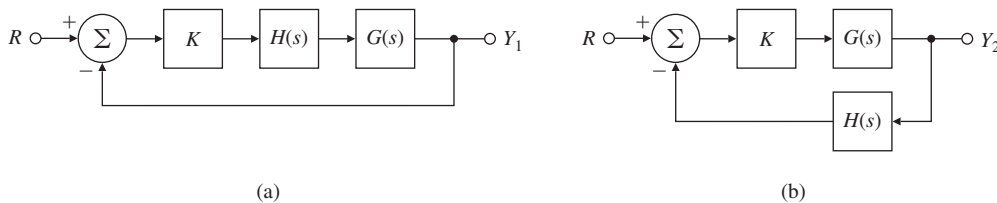
$$G(s) = \frac{K}{s \left( \frac{s}{0.4} + 1 \right) \left( \frac{s^2}{4} + \frac{s}{5} + 1 \right)}$$

- (a) Use Matlab to draw the Bode plots for  $G(j\omega)$  assuming  $K = 1$ .
- (b) What gain  $K$  is required for a PM of  $50^\circ$ ? What is the GM for this value of  $K$ ?
- (c) What is  $K_v$  when the gain  $K$  is set for  $\text{PM} = 50^\circ$ ?
- (d) Create a root locus with respect to  $K$ , and indicate the roots for a PM of  $50^\circ$ .

- 6.32** For the system depicted in Fig. 6.92(a), the transfer-function blocks are defined by

$$G(s) = \frac{1}{(s+2)^2(s+4)} \quad \text{and} \quad H(s) = \frac{1}{s+1}.$$

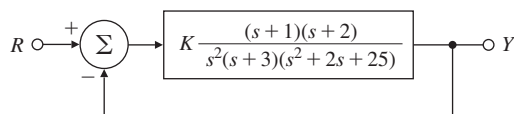
- (a) Using rlocus and rlocfind, determine the value of  $K$  at the stability boundary.
- (b) Using rlocus and rlocfind, determine the value of  $K$  that will produce roots with damping corresponding to  $\zeta = 0.707$ .
- (c) What is the GM of the system if the gain is set to the value determined in part (b)? Answer this question *without* using any frequency-response methods.
- (d) Create the Bode plots for the system, and determine the GM that results for  $\text{PM} = 65^\circ$ . What damping ratio would you expect for this PM?
- (e) Sketch a root locus for the system shown in Fig. 6.92 (b). How does it differ from the one in part (a)?
- (f) For the systems in Figs. 6.92 (a) and (b), how does the transfer function  $Y_2(s)/R(s)$  differ from  $Y_1(s)/R(s)$ ? Would you expect the step response to  $r(t)$  to be different for the two cases?

**Figure 6.92**

Block diagram for Problem 6.32: (a) unity feedback; (b)  $H(s)$  in feedback

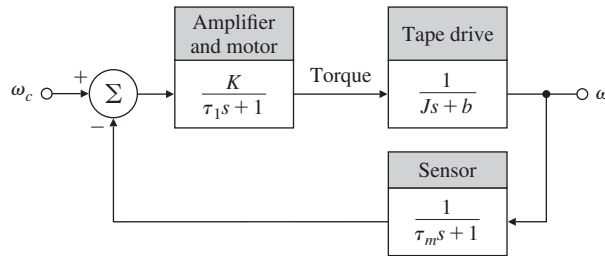
- 6.33** For the system shown in Fig. 6.93, use Bode and root-locus plots to determine the gain and frequency at which instability occurs. What gain (or gains) gives a PM of  $20^\circ$ ? What is the GM when  $\text{PM} = 20^\circ$ ?

**Figure 6.93**  
Control system for  
Problem 6.33



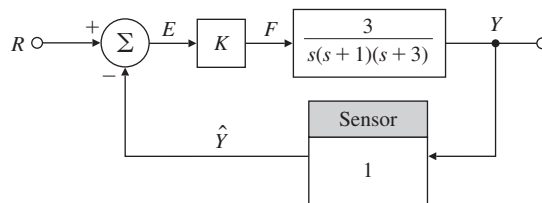
- 6.34** A magnetic tape-drive speed-control system is shown in Fig. 6.94. The speed sensor is slow enough that its dynamics must be included. The speed-measurement time constant is  $\tau_m = 0.5$  sec; the reel time constant is  $\tau_r = J/b = 4$  sec, where  $b$  = the output shaft damping constant = 1 N·m·sec; and the motor time constant is  $\tau_1 = 1$  sec.
- Determine the gain  $K$  required to keep the steady-state speed error to less than 7% of the reference-speed setting.
  - Determine the gain and phase margins of the system. Is this a good system design?

**Figure 6.94**  
Magnetic tape-drive speed control



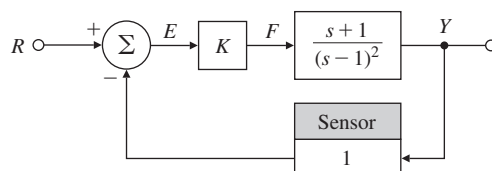
- 6.35** For the system in Fig. 6.95, determine the Nyquist plot and apply the Nyquist criterion
- to determine the range of values of  $K$  (positive and negative) for which the system will be stable, and
  - to determine the number of roots in the RHP for those values of  $K$  for which the system is unstable. Check your answer by using a rough root-locus sketch.

**Figure 6.95**  
Control system for Problems 6.35, 6.69, and 6.70



- 6.36** For the system shown in Fig. 6.96, determine the Nyquist plot and apply the Nyquist criterion
- to determine the range of values of  $K$  (positive and negative) for which the system will be stable, and

**Figure 6.96**  
Control system for Problem 6.36

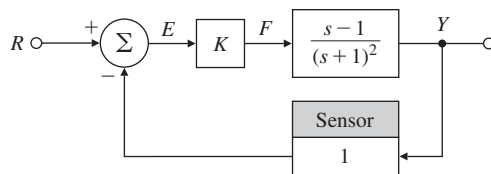


- (b) to determine the number of roots in the RHP for those values of  $K$  for which the system is unstable. Check your answer by using a rough root-locus sketch.

**6.37** For the system shown in Fig. 6.97, determine the Nyquist plot and apply the Nyquist criterion

- (a) to determine the range of values of  $K$  (positive and negative) for which the system will be stable, and  
 (b) to determine the number of roots in the RHP for those values of  $K$  for which the system is unstable. Check your answer by using a rough root-locus sketch.

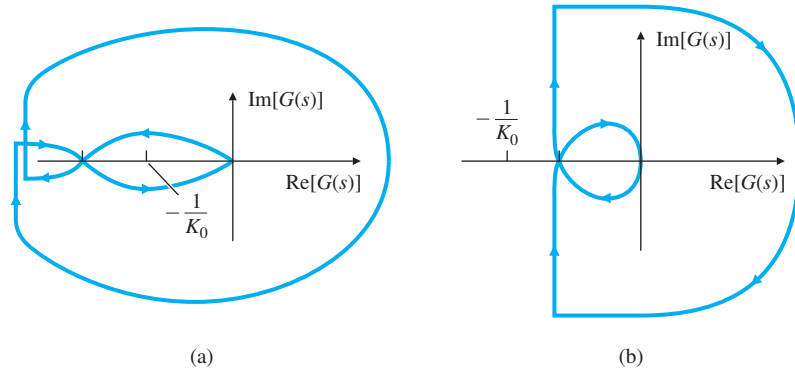
**Figure 6.97**  
Control system for  
Problem 6.37



**6.38** The Nyquist diagrams for two stable, open-loop systems are sketched in Fig. 6.98. The proposed operating gain is indicated as  $K_0$ , and arrows indicate increasing frequency. In each case, give a rough estimate of the following quantities for the closed-loop (unity feedback) system:

- (a) Phase margin;  
 (b) Damping ratio;  
 (c) Range of gain for stability (if any);  
 (d) System type (0, 1, or 2).

**Figure 6.98**  
Nyquist plots for  
Problem 6.38



**6.39** The steering dynamics of a ship are represented by the transfer function

$$\frac{V(s)}{\delta_r(s)} = G(s) = \frac{K[-(s/0.142) + 1]}{s(s/0.325 + 1)(s/0.0362 + 1)},$$

where  $V$  is the ship's lateral velocity in meters per second, and  $\delta_r$  is the rudder angle in radians.

- (a) Use the Matlab command `bode` to plot the log magnitude and phase of  $G(j\omega)$  for  $K = 0.2$ .
- (b) On your plot, indicate the crossover frequency, PM, and GM.
- (c) Is the ship-steering system stable with  $K = 0.2$ ?
- (d) What value of  $K$  would yield a PM of  $30^\circ$ , and what would the crossover frequency be?

**6.40** For the open-loop system

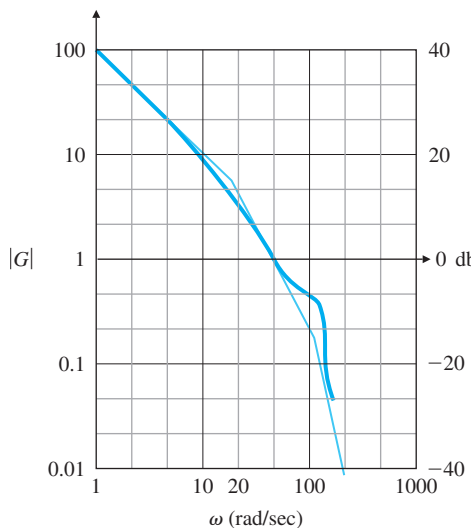
$$KG(s) = \frac{K(s + 0.1)}{s^2(s + 9)^2},$$

determine the value of  $K$  at the stability boundary and the values of  $K$  at the points where PM =  $50^\circ$ .

### Problems for Section 6.5: Bode's Gain-Phase Relationship

- 6.41** The frequency response of a plant in a unity feedback configuration with no controller is sketched in Fig. 6.99. Assume the plant is open-loop stable and is minimum phase, and it has an integrator.
- (a) What is the velocity constant  $K_v$  for the system as drawn?
- (b) What is the damping ratio of the complex poles?
- (c) What is the PM of the system as shown? (Estimate to within  $\pm 10^\circ$ )
- (d) Assuming the reference input is corrupted with a noise consisting of a sinusoidal signal of  $\omega = 20$  rad/sec? Approximately estimate the factor by which the noise is attenuated at the output.

**Figure 6.99**  
Magnitude frequency response for Problem 6.41



**6.42** For the system

$$G(s) = \frac{100(s/a + 1)}{s(s + 1)(s/b + 1)},$$

where  $b = 10a$ , find the approximate value of  $a$  that will yield the best PM by sketching only candidate values of the frequency-response magnitude.

*Problem for Section 6.6: Closed-Loop Frequency Response*

- 6.43** For the open-loop system

$$KG(s) = \frac{K(s + 0.1)}{s^2(s + 9)^2},$$

determine the value for  $K$  that will yield  $\text{PM} \geq 30^\circ$  and the maximum possible closed-loop bandwidth. Use Matlab to find the bandwidth.

*Problems for Section 6.7: Compensation Design*

- 6.44** For the lead compensator

$$D_c(s) = \frac{T_D s + 1}{\alpha T_D s + 1},$$

where  $\alpha < 1$ ,

- (a) Show the phase of the lead compensator is given by

$$\phi = \tan^{-1}(T_D \omega) - \tan^{-1}(\alpha T_D \omega).$$

- (b) Show the frequency where the phase is maximum is given by

$$\omega_{\max} = \frac{1}{T_D \sqrt{\alpha}}$$

and the maximum phase corresponds to

$$\sin \phi_{\max} = \frac{1 - \alpha}{1 + \alpha}.$$

- (c) Rewrite your expression for  $\omega_{\max}$  to show the maximum-phase frequency occurs at the geometric mean of the two corner frequencies on a logarithmic scale:

$$\log \omega_{\max} = \frac{1}{2} \left( \log \frac{1}{T_D} + \log \frac{1}{\alpha T_D} \right).$$

- (d) To derive the same results in terms of the pole–zero locations, rewrite  $D_c(s)$  as

$$D_c(s) = \frac{s + z}{s + p},$$

then show that the phase is given by

$$\phi = \tan^{-1} \left( \frac{\omega}{|z|} \right) - \tan^{-1} \left( \frac{\omega}{|p|} \right),$$

such that

$$\omega_{\max} = \sqrt{|z| |p|}.$$

Hence, the frequency at which the phase is maximum is the square root of the product of the pole and zero locations.

- 6.45** For the third-order servo system

$$G(s) = \frac{10,000}{s(s + 20)(s + 30)},$$

design a lead compensator so that  $PM \geq 60^\circ$  and  $\omega_{BW} \geq 10$  rad/sec using Bode plot sketches.

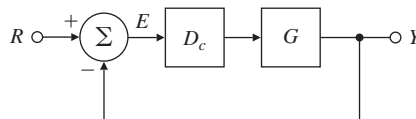
- 6.46** For the system shown in Fig. 6.100, suppose

$$G(s) = \frac{5}{s(s+1)(s/5+1)}.$$

Use Bode plot sketches to design a lead compensation  $D_c(s)$  with unity DC gain so that  $PM \geq 40^\circ$ . Then verify and refine your design by using Matlab. What is the approximate bandwidth of the system?

**Figure 6.100**

Control system for Problem 6.46



- 6.47** Derive the transfer function from  $T_d$  to  $\theta$  for the system in Fig. 6.67. Then apply the Final Value Theorem (assuming  $T_d = \text{constant}$ ) to determine whether  $\theta(\infty)$  is nonzero for the following two cases:

- (a) When  $D_c(s)$  has no integral term:  $\lim_{s \rightarrow 0} D_c(s) = \text{constant}$ ;  
 (b) When  $D_c(s)$  has an integral term:

$$D_c(s) = \frac{D'_c(s)}{s}$$

In this case,  $\lim_{s \rightarrow 0} D'_c(s) = \text{constant}$ .

- 6.48** The inverted pendulum has a transfer function given by Eq. (2.31), which is similar to

$$G(s) = \frac{1}{s^2 - 1}.$$

- (a) Use Bode plot sketches to design a lead compensator to achieve a PM of  $30^\circ$ . Then verify and refine your design by using Matlab.  
 (b) Sketch a root locus and correlate it with the Bode plot of the system.  
 (c) Could you obtain the frequency response of this system experimentally?

- 6.49** The open-loop transfer function of a unity feedback system is

$$G(s) = \frac{K}{s\left(\frac{s}{3} + 1\right)\left(\frac{s}{40} + 1\right)}.$$

- (a) Design a lag compensator for  $G(s)$  using Bode plot sketches so that the closed-loop system satisfies the following specifications:  
 (i) The steady-state error to a unit ramp reference input is less than 0.05.  
 (ii)  $PM \geq 40^\circ$ .  
 (b) Verify and refine your design by using Matlab.

**6.50** The open-loop transfer function of a unity feedback system is

$$G(s) = \frac{K}{(s+10)\left(\frac{s^2}{5} + \frac{s}{6} + 1\right)}.$$

- (a) Design a lead compensator for  $G(s)$  using Bode plot sketches so that the closed-loop system satisfies the following specifications:
- (i) The steady-state error to a unit step reference input is less than 0.01.
  - (ii) For the dominant closed-loop poles the damping ratio  $\zeta \geq 0.4$ .
- (b) Verify your design with a direct computation of the damping of the dominant closed-loop poles.

**6.51** A DC motor with negligible armature inductance is to be used in a position control system. Its open-loop transfer function is given by

$$G(s) = \frac{37}{s\left(\frac{s}{7} + 1\right)}.$$

- (a) Design a compensator for the motor using Bode plot sketches so that the closed-loop system satisfies the following specifications:
- (i) The steady-state error to a unit ramp input is less than  $1/150$ .
  - (ii) The unit step response has an overshoot of less than 20%.
  - (iii) The bandwidth of the compensated system is no less than that of the uncompensated system.
- (b) Verify and/or refine your design including a direct computation step response overshoot.

**6.52** The open-loop transfer function of a unity feedback system is

$$G(s) = \frac{K}{s\left(1 + \frac{s}{0.5}\right)\left(1 + \frac{s}{1.5}\right)}.$$

- (a) Sketch the system block diagram including input reference commands and sensor noise.
- (b) Design a compensator for  $G(s)$  using Bode plot sketches so that the closed-loop system satisfies the following specifications:
- (i) The steady-state error to a unit ramp input is less than 0.03.
  - (ii)  $PM \geq 45^\circ$ .
  - (iii) The steady-state error for sinusoidal inputs with  $\omega < 0.02$  rad/sec is less than  $1/300$ .
  - (iv) Noise components introduced with the sensor signal at frequencies greater than 50 rad/sec are to be attenuated at the output by at least a factor of 1000.
- (c) Verify and/or refine your design including a computation of the closed-loop frequency response to verify (iv).

**6.53** The transfer function for a quadrotor attitude control system between a pitch control input,  $T_{lon}$ , and the pitch angle,  $\theta$ , is

$$\frac{\theta(s)}{T_{lon}(s)} = G_1(s) = \frac{1}{s^2(s+2)}.$$

Design a lead compensator,  $D_c(s)$ , using frequency design so:

$$\begin{aligned}\omega_n &\geq 1 \text{ rad/sec}, \\ \zeta &\geq 0.44.\end{aligned}$$

Compare your design with that arrived at using root locus design in Example 5.12.

- 6.54** Consider a satellite attitude-control system with the transfer function

$$G(s) = \frac{0.05(s + 25)}{s^2(s^2 + 0.1s + 4)}.$$

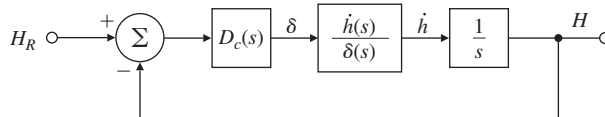
Amplitude-stabilize the system using lead compensation so that  $GM \geq 2$  (6 db), and  $PM \geq 45^\circ$ , keeping the bandwidth as high as possible with a single lead.

- 6.55** In one mode of operation, the autopilot of a jet transport is used to control altitude. For the purpose of designing the altitude portion of the autopilot loop, only the long-period airplane dynamics are important. The linearized relationship between altitude and elevator angle for the long-period dynamics is

$$G(s) = \frac{h(s)}{\delta(s)} = \frac{20(s + 0.01)}{s(s^2 + 0.01s + 0.0025)} \frac{\text{ft/sec}}{\text{deg}}.$$

The autopilot receives from the altimeter an electrical signal proportional to altitude. This signal is compared with a command signal (proportional to the altitude selected by the pilot), and the difference provides an error signal. The error signal is processed through compensation, and the result is used to command the elevator actuators. A block diagram of this system is shown in Fig. 6.101. You have been given the task of designing the compensation. Begin by considering a proportional control law  $D_c(s) = K$ .

**Figure 6.101**  
Control system for  
Problem 6.55



- (a) Use Matlab to draw a Bode plot of the open-loop system for  $D_c(s) = K = 1$ .
- (b) What value of  $K$  would provide a crossover frequency (i.e., where  $|G| = 1$ ) of 0.16 rad/sec?
- (c) For this value of  $K$ , would the system be stable if the loop were closed?
- (d) What is the PM for this value of  $K$ ?
- (e) Sketch the Nyquist plot of the system, and locate carefully any points where the phase angle is  $180^\circ$  or the magnitude is unity.
- (f) Use Matlab to plot the root locus with respect to  $K$ , and locate the roots for your value of  $K$  from part (b).

- (g) What steady-state error would result if the command was a step change in altitude of 1000 ft?

For parts (h) and (i), assume a compensator of the form

$$D_c(s) = \frac{T_D s + 1}{\alpha T_D s + 1}.$$

- (h) Choose the parameters  $K$ ,  $T_D$ , and  $\alpha$  so the crossover frequency is 0.16 rad/sec and the PM is greater than  $50^\circ$ . Verify your design by superimposing a Bode plot of  $D_c(s)G(s)/K$  on top of the Bode plot you obtained for part (a), and measure the PM directly.
- (i) Use Matlab to plot the root locus with respect to  $K$  for the system, including the compensator you designed in part (h). Locate the roots for your value of  $K$  from part (h).
- (j) Altitude autopilots also have a mode in which the rate of climb is sensed directly and commanded by the pilot.
- (i) Sketch the block diagram for this mode.
  - (ii) Modify the  $G(s)$  stated above for the case where the variable to be controlled is the rate of altitude change.
  - (iii) Design  $D_c(s)$  so the system has the same crossover frequency as the altitude hold mode and the PM is greater than  $50^\circ$ .

- 6.56** For a system with open-loop transfer function

$$G(s) = \frac{10}{s[(s/1.4) + 1][(s/3) + 1]},$$

design a lag compensator with unity DC gain so that  $PM \geq 35^\circ$ . What is the approximate bandwidth of this system?

- 6.57** For the ship-steering system in Problem 6.39,

- (a) Design a compensator that meets the following specifications:

- (i) Velocity constant  $K_v = 2$ ,
- (ii)  $PM \geq 50^\circ$ , and
- (iii) Unconditional stability ( $PM > 0$  for all  $\omega \leq \omega_c$ , the crossover frequency).

- (b) For your final design, draw a root locus with respect to  $K$ , and indicate the location of the closed-loop poles.

- 6.58** Consider a unity-feedback system with

$$G(s) = \frac{1}{s(20 + 1)(s^2/100^2 + 0.5s/100 + 1)}. \quad (6.74)$$

- (a) A lead compensator is introduced with  $\alpha = 1/5$  and a zero at  $1/T = 20$ . How must the gain be changed to obtain crossover at  $\omega_c = 31.6$  rad/sec, and what is the resulting value of  $K_v$ ?
- (b) With the lead compensator in place, what is the required value of  $K$  for a lag compensator that will readjust the gain to a  $K_v$  value of 100?
- (c) Place the pole of the lag compensator at 3.16 rad/sec, and determine the zero location that will maintain the crossover frequency at

$\omega_c = 31.6$  rad/sec. Plot the compensated frequency response on the same graph.

- (d) Determine the PM of the compensated design.

- 6.59** Golden Nugget Airlines had great success with their free bar near the tail of the airplane. (See Problem 5.39.) However, when they purchased a much larger airplane to handle the passenger demand, they discovered there was some flexibility in the fuselage that caused a lot of unpleasant yawing motion at the rear of the airplane when in turbulence, which caused the revelers to spill their drinks. The approximate transfer function for the rigid body roll/yawl motion, called the “Dutch roll” mode (see Section 10.3.1) is

$$\frac{r(s)}{\delta_r(s)} = \frac{8.75(4s^2 + 0.4s + 1)}{(s/0.01 + 1)(s^2 + 0.24s + 1)},$$

where  $r$  is the airplane’s yaw rate and  $\delta_r$  is the rudder angle. In performing a finite element analysis (FEA) of the fuselage structure and adding those dynamics to the Dutch roll motion, they found that the transfer function needed additional terms which reflected the fuselage lateral bending that occurred due to excitation from the rudder and turbulence. The revised transfer function is

$$\frac{r(s)}{\delta_r(s)} = \frac{8.75(4s^2 + 0.4s + 1)}{(s/0.01 + 1)(s^2 + 0.24s + 1)} \cdot \frac{1}{(s^2/\omega_b^2 + 2\zeta s/\omega_b + 1)},$$

where  $\omega_b$  is the frequency of the bending mode ( $= 10$  rad/sec) and  $\zeta$  is the bending mode damping ratio ( $= 0.02$ ). Most swept-wing airplanes have a “yaw damper,” which essentially feeds back yaw rate measured by a rate gyro to the rudder with a simple proportional control law. For the new Golden Nugget airplane, the proportional feedback gain  $K = 1$ , where

$$\delta_r(s) = -Kr(s). \quad (6.75)$$

- (a) Make a Bode plot of the open-loop system, determine the PM and GM for the nominal design, and plot the step response and Bode magnitude of the closed-loop system. What is the frequency of the lightly damped mode that is causing the difficulty?
- (b) Investigate remedies to quiet down the oscillations, but maintain the same low-frequency gain in order not to affect the quality of the Dutch roll damping provided by the yaw rate feedback. Specifically, investigate each of the following, one at a time:
- (i) Increasing the damping of the bending mode from  $\zeta = 0.02$  to  $\zeta = 0.04$  and (would require adding energy-absorbing material in the fuselage structure).
  - (ii) Increasing the frequency of the bending mode from  $\omega_b = 10$  rad/sec to  $\omega_b = 20$  rad/sec (would require stronger and heavier structural elements).
  - (iii) Adding a low-pass filter in the feedback—that is, replacing  $K$  in Eq. (6.75) with  $KD_c(s)$ , where

$$D_c(s) = \frac{1}{s/\tau_p + 1}$$

- (iv) Adding a notch filter as described in Section 5.4.3. Pick the frequency of the notch zero to be at  $\omega_b$ , with a damping of  $\zeta = 0.04$ , and pick the denominator poles to be  $(s/100 + 1)^2$ , keeping the DC gain of the filter = 1.
- (c) Investigate the sensitivity of the preceding two compensated designs (iii and iv) by determining the effect of a reduction in the bending mode frequency of  $-10\%$ . Specifically, reexamine the two designs by tabulating the GM, PM, closed-loop bending mode damping ratio, and resonant-peak amplitude, and qualitatively describe the differences in the step response.
- (d) What do you recommend to Golden Nugget to help their customers quit spilling their drinks? (Telling them to get back in their seats is not an acceptable answer for this problem! Make the recommendation in terms of improvements to the yaw damper.)

$\triangle$  **6.60** Consider a system with the open-loop transfer function (loop gain)

$$G(s) = \frac{1}{s(s+1)(s/10+1)}.$$

- (a) Create the Bode plot for the system, and find GM and PM.
- (b) Compute the sensitivity function and plot its magnitude frequency response.
- (c) Compute the vector margin (VM).
- $\triangle$  **6.61** Prove the sensitivity function  $S(s)$  has magnitude greater than 1 inside a circle with a radius of 1 centered at the  $-1$  point. What does this imply about the shape of the Nyquist plot if closed-loop control is to outperform open-loop control at all frequencies?
- $\triangle$  **6.62** Consider the system in Fig. 6.100 with the plant transfer function

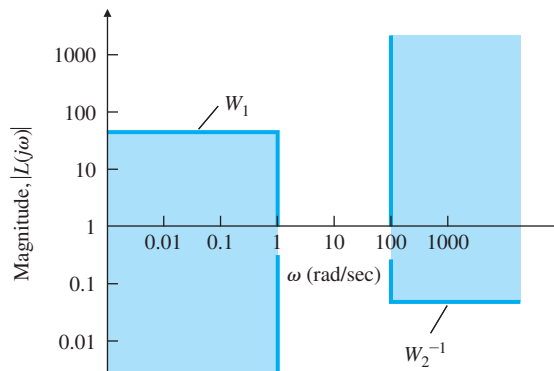
$$G(s) = \frac{10}{s(s/10+1)}.$$

- (a) We wish to design a compensator  $D_c(s)$  that satisfies the following design specifications:
  - (i)  $K_v = 100$ ,
  - (ii)  $PM \geq 45^\circ$ ,
  - (iii) Sinusoidal inputs of up to 1 rad/sec to be reproduced with  $\leq 2\%$  error, and
  - (iv) Sinusoidal inputs with a frequency of greater than 100 rad/sec to be attenuated at the output to  $\leq 5\%$  of their input value.
- (b) Create the Bode plot of  $G(s)$ , choosing the open-loop gain so that  $K_v = 100$ .
- (c) Show a *sufficient* condition for meeting the specification on sinusoidal inputs is that the magnitude plot lies outside the shaded regions in Fig. 6.102. Recall that

$$\frac{Y}{R} = \frac{KG}{1+KG} \quad \text{and} \quad \frac{E}{R} = \frac{1}{1+KG}.$$

**Figure 6.102**

Control system constraints for Problem 6.62



- (d) Explain why introducing a lead network alone cannot meet the design specifications.  
 (e) Explain why a lag network alone cannot meet the design specifications.  
 (f) Develop a full design using a lead-lag compensator that meets all the design specifications without altering the previously chosen low-frequency open-loop gain.
- 6.63** The transfer function for a quadrotor drone between altitude control input,  $F_{alt}$ , and the altitude,  $h$ , is

$$\frac{h(s)}{F_{alt}(s)} = G_h(s) = \frac{1}{s^2(s+10)}.$$

- (a) Based on the rotor arrangements discussed in Example 2.5, determine how to command the four rotors so a vertical force,  $F_{alt}$ , is commanded with no effect on the pitch, roll, or yaw angles.  
 (b) Design a lead compensator,  $D_c(s)$ , with a lead ratio of 20 using frequency design so that  $\zeta \geq 0.6$ , while achieving the maximum possible natural frequency,  $\omega_n$ .

### △ Problems for Section 6.8: Time Delay

- 6.64** Assume the system

$$G(s) = \frac{e^{-T_d s}}{s + 10}$$

has a 0.2-sec time delay ( $T_d = 0.2$  sec). While maintaining a phase margin  $\geq 40^\circ$ , find the maximum possible bandwidth by using the following:

- (a) One lead-compensator section

$$D_c(s) = K \frac{s+a}{s+b},$$

where  $b/a = 100$ .

- (b) Two lead-compensator sections

$$D_c(s) = K \left( \frac{s+a}{s+b} \right)^2,$$

where  $b/a = 10$ .

- (c) Comment on the statement in the text about the limitations on the bandwidth imposed by a delay.

**6.65** Determine the range of  $K$  for which the following systems are stable:

(a)  $G(s) = K \frac{e^{-4s}}{s}$

(b)  $G(s) = K \frac{e^{-s}}{s(s+2)}$

**6.66** Consider the heat exchanger of Example 2.18 with the open-loop transfer function

$$G(s) = \frac{e^{-5s}}{(10s+1)(60s+1)}.$$

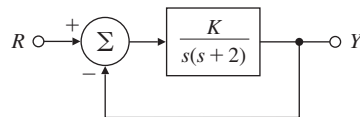
- (a) Design a lead compensator that yields  $\text{PM} \geq 45^\circ$  and the maximum possible closed-loop bandwidth.  
 (b) Design a PI compensator that yields  $\text{PM} \geq 45^\circ$  and the maximum possible closed-loop bandwidth.

### △ Problems for Section 6.9: Alternative Presentations of Data

**6.67** A feedback control system is shown in Fig. 6.103. The closed-loop system is specified to have an overshoot of less than 30% to a step input.

**Figure 6.103**

Control system for Problem 6.67



- (a) Determine the corresponding PM specification in the frequency domain and the corresponding closed-loop resonant-peak value  $M_r$ . (See Fig. 6.37.)

- (b) From Bode plots of the system, determine the maximum value of  $K$  that satisfies the PM specification.

- (c) Plot the data from the Bode plots [adjusted by the  $K$  obtained in part (b)] on a copy of the Nichols chart in Fig. 6.81, and determine the resonant-peak magnitude  $M_r$ . Compare that with the approximate value obtained in part (a).

- (d) Use the Nichols chart to determine the resonant-peak frequency  $\omega_r$  and the closed-loop bandwidth.

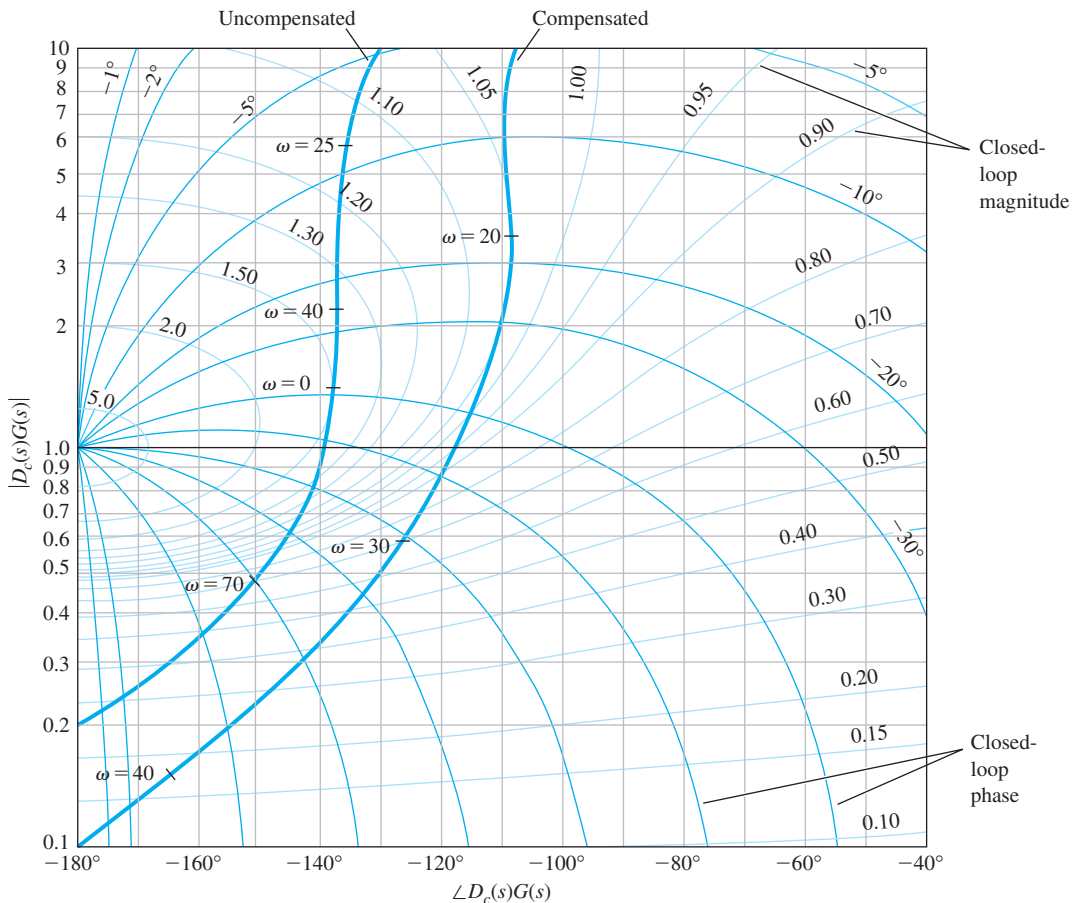
**6.68** The Nichols plots of an uncompensated and a compensated system are shown in Fig. 6.104.

- (a) What are the resonance peaks of each system?

- (b) What are the PM and GM of each system?

- (c) What are the bandwidths of each system?

- (d) What type of compensation is used?

**Figure 6.104**

Nichols plots for Problem 6.68

- 6.69** Consider the system shown in Fig. 6.95.

- Construct an inverse Nyquist plot of  $[Y(j\omega)/E(j\omega)]^{-1}$ . (See Appendix W6.9.2 online at [www.pearsonglobaleditions.com](http://www.pearsonglobaleditions.com).)
- Show how the value of  $K$  for neutral stability can be read directly from the inverse Nyquist plot.
- For  $K = 4, 2$ , and  $1$ , determine the gain and phase margins.
- Construct a root-locus plot for the system, and identify corresponding points in the two plots. To what damping ratios  $\zeta$  do the GM and PM of part (c) correspond?

- 6.70** An unstable plant has the transfer function

$$\frac{Y(s)}{F(s)} = \frac{s+1}{(s-1)^2}.$$

A simple control loop is to be closed around it, in the same manner as in the block diagram in Fig. 6.95.

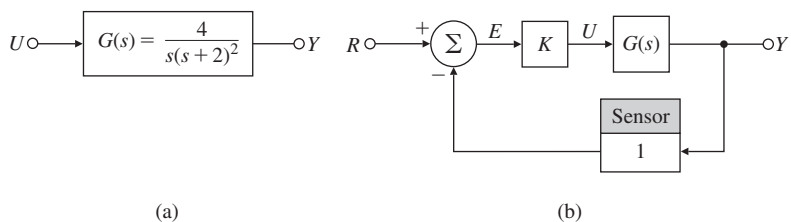
- (a) Construct an inverse Nyquist plot of  $Y/F$ . (See Appendix W6.9.2.)
  - (b) Choose a value of  $K$  to provide a PM of  $45^\circ$ . What is the corresponding GM?
  - (c) What can you infer from your plot about the stability of the system when  $K < 0$ ?
  - (d) Construct a root-locus plot for the system, and identify corresponding points in the two plots. In this case, to what value of  $\zeta$  does  $\text{PM} = 45^\circ$  correspond?

**6.71** Consider the system shown in Fig. 6.105(a).

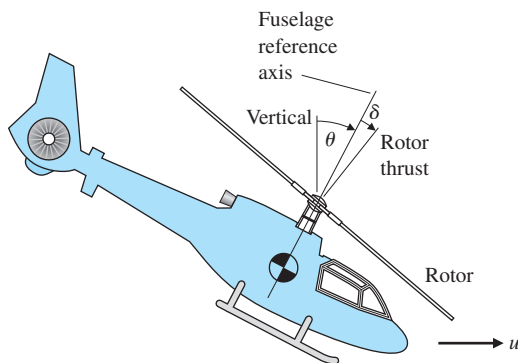
- (a) Construct a Bode plot for the system.
  - (b) Use your Bode plot to sketch an inverse Nyquist plot. (See Appendix W6.9.2.)
  - (c) Consider closing a control loop around  $G(s)$ , as shown in Fig. 6.105(b). Using the inverse Nyquist plot as a guide, read from your Bode plot the values of GM and PM when  $K = 0.7, 1.0, 1.4$ , and  $2$ . What value of  $K$  yields  $PM = 30^\circ$ ?
  - (d) Construct a root-locus plot, and label the same values of  $K$  on the locus. To what value of  $\zeta$  does each pair of PM/GM values correspond? Compare  $\zeta$  versus PM with the rough approximation in Fig. 6.36.

**Figure 6.105**

## Control system for Problem 6.71



# State-Space Design



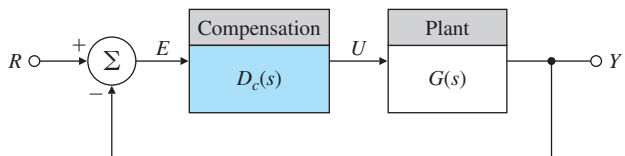
## A Perspective on State-Space Design

In addition to the transform techniques of root locus and frequency response, there is a third major method of designing feedback control systems: the state-space method. We will introduce the state-variable method of describing differential equations. In state-space design, the control engineer designs a dynamic compensation by working directly with the state-variable description of the system. Like the transform techniques, the aim of the state-space method is to find a compensation  $D_c(s)$  (such as that shown in Fig. 7.1) that satisfies the design specifications. Because the state-space method of describing the plant and computing the compensation is so different from the transform techniques, it may seem at first to be solving an entirely different problem. We selected the examples and analysis given toward the end of this chapter to help convince you that, indeed, state-space design results in a compensator with a transfer function  $D_c(s)$  that is equivalent to those  $D_c(s)$  compensators obtained with the other two methods.

Because it is particularly well suited to the use of computer techniques, state-space design is increasingly studied and used today by control engineers.

**Figure 7.1**

A control system design definition



## Chapter Overview

This chapter begins by considering the purposes and advantages of using state-space design. We will discuss selection of state-variables and state-space models for various dynamic systems through several examples in Section 7.2. Models in state-variable form enhance our ability to apply the computational efficiency of computer-aided design tools such as Matlab. In Section 7.3, we will show that it is beneficial to look at the state-variable form in terms of an analog computer simulation model. In Section 7.4, we will review the development of state-variable equations from block diagrams. We then solve for the dynamic response, using state equations for both hand and computer analysis. Having covered these preliminary fundamentals, we next proceed to the major task of control system design via state-space. The steps of the design method are as follows:

1. Select closed-loop pole (root as referred to in previous chapters) locations and develop the control law for the closed-loop system that corresponds to satisfactory dynamic response (see Sections 7.5 and 7.6).
2. Design an estimator (see Section 7.7).
3. Combine the control law and the estimator (see Section 7.8).
4. Introduce the reference input (see Sections 7.5.2 and 7.9).

After working through the central design steps, we will briefly explore the use of integral control in state-space (Section 7.10). The next three sections of this chapter consider briefly some additional concepts pertaining to the state-space method; because they are relatively advanced, they may be considered optional to some courses or readers. Finally, Section 7.15 provides some historical perspective for the material in this chapter.

### 7.1 Advantages of State-Space

The idea of **state-space** comes from the state-variable method of describing differential equations. In this method, the differential equations describing a dynamic system are organized as a set of first-order differential equations in the vector-valued state of the system, and the solution is visualized as a trajectory of this state vector in space. **State-space control design** is the technique in which the control engineer designs a dynamic compensation by working directly with the state-variable description of the system. We will see that the ordinary differential

**Normal form**

equations (ODEs) of physical dynamic systems can be manipulated into state-variable form. In the field of mathematics, where ODEs are studied, the state-variable form is called the **normal form** for the equations. There are several good reasons for studying equations in this form, three of which are listed here:

- *To study more general models:* The ODEs do not have to be linear or stationary. Thus, by studying the equations themselves, we can develop methods that are very general. Having them in state-variable form gives us a compact, standard form for study. Furthermore, the techniques of state-space analysis and design easily extend to systems with multiple inputs and/or multiple outputs. Of course, in this text, we study mainly linear time-invariant (LTI) models with single input and output (for the reasons given earlier).
- *To introduce the ideas of geometry into differential equations:* In physics, the plane of position versus velocity of a particle or rigid body is called the **phase plane**, and the trajectory of the motion can be plotted as a curve in this plane. The state is a generalization of that idea to include more than two dimensions. While we cannot easily plot more than three dimensions, the concepts of distance, of orthogonal and parallel lines, and other concepts from geometry can be useful in visualizing the solution of an ODE as a path in state-space.
- *To connect internal and external descriptions:* The state of a dynamic system often directly describes the distribution of internal energy in the system. For example, for electro-mechanical systems, it is common to select the following as state-variables: position (potential energy), velocity (kinetic energy), capacitor voltage (electric energy), inductor current (magnetic energy), and thermal systems temperature (thermal energy). The internal energy can always be computed from the state-variables. By a system of analysis to be described shortly, we can relate the state to the system inputs and outputs, and thus connect the internal variables to the external inputs and to the sensed outputs. In contrast, the transfer function relates only the input to the output and does not show the internal behavior. The state form keeps the latter information, which is sometimes important.

Use of the state-space approach has often been referred to as **modern control design**, and use of transfer-function-based methods, such as root locus and frequency response, referred to as **classical control design**. However, because the state-space method of description for ODEs has been in use for over 100 years and was introduced to control design in the late 1950s, it seems somewhat misleading to refer to it as modern. We prefer to refer to the two design approaches as the state-space methods and the transform methods.

Advantages of state-space design are especially apparent when the system to be controlled has more than one control input or more than

**Phase plane**

one sensed output. However, in this book, we shall examine the ideas of state-space design using the simpler Single-Input-Single-Output (SISO) systems. The design approach used for the systems described in state form is “divide and conquer.” First, we design the control as if all of the state were measured and available for use in the control law. This provides the possibility of assigning arbitrary dynamics for the system. Having a satisfactory control law based on full-state feedback, we introduce the concept of an observer and construct estimates of the state based on the sensed output. We then show that these estimates can be used in place of the actual state-variables. Finally, we introduce the external reference-command inputs to complete the structure. Only at this point can we recognize that the resulting compensation has the same essential structure as that developed with transform methods.

Before we can begin the design using state descriptions, it is necessary to develop some analytical results and tools from matrix linear algebra for use throughout the chapter. We assume you are familiar with such elementary matrix concepts as the identity matrix, triangular and diagonal matrices, and the transpose of a matrix. We also assume that you have some familiarity with the mechanics of matrix algebra, including adding, multiplying, and inverting matrices. More advanced results will be developed in Section 7.4 in the context of the dynamic response of a linear system. All of the linear algebra results used in this chapter are repeated in Appendix WB available online at [www.pearsonglobaleditions.com](http://www.pearsonglobaleditions.com) for your reference and review.

## 7.2 System Description in State-Space

The motion of any finite dynamic system can be expressed as a set of first-order ODEs. This is often referred to as the state-variable representation. For example, the use of Newton’s law and the free-body diagram in Section 2.1 typically lead to second-order differential equations—that is, equations that contain the second derivative, such as  $\ddot{x}$  in Eq. (2.3) or  $\ddot{\theta}$  in Eq. (2.11). The latter equation can be expressed as

$$\dot{x}_1 = x_2, \quad (7.1)$$

$$\dot{x}_2 = \frac{u}{I}, \quad (7.2)$$

where

$$u = F_c d + M_D,$$

$$x_1 = \theta,$$

$$x_2 = \dot{\theta},$$

$$\dot{x}_2 = \ddot{\theta}.$$

[Standard form of linear differential equations](#)

The output of this system is  $\theta$ , the satellite attitude. These same equations can be represented in the **state-variable form** as the vector equation

$$\dot{\mathbf{x}} = \mathbf{Ax} + \mathbf{Bu}, \quad (7.3)$$

where the input is  $u$  and the output is

$$y = \mathbf{C}\mathbf{x} + Du. \quad (7.4)$$

The column vector  $\mathbf{x}$  is called the **state of the system** and contains  $n$  elements for an  $n$ th-order system. For mechanical systems, the state vector elements usually consist of the positions and velocities of the separate bodies, as is the case for the example in Eqs. (7.1) and (7.2). The quantity  $\mathbf{A}$  is an  $n \times n$  **system matrix**,  $\mathbf{B}$  is an  $n \times 1$  **input matrix**,  $\mathbf{C}$  is a  $1 \times n$  row matrix referred to as the **output matrix**, and  $D$  is a scalar called the **direct transmission term**. To save space, we will sometimes refer to a state vector by its **transpose**,

$$\mathbf{x} = [x_1 \ x_2 \ \dots \ x_n]^T,$$

which is equivalent to

$$\mathbf{x} = \begin{bmatrix} x_1 \\ x_2 \\ \vdots \\ x_n \end{bmatrix}.$$

The differential equation models of more complex systems, such as those developed in Chapter 2 on mechanical, electrical, and electromechanical systems, can be described by state-variables through selection of positions, velocities, capacitor voltages, and inductor currents as suitable state-variables.

In this chapter, we will consider control systems design using the state-variable form. For the case in which the relationships are nonlinear [such as the case in Eqs. (2.22) and (2.97)], the linear form cannot be used directly. One must linearize the equations as we did in Chapter 2 to fit the form (see also Chapter 9).

The state-variable method of specifying differential equations is used by computer-aided control systems design software packages (for example Matlab). Therefore, in order to specify linear differential equations to the computer, you need to know the values of the matrices  $\mathbf{A}$ ,  $\mathbf{B}$ ,  $\mathbf{C}$ , and the constant  $D$ .

## EXAMPLE 7.1

### Satellite Attitude Control Model in State-Variable Form

Determine the  $\mathbf{A}$ ,  $\mathbf{B}$ ,  $\mathbf{C}$ ,  $D$  matrices in the state-variable form for the satellite attitude control model in Example 2.3 with  $M_D = 0$ .

**Solution.** Define the attitude and the angular velocity of the satellite as the state-variables so that  $\mathbf{x} \triangleq [\theta \ \omega]^T$ .<sup>1</sup> The single second-order equation (2.11) can then be written in an equivalent way as two first-order equations:

$$\dot{\theta} = \omega,$$

$$\dot{\omega} = \frac{d}{I} F_c.$$

---

<sup>1</sup>The symbol  $\triangleq$  means “is to be defined.”

These equations are expressed, using Eq. (7.3),  $\dot{\mathbf{x}} = \mathbf{Ax} + \mathbf{Bu}$ , as

$$\begin{bmatrix} \dot{\theta} \\ \dot{\omega} \end{bmatrix} = \begin{bmatrix} 0 & 1 \\ 0 & 0 \end{bmatrix} \begin{bmatrix} \theta \\ \omega \end{bmatrix} + \begin{bmatrix} 0 \\ d/I \end{bmatrix} F_c.$$

The output of the system is the satellite attitude,  $y = \theta$ . Using Eq. (7.4),  $y = \mathbf{Cx} + \mathbf{Du}$ , this relation is expressed as

$$y = [1 \ 0] \begin{bmatrix} \theta \\ \omega \end{bmatrix}.$$

Therefore, the matrices for the state-variable form are

$$\mathbf{A} = \begin{bmatrix} 0 & 1 \\ 0 & 0 \end{bmatrix}, \quad \mathbf{B} = \begin{bmatrix} 0 \\ d/I \end{bmatrix}, \quad \mathbf{C} = [1 \ 0], \quad D = 0,$$

and the input  $u \triangleq F_c$ .

For this very simple example, the state-variable form is a more cumbersome way of writing the differential equation than the second-order version in Eq. (2.11). However, the method is not more cumbersome for most systems, and the advantages of having a standard form for use in computer-aided design have led to widespread use of the state-variable form.

The next example has more complexity and shows how to use Matlab to find the solution of linear differential equations.

## EXAMPLE 7.2

### Cruise Control Step Response

- Rewrite the equation of motion from Example 2.1 in state-variable form, where the output is the car position  $x$ .
- Use Matlab to find the response of the velocity of the car for the case in which the input jumps from being  $u = 0$  at time  $t = 0$  to a constant  $u = 750$  N thereafter. Assume the car mass  $m$  is 1500 kg, and  $b = 60$  N·sec/m.

#### Solution.

- Equations of motion:** First, we need to express the differential equation describing the plant, Eq. (2.3), as a set of simultaneous first-order equations. To do so, we define the position and the velocity of the car as the state-variables  $x$  and  $v$ , so  $\mathbf{x} = [x \ v]^T$ . The single second-order equation, Eq. (2.3), can then be rewritten as a set of two first-order equations:

$$\dot{x} = v,$$

$$\dot{v} = -\frac{b}{m}v + \frac{1}{m}u.$$

Next, we use the standard form of Eq. (7.3),  $\dot{\mathbf{x}} = \mathbf{Ax} + \mathbf{Bu}$ , to express these equations:

$$\begin{bmatrix} \dot{x} \\ \dot{v} \end{bmatrix} = \begin{bmatrix} 0 & 1 \\ 0 & -b/m \end{bmatrix} \begin{bmatrix} x \\ v \end{bmatrix} + \begin{bmatrix} 0 \\ 1/m \end{bmatrix} u. \quad (7.5)$$

The output of the system is the car position  $y = x$ , which is expressed in matrix form as

$$y = [1 \ 0] \begin{bmatrix} x \\ v \end{bmatrix},$$

or

$$y = \mathbf{Cx}.$$

So the state-variable-form matrices defining this example are

$$\mathbf{A} = \begin{bmatrix} 0 & 1 \\ 0 & -b/m \end{bmatrix}, \quad \mathbf{B} = \begin{bmatrix} 0 \\ 1/m \end{bmatrix}, \quad \mathbf{C} = [1 \ 0], \quad D = 0.$$

- (b) **Time response:** The equations of motion are those given in part (a), except that now the output is  $v$ . Therefore, the output matrix is

$$\mathbf{C} = [0 \ 1].$$

The coefficients required are  $b/m = 0.04$  and  $1/m = 6.67 \times 10^{-4}$ . The numerical values for the matrices defining the system are thus

$$\mathbf{A} = \begin{bmatrix} 0 & 1 \\ 0 & -0.04 \end{bmatrix}, \quad \mathbf{B} = \begin{bmatrix} 0 \\ 6.67 \times 10^{-4} \end{bmatrix}, \quad \mathbf{C} = [0 \ 1], \quad D = 0.$$

The step function in Matlab computes the time response of a linear system to a unit-step input. Because the system is linear, the output for this case can be multiplied by the magnitude of the input step to derive a step response of any amplitude. Equivalently, the  $\mathbf{B}$  matrix can be multiplied by the magnitude of the unit step.

#### Step response with Matlab

The statements

```
A = [0 1;0 -0.04];
B = [0; 1/1500];
C = [0 1];
D = 0;
sys = ss(A, 750*B,C,D); % step gives unit step response,
                           % so 750*B gives %u=750 N.
step(sys);               % plots the step response
```

compute and plot the time response for a unit step with a 750-N magnitude. The step response is shown in Fig. 7.2.

### EXAMPLE 7.3

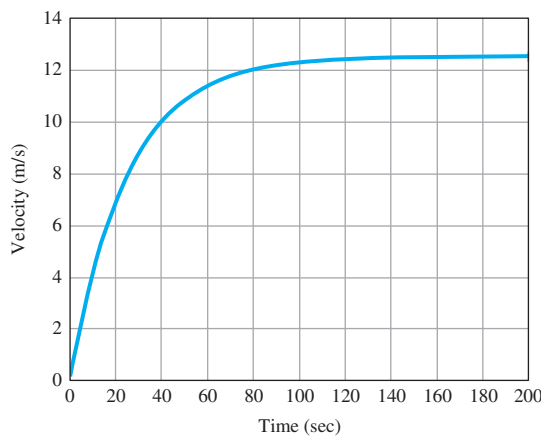
#### Motion of a Hanging Crane in State Variable Form

Based on Example 2.8, determine the state-space equation for the motion of a hanging crane shown in Fig. 2.21. Assume the friction term can be neglected.

**Solution.** In order to write the equations in the state-variable form (that is, a set of simultaneous first-order differential equations), the angular

**Figure 7.2**

Response of the car  
velocity to a step in  $u$



position and velocity for the hanging crane as the state elements (that is  $\mathbf{x} = [x_1 \ x_2] = [\theta \ \dot{\theta}]$  and the force being applied to the trolley is taken as the input  $u$  and the output is  $\theta = [1 \ 0]\mathbf{x}$ . Hence,  $\dot{x}_1 = x_2$ . Before  $\dot{x}_2$  can be defined, Eq. (2.28) can be simplified such that the acceleration term for the trolley can be eliminated and thus,

$$(m_t + m_p)(I + m_p l^2)\ddot{\theta} + (m_t + m_p)m_p g l \theta = (m_p l)^2 \ddot{\theta} - (m_p l)u \quad (7.6)$$

Re-arranging it into the standard form and expressing it in terms of  $x_1$  and  $\dot{x}_2$ , we get

$$\dot{x}_2 = -\frac{(m_t + m_p)m_p g l}{(m_t + m_p)(I + m_p l^2) - (m_p l)^2} x_1 - \frac{m_p l}{(m_t + m_p)(I + m_p l^2) - (m_p l)^2} u \quad (7.7)$$

Therefore, the standard matrices that define the state equations are

$$\mathbf{A} = \begin{bmatrix} 0 & 1 \\ -\frac{(m_t + m_p)m_p g l}{(m_t + m_p)(I + m_p l^2) - (m_p l)^2} & 0 \end{bmatrix},$$

$$\mathbf{B} = \begin{bmatrix} 0 \\ \frac{-m_p l}{(m_t + m_p)(I + m_p l^2) - (m_p l)^2} \end{bmatrix},$$

$$\mathbf{C} = [1 \ 0], \ D = 0.$$

**EXAMPLE 7.4***Loudspeaker with Circuit in State-Variable Form*

For the loudspeaker in Fig. 2.31 and the circuit driving it in Fig. 2.32, find the state-space equations relating the input voltage  $v_a$  to the output cone displacement  $x$ . Assume effective circuit resistance is  $R = 0.5 \Omega$  and the inductance is  $L = 0.15 \text{ mH}$ , and keep the mass  $M$  and friction coefficient  $b$  as unknowns.

**Solution.** Recall the two coupled equations, (2.54) and (2.58), that constitute the dynamic model for the loudspeaker:

$$M\ddot{x} + b\dot{x} = 0.43i,$$

$$L\frac{di}{dt} + Ri = v_a - 0.43\dot{x}.$$

A logical state vector for this third-order system would be  $\mathbf{x} \stackrel{\Delta}{=} [x \ \dot{x} \ i^T]^T$ , which leads to the standard matrices

$$\mathbf{A} = \begin{bmatrix} 0 & 1 & 0 \\ 0 & -b/M & 0.43/M \\ 0 & -2867 & -3333 \end{bmatrix}, \quad \mathbf{B} = \begin{bmatrix} 0 \\ 0 \\ 6667 \end{bmatrix},$$

$$\mathbf{C} = [1 \ 0 \ 0], \quad D = 0,$$

where now the input  $u \stackrel{\Delta}{=} v_a$ .

---

**EXAMPLE 7.5***Modeling a DC Motor in State-Variable Form*

Find the state-space equations for the DC motor with the equivalent electric circuit shown in Fig. 2.34(a).

**Solution.** Recall the equations of motion [Eqs. (2.62) and (2.63)] from Chapter 2:

$$J_m\ddot{\theta}_m + b\dot{\theta}_m = K_t i_a,$$

$$L_a \frac{di_a}{dt} + R_a i_a = v_a - K_e \dot{\theta}_m.$$

A state vector for this third-order system is  $\mathbf{x} \stackrel{\Delta}{=} [\theta_m \ \dot{\theta}_m \ i_a]^T$ , which leads to the standard matrices

$$\mathbf{A} = \begin{bmatrix} 0 & 1 & 0 \\ 0 & -\frac{b}{J_m} & \frac{K_t}{J_m} \\ 0 & -\frac{K_e}{L_a} & -\frac{R_a}{L_a} \end{bmatrix}, \quad \mathbf{B} = \begin{bmatrix} 0 \\ 0 \\ \frac{1}{L_a} \end{bmatrix},$$

$$\mathbf{C} = [1 \ 0 \ 0], \quad D = 0,$$

where the input  $u \stackrel{\Delta}{=} v_a$ .

---

The state-variable form can be applied to a system of any order. Example 7.6 illustrates the method for a fourth-order system.

**EXAMPLE 7.6***Flexible Satellite in State-Variable Form*

Find the state-variable form of the differential equations for Example 2.4, where the output is  $\theta_2$ .

**Solution.** Define the state vector to be

$$\mathbf{x} = [\theta_1 \quad \dot{\theta}_1 \quad \theta_2 \quad \dot{\theta}_2]^T.$$

Then solve the differential equations for  $\ddot{\theta}_1$  and  $\ddot{\theta}_2$  so the state-variable form is more apparent. The resulting matrices for the  $\theta_2$  output are

$$\mathbf{A} = \begin{bmatrix} 0 & 1 & 0 & 0 \\ -\frac{k}{I_1} & -\frac{b}{I_1} & \frac{k}{I_1} & \frac{b}{I_1} \\ 0 & 0 & 0 & 1 \\ \frac{k}{I_2} & \frac{b}{I_2} & -\frac{k}{I_2} & -\frac{b}{I_2} \end{bmatrix}, \quad \mathbf{B} = \begin{bmatrix} 0 \\ \frac{1}{I_1} \\ 0 \\ 0 \end{bmatrix},$$

$$\mathbf{C} = [0 \quad 0 \quad 1 \quad 0], \quad D = 0.$$

Difficulty arises when the differential equation contains derivatives of the input  $u$ . Techniques to handle this situation will be discussed in Section 7.4.

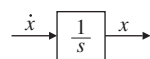
### 7.3 Block Diagrams and State-Space

Perhaps the most effective way of understanding the state-variable equations is via an analog computer block-diagram representation. The structure of the representation uses integrators as the central element, which are quite suitable for a first-order, state-variable representation of dynamic equations for a system. Even though the analog computers are almost extinct, analog computer implementation is still a useful concept for state-variable design, and in the circuit design of analog compensation.<sup>2</sup>

The analog computer was a device composed of electric components designed to simulate ODEs. The basic dynamic component of the analog computer is an **integrator**, constructed from an operational amplifier with a capacitor feedback and a resistor feed-forward as shown in Fig. 2.30. Because an integrator is a device whose input is the derivative of its output (as shown in Fig. 7.3) if, in an analog-computer simulation, we identify the outputs of the integrators as the state, we will then automatically have the equations in state-variable form. Conversely, if a system is described by state-variables, we can construct an

**Figure 7.3**

An integrator



<sup>2</sup>As well as due to its historical significance.

analog-computer simulation of that system by taking one integrator for each state-variable and connecting its input according to the given equation for that state-variable, as expressed in the state-variable equations. The analog-computer diagram is a picture of the state equations.

The components of a typical analog computer used to accomplish these functions are shown in Fig. 7.4. Notice the operational amplifier has a sign change that gives it a negative gain.

### EXAMPLE 7.7

#### *Analogue-Computer Implementation*

Find a state-variable description and the transfer function of the third-order system shown in Fig. 7.5 whose differential equation is

$$\ddot{y} + 7.5\dot{y} + 13y + 6.5y = 7u.$$

**Solution.** We solve for the highest derivative term in the ODE to obtain

$$\ddot{y} = -7.5\dot{y} - 13y - 6.5y + 7u. \quad (7.8)$$

Now we assume we have this highest derivative, and note the lower order terms can be obtained by integration as shown in Fig. 7.6(a). Finally we apply Eq. (7.8) to complete the realization shown in Fig. 7.6(b). To obtain the state description, we simply define the state-variables as the output of the integrators  $x_1 = \dot{y}$ ,  $x_2 = y$ ,  $x_3 = y$ , to obtain

**Figure 7.4**  
Components of an  
analog computer

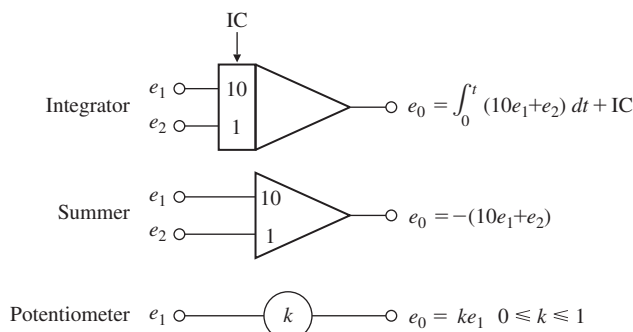


**Figure 7.5**  
Block diagram for a  
third-order system

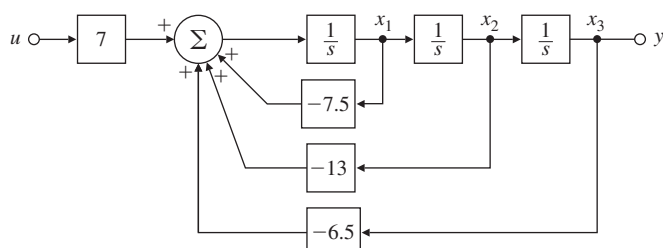
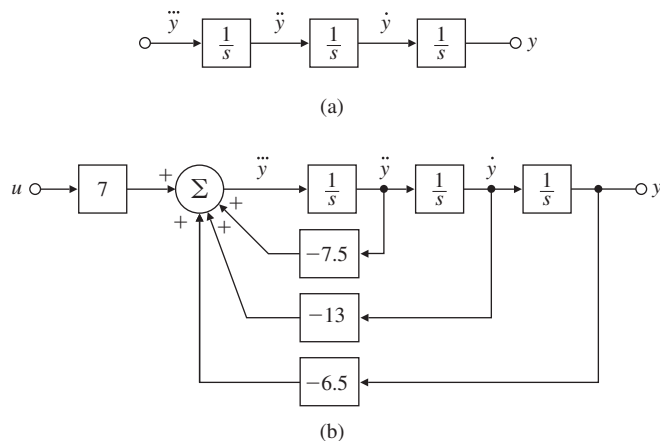


**Figure 7.6**

Block diagram of a system to solve  $\ddot{y} + 7.5\dot{y} + 13y + 6.5y = 7u$ , using only integrators as dynamic elements: (a) intermediate diagram; (b) final diagram



$$\dot{x}_1 = -7.5x_1 - 13x_2 - 6.5x_3,$$

$$\dot{x}_2 = x_1,$$

$$\dot{x}_3 = x_2,$$

which provides the state-variable description

$$\mathbf{A} = \begin{bmatrix} -7.5 & -13 & -6.5 \\ 1 & 0 & 0 \\ 0 & 1 & 0 \end{bmatrix}, \quad \mathbf{B} = \begin{bmatrix} 7 \\ 0 \\ 0 \end{bmatrix}, \quad \mathbf{C} = [0 \ 0 \ 1], \quad D = 0.$$

The Matlab statement

`[num,den] = ss2tf(A,B,C,D);`

will yield the transfer function

$$\frac{Y(s)}{U(s)} = \frac{7}{s^3 + 7.5s^2 + 13s + 6.5}.$$

If the transfer function were desired in factor form, it could be obtained by transforming either the ss or tf description. Therefore, either of the Matlab statements

`[z,p,k] = ss2zp(A,B,C,D)`

and

`[z,p,k] = tf2zp(num,den)`

would result in

$$z = [], \quad p = [-5.26 \ -1.23 \ -1]', \quad k = 7.$$

This means the transfer function could also be written in factored form as

$$\frac{Y(s)}{U(s)} = G(s) = \frac{7}{(s + 5.26)(s + 1.23)(s + 1)}.$$

## 7.4 Analysis of the State Equations

In the previous section, we introduced and illustrated the process of selecting a state and organizing the equations in state form. In this section, we review that process and describe how to analyze the dynamic response using the state description. In Section 7.4.1, we begin by relating the state description to block diagrams and the Laplace transform description and to consider the fact that for a given system the choice of state is not unique. We show how to use this nonuniqueness to select among several canonical forms for the one that will help solve the particular problem at hand; a control canonical form makes feedback gains of the state easy to design. After studying the structure of state equations in Section 7.4.2, we consider the dynamic response and show how transfer-function poles and zeros are related to the matrices of the state descriptions. To illustrate the results with hand calculations, we offer a simple example that represents the model of a thermal system. For more realistic examples, a computer-aided control systems design software package such as Matlab is especially helpful; relevant Matlab commands will be described from time to time.

### 7.4.1 Block Diagrams and Canonical Forms

We begin with a thermal system that has a simple transfer function

$$G(s) = \frac{b(s)}{a(s)} = \frac{s+2}{s^2 + 7s + 12} = \frac{2}{s+4} + \frac{-1}{s+3}. \quad (7.9)$$

The roots of the numerator polynomial  $b(s)$  are the zeros of the transfer function, and the roots of the denominator polynomial  $a(s)$  are the poles. Notice we have represented the transfer function in two forms, as a ratio of polynomials and as the result of a partial-fraction expansion. In order to develop a state description of this system (and this is a generally useful technique), we construct a block diagram that corresponds to the transfer function (and the differential equations) *using only isolated integrators as the dynamic elements*. We present several special forms which we call canonical forms. One such block diagram, structured in **control canonical form**, is illustrated in Fig. 7.7. The central feature of this structure is that each state-variable feeds back to the control input,  $u$ , through the coefficients of the system matrix  $\mathbf{A}_c$ .

Once we have drawn the block diagram in this form, we can identify the state description matrices simply by inspection; this is possible because when the output of an integrator is a state-variable, the input of that integrator is the derivative of that variable. For example, in Fig. 7.7, the equation for the first state-variable is

$$\dot{x}_1 = -7x_1 - 12x_2 + u.$$

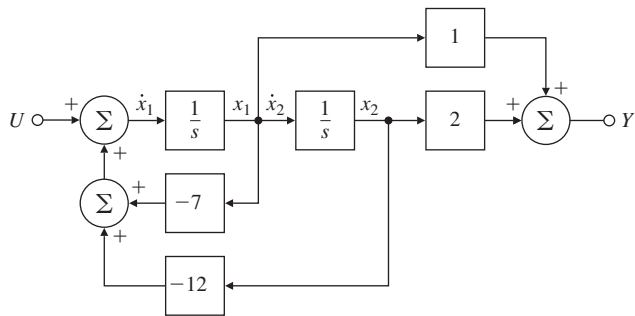
Continuing in this fashion, we get

$$\dot{x}_2 = x_1,$$

$$y = x_1 + 2x_2.$$

**Figure 7.7**

A block diagram representing Eq. (7.9) in control canonical form



These three equations can then be rewritten in the matrix form

$$\dot{\mathbf{x}} = \mathbf{A}_c \mathbf{x} + \mathbf{B}_c u, \quad (7.10)$$

$$y = \mathbf{C}_c \mathbf{x}, \quad (7.11)$$

where

$$\mathbf{A}_c = \begin{bmatrix} -7 & -12 \\ 1 & 0 \end{bmatrix}, \quad \mathbf{B}_c = \begin{bmatrix} 1 \\ 0 \end{bmatrix}, \quad (7.12a)$$

$$\mathbf{C}_c = [1 \ 2], \quad D_c = 0, \quad (7.12b)$$

and where the subscript *c* refers to control canonical form.

Two significant facts about this form are that the coefficients 1 and 2 of the numerator polynomial  $b(s)$  appear in the  $\mathbf{C}_c$  matrix, and (except for the leading term) the coefficients 7 and 12 of the denominator polynomial  $a(s)$  appear (with opposite signs) as the first row of the  $\mathbf{A}_c$  matrix. Armed with this knowledge, we can thus write down by *inspection* the state matrices in control canonical form for any system whose transfer function is known as a ratio of numerator and denominator polynomials. If  $b(s) = b_1 s^{n-1} + b_2 s^{n-2} + \dots + b_n$  and  $a(s) = s^n + a_1 s^{n-1} + a_2 s^{n-2} + \dots + a_n$ , the Matlab steps are

```
num = b = [b1 b2 ... bn]
den = a = [1 a1 a2 ... an]
[Ac, Bc, Cc, Dc] = tf2ss(num,den).
```

[Matlab tf2ss](#)

[Control canonical form](#)

We read tf2ss as “transfer function to state-space.” The result will be

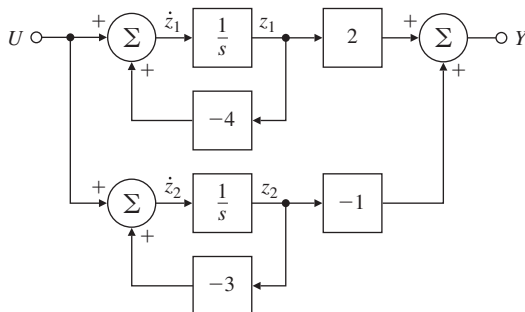
$$\mathbf{A}_c = \begin{bmatrix} -a_1 & -a_2 & \cdots & \cdots & -a_n \\ 1 & 0 & \cdots & \cdots & 0 \\ 0 & 1 & 0 & \cdots & 0 \\ \vdots & & \ddots & 0 & \vdots \\ 0 & 0 & \cdots & \cdots & 1 & 0 \end{bmatrix}, \quad \mathbf{B}_c = \begin{bmatrix} 1 \\ 0 \\ 0 \\ \vdots \\ 0 \end{bmatrix}, \quad (7.13a)$$

$$\mathbf{C}_c = [b_1 \ b_2 \ \dots \ \dots \ b_n], \quad D_c = 0. \quad (7.13b)$$

The block diagram of Fig. 7.7 and the corresponding matrices of Eq. (7.12) are not the only way to represent the transfer function  $G(s)$ . A block diagram corresponding to the partial-fraction expansion of  $G(s)$

**Figure 7.8**

Block diagram for Eq. (7.12) in modal canonical form



is given in Fig. 7.8. Using the same technique as before, with the state-variables marked as shown in the figure, we can determine the matrices directly from the block diagram as being

$$\dot{\mathbf{z}} = \mathbf{A}_m \mathbf{z} + \mathbf{B}_m u,$$

$$y = \mathbf{C}_m \mathbf{z} + D_m u,$$

where

$$\mathbf{A}_m = \begin{bmatrix} -4 & 0 \\ 0 & -3 \end{bmatrix}, \quad \mathbf{B}_m = \begin{bmatrix} 1 \\ 1 \end{bmatrix}, \quad (7.14a)$$

$$\mathbf{C}_m = [ 2 \quad -1 ], \quad D_m = 0, \quad (7.14b)$$

### Modal form

and the subscript *m* refers to **modal canonical form**. The name for this form derives from the fact that the poles of the system transfer function are sometimes called the **normal modes** of the system. The important fact about the matrices in this form is that the system poles (in this case  $-4$  and  $-3$ ) appear as the elements along the diagonal of the  $\mathbf{A}_m$  matrix, and the residues, the numerator terms in the partial-fraction expansion (in this example  $2$  and  $-1$ ), appear in the  $\mathbf{C}_m$  matrix.

Expressing a system in modal canonical form can be complicated by two factors: (1) the elements of the matrices will be complex when the poles of the system are complex, and; (2) the system matrix *cannot* be diagonal when the partial-fraction expansion has repeated poles. To solve the first problem, we express the complex poles of the partial-fraction expansion as conjugate pairs in second-order terms so that all the elements remain real. The corresponding  $\mathbf{A}_m$  matrix will then have  $2 \times 2$  blocks along the main diagonal representing the local coupling between the variables of the complex-pole set. To handle the second difficulty, we also couple the corresponding state-variables so the poles appear along the diagonal with off-diagonal terms indicating the coupling. A simple example of this latter case is the satellite system from Example 7.1, whose transfer function is  $G(s) = 1/s^2$ . The system matrices for this transfer function in a modal form are

$$\mathbf{A}_m = \begin{bmatrix} 0 & 1 \\ 0 & 0 \end{bmatrix}, \quad \mathbf{B}_m = \begin{bmatrix} 0 \\ 1 \end{bmatrix}, \quad \mathbf{C}_m = [ 1 \quad 0 ], \quad D_m = 0. \quad (7.15)$$

**EXAMPLE 7.8***State Equations in Modal Canonical Form*

A “quarter car model” [see Example 2.2] with one resonant model has a transfer function given by

$$G(s) = \frac{5s + 10}{s^2(s^2 + 5s + 10)} = \frac{1}{s^2} - \frac{1}{s^2 + 5s + 10} \quad (7.16)$$

Find state matrices in model form describing this system.

**Solution.** The transfer function has been given in real partial-fraction form. To get state-description matrices, we draw a corresponding block diagram with integrators only, assign the state, and write down the corresponding matrices. This process is not unique, so there are several acceptable solutions to the problem as stated, but they will differ in only trivial ways. A block diagram with a satisfactory assignment of variables is given in Fig. 7.9.

Notice the second-order term to represent the complex poles has been realized in control canonical form. There are a number of other possibilities that can be used as alternatives for this part. This particular form allows us to write down the system matrices by inspection:

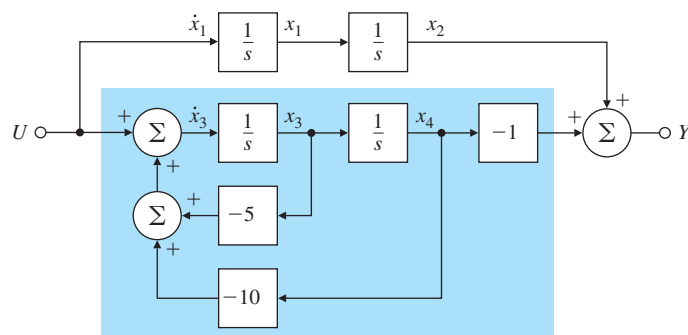
$$\mathbf{A} = \begin{bmatrix} 0 & 0 & 0 & 0 \\ 1 & 0 & 0 & 0 \\ 0 & 0 & -5 & -10 \\ 0 & 0 & 1 & 0 \end{bmatrix}, \quad \mathbf{B} = \begin{bmatrix} 1 \\ 0 \\ 1 \\ 0 \end{bmatrix},$$

$$\mathbf{C} = [0 \ 1 \ 0 \ -1], \quad D = 0. \quad (7.17)$$

Thus far, we have seen that we can obtain the state description from a transfer function in either control or modal form. Because these matrices represent the same dynamic system, we might ask as to what is the relationship between the matrices in the two forms (and their corresponding state-variables)? More generally, suppose we have a set of state equations that describe some physical system in no particular form, and we are given a problem for which the control canonical form would

**Figure 7.9**

Block diagram for a fourth-order system in modal canonical form with shading indicating portion in control canonical form



be helpful. (We will see such a problem in Section 7.5.) Is it possible to calculate the desired canonical form without obtaining the transfer function first? Answering these questions requires a look at the topic of state transformations.

### State description and output equation

Consider a system described by the state equations

$$\dot{\mathbf{x}} = \mathbf{Ax} + \mathbf{Bu}, \quad (7.18a)$$

$$y = \mathbf{Cx} + \mathbf{Du}. \quad (7.18b)$$

As we have seen, this is not a unique description of the dynamic system. We consider a change of state from  $\mathbf{x}$  to a new state  $\mathbf{z}$  that is a linear transformation of  $\mathbf{x}$ . For a nonsingular transformation matrix  $\mathbf{T}$ , we let

$$\mathbf{x} = \mathbf{Tz}. \quad (7.19)$$

By substituting Eq. (7.19) into Eq. (7.18a), we have the dynamic equations in terms of the new state  $\mathbf{z}$ :

$$\dot{\mathbf{x}} = \mathbf{Tz} = \mathbf{ATz} + \mathbf{Bu}, \quad (7.20a)$$

$$\dot{\mathbf{z}} = \mathbf{T}^{-1}\mathbf{ATz} + \mathbf{T}^{-1}\mathbf{Bu}, \quad (7.20b)$$

$$\dot{\mathbf{z}} = \bar{\mathbf{A}}\mathbf{z} + \bar{\mathbf{B}}\mathbf{u}. \quad (7.20c)$$

### Transformation of state

In Eq. (7.20c),

$$\bar{\mathbf{A}} = \mathbf{T}^{-1}\mathbf{AT}, \quad (7.21a)$$

$$\bar{\mathbf{B}} = \mathbf{T}^{-1}\mathbf{B}. \quad (7.21b)$$

We then substitute Eq. (7.19) into Eq. (7.18b) to get the output in terms of the new state  $\mathbf{z}$ :

$$\begin{aligned} y &= \mathbf{Cx} + \mathbf{Du} \\ &= \bar{\mathbf{C}}\mathbf{z} + \bar{\mathbf{D}}\mathbf{u}. \end{aligned}$$

Here

$$\bar{\mathbf{C}} = \mathbf{CT}, \quad \bar{\mathbf{D}} = \mathbf{D}. \quad (7.22)$$

Given the general matrices  $\mathbf{A}$ ,  $\mathbf{B}$ , and  $\mathbf{C}$  and scalar  $D$ , we would like to find the transformation matrix  $\mathbf{T}$  such that  $\bar{\mathbf{A}}$ ,  $\bar{\mathbf{B}}$ ,  $\bar{\mathbf{C}}$ , and  $\bar{\mathbf{D}}$  are in a particular form, for example, control canonical form. To find such a  $\mathbf{T}$ , we assume that  $\mathbf{A}$ ,  $\mathbf{B}$ ,  $\mathbf{C}$ , and  $D$  are already in the required form, further assume the transformation  $\mathbf{T}$  has a general form, and match terms. Here we will work out the third-order case; how to extend the analysis to the general case should be clear from the development. It goes like this.

First, we rewrite Eq. (7.21a) as

$$\bar{\mathbf{A}}\mathbf{T}^{-1} = \mathbf{T}^{-1}\mathbf{A}.$$

If  $\bar{\mathbf{A}}$  is in control canonical form, and we describe  $\mathbf{T}^{-1}$  as a matrix with rows  $\mathbf{t}_1$ ,  $\mathbf{t}_2$ , and  $\mathbf{t}_3$ , then

$$\left[ \begin{array}{ccc} -a_1 & -a_2 & -a_3 \\ 1 & 0 & 0 \\ 0 & 1 & 0 \end{array} \right] \left[ \begin{array}{c} \mathbf{t}_1 \\ \mathbf{t}_2 \\ \mathbf{t}_3 \end{array} \right] = \left[ \begin{array}{c} \mathbf{t}_1\mathbf{A} \\ \mathbf{t}_2\mathbf{A} \\ \mathbf{t}_3\mathbf{A} \end{array} \right]. \quad (7.23)$$

Working out the third and second rows gives the matrix equations

$$\mathbf{t}_2 = \mathbf{t}_3 \mathbf{A}, \quad (7.24a)$$

$$\mathbf{t}_1 = \mathbf{t}_2 \mathbf{A} = \mathbf{t}_3 \mathbf{A}^2. \quad (7.24b)$$

From Eq. (7.21b), assuming  $\bar{\mathbf{B}}$  is also in control canonical form, we have the relation

$$\mathbf{T}^{-1} \mathbf{B} = \bar{\mathbf{B}},$$

or

$$\begin{bmatrix} \mathbf{t}_1 \mathbf{B} \\ \mathbf{t}_2 \mathbf{B} \\ \mathbf{t}_3 \mathbf{B} \end{bmatrix} = \begin{bmatrix} 1 \\ 0 \\ 0 \end{bmatrix}. \quad (7.25)$$

Combining Eqs. (7.24) and (7.25), we get

$$\mathbf{t}_3 \mathbf{B} = 0,$$

$$\mathbf{t}_2 \mathbf{B} = \mathbf{t}_3 \mathbf{A} \mathbf{B} = 0,$$

$$\mathbf{t}_1 \mathbf{B} = \mathbf{t}_3 \mathbf{A}^2 \mathbf{B} = 1.$$

These equations can, in turn, be written in matrix form as

$$\mathbf{t}_3 [ \mathbf{B} \quad \mathbf{AB} \quad \mathbf{A}^2 \mathbf{B} ] = [ 0 \quad 0 \quad 1 ],$$

or

$$\mathbf{t}_3 = [ 0 \quad 0 \quad 1 ] \mathcal{C}^{-1}, \quad (7.26)$$

where the **controllability matrix**  $\mathcal{C} = [ \mathbf{B} \quad \mathbf{AB} \quad \mathbf{A}^2 \mathbf{B} ]$ . Having  $\mathbf{t}_3$ , we can now go back to Eq. (7.24) and construct all the rows of  $\mathbf{T}^{-1}$ .

To sum up, the recipe for converting a general state description of dimension  $n$  to control canonical form is as follows:

- From  $\mathbf{A}$  and  $\mathbf{B}$ , form the controllability matrix

$$\mathcal{C} = [ \mathbf{B} \quad \mathbf{AB} \quad \cdots \quad \mathbf{A}^{n-1} \mathbf{B} ]. \quad (7.27)$$

- Compute the last row of the inverse of the transformation matrix as

$$\mathbf{t}_n = [ 0 \quad 0 \quad \cdots \quad 1 ] \mathcal{C}^{-1}. \quad (7.28)$$

- Construct the entire transformation matrix as

$$\mathbf{T}^{-1} = \begin{bmatrix} \mathbf{t}_n \mathbf{A}^{n-1} \\ \mathbf{t}_n \mathbf{A}^{n-2} \\ \vdots \\ \mathbf{t}_n \end{bmatrix}. \quad (7.29)$$

- Compute the new matrices from  $\mathbf{T}^{-1}$ , using Eqs. (7.21a), (7.21b), and (7.22).

When the controllability matrix  $\mathcal{C}$  is nonsingular, the corresponding  $\mathbf{A}$  and  $\mathbf{B}$  matrices are said to be **controllable**. This is a technical property that usually holds for physical systems and will be important when we consider feedback of the state in Section 7.5. We will also consider a few physical illustrations of loss of controllability at that time.

**Controllability matrix transformation to control canonical form**

**Controllable systems**

Because computing the transformation given by Eq. (7.29) is numerically difficult to do accurately, it is almost never done. The reason for developing this transformation in some detail is to show how such changes of state could be done in theory and to make the following important observation:

One can *always* transform a given state description to control canonical form if (and only if) the controllability matrix  $\mathcal{C}$  is nonsingular.

If we need to test for controllability in a real case with numbers, we use a numerically stable method that depends on converting the system matrices to “staircase” form rather than on trying to compute the controllability matrix. Problem 7.30 at the end of the chapter will call for consideration of this method.

An important question regarding controllability follows directly from our discussion so far: What is the effect of a state transformation on controllability? We can show the result by using Eqs. (7.27), (7.21a), and (7.21b). The controllability matrix of the system ( $\mathbf{A}$ ,  $\mathbf{B}$ ) is

$$\mathcal{C}_x = [ \mathbf{B} \quad \mathbf{AB} \quad \cdots \quad \mathbf{A}^{n-1}\mathbf{B} ]. \quad (7.30)$$

After the state transformation, the new description matrices are given by Eqs. (7.21a) and (7.21b), and the controllability matrix changes to

$$\mathcal{C}_z = [ \bar{\mathbf{B}} \quad \bar{\mathbf{AB}} \quad \cdots \quad \bar{\mathbf{A}}^{n-1}\bar{\mathbf{B}} ] \quad (7.31a)$$

$$= [ \mathbf{T}^{-1}\mathbf{B} \quad \mathbf{T}^{-1}\mathbf{AT}\mathbf{T}^{-1}\mathbf{B} \quad \cdots \quad \mathbf{T}^{-1}\mathbf{A}^{n-1}\mathbf{TT}^{-1}\mathbf{B} ] \quad (7.31b)$$

$$= \mathbf{T}^{-1}\mathcal{C}_x. \quad (7.31c)$$

Thus, we see that  $\mathcal{C}_z$  is nonsingular if and only if  $\mathcal{C}_x$  is nonsingular, yielding the following observation:

A change of state by a nonsingular linear transformation does *not* change controllability.

We return once again to the transfer function of Eq. (7.9), this time to represent it with the block diagram having the structure known as **observer canonical form** (Fig. 7.10). The corresponding matrices for this form are

$$\mathbf{A}_o = \begin{bmatrix} -7 & 1 \\ -12 & 0 \end{bmatrix}, \quad \mathbf{B}_o = \begin{bmatrix} 1 \\ 2 \end{bmatrix}, \quad (7.32a)$$

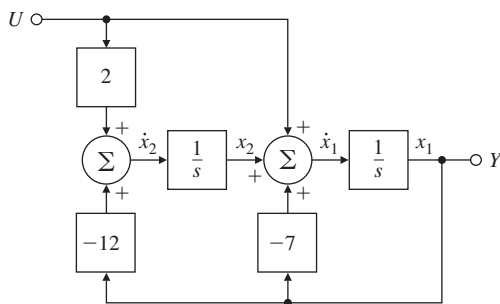
$$\mathbf{C}_o = [ \quad 1 \quad 0 ], \quad D_o = 0. \quad (7.32b)$$

The significant fact about this canonical form is that the output feeds back to each one of the state-variables through the coefficients of the system matrix  $\mathbf{A}_o$ .

### Observer canonical form

**Figure 7.10**

Observer canonical form  
for the second-order  
thermal system



Let us now consider what happens to the controllability of this system as the zero at  $-2$  is varied. For this purpose, we replace the second element  $2$  of  $\mathbf{B}_o$  with the variable zero location  $-z_o$  and form the controllability matrix:

$$\mathcal{C}_x = [ \mathbf{B}_o \quad \mathbf{A}_o \mathbf{B}_o ] \quad (7.33a)$$

$$= \begin{bmatrix} 1 & -7 - z_o \\ -z_o & -12 \end{bmatrix}. \quad (7.33b)$$

The determinant of this matrix is a function of  $z_o$ :

$$\begin{aligned} \det(\mathcal{C}_x) &= -12 + z_o(-7 - z_o) \\ &= -(z_o^2 + 7z_o + 12). \end{aligned}$$

This polynomial is zero for  $z_o = -3$  or  $-4$ , implying that controllability is lost for these values. What does this mean? In terms of the parameter  $z_o$ , the transfer function is

$$G(s) = \frac{s - z_o}{(s + 3)(s + 4)}.$$

If  $z_o = -3$  or  $-4$ , there is a pole-zero cancellation and the transfer function reduces from a second-order system to a first-order one. When  $z_o = -3$ , for example, the mode at  $-3$  is decoupled from the input and control of this mode is lost.

Notice we have taken the transfer function given by Eq. (7.9) and given it two realizations, one in control canonical form, and one in observer canonical form. The control form is always controllable for any value of the zero, while the observer form loses controllability if the zero cancels either of the poles. Thus, these two forms may represent the same transfer function, but it may not be possible to transform the state of one to the state of the other (in this case, from observer to control canonical form). Although a transformation of state cannot affect controllability, the particular state selected from a transfer function can:

Controllability is a function of the *state* of the system and cannot be decided from a transfer function.

To discuss controllability more at this point would take us too far afield. The closely related property of observability and the observer canonical form will be discussed in Section 7.7.1. A more detailed discussion of these properties of dynamic systems is given in Appendix WC available online [www.pearsonglobaleditions.com](http://www.pearsonglobaleditions.com), for those who would like to learn more.

We return now to the modal form for the equations, given by Eqs. (7.14a) and (7.14b) for the example transfer function. As mentioned before, it is not always possible to find a modal form for transfer functions that have repeated poles, so we assume our system has only distinct poles. Furthermore, we assume the general state equations given by Eqs. (7.18a) and (7.18b) apply. We want to find a transformation matrix  $\mathbf{T}$  defined by Eq. (7.19) such that the transformed Eqs. (7.21a) and (7.22) will be in modal form. In this case, we assume the  $\mathbf{A}$  matrix is diagonal, and  $\mathbf{T}$  is composed of the *columns*  $\mathbf{t}_1$ ,  $\mathbf{t}_2$ , and  $\mathbf{t}_3$ . With this assumption, the state transformation Eq. (7.21a) becomes

$$\mathbf{T}\bar{\mathbf{A}} = \mathbf{A}\mathbf{T} \quad (7.34)$$

$$\left[ \begin{array}{ccc} \mathbf{t}_1 & \mathbf{t}_2 & \mathbf{t}_3 \end{array} \right] \left[ \begin{array}{ccc} p_1 & 0 & 0 \\ 0 & p_2 & 0 \\ 0 & 0 & p_3 \end{array} \right] = \mathbf{A} \left[ \begin{array}{ccc} \mathbf{t}_1 & \mathbf{t}_2 & \mathbf{t}_3 \end{array} \right].$$

[Transformation to modal form](#)

[Eigenvectors](#)

[Eigenvalues](#)

[Matlab eig](#)

Equation (7.34) is equivalent to the three vector-matrix equations

$$p_i \mathbf{t}_i = \mathbf{A} \mathbf{t}_i, \quad i = 1, 2, 3. \quad (7.35)$$

In matrix algebra, Eq. (7.35) is a famous equation, whose solution is known as the **eigenvector/eigenvalue problem**. Recall that  $\mathbf{t}_i$  is a vector,  $\mathbf{A}$  is a matrix, and  $p_i$  is a scalar. The vector  $\mathbf{t}_i$  is called an **eigenvector** of  $\mathbf{A}$ , and  $p_i$  is called the corresponding **eigenvalue**. Because we saw earlier that the modal form is equivalent to a partial-fraction-expansion representation with the system poles along the diagonal of the state matrix, it should be clear that these eigenvalues are precisely the poles of our system. The transformation matrix that will convert the state description matrices to modal form has as its columns the eigenvectors of  $\mathbf{A}$ , as shown in Eq. (7.34) for the third-order case. As it happens, there are robust, reliable computer algorithms to compute eigenvalues and the eigenvectors of quite large systems using the QR algorithm. In Matlab, the command `p = eig(A)` is the way to compute the poles if the system equations are in state form.

Notice also that Eq. (7.35) is homogeneous in that, if  $\mathbf{t}_i$  is an eigenvector, so is  $\alpha \mathbf{t}_i$ , for any scalar  $\alpha$ . In most cases, the scale factor is selected so the length (square root of the sum of squares of the magnitudes of the elements) is unity. Matlab will perform this operation. Another option is to select the scale factors so that the input matrix  $\bar{\mathbf{B}}$  is composed of all 1's. The latter choice is suggested by a partial-fraction expansion with each part realized in control canonical form. If the system is real, then each element of  $\mathbf{A}$  is real, and if  $p = \sigma + j\omega$  is a pole, so is the conjugate,  $p^* = \sigma - j\omega$ . For these eigenvalues, the eigenvectors

are also complex and conjugate. It is possible to compose the transformation matrix using the real and complex parts of the eigenvectors separately, so the modal form is real but has  $2 \times 2$  blocks for each pair of complex poles. Later, we will see the result of the Matlab function that does this, but first, let us look at the simple real-poles case.

### EXAMPLE 7.9

#### *Transformation of Thermal System from Control to Modal Form*

Find the matrix to transform the control form matrices in Eq. (7.12) into the modal form of Eq. (7.14).

**Solution.** According to Eqs. (7.34) and (7.35), we need first to find the eigenvectors and eigenvalues of the  $\mathbf{A}_c$  matrix. We take the eigenvectors to be

$$\begin{bmatrix} t_{11} \\ t_{21} \end{bmatrix} \quad \text{and} \quad \begin{bmatrix} t_{12} \\ t_{22} \end{bmatrix}.$$

The equations using the eigenvector on the left are

$$\begin{bmatrix} -7 & -12 \\ 1 & 0 \end{bmatrix} \begin{bmatrix} t_{11} \\ t_{21} \end{bmatrix} = p \begin{bmatrix} t_{11} \\ t_{21} \end{bmatrix}, \quad (7.36a)$$

$$-7t_{11} - 12t_{21} = pt_{11}, \quad (7.36b)$$

$$t_{11} = pt_{21}. \quad (7.36c)$$

Substituting Eq. (7.36c) into Eq. (7.36b) results in

$$-7pt_{21} - 12t_{21} = p^2t_{21}, \quad (7.37a)$$

$$p^2t_{21} + 7pt_{21} + 12t_{21} = 0, \quad (7.37b)$$

$$p^2 + 7p + 12 = 0, \quad (7.37c)$$

$$p = -3, -4. \quad (7.37d)$$

We have found (again!) that the eigenvalues (poles) are  $-3$  and  $-4$ ; furthermore, Eq. (7.36c) tells us that the two eigenvectors are

$$\begin{bmatrix} -4t_{21} \\ t_{21} \end{bmatrix} \quad \text{and} \quad \begin{bmatrix} -3t_{22} \\ t_{22} \end{bmatrix},$$

where  $t_{21}$  and  $t_{22}$  are arbitrary nonzero scale factors. We want to select the two scale factors such that both elements of  $\mathbf{B}_m$  in Eq. (7.14a) are unity. The equation for  $\mathbf{B}_m$  in terms of  $\mathbf{B}_c$  is  $\mathbf{T}\mathbf{B}_m = \mathbf{B}_c$ , and its solution is  $t_{21} = -1$  and  $t_{22} = 1$ . Therefore, the transformation matrix and its inverse<sup>3</sup> are

$$\mathbf{T} = \begin{bmatrix} 4 & -3 \\ -1 & 1 \end{bmatrix}, \quad \mathbf{T}^{-1} = \begin{bmatrix} 1 & 3 \\ 1 & 4 \end{bmatrix}. \quad (7.38)$$

---

<sup>3</sup>To find the inverse of a  $2 \times 2$  matrix, you need only interchange the elements subscripted “11” and “22,” change the signs of the “12” and the “21” elements, and divide by the determinant [= 1 in Eq. (7.38)].

Elementary matrix multiplication shows that, using  $\mathbf{T}$  as defined by Eq. (7.38), the matrices of Eqs. (7.12) and (7.14) are related as follows:

$$\begin{aligned}\mathbf{A}_m &= \mathbf{T}^{-1} \mathbf{A}_c \mathbf{T}, & \mathbf{B}_m &= \mathbf{T}^{-1} \mathbf{B}_c, \\ \mathbf{C}_m &= \mathbf{C}_c \mathbf{T}, & \mathbf{D}_m &= \mathbf{D}_c.\end{aligned}\quad (7.39)$$

These computations can be carried out by using the following Matlab statements:

```
T = [4 -3; -1 1];
Am = inv(T)*Ac*T;
Bm = inv(T)*Bc;
Cm = Cc*T;
Dm = Dc;
```

The next example has four state-variables and, in state-variable form, is too complicated for hand calculations. However, it is a good example for illustrating the use of computer software designed for the purpose. The model we will use is based on a physical state after amplitude and time scaling have been done.

### EXAMPLE 7.10

#### *Using Matlab to Find Poles and Zeros of Piper Dakota Airplane*

The state space representation of the transfer function between the elevator input and pitch attitude for the Piper Dakota, Eq. (5.78), is shown below. Find the eigenvalues of the system matrix. Also, compute the transformation of the equations of the airplane in their given form to the modal canonical form. The system matrices are

$$\mathbf{A} = \begin{bmatrix} -5.03 & -40.21 & -1.5 & -2.4 \\ 1 & 0 & 0 & 0 \\ 0 & 1 & 0 & 0 \\ 0 & 0 & 1 & 0 \end{bmatrix}, \quad \mathbf{B} = \begin{bmatrix} 1 \\ 0 \\ 0 \\ 0 \end{bmatrix}$$

$$\mathbf{C} = [0 \ 160 \ 512 \ 280], \quad \mathbf{D} = 0.0 \quad (7.40)$$

**Solution.** To compute the eigenvalues by using Matlab, we write

$$\mathbf{P} = \text{eig}(\mathbf{A}),$$

which results in

$$\mathbf{P} = \begin{bmatrix} -2.5000 + 5.8095i \\ -2.5000 - 5.8095i \\ -0.0150 + 0.2445i \\ -0.0150 - 0.2445i \end{bmatrix}.$$

Notice that the system has all poles in the left half-plane (LHP).

## Matlab canon

To transform to modal form, we use the Matlab function `canon`:

```
sysG = ss(A,B,C,D);
[sysGm,TI]=canon(sysG,'modal');
[Am,Bm,Cm,Dm]=ssdata(sysGm)
```

The result of this computation is

$$A_m = A_m = \begin{bmatrix} -2.5000 & 5.8090 & 0 & 0 \\ -5.8090 & -2.5000 & 0 & 0 \\ 0 & 0 & -0.0150 & 0.2445 \\ 0 & 0 & -0.2445 & -0.0150 \end{bmatrix}.$$

Notice the two complex poles appear in the  $2 \times 2$  blocks along the diagonal of  $A_m$ . The rest of the computations from `canon` are

$$B_m = B_m = \begin{bmatrix} 7.7760 \\ -22.6800 \\ -3.2010 \\ 0.3066 \end{bmatrix}$$

$$C_m = C_m = [-1.0020 \quad 0.1809 \quad -2.8710 \quad 8.8120]$$

$$D_m = D_m = 0$$

$$\Pi = T^{-1} = \begin{bmatrix} 7.7761 & -112.0713 & -2.9026 & -6.7383 \\ -22.6776 & -102.5493 & -4.4167 & -6.1121 \\ -3.2007 & -15.9764 & -127.8924 & 1.0776 \\ 0.3066 & 2.3199 & 16.1981 & 31.4852 \end{bmatrix}$$

It happens that `canon` was written to compute the *inverse* of the transformation we are working with (as you can see from `TI` in the previous equation), so we need to invert our Matlab results. The inverse is computed from

$$T = \text{inv}(\Pi)$$

and results in

$$T = T = \begin{bmatrix} 0.0307 & -0.0336 & 0.0005 & 0.0000 \\ -0.0068 & -0.0024 & -0.0000 & -0.0019 \\ 0.0001 & 0.0011 & -0.0078 & 0.0005 \\ 0.0002 & -0.0001 & 0.0040 & 0.0316 \end{bmatrix}$$

The eigenvectors computed with `[V,P]=eig(A)` are

$$V = \begin{bmatrix} 0.9874 + 0.0000i & 0.9874 + 0.0000i & 0.0026 - 0.0140i & 0.0026 + 0.0140i \\ -0.0617 - 0.1434i & -0.0617 + 0.1434i & -0.0577 - 0.0071i & -0.0577 + 0.0071i \\ -0.0170 + 0.0179i & -0.0170 - 0.0179i & -0.0145 + 0.2370i & -0.0145 - 0.2370i \\ 0.0037 + 0.0013i & 0.0037 - 0.0013i & 0.9695 + 0.0000i & 0.9695 + 0.0000i \end{bmatrix}.$$


---

## 7.4.2 Dynamic Response from the State Equations

Having considered the structure of the state-variable equations, we now turn to finding the dynamic response from the state description and to the relationships between the state description and our earlier discussion of the frequency response and poles and zeros in Chapter 6. Let us begin with the general state equations given by Eqs. (7.18a) and (7.18b), and consider the problem in the frequency domain. Taking the Laplace transform of

$$\dot{\mathbf{x}} = \mathbf{Ax} + \mathbf{Bu}, \quad (7.41)$$

we obtain

$$s\mathbf{X}(s) - \mathbf{x}(0) = \mathbf{AX}(s) + \mathbf{BU}(s), \quad (7.42)$$

which is now an algebraic equation. If we collect the terms involving  $\mathbf{X}(s)$  on the left side of Eq. (7.42), keeping in mind that in matrix multiplication order is very important, we find that<sup>4</sup>

$$(s\mathbf{I} - \mathbf{A})\mathbf{X}(s) = \mathbf{BU}(s) + \mathbf{x}(0).$$

If we premultiply both sides by the inverse of  $(s\mathbf{I} - \mathbf{A})$ , then

$$\mathbf{X}(s) = (s\mathbf{I} - \mathbf{A})^{-1}\mathbf{BU}(s) + (s\mathbf{I} - \mathbf{A})^{-1}\mathbf{x}(0). \quad (7.43)$$

The output of the system is

$$Y(s) = \mathbf{CX}(s) + DU(s), \quad (7.44a)$$

$$= \mathbf{C}(s\mathbf{I} - \mathbf{A})^{-1}\mathbf{BU}(s) + \mathbf{C}(s\mathbf{I} - \mathbf{A})^{-1}\mathbf{x}(0) + DU(s). \quad (7.44b)$$

This equation expresses the output response to both an initial condition and an external forcing input. Collecting the terms involving  $U(s)$  and assuming zero initial conditions result in the transfer function of the system,

$$G(s) = \frac{Y(s)}{U(s)} = \mathbf{C}(s\mathbf{I} - \mathbf{A})^{-1}\mathbf{B} + D. \quad (7.45)$$

**Transfer function from state equations**

### EXAMPLE 7.11

#### *Thermal System Transfer Function from the State Description*

Use Eq. (7.45) to find the transfer function of the thermal system described by Eqs. (7.12a) and (7.12b).

**Solution.** The state-variable description matrices of the system are

$$\mathbf{A} = \begin{bmatrix} -7 & -12 \\ 1 & 0 \end{bmatrix}, \quad \mathbf{B} = \begin{bmatrix} 1 \\ 0 \end{bmatrix},$$

$$\mathbf{C} = [1 \ 2], \quad D = 0.$$

To compute the transfer function according to Eq. (7.45), we form

$$s\mathbf{I} - \mathbf{A} = \begin{bmatrix} s+7 & 12 \\ -1 & s \end{bmatrix},$$

---

<sup>4</sup>The identity matrix  $\mathbf{I}$  is a matrix of ones on the main diagonal and zeros everywhere else; therefore,  $\mathbf{Ix} = \mathbf{x}$ .

and compute

$$(s\mathbf{I} - \mathbf{A})^{-1} = \frac{\begin{bmatrix} s & -12 \\ 1 & s+7 \end{bmatrix}}{s(s+7)+12}. \quad (7.46)$$

We then substitute Eq. (7.46) into Eq. (7.45) to get

$$G(s) = \frac{\begin{bmatrix} 1 & 2 \end{bmatrix} \begin{bmatrix} s & -12 \\ 1 & s+7 \end{bmatrix} \begin{bmatrix} 1 \\ 0 \end{bmatrix}}{s(s+7)+12} \quad (7.47)$$

$$= \frac{\begin{bmatrix} 1 & 2 \end{bmatrix} \begin{bmatrix} s \\ 1 \end{bmatrix}}{s(s+7)+12} \quad (7.48)$$

$$= \frac{(s+2)}{(s+3)(s+4)}. \quad (7.49)$$

The results can also be found using the Matlab statements,

`[num,den] = ss2tf(A,B,C,D)`

and yield `num = [0 1 2]` and `den = [1 7 12]`, which agrees with the hand calculations above.

---

Because Eq. (7.45) expresses the transfer function in terms of the general state-space descriptor matrices  $\mathbf{A}$ ,  $\mathbf{B}$ ,  $\mathbf{C}$ , and  $D$ , we are able to express poles and zeros in terms of these matrices. We saw earlier that by transforming the state matrices to diagonal form, the poles appear as the eigenvalues on the main diagonal of the  $\mathbf{A}$  matrix. We now take a systems theory point of view to look at the poles and zeros as they are involved in the transient response of a system.

As we saw in Chapter 3, a pole of the transfer function  $G(s)$  is a value of generalized frequency  $s$  such that, if  $s = p_i$ , then the system can respond to an initial condition as  $K_i e^{p_i t}$ , with no forcing function  $u$ . In this context,  $p_i$  is called a **natural frequency** or **natural mode** of the system. If we take the state-space equations (7.18a and 7.18b) and set the forcing function  $u$  to zero, we have

$$\dot{\mathbf{x}} = \mathbf{Ax}. \quad (7.50)$$

If we assume some (as yet unknown) initial condition

$$\mathbf{x}(0) = \mathbf{x}_0, \quad (7.51)$$

and that the entire state motion behaves according to the same natural frequency, then the state can be written as  $\mathbf{x}(t) = e^{p_i t} \mathbf{x}_0$ . It follows from Eq. (7.50) that

$$\dot{\mathbf{x}}(t) = p_i e^{p_i t} \mathbf{x}_0 = \mathbf{Ax} = \mathbf{Ae}^{p_i t} \mathbf{x}_0, \quad (7.52)$$

or

$$\mathbf{Ax}_0 = p_i \mathbf{x}_0. \quad (7.53)$$

We can rewrite Eq. (7.53) as

$$(p_i \mathbf{I} - \mathbf{A}) \mathbf{x}_0 = 0. \quad (7.54)$$

**Transfer function poles  
from state equations**

Equations (7.53) and (7.54) constitute the eigenvector/eigenvalue problem we saw in Eq. (7.35) with eigenvalues  $p_i$  and, in this case, eigenvectors  $\mathbf{x}_0$  of the matrix  $\mathbf{A}$ . If we are just interested in the eigenvalues, we can use the fact that for a nonzero  $\mathbf{x}_0$ , Eq. (7.54) has a solution if and only if

$$\det(p_i \mathbf{I} - \mathbf{A}) = 0. \quad (7.55)$$

These equations show again that the *poles* of the transfer function are the eigenvalues of the system matrix  $\mathbf{A}$ . The determinant equation (7.55) is a polynomial in the eigenvalues  $p_i$  known as the **characteristic equation**. In Example 7.9, we computed the eigenvalues and eigenvectors of a particular matrix in control canonical form. As an alternative computation for the poles of that system, we could solve the characteristic equation (7.55). For the system described by Eqs. (7.12a) and (7.12b), we can find the poles from Eq. (7.55) by solving

$$\det(s \mathbf{I} - \mathbf{A}) = 0, \quad (7.56a)$$

$$\det \begin{bmatrix} s+7 & 12 \\ -1 & s \end{bmatrix} = 0, \quad (7.56b)$$

$$s(s+7) + 12 = (s+3)(s+4) = 0. \quad (7.56c)$$

This confirms again that the poles of the system are the eigenvalues of  $\mathbf{A}$ .

We can also determine the transmission zeros of a system from the state-variable description matrices  $\mathbf{A}$ ,  $\mathbf{B}$ ,  $\mathbf{C}$ , and  $\mathbf{D}$  using a systems theory point of view. From this perspective, a zero is a value of generalized frequency  $s$  such that the system can have a nonzero input and state and yet have an output of zero. If the input is exponential at the zero frequency  $z_i$ , given by

$$u(t) = u_0 e^{z_i t}, \quad (7.57)$$

then the output is identically zero:

$$y(t) \equiv 0. \quad (7.58)$$

The state-space description of Eqs. (7.57) and (7.58) would be

$$u = u_0 e^{z_i t}, \quad \mathbf{x}(t) = \mathbf{x}_0 e^{z_i t}, \quad y(t) \equiv 0. \quad (7.59)$$

Thus

$$\dot{\mathbf{x}} = z_i e^{z_i t} \mathbf{x}_0 = \mathbf{A} e^{z_i t} \mathbf{x}_0 + \mathbf{B} u_0 e^{z_i t}, \quad (7.60)$$

or

$$[z_i \mathbf{I} - \mathbf{A} \quad -\mathbf{B}] \begin{bmatrix} \mathbf{x}_0 \\ u_0 \end{bmatrix} = \mathbf{0}, \quad (7.61)$$

and

$$y = \mathbf{C} \mathbf{x} + \mathbf{D} u = \mathbf{C} e^{z_i t} \mathbf{x}_0 + \mathbf{D} u_0 e^{z_i t} \equiv 0. \quad (7.62)$$

Combining Eqs. (7.61) and (7.62), we get

$$\begin{bmatrix} z_i \mathbf{I} - \mathbf{A} & -\mathbf{B} \\ \mathbf{C} & D \end{bmatrix} \begin{bmatrix} \mathbf{x}_0 \\ u_0 \end{bmatrix} = \begin{bmatrix} \mathbf{0} \\ 0 \end{bmatrix}. \quad (7.63)$$

Transfer function zeros  
from state equations

From Eq. (7.63), we can conclude that a zero of the state-space system is a value of  $z_i$  where Eq. (7.63) has a nontrivial solution. With one input and one output, the matrix is square, and a solution to Eq. (7.63) is equivalent to a solution to

$$\det \begin{bmatrix} z_i \mathbf{I} - \mathbf{A} & -\mathbf{B} \\ \mathbf{C} & D \end{bmatrix} = 0. \quad (7.64)$$

## EXAMPLE 7.12

### Zeros for the Thermal System from a State Description

Compute the zero(s) of the thermal system described by Eq. (7.12).

**Solution.** We use Eq. (7.64) to compute the zeros:

$$\begin{aligned} \det \begin{bmatrix} s+7 & 12 & -1 \\ -1 & s & 0 \\ 1 & 2 & 0 \end{bmatrix} &= 0, \\ -2-s &= 0, \\ s &= -2. \end{aligned}$$

Note this result agrees with the zero of the transfer function given by Eq. (7.9). The result can also be found using the following Matlab statements:

```
sysG = ss(Ac,Bc,Cc,Dc);
[z] = tzero(sysG)
```

and yields  $z = -2.0$ .

Equation (7.55) for the characteristic equation and Eq. (7.64) for the zeros polynomial can be combined to express the transfer function in a compact form from state-description matrices as

$$G(s) = \frac{\det \begin{bmatrix} s\mathbf{I} - \mathbf{A} & -\mathbf{B} \\ \mathbf{C} & D \end{bmatrix}}{\det(s\mathbf{I} - \mathbf{A})}. \quad (7.65)$$

(See Appendix WB available online at [www.pearsonglobaleditions.com](http://www.pearsonglobaleditions.com) for more details.) While Eq. (7.65) is a compact formula for theoretical studies, it is very sensitive to numerical errors. A numerically stable algorithm for computing the transfer function is described in Emami-Naeini and Van Dooren (1982). Given the transfer function, we can compute the frequency response as  $G(j\omega)$ , and as discussed earlier, we can use Eqs. (7.54) and (7.63) to find the poles and zeros, upon which the transient response depends, as we saw in Chapter 3.

**EXAMPLE 7.13***Analysis of the State Equations of Piper Dakota*

Compute the poles, zeros, and the transfer function for the state space equations of the Piper Dakota given in Example 7.10.

**Matlab ss2tf**

**Solution.** There are two different ways to compute the answer to this problem. The most direct is to use the Matlab function `ss2tf` (state-space to transfer function), which will give the numerator and denominator polynomials directly. This function permits multiple inputs and outputs; the fifth argument of the function tells which input is to be used. We have only one input here, but must still provide the argument. The computation of the transfer function is

$$[\text{Num}, \text{Den}] = \text{ss2tf}(A, B, C, D, 1),$$

which results in

$$\text{Num} = [ 0 \quad 0 \quad 160 \quad 512 \quad 280 ]$$

$$\text{Den} = [ 1.00 \quad 5.03 \quad 40.21 \quad 1.50 \quad 2.40 ]$$

**Matlab roots**

It is interesting to check to see whether the poles and zeros determined this way agree with those found by other means. To find the roots of a polynomial such as the one corresponding to `Den`, we use the Matlab function `roots`:

$$\text{roots}(\text{Den}) = \begin{bmatrix} -2.5000 + 5.8095i \\ -2.5000 - 5.8095i \\ -0.0150 + 0.2445i \\ -0.0150 - 0.2445i \end{bmatrix}.$$

which yields the poles of the system. Checking with Example 7.10, we confirm that they agree.

How about the zeros? We can find these by finding the roots of the numerator polynomial. We compute the roots of the polynomial `Num`:

$$\text{roots}(\text{Num}) = \begin{bmatrix} -2.5000 \\ -0.7000 \end{bmatrix}.$$

**Matlab tzero**

The zeros can be computed by the equivalent of Eq. (7.63) with the function `tzero` (transmission zeros).

$$\text{sysG} = \text{ss}(A, B, C, D)$$

$$[\text{ZER}] = \text{tzero}(\text{sysG})$$

yields

$$\text{ZER} = \begin{bmatrix} -2.5000 \\ -0.7000 \end{bmatrix},$$

From these results we can write down, for example, the transfer function as

$$\begin{aligned} G(s) &= \frac{160s^2 + 512s + 280}{s^4 + 5.03s^3 + 40.21s^2 + 1.5s + 2.4} \\ &= \frac{160(s + 2.5)(s + 0.7)}{(s^2 + 5s + 40)(s^2 + 0.03s + 0.06)}. \end{aligned} \quad (7.66)$$

## 7.5 Control-Law Design for Full-State Feedback

One of the attractive features of the state-space design method is that it consists of a sequence of independent steps, as mentioned in the chapter overview. The first step, discussed in Section 7.5.1, is to determine the control law. The purpose of the control law is to allow us to assign a set of pole locations for the closed-loop system that will correspond to satisfactory dynamic response in terms of rise time and other measures of transient response. In Section 7.5.2, we will show how to introduce the reference input with full-state feedback, and in Section 7.6, we will describe the process of finding the poles for good design.

The second step—necessary if the full state is not available—is to design an **estimator** (sometimes called an **observer**), which computes an estimate of the entire state vector when provided with the measurements of the system indicated by Eq. (7.18b). We will examine estimator design in Section 7.7.

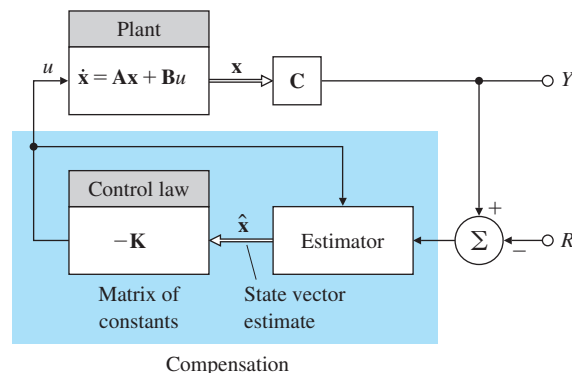
The third step consists of combining the control law and the estimator. Figure 7.11 shows how the control law and the estimator fit together and how the combination takes the place of what we have been previously referring to as **compensation**. At this stage, the control-law calculations are based on the estimated state rather than the actual state. In Section 7.8, we will show that this substitution is reasonable, and also that using the combined control law and estimator results in closed-loop pole locations that are the same as those determined when designing the control and estimator separately.

Estimator/observer

The control law and the estimator together form the compensation

**Figure 7.11**

Schematic diagram of state-space



The fourth and final step of state-space design is to introduce the reference input in such a way that the plant output will track external commands with acceptable rise-time, overshoot, and settling-time values. At this point in the design, all the closed-loop poles have been selected, and the designer is concerned with the zeros of the overall transfer function. Figure 7.11 shows the command input  $r$  introduced in the same relative position as was done with the transform design methods; however, in Section 7.9, we will show how to introduce the reference at another location, resulting in different zeros and (usually) superior control.

### 7.5.1 Finding the Control Law

The first step in the state-space design method, as mentioned earlier, is to find the control law as feedback of a linear combination of the state-variables—that is,

$$u = -\mathbf{K}\mathbf{x} = -[ K_1 \ K_2 \ \dots \ K_n ] \begin{bmatrix} x_1 \\ x_2 \\ \vdots \\ x_n \end{bmatrix}. \quad (7.67)$$

We assume, for feedback purposes, that all the elements of the state vector are at our disposal which is why we refer to this as “full-state,” feedback. In practice, of course, this would usually be a ridiculous assumption; moreover, a well-trained control designer knows that other design methods do not require so many sensors. The assumption that all state-variables are available merely allows us to proceed with this first step.

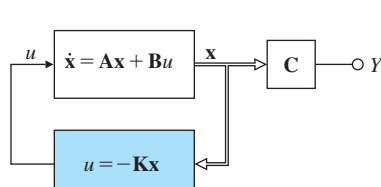
Equation (7.67) tells us that the system has a constant matrix in the state-vector feedback path, as shown in Fig. 7.12. For an  $n$ th-order system, there will be  $n$  feedback gains,  $K_1, \dots, K_n$ , and because there are  $n$  roots of the system, it is possible that there are enough degrees of freedom to select *arbitrarily* any desired root location by choosing the proper values of  $K_i$ . This freedom contrasts sharply with root-locus design, in which we have only one parameter and the closed-loop poles are restricted to the locus.

Substituting the feedback law given by Eq. (7.67) into the system described by Eq. (7.18a) yields

$$\dot{\mathbf{x}} = \mathbf{A}\mathbf{x} + \mathbf{B}\mathbf{u}. \quad (7.68)$$

**Control characteristic equation**

**Figure 7.12**  
Assumed system for control-law



$$\det[s\mathbf{I} - (\mathbf{A} - \mathbf{B}\mathbf{K})] = 0. \quad (7.69)$$

When evaluated, this yields an  $n$ th-order polynomial in  $s$  containing the gains  $K_1, \dots, K_n$ . The control-law design then consists of picking the gains  $\mathbf{K}$  so the roots of Eq. (7.69) are in desirable locations. Selecting desirable root locations is an inexact science that may require some iteration by the designer. Issues in their selection are considered in Examples 7.14 to 7.16 as well as in Section 7.6. For now, we assume the desired locations are known, say,

$$s = s_1, s_2, \dots, s_n.$$

Then the corresponding desired (control) characteristic equation is

$$\alpha_c(s) = (s - s_1)(s - s_2) \dots (s - s_n) = 0. \quad (7.70)$$

Hence, the required elements of  $\mathbf{K}$  are obtained by matching coefficients in Eqs. (7.69) and (7.70). This forces the system's characteristic equation to be identical to the desired characteristic equation and the closed-loop poles to be placed at the desired locations.

### EXAMPLE 7.14

#### *Control Law for a Pendulum*

Suppose you have a pendulum with frequency  $\omega_0$  and a state-space description given by

$$\begin{bmatrix} \dot{x}_1 \\ \dot{x}_2 \end{bmatrix} = \begin{bmatrix} 0 & 1 \\ -\omega_0^2 & 0 \end{bmatrix} \begin{bmatrix} x_1 \\ x_2 \end{bmatrix} + \begin{bmatrix} 0 \\ 1 \end{bmatrix} u. \quad (7.71)$$

Find the control law that places the closed-loop poles of the system so they are both at  $-2\omega_0$ . In other words, you wish to double the natural frequency and increase the damping ratio  $\zeta$  from 0 to 1.

**Solution.** From Eq. (7.70), we find that

$$\alpha_c(s) = (s + 2\omega_0)^2 \quad (7.72a)$$

$$= s^2 + 4\omega_0 s + 4\omega_0^2. \quad (7.72b)$$

Equation (7.69) tells us that

$$\begin{aligned} & \det[s\mathbf{I} - (\mathbf{A} - \mathbf{B}\mathbf{K})] \\ &= \det \left\{ \begin{bmatrix} s & 0 \\ 0 & s \end{bmatrix} - \left( \begin{bmatrix} 0 & 1 \\ -\omega_0^2 & 0 \end{bmatrix} - \begin{bmatrix} 0 \\ 1 \end{bmatrix} [K_1 \ K_2] \right) \right\}, \end{aligned}$$

or

$$s^2 + K_2 s + \omega_0^2 + K_1 = 0. \quad (7.73)$$

Equating the coefficients with like powers of  $s$  in Eqs. (7.72b) and (7.73) yields the system of equations

$$K_2 = 4\omega_0,$$

$$\omega_0^2 + K_1 = 4\omega_0^2,$$

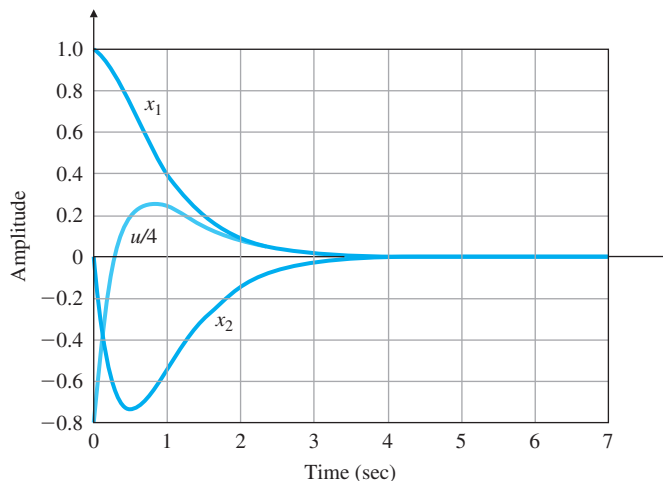
and therefore,

$$K_1 = 3\omega_0^2,$$

$$K_2 = 4\omega_0.$$

**Figure 7.13**

Impulse response of the undamped oscillator with full-state feedback  
 $\omega_0 = 1$



Thus the control law in concise form is

$$\mathbf{K} = [ K_1 \ K_2 ] = [ 3\omega_0^2 \ 4\omega_0 ].$$

Figure 7.13 shows the response of the closed-loop system to the initial conditions  $x_1 = 1.0$ ,  $x_2 = 0.0$ , and  $\omega_0 = 1$ . It shows a very well damped response, as would be expected from having two roots at  $s = -2$ . The Matlab command `impulse` was used to generate the plot.

Calculating the gains using the technique illustrated in Example 7.14 becomes rather tedious when the order of the system is higher than 3. There are, however, special “canonical” forms of the state-variable equations for which the algebra for finding the gains is especially simple. One such canonical form that is useful in control law design is the *control canonical form* as discussed in Section 7.4.1. Consider the third-order system<sup>5</sup>

$$\ddot{y} + a_1\dot{y} + a_2y = b_1\ddot{u} + b_2\dot{u} + b_3u, \quad (7.74)$$

which corresponds to the transfer function

$$G(s) = \frac{Y(s)}{U(s)} = \frac{b_1s^2 + b_2s + b_3}{s^3 + a_1s^2 + a_2s + a_3} = \frac{b(s)}{a(s)}. \quad (7.75)$$

Suppose we introduce an auxiliary variable (referred to as the *partial state*)  $\xi$ , which relates  $a(s)$  and  $b(s)$  as shown in Fig. 7.14(a). The transfer function from  $U$  to  $\xi$  is

$$\frac{\xi(s)}{U(s)} = \frac{1}{a(s)}, \quad (7.76)$$

or

$$\ddot{\xi} + a_1\dot{\xi} + a_2\xi + a_3\xi = u. \quad (7.77)$$

<sup>5</sup>This development is exactly the same for higher-order systems.

It is easy to draw a block diagram corresponding to Eq. (7.77) if we rearrange the equation as follows:

$$\ddot{\xi} = -a_1\ddot{\xi} - a_2\dot{\xi} - a_3\xi + u. \quad (7.78)$$

The summation is indicated in Fig. 7.14(b), where each  $\dot{\xi}$  on the right-hand side is obtained by sequential integration of  $\ddot{\xi}$ . To form the output, we go back to Fig. 7.14(a) and note that

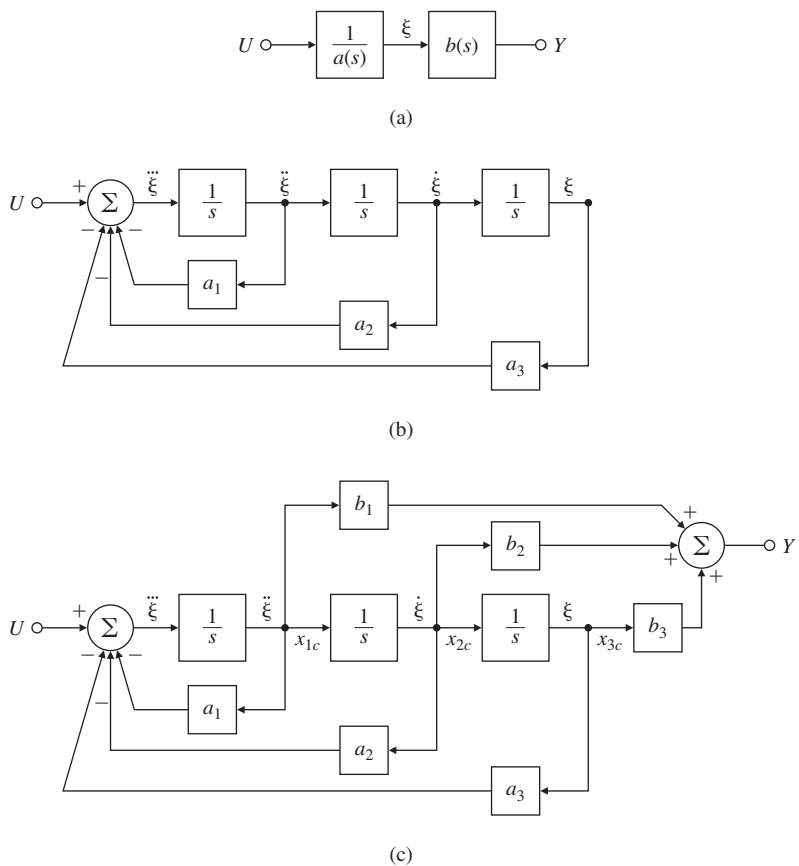
$$Y(s) = b(s)\xi(s), \quad (7.79)$$

which means that

$$y = b_1\ddot{\xi} + b_2\dot{\xi} + b_3\xi. \quad (7.80)$$

We again pick off the outputs of the integrators, multiply them by  $\{b_i\}$ 's, and form the right-hand side of Eq. (7.74) using a summer to yield the output as shown in Fig. 7.14(c). In this case, all the feedback loops return to the point of the application of the input, or “control” variable, and hence the form is referred to as the *control canonical form* as discussed in Section 7.4.1. Reduction of the structure by Mason's rule or by elementary block diagram operations verifies that this structure has the transfer function given by  $G(s)$ .

**Figure 7.14**  
Derivation of control  
canonical form



Taking the state as the outputs of the three integrators numbered, by convention, from the left, namely,

$$x_1 = \ddot{\xi}_1, x_2 = \dot{\xi}, x_3 = \xi, \quad (7.81)$$

we obtain

$$\begin{aligned} \dot{x}_1 &= \ddot{\xi} = -a_1 x_1 - a_2 x_2 - a_3 x_3 + u, \\ \dot{x}_2 &= x_1, \\ \dot{x}_3 &= x_2. \end{aligned} \quad (7.82)$$

We may now write the matrices describing the control canonical form in general:

$$\mathbf{A}_c = \begin{bmatrix} -a_1 & -a_2 & \cdots & \cdots & -a_n \\ 1 & 0 & \cdots & \cdots & 0 \\ 0 & 1 & 0 & \cdots & 0 \\ \vdots & & \ddots & & 0 \\ 0 & 0 & \cdots & 1 & 0 \end{bmatrix}, \quad \mathbf{B}_c = \begin{bmatrix} 1 \\ 0 \\ 0 \\ \vdots \\ 0 \end{bmatrix}, \quad (7.83a)$$

$$\mathbf{C}_c = [b_1 \ b_2 \ \cdots \ \cdots \ b_n], \quad D_c = 0. \quad (7.83b)$$

#### Companion form matrix

The special structure of this system matrix is referred to as the **upper companion form** because the characteristic equation is  $a(s) = s^n + a_1 s^{n-1} + a_2 s^{n-2} + \cdots + a_n$  and the coefficients of this monic “companion” polynomial are the elements in the first row of  $\mathbf{A}_c$ . If we now form the closed-loop system matrix  $\mathbf{A}_c - \mathbf{B}_c \mathbf{K}_c$ , we find that

$$\mathbf{A}_c - \mathbf{B}_c \mathbf{K}_c = \begin{bmatrix} -a_1 - K_1 & -a_2 - K_2 & \cdots & \cdots & -a_n - K_n \\ 1 & 0 & \cdots & \cdots & 0 \\ 0 & 1 & 0 & \cdots & 0 \\ \vdots & & \ddots & & \vdots \\ 0 & 0 & \cdots & 1 & 0 \end{bmatrix}. \quad (7.84)$$

By visually comparing Eqs. (7.83a) and (7.84), we see the closed-loop characteristic equation is

$$s^n + (a_1 + K_1)s^{n-1} + (a_2 + K_2)s^{n-2} + \cdots + (a_n + K_n) = 0. \quad (7.85)$$

Therefore, if the desired pole locations result in the characteristic equation given by

$$\alpha_c(s) = s^n + \alpha_1 s^{n-1} + \alpha_2 s^{n-2} + \cdots + \alpha_n = 0, \quad (7.86)$$

then the necessary feedback gains can be found by equating the coefficients in Eqs. (7.85) and (7.86):

$$K_1 = -a_1 + \alpha_1, \quad K_2 = -a_2 + \alpha_2, \dots, \quad K_n = -a_n + \alpha_n. \quad (7.87)$$

We now have an algorithm for a design procedure: Given a system of order  $n$  described by an arbitrary  $(\mathbf{A}, \mathbf{B})$  and given a desired  $n$ th-order monic characteristic polynomial  $\alpha_c(s)$ , we (1) transform  $(\mathbf{A}, \mathbf{B})$  to control canonical form  $(\mathbf{A}_c, \mathbf{B}_c)$  by changing the state  $\mathbf{x} = \mathbf{Tz}$  and

Ackermann's formula for pole placement

(2) solve for the control gains by inspection using Eq. (7.87) to give the control law  $u = -\mathbf{K}_c \mathbf{z}$ . Because this gain is for the state in the *control* form, we must (3) transform the gain back to the original state to get  $\mathbf{K} = \mathbf{K}_c \mathbf{T}^{-1}$ .

An alternative to this transformation method is given by **Ackermann's formula** (1972), which organizes the three-step process of converting to  $(\mathbf{A}_c, \mathbf{B}_c)$ , solving for the gains, and converting back again into the very compact form

$$\mathbf{K} = [ \begin{array}{cccc} 0 & \cdots & 0 & 1 \end{array} ] \mathcal{C}^{-1} \alpha_c(\mathbf{A}), \quad (7.88)$$

such that

$$\mathcal{C} = [ \mathbf{B} \quad \mathbf{AB} \quad \mathbf{A}^2\mathbf{B} \quad \cdots \quad \mathbf{A}^{n-1}\mathbf{B} ], \quad (7.89)$$

where  $\mathcal{C}$  is the controllability matrix we saw in Section 7.4,  $n$  gives the order of the system and the number of state-variables, and  $\alpha_c(\mathbf{A})$  is a matrix defined as

$$\alpha_c(\mathbf{A}) = \mathbf{A}^n + \alpha_1 \mathbf{A}^{n-1} + \alpha_2 \mathbf{A}^{n-2} + \cdots + \alpha_n \mathbf{I}, \quad (7.90)$$

where the  $\alpha_i$  are the coefficients of the desired characteristic polynomial Eq. (7.86). Note Eq. (7.90) is a matrix equation. Refer to Appendix WD available online at [www.pearsonglobaleditions.com](http://www.pearsonglobaleditions.com) for the derivation of Ackermann's formula.

## EXAMPLE 7.15

### *Ackermann's Formula for Undamped Oscillator*

(a) Use Ackermann's formula to solve for the gains for the undamped oscillator of Example 7.14. (b) Verify the calculations with Matlab for  $\omega_0 = 1$ .

#### Solution

(a) The desired characteristic equation is  $\alpha_c(s) = (s+2\omega_0)^2$ . Therefore, the desired characteristic polynomial coefficients,

$$\alpha_1 = 4\omega_0, \quad \alpha_2 = 4\omega_0^2,$$

are substituted into Eq. (7.90) and the result is

$$\begin{aligned} \alpha_c(\mathbf{A}) &= \begin{bmatrix} -\omega_0^2 & 0 \\ 0 & -\omega_0^2 \end{bmatrix} + 4\omega_0 \begin{bmatrix} 0 & 1 \\ -\omega_0^2 & 0 \end{bmatrix} \\ &\quad + 4\omega_0^2 \begin{bmatrix} 1 & 0 \\ 0 & 1 \end{bmatrix}, \end{aligned} \quad (7.91a)$$

$$= \begin{bmatrix} 3\omega_0^2 & 4\omega_0 \\ -4\omega_0^3 & 3\omega_0^2 \end{bmatrix}. \quad (7.91b)$$

The controllability matrix is

$$\mathcal{C} = [ \mathbf{B} \quad \mathbf{AB} ] = \begin{bmatrix} 0 & 1 \\ 1 & 0 \end{bmatrix},$$

which yields

$$\mathcal{C}^{-1} = \begin{bmatrix} 0 & 1 \\ 1 & 0 \end{bmatrix}. \quad (7.92)$$

Finally, we substitute Eqs. (7.92) and (7.91a) into Eq. (7.88) to get

$$\begin{aligned}\mathbf{K} &= [ K_1 \quad K_2 ] \\ &= [ 0 \quad 1 ] \begin{bmatrix} 0 & 1 \\ 1 & 0 \end{bmatrix} \begin{bmatrix} 3\omega_0^2 & 4\omega_0 \\ -4\omega_0^3 & 3\omega_0^2 \end{bmatrix}.\end{aligned}$$

Therefore

$$\mathbf{K} = [ 3\omega_0^2 \quad 4\omega_0 ],$$

which is the same result we obtained previously.

- (b) The Matlab statements

```
wo = 1;
A = [0 1; -wo*wo 0];
B = [0;1];
pc = [-2*wo;-2*wo];
K = acker(A,B,pc)
```

yield  $\mathbf{K} = [ 3 \quad 4 ]$ , which agrees with the hand calculations above.

#### Matlab Acker, Place

As was mentioned earlier, computation of the controllability matrix has very poor numerical accuracy, and this carries over to Ackermann's formula. Equation (7.88), implemented in Matlab with the function `acker`, can be used for the design of SISO systems with a small ( $\leq 10$ ) number of state-variables. For more complex cases a more reliable formula is available, implemented in Matlab with `place`. A modest limitation on `place` is that, because it is based on assigning closed-loop eigenvectors, none of the desired closed-loop poles may be repeated; that is, the poles must be distinct,<sup>6</sup> a requirement that does not apply to `acker`.

The fact that we can shift the poles of a system by state feedback to any desired location is a rather remarkable result. The development in this section reveals that this shift is possible if we can transform  $(\mathbf{A}, \mathbf{B})$  to the control form  $(\mathbf{A}_c, \mathbf{B}_c)$ , which in turn is possible if the system is controllable. In rare instances, the system may be uncontrollable, in which case no possible control will yield arbitrary pole locations. **Uncontrollable systems** have certain modes, or subsystems, that are unaffected by the control. This usually means that parts of the system are physically disconnected from the input. For example, in modal canonical form for a system with distinct poles, one of the modal state-variables is not connected to the input if there is a zero entry in the  $\mathbf{B}_m$  matrix. A good physical understanding of the system being controlled would prevent any attempt to design a controller for an uncontrollable system. As we saw earlier, there are algebraic tests for controllability; however, no mathematical test can replace the control engineer's understanding of the physical system. Often the physical situation is such that every mode

<sup>6</sup>One may get around this restriction by moving the repeated poles by very small amounts to make them distinct.

An example of weak controllability

is controllable to some degree, and, while the mathematical tests indicate the system is controllable, certain modes are so weakly controllable that designs to control them are virtually useless.

Airplane control is a good example of weak controllability of certain modes. Pitch plane motion  $\mathbf{x}_p$  is primarily affected by the elevator  $\delta_e$  and weakly affected by rolling motion  $\mathbf{x}_r$ . Rolling motion is essentially affected only by the ailerons  $\delta_a$ . The state-space description of these relationships is

$$\begin{bmatrix} \dot{\mathbf{x}}_p \\ \dot{\mathbf{x}}_r \end{bmatrix} = \begin{bmatrix} \mathbf{A}_p & \varepsilon \\ 0 & \mathbf{A}_r \end{bmatrix} \begin{bmatrix} \mathbf{x}_p \\ \mathbf{x}_r \end{bmatrix} + \begin{bmatrix} \mathbf{B}_p & 0 \\ 0 & \mathbf{B}_r \end{bmatrix} \begin{bmatrix} \delta_e \\ \delta_a \end{bmatrix}, \quad (7.93)$$

where the matrix of small numbers  $\varepsilon$  represents the weak coupling from rolling motion to pitching motion. A mathematical test of controllability for this system would conclude that pitch plane motion (and therefore altitude) is controllable by the ailerons as well as by the elevator! However, it is impractical to attempt to control an airplane's altitude by rolling the aircraft with the ailerons.

Another example will illustrate some of the properties of pole placement by state feedback and the effects of loss of controllability on the process.

## EXAMPLE 7.16

### *How Zero Location Can Affect the Control Law*

A specific thermal system is described by Eq. (7.32a) in observer canonical form with a zero at  $s = z_0$ . (a) Find the state feedback gains necessary for placing the poles of this system at the roots of  $s^2 + 2\xi\omega_n s + \omega_n^2$  (that is, at  $-\xi\omega_n \pm j\omega_n\sqrt{1 - \xi^2}$ ). (b) Repeat the computation with Matlab, using the parameter values  $z_0 = 2$ ,  $\xi = 0.5$ , and  $\omega_n = 2$  rad/sec.

#### Solution

(a) The state description matrices are

$$\mathbf{A}_o = \begin{bmatrix} -7 & 1 \\ -12 & 0 \end{bmatrix}, \quad \mathbf{B}_o = \begin{bmatrix} 1 \\ -z_0 \end{bmatrix},$$

$$\mathbf{C}_o = [ \quad 1 \quad 0 ], \quad D_o = 0.$$

First, we substitute these matrices into Eq. (7.69) to get the closed-loop characteristic equation in terms of the unknown gains and the zero position:

$$s^2 + (7 + K_1 - z_0 K_2)s + 12 - K_2(7z_0 + 12) - K_1 z_0 = 0.$$

Next, we equate the coefficients of this equation to the coefficients of the desired characteristic equation to get

$$K_1 - z_0 K_2 = 2\xi\omega_n - 7,$$

$$-z_0 K_1 - (7z_0 + 12) K_2 = \omega_n^2 - 12.$$

The solutions to these equations are

$$K_1 = \frac{z_0(14\zeta\omega_n - 37 - \omega_n^2) + 12(2\zeta\omega_n - 7)}{(z_0 + 3)(z_0 + 4)},$$

$$K_2 = \frac{z_0(7 - 2\zeta\omega_n) + 12 - \omega_n^2}{(z_0 + 3)(z_0 + 4)}.$$

(b) The following Matlab statements can be used to find the solution:

```
Ao = [-7 1;-12 0];
zo = 2;
Bo = [1;-zo];
pc = roots([1 2 4]);
K = place(Ao,Bo,pc)
```

These statements yield  $K = [-3.80 \ 0.60]$ , which agrees with the hand calculations. If the zero were close to one of the open-loop poles, say  $z_0 = -2.99$ , then we find  $K = [2052.5 \ -688.1]$ .

Two important observations should be made from this example. The first is that the gains grow as the zero  $z_0$  approaches either  $-3$  or  $-4$ , the values where this system loses controllability. In other words, as controllability is almost lost, the control gains become very large.

The system has to work harder and harder to achieve control as controllability slips away.

Apart from controllability, any actuator has limited dynamic range and saturation limits. Therefore, even though for a system that is controllable, the poles can be placed in arbitrary locations, some locations may be quite undesirable as they would drive the actuators into saturation.

The second important observation illustrated by the example is that both  $K_1$  and  $K_2$  grow as the desired closed-loop bandwidth given by  $\omega_n$  is increased. From this, we can conclude that

To move the poles a long way requires large gains.

These observations lead us to a discussion of how we might go about selecting desired pole locations in general. Before we begin that topic, we will complete the design with full-state feedback by showing how the reference input might be applied to such a system and what the resulting response characteristics are.

## 7.5.2 Introducing the Reference Input with Full-State Feedback

Thus far, the control has been given by Eq. (7.67), or  $u = -\mathbf{K}\mathbf{x}$ . In order to study the transient response of the pole-placement designs to input commands, it is necessary to introduce the reference input into the system. An obvious way to do this is to change the control to  $u = -\mathbf{K}\mathbf{x} + r$ . However, the system will now almost surely have a nonzero steady-state error to a step input. The way to correct this problem is to compute the steady-state values of the state and the control input that will result in zero output error and then force them to take these values. If the desired final values of the state and the control input are  $\mathbf{x}_{ss}$  and  $u_{ss}$  respectively, then the new control formula should be

$$u = u_{ss} - \mathbf{K}(\mathbf{x} - \mathbf{x}_{ss}), \quad (7.94)$$

so that when  $\mathbf{x} = \mathbf{x}_{ss}$  (no error),  $u = u_{ss}$ . To pick the correct final values, we must solve the equations so that the system will have zero steady-state error to *any* constant input. The system differential equations are the standard ones:

$$\dot{\mathbf{x}} = \mathbf{Ax} + \mathbf{Bu}, \quad (7.95a)$$

$$y = \mathbf{Cx} + \mathbf{Du}. \quad (7.95b)$$

In the constant steady-state, Eqs. (7.95a) and (7.95b) reduce to the pair

$$\mathbf{0} = \mathbf{Ax}_{ss} + \mathbf{Bu}_{ss}, \quad (7.96a)$$

$$y_{ss} = \mathbf{Cx}_{ss} + \mathbf{Du}_{ss}. \quad (7.96b)$$

**Gain calculation for reference input**

We want to solve for the values for which  $y_{ss} = r_{ss}$  for any value of  $r_{ss}$ . To do this, we make  $\mathbf{x}_{ss} = \mathbf{Nx}r_{ss}$  and  $u_{ss} = N_ur_{ss}$ . With these substitutions, we can write Eqs. (7.96) as a matrix equation; the common factor of  $r_{ss}$  cancels out to give the equation for the gains:

$$\begin{bmatrix} \mathbf{A} & \mathbf{B} \\ \mathbf{C} & \mathbf{D} \end{bmatrix} \begin{bmatrix} \mathbf{N}_x \\ N_u \end{bmatrix} = \begin{bmatrix} \mathbf{0} \\ 1 \end{bmatrix}. \quad (7.97)$$

This equation can be solved for  $\mathbf{N}_x$  and  $N_u$  to get

$$\begin{bmatrix} \mathbf{N}_x \\ N_u \end{bmatrix} = \begin{bmatrix} \mathbf{A} & \mathbf{B} \\ \mathbf{C} & \mathbf{D} \end{bmatrix}^{-1} \begin{bmatrix} \mathbf{0} \\ 1 \end{bmatrix}.$$

**Control equation with reference input**

With these values, we finally have the basis for introducing the reference input so as to get zero steady-state error to a step input:

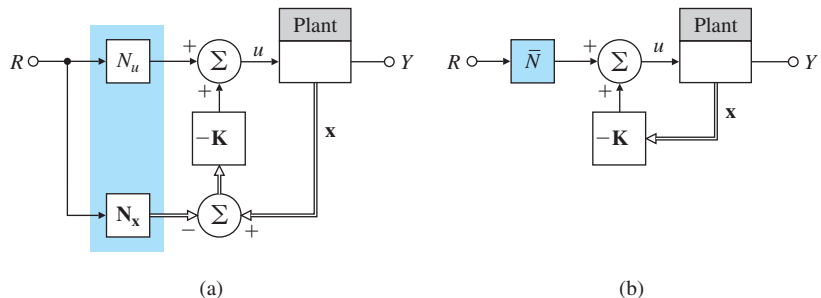
$$u = N_u r - \mathbf{K}(\mathbf{x} - \mathbf{N}_x r) \quad (7.98a)$$

$$= -\mathbf{K}\mathbf{x} + (N_u + \mathbf{K}\mathbf{N}_x)r. \quad (7.98b)$$

The coefficient of  $r$  in parentheses is a constant that can be computed beforehand. We give it the symbol  $\bar{N}$ , so

**Figure 7.15**

Block diagram for introducing the reference input with full-state feedback:  
(a) with state and control gains; (b) with a single composite gain



$$u = -\mathbf{K}\mathbf{x} + \bar{N}r. \quad (7.99)$$

The block diagram of the system is shown in Fig. 7.15.

### EXAMPLE 7.17

#### *Introducing the Reference Input*

Compute the necessary gains for zero steady-state error to a step command at  $x_1$ , and plot the resulting unit step response for the oscillator in Example 7.14 with  $\omega_0 = 1$ .

**Solution.** We substitute the matrices of Eq. (7.71) (with  $\omega_0 = 1$  and  $\mathbf{C} = [1 \ 0]$  because  $y = x_1$ ) into Eq. (7.97) to get

$$\begin{bmatrix} 0 & 1 & 0 \\ -1 & 0 & 1 \\ 1 & 0 & 0 \end{bmatrix} \begin{bmatrix} \mathbf{N}_x \\ \mathbf{N}_u \end{bmatrix} = \begin{bmatrix} 0 \\ 0 \\ 1 \end{bmatrix}. \quad (7.100)$$

The solution is  $\mathbf{x} = \mathbf{a} \setminus \mathbf{b}$  in Matlab (where  $\mathbf{a}$  and  $\mathbf{b}$  are the left- and right-hand side matrices, respectively),

$$\mathbf{N}_x = \begin{bmatrix} 1 \\ 0 \end{bmatrix},$$

$$N_u = 1,$$

and, for the given control law,  $\mathbf{K} = [3\omega_0^2 \ 4\omega_0] = [3 \ 4]$ ,

$$\bar{N} = N_u + \mathbf{K}\mathbf{N}_x = 4. \quad (7.101)$$

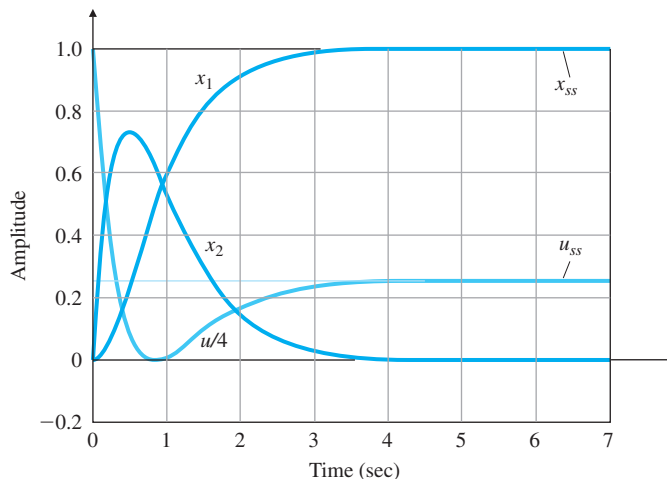
The corresponding step response (using the Matlab step command) is plotted in Fig. 7.16.

---

Note there are two equations for the control—Eqs. (7.98b) and (7.99). While these expressions are equivalent in theory, they differ in practical implementation in that Eq. (7.98b) is usually more robust to parameter errors than Eq. (7.99), particularly when the plant includes a pole at the origin and Type 1 behavior is possible. The difference is most clearly illustrated by the next example.

**Figure 7.16**

Step response of oscillator to a reference input

**EXAMPLE 7.18***Reference Input to a Type 1 System: DC Motor*

DC Motor

Compute the input gains necessary to introduce a reference input with zero steady-state error to a step for the DC motor of Example 5.1, which in state-variable form is described by the matrices:

$$\mathbf{A} = \begin{bmatrix} 0 & 1 \\ 0 & -1 \end{bmatrix}, \quad \mathbf{B} = \begin{bmatrix} 0 \\ 1 \end{bmatrix},$$

$$\mathbf{C} = [1 \quad 0], \quad D = 0.$$

Assume the state feedback gain is  $[K_1 \quad K_2]$ .

**Solution.** If we substitute the system matrices of this example into the equation for the input gains, Eq. (7.97), we find that the solution is

$$\mathbf{N}_x = \begin{bmatrix} 1 \\ 0 \end{bmatrix},$$

$$N_u = 0,$$

$$\bar{N} = K_1.$$

With these values, the expression for the control using  $\mathbf{N}_x$  and  $N_u$  [Eq. (7.98b)] reduces to

$$u = -K_1(x_1 - r) - K_2x_2,$$

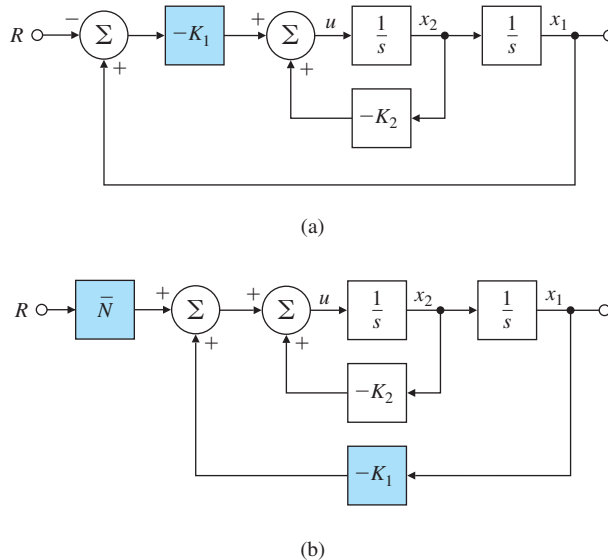
while the one using  $\bar{N}$  [Eq. (7.99)] becomes

$$u = -K_1x_1 - K_2x_2 + K_1r.$$

The block diagrams for the systems using each of the control equations are given in Fig. 7.17. When using Eq. (7.99), as shown in Fig. 7.17(b), it is necessary to multiply the input by a gain  $K_1 (= \bar{N})$  exactly equal to that used in the feedback. If these two gains do not match exactly, there

**Figure 7.17**

Alternative structures for introducing the reference input: (a) Eq. (7.98b); (b) Eq. (7.99)



will be a steady-state error. On the other hand, if we use Eq. (7.98b), as shown in Fig. 7.17(a), there is only one gain to be used on the difference between the reference input and the first state, and zero steady-state error will result even if this gain is slightly in error. The system of Fig. 7.17(a) is more robust than the system of Fig. 7.17(b).

With the reference input in place, the closed-loop system has input  $r$  and output  $y$ . From the state description, we know the system poles are at the eigenvalues of the closed-loop system matrix,  $\mathbf{A} - \mathbf{BK}$ . In order to compute the closed-loop transient response, it is necessary to know where the closed-loop zeros of the transfer function from  $r$  to  $y$  are. They are to be found by applying Eq. (7.64) to the closed-loop description, which we assume has no direct path from input  $u$  to output  $y$ , so  $D = 0$ . The zeros are values of  $s$  such that

$$\det \begin{bmatrix} s\mathbf{I} - (\mathbf{A} - \mathbf{BK}) & -\bar{N}\mathbf{B} \\ \mathbf{C} & 0 \end{bmatrix} = 0. \quad (7.102)$$

We can use two elementary facts about determinants to simplify Eq. (7.102). In the first place, if we divide the last column by  $\bar{N}$ , which is a scalar, then the point where the determinant is zero remains unchanged. The determinant is also not changed if we multiply the last column by  $\mathbf{K}$  and add it to the first (block) column, with the result that the  $\mathbf{BK}$  term is cancelled out. Thus, the matrix equation for the zeros reduces to

$$\det \begin{bmatrix} s\mathbf{I} - \mathbf{A} & -\mathbf{B} \\ \mathbf{C} & 0 \end{bmatrix} = 0. \quad (7.103)$$

Equation (7.103) is the same as Eq. (7.64) for the zeros of the plant *before* the feedback was applied. The important conclusion is that

When full-state feedback is used as in Eq. (7.98b) or (7.99), the zeros remain unchanged by the feedback.

## 7.6 Selection of Pole Locations for Good Design

The first step in the pole-placement design approach is to decide on the closed-loop pole locations. When selecting pole locations, it is always useful to keep in mind that the required control effort is related to how far the open-loop poles are moved by the feedback. Furthermore, when a zero is near a pole, the system may be nearly uncontrollable and, as we saw in Section 7.5, moving such poles requires large control gains and thus a large control effort; however, the designer is able to temper the choices to take control effort into account. Therefore, a pole-placement philosophy that aims to fix only the undesirable aspects of the open-loop response and avoids either large increases in bandwidth or efforts to move poles that are near zeros will typically allow smaller gains, and thus smaller control actuators, than a philosophy that arbitrarily picks all the poles without regard to the original open-loop pole and zero locations.

[Two methods of pole selection](#)

In this section, we discuss two techniques to aid in the pole-selection process. The first approach—dominant second-order poles—deals with pole selection without explicit regard for their effect on control effort; however, the designer is able to temper the choices to take control effort into account. The second method (called optimal control, or symmetric root locus) does specifically address the issue of achieving a balance between good system response and control effort.

### 7.6.1 Dominant Second-Order Poles

The step response corresponding to the second-order transfer function with complex poles at radius  $\omega_n$  and damping ratio  $\zeta$  was discussed in Chapter 3. The rise time, overshoot, and settling time can be deduced directly from the pole locations. We can choose the closed-loop poles for a higher-order system as a desired pair of dominant second-order poles, and select the rest of the poles to have real parts corresponding to sufficiently damped modes, so the system will mimic a second-order response with reasonable control effort. We also must make sure that the zeros are far enough into the LHP to avoid having any appreciable effect on the second-order behavior. A system with several lightly damped high-frequency vibration modes plus two rigid-body low-frequency modes lends itself to this philosophy. Here we can pick the low-frequency modes to achieve desired values of  $\omega_n$  and  $\zeta$  and select the rest of the poles to increase the damping of the high-frequency modes, while holding their frequency constant in order to minimize control effort. To illustrate this design method, we obviously need a system

of higher than second-order; we will use the drone system described in Example 5.12.

### EXAMPLE 7.19

#### *Pole Placement as a Dominant Second-Order System*

Design the feedback control for the drone system (see Example 5.12)

$$G(s) = \frac{1}{s^2(s+2)}$$

by the dominant second-order poles method to have a rise time of 1 sec or less and an overshoot of less than 5%.

**Solution.** We use the Matlab command `ssdata(G)` to find a state space realization for  $G(s)$

$$\mathbf{A} = \begin{bmatrix} -2 & 0 & 0 \\ 1 & 0 & 0 \\ 0 & 1 & 0 \end{bmatrix}, \quad \mathbf{B} = \begin{bmatrix} 1 \\ 0 \\ 0 \end{bmatrix}$$

$$\mathbf{C} = [0 \ 0 \ 1], \quad \mathbf{D} = 0.$$

From the plots of the second-order transients in Fig. 3.19, a damping ratio  $\zeta = 0.7$  will meet the overshoot requirement. We choose a natural frequency of 4 rad/sec and the two dominant poles located at  $-2 \pm j2$ . There are three poles in all, so the other pole needs to be placed far to the left of the dominant pair; for our purposes, “far” means the transients due to the fast pole should be over (significantly faster) well before the transients due to the dominant poles, and we assume a factor of higher than 4 in the respective undamped natural frequencies to be adequate. From these considerations, the desired poles are given by

$$\text{pc} = [-2 + 2*j; -2 - 2*j; -12] \quad (7.104)$$

With these desired poles, we can use the function `acker`, to find the control gains

$$\mathbf{K} = [14 \ 56 \ 96]. \quad (7.105)$$

**Matlab acker**

These are found with the following Matlab statements:

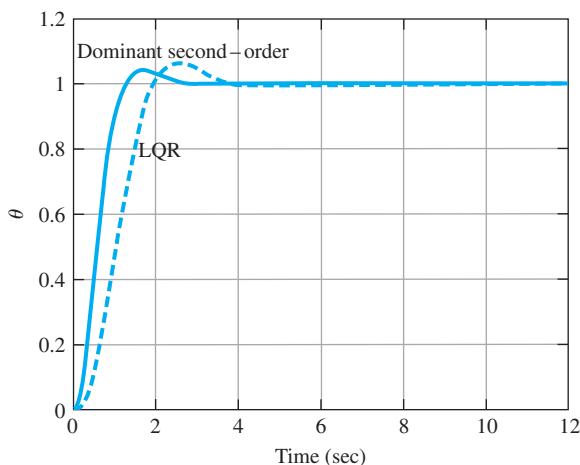
```
A = [-2 0 0; 1 0 0; 0 1 0];
B = [1; 0; 0];
pc = [-2+2*j; -2-2*j; -12];
K= acker(A,B,pc)
```

The step response and the corresponding plots for this and another design (to be discussed in Section 7.6.2) are given in Fig. 7.18 and Fig. 7.19. Notice the rise time is approximately 0.8 sec, and the overshoot is about 4%, as specified.

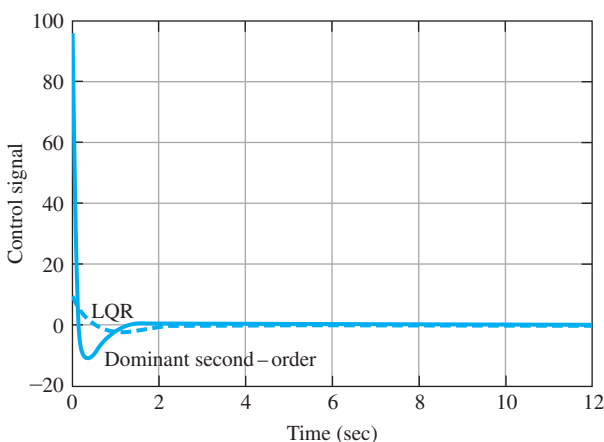
Because the design process is iterative, the poles we selected should be seen as only a first step, to be followed by further modifications to meet the specifications as accurately as necessary. For this example, we happened to select adequate pole locations on the first try.

**Figure 7.18**

Step responses of drone designs

**Figure 7.19**

Control efforts for drone designs



## 7.6.2 Symmetric Root Locus (SRL)

LQR design

A most effective and widely used technique of linear control systems design is the optimal **linear quadratic regulator (LQR)**. The simplified version of the LQR problem is to find the control such that the performance index

$$\mathcal{J} = \int_0^{\infty} [\rho z^2(t) + u^2(t)] dt \quad (7.106)$$

is minimized for the system

$$\dot{\mathbf{x}} = \mathbf{A}\mathbf{x} + \mathbf{B}u, \quad (7.107a)$$

$$z = \mathbf{C}_1\mathbf{x}, \quad (7.107b)$$

where  $\rho$  in Eq. (7.106) is a weighting factor of the designer's choice. A remarkable fact is that the control law that minimizes  $\mathcal{J}$  is given by linear-state feedback

$$u = -\mathbf{K}\mathbf{x}. \quad (7.108)$$

### Symmetric root locus

Here the optimal value of  $\mathbf{K}$  is that which places the closed-loop poles at the stable roots (those in the LHP) of the symmetric root-locus (SRL) equation (Kailath, 1980)

$$1 + \rho G_0(-s)G_0(s) = 0, \quad (7.109)$$

where  $G_0$  is the open-loop transfer function from  $u$  to  $z$ :

$$G_0(s) = \frac{Z(s)}{U(s)} = \mathbf{C}_1(s\mathbf{I} - \mathbf{A})^{-1}\mathbf{B} = \frac{N(s)}{D(s)}. \quad (7.110)$$

Note that this is a root-locus problem as discussed in Chapter 5 with respect to the parameter  $\rho$ , which weighs the relative cost of (tracking error)  $z^2$  with respect to the control effort  $u^2$  in the performance index equation (7.106). Note also that  $s$  and  $-s$  affect Eq. (7.109) in an identical manner; therefore, for any root  $s_0$  of Eq. (7.109), there will also be a root at  $-s_0$ . We call the resulting root locus a **SRL**, since the locus in the LHP will have a mirror image in the right half-plane (RHP); that is, they are symmetric with respect to the imaginary axis. We may thus choose the optimal closed-loop poles by first selecting the matrix  $\mathbf{C}_1$ , which defines the tracking error and which the designer wishes to keep small, then choosing  $\rho$ , which balances the importance of this tracking error against the control effort. Notice the output we select as tracking error does *not* need to be the plant sensor output. That is why we call the output in Eq. (7.107)  $z$  rather than  $y$ .

Selecting a set of stable poles from the solution of Eq. (7.109) results in desired closed-loop poles, which we can then use in a pole-placement calculation such as Ackermann's formula [Eq. (7.88)] to obtain  $\mathbf{K}$ . As with all root loci for real transfer functions  $G_0$ , the locus is also symmetric with respect to the real axis; thus there is symmetry with respect to both the real and imaginary axes. We can write the SRL equation in the standard root-locus form

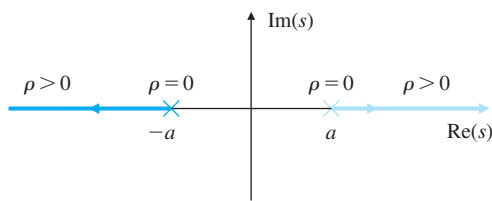
$$1 + \rho \frac{N(-s)N(s)}{D(-s)D(s)} = 0, \quad (7.111)$$

### SRL equation

obtain the locus poles and zeros by reflecting the open-loop poles and zeros of the transfer function from  $U$  to  $Z$  across the imaginary axis (which doubles the number of poles and zeros), then sketch the locus. Note the locus could be either a  $0^\circ$  or  $180^\circ$  locus, depending on the sign of  $G_0(-s)G_0(s)$  in Eq. (7.109). A quick way to determine which type of locus to use ( $0^\circ$  or  $180^\circ$ ) is to pick the one that *has no part on the imaginary axis*. The real-axis rule of root locus plotting will reveal this right away. For the controllability assumptions we have made here, plus the assumption that all the system modes are present in the chosen output  $z$ , the optimal closed-loop system is guaranteed to be stable; thus no part of the locus can be on the imaginary axis.

**Figure 7.20**

SRL for a first-order system

**EXAMPLE 7.20***SRL for Servo Speed Control*

Plot the SRL for the following servo speed control system with  $z = y$ :

$$\dot{y} = -ay + u, \quad (7.112a)$$

$$G_0(s) = \frac{1}{s + a}. \quad (7.112b)$$

**Solution.** The SRL equation [see Eq. (7.109)] for this example is

$$1 + \rho \frac{1}{(-s + a)(s + a)} = 0. \quad (7.113)$$

The SRL, shown in Fig. 7.20, is a  $0^\circ$  locus. The optimal (stable) pole can be determined explicitly in this case as

$$s = -\sqrt{a^2 + \rho}. \quad (7.114)$$

Thus, the closed-loop root location that minimizes the performance index of Eq. (7.106) lies on the real axis at the distance given by Eq. (7.114) and is always to the left of the open-loop root.

**EXAMPLE 7.21***SRL Design for Satellite Attitude Control*

Draw the SRL for the satellite system with  $z = y$ .

**Solution.** The equations of motion are

$$\dot{\mathbf{x}} = \begin{bmatrix} 0 & 1 \\ 0 & 0 \end{bmatrix} \mathbf{x} + \begin{bmatrix} 0 \\ 1 \end{bmatrix} u, \quad (7.115)$$

$$y = [1 \ 0] \mathbf{x}. \quad (7.116)$$

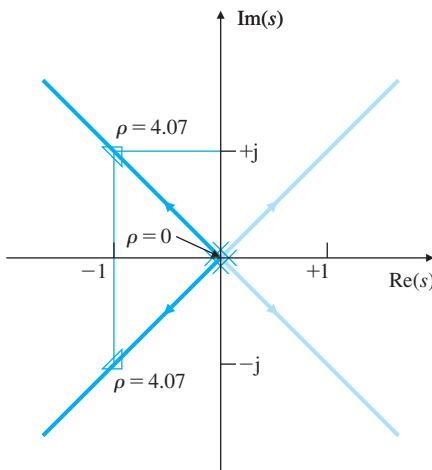
We then calculate from Eqs. (7.115) and (7.116) so

$$G_0(s) = \frac{1}{s^2}. \quad (7.117)$$

The symmetric  $180^\circ$  loci are shown in Fig. 7.21. The Matlab statements to generate the SRL are

```
s=tf('s');
sysGG=1/s^4;
rlocus(sysGG);
```

**Figure 7.21**  
SRL for the satellite



It is interesting to note the (stable) closed-loop poles have damping of  $\zeta = 0.707$ . We would choose two stable roots for a given value of  $\rho$ , for example,  $s = -1 \pm j1$  for  $\rho = 4.07$ , on the SRL and use them for pole-placement and control-law design.

Choosing different values of  $\rho$  can provide us with pole locations that achieve varying balances between a fast response (small values of  $\int z^2 dt$ ) and a low control effort (small values of  $\int u^2 dt$ ). Figure 7.22 shows the design trade-off curve for the satellite (double-integrator) plant [see Eq. (7.15)] for various values of  $\rho$  ranging from 0.01 to 100. The curve has two asymptotes (dashed lines) corresponding to low (large  $\rho$ ) and high (small  $\rho$ ) penalty on the control usage. In practice, usually a value of  $\rho$  corresponding to a point close to the knee

**Figure 7.22**  
Design trade-off curve  
for satellite plant

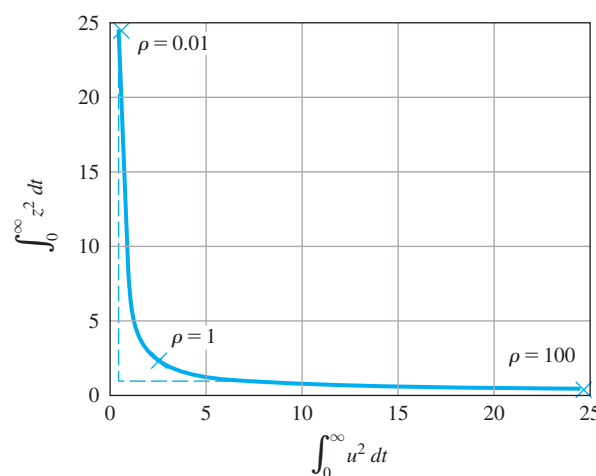
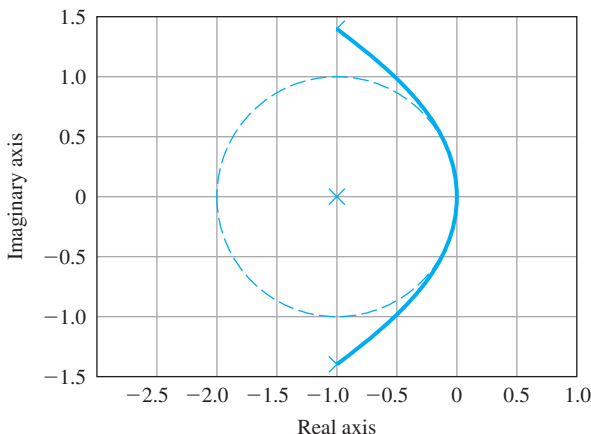


**Figure 7.23**

Nyquist plot for LQR design



of the trade-off curve is chosen. This is because it provides a reasonable compromise between the use of control and the speed of response. For the satellite plant, the value of  $\rho = 1$  corresponds to the knee of the curve. In this case, the closed-loop poles have a damping ratio of  $\zeta = 0.707$ ! Figure 7.23 shows the associated Nyquist plot, which has a phase margin  $PM = 65^\circ$  and infinite gain margin. These excellent stability properties are a general feature of LQR designs. However, recall that this method assumes all the state variables are available (measured) for feedback, which is not the case in general. The state variables that are not measured may be estimated as shown in the next section, but the excellent LQR stability properties may not be attainable.

It is also possible to locate optimal pole locations for the design of an open-loop unstable system using the SRL and LQR method.

## EXAMPLE 7.22

### SRL Design for an Inverted Pendulum

Draw the SRL for the linearized equations of the simple inverted pendulum with  $\omega_o = 1$ . Take the output,  $z$ , to be the sum of twice the position plus the velocity (so as to weight or penalize *both* position and velocity).

**Solution.** The equations of motion are

$$\dot{\mathbf{x}} = \begin{bmatrix} 0 & 1 \\ \omega_0^2 & 0 \end{bmatrix} \mathbf{x} + \begin{bmatrix} 0 \\ -1 \end{bmatrix} u. \quad (7.118)$$

For the specified output of  $2 \times$  position + velocity, we compute the output by

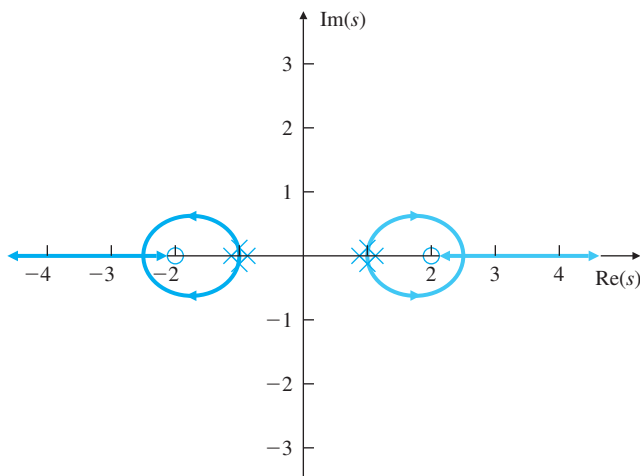
$$z = [2 \ 1] \mathbf{x}. \quad (7.119)$$

We then calculate from Eqs. (7.118) and (7.119) so

$$G_0(s) = -\frac{s+2}{s^2 - \omega_0^2}. \quad (7.120)$$

The symmetric  $0^\circ$  loci are shown in Fig. 7.24. The Matlab statements to generate the SRL are (for  $\omega_o = 1$ ),

**Figure 7.24**  
SRL for the inverted pendulum



```
s=tf('s');
G=-(s+2)/(s^2-1);
G1=-(-s+2)/(s^2-1);
sysGG=G*G1;
rlocus(sysGG);
```

For  $\rho = 1$ , we find that the closed-loop poles are at  $-1.36 \pm j0.606$ , corresponding to  $\mathbf{K} = [ -2.23 \quad -2.73 ]$ . If we substitute the system matrices of this example into the equation for the input gains, Eq. (7.97), we find that the solution is

$$\mathbf{N}_x = \begin{bmatrix} 1 \\ 0 \end{bmatrix}, \\ N_u = 1, \\ \bar{N} = -1.23.$$

With these values, the expression for the control using  $\mathbf{N}_x$  and  $N_u$  [Eq. (7.98b)] the controller reduces to

$$u = -\mathbf{K}\mathbf{x} + \bar{N}r.$$

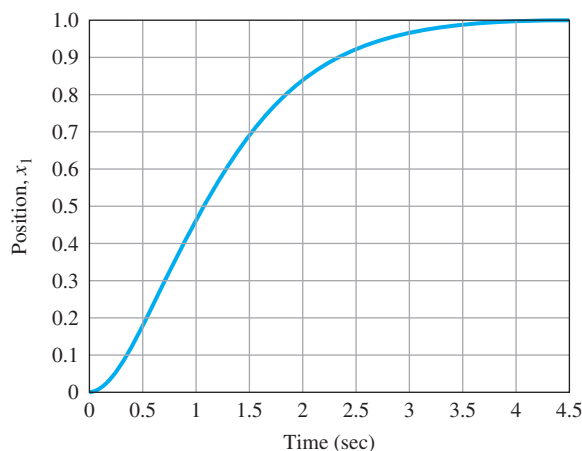
The corresponding step response for position is shown in Fig. 7.25.

As a final example in this section, we consider again the drone system and introduce LQR design using the computer directly to solve for the optimal control law. From Eqs. (7.106) and (7.108), we know that the information needed to find the optimal control is given by the system matrices  $\mathbf{A}$  and  $\mathbf{B}$  and the output matrix  $\mathbf{C}_1$ . Most computer-aided software packages, including Matlab, use a more general form of Eq. (7.106):

$$\mathcal{J} = \int_0^\infty (\mathbf{x}^T \mathbf{Q} \mathbf{x} + \mathbf{u}^T \mathbf{R} \mathbf{u}) dt. \quad (7.121)$$

**Figure 7.25**

Step response for the inverted pendulum



[Matlab lqr](#)

[Bryson's rule](#)

Equation (7.121) reduces to the simpler form of Eq. (7.106) if we take  $\mathbf{Q} = \rho \mathbf{C}_1^T \mathbf{C}_1$  and  $\mathbf{R} = 1$ . The direct solution for the optimal control gain is the Matlab statement

$$\mathbf{K} = \text{lqr}(\mathbf{A}, \mathbf{B}, \mathbf{Q}, \mathbf{R}). \quad (7.122)$$

One reasonable method to start the LQR design iteration is suggested by Bryson's rule (Bryson and Ho, 1969). In practice, an appropriate choice to obtain acceptable values of  $\mathbf{x}$  and  $\mathbf{u}$  is to initially choose diagonal matrices  $\mathbf{Q}$  and  $\mathbf{R}$  such that

$$Q_{ii} = 1/\text{maximum acceptable value of } [x_i^2],$$

$$R_{ii} = 1/\text{maximum acceptable value of } [u_i^2].$$

The weighting matrices are then modified during subsequent iterations to achieve an acceptable trade-off between performance and control effort.

## EXAMPLE 7.23

### LQR Design for a Drone

- (a) Find the optimal control for the drone Example 7.19, using  $\theta$  as the output for the performance index. Let  $\rho = 100$ . Compare the results with that of dominant second-order obtained before.
- (b) Compare the LQR designs for  $\rho = 1, 10, 100$ .

### Solution

- (a) All we need to do here is to substitute the matrices into Eq.(7.122), form the feedback system, and plot the response. The performance index matrix is the scalar  $\mathbf{R} = 1$ ; the most difficult part of the problem is finding the state-cost matrix  $\mathbf{Q}$ . With the output-cost variable  $z = \theta$ , the output matrix from Example 7.19 is

$$\mathbf{C} = [0 \ 0 \ 1],$$

and with  $\rho = 1$ , the required matrix is

$$\begin{aligned}\mathbf{Q} &= \mathbf{C}^T \mathbf{C} \\ &= \begin{bmatrix} 0 & 0 & 0 \\ 0 & 0 & 0 \\ 0 & 0 & 1 \end{bmatrix}.\end{aligned}$$

The gain is given by Matlab, using the following statements:

```
A=[-2 0 0; 1 0 0; 0 1 0];
B=[1; 0; 0];
C=[0 0 1];
R=1;
rho=100;
Q=rho*C'*C;
K=lqr(A,B,Q,R)
```

The Matlab computed gain is

$$\mathbf{K} = [ 2.8728 \quad 9.8720 \quad 10.0000 ]. \quad (7.123)$$

The results of the step responses and the corresponding control efforts are plotted in Fig. 7.18 and Fig. 7.19 (using step) with the earlier responses for comparison. Obviously, there is a vast range of choice for the elements of  $\mathbf{Q}$  and  $\mathbf{R}$ , so substantial experience is needed in order to use the LQR method effectively.

- (b) The LQR designs may be repeated as in part (a) with the same  $\mathbf{Q}$  and  $\mathbf{R}$ , but with  $\rho = 1, 10, 100$ . Figure 7.26 shows a comparison of  $\theta$  step and the corresponding control efforts for the three designs. As seen from the results, the smaller values of  $\rho$  correspond to higher cost on the control and slower response, whereas the larger values of  $\rho$  correspond to lower cost on the control and relatively fast response.
- 

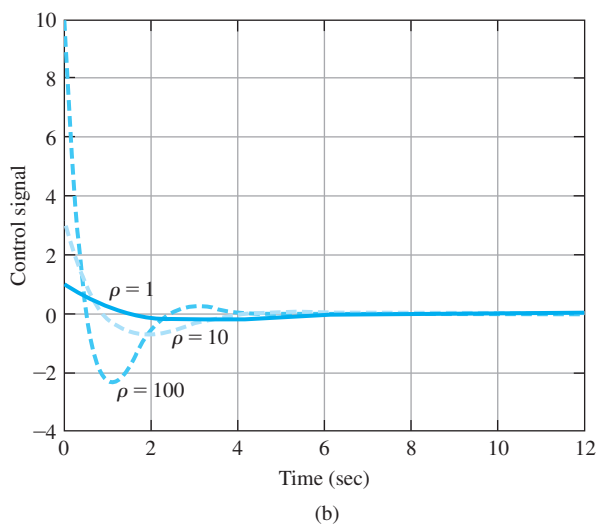
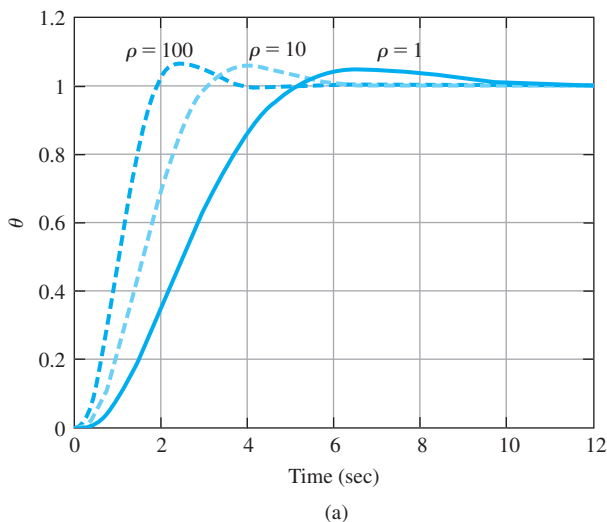
### *Limiting Behavior of LQR Regulator Poles*

It is interesting to consider the limiting behavior of the optimal closed-loop poles as a function of the root-locus parameter (that is,  $\rho$ ) although, in practice, neither case would be used.

“Expensive control” case ( $\rho \rightarrow 0$ ): Equation (7.106) primarily penalizes the use of control energy. If the control is expensive, the optimal control does not move any of the open-loop poles except for those that are in the RHP. The poles in the RHP are simply moved to their mirror images in the LHP. The optimal control does this to stabilize the system using minimum control effort, and makes no attempt to move any of the poles of the system that are already in the LHP. The closed-loop pole locations are simply the starting points on the SRL in the

**Figure 7.26**

- (a) Step responses of drone for LQR designs  
 (b) Control efforts for drone designs



LHP. The optimal control does not speed up the response of the system in this case. For the satellite plant, the vertical dashed line in Fig. 7.22 corresponds to the “expensive control” case and illustrates that the very low control usage results in a very large error in  $z$ .

*“Cheap control” case ( $\rho \rightarrow \infty$ ):* In this case, control energy is no object and arbitrary control effort may be used by the optimal control law. The control law then moves some of the closed-loop pole locations right on top of the zeros in the LHP. The rest are moved to infinity along the SRL asymptotes. If the system is nonminimum phase, some of the closed-loop poles are moved to mirror images of these zeros in

the LHP, as shown in Example 7.22. The rest of the poles go to infinity and do so along a Butterworth filter pole pattern, as shown in Example 7.21. The optimal control law provides the fastest possible response time consistent with the LQR cost function. The feedback gain matrix  $\mathbf{K}$  becomes unbounded in this case. For the double-integrator plant, the horizontal dashed line in Fig. 7.22 corresponds to the “cheap control” case.

### *Robustness Properties of LQR Regulators*

It has been proven (Anderson and Moore, 1990) that the Nyquist plot for LQR design avoids a circle of unity radius centered at the  $-1$  point as shown in Fig. 7.23. This leads to extraordinary phase and gain margin properties. It can be shown (see Problem 7.33) that the return difference must satisfy

$$|1 + \mathbf{K}(j\omega \mathbf{I} - \mathbf{A})^{-1} \mathbf{B}| \geq 1. \quad (7.124)$$

Let us rewrite the loop gain as the sum of its real and imaginary parts:

$$L(j\omega) = \mathbf{K}(j\omega \mathbf{I} - \mathbf{A})^{-1} \mathbf{B} = \text{Re}(L(j\omega)) + j\text{Im}(L(j\omega)). \quad (7.125)$$

Equation (7.124) implies that

$$([\text{Re}(L(j\omega))] + 1)^2 + [\text{Im}(L(j\omega))]^2 \geq 1, \quad (7.126)$$

which means the Nyquist plot must indeed avoid a circle centered at  $-1$  with unit radius. This implies that  $\frac{1}{2} < \text{GM} < \infty$ , which means that the “upward” gain margin is  $\text{GM} = \infty$  and the “downward” gain margin is  $\text{GM} = \frac{1}{2}$  (see also Problem 6.24 of Chapter 6). Hence, the LQR gain matrix,  $\mathbf{K}$ , can be multiplied by a large scalar or reduced by half with guaranteed closed-loop system stability. The phase margin,  $\text{PM}$ , is at least  $\pm 60^\circ$ . These margins are remarkable, and it is not realistic to assume they can be achieved in practice, because of the presence of modeling errors and lack of sensors!

LQR gain and phase margins

### **7.6.3 Comments on the Methods**

The two methods of pole selection described in Sections 7.6.1 and 7.6.2 are alternatives the designer can use for an initial design by pole placement. Note the first method (dominant second-order) suggests selecting closed-loop poles without regard to the effect on the control effort required to achieve that response. In some cases, therefore, the resulting control effort may be unrealistically high. The second method (SRL), on the other hand, selects poles that result in some balance between system errors and control effort. The designer can easily examine the relationship between shifts in that balance (by changing  $\rho$ ) and system root locations, time response, and feedback gains. Whatever initial pole-selection method we use, some modification is almost always necessary to achieve the desired balance of bandwidth, overshoot, sensitivity, control effort, and other practical design requirements. Further insight

into pole selection will be gained from the examples that illustrate compensation in Section 7.8, and from the case studies in Chapter 10.

## 7.7 Estimator Design

The control law designed in Section 7.5 assumed all the state-variables are available for feedback. In most cases, not all the state-variables are measured. The cost of the required sensors may be prohibitive, or it may be physically impossible to measure all of the state-variables, as in, for example, a nuclear power plant. In this section, we demonstrate how to reconstruct all of the state-variables of a system from a few measurements. If the estimate of the state is denoted by  $\hat{x}$ , it would be convenient whether we could replace the true state in the control law given by Eq. (7.99) with the estimates, so the control becomes  $u = -K\hat{x} + \bar{N}r$ . This is indeed possible, as we shall see in Section 7.8, so construction of a state estimate is a key part of state-space control design.

### 7.7.1 Full-Order Estimators

One method of estimating the state is to construct a full-order model of the plant dynamics,

$$\dot{\hat{x}} = A\hat{x} + Bu, \quad (7.127)$$

where  $\hat{x}$  is the estimate of the actual state  $x$ . We know  $A$ ,  $B$ , and  $u(t)$ . Hence this estimator will be satisfactory if we can obtain the correct initial condition  $x(0)$  and set  $\hat{x}(0)$  equal to it. Figure 7.27 depicts this open-loop estimator. However, it is precisely the lack of information about  $x(0)$  that requires the construction of an estimator. Otherwise, the estimated state would track the true state exactly. Thus, if we made a poor estimate for the initial condition, the estimated state would have a continually growing error or an error that goes to zero too slowly to be of use. Furthermore, small errors in our knowledge of the system ( $A$ ,  $B$ ) would also cause the estimate to diverge from the true state.

To study the dynamics of this estimator, we define the error in the estimate to be

$$\tilde{x} \stackrel{\Delta}{=} x - \hat{x}. \quad (7.128)$$

Then, the dynamics of this error system are given by

$$\dot{\tilde{x}} = \dot{x} - \dot{\hat{x}} = Ax - A\hat{x}, \quad \tilde{x}(0) = x(0) - \hat{x}(0). \quad (7.129)$$

We have no ability to influence the rate at which the state estimate converges to the true state.

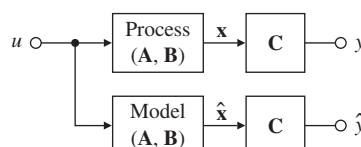
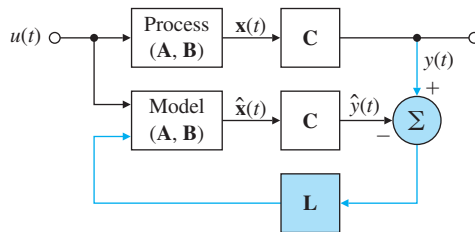


**Figure 7.27**

Block diagram for the open-loop estimator

**Figure 7.28**

Block diagram for the closed-loop estimator



**Feed back the output error to correct the state estimate equation.**

We now invoke the golden rule: When in trouble, use feedback. Consider feeding back the difference between the measured and estimated outputs and correcting the model continuously with this error signal. The equation for this scheme, as shown in Fig. 7.28, is

$$\dot{\hat{x}} = \mathbf{A}\hat{x} + \mathbf{B}u + \mathbf{L}(y - \mathbf{C}\hat{x}). \quad (7.130)$$

Here,  $\mathbf{L}$  is a proportional gain defined as

$$\mathbf{L} = [l_1, l_2, \dots, l_n]^T, \quad (7.131)$$

and is chosen to achieve satisfactory error characteristics. The dynamics of the error can be obtained by subtracting the estimate [see Eq. (7.130)] from the state [see Eq. (7.41)], to get the error equation

$$\dot{\tilde{x}} = (\mathbf{A} - \mathbf{LC})\tilde{x}. \quad (7.132)$$

The characteristic equation of the error is now given by

$$\det[s\mathbf{I} - (\mathbf{A} - \mathbf{LC})] = 0. \quad (7.133)$$

If we can choose  $\mathbf{L}$  so  $\mathbf{A} - \mathbf{LC}$  has stable and reasonably fast eigenvalues,  $\tilde{x}$  will decay to zero and remain there—*independent* of the known forcing function  $u(t)$  and its effect on the state  $x(t)$  and irrespective of the initial condition  $\tilde{x}(0)$ . This means  $\hat{x}(t)$  will converge to  $x(t)$ , regardless of the value of  $\hat{x}(0)$ ; furthermore, we can choose the dynamics of the error to be stable as well as much faster than the open-loop dynamics determined by  $\mathbf{A}$ .

Note in obtaining Eq. (7.132), we have assumed that  $\mathbf{A}$ ,  $\mathbf{B}$ , and  $\mathbf{C}$  are identical in the physical plant and in the computer implementation of the estimator. If we do not have an accurate model of the plant ( $\mathbf{A}$ ,  $\mathbf{B}$ ,  $\mathbf{C}$ ), the dynamics of the error are no longer governed by Eq. (7.132). However, we can typically choose  $\mathbf{L}$  so the error system is still at least stable and the error remains acceptably small, even with (small) modeling errors and disturbing inputs. It is important to emphasize that the nature of the plant and the estimator are quite different. The plant is a physical system such as a chemical process or servomechanism, whereas the estimator is usually a digital processor computing the estimated state according to Eq. (7.130).

The selection of  $\mathbf{L}$  can be approached in exactly the same fashion as  $\mathbf{K}$  is selected in the control-law design. If we specify the desired location of the estimator error poles as

$$s_i = \beta_1, \beta_2, \dots, \beta_n,$$

**Estimate-error characteristic equation**

then the desired estimator characteristic equation is

$$\alpha_e(s) \triangleq (s - \beta_1)(s - \beta_2) \cdots (s - \beta_n). \quad (7.134)$$

We can then solve for  $\mathbf{L}$  by comparing coefficients in Eqs. (7.133) and (7.134).

### EXAMPLE 7.24

#### An Estimator Design for a Simple Pendulum

Design an estimator for the simple pendulum. Compute the estimator gain matrix that will place both the estimator error poles at  $-10\omega_0$  (five times as fast as the controller poles selected in Example 7.14). Verify the result using Matlab for  $\omega_0 = 1$ . Evaluate the performance of the estimator.

**Solution.** The equations of motion are

$$\dot{\mathbf{x}} = \begin{bmatrix} 0 & 1 \\ -\omega_0^2 & 0 \end{bmatrix} \mathbf{x} + \begin{bmatrix} 0 \\ 1 \end{bmatrix} u, \quad (7.135a)$$

$$y = [1 \ 0] \mathbf{x}. \quad (7.135b)$$

We are asked to place the two estimator error poles at  $-10\omega_0$ . The corresponding characteristic equation is

$$\alpha_e(s) = (s + 10\omega_0)^2 = s^2 + 20\omega_0 s + 100\omega_0^2. \quad (7.136)$$

From Eq. (7.133), we get

$$\det[s\mathbf{I} - (\mathbf{A} - \mathbf{LC})] = s^2 + l_1 s + l_2 + \omega_0^2. \quad (7.137)$$

Comparing the coefficients in Eqs. (7.136) and (7.137), we find that

$$\mathbf{L} = \begin{bmatrix} l_1 \\ l_2 \end{bmatrix} = \begin{bmatrix} 20\omega_0 \\ 99\omega_0^2 \end{bmatrix}. \quad (7.138)$$

The result can also be found from Matlab. For example, for  $\omega_0 = 1$ , the following Matlab statements:

```
wo=1;
A=[0 1;-wo*wo 0];
C=[1 0];
pe=[-10*wo;-10*wo];
Lt=acker(A',C',pe);
L=Lt'
```

yield  $\mathbf{L} = [20 \ 99]^T$  and agrees with the preceding hand calculations.

Performance of the estimator can be tested by adding the actual state feedback to the plant and plotting the estimation errors. Note this is not the way the system will ultimately be built, but this approach provides a means of validating the estimator performance. Combining Eq. (7.68) of the plant with state feedback with Eq. (7.130) of the

estimator with output feedback results in the following overall system equations:

$$\begin{bmatrix} \dot{\hat{x}} \\ \dot{\hat{x}} \end{bmatrix} = \begin{bmatrix} A - BK & 0 \\ LC - BK & A - LC \end{bmatrix} \begin{bmatrix} x \\ \hat{x} \end{bmatrix}, \quad (7.139)$$

$$y = [ C \ 0 ] \begin{bmatrix} x \\ \hat{x} \end{bmatrix}, \quad (7.140)$$

$$y - \hat{y} = [ C \ -C ] \begin{bmatrix} x \\ \hat{x} \end{bmatrix}. \quad (7.141)$$

A block diagram of the setup is drawn in Fig. 7.29.

The response of this closed-loop system with  $\omega_0 = 1$  to an initial condition  $x_0 = [1.0, 0.0]^T$  and  $\hat{x}_0 = [0, 0]^T$  is shown in Fig. 7.30, where  $K$  is obtained from Example 7.14 and  $L$  comes from Eq. (7.138). The response may be obtained using the Matlab commands impulse or initial. Note the state estimates converge to the actual state-variables after an initial transient even though the initial value of  $\hat{x}$  had a large error. Also note the estimation error decays approximately five times faster than the decay of the state itself, as we designed it to do.

Matlab commands  
impulse, initial

**Figure 7.29**  
Estimator connected to  
the plant

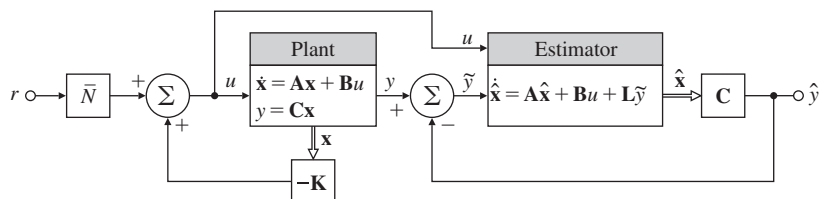
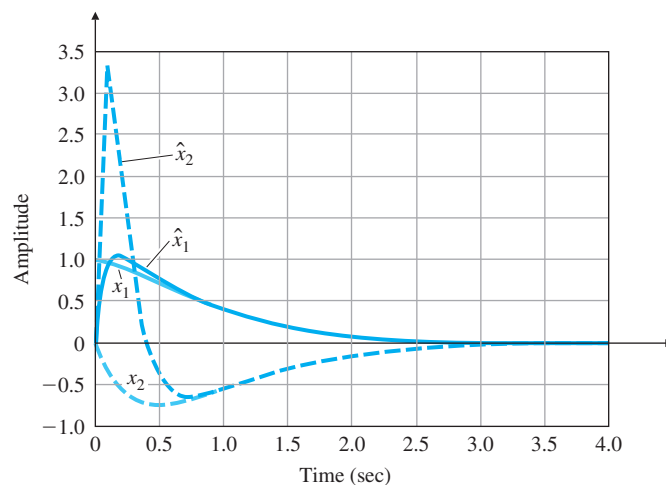


**Figure 7.30**  
Initial-condition  
response of oscillator  
showing  $x$  and  $\hat{x}$



### Observer Canonical Form

As was the case for control-law design, there is a canonical form for which the estimator gain design equations are particularly simple and the existence of a solution is obvious. We introduced this form in Section 7.4.1. The equations are in the observer canonical form and have the structure:

$$\dot{\mathbf{x}}_o = \mathbf{A}_o \mathbf{x}_o + \mathbf{B}_o u, \quad (7.142a)$$

$$y = \mathbf{C}_o \mathbf{x}_o, \quad (7.142b)$$

where

$$\mathbf{A}_o = \begin{bmatrix} -a_1 & 1 & 0 & 0 & \dots & 0 \\ -a_2 & 0 & 1 & 0 & \dots & \vdots \\ \vdots & \vdots & \ddots & & & 1 \\ -a_n & 0 & 0 & 0 & & 0 \end{bmatrix}, \quad \mathbf{B}_o = \begin{bmatrix} b_1 \\ b_2 \\ \vdots \\ b_n \end{bmatrix},$$

$$\mathbf{C}_o = [ \quad 1 \quad 0 \quad 0 \quad \dots \quad 0 ], \quad D_o = 0.$$

#### Observer canonical form

A block diagram for the third-order case is shown in Fig. 7.31. In observer canonical form, all the feedback loops come from the output, or observed signal. Like the control canonical form, the observer canonical form is a “direct” form because the values of the significant elements in the matrices are obtained directly from the coefficients of the numerator and denominator polynomials of the corresponding transfer function  $G(s)$ . The matrix  $\mathbf{A}_o$  is called a **left companion matrix** to the characteristic equation because the coefficients of the equation appear on the left side of the matrix.

One of the advantages of the observer canonical form is that the estimator gains can be obtained from it by inspection. The estimator error closed-loop matrix for the third-order case is

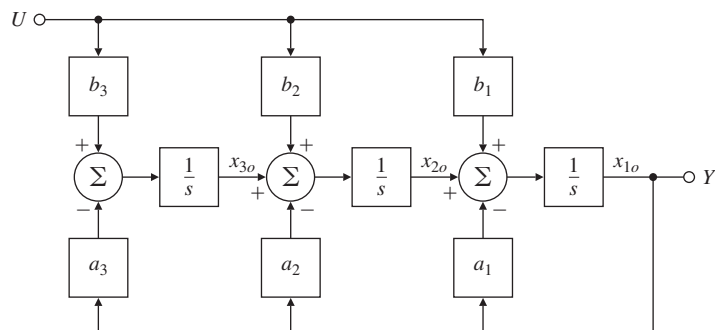
$$\mathbf{A}_o - \mathbf{LC}_o = \begin{bmatrix} -a_1 - l_1 & 1 & 0 \\ -a_2 - l_2 & 0 & 1 \\ -a_3 - l_3 & 0 & 0 \end{bmatrix}, \quad (7.143)$$

which has the characteristic equation

$$s^3 + (a_1 + l_1)s^2 + (a_2 + l_2)s + (a_3 + l_3) = 0, \quad (7.144)$$

**Figure 7.31**

Observer canonical form of a third-order system



and the estimator gain can be found by comparing the coefficients of Eq. (7.144) with  $\alpha_e(s)$  from Eq. (7.134).

In a development exactly parallel with the control-law case, we can find a transformation to take a given system to observer canonical form if and only if the system has a structural property that in this case we call **observability**. Roughly speaking, observability refers to our ability to deduce information about all the modes of the system by monitoring only the sensed outputs. Unobservability results when some mode or subsystem is disconnected physically from the output and therefore no longer appears in the measurements. For example, if only derivatives of certain state-variables are measured, and these state-variables do not affect the dynamics, a constant of integration is obscured. This situation occurs with a plant having the transfer function  $1/s^2$  if only velocity is measured, for then it is impossible to deduce the initial value of the position. On the other hand, for an oscillator, a velocity measurement is sufficient to estimate position because the acceleration, and consequently the velocity observed, are affected by position. The mathematical test for determining observability is that the **observability matrix**,

$$\mathcal{O} = \begin{bmatrix} \mathbf{C} \\ \mathbf{CA} \\ \vdots \\ \mathbf{CA}^{n-1} \end{bmatrix}, \quad (7.145)$$

must have independent columns. In the one output case we will study,  $\mathcal{O}$  is square, so the requirement is that  $\mathcal{O}$  be nonsingular or have a nonzero determinant. In general, we can find a transformation to observer canonical form if and only if the observability matrix is nonsingular. Note this is analogous to our earlier conclusions for transforming system matrices to control canonical form.

As with control-law design, we could find the transformation to observer form, compute the gains from the equivalent of Eq. (7.144), and transform back. An alternative method of computing  $\mathbf{L}$  is to use Ackermann's formula in estimator form, which is

$$\mathbf{L} = \alpha_e(\mathbf{A})\mathcal{O}^{-1} \begin{bmatrix} 0 \\ 0 \\ \vdots \\ 1 \end{bmatrix}, \quad (7.146)$$

where  $\mathcal{O}$  is the observability matrix given in Eq. (7.145).

### Duality

You may already have noticed from this discussion the considerable resemblance between estimation and control problems. In fact, the two problems are mathematically equivalent. This property is called **duality**. Table 7.1 shows the duality relationships between the estimation and control problems. For example, Ackermann's control formula

Ackermann's estimator formula

Duality of estimation and control

**TABLE 7.1**

Duality	
Control	Estimation
A	$A^T$
B	$C^T$
C	$B^T$

[Eq. (7.88)] becomes the estimator formula Eq. (7.146) if we make the substitutions given in Table 7.1. We can demonstrate this directly using matrix algebra. The control problem is to select the row matrix  $\mathbf{K}$  for satisfactory placement of the poles of the system matrix  $\mathbf{A} - \mathbf{BK}$ ; the estimator problem is to select the column matrix  $\mathbf{L}$  for satisfactory placement of the poles of  $\mathbf{A} - \mathbf{LC}$ . However, the poles of  $\mathbf{A} - \mathbf{LC}$  equal those of  $(\mathbf{A} - \mathbf{LC})^T = \mathbf{A}^T - \mathbf{C}^T \mathbf{L}^T$ , and in this form, the algebra of the design for  $\mathbf{L}^T$  is identical to that for  $\mathbf{K}$ . Therefore, where we used Ackermann's formula or the place algorithm in the forms

$$\mathbf{K} = \text{acker}(\mathbf{A}, \mathbf{B}, \mathbf{pc}),$$

$$\mathbf{K} = \text{place}(\mathbf{A}, \mathbf{B}, \mathbf{pc}),$$

for the control problem, we use

$$\mathbf{L} = \text{acker}(\mathbf{A}', \mathbf{C}', \mathbf{pe}),$$

$$\mathbf{L} = \text{place}(\mathbf{A}', \mathbf{C}', \mathbf{pe}),$$

$$\mathbf{L} = \mathbf{L}^T,$$

where  $\mathbf{p}_e$  is a vector containing the desired estimator error poles for the estimator problem.

Thus duality allows us to use the same design tools for estimator problems as for control problems with proper substitutions. The two canonical forms are also dual, as we can see by comparing the triples  $(\mathbf{A}_c, \mathbf{B}_c, \mathbf{C}_c)$  and  $(\mathbf{A}_o, \mathbf{B}_o, \mathbf{C}_o)$ .

### 7.7.2 Reduced-Order Estimators

The estimator design method described in Section 7.7.1 reconstructs the entire state vector using measurements of some of the state-variables. If the sensors have no noise, a full-order estimator contains redundancies, and it seems reasonable to question the necessity for estimating state-variables that are measured directly. Can we reduce the complexity of the estimator using the state-variables that are measured directly and exactly? Yes. However, it is better to implement a full-order estimator if there is significant noise on the measurements because, in addition to estimating unmeasured state-variables, the estimator filters the measurements.

The **reduced-order estimator** reduces the order of the estimator by the number (1 in this text) of sensed outputs. To derive this estimator,

Matlab commands  
acker,  
place

we start with the assumption that the output equals the first state as, for example,  $y = x_a$ . If this is not so, a preliminary step is required. Transforming to observer form is possible but is overkill; any nonsingular transformation with  $\mathbf{C}$  as the first row will do. We now partition the state vector into two parts:  $x_a$ , which is directly measured, and  $\mathbf{x}_b$ , which represents the remaining state-variables that need to be estimated. If we partition the system matrices accordingly, the complete description of the system is given by

$$\begin{bmatrix} \dot{x}_a \\ \dot{\mathbf{x}}_b \end{bmatrix} = \begin{bmatrix} A_{aa} & A_{ab} \\ A_{ba} & A_{bb} \end{bmatrix} \begin{bmatrix} x_a \\ \mathbf{x}_b \end{bmatrix} + \begin{bmatrix} B_a \\ \mathbf{B}_b \end{bmatrix} u, \quad (7.147a)$$

$$y = [1 \ 0] \begin{bmatrix} x_a \\ \mathbf{x}_b \end{bmatrix}. \quad (7.147b)$$

The dynamics of the unmeasured state-variables are given by

$$\dot{\mathbf{x}}_b = \mathbf{A}_{bb}\mathbf{x}_b + \underbrace{\mathbf{A}_{ba}x_a + \mathbf{B}_bu}_{\text{known input}}, \quad (7.148)$$

where the right-most two terms are known and can be considered as an input into the  $\mathbf{x}_b$  dynamics. Because  $x_a = y$ , the measured dynamics are given by the scalar equation

$$\dot{x}_a = \dot{y} = A_{aa}y + \mathbf{A}_{ab}\mathbf{x}_b + B_{au}. \quad (7.149)$$

If we collect the known terms of Eq. (7.149) on one side, yielding

$$\underbrace{\dot{y} - A_{aa}y - B_{au}}_{\text{known measurement}} = \mathbf{A}_{ab}\mathbf{x}_b, \quad (7.150)$$

we obtain a relationship between known quantities on the left side, which we consider measurements, and unknown state-variables on the right. Therefore, Eqs. (7.149) and (7.150) have the same relationship to the state  $\mathbf{x}_b$  that the original equation [see Eq. (7.147b)] had to the entire state  $\mathbf{x}$ . Following this line of reasoning, we can establish the following substitutions in the original estimator equations to obtain a (reduced-order) estimator of  $\mathbf{x}_b$ :

$$\mathbf{x} \leftarrow \mathbf{x}_b, \quad (7.151a)$$

$$\mathbf{A} \leftarrow \mathbf{A}_{bb}, \quad (7.151b)$$

$$\mathbf{B}u \leftarrow \mathbf{A}_{bay} + \mathbf{B}_bu, \quad (7.151c)$$

$$y \leftarrow \dot{y} - A_{aa}y - B_{au}, \quad (7.151d)$$

$$\mathbf{C} \leftarrow \mathbf{A}_{ab}. \quad (7.151e)$$

Therefore, the reduced-order estimator equations are obtained by substituting Eqs. (7.151) into the full-order estimator [see Eq. (7.130)]:

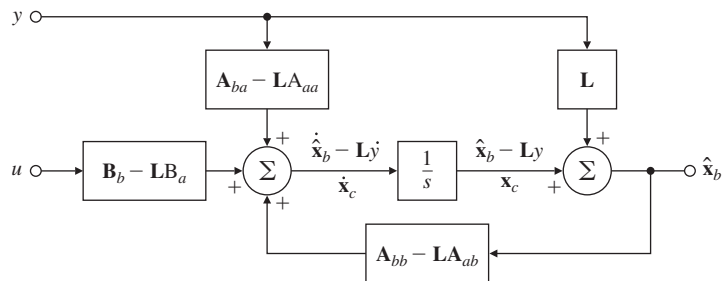
$$\dot{\hat{\mathbf{x}}}_b = \mathbf{A}_{bb}\hat{\mathbf{x}}_b + \underbrace{\mathbf{A}_{bay} + \mathbf{B}_bu}_{\text{input}} + \mathbf{L} \underbrace{(\dot{y} - A_{aa}y - B_{au} - \mathbf{A}_{ab}\hat{\mathbf{x}}_b)}_{\text{measurement}}. \quad (7.152)$$

If we define the estimator error to be

$$\tilde{\mathbf{x}}_b \stackrel{\Delta}{=} \mathbf{x}_b - \hat{\mathbf{x}}_b, \quad (7.153)$$

**Figure 7.32**

Reduced-order estimator structure



then the dynamics of the error are given by subtracting Eq. (7.148) from Eq. (7.152) to get

$$\dot{\tilde{x}}_b = (\mathbf{A}_{bb} - \mathbf{L}\mathbf{A}_{ab})\tilde{x}_b, \quad (7.154)$$

and its characteristic equation is given by

$$\det[s\mathbf{I} - (\mathbf{A}_{bb} - \mathbf{L}\mathbf{A}_{ab})] = 0. \quad (7.155)$$

We design the dynamics of this estimator by selecting  $\mathbf{L}$  so that Eq. (7.155) matches a reduced order  $\alpha_e(s)$ . Now Eq. (7.152) can be rewritten as

$$\dot{\tilde{x}}_b = (\mathbf{A}_{bb} - \mathbf{L}\mathbf{A}_{ab})\tilde{x}_b + (\mathbf{A}_{ba} - \mathbf{L}\mathbf{A}_{aa})y + (\mathbf{B}_b - \mathbf{L}\mathbf{B}_a)u + \mathbf{L}\dot{y}. \quad (7.156)$$

The fact we must form the derivative of the measurements in Eq. (7.156) appears to present a practical difficulty. It is known that differentiation amplifies noise, so if  $y$  is noisy, the use of  $\dot{y}$  is unacceptable. To get around this difficulty, we define the new controller state to be

$$\mathbf{x}_c \triangleq \tilde{x}_b - \mathbf{L}y. \quad (7.157)$$

In terms of this new state, the implementation of the reduced-order estimator is given by

$$\dot{\mathbf{x}}_c = (\mathbf{A}_{bb} - \mathbf{L}\mathbf{A}_{ab})\tilde{x}_b + (\mathbf{A}_{ba} - \mathbf{L}\mathbf{A}_{aa})y + (\mathbf{B}_b - \mathbf{L}\mathbf{B}_a)u, \quad (7.158)$$

and  $\dot{y}$  no longer appears directly. A block-diagram representation of the reduced-order estimator is shown in Fig. 7.32.

## EXAMPLE 7.25

### A Reduced-Order Estimator Design for Pendulum

#### Reduced-order estimator

Design a reduced-order estimator for the pendulum that has the error pole at  $-10\omega_0$ .

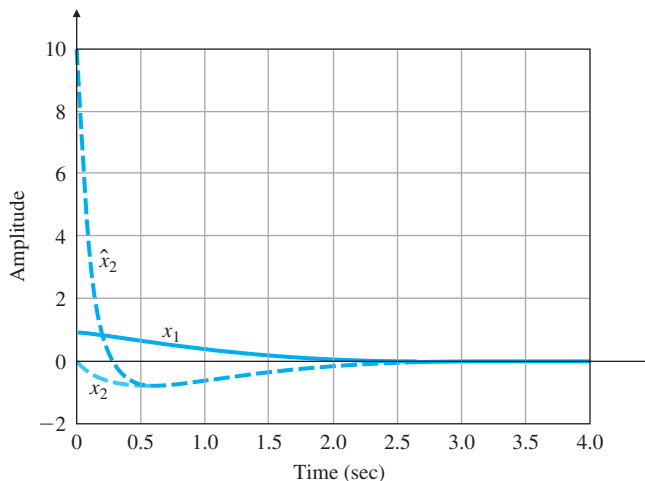
**Solution.** We are given the system equations

$$\begin{bmatrix} \dot{x}_1 \\ \dot{x}_2 \end{bmatrix} = \begin{bmatrix} 0 & 1 \\ -\omega_0^2 & 0 \end{bmatrix} \begin{bmatrix} x_1 \\ x_2 \end{bmatrix} + \begin{bmatrix} 0 \\ 1 \end{bmatrix} u,$$

$$y = [1 \ 0] \begin{bmatrix} x_1 \\ x_2 \end{bmatrix}.$$

**Figure 7.33**

Initial-condition response of the reduced-order estimator



The partitioned matrices are

$$\begin{bmatrix} A_{aa} & A_{ab} \\ A_{ba} & A_{bb} \end{bmatrix} = \begin{bmatrix} 0 & 1 \\ -\omega_0^2 & 0 \end{bmatrix},$$

$$\begin{bmatrix} B_a \\ B_b \end{bmatrix} = \begin{bmatrix} 0 \\ 1 \end{bmatrix}.$$

From Eq. (7.155), we find the characteristic equation in terms of  $L$ :

$$s - (0 - L) = 0.$$

We compare it with the desired equation,

$$\alpha_e(s) = s + 10\omega_0 = 0,$$

which yields

$$L = 10\omega_0.$$

The estimator equation, from Eq. (7.158), is

$$\dot{x}_c = -10\omega_0\hat{x}_2 - \omega_0^2 y + u,$$

and the state estimate, from Eq. (7.157), is

$$\hat{x}_2 = x_c + 10\omega_0 y.$$

We use the control law given in the earlier examples. The response of the estimator to a plant initial condition  $x_0 = [1.0, 0.0]^T$  and an estimator initial condition  $x_{c0} = 0$  is shown in Fig. 7.33 for  $\omega_0 = 1$ . The response may be obtained using the Matlab commands impulse or initial. Note the similarity of the initial-condition response to that of the full-order estimator plotted in Fig. 7.30.

[Matlab impulse, initial](#)

The reduced-order estimator gain can also be found from Matlab using

$$\mathbf{L}_t = \text{acker}(\mathbf{A}_{bb}', \mathbf{A}_{ab}', \mathbf{p}_e),$$

$$\mathbf{L}_t = \text{place}(\mathbf{A}_{bb}', \mathbf{A}_{ab}', \mathbf{p}_e),$$

$$\mathbf{L} = \mathbf{L}_t^T.$$

The conditions for the existence of the reduced-order estimator are the same as for the full-order estimator—namely, observability of  $(\mathbf{A}_{bb}, \mathbf{A}_{ab})$  which can be shown to be the same as the observability of  $(\mathbf{A}, \mathbf{C})$ .

### 7.7.3 Estimator Pole Selection

[Design rules of thumb for selecting estimator poles](#)

We can base our selection of estimator pole locations on the techniques discussed in Section 7.6 for the case of controller poles. As a rule of thumb, the estimator poles can be chosen to be faster than the controller poles by a factor of 2 to 6. This ensures a faster decay of the estimator errors compared with the desired dynamics, thus causing the controller poles to dominate the total response. If sensor noise is large enough to be a major concern, we may choose the estimator poles to be slower than two times the controller poles, which would yield a system with lower bandwidth and more noise smoothing. However, we would expect the total system response in this case to be strongly influenced by the location of the estimator poles. If the estimator poles are slower than the controller poles, we would expect the system response to disturbances to be dominated by the dynamic characteristics of the estimator rather than by those selected by the control law.

In comparison with the selection of controller poles, estimator pole selection requires us to be concerned with a much different relationship than with control effort. As in the controller, there is a feedback term in the estimator that grows in magnitude as the requested speed of response increases. However, this feedback is in the form of an electronic signal or a digital word in a computer, so its growth causes no special difficulty. In the controller, increasing the speed of response increases the control effort; this implies the use of a larger actuator, which in turn increases its size, weight, and cost. The important consequence of increasing the speed of response of an estimator is that the bandwidth of the estimator becomes higher, thus causing more sensor noise to pass on to the control actuator. Of course, if  $(\mathbf{A}, \mathbf{C})$  are not observable, then no amount of estimator gain can produce a reasonable state estimate. Thus, as with controller design, the best estimator design is a balance between good transient response and low-enough bandwidth that sensor noise does not significantly impair actuator activity. Both dominant second-order and optimal control ideas can be used to meet the requirements.

There is a result for estimator gain design based on the SRL. In optimal estimation theory, the best choice for estimator gain is dependent on the ratio of sensor noise intensity  $\nu$  to process (disturbance) noise intensity [ $w$  in Eq. (7.160)]. This is best understood by reexamining the estimator equation

$$\dot{\hat{x}} = \mathbf{A}\hat{x} + \mathbf{B}u + \mathbf{L}(y - \mathbf{C}\hat{x}) \quad (7.159)$$

**Process noise**

to see how it interacts with the system when process noise  $w$  is present. The plant with process noise is described by

$$\dot{x} = \mathbf{Ax} + \mathbf{Bu} + \mathbf{B}_1w, \quad (7.160)$$

**Sensor noise**

and the measurement equation with sensor noise  $v$  is described by

$$y = \mathbf{Cx} + v. \quad (7.161)$$

The estimator error equation with these additional inputs is found directly by subtracting Eq. (7.159) from Eq. (7.160) and substituting Eq. (7.161) for  $y$ :

$$\dot{\tilde{x}} = (\mathbf{A} - \mathbf{LC})\tilde{x} + \mathbf{B}_1w - \mathbf{Lv}. \quad (7.162)$$

In Eq. (7.162), the sensor noise is multiplied by  $\mathbf{L}$  and the process noise is not. If  $\mathbf{L}$  is very small, then the effect of sensor noise is removed, but the estimator's dynamic response will be "slow," so the error will not reject effects of  $w$  very well. The state of a low-gain estimator will not track uncertain plant inputs very well. These results can, with some success, also be applied to model errors in, for example,  $\mathbf{A}$  or  $\mathbf{B}$ . Such model errors will add terms to Eq. (7.162) and act like additional process noise. On the other hand, if  $\mathbf{L}$  is large, then the estimator response will be fast and the disturbance or process noise will be rejected, but the sensor noise, multiplied by  $\mathbf{L}$ , results in large errors. Clearly, a balance between these two effects is required. It turns out that the optimal solution to this balance can be found under very reasonable assumptions by solving an SRL equation for the estimator that is very similar to the one for the optimal control formulation [see Eq. (7.109)]. The estimator SRL equation is

$$1 + qG_e(-s)G_e(s) = 0, \quad (7.163)$$

where  $q$  is the ratio of input disturbance noise intensity to sensor noise intensity and  $G_e$  is the transfer function from the process noise to the sensor output and is given by

$$G_e(s) = \mathbf{C}(s\mathbf{I} - \mathbf{A})^{-1}\mathbf{B}_1. \quad (7.164)$$

Note from Eqs. (7.109) and (7.163) that  $G_e(s)$  is similar to  $G_0(s)$ . However, a comparison of Eqs. (7.110) and (7.164) shows  $G_e(s)$  has the input matrix  $\mathbf{B}_1$  instead of  $\mathbf{B}$ , and  $G_0$  is the transfer function from the control input  $u$  to *cost* output  $z$ , and has output matrix  $\mathbf{C}_1$  instead of  $\mathbf{C}$ .

The use of the estimator SRL [see Eq. (7.163)] is identical to the use of the controller SRL. A root locus with respect to  $q$  is generated, thus yielding sets of optimal estimator poles corresponding more or less to the ratio of process noise intensity to sensor noise intensity. The designer then picks the set of (stable) poles that seems best, considering all aspects of the problem. An important advantage of using the SRL technique is that after the process noise input matrix  $\mathbf{B}_1$  has been selected, the "arbitrariness" is reduced to one degree of freedom, the selection  $q$ , instead of the many degrees of freedom required to select the poles directly in a higher-order system.

**Estimator SRL equation**

A final comment concerns the reduced-order estimator. Because of the presence of a direct transmission term from  $y$  through  $\mathbf{L}$  to  $\mathbf{x}_b$  (see Fig. 7.32), the reduced-order estimator has a much higher bandwidth from sensor to control when compared with the full-order estimator. Therefore, if sensor noise is a significant factor, the reduced-order estimator is less attractive because the potential saving in complexity is more than offset by the increased sensitivity to noise.

### EXAMPLE 7.26

#### *SRL Estimator Design for a Simple Pendulum*

Draw the estimator SRL for the linearized equations of the simple inverted pendulum with  $\omega_o = 1$ . Take the output to be a noisy measurement of position with noise intensity ratio  $q$ .

**Solution.** We are given the system equations

$$\begin{bmatrix} \dot{x}_1 \\ \dot{x}_2 \end{bmatrix} = \begin{bmatrix} 0 & 1 \\ -\omega_0^2 & 0 \end{bmatrix} \begin{bmatrix} x_1 \\ x_2 \end{bmatrix} + \begin{bmatrix} 0 \\ 1 \end{bmatrix} w,$$

$$y = [1 \ 0] \begin{bmatrix} x_1 \\ x_2 \end{bmatrix} + v.$$

We then calculate from Eq. (7.164) that

$$G_e(s) = \frac{1}{s^2 + \omega_0^2}.$$

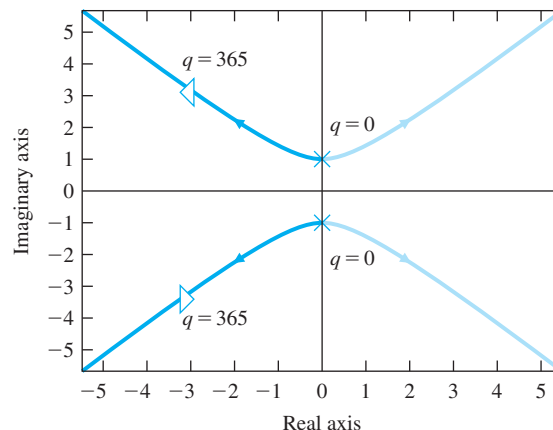
The symmetric  $180^\circ$  loci are shown in Fig. 7.34. The Matlab statements to generate the SRL are (for  $\omega_o = 1$ )

```
s=tf('s');
G=1/(s^2+1);
sysGG=G*G;
rlocus(sysGG);
```

We would choose two stable roots for a given value of  $q$ , for example,  $s = -3 \pm j3.18$  for  $q = 365$ , and use them for estimator pole placement.

**Figure 7.34**

Symmetric root locus for the inverted pendulum estimator design



## Regulator

## 7.8 Compensator Design: Combined Control Law and Estimator

If we take the control-law design described in Section 7.5, combine it with the estimator design described in Section 7.7, and implement the control law by using the estimated state-variables, the design is complete for a **regulator** that is able to reject disturbances but has no external reference input to track. However, because the control law was designed for feedback of the actual (not the estimated) state, you may wonder what effect using  $\hat{\mathbf{x}}$  in place of  $\mathbf{x}$  has on the system dynamics. In this section, we compute this effect. In doing so, we will compute the closed-loop characteristic equation and the open-loop compensator transfer function. We will use these results to compare the state-space designs with root-locus and frequency-response designs.

The plant equation with feedback is now

$$\dot{\mathbf{x}} = \mathbf{Ax} - \mathbf{BK}\hat{\mathbf{x}}, \quad (7.165)$$

which can be rewritten in terms of the state error  $\tilde{\mathbf{x}}$  as

$$\dot{\mathbf{x}} = \mathbf{Ax} - \mathbf{BK}(\mathbf{x} - \tilde{\mathbf{x}}). \quad (7.166)$$

The overall system dynamics in state form are obtained by combining Eq. (7.166) with the estimator error [see Eq. (7.132)] to get

$$\begin{bmatrix} \dot{\mathbf{x}} \\ \dot{\tilde{\mathbf{x}}} \end{bmatrix} = \begin{bmatrix} \mathbf{A} - \mathbf{BK} & \mathbf{BK} \\ \mathbf{0} & \mathbf{A} - \mathbf{LC} \end{bmatrix} \begin{bmatrix} \mathbf{x} \\ \tilde{\mathbf{x}} \end{bmatrix}. \quad (7.167)$$

The characteristic equation of this closed-loop system is

$$\det \begin{bmatrix} s\mathbf{I} - \mathbf{A} + \mathbf{BK} & -\mathbf{BK} \\ \mathbf{0} & s\mathbf{I} - \mathbf{A} + \mathbf{LC} \end{bmatrix} = 0. \quad (7.168)$$

Because the matrix is block triangular (see Appendix WD available online at [www.pearsonglobaleditions.com](http://www.pearsonglobaleditions.com)), we can rewrite Eq. (7.168) as

$$\det(s\mathbf{I} - \mathbf{A} + \mathbf{BK}) \cdot \det(s\mathbf{I} - \mathbf{A} + \mathbf{LC}) = \alpha_c(s)\alpha_e(s) = 0. \quad (7.169)$$

## Poles of the combined control law and estimator

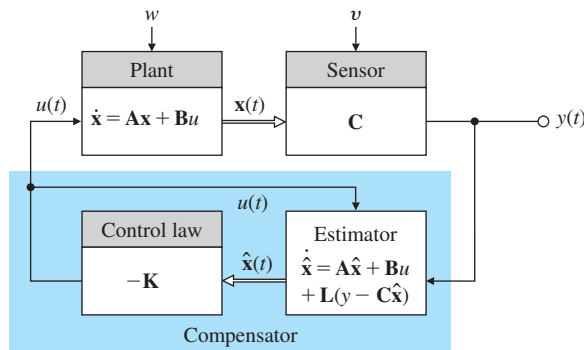
In other words, the set of poles of the combined system consists of the union of the control poles and the estimator poles. This means that the designs of the control law and the estimator can be carried out independently, yet when they are used together in this way, the poles remain unchanged.<sup>7</sup>

To compare the state-variable method of design with the transform methods discussed in Chapters 5 and 6, we note from Fig. 7.35 that the blue shaded portion corresponds to a compensator. The state equation for this compensator is obtained by including the feedback law  $u = -\mathbf{K}\hat{\mathbf{x}}$  (because it is part of the compensator) in the estimator Eq. (7.130) to get

<sup>7</sup>This is a special case of the **separation principle** (Gunckel and Franklin, 1963), which holds in much more general contexts and allows us to obtain an overall optimal design by combining the separate designs of control law and estimator in certain stochastic cases.

**Figure 7.35**

Estimator and controller mechanization



$$\dot{\hat{x}} = (\mathbf{A} - \mathbf{B}\mathbf{K} - \mathbf{L}\mathbf{C})\hat{x} + \mathbf{L}y, \quad (7.170a)$$

$$u = -\mathbf{K}\hat{x}. \quad (7.170b)$$

Note Eq. (7.170a) has the same structure as Eq. (7.18a), which we repeat here:

$$\dot{x} = \mathbf{A}x + \mathbf{B}u. \quad (7.171)$$

Because the characteristic equation of Eq. (7.18a) is

$$\det(s\mathbf{I} - \mathbf{A}) = 0, \quad (7.172)$$

the characteristic equation of the compensator is found by comparing Eqs. (7.170a) and (7.171), and substituting the equivalent matrices into Eq. (7.172) to get

$$\det(s\mathbf{I} - \mathbf{A} + \mathbf{B}\mathbf{K} + \mathbf{L}\mathbf{C}) = 0. \quad (7.173)$$

Note we never specified the roots of Eq. (7.173) nor used them in our discussion of the state-space design technique. (Note also the compensator is not guaranteed to be stable; the roots of Eq. (7.173) can be in the RHP.) The transfer function from  $y$  to  $u$  representing the dynamic compensator is obtained by inspecting Eq. (7.45) and substituting in the corresponding matrices from Eq. (7.173):

$$D_c(s) = \frac{U(s)}{Y(s)} = -\mathbf{K}(s\mathbf{I} - \mathbf{A} + \mathbf{B}\mathbf{K} + \mathbf{L}\mathbf{C})^{-1}\mathbf{L}. \quad (7.174)$$

The same development can be carried out for the reduced-order estimator. Here the control law is

$$u = -[\ K_a \quad \mathbf{K}_b ] \begin{bmatrix} x_a \\ \hat{x}_b \end{bmatrix} = -K_a y - \mathbf{K}_b \hat{x}_b. \quad (7.175)$$

Substituting Eq. (7.175) into Eq. (7.171), and using Eq. (7.158) and some algebra, we obtain

$$\dot{x}_c = \mathbf{A}_r x_c + \mathbf{B}_r y, \quad (7.176a)$$

$$u = \mathbf{C}_r x_c + D_r y, \quad (7.176b)$$

**Compensator transfer function**

where

$$\mathbf{A}_r = \mathbf{A}_{bb} - \mathbf{L}\mathbf{A}_{ab} - (\mathbf{B}_b - \mathbf{L}\mathbf{B}_a)\mathbf{K}_b, \quad (7.177a)$$

$$\mathbf{B}_r = \mathbf{A}_r\mathbf{L} + \mathbf{A}_{ba} - \mathbf{L}\mathbf{A}_{aa} - (\mathbf{B}_b - \mathbf{L}\mathbf{B}_a)\mathbf{K}_a, \quad (7.177b)$$

$$\mathbf{C}_r = -\mathbf{K}_b, \quad (7.177c)$$

$$D_r = -K_a - \mathbf{K}_b\mathbf{L}. \quad (7.177d)$$

Reduced-order  
compensator transfer  
function

The dynamic compensator now has the transfer function

$$D_{cr}(s) = \frac{U(s)}{Y(s)} = \mathbf{C}_r(s\mathbf{I} - \mathbf{A}_r)^{-1}\mathbf{B}_r + D_r. \quad (7.178)$$

When we compute  $D_c(s)$  or  $D_{cr}(s)$  for a specific case, we will find that they are very similar to the classical compensators given in Chapters 5 and 6, in spite of the fact that they are arrived at by entirely different means.

## EXAMPLE 7.27

### Full-Order Compensator Design for Satellite Attitude Control

Design a compensator using pole placement for the satellite plant with transfer function  $1/s^2$ . Place the control poles at  $s = -0.8 \pm 0.8j$  ( $\omega_n = 1.13$  rad/sec,  $\zeta = 0.7$ ) and place the estimator poles at  $\omega_n = 8$  rad/sec,  $\zeta = 0.5$ .

**Solution.** A state-variable description for the given transfer function  $G(s) = 1/s^2$  is

$$\begin{aligned} \dot{\mathbf{x}} &= \begin{bmatrix} 0 & 1 \\ 0 & 0 \end{bmatrix} \mathbf{x} + \begin{bmatrix} 0 \\ 1 \end{bmatrix} u, \\ y &= [1 \ 0] \mathbf{x}. \end{aligned}$$

If we place the control roots at  $s = -0.8 \pm 0.8j$  ( $\omega_n = 1.13$  rad/sec,  $\zeta = 0.7$ ), then

$$\alpha_c = s^2 + 1.6s + 1.28. \quad (7.179)$$

From  $\mathbf{K} = \text{place}(\mathbf{A}, \mathbf{B}, \mathbf{pc})$ , the state feedback gain is found to be

$$\mathbf{K} = [1.28 \ 1.6].$$

If the estimator error roots are at  $\omega_n = 8$  rad/sec and  $\zeta = 0.5$ , the desired estimator characteristic polynomial is

$$\alpha_e(s) = s^2 + 8s + 64 = (s + 4 + 6.93j)(s + 4 - 6.93j), \quad (7.180)$$

and, from  $\mathbf{L}t = \text{place}(\mathbf{A}', \mathbf{C}', \mathbf{pe})$ , the estimator feedback-gain matrix is found to be

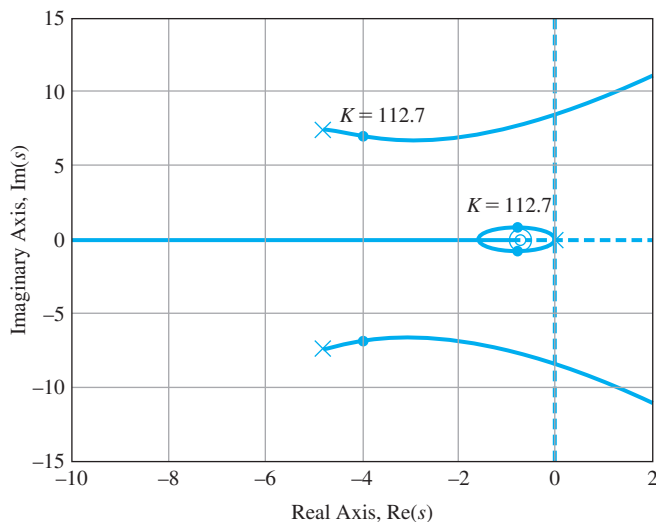
$$\mathbf{L} = \begin{bmatrix} 8 \\ 64 \end{bmatrix}.$$

The compensator transfer function given by Eq. (7.174) is

$$D_c(s) = -112.7 \frac{(s + 0.727)}{s^2 + 9.6s + 78.1}, \quad (7.181)$$

**Figure 7.36**

Root locus for the combined controller and estimator, with process gain as the parameter



which looks very much like a lead compensator in that it has a zero on the real axis to the right of its poles; however, rather than one real pole, Eq. (7.181) has two complex poles. The zero provides the derivative feedback with phase lead, and the two poles provide some smoothing of sensor noise.

The effect of the compensation on this system's closed-loop poles can be evaluated in exactly the same way we evaluated compensation in Chapters 5 and 6 using root-locus or frequency-response tools. The gain of 112.7 in Eq. (7.181) is a result of the pole selection inherent in Eqs. (7.179) and (7.180). If we replace this specific value of compensator gain with a variable gain  $K$ , then the characteristic equation for the closed-loop system of plant plus compensator becomes

$$1 + K \frac{(s + 0.727)}{(s + 4.8 + 7.42j)(s + 4.8 - 7.42j)s^2} = 0. \quad (7.182)$$

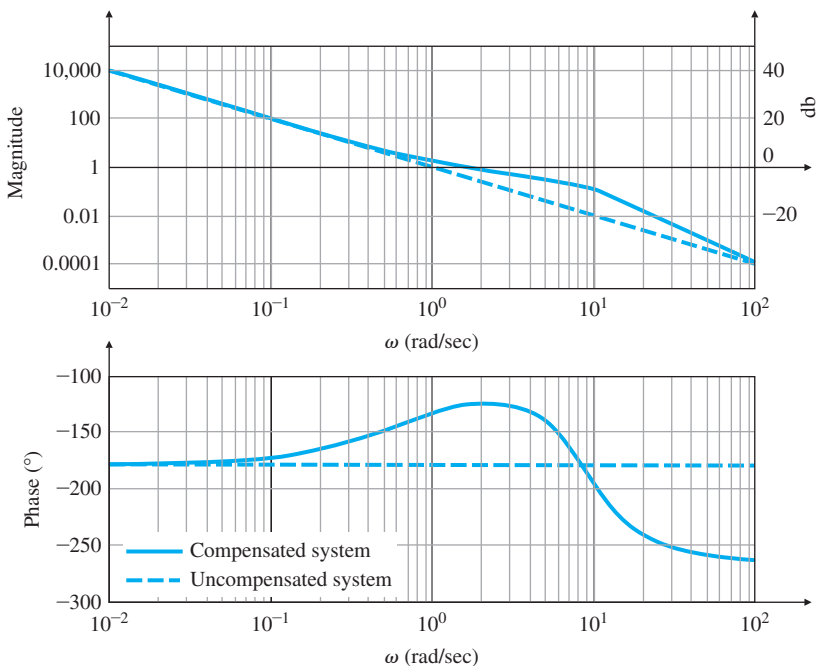
The root-locus technique allows us to evaluate the roots of this equation with respect to  $K$ , as drawn in Fig. 7.36. Note the locus goes through the roots selection for Eqs. (7.179) and (7.180), and, when  $K = 112.7$ , the four roots of the closed-loop system are equal to those specified.

The frequency-response plots given in Fig. 7.37 show that the compensation designed using state-space accomplishes the same results that one would strive for using frequency-response design. Specifically, the uncompensated phase margin of  $0^\circ$  increases to  $53^\circ$  in the compensated case, the gain  $K = 112.7$  produces a crossover frequency  $\omega_c = 1.5$  rad/sec. Both these values are roughly consistent with the controller closed-loop roots, with  $\omega_n = 1.14$  and  $\zeta = 0.7$ , as we would expect, because these slow controller poles are dominant in the system response over the fast estimator poles.

**Identical results of state-space and frequency response design methods**

**Figure 7.37**

Frequency response for the open-loop system for the compensated and uncompensated systems



Now we consider a reduced-order estimator for the same system.

### EXAMPLE 7.28

#### *Reduced-Order Compensator Design for a Satellite Attitude Control*

Repeat the design for the  $1/s^2$  satellite plant, but use a reduced-order estimator. Place the one estimator pole at  $-10$  rad/sec.

**Solution.** From Eq. (7.155), we know that the estimator gain is

$$L = 10,$$

From Eqs. (7.176a, b) and with  $\mathbf{K} = [1.28 \ 1.6]$  from Example 7.27, the scalar compensator equations are

$$\begin{aligned}\dot{x}_c &= -11.6x_c - 117.28y, \\ u &= -1.6x_c - 17.28y,\end{aligned}$$

where from Eq. (7.157),

$$x_c = \hat{x}_2 - 10y.$$

The compensator has the transfer function calculated from Eq. (7.178) to be

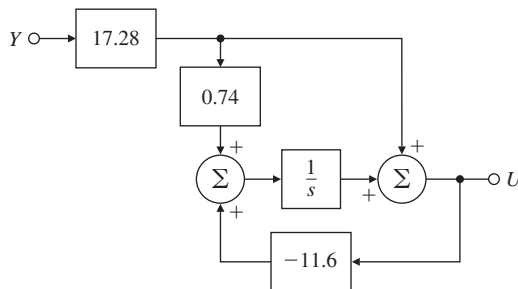
$$D_c = -\frac{17.28(s + 0.74)}{s + 11.6},$$

and is shown in Fig. 7.38.

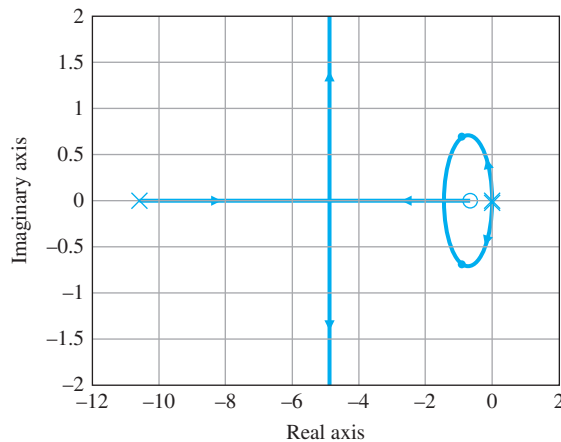
The reduced-order compensator here is precisely a lead network. This is a pleasant discovery, as again it shows that transform and state-variable techniques can result in exactly the same type of compensation. The root locus of Fig. 7.39 shows the closed-loop poles occur at the

**Figure 7.38**

Simplified block diagram of a reduced-order controller that is a lead network

**Figure 7.39**

Root locus of a reduced-order controller and  $1/s^2$  process, roots locations at  $K = 17.28$  shown by the dots.



assigned locations. The frequency response of the compensated system seen in Fig. 7.40 shows a phase margin of about  $60^\circ$ . As with the full-order estimator, analysis by other methods confirms the selected root locations.

More subtle properties of the pole-placement method can be illustrated by a third-order system.

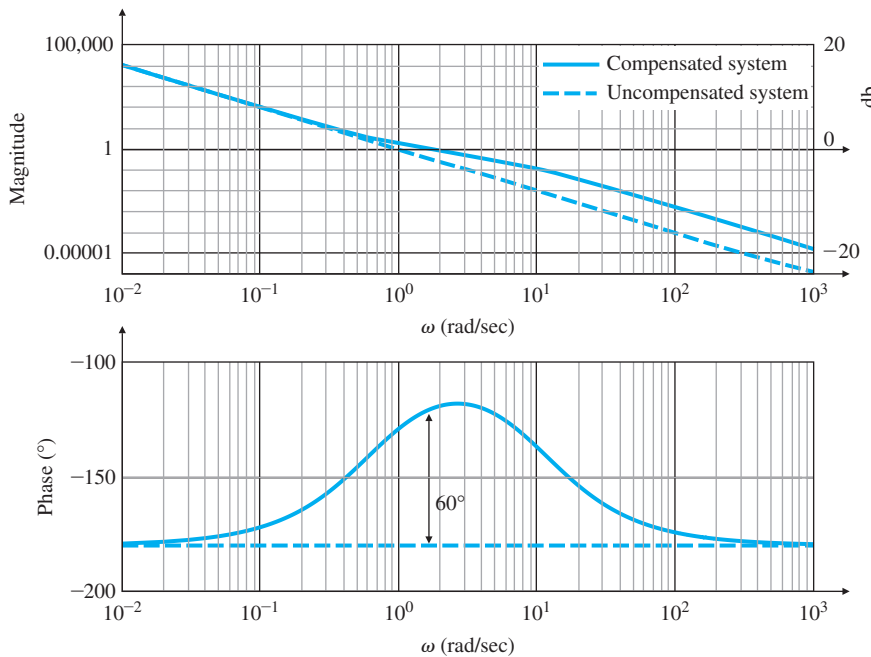
### EXAMPLE 7.29

#### *Full-Order Compensator Design for DC Servo*

Use the state-space pole-placement method to design a compensator for the DC servo system with the transfer function

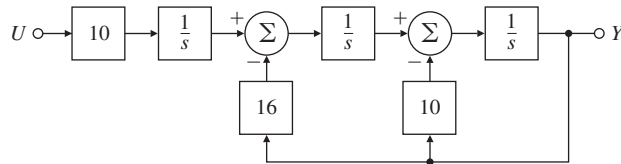
$$G(s) = \frac{10}{s(s+2)(s+8)}.$$

Using a state description in observer canonical form, place the control poles at  $pc = [-1.42; -1.04 \pm 2.14j]$  locations and the full-order estimator poles at  $pe = [-4.25; -3.13 \pm 6.41j]$ .

**Figure 7.40**

Frequency response for  $G(s) = 1/s^2$  with a reduced-order estimator

**Figure 7.41**  
DC servo in observer canonical form



**Solution.** A block diagram of this system in observer canonical form is shown in Fig. 7.41. The corresponding state-space matrices are

$$\mathbf{A} = \begin{bmatrix} -10 & 1 & 0 \\ -16 & 0 & 1 \\ 0 & 0 & 0 \end{bmatrix}, \quad \mathbf{B} = \begin{bmatrix} 0 \\ 0 \\ 10 \end{bmatrix},$$

$$\mathbf{C} = [1 \ 0 \ 0], \quad D = 0.$$

The desired poles are

$$pc = [-1.42; -1.04 + 2.14 * j; -1.04 - 2.14 * j].$$

We compute the state feedback gain to be  $K = \text{place}(A, B, pc)$ ,

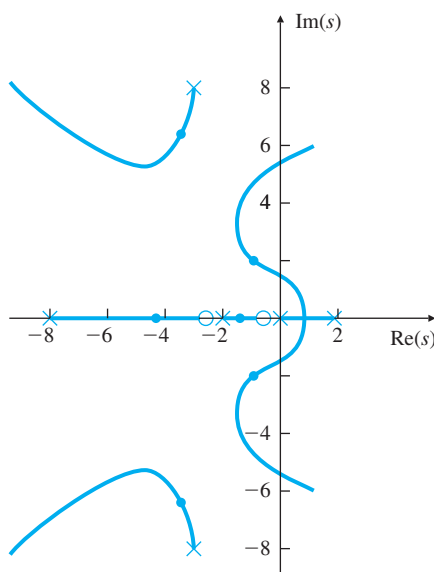
$$K = [-46.4 \ 5.76 \ -0.65].$$

The estimator error poles are at

$$pe = [-4.25; -3.13 + 6.41 * j; -3.13 - 6.41 * j];$$

**Figure 7.42**

Root locus for DC servo  
pole assignment



We compute the estimator gain to be  $L_t = \text{place}(A^t, C^t, pe)$ ,  $L = L_t^t$ ,

$$L = \begin{bmatrix} 0.5 \\ 61.4 \\ 216 \end{bmatrix}.$$

The compensator transfer function, as given by substituting into Eq. (7.174), is

$$D_c(s) = -190 \frac{(s + 0.432)(s + 2.10)}{(s - 1.88)(s + 2.94 \pm 8.32j)}.$$

Figure 7.42 shows the root locus of the system of compensator and plant in series, plotted with the compensator gain as the parameter. It verifies that the roots are in the desired locations specified when the gain  $K = 190$  in spite of the peculiar (unstable) compensation that has resulted. Even though this compensator has an unstable root at  $s = +1.88$ , all system closed-loop poles (controller and estimator) are stable.

---

An unstable compensator is typically not acceptable because of the difficulty in testing either the compensator by itself or the system in open loop during a bench checkout. In some cases, however, better control can be achieved with an unstable compensator; then its inconvenience in checkout may be worthwhile.<sup>8</sup>

Figure 7.33 shows a direct consequence of the unstable compensator is that the system becomes unstable as the gain is reduced from its nominal value. Such a system is called **conditionally stable**, and should be avoided if possible. As we shall see in Chapter 9, actuator saturation in response to large signals has the effect of lowering the effective gain,

Conditionally stable  
compensator

---

<sup>8</sup>There are even systems that cannot be stabilized with a stable compensator.

and in a conditionally stable system, instability can result. Also, if the electronics are such that the control amplifier gain rises continuously from zero to the nominal value during startup, such a system would be initially unstable. These considerations lead us to consider alternative designs for this system.

### EXAMPLE 7.30

#### *Redesign of the DC Servo System with a Reduced-Order Estimator*

Design a compensator for the DC servo system of Example 7.29 using the same control poles, but with a reduced-order estimator. Place the estimator poles at  $-4.24 \pm 4.24j$  positions with  $\omega_n = 6$  rad/sec and  $\zeta = 0.707$ .

**Solution.** The reduced-order estimator corresponds to poles at

$$pe = [-4.24 + 4.24 * j; -4.24 - 4.24 * j].$$

After partitioning we have,

$$\begin{bmatrix} A_{aa} & A_{ab} \\ A_{ba} & A_{bb} \end{bmatrix} = \begin{bmatrix} -10 & 1 & 0 \\ -16 & 0 & 1 \\ 0 & 0 & 0 \end{bmatrix}, \quad \begin{bmatrix} B_a \\ B_b \end{bmatrix} = \begin{bmatrix} 0 \\ 0 \\ 10 \end{bmatrix}.$$

Solving for the estimator error characteristic polynomial,

$$\det(sI - A_{bb} + LA_{ab}) = \alpha_e(s),$$

we find (using place) that

$$L = \begin{bmatrix} 8.5 \\ 36 \end{bmatrix}.$$

The compensator transfer function, given by Eq. (7.178), is computed to be

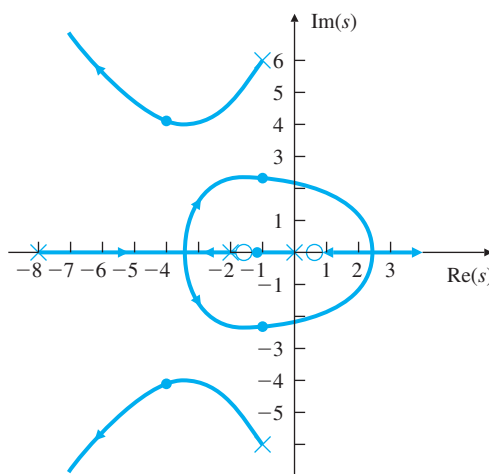
$$D_{cr}(s) = 20.93 \frac{(s - 0.735)(s + 1.871)}{(s + 0.990 \pm 6.120j)}.$$

The associated root locus for this system is shown in Fig. 7.43. Note this time, we have a stable but nonminimum-phase compensator and

A nonminimum-phase compensator

**Figure 7.43**

Root locus for DC servo reduced-order controller



a zero-degree root locus. The RHP portion of the locus will not cause difficulties because the gain has to be selected to keep all closed-loop poles in the LHP.

As a next pass at the design for this system, we attempt a design with the SRL.

### EXAMPLE 7.31

#### *Redesign of the DC Servo Compensator Using the SRL*

Design a compensator for the DC servo system of Example 7.29 using pole placement based on the SRL. For the control law, let the cost output  $z$  be the same as the plant output; for the estimator design, assume the process noise enters at the same place as the system control signal. Select roots for a control bandwidth of about 2.5 rad/sec, and choose the estimator roots for a bandwidth of about 2.5 times faster than the control bandwidth (6.3 rad/sec). Verify the design by plotting the step response and commenting. See Appendix W7.8 available online at [www.pearsonglobaleditions.com](http://www.pearsonglobaleditions.com) for a discrete implementation of the solution.

**Solution.** Because the problem has specified that  $\mathbf{B}_1 = \mathbf{B}$  and  $\mathbf{C}_1 = \mathbf{C}$ , then the SRL is the same for the control as for the estimator, so we need to generate only one locus based on the plant transfer function. The SRL for the system is shown in Fig. 7.44. From the locus, we select  $-2 \pm 1.56j$  and  $-8.04$  as the desired control poles ( $pc=[-2+1.56*j;-2-1.56*j;-8.04]$ ) and  $-4 \pm 4.9j$  and  $-9.169$  ( $pe=[-4+4.9*j;-4-4.9*j;-9.169]$ ) as the desired estimator poles. The state feedback gain is  $K=(A,B,pc)$ , or

$$\mathbf{K} = [-0.285 \quad 0.219 \quad 0.204],$$

and the estimator gain is  $L_t=place(A', C', pe)$ ,  $L=Lt'$ , or

$$\mathbf{L} = \begin{bmatrix} 7.17 \\ 97.4 \\ 367 \end{bmatrix}.$$

**Figure 7.44**

Symmetric root locus  
for DC servo system

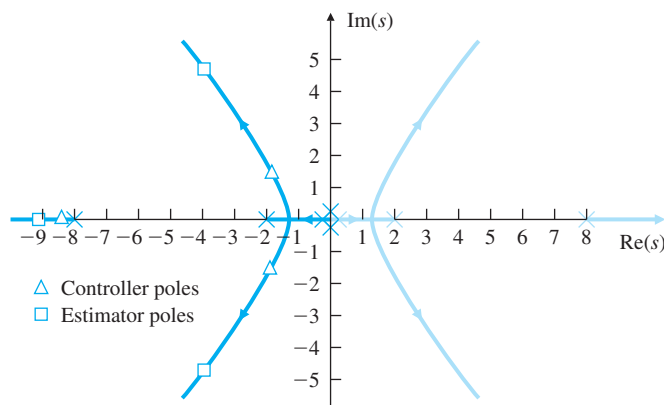
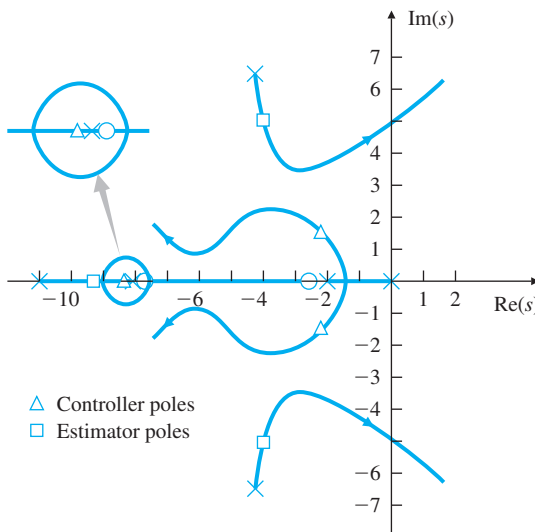


**Figure 7.45**

Root locus for pole assignment from the SRL



Notice the feedback gains are much smaller than before. The resulting compensator transfer function is computed from Eq. (7.174) to be

$$D_c(s) = -\frac{94.5(s + 7.98)(s + 2.52)}{(s + 4.28 \pm 6.42j)(s + 10.6)}.$$

We now take this compensator, put it in series with the plant, and use the compensator gain as the parameter. The resulting ordinary root locus of the closed-loop system is shown in Fig. 7.45. When the root-locus gain equals the nominal gain of 94.5, the roots are at the closed-loop locations selected from the SRL, as they should be. The step response and the associated control effort are shown in Fig. 7.46.

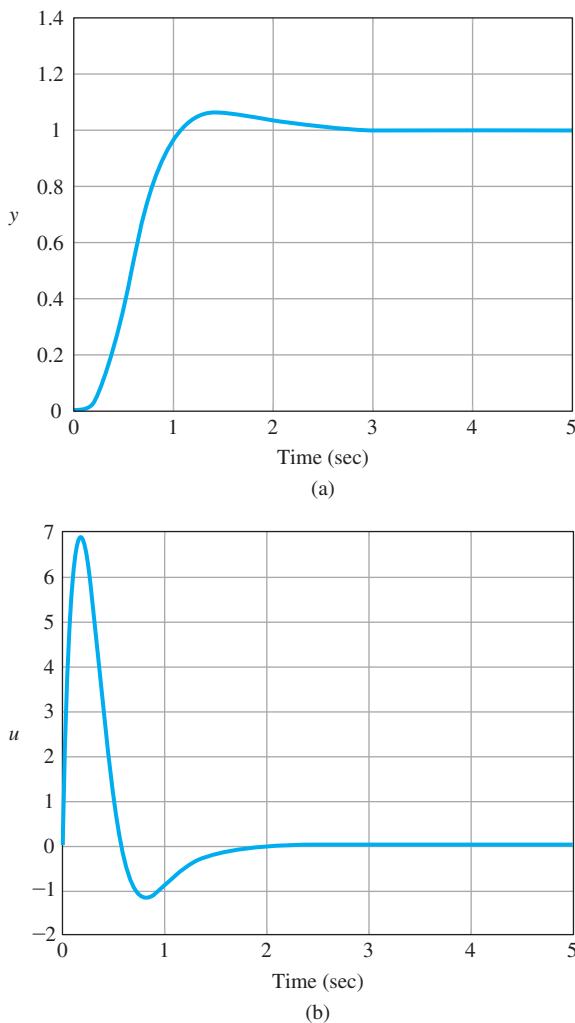
Note the compensator is now stable and minimum phase. This improved design comes about in large part because the plant pole at  $s = -8$  is virtually unchanged by either controller or estimator. It does not need to be changed for good performance; in fact, the only feature in need of repair in the original  $G(s)$  is the pole at  $s = 0$ . Using the SRL technique, we essentially discovered that the best use of control effort is to shift the two low-frequency poles at  $s = 0$  and  $-2$  and to leave the pole at  $s = -8$  virtually unchanged. As a result, the control gains are much lower, and the compensator design is less radical. This example illustrates why LQR design is typically preferable over pole placement.

---

Armed with the knowledge gained from Example 7.31, let us go back, with a better selection of poles, to investigate the use of pole placement for this example. Initially we used the third-order locations, which produced three poles with a natural frequency of about 2 rad/sec. This design moved the pole at  $s = -8$  to  $s = -1.4$ , thus violating the principle that open-loop poles should not be moved unless they are a problem.

**Figure 7.46**

Step response and control effort: (a) step response, (b) control signal



Now let us try it again, this time using dominant second-order locations to shift the slow poles, and leaving the fast pole alone at  $s = -8$ .

### EXAMPLE 7.32

#### *DC Servo System Redesign with Modified Dominant Second-Order Pole Locations*

Design a compensator for the DC servo system of Example 7.29 using pole placement with control poles given by

$$pc = [-1.7 \pm j; -8]$$

and the estimator poles given by

$$pe = [-7 \pm 3j; -8].$$

**Solution.** With these pole locations, we find that the required feedback gain is [using  $K = \text{place}(A, B, pc)$ ]

$$K = [-0.218 \quad 0.109 \quad 0.14],$$

which has a smaller magnitude than the case where the pole at  $s = -8$  was moved.

We find the estimator gain to be [using  $L_t = \text{place}(A, B, pe)$ ,  $L = L_t'$ ]

$$L = \begin{bmatrix} 12 \\ 154 \\ 464 \end{bmatrix}.$$

The compensator transfer function is computed from Eq. (7.174)

$$D_c = -\frac{79.13(s+8)(s+2.28)}{(s+11)(s+6.17 \pm 5.23j)},$$

which is stable and minimum phase. This example illustrates the value of judicious pole selection and of the SRL technique.

The poor pole selection inherent in the initial use of the poles results in higher control effort and produces an unstable compensator. Both of these undesirable features are eliminated using the SRL (or LQR), or by improved pole selection. But we really need to use SRL to guide the proper selection of poles. The bottom line is that *SRL (or LQR) is the method of choice!*

---

As seen from some of the preceding examples, we have shown the use of optimal design via the SRL. However, it is more common in practice to skip that step and use LQR directly.

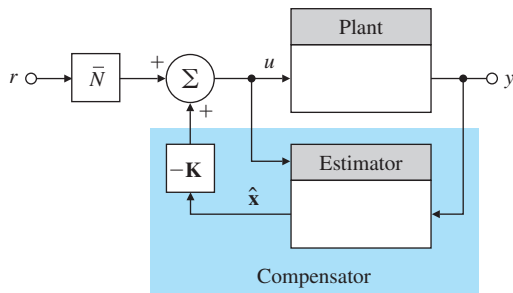
## 7.9 Introduction of the Reference Input with the Estimator

The controller obtained by combining the control law studied in Section 7.5 with the estimator discussed in Section 7.8 is essentially a **regulator design**. This means the characteristic equations of the control and the estimator are chosen for good disturbance rejection—that is, to give satisfactory transients to disturbances such as  $w(t)$ . However, this design approach does not consider a reference input, nor does it provide for **command following**, which is evidenced by a good transient response of the combined system to command changes. In general, good disturbance rejection and good command following both need to be taken into account in designing a control system. Good command following is done by properly introducing the reference input into the system equations.

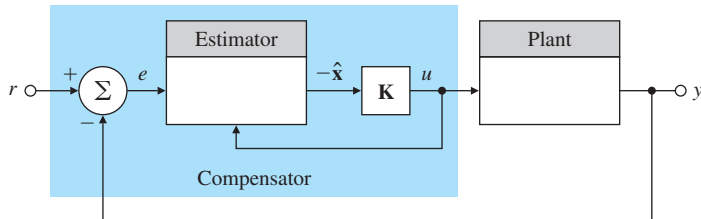
Let us repeat the plant and controller equations for the full-order estimator; the reduced-order case is the same in concept, differing only in detail:

**Figure 7.47**

Possible locations for introducing the command input:  
 (a) compensation in the feedback path;  
 (b) compensation in the feed-forward path



(a)



(b)

$$\text{Plant: } \dot{\mathbf{x}} = \mathbf{A}\mathbf{x} + \mathbf{B}u, \quad (7.183a)$$

$$y = \mathbf{C}\mathbf{x}; \quad (7.183b)$$

$$\text{Controller: } \dot{\hat{\mathbf{x}}} = (\mathbf{A} - \mathbf{B}\mathbf{K} - \mathbf{L}\mathbf{C})\hat{\mathbf{x}} + \mathbf{L}y, \quad (7.184a)$$

$$u = -\mathbf{K}\hat{\mathbf{x}}. \quad (7.184b)$$

Figure 7.47 shows two possibilities for introducing the command input  $r$  into the system. This figure illustrates the general issue of whether the compensation should be put in the feedback or feed-forward path. The response of the system to command inputs is different, depending on the configuration, because the zeros of the transfer functions are different. The closed-loop poles are identical, however, as can be easily verified by letting  $r = 0$  and noting the systems are then identical.

The difference in the responses of the two configurations can be seen quite easily. Consider the effect of a step input in  $r$ . In Fig. 7.47(a), the step will excite the estimator in precisely the same way that it excites the plant; thus the estimator error will remain zero during and after the step. This means that the estimator dynamics are not excited by the command input, so the transfer function from  $r$  to  $y$  must have zeros at the estimator pole locations that cancel those poles. As a result, a step command will excite system behavior that is consistent with the control poles alone—that is, with the roots of  $\det(s\mathbf{I} - \mathbf{A} + \mathbf{B}\mathbf{K}) = 0$ .

In Fig. 7.47(b), a step command in  $r$  enters directly only into the estimator, thus causing an estimation error that decays with the estimator dynamic characteristics in addition to the response corresponding to

the control poles. Therefore, a step command will excite system behavior consistent with both control roots and estimator roots—that is, the roots of

$$\det(s\mathbf{I} - \mathbf{A} + \mathbf{BK}) \cdot \det(s\mathbf{I} - \mathbf{A} + \mathbf{LC}) = 0.$$

For this reason, the configuration shown in Fig. 7.47(a) is typically the superior way to command the system, where  $\bar{N}$  is found using Eqs. (7.97)–(7.99).

In Section 7.9.1, we will show a general structure for introducing the reference input with three choices of parameters that implement either the feed-forward or the feedback case. We will analyze the three choices from the point of view of the system zeros and the implications the zeros have for the system transient response. Finally, in Section 7.9.2, we will show how to select the remaining parameter to eliminate constant errors.

### 7.9.1 General Structure for the Reference Input

Given a reference input  $r(t)$ , the most general linear way to introduce  $r$  into the system equations is to add terms proportional to it in the controller equations. We can do this by adding  $\bar{Nr}$  to Eq. (7.184b) and  $\mathbf{Mr}$  to Eq. (7.184a). Note in this case,  $\bar{N}$  is a scalar and  $\mathbf{M}$  is an  $n \times 1$  vector. With these additions, the **controller equations** become

$$\dot{\hat{x}} = (\mathbf{A} - \mathbf{BK} - \mathbf{LC})\hat{x} + \mathbf{Ly} + \mathbf{Mr}, \quad (7.185a)$$

$$u = -\mathbf{K}\hat{x} + \bar{Nr}. \quad (7.185b)$$

The block diagram is shown in Fig. 7.48(a). The alternatives shown in Fig. 7.47 correspond to different choices of  $\mathbf{M}$  and  $\bar{N}$ . Because  $r(t)$  is an external signal, it is clear that neither  $\mathbf{M}$  nor  $\bar{N}$  affects the characteristic equation of the combined controller-estimator system. In transfer-function terms, the selection of  $\mathbf{M}$  and  $\bar{N}$  will affect only the zeros of transmission from  $r$  to  $y$  and, as a consequence, can significantly affect the transient response but not the stability. How can we choose  $\mathbf{M}$  and  $\bar{N}$  to obtain satisfactory transient response? We should point out that we assigned the poles of the system by feedback gains  $\mathbf{K}$  and  $\mathbf{L}$ , and we are now going to assign zeros by feed-forward gains  $\mathbf{M}$  and  $\bar{N}$ .

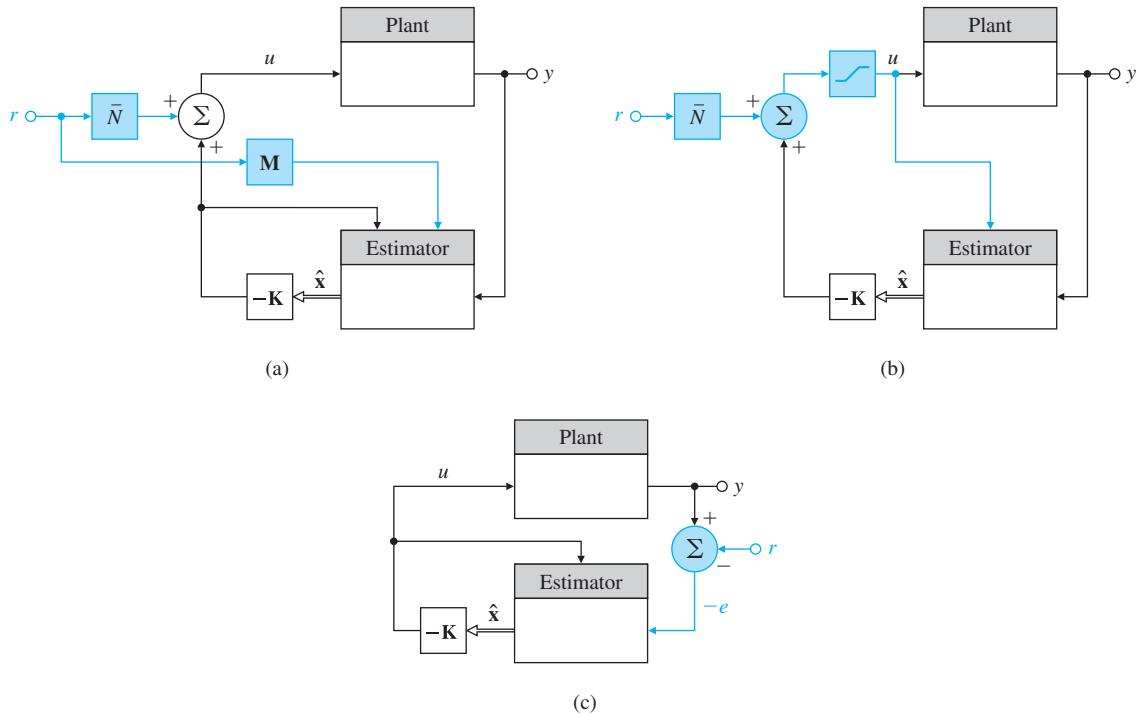
There are three strategies for choosing  $\mathbf{M}$  and  $\bar{N}$ :

1. *Autonomous estimator:* Select  $\mathbf{M}$  and  $\bar{N}$  so the state estimator error equation is independent of  $r$  [Fig. 7.48(b)].
2. *Tracking-error estimator:* Select  $\mathbf{M}$  and  $\bar{N}$  so only the tracking error,  $e = (r - y)$ , is used in the control [Fig. 7.48(c)].
3. *Zero-assignment estimator:* Select  $\mathbf{M}$  and  $\bar{N}$  so  $n$  of the zeros of the overall transfer function are assigned at places of the designer's choice [Fig. 7.48(a)].

CASE 1. From the viewpoint of estimator performance, the first method is quite attractive and the most widely used of the alternatives.

[Controller equations](#)

[Three methods for selecting  \$\mathbf{M}\$  and  \$\bar{N}\$](#)

**Figure 7.48**

Alternative ways to introduce the reference input: (a) general case—zero assignment; (b) standard case—estimator not excited, zeros =  $\alpha_e(s)$ ; (c) error-control case—classical compensation

If  $\hat{x}$  is to generate a good estimate of  $x$ , then surely  $\hat{x}$  should be as free of external excitation as possible; that is,  $\hat{x}$  should be uncontrollable from  $r$ . The computation of  $M$  and  $\bar{N}$  to bring this about is quite easy. The estimator error equation is found by subtracting Eq. (7.185a) from Eq. (7.183a), with the plant output [see Eq. (7.183b)] substituted into the estimator [see Eq. (7.184a)], and the control [see Eq. (7.184b)] substituted into the plant [see Eq. (7.183a)]:

$$\dot{\hat{x}} - \hat{x} = Ax + B(-K\hat{x} + \bar{N}r) - [(A - BK - LC)\hat{x} + Ly + Mr], \quad (7.186a)$$

$$\dot{\hat{x}} = (A - LC)\hat{x} + B\bar{N}r - Mr. \quad (7.186b)$$

If  $r$  is not to appear in Eq. (7.186a), then we should choose

$$M = B\bar{N}. \quad (7.187)$$

Because  $\bar{N}$  is a scalar,  $M$  is fixed to within a constant factor. Note with this choice of  $M$ , we can write the controller equations as

$$u = -K\hat{x} + \bar{N}r, \quad (7.188a)$$

$$\dot{\hat{x}} = (A - LC)\hat{x} + Bu + Ly, \quad (7.188b)$$

which matches the configuration in Fig. 7.48(b). The net effect of this choice is that the control is computed from the feedback gain and the reference input *before* it is applied, then the same control is input to both the plant and the estimator. In this form, if the plant control is subject to saturation (as shown by the inclusion of the saturation nonlinearity in Fig. 7.48(b) and discussed in Chapter 9), the same control limits can be applied in Eq. (7.188) to the control entering the equation for the estimate  $\hat{x}$ , and the nonlinearity cancels out of the  $\dot{\hat{x}}$  equation. This behavior is essential for proper estimator performance. The block diagram corresponding to this technique is shown in Fig. 7.48(b). We will return to the selection of the gain factor on the reference input,  $\bar{N}$ , in Section 7.9.2 after discussing the other two methods of selecting  $\mathbf{M}$ .

CASE 2. The second approach suggested earlier is to use the tracking error. This solution is sometimes forced on the control designer when the sensor measures only the output error. For example, in many thermostats, the output is the difference between the temperature to be controlled and the setpoint temperature, and there is no absolute indication of the reference temperature available to the controller. Also, some radar tracking systems have a reading that is proportional to the pointing error, and this error signal alone must be used for feedback control. In these situations, we must select  $\mathbf{M}$  and  $\bar{N}$  so Eqs. (7.188) are driven by the error only. This requirement is satisfied if we select

$$\bar{N} = 0 \quad \text{and} \quad \mathbf{M} = -\mathbf{L}. \quad (7.189)$$

Then the estimator equation is

$$\dot{\hat{x}} = (\mathbf{A} - \mathbf{B}\mathbf{K} - \mathbf{LC})\hat{x} + \mathbf{L}(y - r). \quad (7.190)$$

The compensator in this case, for low-order designs, is a standard lead compensator in the forward path. As we have seen in earlier chapters, this design can have a considerable amount of overshoot because of the zero of the compensator. This design corresponds exactly to the compensators designed by the transform methods given in Chapters 5 and 6.

CASE 3. The third method of selecting  $\mathbf{M}$  and  $\bar{N}$  is to choose the values so as to assign the system's zeros to arbitrary locations of the designer's choice. This method provides the designer with the maximum flexibility in satisfying transient-response and steady-state gain constraints. The other two methods are special cases of this third method. All three methods depend on the zeros. As we saw in Section 7.5.2, when there is no estimator and the reference input is added to the control, the closed-loop system zeros remain fixed as the zeros of the open-loop plant. We now examine what happens to the zeros when an estimator is present. To do so, we reconsider the controller of Eqs. (7.188). If there is a zero of transmission from  $r$  to  $u$ , then there is necessarily a zero of transmission from  $r$  to  $y$ , unless there is a pole at the same location as the zero. It is therefore sufficient to treat the controller alone to determine what effect the choices of  $\mathbf{M}$  and  $\bar{N}$  will have on the system zeros. The equations for a zero from  $r$  to  $u$  from Eqs. (7.188) are given by

$$\det \begin{bmatrix} s\mathbf{I} - \mathbf{A} + \mathbf{B}\mathbf{K} + \mathbf{L}\mathbf{C} & -\mathbf{M} \\ -\mathbf{K} & \bar{N} \end{bmatrix} = 0. \quad (7.191)$$

(We let  $y = 0$  because we care only about the effect of  $r$ .) If we divide the last column by the (nonzero) scalar  $\bar{N}$  then add to the rest the product of  $\mathbf{K}$  times the last column, we find that the feed-forward zeros are at the values of  $s$  such that

$$\det \begin{bmatrix} s\mathbf{I} - \mathbf{A} + \mathbf{B}\mathbf{K} + \mathbf{L}\mathbf{C} - \frac{\mathbf{M}}{\bar{N}}\mathbf{K} & -\frac{\mathbf{M}}{\bar{N}} \\ \mathbf{0} & 1 \end{bmatrix} = 0,$$

or

$$\det \left( s\mathbf{I} - \mathbf{A} + \mathbf{B}\mathbf{K} + \mathbf{L}\mathbf{C} - \frac{\mathbf{M}}{\bar{N}}\mathbf{K} \right) = \gamma(s) = 0. \quad (7.192)$$

Now Eq. (7.192) is exactly in the form of Eq. (7.133) for selecting  $\mathbf{L}$  to yield desired locations for the estimator poles. Arbitrary zero assignment is possible if the pair  $(\mathbf{A}-\mathbf{B}\mathbf{K}-\mathbf{L}\mathbf{C}, \mathbf{K})$  is observable. Here we have to select  $\mathbf{M}/\bar{N}$  for a desired zero polynomial  $\gamma(s)$  in the transfer function from the reference input to the control. Thus, the selection of  $\mathbf{M}$  provides a substantial amount of freedom to influence the transient response. We can add an arbitrary  $n$ th-order polynomial to the transfer function from  $r$  to  $u$  and hence from  $r$  to  $y$ ; that is, we can assign  $n$  zeros in addition to all the poles that we assigned previously. If the roots of  $\gamma(s)$  are not canceled by the poles of the system, then they will be included in zeros of transmission from  $r$  to  $y$ .

Two considerations can guide us in the choice of  $\mathbf{M}/\bar{N}$ —that is, in the location of the zeros. The first is dynamic response. We have seen in Chapter 3 that the zeros influence the transient response significantly, and the heuristic guidelines given there may suggest useful locations for the available zeros. The second consideration, which will connect state-space design to another result from transform techniques, is steady-state error or velocity-constant control. In Chapter 4, we derived the relationship between the steady-state accuracy of a Type 1 system and the closed-loop poles and zeros. If the system is Type 1, then the steady-state error to a step input will be zero and to a unit-ramp input will be

$$e_{\infty} = \frac{1}{K_v}, \quad (7.193)$$

where  $K_v$  is the velocity constant. Furthermore, it can be shown that if the *closed-loop* poles are at  $\{p_i\}$  and the *closed-loop* zeros are at  $\{z_i\}$ , then (for a Type 1 system) **Truxal's formula** gives

$$\frac{1}{K_v} = \sum \frac{1}{z_i} - \sum \frac{1}{p_i}. \quad (7.194)$$

Equation (7.194) forms the basis for a partial selection of  $\gamma(s)$ , and hence of  $\mathbf{M}$  and  $\bar{N}$ . The choice is based on two observations:

1. If  $|z_i - p_i| \ll 1$ , then the effect of this pole–zero pair on the dynamic response will be small, because the pole is almost canceled by the

zero, and in any transient the residue of the pole at  $p_i$  will be very small.

2. Even though  $z_i - p_i$  is small, it is possible for  $1/z_i - 1/p_i$  to be substantial and thus to have a significant influence on  $K_v$  according to Eq. (7.194). Application of these two guidelines to the selection of  $\gamma(s)$ , and hence of  $\mathbf{M}$  and  $\bar{N}$ , results in a lag-network design. We can illustrate this with an example.

## EXAMPLE 7.33

### *Servomechanism: Increasing the Velocity Constant through Zero Assignment*

Lag compensation by a state-space method

Consider the second-order servomechanism system described by

$$G(s) = \frac{1}{s(s+1)},$$

and with state description

$$\begin{aligned}\dot{x}_1 &= x_2, \\ \dot{x}_2 &= -x_2 + u.\end{aligned}$$

Design a controller using pole placement so both poles are at  $s = -2 \pm j2$  and the system has a velocity constant  $K_v = 10 \text{ sec}^{-1}$ . Verify the design by plotting the step response and the control effort. See Appendix W7.9 available online at [www.pearsonglobaleditions.com](http://www.pearsonglobaleditions.com) for a discrete implementation of the solution.

**Solution.** For this problem, the state feedback gain

$$\mathbf{K} = [8 \ 3],$$

results in the desired control poles. However, with this gain,  $K_v = 2 \text{ sec}^{-1}$ , and we need  $K_v = 10 \text{ sec}^{-1}$ . What effect will using estimators designed according to the three methods for  $\mathbf{M}$  and  $\bar{N}$  selection have on our design? Using the first strategy (the autonomous estimator), we find that the value of  $K_v$  does not change. If we use the second method (error control), we introduce a zero at a location unknown beforehand, and the effect on  $K_v$  will not be under direct design control. However, if we use the third option (zero placement) along with Truxal's formula [Eq. (7.194)], we can satisfy both the dynamic response and the steady-state requirements.

First, we must select the estimator pole  $p_3$  and the zero  $z_3$  to satisfy Eq. (7.194) for  $K_v = 10 \text{ sec}^{-1}$ . We want to keep  $z_3 - p_3$  small, so there is little effect on the dynamic response, and yet have  $1/z_3 - 1/p_3$  be large enough to increase the value of  $K_v$ . To do this, we arbitrarily set  $p_3$  small compared with the control dynamics. For example, we let

$$p_3 = -0.1.$$

Notice this approach is opposite to the usual philosophy of estimation design, where fast response is the requirement. Now, using Eq. (7.194) to get

$$\frac{1}{K_v} = \frac{1}{z_3} - \frac{1}{p_1} - \frac{1}{p_2} - \frac{1}{p_3},$$

where  $p_1 = -2 + 2j$ ,  $p_2 = -2 - 2j$ , and  $p_3 = -0.1$ , we solve for  $z_3$  such that  $K_v = 10$  we obtain

$$\frac{1}{K_v} = \frac{4}{8} + \frac{1}{0.1} + \frac{1}{z_3} = \frac{1}{10},$$

or

$$z_3 = -\frac{1}{10.4} = -0.096.$$

We thus design a reduced-order estimator to have a pole at  $-0.1$  and choose  $\mathbf{M}/\bar{N}$  such that  $\gamma(s)$  has a zero at  $-0.096$ . A block diagram of the resulting system is shown in Fig. 7.49(a). You can readily verify that this system has the overall transfer function

$$\frac{Y(s)}{R(s)} = \frac{8.32(s + 0.096)}{(s^2 + 4s + 8)(s + 0.1)}, \quad (7.195)$$

for which  $K_v = 10 \text{ sec}^{-1}$ , as specified.

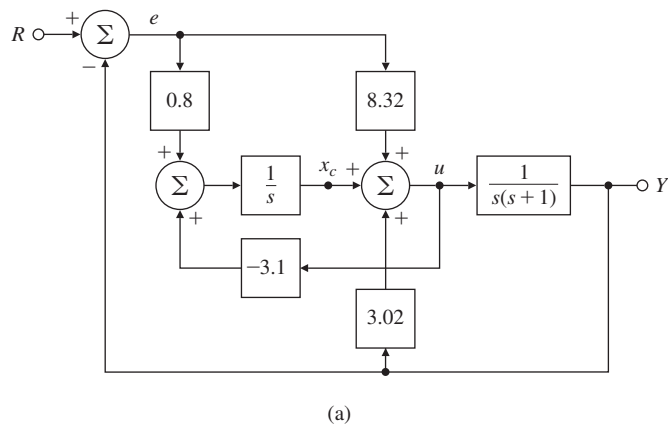
The compensation shown in Fig. 7.49(a) is nonclassical in the sense that it has two inputs ( $e$  and  $y$ ) and one output. If we resolve the equations to provide pure error compensation by finding the transfer function from  $e$  and  $u$ , which would give Eq. (7.195), we obtain the system shown in Fig. 7.49(b). This can be seen as follows: The relevant controller equations are

$$\dot{x}_c = 0.8 e - 3.1 u,$$

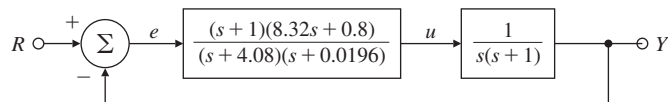
$$u = 8.32 e + 3.02 y + x_c,$$

**Figure 7.49**

Servomechanism with assigned zeros (a lag network): (a) the two-input compensator; (b) equivalent unity-feedback system

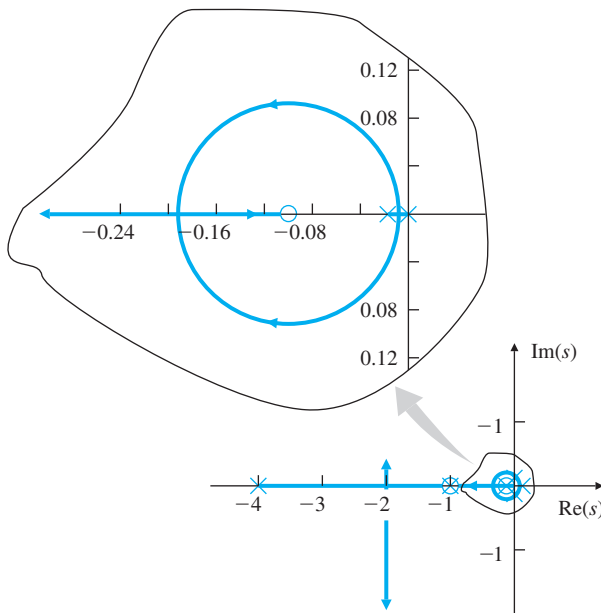


(a)



(b)

**Figure 7.50**  
Root locus of lag–lead compensation



where  $x_c$  is the controller state. Taking the Laplace transform of these equations, eliminating  $X_c(s)$ , and substituting for the output [ $Y(s) = G(s)U(s)$ ], we find the compensator is described by

$$\frac{U(s)}{E(s)} = D_c(s) = \frac{(s + 1)(8.32s + 0.8)}{(s + 4.08)(s + 0.0196)}.$$

This compensation is a classical lag–lead network. The root locus of the system in Fig. 7.49(b) is shown in Fig. 7.50. Note the pole–zero pattern near the origin that is characteristic of a lag network. The Bode plot in Fig. 7.51 shows the phase lag at low frequencies and the phase lead at high frequencies. The step response of the system is shown in Fig. 7.52 (a) and shows the presence of a “tail” on the response due to the slow pole at  $-0.1$ . The associated control effort is shown in Fig. 7.52 (b). Of course, the system is Type 1 and the system will have zero tracking error eventually.

---

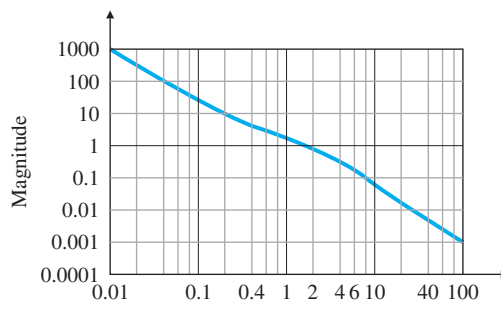
We now reconsider the first two methods for choosing  $\mathbf{M}$  and  $\bar{\mathbf{N}}$ , this time to examine their implications in terms of zeros. Under the first rule (for the autonomous estimator), we let  $\mathbf{M} = \mathbf{B}\bar{\mathbf{N}}$ . Substituting this into Eq. (7.192) yields, for the controller feed-forward zeros,

$$\det(s\mathbf{I} - \mathbf{A} + \mathbf{LC}) = 0. \quad (7.196)$$

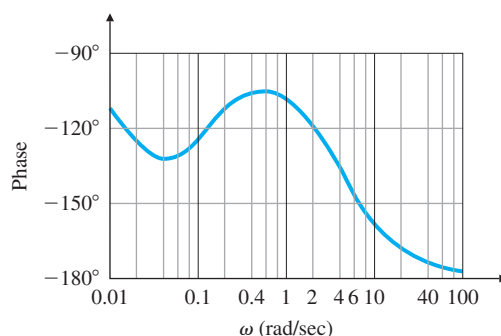
This is exactly the equation from which  $\mathbf{L}$  was selected to make the characteristic polynomial of the estimator equation equal to  $\alpha_e(s)$ . Thus we have created  $n$  zeros in exactly the same locations as the  $n$  poles of the

**Figure 7.51**

Frequency response of lag-lead compensation



(a)



(b)

estimator. Because of this pole-zero cancellation (which causes “uncontrollability” of the estimator modes), the overall transfer function poles consist only of the state feedback controller poles.

The second rule (for a tracking-error estimator) selects  $\mathbf{M} = -\mathbf{L}$  and  $\bar{N} = 0$ . If these are substituted into Eq. (7.191), then the feed-forward zeros are given by

$$\det \begin{bmatrix} s\mathbf{I} - \mathbf{A} + \mathbf{B}\mathbf{K} + \mathbf{L}\mathbf{C} & \mathbf{L} \\ -\mathbf{K} & 0 \end{bmatrix} = 0. \quad (7.197)$$

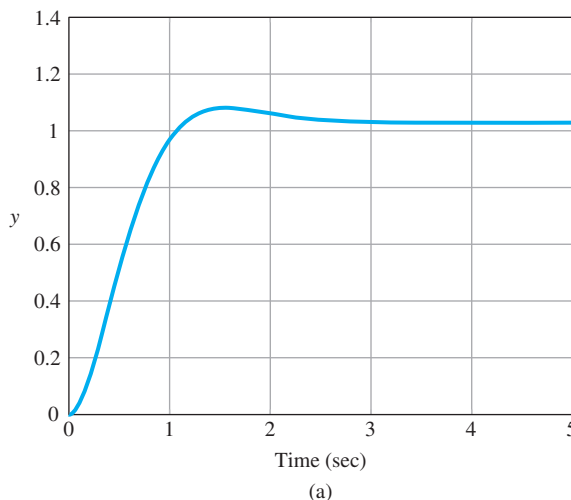
If we postmultiply the last column by  $\mathbf{C}$  and subtract the result from the first  $n$  columns, then premultiply the last row by  $\mathbf{B}$  and add it to the first  $n$  rows, Eq. (7.197) reduces to

$$\det \begin{bmatrix} s\mathbf{I} - \mathbf{A} & \mathbf{L} \\ -\mathbf{K} & 0 \end{bmatrix} = 0. \quad (7.198)$$

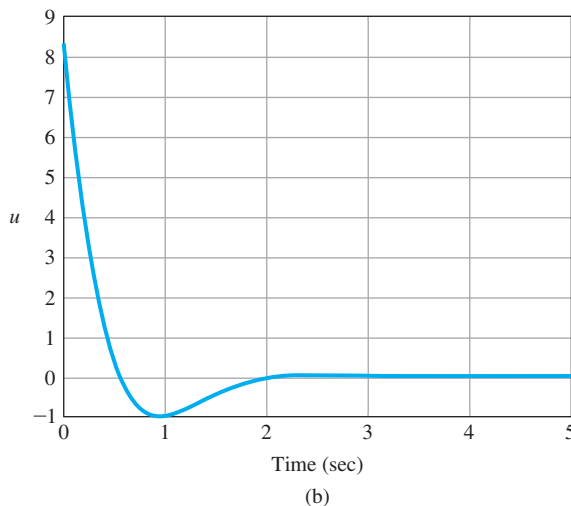
If we compare Eq. (7.198) with the equations for the zeros of a system in a state description, Eq. (7.63), we see the added zeros are those obtained by replacing the input matrix with  $\mathbf{L}$  and the output with  $\mathbf{K}$ . Thus, if we wish to use error control, we have to accept the presence of these compensator zeros that depend on the choice of  $\mathbf{K}$  and  $\mathbf{L}$  and over which we have no direct control. For low-order cases this results, as we said before, in a lead compensator as part of a unity feedback topology.

**Figure 7.52**

Response of the system with lag compensation:  
 (a) step response;  
 (b) control effort



(a)



(b)

**Transfer function for the closed-loop system when reference input is included in controller**

Let us now summarize our findings on the effect of introducing the reference input. When the reference input signal is included in the controller, the overall transfer function of the closed-loop system is

$$\mathcal{T}(s) = \frac{Y(s)}{R(s)} = \frac{K_s \gamma(s) b(s)}{\alpha_e(s) \alpha_c(s)}, \quad (7.199)$$

where  $K_s$  is the total system gain and  $\gamma(s)$  and  $b(s)$  are monic polynomials. The polynomial  $\alpha_c(s)$  results in a control gain  $\mathbf{K}$  such that  $\det[s\mathbf{I} - \mathbf{A} + \mathbf{B}\mathbf{K}] = \alpha_c(s)$ . The polynomial  $\alpha_e(s)$  results in estimator gains  $\mathbf{L}$  such that  $\det[s\mathbf{I} - \mathbf{A} + \mathbf{L}\mathbf{C}] = \alpha_e(s)$ . Because, as designers, we get to choose  $\alpha_c(s)$  and  $\alpha_e(s)$ , we have complete freedom in assigning the poles of the closed-loop system. There are three ways to handle the

polynomial  $\gamma(s)$ : We can select it so  $\gamma(s) = \alpha_e(s)$  by using the implementation of Fig. 7.48(b), in which case  $\mathbf{M}/\bar{N}$  is given by Eq. (7.187); we may accept  $\gamma(s)$  as given by Eq. (7.198), so error control is used; or we may give  $\gamma(s)$  arbitrary coefficients by selecting  $\mathbf{M}/\bar{N}$  from Eq. (7.192). It is important to point out that the plant zeros represented by  $b(s)$  are not moved by this technique, and remain as part of the closed-loop transfer function unless  $\alpha_c$  or  $\alpha_e$  are selected to cancel some of these zeros.

### 7.9.2 Selecting the Gain

We now turn to the process of determining the gain  $\bar{N}$  for the three methods of selecting  $\mathbf{M}$ . If we choose method 1, the control is given by Eq. (7.188a) and  $\hat{x}_{ss} = x_{ss}$ . Therefore, we can use either  $\bar{N} = N_u + \mathbf{K}\mathbf{N}_x$ , as in Eq. (7.99), or  $u = N_u r - \mathbf{K}(\hat{x} - \mathbf{N}_x r)$ . *This is the most common choice.* If we use the second method, the result is trivial; recall that  $\bar{N} = 0$  for error control. If we use the third method, we pick  $\bar{N}$  such that the overall closed-loop DC gain is unity.<sup>9</sup>

The overall system equations then are

$$\begin{bmatrix} \dot{\tilde{x}} \\ \dot{\tilde{x}} \end{bmatrix} = \begin{bmatrix} \mathbf{A} - \mathbf{B}\mathbf{K} & \mathbf{B}\mathbf{K} \\ \mathbf{0} & \mathbf{A} - \mathbf{L}\mathbf{C} \end{bmatrix} \begin{bmatrix} \mathbf{x} \\ \tilde{\mathbf{x}} \end{bmatrix} + \begin{bmatrix} \mathbf{B} \\ \mathbf{B} - \bar{\mathbf{M}} \end{bmatrix} \bar{N}r, \quad (7.200a)$$

$$y = [\mathbf{C} \quad \mathbf{0}] \begin{bmatrix} \mathbf{x} \\ \tilde{\mathbf{x}} \end{bmatrix}, \quad (7.200b)$$

where  $\bar{\mathbf{M}}$  is the outcome of selecting zero locations with either Eq. (7.192) or Eq. (7.187). The closed-loop system has unity DC gain if

$$-[\mathbf{C} \quad \mathbf{0}] \begin{bmatrix} \mathbf{A} - \mathbf{B}\mathbf{K} & \mathbf{B}\mathbf{K} \\ \mathbf{0} & \mathbf{A} - \mathbf{L}\mathbf{C} \end{bmatrix}^{-1} \begin{bmatrix} \mathbf{B} \\ \mathbf{B} - \bar{\mathbf{M}} \end{bmatrix} \bar{N} = 1. \quad (7.201)$$

If we solve Eq. (7.201) for  $\bar{N}$ , we get<sup>10</sup>

$$\bar{N} = -\frac{1}{\mathbf{C}(\mathbf{A} - \mathbf{B}\mathbf{K})^{-1}\mathbf{B}[1 - \mathbf{K}(\mathbf{A} - \mathbf{L}\mathbf{C})^{-1}(\mathbf{B} - \bar{\mathbf{M}})]}. \quad (7.202)$$

The techniques in this section can be readily extended to reduced-order estimators.

<sup>9</sup>A reasonable alternative is to select  $\bar{N}$  such that, when  $r$  and  $y$  are both unchanging, the DC gain from  $r$  to  $u$  is the *negative* of the DC gain from  $y$  to  $u$ . The consequences of this choice are that our controller can be structured as a combination of error control and generalized derivative control, and if the system is capable of Type 1 behavior, that capability will be realized.

<sup>10</sup>We have used the fact that

$$\begin{bmatrix} \mathbf{A} & \mathbf{C} \\ \mathbf{0} & \mathbf{B} \end{bmatrix}^{-1} = \begin{bmatrix} \mathbf{A}^{-1} & -\mathbf{A}^{-1}\mathbf{C}\mathbf{B}^{-1} \\ \mathbf{0} & \mathbf{B}^{-1} \end{bmatrix}.$$

## 7.10 Integral Control and Robust Tracking

The choices of  $\bar{N}$  gain in Section 7.9 will result in zero steady-state error to a step command, but the result is not robust because any change in the plant parameters will cause the error to be nonzero. We need to use integral control to obtain robust tracking.

In the state-space design methods discussed so far, no mention has been made of integral control, and no design examples have produced a compensation containing an integral term. In Section 7.10.1, we will show how integral control can be introduced by a direct method of adding the integral of the system error to the dynamic equations. Integral control is a special case of tracking a signal that does not go to zero in the steady-state. We will introduce (in Section 7.10.2) a general method for robust tracking that will present the internal model principle, which solves an entire class of tracking problems and disturbance-rejection controls. Finally, in Section 7.10.4, we will show that if the system has an estimator and also needs to reject a disturbance of known structure, we can include a model of the disturbance in the estimator equations and use the computer estimate of the disturbance to cancel the effects of the real plant disturbance on the output.

### 7.10.1 Integral Control

We start with an *ad hoc* solution to integral control by augmenting the state vector with the integrator dynamics. For the system

$$\dot{\mathbf{x}} = \mathbf{Ax} + \mathbf{Bu} + \mathbf{B}_1 w, \quad (7.203a)$$

$$y = \mathbf{Cx}, \quad (7.203b)$$

we can feed back the integral of the error,<sup>11</sup>  $e = y - r$ , as well as the state of the plant,  $\mathbf{x}$ , by augmenting the plant state with the extra (integral) state  $x_I$ , which obeys the differential equation

$$\dot{x}_I = \mathbf{Cx} - r (= e).$$

Thus

$$x_I = \int^t e(\tau) d\tau.$$

The augmented state equations become

$$\begin{bmatrix} \dot{x}_I \\ \dot{\mathbf{x}} \end{bmatrix} = \begin{bmatrix} 0 & \mathbf{C} \\ \mathbf{0} & \mathbf{A} \end{bmatrix} \begin{bmatrix} x_I \\ \mathbf{x} \end{bmatrix} + \begin{bmatrix} 0 \\ \mathbf{B} \end{bmatrix} u - \begin{bmatrix} 1 \\ \mathbf{0} \end{bmatrix} r + \begin{bmatrix} 0 \\ \mathbf{B}_1 \end{bmatrix} w, \quad (7.204)$$

and the feedback law is

$$u = -[K_1 \ K_0] \begin{bmatrix} x_I \\ \mathbf{x} \end{bmatrix},$$

or simply

$$u = -\mathbf{K} \begin{bmatrix} x_I \\ \mathbf{x} \end{bmatrix}.$$

**Augmented state equations with integral control**

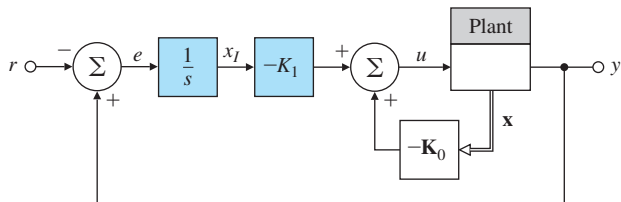
**Feedback law with integral control**

---

<sup>11</sup>Watch out for the sign here; we are using the negative of the usual convention.

**Figure 7.53**

Integral control structure



With this revised definition of the system, we can apply the design techniques from Section 7.5 in a similar fashion; they will result in the control structure shown in Fig. 7.53.

### EXAMPLE 7.34

#### *Integral Control of a Motor Speed System*

Consider the motor speed system described by

$$\frac{Y(s)}{U(s)} = \frac{1}{s+3},$$

that is,  $A = -3$ ,  $B = 1$ , and  $C = 1$ . Design the system to have integral control and two poles at  $s = -5$ . Design an estimator with pole at  $s = -10$ . The disturbance enters at the same place as the control. Evaluate the tracking and disturbance rejection responses.

**Solution.** The pole-placement requirement is equivalent to

$$pc = [-5; -5].$$

The augmented system description, including the disturbance  $w$ , is

$$\begin{bmatrix} \dot{x}_I \\ \dot{x} \end{bmatrix} = \begin{bmatrix} 0 & 1 \\ 0 & -3 \end{bmatrix} \begin{bmatrix} x_I \\ x \end{bmatrix} + \begin{bmatrix} 0 \\ 1 \end{bmatrix} (u + w) - \begin{bmatrix} 1 \\ 0 \end{bmatrix} r.$$

Therefore, we can find  $\mathbf{K}$  from

$$\det \left( s\mathbf{I} - \begin{bmatrix} 0 & 1 \\ 0 & -3 \end{bmatrix} + \begin{bmatrix} 0 \\ 1 \end{bmatrix} \mathbf{K} \right) = s^2 + 10s + 25,$$

or

$$s^2 + (3 + K_0)s + K_1 = s^2 + 10s + 25.$$

Consequently,

$$\mathbf{K} = [ K_1 \ K_0 ] = [ 25 \ 7 ].$$

We may verify this result using acker. The system is shown with feed-backs in Fig. 7.54, along with a disturbance input  $w$ .

The estimator gain  $L = 7$  is obtained from

$$\alpha_e(s) = s + 10 = s + 3 + L.$$

The estimator equation is of the form

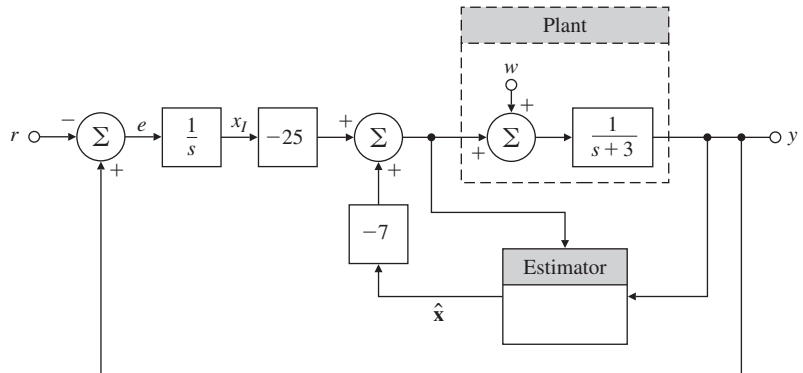
$$\begin{aligned} \dot{\hat{x}} &= (A - LC)\hat{x} + Bu + Ly \\ &= -10\hat{x} + u + 7y, \end{aligned}$$

and

$$u = -K_0\hat{x} = -7\hat{x}.$$

**Figure 7.54**

Integral control example



The step response  $y_1$  due to a step reference input  $r$  and the output disturbance response  $y_2$  due to a step disturbance input  $w$  are shown in Fig. 7.55(a), and the associated control efforts ( $u_1$  and  $u_2$ ) are shown in Fig. 7.55(b). As expected, the system is Type 1 and tracks the step reference input and rejects the step disturbance asymptotically.

### △ 7.10.2 Robust Tracking Control: The Error-Space Approach

In Section 7.10.1, we introduced integral control in a direct way and selected the structure of the implementation so as to achieve integral action with respect to reference and disturbance inputs. We now present a more analytical approach to giving a control system the ability to track (with zero steady-state error) a nondecaying input and to reject (with zero steady-state error) a nondecaying disturbance such as a step, ramp, or sinusoidal input. The method is based on including the equations satisfied by these external signals as part of the problem formulation and solving the problem of control in an **error space**, so we are assured that the error approaches zero even if the output is following a nondecaying, or even a growing, command (such as a ramp signal) and even if some parameters change (the robustness property). The method is illustrated in detail for signals that satisfy differential equations of order 2, but the extension to more complex signals is not difficult.

Suppose we have the system state equations

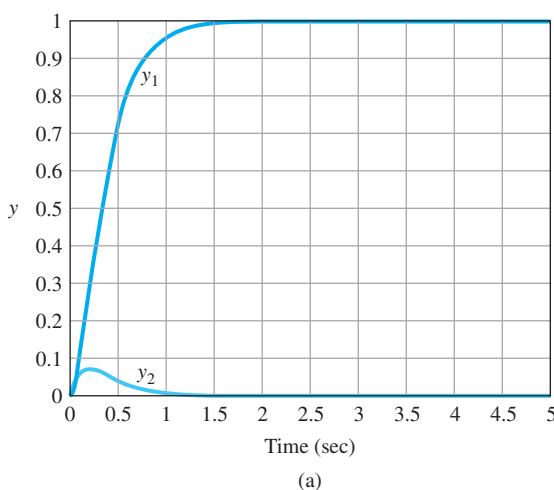
$$\dot{\mathbf{x}} = \mathbf{A}\mathbf{x} + \mathbf{B}u + \mathbf{B}_1w, \quad (7.205a)$$

$$y = \mathbf{C}\mathbf{x}, \quad (7.205b)$$

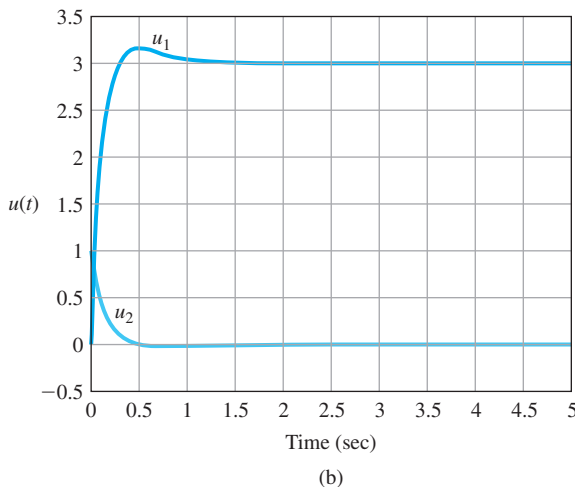
and a reference signal that is known to satisfy a specific differential equation. The initial conditions on the equation generating the input are unknown. For example, the input could be a ramp whose slope and initial value are unknown. Plant disturbances of the same class may also be present. We wish to design a controller for this system so the closed-loop system will have specified poles, and can also track input command

**Figure 7.55**

Transient response for motor speed system:  
 (a) step responses;  
 (b) control efforts



(a)



(b)

signals, and reject disturbances of the type described without steady-state error. We will develop the results only for second-order differential equations. We define the reference input to satisfy the relation

$$\ddot{r} + \alpha_1 \dot{r} + \alpha_2 r = 0, \quad (7.206)$$

and the disturbance to satisfy exactly the same equation:

$$\ddot{w} + \alpha_1 \dot{w} + \alpha_2 w = 0. \quad (7.207)$$

The (tracking) error is defined as

$$e = y - r. \quad (7.208)$$

[The meaning of robust control](#)

The problem of tracking  $r$  and rejecting  $w$  can be seen as an exercise in designing a control law to provide *regulation of the error*, which is to say that the error  $e$  tends to zero as time gets large. The control must also be **structurally stable** or **robust**, in the sense that regulation of  $e$  to zero in the steady-state occurs even in the presence of “small” perturbations

of the original system parameters. Note that, in practice, we never have a perfect model of the plant, and the values of parameters are virtually always subject to some change, so robustness is always very important.

We know that the command input satisfies Eq. (7.206), and we would like to eliminate the reference from the equations in favor of the error. We begin by replacing  $r$  in Eq. (7.206) with the error of Eq. (7.208). When we do this, the reference cancels because of Eq. (7.206), and we have the formula for the error in terms of the state:

$$\ddot{e} + \alpha_1 \dot{e} + \alpha_2 e = \ddot{y} + \alpha_1 \dot{y} + \alpha_2 y \quad (7.209a)$$

$$= \mathbf{C}\ddot{\mathbf{x}} + \alpha_1 \mathbf{C}\dot{\mathbf{x}} + \alpha_2 \mathbf{C}\mathbf{x}. \quad (7.209b)$$

We now replace the plant state vector with the error-space state, defined by

$$\xi \stackrel{\Delta}{=} \ddot{\mathbf{x}} + \alpha_1 \dot{\mathbf{x}} + \alpha_2 \mathbf{x}. \quad (7.210)$$

Similarly, we replace the control with the control in error space, defined as

$$\mu \stackrel{\Delta}{=} \ddot{u} + \alpha_1 \dot{u} + \alpha_2 u. \quad (7.211)$$

With these definitions, we can replace Eq. (7.209b) with

$$\ddot{e} + \alpha_1 \dot{e} + \alpha_2 e = \mathbf{C}\xi. \quad (7.212)$$

The state equation for  $\xi$  is given by<sup>12</sup>

$$\dot{\xi} = \ddot{\mathbf{x}} + \alpha_1 \dot{\mathbf{x}} + \alpha_2 \mathbf{x} = \mathbf{A}\xi + \mathbf{B}\mu. \quad (7.213)$$

Notice the disturbance, as well as the reference, cancels from Eq. (7.213). Equations (7.212) and (7.213) now describe the overall system in an error space. In standard state-variable form, the equations are

$$\dot{\mathbf{z}} = \mathbf{A}_s \mathbf{z} + \mathbf{B}_s \mu, \quad (7.214)$$

where  $\mathbf{z} = [ e \quad \dot{e} \quad \xi^T ]^T$  and

$$\mathbf{A}_s = \begin{bmatrix} 0 & 1 & \mathbf{0} \\ -\alpha_2 & -\alpha_1 & \mathbf{C} \\ \mathbf{0} & \mathbf{0} & \mathbf{A} \end{bmatrix}, \quad \mathbf{B}_s = \begin{bmatrix} 0 \\ 0 \\ \mathbf{B} \end{bmatrix}. \quad (7.215)$$

The error system  $(\mathbf{A}_s, \mathbf{B}_s)$  can be given arbitrary dynamics by state feedback if it is controllable. If the plant  $(\mathbf{A}, \mathbf{B})$  is controllable and does not have a zero at any of the roots of the reference-signal characteristic equation

$$\alpha_r(s) = s^2 + \alpha_1 s + \alpha_2,$$

then the error system  $(\mathbf{A}_s, \mathbf{B}_s)$  is controllable.<sup>13</sup> We assume these conditions hold; therefore, there exists a control law of the form

$$\mu = -[ K_2 \quad K_1 \quad \mathbf{K}_0 ] \begin{bmatrix} e \\ \dot{e} \\ \xi \end{bmatrix} = -\mathbf{K}\mathbf{z}, \quad (7.216)$$

<sup>12</sup>Notice this concept can be extended to more complex equations in  $r$  and to multivariable systems.

<sup>13</sup>For example, it is not possible to add integral control to a plant that has a zero at the origin.

Robust control equations  
in the error space

such that the error system has arbitrary dynamics by pole placement. We now need to express this control law in terms of the actual process state  $\mathbf{x}$  and the actual control. We combine Eqs. (7.216), (7.210), and (7.211) to get the control law in terms of  $u$  and  $\mathbf{x}$  (we write  $u^{(2)}$  to mean  $\frac{d^2u}{dt^2}$ ):

$$(u + \mathbf{K}_0\mathbf{x})^{(2)} + \sum_{i=1}^2 \alpha_i(u + \mathbf{K}_0\mathbf{x})^{(2-i)} = -\sum_{i=1}^2 K_i e^{(2-i)}. \quad (7.217)$$

The structure for implementing Eq. (7.217) is very simple for tracking constant inputs. In that case, the equation for the reference input is  $\dot{r} = 0$ . In terms of  $u$  and  $\mathbf{x}$ , the control law [Eq. (7.217)] reduces to

$$\dot{u} + \mathbf{K}_0\dot{\mathbf{x}} = -K_1 e. \quad (7.218)$$

Here we need only to integrate to reveal the control law and the action of integral control:

$$u = -K_1 \int^t e(\tau) d\tau - \mathbf{K}_0\mathbf{x}. \quad (7.219)$$

A block diagram of the system, shown in Fig. 7.56, clearly shows the presence of a pure integrator in the controller. In this case, the only difference between the internal model method of Fig. 7.56 and the *ad hoc* method of Fig. 7.54 is the relative location of the integrator and the gain.

A more complex problem that clearly shows the power of the error-space approach to robust tracking is posed by requiring that a sinusoid be tracked with zero steady-state error. The problem arises, for instance, in the control of a mass-storage disk-head assembly.

### EXAMPLE 7.35

#### *Disk-Drive Servomechanism: Robust Control to Follow a Sinusoid*

A simple normalized model of a computer disk-drive servomechanism is given by the equations

$$\begin{aligned} \mathbf{A} &= \begin{bmatrix} 0 & 1 \\ 0 & -1 \end{bmatrix}, & \mathbf{B} &= \begin{bmatrix} 0 \\ 1 \end{bmatrix}, \\ \mathbf{B}_1 &= \begin{bmatrix} 0 \\ 1 \end{bmatrix}, & \mathbf{C} &= [1 \ 0], \quad D = 0. \end{aligned}$$

**Figure 7.56**

Integral control using the internal model

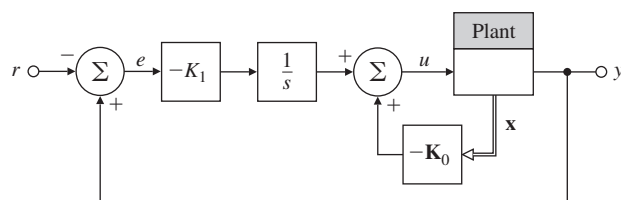
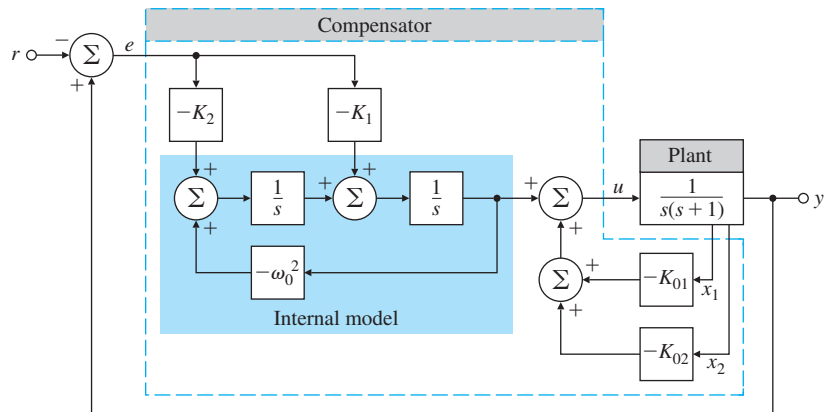


**Figure 7.57**

Structure of the compensator for the servomechanism to track exactly the sinusoid of frequency  $\omega_0$



Because the data on the disk are not exactly on a centered circle, the servo must follow a sinusoid of radian frequency  $\omega_0$  determined by the spindle speed.

- Give the structure of a controller for this system that will follow the given reference input with zero steady-state error.
- Assume  $\omega_0 = 1$  and the desired closed-loop poles are at  $-1 \pm j\sqrt{3}$  and  $-\sqrt{3} \pm j1$ .
- Demonstrate the tracking and disturbance rejection properties of the system using Matlab or Simulink.

### Solution

- The reference input satisfies the differential equation  $\ddot{r} = -\omega_0^2 r$  so  $\alpha_1 = 0$  and  $\alpha_2 = \omega_0^2$ . With these values, the error-state matrices, according to Eq. (7.215), are

$$\mathbf{A}_s = \begin{bmatrix} 0 & 1 & 0 & 0 \\ -\omega_0^2 & 0 & 1 & 0 \\ 0 & 0 & 0 & 1 \\ 0 & 0 & 0 & -1 \end{bmatrix}, \quad \mathbf{B}_s = \begin{bmatrix} 0 \\ 0 \\ 0 \\ 1 \end{bmatrix}.$$

The characteristic equation of  $\mathbf{A}_s - \mathbf{B}_s \mathbf{K}$  is

$$s^4 + (1 + K_{02})s^3 + (\omega_0^2 + K_{01})s^2 + [K_1 + \omega_0^2(1 + K_{02})]s + K_{01}\omega_0^2 K_2 = 0,$$

from which the gain may be selected by pole assignment. The compensator implementation from Eq. (7.217) has the structure shown in Fig. 7.57, which clearly shows the presence of the oscillator with frequency  $\omega_0$  (known as the **internal model of the input generator**) in the controller.<sup>14</sup>

**Internal model principle**

<sup>14</sup>This is a particular case of the **internal model principle**, which requires that a model of the external or exogenous signal be in the controller for robust tracking and disturbance rejection. (see Francis and Wonham (1975) for a systematic treatment of this topic.)

- (b) Now, assume  $\omega_0 = 1$  rad/sec and the desired closed-loop poles are as given:

$$\mathbf{pc} = [-1 + j\sqrt{3}; -1 - j\sqrt{3}; -\sqrt{3} + j; -\sqrt{3} - j].$$

Then the feedback gain is

$$\mathbf{K} = [K_2 \ K_1 : \mathbf{K}_0] = [2.0718 \ 16.3923 : 13.9282 \ 4.4641],$$

which results in the controller

$$\begin{aligned}\dot{\mathbf{x}}_c &= \mathbf{A}_c \mathbf{x}_c + \mathbf{B}_c e, \\ u &= \mathbf{C}_c \mathbf{x}_c - \mathbf{K}_0 \mathbf{x},\end{aligned}$$

with

$$\begin{aligned}\mathbf{A}_c &= \begin{bmatrix} 0 & 1 \\ -1 & 0 \end{bmatrix}, & \mathbf{B}_c &= \begin{bmatrix} -16.3923 \\ -2.0718 \end{bmatrix}, \\ \mathbf{C}_c &= [ \quad 1 \quad 0 ].\end{aligned}$$

The relevant Matlab statements are

```
% plant matrices
A=[0 1; 0 -1];
B=[0;1];
C=[1 0];
D=[0];
% form error space matrices
omega=1;
As=[0 1 0 0; -omega*omega 0 1 0; 0 0 0 1; 0 0 0 -1];
Bs=[0;0;B];

% desired closed-loop poles
j=sqrt(-1);
pc=[-1+sqrt(3)*j ; -1-sqrt(3)*j; -sqrt(3)+j; -sqrt(3)-j];
K=place(As,Bs,pc);
% form controller matrices
K1=K(:,1:2);
Ko=K(:,3:4);
Ac=[0 1; -omega*omega 0];
Bc=-[K(2);K(1)];
Cc=[1 0];
Dc=[0];
```

The controller frequency response is shown in Fig. 7.58 and shows a gain of infinity at the rotation frequency of  $\omega_0 = 1$  rad/sec. The frequency response from  $r$  to  $e$  [that is, the sensitivity function  $S(s)$ ], is shown in Fig. 7.59 and reveals a sharp notch at the rotation frequency  $\omega_0 = 1$  rad/sec. The same notch is also present in the frequency response of the transfer function from  $w$  to  $y$ .

**Figure 7.58**  
Controller frequency response for robust servomechanism

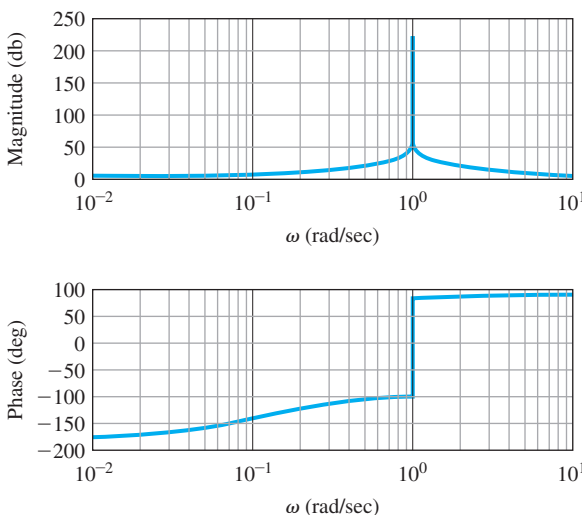
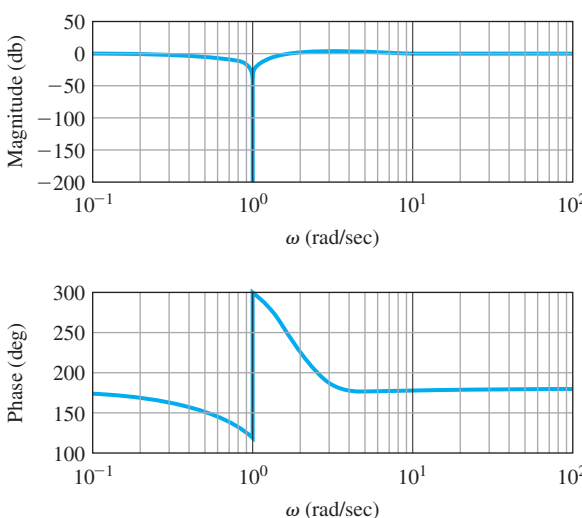


**Figure 7.59**  
Sensitivity function frequency response for robust servomechanism

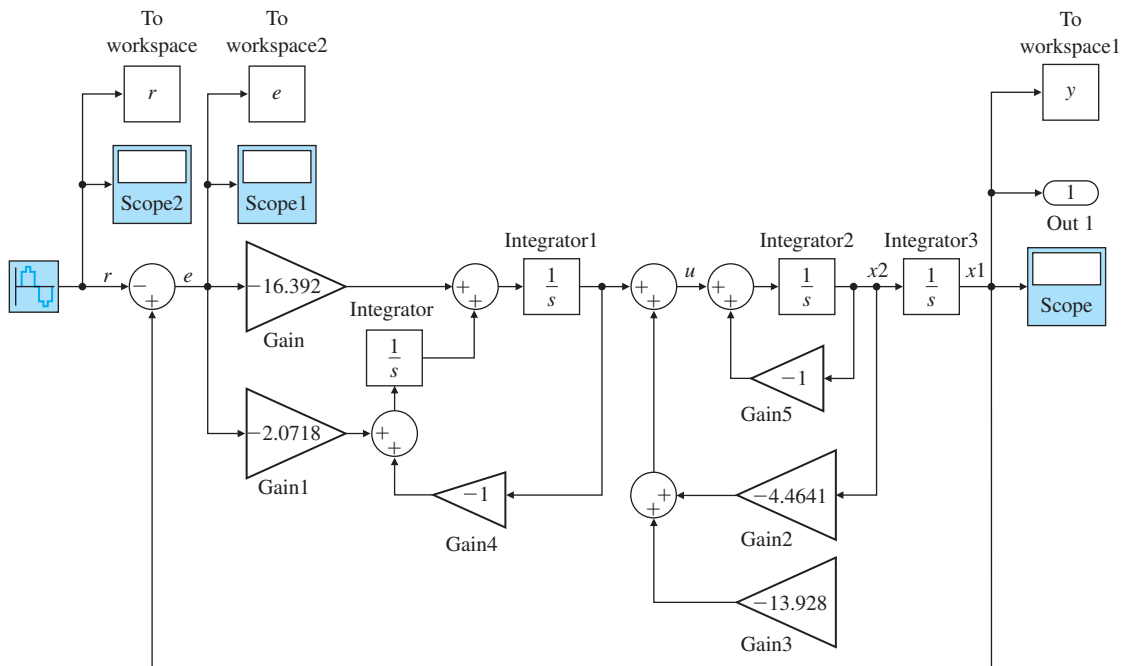


#### Simulink simulation

- (c) Figure 7.60 shows the Simulink simulation diagram for the system. Although the simulations can also be done in Matlab, it is more instructive to use the interactive graphical environment of Simulink. Simulink also provides the capability to add nonlinearities (see Chapter 9) and carry out robustness studies efficiently.<sup>15</sup> The tracking properties of the system are shown in Fig. 7.61(a),

---

<sup>15</sup>In general, the design can be done in Matlab and (nonlinear) simulations can be carried out in Simulink.

**Figure 7.60**

Simulink block diagram for robust servomechanism

*Source: Reprinted with permission of The MathWorks, Inc.*

showing the asymptotic tracking property of the system. The associated control effort and the tracking error signal are shown in Fig. 7.61(b) and (c), respectively. The disturbance rejection properties of the system are illustrated in Fig. 7.62(a), displaying asymptotic disturbance rejection of sinusoidal disturbance input. The associated control effort is shown in Fig. 7.62(b). The closed-loop frequency response [that is, the complementary transfer function  $T(s)$ ] for the robust servomechanism is shown in Fig. 7.63. As seen from the figure, the frequency response from  $r$  to  $y$  is unity at  $\omega_0 = 1$  rad/sec as expected.

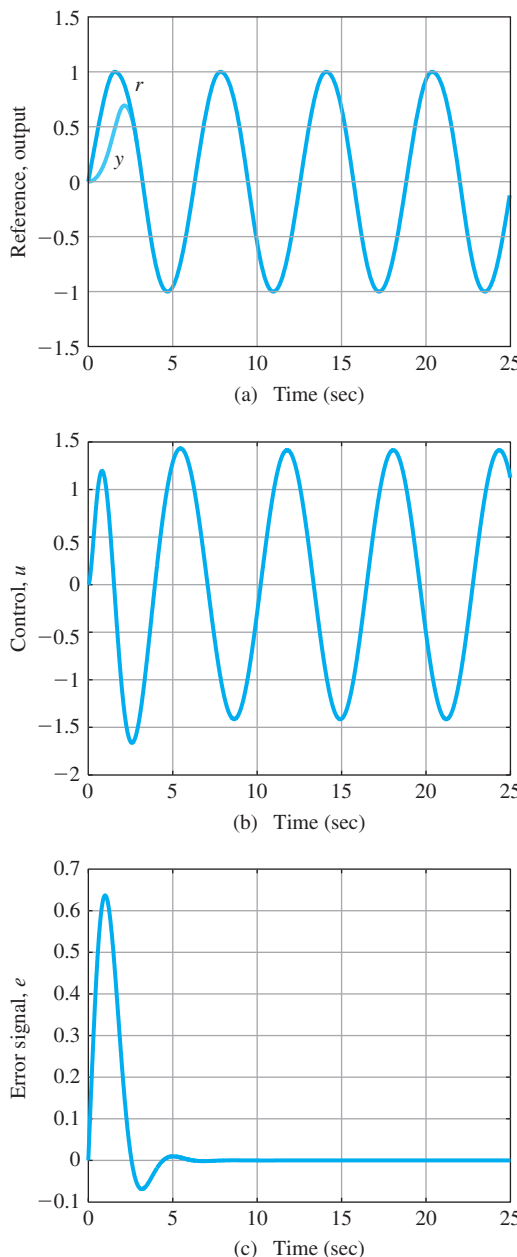
The zeros of the system from  $r$  to  $e$  are located at  $\pm j, -2.7321 \pm j2.5425$ . The robust tracking properties are due to the presence of the blocking zeros at  $\pm j$ . The zeros from  $w$  to  $y$ , both blocking zeros, are located at  $\pm j$ . The robust disturbance rejection properties are due to the presence of these blocking zeros.

**Blocking zeros**

From the nature of the pole-placement problem, the state  $z$  in Eq. (7.214) will tend toward zero for all perturbations in the system parameters as long as  $A_s - B_s K$  remains stable. Notice the signals that are rejected are those that satisfy the equations with the values of  $\alpha_i$

**Figure 7.61**

- (a) Tracking properties for robust servomechanism;  
 (b) control effort;  
 (c) tracking error signal

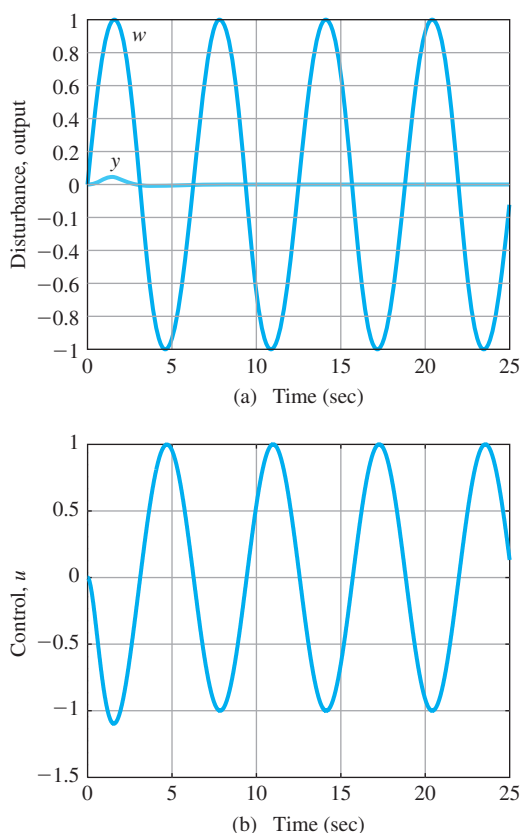


actually implemented in the model of the external signals. The method assumes these are known and implemented exactly. If the implemented values are in error, then a steady-state error will result.

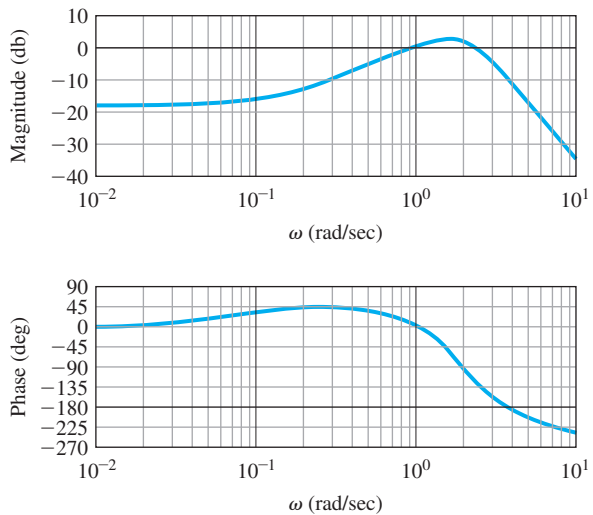
Now let us repeat the example of Section 7.10.1 for integral control.

**Figure 7.62**

(a) Disturbance rejection properties for robust servomechanism;  
 (b) control effort

**Figure 7.63**

Closed-loop frequency response for robust servomechanism



**EXAMPLE 7.36***Integral Control Using the Error-Space Design*

For the system

$$H(s) = \frac{1}{s+3},$$

with the state-variable description

$$A = -3, \quad B = 1, \quad C = 1,$$

construct a controller with poles at  $s = -5$  to track an input that satisfies  $\dot{r} = 0$ .

**Solution.** The error-space system is

$$\begin{bmatrix} \dot{e} \\ \dot{\xi} \end{bmatrix} = \begin{bmatrix} 0 & 1 \\ 0 & -3 \end{bmatrix} \begin{bmatrix} e \\ \xi \end{bmatrix} + \begin{bmatrix} 0 \\ 1 \end{bmatrix} \mu,$$

with  $e = y - r$ ,  $\xi = \dot{x}$ , and  $\mu = \dot{u}$ . If we take the desired characteristic equation to be

$$\alpha_c(s) = s^2 + 10s + 25,$$

then the pole-placement equation for  $\mathbf{K}$  is

$$\det[s\mathbf{I} - \mathbf{A}_s + \mathbf{B}_s \mathbf{K}] = \alpha_c(s). \quad (7.220)$$

In detail, Eq. (7.220) is

$$s^2 + (3 + K_0)s + K_1 = s^2 + 10s + 25,$$

which gives

$$\mathbf{K} = [25 \quad 7] = [K_1 \quad K_0],$$

and the system is implemented as shown in Fig. 7.64. The transfer function from  $r$  to  $e$  for this system, the sensitivity function

$$\frac{E(s)}{R(s)} = \mathcal{S}(s) = -\frac{s(s+10)}{s^2 + 10s + 25},$$

shows a blocking zero at  $s = 0$ , which prevents the constant input from affecting the error. The closed-loop transfer function—that is, the complementary sensitivity function—is

$$\frac{Y(s)}{R(s)} = \mathcal{T}(s) = 1 - \mathcal{S}(s) = \frac{25}{s^2 + 10s + 25}.$$

**Figure 7.64**

Example of internal model with feedforward

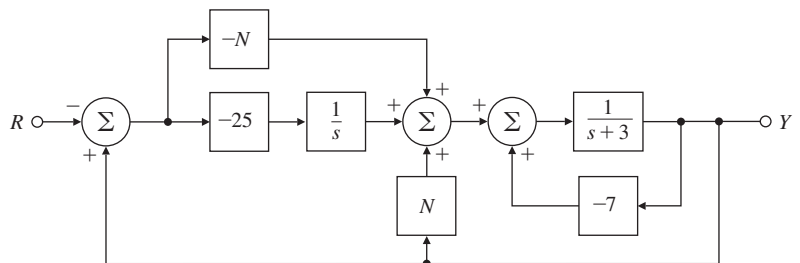
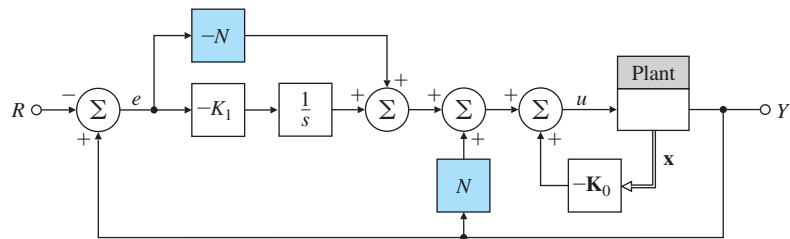


**Figure 7.65**

Internal model as integral control with feedforward



The structure of Fig. 7.65 permits us to add a feedforward of the reference input, which provides one extra degree of freedom in zero assignment. If we add a term proportional to  $r$  in Eq. (7.219), then

$$u = -K_1 \int^t e(\tau) d\tau - \mathbf{K}_0 \mathbf{x} + Nr. \quad (7.221)$$

This relationship has the effect of creating a zero at  $-K_1/N$ . The location of this zero can be chosen to improve the transient response of the system. For actual implementation, we can rewrite Eq. (7.221) in terms of  $e$  to get

$$u = -K_1 \int^t e(\tau) d\tau - \mathbf{K}_0 \mathbf{x} + N(y - e). \quad (7.222)$$

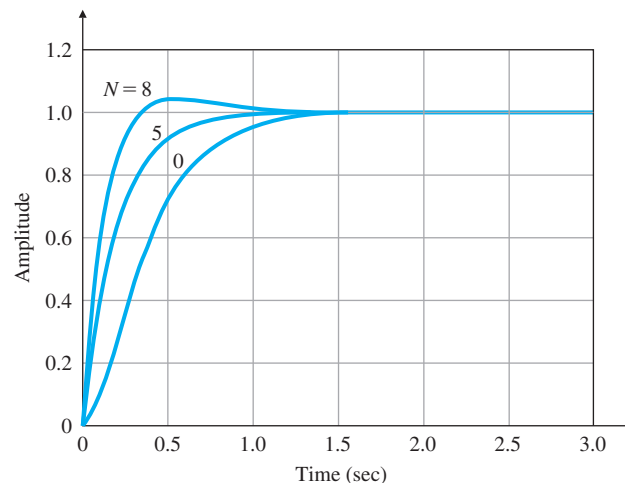
The block diagram for the system is shown in Fig. 7.65. For our example, the overall transfer function now becomes

$$\frac{Y(s)}{R(s)} = \frac{Ns + 25}{s^2 + 10s + 25}.$$

Notice the DC gain is unity for any value of  $N$  and that, through our choice of  $N$ , we can place the zero at any real value to improve the dynamic response. A natural strategy for locating the zero is to have it cancel one of the system poles, in this case at  $s = -5$ . The step response of the system is shown in Fig. 7.66 for  $N = 5$ , as well as for  $N = 0$  and

**Figure 7.66**

Step responses with integral control and feedforward



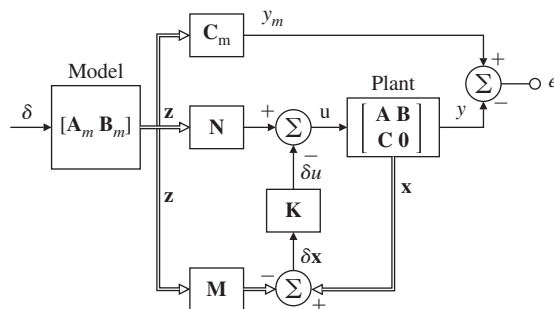
8. With the understanding that one pole can be cancelled in integral control designs, we make sure to choose one of the desired control poles such that it is both real and able to be cancelled through the proper choice of  $N$ .

### △ 7.10.3 Model-Following Design

A related method to track a persistent reference input is called model-following design (see Fig. 7.67). This is an open-loop method that uses the feedforward of the state of the model to construct a specific control input. This control will force the plant output to asymptotically track the output of the desired model which may or may not be persistent. As an example, the desired model can be the specified path that an aircraft is required to track accurately. LTI models with nonzero initial conditions can be used to generate such paths. Alternatively, an impulsive input can be used to establish the initial condition on the desired model (as done here). The technique can produce superior tracking properties to follow such desired paths. The method is described more fully in Bryson (1994), including the case of disturbance rejection, and used to synthesize the landing flare logic for the Boeing 747 aircraft. Assume we have a plant described by the triple  $(A, B, C)$ , having state  $x$  and output  $y$ . Furthermore, assume a given model that produces the desired response of the plant which is described by the triple  $(A_m, B_m, C_m)$ , with state  $z$  and output  $y_m$ . The idea is to use the states  $x$  and  $z$  to construct a control signal so the error  $y - y_m$  “quickly” approaches zero. In other words, we want the plant to follow the model with an error that goes to zero. As you will see in the ensuing development, we will tailor the control input such that the output of the plant is forced to follow the desired reference input. The control law uses the feedforward of the model state,  $z$ , and the feedback of the plant state  $x$ . The constant feed-forward gain matrices  $M$  and  $N$  are obtained from the solution of a set of linear equations. The feedback gain,  $K$ , is designed as usual to stabilize or speed up the plant dynamics. We now derive the model-following design from first principles, and illustrate the results with an example.

**Figure 7.67**

Block diagram for the model-following design



Consider the plant described by

$$\dot{\mathbf{x}} = \mathbf{Ax} + \mathbf{Bu}, \quad (7.223)$$

$$y = \mathbf{Cx}, \quad (7.224)$$

and the desired model given by

$$\dot{\mathbf{z}} = \mathbf{A}_m \mathbf{z} + \mathbf{B}_m \delta(t), \quad (7.225)$$

$$y_m = \mathbf{C}_m \mathbf{z}, \quad (7.226)$$

where  $\mathbf{A}_m$  is  $n_m \times n_m$ . In our case, the model is driven by the impulse,  $\delta(t)$ , or essentially initial conditions only. Assume the dimensions of  $u$ ,  $y$ , and  $y_m$  are the same. Let

$$\mathbf{x} = \mathbf{Mz} + \delta \mathbf{x}, \quad (7.227)$$

$$u = \mathbf{Nz} + \delta u, \quad (7.228)$$

$$y = y_m + \delta y, \quad (7.229)$$

where  $\mathbf{M}$  and  $\mathbf{N}$  are constant matrices. We wish that  $\delta y \rightarrow 0$  rapidly so  $y \rightarrow y_m$ . If we substitute Eqs. (7.227) and (7.228) in Eqs. (7.223) and (7.224), we obtain

$$\mathbf{M}\dot{\mathbf{z}} + \delta \dot{\mathbf{x}} = \mathbf{A}(\mathbf{Mz} + \delta \mathbf{x}) + \mathbf{B}(\mathbf{Nz} + \delta u), \quad (7.230)$$

$$y = y_m + \delta y = \mathbf{C}(\mathbf{Mz} + \delta \mathbf{x}), \quad (7.231)$$

which we can rewrite as

$$\delta \dot{\mathbf{x}} = \mathbf{A}\delta \mathbf{x} + \mathbf{B}\delta u + (\mathbf{AM} - \mathbf{MA}_m + \mathbf{BN})\mathbf{z} - \mathbf{MB}_m \delta(t), \quad (7.232)$$

$$\delta y = \mathbf{C}\delta \mathbf{x} + (\mathbf{CM} - \mathbf{C}_m)\mathbf{z}. \quad (7.233)$$

If we select the matrices  $\mathbf{M}$  and  $\mathbf{N}$  so the matrices multiplying the model state  $\mathbf{z}$  in Eqs. (7.232) and (7.233) vanish, we have the two ensuing matrix equations<sup>16</sup>

$$\mathbf{AM} - \mathbf{MA}_m + \mathbf{BN} = \mathbf{0}, \quad (7.234)$$

$$\mathbf{CM} = \mathbf{C}_m. \quad (7.235)$$

Eq. (7.234) is called a Sylvester equation. In Eqs. (7.234) and (7.235), there are  $n_m(n+1)$  linear equations in the  $n_m(n+1)$  unknown elements of the matrices  $\mathbf{M}$  and  $\mathbf{N}$ . A necessary and sufficient condition for the existence of the solution to Eqs. (7.234) and (7.235) is that the transmission zeros of the plant do not coincide with the eigenvalues of the model  $\mathbf{A}_m$ . Let the control law be

$$u = \mathbf{Nz} - \mathbf{K}(\mathbf{x} - \mathbf{Mz}), \quad (7.236)$$

where  $\mathbf{K}$  is designed in the usual way so  $\mathbf{A} - \mathbf{BK}$  has a satisfactory stable control. We observe that

$$\delta u = u - \mathbf{Nz} = \mathbf{Nz} - \mathbf{K}(\mathbf{x} - \mathbf{Mz}) - \mathbf{Nz} = -\mathbf{K}\delta \mathbf{x}. \quad (7.237)$$

---

<sup>16</sup>Bryson (1994) presents an algorithm to solve Eqs. (7.234) and (7.235), using the Matlab Kronecker product (kron) command.

With the given control law, Eq. (7.236), the plant equations become

$$\begin{aligned}\dot{\mathbf{x}} &= \mathbf{Ax} + \mathbf{B}(\mathbf{Nz} - \mathbf{K}(\mathbf{x} - \mathbf{Mz})), \\ &= (\mathbf{A} - \mathbf{BK})\mathbf{x} + \mathbf{B}(\mathbf{N} + \mathbf{KM})\mathbf{z}.\end{aligned}\quad (7.238)$$

In the frequency domain, noting that  $\mathbf{Z}(s) = (s\mathbf{I} - \mathbf{A}_m)^{-1}\mathbf{B}_m$ , this can be written as

$$\mathbf{X}(s) = (s\mathbf{I} - \mathbf{A} + \mathbf{BK})^{-1}\mathbf{B}(\mathbf{N} + \mathbf{KM})(s\mathbf{I} - \mathbf{A}_m)^{-1}\mathbf{B}_m. \quad (7.239)$$

Now substituting for  $\mathbf{BN}$  from Eq. (7.234) and adding and subtracting  $s\mathbf{M}$ , this can be written as

$$\mathbf{X}(s) = (s\mathbf{I} - \mathbf{A} + \mathbf{BK})^{-1}[\mathbf{MA}_m - \mathbf{AM} + \mathbf{BKM}](s\mathbf{I} - \mathbf{A}_m)^{-1}\mathbf{B}_m, \quad (7.240)$$

$$\mathbf{X}(s) = (s\mathbf{I} - \mathbf{A} + \mathbf{BK})^{-1}[(s\mathbf{I} - \mathbf{A} + \mathbf{BK})\mathbf{M} - \mathbf{M}(s\mathbf{I} - \mathbf{A}_m)](s\mathbf{I} - \mathbf{A}_m)^{-1}\mathbf{B}_m. \quad (7.241)$$

If we now multiply this out, the result is

$$\mathbf{X}(s) = \mathbf{M}(s\mathbf{I} - \mathbf{A}_m)^{-1}\mathbf{B}_m - (s\mathbf{I} - \mathbf{A} + \mathbf{BK})^{-1}\mathbf{MB}_m. \quad (7.242)$$

The output,  $Y(s) = \mathbf{CX}(s)$  is thus

$$Y(s) = \mathbf{CM}(s\mathbf{I} - \mathbf{A}_m)^{-1}\mathbf{B}_m - \mathbf{C}(s\mathbf{I} - \mathbf{A} + \mathbf{BK})^{-1}\mathbf{MB}_m. \quad (7.243)$$

Finally, as  $\mathbf{CM} = \mathbf{C}_m$ , we have

$$Y(s) = \mathbf{C}_m(s\mathbf{I} - \mathbf{A}_m)^{-1}\mathbf{B}_m - \mathbf{C}(s\mathbf{I} - \mathbf{A} + \mathbf{BK})^{-1}\mathbf{MB}_m, \quad (7.244)$$

and therefore, in the time domain,

$$y(t) = y_m(t) - [\text{decaying transient term controlled by } \mathbf{K}], \quad (7.245)$$

which is what we set out to show.

### EXAMPLE 7.37

#### *Model-following for Disk Drive*

Assume the model to be followed is given by an oscillator, that is,

$$\begin{aligned}\mathbf{A}_m &= \begin{bmatrix} 0 & 1 \\ -1 & 0 \end{bmatrix}, \quad \mathbf{B}_m = \begin{bmatrix} 0 \\ 1 \end{bmatrix}, \\ \mathbf{C}_m &= \begin{bmatrix} 1 & 0 \end{bmatrix}.\end{aligned}$$

The plant is the same as given in Example 7.35 and we wish to track the same sine wave signal. Assume the desired closed-loop poles are given by

$$p_c = [-1 + j * \sqrt{3}; -1 - j * \sqrt{3}].$$

**Solution.** The feedback gain is

$$\mathbf{K} = [4 \ 1].$$

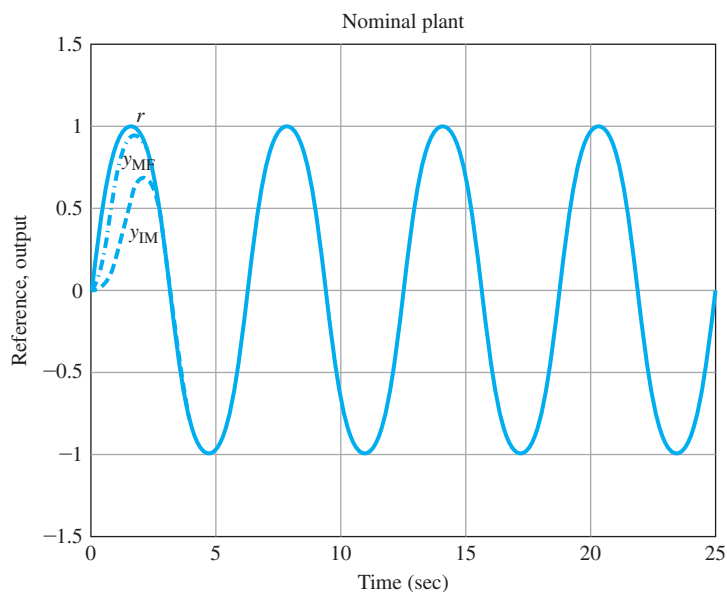
We solve Eqs. (7.234) and (7.235) for this case to obtain

$$\begin{aligned}\mathbf{M} &= \begin{bmatrix} 1 & 0 \\ 0 & 1 \end{bmatrix}, \\ \mathbf{N} &= \begin{bmatrix} -1 & 1 \end{bmatrix}.\end{aligned}$$

The internal model design is the same as in Example 7.35. A comparison of the tracking error for the internal model and model-following designs are shown in Figs. 7.68 and 7.69. Both techniques track the sinusoid exactly in an asymptotic fashion, and the model-following technique has a snappier response and the smaller maximum error as seen from Fig. 7.69.

**Figure 7.68**

Comparison of the tracking properties for the two designs: desired model ( $r$ ), model-following design ( $y_{MF}$ ), and internal model design ( $y_{IM}$ , see Example 7.35) with the nominal plant model

**Figure 7.69**

Comparison of the tracking error signals for the two designs with the nominal plant model

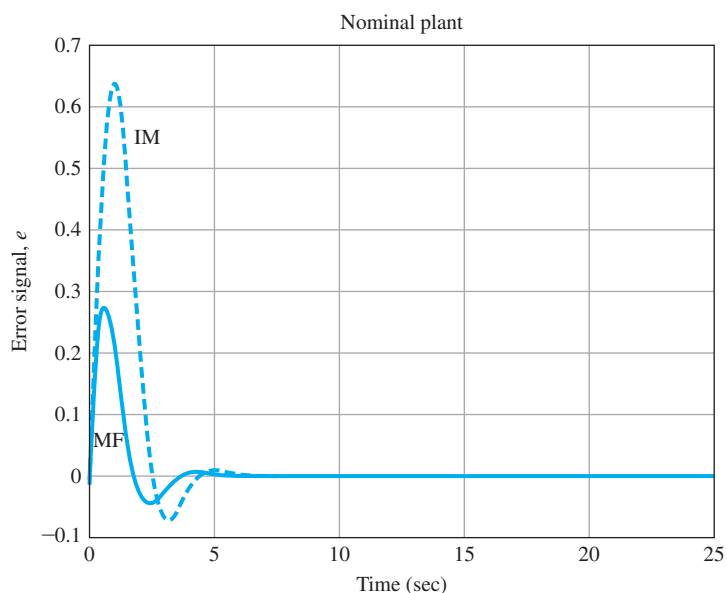
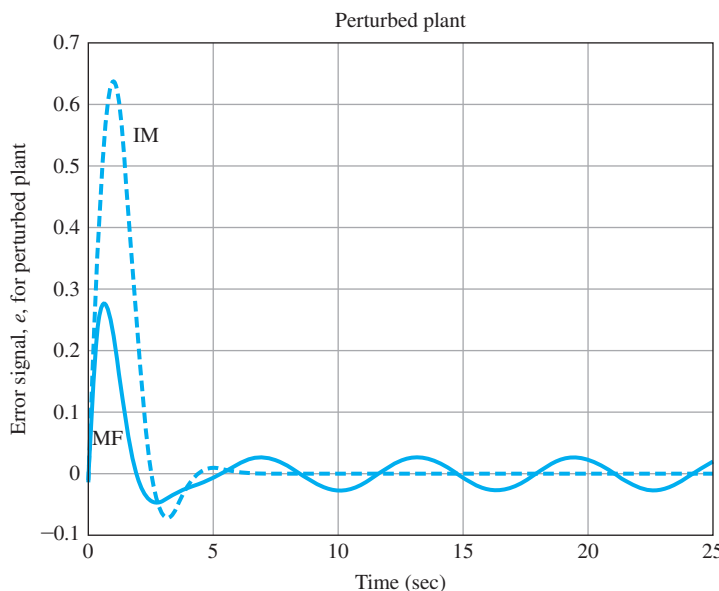


**Figure 7.70**

Comparison of the tracking errors of the two designs with the perturbed plant model



Now let us investigate the robustness of the two techniques with respect to plant perturbations. For comparison of robustness properties, both the model-following system and the internal model closed-loop systems were run but with the plant system matrix perturbed to be

$$\tilde{\mathbf{A}} = \begin{bmatrix} 0 & 1 \\ 0 & -1.1 \end{bmatrix}.$$

The tracking errors for the two cases are plotted in Fig. 7.70. Notice in Fig. 7.70, the model-following design has the smaller maximum error but, being non-robust, has a persistent error while the internal model design continues to track the sine wave exactly.

#### △ 7.10.4 The Extended Estimator

Our discussion of robust control so far has used a control based on full-state feedback. If the state is not available, then as in the regular case, the full-state feedback,  $\mathbf{Kx}$ , can be replaced by the estimates,  $\mathbf{K}\hat{\mathbf{x}}$ , where the estimator is built as before. As a final look at ways to design control with external inputs, in this section, we develop a method for tracking a reference input and rejecting disturbances. The method is based on augmenting the estimator to include estimates from external signals in a way that permits us to cancel out their effects on the system error.

Suppose the plant is described by the equations

$$\dot{\mathbf{x}} = \mathbf{Ax} + \mathbf{Bu} + \mathbf{Bw}, \quad (7.246a)$$

$$y = \mathbf{Cx}, \quad (7.246b)$$

$$e = \mathbf{Cx} - r. \quad (7.246c)$$

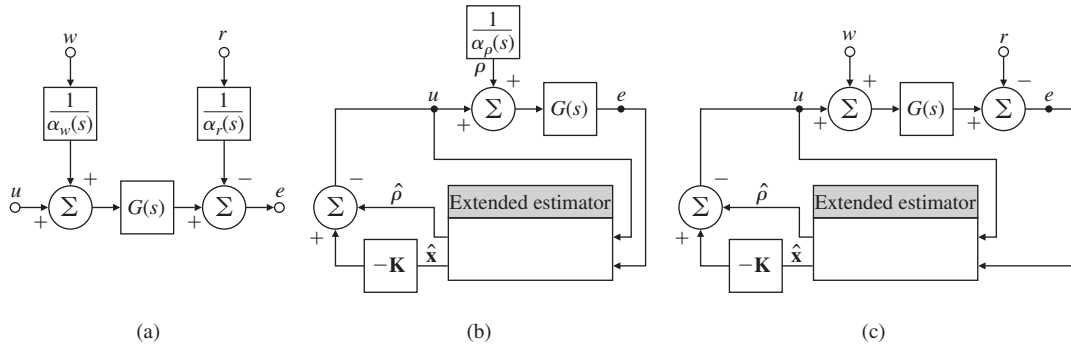


Figure 7.71

Block diagram of a system for tracking and disturbance rejection with extended estimator: (a) equivalent disturbance; (b) block diagram for *design*; (c) block diagram for *implementation*

Furthermore, assume both the reference  $r$  and the disturbance  $w$  are known to satisfy the equations<sup>17</sup>

$$\alpha_w(s)w = \alpha_\rho(s)w = 0, \quad (7.247)$$

$$\alpha_r(s)r = \alpha_\rho(s)r = 0, \quad (7.248)$$

where

$$\alpha_\rho(s) = s^2 + \alpha_1s + \alpha_2,$$

corresponding to polynomials  $\alpha_w(s)$  and  $\alpha_r(s)$  in Fig. 7.71(a). In general, we would select the equivalent disturbance polynomial  $\alpha_\rho(s)$  in Fig. 7.71(b) to be the *least common multiple* of  $\alpha_w(s)$  and  $\alpha_r(s)$ . The first step is to recognize that, as far as the steady-state response of the output is concerned, there is an input-equivalent signal  $\rho$  that satisfies the same equation as  $r$  and  $w$  and enters the system at the same place as the control signal, as shown in Fig. 7.71(b). As before, we must assume the plant does not have a zero at any of the roots of Eq. (7.247). For our purposes here, we can replace Eqs. (7.223) with

$$\dot{\mathbf{x}} = \mathbf{Ax} + \mathbf{B}(u + \rho), \quad (7.249a)$$

$$e = \mathbf{Cx}. \quad (7.249b)$$

If we can estimate this equivalent input, we can add to the control a term  $-\hat{\rho}$  that will cancel out the effects of the real disturbance and reference and cause the output to track  $r$  in the steady-state. To do this, we combine Eqs. (7.223) and (7.247) into a state description to get

$$\dot{\mathbf{z}} = \mathbf{A}_s\mathbf{z} + \mathbf{B}_su, \quad (7.250a)$$

$$e = \mathbf{C}_s\mathbf{z}, \quad (7.250b)$$

---

<sup>17</sup>Again, we develop the results for a second-order equation in the external signals; the discussion can be extended to higher-order equations.

where  $\mathbf{z} = [\rho \quad \dot{\rho} \quad \mathbf{x}^T]^T$ . The matrices are

$$\mathbf{A}_s = \begin{bmatrix} 0 & 1 & \mathbf{0} \\ -\alpha_2 & -\alpha_1 & \mathbf{0} \\ \mathbf{B} & \mathbf{0} & \mathbf{A} \end{bmatrix}, \quad \mathbf{B}_s = \begin{bmatrix} 0 \\ 0 \\ \mathbf{B} \end{bmatrix}, \quad (7.251a)$$

$$\mathbf{C}_s = [0 \quad 0 \quad \mathbf{C}]. \quad (7.251b)$$

The system given by Eqs. (7.251) is not controllable since we cannot influence  $\rho$  from  $u$ . However, if  $\mathbf{A}$  and  $\mathbf{C}$  are observable and if the system  $(\mathbf{A}, \mathbf{B}, \mathbf{C})$  does not have a zero that is also a root of Eq. (7.247), then the system of Eq. (7.251) will be observable, and we can construct an observer that will compute estimates of both the state of the plant and of  $\rho$ . The estimator equations are standard, but the control is not:

$$\dot{\hat{\mathbf{z}}} = \mathbf{A}_s \hat{\mathbf{z}} + \mathbf{B}_s u + \mathbf{L}(e - \mathbf{C}_s \hat{\mathbf{z}}), \quad (7.252a)$$

$$u = -\mathbf{K}\hat{\mathbf{x}} - \hat{\rho}. \quad (7.252b)$$

In terms of the original variables, the estimator equations are

$$\dot{\hat{\mathbf{z}}} = \begin{bmatrix} \dot{\hat{\rho}} \\ \ddot{\hat{\rho}} \\ \dot{\hat{\mathbf{x}}} \end{bmatrix} = \begin{bmatrix} 0 & 1 & \mathbf{0} \\ -\alpha_2 & -\alpha_1 & \mathbf{0} \\ \mathbf{B} & \mathbf{0} & \mathbf{A} \end{bmatrix} \begin{bmatrix} \hat{\rho} \\ \dot{\hat{\rho}} \\ \hat{\mathbf{x}} \end{bmatrix} + \begin{bmatrix} 0 \\ 0 \\ \mathbf{B} \end{bmatrix} u + \begin{bmatrix} l_1 \\ l_2 \\ \mathbf{L}_3 \end{bmatrix} [e - \mathbf{C}\hat{\mathbf{x}}]. \quad (7.253)$$

The overall block diagram of the system for *design* is shown in Fig. 7.71(b). If we write out the last equation for  $\hat{\mathbf{x}}$  in Eq. (7.253) and substitute Eq. (7.252b), a simplification of sorts results because a term in  $\hat{\rho}$  cancels out:

$$\begin{aligned} \dot{\hat{\mathbf{x}}} &= \mathbf{B}\hat{\rho} + \mathbf{A}\hat{\mathbf{x}} + \mathbf{B}(-\mathbf{K}\hat{\mathbf{x}} - \hat{\rho}) + \mathbf{L}_3(e - \mathbf{C}\hat{\mathbf{x}}) \\ &= \mathbf{A}\hat{\mathbf{x}} + \mathbf{B}(-\mathbf{K}\hat{\mathbf{x}}) + \mathbf{L}_3(e - \mathbf{C}\hat{\mathbf{x}}) \\ &= \mathbf{A}\hat{\mathbf{x}} + \mathbf{B}\bar{u} + \mathbf{L}_3(e - \mathbf{C}\hat{\mathbf{x}}). \end{aligned}$$

With the estimator of Eq. (7.253) and the control of Eq. (7.252b), the state equation is

$$\dot{\mathbf{x}} = \mathbf{A}\mathbf{x} + \mathbf{B}(-\mathbf{K}\hat{\mathbf{x}} - \hat{\rho}) + \mathbf{B}\rho. \quad (7.254)$$

In terms of the estimation errors, Eq. (7.254) can be rewritten as

$$\dot{\mathbf{x}} = (\mathbf{A} - \mathbf{B}\mathbf{K})\mathbf{x} + \mathbf{B}\mathbf{K}\tilde{\mathbf{x}} + \mathbf{B}\tilde{\rho}. \quad (7.255)$$

Because we designed the estimator to be stable, the values of  $\tilde{\rho}$  and  $\tilde{\mathbf{x}}$  go to zero in the steady-state, and the final value of the state is not affected by the external input. The block diagram of the system for *implementation* is drawn in Fig. 7.71(c). A simple example will illustrate the steps in this process.

### EXAMPLE 7.38

#### *Steady-State Tracking and Disturbance Rejection of Motor Speed by Extended Estimator*

Construct an estimator to control the state and cancel a constant bias at the output and track a constant reference in the motor speed system described by

$$\dot{x} = -3x + u, \quad (7.256a)$$

$$y = x + w, \quad (7.256b)$$

$$\dot{w} = 0, \quad (7.256c)$$

$$\dot{r} = 0. \quad (7.256d)$$

Place the control pole at  $s = -5$ , and the two extended estimator poles at  $s = -15$ .

**Solution.** To begin, we design the control law by ignoring the equivalent disturbance. Rather, we notice by inspection that a gain of  $-2$  will move the single pole from  $-3$  to the desired  $-5$ . Therefore,  $K = 2$ . The system augmented with equivalent external input  $\rho$ , which replaces the actual disturbance  $w$  and the reference  $r$ , is given by

$$\begin{aligned}\dot{\rho} &= 0, \\ \dot{x} &= -3x + u + \rho, \\ e &= x.\end{aligned}$$

The extended estimator equations are

$$\begin{aligned}\dot{\hat{\rho}} &= l_1(e - \hat{x}), \\ \dot{\hat{x}} &= -3\hat{x} + u + \hat{\rho} + l_2(e - \hat{x}).\end{aligned}$$

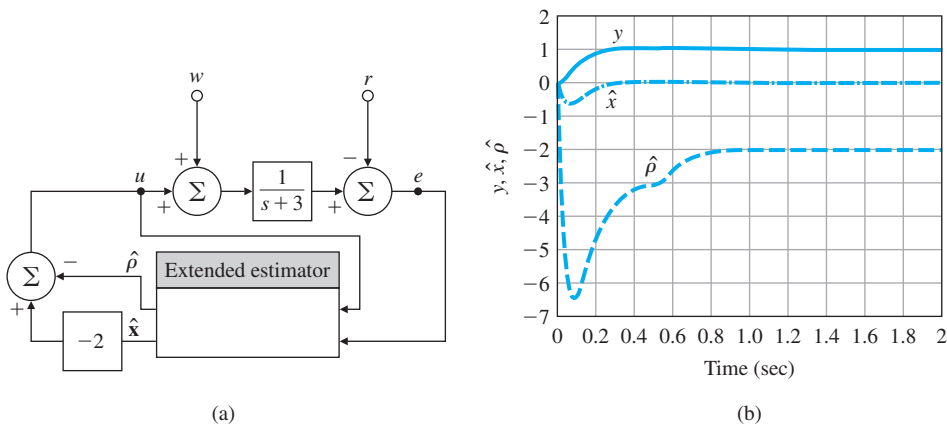
The estimator error gain is found to be  $\mathbf{L} = [ \begin{smallmatrix} 225 & 27 \end{smallmatrix} ]^T$  from the characteristic equation

$$\det \begin{bmatrix} s & l_1 \\ 1 & s + 3 + l_2 \end{bmatrix} = s^2 + 30s + 225.$$

A block diagram of the system is given in Fig. 7.72(a), and the step responses to input at the command  $r$  (applied at  $t = 0$  sec) and at the disturbance  $w$  (applied at  $t = 0.5$  sec) are shown in Fig. 7.72(b).

## △ 7.11 Loop Transfer Recovery

The introduction of an estimator in a state feedback controller loop may adversely affect the stability robustness properties of the system [that is, the phase margin (PM) and gain margin (GM) properties may become arbitrarily poor, as shown by Doyle's famous example (Doyle, 1978)]. However, it is possible to modify the estimator design so as to try to "recover" the LQR stability robustness properties to some extent. This process, called LTR, is especially effective for minimum-phase systems. To achieve the recovery, some of the estimator Loop Transfer Recovery poles are placed at (or near) the zeros of the plant and the remaining

**Figure 7.72**

Motor speed system with extended estimator: (a) block diagram; (b) command step response and disturbance step response

poles are moved (sufficiently far) into the LHP. The idea behind LTR is to redesign the estimator in such a way as to shape the loop gain properties to approximate those of LQR.

The use of LTR means that feedback controllers can be designed to achieve desired sensitivity  $[S(s)]$  and complementary sensitivity functions  $[T(s)]$  at critical (loop-breaking) points in the feedback system (for example, at either the input or output of the plant). Of course, there is a price to be paid for this improvement in stability robustness! The newly designed control system may have worse sensor noise sensitivity properties. Intuitively, one can think of making (some of) the estimator poles arbitrarily fast so the loop gain is approximately that of LQR. Alternatively, one can think of essentially “inverting” the plant transfer function so that all the LHP poles of the plant are cancelled by the dynamic compensator to achieve the desired loop shape. There are obvious trade-offs, and the designer needs to be careful to make the correct choice for the given problem, depending on the control system specifications.

LTR is a well-known technique now, and specific practical design procedures have been identified (Athans, 1986; Stein and Athans, 1987; Saberi et al., 1993). The same procedures may also be applied to non-minimum phase systems, but there is no guarantee on the extent of possible recovery. The LTR technique may be viewed as a systematic procedure to study design trade-offs for linear quadratic-based compensator design (Doyle and Stein, 1981). We will now formulate the LTR problem.

Consider the linear system

$$\dot{\mathbf{x}} = \mathbf{Ax} + \mathbf{Bu} + \mathbf{w}, \quad (7.257a)$$

$$y = \mathbf{Cx} + \mathbf{v}, \quad (7.257b)$$

where  $w$  and  $v$  are uncorrelated zero-mean white Gaussian process and sensor noise with covariance matrices  $\mathbf{R}_w \geq 0$  and  $\mathbf{R}_v \geq 0$ . The estimator design yields

$$\dot{\hat{\mathbf{x}}} = \mathbf{A}\hat{\mathbf{x}} + \mathbf{B}u + \mathbf{L}(y - \hat{y}), \quad (7.258a)$$

$$\hat{y} = \mathbf{C}\hat{\mathbf{x}}, \quad (7.258b)$$

resulting in the usual dynamic compensator

$$D_c(s) = -\mathbf{K}(s\mathbf{I} - \mathbf{A} + \mathbf{B}\mathbf{K} + \mathbf{L}\mathbf{C})^{-1}\mathbf{L}. \quad (7.259)$$

We will now treat the noise parameters,  $\mathbf{R}_w$  and  $\mathbf{R}_v$ , as design “knobs” in the dynamic compensator design. Without loss of generality, let us choose  $\mathbf{R}_w = \Gamma^T\Gamma$  and  $\mathbf{R}_v = 1$ . For LTR, assume  $\Gamma = q\mathbf{B}$ , where  $q$  is a scalar design parameter. The estimator design is then based on the specific design parameters  $\mathbf{R}_w$  and  $\mathbf{R}_v$ . It can be shown that, for a minimum-phase system, as  $q$  becomes large (Doyle and Stein, 1979),

$$\lim_{q \rightarrow \infty} D_c(s)G(s) = \mathbf{K}(s\mathbf{I} - \mathbf{A})^{-1}\mathbf{B}, \quad (7.260)$$

#### Plant inversion

the convergence is pointwise in  $s$  and the degree of recovery can be arbitrarily good. This design procedure in effect “inverts” the plant transfer function in the limit as  $q \rightarrow \infty$ :

$$\lim_{q \rightarrow \infty} D_c(s) = \mathbf{K}(s\mathbf{I} - \mathbf{A})^{-1}\mathbf{B}G^{-1}(s). \quad (7.261)$$

This is precisely the reason that full-loop transfer recovery is not possible for a nonminimum-phase system. This limiting behavior may be explained using the symmetric root loci. As  $q \rightarrow \infty$ , some of the estimator poles approach the zeros of

$$G_e(s) = \mathbf{C}(s\mathbf{I} - \mathbf{A})^{-1}\Gamma, \quad (7.262)$$

#### LTR for nonminimum-phase systems

and the rest tend to infinity<sup>18</sup> [see Eqs. (7.163) and (7.164)]. In practice, the LTR design procedure can still be applied to a nonminimum-phase plant. The degree of recovery will depend on the specific locations of the nonminimum-phase zeros. Sufficient recovery should be possible at many frequencies if the RHP zeros are located outside the specified closed-loop bandwidth. Limits on achievable performance of feedback systems due to RHP zeros are discussed in Freudenberg and Looze (1985). We will next illustrate the LTR procedure by a simple example.

---

<sup>18</sup>In a Butterworth configuration.

**EXAMPLE 7.39***LTR Design for Satellite Attitude Control*

Consider the satellite system with state-space description

$$\mathbf{A} = \begin{bmatrix} 0 & 1 \\ 0 & 0 \end{bmatrix}, \quad \mathbf{B} = \begin{bmatrix} 0 \\ 1 \end{bmatrix},$$

$$\mathbf{C} = [1 \ 0], \quad D = 0.$$

- (a) Design an LQR controller with  $\mathbf{Q} = \rho \mathbf{C}^T \mathbf{C}$  and  $R = 1$ ,  $\rho = 1$ , and determine the loop gain.
- (b) Then design a compensator that recovers the LQR loop gain of part (a) using the LTR technique for  $q = 1, 10, 100$ .
- (c) Compare the different candidate designs in part (b) with respect to the actuator activity due to additive white Gaussian sensor noise.

**Solution.** Using lqr, the selected LQR weights result in the feedback gain  $\mathbf{K} = [1 \ 1.414]$ . The loop transfer function is

$$\mathbf{K}(s\mathbf{I} - \mathbf{A})^{-1}\mathbf{B} = \frac{1.414(s + 0.707)}{s^2}.$$

A magnitude frequency response plot of this LQR loop gain is shown in Fig. 7.73. For the estimator design using lqe, let  $\mathbf{\Gamma} = q\mathbf{B}$ ,  $\mathbf{R}_w = \mathbf{\Gamma}^T \mathbf{\Gamma}$ ,  $\mathbf{R}_v = 1$ , and choose  $q = 10$ , resulting in the estimator gain

$$\mathbf{L} = \begin{bmatrix} 14.142 \\ 100 \end{bmatrix}.$$

The compensator transfer function is

$$\begin{aligned} D_c(s) &= \mathbf{K}(s\mathbf{I} - \mathbf{A} + \mathbf{B}\mathbf{K} + \mathbf{L}\mathbf{C})^{-1}\mathbf{L} \\ &= \frac{155.56(s + 0.6428)}{(s^2 + 15.556s + 121)} = \frac{155.56(s + 0.6428)}{(s + 7.77 + j7.77)(s + 7.77 - j7.77)}, \end{aligned}$$

and the loop transfer function is

$$D_c(s)G(s) = \frac{155.56(s + 0.6428)}{s^2(s + 7.77 + j7.77)(s + 7.77 - j7.77)}.$$

Figure 7.73 shows the frequency response of the loop transfer function for several values of  $q$  ( $q = 1, 10, 100$ ), along with the ideal LQR loop transfer function frequency response. As seen from this figure, the loop gain tends to approach that of LQR as the value of  $q$  increases. As seen in Fig. 7.73, for  $q = 10$ , the “recovered” gain margin is  $GM = 11.1 = 20.9$  db and the  $PM = 55.06^\circ$ . Sample Matlab statements to carry out the preceding LTR design procedure are as follows:

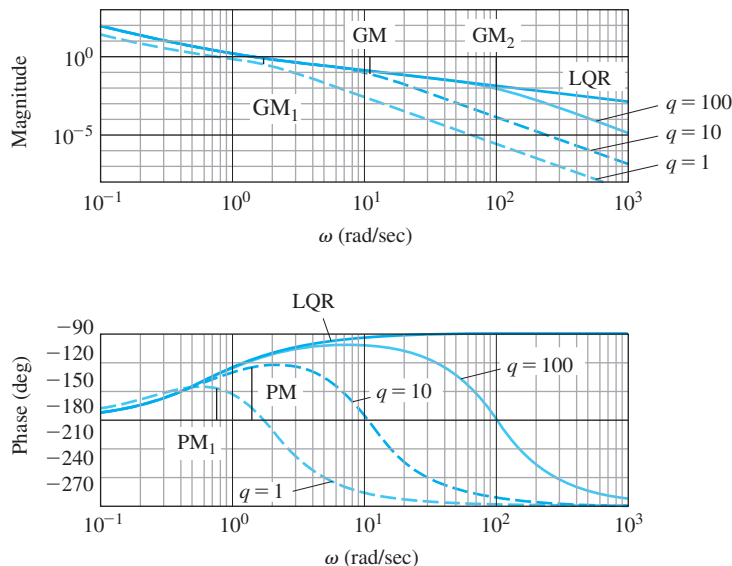
```

A=[0 1; 0 0];
B=[0;1];
C=[1 0];
D=[0];
sys0=ss(A,B,C,D);
C1=[1 0];
sys=ss(A,B,C1,D);

```

**Figure 7.73**

Frequency response plots for LTR design



```
w=logspace(-1,3,1000);
rho=1.0;
Q=rho*C1'*C1;
r=1;
[K]=lqr(A,B,Q,r)
sys1=ss(A,B,K,0);
[maggk1,phsgk1]=bode(sys1,w);
q=10;
gam=q*B;
Q1=gam'*gam;
rv=1;
[L]=lqe(A,gam,C,Q1,rv)
```

[Matlab lqr](#)

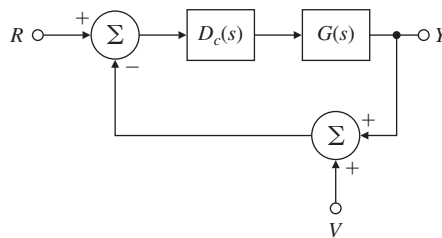
[Matlab bode](#)

[Matlab margin](#)

```
aa=A-B*K-L*C;
bb=L;
cc=K;
dd=0;
sysk=ss(aa,bb,cc,dd);
sysgk=series(sys0,sysk);
[maggk,phsgk,w]=bode(sysgk,w);
[gm,phm,wcp]=margin(maggk,phsgk,w)
loglog(w,[maggk1(:) maggk(:)]);
semilogx(w,[phsgk1(:) phsgk(:)]);
```

To determine the effect of sensor noise,  $\nu$ , on the actuator activity, we determine the transfer function from  $\nu$  to  $u$  as shown in Fig. 7.74. For the selected value of LTR design parameter,  $q = 10$ , we have

**Figure 7.74**  
Closed-loop system for LTR design



$$\begin{aligned}\frac{U(s)}{V(s)} = H(s) &= \frac{-D_c(s)}{1 + D_c(s)G(s)} \\ &= \frac{-155.56s^2(s + 0.6428)}{s^4 + 15.556s^3 + 121s^2 + 155.56s + 99.994}.\end{aligned}$$

RMS value

One reasonable measure of the effect of the sensor noise on the actuator activity is the root-mean-square (RMS) value of the control,  $u$ , due to the additive noise,  $v$ . The RMS value of the control may be computed as

$$\|u\|_{\text{rms}} = \left( \frac{1}{T_0} \int_0^{T_0} u(t)^2 dt \right)^{1/2}, \quad (7.263)$$

where  $T_0$  is the signal duration. Assuming white Gaussian noise  $v$ , the RMS value of the control can also be determined analytically (Boyd and Barratt, 1991). The closed-loop Simulink diagram with band-limited white sensor noise excitation is shown in Fig. 7.75. The values of the RMS control were computed for different values of the LTR design parameter  $q$ , using the Simulink simulations, and are tabulated in Table 7.2. The results suggest increased vulnerability due to actuator wear as  $q$  is increased. Refer to Matlab commands ltry and ltru for the LTR computations.

**Figure 7.75**  
Simulink block diagram for LTR design

Source: Franklin, Gene F. *Feedback Control of Dynamic Systems*, 8E, 2019, Pearson Education, Inc., New York, NY.

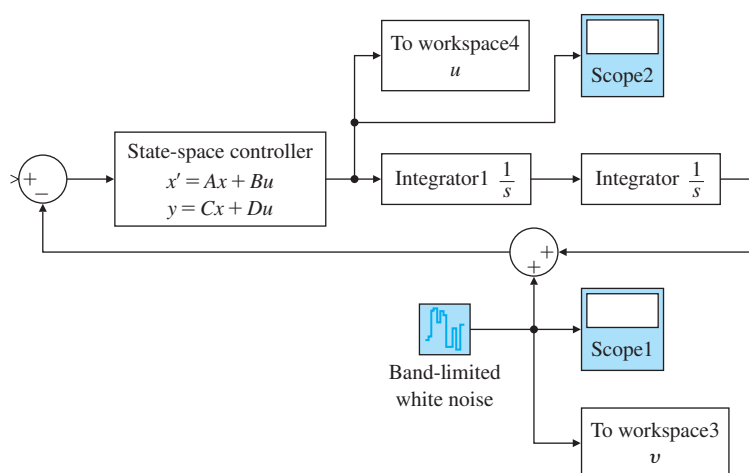


**TABLE 7.2****Computed RMS Control for Various Values of LTR Tuning Parameter  $q$** 

$q$	$\ u\ _{rms}$
1	0.1454
10	2.8054
100	70.5216

**△ 7.12 Direct Design with Rational Transfer Functions**

An alternative to the state-space methods discussed so far is to postulate a general-structure dynamic controller with two inputs ( $r$  and  $y$ ) and one output ( $u$ ) and to solve for the transfer function of the controller to give a specified overall  $r$ -to- $y$  transfer function. A block diagram of the situation is shown in Fig. 7.76. We model the plant as the transfer function

$$\frac{Y(s)}{U(s)} = \frac{b(s)}{a(s)}, \quad (7.264)$$

General controller in polynomial form

rather than by state equations. The controller is also modeled by its transfer function, in this case, a transfer function with two inputs and one output:

$$U(s) = -\frac{c_y(s)}{d(s)} Y(s) + \frac{c_r(s)}{d(s)} R(s). \quad (7.265)$$

Here  $d(s)$ ,  $c_y(s)$ , and  $c_r(s)$  are polynomials. In order for the controller of Fig. 7.76 and Eq. (7.265) to be implemented, the orders of the numerator polynomials  $c_y(s)$  and  $c_r(s)$  must not be higher than the order of the denominator polynomial  $d(s)$ .

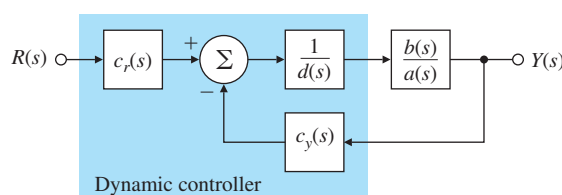
To carry out the design, we require that the closed-loop transfer function defined by Eqs. (7.264) and (7.265) be matched to the desired transfer function

$$\frac{Y(s)}{R(s)} = \frac{c_r(s)b(s)}{\alpha_c(s)\alpha_e(s)}. \quad (7.266)$$

Equation (7.266) tells us that the zeros of the plant must be zeros of the overall system. The only way to change this is to have factors of  $b(s)$  appear in either  $\alpha_c$  or  $\alpha_e$ . We combine Eqs. (7.264) and (7.265) to get

**Figure 7.76**

Direct transfer-function formulation



$$a(s)Y(s) = b(s) \left[ -\frac{c_y(s)}{d(s)} Y(s) + \frac{c_r(s)}{d(s)} R(s) \right], \quad (7.267)$$

which can be rewritten as

$$[a(s)d(s) + b(s)c_y(s)]Y(s) = b(s)c_r(s)R(s). \quad (7.268)$$

Comparing Eq. (7.266), with Eq. (7.267) we immediately see that the design can be accomplished if we can solve the **Diophantine equation**

$$a(s)d(s) + b(s)c_y(s) = \alpha_c(s)\alpha_e(s), \quad (7.269)$$

for given arbitrary  $a$ ,  $b$ ,  $\alpha_c$ , and  $\alpha_e$ . Because each transfer function is a ratio of polynomials, we can assume  $a(s)$  and  $d(s)$  are **monic polynomials**; that is, the coefficient of the highest power of  $s$  in each polynomial is unity. The question is, how many equations and how many unknowns are there, if we match coefficients of equal powers of  $s$  in Eq. (7.269)? If  $a(s)$  is of degree  $n$  (given) and  $d(s)$  is of degree  $m$  (to be selected), then a direct count yields  $2m+1$  unknowns in  $d(s)$  and  $c_y(s)$  and  $n+m$  equations from the coefficients of powers of  $s$ . Thus the requirement is that

$$2m+1 \geq n+m,$$

or

$$m \geq n-1.$$

One possibility for a solution is to choose  $d(s)$  of degree  $n$  and  $c_y(s)$  of degree  $n-1$ . In that case, which corresponds to the state-space design for a full-order estimator, there are  $2n$  equations and  $2n$  unknowns with  $\alpha_c\alpha_e$  of degree  $2n$ . The resulting equations will then have a solution for arbitrary  $\alpha_i$  if and only if  $a(s)$  and  $b(s)$  have no common factors.<sup>19</sup>

## EXAMPLE 7.40

### Pole Placement for Polynomial Transfer Functions

Using the polynomial method, design a controller of order  $n$  for the third-order plant in Example 7.29. Note if the polynomials  $\alpha_c(s)$  and  $\alpha_e(s)$  from Example 7.29 are multiplied, the result is the desired closed-loop characteristic equation:

$$\alpha_c(s)\alpha_e(s) = s^6 + 14s^5 + 122.75s^4 + 585.2s^3 + 1505.64s^2 + 2476.8s + 1728. \quad (7.270)$$

**Solution.** Using Eq. (7.269) with  $b(s) = 10$ , we find that

$$(d_0s^3 + d_1s^2 + d_2s + d_3)(s^3 + 10s^2 + 16s) + 10(c_0s^2 + c_1s + c_2) \equiv \alpha_c(s)\alpha_e(s). \quad (7.271)$$

We have expanded the polynomial  $d(s)$  with coefficients  $d_i$  and the polynomial  $c_y(s)$  with coefficients  $c_i$ .

<sup>19</sup>If they do have a common factor, it will show up on the left side of Eq. (7.269); for there to be a solution, the same factor must be on the right side of Eq. (7.269), and thus a factor of either  $\alpha_c$  or  $\alpha_e$ .

Now we equate the coefficients of the like powers of  $s$  in Eq. (7.271) to find that the parameters must satisfy<sup>20</sup>

$$\begin{bmatrix} 1 & 0 & 0 & 0 & 0 & 0 & 0 \\ 10 & 1 & 0 & 0 & 0 & 0 & 0 \\ 16 & 10 & 1 & 0 & 0 & 0 & 0 \\ 0 & 16 & 10 & 1 & 0 & 0 & 0 \\ 0 & 0 & 16 & 10 & 10 & 0 & 0 \\ 0 & 0 & 0 & 16 & 0 & 10 & 0 \\ 0 & 0 & 0 & 0 & 0 & 0 & 10 \end{bmatrix} \begin{bmatrix} d_0 \\ d_1 \\ d_2 \\ d_3 \\ c_0 \\ c_1 \\ c_2 \end{bmatrix} = \begin{bmatrix} 1 \\ 14 \\ 122.75 \\ 585.2 \\ 1505.64 \\ 2476.8 \\ 1728 \end{bmatrix}. \quad (7.272)$$

The solution to Eq. (7.272) is

$$\begin{aligned} d_0 &= 1, & c_0 &= 190.1, \\ d_1 &= 4, & c_1 &= 481.8, \\ d_2 &= 66.75, & c_2 &= 172.8, \\ d_3 &= -146.3, \end{aligned}$$

**Matlab a\b**

[The solution can be found using  $x = a \backslash b$  command in Matlab, where  $a$  is the Sylvester matrix, and  $b$  is the right-hand side in Eq. (7.272).] Hence the controller transfer function is

$$\frac{c_y(s)}{d(s)} = \frac{190.1s^2 + 481.8s + 172.8}{s^3 + 4s^2 + 66.75s - 146.3}. \quad (7.273)$$

Note the coefficients of Eq. (7.273) are the same as those of the controller  $D_c(s)$  (which we obtained using the state-variable techniques), once the factors in  $D_c(s)$  are multiplied out.

The reduced-order compensator can also be derived using a polynomial solution.

### EXAMPLE 7.41

#### *Reduced-Order Design for a Polynomial Transfer Function Model*

Design a reduced-order controller for the third-order system in Example 7.29. The desired characteristic equation is

$$\alpha_c(s)\alpha_e(s) = s^5 + 12s^4 + 74s^3 + 207s^2 + 378s + 288.$$

**Solution.** The equations needed to solve this problem are the same as those used to obtain Eq. (7.271), except that we take both  $d(s)$  and  $c_y(s)$  to be of degree  $n - 1$ . We need to solve

$$(d_0s^2 + d_1s + d_2)(s^3 + 10s^2 + 16s) + 10(c_0s^2 + c_1s + c_2) \equiv \alpha_c(s)\alpha_e(s). \quad (7.274)$$

<sup>20</sup>The matrix on the left side of Eq. (7.272) is called a **Sylvester matrix**, and is nonsingular if and only if  $a(s)$  and  $b(s)$  have no common factor.

Equating coefficients of like powers of  $s$  in Eq. (7.274), we obtain

$$\begin{bmatrix} 1 & 0 & 0 & 0 & 0 & 0 \\ 10 & 1 & 0 & 0 & 0 & 0 \\ 16 & 10 & 1 & 0 & 0 & 0 \\ 0 & 16 & 10 & 10 & 0 & 0 \\ 0 & 0 & 16 & 0 & 10 & 0 \\ 0 & 0 & 0 & 0 & 0 & 10 \end{bmatrix} \begin{bmatrix} d_0 \\ d_1 \\ d_2 \\ c_0 \\ c_1 \\ c_2 \end{bmatrix} = \begin{bmatrix} 1 \\ 12 \\ 74 \\ 207 \\ 378 \\ 288 \end{bmatrix}. \quad (7.275)$$

The solution is (again using the  $x = a \backslash b$  command in Matlab)

$$d_0 = 1, \quad c_0 = -20.8,$$

$$d_1 = 2.0, \quad c_1 = -23.6,$$

$$d_2 = 38, \quad c_2 = 28.8,$$

and the resulting controller is

$$\frac{c_y(s)}{d(s)} = \frac{-20.8s^2 - 23.6s + 28.8}{s^2 + 2.0s + 38}. \quad (7.276)$$

Again, Eq. (7.276) is exactly the same as  $D_{cr}(s)$  derived using the state-variable techniques in Example 7.30, once the polynomials of  $D_{cr}(s)$  are multiplied out and minor numerical differences are considered.

Notice the reference input polynomial  $c_r(s)$  does not enter into the analysis of Examples 7.40 and 7.41. We can select  $c_r(s)$  so it will assign zeros in the transfer function from  $R(s)$  to  $Y(s)$ . This is the same role played by  $\gamma(s)$  in Section 7.9. One choice is to select  $c_r(s)$  to cancel  $\alpha_e(s)$  so the overall transfer function is

$$\frac{Y(s)}{R(s)} = \frac{K_s b(s)}{\alpha_c(s)}.$$

This corresponds to the first and most common choice of  $\mathbf{M}$  and  $\bar{N}$  for introducing the reference input described in Section 7.9.

It is also possible to introduce integral control and, indeed, internal-model-based robust tracking control into the polynomial design method. What is required is that we have error control, and that the controller has poles at the internal model locations. To get error control with the structure of Fig. 7.76, we need only let  $c_r = c_y$ . To get desired poles into the controller, we need to require that a specific factor be part of  $d(s)$ . For integral control—the most common case—this is almost trivial. The polynomial  $d(s)$  will have a root at zero if we set the last term,  $d_m$ , to zero. The resulting equations can be solved if  $m = n$ . For a more general internal model, we define  $d(s)$  to be the product of a reduced-degree polynomial and a specified polynomial such as Eq. (7.247), and match coefficients in the Diophantine equation as before. The process is straightforward but tedious. Again we caution that, while the polynomial design method can be effective, the numerical problems of this method are often much worse than

**Adding integral control to the polynomial solution**

those associated with methods based on state equations. For higher-order systems, as well as systems with multiple inputs and outputs, the state-space methods are preferable.

## △ 7.13 Design for Systems with Pure Time Delay

In any linear system consisting of lumped elements, the response of the system appears immediately after an excitation of the system. In some feedback systems—for example, process control systems, whether controlled by a human operator in the loop or by computer—there is a **pure time delay** (also called **transportation lag**) in the system. As a result of the distributed nature of these systems, the response remains identically zero until after a delay of  $\lambda$  seconds. A typical step response is shown in Fig. 7.77(a). The transfer function of a pure transportation lag is  $e^{-\lambda s}$ . We can represent an overall transfer function of a SISO system with time delay as

$$G_I(s) = G(s)e^{-\lambda s}, \quad (7.277)$$

where  $G(s)$  has no pure time delay. Because  $G_I(s)$  does not have a finite state description, standard use of state-variable methods is impossible. However, Smith (1958) showed how to construct a feedback structure that effectively takes the delay outside the loop and allows a feedback design based on  $G(s)$  alone, which can be done with standard methods. The result of this method is a design having closed-loop transfer function with delay  $\lambda$  but otherwise showing the same response as the closed-loop design based on no delay. To see how the method works, let us consider the feedback structure shown in Fig. 7.77(b). The overall transfer function is

$$\frac{Y(s)}{R(s)} = \mathcal{T}(s) = \frac{D'_c(s)G(s)e^{-\lambda s}}{1 + D'_c(s)G(s)e^{-\lambda s}}. \quad (7.278)$$

Smith suggested that we solve for  $D'_c(s)$  by setting up a dummy overall transfer function in which the controller transfer function  $D_c(s)$  is in a loop with  $G(s)$  with *no loop* delay but with an overall delay of  $\lambda$ :

$$\frac{Y(s)}{R(s)} = \mathcal{T}(s) = \frac{D_c(s)G(s)}{1 + D_c(s)G(s)}e^{-\lambda s}. \quad (7.279)$$

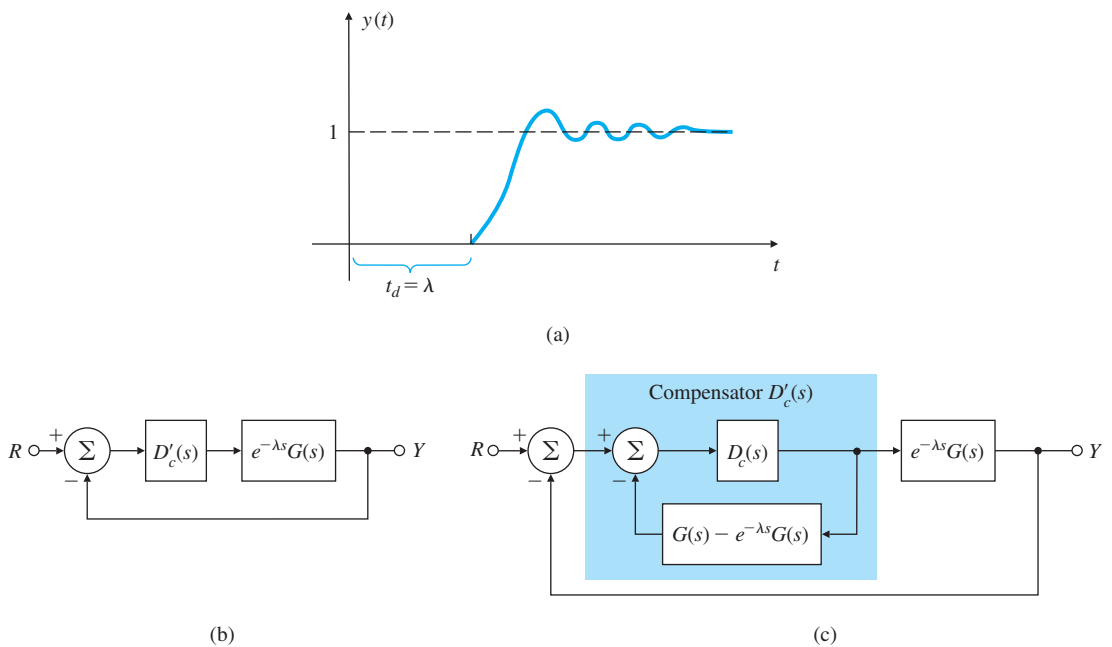
The Smith compensator

We then equate Eqs. (7.278) and (7.279) to solve for  $D'_c(s)$ :

$$D'_c(s) = \frac{D_c(s)}{1 + D_c(s)[G(s) - G(s)e^{-\lambda s}]} \cdot \frac{D_c(s)G(s)}{1 + D_c(s)G(s)}. \quad (7.280)$$

If the plant transfer function and the delay are known,  $D'_c(s)$  can be realized with real components by means of the block diagram shown in Fig. 7.77(c). With this knowledge, we can design the compensator  $D_c(s)$  in the usual way, based on Eq. (7.279), as if there were no delay, then implement it as shown in Fig. 7.77(c). The resulting closed-loop

Overall transfer function  
for a time-delayed system

**Figure 7.77**

A Smith regulator for systems with pure time delay

system would exhibit the behavior of a finite closed-loop system except for the time delay  $\lambda$ . This design approach is particularly suitable when the pure delay,  $\lambda$ , is significant as compared to the process time constant, for example, in pulp and paper process applications.

Notice that, conceptually, the Smith compensator is feeding back a simulated plant output to cancel the true plant output and then adding in a simulated plant output without the delay. It can be demonstrated that  $D'_c(s)$  in Fig. 7.77(c) is equivalent to an ordinary regulator in line with a compensator that provides significant phase lead. To implement such compensators in analog systems, it is usually necessary to approximate the delay required in  $D'_c(s)$  by a Padé approximant; with digital compensators the delay can be implemented exactly (see Chapter 8). It is also a fact that the compensator  $D'_c(s)$  is a strong function of  $G(s)$ , and a small error in the model of the plant used in the controller could lead to large errors in the closed loop, perhaps even to instability. This design is very sensitive both to uncertainties in plant parameters as well as uncertainty in the time delay. If  $D_c(s)$  is implemented as a PI controller, then one could detune (that is, reduce the gain) to try to ensure stability and reasonable performance. For automatic tuning of the Smith regulator and an application to Stanford's quiet hydraulic precision lathe fluid temperature control, refer to Huang and DeBra (2000).

**EXAMPLE 7.42***Heat Exchanger: Design with Pure Time Delay*

Figure 7.78 shows the heat exchanger from Example 2.18. The temperature of the product is controlled by controlling the flow rate of steam in the exchanger jacket. The temperature sensor is several meters downstream from the steam control valve, which introduces a transportation lag into the model. A suitable model is given by

$$G(s) = \frac{e^{-5s}}{(10s + 1)(60s + 1)}.$$

Design a controller for the heat exchanger using the Smith compensator and pole placement. The control poles are to be at

$$p_c = -0.05 \pm 0.087j,$$

and the estimator poles are to be at three times the control poles' natural frequency:

$$p_e = -0.15 \pm 0.26j.$$

Simulate the response of the system with Simulink.

**Solution.** A suitable set of state-space equations is

$$\dot{\mathbf{x}}(t) = \begin{bmatrix} -0.017 & 0.017 \\ 0 & -0.1 \end{bmatrix} \mathbf{x}(t) + \begin{bmatrix} 0 \\ 0.1 \end{bmatrix} u(t - 5),$$

$$y = [1 \ 0] \mathbf{x},$$

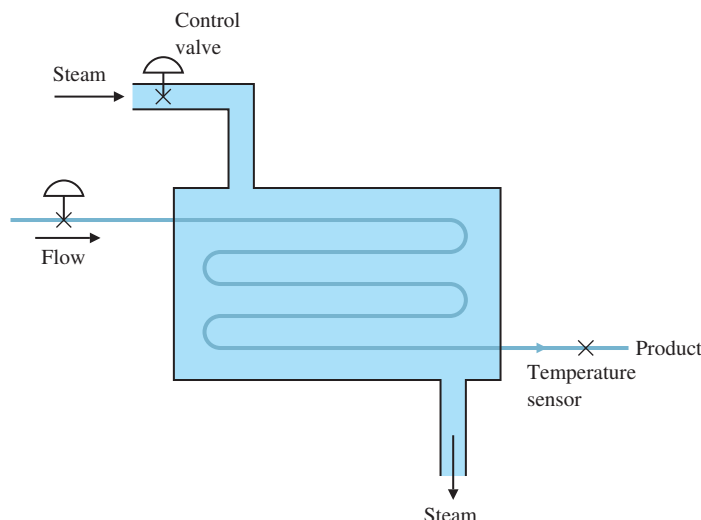
$$\lambda = 5.$$

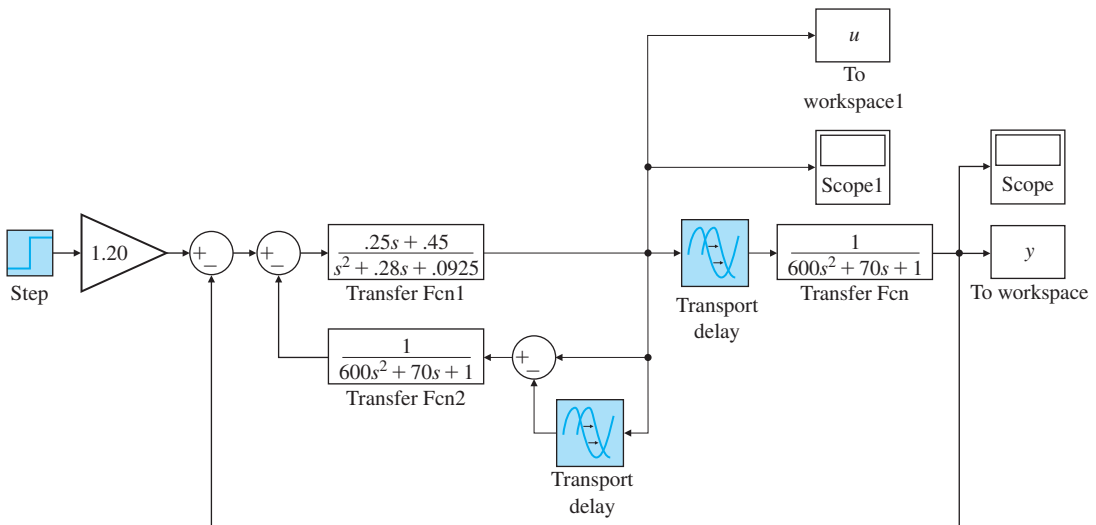
For the specified control pole locations, and for the moment ignoring the time delay, we find that the state feedback gain is

$$\mathbf{K} = [5.2 \ -0.17].$$

**Figure 7.78**

A heat exchanger



**Figure 7.79**

Closed-loop Simulink diagram for a heat exchanger

*Source: Reprinted with permission of The MathWorks, Inc.*

For the given estimator poles, the estimator gain matrix for a full-order estimator is

$$\mathbf{L} = \begin{bmatrix} 0.18 \\ 4.2 \end{bmatrix}.$$

The resulting controller transfer function is

$$D_c(s) = \frac{U(s)}{Y(s)} = \frac{-0.25(s + 1.8)}{s + 0.14 \pm 0.27j}.$$

If we choose to adjust for unity closed-loop DC gain, then

$$\bar{N} = 1.2055.$$

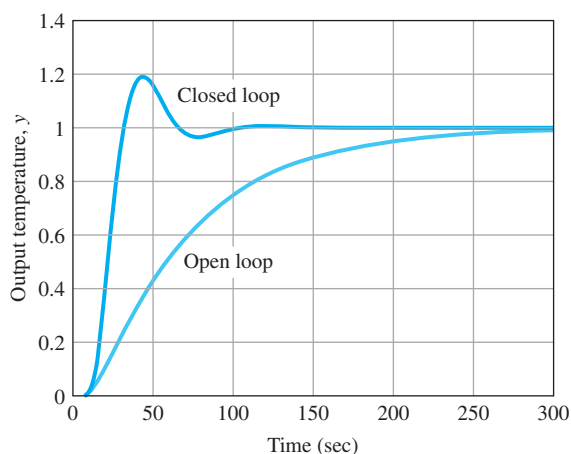
The Simulink diagram for the system is shown in Fig. 7.79. The open-loop and closed-loop step responses of the system and the control effort are shown in Figs. 7.80 and 7.81, and the root locus of the system (without the delay) is shown in Fig. 7.82. Note the time delay of 5 sec in Figs. 7.80 and 7.81 is quite small compared with the response of the system, and is barely noticeable in this case.

## 7.14 Solution of State Equations

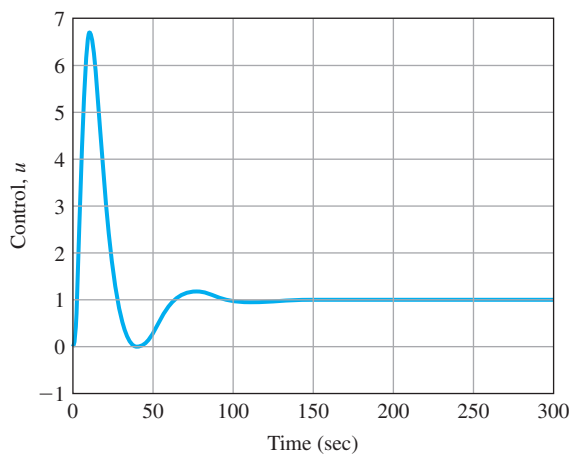
It is possible to write down the solution to the state equations using the matrix exponential. See Appendix W7.13.1 available online at [www.pearsonglobaleditions.com](http://www.pearsonglobaleditions.com).

**Figure 7.80**

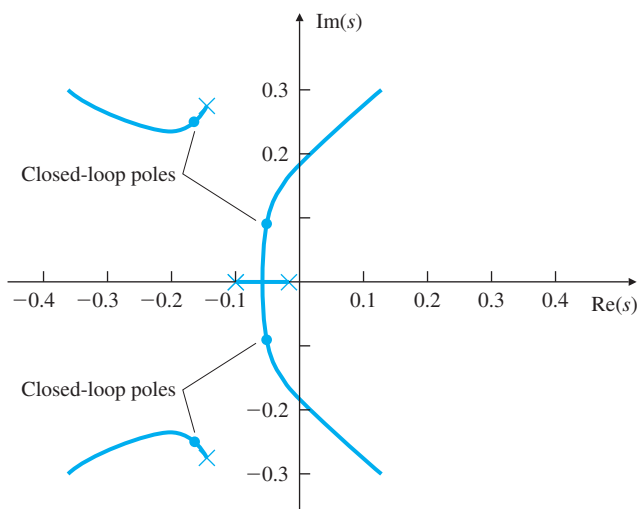
Step response for a heat exchanger

**Figure 7.81**

Control effort for a heat exchanger

**Figure 7.82**

Root locus for a heat exchanger



## 7.15 Historical Perspective

The state-variable approach to solving differential equations in engineering problems was advocated by R. E. Kalman while attending MIT. This was revolutionary and ruffled some feathers as it was going against the grain. The well-established academics, Kalman's teachers, were well-versed in the frequency domain techniques and staunch supporters of it. Beginning in the late 1950s and early 1960s, Kalman wrote a series of seminal papers introducing the ideas of state-variables, controllability, observability, the Linear Quadratic (LQ), and the Kalman Filter (LQF). Gunkel and Franklin (1963) and Joseph and Tou (1961) independently showed the separation theorem, which made possible the Linear Quadratic Gaussian (LQG) problem nowadays referred to as the  $H_2$  formulation. The separation theorem is a special case of the certainty-equivalence theorem of Simon (1956). The solutions to both LQ and LQG problems can be expressed in an elegant fashion in terms of the solutions to Riccati equations. D. G. Luenberger, who was taking a course with Kalman at Stanford University, derived the observer and reduced-order observer over a weekend after hearing Kalman suggesting the problem in a lecture. Kalman, Bryson, Athans, and others contributed to the field of optimal control theory that was widely employed in aerospace problems including the Apollo program. The book by Zadeh and Desoer published in 1962 was also influential in promoting the state-space method. In the 1970s, the robustness of LQ and LQG methods were studied resulting in the celebrated and influential paper of Doyle and Stein in 1981. One of the most significant contributions of Doyle and Safonov was to extend the idea of frequency domain gain to multi-input multi-output systems using the singular value decomposition. Others contributing to this research included G. Zames who introduced the  $H_\infty$  methods that were found to be extensions of the  $H_2$  methods. The resulting design techniques are known as  $H_\infty$  and  $\mu$ -synthesis procedures. During the 1980s, reliable numerical methods were developed for dealing with state-variable designs and computer-aided software for control design was developed. The invention of Matlab by Cleve Moler and its wide distribution by The MathWorks has had a huge impact not only in the control design field but on all interactive scientific computations.

In the mid-1970s, polynomial and matrix fraction descriptions (MFDs) of systems attracted much attention culminating in the celebrated Q-parametrization which characterizes the set of *all stabilizing* controllers for a feedback system.

While the state-variable methods were gaining momentum particularly in the United States, research groups in Europe especially in England led by Rosenbrock, MacFarlane, Munro, and others extended the classical techniques to multi-input multi-output systems. Hence root locus and frequency domain methods such as the (inverse) Nyquist techniques could be used for multi-input multi-output systems. Eventually in the 1980s, there was a realization that the power of both frequency

domain and state-variable methods should be combined for an eclectic control design method employing the best of both approaches.

In the 1970s and 1980s, there was a lot of research on discrete event systems, adaptive control and system identification techniques. In the 1990s, research on control of intelligent autonomous systems and hybrid systems began. Since the turn of the century, research has focused on networked control, cyber-physical systems, control of driverless cars, use of machine learning and convex optimization techniques for control, as well as continued research efforts in control of nonlinear, time-delay, and stochastic systems.

We saw in Chapter 7 that, in contrast to frequency response methods of Bode and Nyquist, the state-variable method not only deals with the input and output variables of the system but also with the internal physical variables. The state-variable methods can be used to study linear and nonlinear, as well as time varying systems. Furthermore, the state-variable method handles the multi-input multi-output problems and high-order systems with equal ease. From a computational perspective, the state-variable methods are far superior to the frequency domain techniques that require polynomial manipulations.

## SUMMARY

- To every transfer function that has no more zeros than poles, there corresponds a differential equation in state-space form.
- State-space descriptions can be in several canonical forms. Among these are **control**, **observer**, and **modal canonical forms**.
- Open-loop poles and zeros can be computed from the state description matrices ( $\mathbf{A}$ ,  $\mathbf{B}$ ,  $\mathbf{C}$ ,  $\mathbf{D}$ ):

$$\text{Poles: } p = \text{eig}(\mathbf{A}), \quad \det(p\mathbf{I} - \mathbf{A}) = 0,$$

$$\text{Zeros: } \det \begin{bmatrix} z\mathbf{I} - \mathbf{A} & -\mathbf{B} \\ \mathbf{C} & \mathbf{D} \end{bmatrix} = 0.$$

- For any controllable system of order  $n$ , there exists a state feedback control law that will place the closed-loop poles at the roots of an arbitrary **control characteristic equation** of order  $n$ .
- The reference input can be introduced so as to result in zero steady-state error to a step command. This property is not expected to be robust to parameter changes.
- Good closed-loop pole locations depend on the desired transient response, the robustness to parameter changes, and a balance between dynamic performance and control effort.
- Closed-loop pole locations can be selected to result in a dominant second-order response, or to minimize a quadratic performance measure.
- For any observable system of order  $n$ , an estimator (or observer) can be constructed with only sensor inputs and a state that

estimates the plant state. The  $n$  poles of the estimator error system can be placed arbitrarily.

- Every transfer function can be represented by a minimal realization, that is, a state-space model that is both controllable and observable.
- A single-input single-output system is completely controllable if and only if the input excites all the natural frequencies of the system, that is, there is no cancellation of the poles in the transfer function.
- The control law and the estimator can be combined into a controller such that the poles of the closed-loop system are the union of the control-law-only poles and the estimator-only poles.
- With the estimator-based controller, the **reference input** can be introduced in such a way as to permit  $n$  arbitrary zeros to be assigned. The most common choice is to assign the zeros to cancel the estimator poles, thus not exciting an estimator error.
- **Integral control** can be introduced to obtain robust steady-state tracking of a step by augmenting the plant state. The design is also robust with respect to rejecting constant disturbances.
- General **robust control** can be realized by combining the equations of the plant and the reference model into an **error space** and designing a control law for the extended system. Implementation of the robust design demonstrates the **internal model principle**. An estimator of the plant state can be added while retaining the robustness properties.
- The **model-following** technique can produce superior tracking properties but suffers from robustness problems.
- The estimator can be extended to include estimates of the equivalent control disturbance, and so result in robust tracking and disturbance rejection.
- Pole-placement designs, including integral control, can be computed using the polynomials of the plant transfer function in place of the state descriptions. Designs using polynomials frequently have problems with numerical accuracy.
- Controllers for plants that include a pure time delay can be designed as if there were no delay, then a controller can be implemented for the plant with the delay. The design can be expected to be sensitive to parameter changes, especially to uncertainty in the delay time.
- Table 7.3 gives the important equations discussed in this chapter. The triangles indicate equations taken from optional sections in the text.
- Determining a model from experimental data, or verifying an analytically based model by experiment, is an important step in system design by state-space analysis, a step that is not necessarily needed for compensator design via frequency-response methods.

**TABLE 7.3****Important Equations in Chapter 7**

Name	Equation	Page
Control canonical form	$\mathbf{A}_c = \begin{bmatrix} -a_1 & -a_2 & \cdots & \cdots & -a_n \\ 1 & 0 & \cdots & \cdots & 0 \\ 0 & 1 & 0 & \cdots & 0 \\ \vdots & & \ddots & 0 & \vdots \\ 0 & 0 & \cdots & 1 & 0 \end{bmatrix}, \quad \mathbf{B}_c = \begin{bmatrix} 1 \\ 0 \\ 0 \\ \vdots \\ 0 \end{bmatrix},$ $\mathbf{C}_c = [b_1 \ b_2 \ \cdots \ \cdots \ b_n], \quad D_c = 0.$	492
State description	$\dot{\mathbf{x}} = \mathbf{Ax} + \mathbf{Bu}$	495
Output equation	$y = \mathbf{Cx} + \mathbf{Du}$	495
Transformation of state	$\bar{\mathbf{A}} = \mathbf{T}^{-1}\mathbf{AT}$ $\bar{\mathbf{B}} = \mathbf{T}^{-1}\mathbf{B}$ $y = \mathbf{CTz} + \mathbf{Du} = \bar{\mathbf{C}}\mathbf{z} + \bar{\mathbf{D}}u,$ where $\bar{\mathbf{C}} = \mathbf{CT}, \bar{\mathbf{D}} = \mathbf{D}$	495
Controllability matrix	$\mathcal{C} = [\mathbf{B} \ \mathbf{AB} \ \cdots \ \mathbf{A}^{n-1}\mathbf{B}]$	496
Transfer function from state equations	$G(s) = \frac{Y(s)}{U(s)} = \mathbf{C}(s\mathbf{I} - \mathbf{A})^{-1}\mathbf{B} + \mathbf{D}$	503
Transfer-function poles	$\det(p_i\mathbf{I} - \mathbf{A}) = 0$	505
Transfer-function zeros	$\alpha_z(s) = \det \begin{bmatrix} z_i\mathbf{I} - \mathbf{A} & -\mathbf{B} \\ \mathbf{C} & \mathbf{D} \end{bmatrix} = 0$	506
Control characteristic equation	$\det[s\mathbf{I} - (\mathbf{A} - \mathbf{BK})] = 0$	510
Ackermann's control formula for pole placement	$\mathbf{K} = [0 \ \cdots \ 0 \ 1]\mathcal{C}^{-1}\alpha_c(\mathbf{A})$	514
Reference input gains	$\begin{bmatrix} \mathbf{A} & \mathbf{B} \\ \mathbf{C} & \mathbf{D} \end{bmatrix} \begin{bmatrix} \mathbf{N_x} \\ \mathbf{N_u} \end{bmatrix} = \begin{bmatrix} \mathbf{0} \\ 1 \end{bmatrix}$	518
Control equation with reference input	$u = N_u r - \mathbf{K}(\mathbf{x} - \mathbf{N_x}r)$ $= -\mathbf{Kx} + (N_u + \mathbf{KN_x})r$ $= -\mathbf{Kx} + \bar{N}r$	518
Symmetric root locus	$1 + \rho G_0(-s)G_0(s) = 0$	525
Estimator error characteristic equation	$\alpha_e(s) = \det[s\mathbf{I} - (\mathbf{A} - \mathbf{LC})] = 0$	535
Observer canonical form	$\dot{\mathbf{x}}_o = \mathbf{A}_o \mathbf{x}_o + \mathbf{B}_o u,$ $y = \mathbf{C}_o \mathbf{x}_o + \mathbf{D}_o u,$ where $\mathbf{A}_o = \begin{bmatrix} -a_1 & 1 & 0 & 0 & \cdots & 0 \\ -a_2 & 0 & 1 & 0 & \cdots & \vdots \\ \vdots & \vdots & \ddots & & & 1 \\ -a_n & 0 & 0 & 0 & & 0 \end{bmatrix}, \quad \mathbf{B}_o = \begin{bmatrix} b_1 \\ b_2 \\ \vdots \\ b_n \end{bmatrix},$ $\mathbf{C}_o = [1 \ 0 \ 0 \ \cdots \ 0], \quad D_o = 0.$	538

**TABLE 7.3****Continued**

Name	Equation	Page
Observability matrix	$\mathcal{O} = \begin{bmatrix} \mathbf{C} \\ \mathbf{CA} \\ \vdots \\ \mathbf{CA}^{n-1} \end{bmatrix},$	539
Ackermann's estimator formula	$\mathbf{L} = \alpha_e(\mathbf{A})\mathcal{O}^{-1} \begin{bmatrix} 0 \\ 0 \\ \vdots \\ 1 \end{bmatrix}$	539
Compensator transfer function	$D_c(s) = \frac{U(s)}{Y(s)} = -\mathbf{K}(s\mathbf{I} - \mathbf{A} + \mathbf{B}\mathbf{K} + \mathbf{LC})^{-1}\mathbf{L}$	548
Reduced-order compensator transfer function	$D_{cr}(s) = \frac{U(s)}{Y(s)} = \mathbf{C}_r(s\mathbf{I} - \mathbf{A}_r)^{-1}\mathbf{B}_r + D_r$	549
Controller equations	$\dot{\hat{\mathbf{x}}} = (\mathbf{A} - \mathbf{B}\mathbf{K} - \mathbf{LC})\hat{\mathbf{x}} + \mathbf{Ly} + \mathbf{Mr}$ $u = -\mathbf{K}\hat{\mathbf{x}} + \bar{N}r$	561
Augmented state equations with integral control	$\begin{bmatrix} \dot{x}_I \\ \dot{x} \end{bmatrix} = \begin{bmatrix} 0 & \mathbf{C} \\ \mathbf{0} & \mathbf{A} \end{bmatrix} \begin{bmatrix} x_I \\ \mathbf{x} \end{bmatrix} + \begin{bmatrix} 0 \\ \mathbf{B} \end{bmatrix} u - \begin{bmatrix} 1 \\ \mathbf{0} \end{bmatrix} r + \begin{bmatrix} 0 \\ \mathbf{B}_1 \end{bmatrix} w$	571
△ General controller in polynomial form	$U(s) = -\frac{c_y(s)}{d(s)} Y(s) + \frac{c_r(s)}{d(s)} R(s)$	598
△ Diophantine equation for closed-loop characteristic equation	$a(s)d(s) + b(s)c_y(s) = \alpha_c(s)\alpha_e(s)$	599

## REVIEW QUESTIONS

The following questions are based on a system in state-variable form with matrices  $\mathbf{A}$ ,  $\mathbf{B}$ ,  $\mathbf{C}$ ,  $\mathbf{D}$ , input  $u$ , output  $y$ , and state  $\mathbf{x}$ .

- 7.1 Why is it convenient to write dynamic equations in state-variable form?
- 7.2 Give an expression for the transfer function of this system.
- 7.3 Give two expressions for the poles of the transfer function of the system.
- 7.4 Give an expression for the zeros of the system transfer function.
- 7.5 Under what condition will the state of the system be controllable?
- 7.6 Under what conditions will the system be observable from the output  $y$ ?
- 7.7 Give an expression for the *closed-loop* poles if state feedback of the form  $u = -\mathbf{K}\mathbf{x}$  is used.
- 7.8 Under what conditions can the feedback matrix  $\mathbf{K}$  be selected so the roots of  $\alpha_c(s)$  are arbitrary?

- 7.9** What is the advantage of using the LQR or SRL in designing the feedback matrix  $\mathbf{K}$ ?
- 7.10** What is the main reason for using an estimator in feedback control?
- 7.11** If the estimator gain  $\mathbf{L}$  is used, give an expression for the closed-loop poles due to the estimator.
- 7.12** Under what conditions can the estimator gain  $\mathbf{L}$  be selected so the roots of  $\alpha_e(s) = 0$  are arbitrary?
- 7.13** If the reference input is arranged so the input to the estimator is identical to the input to the process, what will the overall closed-loop transfer function be?
- 7.14** If the reference input is introduced in such a way as to permit the zeros to be assigned as the roots of  $\gamma(s)$ , what will the overall closed-loop transfer function be?
- 7.15** What are the three standard techniques for introducing integral control in the state feedback design method?

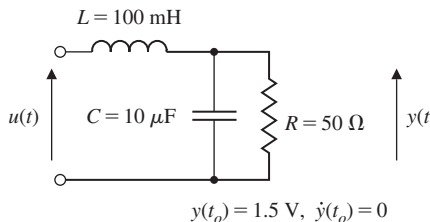
## PROBLEMS

### Problems for Section 7.3: Block Diagrams and State-Space

- 7.1** Write the dynamic equations describing in Fig. 7.83. Write the equations as a second-order differential equation in  $y(t)$ . Assuming zero input, solve the differential equation for  $y(t)$  using Laplace transform methods for the parameters values and initial conditions shown in the figure. Verify your answer using the initial command in Matlab.

**Figure 7.83**

Circuit for Problem 7.1



- 7.2** A schematic for the satellite and scientific probe for the Gravity Probe-B (GP-B) experiment that was launched April 30, 2004 is sketched in Fig. 7.84. Assume that the mass of the spacecraft plus helium tank,  $m_1$ , is 1500 kg and the mass of the probe,  $m_2$ , is 800 kg. A rotor will float inside the probe and will be forced to follow the probe with a capacitive forcing mechanism. The spring constant of the coupling,  $k$ , is  $2.8 \times 10^6$ . The viscous damping  $b$  is  $5.0 \times 10^3$ .
- (a) Write the equations of motion for the system consisting of masses  $m_1$  and  $m_2$  using the inertia position variables,  $y_1$  and  $y_2$ .
- (b) The actual disturbance  $u$  is a micrometeorite, and the resulting motion is very small. Therefore, re-write your equations with the scaled variables  $z_1 = 10^6 y_1$ ,  $z_2 = 10^6 y_2$ , and  $v = 1000u$ .

- (c) Put the equations in state-variable form using the state  $\mathbf{x} = [z_1 \ z_2 \ \dot{z}_1 \ \dot{z}_2]^T$ , the output  $y = z_2$ , and the input an impulse,  $u = 10^{-3}\delta(t)$  N·sec on mass  $m_1$ .

- (d) Using the numerical values, enter the equations of motion into Matlab in the form

$$\dot{\mathbf{x}} = \mathbf{Ax} + \mathbf{Bv} \quad (7.281)$$

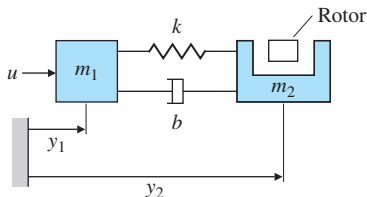
$$y = \mathbf{Cx} + \mathbf{Dv}. \quad (7.282)$$

and define the Matlab system:  $\text{sysGPB} = \text{ss}(A, B, C, D)$ . Plot the response of  $y$  caused by the impulse with the Matlab command `impulse(sysGPB)`. This is the signal the rotor must follow.

- (e) Use the Matlab commands `p=eig(F)` to find the poles (or roots) of the system, and `z=tzero(A,B,C,D)` to find the zeros of the system.

**Figure 7.84**

Schematic diagram of the GP-B satellite and probe



### Problems for Section 7.4: Analysis of the State Equations

- 7.3** Give the state description matrices in control-canonical form for the following transfer functions:

(a)  $G(s) = \frac{1}{7s+1}$ .

(b)  $G(s) = \frac{6(s/3+1)}{(s/10+1)}$ .

(c)  $G(s) = \frac{7s+1}{s^2+3+2}$ .

(d)  $G(s) = \frac{s+7}{s(s^2+2s+2)}$ .

(e)  $G(s) = \frac{(s+7)(s^2+s+25)}{s^2(s+2)(s^2+s+36)}$ .

- 7.4** Use the Matlab function `tf2ss` to obtain the state matrices called for in Problem 7.3.

- 7.5** Give the state description matrices in modal canonical form for the transfer functions of Problem 7.3. Make sure that all entries in the state matrices are real valued by keeping any pairs of complex conjugate poles together, and realize them as a separate subblock in control canonical form.

- 7.6** A certain system with state  $\mathbf{x}$  is described by the state matrices,

$$\mathbf{A} = \begin{bmatrix} -1.5 & 1 \\ -1.5 & 0 \end{bmatrix}, \quad \mathbf{B} = \begin{bmatrix} 1 \\ 5 \end{bmatrix},$$

$$\mathbf{C} = \begin{bmatrix} 1 & 0 \end{bmatrix}, \quad \mathbf{D} = 0.$$

Find the transformation  $\mathbf{T}$  so that if  $\mathbf{x} = \mathbf{T}\mathbf{z}$ , the state matrices describing the dynamics of  $\mathbf{z}$  are in control canonical form. Compute the matrices  $\bar{\mathbf{A}}$ ,  $\bar{\mathbf{B}}$ ,  $\bar{\mathbf{C}}$ , and  $\bar{\mathbf{D}}$ .

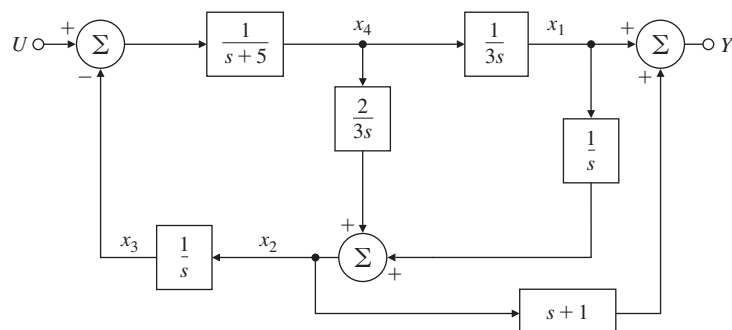
- 7.7 Show that the transfer function is not changed by a linear transformation of state.
- 7.8 Use block-diagram reduction or Mason's rule to find the transfer function for the system in observer canonical form depicted by Fig. 7.31.
- 7.9 Suppose we are given a system with state matrices  $\mathbf{A}$ ,  $\mathbf{B}$ ,  $\mathbf{C}$  ( $D = 0$  in this case). Find the transformation  $\mathbf{T}$  so, under Eqs. (7.21) and (7.22), the new state description matrices will be in observer canonical form.
- 7.10 Use the transformation matrix in Eq. (7.38) to explicitly multiply out the equations at the end of Example 7.9.
- 7.11 Find the state transformation that takes the observer canonical form of Eq. (7.32) to the modal canonical form.
- 7.12 (a) Find the transformation  $\mathbf{T}$  that will keep the description of the airplane system of Example 7.10 in modal canonical form but will convert each element of the input matrix  $\mathbf{B}_m$  to unity.  
 (b) Use Matlab to verify that your transformation does the job.
- 7.13 (a) Find the state transformation that will keep the description of the airplane system of Example 7.10 in modal canonical form but will cause the poles to be displayed in  $\mathbf{A}_m$  in order of increasing magnitude.  
 (b) Use Matlab to verify your result in part (a), and give the complete new set of state matrices as  $\bar{\mathbf{A}}$ ,  $\bar{\mathbf{B}}$ ,  $\bar{\mathbf{C}}$ , and  $\bar{\mathbf{D}}$ .
- 7.14 Find the characteristic equation for the modal-form matrix  $\mathbf{A}_m$  of Eq. (7.14a) using Eq. (7.55).
- 7.15 Given the system

$$\dot{\mathbf{x}} = \begin{bmatrix} -3 & 2 \\ -5 & -1 \end{bmatrix} \mathbf{x} + \begin{bmatrix} 0 \\ 1 \end{bmatrix} u,$$

with zero initial conditions, find the steady-state value of  $x$  for a step input  $u$ .

- 7.16 Consider the system shown in Fig. 7.85:
  - (a) Find the transfer function from  $U$  to  $Y$ .
  - (b) Write state equations for the system using the state-variables indicated.

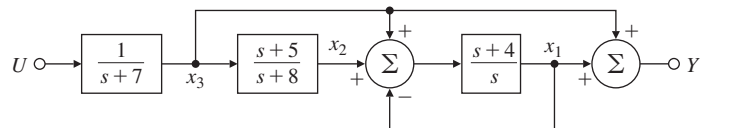
**Figure 7.85**  
Block diagram for  
Problem 7.16



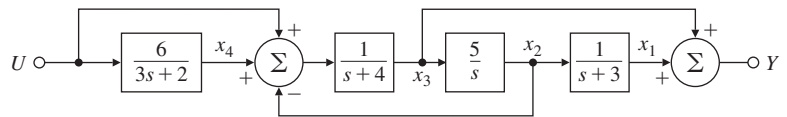
- 7.17** Using the indicated state-variables, write the state equations for each of the system show in Fig. 7.86. Find the transfer function for each system using both block-diagram manipulation and matrix algebra [as in Eq. (7.45)].

**Figure 7.86**

Block diagram for Problem 7.17



(a)



(b)

- 7.18** For each of the listed transfer functions, write the state equations in both control and observer canonical form. In each case, draw a block diagram and given the appropriate expressions for  $\mathbf{A}$ ,  $\mathbf{B}$ , and  $\mathbf{C}$ .

- (a)  $G(s) = \frac{(s^2-2s+7)(s+1)}{s^5+2s^4+7s^3+5s^2+10s+1}$  (voltage equalisation circuit for a solar photovoltaic array using a high-order low-ripple power converter)
- (b)  $G(s) = \frac{s^2-6}{s^2(s^2-2)}$  (control of an inverted pendulum by a force on the cart)

- 7.19** Consider the transfer function

$$G(s) = \frac{s+4}{s^2+3s+2} \quad (7.283)$$

- (a) By re-writing Eq. (7.283) in the form,

$$G(s) = \frac{1}{s+2} \left( \frac{s+4}{s+1} \right),$$

find a series realization of  $G(s)$  as a cascade of two first-order systems.

- (b) Using a partial-fraction expansion of  $G(s)$ , find a parallel realization of  $G(s)$ .

- (c) Realise in control canonical form.

- 7.20** Show that the impulse response of the system  $(\mathbf{A}, \mathbf{B}, \mathbf{C}, \mathbf{D})$  is given by

$$h(t) = \mathbf{C}e^{\mathbf{A}t}\mathbf{B} + \mathbf{D}\delta(t),$$

where  $e^{\mathbf{A}t}$  is the matrix exponential defined by

$$e^{\mathbf{A}t} = \left( \mathbf{I} + \mathbf{A}t + \frac{\mathbf{A}^2 t^2}{2!} + \dots \right) = \sum_{k=0}^{\infty} \frac{\mathbf{A}^k t^k}{k!}.$$

*Problems for Section 7.5: Control Law Design for Full-State Feedback*

7.21 Consider the plant described by,

$$\dot{\mathbf{x}} = \begin{bmatrix} 0 & 1 \\ 2 & -9 \end{bmatrix} \mathbf{x} + \begin{bmatrix} 1 \\ 8 \end{bmatrix} u,$$

$$y = [2 \quad 4] \mathbf{x}.$$

- (a) Draw a block diagram for the plant with one integrator for each state variable.
- (b) Find the transfer function using matrix algebra.
- (c) Find the closed-loop characteristic equation if the feedback is
  - (i)  $u = -[K_1 \quad K_2] \mathbf{x}$ ;
  - (ii)  $u = -Ky$ .

7.22 For the system

$$\dot{\mathbf{x}} = \begin{bmatrix} 0 & 1 \\ -7.2 & -9.3 \end{bmatrix} \mathbf{x} + \begin{bmatrix} 0 \\ 1 \end{bmatrix} u,$$

$$y = [1 \quad 0] \mathbf{x},$$

design a state feedback controller that satisfies the following specifications:

- (a) Closed-loop poles having a damping coefficient  $\zeta = 0.707$ .
- (b) Step-response peak time is under 0.5 sec.

Verify your design with Matlab.

7.23 (a) Design a state feedback controller for the following system so that the closed-loop step response has an overshoot of less than 18% and 1% settling under 0.3 sec:

$$\dot{\mathbf{x}} = \begin{bmatrix} 0 & 1 \\ 0 & -7.5 \end{bmatrix} \mathbf{x} + \begin{bmatrix} 0 \\ 1 \end{bmatrix} u,$$

$$y = [1 \quad 0] \mathbf{x}.$$

- (b) Use the step command in Matlab to verify that your design meets the specifications. If it does not, modify your feedback gains accordingly.

7.24 Consider the system

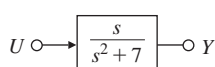
$$\dot{\mathbf{x}} = \begin{bmatrix} -1 & -2 & -2 \\ 0 & -1 & 1 \\ 1 & 0 & -1 \end{bmatrix} \mathbf{x} + \begin{bmatrix} 2 \\ 0 \\ 1 \end{bmatrix} u.$$

- (a) Design a state feedback controller for the system so the closed-loop step response has an overshoot of less than 5% and a 1% settling time under 4.6 sec.
- (b) Use the step command in Matlab to verify that your design meets the specifications. If it does not, modify your feedback gains accordingly.

7.25 Consider the system in Fig. 7.87.

Figure 7.87

System for Problem 7.25



- (a) Write a set of equations that describes this system in the control canonical form as  $\dot{\mathbf{x}} = \mathbf{Ax} + \mathbf{Bu}$  and  $y = \mathbf{Cx}$ .

- (b) Design a control law of the form,

$$u = -[K_1 \ K_2] \begin{bmatrix} x_1 \\ x_2 \end{bmatrix},$$

which will place the closed-loop poles at  $s = -2.5 \pm j2.5$ .

- 7.26 Output Controllability.** In many situations, a control engineer may be interested in controlling the output  $y$  rather than the state  $\mathbf{x}$ . A system is said to be **output controllable** if at any time you are able to transfer the output from zero to any desired output  $y^*$  in a finite time using an appropriate control signal  $u^*$ . Derive necessary and sufficient conditions for a continuous system ( $\mathbf{A}$ ,  $\mathbf{B}$ ,  $\mathbf{C}$ ) to be output controllable. Are output and state controllability related? If so, how?

- 7.27** Consider the system

$$\dot{\mathbf{x}} = \begin{bmatrix} 0 & 4 & 0 & 0 \\ -1 & -4 & 0 & 0 \\ 5 & 7 & 1 & 15 \\ 0 & 0 & 3 & -3 \end{bmatrix} \mathbf{x} + \begin{bmatrix} 0 \\ 0 \\ 1 \\ 0 \end{bmatrix} u.$$

- (a) Find the eigenvalues of this system. (*Hint:* Note the block-triangular structure of  $\mathbf{A}$ .)

- (b) Find the controllable and uncontrollable modes of this system.

- (c) For each of the uncontrollable modes, find a vector  $\mathbf{v}$  such that

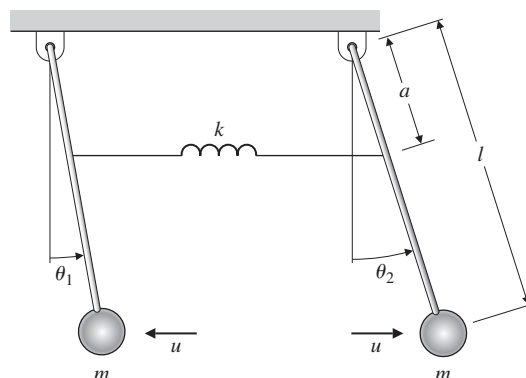
$$\mathbf{v}^T \mathbf{B} = 0, \quad \mathbf{v}^T \mathbf{A} = \lambda \mathbf{v}^T.$$

- (d) Show there are an infinite number of feedback gains  $\mathbf{K}$  that will relocate the modes of the system to  $-5$ ,  $-3$ ,  $-2$ , and  $-2$ .

- (e) Find the unique matrix  $\mathbf{K}$  that achieves these pole locations and prevents initial conditions on the uncontrollable part of the system from ever affecting the controllable part.

- 7.28** Two pendulums, coupled by a spring, are to be controlled by two equal and opposite forces  $u$ , which are applied to the pendulum bobs as shown in Fig. 7.88. The equations of motion are

**Figure 7.88**  
Coupled pendulums for  
Problem 7.28



$$\begin{aligned} ml^2\ddot{\theta}_1 &= -ka^2(\theta_1 - \theta_2) - mgl\theta_1 - lu, \\ ml^2\ddot{\theta}_2 &= -ka^2(\theta_2 - \theta_1) - mgl\theta_2 + lu. \end{aligned}$$

- (a) Show the system is uncontrollable. Can you associate a physical meaning with the controllable and uncontrollable modes?
- (b) Is there any way that the system can be made controllable?
- 7.29 The state-space model for a certain application has been given to us with the following state description matrices:

$$\mathbf{A} = \begin{bmatrix} 0.174 & 0 & 0 & 0 & 0 \\ 0.157 & 0.645 & 0 & 0 & 0 \\ 0 & 1 & 0 & 0 & 0 \\ 0 & 0 & 1 & 0 & 0 \\ 0 & 0 & 0 & 1 & 0 \end{bmatrix}, \quad \mathbf{B} = \begin{bmatrix} -0.207 \\ -0.005 \\ 0 \\ 0 \\ 0 \end{bmatrix},$$

$$\mathbf{C} = [1 \ 0 \ 0 \ 0 \ 0].$$

- (a) Draw a block diagram of the realization with an integrator for each state-variable.
- (b) A student has computed  $\det \mathcal{C} = 2.3 \times 10^{-7}$  and claims that the system is uncontrollable. Is the student right or wrong? Why?
- (c) Is the realization observable?
- 7.30 *Staircase Algorithm (Van Dooren et al., 1978)*: Any realization  $(\mathbf{A}, \mathbf{B}, \mathbf{C})$  can be transformed by an **orthogonal similarity transformation** to  $(\bar{\mathbf{A}}, \bar{\mathbf{B}}, \bar{\mathbf{C}})$ , where  $\bar{\mathbf{A}}$  is an **upper Hessenberg matrix** (having one nonzero diagonal above the main diagonal) given by

$$\bar{\mathbf{A}} = \mathbf{T}^T \mathbf{A} \mathbf{T} = \begin{bmatrix} * & \alpha_1 & 0 & 0 \\ * & * & \ddots & 0 \\ * & * & \ddots & \alpha_{n-1} \\ * & * & \cdots & * \end{bmatrix}, \quad \bar{\mathbf{B}} = \mathbf{T}^T \mathbf{B} = \begin{bmatrix} 0 \\ \vdots \\ 0 \\ g_1 \end{bmatrix},$$

where  $g_1 \neq 0$ , and

$$\bar{\mathbf{C}} = \mathbf{C} \mathbf{T} = [\bar{c}_1 \ \bar{c}_2 \ \cdots \ \bar{c}_n], \quad \mathbf{T}^{-1} = \mathbf{T}^T.$$

Orthogonal transformations correspond to a **rotation** of the vectors (represented by the matrix columns) being transformed with no change in length.

- (a) Prove that if  $\alpha_i = 0$  and  $\alpha_{i+1}, \dots, \alpha_{n-1} \neq 0$  for some  $i$ , then the controllable and uncontrollable modes of the system can be identified after this transformation has been done.
- (b) How would you use this technique to identify the observable and unobservable modes of  $(\mathbf{A}, \mathbf{B}, \mathbf{C})$ ?
- (c) What advantage does this approach for determining the controllable and uncontrollable modes have over transforming the system to any other form?
- (d) How can we use this approach to determine a basis for the controllable and uncontrollable subspaces, as in Problem 7.44?

This algorithm can also be used to design a numerically stable algorithm for pole placement [see Minimis and Paige (1982)]. The name of the algorithm comes from the multi-input version in which the  $\alpha_i$  are the blocks that make  $\tilde{\mathbf{A}}$  resemble a staircase. Refer to `ctrbf`, `obsvf` commands in Matlab.

### Problems for Section 7.6: Selection of Pole Locations for Good Design

- 7.31** The normalized equations of motion for an inverted pendulum at angle  $\theta$  on a cart are

$$\ddot{\theta} = \theta + u, \quad \ddot{x} = -\beta\theta - u,$$

where  $x$  is the cart position, and the control input  $u$  is a force acting on the cart.

- (a) With the state defined as  $\mathbf{x} = [\theta \quad \dot{\theta} \quad x \quad \dot{x}]^T$  find the feedback gain  $\mathbf{K}$  that places the closed-loop poles at  $s = -1, -1, -1 \pm 1j$ . For parts (b) through (d), assume that  $\beta = 0.5$ .

- (b) Use the SRL to select poles with a bandwidth as close as possible to those of part (a), and find the control law that will place the closed-loop poles at the points you selected.

- (c) Compare the responses of the closed-loop systems in parts (a) and (b) to an initial condition of  $\theta = 10^\circ$ . You may wish to use the initial command in Matlab.

- (d) Compute  $N_x$  and  $N_u$  for zero steady-state error to a constant command input on the cart position, and compare the step responses of each of the two closed-loop systems.

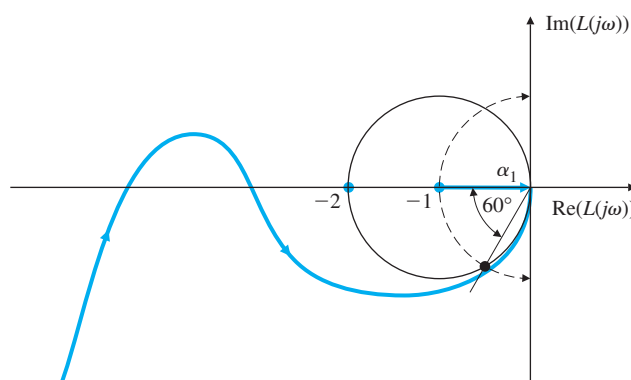
- 7.32** An asymptotically stable Type I system with input  $r$  and output  $y$  is described by the closed-loop system matrices  $(\mathbf{A}, \mathbf{B}, \mathbf{C}, D = 0)$ . Suppose the input is given by the ramp  $r = at$ , for  $t > 0$ . Show the velocity error coefficient is given by

$$K_v = \left[ \mathbf{C}\mathbf{A}^{-2}\mathbf{B} \right]^{-1}.$$

- 7.33** Prove the Nyquist plot for LQR design avoids a circle of radius one centered at the  $-1$  point, as shown in Fig. 7.89. Show this implies that

**Figure 7.89**

Nyquist plot for an optimal regulator



$\frac{1}{2} < GM < \infty$ , the “upward” gain margin is  $GM = \infty$ , and there is a “downward”  $GM = \frac{1}{2}$ , and the phase margin is at least  $PM = \pm 60^\circ$ . Hence the LQR gain matrix,  $\mathbf{K}$ , can be multiplied by a large scalar or reduced by half with guaranteed closed-loop system stability.

### Problems for Section 7.7: Estimator Design

- 7.34 Consider the system

$$\mathbf{A} = \begin{bmatrix} -5 & 3 \\ 1 & 0 \end{bmatrix}, \mathbf{B} = \begin{bmatrix} 1 \\ 0 \end{bmatrix}, \mathbf{C} = [3 \quad 4],$$

and assume that you are using feedback of the form  $u = -\mathbf{K}\mathbf{x} + r$ , where  $r$  is a reference input signal.

- (a) Show that  $(\mathbf{A}, \mathbf{C})$  is observable.
- (b) Show that there exists a  $\mathbf{K}$  such that  $(\mathbf{A} - \mathbf{B}\mathbf{K}, \mathbf{C})$  is unobservable.
- (c) Compute a  $\mathbf{K}$  of the form  $\mathbf{K} = [1, K_2]$  that will make the system unobservable as in part (b); that is, find  $K_2$  so that closed-loop system is not observable.
- (d) Compare the open-loop transfer function with the transfer function of the closed-loop system of part (c). What is the unobservability due to?

- 7.35 Consider a system with the transfer function,

$$G(s) = \frac{s + 15}{s^2 - 15}.$$

- (a) Find  $(\mathbf{A}_o, \mathbf{B}_o, \mathbf{C}_o)$  for this system in observer canonical form.
- (b) Check if this system observable.
- (c) Is  $(\mathbf{A}_o, \mathbf{B}_o)$  controllable?
- (d) Compute  $\mathbf{K}$  so that the closed-loop poles are assigned to  $s = -10 \pm j10$ .
- (e) Design a full-order estimator with estimator-error poles at  $s = -15 \pm j15$ .
- (f) Prove that if  $u = -\mathbf{K}\mathbf{x} + r$  there is a feedback gain  $\mathbf{K}$  that makes the closed-loop system unobservable. Design  $\mathbf{K}$  so that the closed-loop system has no zero and there is only one pole at  $s = -5$ .

- 7.36 Explain how the controllability, observability, and stability properties of a linear system are related.

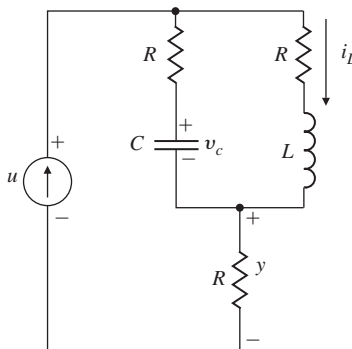
- 7.37 Consider the electric circuit shown in Fig. 7.90.

- (a) Write the internal (state) equations for the circuit. The input  $u$  is a voltage source, and the output  $y$  is a voltage. Let  $x_1 = i_L$  and  $x_2 = v_c$ .
- (b) What condition(s) on  $R$ ,  $L$ , and  $C$  will guarantee that the system is controllable?
- (c) What condition(s) on  $R$ ,  $L$ , and  $C$  will guarantee that the system is observable?

- 7.38 The block diagram of a feedback system is shown in Fig. 7.91. The system state is

$$\mathbf{x} = \begin{bmatrix} \mathbf{x}_p \\ \mathbf{x}_f \end{bmatrix},$$

**Figure 7.90**  
Electric circuit for  
Problem 7.37



and the dimensions of the matrices are as follows:

$$\mathbf{A} = n \times n, \quad \mathbf{L} = n \times 1,$$

$$\mathbf{B} = n \times 1, \quad \mathbf{x} = 2n \times 1,$$

$$\mathbf{C} = 1 \times n, \quad r = 1 \times 1,$$

$$\mathbf{K} = 1 \times n, \quad y = 1 \times 1.$$

(a) Write state equations for the system.

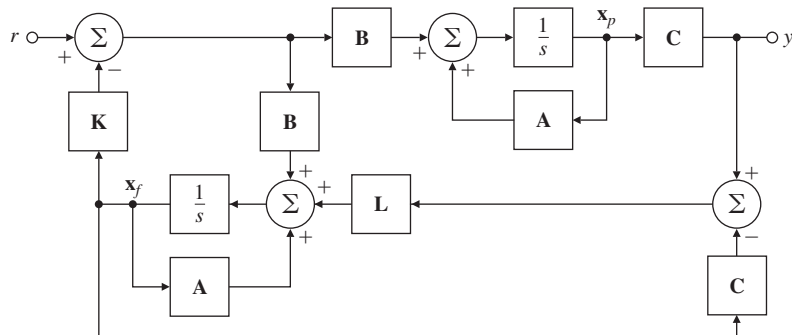
(b) Let  $\mathbf{x} = \mathbf{Tz}$ , where

$$\mathbf{T} = \begin{bmatrix} \mathbf{I} & \mathbf{0} \\ \mathbf{I} & \mathbf{I} \end{bmatrix}.$$

Show the system is not controllable.

(c) Find the transfer function of the system from  $r$  to  $y$ .

**Figure 7.91**  
Block diagram for  
Problem 7.38

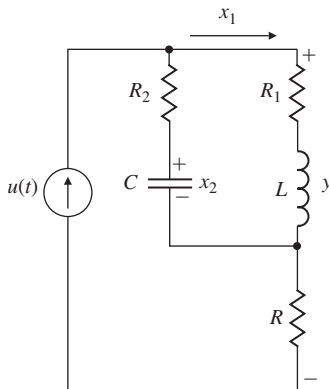


**7.39** This problem is intended to give you more insight into controllability and observability. Consider the circuit in Fig. 7.92, with an input current source  $u(t)$  and an output voltage  $y(t)$ . Note that usually  $R_1$  and  $R_2$  represent the respective internal resistances of  $L$  and  $C$  while  $R$  can be the load.

- (a) Using the capacitor voltage and inductor current as state variables, write state and output equations for the system.
- (b) Find the conditions relating  $R_1$ ,  $R_2$ ,  $R$ ,  $C$ , and  $L$  that render the system uncontrollable. Find a similar set of conditions that result in an unobservable system.

**Figure 7.92**

Electric circuit for Problem 7.39



- (c) Interpret the conditions found in part (b) in terms of the time constants of the system.
- (d) If  $R_1 = 2 \Omega$ ,  $R_2 = 3 \Omega$ , and  $C = 0.01F$ , find the value of  $L$  for the conditions derived in part (b) (that is, when the system is uncontrollable or unobservable). Find the transfer function of the system and show that there is a pole-zero cancellation for this system.

**7.40** The linearized dynamic equations of motion for a satellite are

$$\dot{\mathbf{x}} = \mathbf{Ax} + \mathbf{Bu},$$

$$\mathbf{y} = \mathbf{Cx},$$

where

$$\mathbf{A} = \begin{bmatrix} 0 & 1 & 0 & 0 \\ 3\omega^2 & 0 & 0 & 2\omega \\ 0 & 0 & 0 & 1 \\ 0 & -2\omega & 0 & 0 \end{bmatrix}, \quad \mathbf{B} = \begin{bmatrix} 0 & 0 \\ 1 & 0 \\ 0 & 0 \\ 0 & 1 \end{bmatrix}, \quad \mathbf{C} = \begin{bmatrix} 1 & 0 & 0 & 0 \\ 0 & 0 & 1 & 0 \end{bmatrix},$$

$$\mathbf{u} = \begin{bmatrix} u_1 \\ u_2 \end{bmatrix}, \quad \mathbf{y} = \begin{bmatrix} y_1 \\ y_2 \end{bmatrix}.$$

The inputs  $u_1$  and  $u_2$  are the radial and tangential thrusts, the state-variables  $x_1$  and  $x_3$  are the radial and angular deviations from the reference (circular) orbit, and the outputs  $y_1$  and  $y_2$  are the radial and angular measurements, respectively.

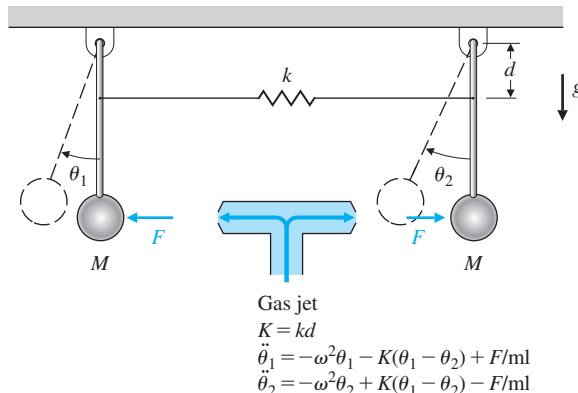
- (a) Show the system is controllable using both control inputs.
- (b) Show the system is controllable using only a single input. Which one is it?
- (c) Show the system is observable using both measurements.
- (d) Show the system is observable using only one measurement. Which one is it?

**7.41** Consider the system in Fig. 7.93.

- (a) Write the state-variable equations for the system, using  $[\theta_1 \ \theta_2 \ \dot{\theta}_1 \ \dot{\theta}_2]^T$  as the state vector and  $F$  as the single input.
- (b) Show all the state-variables are observable using measurements of  $\theta_1$  alone.

**Figure 7.93**

Coupled pendulums for Problem 7.41



- (c) Show the characteristic polynomial for the system is the product of the polynomials for two oscillators. Do so by first writing a new set of system equations involving the state-variables

$$\begin{bmatrix} y_1 \\ y_2 \\ \dot{y}_1 \\ \dot{y}_2 \end{bmatrix} = \begin{bmatrix} \theta_1 + \theta_2 \\ \theta_1 - \theta_2 \\ \dot{\theta}_1 + \dot{\theta}_2 \\ \dot{\theta}_1 - \dot{\theta}_2 \end{bmatrix}.$$

*Hint:* If  $\mathbf{A}$  and  $\mathbf{D}$  are invertible matrices, then

$$\begin{bmatrix} \mathbf{A} & \mathbf{0} \\ \mathbf{0} & \mathbf{D} \end{bmatrix}^{-1} = \begin{bmatrix} \mathbf{A}^{-1} & \mathbf{0} \\ \mathbf{0} & \mathbf{D}^{-1} \end{bmatrix}.$$

- (d) Deduce the fact that the spring mode is controllable with  $F$ , but the pendulum mode is not.

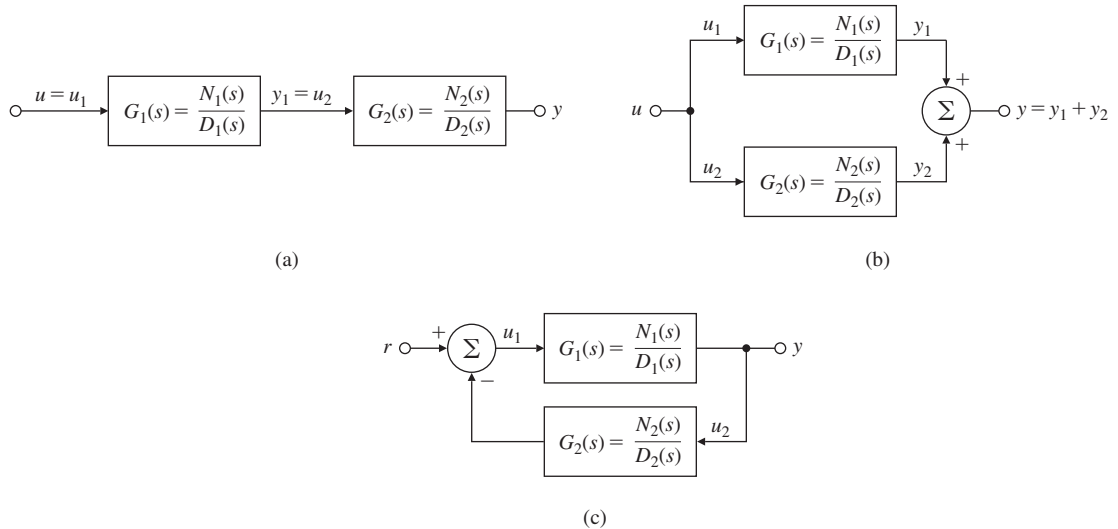
- 7.42** A certain fifth-order system is found to have a characteristic equation with roots at  $0, -1, -2$ , and  $-1 \pm 1j$ . A decomposition into controllable and uncontrollable parts discloses that the controllable part has a characteristic equation with roots  $0$  and  $-1 \pm 1j$ . A decomposition into observable and nonobservable parts discloses that the observable modes are at  $0, -1$ , and  $-2$ .

- (a) Where are the zeros of  $b(s) = \mathbf{C}\text{adj}(s\mathbf{I} - \mathbf{A})\mathbf{B}$  for this system?  
 (b) What are the poles of the reduced-order transfer function that includes only controllable and observable modes?

- 7.43** Consider the systems shown in Fig. 7.94, employing series, parallel, and feedback configurations.  
 (a) Suppose we have controllable-observable realizations for each subsystem:

$$\begin{aligned} \dot{\mathbf{x}}_i &= \mathbf{A}\mathbf{x}_i + \mathbf{B}_i\mathbf{u}_i, \\ \mathbf{y}_i &= \mathbf{C}_i\mathbf{x}_i, \quad \text{where } i = 1, 2. \end{aligned}$$

Give a set of state equations for the combined systems in Fig. 7.94.

**Figure 7.94**

Block diagrams for Problem 7.43: (a) series; (b) parallel; (c) feedback

- (b) For each case, determine what condition(s) on the roots of the polynomials  $N_i$  and  $D_i$  is necessary for each system to be controllable and observable. Give a brief reason for your answer in terms of pole-zero cancellations.

**7.44** Consider the system  $\ddot{y} + 3\dot{y} + 2y = \dot{u} + u$ .

- (a) Find the state matrices  $\mathbf{A}_c$ ,  $\mathbf{B}_c$ , and  $\mathbf{C}_c$  in control canonical form that correspond to the given differential equation.
- (b) Sketch the eigenvectors of  $\mathbf{A}_c$  in the  $(x_1, x_2)$  plane, and draw vectors that correspond to the completely observable  $(\mathbf{x}_0)$  and the completely unobservable  $(\mathbf{x}_{\bar{0}})$  state-variables.
- (c) Express  $\mathbf{x}_0$  and  $\mathbf{x}_{\bar{0}}$  in terms of the observability matrix  $\mathcal{O}$ .
- (d) Give the state matrices in observer canonical form and repeat parts (b) and (c) in terms of controllability instead of observability.

**7.45** The dynamic equations of motion for a station-keeping satellite (such as a weather satellite) are

$$\ddot{x} - 2\omega\dot{y} - 3\omega^2x = 0, \quad \ddot{y} + 2\omega\dot{x} = u,$$

where

$x$  = radial perturbation,

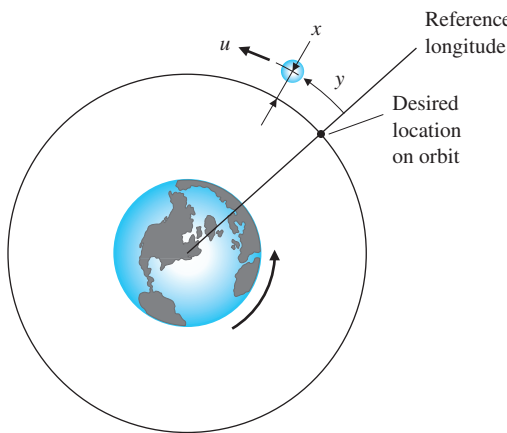
$y$  = longitudinal position perturbation,

$u$  = engine thrust in the  $y$ -direction,

as depicted in Fig. 7.95. If the orbit is synchronous with the earth's rotation, then  $\omega = 2\pi/(3600 \times 24)$  rad/sec.

**Figure 7.95**

Diagram of a station-keeping satellite in orbit for Problem 7.45



(a) Is the state  $\mathbf{x} = [x \quad \dot{x} \quad y \quad \dot{y}]^T$  observable?

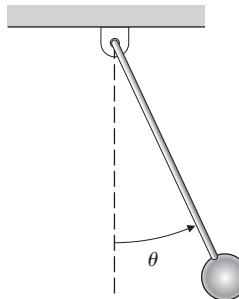
(b) Choose  $\mathbf{x} = [x \quad \dot{x} \quad y \quad \dot{y}]^T$  as the state vector and  $y$  as the measurement, and design a full-order observer with poles placed at  $s = -2\omega, -3\omega$ , and  $-3\omega \pm 3\omega j$ .

- 7.46** The linearized equations of motion of the simple pendulum in Fig. 7.96 are

$$\ddot{\theta} + \omega^2\theta = u.$$

**Figure 7.96**

Pendulum diagram for Problem 7.46



(a) Write the equations of motion in state-space form.

(b) Design an estimator (observer) that reconstructs the state of the pendulum given measurements of  $\dot{\theta}$ . Assume  $\omega = 5$  rad/sec, and pick the estimator roots to be at  $s = -10 \pm 10j$ .

(c) Write the transfer function of the estimator between the measured value of  $\dot{\theta}$  and the estimated value of  $\theta$ .

(d) Design a controller (that is, determine the state feedback gain  $\mathbf{K}$ ) so the roots of the closed-loop characteristic equation are at  $s = -4 \pm 4j$ .

- 7.47** An LCL Butterworth low pass filter is described by the following state equations:

$$\begin{bmatrix} \dot{x}_1 \\ \dot{x}_2 \\ \dot{x}_3 \end{bmatrix} = \begin{bmatrix} 0 & -1/L & 0 \\ 1/C & 0 & -1/C \\ 0 & 1/L & -R/L \end{bmatrix} \begin{bmatrix} x_1 \\ x_2 \\ x_3 \end{bmatrix} + \begin{bmatrix} 1/L \\ 0 \\ 0 \end{bmatrix} u$$

where  $x_1$  and  $x_2$  are the inductor currents,  $x_3$  is the capacitor voltage, and  $u$  is the input voltage. Consider  $L = 0.1$  H,  $C = 0.01$  F and  $R = 10$  Ω.

Design a reduced-order estimator with  $y = x_1$  as the known measurement, and place the observer error poles at  $-200$  and  $-200$ . Be sure to provide all the relevant estimator equations.

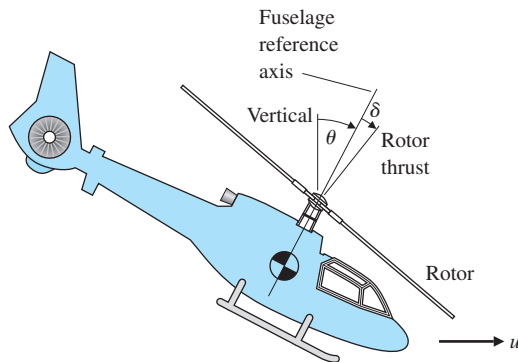
*Problems for Section 7.8: Compensator Design: Combined Control Law and Estimator*

- 7.48** A certain process has a the transfer function  $G(s) = \frac{4.5}{s(s-4.5)}$ .
- (a) Find **A**, **B**, and **C** for this system in observer canonical form.
  - (b) If  $u = -Kx$ , compute **K** so that the closed-loop control poles are located at  $s = -1.8 \pm 2j$ .
  - (c) Compute **L** so that the estimator-error poles are located at  $s = -15 \pm 15j$ .
  - (d) Give the transfer function of the resulting controller (for example, using Eq. (7.174)).
  - (e) What are the gain and phase margins of the controller and the given open-loop system?
- 7.49** The linearized longitudinal motion of a helicopter near hover (see Fig. 7.97) can be modeled by the normalized third-order system

$$\begin{bmatrix} \dot{q} \\ \dot{\theta} \\ \dot{u} \end{bmatrix} = \begin{bmatrix} -0.4 & 0 & -0.01 \\ 1 & 0 & 0 \\ -1.4 & 9.8 & -0.02 \end{bmatrix} \begin{bmatrix} q \\ \theta \\ u \end{bmatrix} + \begin{bmatrix} 6.3 \\ 0 \\ 9.8 \end{bmatrix} \delta,$$

**Figure 7.97**

Helicopter for Problem 7.49



Suppose our sensor measures the horizontal velocity  $u$  as the output; that is,  $y = u$ .

- (a) Find the open-loop pole locations.  
 (b) Is the system controllable?  
 (c) Find the feedback gain that places the poles of the system at  $s = -1 \pm 1j$  and  $s = -2$ .  
 (d) Design a full-order estimator for the system, and place the estimator poles at  $-8$  and  $-4 \pm 4\sqrt{3}j$ .  
 (e) Design a reduced-order estimator with both poles at  $-4$ . What are the advantages and disadvantages of the reduced-order estimator compared with the full-order case?  
 (f) Compute the compensator transfer function using the control gain and the full-order estimator designed in part (d), and plot its frequency response using Matlab. Draw a Bode plot for the closed-loop design, and indicate the corresponding gain and phase margins.  
 (g) Repeat part (f) with the reduced-order estimator.  
 (h) Draw the SRL and select roots for a control law that will give a control bandwidth matching the design of part (c), and select roots for a full-order estimator that will result in an estimator error bandwidth comparable to the design of part (d). Draw the corresponding Bode plot and compare the pole placement and SRL designs with respect to bandwidth, stability margins, step response, and control effort for a unit-step rotor-angle input. Use Matlab for the computations.
- 7.50** Suppose a DC drive motor with motor current is connected to the wheels of a cart in order to control the movement of an inverted pendulum mounted on the cart. The linearized and normalized equations of motion corresponding to this system can be put in the form

$$\begin{aligned}\ddot{\theta} &= \theta + v + u, \\ \dot{v} &= \theta - v - u,\end{aligned}$$

where

$$\begin{aligned}\theta &= \text{angle of the pendulum,} \\ v &= \text{velocity of the cart.}\end{aligned}$$

- (a) We wish to control  $\theta$  by feedback to  $u$  of the form,

$$u = -K_1\theta - K_2\dot{\theta} - K_3v.$$

Find the feedback gains so that the resulting closed-loop poles are located at  $-1.2$ ,  $-1.2 \pm j\sqrt{2}$ .

- (b) Assume  $\theta$  and  $v$  are measured. Construct an estimator for  $\theta$  and  $\dot{\theta}$  of the form,

$$\dot{\hat{x}} = \mathbf{A}\hat{x} + \mathbf{L}(y - \hat{y}),$$

where  $\mathbf{x} = [\theta \quad \dot{\theta}]^T$  and  $y = \theta$ . Treat both  $v$  and  $u$  as known. Select  $\mathbf{L}$  so that the estimator poles are at  $-3.5$ , and  $-3.5$ .

- (c) Based on the above designs, find the transfer function of the controller, and draw the Bode plot of the closed-loop system, indicating the corresponding gain and phase margins.

## 7.51 Consider the control of

$$G(s) = \frac{Y(s)}{U(s)} = \frac{7.5}{s(s+3.5)}.$$

- (a) Let  $y = x_1$  and  $\dot{x}_1 = x_2$ , and write state equations for the system.
- (b) Find  $K_1$  and  $K_2$  so that  $u = -K_1x_1 - K_2x_2$  yields closed-loop poles with a natural frequency  $\omega_n = 5$  and a damping ratio  $\zeta = 0.7$ .
- (c) Design a state estimator for the system that yields estimator error poles with  $\omega_{n1} = 20$  and  $\zeta_1 = 0.7$ .
- (d) What is the transfer function of the controller obtained by combining parts (a) through (c)?
- (e) Sketch the root locus of the resulting closed-loop system as plant gain (nominally 7.5) is varied.

## 7.52 Unstable equations of motion of the form,

$$\ddot{x} = x + u,$$

arise in situations where the motion of an upside-down pendulum (such as a rocket) must be controlled.

- (a) Let  $u = -Kx$  (position feedback alone), and sketch the root locus with respect to the scalar gain  $K$ .
- (b) Consider a compensator of the form,

$$U(s) = K \frac{(s+a)}{s+b} X(s).$$

Select and so that the system will display a rise time of about 1.8 sec and no more than 15% overshoot. Sketch the root locus with respect to  $K$ .

- (c) Sketch the Bode plot (both magnitude and phase) of the uncompensated plant.
- (d) Sketch the Bode plot of the compensated design, and estimate the phase margin and the bandwidth.
- (e) Design state feedback so that the closed-loop poles are the same locations as those of the design in part (b).
- (f) Design an estimator for  $x$  and  $\dot{x}$  using the measurement  $x = y$ , and select the observer gain  $\mathbf{L}$  so that the equation for  $\tilde{x}$  has characteristic roots with a damping ratio the same as chosen for the design in part (e) but the natural frequency is set to be twice larger than that in part (e).
- (g) Draw a Bode plot for the closed-loop system, and compare the resulting bandwidth and stability margins with those obtained using the design of part (b). If the ones with the estimator are worse, re-design by selecting another value of  $\omega_n$  for the estimator. Comment on your designs based on the step responses of each design.

## 7.53 A simplified model for the control of a flexible robotic arm is shown in Fig. 7.98, where

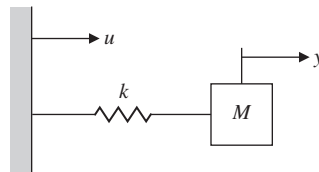
$$k/M = 900 \text{ rad/sec}^2,$$

$y$  = output, the mass position,

$u$  = input, the position of the end of the spring.

**Figure 7.98**

Simple robotic arm for Problem 7.53



- (a) Write the equations of motion in state-space form.  
 (b) Design an estimator with roots at  $s = -100 \pm 100j$ .  
 (c) Could both state-variables of the system be estimated if only a measurement of  $\dot{y}$  was available?  
 (d) Design a full-state feedback controller with roots at  $s = -20 \pm 20j$ .  
 (e) Would it be reasonable to design a control law for the system with roots at  $s = -200 \pm 200j$ . State your reasons.  
 (f) Write equations for the compensator, including a command input for  $y$ . Draw a Bode plot for the closed-loop system and give the gain and phase margins for the design.
- 7.54** The linearized differential equations governing the fluid-flow dynamics for the two cascaded tanks in Fig. 7.99 are

$$\begin{aligned}\delta\dot{h}_1 + \sigma\delta h_1 &= \delta u, \\ \delta\dot{h}_2 + \sigma\delta h_2 &= \sigma\delta h_1,\end{aligned}$$

where

$\delta h_1$  = deviation of depth in tank 1 from the nominal level,

$\delta h_2$  = deviation of depth in tank 2 from the nominal level, and

$\delta u$  = deviation in fluid in flow rate to tank 1 (control).

- (a) Level Controller for Two Cascaded Tanks:** Using state feedback of the form

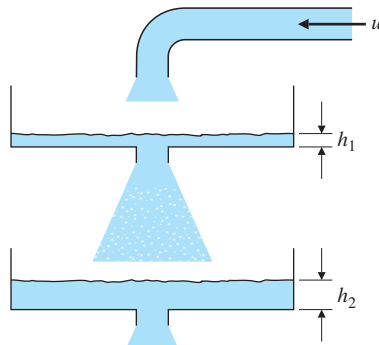
$$\delta u = -K_1\delta h_1 - K_2\delta h_2,$$

choose values of  $K_1$  and  $K_2$  that will place the closed-loop eigenvalues at

$$s = -2\sigma(1 \pm j).$$

**Figure 7.99**

Coupled tanks for Problem 7.54



(b) *Level Estimator for Two Cascaded Tanks:* Suppose only the deviation in the level of tank 2 is measured (that is,  $y = \delta h_2$ ). Using this measurement, design an estimator that will give continuous, smooth estimates of the deviation in levels of tank 1 and tank 2, with estimator error poles at  $-8\sigma(1 \pm j)$ .

(c) *Estimator/Controller for Two Cascaded Tanks:* Sketch a block diagram (showing individual integrators) of the closed-loop system obtained by combining the estimator of part (b) with the controller of part (a).

(d) Using Matlab, compute and plot the response at  $y$  to an initial offset in  $\delta h_1$ . Assume  $\sigma = 1$  for the plot.

**7.55** The lateral motions of a ship that is 100 m long, moving at a constant velocity of 10 m/sec, are described by

$$\begin{bmatrix} \dot{\beta} \\ \dot{r} \\ \dot{\psi} \end{bmatrix} = \begin{bmatrix} -0.0895 & -0.286 & 0 \\ -0.0439 & -0.272 & 0 \\ 0 & 1 & 0 \end{bmatrix} \begin{bmatrix} \beta \\ r \\ \psi \end{bmatrix} + \begin{bmatrix} 0.0145 \\ -0.0122 \\ 0 \end{bmatrix} \delta,$$

where

$\beta$  = side slip angle(deg),

$\psi$  = heading angle(deg),

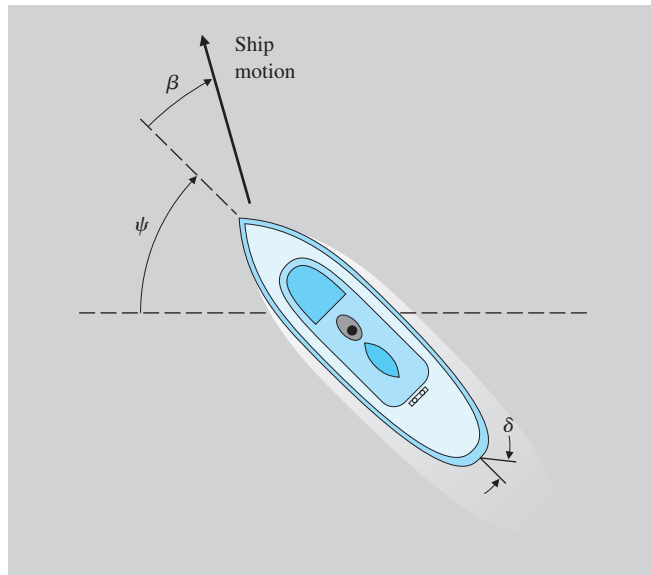
$\delta$  = rudder angle(deg), and

$r$  = yaw rate (see Fig. 7.100).

(a) Determine the transfer function from  $\delta$  to  $\psi$  and the characteristic roots of the uncontrolled ship.

**Figure 7.100**

View of ship from above for Problem 7.55



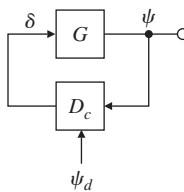
- (b) Using complete state feedback of the form

$$\delta = -K_1\beta - K_2r - K_3(\psi - \psi_d),$$

where  $\psi_d$  is the desired heading, determine values of  $K_1$ ,  $K_2$ , and  $K_3$  that will place the closed-loop roots at  $s = -0.2, -0.2 \pm 0.2j$ .

- (c) Design a state estimator based on the measurement of  $\psi$  (obtained from a gyrocompass, for example). Place the roots of the estimator error equation at  $s = -0.8$  and  $-0.8 \pm 0.8j$ .
- (d) Give the state equations and transfer function for the compensator  $D_c(s)$  in Fig. 7.101, and plot its frequency response.
- (e) Draw the Bode plot for the closed-loop system, and compute the corresponding gain and phase margins.
- (f) Compute the feed-forward gains for a reference input, and plot the step response of the system to a change in heading of  $5^\circ$ .

**Figure 7.101**  
Ship control block diagram for Problem 7.55



### Problem for Section 7.9: Introduction of the Reference Input with the Estimator

- △ 7.56 As mentioned in footnote 9 in Section 7.9.2, a reasonable approach for selecting the feed-forward gain in Eq. (7.202) is to choose  $\bar{N}$  such that when  $r$  and  $y$  are both unchanging, the DC gain from  $r$  to  $u$  is the negative of the DC gain from  $y$  to  $u$ . Derive a formula for  $\bar{N}$  based on this selection rule. Show if the plant is Type 1, this choice is the same as that given by Eq. (7.202).

### Problems for Section 7.10: Integral Control and Robust Tracking

- 7.57 Assume the linearized and time-scaled equation of motion for the ball-bearing levitation device is  $\ddot{x} - x = u + w$ . Here  $w$  is a constant bias due to the power amplifier. Introduce integral error control, and select three control gains  $\mathbf{K} = [K_1 \ K_2 \ K_3]$  so the closed-loop poles are at  $-1$  and  $-1 \pm j$  and the steady-state error to  $w$  and to a (step) position command will be zero. Let  $y = x$  and the reference input  $r \triangleq y_{ref}$  be a constant. Draw a block diagram of your design showing the locations of the feedback gains  $K_i$ . Assume both  $\dot{x}$  and  $x$  can be measured. Plot the response of the closed-loop system to a step command input and the response to a step change in the bias input. Verify that the system is Type 1. Use Matlab (Simulink) software to simulate the system responses.

**7.58** Consider a system with state matrices

$$\mathbf{A} = \begin{bmatrix} -2 & 1 \\ 0 & -3 \end{bmatrix}, \quad \mathbf{B} = \begin{bmatrix} 1 \\ 1 \end{bmatrix}, \quad \mathbf{C} = [1 \ 3].$$

- (a) Use feedback of the form  $u(t) = -\mathbf{Kx}(t) + \bar{N}r(t)$ , where  $\bar{N}$  is a nonzero scalar, to move the poles to  $-3 \pm j$ .
- (b) Choose  $\bar{N}$  so if  $r$  is a constant, the system has zero steady-state error; that is,  $y(\infty) = r$ .
- (c) Show if  $\mathbf{A}$  changes to  $\mathbf{A} + \delta\mathbf{A}$ , where  $\delta\mathbf{A}$  is an arbitrary  $2 \times 2$  matrix, then your choice of  $\bar{N}$  in part(b) will no longer make  $y(\infty) = r$ . Therefore, the system is not robust under changes to the system parameters in  $\mathbf{A}$ .
- (d) The system steady-state error performance can be made robust by augmenting the system with an integrator and using unity feedback—that is, by setting  $\dot{x}_I = r - y$ , where  $x_I$  is the state of the integrator. To see this, first use state feedback of the form  $u = -\mathbf{Kx} - K_1x_I$  so the poles of the augmented system are at  $-3, -2 \pm j\sqrt{3}$ .
- (e) Show the resulting system will yield  $y(\infty) = r$  no matter how the matrices  $\mathbf{A}$  and  $\mathbf{B}$  are changed, as long as the closed-loop system remains stable.
- (f) For part (d), use Matlab (Simulink) software to plot the time response of the system to a constant input. Draw Bode plots of the controller, as well as the sensitivity function ( $S$ ) and the complementary sensitivity function ( $T$ ).

- △ **7.59** Consider a servomechanism for following the data track on a computer-disk memory system. Because of various unavoidable mechanical imperfections, the data track is not exactly a centered circle, and thus the radial servo must follow a sinusoidal input of radian frequency  $\omega_0$  (the spin rate of the disk). The state matrices for a linearized model of such a system are

$$\mathbf{A} = \begin{bmatrix} 0 & 1 \\ 0 & -1 \end{bmatrix}, \quad \mathbf{B} = \begin{bmatrix} 0 \\ 1 \end{bmatrix}, \quad \mathbf{C} = [1 \ 3].$$

The sinusoidal reference input satisfies  $\ddot{r} = -\omega_0^2 r$ .

- (a) Let  $\omega_0 = 1$ , and place the poles of the error system for an internal model design at

$$\alpha_c(s) = (s + 2 \pm j2)(s + 1 \pm j1)$$

and the pole of the reduced-order estimator at

$$\alpha_e(s) = (s + 6).$$

- (b) Draw a block diagram of the system, and clearly show the presence of the oscillator with frequency  $\omega_0$  (the internal model) in the controller. Also verify the presence of the blocking zeros at  $\pm j\omega_0$ .
- (c) Use Matlab (Simulink) software to plot the time response of the system to a sinusoidal input at frequency  $\omega_0 = 1$ .
- (d) Draw a Bode plot to show how this system will respond to sinusoidal inputs at frequencies different from but near  $\omega_0$ .

- △ **7.60** Compute the controller transfer function [from  $Y(s)$  to  $U(s)$ ] in Example 7.38. What is the prominent feature of the controller that allows tracking and disturbance rejection?
- △ **7.61** Consider the pendulum problem with control torque  $T_c$  and disturbance torque  $T_d$ :

$$\ddot{\theta} + 4\theta = T_c + T_d.$$

(Here  $g/l = 4$ .) Assume there is a potentiometer at the pin that measures the output angle  $\theta$ , but with a constant unknown bias  $b$ . Thus the measurement equation is  $y = \theta + b$ .

- (a)** Take the “augmented” state vector to be

$$\begin{bmatrix} \theta \\ \dot{\theta} \\ \theta \\ w \end{bmatrix},$$

where  $w$  is the input-equivalent bias. Write the system equations in state-space form. Give values for the matrices  $\mathbf{A}$ ,  $\mathbf{B}$ , and  $\mathbf{C}$ .

- (b)** Using state-variable methods, show the characteristic equation of the model is  $s(s^2 + 4) = 0$ .
- (c)** Show  $w$  is observable if we assume  $y = \theta$ , and write the estimator equations for

$$\begin{bmatrix} \hat{\theta} \\ \hat{\dot{\theta}} \\ \hat{\theta} \\ \hat{w} \end{bmatrix}.$$

Pick estimator gains  $[\ell_1 \quad \ell_2 \quad \ell_3]^T$  to place all the roots of the estimator error characteristic equation at  $-10$ .

- (d)** Using full-state feedback of the estimated (controllable) state-variables, derive a control law to place the closed-loop poles at  $-2 \pm j2$ .
- (e)** Draw a block diagram of the complete closed-loop system (estimator, plant, and controller) using integrator blocks.
- (f)** Introduce the estimated bias into the control so as to yield zero steady-state error to the output bias  $b$ . Demonstrate the performance of your design by plotting the response of the system to a step change in  $b$ ; that is,  $b$  changes from 0 to some constant value.

### Problems for Section 7.10.3: Model-following Design

- △ **7.62** Consider the servomechanism problem where we wish to track a ramp reference signal. The plant and the desired model equations are

$$\begin{aligned} \dot{\mathbf{x}} &= \begin{bmatrix} 0 & 1 \\ 0 & -1 \end{bmatrix} \mathbf{x} + \begin{bmatrix} 0 \\ 1 \end{bmatrix} u, \\ y &= \begin{bmatrix} 1 & 0 \end{bmatrix} \end{aligned}$$

$$\dot{\mathbf{x}}_m = \begin{bmatrix} 0 & 1 \\ 0 & 0 \end{bmatrix} \mathbf{x}_m,$$

$$y_m = [1 \ 0] \mathbf{x}_m.$$

Design a model-following control law and demonstrate its tracking performance. Place the closed-loop poles at  $s = -2 \pm j2$ .

- $\triangle$  **7.63** *Implicit Model-following:* Suppose we wish the closed-loop system to behave like a desired model, called the implicit model

$$\dot{\mathbf{z}} = \mathbf{A}_m \mathbf{z}.$$

We may minimize a modified LQR performance index

$$\mathcal{J} = \int_0^\infty \left\{ (\dot{\mathbf{y}} - \mathbf{A}_m \mathbf{y})^T \mathbf{Q}_1 (\dot{\mathbf{y}} - \mathbf{A}_m \mathbf{y}) + u^T \mathbf{R} u \right\} dt.$$

Show this performance index is equivalent to the standard one with the addition of a cross-weighting term between the control and the state of the form

$$\mathcal{J} = \int_0^\infty \left\{ \mathbf{x}^T \hat{\mathbf{Q}} \mathbf{x} + 2u^T \hat{\mathbf{S}} \mathbf{x} + u^T \hat{\mathbf{R}} u \right\} dt,$$

where

$$\hat{\mathbf{Q}} = (\mathbf{C}\mathbf{A} - \mathbf{A}_m \mathbf{C})^T \mathbf{Q}_1 (\mathbf{C}\mathbf{A} - \mathbf{A}_m \mathbf{C}),$$

$$\hat{\mathbf{S}} = \mathbf{B}^T \mathbf{C}^T \mathbf{Q}_1 (\mathbf{C}\mathbf{A} - \mathbf{A}_m \mathbf{C}),$$

$$\hat{\mathbf{R}} = \mathbf{R} + \mathbf{B}^T \mathbf{C}^T \mathbf{Q}_1 \mathbf{C}\mathbf{B}.$$

- $\triangle$  **7.64** *Explicit Model-Following:* Suppose in the LQR problem, we wish the closed-loop system to behave as close as possible to a system of the form

$$\dot{\mathbf{z}} = \mathbf{A}_m \mathbf{z},$$

which represents the model of desirable dynamics. We may choose a performance index of the form

$$\mathcal{J} = \int_0^\infty \left\{ (y - \mathbf{z})^T \mathbf{Q}_1 (y - \mathbf{z}) + u^T \mathbf{R} u \right\} dt.$$

- (a)** Show this performance index can be converted to the standard one by augmenting the states of the plant and the model and again choose the augmented state vector,  $\xi = [\mathbf{x}^T \ \mathbf{z}^T]^T$  and write down the system equations to show that

$$\mathcal{J} = \int_0^\infty \left\{ \xi^T \mathbf{Q}_1 \xi + u^T \mathbf{R} u \right\} dt,$$

where

$$\mathbf{Q} = \begin{bmatrix} \mathbf{C}^T \mathbf{Q}_1 \mathbf{C} & -\mathbf{C}^T \mathbf{Q}_1 \\ -\mathbf{Q}_1 \mathbf{C} & \mathbf{Q}_1 \end{bmatrix}.$$

- (b) Which state variables of the system are uncontrollable? Is this result surprising?  
(c) The optimal control is of the form

$$u = -\mathbf{K}_1 \mathbf{x} - \mathbf{K}_2 \mathbf{z},$$

which means that the model's equations must be implemented as part of the control law. Suppose we now drive the model as follows

$$\dot{\mathbf{z}} = \mathbf{A}_m \mathbf{z} + \mathbf{B}_p u_p,$$

where  $u_p$  may be the pilot input in an aircraft system. Show that

$$\frac{Y(s)}{U_p(s)} = \underbrace{-\mathbf{C}(s\mathbf{I} - \mathbf{A} + \mathbf{B}\mathbf{K}_1)^{-1}\mathbf{B}\mathbf{K}_2}_{\text{Closed-loop dynamics}} \underbrace{(s\mathbf{I} - \mathbf{A}_m)^{-1}\mathbf{B}_p}_{\text{Feedforward dynamics}}.$$

This indicates that the feedforward dynamics may be used to improve the transient response of the system.

- (d) What are the transmission zeros of the overall system?  
(e) What is a possible disadvantage of this scheme compared to the standard LQR, that is, with no explicit model?

### *Problem for Section 7.13: Design for Systems with Pure Time Delay*

- △ **7.65** Consider the system with the transfer function  $e^{-Ts}G(s)$ , where

$$G(s) = \frac{1}{s(s+1)(s+2)}.$$

The Smith compensator for this system is given by

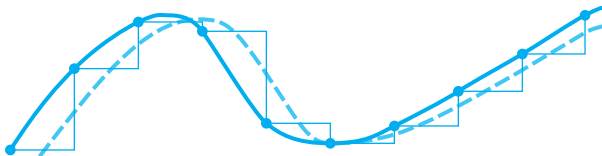
$$D'_c(s) = \frac{D_c(s)}{1 + (1 - e^{-sT})G(s)D_c(s)}.$$

Plot the frequency response of the compensator for  $T = 5$  and  $D_c(s) = 1$ , and draw a Bode plot that shows the gain and phase margins of the system.<sup>21</sup>

---

<sup>21</sup>This problem was given by Åström (1977).

# Digital Control



## A Perspective on Digital Control

Most of the controllers we have studied so far were described by the Laplace transform or differential equations, which, strictly speaking, are assumed to be built using analog electronics, such as that in Fig. 5.31. However, most control systems today use digital computers (usually microprocessors or microcontrollers) to implement the controllers. The intent of this chapter is to show how to implement a control system in a digital computer. The implementation leads to an average delay of half the sample period, and to a phenomenon called **aliasing**, both of which need to be addressed in the controller design.

Analog electronics can integrate and differentiate signals. In order for a digital computer to accomplish these tasks, the differential equations describing compensation must be approximated by reducing them to algebraic equations involving addition, division, and multiplication. This chapter expands on various ways to make these approximations. The resulting design can then be tuned up, if needed, using direct digital analysis. In some cases, it will pay to perform the design directly in the **discrete-time domain**.

You should be able to design, analyze, and implement a digital control system from the material in this chapter. However, our treatment here is a limited version of a complex subject covered in more detail in *Digital Control of Dynamic Systems* by Franklin et al. (1998).

## Chapter Overview

In Section 8.1, we will describe the basic structure of digital control systems and introduce the issues that arise due to the sampling.

A digital implementation based on a discrete approximation of a continuous control law can be evaluated via Simulink to determine the degradation with respect to the continuous-time case. However, to fully understand the effect of sampling, it is useful to learn about discrete linear analysis tools. This requires an understanding of the ***z-transform***, which we will discuss in Section 8.2. In Section 8.3 we will build on this understanding to provide a foundation for design using various **discrete equivalents**. Generally speaking, the discrete equivalents work well if the sampling rate is sufficiently fast. In Sections 8.4 and 8.5, we will discuss hardware characteristics and sample rate issues, both of which need to be addressed in order to implement a digital controller.

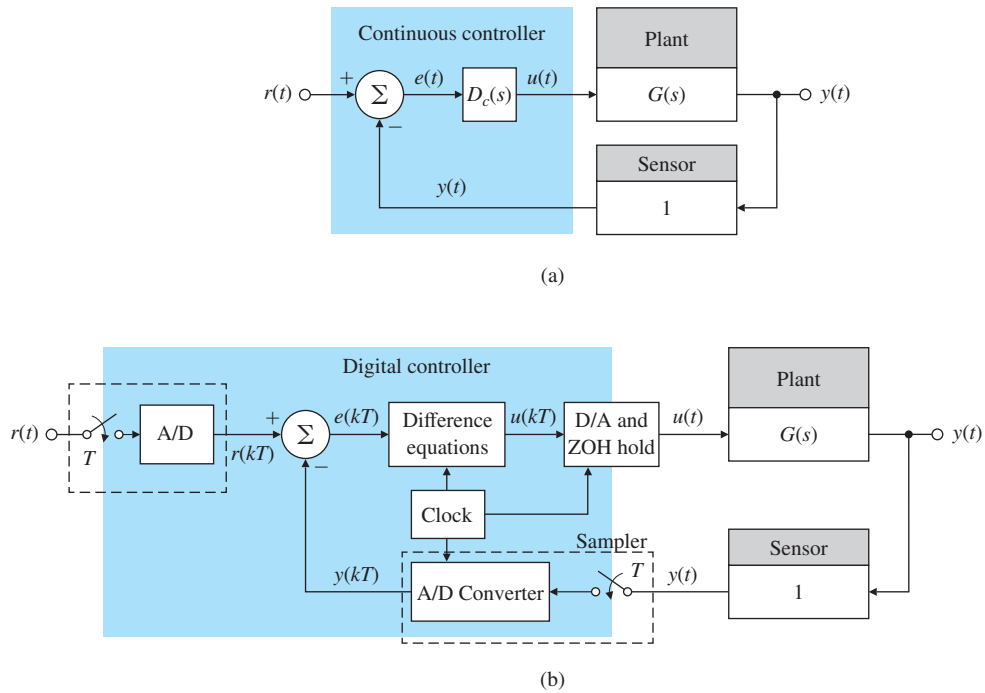
Discrete analysis also allows us to analytically determine the performance of the approximate discrete equivalent design without resorting to a numerical simulation, such as Simulink, as we do in the early examples. This analysis can then serve as a guide to tune up the designs, which will be described in Section 8.6. It is also possible to perform a direct digital design (also called discrete design), which provides an exact design method that is independent of whether the sample rate is fast or not. Direct digital design will be described in Section 8.7.

## 8.1 Digitization

Figure 8.1(a) shows the topology of the typical continuous system that we have been considering in previous chapters. The computation of the error signal  $e$  and the dynamic compensation  $D_c(s)$  can all be accomplished in a digital computer as shown in Fig. 8.1(b). The fundamental differences between the two implementations are that the digital system operates on **samples** of the sensed plant output rather than on the continuous signal, and that the continuous control provided by  $D_c(s)$ , including any differentiation and integration, must be generated at discrete instances in time and *approximated* using numerical methods called **difference equations**. These equations are recursive, algebraic calculations because computers are not capable of performing dynamic functions directly.

Walking through the process in more detail, the analog output of the plant sensor is sampled and converted to a digital number in the **analog-to-digital (A/D converter)**. This device samples a physical variable, most commonly an electrical voltage, and converts the samples of the analog signal into a digital binary number that usually consists of 10 to 16 bits. Conversion from the continuous analog signal  $y(t)$  to the discrete digital samples,  $y(kT)$ , occurs repeatedly at instants of time,  $T$ , apart where  $T$  is the **sample period** and  $1/T$  is the **sample rate**. If  $T$  is in seconds,  $1/T$  is the sample rate in Hertz, denoted by  $f_s$ . The sampled signal is  $y(kT)$ , where  $k$  can take on any integer value. It is often written simply as  $y(k)$ . We call this type of variable a **discrete signal** to

Sample period

**Figure 8.1**

Block diagrams for a basic control system: (a) continuous system; (b) with a digital computer

distinguish it from a continuous signal such as  $y(t)$ , which changes continuously in time. A system having both discrete and continuous signals is called a **sampled-data system**.

We make the assumption in this book that the sample period is fixed. In practice, digital control systems sometimes have varying sample periods and/or different periods in different feedback paths. Usually, the computer logic includes a **clock** that supplies a pulse, or **interrupt**, every  $T$  seconds, and the A/D converter sends a number to the computer each time the interrupt arrives. An alternative implementation, often referred to as **free-running**, is to access the A/D converter after each cycle of code execution has been completed. In the former case, the sample period is precisely fixed; in the latter case, the sample period is fixed essentially by the length of the code, provided that no logic branches are present, which could vary the amount of code executed. There also may be a sampler and an A/D converter for the input command  $r(t)$ , which produces the discrete  $r(kT)$ , from which the sensed output  $y(kT)$  will be subtracted to arrive at the discrete error signal  $e(kT)$ .

The continuous compensation  $D_c(s)$  is approximated by difference equations, which are the discrete version of differential equations and can be made to duplicate the dynamic behavior of  $D_c(s)$  accurately if the sample rate is fast enough. The result of the difference equations

### Zero-order hold (ZOH)

is a discrete control signal  $u(kT)$  at each sample instant. This signal is converted to a continuous signal  $u(t)$  by the **digital-to-analog (D/A) converter** and the **hold**: the D/A converter changes the digital binary number to an analog voltage, and a **zero-order hold** maintains that same voltage throughout the sample period. The resulting control signal  $u(t)$  is then applied to the actuator in precisely the same manner as the continuous implementation. There are two basic techniques for finding the difference equations for the digital controller. One technique, called the **discrete equivalent**, consists of designing a continuous compensation  $D_c(s)$  using methods described in the previous chapters, then approximating that  $D_c(s)$  using one of the methods to be described in Section 8.3. The other technique is **discrete design**, to be described in Section 8.7. Here, the difference equations are found directly without designing  $D_c(s)$  first.

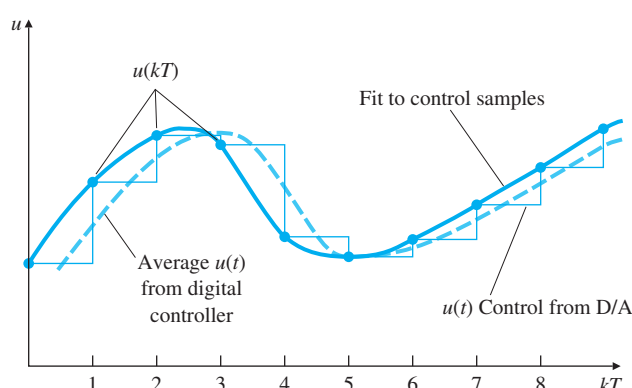
The sample rate required depends on the closed-loop bandwidth of the system. Generally, sample rates should be at least 20 times the bandwidth  $\omega_{BW}$  in order to assure that the digital controller will match the performance of the continuous controller. Slower sample rates can be used if some adjustments are made in the digital controller or some performance degradation is acceptable. Use of the discrete design method allows for a much slower sample rate if that is desirable to minimize hardware costs; however, best performance of a digital controller is obtained when the sample rate is greater than 25 times the bandwidth.

It is worth noting the single most important impact of implementing a control system digitally is the delay associated with the hold. Because each value of  $u(kT)$  in Fig. 8.1(b) is held constant until the next value is available from the computer, the continuous value of  $u(t)$  consists of steps (see Fig. 8.2) that, on average, are delayed from a fit to  $u(kT)$  by  $T/2$ , as shown in the figure. If we simply incorporate this  $T/2$  delay into a continuous analysis of the system, an excellent prediction of the effects of sampling results for sample rates much slower than 20 times bandwidth. We will discuss this further in Section 8.3.5.

### Sample rate selection

**Figure 8.2**

The delay due to the hold operation



## 8.2 Dynamic Analysis of Discrete Systems

The  $z$ -transform is the mathematical tool for the analysis of linear discrete systems. It plays the same role for discrete-time systems that the Laplace transform does for continuous-time systems. This section will give a short description of the  $z$ -transform, describe its use in analyzing discrete systems, and show how it relates to the Laplace transform.

### 8.2.1 $z$ -Transform

In the analysis of continuous-time systems, we use the Laplace transform, which is defined by

$$\mathcal{L}\{f(t)\} = F(s) = \int_0^\infty f(t)e^{-st} dt,$$

which leads directly to the important property that (with zero initial conditions)

$$\mathcal{L}\{\dot{f}(t)\} = sF(s). \quad (8.1)$$

Equation (8.1) enables us easily to find the transfer function of a linear continuous-time system, given the differential equation description of that system.

For discrete systems a similar procedure is available. The  **$z$ -transform** is defined by

$$\mathcal{Z}\{f(k)\} = F(z) = \sum_{k=0}^{\infty} f(k)z^{-k}, \quad (8.2)$$

where  $f(k)$  is the sampled version of  $f(t)$ , as shown in Fig. 8.3, and  $k = 0, 1, 2, 3, \dots$  refers to discrete sample times  $t_0, t_1, t_2, t_3, \dots$ . This leads directly to a property analogous to Eq. (8.1), specifically, that

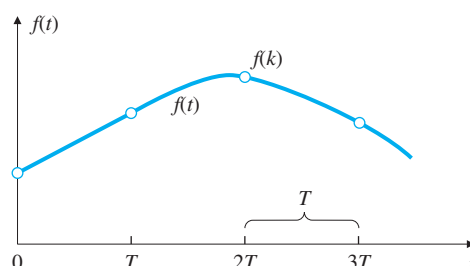
$$\mathcal{Z}\{f(k-1)\} = z^{-1}F(z), \quad (8.3)$$

where  $z^{-1}$  represents one sample delay. This relation allows us to easily find the transfer function of a discrete system, given the difference equations of that system. For example, the general second-order difference equation

$$y(k) = -a_1y(k-1) - a_2y(k-2) + b_0u(k) + b_1u(k-1) + b_2u(k-2)$$

**Figure 8.3**

A continuous, sampled version of signal  $f$



can be converted from this form to the  $z$ -transform of the variables  $y(k)$ ,  $u(k), \dots$  by invoking Eq. (8.3) once or twice to arrive at

$$Y(z) = (-a_1 z^{-1} - a_2 z^{-2}) Y(z) + (b_0 + b_1 z^{-1} + b_2 z^{-2}) U(z). \quad (8.4)$$

### Discrete transfer function

Equation (8.4) then results in the **discrete transfer function**

$$\frac{Y(z)}{U(z)} = \frac{b_0 + b_1 z^{-1} + b_2 z^{-2}}{1 + a_1 z^{-1} + a_2 z^{-2}}.$$

### 8.2.2 $z$ -Transform Inversion

Table 8.1 relates simple discrete-time functions to their  $z$ -transforms and gives the Laplace transforms for the same time functions.

Given a general  $z$ -transform, we could expand it into a sum of elementary terms using partial-fraction expansion (see Appendix A.1.2) and find the resulting time series from the table. These procedures are exactly the same as those used for continuous-time systems. However, as with the continuous case, most designers would use a numerical evaluation of the discrete equations to obtain a time history rather than inverting the  $z$ -transform.

A  $z$ -transform inversion technique that has no continuous counterpart is called **long division**. Given the  $z$ -transform

$$Y(z) = \frac{N(z)}{D_d(z)}, \quad (8.5)$$

we simply divide the denominator into the numerator using long division. The result is a series (perhaps with an infinite number of terms) in  $z^{-1}$ , from which the time series can be found using Eq. (8.2).

For example, a first-order discrete system described by the difference equation

$$y(k) = \alpha y(k-1) + u(k), \quad (8.6)$$

yields the discrete transfer function

$$\frac{Y(z)}{U(z)} = \frac{1}{1 - \alpha z^{-1}}.$$

For a unit-pulse input defined by

$$u(0) = 1,$$

$$u(k) = 0, \quad k \neq 0,$$

the  $z$ -transform is then

$$U(z) = 1, \quad (8.7)$$

so

$$Y(z) = \frac{1}{1 - \alpha z^{-1}}. \quad (8.8)$$

### z-transform inversion: long division

**TABLE 8.1****Laplace Transforms and z-Transforms of Simple Discrete-Time Functions**

No.	$F(s)$	$f(kT)$	$F(z)$
1		$1, k = 0; 0, k \neq 0$	$1$
2		$1, k = k_o; 0, k \neq k_o$	$\frac{1}{z - k_o}$
3	$\frac{1}{s}$	$1(kT)$	$\frac{z}{z-1}$
4	$\frac{1}{s^2}$	$kT$	$\frac{Tz}{(z-1)^2}$
5	$\frac{1}{s^3}$	$\frac{1}{2!}(kT)^2$	$\frac{T^2}{2} \left[ \frac{z(z+1)}{(z-1)^3} \right]$
6	$\frac{1}{s^4}$	$\frac{1}{3!}(kT)^3$	$\frac{T^3}{6} \left[ \frac{z(z^2+4z+1)}{(z-1)^4} \right]$
7	$\frac{1}{s^m}$	$\lim_{a \rightarrow 0} \frac{(-1)^{m-1}}{(m-1)!} \left( \frac{\partial^{m-1}}{\partial a^{m-1}} e^{-akT} \right)$	$\lim_{a \rightarrow 0} \frac{(-1)^{m-1}}{(m-1)!} \left( \frac{\partial^{m-1}}{\partial a^{m-1}} \frac{z}{z - e^{-aT}} \right)$
8	$\frac{1}{s+a}$	$e^{-akT}$	$\frac{z}{z - e^{-aT}}$
9	$\frac{1}{(s+a)^2}$	$kTe^{-akT}$	$\frac{Tze^{-aT}}{(z - e^{-aT})^2}$
10	$\frac{1}{(s+a)^3}$	$\frac{1}{2}(kT)^2 e^{-akT}$	$\frac{T^2}{2} e^{-aT} z \frac{(z + e^{-aT})}{(z - e^{-aT})^3}$
11	$\frac{1}{(s+a)^m}$	$\frac{(-1)^{m-1}}{(m-1)!} \left( \frac{\partial^{m-1}}{\partial a^{m-1}} e^{-akT} \right)$	$\frac{(-1)^{m-1}}{(m-1)!} \left( \frac{\partial^{m-1}}{\partial a^{m-1}} \frac{z}{z - e^{-aT}} \right)$
12	$\frac{a}{s(s+a)}$	$1 - e^{-akT}$	$\frac{z(1 - e^{-aT})}{(z-1)(z - e^{-aT})}$
13	$\frac{a}{s^2(s+a)}$	$\frac{1}{a}(akT - 1 + e^{-akT})$	$\frac{z[(aT-1+e^{-aT})z+(1-e^{-aT}-aTe^{-aT})]}{a(z-1)^2(z - e^{-aT})}$
14	$\frac{b-a}{(s+a)(s+b)}$	$e^{-akT} - e^{-bkT}$	$\frac{(e^{-aT} - e^{-bT})z}{(z - e^{-aT})(z - e^{-bT})}$
15	$\frac{s}{(s+a)^2}$	$(1 - akT)e^{-akT}$	$\frac{z[z - e^{-aT}(1+aT)]}{(z - e^{-aT})^2}$
16	$\frac{a^2}{s(s+a)^2}$	$1 - e^{-akT}(1 + akT)$	$\frac{z[z(1 - e^{-aT} - aTe^{-aT}) + e^{-2aT} - e^{-aT} + aTe^{-aT}]}{(z-1)(z - e^{-aT})^2}$
17	$\frac{(b-a)s}{(s+a)(s+b)}$	$be^{-bkT} - ae^{-akT}$	$\frac{z[z(b-a) - (be^{-aT} - ae^{-bT})]}{(z - e^{-aT})(z - e^{-bT})}$
18	$\frac{a}{s^2+a^2}$	$\sin akT$	$\frac{z \sin aT}{z^2 - (2 \cos aT)z + 1}$
19	$\frac{s}{s^2+a^2}$	$\cos akT$	$\frac{z(z - \cos aT)}{z^2 - (2 \cos aT)z + 1}$
20	$\frac{s+a}{(s+a)^2+b^2}$	$e^{-akT} \cos bkT$	$\frac{z(z - e^{-aT} \cos bT)}{z^2 - 2e^{-aT}(\cos bT)z + e^{-2aT}}$
21	$\frac{b}{(s+a)^2+b^2}$	$e^{-akT} \sin bkT$	$\frac{ze^{-aT} \sin bT}{z^2 - 2e^{-aT}(\cos bT)z + e^{-2aT}}$
22	$\frac{a^2+b^2}{s[(s+a)^2+b^2]}$	$1 - e^{-akT}(\cos bkT + \frac{a}{b} \sin bkT)$	$\frac{z(Az+B)}{(z-1)[z^2 - 2e^{-aT}(\cos bT)z + e^{-2aT}]}$
			$A = 1 - e^{-aT} \cos bT - \frac{a}{b} e^{-aT} \sin bT$
			$B = e^{-2aT} + \frac{a}{b} e^{-aT} \sin bT - e^{-aT} \cos bT$

$F(s)$  is the Laplace transform of  $f(t)$ , and  $F(z)$  is the z-transform of  $f(kT)$ .

Note:  $f(t) = 0$  for  $t = 0$ .

Therefore, to find the time series, we divide the numerator of Eq. (8.8) by its denominator using long division:

$$\begin{array}{r}
 1 + \alpha z^{-1} + \alpha^2 z^{-2} + \alpha^3 z^{-3} + \dots \\
 \hline
 1 - \alpha z^{-1} ) 1 \\
 \hline
 1 - \alpha z^{-1} \\
 \hline
 \alpha z^{-1} + 0 \\
 \alpha z^{-1} - \alpha^2 z^{-2} \\
 \hline
 \alpha^2 z^{-2} + 0 \\
 \alpha^2 z^{-2} - \alpha^3 z^{-3} \\
 \hline
 \alpha^3 z^{-3} \\
 \ddots
 \end{array}$$

This yields the infinite series

$$Y(z) = 1 + \alpha z^{-1} + \alpha^2 z^{-2} + \alpha^3 z^{-3} + \dots \quad (8.9)$$

From Eqs. (8.9) and (8.2), we see the sampled time history of  $y$  is

$$y(0) = 1,$$

$$y(1) = \alpha,$$

$$y(2) = \alpha^2,$$

$$\vdots \quad \vdots$$

$$y(k) = \alpha^k,$$

which also could have been easily calculated for this simple example by directly evaluating Eq. (8.6).

### 8.2.3 Relationship Between $s$ and $z$

For continuous-time systems, we saw in Chapter 3 that certain behaviors result from different pole locations in the  $s$ -plane: oscillatory behavior for poles near the imaginary axis, exponential decay for poles on the negative real axis, and unstable behavior for poles with a positive real part. A similar kind of association would also be useful to know when designing discrete systems. Consider the continuous signal

$$f(t) = e^{-at}, \quad t > 0,$$

which has the Laplace transform

$$F(s) = \frac{1}{s + a},$$

and corresponds to a pole at  $s = -a$ . The  $z$ -transform of  $f(kT)$  is

$$F(z) = \mathcal{Z}\{e^{-akT}\}. \quad (8.10)$$

From Table 8.1, we can see that Eq. (8.10) is equivalent to

$$F(z) = \frac{z}{z - e^{-aT}},$$

which corresponds to a pole at  $z = e^{-aT}$ . This means that a pole at  $s = -a$  in the  $s$ -plane corresponds to a pole at  $z = e^{-aT}$  in the discrete domain. This is true in general, which is shown in more detail in Franklin et al. (1998). The important result is:

### Relationship between z-plane and s-plane characteristics

The equivalent characteristics in the  $z$ -plane are related to those in the  $s$ -plane by the expression

$$z = e^{sT}, \quad (8.11)$$

where  $T$  is the sample period.

Table 8.1 also includes the Laplace transforms, which demonstrates the  $z = e^{sT}$  relationship for the roots of the denominators of the table entries for  $F(s)$  and  $F(z)$ .

Figure 8.4 shows the mapping of lines of constant damping  $\zeta$  and natural frequency  $\omega_n$  from the  $s$ -plane to the upper half of the  $z$ -plane, using Eq. (8.11). The mapping also has several other important features (see Problem 8.4):

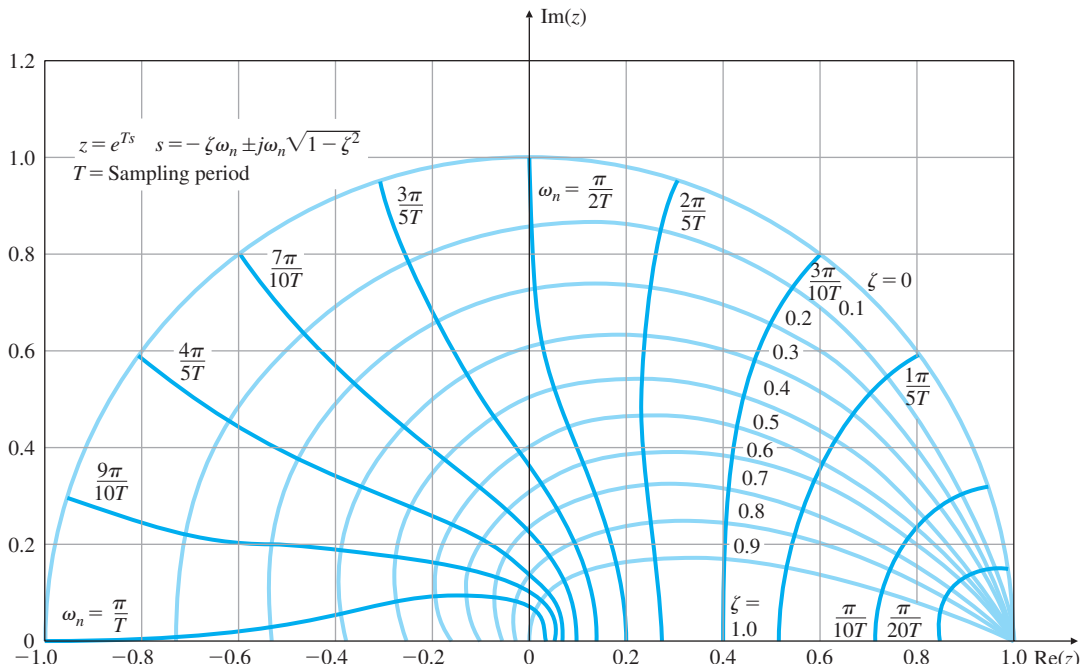


**Figure 8.4**

Natural frequency (solid color) and damping loci (light color) in the  $z$ -plane; the portion below the  $Re(z)$ -axis (not shown) is the mirror image of the upper half shown

1. The stability boundary ( $s = 0 \pm j\omega$  in the  $s$ -plane) becomes the unit circle  $|z| = 1$  in the  $z$ -plane; inside the unit circle is stable, outside is unstable.
2. The small vicinity around  $z = +1$  in the  $z$ -plane is essentially identical to the vicinity around the origin,  $s = 0$ , in the  $s$ -plane.
3. The  $z$ -plane locations give response information normalized to the sample rate rather than to time as in the  $s$ -plane.
4. The negative real  $z$ -axis always represents a frequency of  $\omega_s/2$ , where  $\omega_s = 2\pi/T$  = sample rate in radians per second when  $T$  is in seconds.
5. Vertical lines in the left half of the  $s$ -plane (the constant real part of  $s$  or time constant) map into circles within the unit circle of the  $z$ -plane.
6. Horizontal lines in the  $s$ -plane (the constant imaginary part of  $s$  or frequency) map into radial lines in the  $z$ -plane.
7. Frequencies greater than  $\omega_s/2$ , called the **Nyquist frequency**<sup>1</sup>, appear in the  $z$ -plane on top of corresponding lower frequencies because of the circular character of the trigonometric functions imbedded in Eq. (8.11). This overlap is called **aliasing** or **folding**. As a result it is necessary to sample at least twice as fast as a signal's highest frequency component in order to represent that signal with the samples. (We will discuss aliasing in greater detail in Section 8.4.3.)

To provide insight into the correspondence between  $z$ -plane locations and the resulting time sequence, Fig. 8.5 sketches time responses that would result from poles at the indicated locations. This figure is the discrete counterpart of Fig. 3.16.

### 8.2.4 Final Value Theorem

The Final Value Theorem for continuous-time systems, discussed in Section 3.1.6, states that

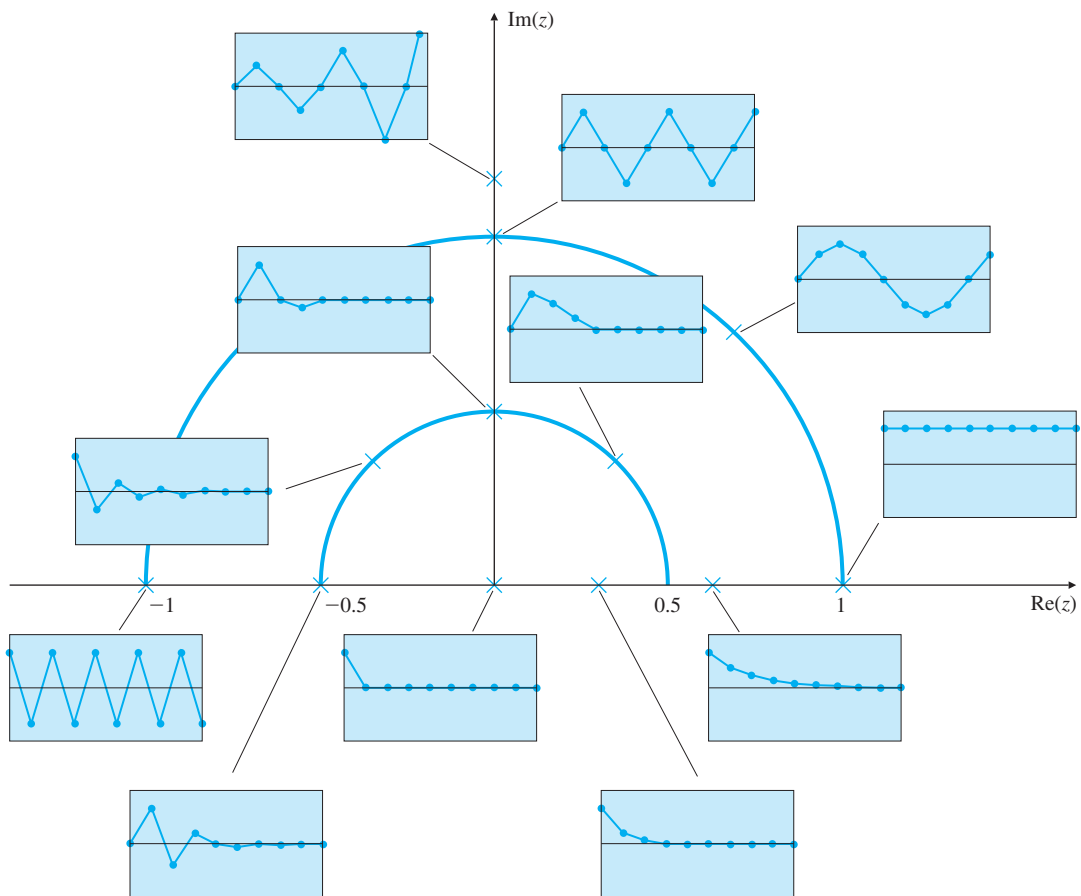
$$\lim_{t \rightarrow \infty} x(t) = x_{ss} = \lim_{s \rightarrow 0} sX(s), \quad (8.12)$$

as long as all the poles of  $sX(s)$  are in the left half-plane (LHP). It is often used to find steady-state system errors and/or steady-state gains of portions of a control system. We can obtain a similar relationship for discrete systems by noting a constant continuous steady-state response is denoted by  $X(s) = A/s$  and leads to the multiplication by  $s$  in Eq. (8.12). Therefore, because the constant steady-state response for discrete systems is

$$X(z) = \frac{A}{1 - z^{-1}},$$

---

<sup>1</sup>Nyquist frequency =  $\omega_s/2$

**Figure 8.5**

Time sequences associated with points in the  $z$ -plane

#### Final Value Theorem for discrete systems

the discrete Final Value Theorem is

$$\lim_{k \rightarrow \infty} x(k) = x_{ss} = \lim_{z \rightarrow 1} (1 - z^{-1}) X(z), \quad (8.13)$$

if all the poles of  $(1 - z^{-1})X(z)$  are inside the unit circle.

For example, to find the DC gain of the transfer function

$$G(z) = \frac{X(z)}{U(z)} = \frac{0.58(1+z)}{z+0.16},$$

we let  $u(k) = 1$  for  $k \geq 0$ , so

$$U(z) = \frac{1}{1 - z^{-1}}$$

and

$$X(z) = \frac{0.58(1+z)}{(1 - z^{-1})(z + 0.16)}.$$

Applying the Final Value Theorem yields

$$x_{ss} = \lim_{z \rightarrow 1} \left[ \frac{0.58(1+z)}{z+0.16} \right] = 1,$$

## DC gain

so the **DC gain** of  $G(z)$  is unity. To find the DC gain of any stable transfer function, we simply substitute  $z = 1$  and compute the resulting gain. Because the DC gain of a system should not change whether represented continuously or discretely, this calculation is an excellent aid to check that an equivalent discrete controller matches a continuous controller. It is also a good check on the calculations associated with determining the discrete model of a system.

## 8.3 Design Using Discrete Equivalents

## Stages in design using discrete equivalents

1. Design a continuous compensation, as described in Chapters 1 through 7.
  2. Find the discrete equivalent that, when implemented with the system described by Fig. 8.1(b), best approximates the continuous compensation.
  3. Use discrete analysis, simulation, or experimentation to verify the design.

Assume we are given a continuous compensation  $D_c(s)$ , as shown in Fig. 8.1(a). We wish to find a set of difference equations or  $D_d(z)$  for the digital implementation of that compensation in Fig. 8.1(b). First, we rephrase the problem as one of finding the best  $D_d(z)$  in the digital implementation shown in Fig. 8.6(a) to match the continuous system represented by  $D_c(s)$  in Fig. 8.6(b). In this section, we examine and compare four methods for solving this problem.

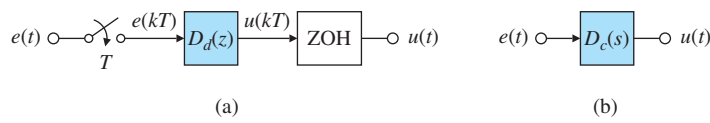
It is important to remember, as stated earlier, that these methods are approximations; there is no exact solution for all possible inputs because  $D_c(s)$  responds to the complete time history of  $e(t)$ , whereas  $D_d(z)$  has access to only the samples  $e(kT)$ . In a sense, the various digitization techniques simply make different assumptions about what happens to  $e(t)$  between the sample points.

### 8.3.1 Tustin's Method

Tustin's method is a digitization technique that approaches the problem as one of numerical integration. Suppose

## Figure 8.6

### Comparison of (a) digital and; (b) continuous implementation



$$\frac{U(s)}{E(s)} = D_c(s) = \frac{1}{s},$$

which is integration. Therefore,

$$u(kT) = \int_0^{kT-T} e(t) dt + \int_{kT-T}^{kT} e(t) dt, \quad (8.14)$$

which can be rewritten as

$$u(kT) = u(kT - T) + \text{area under } e(t) \text{ over last period, } T, \quad (8.15)$$

where  $T$  is the sample period.

For Tustin's method, the task at each step is to use trapezoidal integration, that is, to approximate  $e(t)$  by a straight line between the two samples (see Fig. 8.7). Writing  $u(kT)$  as  $u(k)$  and  $u(kT - T)$  as  $u(k-1)$  for short, we convert Eq. (8.15) to

$$u(k) = u(k-1) + \frac{T}{2}[e(k-1) + e(k)], \quad (8.16)$$

or, taking the  $z$ -transform,

$$\frac{U(z)}{E(z)} = \frac{T}{2} \left( \frac{1+z^{-1}}{1-z^{-1}} \right) = \frac{1}{\frac{2}{T} \left( \frac{1-z^{-1}}{1+z^{-1}} \right)}. \quad (8.17)$$

For  $D_c(s) = a/(s+a)$ , applying the same integration approximation yields

$$D_d(z) = \frac{a}{\frac{2}{T} \left( \frac{1-z^{-1}}{1+z^{-1}} \right) + a}.$$

In fact, substituting

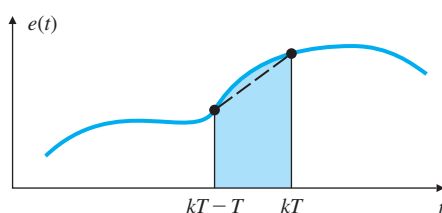
$$s = \frac{2}{T} \left( \frac{1-z^{-1}}{1+z^{-1}} \right)$$

for every occurrence of  $s$  in any  $D_c(s)$  yields a  $D_d(z)$  based on the trapezoidal integration formula. This is called **Tustin's method** or the **bilinear approximation**. Finding Tustin's approximation by hand for even a simple transfer function requires fairly extensive algebraic manipulations. The `c2d` function of Matlab expedites the process, as shown in the next example.

**Tustin's method or bilinear approximation**

**Figure 8.7**

Trapezoidal integration in Tustin's method



**EXAMPLE 8.1***Digital Controller for Example 6.15 Using Tustin's Approximation*

Determine the difference equations to implement the compensation from Example 6.15,

$$D_c(s) = 10 \frac{s/2 + 1}{s/10 + 1},$$

at a sample rate of 25 times bandwidth using Tustin's approximation. Compare the performance against the continuous system done in Example 6.15.

**Solution.** The bandwidth,  $\omega_{BW}$ , for Example 6.15 is approximately 10 rad/sec, as can be deduced by observing that the crossover frequency ( $\omega_c$ ) is approximately 5 rad/sec and noting the relationship between  $\omega_c$  and  $\omega_{BW}$  in Fig. 6.50. Therefore, the sample frequency should be

$$\omega_s = 25 \times \omega_{BW} = (25)(10) = 250 \text{ rad/sec.}$$

Normally, when a frequency is indicated with the units of cycles per second, or Hz, it is given the symbol  $f$ , so with this convention, we have

$$f_s = \omega_s / (2\pi) \simeq 40 \text{ Hz,} \quad (8.18)$$

and the sample period is then

$$T = 1/f_s = 1/40 = 0.025 \text{ sec.}$$

The discrete compensation is computed by the Matlab statement

```
s=tf('s');
sysDc = tf(10*(s/2 + 1)/(s/10 + 1));
T = 0.025;
sysDd = c2d(sysDc,T,'tustin')
```

which produces

$$D_d(z) = \frac{45.56 - 43.33 z^{-1}}{1 - 0.7778 z^{-1}}. \quad (8.19)$$

We can then write the difference equation by inspecting Eq. (8.19) to get

$$u(k) = 0.7778u(k-1) + 45.56e(k) - 43.33e(k-1),$$

or,

$$u(k) = 0.7778u(k-1) + 45.56[e(k) - 0.9510e(k-1)]. \quad (8.20)$$

Equation (8.20) computes the new value of the control,  $u(k)$ , given the past value of the control,  $u(k-1)$ , and the new and past values of the error signal,  $e(k)$  and  $e(k-1)$ .

In principle, the difference equation is evaluated initially with  $k = 0$ , then  $k = 1, 2, 3, \dots$ . However, there is usually no requirement that values for all times be saved in memory. Therefore, the computer only needs

to have variables defined for the current and past values. The instructions to the computer to implement the feedback loop in Fig. 8.1(b) with the difference equation from Eq. (8.20) would call for a continual looping through the following code:

```

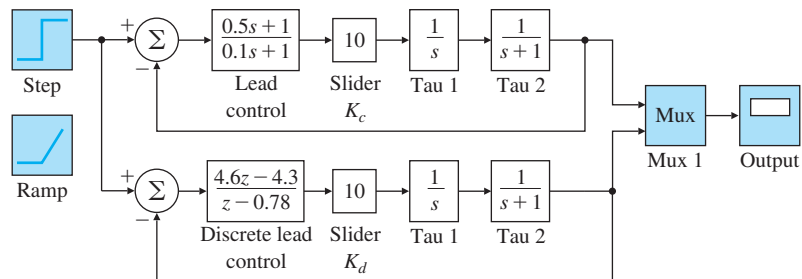
READ A/D:  $y, r$ 
 $e = r - y$ 
 $u = 0.7778u_p + 45.56[e - 0.9510e_p]$ 
OUTPUT D/A:  $u$ 
 $u_p = u$  (where  $u_p$  will be the past value for the next loop through)
 $e_p = e$ 
go back to READ when  $T$  sec have elapsed since last READ.

```

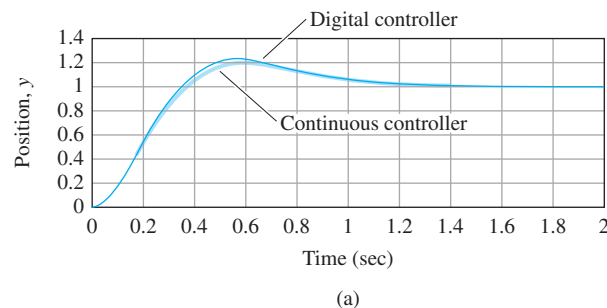
To evaluate this discrete controller, we use Simulink to compare the two implementations. Figure 8.8 shows the block diagram for the comparison, and the results of the step responses are shown in Fig. 8.9.

**Figure 8.8**

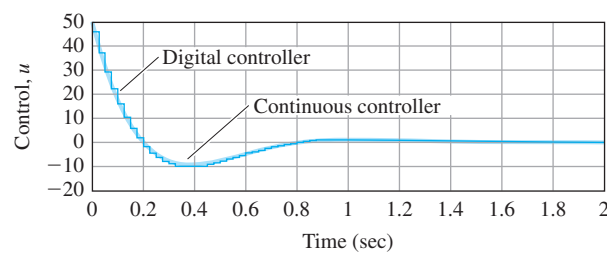
Simulink block diagram for transient response of lead-compensation designs with discrete and analog implementations

**Figure 8.9**

Comparison between the digital (using Tustin's) and the continuous controller step response with a sample rate 25 times the bandwidth:  
(a) position; (b) control signal



(a)



(b)

Note sampling at 25 times the bandwidth causes the digital implementation to match the continuous one quite well. Generally speaking, if you want to match a continuous system with a digital approximation of the continuous compensation, a conservative approach is to sample at approximately 25 times the bandwidth or faster.

---

### 8.3.2 Zero-Order Hold (ZOH) Method

Tustin's method essentially assumed the input to the controller varied linearly between the past sample rate and the current one, as shown in Fig. 8.7. Another assumption is the input to the controller remains constant throughout the sample period. In other words, for purposes of this design approximation, we assume that the  $D_c(s)$  in Fig. 8.1(a) is preceded by a ZOH whose function is to accept the value of  $e$  at sample time,  $k$ , and hold that value constant until  $k + 1$ . This is *not* the actual case; rather, the only ZOH in the system is the one preceding the plant,  $G(s)$ , as shown in Fig. 8.1(b). With this assumption, there is an *exact* discrete equivalent for this system because the ZOH precisely describes what happens between samples of  $e$  and the output  $u$  is dependent only on the input at the sample times  $e(k)$ .

For a controller described by  $D_c(s)$  preceded by a ZOH, given an input,  $e(k)$ , the system is essentially responding to a positive step at sample time,  $k$ , followed by a negative step one cycle delayed. In other words, one input sample produces a square pulse of height,  $e$ , that lasts for one sample period. For a constant positive step input,  $e$ , at time  $k$ ,  $E(s) = e(k)/s$ , so the result would be,

$$D_d(z) = \mathcal{Z} \left\{ \frac{D_c(s)}{s} \right\}, \quad (8.21)$$

where  $\mathcal{Z}\{F(s)\}$  is the  $z$ -transform of the sampled time series whose Laplace transform is the expression for  $F(s)$ , that is, it is given on the same line in Table 8.1. Furthermore, a constant negative step, one cycle delayed, would be

$$D_d(z) = z^{-1} \mathcal{Z} \left\{ \frac{D_c(s)}{s} \right\}. \quad (8.22)$$

Therefore, the discrete transfer function for the square pulse is

$$D_d(z) = (1 - z^{-1}) \mathcal{Z} \left\{ \frac{D_c(s)}{s} \right\}. \quad (8.23)$$

For a more complete derivation, see Chapter 4 in Franklin et al. (1998). Equation (8.23) provides us with a discrete approximation to  $D_c(s)$  and determines the difference equations to be used in Fig. 8.1(b).

ZOH approximation

ZOH transfer function

**EXAMPLE 8.2***Digital Controller for Example 6.15 Using the ZOH Approximation*

Again, determine the difference equations to implement the compensation from Example 6.15,

$$D_c(s) = 10 \frac{s/2 + 1}{s/10 + 1},$$

at a sample rate of 25 times the bandwidth using the ZOH approximation. Compare the performance against the continuous system done in Example 6.15 and with the results of Example 8.1.

**Solution.** The bandwidth is the same as the previous example, so the sample period is unchanged

$$T = 0.025 \text{ sec.}$$

The discrete compensation is computed by the Matlab statement, but this time we use the ZOH version of c2d

```
s = tf('s');
sysDc = 10*(s/2 + 1)/(s/10 + 1);
T = 0.025;
sysDd = c2d(sysDc,T,'zoh');
```

which produces

$$D_d(z) = \frac{(50 - 47.79 z^{-1})}{1 - 0.7788 z^{-1}}. \quad (8.24)$$

We can then write the difference equation by inspecting Eq. (8.24) to get

$$u(k) = 0.7788u(k-1) + 50e(k) - 47.79e(k-1),$$

or,

$$u(k) = 0.7788u(k-1) + 50[e(k) - 0.9558e(k-1)]. \quad (8.25)$$

Note the similarity between Eq. (8.25) and Eq. (8.20). There are very small differences in the zero and pole locations and the overall gain. The difference equations to be implemented in the digital controller are:

READ A/D:  $y, r$

$$e = r - y$$

$$u = 0.7788u_p + 50[e - 0.9510e_p]$$

OUTPUT D/A:  $u$

$u_p = u$  (where  $u_p$  will be the past value for the next loop through)

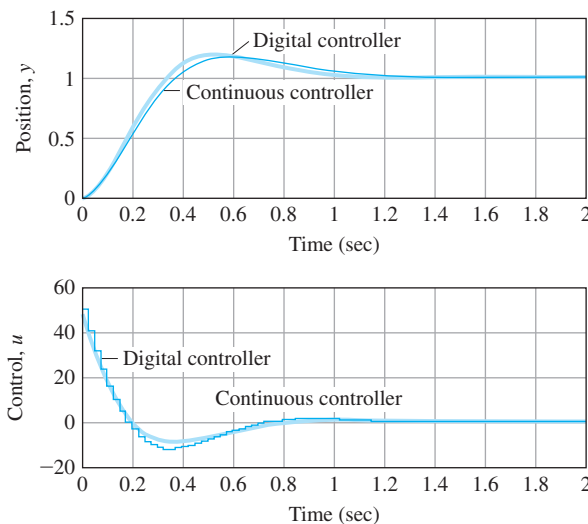
$$e_p = e$$

go back to READ when  $T$  sec have elapsed since last READ.

Use of Simulink to compare the two implementations, in a manner similar to that used for Example 8.1, yields the step responses shown in Fig. 8.10. Note, again, that sampling at 25 times the bandwidth again

**Figure 8.10**

Comparison between the digital (using ZOH approximation) and the continuous controller step response with a sample rate 25 times bandwidth: (a) position; (b) control



causes the digital implementation to match the continuous one quite well, although for this case, use of the Tustin approximation matched slightly better than the ZOH approximation. Historically, the advantage of the ZOH method was that it involved simpler algebraic manipulations; however, with the availability of control software such as Matlab, that advantage has diminished. A comparison of all the methods will be contained in Section 8.3.5.

### 8.3.3 Matched Pole-Zero (MPZ) Method

Another digitization method, called the **matched pole-zero** (MPZ) method, is found by extrapolating from the relationship between the  $s$ - and  $z$ -planes stated in Eq. (8.11). If we take the  $z$ -transform of a sampled function  $x(k)$ , the poles of  $X(z)$  are related to the poles of  $X(s)$  according to the relation  $z = e^{sT}$ . The MPZ technique applies the relation  $z = e^{sT}$  to the poles and zeros of a transfer function, even though, strictly speaking, this relation applies neither to transfer functions nor even to the zeros of a time sequence. Like all transfer-function digitization methods, the MPZ method is an approximation; here the approximation is motivated partly by the fact that  $z = e^{sT}$  is the correct  $s$  to  $z$  transformation for the poles of the transform of a time sequence and partly by the minimal amount of algebra required to determine the digitized transfer function by hand, in the event that one wanted to check the computer calculations.

Because physical systems often have more poles than zeros, it is useful to arbitrarily add zeros at  $z = -1$ , resulting in a  $1 + z^{-1}$  term in  $D_d(z)$ . This causes an averaging of the current and past input values,

as in Tustin's method. We select the low-frequency gain of  $D_d(z)$  so it equals that of  $D_c(s)$ .

### MPZ Method Summary

1. Map poles and zeros according to the relation  $z = e^{sT}$ .
2. If the numerator is of lower order than the denominator, add powers of  $(z + 1)$  to the numerator until numerator and denominator are of equal order.
3. Set the DC or low-frequency gain of  $D_d(z)$  equal to that of  $D_c(s)$ .

For example, the MPZ approximation of

$$D_c(s) = K_c \frac{s + a}{s + b}, \quad (8.26)$$

is

$$D_d(z) = K_d \frac{z - e^{-aT}}{z - e^{-bT}}, \quad (8.27)$$

where  $K_d$  is found by causing the DC gain of  $D_d(z)$  to equal the DC gain of  $D_c(s)$  using the continuous and discrete versions of the Final Value Theorem. The result is

$$K_c \frac{a}{b} = K_d \frac{1 - e^{-aT}}{1 - e^{-bT}},$$

or

$$K_d = K_c \frac{a}{b} \left( \frac{1 - e^{-bT}}{1 - e^{-aT}} \right). \quad (8.28)$$

For a  $D_c(s)$  with a higher-order denominator, Step 2 in the method calls for adding the  $(z + 1)$  term. For example,

$$D_c(s) = K_c \frac{s + a}{s(s + b)} \Rightarrow D_d(z) = K_d \frac{(z + 1)(z - e^{-aT})}{(z - 1)(z - e^{-bT})}, \quad (8.29)$$

however, because the DC gains of these transfer functions are infinite, it is necessary to match the low frequency gains instead. This can be accomplished by deleting the pure integral terms, that is, the poles at  $s = 0$  and  $z = 1$ , and proceeding as before to match the DC gains of the remaining transfer functions for the two cases. Doing this, we find that

$$K_d = K_c \frac{a}{2b} \left( \frac{1 - e^{-bT}}{1 - e^{-aT}} \right). \quad (8.30)$$

In the digitization methods described so far, the same power of  $z$  appears in the numerator and denominator of  $D_d(z)$ . This implies that the difference equation output at time  $k$  will require a sample of the input at time  $k$ . For example, the  $D_d(z)$  in Eq. (8.27) can be written

$$\frac{U(z)}{E(z)} = D_d(z) = K_d \frac{1 - \alpha z^{-1}}{1 - \beta z^{-1}}, \quad (8.31)$$

where  $\alpha = e^{-aT}$  and  $\beta = e^{-bT}$ . By inspection, we can see that Eq. (8.31) results in the difference equation

$$u(k) = \beta u(k - 1) + K_d[e(k) - \alpha e(k - 1)]. \quad (8.32)$$

**EXAMPLE 8.3***Design of a Space Station Attitude Digital Controller Using the Matched Pole-Zero Approximation*

A very simplified model of the space station attitude control dynamics has the plant transfer function

$$G(s) = \frac{1}{s^2}.$$

Design a digital controller to have a closed-loop natural frequency  $\omega_n \cong 0.3$  rad/sec and a damping ratio  $\zeta = 0.7$ .

**Solution.** The first step is to find the proper  $D_c(s)$  for the system defined in Fig. 8.11. After some trial and error, we find that the specifications can be met by the lead compensation

$$D_c(s) = 0.81 \frac{s + 0.2}{s + 2}. \quad (8.33)$$

The root locus in Fig. 8.12 verifies the appropriateness of using Eq. (8.33).

To digitize this  $D_c(s)$ , we first need to select a sample rate. For a system with  $\omega_n = 0.3$  rad/sec, the bandwidth will also be about 0.3 rad/sec. Let's try a sample rate slightly slower than the previous examples to obtain a sense of the effect. So let's use approximately 20 times  $\omega_n$ . Thus

$$\omega_s = 0.3 \times 20 = 6 \text{ rad/sec.}$$

A sample rate of 6 rad/sec is about 1 Hertz; therefore, the sample period should be  $T = 1$  sec. The MPZ digitization of Eq. (8.33), given by Eqs. (8.27) and (8.28), yields

$$\begin{aligned} D_d(z) &= 0.389 \frac{z - 0.82}{z - 0.135} \\ &= \frac{0.389 - 0.319z^{-1}}{1 - 0.135z^{-1}}. \end{aligned} \quad (8.34)$$

**Figure 8.11**  
Continuous-design definition for Example 8.3

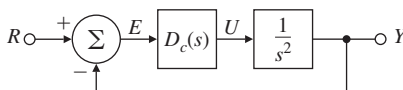


**Figure 8.12**  
s-Plane locus with respect to  $K$

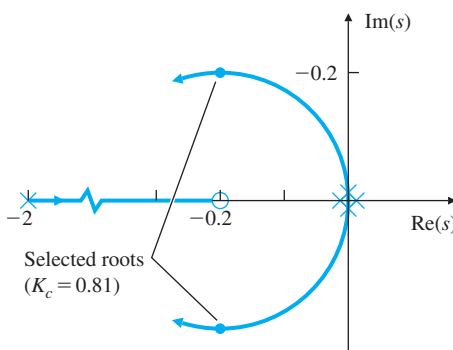
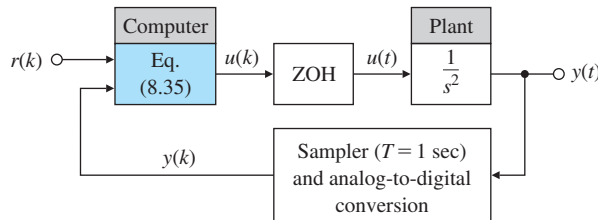


**Figure 8.13**

A digital control system that is equivalent to Fig. 8.11



Inspection of Eq. (8.34) gives us the difference equation

$$u(k) = 0.135u(k - 1) + 0.389e(k) - 0.319e(k - 1), \quad (8.35)$$

where

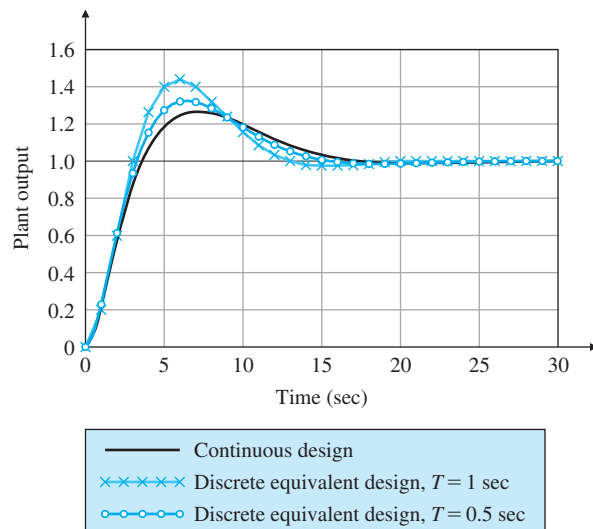
$$e(k) = r(k) - y(k),$$

and this completes the digital algorithm design. The complete digital system is shown in Fig. 8.13.

The last step in the design process is to verify the design by implementing it on the computer. Figure 8.14 compares the step response of the digital system using  $T = 1$  sec ( $20 \times \omega_{BW}$ ) with the step response of the continuous compensation. Note there is greater overshoot in the digital system, which suggests a decrease in the damping due to the digital implementation. The average  $T/2$  delay shown in Fig. 8.2 is the cause of the reduced damping. For a better match to the continuous system, it may be prudent to increase the sample rate. Figure 8.14 also shows the response with sampling that is twice as fast ( $40 \times \omega_{BW}$ ) and it can be seen that it comes much closer to the continuous system. Note the discrete compensation needs to be recalculated for this faster sample rate according to Eqs. (8.27) and (8.28).

**Figure 8.14**

Step responses of the continuous and digital implementations using the MPZ equivalent with slower sampling



All the methods thus far required knowing  $e(k)$  in order to compute  $u(k)$ ; however, it is impossible to sample  $e(k)$ , compute  $u(k)$ , then output  $u(k)$  all in zero elapsed time; therefore, Eq. (8.35) is impossible to implement precisely. However, if the equation is simple enough and/or the computer is fast enough, a slight computational delay between the  $e$  read and the  $u$  output will have a negligible effect on the actual response of the system compared with that expected from the original design. A rule of thumb would be to keep the computational delay on the order of  $1/10$  of  $T$ . The real-time code and hardware can be structured so this delay is minimized by making sure that computations between READ A/D and OUTPUT D/A are minimized, and  $u$  is sent to the ZOH immediately after its calculation.

### 8.3.4 Modified Matched Pole-Zero (MMPZ) Method

The  $D_d(z)$  in Eq. (8.29) would also result in  $u(k)$  being dependent on  $e(k)$ , the input at the same time point. If the structure of the computer hardware prohibits minimizing the time between the READ and the OUTPUT, or if the computations are particularly lengthy, it may be desirable to derive a  $D_d(z)$  that has one less power of  $z$  in the numerator than in the denominator; hence, the computer output  $u(k)$  would require only input from the previous time, that is,  $e(k - 1)$ . To do this, we simply modify Step 2 in the matched pole-zero procedure so the numerator is of lower order than the denominator by 1. We call this the Modified Matched Pole-Zero (MMPZ) method. For example, if

$$D_c(s) = K_c \frac{s + a}{s(s + b)},$$

we skip Step 2 to get

$$\begin{aligned} D_d(z) &= K_d \frac{z - e^{-aT}}{(z - 1)(z - e^{-bT})}, \\ K_d &= K_c \frac{a}{b} \left( \frac{1 - e^{-bT}}{1 - e^{-aT}} \right). \end{aligned} \quad (8.36)$$

To find the difference equation, we multiply the top and bottom of Eq. (8.36) by  $z^{-2}$  to obtain

$$D_d(z) = K_d \frac{z^{-1}(1 - e^{-aT}z^{-1})}{1 - z^{-1}(1 + e^{-bT}) + z^{-2}e^{-bT}}. \quad (8.37)$$

By inspecting Eq. (8.37) we can see the difference equation is  $u(k) = (1 + e^{-bT})u(k - 1) - e^{-bT}u(k - 2) + K_d[e(k - 1) - e^{-aT}e(k - 2)]$ .

In this equation, an entire sample period is available to perform the calculation and to output  $u(k)$ , because it depends only on  $e(k - 1)$ . A discrete analysis of this controller would therefore more accurately explain the behavior of the actual system. However, because this controller is using data that are one cycle old, it will typically not perform as well as the MPZ controller in terms of the deviations of the desired system output in the presence of random disturbances.

### 8.3.5 Comparison of Digital Approximation Methods

A numerical comparison of the magnitude of the frequency response for a first-order lag,

$$D_c(s) = \frac{5}{s+5},$$

is made in Fig. 8.15 for the four approximation techniques at two different sample rates. The results of the  $D_d(z)$  computations used in Fig. 8.15 are shown in Table 8.2. Note the MMPZ and ZOH methods are identical in this example; however, this will not always be the case when there are zeros and poles. The MPZ and Tustin's methods also appear to be identical; however, there are minor differences as you can see from their  $D_d(z)$  in Table 8.2. The major difference between the four approximations is that the two with the  $(z + 1)$  zeros yield a deep notch at  $\omega_s/2$ , which is often a desirable feature.

Figure 8.15, which shows three of the four approximations, shows that all the approximations are quite good at frequencies below about  $1/5$  the sample rate, or  $\omega_s/5$ . If  $\omega_s/5$  is sufficiently faster than the filter break-point frequency—that is, if the sampling is fast enough—the break-point characteristics of the lag will be accurately reproduced.

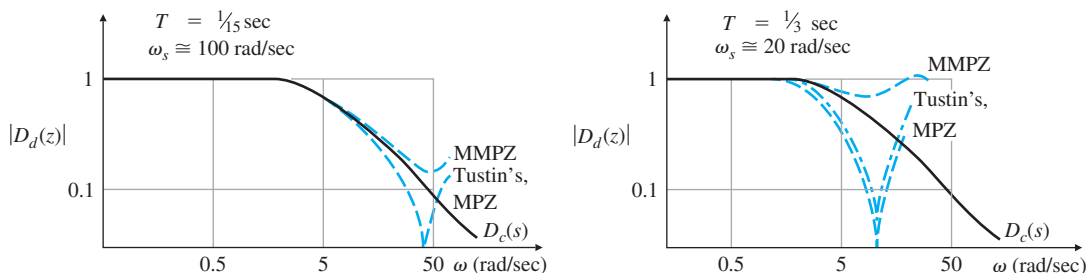


**Figure 8.15**

A comparison of the frequency response of 3 discrete approximations at two sample rates

**TABLE 8.2**

Comparing Digital Approximations of  $D_d(z)$  for  $D_c(s) = 5/(s + 5)$

Method	$\omega_s$	
	150 rad/sec	750 rad/sec
Matched pole-zero (MPZ)	$0.0945 \frac{z+1}{z-0.811}$	$0.1715 \frac{z+1}{z-0.657}$
Modified MPZ (MMPZ)	$0.189 \frac{1}{z-0.811}$	$0.343 \frac{1}{z-0.657}$
Tustin's	$0.0950 \frac{z+1}{z-0.810}$	$0.1735 \frac{z+1}{z-0.653}$
ZOH	$0.189 \frac{1}{z-0.811}$	$0.343 \frac{1}{z-0.657}$

Tustin's technique and the MPZ method show a notch at  $\omega_s/2$  because of their zero at  $z = -1$  from the  $z + 1$  term. Other than the large difference in the vicinity approaching  $\omega_s/2$  and higher, which is typically outside the range of interest, the four methods have similar accuracies.

### 8.3.6 Applicability Limits of the Discrete Equivalent Design Method

If we performed an exact discrete analysis or a simulation of a system and determined the digitization for a wide range of sample rates, the system could often be unstable for rates slower than approximately  $5\omega_{BW}$ , and the damping would be degraded significantly for rates slower than about  $10\omega_{BW}$ . At sample rates  $\gtrsim 20\omega_{BW}$ , design by discrete equivalents yields reasonable results, and at sample rates of 25 times the bandwidth or higher, discrete equivalents can be used with confidence.

As illustrated in Fig. 8.2, the errors partly come about because the technique ignores the lagging effect of the ZOH that precedes the plant which, on the average, is  $T/2$ . The other source of error is the behavior of the input signal between sample times. A method to account for the  $T/2$  delay is to include an approximation of the delay due to the ZOH:<sup>2</sup>

$$G_{ZOH}(s) = \frac{2/T}{s + 2/T}. \quad (8.38)$$

Once an initial design is carried out and the sampling rate has been selected, we could improve on our discrete design by inserting Eq. (8.38) into the original plant model and adjusting  $D_c(s)$  so that a satisfactory response in the presence of the approximate sampling delay is achieved. Therefore, we see that use of Eq. (8.38) partially alleviates the approximate nature of using discrete equivalents.

For sample rates slower than about  $10\omega_{BW}$  it is advisable to analyze the entire system using an exact discrete analysis. If a discrete analysis shows an unacceptable degradation of performance due to the sampling, the design can then be refined using exact discrete methods. We will cover this approach in Section 8.6.

## 8.4 Hardware Characteristics

A digital control system includes several unique components not found in continuous control systems: an **A/D converter** is a device to sample the continuous signal voltage from the sensor and to convert that signal to a digital word; a **D/A converter** is a device to convert the digital word from the computer to an analog voltage, an **anti-alias prefilter** is an analog device designed to reduce the effects of aliasing, and the **computer** is the device where the compensation  $D_d(z)$  is programmed and the calculations are carried out. This section provides a brief description of each of these.

---

<sup>2</sup>This is the lowest order Padé approximate to a pure time delay. See Appendix W5.6.3 available online at [www.pearsonglobaleditions.com](http://www.pearsonglobaleditions.com).

### 8.4.1 Analog-to-Digital (A/D) Converters

As discussed in Section 8.1, A/D converters are devices that convert a voltage level from a sensor to a digital word usable by the computer. At the most basic level, all digital words are binary numbers consisting of many bits that are set to either 1 or 0. Therefore, the task of the A/D converter at each sample time is to convert a voltage level to the correct bit pattern and often to hold that pattern until the next sample time.

Of the many A/D conversion techniques that exist, the most common are based on counting schemes or a successive-approximation technique. In counting methods, the input voltage may be converted to a train of pulses whose frequency is proportional to the voltage level. The pulses are then counted over a fixed period using a binary counter, thus resulting in a binary representation of the voltage level. A variation on this scheme is to start the count simultaneously with a voltage that is linear in time and to stop the count when the voltage reaches the magnitude of the input voltage to be converted.

The successive-approximation technique tends to be much faster than the counting methods. It is based on successively comparing the input voltage to reference levels representing the various bits in the digital word. The input voltage is first compared with a reference value that is half the maximum. If the input voltage is greater, the most significant bit is set, and the signal is then compared with a reference level that is  $\frac{3}{4}$  the maximum to determine the next bit, and so on. One clock cycle is required to set each bit, so an  $n$ -bit converter would require  $n$  cycles. At the same clock rate, a counter-based converter might require as many as  $2^n$  cycles, which would usually be much slower.

With either technique, the greater the number of bits, the longer it will take to perform the conversion. The price of A/D converters generally goes up with both speed and bit size. In 2017, a 12-bit (resolution of 0.025%) converter with a high performance capability of 170 million samples per sec (170 MHz) sold for approximately \$15 while a 12-bit converter with a good performance capability of 1 MHz sold for approximately \$2. Also now becoming common are 16-bit A/D converters (0.0015% resolution). A 16 bit A/D with 500 KHz capability sold for approximately \$5 in 2017. The performance has been improving considerably every year and these numbers change substantially with each edition of this book!

If more than one channel of data needs to be sampled and converted to digital words, it is usually accomplished using a multiplexer rather than by multiple A/D converters. The multiplexer sequentially connects the converter into the channel being sampled.

### 8.4.2 Digital-to-Analog Converters

D/A converters, as mentioned in Section 8.1, are used to convert the digital words from the computer to a voltage level, and are sometimes

referred to as **Sample and Hold** devices. They provide analog outputs from a computer for driving actuators or perhaps a recording device such as an oscilloscope or strip-chart recorder. The basic idea behind their operation is that the binary bits cause switches (electronic gates) to open or close, thus routing the electric current through an appropriate network of resistors to generate the correct voltage level. Because no counting or iteration is required for such converters, they tend to be much faster than A/D converters. In fact, A/D converters that use the successive-approximation method of conversion include D/A converters as components. The price of D/A converters is comparable to A/D converters, but usually somewhat lower.

### 8.4.3 Anti-Alias Prefilters

An analog **anti-alias prefilter** is often placed between the analog sensor and the A/D converter. Its function is to reduce the higher-frequency noise components in the analog signal in order to prevent aliasing, that is, having the noise be modulated to a lower frequency by the sampling process.

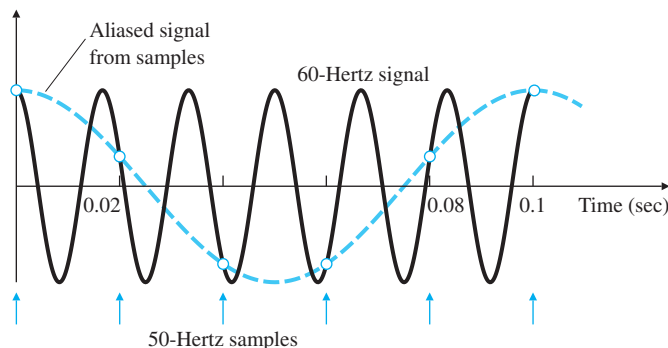
An example of aliasing is shown in Fig. 8.16, where a 60 Hertz oscillatory signal is being sampled at 50 Hertz. The figure shows the result from the samples as a 10 Hertz signal, and also shows the mechanism by which the frequency of the signal is aliased from 60 to 10 Hertz. Aliasing will occur any time the sample rate is not at least twice as fast as any of the frequencies in the signal being sampled. Therefore, to prevent aliasing of a 60 Hertz signal, the sample rate would have to be faster than 120 Hertz, clearly much higher than the 50 Hertz rate in the figure.

Aliasing can be explained from the **sampling theorem of Nyquist and Shannon**. Their theorem basically states that, for the signal to be accurately reconstructed from the samples, it must have no frequency component greater than half the sample rate ( $\omega_s/2$ ). Another result of their theorem is that the highest frequency that can be unambiguously represented by discrete samples is the **Nyquist rate** of  $\omega_s/2$ , an idea discussed in Section 8.2.3.

**Analog prefilters reduce aliasing**

**Nyquist-Shannon sampling theorem**

**Figure 8.16**  
An example of aliasing



The result of aliasing on a digital control system can be substantial. In a continuous system, noise components with a frequency much higher than the control-system bandwidth normally have a small effect because the system will not respond at the high frequency. However, in a digital system, the frequency of the noise can be aliased down to the vicinity of, or less than, the system bandwidth so the closed-loop system would respond to the noise. Thus, the noise in a poorly designed digitally controlled system could have a substantially greater effect than if the control had been implemented using analog electronics.

The solution is to place an *analog* prefilter before the sampler. In many cases, a simple first-order low-pass filter will do—that is,

$$H_p(s) = \frac{a}{s + a}, \quad (8.39)$$

where the break point  $a$  is selected to be lower than  $\omega_s/2$  so any noise present with frequencies greater than  $\omega_s/2$  is attenuated by the prefilter. The lower the break-point frequency selected, the more the noise above  $\omega_s/2$  is attenuated. For example, if  $\omega_s$  is chosen to be  $25\omega_{BW}$ , the anti-aliasing filter breakpoint,  $a$ , should be selected lower than  $\omega_s/2$ , so that  $a = 10\omega_{BW}$  would be a reasonable choice. A breakpoiont 10 × higher than the bandwidth should not affect the stability or performance of the closed-loop system; however, too low a break point may force the designer to reduce the control system's bandwidth or add more phase lead to the compensation. The prefilter does not completely eliminate the aliasing; however, it does attenuate the magnitude of the high frequency noise that will be aliased. Through judicious choice of the prefilter break point and the sample rate, the designer has the ability to reduce the magnitude of the aliased noise to some acceptable level.

#### 8.4.4 The Computer

The computer is the unit that does all the computations. Most digital controllers used today are built around a microcontroller that contains both a microprocessor and most of the other functions needed, including the A/D and D/A conversion. For development purposes in a laboratory, a digital controller could be a laptop or PC. The relatively low cost of microprocessor technology has accounted for the large increase in the use of digital control systems, which started in the 1980s and has continued into the 2010s.

The computer consists of a central processor unit (CPU), which does the computations and provides the system logic; a clock to synchronize the system; memory modules for data and instruction storage; and a power supply to provide the various required voltages. The memory modules come in three basic varieties:

1. **Read-only memory (ROM)** is the least expensive, but after its manufacture, its contents cannot be changed. Most of the memory in

products manufactured in quantity is ROM. It retains its stored values when power is removed.

2. **Random-access memory (RAM)** is the most expensive, but its values can be changed by the CPU. It is required only to store the values that will be changed during the control process and typically represents only a small fraction of the total memory of a developed product. The values in memory are lost when power is removed.
3. **Programmable read-only memory (EPROM) or Flash Memory** is similar to a ROM, but whose values can be changed. It retains its stored values when power is removed but values are changed at a slower speed than RAM. The readout speed is about the same as ROM. Flash memory is becoming very common and is used in cameras, USB memory sticks, smart phones, and so on.

Microprocessors for control applications generally come with a digital word size of 8, 16, or 32 bits, although some have been available with 12 bits. Larger word sizes give better accuracy, but at an increase in cost. The most economical solution is often to use an 8-bit microprocessor, but to use two digital words to store one value (**double precision**) in the areas of the controller that are critical to the system accuracy. Many digital control systems use computers originally designed for digital signal-processing applications, so-called DSP chips, which give the control designer full freedom to implement computationally advanced control schemes at high sample rates on the order of MHz. For even higher sample rates, Field Programmable Gate Arrays are sometimes preferred.

## 8.5 Sample-Rate Selection

The selection of the best sample rate for a digital control system is the result of a compromise of many factors. Sampling too fast can cause a loss of accuracy while the basic motivation for lowering the sample rate  $\omega_s$  is cost, both of the digital hardware and the sensors. A decrease in sample rate means more time is available for the control calculations; hence, slower computers can be used for a given control function or more control capability can be achieved from a given computer. Either way, the cost per function is lowered. For systems with A/D converters, less demand on conversion speed will also lower cost. These economic arguments indicate that the best engineering choice is the slowest possible sample rate that still meets all performance specifications.

There are several factors that could provide a lower limit on the acceptable sample rate:

1. Tracking effectiveness as measured by closed-loop bandwidth or by time-response requirements, such as rise time and settling time;
2. Regulation effectiveness as measured by the error response to random plant disturbances; and

3. Error due to measurement noise and the associated prefilter.

A fictitious limit occurs when using discrete equivalents. The inherent approximation in the method may give rise to decreased performance or even system instabilities as the sample rate is lowered. This can lead the designer to conclude that a faster sample rate is required. However, there are two solutions:

1. Sample faster, and
2. Recognize that the approximations are invalid and refine the design using discrete analysis design methods described in the subsequent sections.

The ease of designing digital control systems with fast sample rates and the low cost of very capable computers often drives the designer to select a sample rate that is  $40 \times \omega_{BW}$  or higher. For computers with fixed-point arithmetic, very fast sample rates can lead to multiplication errors that have the potential to produce significant offsets or limit cycles in the control (see Franklin et al., 1998).

### 8.5.1 Tracking Effectiveness

An absolute lower bound on the sample rate is set by a specification to track a command input with a certain frequency (the system bandwidth). The sampling theorem (see Section 8.4.3 and Franklin et al., 1998) states that in order to reconstruct an unknown, band-limited, continuous signal from samples of that signal, we must sample at least twice as fast as the highest frequency contained in the signal. Therefore, in order for a closed-loop system to track an input at a certain frequency, it must have a sample rate twice as fast; that is,  $\omega_s$  must be at least twice the system bandwidth ( $\omega_s \Rightarrow 2 \times \omega_{BW}$ ). We also saw from the results of mapping the  $s$ -plane into the  $z$ -plane ( $z = e^{sT}$ ) that the highest frequency that can be represented by a discrete system is  $\omega_s/2$ , which supports the conclusion of the theorem.

For systems with resonances, it is sometimes required to sample fast enough to provide stabilization of the resonant modes. This topic is covered in Franklin et al. (1998).

The closed-loop-bandwidth limitation provides the fundamental lower bound on the sample rate. In practice, however, the theoretical lower bound of sampling at twice the bandwidth of the reference input signal would not be judged sufficient in terms of the quality of the desired time responses. For a system with a rise time on the order of 1 sec (thus yielding a closed-loop bandwidth on the order of 0.5 Hertz), it is reasonable to insist on a sampling rate of 10 to 20 Hertz, which is a factor of 20 to 40 times  $\omega_{BW}$ . The purposes of choosing a sample rate much greater than the bandwidth are to reduce the delay between a command and the system response to the command, and also to smooth the system output to the control steps coming out of the ZOH.

### 8.5.2 Disturbance Rejection

Disturbance rejection is an important—if not the most important—aspect of any control system. Disturbances enter a system with various frequency characteristics ranging from steps to white noise. For the purpose of sample-rate selection, the higher-frequency random disturbances are the most influential. However, the impact of high frequency disturbances is affected by the anti-aliasing filter as well as the sample rate. For a very high frequency noise, it would be foolish to sample fast enough to attenuate the disturbance without the use of a prefilter for reasons discussed in the next subsection.

Assuming the prefilter is well designed so there is little or no aliasing of noise with a frequency greater than  $\omega_s/2$ , the sample rate selection pretty much follows the same rule of thumb as Tracking Effectiveness; that is, sample rates on the order of 25 times  $\omega_{BW}$  or higher are typical.

### 8.5.3 Effect of Anti-Alias Prefilter

Digital control systems with analog sensors typically include an analog anti-alias prefilter between the sensor and the sampler as described in Section 8.4.3. The prefilters are low-pass, and the simplest transfer function is

$$H_p(s) = \frac{a}{s+a}. \quad (8.40)$$

so the noise above the prefilter break point  $a$  is attenuated. The goal is to provide enough attenuation at half the sample rate ( $\omega_s/2$ ) such that the noise above  $\omega_s/2$ , when aliased into lower frequencies by the sampler, will not be detrimental to control system performance.

A conservative design procedure is to select the prefilter break point to be sufficiently higher than the system bandwidth that the phase lag from the prefilter does not significantly alter the system stability. This procedure allows the prefilter to be ignored in the basic control system design. For example, selecting  $a = 10\omega_{BW}$  would be a reasonable choice. Furthermore, for a good reduction in the high-frequency noise at  $\omega_s/2$ , we might choose a sample rate that is about 10 times higher than the prefilter break point. This selection would reduce the high frequency noise above  $\omega_s/2$  that would be aliased into a lower frequency by at least a factor of 5. The result of this conservative prefilter design example is that the sample rate would be on the order 100 times faster than the system bandwidth! Using this sort of design procedure, the prefilter influence will likely provide the lower bound on the selection of the sample rate. This kind of process was carried out in past years when one group of a company designed the analog control system, then gave the design to the digital group to put it in the computer. In fact, this is still the current practice in some industries where the performance of the control system is critical.

An alternative design procedure is to allow significant phase lag from the prefilter at the system bandwidth. This requires us to include

the analog prefilter characteristics in the plant model when carrying out the control design, and requires an integrated design effort between the analog and digital design groups, or better yet, one group to do it all. It allows the use of lower sample rates, but at the possible expense of increased complexity in the compensation because additional phase lead must be provided to counteract the prefilter's phase lag. If this procedure is used and low prefilter break points are allowed, the effect of aliased sensor noise is small, and the prefilter essentially has no effect on the sample rate.

It may seem counterintuitive that placing a lag (the analog prefilter) in one portion of the controller and a counteracting lead [extra lead in  $D_d(z)$ ] in another portion of the controller provides a net positive effect on the overall system. The net gain is a result of the fact that the lag is in the analog part of the system where high frequencies can exist. The counteracting lead is in the digital part of the system where frequencies above the Nyquist rate do not exist. The result is a reduction in the high frequencies before the sampling which are not reamplified by the counteracting digital lead, thus producing net reduction in high frequency disturbances. Furthermore, these high frequencies are particularly insidious with a digital controller because of the aliasing that would result from the sampling.

#### 8.5.4 Asynchronous Sampling

As noted in the previous paragraphs, separating the prefilter design from the control-law design may require using a faster sample rate than otherwise. This same result may show up in other architecture types. For example, a smart sensor with its own computer running asynchronously relative to the primary control computer will not be amenable to direct digital design because the overall system transfer function depends on the phasing between the smart sensor and the primary digital controller. Therefore, if asynchronous digital subsystems are present, sample rates on the order of  $20 \times \omega_{BW}$  or slower in any module should be used with caution, and the system performance checked through simulation or experiment.

### △ 8.6 Discrete Design

It is possible to obtain an exact discrete model that relates the samples of the continuous plant  $y(k)$  to the input control sequence  $u(k)$ . This plant model can be used as part of a discrete model of the feedback system including the compensation  $D_d(z)$ . Analysis and design using this discrete model is called **discrete design** or, alternatively, **direct digital design**. Once a discrete model of the entire system is obtained, the designer can develop a discrete controller entirely in the discrete domain. This process is particularly advantageous for systems whose sample rates are

constrained to be very slow compared to their bandwidth, that is, with sample rates ( $\omega_s < 10 \times \omega_n$ ). This would normally only occur if the sample rate was limited by the sampling process or sensor characteristics rather than the microcontroller, which have become very fast and inexpensive. The following subsections will describe how to find the discrete plant model (see Section 8.6.1), what the feedback compensation looks like when designing with a discrete model (see Section 8.6.2), how the design process is carried out (see Section 8.6.3), and how various discrete designs can be analyzed (see Section 8.6.4).

### 8.6.1 Analysis Tools

The first step in performing a discrete analysis of a system with some discrete elements is to find the discrete transfer function of the continuous portion. For a system similar to that shown in Fig. 8.1(b), we wish to find the transfer function between  $u(kT)$  and  $y(kT)$ . This is precisely the case discussed in Section 8.3.2; however, here the ZOH is real so there is no approximation involved. It is an *exact* discrete equivalent for this system; the ZOH precisely describes what happens between samples of  $u(kT)$  and the output  $y(kT)$  is dependent only on the input at the sample times  $u(kT)$ .

For a plant described by  $G(s)$  and preceded by a ZOH, the discrete transfer function was essentially given by Eq. (8.23), and is repeated here with  $D_c(s)$  replaced by  $G(s)$ .

$$G(z) = (1 - z^{-1})\mathcal{Z} \left\{ \frac{G(s)}{s} \right\}, \quad (8.41)$$

The exact discrete equivalent

where  $\mathcal{Z}\{F(s)\}$  is the  $z$ -transform of the sampled time series whose Laplace transform is the expression for  $F(s)$ , given on the same line in Table 8.1. Equation (8.41) allows us to replace the mixed (continuous and discrete) system shown in Fig. 8.17(a) with the equivalent pure discrete system shown in Fig. 8.17(b).

The analysis and design of discrete systems is very similar to the analysis and design of continuous systems; in fact, all the same rules apply. The closed-loop transfer function of Fig. 8.17(b) is obtained using the same rules of block-diagram reduction—that is,

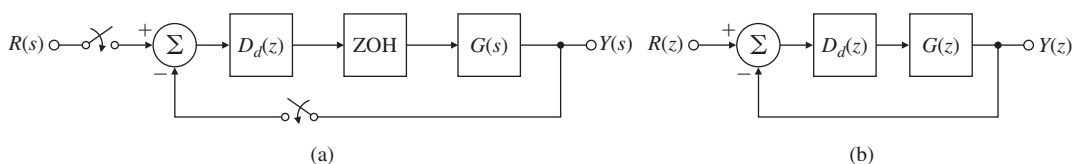


**Figure 8.17**

Comparison of: (a) a mixed system; and (b) its pure discrete equivalent

$$\frac{Y(z)}{R(z)} = \frac{D_d(z)G(z)}{1 + D_d(z)G(z)}. \quad (8.42)$$

To find the characteristic behavior of the closed-loop system, we need to find the factors in the denominator of Eq. (8.42)—that is, the closed-loop poles or the roots of the discrete characteristic equation

$$1 + D_d(z)G(z) = 0.$$

The root-locus techniques used in continuous systems to find roots of a polynomial in  $s$  apply equally well and without modification to the polynomial in  $z$ ; however, the interpretation of the results is quite different, as illustrated in Fig. 8.4. A major difference is that the stability boundary is now the unit circle instead of the imaginary axis.

## EXAMPLE 8.4

### *Discrete Root Locus*

For the case in which  $G(s)$  in Fig. 8.17(a) is

$$G(s) = \frac{a}{s+a}$$

and  $D_d(z) = K$ , draw the root locus with respect to  $K$ , and compare your results with a root locus of a continuous version of the system. Discuss the implications of your loci.

**Solution.** It follows from Eq. (8.41) that

$$\begin{aligned} G(z) &= (1 - z^{-1})\mathcal{Z}\left[\frac{a}{s(s+a)}\right] \\ &= (1 - z^{-1})\left[\frac{(1 - e^{-aT})z^{-1}}{(1 - z^{-1})(1 - e^{-aT}z^{-1})}\right] \\ &= \frac{1 - \alpha}{z - \alpha}, \end{aligned}$$

where

$$\alpha = e^{-aT}.$$

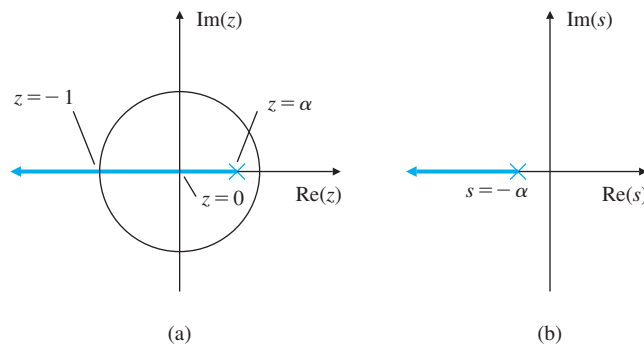
To analyze the performance of the closed-loop system, standard root-locus rules apply. The result is shown in Fig. 8.18(a) for the discrete case and in Fig. 8.18(b) for the continuous case. In contrast to the continuous case, in which the system remains stable for all values of  $K$ , in the discrete case the system becomes oscillatory with decreasing damping ratio as  $z$  goes from 0 to  $-1$  and eventually becomes unstable. This instability is due to the lagging effect of the ZOH, which is properly accounted for in the discrete analysis.

### 8.6.2 Feedback Properties

In continuous systems, we typically start the design process using the following basic design elements: proportional, derivative, or integral

**Figure 8.18**

Root loci for: (a) the  $z$ -plane; and (b) the  $s$ -plane



control laws, or some combination of these, sometimes with a lag included. The same ideas can be used in discrete design. Alternatively, the  $D_d(z)$  resulting from the digitization of a continuously designed  $D_c(s)$  will produce these basic design elements, which will then be used as a starting point in a discrete design. The discrete control laws are as follows:

### *Proportional*

$$u(k) = K e(k) \Rightarrow D_d(z) = K. \quad (8.43)$$

### *Derivative*

$$u(k) = K T_D [e(k) - e(k-1)], \quad (8.44)$$

for which the transfer function is

$$D_d(z) = K T_D (1 - z^{-1}) = K T_D \frac{z - 1}{z} = k_D \frac{z - 1}{z}. \quad (8.45)$$

### *Integral*

$$u(k) = u(k-1) + \frac{K_p}{T_I} e(k), \quad (8.46)$$

for which the transfer function is

$$D_d(z) = \frac{K}{T_I} \left( \frac{1}{1 - z^{-1}} \right) = \frac{K}{T_I} \left( \frac{z}{z - 1} \right) = k_I \left( \frac{z}{z - 1} \right). \quad (8.47)$$

### *Lead Compensation*

The examples in Section 8.3 showed that a continuous lead compensation leads to difference equations of the form

$$u(k+1) = \beta u(k) + K[e(k+1) - \alpha e(k)], \quad (8.48)$$

for which the transfer function is

$$D_d(z) = K \frac{1 - \alpha z^{-1}}{1 - \beta z^{-1}}. \quad (8.49)$$

### 8.6.3 Discrete Design Example

Digital control design consists of using the basic feedback elements of Eqs. (8.43) to (8.49) and iterating on the design parameters until all specifications are met.

#### EXAMPLE 8.5

#### *Direct Discrete Design of the Space Station Digital Controller*

Design a digital controller to meet the same specifications as in Example 8.3 using discrete design.

**Solution.** The discrete model of the  $1/s^2$  plant, preceded by a ZOH, is found through Eq. (8.41) to be

$$G(z) = \frac{T^2}{2} \left[ \frac{z+1}{(z-1)^2} \right],$$

which, with  $T = 1$  sec, becomes

$$G(z) = \frac{1}{2} \left[ \frac{z+1}{(z-1)^2} \right].$$

Proportional feedback in the continuous case yields pure oscillatory motion, so in the discrete case we should expect even worse results. The root locus in Fig. 8.19 verifies this. For very low values of  $K$  (where the locus represents roots at very low frequencies compared to the sample rate), the locus is tangent to the unit circle ( $\zeta \cong 0$  indicating pure oscillatory motion), thus matching the proportional continuous design.

For higher values of  $K$ , Fig. 8.19 shows that the locus diverges into the unstable region because of the effect of the ZOH and sampling. To compensate for this, we will add a derivative term to the proportional term so the control law is

$$U(z) = K[1 + T_D(1 - z^{-1})]E(z), \quad (8.50)$$

which yields compensation of the form

$$D_d(z) = K \frac{z - \alpha}{z}, \quad (8.51)$$

**Figure 8.19**

*z*-plane root locus for a  $1/s^2$  plant with proportional feedback

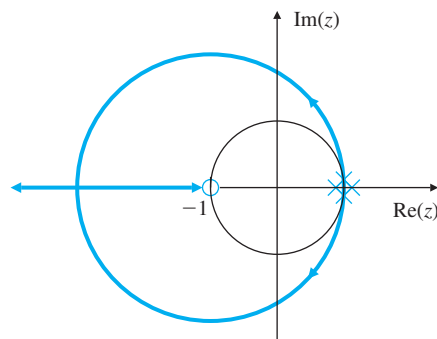
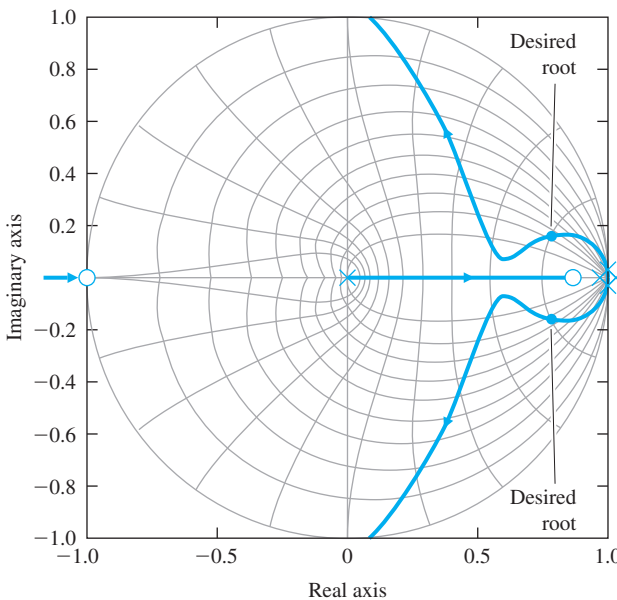


**Figure 8.20**

$z$ -plane locus for the  $1/s^2$  plant with  $D_d(z) = K(z - 0.85)/z$



where the new  $K$  and  $\alpha$  replace the  $K$  and  $T_D$  in Eq. (8.50). Now, the task is to find the values of  $\alpha$  and  $K$  that yield good performance. The specifications for the design are that  $\omega_n = 0.3$  rad/sec and  $\zeta = 0.7$ . Figure 8.4 indicates that this  $s$ -plane root location maps into a desired  $z$ -plane location of

$$z = 0.78 \pm 0.18j.$$

Figure 8.20 is the locus with respect to  $K$  for  $\alpha = 0.85$ . The location of the zero (at  $z = 0.85$ ) was determined by trial and error until the locus passed through the desired  $z$ -plane locations. The value of the gain when the locus passes through  $z = 0.78 \pm 0.18j$  is  $K = 0.374$ . Equation (8.51) now becomes

$$D_d(z) = 0.374 \frac{z - 0.85}{z}. \quad (8.52)$$

Normally, it is not particularly advantageous to match specific  $z$ -plane root locations; rather it is necessary only to pick  $K$  and  $\alpha$  (or  $T_D$ ) to obtain acceptable  $z$ -plane roots, a much easier task. In this example, we want to match a specific location only so we can compare the result with the design in Example 8.3.

The control law that results is

$$U(z) = 0.374(1 - 0.85z^{-1})E(z),$$

or

$$u(k) = 0.374e(k) - 0.318e(k-1), \quad (8.53)$$

which is similar to the control equation (8.35) previously obtained.

The controller in Eq. (8.53) basically differs from the continuously designed controller [see Eq. (8.35)] only in the absence of the  $u(k - 1)$  term. The  $u(k - 1)$  term in Eq. (8.35) results from the lag term  $(s + b)$  in the compensation [see Eq. (8.33)]. The lag term is typically included in analog controllers both because it supplies noise attenuation, and because pure analog differentiators are difficult to build. Some equivalent lag in discrete design naturally appears as a pole at  $z = 0$  (see Fig. 8.20) and represents the one-sample delay in computing the derivative by a first difference. For more noise attenuation, we could move the pole to the right of  $z = 0$ , thus resulting in less derivative action and more smoothing, the same trade-off that exists in continuous control design.

### 8.6.4 Discrete Analysis of Designs

Any digital controller, whether designed by discrete equivalents or directly in the  $z$ -plane, can be analyzed using discrete analysis, which consists of the following steps:

1. Find the discrete model of the plant and ZOH using Eq. (8.41).
2. Form the feedback system including  $D_d(z)$ .
3. Analyze the resulting discrete system.

We can determine the roots of the system using a root locus (as described in Section 8.6.3) or we can determine the time history (at the sample instants) of the discrete system.

## EXAMPLE 8.6

### *Damping and Step Response in Digital versus Continuous Design*

Use discrete analysis to determine the equivalent  $s$ -plane damping and the step responses of the digital designs in Examples 8.3 and 8.5, and compare your results with the damping and step response of the continuous case in Example 8.3.

**Solution.** The Matlab statements to evaluate the damping and step response of the continuous case in Example 8.3 are

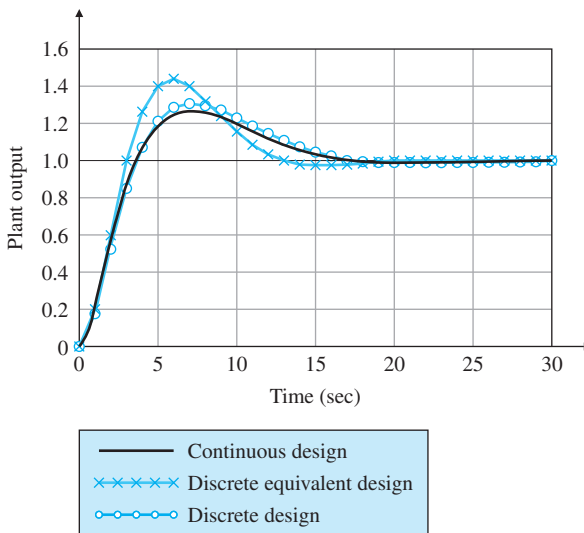
```
s=tf('s');
sysGc = 1/(s^2);
sysDc = 0.81*(s+0.2)/(s+2);
sysGDc = series(sysGc,sysDc);
sysCLc = feedback(sysGDc,1);
step(sysCLc)
damp(sysCLc)
```

To analyze the digital control cases, the model of the plant preceded by the ZOH is found using the following statements:

```
T = 1;
sysGz = c2d(sysGc,T,'zoh');
```

**Figure 8.21**

Step response of the continuous and digital systems in Examples 8.3 and 8.6



Analysis of the digital control designed using the discrete equivalent [see Eq. (8.35)] in Example 8.3 is performed by the statements

```

z = tf('z',T); % specifies z-transform based on input T
sysDz = .389*(z - .82)/(z - .135);
sysDGz = series(sysGz,sysDz);
sysCLz = feedback(sysDGz,1);
step(sysCLz)
damp(sysCLz)

```

Likewise, the discrete design of  $D_d(z)$  from Eq. (8.52) can be analyzed by the same sequence.

The resulting step responses are shown in Fig. 8.21. The calculated damping  $\zeta$  and complex root natural frequencies  $\omega_n$  of the closed-loop systems are

$$\text{Continuous case : } \zeta = 0.705, \quad \omega_n = 0.324;$$

$$\text{Discrete equivalent : } \zeta = 0.645, \quad \omega_n = 0.441;$$

$$\text{Discrete design : } \zeta = 0.733, \quad \omega_n = 0.306.$$

The figure shows increased overshoot for the discrete equivalent method that occurred because of the decreased damping of that case. Very little increased overshoot occurred in the discrete design, because that compensation was adjusted specifically so that the equivalent  $s$ -plane damping of the discrete system was approximately at the desired damping value of  $\zeta = 0.7$ .

---

Although the analysis showed some differences between the performance of the digital controllers designed by the two methods, neither

the performance nor the control equations [see Eqs. (8.35) and (8.53)] are substantially different. This similarity results because the sample rate is fairly fast compared to  $\omega_n$ —that is,  $\omega_s \cong 20 \times \omega_n$ . If we were to decrease the sample rate, the numerical values in the compensations would become increasingly different, and the performance would degrade considerably for the discrete equivalent case.

As a general rule, discrete design should be used if the sampling frequency is slower than  $10 \times \omega_n$ . At the very least, a discrete equivalent design with slow sampling ( $\omega_s < 10 \times \omega_n$ ) should be verified by a discrete analysis or by simulation, as described in this Section, and the compensation adjusted if needed. A simulation of a digital control system is a good idea in any case. If it properly accounts for all delays and possibly asynchronous behavior of different modules, it may expose instabilities that are impossible to detect using continuous or discrete linear analysis. A more complete discussion regarding the effects of sample rate on the design was discussed in Section 8.5.

## 8.7 Discrete State-Space Design Methods

Chapter 7 described the design options available for carrying out continuous designs using the state-space description of the system. These methods can also be applied to discrete models, a subject that is described in Section W8.7 on our website [www.pearsonglobaleditions.com](http://www.pearsonglobaleditions.com). It is also discussed in much greater detail in Franklin et al. (1998).

## 8.8 Historical Perspective

One of the earliest examples of actual control of systems based on sampled data came with the use of search RADAR in WWII. In that case, the position of the target was available only once each revolution of the antenna. The theory of sampled data systems was developed by the mathematician W. Hurewicz<sup>3</sup> and published as a chapter in H. M. James, N. B. Nichols, and R. S. Phillips, *Theory of Servomechanisms*, vol. 25, Rad Lab Series, New York, McGraw Hill, 1947. The historical perspective for Chapter 5 discussed the introduction of computers for engineers performing design activities. The possibility of using computers for direct digital control motivated the continuation of work on sampled-data systems during the 1950s, especially at Columbia University under Professor J. R. Ragazzini. That work was published in Ragazzini and Franklin (1958). Early applications were in the process control industry where the relatively large and expensive computers

---

<sup>3</sup>Hurewicz died in 1956 falling off a ziggurat (a Mexican pyramid) on a conference outing at the International Symposium on algebraic topology in Mexico. It is suggested that he was “... a paragon of absentmindedness, a failing that probably led to his death.”

available at the time could be justified. Professor Karl Åström introduced direct digital control of a paper mill in Sweden in the early 1960s.

In 1961, when President Kennedy announced the goal of sending a man to the moon, there were no digital autopilots for aerospace vehicles. In fact, small digital computers suitable for implementing control systems were virtually nonexistent. The team at the MIT Draper Labs (called the Instrumentation Lab at that time) in charge of designing and building the Apollo control systems initially designed the control systems for the lunar and command modules with conventional analog electronics. However, they discovered that those systems would be too heavy and complex for the mission. So the decision was made to design and build the first aerospace digital control system. Bill Widnall, Dick Battin, and Don Fraser were all key players in the successful design and execution of that system for the Apollo flights in late 1960s. The group went on to demonstrate a digital autopilot for NASA's F-8 in the 1970s, and digital autopilots went on to become dominant over the 1980s and beyond. In fact, with the introduction of inexpensive digital signal processors, most control systems of any kind became digital by the turn of the century and, today, very few control systems are being implemented with analog electronics. This evolution has had an effect on the training for controls engineers. In the past, the ability to design and build the specialized circuitry for analog electronic controls caused many controls engineers to have an Electrical Engineering background. Now, with easily programmable digital computers being readily available, the background of controls engineers tends more toward the specialties that are most familiar with the systems being controlled.

## SUMMARY

- The simplest and most expedient digital control design technique is to transform a continuous controller design to its discrete form—that is, to use its **discrete equivalent**.
- **Design using discrete equivalents** entails (a) finding the continuous compensation  $D_c(s)$  using the ideas in Chapters 1 to 7, and (b) approximating  $D_c(s)$  with difference equations using a discretization methods such as Tustin's method, the ZOH method, or the matched-pole–zero method.
- In order to analyze a discrete controller design, or any discrete system, the  **$z$ -transform** is used to determine the system's behavior. The  $z$ -transform of a time sequence  $f(k)$  is given by

$$\mathcal{Z}\{f(k)\} = F(z) = \sum_{k=0}^{\infty} f(k)z^{-k},$$

and has the key property that

$$\mathcal{Z}\{f(k-1)\} = z^{-1}F(z).$$

This property allows us to find the discrete transfer function of a **difference equation**, which is the digital equivalent of a differential equation for continuous systems. Analysis using  $z$ -transforms closely parallels that using Laplace transforms.

- Normally  $z$ -transforms are found using the computer (Matlab) or using the look-up Table 8.1.
- The discrete Final Value Theorem is

$$\lim_{k \rightarrow \infty} x(k) = \lim_{z \rightarrow 1} (1 - z^{-1}) X(z),$$

provided that all poles of  $(1 - z^{-1}) X(z)$  are inside the unit circle.

- For a continuous signal  $f(t)$  whose samples are  $f(k)$ , the poles of  $F(s)$  are related to the poles of  $F(z)$  by

$$z = e^{sT}.$$

- The following are the most common discrete equivalents:

1. **Tustin's approximation:**

$$D_d(z) = D_c(s) \Big|_{s=\frac{2}{T}\left(\frac{z-1}{z+1}\right)}.$$

2. **The matched pole-zero (MPZ) approximation:**

- Map poles and zeros by  $z = e^{sT}$ .
- Add powers of  $(z + 1)$  to the numerator until numerator and denominator are of equal order or the numerator is one order less than the denominator.
- Set the low-frequency gain of  $D_d(z)$  equal to that of  $D_c(s)$ .
- If designing by discrete equivalents, a minimum **sample rate** of 20 times the bandwidth is recommended. Typically, even faster sampling is useful for best performance.
- Analog **prefilters** are commonly placed before the **sampler** in order to attenuate the effects of high-frequency measurement noise. A sampler **aliases** all frequencies in the signal that are greater than half the sample frequency to lower frequencies; therefore, prefilter break points should be selected so that no significant frequency content remains above half the sample rate.
- The discrete model of the continuous plant  $G(s)$  preceded by a **ZOH** is

$$G(z) = (1 - z^{-1}) \mathcal{Z} \left\{ \frac{G(s)}{s} \right\}.$$

The discrete plant model plus the discrete controller can be analyzed using the  **$z$ -transform** or simulated using Simulink.

- **Discrete design** is an exact design method and avoids the approximations inherent with discrete equivalents. The design procedure entails (a) finding the discrete model of the plant  $G(s)$ , and (b) using the discrete model to design the compensation directly in its discrete form. The design process is more cumbersome than discrete equivalent design, and requires that a sample rate be selected before

commencing the design. A practical approach is to commence the design using discrete equivalents, then tune up the result using discrete design.

- Discrete design using  $G(z)$  closely parallels continuous design, but the stability boundary and interpretation of  $z$ -plane root locations are different. Figure 8.5 summarizes the response characteristics.
- If using discrete design, system stability can theoretically be assured when **sampling** at a rate as slow as twice the bandwidth. However, for good transient performance and (random) disturbance rejection, best results are obtained by sampling at 10 times the closed-loop bandwidth or faster. In some cases, for example with troublesome vibrational modes, it is sometimes useful to sample more than twice as fast as the vibrational mode.

## REVIEW QUESTIONS

- 8.1** What is the Nyquist rate? What are its characteristics?
- 8.2** Describe the discrete equivalent design process.
- 8.3** Describe how to arrive at a  $D_d(z)$  if the sample rate is  $30 \times \omega_{BW}$ .
- 8.4** For a system with a 1 rad/sec bandwidth, describe the consequences of various sample rates.
- 8.5** Give two advantages for selecting a digital processor rather than analog circuitry to implement a controller.
- 8.6** Give two disadvantages for selecting a digital processor rather than analog circuitry to implement a controller.
- 8.7** Describe how to arrive at a  $D_d(z)$  if the sample rate is  $5 \times \omega_{BW}$ .

## PROBLEMS

### *Problems for Section 8.2: Dynamic Analysis of Discrete Systems*

- 8.1** The  $z$ -transform of a discrete-time filter  $h(k)$  at a 1.5 Hz sample rate is

$$H(z) = \frac{(1 + (1/5)z^{-1})}{[1 - (1/7)z^{-1}][1 + (1/2)z^{-1}]}.$$

- (a) Let  $u(k)$  and  $y(k)$  be the discrete input and output of this filter. Find a difference equation relating  $u(k)$  and  $y(k)$ .
  - (b) Find the natural frequency and damping coefficient of the filter's poles.
  - (c) Is the filter stable?
- 8.2** Use the  $z$ -transform to solve the difference equation

$$y(k) - 0.5y(k-1) - 7.5y(k-2) = 3u(k-1) + 7.5u(k-2),$$

where

$$u(k) = \begin{cases} k, & k \geq 0, \\ 0, & k < 0, \end{cases}$$

$$y(k) = 0, \quad k < 0.$$

- 8.3** The one-sided  $z$ -transform is defined as

$$F(z) = \sum_0^{\infty} f(k)z^{-k}.$$

- (a) Show that the one-sided transform of  $f(k + 1)$  is  $\mathcal{Z}\{f(k + 1)\} = zF(z) - zf(0)$ .
  - (b) Use the one-sided transform to solve for the transforms of the Fibonacci numbers generated by the difference equation  $u(k + 2) = u(k + 1) + u(k)$ . Let  $u(0) = u(1) = 1$ . [Hint: You will need to find a general expression for the transform of  $f(k + 2)$  in terms of the transform of  $f(k)$ .]
  - (c) Compute the pole locations of the transform of the Fibonacci numbers.
  - (d) Compute the inverse transform of the Fibonacci numbers.
  - (e) Show that, if  $u(k)$  represents the  $k$ th Fibonacci number, then the ratio  $u(k + 1)/u(k)$  will approach  $\left(\frac{1+\sqrt{5}}{2}\right)$ . This is the golden ratio valued so highly by the Greeks.
- 8.4** Prove the seven properties of the  $s$ -plane-to- $z$ -plane mapping listed in Section 8.2.3.

### Problems for Section 8.3: Design Using Discrete Equivalents

- 8.5** A unity feedback system has an open-loop transfer function given by

$$G(s) = \frac{178}{s[s + 17]}.$$

The following lag compensator added in series with the plant yields a phase margin of  $50^\circ$  and a crossover frequency of 30.6 rad/sec:

$$D_c(s) = 4.141 \frac{(0.0475s + 1)}{0.02246s + 1}.$$

Using the matched pole-zero approximation, determine an equivalent digital realization of this compensator for a sample rate of 40 Hz.

- 8.6** The following transfer function is a lead network designed to add about  $33.7^\circ$  of phase at  $\omega_1 = 2.47$  rad/sec:

$$H(s) = \frac{0.7s + 1}{0.2s + 1}.$$

- (a) Assume a sampling period of  $T = 2/3$  sec, and compute and plot in the  $z$ -plane the pole and zero locations of the digital implementations of  $H(s)$  obtained using (1) Tustin's method and (2) pole-zero mapping. For each case, compute the amount of phase lead provided by the network at  $z_1 = e^{j\omega_1 T}$ .

- (b) Using a log–log scale for the frequency range  $\omega = 0.5$  to  $\omega = 100$  rad/sec, plot the magnitude Bode plots for each of the equivalent digital systems you found in part (a), and compare with  $H(s)$ . (*Hint:* Magnitude Bode plots are given by  $H(z) = |H(e^{j\omega T})|$ .)
- 8.7** The following transfer function is a lag network designed to introduce a gain attenuation of  $2(-6$  dB) at  $\omega_1 = 0.025$  rad/sec:

$$H(s) = \frac{20s + 1}{80s + 1}.$$

- (a) Assume a sampling period of  $T = 0.5$  sec, and compute the plot in the  $s$ -plane the pole and zero locations of the digital implementations  $H(s)$  obtained using (1) Tustin's method and (2) pole–zero mapping. For each case, compute the amount of gain attenuation provided by the network at  $z_1 = e^{j\omega_1 T}$ .
- (b) For each of the equivalent digital system in part (a), plot the Bode magnitude curves over the frequency range  $\omega = 0.001$  to  $1$  rad/sec.

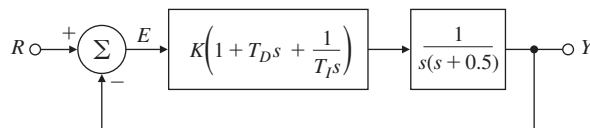
### Problem for Section 8.5: Sample Rate Selection

- 8.8** For the system shown in Fig. 8.22, find values for  $K$ ,  $T_D$ , and  $T_I$  so the closed-loop poles satisfy  $\zeta > 0.7$  and  $\omega_n > 0.5$  rad/sec. Discretize the PID controller using

- (a) Tustin's method  
 (b) The matched pole–zero method

Use MATLAB to simulate the step response of each of these digital implementations for sample times of  $T = 0.5$ ,  $0.05$ , and  $0.005$  sec.

**Figure 8.22**  
 Control system for  
 Problem 8.8



### △ Problems for Section 8.6: Discrete Design

- 8.9** Consider the system configuration shown in Fig. 8.23, where

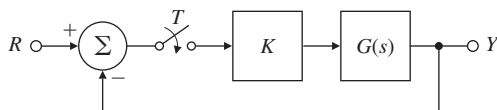
$$G(s) = \frac{60(0.5s + 3)}{(s - 0.1)(s^2 + 5s + 12)(s + 5)}.$$

- (a) Find the transfer function  $G(z)$  for  $T = 0.5$  assuming the system is preceded by a ZOH.  
 (b) Use MATLAB to draw the root locus of the discrete system with respect to  $K$ .  
 (c) What is the range of  $K$  for which the closed-loop discrete system is stable?  
 (d) Compare your results of part (c) to the case where an analog controller is used (that is, where the sampling switch is always closed).

- (e) Use MATLAB to find the  $K$  value to yield a damping factor of  $\zeta = 0.6$  for both the continuous and discrete systems. Plot the step response of both cases.

**Figure 8.23**

Control system for Problem 8.9



- 8.10 Single-axis Satellite Attitude Control:** Satellites often require attitude control for proper orientation of antennas and sensors with respect to Earth. Figure 2.7 shows a communication satellite with a three-axis attitude-control system. To gain insight into the three-axis problem, we often consider one axis at a time. Figure 8.24 depicts this case, where motion is only allowed about an axis perpendicular to the page. The equations of motion of the system are given by

$$I\ddot{\theta} = M_C + M_D,$$

where

$I$  = motion of inertia of the satellite about its mass center,

$M_C$  = control torque applied by the thrusters,

$M_D$  = disturbance torques,

$\theta$  = angle of the satellite axis with respect to an inertial reference with no angular acceleration.

We normalize the equations of motion by defining

$$u = \frac{M_C}{I}, \quad w_d = \frac{M_D}{I},$$

and obtain

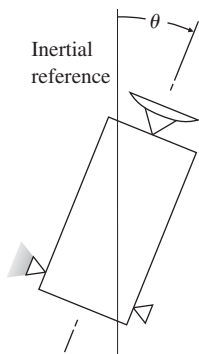
$$\ddot{\theta} = u + w_d.$$

Taking the Laplace transform yields

$$\theta(s) = \frac{1}{s^2}[u(s) + w_d(s)],$$

**Figure 8.24**

Satellite control schematic for Problem 8.10



which with no disturbance becomes

$$\frac{\theta(s)}{u(s)} = \frac{1}{s^2} = G_1(s).$$

In the discrete case where  $u$  is applied through a ZOH, we can use the methods described in this chapter to obtain the discrete transfer function

$$G_1(z) = \frac{\theta(z)}{u(z)} = \frac{T^2}{2} \left[ \frac{z+1}{(z-1)^2} \right].$$

- (a) Sketch the root locus of this system by hand assuming proportional control.
  - (b) Draw the root locus using MATLAB to verify the hand sketch.
  - (c) Add a discrete controller to the position feedback so that the dominant poles correspond to  $\zeta = 0.57$  and  $\omega_n = \frac{2.5\pi}{10T}$ .
  - (d) What is the controller gain if  $T = 0.5$  sec? If  $T = 1$  sec.
  - (e) Plot the closed-loop step response and the associated control time history for  $T = 1$  sec.
- 8.11** It is possible to suspend a mass of magnetic material by means of an electromagnet whose current is controlled by the position of the mass (Woodson and Melcher, 1968). The schematic of a possible setup is illustrated in Fig. 8.25, and a photo of a working system at Stanford University is shown in Fig. 9.1. The equations of motion are

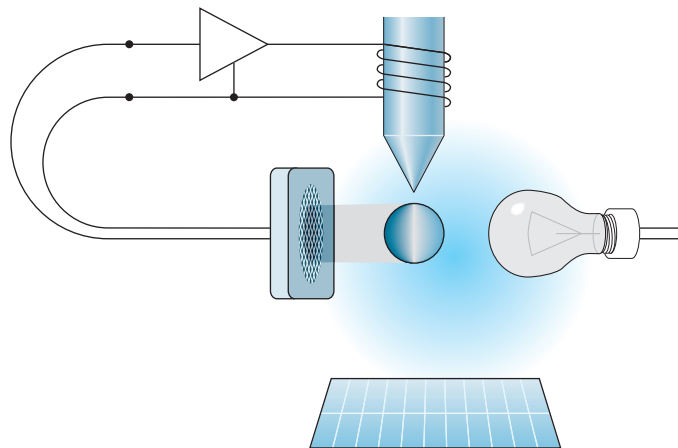
$$m\ddot{x} = -mg + f(x, I),$$

where the force on the ball due to the electromagnet is given by  $f(x, I)$ . At equilibrium, the magnet force balances the gravity force. Suppose we let  $I_0$  represent the current at equilibrium. If we write  $I = I_0 + i$ , where  $i$  represents a deviation from the nominal current,  $I_0$ , expand  $f$  about  $x = 0$  and  $I = I_0$ , and neglect higher-order terms, we obtain the linearized equation

$$m\ddot{x} = k_1x + k_2i. \quad (8.54)$$

**Figure 8.25**

Schematic of magnetic levitation device for Problem 8.11



Reasonable values for the constants in Eq. (8.54) are  $m = 0.02$  kg,  $k_1 = 20$  N/m, and  $k_2 = 0.4$  N/A.

- (a) Compute the transfer function from  $I$  to  $x$ , and draw the (continuous) root locus for the simple feedback  $i = -Kx$ .
- (b) Assume the input is passed through a ZOH, and let the sampling period be 0.02 sec. Compute the transfer function of the equivalent discrete-time plant.
- (c) Design a digital control for the magnetic levitation device so the closed-loop system meets the following specifications:  $t_r \leq 0.1$  sec,  $t_s \leq 0.4$  sec, and overshoot  $\leq 20\%$ .
- (d) Plot a root locus with respect to  $k_1$  for your design, and discuss the possibility of using your closed-loop system to balance balls of various masses.
- (e) Plot the step response of your design to an initial disturbance displacement on the ball, and show both  $x$  and the control current  $i$ . If the sensor can measure  $x$  only over a range of  $\pm 1/4$  cm and the amplifier can provide a current of only 1 A, what is the *maximum* displacement possible for control, neglecting the nonlinear terms in  $f(x, I)$ ?

**8.12** Repeat Problem 5.26 in Chapter 5 by constructing discrete root loci and performing the designs directly in the  $z$ -plane. Assume the output  $y$  is sampled, the input  $u$  is passed through a ZOH as it enters the plant, and the sample rate is 15 Hz.

**8.13** Design a digital controller for the antenna servo system shown in Figs. 3.60 and 3.61 and described in Problem 3.35. The design should provide a step response with an overshoot of less than 8% and a rise time of less than 95 sec.

- (a) What should the sample rate be?
- (b) Use the matched pole-zero discrete equivalent method.
- (c) Use discrete design and the  $z$ -plane root locus.

**8.14** The system

$$G(s) = \frac{100}{(13s + 1)(0.7s + 1)}$$

is to be controlled with a digital controller having a sampling period of  $T = 0.4$  sec. Using a  $z$ -plane root locus, design compensation that will respond to a step with a rise time  $t_r \leq 2.24$  sec and an overshoot  $M_p \leq 6.5\%$ . What can be done to reduce the steady-state error?

**8.15** The discrete transfer function for pure derivative control is

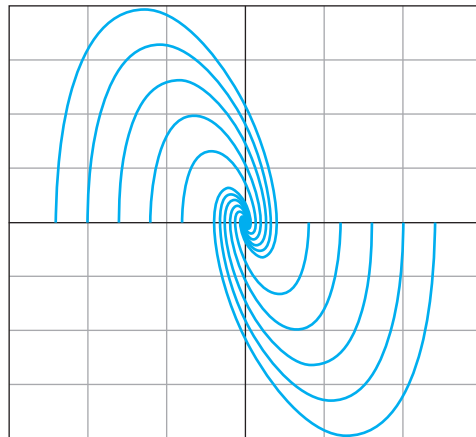
$$D_d(z) = KT_D \frac{z - 1}{Tz},$$

where the pole at  $z = 0$  adds some destabilizing phase lag. Can this phase lag be removed by using derivative control of the form

$$D_d(z) = KT_D \frac{(z - 1)}{T}?$$

Support your answer with the difference equation that would be required and discuss the requirements to implement it.

# Nonlinear Systems



## A Perspective on Nonlinear Systems

All systems are nonlinear, especially if large signals are considered. On the other hand, almost all physical systems can be well approximated by linear models if the signals are small. For example, if  $\theta$  is small, then  $\sin(\theta) \approx \theta$  and  $\cos(\theta) \approx 1$ . Similarly, in analog electronic devices such as amplifiers, the operation will be nearly linear if the signals are small with respect to the supply voltage. Finally, as we will consider later in this chapter in an optional section, Lyapunov showed that if the linear approximation of a system is stable near an equilibrium point, then the truly nonlinear system will be stable for some neighborhood of the equilibrium point. For all these reasons, the analysis and design methods presented thus far in this book have considered only the enormously powerful techniques available for linear models. However, if the signals cause a device to saturate or if the system includes nonlinearities that are active for small signals, such as certain kinds of friction, then the nonlinear effects must be taken into account to explain the behavior of the system. In this chapter, a few of the tools available for this purpose will be described.

## Chapter Overview

Because every nonlinear system is in many ways unique, a vast number of approaches are used in nonlinear control design. The approaches to analysis and design of nonlinear systems that we will describe may be classified under four categories. In Section 9.2, methods of reducing the problem to a linear model will be discussed. In most cases, considering the small signal approximation is adequate. In some cases there are nonlinearities for which an inverse can be found, and placing the inverse before the physical nonlinearity results in an overall system that responds linearly. In yet other cases, some nonlinear models can be reduced to an exact linear form by the clever use of feedback, in a technique called “computed torque” in the field of robotics.

The second category is a heuristic approach based on considering the nonlinearity to be a varying gain. In Section 9.3, cases will be considered for which the nonlinearity has no memory as, for example, with an amplifier whose output saturates when the signal gets large. The idea is to consider the amplifier as if its gain begins to be reduced as the signal gets large. Because the root locus is based on evaluating the system characteristic roots as gain changes, this point of view leads to a heuristic use of the root locus to predict how such a system will respond to changing input signal sizes. Section 9.4 treats cases in which the nonlinearity has dynamics or memory; then the root locus is not useful. For these cases, a technique introduced by Kochenburger in 1950 known as the describing function can be used. To apply this method, a sinusoid is applied to the nonlinear part of the system and the first harmonic of the periodic response is computed. The ratio of the input to the output is taken as if it were a linear but variable frequency response. Thus the Nyquist plot is the natural domain in which to consider the system behavior.

While the heuristic approaches may give very useful insight into the system’s behavior, they cannot be used to decide if the system is guaranteed to be stable. For this, one must turn to the analysis of stability as studied in control theory. The most famous of these theories is that of internal stability developed by Lyapunov. As an introduction to the idea of a system response as a trajectory in space, Section 9.5 describes analysis in the phase plane then presents the stability theory. Examples are given of using the stability theorem to guide design of a controller so the system is guaranteed to be stable if the initial assumptions about the system hold. With these methods, the control engineer is given a start on the path to the effective understanding and design of real control problems. Finally, Section 9.6 provides a historical perspective for the material in this chapter.

## 9.1 Introduction and Motivation: Why Study Nonlinear Systems?

It is intuitively clear that at some level of signal strength any physical system will be nonlinear, and that some systems are nonlinear at any and all signal levels. On the other hand, we began our study by developing linear approximate models, and all our design methods thus far have been based on the assumption that the plant can be represented by a linear transfer function. In this chapter, we shall give some of the reasons for believing that all the time spent studying linear techniques was not a waste of time, but we shall also try to explain why it is very important to understand how to take nonlinear effects into account in control system design.

We begin by showing that we can combine the root-locus technique, which plots roots of the characteristic equation as a function of various gain values, with the observation that many nonlinear elements can be viewed as a gain that changes as signal level changes. While the method is, at this point, entirely heuristic, the simulation results are very promising. Many properties of systems containing such zero-memory nonlinear elements can be predicted by plotting a root locus versus gain at the point of the nonlinearity. However, the method, as presented, is not on a firm foundation, and the designer is left to wonder if there is some unexplored region of the real state space or the signal spaces where catastrophe awaits. After all, the model is an approximation, and no matter how extensive the simulation, it is not possible to cover every situation.

Following the use of the root locus, we turn to methods based on the frequency response. One of the great advantages of the frequency response is that, in many cases, one can obtain the transfer function experimentally on the real system. In the most basic approach, a sinusoidal signal is applied to the system and the amplitude and phase of the output sinusoid are measured. However, noise and inevitable nonlinear effects cause the output to be more complicated than a simple sinusoid, so the designer extracts the fundamental component and treats it as if it is the whole story. One gets the same result if a spectrum analyzer is used to compute a transfer function. The approach computes what Kochenburger called the **describing function**. From this point of view, a describing function can be defined for nonlinear elements, including those with memory. Again, simulations are promising and many useful designs are done with this technique but, as with the use of root locus to design nonlinear systems, this method is also on shaky ground.<sup>1</sup>

So what is to be made of this situation? The only possibility is to face up to the facts and take on nonlinear behavior directly. Fortunately, a firm foundation in mathematics was established when A. M. Lyapunov published his work on the stability of motion in 1892.

---

<sup>1</sup> And as we live in California, we know how dangerous it is to be on shaky ground.

This work was translated into French in 1907 and recovered in a control context by Kalman and Bertram in 1960. Lyapunov gave two methods for the study of stability. For his first method, he considered stability based on the linear approximation, the very thing required to justify our concentration on that approach in this book. He proved the remarkable result that if the linear approximation is strictly stable, having all roots in the left half-plane (LHP), then the nonlinear system will have a region of stability around the equilibrium point where the linear approximation applies. Furthermore, he proved that if the linear approximation has at least one root in the right half-plane (RHP), then the nonlinear system cannot have any region of stability in the neighborhood of the equilibrium. The size of the stable region in the state space is not given by the linear terms, but is included in the construction used for the proof. That construction constituted his second method. Lyapunov's second method is based on the mathematical equivalent of finding a scalar function that describes the internal energy stored in the system. He proved that if such a function is constructed, and if the derivative of the function is negative on trajectories of the dynamic equations of the system, then the function and the state on which it depends will eventually drain away and the state will come to rest at the equilibrium point. A function having these properties is called a *Lyapunov function*. Of course, this simple description omits a great deal of complexity; for example, there are dozens of definitions of stability. However, the concept remains that if a Lyapunov function can be found, then the system on which it is based will be stable. As described, the theory gives a sufficient condition for stability. If a Lyapunov function is not found, the designer does not know if one does not exist, or if the search has just been inadequate. A great deal of research has been directed toward finding Lyapunov functions for particular classes of nonlinear systems.

Lyapunov's methods are based on differential equations in normal or state form and are thus concerned with internal stability. Frequency-response methods, on the other hand, are external measures, and there has been interest in developing stability results based on the external response of the system. One such method is the circle criterion, which we will describe in this chapter. The method can be described as considering the energy seen at the terminal of the system and noting if it is always flowing *into* the terminals. If so, it is reasonable to assume that eventually all energy will be gone and the system will be stable. For a formal proof of the method, researchers have turned to Lyapunov's second method, but the result is expressed in terms of external properties, such as the Nyquist plot of the linear portion of the system that faces the nonlinear elements. Again, this tool gives a basis for setting a firm foundation under a method of design for a particular class of nonlinear systems.

As should be clear at this point, the theory of nonlinear control is a vast and sophisticated topic, and in this text we can give only a brief introduction to a small part of it. However, the foundation of control

design rests on this theory, and the more the designer understands of the theory, the better he or she understands both the limits and the opportunities of problems. It is our hope that by considering this material, students will be stimulated to further their profitable study of this fascinating topic.

## 9.2 Analysis by Linearization

Three methods of reducing some nonlinear systems to a suitable linear model are presented in this section. The differential equations of motion for almost all processes selected for control are nonlinear. On the other hand, both analysis and control design methods we have discussed so far are much easier for linear than for nonlinear models. **Linearization** is the process of finding a linear model that approximates a nonlinear one. Fortunately, as Lyapunov proved over 100 years ago, if a small-signal linear model is valid near an equilibrium and is stable, then there is a region (which may be small, of course) containing the equilibrium within which the nonlinear system is stable. So we can safely make a linear model and design a linear control for it such that, at least in the neighborhood of the equilibrium, our design will be stable. Since a very important role of feedback control is to maintain the process variables near equilibrium, such small-signal linear models are a frequent starting point for control design.

An alternative approach to obtain a linear model for use as the basis of control system design is to use part of the control effort to cancel the nonlinear terms and to design the remainder of the control based on linear theory. This approach—linearization by feedback—is popular in the field of robotics, where it is called the **method of computed torque**. It is also a research topic for control of aircraft. Section 9.2.2 takes a brief look at this method. Finally, some nonlinear functions are such that an **inverse nonlinearity** can be found to be placed in series with the nonlinearity so that the combination is linear. This method is often used to correct mild nonlinear characteristics of sensors or actuators that have small variations in use, as will be discussed in Section 9.2.3.

### 9.2.1 Linearization by Small-Signal Analysis

For a system with smooth nonlinearities and a continuous derivative, one can compute a linear model that is valid for small signals. In many cases, these models can be used for design. A nonlinear differential equation is an equation for which the derivatives of the state have a nonlinear relationship to the state itself and/or the control. In other words, the differential equations *cannot* be written in the form<sup>2</sup>

$$\dot{\mathbf{x}} = \mathbf{A}\mathbf{x} + \mathbf{B}u,$$

---

<sup>2</sup>This equation assumes the system is time invariant. A more general expression would be  $\dot{\mathbf{x}} = \mathbf{f}(\mathbf{x}, u, t)$ .

but must be left in the form

$$\dot{\mathbf{x}} = \mathbf{f}(\mathbf{x}, u). \quad (9.1)$$

For small-signal linearization, we first determine equilibrium values of  $\mathbf{x}_o$ ,  $u_o$ , such that  $\dot{\mathbf{x}}_o = \mathbf{0} = \mathbf{f}(\mathbf{x}_o, u_o)$ , and we let  $\mathbf{x} = \mathbf{x}_o + \delta\mathbf{x}$  and  $u = u_o + \delta u$ . We then expand the nonlinear equation in terms of the perturbations from these equilibrium values, which yields

$$\dot{\mathbf{x}}_o + \delta\dot{\mathbf{x}} \cong \mathbf{f}(\mathbf{x}_o, u_o) + \mathbf{A}\delta\mathbf{x} + \mathbf{B}\delta u,$$

where  $\mathbf{A}$  and  $\mathbf{B}$  are the best linear fits to the nonlinear function  $\mathbf{f}(\mathbf{x}, u)$  at  $\mathbf{x}_o$  and  $u_o$ , computed as

$$\mathbf{A} = \left[ \frac{\partial \mathbf{f}}{\partial \mathbf{x}} \right]_{x_o, u_o} \quad \text{and} \quad \mathbf{B} = \left[ \frac{\partial \mathbf{f}}{\partial u} \right]_{x_o, u_o}. \quad (9.2)$$

Subtracting out the equilibrium solution, this reduces to

$$\delta\dot{\mathbf{x}} = \mathbf{A}\delta\mathbf{x} + \mathbf{B}\delta u, \quad (9.3)$$

which is a linear differential equation approximating the dynamics of the state *about* the equilibrium point. Normally, the  $\delta$  notation is dropped and it is understood that  $\mathbf{x}$  and  $u$  refer to the deviation from the equilibrium.

In developing the models discussed thus far in this book, we have encountered nonlinear equations on several occasions: the pendulum in Example 2.6, the hanging crane in Example 2.8, the AC induction motor in Section 2.2, the tank flow in Example 2.19, and the hydraulic actuator in Example 2.20. In each case, we assumed either that the motion was small or that motion from some operating point was small, so nonlinear functions were approximated by linear functions. The steps followed in those examples essentially involved finding  $\mathbf{A}$  and  $\mathbf{B}$  in order to linearize the differential equations to the form of Eq. (9.3), as illustrated in the next several examples. The linearization functions in Matlab include `linmod` and `linmod2`.

## EXAMPLE 9.1

### *Linearization of Nonlinear Pendulum*

Consider the nonlinear equations of motion of the simple pendulum in Example 2.5. Derive the equilibrium points for the system and determine the corresponding small-signal linear models.

**Solution.** The equation of motion is

$$\ddot{\theta} + \frac{g}{\ell} \sin \theta = \frac{T_c}{m\ell^2}. \quad (9.4)$$

We can rewrite the equation of motion in state-variable form, with  $\mathbf{x} = [x_1 \ x_2]^T = [\theta \ \dot{\theta}]^T$ , as

$$\dot{\mathbf{x}} = \begin{bmatrix} x_2 \\ -\omega_o^2 \sin x_1 + u \end{bmatrix} = \begin{bmatrix} f_1(\mathbf{x}, u) \\ f_2(\mathbf{x}, u) \end{bmatrix} = \mathbf{f}(\mathbf{x}, u),$$

where  $\omega_o = \sqrt{\frac{g}{\ell}}$  and  $u = \frac{T_c}{m\ell^2}$ . To determine the equilibrium state, suppose the (normalized) input torque has a nominal value of  $u_o = 0$ . Then

$$\begin{aligned}\dot{x}_1 &= \dot{\theta} = 0, \\ \dot{x}_2 &= \ddot{\theta} = -\frac{g}{\ell} \sin \theta = 0,\end{aligned}$$

so the equilibrium conditions correspond to  $\theta_o = 0, \pi$  (that is, the downward and the inverted pendulum at rest configurations, respectively). The equilibrium state and the input are  $\mathbf{x}_o = [\theta_o \ 0]^T$ ,  $u_o = 0$ , and the state-space matrices are given by

$$\begin{aligned}\mathbf{A} &= \left[ \begin{array}{cc} \frac{\partial f_1}{\partial x_1} & \frac{\partial f_1}{\partial x_2} \\ \frac{\partial f_2}{\partial x_1} & \frac{\partial f_2}{\partial x_2} \end{array} \right]_{x_o, u_o} = \left[ \begin{array}{cc} 0 & 1 \\ -\omega_o^2 \cos \theta_o & 0 \end{array} \right], \\ \mathbf{B} &= \left[ \begin{array}{c} \frac{\partial f_1}{\partial u} \\ \frac{\partial f_2}{\partial u} \end{array} \right]_{x_o, u_o} = \left[ \begin{array}{c} 0 \\ 1 \end{array} \right].\end{aligned}$$

The linear system has eigenvalues of  $\pm j\omega_o$  and  $\pm\omega_o$  corresponding to  $\theta_o = 0$  and  $\pi$ , respectively, with the latter inverted case being unstable as expected.

## EXAMPLE 9.2

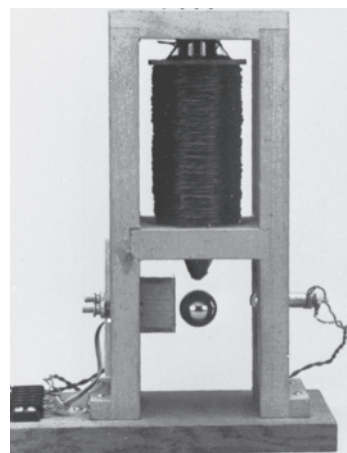
### *Linearization of Motion in a Ball Levitator*

A simplified version of a magnetic bearing that can be built in a laboratory is shown in Fig. 9.1, where one electromagnet is used to levitate

**Figure 9.1**

Magnetic ball levitator used in the laboratory

*Source: Photo courtesy of Gene Franklin*



a metal ball. The physical arrangement of the levitator is depicted in Fig. 9.2. The equation of motion of the ball, derived from Newton's law, Eq. (2.1), is

$$m\ddot{x} = f_m(x, i) - mg, \quad (9.5)$$

where the force  $f_m(x, i)$  is caused by the field of the electromagnet. Theoretically, the force from an electromagnet falls off with an inverse square relationship to the distance from the magnet, but the exact relationship for the laboratory levitator is difficult to derive from physical principles because its magnetic field is so complex. However, the forces can be measured with a scale. Figure 9.3 shows the experimental curves for a ball with a 1-cm diameter and a mass of  $8.4 \times 10^{-3}$  kg. For the current of  $i_2 = 600$  mA and the displacement  $x_1$  shown in the figure, the magnetic force  $f_m$  just cancels the gravity force,  $mg = 82 \times 10^{-3}$  N. (The mass of the ball is  $8.4 \times 10^{-3}$  kg, and the acceleration of gravity is  $9.8 \text{ m/sec}^2$ .) Therefore, the point  $(x_1, i_2)$  represents an equilibrium. Using the data, find the linearized equations of motion about the equilibrium point.

**Figure 9.2**

Model for ball levitation

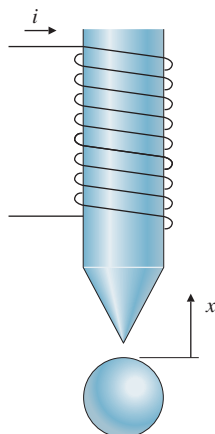
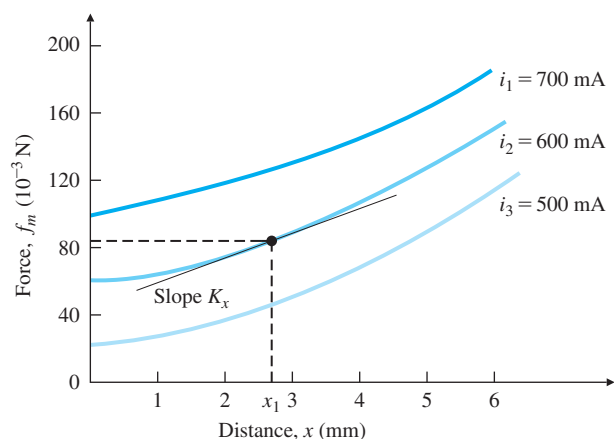


**Figure 9.3**

Experimentally determined force curves



**Solution.** First we write, in expanded form, the force in terms of deviations from the equilibrium values  $x_1$  and  $i_2$ :

$$f_m(x_1 + \delta x, i_2 + \delta i) \cong f_m(x_1, i_2) + K_x \delta x + K_i \delta i. \quad (9.6)$$

The linear gains are found as follows:  $K_x$  is the slope of the force versus  $x$  along the curve  $i = i_2$ , as shown in Fig. 9.3, and is found to be about 14 N/m.  $K_i$  is the change of force with current for the value of fixed  $x = x_1$ . We find that for  $i = i_1 = 700$  mA at  $x = x_1$ , the force is about  $122 \times 10^{-3}$  N, and at  $i = i_3 = 500$  mA at  $x = x_1$ , it is about  $42 \times 10^{-3}$  N. Thus

$$\begin{aligned} K_i &\cong \frac{122 \times 10^{-3} - 42 \times 10^{-3}}{700 - 500} = \frac{80 \times 10^{-3} \text{ N}}{200 \text{ mA}} \\ &\cong 400 \times 10^{-3} \text{ N/A} \\ &\cong 0.4 \text{ N/A}. \end{aligned}$$

Substituting these values into Eq. (9.6) leads to the following linear approximation for the force in the neighborhood of equilibrium:

$$f_m \cong 82 \times 10^{-3} + 14\delta x + 0.4\delta i.$$

Substituting this expression into Eq. (9.5) and using the numerical values for mass and gravity force, we get for the linearized model

$$(8.4 \times 10^{-3})\ddot{x} = 82 \times 10^{-3} + 14\delta x + 0.4\delta i - 82 \times 10^{-3}.$$

Because  $x = x_1 + \delta x$ , then  $\ddot{x} = \delta\ddot{x}$ . The equation in terms of  $\delta x$  is thus

$$\begin{aligned} (8.4 \times 10^{-3})\delta\ddot{x} &= 14\delta x + 0.4\delta i, \\ \delta\ddot{x} &= 1667\delta x + 47.6\delta i, \end{aligned} \quad (9.7)$$

which is the desired linearized equation of motion about the equilibrium point. A logical state vector is  $\mathbf{x} = [\delta x \ \delta\dot{x}]^T$ , which leads to the standard matrices

$$\mathbf{A} = \begin{bmatrix} 0 & 1 \\ 1667 & 0 \end{bmatrix} \quad \text{and} \quad \mathbf{B} = \begin{bmatrix} 0 \\ 47.6 \end{bmatrix},$$

and the control  $u = \delta i$ .

A real-world example of this technology is the Shanghai Maglev Train (SMT) in Figure 9.4 that was built in 2004. It travels at 431 Km/hour, but the high cost of building the required precision track has, to date, kept any extensions from being built.

## EXAMPLE 9.3

### Linearization of the Water Tank Revisited

Repeat the linearization of Example 2.19 using the concepts presented in this section.

**Solution.** Equation (2.94) may be written as

$$\dot{x} = f(x, u), \quad (9.8)$$

**Figure 9.4**

Shanghai Maglev Train



where  $x \triangleq h$ ,  $u \triangleq w_{in}$ , and  $f(x, u) = -\frac{1}{RA\rho}\sqrt{p_1 - p_a} + \frac{1}{A\rho}w_{in} = -\frac{1}{RA\rho}\sqrt{\rho gh - p_a} + \frac{1}{A\rho}w_{in}$ . The linearized equations are of the form

$$\delta\dot{x} = A\delta x + B\delta u, \quad (9.9)$$

where

$$[A]_{x_o, u_o} = \frac{\partial f}{\partial x} = \left[ \frac{\partial f}{\partial h} \right]_{h_o, u_o} = \frac{\partial}{\partial h} \left[ -\frac{1}{RA\rho}\sqrt{\rho gh - p_a} \right]_{h_o, u_o} \quad (9.10)$$

$$= -\frac{g}{2AR} \frac{1}{\sqrt{\rho gh_o - p_a}} = -\frac{g}{2AR} \frac{1}{\sqrt{p_o - p_a}}, \quad (9.11)$$

and

$$[B]_{x_o, u_o} = \frac{\partial f}{\partial u} = \frac{\partial f}{\partial w_{in}} = \frac{1}{A\rho}. \quad (9.12)$$

However, note some flow is required to maintain the system in equilibrium so that Eq. (9.9) is valid; specifically, we see from Eq. (2.94) that

$$u_o = w_{in_o} = \frac{1}{R}\sqrt{p_o - p_a} \quad \text{for } \dot{h} = 0, \quad (9.13)$$

and the  $\delta u$  in Eq. (9.9) is  $\delta w_{in}$ , where  $w_{in} = w_{in_o} + \delta w_{in}$ . Therefore, Eq. (9.9) becomes

$$\delta\dot{h} = A\delta h + B\delta w_{in} = A\delta h + Bw_{in} - B\frac{1}{R}\sqrt{p_o - p_a} \quad (9.14)$$

and matches Eq. (2.97) precisely.

### 9.2.2 Linearization by Nonlinear Feedback

#### Nonlinear feedback

Linearization by feedback is accomplished by subtracting the nonlinear terms out of the dynamic equations and adding them to the control. The result is a linear system, provided that the computer implementing the control has enough capability to compute the nonlinear terms fast

enough and the resulting control does not cause the actuator to saturate. A more detailed understanding of the method is best achieved through an example.

### EXAMPLE 9.4

#### *Linearization of the Nonlinear Pendulum*

Consider the equation of a simple pendulum developed in Example 2.6 [see Eq. (2.21)]. Linearize the system by using nonlinear feedback.

**Solution.** The equation of motion is

$$ml^2\ddot{\theta} + mgl \sin \theta = T_c. \quad (9.15)$$

If we compute the torque to be

$$T_c = mgl \sin \theta + u, \quad (9.16)$$

then the motion is described by

$$ml^2\ddot{\theta} = u. \quad (9.17)$$

Equation (9.17) is a linear equation *no matter how large the angle  $\theta$  becomes*. We use it as the model for purposes of control design because it enables us to use linear analysis techniques. The resulting linear control will provide the value of  $u$  based on measurements of  $\theta$ ; however, the value of the torque actually sent to the equipment would derive from Eq. (9.16). For robots with two or three rigid links, this **computed-torque** approach has led to effective control. It is also being researched for the control of aircraft, where the linear models change considerably in character with the flight regime.

### 9.2.3 Linearization by Inverse Nonlinearity

#### Inverse nonlinearity

The simplest case of the introduction of nonlinearities into a control design is that of **inverse nonlinearities**. It is sometimes possible to reverse the effect of some nonlinearities. For example, suppose we have a system whose output is the square of the signal of interest:

$$y = x^2. \quad (9.18)$$

One clever and rather obvious technique is to undo the nonlinearity by preceding the physical nonlinearity with a square root nonlinearity,

$$x = \sqrt{(.)}, \quad (9.19)$$

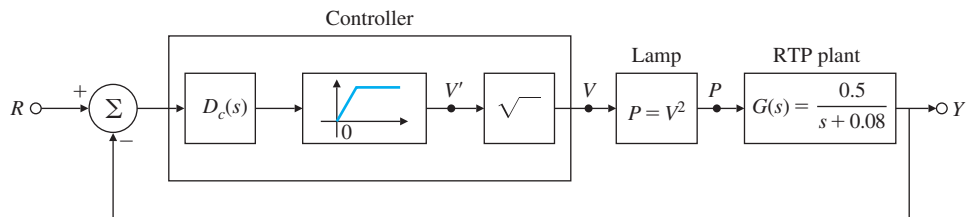
as shown in the next example. The overall cascaded system would then be linear.

### EXAMPLE 9.5

#### *Linearization of the Rapid Thermal Processing (RTP) System*

Consider the RTP system that uses a nonlinear lamp as an actuator, as shown in Fig. 9.5. Suppose the input to the lamp is voltage  $V$  and the output is power  $P$ , and they are related by

$$P = V^2.$$

**Figure 9.5**

Linearization through inverse nonlinearity

Design an inverse nonlinearity to linearize the system.

**Solution.** We simply precede the lamp input nonlinearity with a square root nonlinearity

$$V = \sqrt{V'}.$$

The overall open-loop cascaded system is now linear for any value of the voltage:

$$Y = G(s)P = G(s)V^2 = G(s)V'.$$

Thus we can use linear control design techniques for the dynamic compensator,  $D_c(s)$ . Note a nonlinear element has been inserted in front of the square root element to ensure that the input to this block remains nonnegative at all times. The controller is then implemented as shown in Fig. 9.5. For a detailed application of this method for control design, refer to the RTP case study in Section 10.6.

### 9.3 Equivalent Gain Analysis Using the Root Locus

As we have tried to make clear, every real control system is nonlinear, and the linear analysis and design methods we have described thus far use linear approximations to the real models. There is one important category of nonlinear systems for which linearization is not appropriate and for which some significant analysis (and design) can be done. This category comprises systems in which the nonlinearity has no dynamics and is well approximated as a gain that varies as the size of its input signal varies, so-called memoryless nonlinearities. Sketches of a few such nonlinear system elements and their common names are shown in Fig. 9.6.

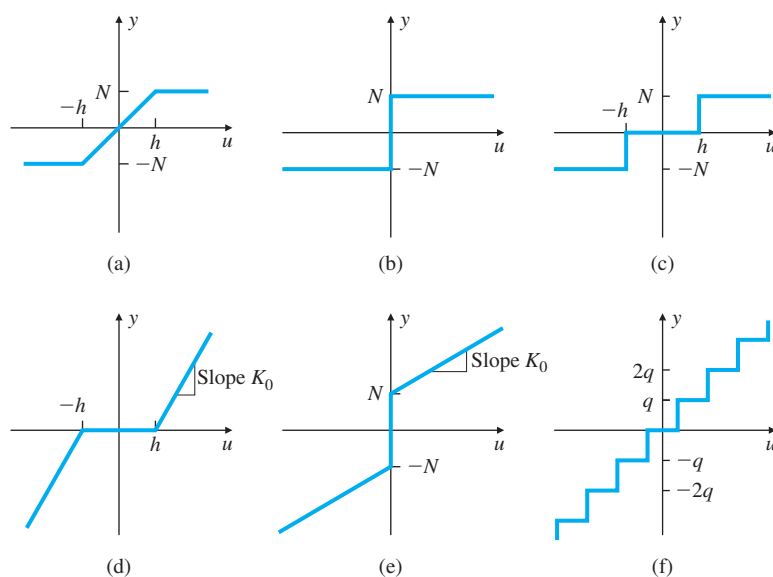
Memoryless nonlinearity

The stability of systems with memoryless nonlinearities can be studied heuristically using the root locus. The technique is to replace the memoryless nonlinearity by an equivalent gain  $K$ , and a root locus is plotted versus this gain. For a range of input signal amplitudes, the equivalent gain will take on a range of values, and the closed-loop roots of the system are examined in this range as if the gain were fixed. This is illustrated by the next several examples.

**Figure 9.6**

Nonlinear elements without dynamics:

- (a) saturation;
- (b) relay;
- (c) relay with dead zone;
- (d) gain with dead zone;
- (e) preloaded spring, or coulomb plus viscous friction;
- (f) quantization



### EXAMPLE 9.6

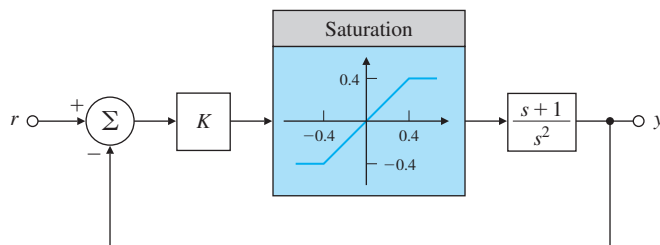
#### *Changing Overshoot and Saturation Nonlinearity*

Consider the system with saturation shown in Fig. 9.7. Determine the stability properties of the system using the root-locus technique.

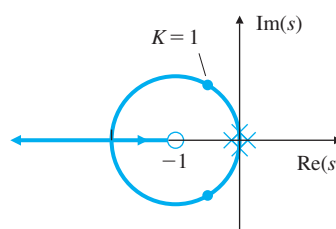
**Solution.** The root locus of this system versus  $K$  with the saturation removed is shown in Fig. 9.8. At  $K = 1$ , the damping ratio is  $\zeta = 0.5$ . As the gain is reduced, the locus shows that the roots move toward the origin of the  $s$ -plane with less and less damping. Plots of the step responses of this system were obtained using Simulink. A series of step inputs  $r$  with magnitudes  $r = 2, 4, 6, 8, 10$ , and 12 was introduced

**Figure 9.7**

Dynamic system with saturation

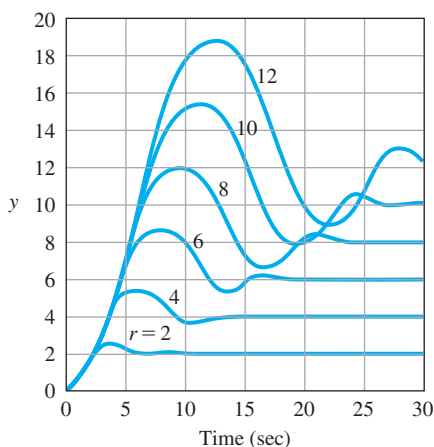
**Figure 9.8**

Root locus of  $(s + 1)/s^2$ , the system in Fig. 9.7 with the saturation removed

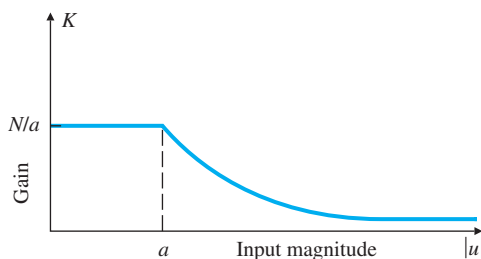


**Figure 9.9**

Step responses of system in Fig. 9.7 for various input step sizes

**Figure 9.10**

General shape of the effective gain of saturation



to the system, and the results are shown in Fig. 9.9. As long as the signal entering the saturation remains less than 0.4, the system will be linear and should behave according to the roots at  $\zeta = 0.5$ . However, notice that as the input gets larger, the response has more and more overshoot and slower and slower recovery. This can be explained by noting that larger and larger input signals correspond to smaller and smaller effective gain  $K$ , as seen in Fig. 9.10. From the root-locus plot of Fig. 9.8, we see as  $K$  decreases, the closed-loop poles move closer to the origin and have a smaller damping  $\zeta$ , which explains the longer rise and settling times, increased overshoot, and greater oscillatory response.

## EXAMPLE 9.7

A nonlinear example:  
stability depends on input  
magnitude

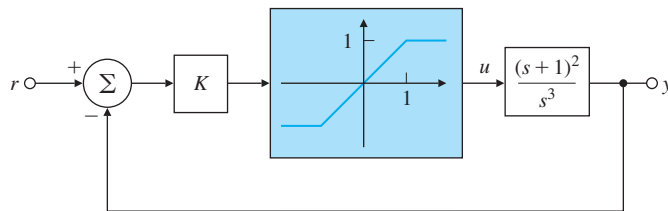
### *Stability of Conditionally Stable System Using the Root Locus*

As a second example of a nonlinear response described by signal-dependent gain, consider the system with a saturation nonlinearity as shown in Fig. 9.11. Determine whether the system is stable.

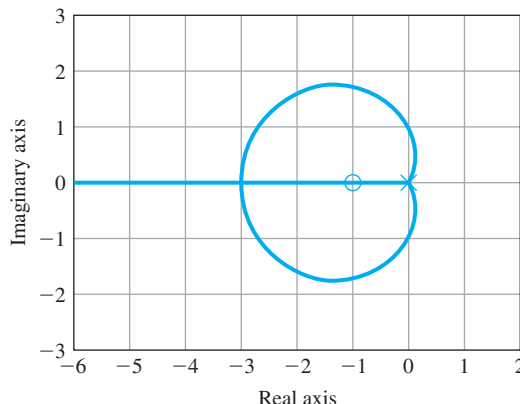
**Solution.** The root locus for the system, excluding the saturation, is plotted in Fig. 9.12. From this locus, we can readily calculate that the imaginary axis crossing occurs at  $\omega_0 = 1$  and  $K = \frac{1}{2}$ . Systems such as this, which are stable for (relatively) large gains but unstable for smaller

**Figure 9.11**

Block diagram of a conditionally stable system

**Figure 9.12**

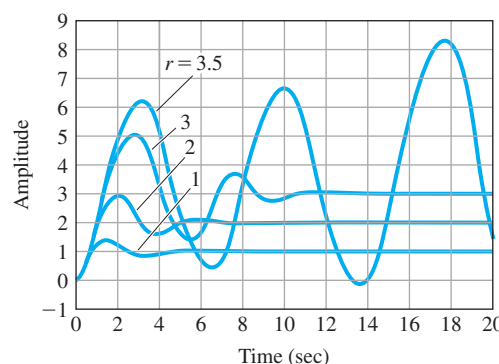
Root locus for  $G(s) = (s + 1)^2 / s^3$  from system in Fig. 9.11

**Conditional stability**

gains, are called **conditionally stable systems**. If  $K = 2$ , which corresponds to  $\zeta = 0.5$  on the locus, the system would be expected to show responses consistent with  $\zeta = 0.5$  for small reference input signals. However, as the reference input size gets larger, the equivalent gain would get smaller due to the saturation, and the system would be expected to become less well damped. Finally, the system would be expected to become unstable at some point for large inputs. Step responses from nonlinear simulation of the system with  $K = 2$  for input steps of size  $r = 1.0, 2.0, 3.0$ , and  $3.5$  are shown in Fig. 9.13. These responses confirm our predictions. Furthermore, the marginally stable case shows oscillations near 1 rad/sec, which is predicted by the frequency at the point at which the root locus crosses into the RHP.

**Figure 9.13**

Step responses of the system in Fig. 9.11



**EXAMPLE 9.8***Analysis and Design of System with Limit Cycle Using the Root Locus*

A nonlinear example: an oscillatory system with saturation

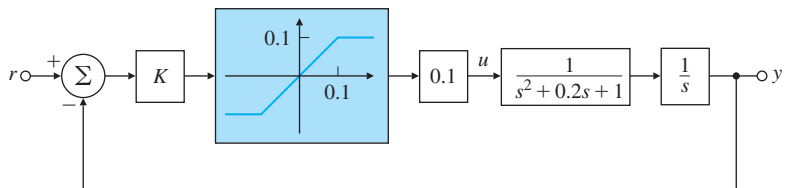
The final illustration of the use of the root locus to give a qualitative description of the response of a nonlinear system is based on the block diagram in Fig. 9.14. Determine whether the system is stable and find the amplitude and the frequency of the limit cycle. Modify the controller design to minimize the effect of limit-cycle oscillations.

**Solution.** This system is typical of electromechanical control problems in which the designer perhaps at first is not aware of the resonant mode corresponding to the denominator term  $s^2 + 0.2s + 1$ , ( $\omega = 1$ ,  $\zeta = 0.1$ ). The root locus for this system versus  $K$ , excluding the saturation, is illustrated in Fig. 9.15. The imaginary axis crossing can be verified to be at  $\omega_0 = 1$ ,  $K = 0.2$ ; thus a gain of  $K = 0.5$  is enough to force the roots of the resonant mode into the RHP, as shown by the dots. If the system gain is set at  $K = 0.5$ , our analysis predicts a system that is initially unstable but becomes stable as the gain decreases. Thus we would expect the response of the system with the saturation to build up due to the instability until the magnitude is sufficiently large that the effective gain is lowered to  $K = 0.2$  and then stop growing!

Plots of the step responses with  $K = 0.5$  for three steps of size  $r = 1, 4$ , and  $8$  are shown in Fig. 9.16(a). The control signal is shown in Fig. 9.16(b) for  $r = 1$  and a similar saturation situation occurs for the other two cases, but with the onset of the limit cycle later depending on the value of  $r$ . Again our heuristic analysis is exactly correct: The error builds up to a fixed amplitude then starts to oscillate at a fixed

**Figure 9.14**

Block diagram of a system with an oscillatory mode

**Figure 9.15**

Root locus for the system in Fig. 9.14

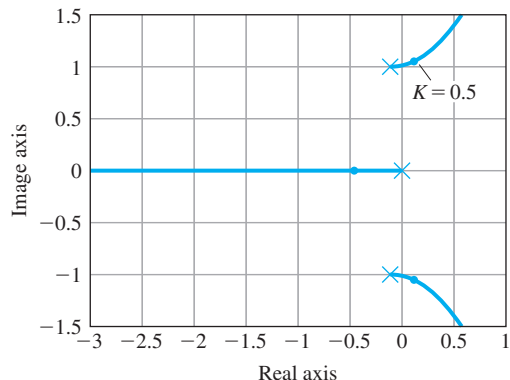
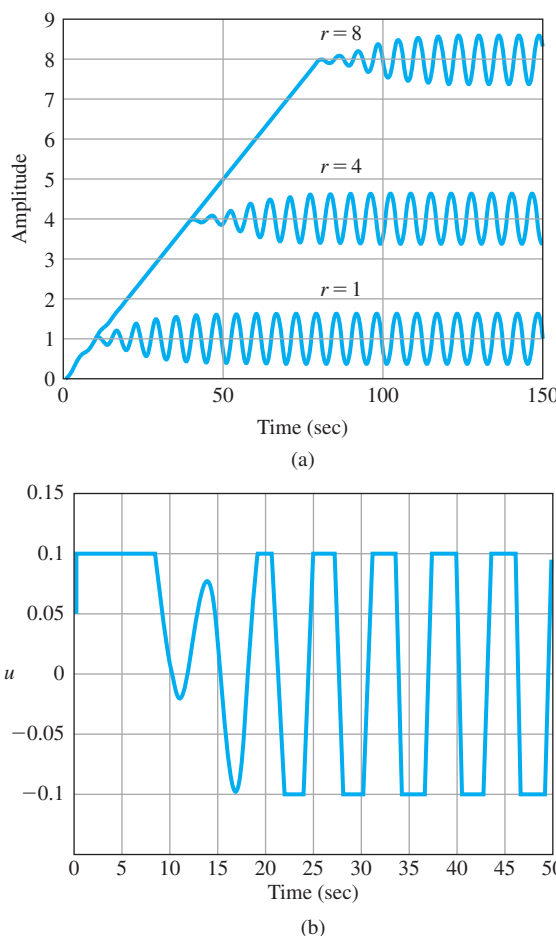


**Figure 9.16**

(a) Step responses of the system in Fig. 9.14,  
 (b) control signal for  $r = 1$



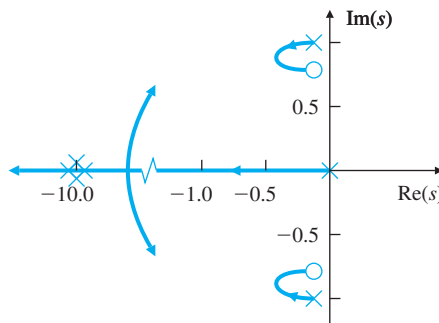
### Limit cycle

amplitude. The oscillations have a frequency of  $\approx 1$  rad/sec and hold constant amplitude regardless of the step sizes of the input. In this case, the response always approaches a periodic solution of fixed amplitude known as a **limit cycle**, so-called because the response is cyclic and is approached in the limit as time grows large.

Returning to Fig. 9.13 in Example 9.7, we can be easily convinced that the first transient to a step of size 3 is nearly a sinusoid. We can predict that the system is just on the border of stability for an equivalent gain corresponding to a root-locus gain of  $1/2$  when the locus crosses into the RHP. In order to prevent the limit cycle, the locus has to be modified by compensation so no branches cross into the RHP. One common method of doing this for a lightly damped oscillatory mode is to place compensation zeros near the poles at a frequency such that the angle of departure of the root-locus branch from these poles is toward the LHP, a procedure called phase stabilization earlier. Example 5.8 for collocated mechanical motion demonstrated that

**Figure 9.17**

Root locus including compensation



a pole–zero pair located in this manner will often cause a locus branch to go from the pole to the zero, looping to the left, and thus staying away from the RHP. Figure 9.17 shows the root locus for the system,  $1/[s(s^2 + 0.2s + 1.0)]$ , including a **notch compensation** with zeros located as just discussed. In addition, the compensation also includes two poles to make the compensation physically realizable. In this case, both poles were placed at  $s = -10$ , fast enough to not cause stability problems with the system, yet slow enough that high-frequency noise would not be amplified too much. Thus, the compensation used for the root locus is

$$D_c(s) = 123 \frac{s^2 + 0.18s + 0.81}{(s + 10)^2},$$

where the gain of 123 has been selected to make the compensation's DC gain equal to unity. This notch filter compensation attenuates inputs in the vicinity of  $\omega_n^2 = 0.81$  or  $\omega_n = 0.9$  rad/sec, so that any input from the plant resonance is attenuated, and is thus prevented from detracting from the stability of the system. Figure 9.18 shows the system, including the notch filter, and Fig. 9.19 shows the time response for two step inputs. Both inputs,  $r = 2$  and  $4$ , are sufficiently large that the nonlinearity is saturated initially; however, because the system is unconditionally stable, the saturation results only in lowering the gain, so the response is slower than predicted by linear analysis but still stable, as also predicted by our piecewise linear analysis. In both cases, the nonlinearity eventually becomes unsaturated, and the system stabilizes to its new commanded value of  $r$ .

**Figure 9.18**

Block diagram of the system with a notch filter

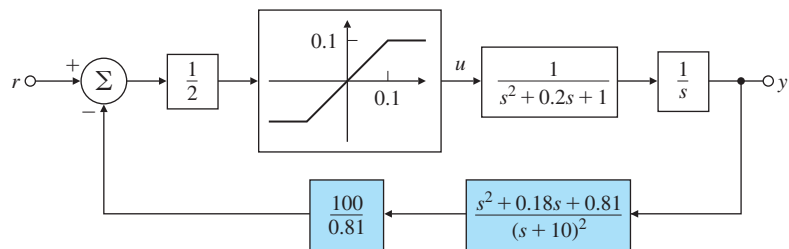
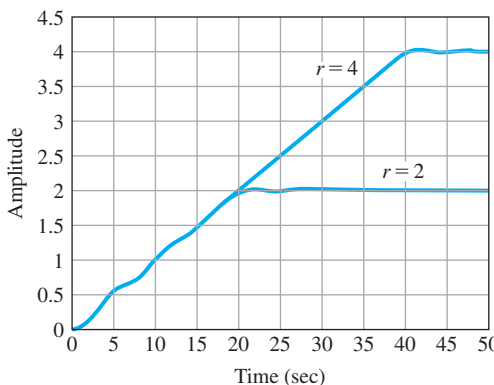


**Figure 9.19**

Step responses of the system in Fig. 9.18



### 9.3.1 Integrator Antiwindup

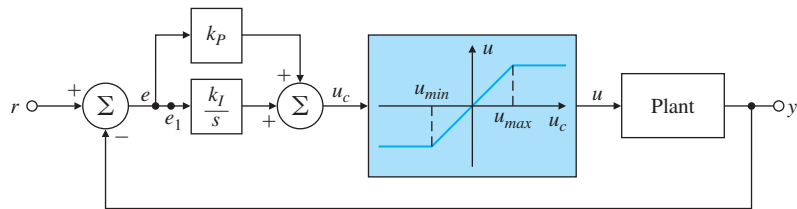
In any control system, the output of the actuator can saturate because the dynamic range of all real actuators is limited. For example, a valve saturates when it is fully open or closed, the control surfaces on an aircraft cannot be deflected beyond certain angles from their nominal positions, electronic amplifiers can produce only finite voltage outputs, etc. Whenever actuator saturation happens, the control signal to the process stops changing and the feedback path is effectively opened. If the error signal continues to be applied to the integrator input under these conditions, the integrator output will grow (windup) until the sign of the error changes and the integration turns around. The result can be a very large overshoot, as the output must grow to produce the necessary unwinding error, and poor transient response is the result. In effect, the integrator is an unstable element in open-loop and must be stabilized when saturation occurs.<sup>3</sup>

Consider the feedback system shown in Fig. 9.20. Suppose a given reference step is more than large enough to cause the actuator to saturate at  $u_{max}$ . The integrator continues integrating the error  $e$ , and the signal  $u_c$  keeps growing. However, the input to the plant is stuck at its maximum value, namely  $u = u_{max}$ , so the error remains large until the plant output exceeds the reference and the error changes sign. The increase in  $u_c$  is not helpful, since the input to the plant is not changing, but  $u_c$  may become quite large if saturation lasts a long time. It will then take a considerable negative error  $e$  (and the resulting poor transient response) to bring the integrator output back to within the linear band where the control is not saturated.

<sup>3</sup>In process control, integral control is usually called **reset control**, and so integrator windup is often called **reset windup**. Without integral control, a given setpoint of, say, 10 results in a response of less value, say, 9.9. The operator must then *reset* to 10.1 to bring the output to the desired value of 10. With integral control the controller automatically brings the output to 10 with a setpoint of 10; hence the integrator does *automatic reset*.

**Figure 9.20**

Feedback system with actuator saturation



The solution to this problem is an **integrator antiwindup** circuit, which “turns off” the integral action when the actuator saturates. (This can be done quite easily with logic, if the controller is implemented digitally, by including a statement such as “if  $|u| = u_{max}$ ,  $k_I = 0$ ;” see Chapter 8.) Two equivalent antiwindup schemes are shown in Fig. 9.21(a, b) for a PI controller. The method in Fig. 9.21(a) is somewhat easier to understand, whereas the one in Fig. 9.21(b) is easier to implement, as it does not require a separate nonlinearity but uses the saturation itself.<sup>4</sup> In these schemes, as soon as the actuator saturates, the feedback loop around the integrator becomes active and acts to keep the input to the integrator at  $e_1$  small. During this time, the integrator essentially becomes a fast first-order lag. To see this, note we can redraw the portion of the block diagram in Fig. 9.21(b) from  $e$  to  $u_c$ , as shown in Fig. 9.21(c). The integrator part then becomes the first-order lag shown in Fig. 9.21(d). The antiwindup gain,  $K_a$ , should be chosen to be large enough that the antiwindup circuit keeps the input to the integrator small under all error conditions.

The effect of the antiwindup is to reduce both the overshoot and the control effort in the feedback system. Implementation of such antiwindup schemes is a necessity in any practical application of integral control, and omission of this technique may lead to serious deterioration of the response. From the point of view of stability, the effect of the saturation is to open the feedback loop and leave the open-loop plant with a constant input and the controller as an open-loop system with the system error as input.

#### Purpose of antiwindup

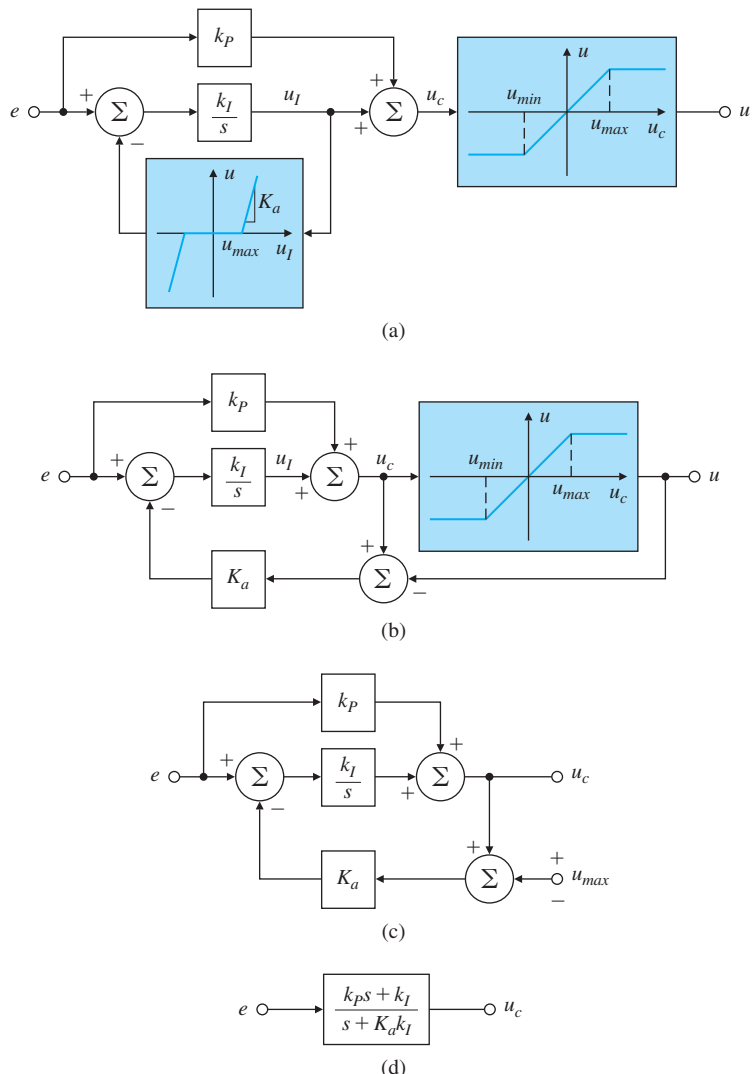
The purpose of the antiwindup is to provide local feedback to stabilize the controller only when the main loop is opened by signal saturation, and any circuit that does this will perform as antiwindup.<sup>5</sup>

<sup>4</sup>In some cases, especially with mechanical actuators such as an aircraft control surface or a flow control valve, it is not desirable and may cause damage to have the physical device bang against its stops. In such cases, it is common practice to include an *electronic* saturation with lower limits than those of the physical device, so that the system hits the electrical stops just before the physical device will saturate.

<sup>5</sup>A more sophisticated scheme might use an antiwindup feedback at a lower level of saturation than that imposed by the actuator, so PD control continues for a time after

**Figure 9.21**

Integrator antiwindup  
techniques

**EXAMPLE 9.9***Antiwindup Compensation for a PI Controller*

Consider a plant with the transfer function for small signals,

$$G(s) = \frac{1}{s},$$

and a PI controller,

$$D_c(s) = k_p + \frac{k_I}{s} = 2 + \frac{4}{s},$$

---

integration has been stopped. Any such scheme needs to be analyzed carefully to evaluate its performance and to assure stability.

in the unity feedback configuration. The input to the plant is limited to  $\pm 1.0$ . Study the effect of antiwindup on the response of the system.

**Solution.** Suppose we use an antiwindup circuit with a feedback gain of  $K_a = 10$ , as shown in the Simulink block diagram of Fig. 9.22. Figure 9.23(a) shows the step response of the system with and without the antiwindup element. Figure 9.23(b) shows the corresponding control effort. Note the system with antiwindup has substantially less overshoot and less control effort.

A careful look at Figures 9.23 and 9.24 provides insight into how the integrator antiwindup scheme works. Let us first consider the system without antiwindup. The value of the initial tracking error is so large that the proportional controller goes “full blast” and the actuator saturates at its maximum value (“high-sat”) immediately as shown in Fig. 9.23(b). The value of the component of the control signal due to

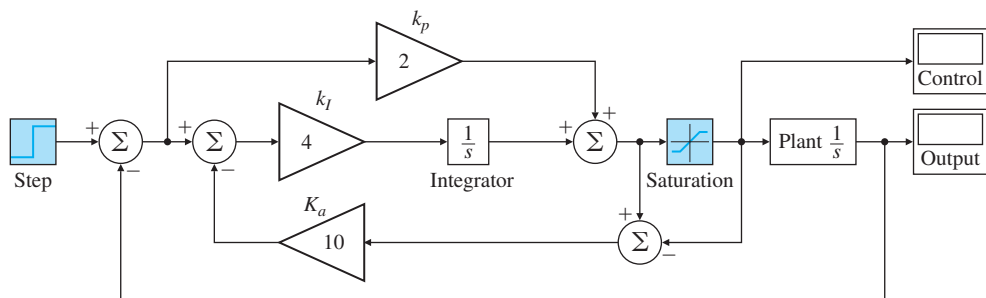
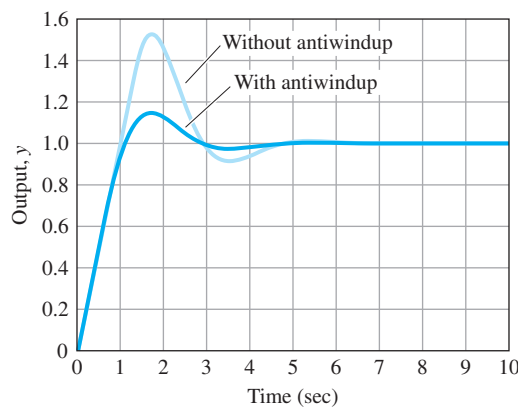


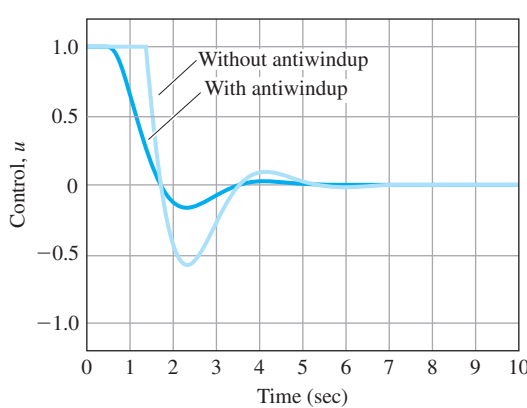
**Figure 9.22**

Simulink diagram for the antiwindup example

Source: Franklin, Gene F. *Feedback Control of Dynamic Systems*, 8E, 2019, Pearson Education, Inc., New York, NY.



(a)



(b)

**Figure 9.23**

Integrator antiwindup: (a) step response; (b) control effort

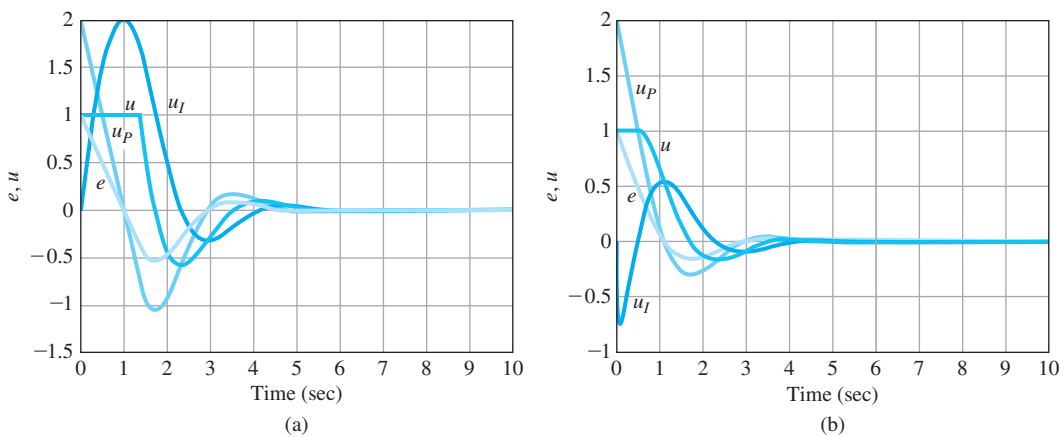


**Figure 9.24**

Explanation of the antiwindup scheme (a) error and control signals without antiwindup (b) error and control signals with antiwindup

integral control,  $u_I$ , starts off as **positive** because the value of the tracking error signal is positive as seen in Fig. 9.24(a). The signal  $u_I$  builds up over time and reaches its maximum value of 2.0 at  $t = 1.1$  sec when the tracking error goes through zero and starts to decrease afterwards as shown in Fig. 9.24(a). However, the system remains in saturation because of the large value of  $u_I$ . It does not come out of saturation until the tracking error has been negative for sufficient amount of time and the value of  $u_I$  has decreased enough so the overall control signal ( $u = u_P + u_I$ ) is below its maximum saturation value of unity. Eventually the system does come out of saturation. Meanwhile the tracking error signal  $e(t)$  changes sign, that is it goes from positive to negative, around  $t = 1$  sec as seen in Fig. 9.24(a). At  $t = 3$  sec, the tracking error goes through zero again and the overshoot is gone. Note the system never reaches the lower saturation limit (“low-sat”). The effects of not having the antiwindup are large overshoot of 53% and considerable control effort, as seen in Figure 9.23.

The system’s response is quite different with the antiwindup scheme in place. The system again saturates immediately at its maximum value due to the large initial tracking error signal. However, in sharp contrast to the previous case, the control signal component due to the integral term,  $u_I$ , goes **negative** as shown in Fig. 9.24(b). The antiwindup scheme works rapidly to produce an input signal to the integrator so the system is led out of saturation faster by almost a factor of 3 at  $t = 0.52$  sec before the tracking error changes sign at  $t = 1.2$  sec [see Fig. 9.24(b)]. The tracking error goes through zero again at  $t = 2.8$  sec, and the overshoot is gone. In this case, the overall magnitude of the tracking error is smaller, the overshoot has been reduced from around 53% to 15% and the control effort is also

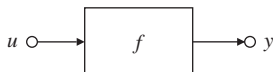
lower as seen in Fig. 9.23(b). Hence the antiwindup technique produces superior performance.

## 9.4 Equivalent Gain Analysis Using Frequency Response: Describing Functions

The behavior of systems containing any one of the nonlinearities shown in Fig. 9.6 can be qualitatively described by considering the nonlinear element as a varying signal-dependent gain. For example, with the saturation element (see Fig. 9.6(a)), it is clear that for input signals with magnitudes of less than  $h$ , the nonlinearity is linear with the gain  $N/h$ . However, for signals larger than  $h$ , the output size is bounded by  $N$ , while the input size can get much larger than  $h$ , so once the input exceeds  $h$ , the ratio of output to input goes down. Thus, saturation has the gain characteristics shown in Fig. 9.10. All actuators saturate at some level. If they did not, their output would increase to infinity, which is physically impossible. An important aspect of control system design is **sizing the actuator**, which means picking the size, weight, power required, cost, and saturation level of the device. Generally, higher saturation levels require bigger, heavier, and more costly actuators. From a control point of view, the key factor that enters into the sizing is the effect of the saturation on the control system's performance.

A nonlinear analysis method known as **describing functions**, based on the assumption that the input to the nonlinearity is sinusoidal, can be used to predict the behavior of a class of nonlinear systems. A nonlinear element does not have a transfer function. However, for a certain class of nonlinearities, it is possible to replace the nonlinearity by a frequency-dependent equivalent gain for analysis purposes. We can then study the properties of the loop, such as its stability. The describing function method is mostly a heuristic method, and its aim is to try to find something akin to a “transfer function” for a nonlinear element. The idea is that in response to a sinusoidal excitation, most nonlinearities will produce a *periodic* signal (not necessarily sinusoidal) with frequencies being the harmonics of the input frequency. Hence one may view the describing function as an extension of the frequency response to nonlinearities. We can *assume* that, in many cases, we may approximate the output by the first harmonic alone, and the rest can be neglected. This basic assumption means that the plant behaves approximately as a low-pass filter, and this is luckily a good assumption in most practical situations. The other assumptions behind the describing function are that the nonlinearity is time invariant and that there is a single nonlinear element in the system. Indeed, the describing function is a special case of the more sophisticated harmonic balance analysis. Its roots go back to the early studies in the Soviet Union and elsewhere. The method was introduced by Kochenburger in 1950 in the United States.

**Figure 9.25**  
Nonlinear element



He proposed that the Fourier series be used to define an equivalent gain,  $K_{eq}$  (Truxal, 1955, p. 566). This idea has proved to be very useful in practice. The method is heuristic, but there are attempts at establishing a theoretical justification for the technique (Bergen and Franks, 1971; Khalil, 2002; Sastry, 1999). In fact, the method works much better than is warranted by the existing theory!

Consider the nonlinear element  $f(u)$  shown in Fig. 9.25. If the input signal  $u(t)$  is sinusoidal of amplitude  $a$ , or

$$u(t) = a \sin(\omega t), \quad (9.20)$$

then the output  $y(t)$  will be *periodic* with a fundamental period equal to that of the input and consequently with a Fourier series described by

$$\begin{aligned} y(t) &= a_0 + \sum_{i=1}^{\infty} a_i \cos(j\omega t) + b_i \sin(j\omega t), \\ &= a_0 + \sum_{i=1}^{\infty} Y_i \sin(j\omega t + \theta_i), \end{aligned} \quad (9.21)$$

where

$$a_i = \frac{2}{\pi} \int_0^{\pi} y(t) \cos(j\omega t) d(\omega t), \quad (9.22)$$

$$b_i = \frac{2}{\pi} \int_0^{\pi} y(t) \sin(j\omega t) d(\omega t), \quad (9.23)$$

$$Y_i = \sqrt{a_i^2 + b_i^2}, \quad (9.24)$$

$$\theta_i = \tan^{-1} \left( \frac{a_i}{b_i} \right). \quad (9.25)$$

Kochenburger suggested that the nonlinear element could be described by the first fundamental component of this series as if it were a linear system with a gain of  $Y_1$  and phase of  $\theta_1$ . If the amplitude is varied, the Fourier coefficients and the corresponding phases will vary as a function of the input signal amplitude, due to the nonlinear nature of the element. He called this approximation a **describing function (DF)**. The describing function is defined as the (complex) quantity that is a ratio of the amplitude of the fundamental component of the output of the nonlinear element to the amplitude of the sinusoidal input signal and is essentially an “equivalent frequency response” function:

$$DF = K_{eq}(a, \omega) = \frac{b_1 + ja_1}{a} = \frac{Y_1(a, \omega)}{a} e^{j\theta_1} = \frac{Y_1(a, \omega)}{a} \angle \theta_1. \quad (9.26)$$

Hence the describing function is defined only on the  $j\omega$  axis. In the case of memoryless nonlinearities that are also an odd function [that

### Describing function

is,  $f(-a) = -f(a)$ ], then the coefficients of the Fourier series cosine terms are all zeros, and the describing function is simply

$$DF = K_{\text{eq}}(a) = \frac{b_1}{a}, \quad (9.27)$$

and is *independent* of the frequency  $\omega$ . This is the usual case in control, and saturation, relay, and dead-zone nonlinearities all result in such describing functions. Computation of the describing function for the nonlinear characteristics of Fig. 9.6 is generally straightforward, but tedious. It can be done either analytically or numerically, and may also be determined by an experiment. We will now focus on computation of several describing functions for some very common nonlinearities.

### EXAMPLE 9.10

#### Describing Function for a Saturation Nonlinearity

A saturation nonlinearity is shown in Fig. 9.26(a) and is the most common nonlinearity in control systems. The saturation function (sat) is defined as

$$\text{sat}(u) = \begin{cases} +1, & u > 1, \\ u, & |u| \leq 1, \\ -1, & u < -1. \end{cases}$$

If the slope of the linear region is  $k$  and the final saturated values are  $\pm N$ , then the function is

$$y = N \text{ sat}\left(\frac{k}{N}u\right).$$

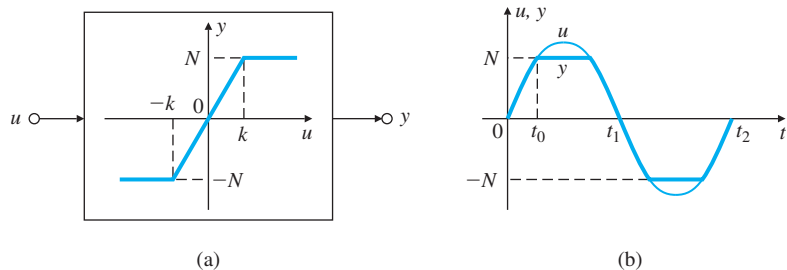
Find the describing function for this nonlinearity.

**Solution.** Consider the input and output signals of the saturation element shown in Fig. 9.26. For an input sinusoid of  $u = a \sin \omega t$  with amplitude  $a \leq \frac{N}{k}$ , the output is such that the DF is just a gain of unity. With  $a \geq \frac{N}{k}$ , we need to compute the amplitude and phase of the fundamental component of the output. Since saturation is an odd function, all the cosine terms in Eq. (9.21) are zeros and  $a_1 = 0$ . According to Eq. (9.27),

$$K_{\text{eq}}(a) = \frac{b_1}{a},$$

**Figure 9.26**

(a) Saturation nonlinearity; (b) input and output signals



so

$$b_1 = \frac{2}{\pi} \int_0^\pi N \operatorname{sat}\left(\frac{k}{N}a \sin \omega t\right) \sin \omega t d(\omega t),$$

since the integral for the coefficient  $b_1$  over the interval  $\omega t = [0, \pi]$  is simply twice that of the interval  $\omega t = [0, \pi/2]$ . Then

$$b_1 = \frac{4N}{\pi} \int_0^{\frac{\pi}{2}} \operatorname{sat}\left(\frac{k}{N}a \sin \omega t\right) \sin \omega t d(\omega t).$$

We can now divide the integral into two parts corresponding to the linear and saturation parts. Let us define the saturation time  $t_s$  as the time when

$$t_s = \frac{1}{\omega} \sin^{-1}\left(\frac{N}{ak}\right) \quad \text{or} \quad \omega t_s = \sin^{-1}\left(\frac{N}{ak}\right). \quad (9.28)$$

Then

$$\begin{aligned} b_1 &= \frac{4N\omega}{\pi a} \left( \int_0^{\omega t_s} \operatorname{sat}\left(\frac{k}{N}a \sin \omega t\right) \sin \omega t dt + \int_{\omega t_s}^{\frac{\pi}{2}} \sin \omega t dt \right) \\ &= \frac{4N\omega}{\pi a} \left( \int_0^{\omega t_s} \frac{k}{N}a \sin^2 \omega t dt + \int_{\omega t_s}^{\frac{\pi}{2}} \sin \omega t dt \right) \\ &= \frac{4N\omega}{\pi a} \left( \int_0^{\omega t_s} \frac{k}{2N}a(1 - \cos 2\omega t) dt + \int_{\omega t_s}^{\frac{\pi}{2}} \sin \omega t dt \right) \\ &= \frac{4N\omega}{\pi a} \left( \frac{k}{2N}at \Big|_0^{t_s} - \frac{k}{2N}a \sin 2\omega t \Big|_0^{t_s} - \frac{1}{\omega}(\cos \frac{\pi}{2} - \cos t_s) \right). \end{aligned}$$

But using Eq. (9.28), we have

$$\sin \omega t_s = \frac{N}{ka} \quad \text{and} \quad \cos \omega t_s = \sqrt{1 - \left(\frac{N}{ka}\right)^2}.$$

We finally obtain

$$K_{eq}(a) = \begin{cases} \frac{2}{\pi} \left( k \sin^{-1}\left(\frac{N}{ak}\right) + \frac{N}{a} \sqrt{1 - \left(\frac{N}{ka}\right)^2} \right), & \frac{ka}{N} > 1, \\ k, & \frac{ka}{N} \leq 1. \end{cases} \quad (9.29)$$

Figure 9.27 shows a plot of  $K_{eq}(a)$  indicating it is a real function independent of frequency and results in no phase shifts. It is seen that the describing function is initially a constant, then decays essentially as a function of the reciprocal of the input signal amplitude,  $a$ .

### EXAMPLE 9.11

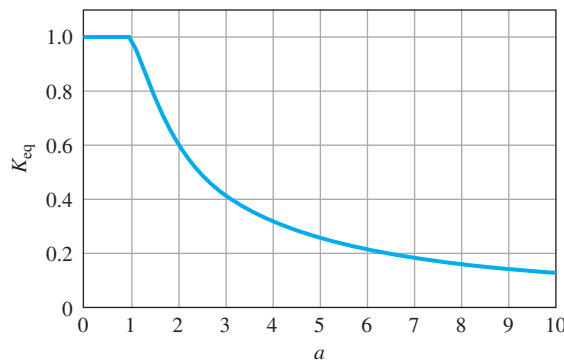
#### *Describing Function for a Relay Nonlinearity*

Find the describing function for the relay or sgn function shown in Fig. 9.6(b) and defined as

$$\operatorname{sgn}(u) = \begin{cases} +1 & \text{if } u > 0, \\ 0 & \text{if } u = 0, \\ -1 & \text{if } u < 0. \end{cases}$$

**Figure 9.27**

Describing function for saturation nonlinearity with  $k = N = 1$



**Solution.** The output is a square wave of amplitude  $N$  for every size input; thus  $Y_1 = \frac{4N}{\pi}$  and  $K_{eq} = \frac{4N}{\pi a}$ . The solution can also be obtained from Eq. (9.29) if we let  $k \rightarrow \infty$ . For small angles,

$$\sin^{-1}\left(\frac{N}{ak}\right) \cong \frac{N}{ak},$$

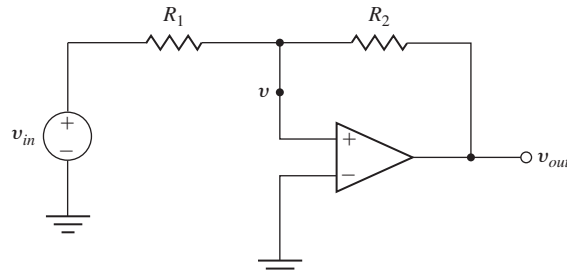
and thus, from Eq. (9.27), we have

$$K_{eq}(a) = \frac{2}{\pi} \left( k \left( \frac{N}{ak} \right) + \frac{N}{a} \right) = \frac{4N}{\pi a}. \quad (9.30)$$

The preceding two nonlinearities were memoryless. Next we consider a nonlinearity with memory. Nonlinearities with memory occur in many applications, including magnetic recording devices, backlash in mechanical systems, and in electronic circuits. Consider the bistable electronic circuit in Fig. 9.28 that is called a Schmitt trigger (Sedra and Smith, 1991). This circuit has memory. Referring to Fig. 9.29, if the circuit is in the state where  $v_{out} = +N$ , then positive values of  $v_{in}$  do not change the state. To “trigger” the circuit into the state  $v_{out} = -N$ , we must make  $v_{in}$  negative enough to make  $v$  negative. The threshold value is  $h = \frac{NR_1}{R_2}$ . The Schmitt trigger is employed commonly in space-craft control (Bryson, 1994). We next find the describing function for a hysteresis nonlinearity.

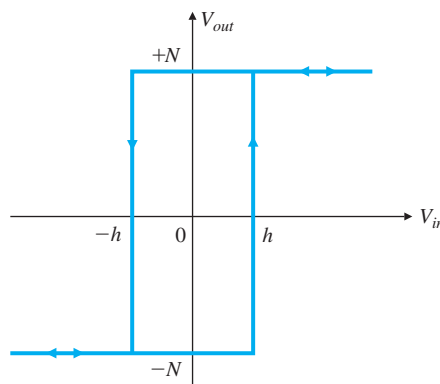
**Figure 9.28**

Schmitt trigger circuit



**Figure 9.29**

Hysteresis nonlinearity for Schmitt trigger circuit

**EXAMPLE 9.12***Describing Function for a Relay with Hysteresis Nonlinearity*

Consider the relay function with hysteresis shown in Fig. 9.30(a). Find the describing function for this nonlinearity.

**Solution.** A system with hysteresis tends to stay in its current state. Until the input to the signum function is past the value  $h$ , it is not possible to determine the output uniquely without knowing its past history. That implies that we have a nonlinearity with memory. The output is a square wave with amplitude  $N$  as long as the input amplitude  $a$  is greater than the hysteresis level  $h$ . From Fig. 9.30(b), it is seen that the square wave lags the input in time. The lag time can be computed as the time when

$$a \sin \omega t = h \quad \text{or} \quad \omega t = \sin^{-1} \left( \frac{h}{a} \right). \quad (9.31)$$

Because the phase angle is known for all frequencies,

$$K_{\text{eq}}(a) = \frac{4N}{\pi a} \angle -\sin^{-1} \left( \frac{h}{a} \right) = \frac{4N}{\pi a} e^{-j \sin^{-1} \left( \frac{h}{a} \right)}, \quad (9.32)$$

$$= \frac{4N}{\pi a} \left( \sqrt{1 - \left( \frac{h}{a} \right)^2} - j \frac{h}{a} \right). \quad (9.33)$$

**Figure 9.30**

(a) Hysteresis nonlinearity; (b) input and output to the nonlinearity

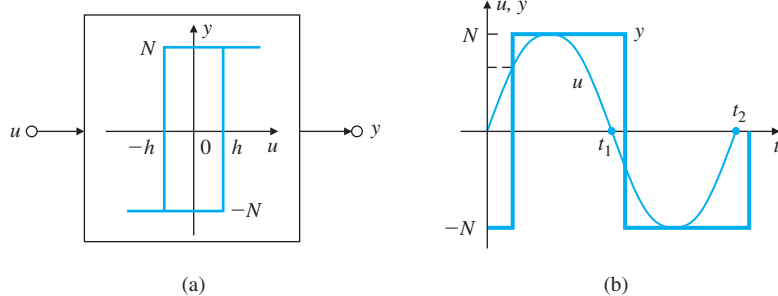
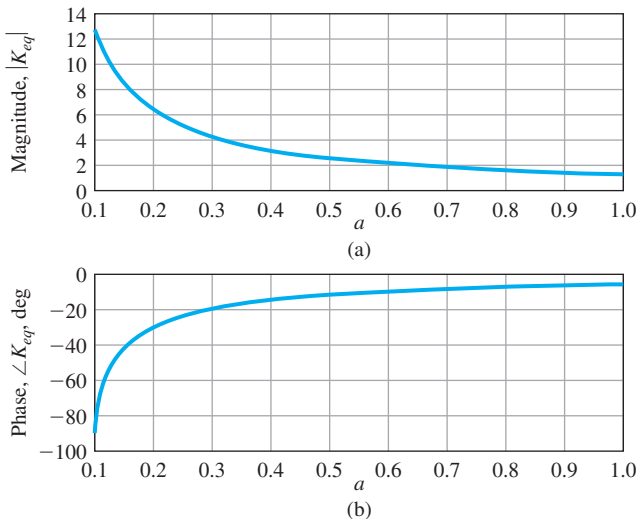


**Figure 9.31**

Describing function for the hysteresis nonlinearity for  $h = 0.1$  and  $N = 1$ : (a) magnitude; (b) phase



The describing function is then given by

$$K_{eq}(a) = \begin{cases} \frac{4N}{\pi a} \left( \sqrt{1 - \left(\frac{h}{a}\right)^2} - j\frac{h}{a} \right), & a \geq h, \\ 0, & a < h. \end{cases} \quad (9.34)$$

The describing function is plotted in Fig. 9.31. The magnitude is proportional to the reciprocal of the input signal amplitude, and the phase varies between  $-90^\circ$  and  $0^\circ$ .

### 9.4.1 Stability Analysis Using Describing Functions

The Nyquist theorem can be extended to deal with nonlinear systems whose nonlinearities have been approximated by describing functions. In the standard linear system analysis, the characteristic equation is  $1 + KL = 0$ , where the loop gain is  $L = D_c G$  and

$$L = -\frac{1}{K}. \quad (9.35)$$

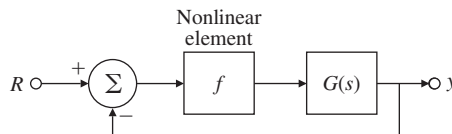
As described in Section 6.3, we look at the encirclements of the  $-1/K$  point to determine stability. With a nonlinearity represented by the describing function,  $K_{eq}(a)$ , the characteristic equation is of the form  $1 + K_{eq}(a)L = 0$ , and it follows that

$$L = -\frac{1}{K_{eq}(a)}. \quad (9.36)$$

Now we have to look at the intersection of  $L$  with a plot of  $-1/K_{eq}(a)$ . If the curve  $L$  intersects  $-1/K_{eq}(a)$ , then the system will oscillate at the crossing amplitude,  $a_l$ , and the corresponding frequency,  $\omega_l$ , keeping

**Figure 9.32**

Closed-loop system with a nonlinearity



in mind the approximate nature of the describing function. We then look for encirclements to decide whether the system would be stable for that particular value of the gain, as if it were a linear system. If so, we deduce that the nonlinear system is stable. Otherwise, we infer that the nonlinear system is unstable.

Figure 9.32 shows an example of an otherwise linear system, except for a single nonlinearity. The nonlinear elements may indeed have a beneficial effect and may limit the amplitude of oscillations. The describing function analysis can be used to determine the amplitude and frequency of the limit cycle. Strictly speaking, a limit cycling system can be considered to be unstable. In reality, the trajectory of the limit cycling is confined to a finite region of the state space. If this region is within allowable performance, then the response is tolerable. In some cases, the limit cycling is a beneficial effect (see the case study in Section 10.4). The system does not possess asymptotic stability, since the system does not come to a rest at the origin of the state space. The describing function can be beneficial in determining the conditions under which instability results and can even suggest remedies in eliminating instability, as illustrated in the next example, in which the Nyquist plot of the linear loop gain,  $L$ , as well as the negative reciprocal of the describing function,  $-1/K_{eq}(a)$ , are superimposed. The point at which they cross corresponds to the limit cycle. To determine the amplitude and frequency of the limit cycle, we can rewrite Eq. (9.36) as follows:

$$\begin{aligned} \operatorname{Re}\{L(j\omega)\}\operatorname{Re}\{K_{eq}(a)\} - \operatorname{Im}\{L(j\omega)\}\operatorname{Im}\{K_{eq}(a)\} + 1 &= 0, \quad (9.37) \\ \operatorname{Re}\{L(j\omega)\}\operatorname{Im}\{K_{eq}(a)\} + \operatorname{Im}\{L(j\omega)\}\operatorname{Re}\{K_{eq}(a)\} &= 0. \end{aligned}$$

We can then solve these two equations for the possible two unknown values of the limit-cycle frequency,  $\omega_l$ , and the corresponding amplitude,  $a_l$ , as illustrated in the ensuing examples.

## EXAMPLE 9.13

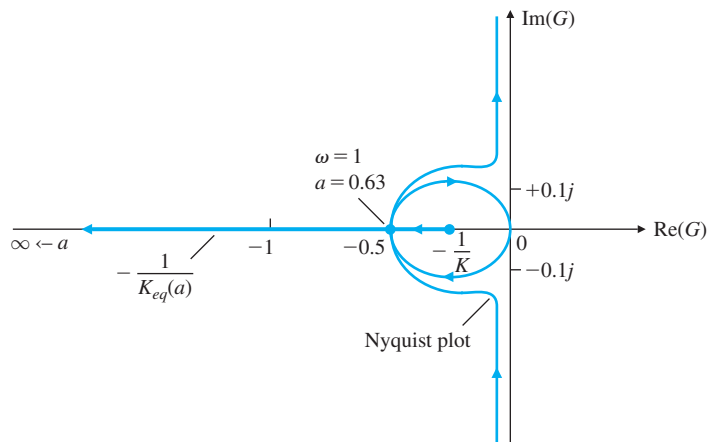
### Conditionally Stable System

Consider the feedback system in Fig. 9.14. Determine the amplitude and the frequency of the limit cycle using the Nyquist plot.

**Solution.** The Nyquist plot of the system is superimposed on  $-1/K_{eq}(a)$  as shown in Fig. 9.33. Note the negative of the reciprocal of the describing function, using Eq. (9.29), is

**Figure 9.33**

Nyquist plot and  
describing function to  
determine limit cycle



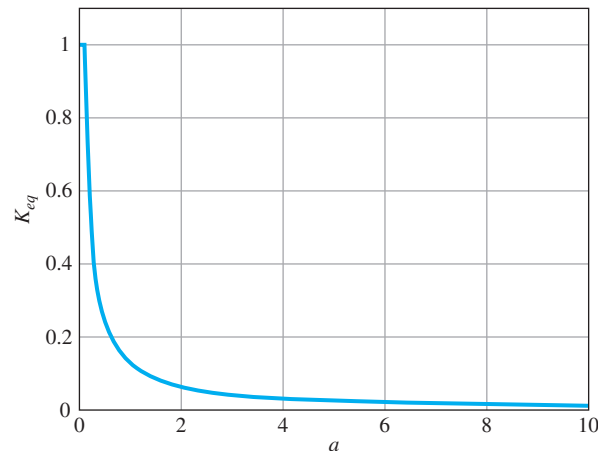
$$\begin{aligned} -\frac{1}{K_{eq}(a)} &= -\frac{1}{\frac{2}{\pi} \left( k \sin^{-1} \left( \frac{N}{ak} \right) + \frac{N}{a} \sqrt{1 - \left( \frac{N}{ka} \right)^2} \right)} \\ &= -\frac{1}{\frac{2}{\pi} \left( \sin^{-1} \left( \frac{0.1}{a} \right) + \frac{0.1}{a} \sqrt{1 - \left( \frac{0.1}{a} \right)^2} \right)}, \end{aligned}$$

which is a straight line that is coincident with the negative real axis and is parameterized as a function of the input signal amplitude,  $a$ . The point of the intersection of the two curves at  $-0.5$  corresponds to the limit-cycle frequency of  $\omega_l = 1$ . A plot of the describing function for  $k = 1$  and  $N = 0.1$  is shown in Fig. 9.34, and a magnitude of  $K_{eq} = 0.2$  corresponds to a limit-cycle amplitude of  $a_l = 0.63$ .

Alternatively, from the root locus of our example shown in Fig. 9.15, the gain at the imaginary-axis crossover is 0.2; then, from Eq. (9.29), we have

**Figure 9.34**

Describing function for  
saturation nonlinearity  
with  $N = 0.1$  and  $k = 1$



$$K_{eq} = \frac{2}{\pi} \left( \sin^{-1} \left( \frac{0.1}{a} \right) + \frac{0.1}{a} \sqrt{1 - \left( \frac{0.1}{a} \right)^2} \right) = 0.2.$$

If we approximate the arcsine function by its argument as

$$\sin^{-1} \left( \frac{0.1}{a} \right) \approx \frac{0.1}{a},$$

then

$$\frac{2}{\pi} \left( \left( \frac{0.1}{a} \right) + \frac{0.1}{a} \sqrt{1 - \left( \frac{0.1}{a} \right)^2} \right) = 0.2,$$

which leads to the polynomial equation

$$\pi^2 a^4 - 2\pi a^3 + (0.1)^2 = 0,$$

and we find the relevant solution to be  $a = 0.63$ . By measurement on the time history of Fig. 9.16, the amplitude of the oscillation is 0.62, which is in good agreement with our prediction.

For systems with nonlinearities that have memory, we can also use the Nyquist technique, as illustrated in the next example.

### EXAMPLE 9.14

#### *Determination of Stability with a Hysteresis Nonlinearity*

Consider the system with a hysteresis nonlinearity shown in Fig. 9.35. Determine whether the system is stable and find the amplitude and the frequency of the limit cycle.

**Solution.** The Nyquist plot for the system is shown in Fig. 9.36. The negative reciprocal of the describing function for the hysteresis nonlinearity is

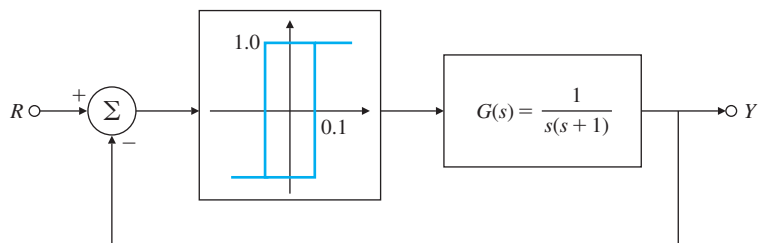
$$-\frac{1}{K_{eq}(a)} = -\frac{1}{\frac{4N}{\pi a} \left( \sqrt{1 - \left( \frac{h}{a} \right)^2} - j \frac{h}{a} \right)} = -\frac{\pi}{4N} \left[ \sqrt{a^2 - h^2} + jh \right].$$

In this case,  $N = 1$  and  $h = 0.1$ , and we have

$$-\frac{1}{K_{eq}(a)} = -\frac{\pi}{4} \left[ \sqrt{a^2 - 0.01} + j0.1 \right].$$

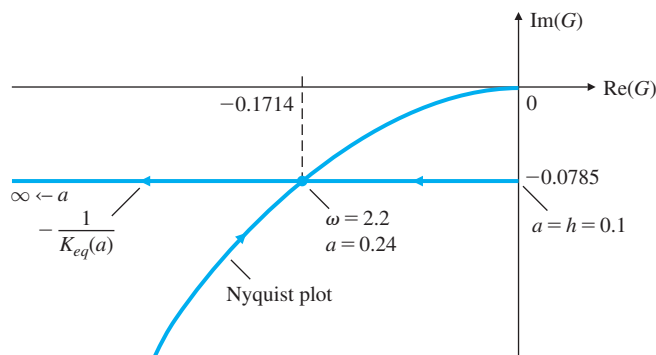
**Figure 9.35**

Feedback system with hysteresis nonlinearity



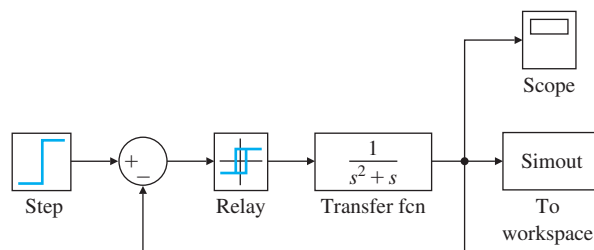
**Figure 9.36**

Nyquist plot and DF to determine limit-cycle properties

**Figure 9.37**

Simulink diagram for system with hysteresis

Source: Franklin, Gene F.  
*Feedback Control of Dynamic Systems*, 8E, 2019, Pearson  
Education, Inc., New York, NY.



This is a straight line parallel to the real axis that is parameterized as a function of the input signal amplitude  $a$  and is also plotted in Fig. 9.36. The intersection of this curve with the Nyquist plot yields the frequency and the corresponding amplitude of the stable limit cycle. We can also determine the limit-cycle information analytically:

$$-\frac{1}{K_{eq}(a)} = -\frac{\pi}{4} \left[ \sqrt{a^2 - 0.01} + j0.1 \right] = G(j\omega) = \frac{1}{j\omega(j\omega + 1)}.$$

Clearing the denominator in the preceding equation, we have

$$\frac{\pi}{4} \sqrt{a^2 - 0.01} \omega^2 + \frac{0.1\pi}{4} \omega - 1 + j \left[ \frac{0.1\pi}{4} \omega^2 - \frac{\pi}{4} \sqrt{a^2 - 0.01} \omega \right] = 0.$$

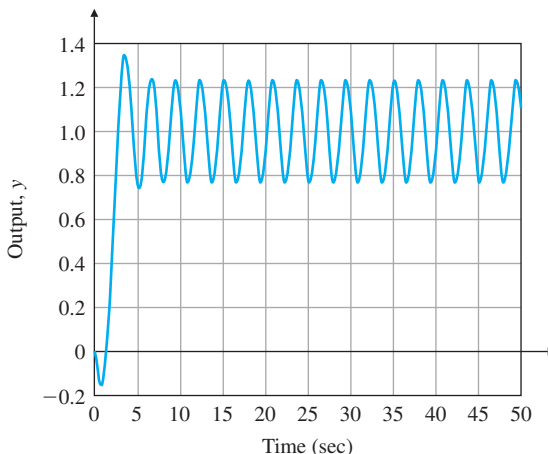
Setting the real and imaginary parts equal to zero yields two equations and two unknowns. The relevant solution is  $\omega_l = 2.2$  rad/sec and  $a_l = 0.24$ . A Simulink implementation of the closed-loop system is shown in Fig. 9.37. The step response of the system is shown in Fig. 9.38, and the limit cycle has an amplitude of  $a_l = 0.24$  and a frequency of  $\omega_l = 2.2$  rad/sec and is well predicted by our analysis.

## △ 9.5 Analysis and Design Based on Stability

The central requirement of any control system is stability, and the design methods we have studied are based on this fact. The root locus is a plot of closed-loop poles in the  $s$ -plane, and the designer is always aware of

**Figure 9.38**

Step response displaying limit-cycle oscillations



the fact that if a root strays into the right half of the plane, the system will be unstable. Designs based on the state representation include pole placement, where the desired locations of the poles are, of course, selected to be well within the stable region. In a similar fashion, Nyquist proved conditions for stability based on the frequency response, and designers are aware of the encirclement requirements of their plots or, equivalently, of the gain and phase margins of stability margins in the Bode plots. Prior to either of these methods, mathematicians studied the stability of ordinary differential equations (ODE), and these and other sophisticated techniques are needed to face the problems of nonlinear systems. We begin with a graphical representation of ODE solutions known as the phase plane and introduce the methods of Lyapunov and others as an introduction to this area of control design.

### 9.5.1 The Phase Plane

Whereas the root locus and the frequency-response methods consider the system response indirectly via either the poles and zeros of the transfer function or the gain and phase of the frequency response, the phase plane considers the time response directly by plotting the trajectory of the state variables. Although direct visualization restricts the method to second-order systems having only two state variables, the ability of the method to consider nonlinearities, as well as to give new insight into linear systems, makes a quick look at the technique well worthwhile.

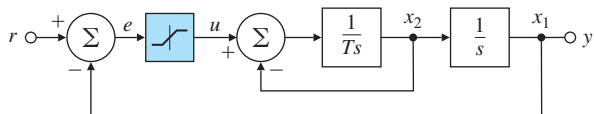
To illustrate the ideas of the phase plane, consider a fictional motor system shown in Fig. 9.39 with the open-loop transfer function

$$G(s) = \frac{1}{s(Ts + 1)}.$$

If we assume  $T = 1/6$  and the amplifier is (for the moment) not subject to saturation and has gain  $K$  where  $K = 5T$ , the state equations for the closed-loop system can be written as

**Figure 9.39**

An elementary position feedback system with a nonlinear actuator



$$\dot{x}_1 = x_2, \quad (9.38)$$

$$\dot{x}_2 = -5x_1 - 6x_2, \quad (9.39)$$

$$y = x_1. \quad (9.40)$$

Because these equations are time invariant, the time can be eliminated by dividing Eq. (9.38) into Eq. (9.39), with the result that

$$\frac{dx_2}{dx_1} = \frac{-5x_1 - 6x_2}{x_2}. \quad (9.41)$$

The solution to this equation gives a plot of  $x_2$  versus  $x_1$  or, in other words, a trajectory in the phase plane of coordinates  $(x_1, x_2)$ .<sup>6</sup> Before plotting Eq. (9.41), it is useful to consider the system equations first in matrix form as  $\dot{\mathbf{x}} = \mathbf{Ax}$  for which

$$\mathbf{A} = \begin{bmatrix} 0 & 1 \\ -5 & -6 \end{bmatrix}.$$

If in this equation we assume  $\mathbf{x} = \mathbf{x}_o e^{st}$ , where both  $s$  and  $\mathbf{x}_o$  are constants, then  $\dot{\mathbf{x}} = \mathbf{x}_o s e^{st}$ , and the equation can be reduced as follows:

$$\dot{\mathbf{x}} = \mathbf{Ax}, \quad (9.42)$$

$$\mathbf{x}_o s e^{st} = \mathbf{Ax}_o e^{st}, \quad (9.43)$$

$$[s\mathbf{I} - \mathbf{A}]\mathbf{x}_o e^{st} = \mathbf{0}, \quad (9.44)$$

$$[s\mathbf{I} - \mathbf{A}]\mathbf{x}_o = \mathbf{0}. \quad (9.45)$$

Here it should be recognized that Eq. (9.45) is the eigenvector equation for the matrix  $\mathbf{A}$ , which, in component form, is

$$\begin{bmatrix} s & -1 \\ 5 & s+6 \end{bmatrix} \begin{bmatrix} x_{01} \\ x_{02} \end{bmatrix} = \begin{bmatrix} 0 \\ 0 \end{bmatrix}. \quad (9.46)$$

As described in Appendix WE available online Eq. (9.46) has a solution only if the determinant of the coefficient matrix is zero, for which

$$s(s + 6) + 5 = 0, \quad (9.47)$$

$$(s + 1)(s + 5) = 0. \quad (9.48)$$

<sup>6</sup>If the slope  $dx_2/dx_1$  is set to a constant, the relation between  $x_2$  and  $x_1$  is a straight line. If the known values of slopes are marked along a set of these lines, the trajectories can be readily sketched. For example, along the  $x_1$  axis, where  $x_2 = 0$ , the slope is  $\infty$  and the trajectories are vertical. This method is called the method of isoclines.

The two values of  $s$  for which the equation has a solution are the eigenvalues  $s = -1$  and  $s = -5$ . If we substitute  $s = -1$  into Eq. (9.46), we obtain

$$\begin{bmatrix} -1 & -1 \\ 5 & -1+6 \end{bmatrix} \begin{bmatrix} x_{01} \\ x_{02} \end{bmatrix} = \begin{bmatrix} 0 \\ 0 \end{bmatrix}, \quad (9.49)$$

from which the solution for the initial state vector is  $x_{02} = -x_{01}$ . This line in the state space is the eigenvector corresponding to the eigenvalue  $s = -1$ . If we repeat this process with  $s = -5$ , the result is

$$\begin{bmatrix} -5 & -1 \\ 5 & -5+6 \end{bmatrix} \begin{bmatrix} x_{01} \\ x_{02} \end{bmatrix} = \begin{bmatrix} 0 \\ 0 \end{bmatrix}, \quad (9.50)$$

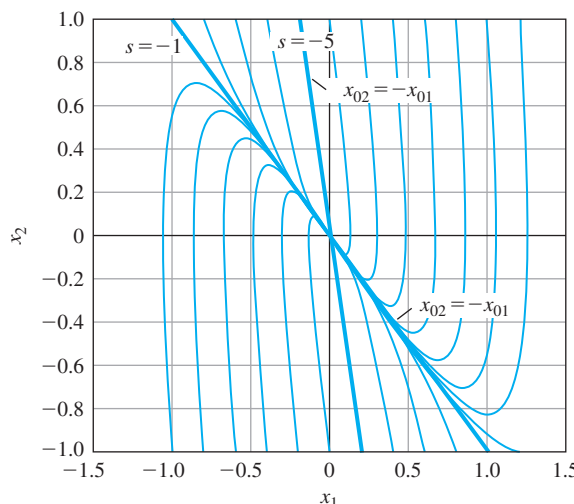
and, in this case, the solution for the eigenvector is  $x_{02} = -5x_{01}$ .

Consider what all this means. We started with the assumption that the time solution for the state is a constant times an exponential. We found that this is possible only if the exponential is either  $e^{-t}$  or  $e^{-5t}$ . In the first case, the state *must* lie along the vector  $x_{02} = -x_{01}$ , and in the second, the state *must* lie along the vector  $x_{02} = -5x_{01}$ . With this knowledge, we compute the solutions to Eq. (9.38) and Eq. (9.39) for different initial conditions and plot  $x_1(t)$  versus  $x_2(t)$  in Fig. 9.40. In the figure, the two eigenvectors are identified by the thick lines. When we look at these curves, it is clear that all the paths start parallel to the (fast!) eigenvector corresponding to  $s = -5$ , and quickly move to the (slow!) one corresponding to  $s = -1$ . All trajectories approach the equilibrium point at the origin of the state space.

The plot will be substantially changed if the amplifier saturates. For example, if the amplifier saturates at a value of  $u = 0.5$ , then the velocity,  $x_2$ , will rapidly approach this value and will be stuck there until the position reaches a value that brings the amplifier out of saturation. The new plot is shown in Fig. 9.41.

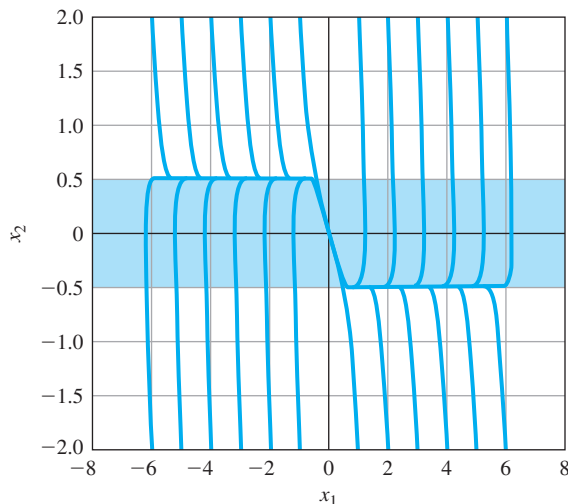
**Figure 9.40**

Phase-plane plot of a system with poles at  $s = -1$  and  $s = -5$

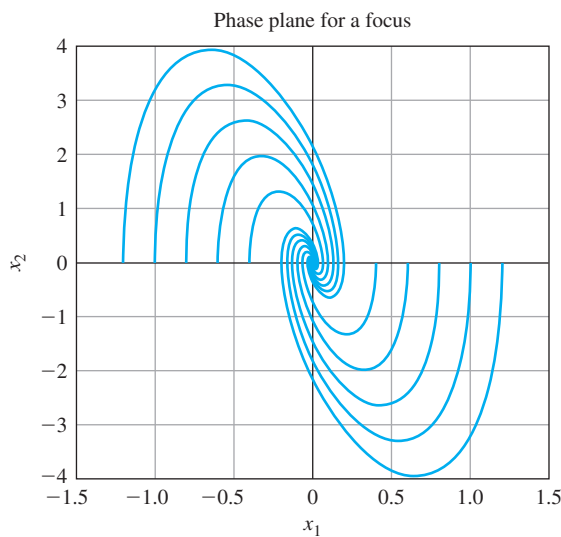


**Figure 9.41**

Phase-plane plot with saturation

**Figure 9.42**

Phase-plane plot for a system with complex poles



Notice in the linear region the motion is almost entirely along the slow eigenvector. Finally, we note the phase-plane portrait changes again when the poles are complex. In that case, the motion of the state variables are composed of damped sinusoids and the plot of  $x_1$  versus  $x_2$  is along a spiral. A collection of trajectories for various initial conditions is shown in Fig 9.42.

These few examples just scratch the surface of phase-plane analysis but give some idea of the use of this format in helping a designer to visualize dynamic responses. Note this visualization is mostly useful for systems with two (dominant) modes. For higher order systems, the concept still holds, but visualization becomes significantly more difficult.

### Bang-Bang Control

One example of design for a nonlinear system based on the phase plane is that of optimal minimum-time control in the face of control saturation. For our purposes here, the simplest version of this widely used technique is introduced: that of the  $1/s^2$  plant. The equations are

$$\ddot{y} = u, \quad (9.51)$$

$$e = y - y_f, \quad (9.52)$$

where  $y(0) = \dot{y}(0) = 0$ ,  $y_f$  is a constant, and the control is constrained to be  $|u| \leq 1$ . The problem is to drive the error to be identically zero in minimum time. If we define state variables as  $x_1 = e$  and  $x_2 = \dot{e} = \dot{y}$ , the equations reduce to

$$\dot{x}_1 = x_2, \quad (9.53)$$

$$\dot{x}_2 = u, \quad (9.54)$$

$$x_1(0) = -y_f, \quad (9.55)$$

$$x_1(t_f) = x_2(t_f) = 0, \quad (9.56)$$

and the problem is to minimize  $t_f$ . Intuitively, this is the problem of the eager driver who wishes to speed from one stop to the next in minimum time. She would put the pedal to the metal for a time then switch to stand on the brakes as the car skids to a stop at just the right place. A basic result of the theory of optimal control confirms this intuitive idea that the solution to this problem is, if  $y_f > 0$ , to apply full positive control for a time, then to switch to full negative control at just the right time to cause the error to reach the origin and stop there. To study the case, a plot of the trajectories of the plant in the phase plane for the two cases of  $u = 1$  and  $u = -1$  is given in Fig. 9.43. For  $u = +1$ , the

**Figure 9.43**

Phase-plane of the  $1/s^2$  plant for  $\pm 1$  controls

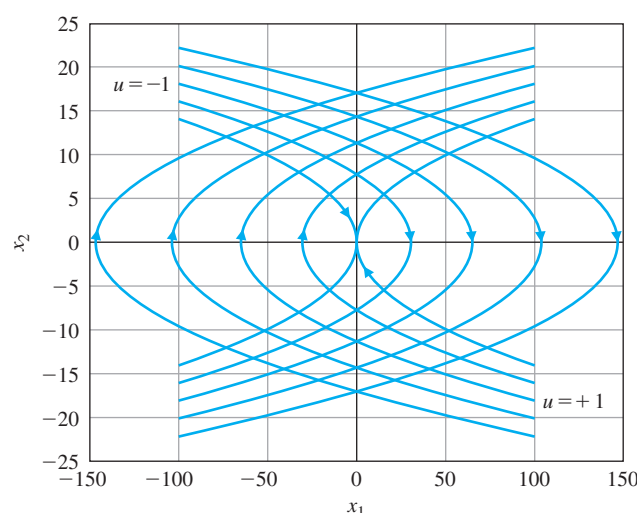
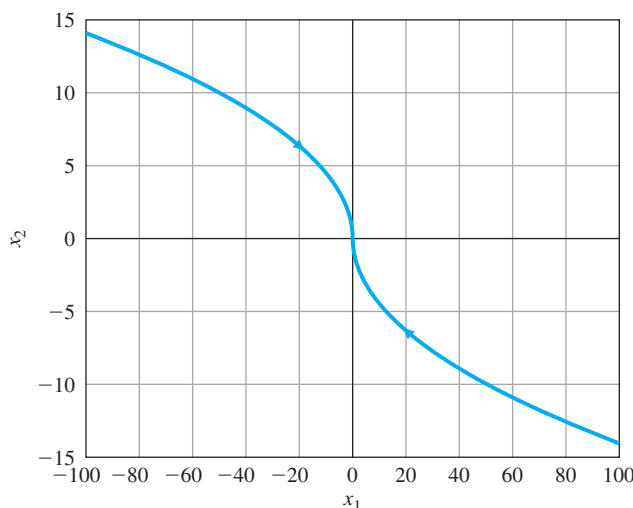


**Figure 9.44**

Switching curve for the  $1/s^2$  plant



trajectories start in the fourth quadrant and move up to the first. For  $u = -1$ , they start in the second quadrant and move down to the third.

Two segments of this family are of particular interest: those that pass through the origin. Once the path reaches one of these, a constant control will bring the state to the desired final resting place. Therefore, for any initial condition, once the trajectory reaches one of the two curves going through the origin, the correct action is to switch the control ( $u = +1$  to  $-1$ , or  $u = -1$  to  $+1$ ) so the trajectory will follow that curve to the origin. The “switching curve” is plotted in Fig. 9.44.

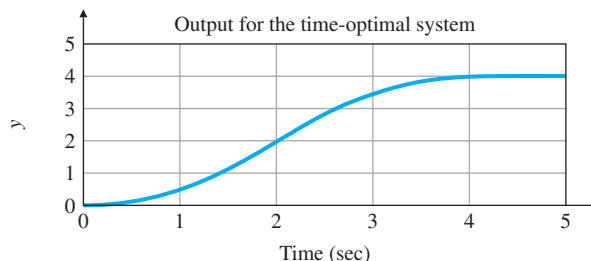
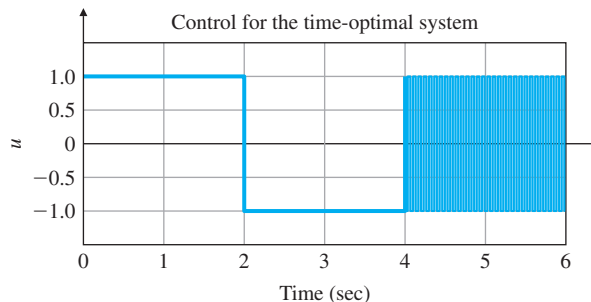
For a second-order plant, the switching curve can be found by reversing the time in the equations of motion, setting the initial state to zero and applying the maximum control. The process can be repeated with minimum control to sweep out the other branch of the curve.

For any initial condition above the curve,  $u = -1$  is applied and for any initial condition below the curve,  $u = +1$  is used. As described, the result will be a minimum-time response. Notice the curve has vertical slope at the origin; as a result, the implementation is extremely sensitive in this neighborhood. A modified version known as the proximate time-optimal system (PTOS) used in the computer disk drive industry was studied by Workman (1987). The modification consists of shifting the curves a bit and replacing the infinite slope at the origin with a finite-slope, linear control region. The result has been widely used for hard-disk drives and similar systems, and is also called “sliding mode” control.

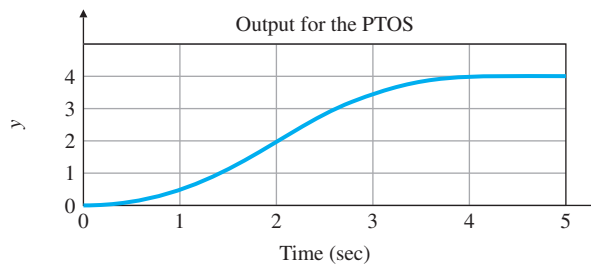
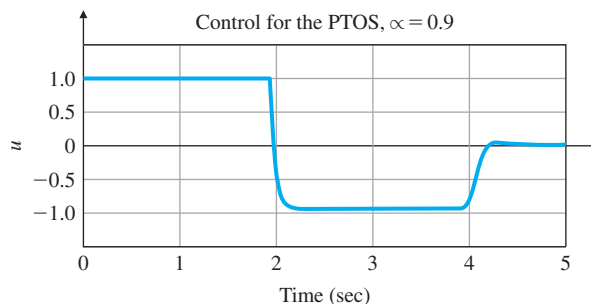
Typical responses for a time-optimal system and for a PTOS system generated with Simulink are given in Figs. 9.45 to 9.47. Notice the response times are almost exactly the same, but while the time-optimal system control has a violent chatter at the end where the switching curve has infinite slope, the output of the PTOS system slips into its final value

**Figure 9.45**

Response of a time-optimal system

**Figure 9.46**

Response of a PTOS system



smoothly. For a more exact study, we need to turn to the nonlinear equations.

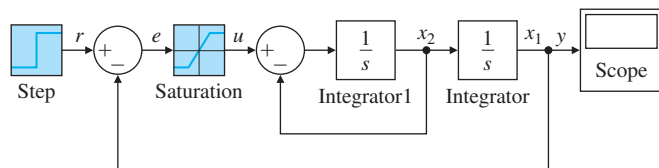
### 9.5.2 Lyapunov Stability Analysis

The stability of motion as studied by Lyapunov involves sophisticated mathematics beyond the scope of this text. Here we will present heuristic arguments giving the flavor of the theory and state a few of the most

**Figure 9.47**

Simulink diagram for position feedback system

*Source: Reprinted with permission of The MathWorks, Inc.*



basic results. Lyapunov presented two methods for the study of stability of motion described by systems of ODEs. His indirect or **first method** is based on linearization of the equations and drawing conclusions about the stability of the nonlinear system by considering the stability of the linear approximation. He proved the results of the first method by use of his direct or **second method**, in which the nonlinear equations are considered directly. A discussion of the indirect method serves to introduce both methods. The problem requires a new definition of stability suitable for vector-matrix equations. Intuitively, we say a system is stable if initial conditions of moderate size result in a response that remains of moderate size. To express this mathematically, first we need a definition of "size." For this, we use the norm of a vector for which the symbol is  $\|\mathbf{x}\|$ . Of the many possible definitions, the familiar Euclidean measure is selected and defined by its square as  $\|\mathbf{x}\|^2 = \mathbf{x}^T \mathbf{x} = \sum_{i=1}^n x_i^2$ . With this idea, the definition of stability used is that if one is given a sphere of any radius  $\epsilon$ , one can find a smaller sphere of radius  $\delta$  such that if the initial state is inside  $\delta$ , then the trajectory will, for all time, remain inside  $\epsilon$ . A bit more formally, the system is **stable** if, for any given  $\epsilon > 0$ , one can find a  $\delta > 0$  such that if  $\|\mathbf{x}(0)\| < \delta$ , then  $\|\mathbf{x}(t)\| < \epsilon$  for all  $t$ . If the state is not only stable, but in the limit as  $t \rightarrow \infty$ ,  $\|\mathbf{x}(t)\| \rightarrow 0$ , the system is said to be **asymptotically stable**. If, for any  $\epsilon$ , it is possible to select  $\delta$  arbitrarily large, then the system is said to be **stable in the large**.

Study of these matters begins with the time-invariant ODE equation

$$\dot{\mathbf{x}} = \mathbf{f}(\mathbf{x}), \quad (9.57)$$

for which the linear approximation is

$$\dot{\mathbf{x}} = \mathbf{A}\mathbf{x} + \mathbf{g}(\mathbf{x}). \quad (9.58)$$

In this equation, it is assumed all the linear terms are in  $\mathbf{A}\mathbf{x}$  and higher-order terms are in  $\mathbf{g}(\mathbf{x})$ , in the sense that when  $\mathbf{x}$  gets small,  $\mathbf{g}(\mathbf{x})$  gets small faster, as expressed by

$$\lim_{\|\mathbf{x}\| \rightarrow 0} \frac{\|\mathbf{g}(\mathbf{x})\|}{\|\mathbf{x}\|} = 0. \quad (9.59)$$

Lyapunov's second method begins with the intuitive notion that one measure of the size of the state of a physical system is the total energy stored in the system at any instant, and the observation that when the stored energy is no longer changing, the system must be at rest. For an electric circuit, for example, the electric energy is proportional to the square of the capacitor voltages and the magnetic energy is proportional to the square of the inductor currents. Lyapunov extracted the

**Stability in the sense of Lyapunov**

**Lyapunov function**

abstract essence of this idea and defined a scalar function of the state  $V(\mathbf{x})$ , called a Lyapunov function, having the following properties:

1.  $V(\mathbf{0}) = 0$ ;
2.  $V(\mathbf{x}) > 0$ ,  $\|\mathbf{x}\| \neq 0$ ;
3.  $V$  is continuous and has continuous derivatives with respect to all components of  $\mathbf{x}$ ;
4.  $\dot{V}(\mathbf{x}) = \frac{\partial V}{\partial \mathbf{x}} \dot{\mathbf{x}} = \frac{\partial V}{\partial \mathbf{x}} \mathbf{f}(\mathbf{x}) \leq 0$  along trajectories of the equation.

The first three conditions ensure that in a neighborhood of the origin the function is like a smooth bowl sitting at the origin of the state space. The fourth condition, which obviously depends on the equations of motion, ensures that if  $\delta$  is selected so the initial conditions are deeper in the bowl than any part of the ball defined by  $\epsilon$ , the trajectory never climbs higher on the bowl than it was at the start and so remains within  $\epsilon$ , and the system will be stable. Furthermore, if condition 4 is strengthened to be  $V(\mathbf{x}) < 0$ , then the value of the function must fall to zero and, by condition 1, the state also goes to zero. The stability theorem, which is the basis for Lyapunov's second method, states that

**Lyapunov's second method**

If a Lyapunov function can be found for a system, then the motion is stable and, furthermore, if  $V(\mathbf{x}) < 0$ , the motion is asymptotically stable. The second method is to search for a Lyapunov function.

The hard part for the application of this theory is the statement "If a Lyapunov function can be found." Only in the linear case is a prescription given for finding a Lyapunov function; otherwise the theory only gives the engineer a hunting license to look for such a function. We are now in a position to consider the indirect method for stability of Eq. (9.58).

Perhaps because energy in simple systems is a sum of the squares of the variables, for this problem, Lyapunov considers a quadratic candidate for  $V$  by assuming that a symmetric positive definite matrix  $\mathbf{P}$  can be found and the function defined as  $V(\mathbf{x}) = \mathbf{x}^T \mathbf{P} \mathbf{x}$ . Clearly the first three conditions are satisfied by this function; the fourth condition must be tested before it can be concluded that we have a Lyapunov function. The calculation of  $\dot{V}$  is

$$V(\mathbf{x}) = \mathbf{x}^T \mathbf{P} \mathbf{x}, \quad (9.60)$$

$$\dot{V}(\mathbf{x}) = \dot{\mathbf{x}}^T \mathbf{P} \mathbf{x} + \mathbf{x}^T \mathbf{P} \dot{\mathbf{x}} \quad (9.61)$$

$$= (\mathbf{A}\mathbf{x} + \mathbf{g}(\mathbf{x}))^T \mathbf{P} \mathbf{x} + \mathbf{x}^T \mathbf{P} (\mathbf{A}\mathbf{x} + \mathbf{g}(\mathbf{x})) \quad (9.62)$$

$$= \mathbf{x}^T (\mathbf{A}^T \mathbf{P} + \mathbf{P} \mathbf{A}) \mathbf{x} + 2\mathbf{x}^T \mathbf{P} \mathbf{g}(\mathbf{x}). \quad (9.63)$$

A basic matrix result, known as a Lyapunov equation, is

$$\mathbf{A}^T \mathbf{P} + \mathbf{P} \mathbf{A} = -\mathbf{Q}, \quad (9.64)$$

and he showed that if  $\mathbf{A}$  is a stability matrix having all its eigenvalues in the LHP, then for *any* positive definite matrix  $\mathbf{Q}$ , the solution  $\mathbf{P}$  of this equation will also be positive definite. The argument from here is to select  $\mathbf{Q}$  and solve for  $\mathbf{P}$ . Then, if the eigenvalues of  $\mathbf{A}$  are in the LHP,  $\mathbf{P}$  will be positive definite, so  $V(\mathbf{x})$  is a possible Lyapunov function and

$$\dot{V}(\mathbf{x}) = -\mathbf{x}^T \mathbf{Q} \mathbf{x} + 2\mathbf{x}^T \mathbf{P} \mathbf{g}. \quad (9.65)$$

The final part of the argument is to note that, by Eq. (9.59), if  $\mathbf{x}$  is small enough, then the first term of Eq. (9.65) will dominate, the fourth condition is satisfied,  $V$  is a Lyapunov function, and the system has been proven to be stable. Note the requirement that  $\mathbf{x}$  be small enough guarantees only that there is a *neighborhood* of the origin which is stable. Further conditions are needed to show that the bowl defined by  $V$  extends to  $\infty$  in all directions as  $\|\mathbf{x}\|$  tends to  $\infty$  (and not before!), so stability holds for all states and is “in the large.”

There is also an instability theorem which shows that if *any* eigenvalue of  $\mathbf{A}$  is in the RHP, then the origin will be unstable. If all the poles of  $\mathbf{A}$  are in the LHP except for some simple poles on the imaginary axis, then stability depends on further properties of the nonlinear terms,  $\mathbf{g}(\mathbf{x})$ . With this result in hand, the first or indirect method of Lyapunov can be stated:

1. Find the linear approximation and compute the eigenvalues of  $\mathbf{A}$ .
2. If all the eigenvalues are in the LHP, then there is a region of stability about the origin.
3. If at least one of the eigenvalues is in the RHP, then the origin is unstable.
4. If there are simple eigenvalues on the imaginary axis and all other values are in the LHP, then no statement about stability can be made based on this method.

#### Lyapunov's first method

### EXAMPLE 9.15

#### *Lyapunov Stability for a Second-Order System*

Use Lyapunov's method to find conditions for the stability of a second-order linear system described by the state matrix

$$\mathbf{A} = \begin{bmatrix} -\alpha & \beta \\ -\beta & -\alpha \end{bmatrix}.$$

**Solution.** For the linear case, we can take any positive definite  $\mathbf{Q}$  we like; the simplest is  $\mathbf{Q} = \mathbf{I}$ . The corresponding Lyapunov equation is

$$\begin{bmatrix} -\alpha & -\beta \\ \beta & -\alpha \end{bmatrix} \begin{bmatrix} p & q \\ q & r \end{bmatrix} + \begin{bmatrix} p & q \\ q & r \end{bmatrix} \begin{bmatrix} -\alpha & \beta \\ -\beta & -\alpha \end{bmatrix} = \begin{bmatrix} -1 & 0 \\ 0 & -1 \end{bmatrix}. \quad (9.66)$$

Multiplying out Eq. (9.66) and equating coefficients, we get

$$-\alpha p - \beta q - \alpha p - \beta q = -1, \quad (9.67)$$

$$-\alpha q - \beta r + \beta p - \alpha q = 0, \quad (9.68)$$

$$\beta q - \alpha r + \beta q - \alpha r = -1. \quad (9.69)$$

Equations (9.67) to (9.69) are readily solved to get  $p = r = 1/2\alpha$ ,  $q = 0$ , so

$$\mathbf{P} = \begin{bmatrix} \frac{1}{2\alpha} & 0 \\ 0 & \frac{1}{2\alpha} \end{bmatrix},$$

and the determinants are  $1/2\alpha > 0$  and  $1/4\alpha^2 > 0$ . Thus  $\mathbf{P} > 0$ , so we conclude that the system is stable if  $\alpha > 0$ .

For systems with many state variables and nonnumeric parameters, solution of the Lyapunov equation can be burdensome, but the result is an equivalent alternative to Routh's method for computing the conditions for stability in a system with literal parameters.

### EXAMPLE 9.16

#### *Lyapunov's Direct Method for a Position Feedback System*

Consider the position feedback system modeled in Fig. 9.39. Illustrate the use of the direct method on this nonlinear system. Simulate the system using Simulink, assuming  $T = 1$ , and evaluate the step response of the system.

**Solution.** We assume the actuator, which is perhaps only an amplifier in this case, has a significant nonlinearity, which is shown in the figure as a saturation but is possibly more complex. We will assume only that  $u = f(e)$ , where the function lies in the first and third quadrants so that  $\int_0^e f(e) de > 0$ . We also assume  $f(e) = 0$  implies that  $e = 0$ , and we will assume  $T > 0$ , so the system is open-loop stable. The equations of motion are

$$\dot{e} = -x_2, \quad (9.70a)$$

$$\dot{x}_2 = -\frac{1}{T}x_2 + \frac{f(e)}{T}. \quad (9.70b)$$

For a Lyapunov function, consider something like kinetic plus potential energy:

$$V = \frac{T}{2}x_2^2 + \int_0^e f(\sigma) d\sigma. \quad (9.71)$$

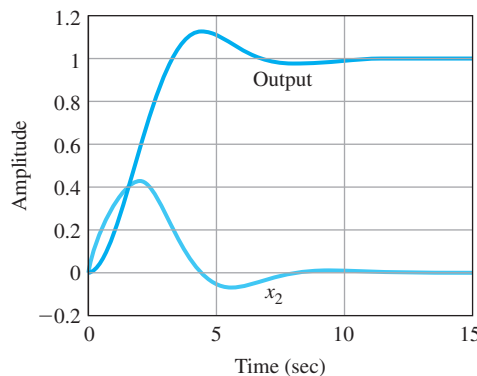
Clearly,  $V = 0$  if  $x_2 = e = 0$  and, because of the assumptions about  $f$ ,  $V > 0$  if  $x_2^2 + e^2 \neq 0$ . To see whether the  $V$  in Eq. (9.71) is a Lyapunov function, we compute  $\dot{V}$  as follows:

$$\begin{aligned} \dot{V} &= Tx_2\dot{x}_2 + f(e)\dot{e} \\ &= Tx_2\left[-\frac{1}{T}x_2 + \frac{f(e)}{T}\right] + f(e)(-x_2) \\ &= -x_2^2. \end{aligned}$$

Hence  $\dot{V} \leq 0$  and the origin is Lyapunov stable. Moreover,  $\dot{V}$  is always decreasing if  $x_2 \neq 0$ , and Eq. (9.70b) indicates that the system has no trajectory with  $x_2 \equiv 0$ , except  $x_2 = 0$ . Thus we can conclude that the system is asymptotically stable for every  $f$  that satisfies two conditions:

**Figure 9.48**

Step response for position control system



(1)  $\int f d\sigma > 0$  and (2)  $f(e) = 0$  implies that  $e = 0$ . The Simulink diagram for the system is shown in Fig. 9.47 for  $T = 1$ . The step response of the system is shown in Fig. 9.48.

As we mentioned earlier, the study of the stability of nonlinear systems is vast, so we have only touched here on some important points and methods. Further material for study can be found in LaSalle and Lefschetz (1961), Kalman and Bertram (1960), Vidyasagar (1993), Khalil (2002), and Sastry (1999).

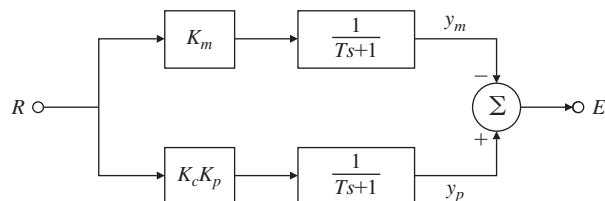
### *Lyapunov Redesign of Adaptive Control*

One of the classical applications of Lyapunov stability theory to control is a technique known as Lyapunov redesign. The idea is to construct the system with some key control parameters unspecified, propose a candidate Lyapunov function, then select the available components to force the candidate to succeed and be an actual Lyapunov function from which stability can be concluded. The method was applied in an early paper by Parks (1966) to a model reference adaptive control system. A block diagram of the simple system first considered is drawn in Fig. 9.49.

In this system, the model and the plant have the same dynamics but different gains. The objective is to adjust the control gain,  $K_c$ , so  $K_c K_p = K_m$ , and the plant output,  $y_p$ , will equal the model output,  $y_m$ . A proposed heuristic rule, known as the “MIT” rule, was based on the

**Figure 9.49**

Block diagram of a simple model reference adaptive control system



idea that if we define the cost as the square of the instantaneous error and move  $K_c$  so as to make this cost smaller, the result should drive  $K_c$  to the right value. If the gradient of the cost is positive (pointing uphill, so to speak), the gain should be reduced, and if the gradient is negative, the gain should be increased. Thus the time derivative of the gain should be proportional to the *negative* of the gradient. In equation form,

$$J = e^2, \quad (9.72)$$

$$\frac{\partial J}{\partial K_c} = 2e \frac{\partial e}{\partial K_c}, \quad (9.73)$$

$$\frac{dK_c}{dt} = -Be \frac{\partial e}{\partial K_c}, \quad (9.74)$$

where  $B$  is the “adaptive gain” to be chosen. From the block diagram,

$$E(s) = \frac{K_c K_p - K_m}{Ts + 1} R(s), \quad (9.75)$$

$$\frac{\partial E}{\partial K_c} = \frac{K_p}{Ts + 1} R \quad (9.76)$$

$$= \frac{K_p}{K_m} Y_m. \quad (9.77)$$

If we substitute the result of Eq. (9.77) into Eq. (9.74), the result is the MIT rule,

$$\frac{dK_c}{dt} = -B' e Y_m, \quad (9.78)$$

where there is a new adaptive gain,  $B'$ . Unfortunately, the stability of this rule is not established, and some analysis showed that it could be unstable under reasonable circumstances, such as if there are unmodeled dynamics or disturbances. Parks proposed that Lyapunov redesign would be a better idea and also proposed that, rather than taking  $\dot{K}_c$  given by Eq. (9.74), this choice be made in a way that guarantees stability. His idea begins with the differential equations where  $r = r_o$  is a constant:

$$T\dot{e} + e = (K_c K_p - K_m)r_o, \quad (9.79)$$

$$\dot{K}_c = -B' e Y_m. \quad (9.80)$$

To simplify things, the definition is made that  $x = (K_c K_p - K_m)$  and  $\dot{x}$  is to be found. Parks selects  $V = e^2 + \lambda x^2$  as a candidate Lyapunov function and computes

$$\dot{V} = 2e\dot{e} + 2\lambda x\dot{x} \quad (9.81)$$

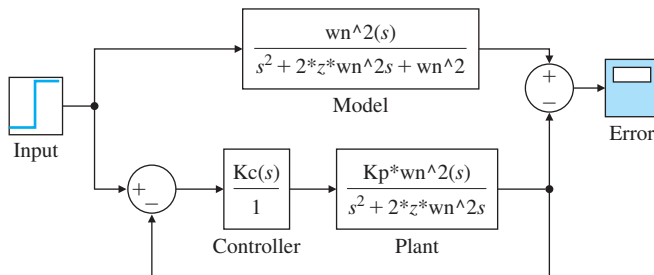
$$= 2e \left( \frac{xr_o}{T} - \frac{e}{T} \right) + 2\lambda x\dot{x}. \quad (9.82)$$

If  $\dot{x}$  in the last equation is selected to be  $\dot{x} = -\frac{er_o}{\lambda T}$ , then  $\dot{V} = -2\frac{e^2}{T}$ , the conditions for a Lyapunov function are satisfied, and stability is assured for the given assumptions. Working back, we find that the new algorithm is

$$\dot{K}_c = -B'' e r_o. \quad (9.83)$$

**Figure 9.50**

Block diagram of adaptive control of a motor



Obviously, this result does not address issues arising from unmodeled dynamics or disturbances, but the principle is clear: Leaving key control equations to be defined so as to obtain a Lyapunov function can put the stability of a system on a firm foundation.

As a second example of Lyapunov redesign, consider the adaptive control of a motor shown in Fig. 9.50. Defining the model output as  $y_m$  and the plant output as  $y_p$ , the equations are

$$\ddot{y}_m + 2\zeta\omega_n\dot{y}_m + \omega_n^2 y_m = \omega_n^2 r, \quad (9.84)$$

$$\ddot{y}_p + 2\zeta\omega_n\dot{y}_p + \omega_n^2 y_p = K_c K_p \omega_n^2 (r - y_p) + \omega_n^2 y_p. \quad (9.85)$$

(In the equation for  $y_p$ , the term  $\omega_n^2 y_p$  has been added to both sides to make the error equation simpler.) The error is defined as  $e = y_m - y_p$  and an equation for error can be obtained by subtracting the equation for  $y_p$  from that for  $y_m$ . The result is

$$\ddot{e} + 2\zeta\omega_n\dot{e} + \omega_n^2 e = \omega_n^2 (1 - K_c K_p)(r - y_p). \quad (9.86)$$

The idea now is to find an equation for  $K_c$  that will result in a Lyapunov function for the error equation. To simplify the calculation, we define the parameter  $x = 1 - K_c K_p$ , for which  $\dot{x} = -K_p \dot{K}_c$  and in terms of which the error equation is

$$\ddot{e} + 2\zeta\omega_n\dot{e} + \omega_n^2 e = \omega_n^2 x(r - y_p). \quad (9.87)$$

At this point, Parks suggests consideration of  $V = e^2 + \alpha\dot{e}^2 + \beta x^2$  as a possible function. We need to find  $\dot{x}$  so this  $V$  will be a Lyapunov function. The equation for the derivative is

$$\dot{V} = 2e\dot{e} + 2\alpha\dot{e}\ddot{e} + 2\beta x\dot{x} \quad (9.88)$$

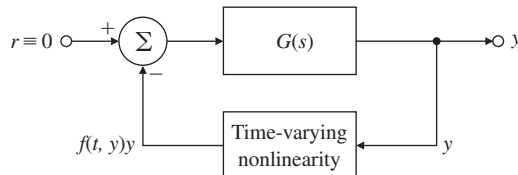
$$= 2e\dot{e} + 2\alpha\dot{e}\{-2\zeta\omega_n\dot{e} - \omega_n^2 e + \omega_n^2 x(r - y_p)\} + 2\beta x\dot{x} \quad (9.89)$$

$$= -4\alpha\zeta\omega_n\dot{e}^2 + 2e\dot{e}(1 - \alpha\omega_n^2) + x\{2\alpha\dot{e}\omega_n^2(r - y_p) + 2\beta\dot{x}\}. \quad (9.90)$$

If we take  $1 - \alpha\omega_n^2 = 0$  and  $2\alpha\dot{e}\omega_n^2(r - y_p) + 2\beta\dot{x} = 0$ , then the equation for  $\dot{V}$  simplifies to  $\dot{V} = -4\alpha\zeta\omega_n\dot{e}^2$ , which is always negative, and  $V$  is a Lyapunov function and the system is stable. Substituting for  $x$ , we get the adaptive control law

**Figure 9.51**

Block diagram of a nonlinear system



$$\dot{K}_c = -\beta' \dot{e}(r - y_p), \quad (9.91)$$

where  $\beta'$  is a new constant equal to  $\frac{\alpha\omega_n^2}{K_p\beta}$ . Clearly, we have only touched on Lyapunov's theory of stability, and our examples of redesign are ancient history from 1966, but they illustrate the principle very well and give a good start to further study of this important area.

### 9.5.3 The Circle Criterion

A nonlinear system with only one single-input–single-output nonlinearity may be represented as shown in Fig. 9.51 by drawing the block diagram from the points of the input and output of the nonlinearity. In the literature, this is referred to as the Lur'e problem after the Soviet scientist who first studied it.

We assume the system is unforced and thus  $r \equiv 0$ . It is possible to derive a graphical sufficient condition for stability of such systems. Even though this method is practical, it may lead to conservative results in some cases, although extensions exist that yield less conservative results (see Safonov and Wyetzner 1987). First, we define sector conditions for memoryless nonlinearities.

#### *Sector Conditions*

A function  $f(x)$  with a scalar input and a scalar output belongs to the sector  $[k_1, k_2]$  if, for all inputs  $x$ ,

$$k_1 x^2 \leq f(x)x \leq k_2 x^2. \quad (9.92)$$

This relationship may be rewritten as

$$k_1 \leq \frac{f(x)}{x} \leq k_2, \quad x \neq 0. \quad (9.93)$$

Basically, the definition says that the graph of  $f(x)$  lies between two straight lines of slopes  $k_1$  and  $k_2$  going through the origin, as shown in Fig. 9.52. In this definition,  $k_1$  and  $k_2$  are allowed to be  $-\infty$  or  $+\infty$ . Note that the sector conditions place no limits on the incremental gain or slope of the function  $f(x)$ . The ensuing examples illustrate how  $k_1$  and  $k_2$  are determined.

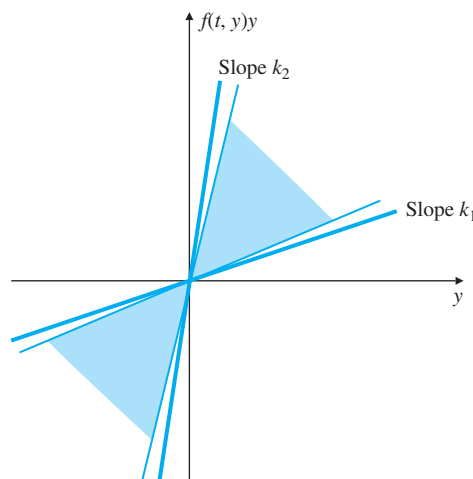
### EXAMPLE 9.17

#### *Computation of a Sector for Signum Nonlinearity*

Determine a sector that contains the signum function  $y = f(u)$ , shown in Fig. 9.6(b).

**Figure 9.52**

Output of the nonlinearity confined in a sector



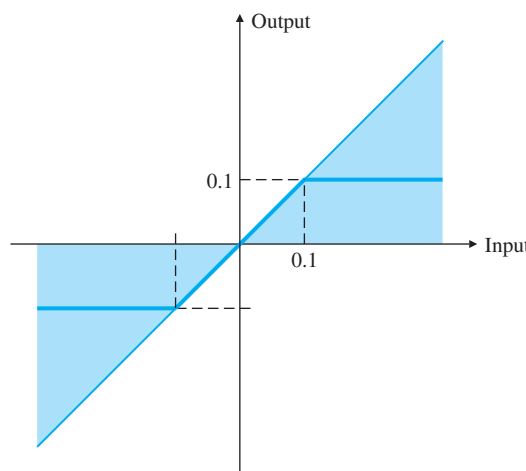
**Solution.** Since  $\text{sgn}(0) = 0$ , we know the only line going through the origin that bounds the signum function from above is the  $y$ -axis, corresponding to a slope of  $k_2 = \infty$ . Similarly, the line going through the origin that bounds the signum function from below has a slope of zero and corresponds to the  $x$ -axis; therefore,  $k_1 = 0$ . Hence, the sector for the signum function is  $[0, \infty]$ .

**EXAMPLE 9.18***Sector for a Saturation Nonlinearity*

Consider the saturation nonlinearity shown in Fig. 9.53. Determine a sector for this function.

**Figure 9.53**

Sector for saturation



**Solution.** The function is bounded above by a line of slope 1,  $k_2 = 1$ , and is bounded below by the  $x$ -axis,  $k_1 = 0$ , as shown in the figure. Therefore, the sector for this function is  $[0, 1]$ .

---

### Circle Criterion

In 1949, the Russian scientist Aizermann conjectured that if a Lur'e system is stable with  $f$  replaced by any linear gain between the limits  $k_1 < k < k_2$ , then the system will be stable, with the gain replaced by a nonlinearity in the sector  $[k_1, k_2]$ . That means if a single-loop (strictly proper) continuous-time feedback system as shown in Fig. 9.51 with a linear forward path (**A**, **B**, **C**) is stable for all linear fixed feedback gains  $k$  in the range  $k_1 < k < k_2$ , such that the resultant closed-loop system matrix  $\mathbf{A} + k\mathbf{BC}$  is stable, then the nonlinear system having a memoryless nonlinear time-varying feedback term  $f(t, y)$  in the sector  $[k_1, k_2]$ , shown in Fig. 9.51, is also stable. Unfortunately, this conjecture is *not* true as counterexamples exist.<sup>7</sup> However, a variation of Aizermann's conjecture *is* true and is known as the circle criterion.

Rather than giving a rigorous proof of the criterion, we describe a heuristic argument that gives insight into the problem and motivates the proof. An electric circuit with a linear impedance,  $Z(j\omega) = R(\omega) + jX(\omega)$ , is described by Ohm's law as  $V = IZ(s)$ . We assume  $Z$  is composed of real components, which means that the real part  $R$  is even and the imaginary part  $X$  is odd; that is  $R(-\omega) = R(\omega)$  and  $X(-\omega) = -X(\omega)$ . If  $R(\omega) \geq \delta > 0$  for all  $\omega$ , the impedance is called strictly passive. It will dissipate energy. The instantaneous power *into* the circuit is  $p = v(t)i(t)$ , and the total energy absorbed by the circuit is  $e = \int_0^\infty v(t)i(t) dt$ . Referring to the figure, Ohm's law is equivalent to the plant equation  $Y = UG(s)$  with  $Y$  as voltage,  $U$  as current, and  $G(s) = R + jX$  as the impedance. Applying the expression for energy to the plant equation and using the theorem by Parseval<sup>8</sup> to convert this to the frequency domain yields

$$\int_0^\infty y(t)u(t) dt = \frac{1}{2\pi} \int_{-\infty}^\infty U(j\omega) Y(-j\omega) d\omega \quad (9.94)$$

$$= \frac{1}{2\pi} \int_{-\infty}^\infty U(j\omega) U(-j\omega) G(-j\omega) d\omega \quad (9.95)$$

$$= \frac{1}{2\pi} \int_{-\infty}^\infty |U(j\omega)|^2 (R - jX) d\omega \quad (9.96)$$

$$= \frac{1}{2\pi} \int_{-\infty}^\infty |U(j\omega)|^2 R(\omega) d\omega. \quad (9.97)$$

---

<sup>7</sup>Aizermann's conjecture spurred a lot of research in this area and led to the development of the Kalman–Yakubovich–Popov lemma, giving state-space conditions for a passive system. The lemma is used in a proof of the circle criterion.

<sup>8</sup>See Appendix A.

In the last step, the fact that  $X$  is odd was used. At this point, the use of more or less conventional notation will simplify the equations substantially. We define inner products and norms as

$$\int_0^\infty y(t)u(t) dt = \langle y, u \rangle, \quad (9.98)$$

$$\|u\|^2 = \int_0^\infty [u(t)]^2 dt = \langle u, u \rangle. \quad (9.99)$$

With this notation, and with the assumption that  $R \geq \delta > 0$ , Eq. (9.97) is reduced to

$$\langle y, u \rangle \geq \delta \|u\|^2. \quad (9.100)$$

Turning now to the nonlinear component, using the same concept of “energy” and assuming that  $f$  is in the sector  $[0, K]$ , we have

$$\int_0^\infty y(t)f(y, t) dt = \int_0^\infty \frac{[f(y, t)]^2}{y(t)} dt \quad (9.101)$$

$$\geq \frac{\|f(y, t)\|^2}{K} \quad (9.102)$$

$$\geq \frac{\|u(t)\|^2}{K}. \quad (9.103)$$

The assumption now is that if the total energy given by the sum of Eq. (9.100) and Eq. (9.102) is positive, then the system *must be stable*, as energy is being steadily lost. The actual value of the energy lost would be equal to the initial energy stored in the elements of the system. From this one would conclude that if  $\delta \|u\|^2 + \frac{\|u(t)\|^2}{K} > 0$ , then the system is stable. Thus, the criterion is

$$\delta \|u\|^2 + \frac{\|u(t)\|^2}{K} > 0, \quad (9.104)$$

$$\left[ \operatorname{Re}\{G(j\omega)\} + \frac{1}{K} \right] \|u(t)\|^2 > 0, \quad (9.105)$$

$$\operatorname{Re}\{KG(j\omega) + 1\} > 0. \quad (9.106)$$

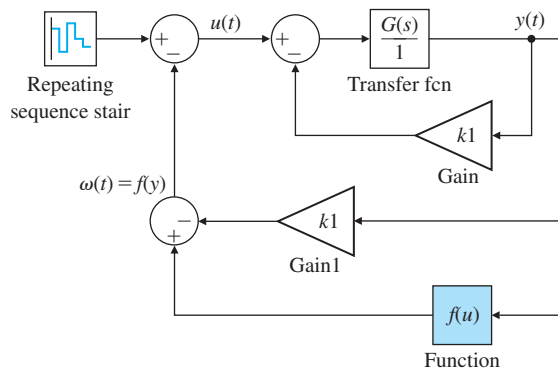
In deriving Eq. (9.106), the assumption was made that the nonlinearity was in a zero sector,  $[0, K]$ . If the function is actually in the sector  $[k_1, k_2]$ , it can be reduced to a zero sector by adding and subtracting  $k_1$  in the block diagram as shown in Fig. 9.54. With this change, the dynamic system is replaced by  $H = \frac{G}{1+k_1G}$  and the function by  $f' = f - k_1$ , which is in the sector  $[k_2 - k_1, 0]$ . With these changes, the stability criterion is transformed to

$$\operatorname{Re} \left\{ 1 + (k_2 - k_1) \frac{G}{1+k_1G} \right\} > 0, \quad (9.107)$$

$$\operatorname{Re} \left\{ \frac{1 + k_1G + (k_2 - k_1)G}{1+k_1G} \right\} > 0, \quad (9.108)$$

**Figure 9.54**

Block diagram manipulation for sector



$$\operatorname{Re} \left\{ \frac{1 + k_2 G(j\omega)}{1 + k_1 G(j\omega)} \right\} > 0. \quad (9.109)$$

A bilinear function such as  $F = \frac{1 + k_2 G(j\omega)}{1 + k_1 G(j\omega)}$  in Eq. (9.109) will map a circle in the  $F$  plane into another circle in the  $G$  plane (see Appendix WD, available online at [www.pearsonglobaleditions.com](http://www.pearsonglobaleditions.com)). In this case, the acceptable region is  $\operatorname{Re}\{F\} > 0$ , of which the boundary is the imaginary axis, so the map is from the *imaginary* axis, a circle of infinite radius, into a finite circle. Because the functions are real, the circle must be centered on the real axis and we need only locate the two points on the real axis. For example, when  $F = 0$ , we have  $1 + k_2 G = 0$  or  $G = -\frac{1}{k_2}$ . The other point on the real axis is when the function is infinite, at which point  $1 + k_1 G = 0$  or  $G = -\frac{1}{k_1}$ . Thus the circle in the  $G$  plane is centered on the real axis and goes through the points  $\left[ -\frac{1}{k_2}, -\frac{1}{k_1} \right]$  as plotted in Fig. 9.55. Since  $F$  had to avoid the LHP, if we set  $F = -1$ , which is in the forbidden region, and solve, we find that  $G = \frac{-2}{k_1 + k_2}$ , which is *inside* the circle, from which we conclude that the system will be stable if the plot of  $G(j\omega)$  avoids this circle.

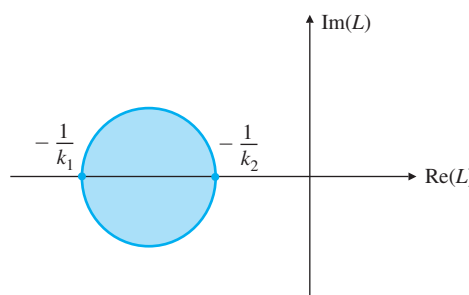
The actual theorem is as follows:

The nonlinear system described is asymptotically stable given that

1.  $f(t, y)$  lies in the sector  $[k_1, k_2]$  with  $0 \leq k_1 < k_2$  and

**Figure 9.55**

Illustration of circle criterion



2. the Nyquist plot of the transfer function  $G(j\omega) = \mathbf{C}(j\omega\mathbf{I} - \mathbf{A})^{-1}\mathbf{B}$  does not intersect or encircle the “critical circle,” which is centered on the real axis and passes through the two points  $-1/k_1$  and  $-1/k_2$ , as shown in Fig. 9.55.

### Circle criterion

In effect, the usual Nyquist “ $-1$ ” point is replaced by the critical disk. This result is known as the **circle criterion** or circle theorem and is due to Sandberg (1964) and Zames (1966). Note these conditions are *sufficient* but not necessary, because intersection of the transfer function  $G(s)$  with the circle as defined does not prove instability. The critical circle is centered at

$$c = \frac{1}{2} \left[ -\frac{1}{k_1} - \frac{1}{k_2} \right] = -\frac{k_1 + k_2}{2k_1 k_2},$$

and has a radius of

$$\frac{k_2 - k_1}{2k_1 k_2}.$$

If  $k_1 = 0$ , then the critical circle degenerates into a half plane defined by  $\text{Re}\{G\} \geq -1/k_2$ .

The circle criterion and the describing function are related. In fact, for the case of time-invariant odd nonlinearities that are within a sector and whose describing functions are real, the describing function satisfies the relationship

$$k_1 \leq K_{eq}(a) \leq k_2 \quad \text{for all } a, \quad (9.110)$$

so

$$-\frac{1}{k_1} \leq -\frac{1}{K_{eq}(a)} \leq -\frac{1}{k_2}, \quad (9.111)$$

and the plot of the negative reciprocal of the describing function will lie inside the critical circle. This can be seen by the following lower and upper bounds:

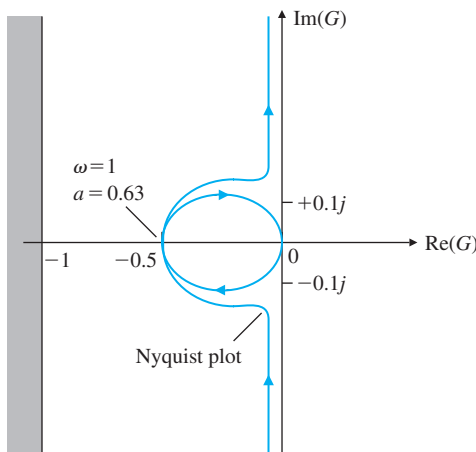
$$\begin{aligned} K_{eq}(a) &= \frac{2}{\pi a} \int_0^\pi f(a \sin(\omega t)) \sin(\omega t) d(\omega t) \\ &\geq \frac{2k_1}{\pi} \int_0^\pi \sin^2(\omega t) d(\omega t) = k_1, \end{aligned} \quad (9.112)$$

$$\begin{aligned} K_{eq}(a) &= \frac{2}{\pi a} \int_0^\pi f(a \sin(\omega t)) \sin(\omega t) d(\omega t) \\ &\leq \frac{2k_2}{\pi} \int_0^\pi \sin^2(\omega t) d(\omega t) = k_2. \end{aligned} \quad (9.113)$$

The equivalent gain analysis and describing functions yield the same results. If we take the gain of the describing function, then the amplitude of the limit cycle can be predicted as with the describing functions. Both equivalent gain techniques can be used to determine stability, but as we have seen, the circle criterion allows for time-varying nonlinearities.

**Figure 9.56**

Nyquist plot and circle criterion



### EXAMPLE 9.19

#### *Determination of Stability Using the Circle Criterion*

Consider the system in Example 9.7. Determine the stability properties of the system using the circle criterion.

**Solution.** The related sector is the same one found in Example 9.18. The critical circle degenerates into a half plane defined by  $\text{Re}(G) \leq -1$ , as shown in Fig. 9.56. Since the Nyquist plot lies entirely to the right of the critical circle, the system is stable.

## 9.6 Historical Perspective

Almost all physical dynamic systems are nonlinear; hence, it is not surprising that the study of nonlinear systems has a long and rich history. The study of nonlinear systems goes back to astronomy and the study of the stability of the solar system dating back to Torricelli (1608–1647), Laplace, and Lagrange. The field received a jolt of “energy” with the doctoral dissertation of A. M. Lyapunov in Russia in 1892. He was trying to solve the stability of rotating bodies of fluids posed by Poincaré and recognized that if he could show that system-stored energy was always decreasing, then the system would be stable and eventually come to rest. The study of Lyapunov functions was introduced to the control field in 1960 by Kalman and Bertram, and has evolved rapidly since then.

Maxwell was the first to study stability by linearization about an equilibrium point by the derivation of the linear model for the Watt's fly-ball governor and stating that the system will be stable if the characteristic roots have negative real parts. Kochenburger derived the describing function method in 1950 in an attempt to handle nonlinearities based on frequency-response ideas. Lur'e proposed the absolute

stability problem in 1944, and in 1961, Popov developed the circle criterion for nonlinear stability analysis. Yakubovich (1962) and Kalman (1963) later established connections between Lur'e and Popov's results.

The study of adaptive control received a lot of attention during the three decades of the 1960s, 1970s, and 1980s. Adaptive controllers are both time varying and nonlinear in general. During the 1960s sensitivity methods and the MIT rule for adaptive adjustments were developed by Draper and others. Methods to study adaptive systems based on Lyapunov's methods and passivity were developed in the 1970s. Robust adaptive control methods were studied in the 1980s. Also, there has been a lot of research on systems, such as the weather, where a minute change in initial conditions or parameters can cause drastic changes in the response of the system. Such systems are said to be chaotic. In all recent studies of nonlinear systems, the availability of powerful computers to solve the equations and to graph the results has been critical. Development of a general theory of nonlinear control continues to be a dream of control theorists and is an ongoing quest.

## SUMMARY

- The nonlinear equations of motion may be approximated by linear ones by considering a small-signal linear model that is accurate near an equilibrium.
- In many cases, the inverse of a nonlinearity may be used to linearize a system.
- Nonlinearities without dynamics, such as saturation, can be analyzed using the root locus by considering the nonlinearity to be a variable gain.
- The root-locus technique can be used to determine the limit-cycle properties for memoryless nonlinearities, and yields the same results as the describing function.
- The describing function is essentially a heuristic method with the goal of finding a frequency-response function for a nonlinear element.
- The stability of systems with a single nonlinearity can be studied using the describing function method.
- The describing function can be used to predict periodic solutions in feedback systems.
- The Nyquist plot together with the describing function can be used to determine limit-cycle properties.
- The phase plane considers the time response directly by plotting the trajectory of the state variables and allows nonlinear behavior to be displayed.
- The stability of a nonlinear system in state-space description can be studied by the methods of Lyapunov.
- The circle criterion provides a sufficient condition for stability.

## REVIEW QUESTIONS

- 9.1** Why do we approximate a physical model of the plant (which is *always* nonlinear) with a linear model?
- 9.2** How would you linearize the nonlinear system equation for radiation heat transfer  $\dot{T} = T^4 + T + u$ ?
- 9.3** A lamp used as a thermal actuator has a nonlinearity such that the experimentally measured output power is related to the input voltage by  $P = V^{1.6}$ . How would you deal with such a nonlinearity in feedback control design?
- 9.4** What is integrator windup?
- 9.5** Why is an antiwindup circuit important?
- 9.6** Using the nonlinear saturation function having gain 1 and limits  $\pm 1$ , sketch the block diagram of saturation for an actuator that has gain 7 and limits of  $\pm 20$ .
- 9.7** What is a describing function and how is it related to a transfer function?
- 9.8** What are the assumptions behind the use of the describing function?
- 9.9** What is a limit cycle in a nonlinear system?
- 9.10** How can one determine the describing function for a nonlinear system in the laboratory?
- 9.11** What is the minimum-time control strategy for a satellite attitude control with bounded controls?
- 9.12** How are the two Lyapunov methods used?

## PROBLEMS

### *Problems for Section 9.2: Analysis by Linearization*

- 9.1** An electric field transducer that can be used as a microphone or a speaker can be described by the following equations:

Mechanical:

$$M \frac{d^2x}{dt^2} + B \frac{dx}{dt} + K(x - \ell) + \frac{\epsilon_0}{2} A \left( \frac{v}{x} \right)^2 = f(t) \quad (9.114)$$

Electrical:

$$\frac{d}{dt} \left( \frac{\epsilon_0}{x} Av \right) = \frac{v_s - v}{R} \quad (9.115)$$

where

$M$  = mass of the moving plate,

$B$  = damping coefficient,

$K$  = spring constant,

$x$  = separation of plates,

$\ell$  = natural length of spring,

$A$  = area of plate,

$v$  = voltage across plates,

$f$  = force on plate (input),

$V_s$  = bias voltage,

$R$  = resistance

The output is

$$y = -R \frac{d}{dt} \left( \frac{\epsilon_0 A v}{x} \right). \quad (9.116)$$

- (a) Using the state variables  $x_1 = x$ ,  $x_2 = \dot{x}$ ,  $x_3 = \frac{v}{x}$ , write the equations in state variable form.

- (b) Find the equations which describe equilibrium points for  $x$  and  $v$  if  $f(t) = 0$ .

- (c) Let the equilibrium points be  $X$  and  $V$ , and find a set of linearized equations about  $X$  and  $V$ .

- 9.2 Figure 9.57 shows a simple pendulum system in which a cord is wrapped around a fixed cylinder. The motion of the system that results is described by the differential equation

$$(l + R\theta)\ddot{\theta} + g \sin \theta + R\dot{\theta}^2 = 0,$$

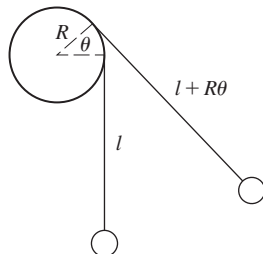
where

$l$  = length of the cord in the vertical (down) position,

$R$  = radius of the cylinder.

**Figure 9.57**

Motion of cord wrapped around a fixed cylinder



- (a) Write the state-variable equations for this system.

- (b) Linearize the equation around the point  $\theta = 0$ , and show for small values of  $\theta$ , the system equation reduces to an equation for a simple pendulum—that is,

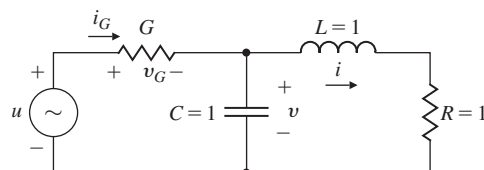
$$\ddot{\theta} + (g/\ell) = 0.$$

- 9.3 The circuit shown in Fig. 9.58 has a nonlinear conductance  $G$  such that  $i_G = g(v_G) = v_G(v_G - 1)(v_G - 4)$ . The state differential equations are

$$\frac{di}{dt} = -i + v,$$

**Figure 9.58**

Nonlinear circuit for Problem 9.3



$$\frac{dv}{dt} = -i + g(u - v),$$

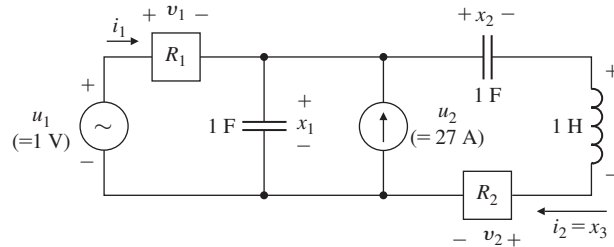
where  $i$  and  $v$  are the state variables and  $u$  is the input.

- (a) One equilibrium state occurs when  $u = 1$ , yielding  $i_1 = v_1 = 0$ . Find the other two pairs of  $v$  and  $i$  that will produce equilibrium.
- (b) Find the linearized model of the system about the equilibrium point  $u = 1$ ,  $i_1 = v_1 = 0$ .
- (c) Find the linearized models about the other two equilibrium points.
- 9.4** Consider the circuit shown in Fig. 9.59;  $u_1$  and  $u_2$  are voltage and current sources, respectively, and  $R_1$  and  $R_2$  are nonlinear resistors with the following characteristics:

$$\text{Resistor 1: } i_1 = G(v_1) = v_1^3,$$

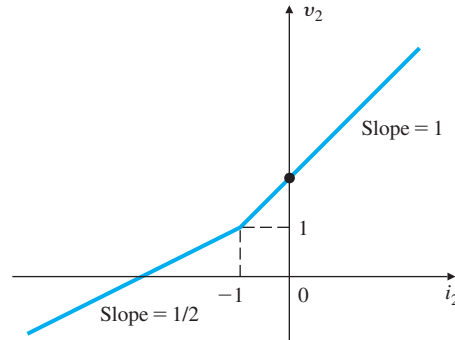
$$\text{Resistor 2: } v_2 = r(i_2).$$

**Figure 9.59**  
A nonlinear circuit



Here, the function  $r$  is defined in Fig. 9.60.

**Figure 9.60**  
Nonlinear resistance



- (a) Show that the circuit equations can be written as

$$\dot{x}_1 = G(u_1 - x_1) + u_2 - x_3,$$

$$\dot{x}_2 = x_3,$$

$$\dot{x}_3 = x_1 - x_2 - r(x_3).$$

Suppose we have a constant voltage source of 1 volt at  $u_1$  and a constant current source of 27 amps (that is,  $u_1^0 = 1$ ,  $u_2^0 = 27$ ). Find the

*equilibrium state*  $\mathbf{x}^0 = [x_1^0, x_2^0, x_3^0]^T$  for the circuit. For a particular input  $u^0$ , an equilibrium state of the system is defined to be any constant state vector whose elements satisfy the relation

$$\dot{x}_1 = \dot{x}_2 = \dot{x}_3 = 0.$$

Consequently, any system started in one of its equilibrium states will remain there indefinitely until a different input is applied.

- (b) Due to disturbances, the initial state (capacitance, voltages, and inductor current) is slightly different from the equilibrium, and so are the independent sources; that is,

$$u(t) = u^0 + \delta u(t),$$

$$x(t_0) = x^0(t_0) + \delta x(t_0).$$

Do a small-signal analysis of the network about the equilibrium found in (a), displaying the equations in the form

$$\dot{\delta x}_1 = f_{11}\delta x_1 + f_{12}\delta x_2 + f_{13}\delta x_3 + g_1\delta u_1 + g_2\delta u_2.$$

- (c) Draw the circuit diagram that corresponds to the linearized model. Give the values of the elements.

### 9.5 Consider the nonlinear system

$$\dot{x} = -x^2 e^{-\frac{1}{x}} + \sin u, \quad x(0) = 1.$$

- (a) Assume  $u^0 = 0$  and solve for  $x^0(t)$ .

- (b) Find the linearized model about the nominal solution in part (a).

### 9.6 *Linearizing effect of feedback:* We have seen that feedback can reduce the sensitivity of the input–output transfer function with respect to changes in the plant transfer function, and reduce the effects of a disturbance acting on the plant. In this problem, we explore another beneficial property of feedback: It can make the input–output response *more linear* than the open-loop response of the plant alone. For simplicity, let us ignore all the dynamics of the plant and assume the plant is described by the static nonlinearity

$$y(t) = \begin{cases} u, & u \leq 1, \\ \frac{u+1}{2}, & u > 1. \end{cases}$$

- (a) Suppose we use proportional feedback

$$u(t) = r(t) + \alpha(r(t) - y(t)),$$

where  $\alpha \geq 0$  is the feedback gain. Find an expression for  $y(t)$  as a function of  $r(t)$  for the closed-loop system. (This function is called the *nonlinear characteristic* of the system.) Sketch the nonlinear transfer characteristic for  $\alpha = 0$  (which is really open loop),  $\alpha = 1$ , and  $\alpha = 2$ .

- (b) Suppose we use integral control:

$$u(t) = r(t) + \int_0^t (r(\tau) - y(\tau)) d\tau.$$

The closed-loop system is therefore nonlinear and dynamic. Show that if  $r(t)$  is a constant, say  $r$ , then  $\lim_{t \rightarrow \infty} y(t) = r$ . Thus, the integral control makes the steady-state transfer characteristic of the closed-loop system *exactly linear*. Can the closed-loop system be described by a transfer function from  $r$  to  $y$ ?

- 9.7** This problem shows that linearization does not always work. Consider the system

$$\dot{x} = \alpha x^3, \quad x(0) \neq 0.$$

- (a) Find the equilibrium point and solve for  $x(t)$ .
- (b) Assume  $\alpha = 1$ . Is the linearized model a valid representation of the system?
- (c) Assume  $\alpha = -1$ . Is the linearized model a valid representation of the system?

- 9.8** Consider the object moving in a straight line with constant velocity shown in Fig. 9.61. The only available measurement is the range to the object. The system equations are

$$\begin{bmatrix} \dot{x} \\ \dot{v} \\ \dot{z} \end{bmatrix} = \begin{bmatrix} 0 & 1 & 0 \\ 0 & 0 & 0 \\ 0 & 0 & 0 \end{bmatrix} \begin{bmatrix} x \\ v \\ z \end{bmatrix},$$

where

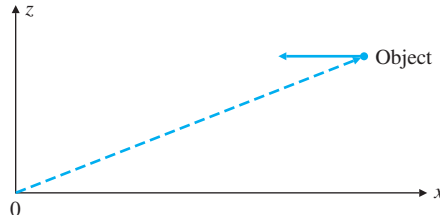
$$z = \text{constant},$$

$$\dot{x} = \text{constant} = v_0,$$

$$r = \sqrt{x^2 + z^2}.$$

Derive a linear model for this system.

**Figure 9.61**  
Diagram of the moving object for Problem 9.8



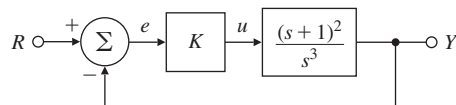
### Problems for Section 9.3: Equivalent Gain Analysis Using the Root Locus

- 9.9** Consider the third-order system shown in Fig. 9.62.

- (a) Sketch the root locus for this system with respect to  $K$ , showing your calculations for the asymptote angles, departure angles, and so on.
- (b) Using graphical techniques, locate carefully the point at which the locus crosses the imaginary axis. What is the value of  $K$  at that point?

**Figure 9.62**

Control system for Problem 9.9



- (c) Assume due to some unknown mechanism, the amplifier output is given by the following saturation non-linearity (instead of by a proportional gain  $K$ ):

$$u = \begin{cases} e, & |e| \leq 1, \\ 1, & e > 1, \\ -1, & e < -1. \end{cases}$$

*Qualitatively* describe how you would expect the system to respond to a unit-step input.

- 9.10** Consider the system with the plant transfer function

$$G(s) = \frac{1}{s^2 + 1}.$$

We would like to use PID control of the form

$$D_c(s) = 10 \left( 1 + \frac{1}{2s} + 2s \right),$$

to control this system. It is known that the system's actuator is a saturation nonlinearity with a slope of unity and  $|u| \leq 10$ . Compare the system response for a step input of size 10 with and without antiwindup circuit. Plot both the step response and the control effort using Simulink. Qualitatively describe the effect of the antiwindup circuit.

- 9.11** Consider the system with the open-loop plant

$$G(s) = \frac{1}{(s + 1)^3}$$

and the nominal PID controller

$$D_c(s) = 2 + \frac{1}{s} + \frac{s}{0.01s + 1}$$

The system has an actuator saturation nonlinearity with the slope of one and  $|u| \leq 2$ . Design an antiwindup scheme for this feedback system. Compare the step responses and control efforts for the system with and without antiwindup.

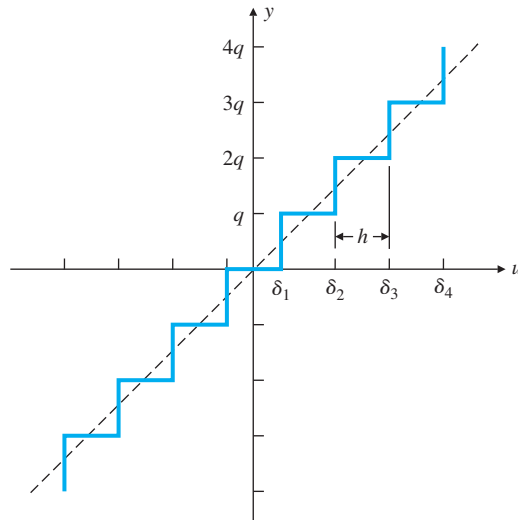
### Problems for Section 9.4: Equivalent Gain Analysis Using Frequency Response: Describing Functions

- 9.12** Compute the describing function for the relay with dead-zone nonlinearity shown in Fig. 9.6(c).
- 9.13** Compute the describing function for gain with dead-zone nonlinearity shown in Fig. 9.6(d).

- 9.14** Compute the describing function for the preloaded spring or Coulomb plus viscous friction nonlinearity shown in Fig. 9.6(e).
- 9.15** Consider the quantizer function shown in Fig. 9.63 that resembles a staircase. Find the describing function for this nonlinearity then write a Matlab .m function to generate it.

**Figure 9.63**

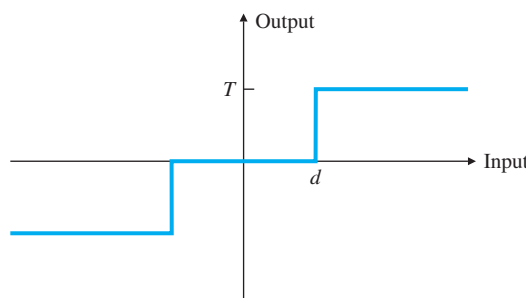
Quantizer nonlinearity  
for Problem 9.15



- 9.16** Derive the describing function for the ideal contactor controller shown in Fig. 9.64. Is it frequency dependent? Would it be frequency dependent if it had a time delay or hysteresis? Graphically sketch the time histories of the output for several amplitudes of the input and determine the describing function values for those inputs.

**Figure 9.64**

Contactor for  
Problem 9.16



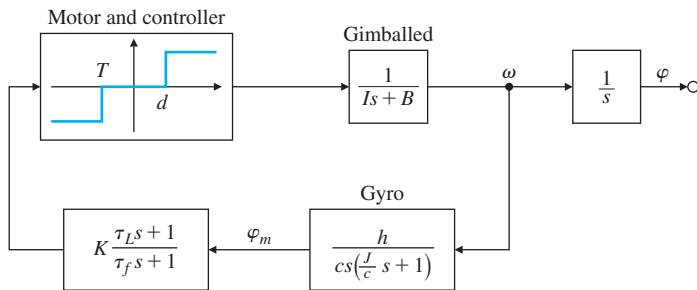
- 9.17** A contactor controller of an inertial platform is shown in Fig. 9.65, where

$$I = 0.1 \text{ kg} \cdot \text{m}^2, \frac{I}{B} = 10 \text{ sec}, \frac{h}{c} = 1,$$

$$\frac{J}{c} = 0.01 \text{ sec}, \tau_L = 0.1 \text{ sec}, \tau_f = 0.01 \text{ sec},$$

**Figure 9.65**

Block diagram of the system for Problem 9.17



$$d = 10^{-5} \text{ rad}, \quad T = 1 \text{ N} \cdot \text{m}.$$

The required stabilization resolution is approximately  $10^{-6}$  rad:

$$K\varphi_m > d \quad \text{for} \quad \varphi_m > 10^{-6} \text{ rad.}$$

Discuss the existence, amplitude, and frequency of possible limit cycles as a function of the gain  $K$  and the DF of the controller. Repeat the problem for a deadband with hysteresis.

- 9.18** *Nonlinear Clegg Integrator:* There have been some attempts over the years to improve upon the linear integrator. A linear integrator has the disadvantage of having a phase lag of  $90^\circ$  at all frequencies. In 1958, J. C. Clegg suggested that we modify the linear integrator to reset its state,  $x$ , to zero whenever the input to the integrator,  $e$ , crosses zero (that is, changes sign). The Clegg integrator has the property that it acts like a linear integrator whenever its input and output have the same sign. Otherwise, it *resets* its output to zero. The Clegg integrator can be described by

$$\begin{aligned} x(t) &= e(t), & \text{if } e(t) \neq 0, \\ x(t+) &= 0, & \text{if } e(t) = 0, \end{aligned}$$

where the latter equation implies that the state of the integrator,  $x$ , is reset to zero immediately after  $e$  changes sign. It can be implemented with opamps and diodes. A potential disadvantage of the Clegg integrator is that it may induce oscillations.

- (a) Sketch the output of the Clegg integrator if the input is  $e = a \sin(\omega t)$ .  
(b) Prove that the DF for the Clegg integrator is

$$N(a, \omega) = \frac{4}{\pi \omega} - j \frac{1}{\omega}$$

and this amounts to a phase lag of only  $38^\circ$ .

### △ Problems for Section 9.5: Analysis and Design Based on Stability

- 9.19** Compute and sketch the optimal reversal curve and optimal control for the minimal-time control of the plant

$$\begin{aligned} \dot{x}_1 &= x_2, \\ \dot{x}_2 &= -x_2 + u, \\ |u| &\leq 1. \end{aligned}$$

Use the reverse-time method and eliminate the time.

- 9.20** Sketch the optimal reversal curve for the minimal-time control with  $|u| \leq 1$  of the linear plant

$$\begin{aligned}\dot{x}_1 &= x_2, \\ \dot{x}_2 &= -2x_1 - 3x_2 + u.\end{aligned}$$

- 9.21** Sketch the time-optimal control law for

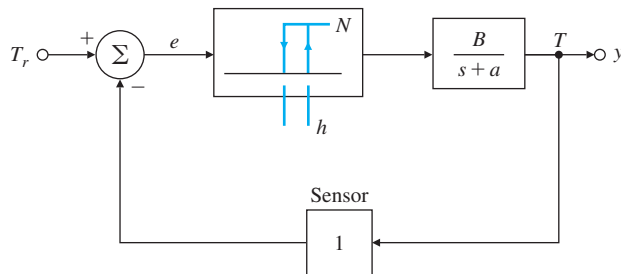
$$\begin{aligned}\dot{x}_1 &= x_2, \\ \dot{x}_2 &= -x_1 + u, \\ |u| &\leq 1,\end{aligned}$$

and show a trajectory for  $x_1(0) = 3$  and  $x_2(0) = 0$ .

- 9.22** Consider the thermal control system shown in Fig. 9.66. The physical plant can be a room, an oven, etc.

- (a) What is the limit-cycle period?
- (b) If  $T_r$  is commanded as a slowly increasing function, sketch the output of the system,  $T$ . Show the solution for  $T_r$  “large.”

**Figure 9.66**  
Thermal system for  
Problem 9.22



- 9.23** Several systems, such as a spacecraft, a spring-mass system with resonant frequency well below the frequency of switching, and a large motor-driven load with very small friction can be modeled as just an inertia. For an ideal switching curve, sketch the phase portraits of the system. The switching function is  $e = \theta + \tau\omega$ . Assume  $\tau = 10$  sec and the control signal  $= 10^{-3}$  rad/sec<sup>2</sup>. Now sketch the results with
- (a) deadband,
  - (b) deadband plus hysteresis,
  - (c) deadband plus time delay  $T$ ,
  - (d) deadband plus a constant disturbance.

- 9.24** Compute the amplitude of the limit cycle in the case of satellite attitude control with delay

$$I \ddot{\theta} = N u(t - \Delta),$$

using

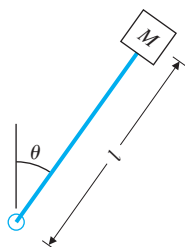
$$u = -\text{sgn}(\tau \dot{\theta} + \theta).$$

Sketch the phase-plane trajectory of the limit cycle and time history of  $\theta$  giving the maximum value of  $\theta$ .

- 9.25** Consider the point mass pendulum with zero friction as shown in Fig. 9.67. Using the method of isolines as a guide, sketch the phase-plane portrait of the motion. Pay particular attention to the vicinity of  $\theta = \pi$ . Indicate a trajectory corresponding to spinning of the bob around and around rather than oscillating back and forth.

**Figure 9.67**

Pendulum for  
Problem 9.25



- 9.26** Draw the phase trajectory for a system

$$\ddot{x} = 10^{-6} \text{ m/sec}^2$$

between  $\dot{x}(0) = 0$ ,  $x(0) = 0$ , and  $x(t) = 1 \text{ mm}$ . Find the transition time  $t_f$  by graphical means from the parabolic curve by comparing your solution with two different interval sizes and the exact solution.

- 9.27** Consider the system with equations of motion

$$\ddot{\theta} + \dot{\theta} + \sin \theta = 0.$$

- (a) What physical system does this correspond to?
- (b) Draw the phase portraits for this system.
- (c) Show a specific trajectory for  $\theta(0) = 0.5 \text{ rad}$  and  $\dot{\theta} = 0$ .

- 9.28** Consider the nonlinear upright pendulum with a motor at its base as an actuator. Design a feedback controller to stabilize this system.

- 9.29** Consider the system

$$\dot{x} = -\sin x.$$

Prove that the origin is an asymptotically stable equilibrium point.

- 9.30** A first-order nonlinear system is described by the equation  $\dot{x} = -f(x)$ , where  $f(x)$  is a continuous and differentiable nonlinear function that satisfies the following:

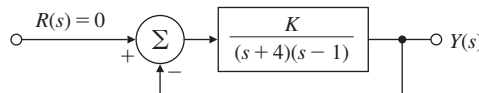
$$\begin{aligned} f(0) &= 0, \\ f(x) &> 0, \quad \text{for } x > 0, \\ f(x) &< 0, \quad \text{for } x < 0. \end{aligned}$$

Use the Lyapunov function  $V(x) = x^2/2$  to show that the system is stable near the origin ( $x = 0$ ).

- 9.31** Use the Lyapunov equation

$$\mathbf{A}^T \mathbf{P} + \mathbf{P} \mathbf{A} = -\mathbf{Q} = -\mathbf{I},$$

**Figure 9.68**  
Control system for  
Problem 9.31



to find the range of  $K$  for which the system in Fig. 9.68 will be stable. Compare your answer with the stable values for  $K$  obtained using Routh's stability criterion.

- 9.32** Consider the system

$$\frac{d}{dt} \begin{bmatrix} x_1 \\ x_2 \end{bmatrix} = \begin{bmatrix} x_1 + x_2 u \\ x_2(x_2 + u) \end{bmatrix}, \quad y = x_1.$$

Find all values of  $\alpha$  and  $\beta$  for which the input  $u(t) = \alpha y(t) + \beta$  will achieve the goal of maintaining the output  $y(t)$  near 1.

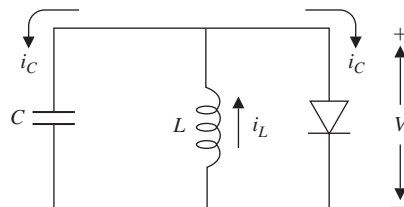
- 9.33** Consider the nonlinear autonomous system

$$\frac{d}{dt} \begin{bmatrix} x_1 \\ x_2 \\ x_3 \end{bmatrix} = \begin{bmatrix} x_2(x_3 - x_1) \\ x_1^2 - 1 \\ -x_1 x_3 \end{bmatrix}.$$

- (a) Find the equilibrium point(s).
- (b) Find the linearized system about each equilibrium point.
- (c) For each case in part (b), what does Lyapunov theory tell us about the stability of the nonlinear system near the equilibrium point?

- 9.34** Consider the circuit shown in Fig. 9.69. For what diode characteristics will this system be stable?

**Figure 9.69**  
Circuit diagram for  
Problem 9.34



- 9.35** *Van der Pol's equation:* Consider the system described by the nonlinear differential equation

$$\ddot{x} + \varepsilon(1 + x^2)\dot{x} + x = 0$$

with the constant  $\varepsilon > 0$ . This nonlinear equation represents the model of electrical activity of the heart and oscillations in some electrical circuits.

- (a) Show that the equations can be put in the form [Liénard or (x,y) plane]

$$\begin{aligned} \dot{x} &= y + \varepsilon \left( \frac{x^3}{3} - x \right), \\ \dot{y} &= -x. \end{aligned}$$

- (b) Use the Lyapunov function  $V = \frac{1}{2}(x^2 + \dot{x}^2)$ , and sketch the *region* of stability as predicted by this  $V$  in the Liénard plane.

- (c) Plot the trajectories of part (b) and show the initial conditions that tend to the origin. Simulate the system in Simulink using various initial conditions on  $x(0)$  and  $\dot{x}(0)$ . Consider two cases, with  $\varepsilon = 0.5$  and  $\varepsilon = 1.0$ .

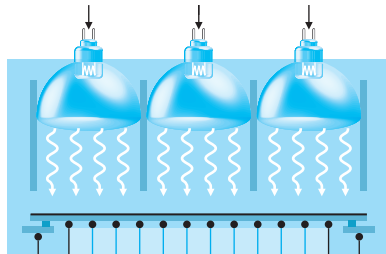
- 9.36 Duffing's equation:** Consider the system described by the nonlinear differential equation

$$\ddot{x} + k\dot{x} + \varepsilon x^3 = u,$$

where  $u = A \cos(t)$ . This equation represents the model of a hard spring where  $k$  is the spring constant and if  $\varepsilon > 0$ , the spring gets stiffer as the displacement increases. Let  $k = 0.05$ ,  $\varepsilon = 1$ , and  $A = 7.5$ .

- (a) Build a simulation of the system in Simulink. Show the system response can be very sensitive to slight perturbations on the initial conditions  $x(0)$ ,  $\dot{x}(0)$  (the system is said to be *chaotic*). Simulate the response of the system with  $x(0) = 3$  and  $\dot{x}(0) = 4$  for  $t = 30$  sec. Repeat the simulation for slightly perturbed initial conditions  $x(0) = 3.01$  and  $\dot{x}(0) = 4.01$ . Compare the two results.
- (b) Consider the unforced Duffing equation ( $u = 0$ ). Plot the time response of the system for  $x(0) = 1$ ,  $\dot{x}(0) = 1$  for  $t = 200$  sec. Draw the phase-plane plot for the system. Show the origin is an equilibrium point.
- (c) Now consider the forced Duffing equation ( $u \neq 0$ ). Find the solution to the Duffing equation for  $x(0) = -1$ ,  $\dot{x}(0) = 1$  for  $t = 30$  sec. Draw the phase-plane plot ( $\dot{x}(t)$  versus  $x(t)$ ) for this case.
- (d) Repeat part (c) for  $k = 0.25$ ,  $\varepsilon = 1$ , and  $A = 8.5$ .
- (e) Repeat part (c) for  $k = 0.1$ ,  $\varepsilon = 1$ , and  $A = 11$ .
- (f) We can get more insight into the system by plotting  $\dot{x}(t_j)$  versus  $x(t_j)$  at several hundred points at  $2\pi$  periodic observation times. In other words, rather than looking at the system continuously, we “strobe” the system and plot the behavior at strobe times only. Show that unlike the phase-plane plots in parts (c)-(e), the points fall on a well-structured plot referred to as a Poincaré section (also called a strange attractor). Plot the Poincaré sections for parts (c)-(e). Simulate the system using the initial conditions  $x(0) = -1$  and  $\dot{x}(0) = 1$  for  $t = 10,000$  sec in order to plot the Poincaré sections.
- (g) What can you conclude about the nature of the solution of the Duffing equation from the results of the previous parts?
- (h) Characterize the system behavior in terms of the ranges of the system parameters  $k$ ,  $\varepsilon$ , and  $A$ .

# Control System Design: Principles and Case Studies



## A Perspective on Design Principles

In Chapters 5, 6, and 7, we presented techniques for analyzing and designing feedback systems based on the root-locus, frequency-response, and state-variable methods. Thus far, we have had to consider somewhat isolated, idealized aspects of larger systems and to focus on applying one analysis method at a time. In this chapter, we return to the theme of Chapter 4—the advantages of feedback control—to reconsider the overall problem of control systems design with the sophisticated tools developed in Chapters 5 to 7 and 9 in hand. We will apply these tools to several complex, real-world applications in a case study-type format.

Having an overarching, step-by-step design approach serves two purposes: It provides a useful starting point for any real-world controls problem, and it provides meaningful checkpoints once the design process is underway. This chapter develops just such a general approach, which will be applied in the case studies.

## Chapter Overview

Section 10.1 opens the chapter with a step-by-step design process that is sufficiently general to apply to any control design process,

but which also provides useful definitions and directions. We will then apply the design process to four practical, complex applications: design of an attitude control system for a satellite (Section 10.2), lateral and longitudinal control of a Boeing 747 (Section 10.3), and control of the fuel-air ratio in an automotive engine (Section 10.4), control of a quadrotor drone (Section 10.5), and control of a rapid thermal processing (RTP) system (Section 10.6). The satellite case study is representative of the control of geosynchronous communications satellite systems. The study addresses the design of robust control systems in which the physical parameters are known to vary within a given range. In this system, the control system needs to meet specifications from the “beginning-of-life” (BOL) to the “end-of-life” (EOL) that spans a period of 12–15 years. The satellite’s moment of inertia and mass will vary as fuel is expended for attitude control, and by deployment and re-orientation of satellite antennas.

The satellite case study illustrates the use of notch compensation for a system with lightly damped resonances. We will see from this case study that collocated actuator and sensor systems are much easier to control than noncollocated systems. The Boeing 747 case study addresses the familiar flight control system of commercial passenger aircraft. The nonlinear equations of motion are given and are linearized about a particular flight condition. The rigid body dynamics, longitudinal and lateral-directional, are each fourth order. Of course, the flexible modes need also be considered for a more accurate model. The Boeing 747 lateral-stabilization case study will illustrate the use of feedback as an inner-loop designed to aid the pilot, who will provide the primary outer-loop control. The altitude control study will show how to combine inner-loop feedback with outer-loop compensation to design a complete control system. The air-to-fuel ratio automotive case study is a real-world example that includes a nonlinear, sensor and a pure time delay. We will use the describing function method of Chapter 9 to analyze the behavior of this system. Another familiar example to most airplane enthusiasts is the quadrotor drone. This case study from an emerging field demonstrates how the four control axes can be designed independently by proper commands to the four rotors. The RTP case study from semiconductor wafer fabrication is remarkably close to an industrial application. The problem concerns temperature tracking and disturbance rejection for a highly nonlinear thermal system. The actuator (lamp) is also nonlinear and we will use the technique from Chapter 9 to try to cancel the effect of this nonlinearity. Another key aspect of this system is actuator saturation and the fact that the control signal cannot go negative. In all these case studies, the designer needs to be able to use multiple tools from previous chapters, including the root locus, the frequency response, pole placement by state feedback, and (nonlinear) simulation of time responses to obtain a satisfactory design. In Section 10.7,

we will present a case study from the emerging field of systems biology and describe chemotaxis or how *Escherichia coli* (*E. coli*) swims away from trouble. Section 10.7 will provide a historical perspective on applications of feedback control.

## 10.1 An Outline of Control Systems Design

Control engineering is an important part of the design process of many dynamic systems. As suggested in Chapter 4, the deliberate use of feedback can stabilize an otherwise unstable system, reduce the error due to disturbance inputs, reduce the tracking error while following a command input, and reduce the sensitivity of a closed-loop transfer function to small variations in internal system parameters. In those situations for which feedback control is required, it is possible to outline an approach to control systems design that often leads to a satisfactory solution.

Before describing this approach, we wish to emphasize that the purpose of control is to aid the product or process—the mechanism, the robot, the chemical plant, the aircraft, or whatever—to do its job. Engineers engaged in other areas of the design process are increasingly taking the contribution of control into account early in their plans. As a result, more and more systems have been designed so they will not work at all without feedback. This is especially significant in the design of high-performance aircraft, where control has taken its place along with structures and aerodynamics as essential to assure that the craft will even fly at all. It is impossible to give a description of such overall design in this book, but recognizing the existence of such cases places in perspective not only the specific task of control system design, but also the central role this task can play in an enterprise.

Control system design begins with a proposed product or process whose satisfactory dynamic performance depends on feedback for stability, disturbance regulation, tracking accuracy, or reduction of the effects of parameter variations. We will give an outline of the design process that is general enough to be useful whether the product is an electronic amplifier or a large structure to be placed in earth orbit. Obviously, to be so widely applicable, our outline has to be vague with respect to physical details and specific only with respect to the feedback-control problem. To present our results, we will divide the control design problem into a sequence of characteristic steps.

**STEP 1. Understand the process and translate dynamic performance requirements into time, frequency, or pole-zero specifications.** The importance of understanding the process, what it is intended to do, how much system error is permissible, how to describe the class of command and disturbance signals to be expected, and what the physical capabilities and limitations are can hardly be overemphasized. Regrettably, in a book such as this, it is easy to view the process as a linear, time-invariant transfer function capable of responding to inputs of arbitrary size, and

we tend to overlook the fact that the linear model is a *very* limited representation of the real system, valid only for small signals, short times, and particular environmental conditions. Do not confuse the approximation with reality. You must be able to use the simplified model for its intended purpose, and to return to an accurate model or the actual physical system to really verify the design performance.

Typical results of this step are specifications that the system have a step response inside some constraint boundaries (as shown in Fig. 10.1a), an open-loop frequency response satisfying certain constraints (Fig. 10.1b), or closed-loop poles to the left of some constraint boundary (Fig. 10.1c).

### Sensors

**STEP 2. Select sensors.** In **sensor** selection, consider which variables are important to control and which variables can physically be measured. For example, in a jet engine, there are critical internal temperatures that must be controlled, but that cannot be measured directly in an operational engine. Select sensors that indirectly allow a good estimate to be made of these critical variables. It is important to consider sensors for the disturbance. Sometimes, especially in chemical processes, it is beneficial to sense a load disturbance directly, because improved performance can be obtained if this information is fed forward to the controller.

Following are some factors that influence sensor selection:

Number of sensors and locations:	Select minimum required number of sensors and their optimal locations
Technology:	Electric or magnetic, mechanical, electromechanical, electro-optical, piezoelectric
Functional performance:	Linearity, bias, accuracy, bandwidth, resolution, dynamic range, noise
Physical properties:	Weight, size, strength
Quality factors:	Reliability, durability, maintainability
Cost:	Expense, availability, facilities for testing and maintenance

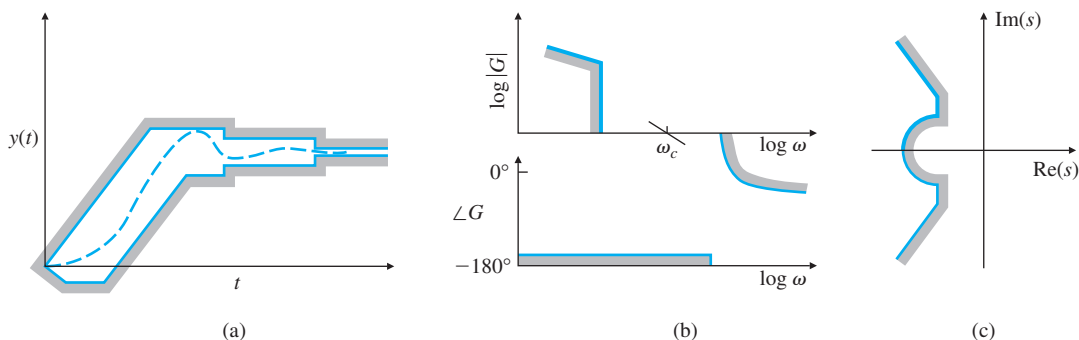


**Figure 10.1**

Examples of: (a) time-response; (b) frequency-response; and (c) pole-zero specifications resulting from Step 1

**Actuators**

**STEP 3. Select actuators.** In order to control a dynamic system, obviously you must be able to influence the response. The device that does this is the **actuator**. Before choosing a specific actuator, consider which variables can be influenced. For example, in a flight vehicle, many configurations of movable surfaces are possible, and the influence these have on the performance and controllability of the craft can be profound. The locations of jets or other torque devices are also a major part of the control design of spacecraft.

Having selected a particular variable to control, you may need to consider other factors:

Number of actuators and locations:	Select minimum required actuators and their optimal locations
Technology:	Electric, hydraulic, pneumatic, thermal, other
Functional performance:	Maximum force possible, extent of the linear range, maximum speed possible, power, efficiency, etc.
Physical properties:	Weight, size, strength
Quality factors:	Reliability, durability, maintainability
Cost:	Expense, availability, facilities for testing and maintenance

**Linearization**

**STEP 4. Construct a linear model.** Here you take the best choice for process, actuator, and sensor; identify the equilibrium point of interest; and construct a small-signal dynamic model valid over the range of frequencies included in the specifications of Step 1. You should also validate the model with experimental data where possible. To be able to make use of all the available tools, express the model in state-variable and pole-zero form as well as in frequency-response form. As we have seen, Matlab and other computer-aided control systems design software packages have the means to perform the transformations among these forms. Simplify and reduce the order of the model if necessary. Quantify model uncertainty.

**Simple compensation  
PID/lead-lag design**

**STEP 5. Try a simple proportional-integral-derivative (PID) or lead-lag design.** To form an initial estimate of the complexity of the design problem, sketch a frequency response (Bode plot) and a root locus with respect to plant gain. If the plant-actuator-sensor model is stable and minimum-phase, the Bode plot will probably be the most useful; otherwise, the root locus shows very important information with respect to behavior in the right half-plane (RHP). In any case, try to meet the specifications with a simple controller of the lead-lag variety, including integral control if steady-state error response requires it. Do not overlook feedforward of the disturbances if the necessary sensor information is available. Consider the effect of sensor noise, and compare a lead network to a direct sensor of velocity to see which gives a better design.

**STEP 6. Evaluate/modify plant.** Based on the simple control design, evaluate the source of the undesirable characteristics of the system performance. Reevaluate the specifications, the physical configuration of

the process, and the actuator and sensor selections in light of the preliminary design, and return to Step 1 if improvement seems necessary or feasible. For example, in many motion-control problems, after testing the first-pass design, you might find vibrational modes that prevent the design from meeting the initial specifications of the problem. It may be much easier to meet the specifications by altering the structure of the plant through the addition of stiffening members, or by passive damping than to meet them by control strategies alone. An alternative solution may be to move a sensor so it is at a node of a vibration mode, thus providing no feedback of the motion. Also, some actuator technologies (such as hydraulic) have many more low-frequency vibrations than others (such as electric) do and changing the actuator technology may be indicated. In a digital implementation, it may be possible to revise the sensor-controller-actuator system structure so as to reduce time delay, which is always a destabilizing element. In thermal systems, it is often possible to change heat capacity or conductivities by material substitution that will enhance the control design. It is important to consider all parts of the design, not only the control logic, to meet the specifications in the most cost-effective way. If the plant is modified, go back to Step 1. If the design now seems satisfactory, go to Step 8; otherwise, try Step 7.

#### Optimal design

**STEP 7. Try an optimal design.** If the trial-and-error compensators do not give entirely satisfactory performance, consider a design based on optimal control. The symmetric root locus (SRL) will show possible root locations from which to select locations for the control poles that meet the response specifications; you can select locations for the estimator poles that represent a compromise between sensor and process noise. Plot the corresponding open-loop frequency response and the root locus to evaluate the stability margins of this design and its robustness to parameter changes. You can modify the pole locations until a best compromise results. Returning to the SRL with different cost measures is often a part of this step, or computations via the direct functions `lqr` and `lqe` can be used. Another variation of optimal control is to propose a fixed structure controller with unknown parameters, formulate a performance cost function, and use parameter optimization to find a good set of parameter values.

Compare the optimal design yielding the most satisfactory frequency response with the transform-method design you derived in Step 5. Select the better of the two before proceeding to Step 8.

**STEP 8. Build a computer model, and compute (simulate) the performance of the design.** After reaching the best compromise among process modification, actuator and sensor selection, and controller design choice, run a computer model of the system. This model should include important nonlinearities, such as actuator saturation, realistic noise sources, and parameter variations you expect to find during operation of the system. The simulation will often identify sensitivities that

may lead to going back to Step 5 or even to Step 2. Design iterations should continue until the simulation confirms acceptable stability and robustness. As part of this simulation, you can often include parameter optimization, in which the computer tunes the free parameters for best performance. In the early stages of design, the model you simulate will be relatively simple; as the design progresses, you will study more complete and detailed models. At this step it is also possible to compute a digital equivalent of the analog controller as described in Chapters 4 and 8. Some refinement of the controller parameters may be required to account for the effects of digitization. This allows the final design to be implemented with digital processor logic.

If the results of the simulation prove the design satisfactory, go to Step 9; otherwise return to Step 1.

### Prototype Prototype testing

**STEP 9. Build a prototype.** As the final test before production, it is common to build and test a prototype. At this point, you verify the quality of the model, discover unsuspected unmodelled dynamics such as vibration and other modes, and consider ways to improve the design. Implement the controller using embedded software/hardware. Tune the controller if necessary. After these tests, you may want to reconsider the sensors, actuators, and process and return to Step 1—unless time, money, or ideas have run out.

This outline is an approximation of good practice; other engineers will have variations on these themes. In some cases, you may wish to carry out the steps in a different order, to omit a step, or to add one. The stages of simulation and prototype construction vary widely, depending on the nature of the system. For systems for which a prototype is difficult to test and rework (for example, a satellite) or where a failure is dangerous (for example, active stabilization of a high-speed centrifuge or landing a human on the moon), most of the design verification is done through simulation of some sort. It may take the form of a digital numerical simulation, a laboratory scale model, or a full-size laboratory model with a simulated environment. For systems that are easy to build and modify (for example, feedback control for an automotive fuel system), the simulation step is often skipped entirely; design verification and refinement are instead accomplished by working with prototypes.

One of the issues raised in the preceding discussion (see Step 6) was the important consideration for **changing the plant itself**. In many cases, proper plant modifications can provide additional damping or increase in stiffness, change in mode shapes, reduction of system response to disturbances, reduction of Coulomb friction, change in thermal capacity or conductivity, etc. It is worth elaborating on this by way of specific examples from the authors' experiences. In a semiconductor wafer-processing example, the edge ring holding the wafer was identified as a limiting factor in closed-loop control. Modifying the thickness of the edge ring and using a different coating material reduced the heat

losses and, together with relocating one of the temperature sensors closer to the edge ring, resulted in significant improvement in control performance. In another application, thin film processing, simply changing the order of the two incoming flows resulted in significant improvement in the mixing of the precursor and oxidizer materials, and led to improvement in uniformity of the film. In an application on physical vapor deposition using RF-plasma, the shape of the target was modified to be curved to counter the geometry effects of the chamber, and yielded substantial improvements in deposition uniformity. As the last example, in a hydraulic spindle control problem, adding oil temperature control with ceramic insulation and a temperature sink for the bell housing resulted in several orders of magnitude reduction in disturbances not achievable by feedback control alone.<sup>1</sup> One can also mention aerospace applications for which the control was an afterthought, and the feedback control problem became exceedingly difficult and resulted in poor closed-loop performance. The moral of this discussion is that one must not forget the option of modifying the plant itself to make the control problem easier and provide maximum closed-loop performance.

The usual approach of designing the system and “throwing it over the fence” to the control group has proved to be inefficient and flawed. A better approach that is gaining momentum is to get the control engineer involved from the onset of a project to provide early feedback on whether or not it is difficult to control the system. The control engineer can provide valuable feedback on the choice of actuators and sensors and can even suggest modifications to the plant. It is often much more efficient to change the plant design while it is on the drawing board before “any metal has been bent.” Closed-loop performance studies can then be performed on a simple model of the system early on.

Implicit in the process of design is the well-known fact that designs within a given category often draw on experience gained from earlier models. Thus, good designs evolve rather than appear in their best form after the first pass. We will illustrate the method with several cases (see Sections 10.2 to 10.6). For easy reference, we summarize the steps here.

### *Summary of Control Design Steps*

1. Understand the process and its performance requirements.
2. Select the types and number of sensors considering location, technology, and noise.
3. Select the types and number of actuators considering location, technology, noise, and power.
4. Construct a linear model of the process, actuator, and sensor.
5. Try a simple trial design based on the concepts of lead-lag compensation or PID control. If satisfied, go to Step 8.

---

<sup>1</sup>Our colleague Prof. Daniel DeBra strongly believes in considering modifying the plant itself as an option for improved control. He cites this particular application to make the point. Of course, we agree with him!

6. Consider modifying the plant itself for improved closed-loop control.
7. If the performance from the simple compensator in Step 5 is not adequate, perform a trial pole-placement design based on optimal control or other criteria.
8. Simulate the design, including the effects of nonlinearities, noise, and parameter variations. If the performance is not satisfactory, return to Step 1 and repeat. Consider modifying the plant itself for improved closed-loop control.
9. Build a prototype and test it. If not satisfied, return to Step 1 and repeat.

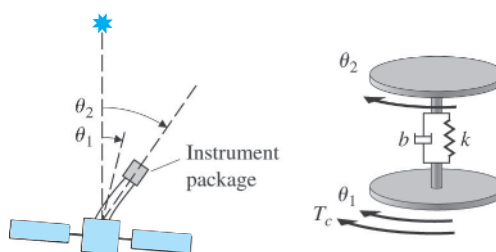
## 10.2 Design of a Satellite's Attitude Control

Our first example, taken from the space program, is suggested by the need to control the pointing direction, or attitude, of a satellite in orbit about the earth. Figure 2.7 shows a picture of a geosynchronous communications satellite. We will go through each step in our design outline and touch on some of the factors that might be considered for the control of such a system.

**STEP 1. Understand the process and its performance specifications.** A satellite is sketched in Fig. 10.2. We imagine the vehicle has an astronomical survey mission requiring accurate pointing of a scientific sensor package. This package must be maintained in the quietest possible environment, which entails isolating it from the vibrations and electrical noise of the main service body and from its power supplies, thrusters, and communication gear. We model the resulting structure as two masses connected by a flexible boom. In Fig. 10.2, the satellite attitude  $\theta_2$  is the angle between the star sensor and the instrument package, and  $\theta_1$  is the angle of the main satellite with respect to the star. Figure 10.2 shows the equivalent mechanical system diagram for the satellite, where the sensor is mounted to the disk associated with  $\theta_2$ . Disturbance torques due to solar pressure, micrometeorites, and orbit perturbations are computed to be negligible. The pointing requirement arises when it is necessary to point the unit in another direction. It can be met by dynamics with a transient settling time of 20 sec and an overshoot of no

**Figure 10.2**

Diagram of a satellite and its two-body model



more than 15%. The dynamics of the satellite include parameters that can vary. The control must be satisfactory for any parameter values in a prespecified range to be given when the equations are written.

**STEP 2. Select sensors.** In order to orient the scientific package, it is necessary to measure the attitude angles of the package. For this purpose, we propose to use a **star tracker**, a system based on gathering an image of a specific star and keeping it centered on the focal plane of a telescope. This sensor gives a relatively noisy but very accurate (on the average) reading proportional to  $\theta_2$ , the angle of deviation of the instrument package from the desired angle. To stabilize the control, we include a rate gyro to give a clean reading of  $\dot{\theta}_2$ , because a lead network on the star-tracker signal would amplify the noise too much. Furthermore, the rate gyro can stabilize large motions before the star tracker has acquired the target star image.

**STEP 3. Select actuators.** Major considerations in selecting the actuator are precision, reliability, weight, power requirements, and lifetime. Alternatives for applying torque are cold-gas jets, reaction wheels or gyros, magnetic torquers, and a gravity gradient. The jets have the most power and are the least accurate. Reaction wheels are precise but can transfer only momentum, so jets or magnetic torquers are required to “dump” momentum from time to time. Magnetic torquers provide relatively low levels of torque and are suitable only for some low-altitude satellite missions. A gravity gradient also provides a very small torque that limits the speed of response and places severe restrictions on the shape of the satellite. For purposes of this mission, we select cold-gas jets as being fast and adequately accurate.

**STEP 4. Make a linear model.** For the satellite, we assume two masses connected by a spring with torque constant  $k$  and viscous-damping constant  $b$  as shown in Fig. 10.2. The equations of motion are

$$J_1 \ddot{\theta}_1 + b(\dot{\theta}_1 - \dot{\theta}_2) + k(\theta_1 - \theta_2) = T_c, \quad (10.1a)$$

$$J_2 \ddot{\theta}_2 + b(\dot{\theta}_2 - \dot{\theta}_1) + k(\theta_2 - \theta_1) = 0, \quad (10.1b)$$

where  $T_c$  is the control torque on the main body. With inertias  $J_1 = 1$  and  $J_2 = 0.1$ , the transfer function is

$$G(s) = \frac{10bs + 10k}{s^2(s^2 + 11bs + 11k)}. \quad (10.2)$$

If we choose

$$\mathbf{x} = [\theta_2 \quad \dot{\theta}_2 \quad \theta_1 \quad \dot{\theta}_1]^T,$$

as the state vector, then, using Eq. (10.1a) and assuming  $T_c \equiv u$ , we find that the equations of motion in state-variable form are

$$\dot{\mathbf{x}} = \begin{bmatrix} 0 & 1 & 0 & 0 \\ -\frac{k}{J_2} & -\frac{b}{J_2} & \frac{k}{J_2} & \frac{b}{J_2} \\ 0 & 0 & 0 & 1 \\ \frac{k}{J_1} & \frac{b}{J_1} & -\frac{k}{J_1} & -\frac{b}{J_1} \end{bmatrix} \mathbf{x} + \begin{bmatrix} 0 \\ 0 \\ 0 \\ \frac{1}{J_1} \end{bmatrix} u, \quad (10.3a)$$

$$y = [1 \ 0 \ 0 \ 0] \mathbf{x}. \quad (10.3b)$$

Physical analysis of the boom leads us to assume that the parameters  $k$  and  $b$  vary as a result of temperature fluctuations but are bounded by

$$0.09 \leq k \leq 0.4, \quad (10.4a)$$

$$0.038\sqrt{\frac{k}{10}} \leq b \leq 0.2\sqrt{\frac{k}{10}}. \quad (10.4b)$$

As a result, the vehicle's natural resonance frequency  $\omega_n$  can vary between 1 and 2 rad/sec, and the damping ratio  $\zeta$  varies between 0.02 and 0.1.

One approach to control design when parameters are subject to variation is to select nominal values for the parameters, construct the design for this model, and then test the controller performance with other parameter values. In the present case, we choose nominal values of  $\omega_n = 1$  and  $\zeta = 0.02$ . The choice is somewhat arbitrary, being based on experience and heuristic analysis. However, note these are the lowest values in their respective ranges and thus correspond to the plant that is probably the most difficult to control so as to meet the specifications. We assume a design for this model has a good chance to meet the specifications for other parameter values as well. (Another choice would be to select a model with average values for each parameter.) The selected parameter values are  $k = 0.091$  and  $b = 0.0036$ ; with  $J_1 = 1$  and  $J_2 = 0.1$ , the nominal equations become

$$\dot{\mathbf{x}} = \begin{bmatrix} 0 & 1 & 0 & 0 \\ -0.91 & -0.036 & 0.91 & 0.036 \\ 0 & 0 & 0 & 1 \\ 0.091 & 0.0036 & -0.091 & -0.0036 \end{bmatrix} \mathbf{x} + \begin{bmatrix} 0 \\ 0 \\ 0 \\ 1 \end{bmatrix} u, \quad (10.5a)$$

$$y = [1 \ 0 \ 0 \ 0] \mathbf{x}. \quad (10.5b)$$

The corresponding transfer function, using the Matlab ss2tf function, is then

### Selecting nominal values for varying parameters

$$G(s) = \frac{0.036(s + 25)}{s^2(s^2 + 0.04s + 1)}. \quad (10.6)$$

When a trial design is completed, the computer simulation should be run with a range of possible parameter values to ensure that the design has adequate robustness to tolerate these changes. Equations (3.74) to (3.76) tell us that the dynamic performance specifications will be met if the closed-loop poles have a natural frequency of 0.5 rad/sec and a closed-loop damping ratio of 0.5; these correspond to an open-loop crossover frequency of  $\omega_c \cong 0.5$  rad/sec and a phase margin of about  $PM = 50^\circ$ . We will try to meet these design criteria.

**STEP 5. Try a lead-lag or PID controller.** The proportional-gain root locus for the nominal plant is drawn in Fig. 10.3, and the Bode plot is given in Fig. 10.4. We can see from Fig. 10.4 that this may be a difficult design problem because the frequency of the lightly damped resonance is greater than the crossover-frequency design point by only a factor of 2. This situation will require that the compensation can correct for the phase lag of the plant at the resonance frequency. Such a correction is very dependent on knowing the resonance frequency, which is subject to change in this case. There may be trouble ahead.

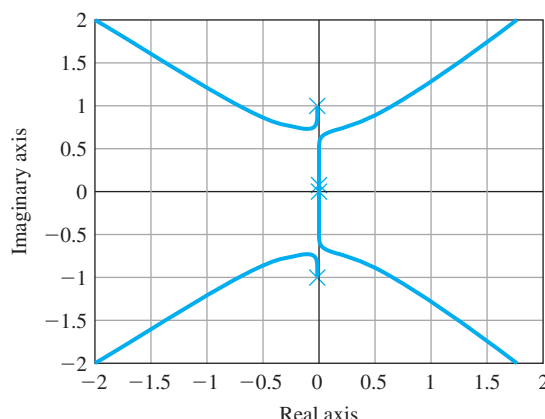
In order to illustrate some important aspects of compensation design, we will at first ignore the resonance and generate a design that would be acceptable for the rigid body alone. We take the process transfer function to be  $1/s^2$ , the feedback to be position plus derivative (star tracker plus rate gyro) or PD control with the transfer function  $D_c(s) = K(sT_D + 1)$ , and the response objective to be  $\omega_n = 0.5$  rad/sec and  $\zeta = 0.5$ . A suitable controller would be

$$D_{c1}(s) = 0.25(2s + 1). \quad (10.7)$$

The root locus for the actual plant with  $D_{c1}$  is shown in Fig. 10.5, and the Bode plot in Fig. 10.6. From these plots, we can see that the low-frequency poles are reasonable, but that the system will be unstable

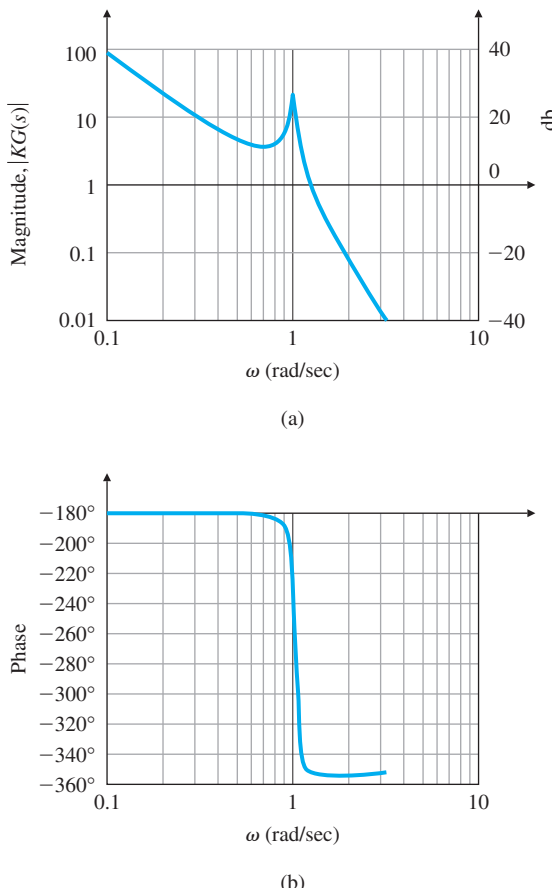
**Figure 10.3**

Root locus of  $KG(s)$

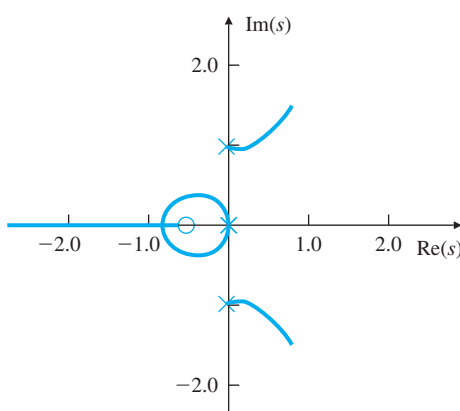


**Figure 10.4**

Open-loop Bode plot of  $G(s)$

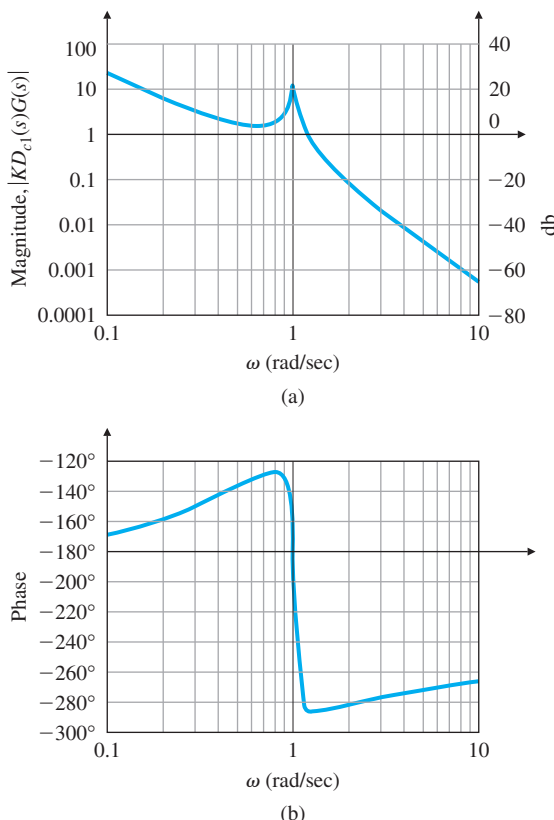
**Figure 10.5**

Root locus of  $D_{c1}(s)G(s)$



because of the resonance.<sup>2</sup> At this point, we take the simple action of reducing our expectation with respect to bandwidth, and we slow the

<sup>2</sup>If this system were built, the actuator jets would saturate as the response grew. We could analyze the response using the method described in Section 9.3 for nonlinear systems. From the analysis, we would expect the signal to grow and the equivalent gain of the

**Figure 10.6**Bode plot of  $D_{c1}(s)\hat{G}(s)$ 

system down by lowering the gain until the system is stable. With so little damping, we must really go slowly. A bit of experimentation leads to

$$D_{c2}(s) = 0.001(30s + 1), \quad (10.8)$$

for which the root locus is drawn in Fig. 10.7 and the Bode plot given in Fig. 10.8. The Bode plot shows that we have a phase margin of  $50^\circ$  but a crossover frequency of only  $\omega_c = 0.04$  rad/sec. While this is too low to meet the settling-time specification, a low crossover frequency is unavoidable if we expect to keep the gain at the resonance frequency below unity so that it is gain stabilized.

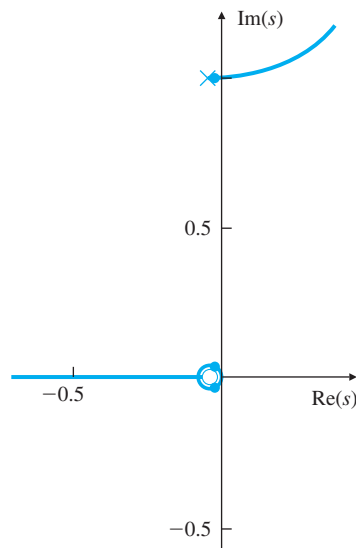
An alternative approach to the problem is to place zeros near the lightly damped poles and use them to hold these poles back from the RHP. Such a compensation has a frequency response with a very low gain near the frequency of the offending poles and a reasonable gain elsewhere. Because the frequency response seems to have a dent or notch in it, this compensation is called a **notch filter**. (It is also called a **band reject filter** in electric network theory.) An RC

### Notch filter

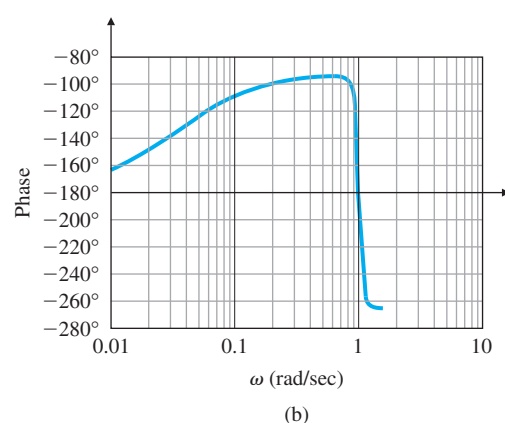
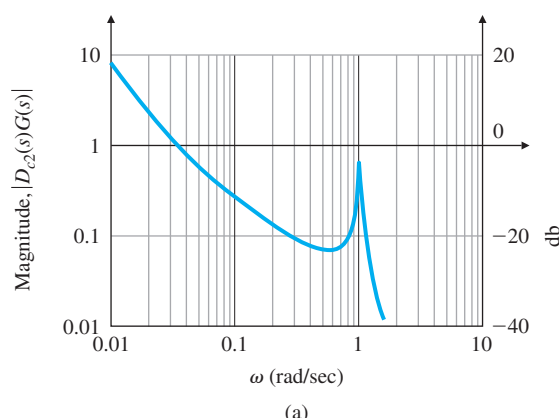
---

actuator to fall until the roots return to the imaginary axis near  $\omega_n$ . The resulting limit cycle would rapidly deplete the control gas supply.

**Figure 10.7**  
Root locus of  $D_{c2}(s)G(s)$

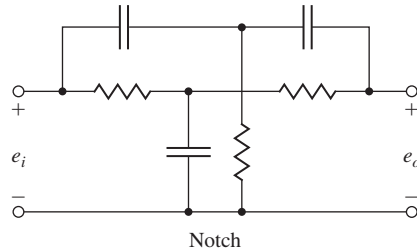


**Figure 10.8**  
Bode plot of  $D_{c2}(s)G(s)$

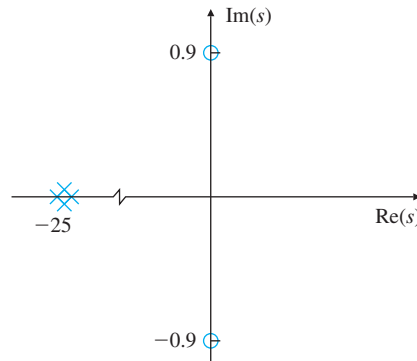


**Figure 10.9**

Twin-tee realization  
of a notch filter

**Figure 10.10**

Notch filter pole-zero  
pattern



circuit with a notch characteristic is shown in Fig. 10.9, its pole-zero pattern in Fig. 10.10, and its frequency response in Fig. 10.11. The  $+180^\circ$  phase lead of the notch can be used to correct for the  $180^\circ$  phase lag of the resonance; if the notch frequency is *lower* than the plant's resonance frequency, the system phase is kept above  $180^\circ$  near resonance.

With this idea, we return to the compensation given by Eq. (10.7) and add the notch, producing the revised compensator transfer function

$$D_{c3}(s) = 0.25(2s + 1) \frac{(s/0.9)^2 + 1}{[(s/25) + 1]^2}. \quad (10.9)$$

The Bode plot for this case is shown in Fig. 10.12, the root locus in Fig. 10.13, and the unit step response in Fig. 10.14. The settling time of the design is too long for the specification and the overshoot is too large, but this design approach seems promising; with iteration it could lead to a satisfactory compensator.

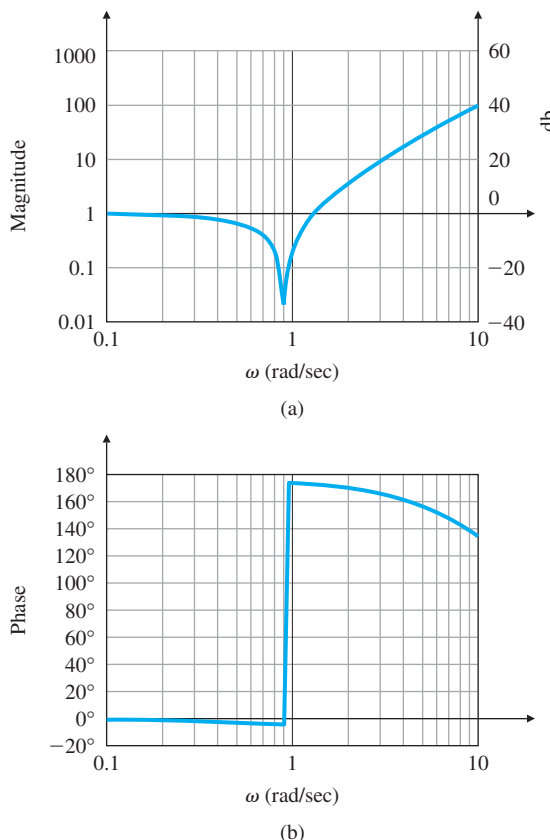
We now recall that the compensator is expected to provide adequate performance as the parameters vary over the ranges given by Eq. (10.3a). An examination of the robustness of the design can be made by looking at the root locus shown in Fig. 10.15, which is drawn using the compensator of Eq. (10.9) and the plant with  $\omega_n = 2$ , rather than 1, such that

$$\hat{G}(s) = \frac{(s/50 + 1)}{s^2(s^2/4 + 0.02s + 1)}. \quad (10.10)$$

This assumes the boom is as stiff as possible. Notice now the low-frequency poles have a damping ratio of only 0.02. Combining the

**Figure 10.11**

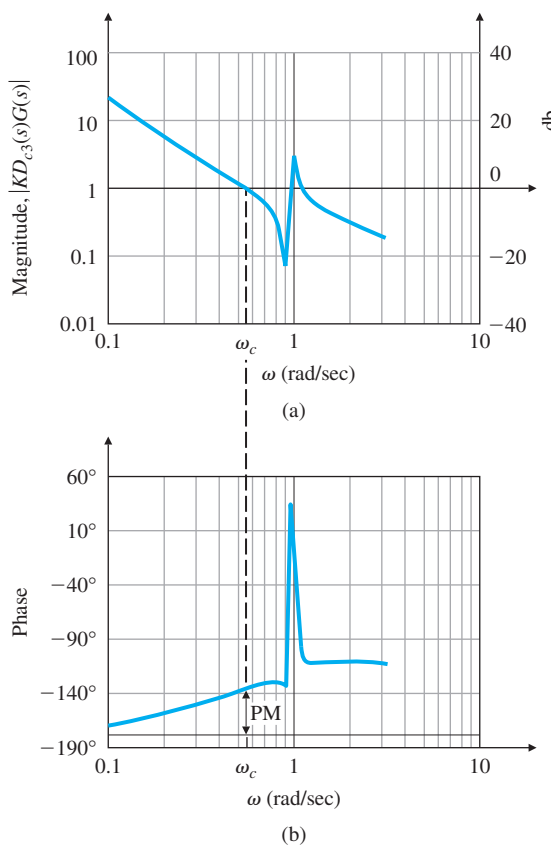
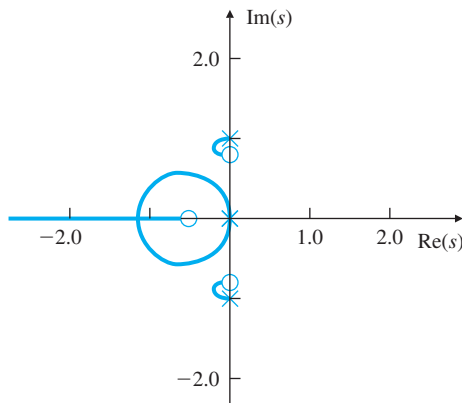
Bode plot of a notch filter



various parameter values, we get the frequency response and transient response shown in Figs. 10.16 and 10.17. We could make a few more trial-and-error iterations with the notch filter and rate feedback, but the system is complex enough that a look at state-space designs now seems reasonable. We go to Step 7.

**STEP 6. Evaluate/modify plant.** Refer to the collocated control discussion after Step 8.

**STEP 7. Try an optimal design using pole placement.** Using the state-variable formulation of the equations of motion in Eq. (10.4a), we devise a controller that will place the closed-loop poles in arbitrary locations. Of course, used without thought, the method of pole placement can also result in a design that requires unreasonable levels of control effort or is very sensitive to changes in the plant transfer function. Guidelines for pole placement were given in Chapter 7; an often successful approach is to derive optimal pole locations using the SRL. Figure 10.18 shows the SRL for the problem at hand. To obtain a bandwidth of about 0.5 rad/sec, we select closed-loop control poles from this locus at  $-0.45 \pm 0.34j$  and  $-0.15 \pm 1.05j$ .

**Figure 10.12**Bode plot of  $D_{c3}(s)G(s)$ **Figure 10.13**Root locus of  $D_{c3}(s)G(s)$ 

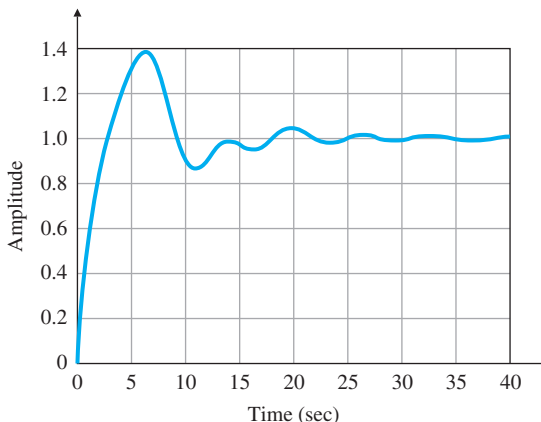
If we select  $\alpha_c(s)$ , as discussed earlier, from the SRL, the control gain using the Matlab function place is

$$\mathbf{K} = \begin{bmatrix} -0.2788 & 0.0546 & 0.6814 & 1.1655 \end{bmatrix}. \quad (10.11)$$

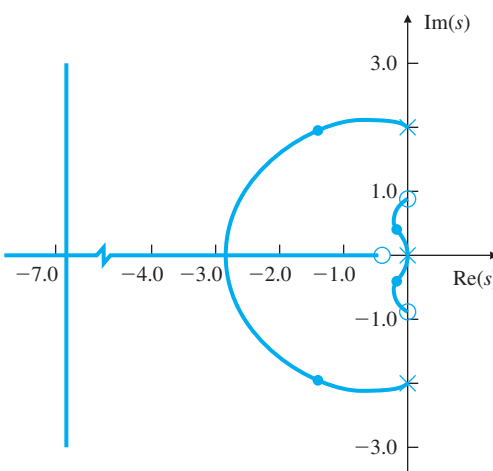
Figure 10.19 shows the step responses for the nominal plant parameters and stiff-spring plant models. The Bode plot of the SRL controller

**Figure 10.14**

Closed-loop step response of  $D_{c3}(s)G(s)$  where  $\theta_2(0) = 0.2 \text{ rad}$

**Figure 10.15**

Root locus of  $D_{c3}(s)\hat{G}(s)$

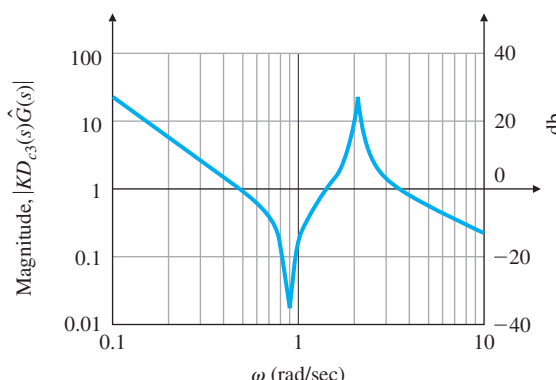


design with the nominal plant parameters can be computed from the loop transfer function (by breaking the loop at  $u$ )

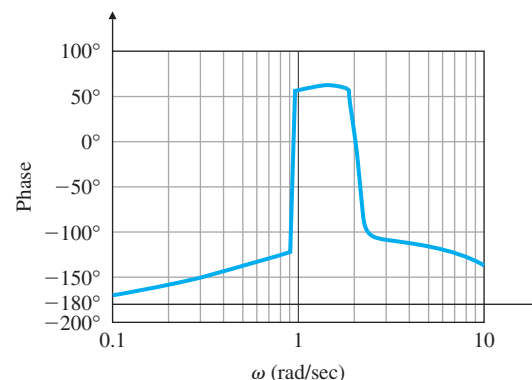
$$\frac{\mathbf{KX}(s)}{U(s)} = \mathbf{K}(s\mathbf{I} - \mathbf{A})^{-1}\mathbf{B},$$

and results in a phase margin of about  $60^\circ$ , as shown in Fig. 10.20. While the speed of response of the design meets the specifications with the nominal plant, the settling time when the plant has the stiff spring is a bit longer than the specifications call for. We might be able to get a better compromise between the nominal and the stiff-spring cases by selecting another point on the SRL; at this point, we do not know. The designer must face alternatives such as these and select the best compromise for the problem at hand.

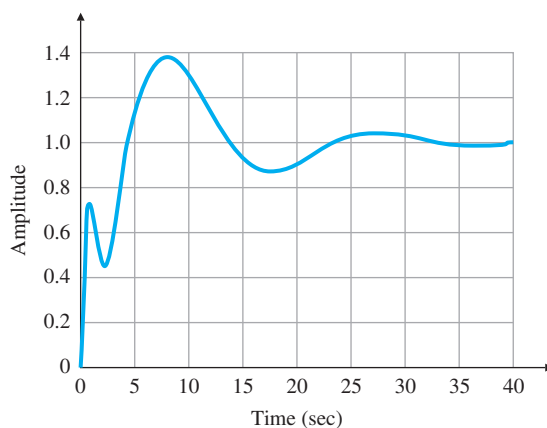
The design of Fig. 10.19 is based on full-state feedback. To complete the optimal design, we need an estimator. We select the closed-loop estimator error poles to be about eight times faster than the control poles. The reason for this is to keep the error poles from reducing the

**Figure 10.16**Bode plot of  $D_{c3}(s)\hat{G}(s)$ 

(a)



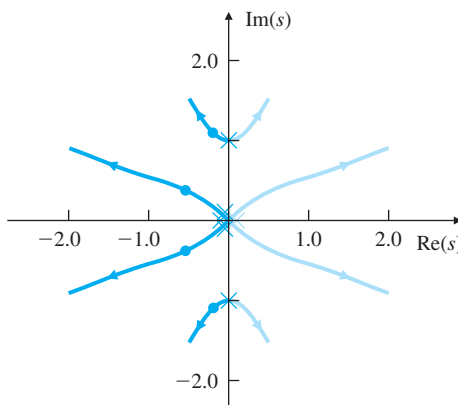
(b)

**Figure 10.17**Closed-loop step response of  $D_{c3}(s)\hat{G}(s)$ 

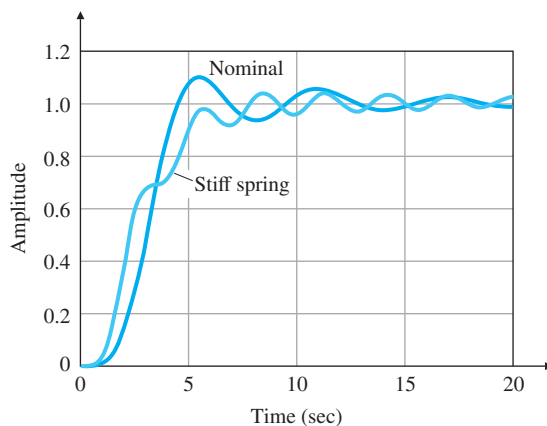
robustness of the design; a fast estimator will have almost the same effect on the response as no estimator at all. We choose the error poles from the SRL at  $-7.7 \pm 3.12j$  and  $-3.32 \pm 7.85j$ . Pole placement with these values leads to an estimator (filter) gain, using the Matlab function `place`:

**Figure 10.18**

Symmetric root locus of the satellite system

**Figure 10.19**

Closed-loop step response of the SRL design



$$\mathbf{L} = \begin{bmatrix} 22 \\ 242.3 \\ 1515.4 \\ 5503.9 \end{bmatrix}. \quad (10.12)$$

After we combine the control gain and estimator, as described in Section 7.8, the compensator transfer function that results from Eq. (7.174) is

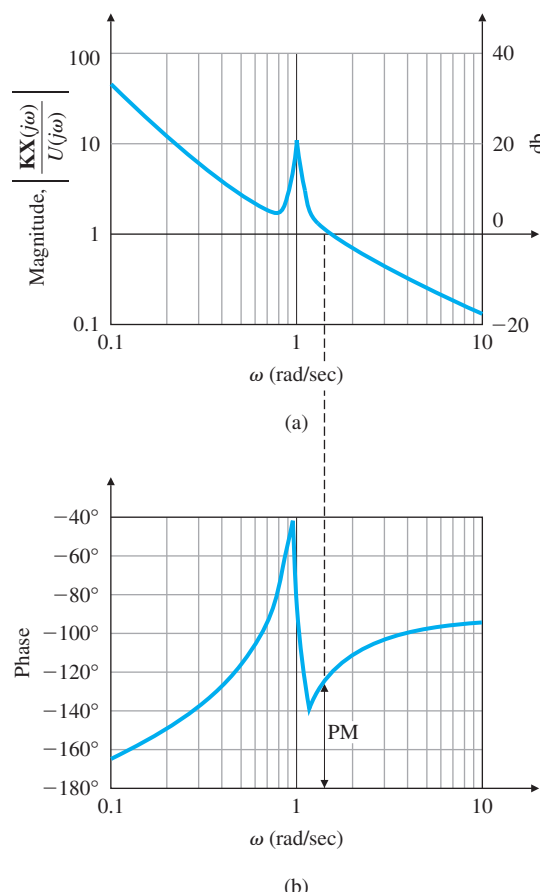
$$D_{c4}(s) = \frac{-745(s + 0.3217)(s + 0.0996 \pm 0.9137j)}{(s + 3.1195 \pm 8.3438j)(s + 8.4905 \pm 3.6333j)}. \quad (10.13)$$

The frequency response of this compensator (see Fig. 10.21) shows that pole placement has introduced a notch implicitly. The frequency response and the root locus of the combined system  $D_{c4}(s)G(s)$  are given in Figs. 10.22 and 10.23, while Fig. 10.24 shows the step response for both the nominal and the stiff-spring plants. Notice the design almost meets the specifications.

**STEP 8. Simulate the design, and compare the alternatives.** At this point we have two designs, with differing complexities and different

**Figure 10.20**

Frequency response of the SRL design from  $u$  to  $KX$



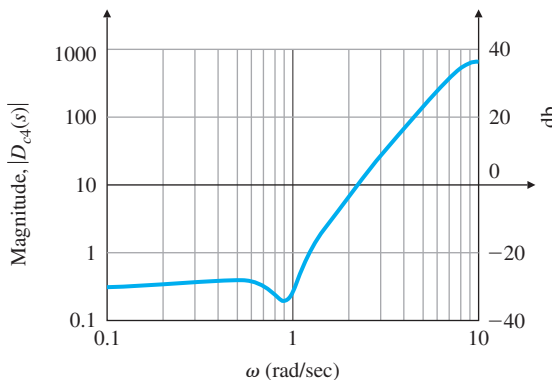
robustness properties. The notch-filter design might be improved with further iterations or by starting with a different nominal case. The SRL design meets the specifications for the nominal plant but is too slow for the stiff-spring case, although alternative selections for the pole locations might lead to a better design. In either case, much more extensive studies need to be made to explore the robustness and noise-response properties. Rather than follow any of these paths, we consider some aspects of the physical system.

Both designs are strongly influenced by the presence of the lightly damped resonant mode caused by the coupled masses. However, the transfer function of this system is strongly dependent on the fact that the actuator is on one body and the sensor is on the other (that is, not collocated). Suppose, rather than considering pointing the star tracker on the small mass, we have the mission of pointing the main mass, perhaps toward an Earth station for communications purposes. For this purpose, we can put the sensor on the *same* mass that holds the actuator—to give control with a collocated actuator and sensor. Due to the physics of the situation, the system's transfer function now has

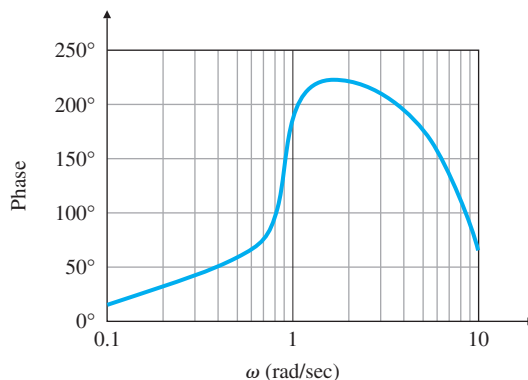
**Collocated actuator and sensor**

**Figure 10.21**

Bode plot of the optimal compensator  $D_{c4}(s)$



(a)



(b)

zeros close to the flexible modes, so control can be achieved using PD feedback alone, because the plant already has the effect of a notch compensator. Consider the transfer function of the satellite with collocated actuator and sensor (to measure  $\theta_1$ ) for which the state matrices are

$$\mathbf{A} = \begin{bmatrix} 0 & 1 & 0 & 0 \\ -0.91 & -0.036 & 0.91 & 0.036 \\ 0 & 0 & 0 & 1 \\ 0.091 & 0.0036 & -0.091 & -0.0036 \end{bmatrix}, \quad \mathbf{B} = \begin{bmatrix} 0 \\ 0 \\ 0 \\ 1 \end{bmatrix},$$

$$\mathbf{C} = [0 \ 0 \ 1 \ 0].$$

The transfer function of the system using the Matlab `ss2tf` function is

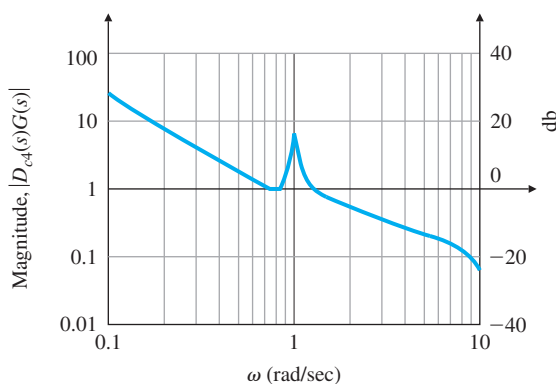
$$G_{co}(s) = \mathbf{C}(s\mathbf{I} - \mathbf{A})^{-1}\mathbf{B} = \frac{(s + 0.018 \pm 0.954j)}{s^2(s + 0.02 \pm j)}. \quad (10.14)$$

Notice the presence of the zeros in the vicinity of the complex conjugate poles. If we now use the same PD feedback as before, namely,

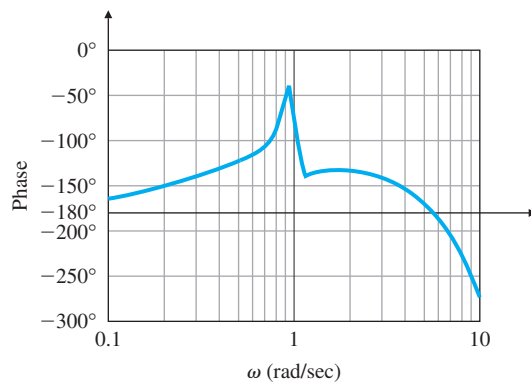
$$D_{c5}(s) = 0.25(2s + 1), \quad (10.15)$$

**Figure 10.22**

Bode plot of the compensated system  
 $D_{c4}(s)G(s)$



(a)



(b)

**Figure 10.23**

Root locus of  $D_{c4}(s)G(s)$

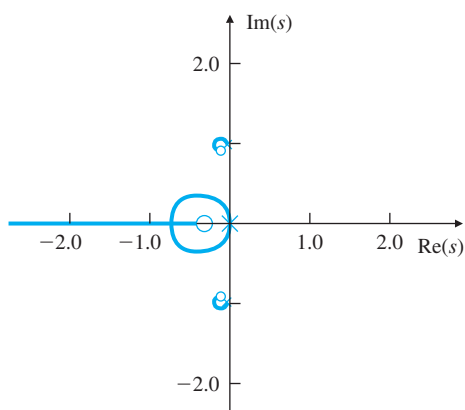
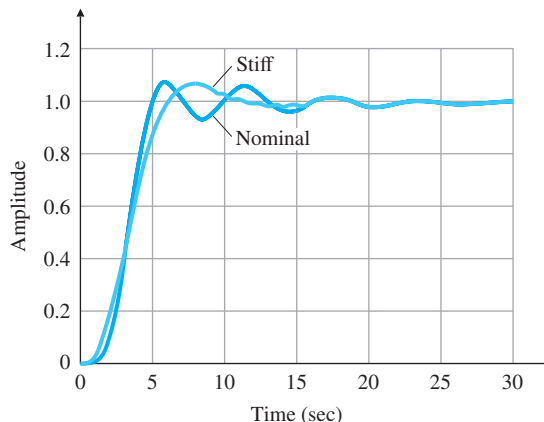


**Figure 10.24**

Closed-loop step response of  $D_{c4}(s)G(s)$

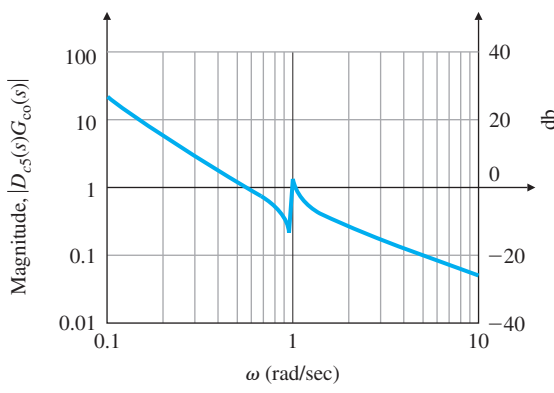


then the system will not only be stabilized, but will also have a satisfactory response (if we consider  $\theta_1$  as the output), because the resonant poles tend to be cancelled by the complex conjugate zeros.

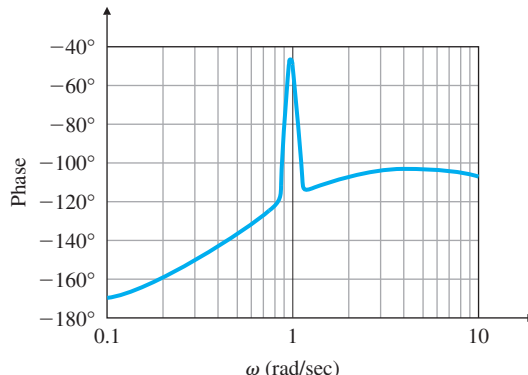
Figures 10.25 to 10.27 show the frequency response, the root locus, and the step response, respectively, for this system. Note from Fig. 10.27

**Figure 10.25**

Bode plot of  $D_{c5}(s)G_{co}(s)$



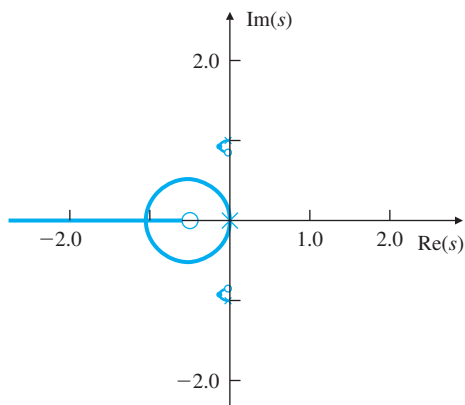
(a)



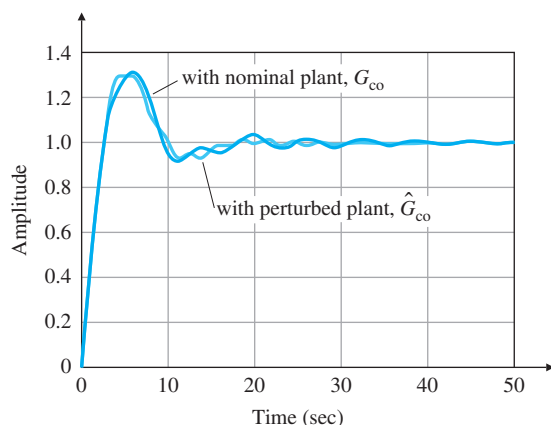
(b)

**Figure 10.26**

Root locus for  
 $D_{c5}(s)G_{co}(s)$

**Figure 10.27**

Closed-loop step response of the system with collocated control,  $D_{c5}(s)G_{co}(s)$  and  $D_{c5}(s)\hat{G}_{co}(s)$



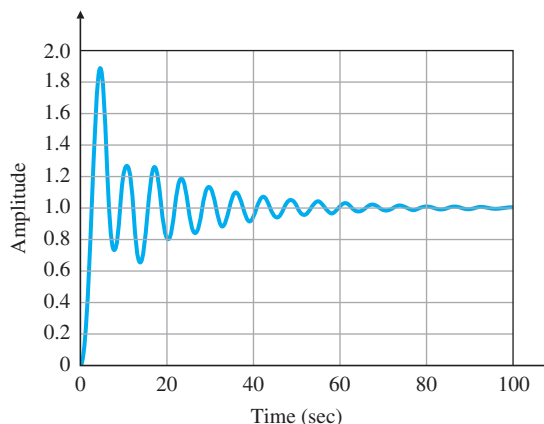
the step response has the excess overshoot associated with the zero of the compensator in the forward path of the transfer function.

The result is a very simple robust design achieved by moving the sensor from a noncollocated position to one collocated with the actuator. The result illustrates that, to achieve good feedback control, it is very important to consider sensor location and other features of the physical problem. However, this last control design will *not* do for pointing the star tracker. This is evident from plotting the output  $\theta_2$  corresponding to the nice step response of Fig. 10.27. The result is shown in Fig. 10.28.

An architecture suggested by these results is to place a coarse star tracker on the satellite body to be used for search and initial settling. Then switch to a star tracker on the instrument package with longer settling time for fine control.

**Figure 10.28**

Response at  $\theta_2$  of the collocated design



### 10.3 Lateral and Longitudinal Control of a Boeing 747

The Boeing 747 (see Fig. 10.29) is a large wide-body transport jet. A schematic with the relevant coordinates that move with the airplane is shown in Fig. 10.30. The linearized equations of (rigid-body) motion<sup>3</sup> for the Boeing 747 are of eighth order, but are separated into two fourth-order sets representing the perturbations in longitudinal ( $U$ ,  $W$ ,  $\theta$ , and  $q$  in Fig. 10.30) and lateral ( $\phi$ ,  $\beta$ ,  $r$ , and  $p$ ) motion. The longitudinal motion consists of axial ( $X$ ), vertical ( $Z$ ), and pitching ( $\theta$ ,  $q$ ) motion, while the lateral motion consists of rolling ( $\phi$ ,  $p$ ) and yawing ( $r$ ,  $\beta$ ) movement. The side-slip angle  $\beta$  is a measure of the direction of forward velocity relative to the direction of the nose of the airplane. The elevator control surfaces and the throttle affect the longitudinal motion, whereas the aileron and rudder primarily affect lateral motion. Although there is a small amount of coupling of lateral motion into longitudinal motion, this is usually ignored, so the equations of motion

**Figure 10.29**

Boeing 747

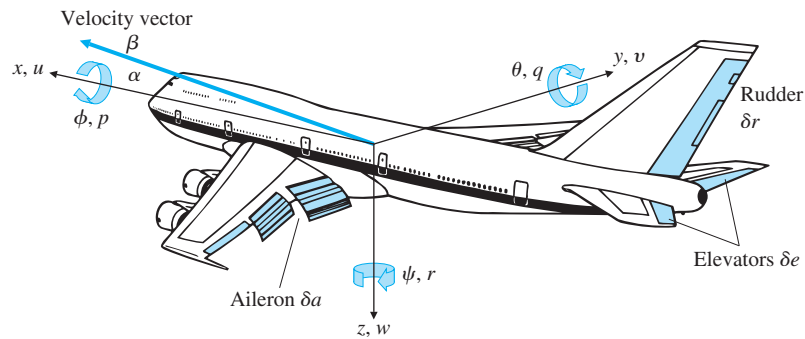
*Source: ClassicStock/Alamy Stock Photo*



<sup>3</sup>For derivation of equations of motion for an aircraft, refer to Bryson (1994), Etkin and Reid (1996), and McRuer et al. (1973).

**Figure 10.30**

Definition of aircraft coordinates



$x, y, z$  = position coordinates

$u, v, w$  = velocity coordinates

$p$  = roll rate

$q$  = pitch rate

$r$  = yaw rate

$\phi$  = roll angle

$\theta$  = pitch angle

$\psi$  = yaw angle

$\beta$  = side-slip angle

$\alpha$  = angle of attack

are treated as two decoupled fourth-order sets for designing the control, or **stability augmentation**, for the aircraft.

The nonlinear rigid body equations of motion in body-axis coordinates, under proper assumptions,<sup>4</sup> can be derived as (Bryson, 1994)

$$m(\dot{U} + qW - rV) = X - mg \sin \theta + \kappa T \cos \theta, \quad (10.16)$$

$$m(\dot{V} + rU - pW) = Y + mg \cos \theta \sin \phi,$$

$$m(\dot{W} + pV - qU) = Z + mg \cos \theta \cos \phi - \kappa T \sin \theta,$$

$$I_x \dot{p} + I_{xz} \dot{r} + (I_z - I_y)qr + I_{xz}qp = L, \quad (10.17)$$

$$I_y \dot{q} + (I_x - I_z)pr + I_{xz}(r^2 - p^2) = M,$$

$$I_z \dot{r} + I_{xz} \dot{p} + (I_y - I_x)qp - I_{xz}qr = N,$$

where

$m$  = mass of the aircraft,

$[U, V, W]$  = body-axis components of the velocity of the center of mass (c.m.),

$$\beta = \tan^{-1} \left( \frac{V}{U} \right),$$

$[U_o, V_o, W_o]$  = reference velocities,

$[p, q, r]$  = the body-axis components of the angular velocity of the aircraft,

$[X, Y, Z]$  = the body-axis aerodynamic forces about the c.m.,

$[L, M, N]$  = the body-axis aerodynamic torques about the c.m.,

---

<sup>4</sup> $x-z$  is the body-axis plane of mass symmetry.

- $g_o$  = the gravitational force per unit mass,  
 $I_i$  = the inertias in body axes,  
 $(\theta, \phi)$  = the Euler pitch and roll angles of the aircraft body,  
 $V_{\text{ref}}$  = reference flight speed,  
 $T$  = the propulsive thrust resultant, and  
 $\kappa$  = the angle between thrust and body  $x$ -axis.

The linearization of these equations can be carried out as follows: In the steady-state straight, level, and constant speed flight condition,  $\dot{U} = \dot{V} = \dot{W} = \dot{p} = \dot{q} = \dot{r} = 0$ . Furthermore, there is no turning in any axis so that  $p_o = q_o = r_o = 0$ , and the wings will be level so that  $\phi = 0$ . However, there will be an angle of attack in order to provide some lift from the wings to counteract the aircraft's weight, so  $\theta_o$  and  $W_o \neq 0$ , where

$$\begin{aligned} U &= U_o + u, \\ V &= V_o + v, \\ W &= W_o + w. \end{aligned} \quad (10.18)$$

The steady-state velocity body axis components will be

$$\begin{aligned} U_o &= V_{\text{ref}} \cos(\theta_o), \\ V_o &= 0 (\beta_o = 0), \\ W_o &= V_{\text{ref}} \sin(\theta_o), \end{aligned} \quad (10.19)$$

as depicted in Fig. 10.31. With these conditions, the *equilibrium* (see Chapter 9) equations are

$$\begin{aligned} 0 &= X_0 - mg_o \sin \theta_0 + \kappa T \cos \theta_0, \\ 0 &= Y_0, \\ 0 &= Z_0 + mg_o \cos \theta_0 - \kappa T \sin \theta_0, \\ 0 &= L_0, \\ 0 &= M_0, \\ 0 &= N_0. \end{aligned} \quad (10.20)$$

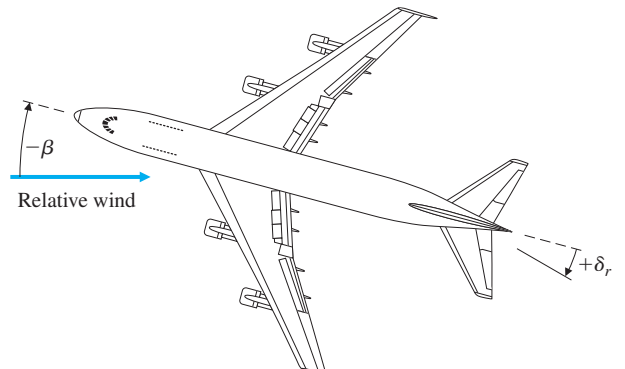
With the assumptions (Bryson, 1994)

$$\begin{aligned} (v^2, w^2) &\ll u^2, \\ (\phi^2, \theta^2) &\ll 1, \\ (p^2, q^2, r^2) &\ll \frac{u^2}{b^2}, \end{aligned} \quad (10.21)$$

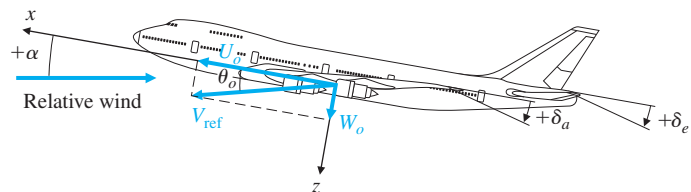
where  $b$  denotes the wingspan, many of the nonlinear terms in Eqs. (10.16) and (10.17) can be neglected. Substitution of Eq. (10.20) in

**Figure 10.31**

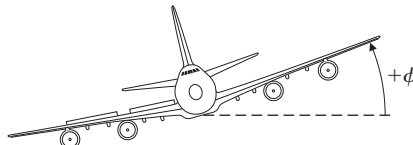
Steady-state flight condition



(a)



(b)



(c)

the nonlinear equations of motion leads to a set of linear perturbational equations that describe small deviations from constant speed, straight and level flight. The equations of motion then divide into two uncoupled sets of *longitudinal* and *lateral* equations of motion.

For linearized longitudinal motion, the results are

$$\begin{bmatrix} \dot{u} \\ \dot{w} \\ \dot{q} \\ \dot{\theta} \end{bmatrix} = \begin{bmatrix} X_u & X_w & -W_o & -g_o \cos \theta_o \\ Z_u & Z_w & U_o & -g_o \sin \theta_o \\ M_u & M_w & M_q & 0 \\ 0 & 0 & 1 & 0 \end{bmatrix} \begin{bmatrix} u \\ w \\ q \\ \theta \end{bmatrix} + \begin{bmatrix} X_{\delta e} \\ Z_{\delta e} \\ M_{\delta e} \\ 0 \end{bmatrix} \delta e, \quad (10.22)$$

where

$u$  = forward velocity perturbation in the aircraft in  $x$  direction (see Fig. 10.30),

$w$  = velocity perturbation in the  $z$  direction (also proportional to perturbations in the angle of attack,  $\alpha = \frac{w}{U_0}$ ),

$q$  = angular rate about the positive  $y$ -axis, or pitch rate,

$\theta$  = pitch-angle perturbation from the reference  $\theta_o$  value,

$X_{u,w,\delta e}$  = partial derivative of the aerodynamic force in  $x$  direction with respect to perturbations in  $u$ ,  $w$ , and  $\delta e$ ,<sup>5</sup>

$Z_{u,w,\delta e}$  = partial derivative of the aerodynamic force in  $z$  direction with respect to perturbations in  $u$ ,  $w$ , and  $\delta e$ ,

$M_{u,w,q,\delta e}$  = partial derivative of the aerodynamic (pitching) moment with respect to perturbations in  $u$ ,  $w$ ,  $q$ , and  $\delta e$ ,

$\delta e$  = movable tail-section, or “elevator,” angle for pitch control.

$W_o q$ ,  $U_o q$  terms in the equations are due to the angular velocity of the body fixed (rotating) reference frame and arise directly from the left-hand side of Eq. (10.16).

To determine altitude changes, we need to add the following equation to the longitudinal equations of motion:

$$\dot{h} = V_{ref} \sin \theta - w \cos \theta. \quad (10.23)$$

This equation will result in the linearized altitude equation

$$\dot{h} = V_{ref} \theta - w, \quad (10.24)$$

which is to be augmented with Eq. (10.22).

For linearized lateral motion, the results are

$$\begin{bmatrix} \dot{\beta} \\ \dot{r} \\ \dot{p} \\ \dot{\phi} \end{bmatrix} = \begin{bmatrix} Y_v & -U_o & V_o & g_o \cos \theta_o \\ N_v & N_r & N_p & 0 \\ L_v & L_r & L_p & 0 \\ 0 & \tan \theta_o & 1 & 0 \end{bmatrix} \begin{bmatrix} \beta \\ r \\ p \\ \phi \end{bmatrix} + \begin{bmatrix} Y_{\delta r} & Y_{\delta a} \\ N_{\delta r} & N_{\delta a} \\ L_{\delta r} & L_{\delta a} \\ 0 & 0 \end{bmatrix} \begin{bmatrix} \delta r \\ \delta a \end{bmatrix}, \quad (10.25)$$

where

$\beta$  = side-slip angle, defined to be  $\frac{v}{U_o}$ ,

$r$  = yaw rate,

$p$  = roll rate,

$\phi$  = roll angle,

$Y_{v,\delta r,\delta a}$  = partial derivative of the aerodynamic force in the  $y$  direction with respect to perturbations in  $\beta$ ,  $\delta r$ , and  $\delta a$ ,

$N_{v,r,p,\delta r,\delta a}$  = aerodynamic (yawing) moment stability derivatives,

$L_{v,r,p,\delta r,\delta a}$  = aerodynamic (rolling) moment stability derivatives,

$\delta r$  = rudder deflection,

$\delta a$  = aileron deflection.

---

<sup>5</sup>  $X$ ,  $Z$ , and  $M$  are stability derivatives and are identified from wind tunnel and flight tests.

We will next discuss the design of a stability-augmentation system for the lateral dynamics, called a **yaw damper**, and the autopilot affecting the longitudinal behavior.

### 10.3.1 Yaw Damper

**STEP 1. Understand the process and its performance specifications.** Swept-wing aircraft have a natural tendency to be lightly damped in the lateral modes of motion. At typical commercial-aircraft cruising speeds and altitudes, this dynamic mode is sufficiently difficult to control that virtually every swept-wing aircraft has a feedback system to help the pilot. Therefore, the goal of our control system is to modify the natural dynamics so the plane is acceptable for the pilot to fly.<sup>6</sup> Studies have shown that pilots like natural frequencies in the range of  $\omega_n \lesssim 0.5$  and damping ratio of  $\zeta \geq 0.5$ . Aircraft with dynamics that violate these guidelines are generally considered fatiguing to fly and highly undesirable. With the pilot being a key part of the closed-loop system, we want to make his or her job as easy as possible. Thus our system specifications are to achieve lateral dynamics that meet these constraints.

**STEP 2. Select sensors.** The easiest measurement of aircraft motion to take is the angular rate. The side-slip angle can be measured with a wind-vane device, but it is noisier and less reliable for stabilization. Two angular rates—roll and yaw—partake in the lateral motion. Study of the lightly damped lateral mode indicates that it is primarily a yawing phenomenon, so measurement of the yaw rate is a logical starting point for the design. Until the early 1980s the measurement was made with a **gyroscope** with a small, fast-spinning rotor that can yield an electric output proportional to the angular yaw rate of the aircraft. Since the early 1980s, most new aircraft systems have relied on a laser device (called a **ring-laser gyroscope**) for the measurement. Here, two laser beams traverse a closed path (often a triangle) in opposite directions. As the triangular device rotates, the detected frequencies of the two beams appear to shift, and this frequency shift is measured, producing a measure of rotational rate. These devices have fewer moving parts and are more reliable at less cost than the spinning-rotor variety of gyroscopes.

**STEP 3. Select actuators.** Two aerodynamic surfaces typically influence the lateral aircraft motion: the rudder and the ailerons (see Fig. 10.30). The lightly damped yaw mode that will be stabilized by the yaw damper is most affected by the rudder. Therefore, use of that single control input is a logical starting point for the design. Hence, it is best to choose the rudder as our actuator. Hydraulic devices are universally employed in

---

<sup>6</sup>The mode is sufficiently difficult to control manually that, if the yaw damper fails in cruise, the pilot is instructed to descend and slow down where the mode is more manageable.

large aircraft to provide the force that moves the aerodynamic surfaces. No other kind of device has been developed to provide the combination of high force, high speed, and light weight desirable for the actuation of the controlling aerodynamic surfaces. On the other hand, the low-speed flaps, which are extended slowly prior to landing, are typically actuated by an electric motor with a worm gear. For small aircraft with no autopilot, no actuator is required at all; the pilot yoke is directly connected to the aerodynamic surface by means of wire cables, and all the force required to move the surfaces is provided by the pilot.

**STEP 4. Make a linear model.** The lateral-perturbation equations of motion for a Boeing 747 in horizontal flight at 40,000 ft and nominal forward speed  $U_0 = 774$  ft/sec (Mach 0.8) (Heffley and Jewell, 1972), with the rudder chosen as the actuator (Step 3), are

$$\begin{bmatrix} \dot{\beta} \\ \dot{r} \\ \dot{p} \\ \dot{\phi} \end{bmatrix} = \begin{bmatrix} -0.0558 & -0.9968 & 0.0802 & 0.0415 \\ 0.598 & -0.115 & -0.0318 & 0 \\ -3.05 & 0.388 & -0.4650 & 0 \\ 0 & 0.0805 & 1 & 0 \end{bmatrix} \begin{bmatrix} \beta \\ r \\ p \\ \phi \end{bmatrix} + \begin{bmatrix} 0.00729 \\ -0.475 \\ 0.153 \\ 0 \end{bmatrix} \delta r,$$

$$y = [0 \ 1 \ 0 \ 0] \begin{bmatrix} \beta \\ r \\ p \\ \phi \end{bmatrix},$$

where  $\beta$  and  $\phi$  are in radians, and  $r$  and  $p$  are in radians per second. The transfer function, using the Matlab ss2tf function, is

$$G(s) = \frac{r(s)}{\delta r(s)} = \frac{-0.475(s + 0.498)(s + 0.012 \pm 0.488j)}{(s + 0.0073)(s + 0.563)(s + 0.033 \pm 0.947j)}, \quad (10.26)$$

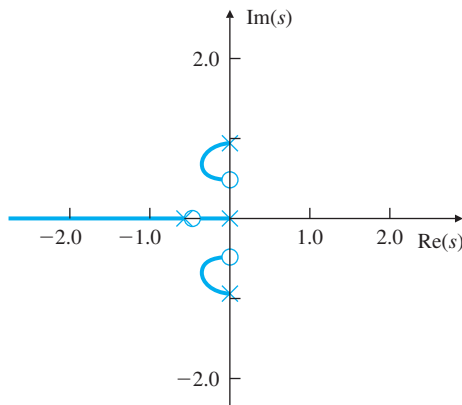
so the system has two stable real poles and a pair of stable complex poles. Notice first the low-frequency gain is negative, corresponding to the simple physical fact that a positive or clockwise rudder motion causes a negative or counter-clockwise yaw rate. In other words, turning the rudder left (clockwise) causes the front of the aircraft to rotate left (counter-clockwise). The natural motion corresponding to the complex poles is referred to as the **Dutch roll**; the name comes from the motions of a person skating on the frozen canals of the Netherlands. The motion corresponding to the stable real poles is referred to as the **spiral mode** ( $s_1 = -0.0073$ ) and the **roll mode** ( $s_2 = -0.563$ ). From looking at the system poles, we see the offending mode that needs repair for good pilot handling is the Dutch roll, with the poles at  $s = -0.033 \pm 0.95j$ . The roots have an acceptable frequency, but their damping ratio  $\zeta \cong 0.03$  is far short of the desired value  $\zeta \cong 0.5$ .

[Dutch roll](#)

[Spiral mode](#)  
[Roll mode](#)

**Figure 10.32**

Root locus for yaw damper with proportional feedback



**STEP 5. Try a lead-lag or PID design.** As a first try at the design, we will consider proportional feedback of the yaw rate to the rudder. The root locus with respect to the gain of this feedback is shown in Fig. 10.32, and its frequency response is shown in Fig. 10.33. The figures show that  $\zeta \cong 0.45$  is achievable and can be computed to occur at a gain of about 3.0.

This feedback, however, creates an objectionable situation during a steady turn when the yaw rate is constant: Because the feedback produces a steady rudder input opposite the yaw rate, the pilot must introduce a much larger steady command for the same yaw rate than is necessary in the open-loop case. This dilemma is solved by attenuating the feedback at DC (that is, “washing out” the feedback). This is accomplished by inserting

$$H(s) = \frac{s}{s + 1/\tau},$$

in the feedback, which passes the yaw-rate feedback at frequencies above  $1/\tau$  and provides no feedback at DC. Therefore, in a steady turn, the damper will provide no correction. Figure 10.34 shows a block diagram of the yaw damper with the washout.

For a more complete model, we include the rudder servo, which represents the actuator dynamics and has the transfer function

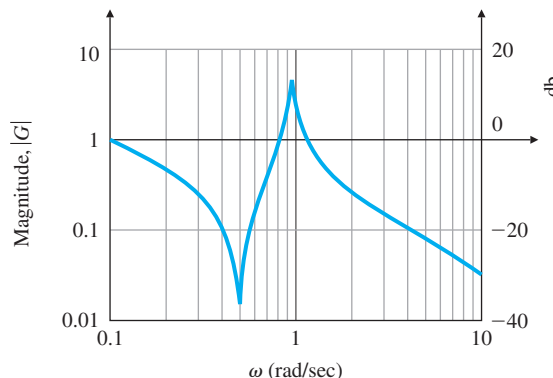
$$A(s) = \frac{\delta r(s)}{e_{\delta r}(s)} = \frac{10}{s + 10},$$

which is fast compared with the dynamics of the rest of the system and is not expected to change the response very much. The root locus, including actuator dynamics and a washout circuit with  $\tau = 3$ , is shown in Fig. 10.35. As seen from the root locus, the addition of the yaw-rate feedback, including the washout, allows the damping ratio to be increased from 0.03 to about 0.35. The associated frequency response of the system is shown in Fig. 10.36. The response of the closed-loop system to an initial condition of  $\beta_0 = 1^\circ$  is shown in Fig. 10.37 for

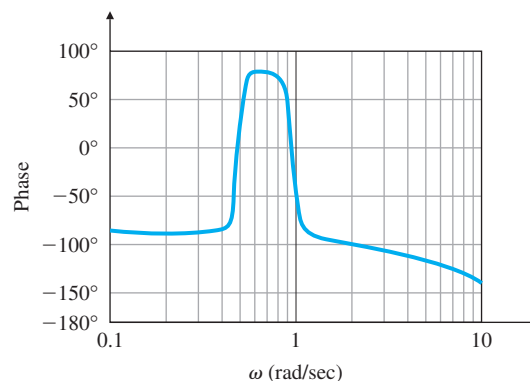
Washout

**Figure 10.33**

Bode plot of yaw damper with proportional feedback



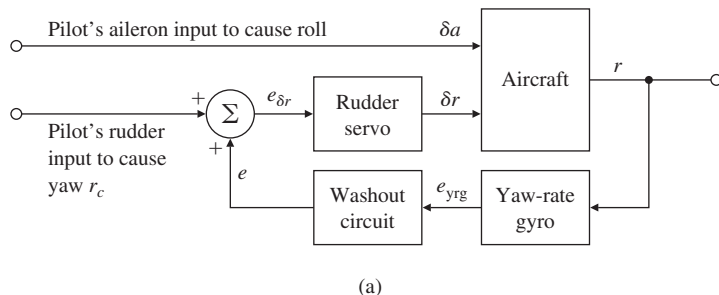
(a)



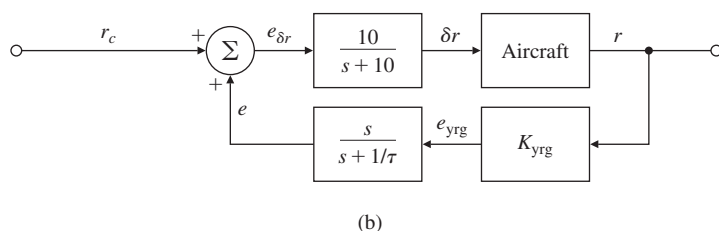
(b)

**Figure 10.34**

Yaw damper:  
(a) functional block diagram; (b) block diagram for analysis



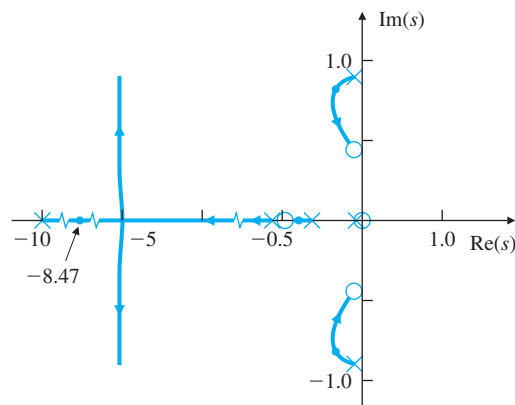
(a)



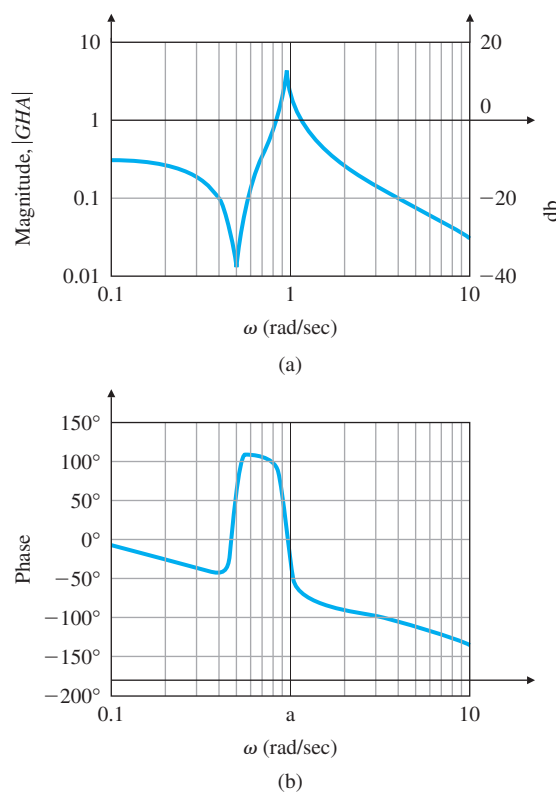
(b)

**Figure 10.35**

Root locus with washout circuit,  $\tau = 3$

**Figure 10.36**

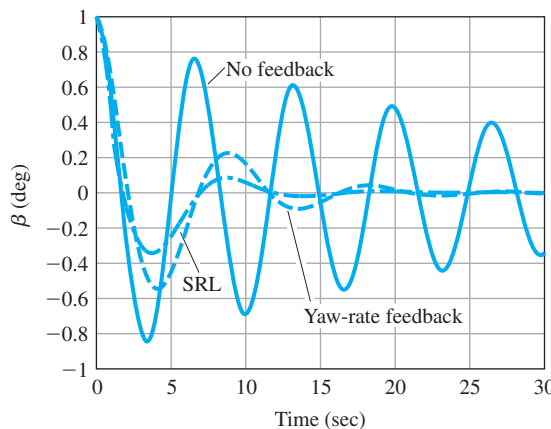
Bode plot of yaw damper, including washout and actuator



a root-locus gain of 2.6. For reference, the response of yaw rate without feedback is also given. Although feedback of yaw rate through the washout circuit results in a considerable improvement over the original aircraft control, the response is not as good as originally specified. Further iterations (not included here) could include other gain values or more complex compensations.

**Figure 10.37**

Initial-condition response with yaw damper and washout, and SRL design, for  $\beta(0) = 1^\circ$



**STEP 6.** *Evaluate/modify plant.* The solution would be to unsweep the wings, which would cause a large drag penalty.

**STEP 7.** *Try an optimal design using pole placement.* If we augment the dynamic model of the system by adding the actuator and washout, we obtain the state-variable model

$$\begin{bmatrix} \dot{x}_A \\ \dot{\beta} \\ \dot{r} \\ \dot{p} \\ \dot{\phi} \\ \dot{x}_{wo} \end{bmatrix} = \begin{bmatrix} -10 & 0 & 0 & 0 & 0 & 0 \\ 0.0729 & -0.0558 & -0.997 & 0.0802 & 0.0415 & 0 \\ -4.75 & 0.598 & -0.1150 & -0.0318 & 0 & 0 \\ 1.53 & -3.05 & 0.388 & -0.465 & 0 & 0 \\ 0 & 0 & 0.0805 & 1 & 0 & 0 \\ 0 & 0 & 1 & 0 & 0 & -0.333 \end{bmatrix} \times \begin{bmatrix} x_A \\ \beta \\ r \\ p \\ \phi \\ \dot{x}_{wo} \end{bmatrix} + \begin{bmatrix} 10 \\ 0 \\ 0 \\ 0 \\ 0 \\ 0 \end{bmatrix} e_{\delta r},$$

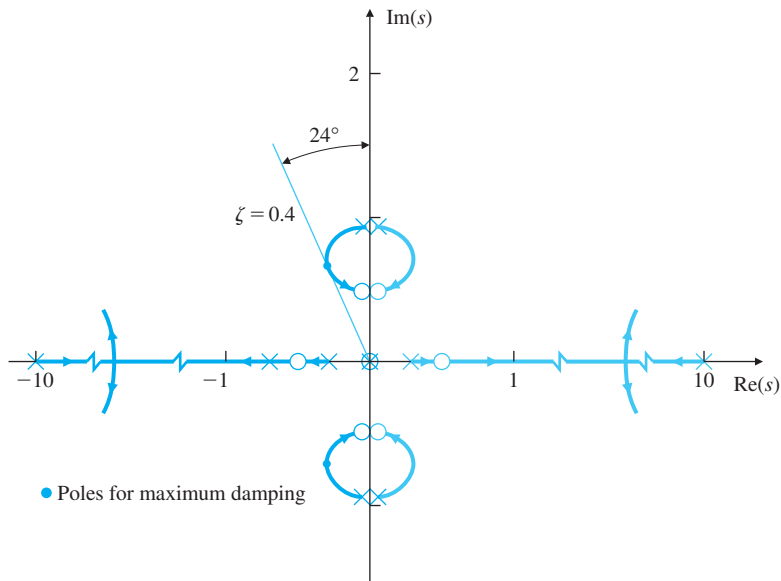
$$e = [0 \ 0 \ 1 \ 0 \ 0 \ -0.333]^T, \begin{bmatrix} x_A \\ \beta \\ r \\ p \\ \phi \\ x_{wo} \end{bmatrix},$$

where  $e_{\delta r}$  is the input to the actuator and  $e$  is the output of the washout. The SRL for the augmented system is as shown in Fig. 10.38. If we select the state-feedback poles from the SRL so that the complex roots have maximum damping ( $\zeta = 0.4$ ), we find that

$$pc = [-0.0051; -0.468; 0.279+0.628*j; 0.279-0.628*j; -1.106; -9.89].$$

**Figure 10.38**

SRL of lateral dynamics,  
including washout filter  
and actuator



Then we can compute the state-feedback gain, using the Matlab function place, to be

$$\mathbf{K} = [1.059 \quad -0.191 \quad -2.32 \quad 0.0992 \quad 0.0370 \quad 0.486].$$

Note that the third entry in  $\mathbf{K}$  is larger than the others, so the feedback of all six state variables is essentially the same as proportional feedback of  $r$ . This is also evident from the similarity of the root locus in Fig. 10.32 and the SRL of Fig. 10.38. If we select the estimator poles to be five times faster than the controller poles, then

$$\text{pe} = [-0.0253; -2.34; -1.39 + 3.14j; -1.39 - 3.14j; -5.53; -49.5]$$

and the estimator gain, again using the Matlab function place, is found to be

$$\mathbf{L} = \begin{bmatrix} 25.0 \\ -2,044 \\ -5,158 \\ -24,843 \\ -40,113 \\ -15,624 \end{bmatrix}.$$

The compensator transfer function from Eq. (7.177) is

$$D_c(s) = \frac{-844(s+10.0)(s-1.04)(s+0.974 \pm 0.559j)(s+0.0230)}{(s+0.0272)(s+0.837 \pm 0.671j)(s+4.07 \pm 10.1j)(s+51.3)}. \quad (10.27)$$

Figure 10.37 also shows the response of the yaw rate to an initial condition of  $\beta_0 = 1^\circ$ . It is clear from the root locus that the damping can be improved by the SRL approach, and this is borne out by the

reduced oscillatory behavior in the transient response of the system. However, this improvement has come at a considerable price. Note the order of the compensator has increased from one in the original design (see Fig. 10.33) to six and washout in the design obtained using the controller-estimator-SRL approach.

Aircraft yaw dampers in use today generally employ a proportional feedback of yaw rate to rudder through a washout or through minor modifications to this design. The improved performance achievable with an optimal design approach utilizing full-state feedback and estimation is not judged to be worth the increase in complexity.

Perhaps a more fruitful approach to improving the design would be to add the aileron surface as a control variable along with the rudder.

**STEPS 8 and 9. Verify the design.** Linear models of aircraft motion are reasonably accurate as long as the motion is small enough that the actuators and surfaces do not saturate. Because actuators are sized for safety in order to handle large transients, such saturation is very rare. Therefore, the linear-analysis-based design is reasonably accurate, and we will not pursue a nonlinear simulation or further design verification. However, aircraft manufacturers do carry out extensive nonlinear simulations and flight testing under all possible flight conditions before obtaining Federal Aviation Administration (FAA) certification to carry passengers.

### 10.3.2 Altitude-Hold Autopilot

**STEP 1. Understand the process and its performance specifications.** One of the pilot's many tasks is to hold a specific altitude. As an aid to keeping aircraft from colliding, those craft on an easterly path are required to be on an odd multiple of 1000 ft, and those on a westerly path on an even multiple of 1000 ft. Therefore, the pilot needs to be able to hold the altitude to less than a hundred feet. A well-trained, attentive pilot can easily accomplish this task manually to within  $\pm 50$  ft, and air-traffic controllers expect pilots to maintain this kind of tolerance. However, since this task requires the pilot to be fairly diligent, sophisticated aircraft often have an altitude-hold autopilot to lessen the pilot's work. This system differs fundamentally from the yaw damper because its role is to replace the pilot for a certain period, while the yaw damper's role is to help the pilot fly. Dynamic specifications, therefore, need not require that pilots like the craft's "feel" (how it responds to their handling of the controls); instead, the design should provide the kind of ride that pilots and passengers like. The damping ratio should still be in the vicinity of  $\zeta \cong 0.5$ , but for a smooth ride, the natural frequency should be much slower than  $\omega_n = 1$  rad/sec.

**STEP 2. Select sensors.** Clearly needed is a device to measure altitude, a task most easily done by measuring the atmospheric pressure. Almost from the time of the first Wright brothers' flight, this basic idea has been

used in a device called a **barometric altimeter**. Before autopilots, the device consisted of a bellows whose free end was connected to a needle that directly indicated altitude on a dial. The same bellows concept is used today for the altitude display, but the pressure is sensed electrically for the autopilot.

Because the transfer function from the controlling elevator input to the altitude control consists of five poles [see Eq. (10.30)], stabilization of the feedback loop cannot be accomplished by simple proportional feedback. Therefore the pitch rate  $q$  is also used as a stabilizing feedback; it is measured by a gyroscope or ring-laser gyro identical to that used for yaw-rate measurement. Further stabilization using pitch-angle feedback is also helpful. It is obtained either from an inertial reference system based on a ring-laser gyro or from a rate-integrating gyro. The latter is a device similar to the rate gyro, but structured differently so its outputs are proportional to the angles of the aircraft's pitch  $\theta$  and roll  $\phi$ .

**STEP 3. Select actuators.** The only aerodynamic surface typically used for pitch control on most aircraft is the elevator  $\delta e$ . It is located on the horizontal tail, well removed from the aircraft's center of gravity, so its force produces an angular pitch rate and thus a pitch angle, which acts to change the lift from the wing. In some high-performance aircraft, there are direct-lift control devices on the wing or perhaps small canard surfaces, which are like tiny wings forward of the main wing, which produce vertical forces on the aircraft that are much faster than elevators on the tail are able to generate. However, for purposes of our altitude hold, we will consider only the typical case of an elevator surface on the tail.

As for the rudder, hydraulic actuators are the preferred devices to move the elevator surface, mainly because of their favorable force-to-weight ratio.

**STEP 4. Make a linear model.** The longitudinal perturbation equations of motion for the Boeing 747 in horizontal flight at a nominal speed  $U_0 = 830$  ft/sec at 20,000 ft (Mach 0.8) with a weight of 637,000 lb are

$$\dot{\mathbf{x}} = \mathbf{Ax} + \mathbf{B}\delta e, \quad (10.28)$$

$$\begin{bmatrix} \dot{u} \\ \dot{w} \\ \dot{q} \\ \dot{\theta} \\ \dot{h} \end{bmatrix} = \begin{bmatrix} -0.00643 & 0.0263 & 0 & -32.2 & 0 \\ -0.0941 & -0.624 & 820 & 0 & 0 \\ -0.000222 & -0.00153 & -0.668 & 0 & 0 \\ 0 & 0 & 1 & 0 & 0 \\ 0 & -1 & 0 & 830 & 0 \end{bmatrix} \begin{bmatrix} u \\ w \\ q \\ \theta \\ h \end{bmatrix} + \begin{bmatrix} 0 \\ -32.7 \\ -2.08 \\ 0 \\ 0 \end{bmatrix} \delta e,$$

where the desired output for an altitude-hold autopilot is

$$h = \mathbf{Cx},$$

$$h = [ \begin{array}{ccccc} 0 & 0 & 0 & 0 & 1 \end{array} ] \begin{bmatrix} u \\ w \\ q \\ \theta \\ h \end{bmatrix}, \quad (10.29)$$

and

$$\frac{h(s)}{\delta e(s)} = \frac{32.7(s + 0.0045)(s + 5.645)(s - 5.61)}{s(s + 0.003 \pm 0.0098j)(s + 0.6463 \pm 1.1211j)}. \quad (10.30)$$

The system has two pairs of stable complex poles and a pole at  $s = 0$ . The complex pair at  $-0.003 \pm 0.0098j$  are referred to as the **phugoid mode**,<sup>7</sup> and the poles at  $-0.6463 \pm 1.1211$  are the **short-period modes**, as computed using the Matlab eig command.

**Phugoid mode**  
**Short-period modes**

**Inner-loop design**

STEP 5. Try a lead-lag or PID controller. As a first step in the design, it is typically helpful to use an inner-loop feedback of pitch rate  $q$  to  $\delta e$  so as to improve the damping of the short-period mode of the aircraft (see Fig. 10.39). The transfer function from  $\delta e$  to  $q$ , using the Matlab ss2tf function, is

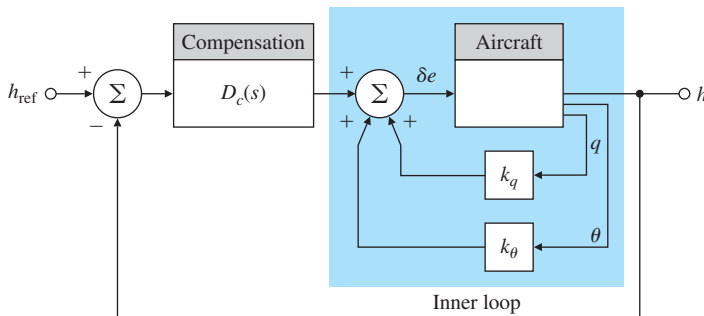
$$\frac{q(s)}{\delta e(s)} = -\frac{2.08s(s + 0.0105)(s + 0.596)}{(s + 0.003 \pm 0.0098j)(s + 0.646 \pm 1.21j)}. \quad (10.31)$$

The inner loop root locus for  $q$  feedback using Eq. (10.31) is as shown in Fig. 10.40. Because  $k_q$  is the root-locus parameter, the system matrix [Eq. (10.28)] is now modified to

$$\mathbf{A}_q = \mathbf{A} + k_q \mathbf{BC}_q, \quad (10.32)$$

where  $\mathbf{A}$  and  $\mathbf{B}$  are defined in Eq. (10.28) and  $\mathbf{C}_q = [ \begin{array}{ccccc} 0 & 0 & 1 & 0 & 0 \end{array} ]$ . The process of picking a suitable gain  $k_q$  is an iterative one. The

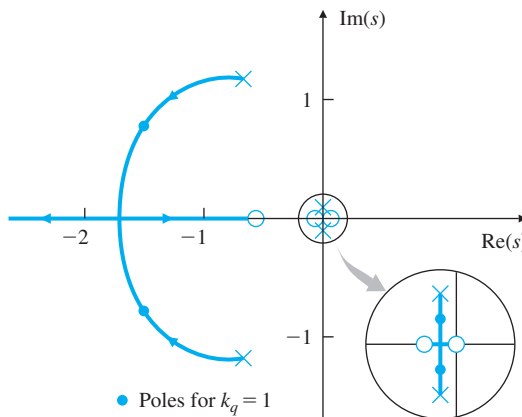
**Figure 10.39**  
Altitude-hold feedback system



<sup>7</sup>The name was adopted by F. W. Lanchester (1908), who was the first to study the dynamic stability of aircraft analytically. It is apparently an incorrect version of a Greek word.

**Figure 10.40**

## Inner-loop root locus for altitude-hold dynamics with $q$ feedback



selection procedure is the same as discussed in Chapter 5. (Recall the tachometer feedback example in Section 5.6.2.) If we choose  $k_q = 1$ , then the closed-loop poles will be located at  $-0.0039 \pm 0.0067j$ ,  $-1.683 \pm 0.277j$  on the root locus, and

$$\mathbf{A}_q = \begin{bmatrix} -0.00643 & 0.0263 & 0 & -32.2 & 0 \\ -0.0941 & -0.624 & 787.3 & 0 & 0 \\ -0.000222 & -0.00153 & -2.75 & 0 & 0 \\ 0 & 0 & 1 & 0 & 0 \\ 0 & -1 & 0 & 830 & 0 \end{bmatrix}. \quad (10.33)$$

Note only the third column of  $\mathbf{A}_q$  is different from  $\mathbf{A}$ . To further improve the damping, it is useful to feed back the pitch angle of the aircraft. By trial and error, we select

$$\mathbf{K}_{\theta q} = [ \begin{array}{ccccc} 0 & 0 & -0.8 & -6 & 0 \end{array} ],$$

in order to feed back  $\theta$  and  $q$ , and the system matrix becomes

$$\mathbf{A}_{\theta q} = \mathbf{A}_q - \mathbf{B}\mathbf{K}_{\theta q},$$

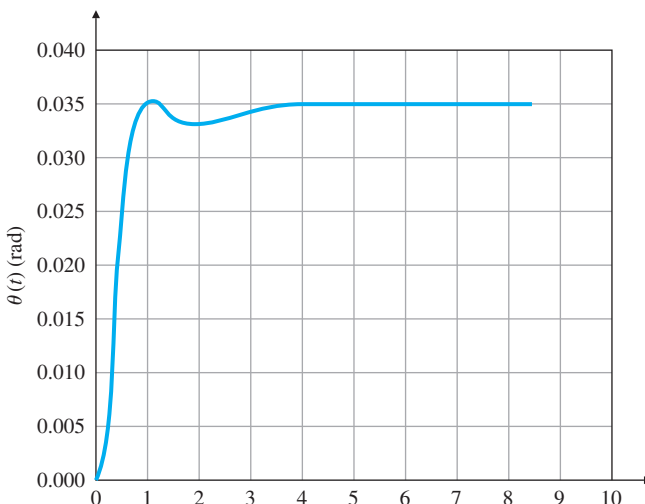
$$= \begin{bmatrix} -0.0064 & 0.0263 & 0 & -32.2 & 0 \\ -0.0941 & -0.624 & 761 & -196.2 & 0 \\ -0.0002 & -0.0015 & -4.41 & -12.48 & 0 \\ 0 & 0 & 1 & 0 & 0 \\ 0 & -1 & 0 & 830 & 0 \end{bmatrix},$$

with poles at  $s = 0, -2.25 \pm 2.99j, -0.531, -0.0105$ .

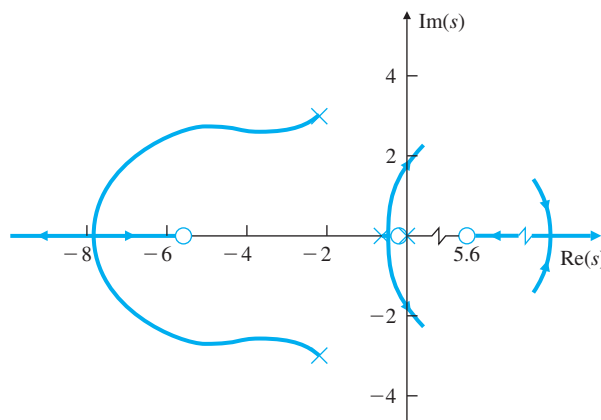
So far, the inner loop of the aircraft has been stabilized significantly. The uncontrolled aircraft has a natural tendency to return to equilibrium in level flight, as evidenced by the open-loop roots in the LHP. The inner-loop stabilization is necessary to enable an outer-loop feedback of  $h$  and  $\dot{h}$  to be successful; furthermore, the feedbacks of  $\theta$  and  $q$  can be used by themselves in an attitude-hold mode of the autopilot, when a pilot wishes to control  $\theta$  directly through an input command. Figure 10.41 shows the response of the inner loop to a  $2^\circ$  ( $0.035\text{-rad}$ )

**Figure 10.41**

Response of altitude-hold autopilot to a command in  $\theta$

**Figure 10.42**

$0^\circ$  root locus with feedback of  $h$  only



step command in  $\theta$ . With the inner loop in place, the transfer function of the system from elevator angle to altitude is now

$$\frac{h(s)}{\delta e(s)} = \frac{32.7(s + 0.0045)(s + 5.645)(s - 5.61)}{s(s + 2.25 \pm 2.99j)(s + 0.0105)(s + 0.0531)}. \quad (10.34)$$

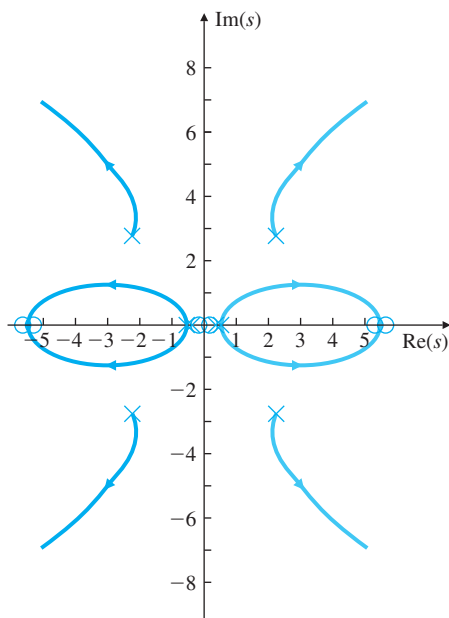
The root locus for this system, given in Fig. 10.42, shows that proportional feedback of altitude by itself does not yield an acceptable design. For stabilization, we may also feed back the rate of change in the altitude in a PD controller. The root locus of the system with feedback of both  $h$  and  $\dot{h}$  is shown in Fig. 10.43. After some iteration we find that the best ratio of  $\dot{h}$  to  $h$  is 10:1, that is,

$$D_{ce}(s) = K_h(s + 0.1).$$

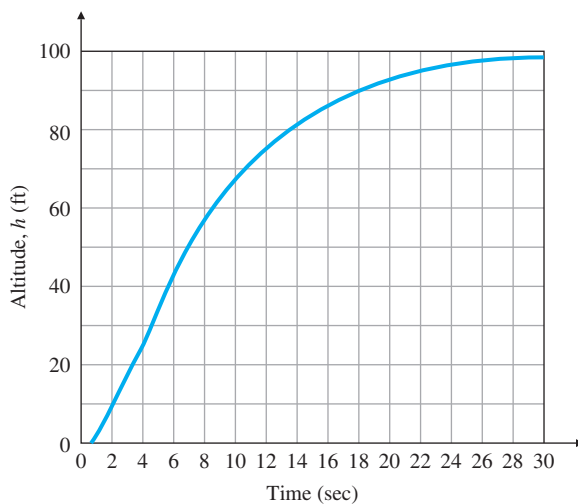
The final design is the result of iterations between the  $q$ ,  $\theta$ ,  $\dot{h}$ , and  $h$  feedback gains, obviously a lengthy process. Although this trial

**Figure 10.43**

SRL for altitude-hold design

**Figure 10.44**

Step response of altitude-hold autopilot to a 100-ft step command



design was successful, use of the SRL approach promises to expedite the process.

**STEP 6. Evaluate/modify plant.** Not applicable here.

**STEP 7. Do an optimal design.** The SRL of the system is shown in Fig. 10.43. If we choose the closed-loop poles at

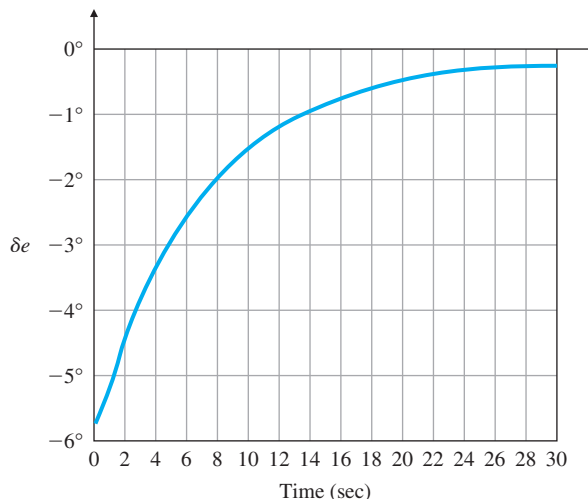
$$\text{pc} = [-0.0045; -0.145; -0.513; -2.25 - 2.98 * j; -2.25 + 2.98 * j],$$

then the required feedback gain, using the Matlab function place, is

$$\mathbf{K} = [ -0.0009 \quad 0.0016 \quad -1.883 \quad -7.603 \quad -0.001 ].$$

**Figure 10.45**

Control effort for 100-ft step command in altitude



The step response of the system to a 100-ft step command in  $h$  is shown in Fig. 10.44, and the associated control effort is shown in Fig. 10.45.

This design has been carried out with the assumption that the linear model is valid for the altitude changes under consideration. We should perform simulations to verify this or to determine the range of validity of the linear model.

STEPS 8 and 9. *Verify the design.* The comments in Steps 7 and 8 of Section 10.3.1 apply to this design as well.

For small-airplane autopilots now in production, such as the one described in Chapter 5, it is interesting to note, for the inner loop, some manufacturers employ only  $\theta$  feedback while others use  $q$  feedback. The use of  $\theta$  enables faster response, but use of  $q$  is less costly. Both, of course, use the altimeter for  $h$  feedback.

## 10.4 Control of the Fuel-Air Ratio in an Automotive Engine

Until the 1980s, most automobile engines had a carburetor to meter the fuel so the ratio of the gasoline-mass flow to air-mass flow, or fuel-to-air ratio (F/A), remained in the vicinity of 1:15. This device metered the fuel by relying on a pressure drop produced by the air flowing through a venturi. The device performed adequately in terms of keeping the engine running satisfactorily, but it historically allowed excursions of up to 20% in the F/A. After the implementation of federal exhaust-pollution regulations, this level of inaccuracy in the F/A was unacceptable because neither excess hydrocarbons (HCs) nor excess carbon monoxide (CO) could be accepted. During the 1970s, automobile companies improved the design and manufacturing process of the carburetors so they became more accurate and delivered a F/A accuracy in the vicinity of 3% to 5%.

Through a combination of factors, this improved F/A accuracy helped lower the exhaust pollution levels. However, the carburetors were still open-loop devices because the system did not measure the F/A of the mixture entering the engine for subsequent feedback into the carburetor. During the 1980s, almost all manufacturers turned to feedback control systems to provide a much-improved level of F/A accuracy, an action made necessary by the decreasing levels of allowable exhaust pollutants. In essence, the same scheme is used currently (2018) so the catalytic converters attached to the exhaust system can remove the pollutants from the exhaust and meet the federal standards.

We now turn to the design of a typical feedback system for engine control, again using the step-by-step design outline given in Section 10.1.

**STEP 1. Understand the process and its performance.** The method chosen to meet the exhaust-pollution standards has been to use a catalytic converter that simultaneously oxidizes excess levels of exhaust carbon monoxide (CO) and unburned HCs and reduces excess levels of the oxides of nitrogen (NO and NO<sub>2</sub>, or NO<sub>x</sub>). This device is usually referred to as a three-way catalyst because of its effect on all three pollutants. This catalyst is ineffective when the F/A is much different from the stoichiometric level of 1:14.7; therefore, a feedback control system is required to maintain the F/A within  $\pm 1\%$  of that desired level. The system is depicted in Fig. 10.46.

The dynamic phenomena that affect the relationship between the sensed F/A output from the exhaust and the fuel-metering command in the intake manifold are (1) intake fuel and air mixing, (2) cycle delays due to the piston strokes in the engine, and (3) the time required for the exhaust to travel from the engine to the sensor. All these effects are strongly dependent on the speed and load of the engine. For example, engine speeds typically vary from 600 to 6000 rpm. The result of these variations is that the time delays in the system that will affect the feedback control-system behavior will also vary by at least 10:1, depending on the operating condition. The system undergoes transients as the

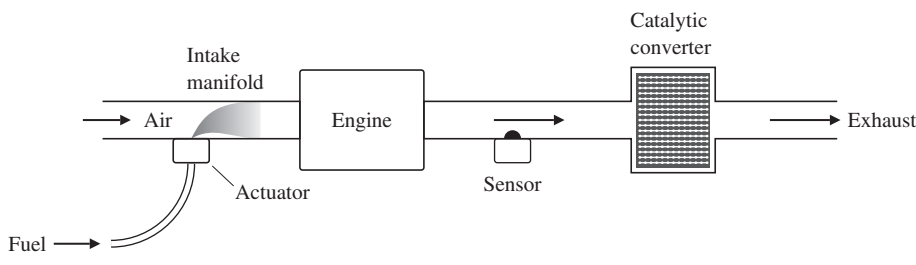
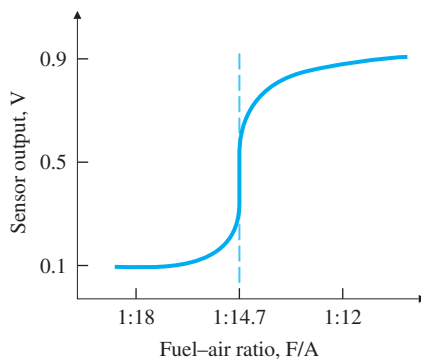


**Figure 10.46**  
F/A feedback control system

**Figure 10.47**

Exhaust sensor output



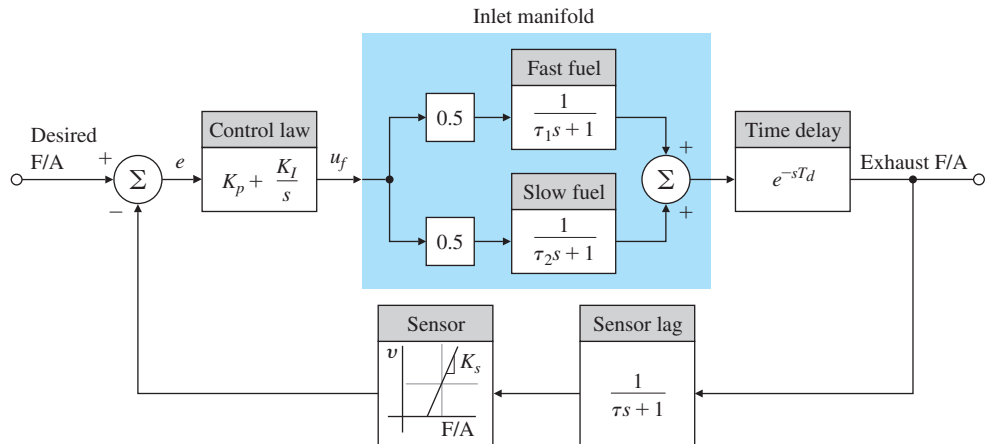
driver demands more or less power through changes in the accelerator pedal, with the changes taking place over fractions of a second. Ideally, the feedback control system should be able to keep up with these transients.

**STEP 2. Select sensors.** The discovery and development of the exhaust sensor was the key technological step that made possible this concept of exhaust-emission reduction by feedback control. The active element in the device, zirconium oxide, is placed in the exhaust stream, where it yields a voltage that is a monotonic function of the oxygen content of the exhaust gas. The F/A is uniquely related to the oxygen level. The voltage of the sensor is highly nonlinear with respect to F/A (see Fig. 10.47); almost all the change in voltage occurs precisely at the F/A value at which the feedback system must operate for effective performance of the catalyst. Therefore, the gain of the sensor will be very high when the F/A is at the desired point (1:14.7), but will fall off considerably for F/A excursions away from 1:14.7.

Although other sensors have been under development for possible use in F/A feedback control, no other cost-effective sensor has so far demonstrated the capability to perform adequately. All manufacturers of production-line automobiles currently use zirconium oxide sensors in their feedback control systems.

**STEP 3. Select actuators.** Fuel metering is accomplished by fuel injectors in current day automobiles. The fuel injectors are either placed in the inlet port near the entrance to each cylinder or the injectors spray the fuel at high pressures directly into the combustion chamber after the inlet valve is closed. These arrangements drastically improve the accuracy of the fuel control to each cylinder compared to the throttle body injection used when feedback control was first introduced in the 1980s. Direct injection into the combustion chambers has always been used for diesel engines, but started to be used for gasoline engines about 5 years ago. It has now become quite common due to its ability to carefully shape the fuel spray and timing of the fuel injection pattern, thus allowing higher compression ratios which lead to significant improvements in fuel economy along with reductions in particulates and the

Nonlinear sensor

**Figure 10.48**

Block diagram of an F/A control system

other exhaust emissions. Direct injection also minimizes the time delay thus providing better engine response and more accurate fuel control, which also helps economy and emissions.

**STEP 4. Make a linear model.** The sensor nonlinearity shown in Fig. 10.47 is severe enough that any design effort based on a linearized model of it should be used with caution. Figure 10.48 shows a block diagram of the system, with the sensor shown to have a gain  $K_s$ . The time constants  $\tau_1$  and  $\tau_2$  indicated for the inlet-manifold dynamics represent, respectively, fast-fuel flow in the form of vapor or droplets and slow-fuel flow in the form of a liquid film on the manifold walls. The time delay is the sum of (1) the time it takes the pistons to move through the four strokes from the intake process until the exhaust process and (2) the time required for the exhaust to travel from the engine to the sensor located roughly 1 ft away. A sensor lag with time constant  $\tau$  is also included in the process to account for the mixing that occurs in the exhaust manifold. Although the time constants and the delay time change considerably, primarily as a function of engine load and speed, we will examine the design at a specific point where the values are

$$\tau_1 = 0.02 \text{ sec}, \quad T_d = 0.2 \text{ sec},$$

$$\tau_2 = 1 \text{ sec}, \quad \tau = 0.1 \text{ sec}.$$

In an actual engine, designs would be carried out for all speed loads.

**STEP 5. Try a lead-lag or PID controller.** Given the tight error specifications and the wide variations in the required fuel command  $u_f$  due to varying engine-operating conditions, an integral-control term is mandatory. With integral control, any required steady-state  $u_f$  can be provided when the error signal  $e = 0$ . The addition of a proportional term, although not often used, allows for an increase (doubling) in the

bandwidth without degrading steady-state characteristics. In this example, we use a control law that is proportional plus integral (PI). The output from the control law is a voltage that drives the injector's pulse former to give a fuel pulse whose duration is proportional to the voltage. The controller transfer function can be written as

$$D_c(s) = K_p + \frac{K_I}{s} = \frac{K_p}{s}(s + z), \quad (10.35)$$

where

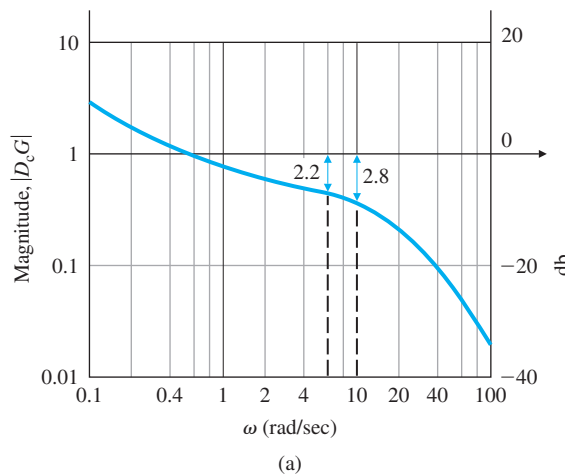
$$z = \frac{K_I}{K_p},$$

and  $z$  can be chosen as desired.

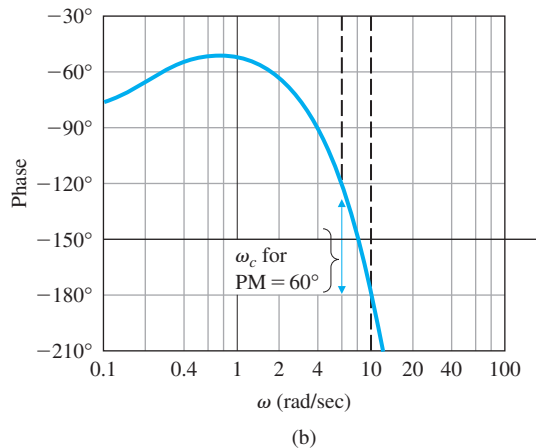
First, let us assume the sensor is linear and can be represented by a gain  $K_s$ . Then, we can choose  $z$  for good stability and good response of the system. Figure 10.49 shows the frequency response of the system for  $K_s K_p = 1.0$  and  $z = 0.3$ , while Fig. 10.50 shows a root locus

**Figure 10.49**

Bode plot of a PI F/A controller



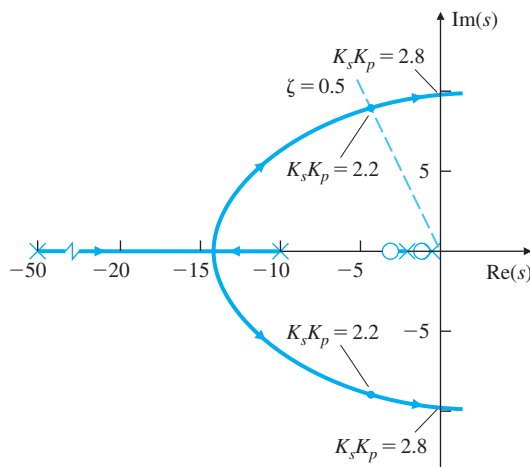
(a)



(b)

**Figure 10.50**

Root locus of a PI F/A controller



of the system with respect to  $K_s K_p$  with  $z = 0.3$ . Both analyses show the system becomes unstable for  $K_s K_p \cong 2.8$ . Figure 10.49 shows to achieve a phase margin of approximately  $60^\circ$ , the gain  $K_s K_p$  should be  $\sim 2.2$ . Figure 10.49 also shows this produces a crossover frequency of  $6.0 \text{ rad/sec} (\sim 1 \text{ Hz})$ . The root locus in Fig. 10.50 verifies this candidate design will achieve acceptable damping ( $\zeta \cong 0.5$ ).

Although this linear analysis shows that acceptable stability at a reasonable bandwidth ( $\sim 1 \text{ Hz}$ ) can be achieved with a PI controller, a look at the nonlinear sensor characteristics (see Fig. 10.47) shows that this indeed may not be achievable. Note the slope of the sensor output is extremely high near the desired setpoint, thus producing a very high value of  $K_s$ . Therefore, lower values of the controller gain  $K_p$  need to be used to maintain the overall  $K_s K_p$  value of 2.2 when including the effect of the high sensor gain. On the other hand, a value of  $K_p$  low enough to yield a stable system at F/A = 1 : 14.7 (= 0.068) will yield a very sluggish response to transient errors that deviate much from the setpoint, because the effective sensor gain will be reduced substantially. It is therefore necessary to account for the sensor nonlinearity in order to obtain satisfactory response characteristics of the system for anything other than minute disturbances about the setpoint. A first approximation to the sensor is shown in Fig. 10.51. Because the actual sensor gain at the setpoint is still quite different from its approximation, this approximation will yield erroneous conclusions regarding stability about the setpoint; however, it will be useful in a simulation to determine the response to initial conditions.

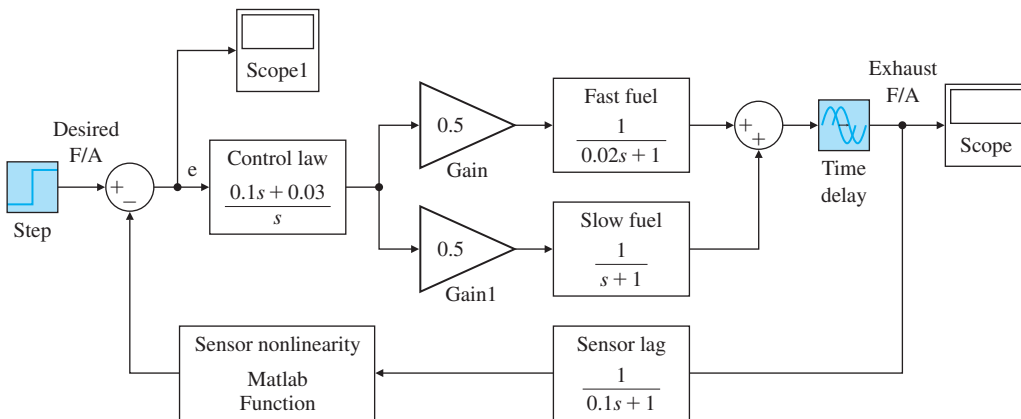
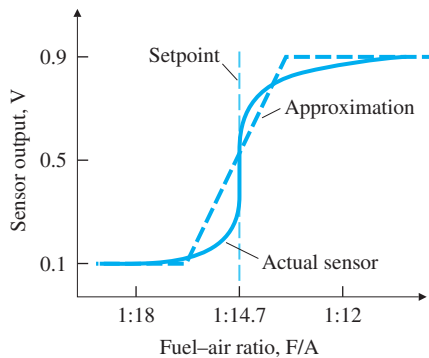
**STEP 6. Evaluate/modify plant.** The nonlinear sensor is undesirable; however, no suitable linear sensor has been found.

**STEP 7. Try an optimal controller.** The response of this system is dominated by the sensor nonlinearity, and any fine tuning of the control needs to account for that feature. Furthermore, the system dynamics

### Complications of nonlinearity

**Figure 10.51**

Sensor approximation

**Figure 10.52**

Closed-loop nonlinear simulation implemented in Simulink

Source: Reprinted with permission of The MathWorks, Inc.

are relatively simple, and it is unlikely that an optimal design approach will yield any improvement over the PI controller used. We will thus omit this step.

#### Simulink nonlinear simulation

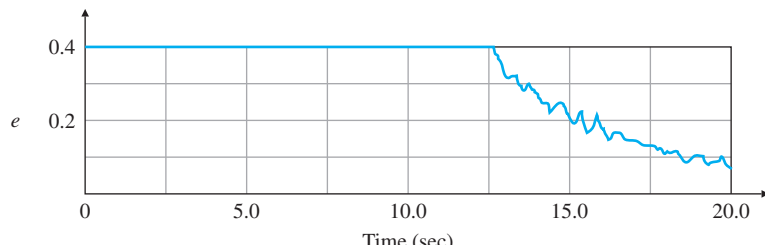
**STEP 8. Simulate design with nonlinearities.** The nonlinear closed-loop simulation of the system implemented in Simulink is shown in Fig. 10.52. The Matlab function `fas` implements the approximate nonlinear sensor characteristics of Fig. 10.51,

```
function y = fas(u)
if u < 0.0606,
    y = 0.1;
elseif u < 0.0741,
    y = 0.1 + (u - 0.0606) * 20;
else y = 0.9;
end
```

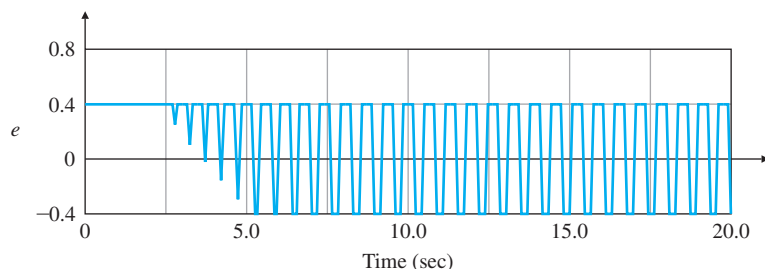
Figure 10.53(a) is a plot of the system error using the approximate sensor of Fig. 10.51 and  $K_p K_s = 2.0$ . The slow response is apparent with

**Figure 10.53**

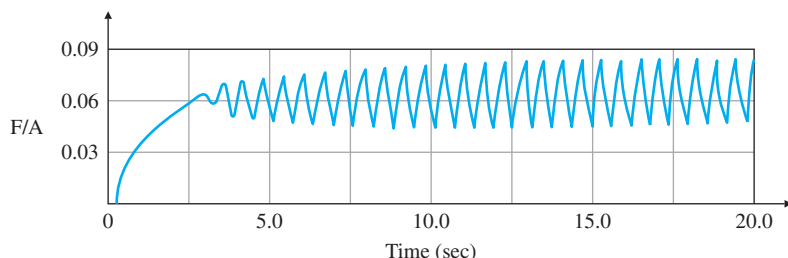
System response with  
nonlinear sensor  
approximation



(a)



(b)



(c)

12.5 sec before the error comes out of saturation and a time constant of almost 5 sec once the linear region is reached. In real automobiles, these systems are operated with much higher gains. To show these effects, a simulation with  $K_p K_s = 6.0$  is plotted in Fig. 10.53(b, c). At this gain the linear system is unstable, and up until about 5 sec, the signals grow. The growth halts after 5 sec due to the fact that, as the input to the sensor nonlinearity gets large, the *effective gain* of the sensor decreases due to the saturation, and eventually, a limit cycle is reached. The frequency of this limit cycle corresponds to the point at which the root locus crosses the imaginary axis and has an amplitude such that the total effective gain of  $K_p K_{s,eq} = 2.8$ . As described in Section 9.3, the effective gain of a saturation for moderately large inputs can be computed and is given by the describing function to be approximately  $4N/\pi a$ , where  $N$  is the saturation level and  $a$  is the amplitude of the input signal. Here  $N = 0.4$ , and if  $K_p = 0.1$ , then  $K_{s,eq} = 28$ . Thus, we predict an input signal amplitude of  $a = 4(0.4)/28\pi = 0.018$ . This value is closely verified by

the plot of Fig. 10.53(c), the input to the nonlinearity in this case. The frequency of oscillation is also nearly 10.1 rad/sec, as predicted by the root locus in Fig. 10.50.

In the actual implementation of F/A feedback controllers in automobile engines, sensor degradation over thousands of miles of use is of primary concern, because the federal government mandates that the engines meet the exhaust-pollution standards for the first 50,000 mi. In order to reduce the sensitivity of the average setpoint to changes in the sensor output characteristics, manufacturers typically modify the design discussed here. One approach is to feed the sensor output into a relay function [see Fig. 9.6(b)], thus completely eliminating any dependency on the sensor gain at the setpoint. The frequency of the limit cycle is then solely determined by controller constants and engine characteristics. Average steady-state F/A accuracy is also improved. The oscillations in the F/A are acceptable because they are not noticeable to the car's occupants. In fact, the F/A excursions are beneficial to the catalyst operation in reducing pollutants.

Feedback systems have also been used in many other areas of modern automobiles. A car's desired inside temperature is set by the passengers and a feedback system maintains that temperature. Cruise control systems have been augmented with radar so the cruise control will maintain a certain distance behind the car ahead by feedback of that distance to the cruise control. Systems are being developed whereby traffic lane marking sensors are being fed back to the steering to maintain a car in the correct lane. Stability augmentation systems use differential braking based on accelerometer measurements to keep a car upright in violent maneuvers. The list goes on and on, many of which are described in a book by Ulsoy, Peng, and Cakmakci (2012). It is possible that platoons of cars on a freeway will be tightly controlled with small distances between them in order to increase the capacity of freeways in the future. Such a scheme will be a victory for feedback control, but could put a tough test on our legal system if there are serious accidents.

## 10.5 Control of a Quadrotor Drone

Drones, or Unmanned Aerial Vehicles (UAVs) are aircraft that are pilotless. They can be either controlled from the ground or are completely autonomous and have onboard control algorithms that primarily determine their path. Some are winged aircraft, and some are helicopters that rely on one or more rotor blades for lift. Drones are being developed for a very large number of applications. Some of the many examples of current use are aerial photography and video, surveillance, security/police work, search and rescue, farming, defense, and, of course, entertainment. Many other applications are being investigated from package delivery to flying cars. More general research includes optimization of onboard control, artificial intelligence, and swarming approaches where

dozens of drones are in a networked communication system and are being controlled to perform a particular task.

Helicopters with multiple rotors are a popular platform for these vehicles due to the simplicity of the vehicle hardware and maintenance, ability to hover, and the vertical takeoff and landing capability. As a result, much of the sophistication is in the control and navigation software.

**STEP 1. Understand the process.** The quadrotor consists of four rotors, with one pair rotating clockwise (CW), and the other pair rotating counter-clockwise (CCW). An example is shown in Figure 10.54. By independently controlling each rotor's speed, it is possible to command the attitude of the vehicle along with the translation and altitude. By using two CW rotors and two CCW rotors, the reaction torques on the vehicle are canceled, thus eliminating the need for the tail rotor that is required for the typical single-rotor helicopters and simplifying the hardware considerably.

**STEP 2. Select sensors.** 3-D position and velocity sensing is readily available via GPS (or other satellite-based navigation systems) in an earth-fixed coordinate system. In addition, it is reasonably affordable to have inertial sensors (aided by GPS in some cases) that provide pitch, roll, and yaw angles, plus their angular rates. These Inertial Measurement Units (IMUs) contain 3-D accelerometers and 3-D gyros at a minimum, but sometimes contain 3-D magnetometers as well. A package with all these sensors will have the capability to supply accurate attitudes and rates, earth-fixed position and velocity, and body-fixed position and velocity. Having all these sensors in the unit allows the utilization of inexpensive sensors because the redundancy in the sensed

**Figure 10.54**

Quadrotor drone

Source: Slavoljub Pantelic/Shutterstock



quantities allows for the estimation of individual sensor errors. Small quadrotor drones without GPS that only include 3-axis angular rate gyros and 3-axis accelerometers are available for less than \$100; however, they require considerable practice to fly them well via remote control. Depending upon UAV requirements and accuracy requirements, sensor packages can range in cost from \$100 to \$3000 and even greater if very precise positioning is required. For purposes of this example, we will assume the existence of position and velocity in both earth- and body-frames, plus pitch, roll, and yaw angles and rates.

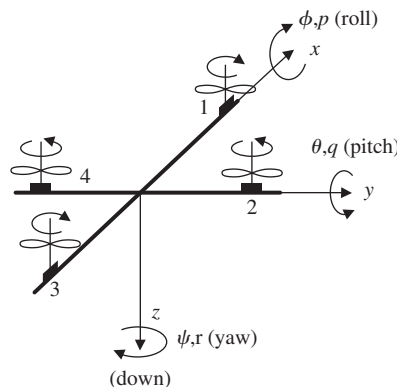
**STEP 3. Select actuators.** The actuators were discussed in STEP 1. The quadrotor drone can be completely controlled by the individual commands to the four motors driving the rotors. As will become apparent in Steps 5 and 8, the 3-D position-time history and yaw angle are controllable with these four inputs. Example 2.5 in Chapter 2 explains the commands necessary to each rotor in order to achieve proper control of roll, pitch, and yaw. Example 5.16 in Chapter 5 explains the use of the actuators to control position as well.

**STEP 4. Make a linear model.** The coordinate system for a quadrotor is shown in Fig. 10.55. It follows the airplane axes in Section 10.3 to some extent; however, in this case, it is arbitrary how the  $x$  and  $y$  axes are oriented in the plane of the rotors. Note rotors 1 and 3 are rotating in a CW direction, while rotors 2 and 4 are rotating in a CCW direction. Selecting the  $x$ -axis to be aligned with two of the rotors simplifies the control logic to some extent for purposes of this example; however, most drones normally fly with the rotor arms at  $45^\circ$  to the direction of flight. Quadrotor drones often have cameras installed that are not able to swivel in the  $x$ - $y$  plane of the drone; rather, they are only able to swivel up and down. Furthermore, the cameras are typically aligned so they look forward in the direction of flight. Therefore, the only way to control the camera viewing azimuth is to yaw the drone.

The quadrotor longitudinal  $x$ -axis equations, linearized and partially modified for drone use of the full nonlinear aircraft Eqs (10.16)

**Figure 10.55**

Definition of drone coordinates



and (10.17), are contained in Eqs. (10.36a). These linearized equations assume the body-fixed coordinate system stays essentially level through the motion and the pitch and roll angles remain small; that is, the drone stays close to level. Also, for the linear assumptions to be valid, we assume the angular motions are reasonably small. If that were not the case, one would have to use the full equations as shown for the airplane in Eqs. (10.16) and (10.17) where there are multiple nonlinearities involving the angular rates and angles. Another simplification below is that the longitudinal motion ( $x, u, \theta$ , and  $q$ ) is uncoupled from the lateral motion ( $y, v, \phi$ , and  $p$ ). If the vehicle is yawing ( $r \neq 0$ ), there will be coupling between the longitudinal and lateral motion as can be seen from Eqs. (10.16) and (10.17). This coupling is ignored in the equations below, and the examples to follow will assume trajectories that do not produce any coupling for purposes of control design. The longitudinal  $x$ -axis equations are:

$$\begin{bmatrix} \dot{x} \\ \dot{u} \\ \dot{q} \\ \dot{\theta} \\ \dot{T}_\theta \end{bmatrix} = \begin{bmatrix} 0 & 1 & 0 & 0 & 0 \\ 0 & X_u & 0 & -g_o & 0 \\ 0 & M_u & 0 & 0 & M_\theta \\ 0 & 0 & 1 & 0 & 0 \\ 0 & 0 & 0 & 0 & -a \end{bmatrix} \begin{bmatrix} x \\ u \\ q \\ \theta \\ T_\theta \end{bmatrix} + \begin{bmatrix} 0 \\ 0 \\ 0 \\ 0 \\ a \end{bmatrix} T_{lon}, \quad (10.36a)$$

$$\begin{bmatrix} \theta_m \\ x_m \end{bmatrix} = \begin{bmatrix} 0 & 0 & 0 & 1 & 0 \\ 1 & 0 & 0 & 0 & 0 \end{bmatrix} \begin{bmatrix} x \\ u \\ q \\ \theta \\ T_\theta \end{bmatrix}$$

where

$x = x_m$  = measured position in the drone frame  $x$  direction

(see Fig. 10.55),

$u$  = velocity in the drone frame  $x$  direction (see Fig. 10.55),

$q$  = angular rate about the positive drone frame  $y$ -axis, or pitch rate,

$\theta = \theta_m$  = measured pitch angle from horizontal,

$X_u$  = partial derivative of the aerodynamic force in  $x$ ,

direction with respect to perturbations in  $u$ ,

$M_u$  = partial derivative of the aerodynamic (pitching) moment with respect to perturbations in  $u$ ,

$M_\theta = 1/I_y$ ,

$T_\theta$  = pitching moment around  $+y$  axis from rotors 1 and 3,

$T_{lon}$  = pitching torque command for rotors 1 and 3, produced by

$\delta T_1 \cdot d$  and  $-\delta T_3 \cdot d$ , where  $\delta T$  is the thrust change

commanded to the rotor and  $d$  is the moment arm,  
 $a$  = lag term representing the delay in the rotors producing the  
changed thrust and resulting torque,  
 $g_o$  = gravity (assumes pitch angle is small, hence  $\cos(\theta) \simeq 1$ ).

If there are no aerodynamic terms, i.e.,  $M_u = 0$ ,  $X_u = 0$ , and there is no lag from the rotor commands, this yields  $\Theta_m(s)/T_\theta(s) = 1/I_y s^2$  as was the case considered in Example 2.5, Eq. (2.15). If the thrust lag is included as shown in Eq. (10.36a), but again without aero terms, then it produces the transfer function  $\Theta_m(s)/T_{lon}(s) = a/I_y/(s^2(s+a))$  as in Examples 5.12 and 5.16.

The lateral  $y$ -axis equations are:

$$\begin{bmatrix} \dot{y} \\ \dot{v} \\ \dot{p} \\ \dot{\phi} \\ \dot{T}_\phi \end{bmatrix} = \begin{bmatrix} 0 & 1 & 0 & 0 & 0 \\ 0 & Y_v & 0 & g_o & 0 \\ 0 & L_v & 0 & 0 & L_\phi \\ 0 & 0 & 1 & 0 & 0 \\ 0 & 0 & 0 & 0 & -a \end{bmatrix} \begin{bmatrix} y \\ v \\ p \\ \phi \\ T_\phi \end{bmatrix} + \begin{bmatrix} 0 \\ 0 \\ 0 \\ 0 \\ a \end{bmatrix} T_{lat}, \quad (10.36b)$$

$$\begin{bmatrix} \phi_m \\ y_m \end{bmatrix} = \begin{bmatrix} 0 & 0 & 0 & 1 & 0 \\ 1 & 0 & 0 & 0 & 0 \end{bmatrix} \begin{bmatrix} y \\ v \\ p \\ \phi \\ T_\phi \end{bmatrix}$$

where

$y = y_m$  = measured position in the drone frame  $y$  direction  
(see Fig. 10.55),

$v$  = velocity in the drone frame  $y$  direction (see Fig. 10.55),

$p$  = angular rate about the positive drone frame  $x$ -axis, or roll rate,

$\phi = \phi_m$  = measured roll-angle from horizontal,

$Y_v$  = partial derivative of the aerodynamic force in  $y$  direction with  
respect to perturbations in  $v$ ,

$L_v$  = partial derivative of the aerodynamic (rolling) moment with respect  
to perturbations in  $v$ ,

$L_\phi = 1/I_x$ ,

$T_\phi$  = rolling moment around  $+x$ -axis from rotors 2 and 4,

$T_{lat}$  = rolling torque command for rotors 2 and 4, produced by

$\delta T_2 \cdot d$  and  $-\delta T_4 \cdot d$ , where  $\delta T$  is the thrust change commanded

to the rotor and  $d$  is the moment arm,

$a$  = lag term representing the delay in the rotors producing the changed thrust and resulting torque,

$g_o$  = gravity (assumes roll angle is small, hence  $\cos(\phi) \approx 1$ ).

The rotational -  $z$ -axis equations are:

$$\begin{bmatrix} \dot{r} \\ \dot{\psi} \end{bmatrix} = \begin{bmatrix} 0 & 0 \\ 1 & 0 \end{bmatrix} \begin{bmatrix} r \\ \psi \end{bmatrix} + \begin{bmatrix} 1/I_z \\ 0 \end{bmatrix} T_\psi, \quad (10.36c)$$

$$[\psi_m] = [0 \ 1] \begin{bmatrix} r \\ \psi \end{bmatrix}$$

where

$r$  = angular rate about positive drone frame  $z$ -axis, or yaw rate,  
(see Fig. 10.55),

$\psi = \psi_m$  = measured azimuth angle of the drone frame  $x$ -axis with respect to North,

$T_\psi$  = commanded yawing moment from all rotors around +  $z$ -axis, produced by  $\delta T_1, \delta T_2, \delta T_3$  and  $\delta T_4 = -T_\psi$ .

(There is no lag here because the torque is applied directly by the motors.)

For the final dimension, altitude, all the rotors need their speed increased. However, because of the different rotational directions, the torques applied to rotors 1 and 3 will be in the opposite direction compared to rotors 2 and 4. Aerodynamic terms have little effect on these dynamics; therefore, the complete equations are

$$\begin{bmatrix} \dot{h} \\ \dot{w} \\ \dot{F}_h \end{bmatrix} = \begin{bmatrix} 0 & 1 & 0 \\ 0 & 0 & Z_h \\ 0 & 0 & -a \end{bmatrix} \begin{bmatrix} h \\ w \\ F_h \end{bmatrix} + \begin{bmatrix} 0 \\ 0 \\ a \end{bmatrix} F_{alt}, \quad (10.36d)$$

$$h_m = [1 \ 0 \ 0] \begin{bmatrix} h \\ w \\ F_h \end{bmatrix}$$

where

$h = h_m$  = vertical position,

$w$  = vertical,  $z$ -axis, velocity,

$Z_h = 1/m_o$ ,  $m_o$  = mass of the vehicle,

$F_h$  = vertical thrust,

$F_{alt}$  = commanded thrust from all rotors, produced by

$$\delta T_1 = \delta T_3 = +F_{alt} \text{ and } \delta T_2 = \delta T_4 = -F_{alt}.$$

To determine the position in an earth-fixed frame for the case when there is no yaw rate,  $r$ , the transformation matrix based on the rotation of the level body-fixed frame is required, thus

$$\begin{bmatrix} \dot{x}_E \\ \dot{y}_E \end{bmatrix} = \begin{bmatrix} \cos(\psi) & -\sin(\psi) \\ \sin(\psi) & \cos(\psi) \end{bmatrix} \begin{bmatrix} u \\ v \end{bmatrix}, \quad (10.37)$$

where

$x_E$  = position in the earth-fixed frame with the  $x$ -axis pointing north,

$y_E$  = position in the earth-fixed frame with the  $y$ -axis pointing east.

For a fixed azimuth of  $\psi = 0$ , i.e. the  $x$ -axis is pointing north, and if there are no aero terms,  $x_E(s)/\theta(s) = -g_o/s^2$  as we assumed in Example 5.16. As discussed above, for the case when there is a yaw rate, there are cross-coupling terms into the longitudinal and lateral axes as can be seen from Eqs (10.16), plus the kinematic relationships between the body-fixed and earth-fixed frames are significantly more complex (see Greenwood, 1988). For our ensuing example, we have chosen to select a trajectory where the equations above [10.36 and 10.37] are satisfactory. For arbitrary motion of a drone, substantial additional complexity is required to accurately simulate the motion in the body and earth-fixed frames. However, for design of feedback control laws of a drone, use of the four independent axes represented by Eqs. (10.36) are usually adequate.

Note, in the linear models above, the four axes are independent of each other providing the rotor commands are implemented as shown in the equations above, and as diagrammed in Fig. 10.56.

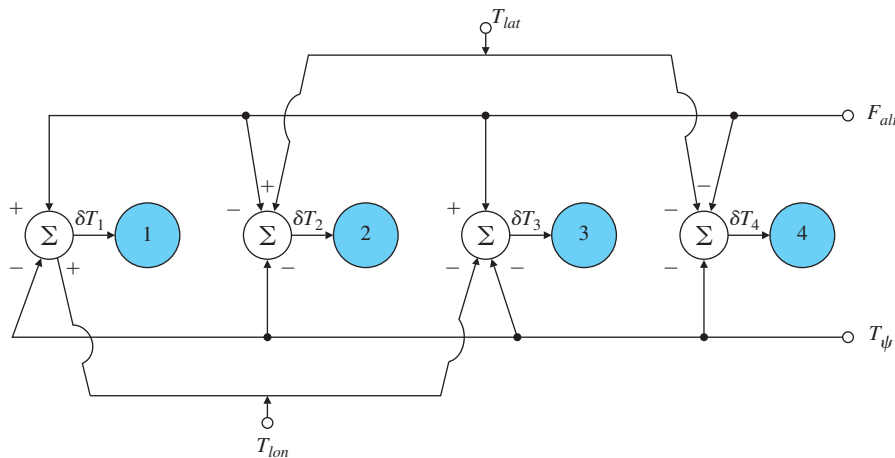


**Figure 10.56**

Required rotor commands for each of the four axes

STEP 5a. Try a PID controller for a single axis. For a set of aerodynamic and inertia terms that are representative of a small drone approximately 3 ft in diameter (Berrios, 2017), the parameters used were

$$\begin{aligned} Mu &= 1.1, \\ Xu &= -0.25, \\ M_\theta &= 0.02, \\ g_o &= 32.2, \\ a &= 20. \end{aligned}$$

These values in Eqs. (10.36a) produce the transfer functions,

$$\frac{\theta_m(s)}{T_{lon}(s)} = 0.4 \frac{(s + 0.25)}{(s - 1.6 \pm 2.8j)(s + 3.4)(s + 20)}. \quad (10.38a)$$

$$\frac{x_m(s)}{T_{lon}(s)} = -13 \frac{1}{s(s - 1.6 \pm 2.8j)(s + 3.4)(s + 20)}. \quad (10.38b)$$

Note there are unstable open-loop poles in this loop. This is typical of helicopters flying near hover and account for the fact that helicopters tend to be difficult to fly near hover. The  $(s + 20)$  term is due to the lag in the rotor coming up to the newly commanded speed and thrust; however the remaining set of poles and zero are often referred to as the “hovering cubic”.

The use of sisotool allows us to find the PD controller (feedback of  $\theta$  and  $\dot{\theta}$ ),

$$D_{c1lon}(s) = 500(s + 4) \quad (10.39a)$$

that produces a damping,  $\zeta \approx 0.6$ , and  $\omega_n \approx 10$  rad/sec for the oscillatory roots of the this inner loop, as shown by the root locus in Fig. 10.57.

However, we see from the frequency response in Fig. 10.58 that the system is conditionally stable due to the RHP open-loop roots that resulted from the aerodynamic terms.

**Figure 10.57**

Root locus of the inner loop with compensation given by Eq. 10.39a

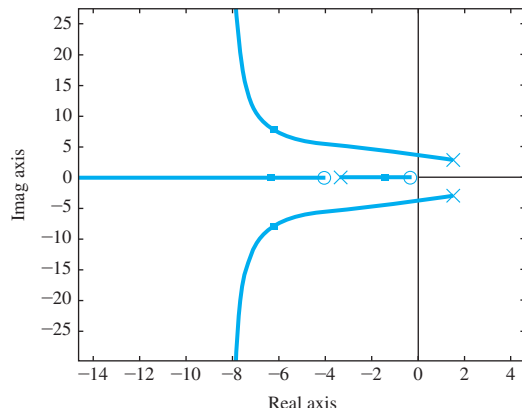
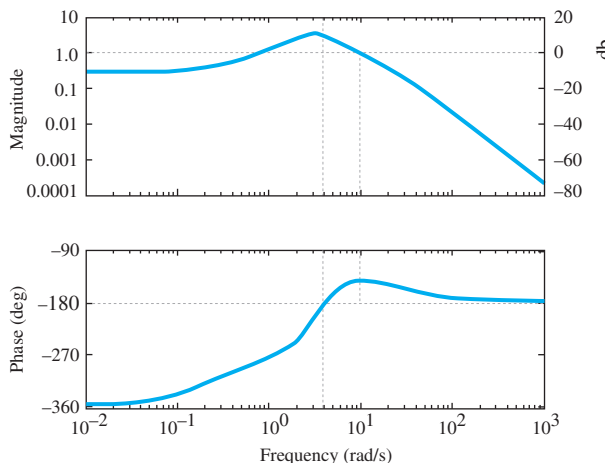


**Figure 10.58**

Open-loop frequency response plots for the inner  $\theta$  loop



With the compensator as designed, the PM is  $40^\circ$ . Lowering the gain by a factor of 3.2 would cause an instability while there is no upper limit of the gain before instability is reached. Some researchers have found that additional lead in this inner loop substantially improves the performance in the presence of gusty wind conditions.

For the outer loop, we wish to command a change in position; therefore our measurement will be  $x$ . Using Eq. (10.36a) with the addition of the inner-loop feedback from Eq. (10.39a), we find that an outer-loop PD controller

$$D_{c2lon}(s) = 0.4(s + 2.2), \quad (10.39b)$$

produces the root locus as shown in Fig. 10.59, where the closed-loop roots for the selected gain are indicated. The system response to a step command in  $x$  yields a satisfactory response as shown in Fig. 10.60. The rise time is approximately 0.6 seconds and the settling time is approximately 3 seconds, with an overshoot of less than 5%.

**Figure 10.59**

Root locus for the outer  $x$ -loop including the PD controller

$$D_{c2lon}(s) = 0.4(s + 2.2)$$

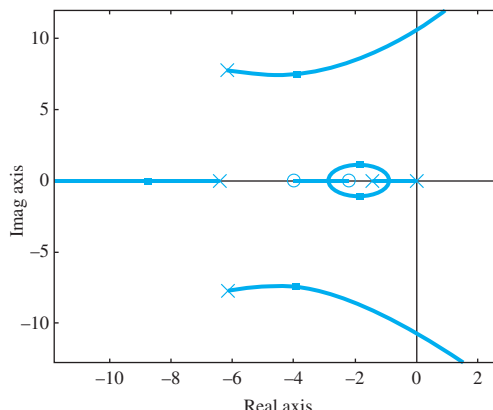
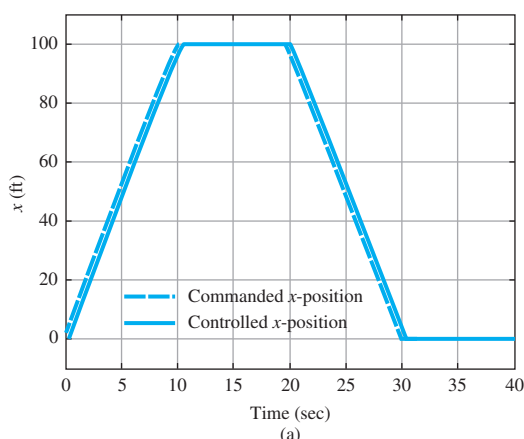
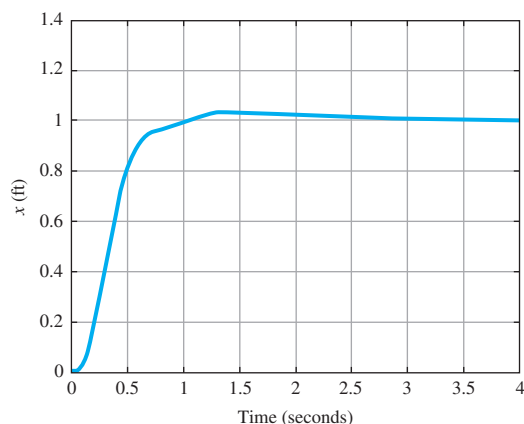
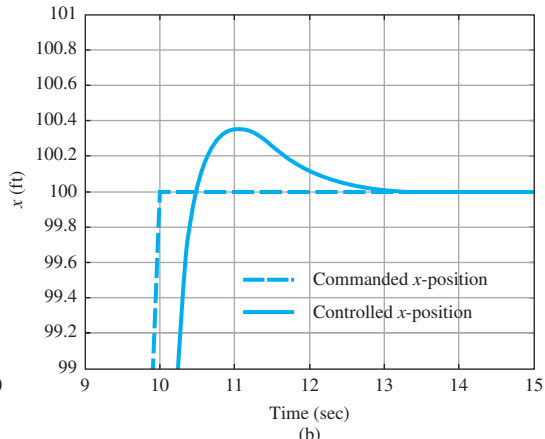


**Figure 10.60**

Step response of  $x$  with the PD controller  
 $D_{c2lon}(s) = 0.4(s + 2.2)$   
 for the outer loop



(a)



(b)

**Figure 10.61**

(a)  $x$  response to a commanded trajectory (b) zoom in to a transition

However, a typical trajectory for a drone would involve moving to some location, performing a function, then returning to the starting point. As a partial test of this sort of trajectory in the  $x$ -direction only, we enter an  $x$ -command to leave the starting point with a speed of 10 ft/sec for 10 seconds, move along at that speed for 10 seconds, stop for 10 seconds, return at -10 ft/sec and stop after 10 seconds and stay stationary for 10 seconds. Fig. 10.61(a) is a plot that includes the commanded  $x$ -position, and the system's response to that command. To exhibit the accuracy better, a blow-up of the area near the transition from forward flight to the position hold at 10 seconds is shown in Fig. 10.61(b).

We see that the drone follows the commanded position very well, including the transition where a step change in velocity of 10 ft/sec is commanded and the resulting position error is less than 0.4 ft.

**STEP 5b.** Try PID controllers for 2-D motion in the horizontal plane. Unlike an airplane, a drone is equally comfortable traveling in the  $y$ -direction as it is traveling in the  $x$ -direction and equally comfortable going in the positive or negative directions! However, as stated earlier, most drones are equipped with a camera or other sensors that are pointing forward in a particular  $x$ - $y$  direction fixed in the drone. So there is a preferred direction of flight due to the placement of the observation sensors on the drone and the preferred method of guiding the craft is to rotate the vehicle about the  $z$ -axis so its sensors point in the direction of flight. Continuing with the evaluation for a trajectory over a path in the  $x$ - $y$  plane, let's assume the camera is oriented to point along the  $x$ -axis and can swing down in the  $x$ - $z$  plane. Initially, we want the drone to start going north so that  $\psi = 0$  for the first portion of the trajectory. At a certain point, the camera detects something interesting, stops with the camera pointing straight down, rotates by  $180^\circ$ , moves sideways toward the east (which will be in the  $-y$ -direction due to the body-frame rotation by  $180^\circ$ ), then moves back to the starting place without yaw rotation ( $\psi = 180^\circ$ ) and translation mostly in the  $+x$ -direction, but enough in the  $+y$ -direction so it returns to the starting location. For the  $y$ -direction flight, since the drone is not quite symmetric, the parameters used are:

$$\begin{aligned} Lv &= -0.5, \\ Yv &= -0.2, \\ L_\phi &= 0.016, \\ g_o &= 32.2, \\ a &= 20. \end{aligned}$$

These result in the transfer function of the inner loop

$$\frac{\phi_m(s)}{T_{lat}(s)} = 0.32 \frac{(s + 0.2)}{(s - 1.2 \pm 2.2j)(s + 2.6)(s + 20)}.$$

The use of sisotool allows us to find the inner loop PD controller (feedback of  $\phi$  and  $p$ ),

$$D_{c1lat}(s) = 500(s + 3), \quad (10.40a)$$

that gives acceptable speed of response and damping. Then closing the outer loop with a PD controller (feedback of  $y$  and  $v$ ),

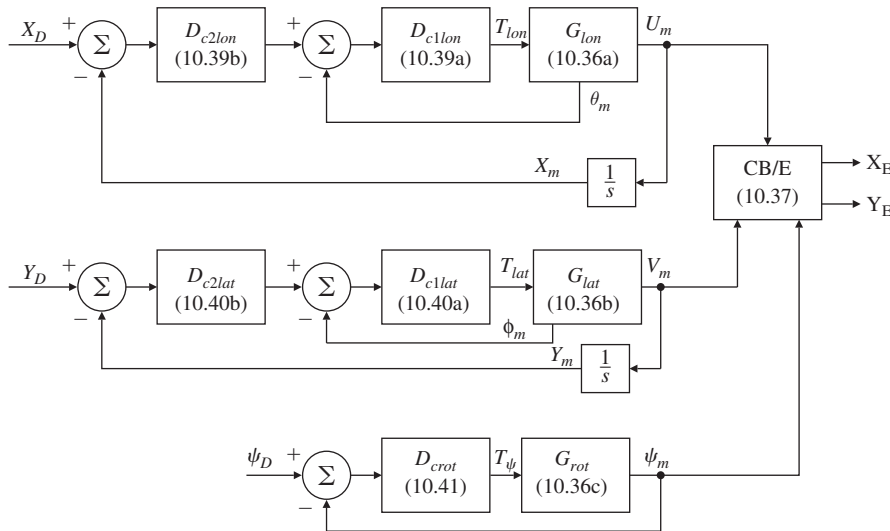
$$D_{c2lat}(s) = 0.25(s + 3), \quad (10.40b)$$

completes the controller for commanding movement in the body-frame  $y$ -direction.

Control of the yaw angle (the azimuth of the body  $x$ -frame axis) is relatively straight forward since Eqs. (10.36c) show that

$$\frac{\psi_m(s)}{T_\psi(s)} = 0.005 \frac{1}{s^2}.$$

The controller,

**Figure 10.62**

Block diagram of the controllers for motion in the  $x$ - $y$  plane

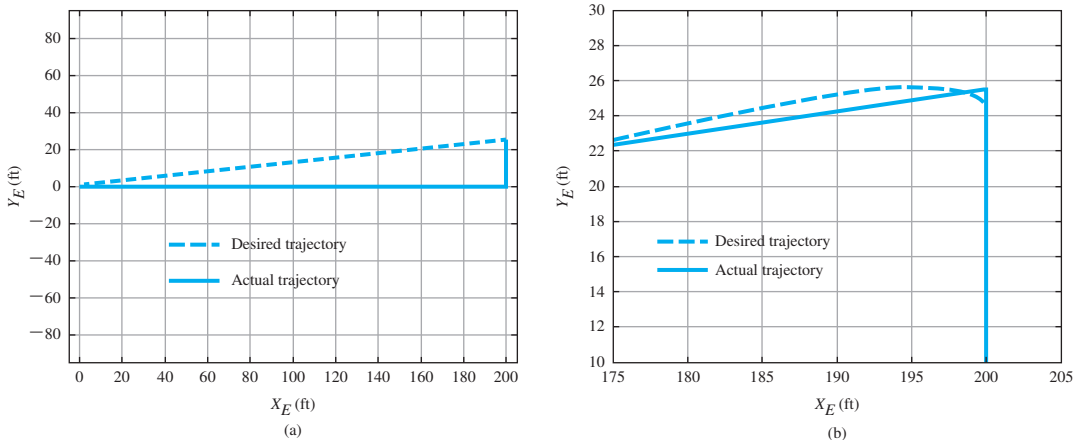
$$D_{crot}(s) = 1500(s + 3), \quad (10.41)$$

provides a fast and well damped response, so the complete controller for motion in the  $x$ - $y$  plane is now designed. Fig. 10.62 shows these control loops in a block diagram.

The specific path chosen is one that goes away from the starting point at 20 ft/sec for 10 seconds along the  $x$ -axis pointing north, then stops and rotates for 5 seconds around the  $z$ -axis by  $180^\circ$ , then slides sideways to the east (negative  $y$ -axis) for 5 seconds at 5 ft/sec, and finally flies for 10 seconds with a velocity along the  $+x$ -axis of 20 ft/sec (which is now pointing south) and a velocity of 2.5 ft/sec along the  $+y$ -axis (which is now pointing west) so that the drone will return to the starting point. Fig. 10.63(a) shows the overall trajectory of the drone while 10.63(b) shows a scale change of the trajectory as it starts the trip back to the starting point to illustrate the errors better. The figure shows that the trajectory error never appears to exceed about a foot.

Based on the definition of the  $x$ - $y$  plane in Fig. 10.55 with the  $z$ -axis pointing down, and the fact that Matlab plots axes as in Figs. 10.63 as if the  $z$ -axis was coming out of the page, the trajectories in Figs. 10.63 are based on an observer who is looking up at the  $x$ - $y$  plane from underneath. That means that, indeed, the  $x_E$ -axis is pointing north and  $y_E$ -axis is pointing east as described above.)

Summarizing, we saw from this example that it is not necessary to command changes in the azimuth angle ( $\psi$ ) as it would be for an airplane. However, there are reasons that one would want to command changes in the azimuth, such as orienting a camera which are typically not gimbaled to swivel around the body-frame  $z$ -axis. In general, if

**Figure 10.63**

(a) Trajectory in the earth-fixed frame, (b) blow-up of the trajectory showing errors.

there is continuous motion in the body axis  $x$ -direction and continual changes in the direction of the body  $x$ -axis (that is, continual changes in  $\psi$ ), there will be accelerations imparted in the body frame  $y$ -axis direction thus necessitating adding the coupling terms between the Eqs. (10.36a, b, and c). The trajectory selected above was chosen so those terms did not appear and, therefore, there were no errors induced by the motion. To accurately simulate a more general motion, the nonlinear terms and coupling need to be added; however, it is generally acceptable to use the uncoupled equations for purposes of control system design.

STEP 6. Try an optimal design: The quadrotor longitudinal  $x$ -axis state-space equations are given by Eq. (10.36a) and with  $x$  selected as the system output, the resulting longitudinal transfer function is

$$\frac{x(s)}{T_{lon}(s)} = \frac{-12.88}{s(s - 1.6 \pm j2.8)(s + 3.37)(s + 20)}.$$

Selecting the following LQR weighting matrices,

$$\mathbf{Q} = \rho \mathbf{C}^T \mathbf{C}, \mathbf{R} = 1, \mathbf{C} = [ \begin{array}{ccccc} 0 & 0 & 0 & 1 & 0 \end{array} ],$$

the symmetric root locus (SRL) for the system is shown in Figure 10.64. Choosing  $\rho = 1e11$ , we compute the state feedback gain matrix as

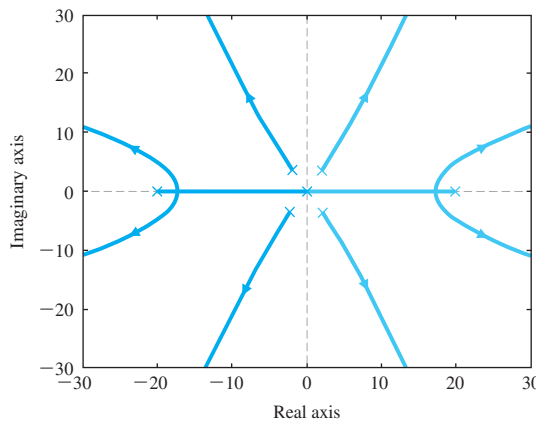
$$\mathbf{K} = [ \begin{array}{ccccc} -49020 & 6204 & 126690 & -316230 & 2.66 \end{array} ].$$

The feedforward gain matrices are computed as

$$\mathbf{N}_x = \begin{bmatrix} 0 \\ 0 \\ 0 \\ 1 \\ 0 \end{bmatrix}, N_u = 0, \bar{N} = N_u + \mathbf{K}\mathbf{N}_x = -3.1623e5, \mathbf{M} = \mathbf{B}\bar{N}.$$

**Figure 10.64**

Longitudinal SRL for quadrotor



Choosing the following estimator design weighting parameters

$$q = 1e7, \quad \mathbf{B}_1 = \mathbf{B},$$

the estimator gain matrix is determined to be

$$\mathbf{L} = \begin{bmatrix} 148 \\ -44 \\ -23 \\ 17 \\ -170 \end{bmatrix},$$

and results in the dynamic controller transfer function for the longitudinal axis given by

$$D_c(s) = \frac{1.59e7(s + 0.93 \pm j3.1)(s + 3.8)(s + 20)}{(s + 36.9)(s + 24.7 \pm j22.2)(s + 2.2 \pm j24.5)}.$$

The overall closed-loop system equations are

$$\begin{bmatrix} \dot{\mathbf{x}} \\ \dot{\hat{\mathbf{x}}} \end{bmatrix} = \begin{bmatrix} \mathbf{A} & -\mathbf{BK} \\ \mathbf{LC} & \mathbf{A} - \mathbf{BK} - \mathbf{LC} \end{bmatrix} \begin{bmatrix} \mathbf{x} \\ \hat{\mathbf{x}} \end{bmatrix} + \begin{bmatrix} \mathbf{B}\bar{\mathbf{N}} \\ \mathbf{M} \end{bmatrix} r,$$

$$y = [\mathbf{C} \quad 0] \begin{bmatrix} \mathbf{x} \\ \hat{\mathbf{x}} \end{bmatrix}.$$

The step response of the longitudinal control is shown in Figures 10.65. The rise time is 0.15 sec, the settling time is 0.8 sec, and there is less than 12% overshoot.

The lateral  $y$ -axis state-space equations are as in Eq. (10.36b) and result in the transfer function

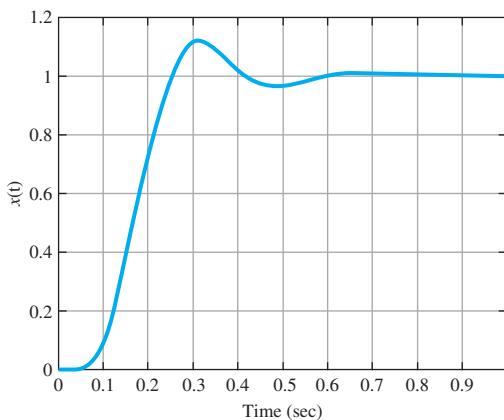
$$\frac{y(s)}{T_{lat(s)}} = \frac{10.3}{s(s - 1.2 \pm j2.2)(s + 2.6)(s + 20)}.$$

Choosing the following LQR weighting matrices,

$$\mathbf{Q} = \rho \mathbf{C}^T \mathbf{C}, \mathbf{R} = 1, \mathbf{C} = \begin{bmatrix} 0 & 0 & 0 & 1 & 0 \end{bmatrix},$$

**Figure 10.65**

Longitudinal step response for state-space design



with  $\rho = 1e10$ , the state feedback gain matrix is computed as

$$\mathbf{K} = \begin{bmatrix} 51641 & 7147 & 139480 & 316230 & 2.5 \end{bmatrix}.$$

The solution to the feedforward gain matrices yields

$$\mathbf{N}_x = \begin{bmatrix} 0 \\ 0 \\ 0 \\ 1 \\ 0 \end{bmatrix}, N_u = 0, \bar{N} = N_u + \mathbf{K}\mathbf{N}_x = 3.16e5, \mathbf{M} = \mathbf{B}\bar{N}.$$

Selection of the ensuing estimator design weighting parameters

$$q = 1e10, \quad \mathbf{B}_1 = \mathbf{B},$$

yields the estimator gain matrix

$$\mathbf{L} = \begin{bmatrix} 733 \\ 1539 \\ 261 \\ 38 \\ 52342 \end{bmatrix},$$

and results in the lateral dynamic controller transfer function

$$D_c(s) = \frac{-9.76e7(s+2 \pm j5.4)(s+5)(s+20)}{(s+46)(s+30.6 \pm j28.9)(s+0.78 \pm j31)}.$$

The step response of the lateral-axis and its associated control effort are very similar to Figures 10.65. The rise time is less than 0.15 sec, the settling time is around 0.8 sec, and the overshoot is less than 12%. As expected there is tremendous amount of symmetry between the longitudinal and lateral axes. The rotational  $z$ -axis state-space equations are as in Eq. (10.36c).

Selecting the ensuing LQR weighting matrices,

$$\mathbf{Q} = \rho \mathbf{C}^T \mathbf{C}, \mathbf{R} = 1, \mathbf{C} = [0 \quad 1],$$

with  $\rho = 1e10$ , the state feedback gain is computed to be

$$\mathbf{K} = \begin{bmatrix} 11246 & 316227 \end{bmatrix}.$$

The feedforward gain matrices are determined as

$$\mathbf{N}_x = \begin{bmatrix} 0 \\ 1 \end{bmatrix}, N_u = 0, \bar{N} = N_u + \mathbf{K}\mathbf{N}_x = 3.16e5, \mathbf{M} = \mathbf{B}\bar{N}.$$

Selecting the ensuing estimator design parameters

$$q = 1e10, \mathbf{B}_1 = \mathbf{B},$$

gives the estimator gain matrix

$$\mathbf{L} = \begin{bmatrix} 500 \\ 31 \end{bmatrix},$$

and the dynamic controller transfer function for the rotational dynamics is given by

$$D_c(s) = \frac{-1.56e7(s+10)}{(s+43.9 \pm j43.9)}.$$

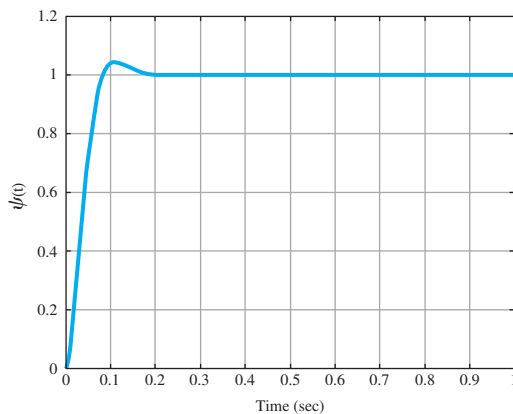
The rotational step response is shown in Figure 10.66. The system has a rise time of 0.05 sec, a settling time of 0.2 sec and less than 5% overshoot.

Figure 10.67 shows the trajectory following response of the quadrotor for the same desired trajectory as before. The quadrotor can follow the desired path very accurately and outperforms the classical design as seen from Figure 10.67. To be fair, iterations on the classical design could match this performance.

This example shows the essence of the control issues for the axes involving motion in the  $x$ - $y$  (horizontal) plane. In addition, there will be a requirement to control the altitude as well, but unlike an airplane

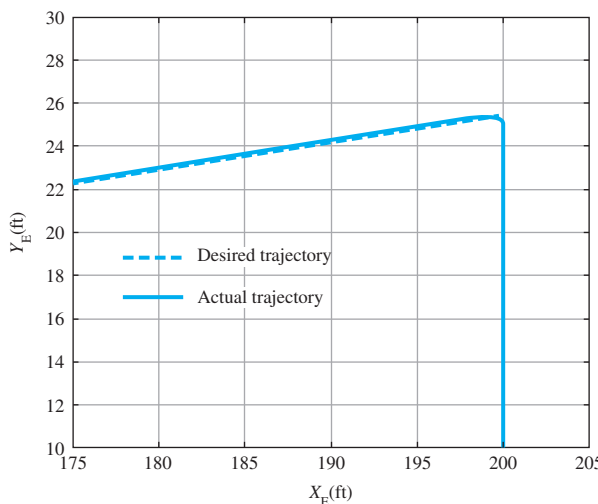
**Figure 10.66**

Rotational axis step response for state-space design



**Figure 10.67**

Trajectory-following response for state-space design

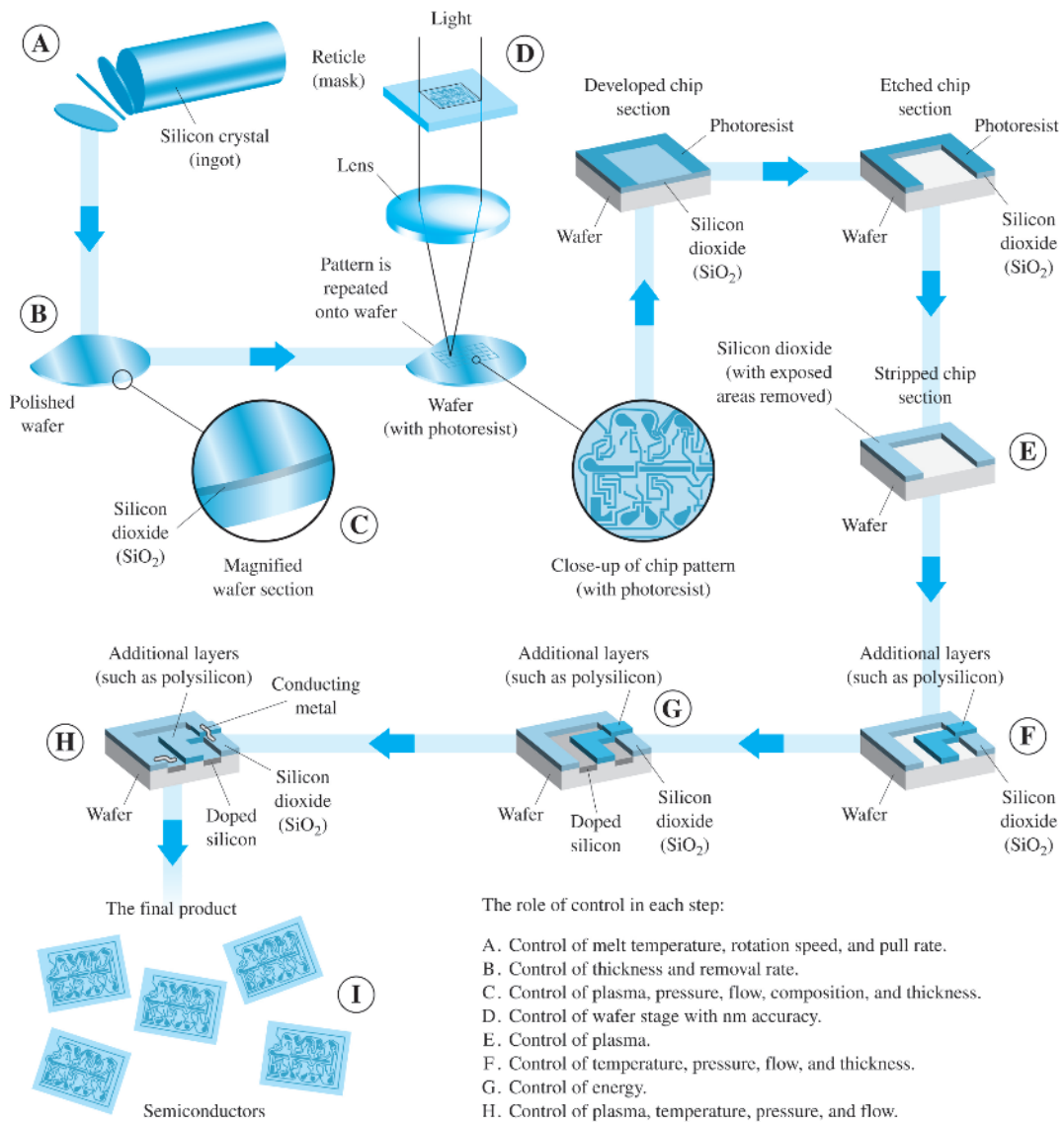


that requires pitch for altitude control, this motion is uncoupled from the other motions for normal flight.

STEP 7. As stated for STEP 5, the control laws determined by any method should be evaluated by a complete and accurate nonlinear simulation to determine the performance considering all known disturbances and the effect of all known model approximations.

## 10.6 Control of RTP Systems in Semiconductor Wafer Manufacturing

Figure 10.68 diagrams the major steps in the manufacture of an ultra-large-scale integrated (ULSI) circuit such as a microprocessor and some of the associated control aspects. Many of the steps described in this process, such as chemical vapor deposition or etching, must be done at closely controlled and timed temperature sequences (Sze, 1988). The standard practice for many years has been to perform these steps in batches on many wafers (silicon disks that contain many chips) at a time to produce large numbers of identical chips. In response to the demand for ever smaller critical dimensions of the devices on the chip, and to give more flexibility in the variety and number of chips to be produced, the makers of the tools for fabrication of integrated circuits are asked to provide more and more precise control of temperature and time profiles during thermal processing. In response to these demands, an important trend is to perform the thermal steps on one wafer at a time in a chamber with cold walls

**Figure 10.68**

Steps in making an integrated circuit

Source: Adapted from International Sematech, *Steps in making an integrated circuit*.

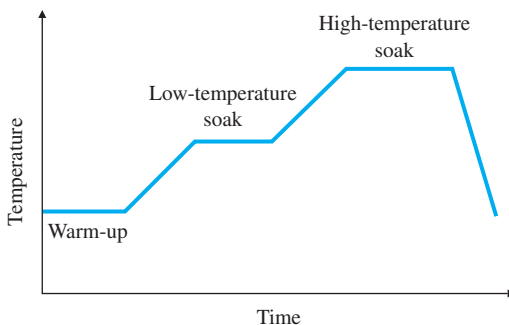
RTP

and a flexible heat source called a rapid thermal processing (RTP) system.

The demands on an RTP system are illustrated by the requirement that the temperature of the wafer needs to rapidly increase or decrease according to a profile such as that shown in Fig. 10.69, where the

**Figure 10.69**

Typical RTP temperature trajectory



ramp-up speeds are at rates of  $25^{\circ}$  to  $150^{\circ}\text{C/sec}$ , and the soak temperatures range from  $600^{\circ}\text{C}$  to  $1100^{\circ}\text{C}$  and last from a few to as many as 120 sec. The ramp-up rates are limited by the danger of causing damage to the crystal structure if the temperature gradients become too large. The ability of the RTP system to change temperature rapidly permits fabrication of devices with very small critical lengths by being able to stop the processes such as deposition or etching quickly and accurately. An important performance consideration is control of temperature uniformity. Hence the actual control is multivariable. However, we will simplify the situation to a single-input single-output case for this study.

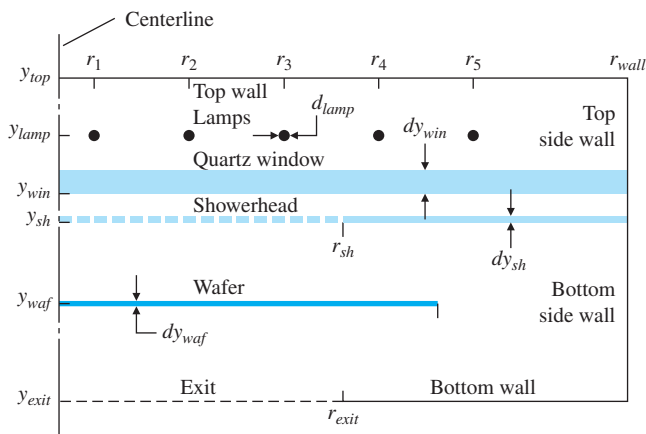
Figure 10.70 shows a generic RTP reactor with tungsten halogen lamps, stainless steel walls that are water cooled, and quartz windows. Temperature measurement can be done by a variety of methods, including thermocouples, RTDs, and pyrometers. For various reasons (particle generation, minimal disturbance, etc.), it is desirable to use noncontact temperature sensing; therefore, pyrometric techniques are the most commonly employed. A pyrometer is a noncontact temperature sensor that measures infrared (IR) radiation, which is directly a function of the temperature. It is known that objects emit radiant energy proportional to  $T^4$ , where  $T$  is the temperature of the object. Among the advantages of pyrometers are they have very fast response time, and can be used to measure the temperature of moving objects (for example, a rotating semiconductor wafer), and in a vacuum for semiconductor manufacturing.

The selection of the actuator depends on the choice of techniques for supplying power (tungsten halogen lamps, arc lamps, hot susceptor, etc.) to heat the wafer. Tungsten halogen lamps are now commonly used in RTP in semiconductor manufacturing (Emami-Naeini et al., 2003). Figure 10.71(a) shows a system with two-sided heating by linear tungsten halogen lamps (typical of systems produced by Mattson). The lamp

**Pyrometer**

**Tungsten halogen lamp**

**Figure 10.70**  
Generic RTP system



arrays on the top and bottom are at right angles to provide more of an axisymmetric configuration. Fig. 10.71(b) shows one-sided heating with lamps in a honeycomb configuration (typical of the Applied Materials systems). Finally, Fig. 10.71(c) shows a configuration of lamps arranged in concentric rings (typical of the Stanford-TI MMST chamber, Gyugyi et al., 1993). The lamps do saturate and, for practical reasons, it is desired to operate them within 5%–95% of maximum power settings.

To illustrate the design of an RTP system, we present the results of a specific design carried out at SC Solutions as a laboratory model constructed to study problems associated with RTP design and operation (Emami-Naeini et al., 2003). The laboratory model is shown schematically in Fig. 10.72. It is made of aluminum and consists of three standard 35-W 12-V tungsten halogen lamps heating a rectangular plate

**Figure 10.71**  
Various lamp geometries for RTP  
*Source: Norman, S.A., "Wafer temperature control in rapid thermal processing," Ph.D. Dissertation, Stanford University, Stanford, CA, 1992.*

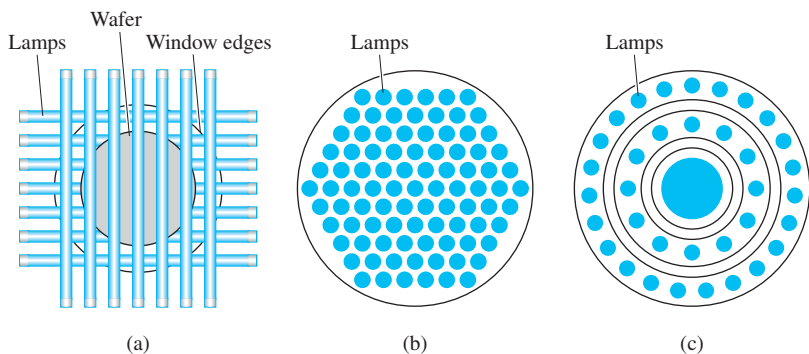
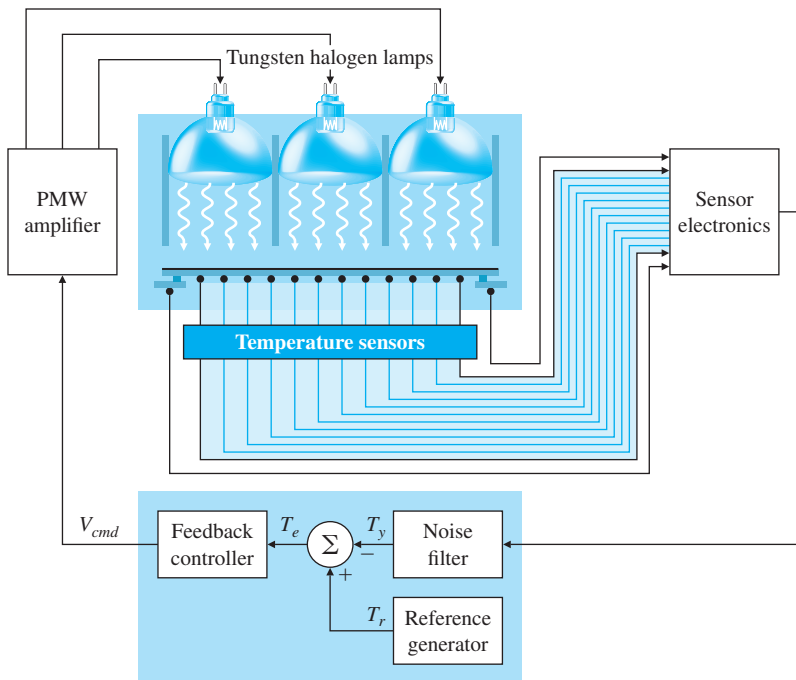


**Figure 10.72**

Block diagram of the RTP laboratory model



that simulates the wafer. The plate measures  $4 \text{ in} \times 1\frac{3}{4} \text{ in}$  and is blackened to increase its radiation absorption. The plate is mounted parallel to the lamps. The lamps are mounted in the lamp housing. The lamp assembly is mounted on a railing so the distance from the lamps to the plate is adjustable. As the lamps are moved out the gain of the system decreases, but the radiation cross talk (coupling) increases. On the other hand, as the lamps are moved closer to the plate, the gain of the system increases and the coupling is reduced. The nominal distance from the lamps to the plate is 1 in., but it is adjustable to several inches. The lamps are driven by a pulse-width modulated (PWM) amplifier driver. There is a separate power supply unit. There are three dials mounted on the side for open-loop and manual system operations. There are fourteen resistive temperature detector (RTD) strips mounted vertically behind the back of the plate: twelve on the plate and two on each support on either side. There is a noise source filter that generates periodic sensor noise at 1.5 Hertz so as to represent wafer rotation noise seen in real RTP systems. All electronics (that is, sensor signal processing and PWM amplifier) reside in the enclosure at the bottom of the unit. Because there is exposure to the outside, the surrounding environment provides sources of disturbance.

#### RTP laboratory model

**STEP 1. Understand the process and its performance specifications.** RTP is an inherently dynamic and nonlinear process. Among interesting

properties of the system are multiple time scales (time constants for lamps, wafer, showerhead, and quartz window are different); nonlinear (radiation dominant) behavior; nonlinear lamps; effects of power supplies; number and placement of sensors; number, placement, and grouping of lamps; and large temperature variations. The DC gain in the system ( $\delta$  temperature/ $\delta$  power) decreases with increasing temperature due to the nonlinear increase in radiative losses. Various types of physical models are needed. Detailed physical models are required for equipment design, but reduced-order models are needed for fast evaluation of geometry changes, recipe development, and for feedback control design. Smooth transition between manual and automatic control is also required.

**STEP 2. Select sensors.** This was discussed earlier. For the laboratory model, the sensors were a set of fourteen RTDs, but three (located at the center and the support edges of the plate) can be used for feedback, and the rest can be used for temperature monitoring purposes. In our case, we will use *only the center temperature* for feedback control. (Another alternative would be to sum the three temperatures into one signal and control the *average* temperature.)

**STEP 3. Select actuators.** This was also discussed earlier. For the laboratory model, the actuators were composed of three standard tungsten halogen lamps previously described. In our case, we shall tie up all three lamps *into a single actuator* by applying the same input command to each lamp.

**STEP 4. Make a linear model.** The laboratory model was built (see Step 9). The nonlinear system equations involve both conduction (see Chapter 2) and radiation terms (see Emami-Naeini et al., 2003). Nonlinear system identification approaches were used to derive a model for the system. Specifically, the three lamps were stepped up, held constant, and then stepped down sequentially, and the three output temperatures were recorded. System identification studies<sup>8</sup> resulted in the following nonlinear model for the system that contains the radiation and conduction terms ( $\mathbf{A}_r$  and  $\mathbf{A}_{con}$ , respectively):

$$\mathbf{M} \dot{\mathbf{T}} = \mathbf{A}_r \begin{bmatrix} \mathbf{T} \\ T_\infty \end{bmatrix}^4 + \mathbf{A}_{con} \begin{bmatrix} \mathbf{T} \\ T_\infty \end{bmatrix} + \mathbf{B} \mathbf{u}. \quad (10.42)$$

Here  $\mathbf{T} = [T_1 \ T_2 \ T_3]^T$  denote the temperatures,  $T_\infty$  = constant ambient temperature ( $\dot{T}_\infty = 0$ ),  $\mathbf{u} = [v_{cmd1} \ v_{cmd2} \ v_{cmd3}]^T$  are the voltage commands, and the system matrices are

$$\mathbf{M}^{-1} = \begin{bmatrix} 1.000040 & 0 & 0 \\ 0 & 5.557443 & 0 \\ 0 & 0 & 13.638218 \end{bmatrix},$$

---

<sup>8</sup>Performed by Dr. G. van der Linden.

$$\mathbf{A}_r = \begin{bmatrix} 5.4762e-2 & -8.5706e-3 & -8.2961e-4 & -4.5361e-2 \\ -8.5706e-3 & 8.5709e-3 & -1.6213e-7 & -8.9134e-8 \\ -8.2961e-4 & -1.6213e-7 & 8.2998e-4 & 2.0976e-7 \end{bmatrix},$$

$$\mathbf{A}_{con} = \begin{bmatrix} 3.5599e-7 & -1.1136e-7 & -1.1976e-7 & -4.7011e-8 \\ -1.1136e-7 & 1.1602e-2 & -2.5027e-3 & -9.0992e-3 \\ -1.9761e-7 & -2.5027e-3 & 6.3736e-3 & -3.8707e-3 \end{bmatrix},$$

$$\mathbf{B} = \begin{bmatrix} 3.4600e-1 & 1.1772e-1 & 2.8380e-2 \\ 3.8803e-11 & 8.0249e-2 & 1.8072e-2 \\ 8.0041e-9 & 2.7216e-3 & 3.1713e-2 \end{bmatrix}.$$

RTP linear model

A linear model for the system was derived as

$$\dot{\mathbf{T}} = \mathbf{A}_3 \mathbf{T} + \mathbf{B}_3 \mathbf{u}, \quad (10.43)$$

$$\mathbf{y} = \mathbf{C}_3 \mathbf{T} + \mathbf{D}_3 \mathbf{u},$$

where  $\mathbf{y} = [T_{y1} \ T_{y2} \ T_{y3}]^T$  and

$$\mathbf{A}_3 = \begin{bmatrix} -0.0682 & 0.0149 & 0.0000 \\ 0.0458 & -0.1181 & 0.0218 \\ 0.0000 & 0.04683 & -0.1008 \end{bmatrix}, \quad \mathbf{B}_3 = \begin{bmatrix} 0.3787 & 0.1105 & 0.0229 \\ 0.0000 & 0.4490 & 0.0735 \\ 0.0000 & 0.0007 & 0.4177 \end{bmatrix},$$

$$\mathbf{C}_3 = \begin{bmatrix} 1 & 0 & 0 \\ 0 & 1 & 0 \\ 0 & 0 & 1 \end{bmatrix}, \quad \mathbf{D}_3 = \begin{bmatrix} 0 & 0 & 0 \\ 0 & 0 & 0 \\ 0 & 0 & 0 \end{bmatrix}.$$

The three open-loop poles are computed from Matlab and are located at  $-0.0527$ ,  $-0.0863$ , and  $-0.1482$ . For our case, because we tied the three lamps into one actuator and are using only the center temperature for feedback, the linear model is then

$$\mathbf{A} = \begin{bmatrix} -0.0682 & 0.0149 & 0.0000 \\ 0.0458 & -0.1181 & 0.0218 \\ 0.0000 & 0.04683 & -0.1008 \end{bmatrix}, \quad \mathbf{B} = \begin{bmatrix} 0.5122 \\ 0.5226 \\ 0.4185 \end{bmatrix},$$

$$\mathbf{C} = [0 \ 1 \ 0], \quad D = [0],$$

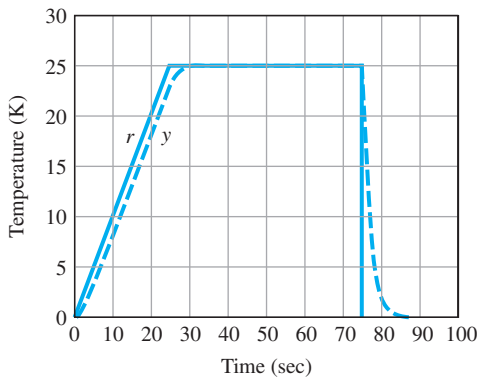
resulting in the transfer function

$$G(s) = \frac{T_{y2}(s)}{V_{cmd}(s)} = \frac{0.5226(s + 0.0876)(s + 0.1438)}{(s + 0.1482)(s + 0.0527)(s + 0.0863)}.$$

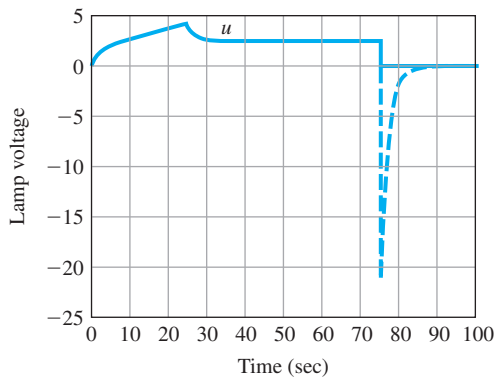
STEP 5. Try a lead-lag or PID controller. We may try a simple PI controller of the form

$$D_c(s) = \frac{(s + 0.0527)}{s},$$

so as to cancel the effect of one of the slower poles. The linear closed-loop response is shown in Fig. 10.73(a) and the associated control effort is shown in Fig. 10.73(b). The system response follows the commanded trajectory with a time delay of approximately 2 sec and no overshoot. The lamp has its normal response until 75 sec and goes negative (shown dashed) to try to follow the sharp drop in commanded temperature.



(a) Temperature tracking response



(b) Control effort

**Figure 10.73**

Linear closed-loop RTP response for PI controller

This behavior is not possible in the system, as there is no means of active cooling and the lamps do saturate low. Note there is no explicit means of controlling the temperature nonuniformity in this approach.

**STEP 6. Evaluate/modify plant.** This was discussed already in connection with actuator and sensor selection.

**STEP 7. Try an optimal design.** We use the error-space approach for inclusion of integral control and employ the linear quadratic Gaussian technique of Chapter 7. The error system is

$$\begin{bmatrix} \dot{e} \\ \dot{\xi} \end{bmatrix} = \begin{bmatrix} 0 & \mathbf{C} \\ \mathbf{0} & \mathbf{A} \end{bmatrix} \begin{bmatrix} e \\ \xi \end{bmatrix} + \begin{bmatrix} D \\ \mathbf{B} \end{bmatrix} \mu, \quad (10.44)$$

where

$$\mathbf{A}_s = \begin{bmatrix} 0 & \mathbf{C} \\ \mathbf{0} & \mathbf{A} \end{bmatrix}, \quad \mathbf{B}_s = \begin{bmatrix} D \\ \mathbf{B} \end{bmatrix},$$

$e = y - r$ ,  $\xi = \dot{T}$ , and  $\mu = \dot{u}$ . For state feedback design, the LQR formulation of Chapter 7 is used; that is,

$$\mathcal{J} = \int_0^{\infty} \{ \mathbf{z}^T \mathbf{Q} \mathbf{z} + \rho \mu^2 \} dt,$$

where  $\mathbf{z} = [e \ \xi^T]^T$ . Note  $\mathcal{J}$  needs to be chosen in such a way as to penalize the tracking error  $e$  and the control  $u$ , as well as the differences in the three temperatures. Therefore, the performance index should include a term of the form

$$10 \left\{ (\dot{T}_1 - \dot{T}_2)^2 + (\dot{T}_1 - \dot{T}_3)^2 + (\dot{T}_2 - \dot{T}_3)^2 \right\},$$

which minimizes a measure of the *temperature nonuniformity*. The factor of 10 was determined by trial and error as the relative weighting between the error state and the plant state. The state and control weighting matrices,  $\mathbf{Q}$  and  $R$ , respectively, are then

### Temperature uniformity

$$\mathbf{Q} = \begin{bmatrix} 1 & 0 & 0 & 0 \\ 0 & 20 & -10 & -10 \\ 0 & -10 & 20 & -10 \\ 0 & -10 & -10 & 20 \end{bmatrix}, \quad R = \rho = 1.$$

The following Matlab command is used to design the feedback gain:

$$[K] = lqr(As, Bs, Q, R).$$

The resulting feedback gain matrix computed from Matlab is

$$\mathbf{K} = [K_1 : \mathbf{K}_0],$$

where

$$K_1 = 1, \quad \mathbf{K}_0 = \begin{bmatrix} 0.1221 & 2.0788 & -0.2140 \end{bmatrix},$$

which results in the internal model controller of the form

$$\begin{aligned} \dot{x}_c &= B_c e, \\ u &= C_c x_c - \mathbf{K}_0 \mathbf{T}, \end{aligned} \tag{10.45}$$

with  $x_c$  denoting the controller state and

$$B_c = -K_1 = -1, \quad C_c = 1.$$

The resulting state-feedback closed-loop poles computed from Matlab are at  $-0.5574 \pm 0.4584j$ ,  $-0.1442$ , and  $-0.0877$ . The full-order estimator was designed with the process and sensor noise intensities selected as the estimator design knobs:

$$R_w = 1, \quad R_v = 0.001.$$

The following Matlab command is used to design the estimator:

$$[L] = lqe(A, B, C, R_w, R_v).$$

The resulting estimator gain matrix is

$$\mathbf{L} = \begin{bmatrix} 16.1461 \\ 16.4710 \\ 13.2001 \end{bmatrix},$$

with estimator error poles at  $-16.5268$ ,  $-0.1438$ , and  $-0.0876$ . The estimator equation is

$$\dot{\hat{\mathbf{T}}} = \mathbf{A}\hat{\mathbf{T}} + \mathbf{B}u + \mathbf{L}(y - \mathbf{C}\hat{\mathbf{T}}). \tag{10.46}$$

With the estimator, the internal model controller equation is modified as

$$\dot{x}_c = B_c e, \tag{10.47}$$

$$u = C_c x_c - \mathbf{K}_0 \hat{\mathbf{T}}.$$

The closed-loop system equations are given by

$$\begin{aligned} \dot{\mathbf{x}}_{cl} &= \mathbf{A}_{cl} \mathbf{x}_{cl} + \mathbf{B}_{cl} r, \\ y &= \mathbf{C}_{cl} \mathbf{x}_{cl} + \mathbf{D}_{cl} r, \end{aligned} \tag{10.48}$$

where  $r$  is the reference input temperature trajectory, the closed-loop state vector is  $\mathbf{x}_{\text{cl}} = [\mathbf{T}^T \mathbf{x}_c^T \hat{\mathbf{T}}^T]^T$  and the system matrices are

$$\mathbf{A}_{\text{cl}} = \begin{bmatrix} \mathbf{A} & \mathbf{B}\mathbf{C}_c & -\mathbf{B}\mathbf{K}_0 \\ \mathbf{B}_c\mathbf{C} & \mathbf{0} & \mathbf{0} \\ \mathbf{L}\mathbf{C} & \mathbf{B}\mathbf{C}_c & \mathbf{A} - \mathbf{B}\mathbf{K}_0 - \mathbf{L}\mathbf{C} \end{bmatrix}, \quad \mathbf{B}_{\text{cl}} = \begin{bmatrix} \mathbf{0} \\ -\mathbf{B}_c \\ \mathbf{0} \end{bmatrix},$$

$$\mathbf{C}_{\text{cl}} = [\mathbf{C} \quad \mathbf{0} \quad \mathbf{0}], \quad D_{\text{cl}} = [0],$$

with closed-loop poles (computed with Matlab) located at  $-0.5574 \pm 0.4584j$ ,  $-0.1442$ ,  $-0.0877$ ,  $-16.5268$ ,  $-0.1438$  and  $-0.0876$  as expected. The closed-loop control structure is shown in Fig. 10.74.

The closed-loop control system diagram implemented in Simulink is shown in Fig. 10.75. The linear closed-loop response is shown in Fig. 10.76(a), and the associated control effort is shown in Fig. 10.76(b). The commanded temperature trajectory,  $r$ , is a ramp from  $0^\circ\text{C}$  to  $25^\circ\text{C}$ , with a  $1^\circ\text{C/sec}$  slope followed by a 50 sec. soak time and a drop back to  $0^\circ\text{C}$ . (Note the ramp rate is very slow here because we have only three lamps for our RTP laboratory model, whereas a real RTP system

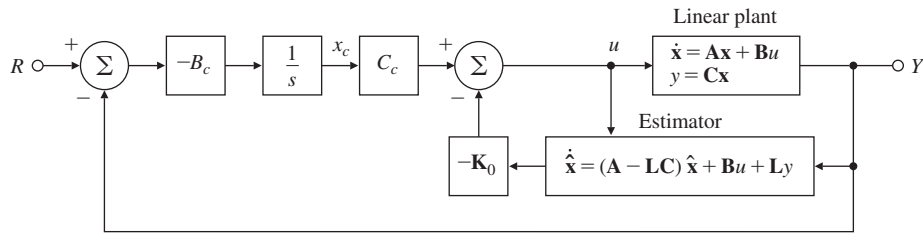


**Figure 10.74**

Closed-loop control structure diagram

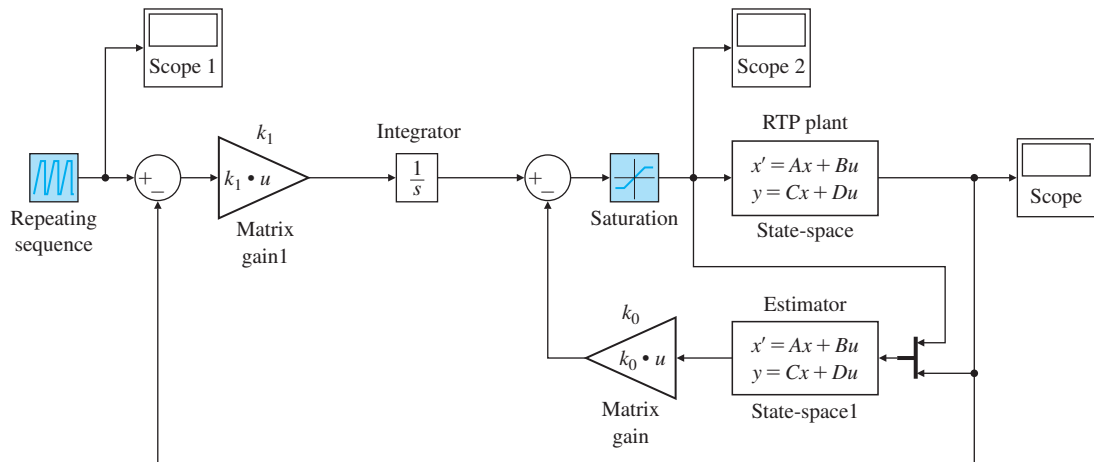


**Figure 10.75**

Simulink block diagram for RTP closed-loop control

Source: Reprinted with permission of The MathWorks, Inc.

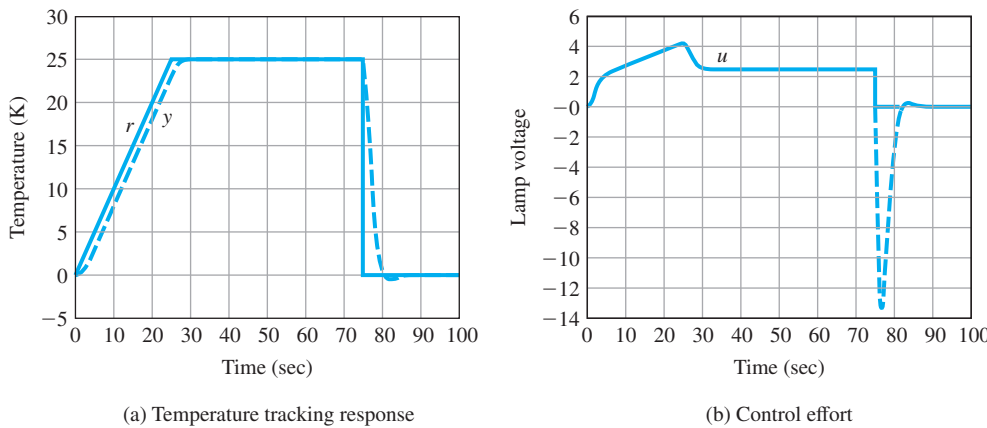


**Figure 10.76**  
Linear closed-loop RTP response for robust servomechanism controller

Temperature trajectory  
following

Simulink nonlinear  
simulation

Prefilter

Lamp nonlinearity

would have hundreds of lamps, and the much faster ramp rates mentioned earlier would be relevant.) The system tracks the commanded temperature trajectory—albeit with a time delay of approximately 2 sec for the ramp and a maximum of  $0.089^{\circ}\text{C}$  overshoot. As expected, the system tracks a constant input asymptotically, with zero steady-state error. The lamp command increases as expected to allow for tracking the ramp input, reaches a maximum value at 25 sec, then drops to a steady-state value around 35 sec. The normal response of the lamp is seen from 0 to 75 sec, followed by a negative commanded voltage for a few seconds corresponding to fast cooling. Again, the negative control effort voltage (shown in dashed lines) is physically impossible as there is no active cooling in the system. Hence, in the nonlinear simulations, commanded lamp power must be constrained to be strictly nonnegative (Step 8). Note the response from 75 to 100 sec is that of the (negative) step response of the system.

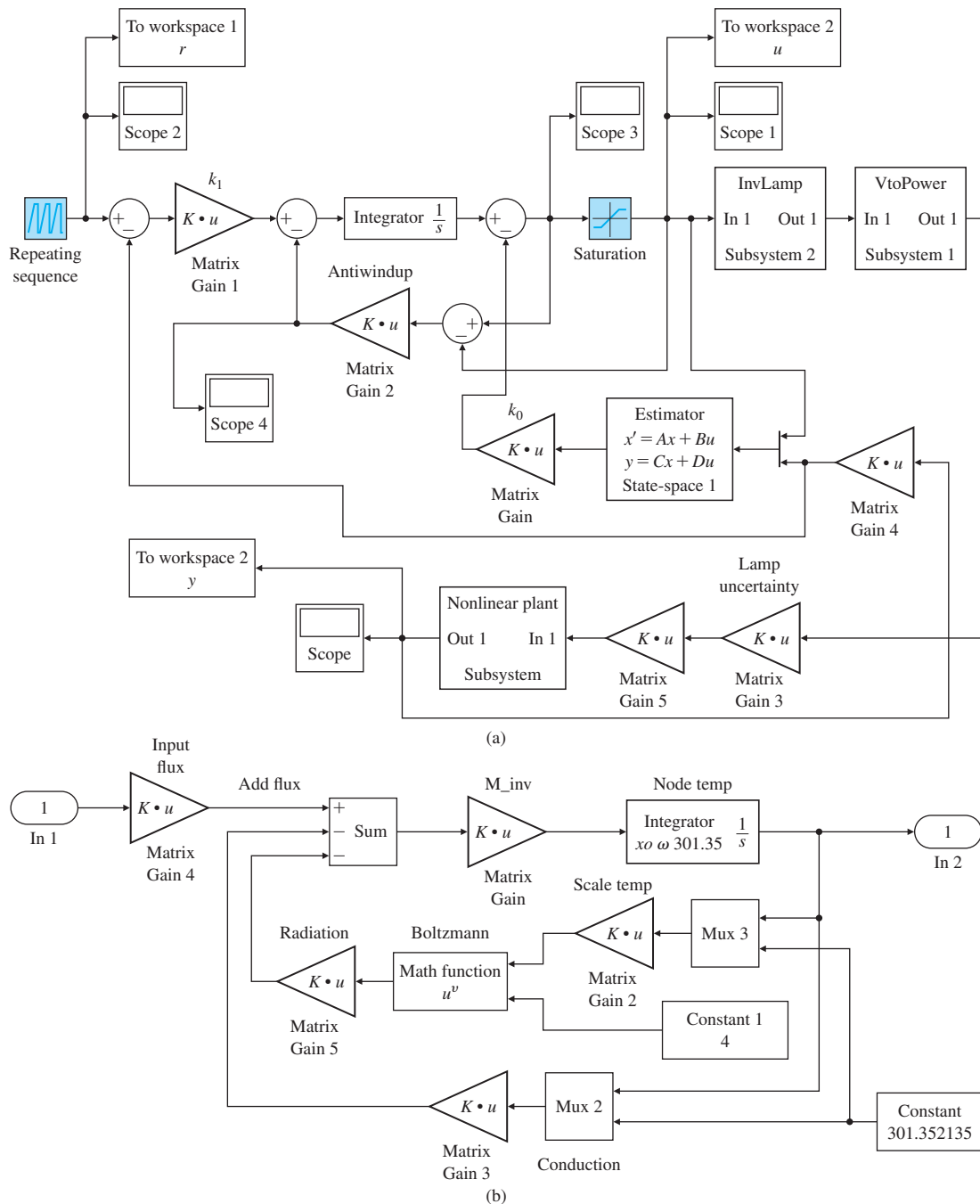
**STEP 8. Simulate the design with nonlinearities.** The nonlinear closed-loop system was simulated in Simulink as shown in Fig. 10.77. The model was implemented in temperature units of degrees Kelvin and the ambient temperature is  $301\text{K}$ .<sup>9</sup> The nonlinear plant model is the implementation of Eq. (10.42). There is a prefilter following the reference temperature trajectory (to smoothen the sharp corners) with the transfer function

$$G_{\text{pf}}(s) = \frac{0.2}{s + 0.2}. \quad (10.49)$$

Note conversion from voltage to power was determined experimentally to be given by

$$P = V^{1.6}, \quad (10.50)$$

<sup>9</sup>[K] = [°C] + 273.

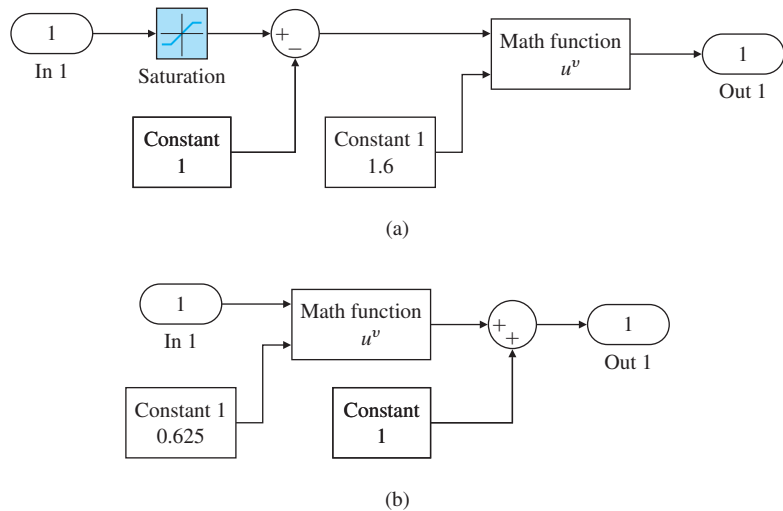
**Figure 10.77**

Simulink diagram for nonlinear closed-loop RTP system: (a) nonlinear closed-loop; (b) nonlinear plant  
Source: Reprinted with permission of The MathWorks, Inc.

**Figure 10.78**

Simulink diagram for nonlinear closed-loop RTP system:  
 (a) subsystem to convert voltage to power;  
 (b) subsystem for lamp model

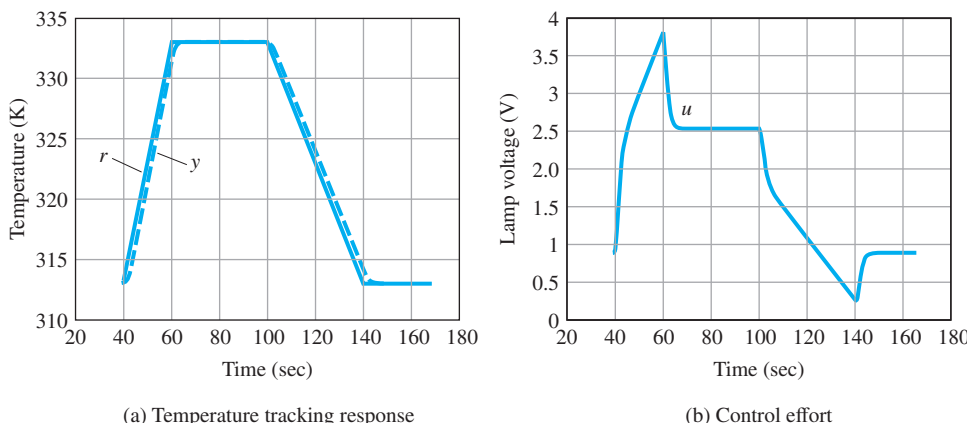
*Source: Reprinted with permission of The MathWorks, Inc.*



and is implemented as a nonlinear block (named VtoPower) in the Simulink diagram accordingly (see Fig. 10.78). The inverse of the static nonlinear lamp model is also included as a block (named InvLamp):

$$V = P^{0.625}. \quad (10.51)$$

This will cancel the lamp nonlinearity. The voltage range for system operation is between 1 and 4 volts, as seen from the diagram. A saturation nonlinearity is included for the lamp as well as integrator antiwindup logic to deal with lamp saturation. The nonlinear dynamic response is shown in Fig. 10.79(a), and the control effort is shown in Fig. 10.79(b). Note the nonlinear response is in general agreement with the linear response.

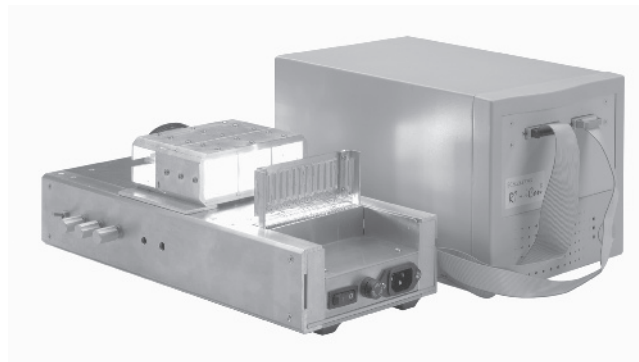
**Figure 10.79**

Nonlinear closed-loop response for robust servomechanism controller

**Figure 10.80**

RTP temperature control laboratory model

*Source: Photo courtesy of Abbas Emami-Naeini*



A prototype of the RTP laboratory model was designed, built,<sup>10</sup> and demonstrated at the Sematech AEC/APC'98 Conference. Figure 10.80 shows a photograph of the operational system. This system is really multivariable in nature. The three-input–three-output multivariable controller used on the prototype system was designed using the same approach discussed in Step 7, and was implemented on an embedded controller platform that uses a real-time operating system.

The continuous controller (that is, the combined internal model controller and the estimator) is of the form

$$\begin{aligned}\dot{\mathbf{x}}^c &= \mathbf{A}^c \mathbf{x}^c + \mathbf{B}^c \mathbf{e}, \\ \mathbf{u} &= \mathbf{C}^c \mathbf{x}^c,\end{aligned}\quad (10.52)$$

where  $\mathbf{x}^c = [\mathbf{x}_c^T \hat{\mathbf{T}}^T]^T$ ,

$$\mathbf{A}^c = \begin{bmatrix} \mathbf{0} & \mathbf{0} \\ \mathbf{B}\mathbf{C}_c & \mathbf{A} - \mathbf{B}\mathbf{K}_0 - \mathbf{L}\mathbf{C} \end{bmatrix}, \quad \mathbf{B}^c = \begin{bmatrix} \mathbf{B}_c \\ \mathbf{L} \end{bmatrix}, \quad (10.53)$$

and

$$\mathbf{C}^c = [\mathbf{C}_c \quad -\mathbf{K}_0].$$

The controller was discretized (see Chapter 8) with a sampling period of  $T_s = 0.1$  sec and implemented digitally (with appropriate antiwindup logic) as

$$\begin{aligned}\mathbf{x}_{k+1}^c &= \Phi^c \mathbf{x}_k^c + \Gamma^c \mathbf{e}_k, \\ \mathbf{u}_k &= \mathbf{C}^c \mathbf{x}_k^c.\end{aligned}\quad (10.54)$$

The response of the actual system to the reference temperature trajectory, along with the three lamp voltages, is shown in Fig. 10.81. It is in good agreement with the nonlinear closed-loop simulation of the system (once noise is accounted for).

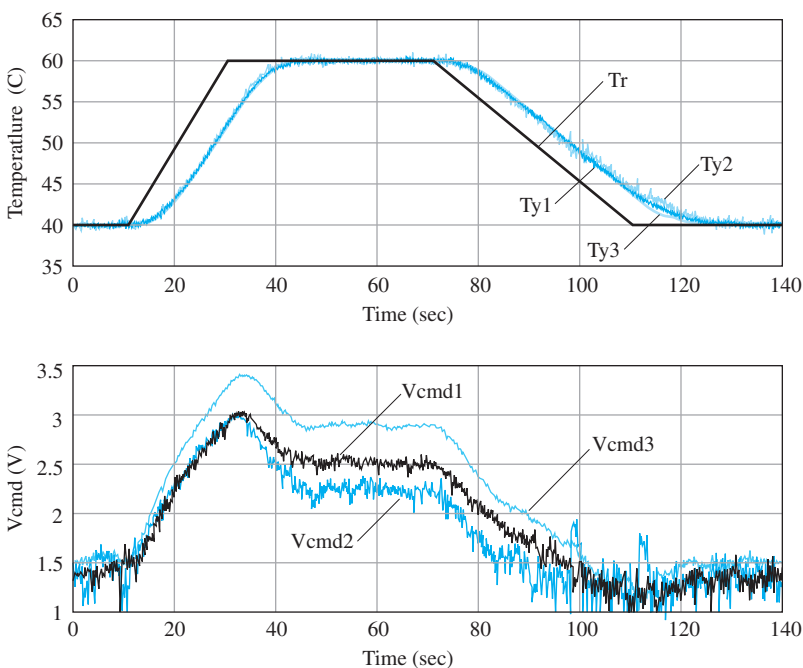
For further information on modeling and control of RTP systems, refer to Emami-Naeini et al. (2003), Ebert et al. (1995a,b), de Roover et al. (1998), and Gyugyi et al. (1993).

---

<sup>10</sup>By Dr. J. L. Ebert.

**Figure 10.81**

Response of the RTP temperature control laboratory model



## 10.7 Chemotaxis, or How *E. Coli* Swims Away from Trouble

Biological systems have numerous feedback loops. One such system is the human body, which implements feedback mechanisms to regulate its core temperature (98.6°F), hormone levels, and eye response to light levels, as well as the pH, arterial blood pressure, and sugar levels of circulating blood. Core temperature is regulated by the hypothalamus region of the brain which, in part, signals the secretion of fluid from sweat glands to lower body temperature, and conversely stimulates skeletal muscles to shiver in order to raise the temperature. Blood sugar levels are controlled using a tight negative feedback loop. If the blood sugar level rises, the pancreas secretes insulin to bring the level back to normal. Meanwhile, downward deflections in blood sugar levels result in the secretion of fluids from the adrenal gland and pancreas to maintain the proper balance. Furthermore, the human heart is a nonlinear feedback control system which has methods for maintaining a regular heartbeat and the proper voltage potential in the membranes. Understanding these biological feedback loops is an important step towards maintaining human health and developing therapies for disease.

Attempts are underway to characterize and model a whole biological organism's behavior as a system of interconnected subsystems. Toward that end, deriving a detailed understanding of a simple cellular system, such as a single *Escherichia coli* bacterium, is a significant effort.

Unlike the previous case studies, this example is not a feedback design example, but rather an illustration of a natural feedback mechanism which has evolved in biological systems.

### Systems biology

### Background

The *cell* is the basic structural and physiological subsystem of all living organisms, and most of the biochemical activities necessary for life are performed in cells. Some organisms, such as the bacteria in Fig. 10.82, consist of only a single cell. *Escherichia coli* (*E. coli*), photographed in Fig. 10.83, is one of these single-cell organisms that has been extensively studied and whose interesting motion and control will be described in a highly simplified way in this case study. The technical results for the study come from the field of systems biology. *Systems biology* is an emerging field with the goal of creating dynamic models to describe the incredibly complex processes in many biological systems. The aim is to determine how shifting variables in one part impact the whole. In this case study, a model is presented to suggest how ideas from control can contribute to this effort. In preparing the study, we have tried to minimize the use of technical terms from biology and to define clearly those found useful and necessary for the presentation. It is hoped that this simple introduction will inspire control engineers to conduct direct study of this important field. First, a bit of background.

### *Escherichia coli*

*Escherichia coli* was discovered by German pediatrician and bacteriologist Theodor Escherich in 1885. The bacterium is a cylindrical organism with hemispherical endcaps, as depicted in Fig. 10.83. It is approximately 1 micron ( $\mu$ ) in diameter and 2 microns ( $\mu$ ) in length and weighs about 1 picogram (pg). *E. coli* lives in the large intestine

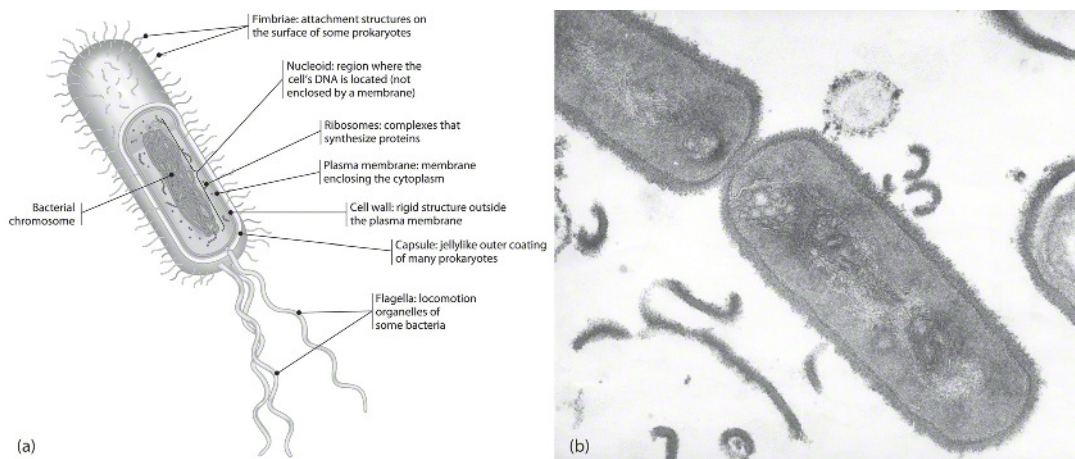


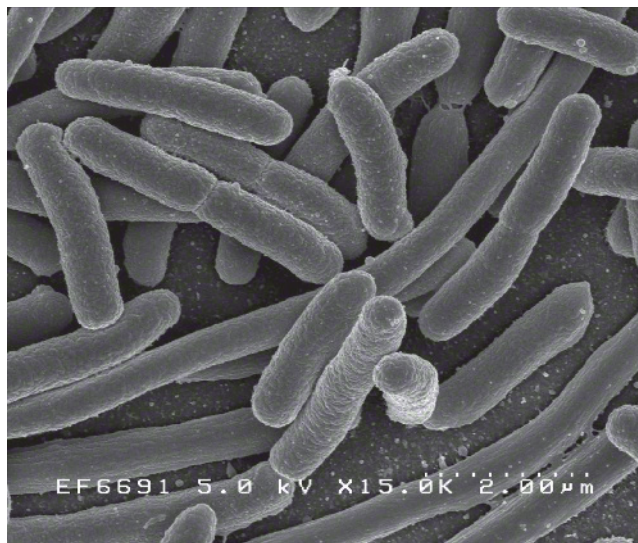
**Figure 10.82**

(a) A typical bacterium; (b) TEM of bacterium *Bacillus coagulans*

Source: Campbell, Neil A.; Reece, Jane B., *Biology*, 8th Ed., © 2008, p. 98. Reprinted and Electronically reproduced by permission of Pearson Education, Inc., Upper Saddle River, New Jersey.

**Figure 10.83***E. coli* bacteria

Source: United States  
Department of Health and  
Human Services, National  
Institutes of Health



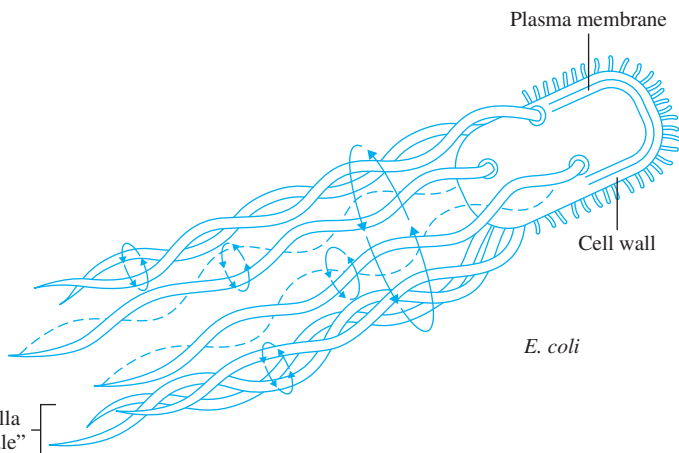
of warm blooded “host” animals, including humans. The bacterium can help in maintaining the balance of healthful intestinal flora (that is, the population of microbial organisms) in the gut and can also synthesize vitamins that benefit its host. *E. coli* has been studied extensively by geneticists because of its rather small genome size and the ease of growth in a laboratory. *E. coli* grows longer and divides by binary fission to create two genetically identical “daughter” bacteria. Under optimal nutritional and environmental conditions, a population of *E. coli* can double every 20 minutes. While most *E. coli* “strains,” or variants of the *E. coli* species, are harmless, a particular strain (*E. coli* O157:H7) can cause food poisoning in humans if ingested. The entire genome, or the “library” of inherited genetic information, has been sequenced for different *E. coli* strains: for example, “lab strain” *E. coli* K12 MG1655 contains approximately 4.64 million of the adenosine-thymine (A-T) and cytosine-guanine (C-G) DNA base pairs arranged into a total of 4466 predicted genes. These genes serve as instructions for the synthesis of specific proteins. Proteins are the primary tools that cells use to implement biochemical and biophysical processes. Highly regulated networks of Protein-Protein Interactions (PPI) give rise to higher order functions essential for the survival of the cell, including, in the case of *E. coli*, motility. In 2003, researchers demonstrated that solitary *E. coli* cells exhibit “quorum sensing” via positive chemotaxis, meaning that they are attracted to like cells in order to perform tasks requiring multiple *E. coli*, such as the formation of a “biofilm.”

*Escherichia coli* has a set of 6 to 10 rotary motors, each driving a thin helical filament about  $10 \mu\text{m}$  long through a short, flexible and proximal hook that acts as a universal joint. This entire assembly is called a flagellum (Berg, 2004). The motor runs either clockwise (CW),

**Figure 10.84**

Flagella motors turning CCW resulting in a run

Source: Courtesy Nima Cyrus Emami



as seen by an observer outside of the cell looking down at the hook, or counter-clockwise (CCW). When all the motors rotate CCW, the flagella filaments bundle together and the cell swims steadily forward in a “run,” as suggested in Fig. 10.84. When one or more motors switch to CW rotation, the corresponding flagella unbundle and reorient the cell in a “tumble” resulting in little displacement, as shown in Fig. 10.85. The two modes of motion alternate and, in a state of equilibrium with

**Figure 10.85**

Flagella motors turning CW resulting in a tumble

Source: Courtesy Nima Cyrus Emami

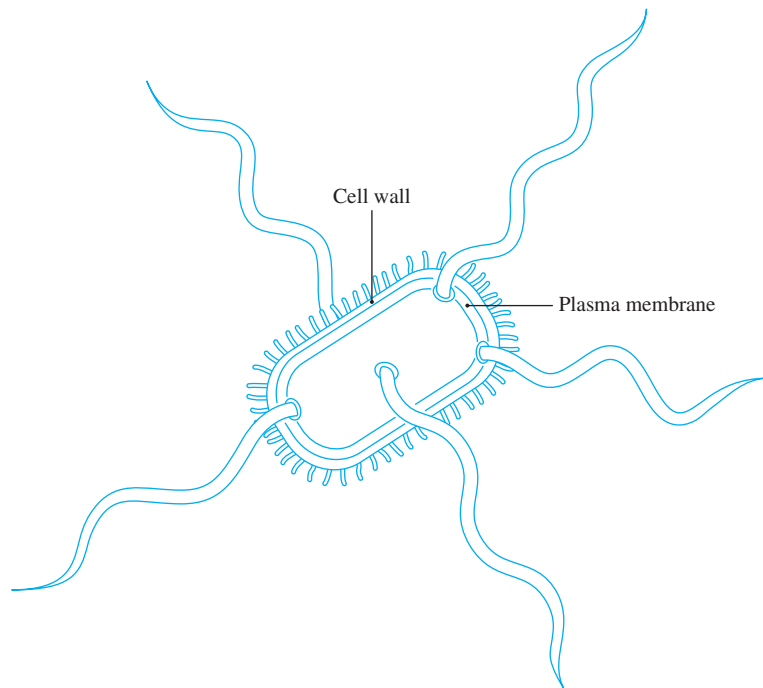
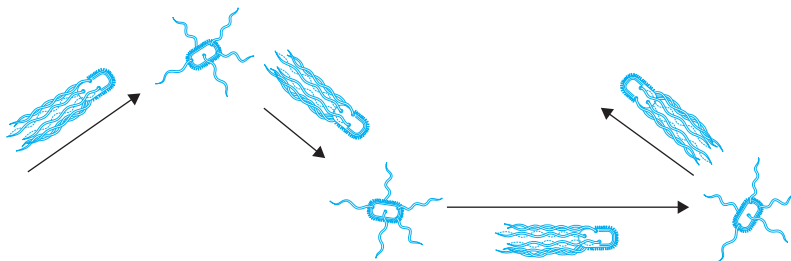


**Figure 10.86**

*Escherichia coli*  
movements resembling  
a biased random walk



its environment, the *E. coli* alternates between both modes with runs lasting about 1 sec and tumbles about 0.1 sec, resulting in a 3-D random walk. Through control of tumbling frequency, the bacteria can direct their motion toward a relatively high concentration of attractant molecules or away from a relatively high concentration of repellent molecules, as suggested in Fig. 10.86.

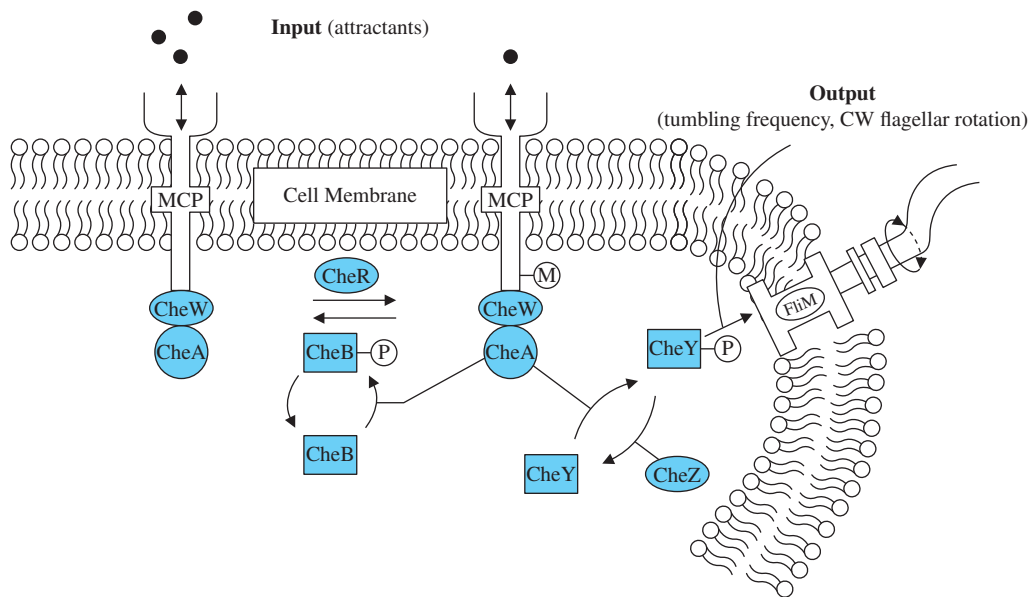
### The Problem

#### Chemotaxis

*Chemotaxis* is the name given to the process by which a motile bacterium senses the changes in its environment and moves toward places with a more favorable environment. Chemotaxis is important for proper functioning of the cell. An *E. coli* bacterium compares the current attractant concentration with the past attractant concentration. If it detects a positive change in the attractant concentration, it should move up the gradient. To do so, the probability of a tumble, and hence its tumbling frequency, is reduced and the runs are correspondingly longer. In contrast, if it detects an increase in repellent concentration, the assumption seems to be that it must have been swimming in a bad direction; consequently, the bacterium increases its tumbling frequency and tries to change direction so as to swim away from the repellents. The dynamics of this *chemotaxis* are the subject of our case study.

Several different models of bacterial chemotaxis have been developed by researchers in systems biology. Our discussion is based on two of these (Barkai & Libler, 1997; Yi et al., 2000). The different proteins involved in chemotactic response have been well studied and their interactions have been characterized in some detail as shown in Fig. 10.87. Biologists have named the proteins involved in chemotaxis by letters of the alphabet prefixed by “Che” (for example, CheA, CheB). In biology, signal transduction is a process by which molecular stimuli outside of the cell react with receptor proteins in the cell membrane, which in turn activate “second messenger” proteins within the cell to carry out some task (for example, expression of a gene, and biochemical synthesis). On the surface of the bacterium is a class of receptor proteins called MCPs, or methyl-accepting chemotaxis proteins. The MCPs contain extracellular, transmembrane, and intracellular domains, meaning they have sub-units which sense chemical stimuli outside of the cell and subsequently activate proteins inside of the cell. These chemicals constitute the input to the system and are collectively called *ligands*. The system is

#### Ligand

**Figure 10.87**

The chemotaxis signal transduction pathway in *E. coli*

Source: Courtesy of Nima Cyrus Emami

set up to control the frequency of tumbling, which is done by control of the activity of CheY, the protein that acts directly on the motor of the flagella.

The MCPs bind CheA and CheW within the cell to form a receptor complex which, through feedback regulation, maintains sensitivity to changes in attractant binding over a wide range of ligand concentrations. Here the input and output conditions, PPI, and biochemical transformations that induce this regulatory process are described. Receptors are considered either active and awaiting a ligand or are inactive and not accepting any ligand. In biochemistry, phosphorylation, or the transfer of a negatively charged phosphate group ( $-PO_4^{3-}$ ) to a protein, is a common method for activating a protein for some task by inducing a transformation in its structural and biochemical properties. In chemotaxis, a decrease in attractant binding results in increased phosphorylation of CheA (denoted by CheA-P), while increased attractant binding causes decreased CheA phosphorylation. Receptors with CheA-P are considered active (more frequent tumbles), while those with dephosphorylated CheA are inactive (more frequent runs). The mechanism behind this change in motility is the phosphorylation of CheY: CheA-P transfers its phosphate group to CheY, yielding CheY-P, which binds the FliM protein in the flagellar basal body (motor) to produce more frequent tumbling.

As part of the steady-state dynamics of chemotaxis, methyl groups ( $-CH_3$ ) are regularly being added to the MCP by CheR (methylation)

and equally removed by CheB (demethylation). Because CheA–P also phosphorylates CheB and CheB–P more frequently demethylates the MCP, this balance is upset when a ligand binds to an active receptor complex. If the ligand is an attractant, the activity of CheA is reduced (less CheA–P), the action of CheB in MCP demethylation is reduced (less CheB–P), more receptors are made active and the activity of CheA slowly returns to the steady-state. This is the feedback loop in chemotaxis. Meanwhile, CheA reduces its rate of activating CheY (less CheY–P) and this causes the tumbling frequency to be reduced. As a consequence, the bacteria swim more and presumably swim toward the attractant concentration. Now, if the ligand is a repellent, the activity of CheA is increased, which causes increased rate of CheY activity and increased frequency of tumbling. The bacterium swims less while it “looks” for a new direction in order to escape the concentration of repellents. At the same time, in the feedback loop, CheB is also more active, receptors are made inactive at a greater rate, and again CheA and the tumble frequency return to their steady-state values. The fact that the activity and the tumble frequency return to exactly the same value after a change in ligand concentration is a remarkable property called **exact adaptation** by system biologists. As we will see, to a control engineer, this is a very common control method.

### Exact adaptation

#### The Model

The problem, then, is to develop a model as a control system block diagram that will describe the average motion of this chemotaxis situation. We represent the averages as if they were one receptor complex with the related proteins acting on the flagella. As the research shows, the equations are complex and highly nonlinear. Also, the surface of the bacterium contains hundreds of receptor complexes, and these interact as suggested already in Fig. 10.87. For our study, the variables for the block diagram are selected as linear, small-signal deviations of the averages of the several quantities away from their equilibrium values. The input is taken to be the concentration of ligand, with attractors being positive and repellents being negative. The outputs of the system are the activity of CheA–P and resulting motion in the single  $x$  direction. The parameters of our model were selected so the responses matched the curves given in Fig. 10 of (Mello et al., 2004). The mechanics of one-dimensional motion assume the viscous friction dominates the mass so the dynamics are a single integrator. The model is based on the following facts:

- It is observed that when a ligand binds to an active receptor site, the changes in concentrations of CheA–P and resulting CheB–P and CheY–P are almost instantaneous.
- However, the CheB phosphorylation only changes the rate of demethylation, not the extent of demethylation itself. The changes

in methylation level take place much more slowly than the changes in tumble rate.

- Upon insertion of a concentration of attractants, the “activity” as measured by the concentration of CheA-P drops quickly, then slowly recovers to exactly the same steady-state level. This property is called *adaptation* of activity.

### Adaptation

A control block diagram shown in Fig. 10.88 implements these facts, including the adaptation. As seen, the adaptation result is accomplished by the standard control scheme of integral control. A Simulink schematic is shown in Fig. 10.89, and the responses in Figs 10.90–10.92 for fixed concentrations of CheR. If the value of CheR is changed, the steady-state intensity of the activity changes and the time constant of the methylation also changes. Fig. 10.90 shows that if attractant is added at time  $t = 20$  sec, the tumble activity drops but recovers to its

**Figure 10.88**

Simplified block diagram of *E. coli* chemotaxis.  $\ell$  represents ligand,  $m$  the methylation, CheR the steady-state rate of methylation,  $\bar{y}$  the steady-state activity, and  $w$  the steady-state random walk motion

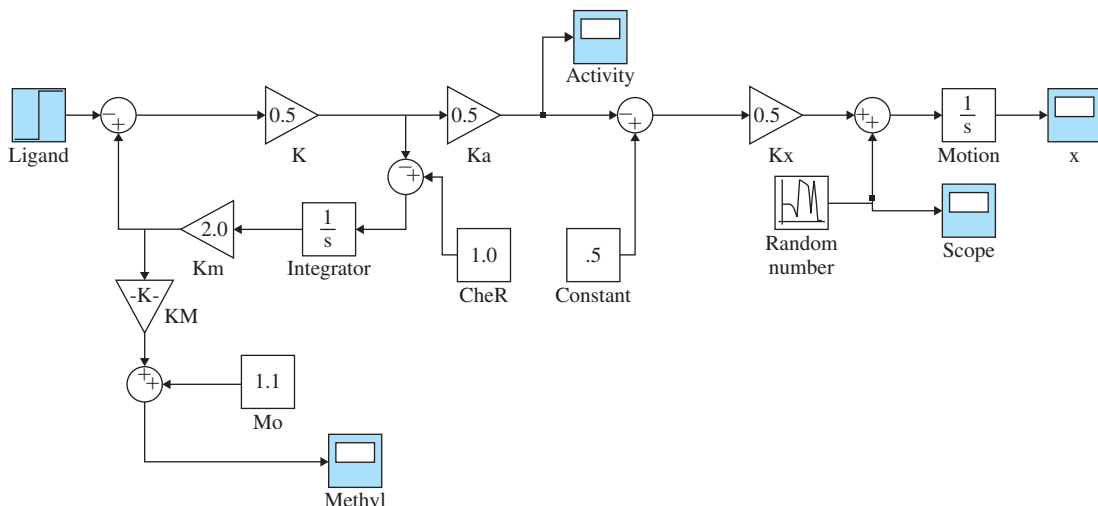
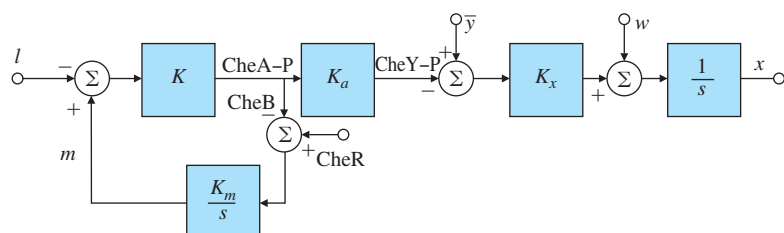


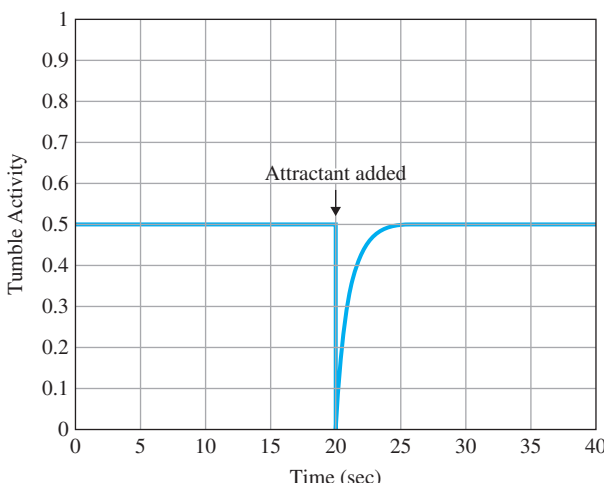
**Figure 10.89**

A Simulink schematic diagram for simulating *E. coli* chemotaxis

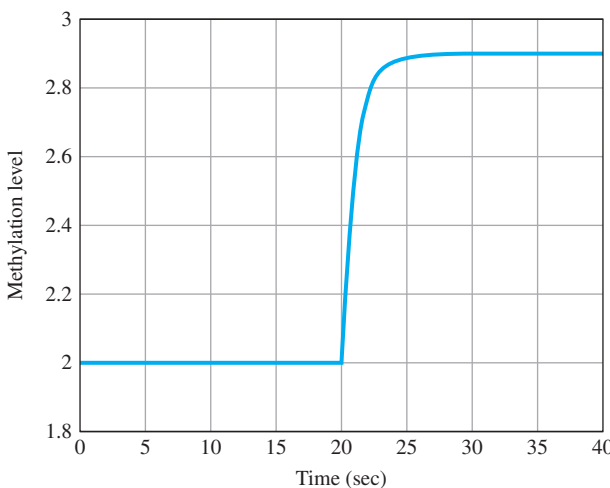
Source: Reprinted with permission of The MathWorks, Inc.

**Figure 10.90**

Simulated tumble frequency of the chemotaxis model following insertion of attractant at  $t = 20$  sec

**Figure 10.91**

Methylation of the chemotaxis model following insertion of attractant at  $t = 20$  sec



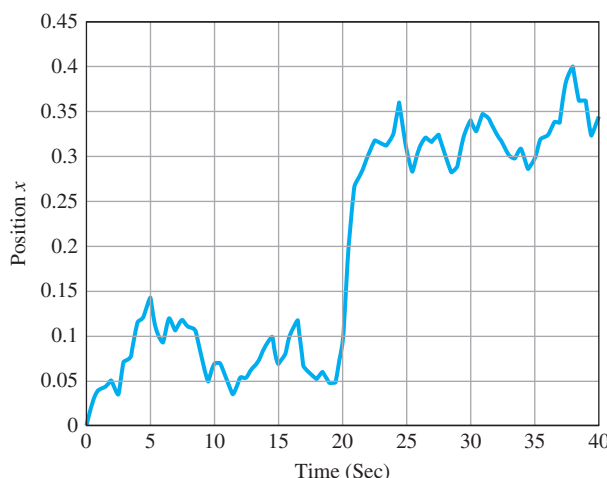
initial value within approximately 5 seconds. Fig. 10.91 shows the corresponding behavior of the methylation level, and Fig. 10.92 shows the motion response of the chemotaxis model.

In the end, we leave this case study with more questions than answers. For example, one should be able to derive the model by a small-signal analysis from the basic chemical and physical equations of the processes. The model as presented could be modified to account for changes in the concentration of CheR, for example. Finally, how would the model be extended to describe the motion in three dimensions? We hope someone using this book is inspired to find the answers to these questions.

While many years of research aimed at characterizing the biophysical regulatory mechanisms of bacterial chemotaxis have resulted in detailed biological models, ongoing research continues to reveal further

**Figure 10.92**

Motion response of the chemotaxis model following insertion of attractant at  $t = 20$  sec



intricacies of this pathway. For instance, while the MCPs in this case study are represented as autonomous single-protein molecules, in fact the MCP is a complex molecule composed of multiple-protein subunits which must bind to one another to give rise to its higher order properties. Similarly, it is known that chemotaxis involves the binding of two CheA proteins to one another, forming a “dimer” (or a complex comprised of two molecular subunits). Biophysicists have recently exploited multiple methodologies for visualizing the structures of and interactions between proteins and macromolecules to uncover a more detailed interaction model whereby MCPs complexes consist of a hexagonal lattice of numerous subunits and are connected by interactions with multiple CheW proteins and CheA dimers [A. Briegel, et al., 2012]. Hence, the dynamics of this system may be subject to the dynamics of binding for numerous subunit molecules in the formation of a very complex macromolecular structure. Although biological details such as these may introduce complexities into the modeling of such systems, they also empower systems biologists to more accurately model the behaviors of these systems, these organisms, and their emergent properties.

### Summary

For years, biologists had been focusing on studying various parts of living organisms. Recently, the focus has shifted to studying the whole organism’s behavior as a system of interconnected parts. Since the 1970s, it had been known experimentally that many biological systems adjust to their environment in an adaptive way. Recently, analytical models have been developed to explain this phenomenon as we discussed in this case study. The new analytical models can explain the inherent properties of the biological system such as robust perfect adaptation as given by the integral control of the receptor sensitivity. Control theory methods and interpretations have proved helpful in increasing

the level of our understanding of the behavior and properties of biological systems. We hope this simple example helps stimulate interest in this exciting field.

## 10.8 Historical Perspective

The first autopilot was tested on a Curtis flying boat in 1912, just nine years after the first Wright brothers' flight. It consisted of a gyroscope to measure the attitude and servo motors to activate the control surfaces, and was designed by Elmer Sperry. In part, it was a result of the Wright brothers' design to intentionally make the aircraft slightly unstable in order to make it more controllable by the pilot. This system gained fame in 1914 when it won a prize in France by demonstrating its capabilities by flying close to the ground with the mechanic walking back and forth along the wing with the pilot, Lawrence Sperry, standing in the cockpit with his hands in the air. Sperry was clearly signifying there was no mechanical connection from the stick to the control surfaces.

Autopilot development went underground in 1915 due to military security for WWI. The next public display was an adaptation of the Sperry system for Wiley Post in his 1933 flight around the world in "Winnie Mae." The flight would have been near impossible without the autopilot because it allowed Post to doze off on occasion. It has been reported that Post had a system consisting of a wrench and string tied to his finger that would wake him up if he slept too soundly. The success of this flight led to the development of an autopilot that included some navigational capabilities as well as attitude control and, in 1947, the Air Force demonstrated an automatic trans-Atlantic flight in a DC-3 type airplane from take-off to landing.

Subsequently, airplanes developed swept wings and higher speeds which required stability augmentation systems to help the pilot control the aircraft even when not on the autopilot. These systems are on all high-performance military and commercial airliners today. In 1974, the F-16 became the first airplane to have aerodynamically unstable regimes and was, therefore, highly dependent on the stability augmentation for sustained flight. This was implemented in order to make the airplane more maneuverable, but required a "fly-by-wire" and quad redundancy for acceptable reliability.

The first spacecraft in the late 1950s had no attitude control, since their only mission was to take measurements and broadcast the information back to earth. However, they were followed in the early 1960s with the Corona spacecraft, whose mission was to take photographs of the earth, which required that the camera be pointed and stabilized very accurately. At the time, these missions were classified for military purposes and called Discoverer for public consumption, but since then have been declassified and described in some detail.<sup>11</sup>

---

<sup>11</sup>Taubman (2003).

The first digital autopilots were in the Apollo program lunar module and the command module in the late 1960s. They were developed primarily by MIT's Instrumentation Lab under the direction of Bill Widnall, Don Fraser, and Dick Battin. The decision to take the bold step of using digital technology for the first time rather than the traditional analog implementation was made by NASA in order to handle the complexity required at a reasonable weight.

Prior to 1980, automobile engine control systems consisted of a mechanical arrangement in the distributor to vary the spark timing and a fluidic system in the carburetor that varied fuel flow in response to the airflow rate or sudden changes in the accelerator pedal position. These were open-loop systems that essentially programmed the proper control setting based on the operating condition of the engine. In 1980, cars were required to improve their polluting characteristics; therefore, it was essential to improve the controls using feedback as described in Section 10.4. These systems still exist today along with variable valve timing, variable fuel injection timing, tailored high pressure injection, and variable valve opening levels. Large strides have also been made in the vehicle's control: stability augmentation has substantially reduced SUV rollovers, cruise control now includes radar for keeping a reasonable distance behind the car in front, and sensors to maintain the car in the lane. A feedback controlled automobile is becoming a reality (for example, the Google car).

Application of control to semiconductor wafer manufacturing automation is gaining momentum. Many important process steps such as RTP, chemical-mechanical planarization, and lithography use advanced real-time controllers. It is anticipated that during the next decade, many more of the semiconductor fabrication equipment will employ sophisticated *in-situ* feedback control as new sensors become available. This adoption of sophisticated closed-loop control systems by the semiconductor industry presents new challenges and opportunities for control system engineers especially for the upcoming 450-mm diameter wafers. Application of control to magnetic resonance force microscopy for imaging atomic structure of materials (de Roover et al., 2008) can fundamentally change our understanding of atomic structures of devices and enable imaging of biological subsystems.

The emerging field of systems biology marks the coming of age of the life sciences. The usual approach of studying individual components is being replaced by a new approach focused on understanding the behavior of the whole biological system. Among the admirable goals are understanding the behavior of biological systems and discovering cures for diseases such as cancer, as well as developing novel approaches to the discovery of new drugs, production of antibiotics, and vaccines.

The applications of control theory have never been more exciting than they are today. Applications of feedback control ideas to biological systems, network congestion control, and new aerospace systems

are emerging. Applications in genomics treating the human body as a dynamic system are underway. The Internet has attracted the attention of many control-systems researchers eager to understand the tremendous success of this technology and how to improve it. Network design and control including Internet modeling, and development of congestion routing and control are under study. A number of our colleagues are enthusiastic about application of control theory to the financial field; however, to date, none of them have profited enough to quit their day job!

## SUMMARY

- In this chapter, we have laid out a basic outline of control systems design and applied it to six typical case studies. The design outline calls for a number of explicit steps.
  1. *Make a system model and determine the required performance specifications.* The purpose of this step is to answer the question: What is the system, and what is it supposed to do?
  2. *Select sensors.* A basic rule of control is that if you can't observe it, you typically can't control it. Following are some factors to consider in the selection of sensors:
    - (a) Number and location of sensors;
    - (b) Technology to be used;
    - (c) Performance of the sensor, such as its accuracy;
    - (d) Physical size and weight;
    - (e) Quality of the sensor, such as lifetime and robustness to environment changes, and;
    - (f) Cost.
  3. *Select actuators.* The actuators must be capable of driving the system so as to meet the required performance specifications. The selection is governed by the same factors that apply to sensor selection.
  4. *Make a linear model.* All our design methods are based on linear models. Both small-signal perturbation models and feedback-linearization methods can be used.
  5. *Try a simple PID controller.* An effort to meet the specifications with a PID or its cousin, the lead-lag compensator, may succeed; in any case such an effort will expose the nature of the control problem.
  6. *Evaluate/modify plant.* Evaluate whether plant modifications enhance closed-loop performance; if so, return to Step 1 or 4.
  7. *Try an optimal design.* The SRL method for control-law selection and estimator design based on state equations is guaranteed to produce a stable control system and can be

structured to show a trade-off between error reduction and control effort. A related alternative is arbitrary pole placement, which gives the designer direct control over the dynamic response. Both the SRL and the pole-placement methods may result in designs that are not robust to parameter changes.

8. *Simulate the design, and verify its performance.* All the tools of analysis should be used here, including the root locus, the frequency response, GM and PM measurements, and transient responses. Also, the performance of the design can be tested in simulation against changes in model parameters and the effects of approximating the compensator with a discrete model if digital control is to be used.
9. *Build a prototype, and measure the performance with typical input signals.* No control design is acceptable until it has been tested. No model can include all the features of a real physical device; so the final step before fixing the design is to try it out on a physical prototype if time and budget permit.

- The satellite case study illustrated particularly the use of a notch compensation for a system with lightly damped resonance. It was also shown that collocated actuator and sensor systems are much easier to control than noncollocated systems.
- The Boeing 747 lateral-stabilization case study illustrated the use of feedback as an inner-loop designed to aid the pilot, who provides the primary outer-loop control.
- The Boeing 747 altitude control showed how to combine inner-loop feedback with outer-loop compensation to design a complete control system.
- The automobile fuel-air ratio control illustrated the use of the Bode plot to design a system that includes time delay. Simulation of the design with the nonlinear sensor verified our heuristic analysis of limit cycles using the concept of equivalent gain with a root locus.
- The drone example illustrated control design for this emerging field and the advantage of having four rotors, which allows uncoupling the control of the four degrees of freedom.
- The RTP case study illustrated modeling and control of a nonlinear thermal system.
- The *E. coli* chemotaxis case study illustrated a simple example of the application of ideas from control theory to the emerging field of systems biology.
- In all cases, the designer needs to be able to use multiple tools, including the root locus, the frequency response, pole placement by state feedback, and (nonlinear) simulation of time responses to get a good design. We promised an understanding of these tools at the beginning of the text, and we trust you are now ready to practice the art of control engineering.

## REVIEW QUESTIONS

- 10.1** Why is a collocated actuator and sensor arrangement for a lightly damped structure (such as a robot arm) easier to design than a non-collocated setup?
- 10.2** Why should the control engineer be involved in the design of the process to be controlled?
- 10.3** Give examples of an actuator and a sensor for the following control problems:
- Attitude control of a geosynchronous communication satellite.
  - Pitch control of a Boeing 747 airliner.
  - Pitch control of a quadcopter.
  - Fuel-air ratio control of a spark-ignited automobile engine.
  - Position control for an arm of a robot used to paint automobiles.
  - Heading control of a ship.
  - Attitude control of a helicopter.

## PROBLEMS

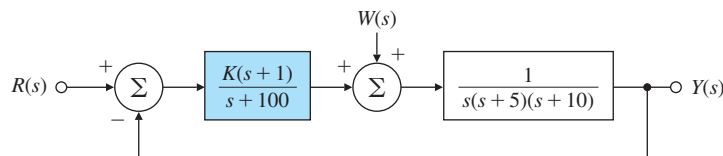
- 10.1** Of the three components of the PID controller (proportional, integral, or derivative), which one is the most effective in reducing the error resulting from a constant disturbance? Explain.
- 10.2** Is there a greater chance of instability when the sensor in a feedback control system for a mechanical structure is not collocated with the actuator? Explain.
- 10.3** The transfer function of a magnetic levitation system can be expressed as

$$G(S) = \frac{5}{s^2}$$

- Is it possible to stabilize this system with a P-type controller? If not, why?
  - Is it possible to stabilize this system with a PD controller? Examine the disturbance rejection if stabilization is possible.
  - Design a PID controller. Compare its disturbance rejection with that of the PD controller.
- 10.4** Consider the closed-loop system shown in Fig. 10.93.
- What is the phase margin if  $K = 70,000$ ?
  - What is the gain margin if  $K = 70,000$ ?
  - What value of  $K$  will yield a phase margin of  $\sim 70^\circ$ ?
  - What value of  $K$  will yield a phase margin of  $\sim 0^\circ$ ?
  - Sketch the root locus with respect to  $K$  for the system, and determine what value of  $K$  causes the system to be on the verge of instability.

**Figure 10.93**

Control system for  
Problem 10.4



- (f) If the disturbance  $w$  is a constant and  $K = 10,000$ , what is the maximum allowable value for  $w$  if  $y(\infty)$  is to remain less than 0.1? (Assume  $r = 0$ .)

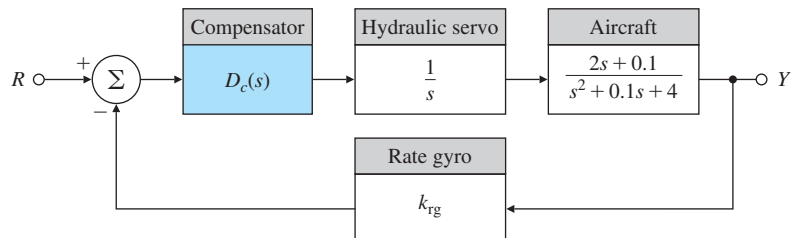
- (g) Suppose the specifications require you to allow larger values of  $w$  than the value you obtained in part (f), but with the same error constraint  $[|y(\infty)| < 0.1]$ . Discuss what steps you could take to alleviate the problem.

- 10.5** Consider the system shown in Fig. 10.94, which represents the attitude rate control for a certain aircraft.

- (a) Design a compensator so that the dominant poles are at  $-2 \pm 2j$ .  
 (b) Sketch the Bode plot for your design, and select the compensation so the crossover frequency is at least  $2\sqrt{2}$  rad/sec and  $PM \geq 50^\circ$ .  
 (c) Sketch the root locus for your design, and find the velocity constant when  $\omega_n > 2\sqrt{2}$  and  $\zeta \geq 0.5$ .

**Figure 10.94**

Block diagram for  
aircraft-attitude rate  
control

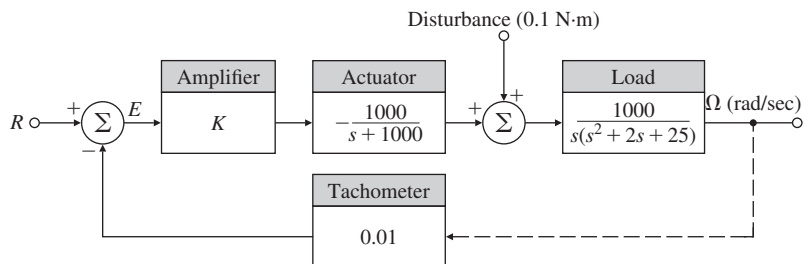


- 10.6** Consider the block diagram for the servomechanism drawn in Fig. 10.95. Which of the following claims are true?

- (a) The actuator dynamics (the pole at 1000 rad/sec) must be included in an analysis to evaluate a usable maximum gain for which the control system is stable.  
 (b) The gain  $K$  must be negative for the system to be stable.  
 (c) There exists a value of  $K$  for which the control system will oscillate at a frequency between 4 and 6 rad/sec.  
 (d) The system is unstable if  $|K| > 10$ .  
 (e) If  $K$  must be negative for stability, the control system cannot counteract a positive disturbance.  
 (f) A positive constant disturbance will speed up the load, thereby making the final value of  $e$  negative.  
 (g) With only a positive constant command input  $r$ , the error signal  $e$  must have a final value greater than zero.

**Figure 10.95**

Servomechanism for Problem 10.6



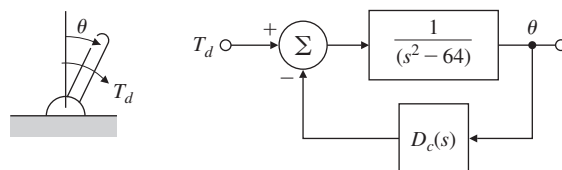
- (h) For  $K = -1$  the closed-loop system is stable, and the disturbance results in a speed error whose steady-state magnitude is less than 5 rad/sec.

- 10.7** A stick balancer and its corresponding control block diagram are shown in Fig. 10.96. The control is a torque applied about the pivot.

- (a) Using root-locus techniques, design a compensator  $D_c(s)$  that will place the dominant roots at  $s = -5 \pm 5j$  (corresponding to  $\omega_n = 7$  rad/sec,  $\zeta = 0.707$ ).
- (b) Use Bode plotting techniques to design a compensator  $D_c(s)$  to meet the following specifications:
- Steady-state  $\theta$  displacement of less than 0.001 for a constant input torque  $T_d = 1$ ,
  - Phase margin  $\geq 50^\circ$ , and
  - Closed-loop bandwidth  $\cong 7$  rad/sec.

**Figure 10.96**

Stick balancer for Problem 10.7



- 10.8** Consider the standard feedback system drawn in Fig. 10.97.

- (a) Suppose

$$G(s) = \frac{2500K}{s(s+25)}.$$

Design a lead compensator so the phase margin of the system is more than  $45^\circ$ ; the steady-state error due to a ramp should be less than or equal to 0.01.

- (b) Using the plant transfer function from part (a), design a lead compensator so the overshoot is less than 25% and the 1% settling time is less than 0.1 sec.

- (c) Suppose

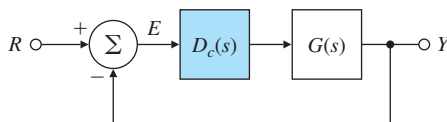
$$G(s) = \frac{K}{s(1+0.1s)(1+0.2s)},$$

and let the performance specifications now be  $K_v = 100$  and  $\text{PM} \geq 40^\circ$ . Is the lead compensation effective for this system? Find a lag compensator, and plot the root locus of the compensated system.

- (d) Using  $G(s)$  from part (c), design a lag compensator such that the peak overshoot is less than 20% and  $K_v = 100$ .
- (e) Repeat part (c) using a lead–lag compensator.
- (f) Find the root locus of the compensated system in part (e), and compare your findings with those from part (c).

**Figure 10.97**

Block diagram of a standard feedback control system



- 10.9** Consider the system in Fig. 10.97, where

$$G(s) = \frac{300}{s(s + 0.225)(s + 4)(s + 180)}.$$

The compensator  $D_c(s)$  is to be designed so the closed-loop system satisfies the following specifications:

- Zero steady-state error for step inputs,
- $\text{PM} = 55^\circ$ ,  $\text{GM} \geq 6 \text{ db}$ ,
- Gain crossover frequency is not smaller than that of the uncompensated plant.

- (a) What kind of compensation should be used and why?
- (b) Design a suitable compensator  $D_c(s)$  to meet the specifications.

- 10.10** We have discussed three design methods: the root-locus method of Evans, the frequency-response method of Bode, and the state-variable pole-assignment method. Explain which of these methods is *best* described by the following statements (if you feel more than one method fits a given statement equally well, explain why):

- (a) This method is the one most commonly used when the plant description must be obtained from experimental data.
- (b) This method provides the most direct control over dynamic response characteristics such as rise time, percent overshoot, and settling time.
- (c) This method lends itself most easily to an automated (computer) implementation.
- (d) This method provides the most direct control over the steady-state error constants  $K_p$  and  $K_v$ .
- (e) This method is most likely to lead to the *least complex* controller capable of meeting the dynamic and static accuracy specifications.
- (f) This method allows the designer to guarantee that the final design will be unconditionally stable.
- (g) This method can be used without modification for plants that include transportation lag terms—for example,

$$G(s) = \frac{e^{-2s}}{(s + 3)^2}.$$

- 10.11** Lead and lag networks are typically employed in designs based on frequency-response (Bode) methods. Assuming a Type 1 system, indicate the effect of these compensation networks on each of the listed performance specifications. In each case, indicate the effect as “an increase,” “substantially unchanged,” or “a decrease.” Use the second-order plant  $G(s) = K/[s(s + 1)]$  to illustrate your conclusions.

- (a)  $K_v$ ,
- (b) Phase margin,
- (c) Closed-loop bandwidth,
- (d) Percent overshoot, and
- (e) Settling time.

- 10.12** *Altitude Control of a Hot-Air Balloon:* American solo balloonist Steve Fossett landed in the Australian outback aboard *Spirit of Freedom* on July 3rd, 2002, becoming the first solo balloonist to circumnavigate the globe (see Fig. 10.98). The equations of vertical motion for a hot-air balloon (see Fig. 10.99), linearized about vertical equilibrium, are

$$\begin{aligned}\delta \dot{T} + \frac{1}{\tau_1} \delta T &= \delta q, \\ \tau_2 \ddot{z} + \dot{z} &= -a \delta T + w,\end{aligned}$$

**Figure 10.98**

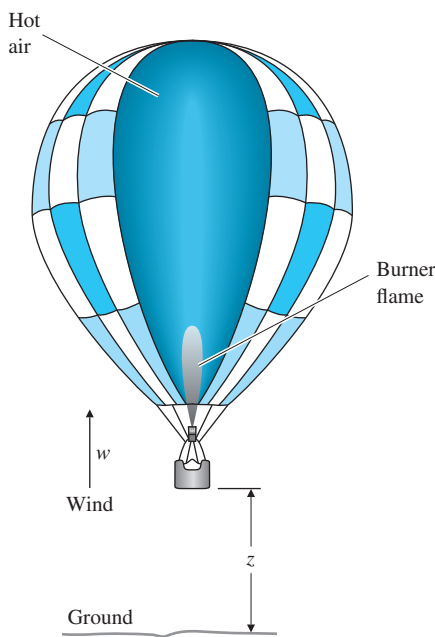
Spirit of Freedom  
balloon

Source: Pool/Getty Images  
News/Getty Images



**Figure 10.99**

Hot-air balloon



where

$\delta T$  = deviation of the hot-air temperature from the equilibrium temperature where buoyant force equals weight,

$z$  = altitude of the balloon,

$\delta q$  = deviation in the burner heating rate from the equilibrium rate (normalized by the thermal capacity of the hot air),

$w$  = vertical component of wind velocity,

$\tau_1, \tau_2, a$  = parameters of the equations.

An altitude-hold autopilot is to be designed for a balloon whose parameters are

$$\tau_1 = 250 \text{ sec} \quad \tau_2 = 25 \text{ sec} \quad a = 0.3 \text{ m}/(\text{sec} \cdot ^\circ\text{C}).$$

Only altitude is sensed, so a control law of the form

$$\delta q(s) = D_c(s)[z_d(s) - z(s)],$$

will be used, where  $z_d$  is the desired (commanded) altitude.

(a) Sketch a root locus of the closed-loop eigenvalues with respect to the gain  $K$  for a proportional feedback controller,  $\delta q = -K(z - z_d)$ .

Use Routh's criterion (or let  $s = j\omega$  and find the roots of the characteristic polynomial) to determine the value of the gain and the associated frequency at which the system is marginally stable.

(b) Our intuition and the results of part (a) indicate that a relatively large amount of lead compensation is required to produce a satisfactory autopilot. Because Steve Fossett was a millionaire, he could afford a more complex controller implementation. Sketch a root

locus of the closed-loop eigenvalues with respect to the gain  $K$  for a double-lead compensator,  $\delta q = D_c(s)(z_d - z)$ , where

$$D_c(s) = K \left( \frac{s + 0.03}{s + 0.12} \right)^2.$$

- (c) Sketch the magnitude portions of the Bode plots (straight-line asymptotes only) for the open-loop transfer functions of the proportional feedback and lead-compensated systems.
  - (d) Select a gain  $K$  for the lead-compensated system to give a crossover frequency of 0.06 rad/sec.
  - (e) Select a gain  $K$  for the lead-compensated system to give a crossover frequency of 0.06 rad/sec.
  - (f) If the error in part (e) is too large, how would you modify the compensation to give higher low-frequency gain? (Give a qualitative answer only.)
- 10.13** Satellite-attitude control systems often use a reaction wheel to provide angular motion. The equations of motion for such a system are

$$\text{Satellite : } I\ddot{\phi} = T_c + T_{ex},$$

$$\text{Wheel : } J\dot{r} = -T_c,$$

$$\text{Measurement : } \dot{Z} = \dot{\phi} - aZ,$$

$$\text{Control : } T_c = -D_c(s)(Z - Z_d),$$

where

$J$  = moment of inertia of the wheel,

$r$  = wheel speed,

$T_c$  = control torque,

$T_{ex}$  = disturbance torque,

$\phi$  = angle to be controlled,

$Z$  = measurement from the sensor,

$Z_d$  = reference angle,

$I$  = satellite inertia ( $1000 \text{ kg/m}^2$ ),

$a$  = sensor constant (1 rad/sec),

$D_c(s)$  = compensation.

- (a) Suppose  $D_c(s) = K_0$ , a constant. Draw the root locus with respect to  $K_0$  for the resulting closed-loop system.
- (b) For what range of  $K_0$  is the closed-loop system stable?
- (c) Add a lead network with a pole at  $s = -1$  so the closed-loop system has a bandwidth  $\omega_{BW} = 0.04 \text{ rad/sec}$ , a damping ratio  $\zeta = 0.5$ , and compensation given by

$$D_c(s) = K_1 \frac{s + z}{s + 1}.$$

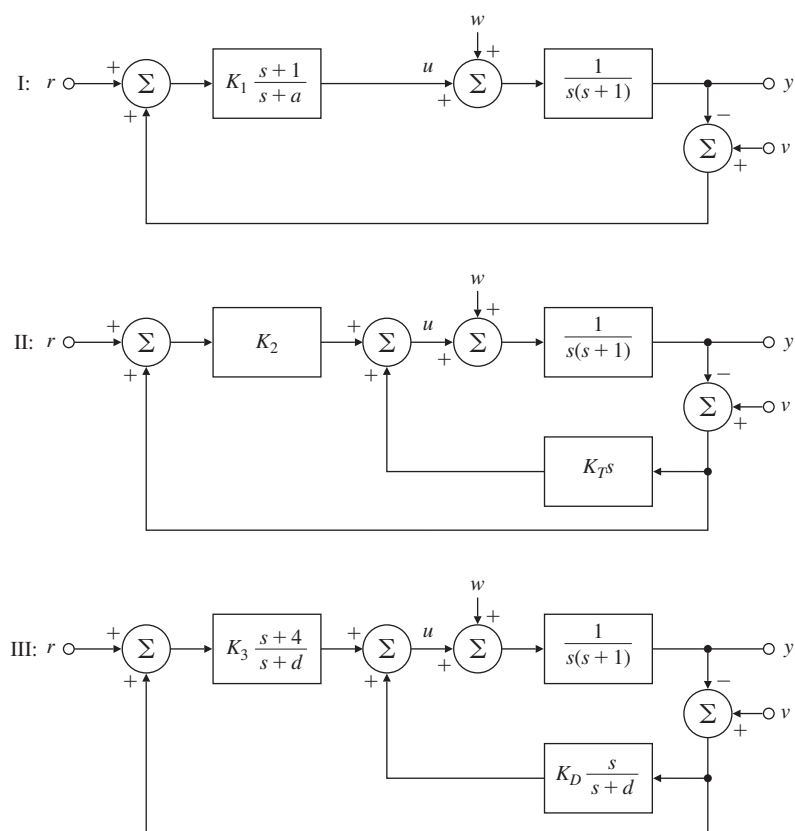
Where should the zero of the lead network be located? Draw the root locus of the compensated system, and give the value of  $K_1$  that allows the specifications to be met.

- (d) For what range of  $K_1$  is the system stable?
- (e) What is the steady-state error (the difference between  $Z$  and some reference input  $Z_d$  to a constant disturbance torque  $T_{ex}$  for the design of part (c)?)
- (f) What is the type of this system with respect to rejection of  $T_{ex}$ ?
- (g) Draw the Bode plot asymptotes of the *open-loop* system, with the gain adjusted for the value of  $K_1$  computed in part (c). Add the compensation of part (c), and compute the phase margin of the closed-loop system. What is the type of this system with respect to rejection of  $T_{ex}$ ?
- (h) Write state equations for the open-loop system, using the state variables  $\phi$ ,  $\dot{\phi}$ , and  $Z$ . Select the gains of a state-feedback controller  $T_c = -K_\phi\phi - K_{\dot{\phi}}\dot{\phi}$  to locate the closed-loop poles at  $s = -0.02 \pm 0.02\sqrt{3}j$ .

- 10.14** Three alternative designs are sketched in Fig. 10.100 for the closed-loop control of a system with the plant transfer function  $G(s) = 1/s(s+1)$ . The signal  $w$  is the plant noise and may be analyzed as if it were a step;

**Figure 10.100**

Alternative feedback structures for Problem 10.14



the signal  $v$  is the sensor noise and may be analyzed as if it contained power to very high frequencies.

- (a) Compute values for the parameters  $K_1$ ,  $a$ ,  $K_2$ ,  $K_T$ ,  $K_3$ ,  $d$ , and  $K_D$  so in each case (assuming  $w = 0$  and  $v = 0$ ),

$$\frac{Y}{R} = \frac{16}{s^2 + 4s + 16}.$$

Note in system III, a pole is to be placed at  $s = -4$ .

- (b) Complete the following table, expressing the last entries as  $A/s^k$  to show how fast noise from  $v$  is attenuated at high frequencies:

System	$K_V$	$\left. \frac{y}{w} \right _{s=0}$	$\left. \frac{y}{v} \right _{s \rightarrow \infty}$
I			
II			
III			

- (c) Rank the three designs according to the following characteristics (the best as “1,” the poorest as “3”):

Performance	I	II	III
Tracking			
Plant-noise rejection			
Sensor-noise rejection			

- 10.15** The equations of motion for a cart–stick balancer with state variables of stick angle, stick angular velocity, and cart velocity are

$$\dot{\mathbf{x}} = \begin{bmatrix} 0 & 1 & 0 \\ 31.33 & 0 & 0.016 \\ -31.33 & 0 & -0.216 \end{bmatrix} \mathbf{x} + \begin{bmatrix} 0 \\ -0.649 \\ 8.649 \end{bmatrix} u,$$

$$y = [10 \ 0 \ 0] \mathbf{x},$$

where the output is stick angle, and the control input is voltage on the motor that drives the cart wheels.

- (a) Compute the transfer function from  $u$  to  $y$ , and determine the poles and zeros.  
 (b) Determine the feedback gain  $\mathbf{K}$  necessary to move the poles of the system to the locations  $-2.832$  and  $-0.521 \pm 1.068j$ , with  $\omega_n = 4$  rad/sec.  
 (c) Determine the estimator gain  $\mathbf{L}$  needed to place the three estimator poles at  $-10$ .  
 (d) Determine the transfer function of the estimated-state-feedback compensator defined by the gains computed in parts (b) and (c).  
 (e) Suppose we use a reduced-order estimator with poles at  $-10$  and  $-10$ . What is the required estimator gain?  
 (f) Repeat part (d) using the reduced-order estimator.  
 (g) Compute the frequency response of the two compensators.

- 10.16** A 282-ton Boeing 747 is approaching land at sea level. If we use the state given in the case study (see Section 10.3) and assume a velocity of 221 ft/sec (Mach 0.198), then the lateral-direction perturbation equations are

$$\begin{bmatrix} \dot{\beta} \\ \dot{r} \\ \dot{p} \\ \dot{\phi} \end{bmatrix} = \begin{bmatrix} -0.0890 & -0.989 & 0.1478 & 0.1441 \\ 0.168 & -0.217 & -0.166 & 0 \\ -1.33 & 0.327 & -0.975 & 0 \\ 0 & 0.149 & 1 & 0 \end{bmatrix} \begin{bmatrix} \beta \\ r \\ p \\ \phi \end{bmatrix} + \begin{bmatrix} 0.0148 \\ -0.151 \\ 0.0636 \\ 0 \end{bmatrix} \delta r,$$

$$y = [0 \ 1 \ 0 \ 0] \begin{bmatrix} \beta \\ r \\ p \\ \phi \end{bmatrix}.$$

The corresponding transfer function is

$$G(s) = \frac{r(s)}{\delta r(s)} = \frac{-0.151(s+1.05)(s+0.0328 \pm 0.414j)}{(s+1.109)(s+0.0425)(s+0.0646 \pm 0.731j)}.$$

- (a) Draw the uncompensated root locus [for  $1 + KG(s)$ ] and the frequency response of the system. What type of classical controller could be used for this system?  
 (b) Try a state-variable design approach by drawing a SRL for the system. Choose the closed-loop poles of the system on the SRL to be

$$\alpha_c(s) = (s+1.12)(s+0.165)(s+0.162 \pm 0.681j),$$

and choose the estimator poles to be five times faster at

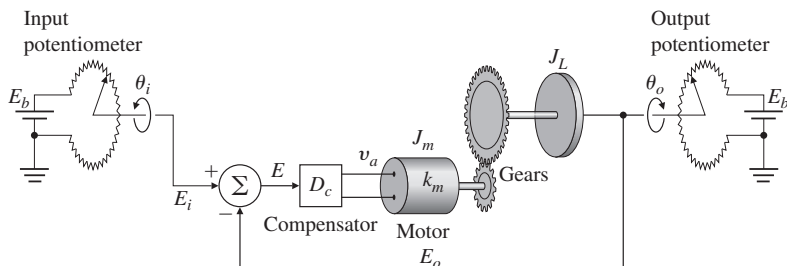
$$\alpha_e(s) = (s+5.58)(s+0.825)(s+0.812 \pm 3.40j).$$

- (c) Compute the transfer function of the SRL compensator.  
 (d) Discuss the robustness properties of the system with respect to parameter variations and unmodeled dynamics.  
 (e) Note the similarity of this design to the one developed for different flight conditions earlier in the chapter. What does this suggest about providing a continuous (nonlinear) control throughout the operating envelope?

- 10.17** (Contributed by Prof. L. Swindlehurst) The feedback control system shown in Fig. 10.101 is proposed as a position-control system. A key component of this system is an armature-controlled DC motor. The input potentiometer produces a voltage  $E_i$  that is proportional to the desired shaft position:  $E_i = K_p\theta_i$ . Similarly, the output potentiometer produces a voltage  $E_0$  that is proportional to the actual shaft position:  $E_0 = K_p\theta_0$ . Note we have assumed both potentiometers have the same proportionality constant. The error signal  $E_i - E_0$  drives a compensator, which in turn produces an armature voltage that drives the motor. The motor has an armature resistance  $R_a$ , an armature inductance  $L_a$ , a torque constant  $K_t$ , and a back emf constant  $K_e$ . The moment of inertia of the motor shaft is  $J_m$ , and the rotational damping due to bearing friction is  $B_m$ . Finally, the gear ratio is  $N : 1$ , the moment of inertia of the load is  $J_L$ , and the load damping is  $B_L$ .

**Figure 10.101**

A servomechanism with gears on the motor shaft and potentiometer sensors



$$\begin{aligned}
 E_i &= \text{voltage from input potentiometer} \\
 &= K_p \theta_i \\
 E_o &= \text{voltage from output potentiometer} \\
 &= K_p \theta_o \\
 E &= E_i - E_o = \text{error voltage} = K_p(\theta_i - \theta_o) \\
 v_a &= \text{armature voltage applied to motor} \\
 E_b &= \text{battery voltage applied to potentiometers}
 \end{aligned}$$

- (a) Write the differential equations that describe the operation of this feedback system.
- (b) Find the transfer function relating  $\theta_0$  and  $\theta_i(s)$  for a general compensator  $D_c(s)$ .
- (c) The open-loop frequency-response data shown in Table 10.1 were taken using the armature voltage  $v_a$  of the motor as an input and the output potentiometer voltage  $E_0$  as the output. Assuming the motor is linear and minimum-phase, make an estimate of the transfer function of the motor,

$$G(s) = \frac{\Theta_m(s)}{V_a(s)},$$

where  $\theta_m$  is the angular position of the motor shaft.

**TABLE 10.1****Frequency-Response Data for Problem 10.17**

Frequency (rad/sec)	$\left  \frac{E_0(s)}{V_a(s)} \right $ (db)	Frequency (rad/sec)	$\left  \frac{E_0(s)}{V_a(s)} \right $ (db)
0.1	60.0	10.0	14.0
0.2	54.0	20.0	2.0
0.3	50.0	40.0	-10.0
0.5	46.0	60.0	-20.0
0.8	42.0	65.0	-21.0
1.0	40.0	80.0	-24.0
2.0	34.0	100.0	-30.0
3.0	30.5	200.0	-48.0
4.0	27.0	300.0	-59.0
5.0	23.0	500.0	-72.0
7.0	19.5		

- (d) Determine a set of performance specifications that are appropriate for a position control system and will yield good performance. Design  $D_c(s)$  to meet these specifications.

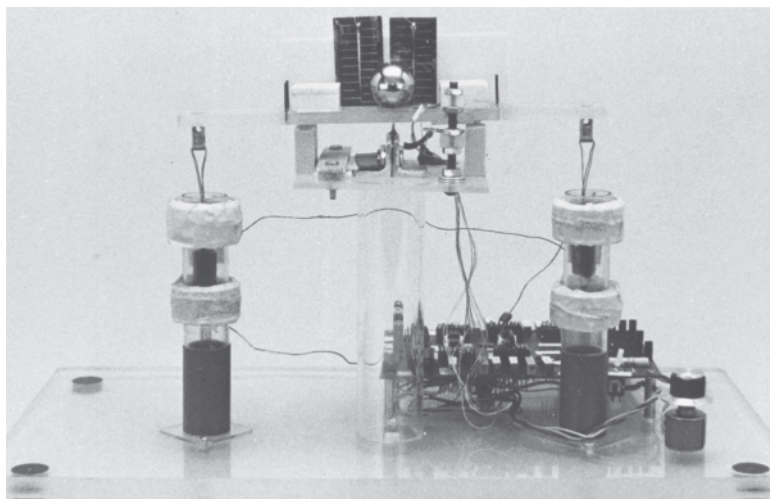
- (e) Verify your design through analysis and simulation using Matlab.

- 10.18** Design and construct a device to keep a ball centered on a freely swinging beam. An example of such a device is shown in Fig. 10.102. It uses coils surrounding permanent magnets as the actuator to move the beam, solar cells to sense the ball position, and a hall-effect device to sense the beam position. Research other possible actuators and sensors as part of your design effort. Compare the quality of the control achievable for ball-position feedback only with that of multiple-loop feedback of both ball and beam position.

**Figure 10.102**

Ball-balancer design example

Source: Photo courtesy of David Powell



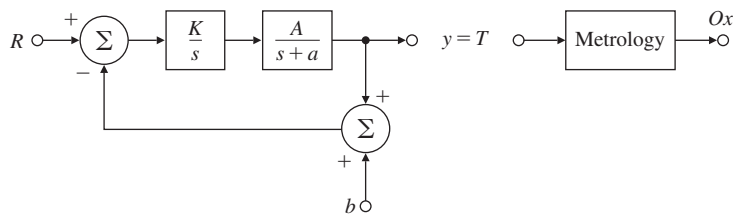
- 10.19** Design and construct the magnetic levitation device shown in Fig. 9.1. You may wish to use LEGO components in your design.

- 10.20** Design and build a Sun tracker using an Arduino board and related software.

- 10.21** *Run-to-Run Control:* Consider the RTP system shown in Fig. 10.103. We wish to heat up a semiconductor wafer, and control the wafer surface temperature accurately using rings of tungsten halogen lamps. The output of the system is temperature  $T$  as a function of time:  $y = T(t)$ . The system reference input  $R$  is a desired step in temperature ( $700^\circ \text{C}$ ), and the control input is lamp power. A pyrometer is used to measure the wafer center temperature. The model of the system is first order, and an integral controller is used as shown in Fig. 10.103. Normally, there is no sensor bias ( $b = 0$ ).

- (a) Suppose the system suddenly develops a sensor bias  $b \neq 0$ , where  $b$  is known. What can be done to ensure zero steady-state tracking of temperature command  $R$ , despite the presence of the sensor bias?

**Figure 10.103**  
RTP system



- (b) Now assume  $b = 0$ . In reality, we are trying to control the thickness of the oxide film grown ( $Ox$ ) on the wafer and not the temperature. At present, no sensor can measure  $Ox$  in real time. The semiconductor process engineer must use off-line equipment (called *metrology*) to measure the thickness of the oxide film grown on the wafer. The relationship between the system output temperature and  $Ox$  is nonlinear and given by the integral of the Arrhenius equation:

$$\text{Oxide thickness} = \int_0^{t_f} p e^{-\frac{c}{T(t)}} dt,$$

where  $t_f$  is the process duration, and  $p$  and  $c$  are known constants. Suggest a scheme in which the center wafer oxide thickness  $Ox$  can be controlled to a desired value (say,  $Ox = 5000 \text{ \AA}$ ) by employing the temperature controller and the output of the metrology.

- 10.22** Develop a nonlinear model for a tungsten halogen lamp and simulate it in Simulink.  
**10.23** Develop a nonlinear model for a pyrometer. Show how temperature can be deduced from the model.  
**10.24** Repeat the RTP case study design by summing the three sensors to form a single signal to control the average temperature. Demonstrate the performance of the linear design, and validate the performance on the nonlinear Simulink simulation.  
**10.25** One of the steps in semiconductor wafer manufacturing during photolithography is performed by placement of the wafer on a heated plate for a certain period of time. Laboratory experiments have shown that the transfer function from the heater power,  $u$ , to the wafer temperature,  $y$ , can be given by

$$\frac{Y(s)}{U(s)} = G(s) = \frac{0.09}{(s + 0.19)(s + 0.78)(s + 0.00018)}.$$

- (a) Sketch the  $180^\circ$  root locus for the uncompensated system.  
(b) Using the root-locus design techniques, design a *dynamic* compensator,  $D_C(s)$ , such that the system meets the following time-domain specifications
- i.  $M_p \leq 5\%$ ,
  - ii.  $t_r \leq 20 \text{ sec}$ ,
  - iii.  $t_s \leq 60 \text{ sec}$ ,
  - iv. Steady-state error to a  $1^\circ\text{C}$  step input command  $< 0.1^\circ\text{C}$ .

Draw the  $180^\circ$  root locus for the compensated system.

- 10.26** *Excitation-Inhibition Model from Systems Biology* (Yang and Iglesias, 2005): In *Dictyostelium* cells, the activation of key signaling molecules involved in chemoattractant sensing can be modeled by the following third-order linearized model. The external disturbance to the output transfer function is:

$$\frac{Y(s)}{W(s)} = \mathcal{S}(s) = \frac{(1-\alpha)s}{(s+\alpha)(s+1)(s+\gamma)},$$

where,  $w$  is the external disturbance signal proportional to chemoattractant concentration, and  $y$  is the output which is the fraction of active response regulators. Show there is an alternate representation of the system with the “plant” transfer function

$$G(s) = \frac{(1-\alpha)}{s^2 + (1+\alpha+\gamma)s + (\alpha+\gamma+\alpha\gamma)},$$

and the “feedback regulator”

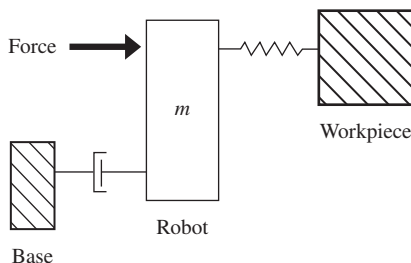
$$D_c(s) = \frac{\alpha\gamma}{(1-\alpha)s}.$$

It is known  $\alpha \neq 1$  for this version of the model. Draw the feedback block diagram of the system showing the locations of the disturbance input and the output. What is the significance of this particular representation of the system? What hidden system property does it reveal? Is the disturbance rejection a robust property for this system? Assume the system parameter values are  $\alpha = 0.5$  and  $\gamma = 0.2$ , then plot the disturbance rejection response of the system for a unit step disturbance input.

- 10.27** When a powerful industrial robot is used for delicate tasks such as polishing glass, it needs to be able to precisely control the force applied to the workpiece (see Figure 10.104). One way to approximately measure the applied force is to measure the deflection of a stiff spring on the robot’s end-effector. The robot-workpiece interaction can be modeled as shown in Fig. 10.104, where it is assumed the workpiece and the base are both fixed in place, and only the robot moves:

**Figure 10.104**

Robot system for Problem 10.27



Assume the robot’s mass is  $m = 8\text{kg}$ , the damping friction in the robot is  $b = 150 \text{ Nsec/m}$ , and the spring constant for the force sensor is  $k = 8000 \text{ N/m}$ . The robot’s motor dynamics (the transfer function from control command to applied force) can be modeled as a first-order system with

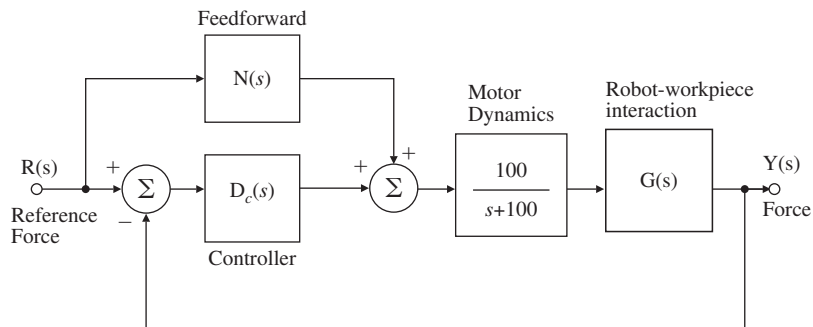
a pole at -100. Hence the plant transfer function relating the applied force to the robot-workpiece interaction force is:

$$G(s) = \frac{k}{ms^2 + bs + k}.$$

A closed-loop system is to be designed to control the robot-workpiece interaction force, as shown in Figure 10.105:

**Figure 10.105**

Feedback control system for Problem 10.27



(a) Sketch the open-loop step response for the combined actuator/robot system (without feedback control).

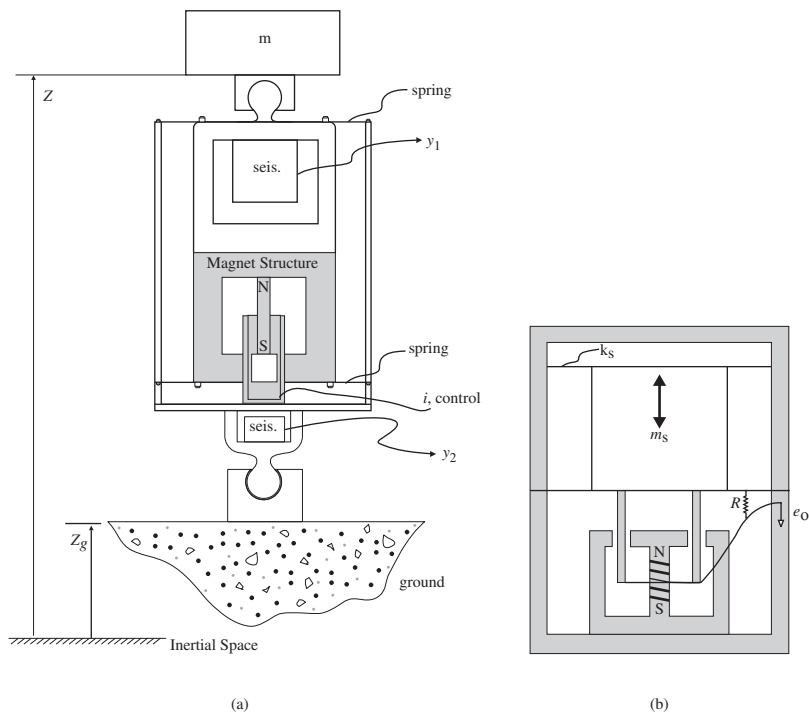
(b) Let  $N(s) = 0$ . Sketch the root locus for the combined actuator/robot system assuming  $D_c(s) = K$ . Discuss the usefulness of a proportional control for decreasing the settling time. Discuss the effect of actuator dynamics on closed-loop stability with proportional control.

(c) Now let  $N(s) = N = \text{constant}$ . Derive the closed-loop transfer function for a generic controller  $D_c(s)$ . Using your derivation, explain why this feedback control structure employing the feedforward term  $N(s)$ , with the reference force entering the dynamics in two places, may be preferable to the standard feedback only structure for this problem. For which value of  $N$  is the system able to track a step reference input with zero steady-state error?

- 10.28** A vibration isolation strut uses a voice coil actuator. It is in parallel with a spring that has a natural frequency with the load of 10 Hz. A seismometer has been chosen for the feedback and one for feedforward. Each seismometer proof mass is supported on a spring which produces a natural frequency of the instrument of 4 Hz and a shunt resistor provides eddy current damping to give a damping factor  $\zeta=1$ . See Figures 10.106(a) and (b).
- (a) Include this instrument dynamics in the sensing (feedback) loop and modify the compensation to provide a factor of 30 attenuation of ground motion at 10 Hz.

**Figure 10.106**

- (a) Strut schematic to isolate mass  $m$  from ground motion  $Z_g$ , (b) Schematic of seismometer



**(b)** Assuming you can match scale factors and model parameters to 5%, how much improvement could you make to the feedback attenuation by using feedforward from a second seismometer mounted on the ground?

**(c)** How would you handle the instrument dynamics if you want to feedforward ground motion at low frequencies ( $\omega < 10$  Hz)?

**10.29** Suppose the load in Problem 10.28 is now elastic. Model the isolated mass as having two parts separated by a spring stiffness such that the free vibration frequency is 50 Hz as shown in Figure 10.107.

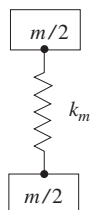
**(a)** How would you alter your feedback control law from Problem 10.28?

**(b)** What effect would this have on your feedforward implementation?

**(c)** Would you need another sensor to control  $Z_2$ , the position of the upper half of the isolated mass? What would you measure? How would you put it into the feedback control law?

**Figure 10.107**

- Schematic of elastic load for Problem 10.29



- 10.30** The six transfer functions for the Mikrokopter quadrotor (Bergamasco and Lovera, 2014) identified from flight experiments are:

$$G_h = \frac{a_z}{f_h} = \frac{1.2498(s + 0.3451)}{(s + 16.49)(s + 5.309)(s + 1.933)},$$

$$G_\psi = \frac{r}{u_\psi} = \frac{0.077646(s + 5.475)(s - 0.2086)}{(s + 11.03)(s^2 + 0.2838s + 0.06947)},$$

$$G_{\theta 1} = \frac{q}{u_\theta} = \frac{0.22016(s + 0.2579)(s - 0.2596)}{(s + 1.865)(s^2 - 1.285s + 8.067)},$$

$$G_{\theta 2} = \frac{a_x}{u_\theta} = \frac{-0.011659(s - 3.271)(s + 3.681)}{(s + 1.865)(s^2 - 1.285s + 8.067)},$$

$$G_{\varphi 1} = \frac{p}{u_\varphi} = \frac{-0.20194(s^2 + 0.09235s + 0.2532)}{(s + 1.82)(s^2 - 1.388s + 10.02)},$$

$$G_{\varphi 2} = \frac{a_y}{u_\varphi} = \frac{-0.00359(s - 9.182)(s + 4.164)}{(s + 1.82)(s^2 - 1.388s + 10.02)}.$$

where  $\varphi$  is roll angle,  $\theta$  is pitch angle,  $\psi$  is yaw angle and  $p = \dot{\phi}$  = roll rate,  $q = \dot{\theta}$  = pitch rate,  $r = \dot{\psi}$  = yaw rate as discussed in Chapter 2.  $a_x$ ,  $a_y$ , and  $a_z$  are the measurements of the components of the acceleration of the quadrotor along the three body axes.  $f_h$  is the control input for the vertical (up and down) motion. The outputs provided by the inertial sensors are  $a_x$ ,  $a_y$ ,  $a_z$ ,  $p$ ,  $q$ , and  $r$ .

- (a) Find the order of the system and the number of transmission zeros at infinity for each of the six transfer functions.
- (b) Find the DC gain for each of the six transfer functions.
- (c) Use Matlab to plot the unit impulse and step responses for each of the six transfer functions. Is there anything peculiar about the yaw step response?
- (d) Classify each of the six transfer functions with regard to stability, minimum-phase or non-minimum phase system.

- 10.31** For the quadrotor Problem 10.30,

- (a) Find a second-order transfer function approximation for the third-order transfer function from  $f_h$  to  $a_z$ .
- (b) Find a second-order transfer function approximation for the third-order transfer function from  $u_\psi$  to  $r$ .

For each part, compare step responses (using Matlab) to demonstrate how good your approximation is as compared to the original transfer function.

- 10.32** For the quadrotor Problem 10.30, design a dynamic controller (PI or PID) for the transfer function from  $f_h$  to  $a_z$  so the rise time ( $t_r$ ) is one sec or less and there is zero steady-state error to a step reference input. Use Matlab to show the resulting closed-loop step response

for your design, and demonstrate that the design specifications have been met.

- 10.33** For the quadrotor Problem 10.30, draw the  $180^\circ$  root locus for the six transfer functions for this system using Matlab. In each case, specify the range of the root locus gain,  $K$ , for which the closed-loop system is stable.
- 10.34** For the quadrotor Problem 10.30, using root locus techniques, design a dynamic controller for the transfer function from  $f_h$  to  $a_z$  so the rise time ( $t_r$ ) is one sec or less and there is zero steady-state error to a step reference input. Use Matlab to show the resulting closed-loop step response for your design. Demonstrate that the design specifications have been met.
- 10.35** For the quadrotor Problem 10.30, draw the Bode plot for the transfer function from  $f_h$  to  $a_z$ . Adjust the transfer function gain so the low-frequency gain is unity (0-db) prior to plotting the Bode frequency response.
- 10.36** For the quadrotor Problem 10.30, draw the Nyquist plots for the six transfer functions for this system using Matlab. In each case, specify the range of the gain,  $K$  (both positive and negative), for which the closed-loop system is stable.
- 10.37** For the quadrotor Problem 10.30, draw the Bode plot for the transfer function from  $f_h$  to  $a_z$ . Adjust the transfer function gain so the low-frequency gain is unity (0-db) prior to plotting the Bode frequency response. Compute the values of the PM and GM from the Bode plot, and the corresponding Nyquist plot. How do the values from Bode and Nyquist compare?

# Appendix A Laplace Transforms

## A.1 The $\mathcal{L}_-$ Laplace Transform

Laplace transforms can be used to study the complete response characteristics of feedback systems, including the transient response. This is in contrast to Fourier transforms, in which the steady-state response is the main concern. In many applications, it is useful to define the Laplace transform of  $f(t)$ , denoted by  $\mathcal{L}_-\{f(t)\} = F(s)$ , as a function of the complex variable  $s = \sigma_1 + j\omega$ , where

$$F(s) \triangleq \int_{0^-}^{\infty} f(t)e^{-st} dt, \quad (\text{A.1})$$

which uses  $0^-$  (that is, a value just before  $t = 0$ ) as the lower limit of integration and is referred to as the **unilateral** (or **one-sided**) **Laplace transform**.<sup>1</sup> A function  $f(t)$  will have a Laplace transform if it is of **exponential order**, which means that there exists a real number  $\sigma_1$  such that

$$\lim_{t \rightarrow \infty} |f(t)e^{-\sigma_1 t}| = 0. \quad (\text{A.2})$$

The decaying exponential term in the integrand in effect provides a built-in convergence factor. This means even if  $f(t)$  does not vanish as  $t \rightarrow \infty$ , the integrand will vanish for sufficiently large values of  $\sigma_1$  if  $f$  does not grow at a faster-than-exponential rate. For example,  $ae^{bt}$  is of exponential order, whereas  $e^{t^2}$  is not. If  $F(s)$  exists for some  $s_0 = \sigma_0 + j\omega_0$ , then it exists for all values of  $s$  such that

$$\operatorname{Re}(s) \geq \sigma_0. \quad (\text{A.3})$$

The smallest value of  $\sigma_0$  for which  $F(s)$  exists is called the **abscissa of convergence**, and the region to the right of  $\operatorname{Re}(s) \geq \sigma_0$  is called the **region of convergence**. Typically, two-sided Laplace transforms exist for a specified range

$$\alpha < \operatorname{Re}(s) < \beta, \quad (\text{A.4})$$

which defines the strip of convergence. Table A.2 gives some Laplace transform pairs. Each entry in the table follows from direct application of the transform definition.<sup>2</sup>

<sup>1</sup> **Bilateral** (or **two-sided**) **Laplace transforms** and the so-called  $\mathcal{L}_+$  transforms, in which the lower value of integral is  $0^+$ , also arise elsewhere.

<sup>2</sup> As for the one-sided Laplace transform, an astute reader would wonder what happens to the validity of the Laplace transform for the rest of the  $s$ -plane, namely, the region where  $\operatorname{Re}(s) < \sigma_0$ . Indeed it would be disappointing if  $F(s)$  was only valid for  $\operatorname{Re}(s) \geq \sigma_0$  and not elsewhere in the  $s$ -plane. Fortunately, except for some pathological cases (which do not arise in practice), one can invoke an important result from the theory of complex variables known as the **Analytic Continuation Theorem** to extend the region of the validity of  $F(s)$  to the whole  $s$ -plane excluding the locations of the poles.

## A.1.1 Properties of Laplace Transforms

In this section, we will address and prove each of the significant properties of the Laplace transform as discussed in Chapter 3 and listed in Table A.1. In addition, we will show examples how these properties can be used.

### 1. Superposition

One of the more important properties of the Laplace transform is that it is linear. We can prove this as follows:

$$\begin{aligned}\mathcal{L}\{\alpha f_1(t) + \beta f_2(t)\} &= \int_0^\infty [\alpha f_1(t) + \beta f_2(t)] e^{-st} dt \\ &= \alpha \int_0^\infty f_1(t) e^{-st} dt + \beta \int_0^\infty f_2(t) e^{-st} dt \\ &= \alpha F_1(s) + \beta F_2(s).\end{aligned}\quad (\text{A.5})$$

The scaling property is a special case of linearity; that is,

$$\mathcal{L}\{\alpha f(t)\} = \alpha F(s). \quad (\text{A.6})$$

**TABLE A.1**

Properties of Laplace Transforms

Number	Laplace Transform	Time Function	Comment
—	$F(s)$	$f(t)$	Transform pair
1	$\alpha F_1(s) + \beta F_2(s)$	$\alpha f_1(t) + \beta f_2(t)$	Superposition
2	$F(s)e^{-s\lambda}$	$f(t - \lambda)$	Time delay ( $\lambda \geq 0$ )
3	$\frac{1}{ a } F\left(\frac{s}{a}\right)$	$f(at)$	Time scaling
4	$F(s+a)$	$e^{-at}f(t)$	Shift in frequency
5	$s^m F(s) - s^{m-1}f(0)$ $-s^{m-2}\dot{f}(0) - \dots - f^{(m-1)}(0)$	$f^{(m)}(t)$	Differentiation
6	$\frac{1}{s} F(s)$	$\int_0^t f(\zeta) d\zeta$	Integration
7	$F_1(s)F_2(s)$	$f_1(t) * f_2(t)$	Convolution
8	$\lim_{s \rightarrow \infty} sF(s)$	$f(0^+)$	Initial Value Theorem
9	$\lim_{s \rightarrow 0} sF(s)$	$\lim_{t \rightarrow \infty} f(t)$	Final Value Theorem
10	$\frac{1}{2\pi j} \int_{\sigma_c-j\infty}^{\sigma_c+j\infty} F_1(\zeta)F_2(s-\zeta) d\zeta$	$f_1(t)f_2(t)$	Time product
11	$\frac{1}{2\pi} \int_{-j\infty}^{+j\infty} Y(-j\omega)U(j\omega) d\omega$	$\int_0^\infty y(t)u(t) dt$	Parseval's Theorem
12	$-\frac{d}{ds} F(s)$	$tf(t)$	Multiplication by time

**TABLE A.2****Table of Laplace Transforms**

Number	$F(s)$	$f(t), t \geq 0$
1	1	$\delta(t)$
2	$1/s$	$1(t)$
3	$1/s^2$	$t$
4	$2!/s^3$	$t^2$
5	$3!/s^4$	$t^3$
6	$m!/s^{m+1}$	$t^m$
7	$\frac{1}{s+a}$	$e^{-at}$
8	$\frac{1}{(s+a)^2}$	$te^{-at}$
9	$\frac{1}{(s+a)^3}$	$\frac{1}{2!}t^2e^{-at}$
10	$\frac{1}{(s+a)^m}$	$\frac{1}{(m-1)!}t^{m-1}e^{-at}$
11	$\frac{a}{s(s+a)}$	$1 - e^{-at}$
12	$\frac{a}{s^2(s+a)}$	$\frac{1}{a}(at - 1 + e^{-at})$
13	$\frac{b-a}{(s+a)(s+b)}$	$e^{-at} - e^{-bt}$
14	$\frac{s}{(s+a)^2}$	$(1-at)e^{-at}$
15	$\frac{a^2}{s(s+a)^2}$	$1 - e^{-at}(1+at)$
16	$\frac{(b-a)s}{(s+a)(s+b)}$	$be^{-bt} - ae^{-at}$
17	$\frac{a}{s^2+a^2}$	$\sin at$
18	$\frac{s}{s^2+a^2}$	$\cos at$
19	$\frac{s+a}{(s+a)^2+b^2}$	$e^{-at} \cos bt$
20	$\frac{b}{(s+a)^2+b^2}$	$e^{-at} \sin bt$
21	$\frac{a^2+b^2}{s[(s+a)^2+b^2]}$	$1 - e^{-at} \left( \cos bt + \frac{a}{b} \sin bt \right)$

**EXAMPLE A.1***Sinusoidal Signal*

Find the Laplace transform of  $f(t) = 1 + 2 \sin(\omega t)$ .

**Solution.** The Laplace transform of  $\sin(\omega t)$  is

$$\mathcal{L}\{\sin(\omega t)\} = \frac{\omega}{s^2 + \omega^2}.$$

Therefore, using Eq. (A.5) we obtain

$$F(s) = \frac{1}{s} + \frac{2\omega}{s^2 + \omega^2} = \frac{s^2 + 2\omega s + \omega^2}{s^3 + \omega^2 s}.$$

The following commands from the Symbolic Math Toolbox in Matlab yield the same result,

```
syms s t w
laplace(1+2*sin(w*t)).
```

---

## 2. Time Delay

Suppose a function  $f(t)$  is delayed by  $\lambda > 0$  units of time. Its Laplace transform is

$$F_1(s) = \int_0^\infty f(t - \lambda) e^{-st} dt.$$

Let us define  $t' = t - \lambda$ . Then  $dt' = dt$ , because  $\lambda$  is a constant and  $f(t) = 0$  for  $t < 0$ . Thus

$$F_1(s) = \int_{-\lambda}^\infty f(t') e^{-s(t'+\lambda)} dt' = \int_0^\infty f(t') e^{-s(t'+\lambda)} dt'.$$

Because  $e^{-s\lambda}$  is independent of time, it can be taken out of the integrand, so

$$F_1(s) = e^{-s\lambda} \int_0^\infty f(t') e^{-st'} dt' = e^{-s\lambda} F(s). \quad (\text{A.7})$$

From this result, we see a time delay of  $\lambda$  corresponds to multiplication of the transform by  $e^{-s\lambda}$ .

### EXAMPLE A.2

#### *Delayed Sinusoidal Signal*

Find the Laplace transform of  $f(t) = A \sin(t - t_d)$ .

**Solution.** The Laplace transform of  $\sin(t)$  is

$$\mathcal{L}\{\sin(t)\} = \frac{1}{s^2 + 1}.$$

Therefore, using Eq. (A.7) we obtain

$$F(s) = \frac{A}{s^2 + 1} e^{-std}.$$


---

## 3. Time Scaling

If the time  $t$  is scaled by a factor  $a$ , then the Laplace transform of the time-scaled signal is

$$F_1(s) = \int_0^\infty f(at) e^{-st} dt.$$

Again, we define  $t' = at$ . As before,  $dt' = a dt$  and

$$F_1(s) = \int_0^\infty f(t') \frac{e^{-st'/a}}{|a|} dt' = \frac{1}{|a|} F\left(\frac{s}{a}\right). \quad (\text{A.8})$$

### EXAMPLE A.3

#### *Sinusoid with Frequency $\omega$*

Find the Laplace transform of  $f(t) = A \sin(\omega t)$ .

**Solution.** The Laplace transform of  $\sin(t)$  is

$$\mathcal{L}\{\sin(t)\} = \frac{1}{s^2 + 1}.$$

Therefore, using Eq. (A.8) we obtain

$$\begin{aligned} F(s) &= \frac{A}{|\omega|} \frac{1}{\left(\frac{s}{\omega}\right)^2 + 1} \\ &= \frac{A\omega}{s^2 + \omega^2}, \end{aligned}$$

as expected. The following commands in Matlab yield the same result,

```
syms s t w A
laplace(A*sin(w*t)).
```

---

#### *4. Shift in Frequency*

Multiplication (modulation) of  $f(t)$  by an exponential expression in the time domain corresponds to a shift in frequency:

$$F_1(s) = \int_0^\infty e^{-at} f(t) e^{-st} dt = \int_0^\infty f(t) e^{-(s+a)t} dt = F(s+a). \quad (\text{A.9})$$

### EXAMPLE A.4

#### *Exponentially Decaying Sinusoid*

Find the Laplace transform of  $f(t) = A \sin(\omega t) e^{-at}$ .

**Solution.** The Laplace transform of  $\sin(\omega t)$  is

$$\mathcal{L}\{\sin(\omega t)\} = \frac{\omega}{s^2 + \omega^2}.$$

Therefore, using Eq. (A.9), we obtain

$$F(s) = \frac{A\omega}{(s+a)^2 + \omega^2}.$$


---

### 5. Differentiation

The transform of the derivative of a signal is related to its Laplace transform and its initial condition as follows:

$$\mathcal{L}\left\{\frac{df}{dt}\right\} = \int_{0^-}^{\infty} \left(\frac{df}{dt}\right) e^{-st} dt = e^{-st} f(t)|_{0^-}^{\infty} + s \int_{0^-}^{\infty} f(t) e^{-st} dt. \quad (\text{A.10})$$

Because  $f(t)$  is assumed to have a Laplace transform,  $e^{-st}f(t) \rightarrow 0$  as  $t \rightarrow \infty$ . Thus,

$$\mathcal{L}\{\dot{f}\} = -f(0^-) + sF(s). \quad (\text{A.11})$$

Another application of Eq. (A.11) leads to

$$\mathcal{L}\{\ddot{f}\} = s^2 F(s) - sf(0^-) - \dot{f}(0^-). \quad (\text{A.12})$$

Repeated application of Eq. (A.11) leads to

$$\mathcal{L}\{f^m(t)\} = s^m F(s) - s^{m-1}f(0^-) - s^{m-2}\dot{f}(0^-) - \dots - f^{(m-1)}(0^-), \quad (\text{A.13})$$

where  $f^m(t)$  denotes the  $m$ th derivative of  $f(t)$  with respect to time.

### EXAMPLE A.5

#### *Derivative of Cosine Signal*

Find the Laplace transform of  $g(t) = \frac{d}{dt}f(t)$ , where  $f(t) = \cos(\omega t)$ .

**Solution.** The Laplace transform of  $\cos(\omega t)$  is

$$F(s) = \mathcal{L}\{\cos(\omega t)\} = \frac{s}{s^2 + \omega^2}.$$

Using Eq. (A.11) with  $f(0^-) = 1$ , we have

$$G(s) = \mathcal{L}\{g(t)\} = s \cdot \frac{s}{s^2 + \omega^2} - 1 = -\frac{\omega^2}{s^2 + \omega^2}.$$


---

### 6. Integration

Let us assume we wish to determine the Laplace transform of the integral of a time function—that is, to find

$$F_1(s) = \mathcal{L}\left\{\int_0^t f(\xi) d\xi\right\} = \int_0^{\infty} \left[\int_0^t f(\xi) d\xi\right] e^{-st} dt.$$

Employing integration by parts, where

$$u = \int_0^t f(\xi) d\xi \quad \text{and} \quad dv = e^{-st} dt,$$

we get

$$F_1(s) = \left[ -\frac{1}{s} e^{-st} \left( \int_0^t f(\xi) d\xi \right) \right]_0^{\infty} - \int_0^{\infty} -\frac{1}{s} e^{-st} f(t) dt = \frac{1}{s} F(s). \quad (\text{A.14})$$

**EXAMPLE A.6***Time Integral of Sinusoidal Signal*

Find the Laplace transform of  $f(t) = \int_0^t \sin \omega \tau d\tau$ .

**Solution.** The Laplace transform of  $\sin(\omega t)$  is

$$\mathcal{L}\{\sin(\omega t)\} = \frac{\omega}{s^2 + \omega^2}.$$

Therefore, using Eq. (A.14),

$$F(s) = \frac{\omega}{s^3 + \omega^2 s}.$$

*7. Convolution*

Convolution in the time domain corresponds to multiplication in the frequency domain. Assume  $\mathcal{L}\{f_1(t)\} = F_1(s)$  and  $\mathcal{L}\{f_2(t)\} = F_2(s)$ . Then

$$\begin{aligned}\mathcal{L}\{f_1(t) * f_2(t)\} &= \int_0^\infty f_1(t) * f_2(t) e^{-st} dt \\ &= \int_0^\infty \left[ \int_0^t f_1(\tau) f_2(t - \tau) d\tau \right] e^{-st} dt.\end{aligned}$$

We see  $t$  varies from zero to infinity and  $\tau$  varies from zero to  $t$ . With the aid of Fig. A.1, we reverse the order of integration and change the limits of integration accordingly so  $\tau$  varies from zero to infinity and  $\infty \geq t \geq \tau$ , to yield

$$\mathcal{L}\{f_1(t) * f_2(t)\} = \int_0^\infty \int_\tau^\infty f_1(\tau) f_2(t - \tau) e^{-st} dt d\tau.$$

Multiplying by  $e^{-s\tau} e^{s\tau}$  results in

$$\mathcal{L}\{f_1(t) * f_2(t)\} = \int_0^\infty f_1(\tau) e^{-s\tau} \left[ \int_\tau^\infty f_2(t - \tau) e^{-s(t-\tau)} dt \right] d\tau.$$

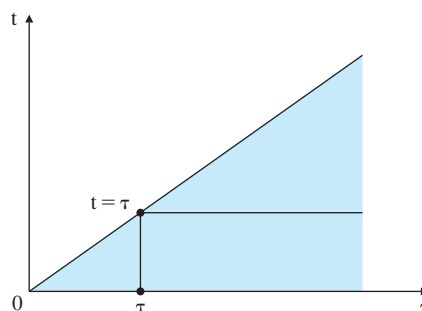
If we change variables  $t' \triangleq t - \tau$ , then

$$\mathcal{L}\{f_1(t) * f_2(t)\} = \int_0^\infty f_1(\tau) e^{-s\tau} d\tau \int_0^\infty f_2(t') e^{-st'} dt',$$

$$\mathcal{L}\{f_1(t) * f_2(t)\} = F_1(s) F_2(s).$$

**Figure A.1**

Diagram illustrating reversal of the order of integration



This implies that

$$\mathcal{L}^{-1}\{F_1(s)F_2(s)\} = f_1(t) * f_2(t). \quad (\text{A.15})$$

## EXAMPLE A.7

### Ramp Response of a First-Order System

Find the ramp response of a first-order system with a pole at  $+a$ .

**Solution.** Let  $f_1(t) = t$  be the ramp input and  $f_2(t) = e^{at}$  be the impulse response of the first-order system. Then, using Eq. (A.15) we find that

$$\begin{aligned} \mathcal{L}^{-1}\left\{\frac{1}{s^2} \frac{1}{s-a}\right\} &= f_1(t) * f_2(t) \\ &= \int_0^t f_1(\tau) f_2(t-\tau) d\tau \\ &= \int_0^t \tau e^{a(t-\tau)} d\tau \\ &= \frac{1}{a^2}(e^{at} - at - 1). \end{aligned}$$

The following commands in Matlab yield the same result,

```
syms s t a
ilaplace(1/(s^3-a*s^2)).
```

---

### 8. Time Product

Multiplication in the time domain corresponds to convolution in the frequency domain:

$$\mathcal{L}\{f_1(t)f_2(t)\} = \frac{1}{2\pi j} \int_{\sigma_c-j\infty}^{\sigma_c+j\infty} F_1(\xi)F_2(s-\xi) d\xi.$$

To see this, consider the relation

$$\mathcal{L}\{f_1(t)f_2(t)\} = \int_0^\infty f_1(t)f_2(t)e^{-st} dt.$$

Substituting the expression for  $f_1(t)$  given by Eq. (3.33) yields

$$\mathcal{L}\{f_1(t)f_2(t)\} = \int_0^\infty \left[ \frac{1}{2\pi j} \int_{\sigma_c-j\infty}^{\sigma_c+j\infty} F_1(\xi)e^{\xi t} d\xi \right] f_2(t)e^{-st} dt.$$

Changing the order of integration results in

$$\mathcal{L}\{f_1(t)f_2(t)\} = \frac{1}{2\pi j} \int_{\sigma_c-j\infty}^{\sigma_c+j\infty} F_1(\xi) \int_0^\infty f_2(t)e^{-(s-\xi)t} dt d\xi.$$

Using Eq. (A.9), we get

$$\mathcal{L}\{f_1(t)f_2(t)\} = \frac{1}{2\pi j} \int_{\sigma_c-j\infty}^{\sigma_c+j\infty} F_1(\xi)F_2(s-\xi) d\xi = \frac{1}{2\pi j} F_1(s) * F_2(s). \quad (\text{A.16})$$

### 9. Parseval's Theorem

Parseval's famous theorem is used to compute the “energy” in a signal or “correlation” between two signals. It tells us that mentioned quantities can be computed either in the time domain or in the frequency domain. If

$$\int_0^\infty |y(t)|^2 dt < 1 \quad \text{and} \quad \int_0^\infty |u(t)|^2 dt < 1 \quad (\text{A.17})$$

(i.e.,  $y(t)$  and  $u(t)$  are square integrable), then

$$\int_0^\infty y(t)u(t)dt = \frac{1}{2\pi} \int_{-\infty}^\infty Y(-j\omega)U(j\omega) d\omega. \quad (\text{A.18})$$

Parseval's result involves only a substitution of the transform for the time functions and an exchange of integration:

$$\int_0^\infty y(t)u(t) dt = \int_0^\infty y(t) \left[ \frac{1}{2\pi} \int_{-\infty}^\infty U(j\omega)e^{j\omega t} d\omega \right] dt \quad (\text{A.19})$$

$$= \frac{1}{2\pi} \int_{-\infty}^\infty U(j\omega) \left[ \int_0^\infty y(t)e^{j\omega t} dt \right] d\omega \quad (\text{A.20})$$

$$= \frac{1}{2\pi} \int_{-\infty}^\infty U(j\omega)Y(-j\omega) d\omega. \quad (\text{A.21})$$

### 10. Multiplication by Time

Multiplication by time corresponds to differentiation in the frequency domain. Let us consider

$$\begin{aligned} \frac{d}{ds}F(s) &= \frac{d}{ds} \int_0^\infty e^{-st}f(t) dt \\ &= \int_0^\infty -te^{-st}f(t) dt \\ &= - \int_0^\infty e^{-st}[tf(t)] dt \\ &= -\mathcal{L}\{tf(t)\}. \end{aligned}$$

Then

$$\mathcal{L}\{tf(t)\} = -\frac{d}{ds}F(s), \quad (\text{A.22})$$

which is the desired result.

## EXAMPLE A.8

### Time Product of Sinusoidal Signal

Find the Laplace transform of  $f(t) = t \sin \omega t$ .

**Solution.** The Laplace transform of  $\sin \omega t$  is

$$\mathcal{L}\{\sin(\omega t)\} = \frac{\omega}{s^2 + \omega^2}.$$

Hence, using Eq. (A.22), we obtain

$$F(s) = -\frac{d}{ds} \left[ \frac{\omega}{s^2 + \omega^2} \right] = \frac{2\omega s}{(s^2 + \omega^2)^2}.$$

The following commands in Matlab yield the same result,

```
syms s t w
laplace(t*sin(w*t)).
```

---

### A.1.2 Inverse Laplace Transform by Partial-Fraction Expansion

As we saw in Chapter 3, the easiest way to find  $f(t)$  from its Laplace transform  $F(s)$ , if  $F(s)$  is rational, is to expand  $F(s)$  as a sum of simpler terms that can be found in the tables via partial-fraction expansion. We have already discussed this method in connection with simple roots in Section 3.1.5. In this section, we will discuss partial-fraction expansion for cases of complex and repeated roots.

*Complex Poles* In the case of quadratic factors in the denominator, the numerator of the quadratic factor is chosen to be first order as shown in Example A.9. Whenever there exists a complex conjugate pair of poles such as

$$F(s) = \frac{C_1}{s - p_1} + \frac{C_2}{s - p_1^*},$$

we can show

$$C_2 = C_1^*$$

(see Problem 3.1) and

$$f(t) = C_1 e^{p_1 t} + C_1^* e^{p_1^* t} = 2\operatorname{Re}(C_1 e^{p_1 t}).$$

Assuming  $p_1 = \alpha + j\beta$ , we may rewrite  $f(t)$  in a more compact form as

$$\begin{aligned} f(t) &= 2\operatorname{Re}\{C_1 e^{p_1 t}\} = 2\operatorname{Re}\{|C_1|e^{j\arg(C_1)} e^{(\alpha+j\beta)t}\} \\ &= 2|C_1|e^{\alpha t} \cos[\beta t + \arg(C_1)]. \end{aligned} \quad (\text{A.23})$$

#### EXAMPLE A.9

#### Partial-Fraction Expansion: Distinct Complex Roots

Find the function  $f(t)$  for which the Laplace transform is

$$F(s) = \frac{1}{s(s^2 + s + 1)}.$$

**Solution.** We rewrite  $F(s)$  as

$$F(s) = \frac{C_1}{s} + \frac{C_2 s + C_3}{s^2 + s + 1}.$$

Using the cover-up method, we find

$$C_1 = sF(s)|_{s=0} = 1.$$

Setting  $C_1 = 1$  then equating the numerators in the partial-fraction expansion relation, we obtain

$$(s^2 + s + 1) + (C_2s + C_3)s = 1.$$

After solving for  $C_2$  and  $C_3$ , we find  $C_2 = -1$  and  $C_3 = -1$ . To make it more suitable for using the Laplace transform tables, we rewrite the partial fraction as

$$F(s) = \frac{1}{s} - \frac{s + \frac{1}{2} + \frac{1}{2}}{\left(s + \frac{1}{2}\right)^2 + \frac{3}{4}}.$$

From the tables we have,

$$\begin{aligned} f(t) &= \left(1 - e^{-t/2} \cos \sqrt{\frac{3}{4}} t - \frac{1}{\sqrt{3}} e^{-t/2} \sin \sqrt{\frac{3}{4}} t\right) 1(t) \\ &= \left(1 - \frac{2}{\sqrt{3}} e^{-t/2} \cos \left(\frac{\sqrt{3}}{2}t - \frac{\pi}{6}\right)\right) 1(t). \end{aligned}$$

Alternatively, we may write  $F(s)$  as

$$F(s) = \frac{C_1}{s} + \frac{C_2}{s - p_1} + \frac{C_2^*}{s - p_1^*}, \quad (\text{A.24})$$

where  $p_1 = -\frac{1}{2} + j\frac{\sqrt{3}}{2}$ .  $C_1 = 1$ , as before, and now

$$C_2 = (s - p_1)F(s)|_{s=p_1} = -\frac{1}{2} + j\frac{1}{2\sqrt{3}},$$

$$C_2^* = -\frac{1}{2} - j\frac{1}{2\sqrt{3}},$$

and

$$\begin{aligned} f(t) &= (1 + 2|C_2|e^{\alpha t} \cos[\beta t + \arg(C_2)]) 1(t) \\ &= \left(1 + \frac{2}{\sqrt{3}} e^{-t/2} \cos \left[\frac{\sqrt{3}}{2}t + \frac{5\pi}{6}\right]\right) 1(t) \\ &= \left(1 - \frac{2}{\sqrt{3}} e^{-t/2} \cos \left[\frac{\sqrt{3}}{2}t - \frac{5\pi}{6}\right]\right) 1(t). \end{aligned}$$

The latter partial-fraction expansion can be readily computed using the following Matlab statements:

```
num = 1; % form numerator
den = conv([1 0],[1 1 1]); % form denominator
[r,p,k] = residue(num,den) % compute residues
```

which yields the result

```
r = [-0.5000 + 0.2887i - 0.5000 - 0.2887i 1.0000]';
p = [-0.5000 + 0.8660i - 0.5000 - 0.8660i 0]';k = []
```

and agrees with the previous hand calculations. Note if we are using the tables, the first method is preferable, while the second method is preferable for checking Matlab results.

The following commands in Matlab yield the same result for the inverse Laplace transform,

```
syms s t
ilaplace(1/(s*(s^2+s+1))).
```

---

*Repeated Poles* For the case in which  $F(s)$  has repeated roots, the procedure to compute the partial-fraction expansion must be modified. If  $p_1$  is repeated three times, we write the partial fraction as

$$F(s) = \frac{C_1}{s - p_1} + \frac{C_2}{(s - p_1)^2} + \frac{C_3}{(s - p_1)^3} + \frac{C_4}{s - p_4} + \cdots + \frac{C_n}{s - p_n}.$$

We determine the constants  $C_4$  through  $C_n$  as discussed previously. If we multiply both sides of the preceding equation by  $(s - p_1)^3$ , we obtain

$$(s - p_1)^3 F(s) = C_1(s - p_1)^2 + C_2(s - p_1) + C_3 + \cdots + \frac{C_n(s - p_1)^3}{s - p_n}. \quad (\text{A.25})$$

If we then set  $s = p_1$ , all the factors on the right side of Eq. (A.25) will go to zero except  $C_3$ , which is

$$C_3 = (s - p_1)^3 F(s)|_{s=p_1},$$

as before. To determine the other factors, we differentiate Eq. (A.25) with respect to the Laplace variable  $s$ :

$$\frac{d}{ds}[(s - p_1)^3 F(s)] = 2C_1(s - p_1) + C_2 + \cdots + \frac{d}{ds} \left[ \frac{C_n(s - p_1)^3}{s - p_n} \right]. \quad (\text{A.26})$$

Again, if we set  $s = p_1$ , we have

$$C_2 = \frac{d}{ds} [(s - p_1)^3 F(s)]|_{s=p_1}.$$

Similarly, if we differentiate Eq. (A.26) again and set  $s = p_1$  a second time, we get

$$C_1 = \frac{1}{2} \frac{d^2}{ds^2} [(s - p_1)^3 F(s)]|_{s=p_1}.$$

In general, we may compute  $C_i$  for a factor with multiplicity  $k$  as

$$C_{k-i} = \frac{1}{i!} \left[ \frac{d^i}{ds^i} [(s - p_1)^k F(s)] \right]_{s=p_1}, \quad i = 0, \dots, k-1.$$

## EXAMPLE A.10

### Partial-Fraction Expansion: Repeated Real Roots

Find the function  $f(t)$  that has the Laplace transform

$$F(s) = \frac{s + 3}{(s + 1)(s + 2)^2}.$$

**Solution.** We write the partial fraction as

$$F(s) = \frac{C_1}{s+1} + \frac{C_2}{s+2} + \frac{C_3}{(s+2)^2}.$$

Then

$$\begin{aligned} C_1 &= (s+1)F(s)|_{s=-1} = \frac{s+3}{(s+2)^2}|_{s=-1} = 2, \\ C_2 &= \frac{d}{ds} \left[ (s+2)^2 F(s) \right] |_{s=-2} = -2, \\ C_3 &= (s+2)^2 F(s) |_{s=-2} = \frac{s+3}{s+1} |_{s=-2} = -1. \end{aligned}$$

The function  $f(t)$  is

$$f(t) = (2e^{-t} - 2e^{-2t} - te^{-2t})1(t).$$

The partial fraction computation can also be carried out using Matlab's residue function,

```
num = [1 3]; % form numerator
den = conv([1 1],[1 4 4]); % form denominator
[r,p,k] = residue(num,den) % compute residues
```

which yields the result

$r = [-2 -1 2]', p = [-2 -2 -1]',$  and  $k = [];$

and agrees with the hand calculations.

The following commands in Matlab yield the same result for the inverse Laplace transform,

```
syms s t
ilaplace((s+3)/((s+1)*(s+2)^2)).
```

### A.1.3 The Initial Value Theorem

We discussed the Final Value Theorem in Chapter 3. A second valuable Laplace transform theorem is the **Initial Value Theorem**, which states that it is always possible to determine the initial value of the time function  $f(t)$  from its Laplace transform. We may also state the theorem in this way:

#### The Initial Value Theorem

For any Laplace transform pair,

$$\lim_{s \rightarrow \infty} sF(s) = f(0^+). \quad (\text{A.27})$$

We may show this as follows.

Using Eq. (A.11), we get

$$\mathcal{L} \left\{ \frac{df}{dt} \right\} = sF(s) - f(0^-) = \int_{0^-}^{\infty} e^{-st} \frac{df}{dt} dt. \quad (\text{A.28})$$

Let us consider the case in which  $s \rightarrow \infty$  and rewrite the integral as

$$\int_{0^-}^{\infty} e^{-st} \frac{df(t)}{dt} dt = \int_{0^+}^{\infty} e^{-st} \frac{df(t)}{dt} dt + \int_{0^-}^{0^+} e^{-st} \frac{df(t)}{dt} dt.$$

Taking the limit of Eq. (A.28) as  $s \rightarrow \infty$ , we get

$$\lim_{s \rightarrow \infty} [sF(s) - f(0^-)] = \lim_{s \rightarrow \infty} \left[ \int_{0^-}^{0^+} e^0 \frac{df(t)}{dt} dt + \int_{0^+}^{\infty} e^{-st} \frac{df(t)}{dt} dt \right].$$

The second term on the right side of the preceding equation approaches zero as  $s \rightarrow \infty$ , because  $e^{-st} \rightarrow 0$ . Hence

$$\lim_{s \rightarrow \infty} [sF(s) - f(0^-)] = \lim_{s \rightarrow \infty} [f(0^+) - f(0^-)] = f(0^+) - f(0^-)$$

or

$$\lim_{s \rightarrow \infty} sF(s) = f(0^+).$$

In contrast with the Final Value Theorem, the Initial Value Theorem can be applied to any function  $F(s)$ .

## EXAMPLE A.11

### *Initial Value Theorem*

Find the initial value of the signal in Example 3.13.

**Solution.** From the Initial Value Theorem, we get

$$y(0^+) = \lim_{s \rightarrow \infty} sY(s) = \lim_{s \rightarrow \infty} s \frac{3}{s(s-2)} = 0,$$

which checks with the expression for  $y(t)$  computed in Example 3.13.

## A.1.4 Final Value Theorem

### The Final Value Theorem

If all poles of  $sY(s)$  are in the left half of the  $s$ -plane, then

$$\lim_{t \rightarrow \infty} y(t) = \lim_{s \rightarrow 0} sY(s). \quad (3.54)$$

### *Proof of the Final Value Theorem*

We may prove this result as follows. The derivative relationship developed in Eq. (3.41) is

$$\mathcal{L} \left\{ \frac{dy}{dt} \right\} = sY(s) - y(0^-) = \int_{0^-}^{\infty} e^{-st} \frac{dy}{dt} dt.$$

We assume we are interested in the case where  $s \rightarrow 0$ . Then

$$\lim_{s \rightarrow 0} [sY(s) - y(0)] = \lim_{s \rightarrow 0} \left( \int_{0^-}^{\infty} e^{-st} \frac{dy}{dt} dt \right) = \lim_{t \rightarrow \infty} [y(t) - y(0)],$$

and we have

$$\lim_{t \rightarrow \infty} y(t) = \lim_{s \rightarrow 0} s Y(s).$$

Another way to see this same result is to note the partial-fraction expansion of  $Y(s)$  [Eq. (3.51)] is

$$Y(s) = \frac{C_1}{s - p_1} + \frac{C_2}{s - p_2} + \cdots + \frac{C_n}{s - p_n}.$$

Let us say  $p_1 = 0$  and all other  $p_i$  are in the left half-plane so that  $C_1$  is the steady-state value of  $y(t)$ . Using Eq. (3.53), we see

$$C_1 = \lim_{t \rightarrow \infty} y(t) = s Y(s)|_{s=0},$$

which is the same as the previous result.

For a thorough study of Laplace transforms and extensive tables, see Churchill (1972) and Campbell and Foster (1948); for the two-sided transform, see Van der Pol and Bremmer (1955).

# Appendix B Solutions to the Review Questions

## Chapter 1

- 1.1 What are the main components of a feedback control system?

*The process, the actuator, the sensor, and the controller*

- 1.2 What is the purpose of the sensor?

*To measure the output variable and, usually, to convert it to an electrical voltage*

- 1.3 Give three important properties of a good sensor.

*A good sensor is linear (the output is proportional to the input signal) over a large range of amplitudes and a large range of frequencies at its input, has low noise, is unbiased, is easy to calibrate, and has low cost. The relative values of these properties varies with the particular application.*

- 1.4 What is the purpose of the actuator?

*The actuator takes an input, usually electrical, and converts it to a signal such as a force or torque that causes the process output to move or change over the required range.*

- 1.5 Give three important properties of a good actuator.

*A good actuator has fast response, and adequate power, energy, speed, torque, and so on, to be able to cause the process output to meet the design specifications and is efficient, lightweight, small, cheap, and so on. As with sensors, the relative value of these properties varies with the application.*

- 1.6 What is the purpose of the controller? Give the input(s) and output(s) of the controller.

*The controller is to take the sensor output (the input to the controller) and compute the control signal (the output of the controller) to be sent to the actuator.*

- 1.7 What physical variable is measured by a tachometer?

*A tachometer measures speed of rotation or angular velocity.*

- 1.8 Describe three different techniques for measuring temperature.

*In each of the following cases, it is important to realize that the devices mentioned need to be calibrated and often corrected for nonlinearity in order to give a reliable, accurate measure of temperature.*

- (a) *An early technique still used in many home thermostats is based on the bimetallic strip composed of two strips of different metals that expand with different coefficients with temperature. As a result, the strip bends with temperature and the resulting motion can be used as a measure of temperature. This principle was introduced in the 18th century to maintain a constant length to a clock pendulum for precision time keeping.*
- (b) *A technique related to the bimetallic strip is based on the fact that metals with different work functions placed in contact will produce a voltage that is proportional to temperature. Such a device is called a thermocouple and is the basis of a standard laboratory technique for measuring temperature.*
- (c) *A number of materials have electrical resistance that is dependent in a monotonic way on temperature, and a resistance bridge can be used with one of these to indicate temperature. Such devices are called thermistors.*
- (d) *For high temperatures, it is well known that the color of the radiation due to heat depends on temperature. A piece of iron placed in a fire will glow orange, then red, and finally become white hot at high temperatures. An instrument for measuring the frequency of the radiation, and thus the temperature, is a pyrometer.*
- (e) *In ceramic kilns, cones of different materials that melt at different and known temperatures are placed near the products in the kiln to indicate when the design temperature has been reached. The potter watches until the cone of importance begins to sag and then knows that the products should be removed. These give a quantized measure of temperature.*

- 1.9 Why do most sensors have an electrical output, regardless of the physical nature of the variable being measured?

*Electrical signals are the most easily manipulated; therefore, most controllers are electrical devices, either analog or digital. To provide the signal input to such a device, the sensor needs to produce an electrical output.*

## Chapter 2

- 2.1 What is a “free-body” diagram?

*To write the equations of motion of a system of connected bodies, it is useful to draw each body in turn with the influence of all other bodies represented by forces and torques on the body in question. A drawing of the collection of such isolated bodies is called a “free-body diagram.”*

- 2.2 What are the two forms of Newton’s law?

*Translational motion is described by  $F = ma$ . Rotational motion is described by  $M = I\alpha$ .*

- 2.3 For a structural process to be controlled, such as a robot arm, what is the meaning of “collocated control”? “Noncollocated control”?

*When the actuator and the sensor are located on the same rigid body, the control is said to be “collocated.” When they are on different bodies that are connected by springs, the control is “noncollocated.”*

- 2.4 State Kirchhoff’s current law.

*The algebraic sum of all currents entering a junction or circuit is zero.*

- 2.5 State Kirchhoff’s voltage law.

*The algebraic sum of voltages around a closed path in an electric circuit is zero.*

- 2.6 When, why, and by whom was the device named an “operational amplifier”?

*In a paper in 1947, Ragazzini, Randall, and Russell named the high-gain, wide-bandwidth amplifier used in feedback to realize operational calculus “operations” the operational amplifier.*

- 2.7 What is the major benefit of having zero input current to an operational amplifier?

*With zero input current the amplifier does not load the input circuit; thus, the transfer function on the device is not dependent on the amplifier characteristics. Also, the analysis of the circuit is simplified in this case.*

- 2.8 Why is it important to have a small value for the armature resistance  $R_a$  of an electric motor?

*The armature resistance causes power loss when the armature current flows and thus reduces the efficiency of the motor.*

- 2.9 What are the definition and units of the electric constant of a motor?

*A rotating motor produces a voltage (called the back emf) in its armature proportional to the rotational speed. The electric constant  $K_e$  is the ratio of this voltage to the speed, so  $e = K_e \dot{\theta}$ . The units are volt-sec/radians.*

- 2.10 What are the definition and units of the torque constant of an electric motor?

*When current  $i_a$  flows in the armature of an electrical motor, a torque  $\tau$  is produced that is proportional to the current. The torque constant  $K_t$  is the constant of proportionality, so  $\tau = K_t i_a$ . The units are Newton-meters/amp.*

- 2.11 Why do we approximate a physical model of the plant (which is *always* nonlinear) with a linear model?

*Analysis and design of linear models is vastly simpler than with nonlinear models. Furthermore, it has been shown (by Lyapunov) that, if the linear approximation is stable, then there is at least some region of stability for the nonlinear model.*

- △ 2.12 Give the relationships for (a) heat flow across a substance and (b) heat storage in a substance.

- (a) *Heat flow is proportional to the temperature difference divided by the thermal resistance; that is,*

$$q = \frac{1}{R} (T_1 - T_2).$$

- (b) *The differential equation describing the heat storage is*

$$\dot{T} = \frac{1}{C} q,$$

*where C is the thermal capacity of the material.*

- △ 2.13 Name and give the equations for the three relationships governing fluid flow.

*Continuity:*  $\dot{m} = w_{in} - w_{out}$ .

*Force equilibrium:*  $f = pA$ .

*Resistance:*  $w = \frac{1}{R} (p_1 - p_2)^{1/\alpha}$ .

## Chapter 3

- 3.1 What is the definition of “transfer function”?

*The Laplace transform of the output of a linear, time-invariant system,  $Y(s)$ , is proportional to the transform of its input,  $U(s)$ . The function of proportionality is the transfer function  $F(s)$ , so that  $Y(s) = F(s)U(s)$ . It is assumed all initial conditions are zero.*

- 3.2 What are the properties of systems whose responses can be described by transfer functions?

*The system must be both linear (superposition applies) and time invariant (the parameters do not vary with time).*

- 3.3 What is the Laplace transform of  $f_1(t) = f(t - \lambda)1(t - \lambda)$  if the transform of  $f(t)$  is  $F(s)$ ?

$$\mathcal{L}\{f_1(t)\} = e^{-s\lambda} F(s).$$

- 3.4 State the Final Value Theorem.

*If all the poles of  $sF(s)$  are in the LHP, then the final value of  $f(t)$  is given by  $\lim_{t \rightarrow \infty} f(t) = \lim_{s \rightarrow 0} sF(s)$ .*

- 3.5 What is the most common use of the Final Value Theorem in control?

*A standard test of a control system is the step response, and the FVT is used to determine the steady-state error to such an input.*

- 3.6 Given a second-order transfer function with damping ratio  $\zeta$  and natural frequency  $\omega_n$ , what is the estimate of the step response rise time? What is the estimate of the percent overshoot in the step response? What is the estimate of the settling time?

*These are given by  $t_r \cong 1.8/\omega_n$ ,  $M_p$  is set by the damping ratio (see the curve in Fig. 3.24) and  $t_s \cong 4.6/\sigma$ .*

- 3.7 What is the major effect of an extra zero in the LHP on the second-order step response?

*Such a zero causes additional overshoot, and the closer the zero is to the imaginary axis, the higher the overshoot. If the zero is more than six times the real part of the complex poles, the effect is negligible.*

- 3.8 What is the most noticeable effect of a zero in the RHP on the step response of the second-order system?

*Such a zero often causes an initial undershoot of the response.*

- 3.9 What is the main effect of an extra real pole on the second-order step response?

*A pole slows down the response and makes the rise time longer. The closer the pole is to the imaginary axis, the more pronounced is the effect. If the pole is more than six times the real part of the complex poles, the effect is negligible.*

- 3.10 Why is stability an important consideration in control system design?

*Almost any useful dynamic system must be stable to perform its function. Feedback around a system that is normally stable can actually introduce instability, so control designers must be able to assure the stability of their designs.*

- 3.11 What is the main use of Routh's criterion?

*With this method, we can find (symbolically) the range of a parameter such as the loop gain for which the system will be stable.*

- 3.12 Under what conditions might it be important to know how to estimate a transfer function from experimental data?

*In many cases, the equations of motion are either extremely complex or not known at all. Chemical processes such as a paper-making machine are often of this kind. In these cases, if one wishes to build a good control, it is very useful to be able to take transient data or steady-state frequency-response data and to estimate a transfer function from these.*

## Chapter 4

- 4.1 Give three advantages of feedback in control.

(a) *Feedback can reduce the steady-state error in response to disturbances.*

- (b) *Feedback can reduce the steady-state error in tracking a reference.*
- (c) *Feedback can reduce the sensitivity of a transfer function to parameter changes.*
- (d) *Feedback can stabilize an unstable process.*

4.2 Give two disadvantages of feedback in control.

- (a) *Feedback requires a sensor, which can be very expensive and may introduce additional noise.*
- (b) *Feedback systems are often more difficult to design and operate than open-loop systems.*

4.3 A temperature control system is found to have zero error to a constant tracking input and an error of  $0.5^{\circ}\text{C}$  to a tracking input that is linear in time, rising at the rate of  $40^{\circ}\text{C/sec}$ . What is the system type of this control system and what is the relevant error constant ( $K_p$  or  $K_v$  or  $K_a$ )?

*The system is Type 1 and  $K_v$  is the ratio of input rate to error or  $K_v = 40/0.5 = 80/\text{sec}$ .*

4.4 What are the units of  $K_p$ ,  $K_v$ , and  $K_a$ ?

*$K_p$  is dimensionless,  $K_v$  is  $\text{sec}^{-1}$ , and  $K_a$  is  $\text{sec}^{-2}$ .*

4.5 What is the definition of system type with respect to reference inputs?

*With only a polynomial of degree  $k$  reference input (no disturbances), the type is the largest value of  $k$  for which the steady-state error is a constant.*

4.6 What is the definition of system type with respect to disturbance inputs?

*With only a polynomial of degree  $k$  disturbance input (no reference), the type is the largest value of  $k$  for which the steady-state error is a constant.*

4.7 Why does system type depend on where the external signal enters the system?

*Because the error depends on where the input enters, so does the type.*

4.8 What is the main objective of introducing integral control?

*Integral control will make the error to a constant input go to zero. It removes the effects of process noise bias. It cannot remove the effects of sensor bias.*

4.9 What is the major objective of adding derivative control?

*Derivative control typically makes the system better damped and more stable.*

- 4.10 Why might a designer wish to put the derivative term in the feedback rather than in the error path?

*When a reference input includes sudden changes, including it in the derivative action might cause unnecessary large controls.*

- 4.11 What is the advantage of having a “tuning rule” for PID controllers?

*PID controllers are typically packaged as a unit with knobs on the front for the several gain constants. These devices are widely installed in factories and operated by technicians with modest knowledge of control theory. A tuning rule permits such a person to measure parameters of the process experimentally and use this data to set the parameters in such a way as to give good response.*

- 4.12 Give two reasons to use a digital controller rather than an analog controller.

- (a) *The control law is easier to change if the controller is digital.*
- (b) *A digital controller can perform logic and other nonlinear operations much easier than an analog controller.*
- (c) *The hardware of a digital controller can be fixed in the design before the details of the actual control design are finished.*

- 4.13 Give two disadvantages to using a digital controller.

- (a) *The bandwidth of a digital controller is limited by the possible sample frequency.*
- (b) *The digital controller introduces noise by the quantization process.*

## Chapter 5

- 5.1 Give two definitions for the root locus.

- (a) *The root locus is the locus of points in the s-plane where the equation  $a(s) + Kb(s) = 0$  has a solution.*
- (b) *The root locus is the locus of points in the s-plane where the angle of  $G(s) = b(s)/a(s)$  is  $180^\circ$ .*

- 5.2 Define the negative root locus.

*The negative root locus is the locus of points where the equation  $a(s) - Kb(s) = 0$  has a solution or where the angle of  $G(s) = b(s)/a(s)$  is  $0^\circ$ .*

- 5.3 Where are the sections of the (positive) root locus on the real axis?

*Segments of the real axis to the left of an odd number of zeros and poles are on the root locus.*

- 5.4 What are the angles of departure from two coincident poles at  $s = -a$  on the real axis? Assume there are no poles or zeros to the right of  $-a$ .  
*The loci depart at  $\pm 90^\circ$ .*
- 5.5 What are the angles of departure from *three* coincident poles at  $s = -a$  on the real axis? Assume there are no poles or zeros to the right of  $-a$ .  
*The loci depart at  $\pm 60^\circ$  and  $180^\circ$ .*
- 5.6 What is the principal effect of a lead compensation on a root locus?  
*The lead compensation generally causes the locus to bend toward the LHP, moving the dominant roots to a place of higher damping.*
- 5.7 What is the principal effect of a lag compensation on a root locus in the vicinity of the dominant closed-loop roots?  
*The lag compensation is normally placed so near the origin that it has negligible effect on the root locus in the vicinity of the dominant closed-loop roots.*
- 5.8 What is the principal effect of a lag compensation on the steady-state error to a reference input?  
*A lag compensation normally raises the gain at  $s = 0$  and thus lowers the errors.*
- 5.9 Why is the angle of departure from a pole near the imaginary axis especially important?  
*If the locus starts toward the RHP, then feedback will make the system less stable. On the other hand, if the locus departs toward the LHP, then feedback is going to make the system more stable.*
- 5.10 Define a conditionally stable system.  
*A system that becomes **unstable** as gain is reduced is considered to be conditionally stable. That is, its stability is conditioned on having an operating compensator with at least a minimum value of gain.*
- 5.11 Show, with a root locus argument, that a system having three poles at the origin *must* be conditionally stable.  
*With three poles at the origin, the angles of departure ensure that two poles leave the origin at  $180^\circ$ ,  $\pm 60^\circ$ , or, if there are poles on the real axis in the RHP, they may leave at  $0^\circ$ ,  $\pm 120^\circ$  which is to say that at least one pole begins by moving into the RHP. As gain is reduced from the operating level, at least one root must pass into the RHP for gain low enough; therefore, the system must be conditionally stable.*

## Chapter 6

- 6.1 Why did Bode suggest plotting the magnitude of a frequency response on log–log coordinates?

*In log-log coordinates, the plot for a rational transfer function can be well guided by linear asymptotes and thus easily plotted and visualized.*

6.2 Define a decibel.

*If a power ratio is  $P_1/P_2$ , then the measure in decibels is  $10 \log(P_1/P_2)$ . Because power is proportional to voltage squared, and a transfer function would give a ratio of voltages, then the gain of a transfer function  $G(j\omega)$  in decibels is  $G_{db} = 20 \log |G(j\omega)|$ .*

6.3 What is the transfer function magnitude if the gain is listed as 14 db?

$$14 = 20 \log M, \text{ therefore } M = 5.01.$$

6.4 Define gain crossover.

*The gain crossover  $\omega_c$  is the value of frequency where the magnitude gain is 1 (or 0 db).*

6.5 Define phase crossover.

*The phase crossover  $\omega_{cp}$  is the value of the frequency where the phase crosses  $-180^\circ$ .*

6.6 Define phase margin PM.

*The phase margin PM is a measure of how far in phase the Nyquist plot is from instability. In the typical case, if the phase of the system at gain crossover is  $\phi$ , then the phase margin is  $180^\circ + \phi$ . For example, if  $\phi = -150^\circ$ , then the phase margin is  $30^\circ$ .*

6.7 Define gain margin GM.

*The gain margin GM is a measure of how far the system is from instability by changes in gain alone. If the gain at phase crossover, where the system phase is  $180^\circ$ , is  $|G(j\omega_{cp})|$ , then the gain margin is calculated from  $GM * |G(j\omega_{cp})| = 1.0$  or  $GM = 1/|G(j\omega_{cp})|$ .*

6.8 What Bode plot characteristic is the best indicator of the closed-loop step response overshoot?

*The phase margin is related to the equivalent closed-loop damping ratio approximately by  $\zeta_{eq} = PM/100$ . As we saw in Chapter 3, the step response overshoot is monotonically related to the damping ratio.*

6.9 What Bode plot characteristic is the best indicator of the closed-loop step response rise time?

*The rise time is measured by the closed-loop natural frequency, which in turn is adequately approximated by the gain crossover. Thus, the best indicator of rise time is  $\omega_c$ .*

6.10 What is the principal effect of a lead compensation on Bode plot performance measures?

*The lead compensation usually is used to raise the phase margin at a desired gain crossover frequency.*

- 6.11 What is the principal effect of a lag compensation on Bode plot performance measures?

*The lag compensation is usually used to raise the low-frequency gain to reduce the steady-state error to polynomial or low-frequency sinusoidal inputs. It can also be used to lower the crossover frequency  $\omega_c$ , where a more favorable phase exists.*

- 6.12 How do you find the  $K_v$  of a type 1 system from its Bode plot?

*The  $K_v$  is determined by the low-frequency asymptote, which has a slope of  $-1$  for a type 1 system and is given by the expression  $K_v/\omega$ . The value of the constant may be found either from the frequency where the asymptote reaches  $1.0$  (or  $0$  db) or else as the value of the asymptote at the frequency of  $\omega = 1$ .*

- 6.13 Why do we need to know beforehand the number of open-loop unstable poles in order to tell stability from the Nyquist plot?

*The number of Nyquist plot encirclements counts the difference in the number of zeros and the number of poles in the RHP of  $1 + KD_cG$ . In order to know the number of zeros of this function (which are closed-loop poles and thus unstable poles of the closed loop), we must know the number of unstable open-loop poles for the plot.*

- 6.14 What is the main advantage in control design of counting the encirclements of  $-1/K$  of  $D_c(j\omega)G(j\omega)$  rather than encirclements of  $-1$  of  $KD_c(j\omega)G(j\omega)$ ?

*If we plot  $D_cG$  alone, then the stability depends on the encirclements of  $-1/K$ . The designer can thus easily look at the entire range of real  $K$  and determine the best value of gain for the design without having to make any more plots.*

- 6.15 Define a conditionally stable feedback system. How can you identify one on a Bode plot?

*A conditionally stable system becomes unstable as gain is reduced. If the low-frequency phase drops below  $-180^\circ$  then a reduction in gain until gain crossover occurs where there is no phase margin, in which case the system is almost surely unstable. A look at the Nyquist plot is necessary to be certain. This condition can also be seen easily from a root locus; the locus will have segments in the RHP for low values of gain.*

- △ 6.16 A certain control system is required to follow sinusoids, which may be any frequency in the range  $0 \leq \omega_t \leq 450$  rad/sec and have amplitudes up to 5 units with (sinusoidal) steady-state error to be never more than 0.01. Sketch (or describe) the corresponding performance function  $W_1(\omega)$ .

The magnitude of  $W_1$  is given by the ratio  $|R|/e_b = 5/0.01 = 500$ . The performance function would then have the value 500 for frequencies up to 450 rad/sec. The Bode magnitude plot would be required to be above this curve for these frequencies.

## Chapter 7

The following questions are based on a system in state-variable form with matrices  $\mathbf{A}$ ,  $\mathbf{B}$ ,  $\mathbf{C}$ , and constant  $D$ , input  $u$ , output  $y$ , and state  $\mathbf{x}$ :

- 7.1 Why is it convenient to write dynamic equations in state-variable form?

*It provides a standard way to describe the differential equations for any dynamic system so that computer-aided analysis can be carried out more conveniently. It is also more convenient to analyze linear systems in terms of the standard description matrices.*

- 7.2 Give an expression for the transfer function of this system.

$$G(s) = \mathbf{C}(s\mathbf{I} - \mathbf{A})^{-1}\mathbf{B} + D.$$

- 7.3 Give two expressions for the poles of the transfer function of the system.

- (a)  $p = \text{eig}(\mathbf{A})$ .
- (b)  $p = \text{roots of } \det[s\mathbf{I} - \mathbf{A}] = a(s) = 0$ .

- 7.4 Give an expression for the zeros of the system transfer function.

$$z = \text{roots of } \det \begin{bmatrix} s\mathbf{I} - \mathbf{A} & -\mathbf{B} \\ \mathbf{C} & D \end{bmatrix} = b(s) = 0.$$

- 7.5 Under what condition will the state of the system be controllable?

- (a) *If the pair  $(\mathbf{A}, \mathbf{B})$  is controllable—that is, if the matrix*

$$\mathcal{C} = [\mathbf{B} \quad \mathbf{AB} \quad \dots \quad \mathbf{A}^{n-1}\mathbf{B}]$$

*is full rank.*

- (b) *If the system can be transformed into control canonical form.*

- 7.6 Under what conditions will the system be observable from the output  $y$ ?

- (a) *If the matrices  $(\mathbf{A}, \mathbf{C})$  are observable—that is, if the matrix*

$$\mathcal{O} = \begin{bmatrix} \mathbf{C} \\ \mathbf{CA} \\ \vdots \\ \mathbf{CA}^{n-1} \end{bmatrix}$$

*has full rank.*

- (b) *If the system can be transformed into observable canonical form.*

7.7 Give an expression for the *closed-loop* poles if state feedback of the form  $u = -\mathbf{Kx}$  is used.

(a)  $p_c = \text{eig}(A - B * K)$ .

(b)  $p_c = \text{roots of } \det(sI - A + BK) = \alpha_c(s) = 0$ .

7.8 Under what conditions can the feedback matrix  $\mathbf{K}$  be selected so that the roots of  $\alpha_c(s)$  are placed arbitrarily?  
*If the system is controllable.*

7.9 What is the advantage of using the LQR or symmetrical root locus in designing the feedback matrix  $\mathbf{K}$ ?  
*With LQR, the closed-loop system will be more robust to parameter changes, and the designer has some control over the control effort used by the closed-loop system.*

7.10 What is the main reason for using an estimator in feedback control?

*When the state is not available (usually because it is too expensive or impractical to put sensors on each state variable), then an estimator using only the output  $y$  can give an estimate that can be used in place of the actual state.*

7.11 If the estimator gain  $\mathbf{L}$  is used, give an expression for the closed-loop poles due to the estimator.

(a)  $p_e = \text{eig}(A - L * C)$ .

(b)  $p_e = \text{roots of } \det(sI - A + LC) = \alpha_e(s) = 0$ .

7.12 Under what conditions can the estimator gain  $\mathbf{L}$  be selected so the roots of  $\alpha_e(s) = 0$  are placed arbitrarily?

*If the system is observable.*

7.13 If the reference input is arranged so the input to the estimator is identical to the input to the process, what will be the overall closed-loop transfer function?

$$T(s) = K_s \frac{b(s)}{\alpha_c(s)}.$$

7.14 If the reference input is introduced in such a way as to permit the zeros to be assigned as the roots of  $\gamma(s)$ , what will the overall closed-loop transfer function be?

$$T(s) = K_s \frac{\gamma(s)b(s)}{\alpha_e(s)\alpha_c(s)},$$

*usually  $\gamma(s) = \alpha_e(s)$ .*

7.15 What are the three standard techniques for introducing integral control in the state-feedback design method?

(a) *By augmenting the process state to include an integrator state variable*

- (b) By the internal-model approach
- (c) By using the extended-estimator approach

## Chapter 8

- 8.1 What is the Nyquist rate? What are its characteristics?  
*The Nyquist rate is half the sample rate, or  $= \omega_s/2$ . Above this rate, no frequencies can be represented by a sampled signal.*
- 8.2 Describe the discrete equivalent design process.  
*The controller for a system is designed as if the controller will be analog. The resulting controller is then approximated by a digital equivalent.*
- 8.3 Describe how to arrive at a  $D_d(z)$  if the sample rate is  $30 \times \omega_{BW}$ .  
*Use the discrete-equivalent design method. It typically yields satisfactory results for such a high sample rate. But after using the discrete equivalent, check the result using a simulation that includes the effect of sampling or else perform an exact discrete linear analysis. It is best to use a simulation that includes all known sampling effects and system delays.*
- 8.4 For a system with a 1 rad/sec bandwidth, describe the consequences of various sample rates.  
*An absolute minimum sample rate is 2 rad/sec (or 0.32 Hz and  $T = 3$  sec). From 2 rad/sec to 10 or 20 rad/sec, the control will be jerky with noticeable steps in the control and the design needs to be done very carefully. Between 20 and 30 rad/sec, the magnitude of the control steps become progressively smaller and design using discrete equivalents works reasonably well. Above 30 rad/sec, the control steps are hardly noticeable and the discrete equivalent can be used with confidence.*
- 8.5 Give two advantages for selecting a digital processor rather than analog circuitry to implement a controller.
- (a) *The physical layout of a digital controller can be done before the final design is complete, often resulting in completing the hardware implementation in much less time than required to get an analog controller specified and constructed.*
  - (b) *A digital processor is more flexible in making design changes as software is easier to reprogram than rewiring and/or adding op-amps to a printed circuit board.*
  - (c) *A digital processor can much more easily include nonlinear terms and logic decision steps in the overall controller design to permit adaptive control or gain scheduling, for example.*
  - (d) *Many models of the same basic controller can be accommodated by simply using different PROMS with the same hardware*

*design. For example, an automobile manufacturer might have one engine controller hardware design for its entire product line; but have a different PROM for each engine/vehicle combination.*

- (e) *Digital controllers are less sensitive to temperature variations than analog controllers.*

8.6 Give two disadvantages of selecting a digital processor rather than analog circuitry to implement a controller.

- (a) *The finite sampling rate of the A/D and D/A converters and the finite computational speed of the processor limit the bandwidth of the controller to about 1/10 of the sample frequency.*
- (b) *The finite accuracy or bit length of the converters introduce extra noise or offsets into the control loop if using low-end controllers.*
- (c) *Cost. For simple controllers, a digital implementation will typically be more expensive than an analog implementation.*

△ 8.7 Describe how to arrive at a  $D_d(z)$  if the sample rate is  $5 \times \omega_{BW}$ .  
*Start by using the discrete equivalent, but include an approximation of the effect of the delay in the plant model when carrying out the analog design. Then check the result via an exact discrete analysis by converting the plant to its discrete equivalent and combining that with the discrete controller. If performance is degraded from that desired, modify the discrete controller using discrete design methods. Finish by using a simulation that includes all known sampling effects and system delays.*

## Chapter 9

9.1 Why do we approximate a physical model of the plant (which is always nonlinear) with a linear model?

*Analysis and design of linear models is vastly simpler than nonlinear models. Furthermore, it has been shown (by Lyapunov) that if the linear approximation is stable, then there is at least some region of stability for the nonlinear model.*

9.2 How would you linearize the nonlinear system equation for radiation heat transfer  $\dot{T} = T^4 + T + u$ ?

$$\delta\dot{T} = (4T_o^3 + 1)\delta T + \delta u,$$

*where  $T_o$  is the nominal operating temperature. (see the RTP case study in Chapter 10.)*

9.3 A lamp used as a thermal actuator has a nonlinearity such that the experimentally measured output power is related to the input voltage by  $P = V^{1.6}$ . How would you deal with such a nonlinearity in feedback control design?

We precede the lamp with an inverse nonlinearity—that is,  $V = P^{0.625}$ —so as to linearize the cascaded system (see the RTP case study in Chapter 10).

#### 9.4 What is integrator windup?

If the plant actuator output signal saturates, then it may take a long time for the error to be brought back to zero from an initial upset and during this time the integrator output may grow or “windup” much more than it would if the system were linear. Special “antiwindup” circuits are designed to prevent windup.

#### 9.5 Why is an antiwindup circuit important?

When a control includes integral action and is subject to saturation, large inputs can cause large overshoots and slow recovering unless an antiwindup circuit is included.

#### 9.6 Using the nonlinear saturation function having gain 1 and limits $\pm 1$ , sketch the block diagram of saturation for an actuator that has gain 7 and limits $\pm 20$ .

If the output of the actuator is  $u_{out}$  and its input is  $u_{in}$ , the control is given by

$$u_{out} = 20 \operatorname{sat}\left(\frac{7u_{in}}{20}\right).$$

#### 9.7 What is a describing function, and how is it related to a transfer function?

The goal of the describing function approach is to find something like a “transfer function” for a nonlinear element. One may view the describing function as an extension of the frequency response to nonlinearities.

#### 9.8 What are the assumptions behind the use of the describing function?

The basic assumption is that the plant behaves approximately as a low-pass filter. The other assumptions are that the nonlinearity is time invariant, and there is a single nonlinear element in the system.

#### 9.9 What is a limit cycle in a nonlinear system?

In some nonlinear systems, the error builds up and the response approaches a periodic solution of fixed amplitude, the limit cycle, as time grows large.

#### 9.10 How can one determine the describing function for a nonlinear system in the laboratory?

One can inject sinusoidal signals into the system and place a low-pass filter with a sharp cutoff at the output of the system to measure the fundamental component of the output. The describing function is then computed as the ratio of the amplitude of the fundamental

*component of the output of the nonlinear system over the amplitude of the sinusoidal input signal.*

- 9.11 What is the minimum-time-control strategy for a satellite attitude control with bounded controls?

*Bang-bang.*

- 9.12 How are the two Lyapunov methods used?

*His indirect or first method is based on linearization of the equations of motion and drawing conclusions about the stability of the nonlinear system by considering the stability of the linear approximation. In his direct or second method, the nonlinear equations are considered directly.*

## Chapter 10

- 10.1 Why is a collocated actuator and sensor arrangement for a lightly damped structure such as a robot arm easier to design than a noncollocated setup?

*In the collocated case, the process naturally has zeros near the lightly damped poles, which keep the root loci in the LHP.*

- 10.2 Why should the control engineer be involved in the design of the process to be controlled?

*In many cases, the characteristics and locations of the actuators and sensors can have a major impact on the complexity and difficulty in design of the controller. If the needs of control are included in the process design, the final systems are often more effective (better closed-loop performance) and less expensive.*

- 10.3 Give examples of an actuator and a sensor for the following control problems:

- (a) Attitude control of a geosynchronous communication satellite

*Actuators: Cold gas-jet thrusters, momentum wheels, magnetic torquers (coils, torque rod), plasma thruster*

*Sensors: Earth sensor (roll, pitch), digital integrated rate assembly (DIRA) gyro (for rates), star tracker*

- (b) Pitch control of a Boeing 747 airliner

*Actuators: Elevator*

*Sensors: Pitch rate and/or pitch angle is measured using a gyro or a ring-laser gyro*

- (c) Pitch control of a quadcopter:

*Actuators: the #1 and #3 rotor motors as defined by Fig. 2.14*

*Sensor: usually a gyro measuring the angular motion about the  $y$ -axis*

- (d) Fuel-air ratio control of a spark-ignited automobile engine

*Actuators: Fuel injection*

*Sensors: Zirconium oxide sensor*

- (e) Position control for an arm of a robot used to paint automobiles

*Actuators: Hydraulic actuators or electric motors*

*Sensors: Encoders to measure arm rotations, pressure sensors, and force sensors*

- (f) Heading control of a ship

*Actuators: Rudder*

*Sensors: Gyrocompass*

- (g) Attitude control of a helicopter

*Actuators: Moving swash plate (either via direct link or servo rotates main blade angle of attack)*

*Sensors: Same as aircraft (pitot tube, accelerometers, rate gyros)*

# Appendix C Matlab Commands

Matlab function (.m file) or Variable	Description	Page (s)
\	Backslash or left matrix divide	600, 601
A(:)	Vectorize matrix A	
allmargin	All stability margins and crossover frequencies	
abs	Absolute value	
acker	Ackermann's formula for pole placement	515, 523, 536, 540
angle	Phase angle	
ans	Most recent answer	
atan	Inverse tangent	
atan2	Four quadrant inverse tangent	
atan2d	Four quadrant inverse tangent, result in degrees	
axis	Control axis scaling	313, 314, 358, 389
bilin	Bilinear transform	
bode	Bode frequency response	124, 358, 373, 443
bodemag	Bode magnitude frequency response	
break	Terminate execution of WHILE or FOR loop	
c2d	Continuous-to-discrete conversion	649, 652, 672
canon	State-space canonical forms	502
clear	Clear variables and functions	
clc	Clear command window	
clf	Clear current figure	
close	Close figure	
close all	Close all figures	
colon(:)	Create vector of indices or reshape matrices	63
conj	Complex conjugate	
conv	Polynomial multiplication	134, 875, 877
cos	Cosine	
cross	Cross product of the vectors	
ctrb	Controllability matrix	
ctrbf	Staircase canonical form, controllability	619
damp	Damping and natural frequency	673
dcgain	Computes DC gain of LTI system	
deconv	Division of polynomials	

Matlab function (.m file) or Variable	Description	Page (s)
delete	Delete file or graphics object	
det	Determinant of a matrix	
diag	Diagonal matrix, diagonals of a matrix	
diary	Save text of Matlab session	
disp	Displays the array	
dlyap	Solution to discrete-time Lyapunov equation	
dot	Vector dot product	
dstep	Step response of a discrete system	
d2c	Discrete to continuous-time model	
eig	Eigenvalues and eigenvectors	501, 502, 891
eigs	Find a few eigenvalues and eigenvectors	
eps	Precision parameter	
eval	Execute string with Matlab expression	
exp	Exponential	
expm	Matrix exponential	
eye	Identity matrix	
ezplot	Easy to use function plotter	182
feedback	Feedback connection of two systems	150, 305, 318
feval	Execute the specified function	
figure	Create figure window	
figure(i)	Make i the current figure, or create figure i	
find	Find indices of nonzero elements	
format	Set output format	
freqresp	Frequency response of LTI systems	
function	Add new function	801
gensig	Generate signals	
gram	Controllability/observability Gramian	
grid	Grid lines	305, 313, 314, 315
gtext	Place text with mouse	
help	Display help text in Command Window	
hold	Hold current hold, toggles hold state	
i	$\sqrt{-1}$	
ilaplace	Inverse Laplace transform	872, 876, 877
imag	Complex imaginary part	
impulse	Impulse response of LTI system	154, 158, 170, 537
impulseplot	Plot impulse response and return handle	
inf	Infinity	
input	Prompt for user input	
initial	Initial-condition response of state-space system	537, 543
inv	Matrix inverse	501, 502
j	$\sqrt{-1}$	523, 553, 555, 787

<b>Matlab function (.m file) or Variable</b>	<b>Description</b>	<b>Page (s)</b>
kron	Kronecker tensor product	586
laplace	Laplace transform	868, 869, 874
length	Length of vector	
linmod	Linearization	688
linmod2	Linearization (advanced)	688
line	Create a line	
linspace	Create linearly spaced vector	
load	Load in workspace variables	
log	Natural logarithm	
log10	Logarithm to the base 10	
loglog	Log-log plot	124, 358, 373, 417
logspace	Create logarithmically spaced vector	124, 358, 596
lqe	Linear Quadratic Estimator design	596, 827
lqr	Linear Quadratic Regulator design	531, 596, 827
lqry	Linear Quadratic Regulator design with output weighting	
lsim	Simulation of LTI system with arbitrary input	143, 144
ltiview	Opens the LTI viewer GUI	
ltru	Loop transfer recovery (LTR)	597
ltry	Loop transfer recovery (LTR)	597
lyap	Solution to continuous-time Lyapunov equation	
margin	Gain and phase margins	417, 462, 596
max	Largest component	443
mean	Average or mean value	
median	Median value	
min	Smallest component	
minreal	Minimal realization of a system	
nan	Not-a-number	
ngrid	Nichol's chart grid	
nichols	Nichol's chart	447
norm	Matrix or vector norm	
nyquist	Nyquist plot	385, 389, 392
obsv	Observability matrix	
obsvf	Staircase canonical form, observability	619
ones	Array of ones	143, 144
ord2	Generate continuous second-order system	
ode23	Solution to nonstiff differential equations	

Matlab function (.m file) or Variable	Description	Page (s)
ode45	Solution to nonstiff differential equations	
pade	Pade approximation for time delay	
parallel	Parallel connection of two LTI systems	150
pause	Wait for user response	
place	Pole placement	517, 553, 556, 559, 578
pi	3.141592653589793	143, 144
pid	Create a PID controller in parallel form	
pidstd	Create a PID controller in standard form	
pidtune	Designs a PID controller	
pidTuner	PID Tuner app	241
plot	Plot function	63, 141, 143, 144
pole	Poles of LTI system	
poly	Form polynomial from its roots	138
polyfit	Fit polynomial to data	
polyval	Evaluate polynomial	
prescale	Optimal scaling of state-space models	
print	Print figure or model	
printsys	Print system in pretty format	
pzmap	Pole-zero map	
rand	Uniformly distributed random numbers	152
randn	Normally distributed random numbers	
rank	Matrix rank	
readtable	Create a table by reading from a file	
real	Complex real part	
reshape	Reshape array	
residue	Residues in partial fraction expansion	134, 138, 875, 877
return	Return to invoking function	
rlocfind	Find root-locus gain	298, 464
rlocus	Root locus	284, 289, 291, 292
rlocusplot	Plot root locus and return handle	
sisotool	Opens sisotool for root-locus design	294
roots	Roots of a polynomial	179, 180, 182, 507, 517
save	Save workspace variables	
semilogx	Semi-log plot	124, 358, 373, 417, 596
semilogy	Semi-log plot	

<b>Matlab function (.m file) or Variable</b>	<b>Description</b>	<b>Page (s)</b>
series	Series connection of two LTI systems	150, 596, 672, 673
sgrid	s-plane grid lines	
shg	Show graph window	
sign	Signum function	
sin	Sine	
sim	Simulate a Simulink model	
sisotool	SISO design tool	294
size	Size of an array	
sort	Sort in ascending or descending order	
sprintf	Write formatted data to string	
sqrt	Square root	578
squeeze	Remove singleton dimensions	124, 358, 373, 417
std	Standard deviation	
ss2tf	State space to transfer function conversion	490, 504, 507, 783
ss2zp	State space to pole-zero conversion	490
ss	Conversion to state space	485, 502, 506, 507, 595
ssdata	Create a state space model	502
std	Standard deviation	
step	Step response	50, 63, 141, 181, 672
stepinfo	Returns information on the step response	
subplot	Multiple plots on the same window	
sum	Sum of elements	
svd	Singular value decomposition	
syms	Declaration of symbolic variables	868, 869, 872, 874
table	Create a table from Matlab variables	
tan	Tangent of argument in radians	
text	Text annotation	
tf2ss	Transfer function to state space conversion	492
tf2zp	Transfer function to pole-zero conversion	490
tf	Creation or conversion to transfer function	50, 63, 124, 140, 141
tfdata	Transfer function data	
title	Plot title	
tzero	Transmission zeros and gain for SISO systems	506, 507
var	Variance	
what	List Matlab-specific files in directory	
who	List of current variables	

Matlab function (.m file) or Variable	Description	Page (s)
why	Answers any question you may have	
whos	List of current variables, long form	
xlabel	x-axis label	
xlim	x-axis limits	
xlsread	Get data from an Excel spreadsheet	
ylabel	y-axis label	
ylim	y-axis limits	
zero	Transmission zeros and gain for SISO systems	140, 141
zeros	Array of zeros	143, 144
zgrid	z-plane grid lines	
zlabel	z-axis label	
zlim	z-axis limits	
zpk	Zero-pole-gain	
zp2ss	Zero-pole to state-space conversion	
zp2tf	Zero-pole to transfer function conversion	

# Bibliography

- Ackermann, J., “Der entwurf linearer regelungssysteme im zustand-  
raum,” *Regelungstech. Prozess-Datenverarb.*, Vol. 7, pp. 297–300,  
1972.
- Airy, G. B., “On the regulator of the clock-work for effecting uniform  
movement of equatorials,” *Mem. R. Astron. Soc.*, Vol. 11, pp. 249–267,  
1840.
- Alon, U., *An Introduction to Systems Biology*. Boca Raton, FL:  
Chapman & Hall/CRC, 2007.
- Alon, U., M. G. Surette, N. Barkai, and S. Leibler, “Robustness in  
bacterial chemotaxis,” *Nature*, Vol. 397, pp. 168–171, January 1999.
- Anderson, B. D. O. and J. B. Moore, *Optimal Control: Linear Quadratic  
Methods*. Upper Saddle River, NJ: Prentice Hall, 1990.
- Åström, K. J., *Introduction to Stochastic Control Theory*. Princeton, NJ:  
Academic Press, 1970.
- Åström, K. J., “Frequency domain properties of Otto Smith regula-  
tors,” *International Journal of Control*, Vol. 26, No. 2, pp. 307–314,  
1977.
- Åström, K. J. and T. Hägglund, *PID Controllers: Theory, Design,  
and Tuning*, 2nd ed., Research Triangle, NC: International Society for  
Measurement and Control, 1995.
- Åström, K. J. and T. Hägglund, *Advanced PID Control*. Research  
Triangle, NC: International Society for Measurement and Control,  
2006.
- Åström, K. J. and Kumar, P. R., “Control: A Perspective,” *Automatica*,  
Vol. 50, No. 3, 2014.
- Athans, M., “A tutorial on the LQG/LTR method,” *Proceedings of the  
American Control Conference*, Seattle, WA, pp. 1289–1296, June 1986.
- Barkai, N. and S. Leibler, “Robustness in simple biochemical net-  
works,” *Nature*, Vol. 387, pp. 913–917, 1997.
- Bellman, R. and R. Kalaba, eds., *Mathematical Trends in Control  
Theory*. New York: Dover, 1964.
- Berg, H. C., *E. coli in Motion*. New York, NY: Springer-Verlag, 2004.
- Berg, H. C. and D. A. Brown, “Chemotaxis in *Escherichia coli* ana-  
lyzed by three-dimensional tracking,” *Nature*, Vol. 239, pp. 500–504,  
1972.
- Bergamasco, M. and M. Lovera, “Identification of Linear Models for  
the Dynamics of a Hovering Quadrotor,” *IEEE Trans. Control Systems  
Technology*, Vol. 22, No. 5, pp. 1696–1707, September 2014.

- Bergen, A. R. and R. L. Franks, "Justification of the describing function method," *SIAM J. Control*, Vol. 9, pp. 568–589, 1971.
- Berrios, M. G., et al, "Hover Flight Control Design for UAS Using Performance-based Disturbance Rejection Requirements," presented at 73rd Annual Forum, American Helicopter Society, 2017.
- Blakelock, J. H., *Automatic Control of Aircraft and Missiles*. 2nd ed., New York: John Wiley, 1991.
- Bodenis, D., *E = MC<sup>2</sup>: A Biography of the World's Most Famous Equation*. New York: Walker and Co., 2000.
- Bode, H. W., *Network Analysis and Feedback Amplifier Design*. New York: Van Nostrand, 1945.
- Bode, H. W., "Feedback: The history of an idea," *Conference on Circuits and Systems*. New York (1960): Reprinted in Bellman and Kalaba, 1964.
- Boyd, S. P. and C. H. Barratt, *Linear Controller Design: Limits of Performance*. Upper Saddle River, NJ: Prentice Hall, 1991.
- Brennan, R. P., *Heisenberg Probably Slept Here*. New York, NY: John Wiley & Sons, 1997.
- Briegel, A. et al., "Bacterial chemoreceptor arrays are hexagonally packed trimers of receptor dimers networked by rings of kinase and coupling proteins," *PNAS*, Vol. 109, No. 19, pp. 3766–3771, March 2012.
- Brown, J. W. and R. V. Churchill, *Complex Variables and Applications*. 6th ed., New York, NY: McGraw-Hill, 1996.
- Bryson, A. E., Jr., *Control of Spacecraft and Aircraft*. Princeton, NJ: Princeton University Press, 1994.
- Bryson, A. E., Jr. and W. F. Denham, "A steepest-ascent method for solving optimum programming problems," *J. Appl. Mech.*, Vol. 29, pp. 247–257, June 1962.
- Bryson, A. E., Jr. and Y. C. Ho, *Applied Optimal Control*. Waltham, MA: Blaisdell, 1969.
- Callender, A., D. R. Hartree, and A. Porter, "Time lag in a control system," *Philos. Trans. R. Soc. London A*, London, UK: Cambridge University Press, 1936.
- Campbell, G. A. and R. N. Foster, *Fourier Integrals for Practical Applications*. New York, NY: Van Nostrand, 1948.
- Campbell, N. A. and J. B. Reece, *Biology*. 8th ed., Benjamin Cummings, 2008.
- Cannon, R. H., Jr., *Dynamics of Physical Systems*. New York, NY: McGraw-Hill, 1967.
- Chien, K. L., J. A. Hrones, and J. B. Reswick, "On the automatic control of generalized passive systems," *Trans. ASME*, 74, pp. 175–185, 1952.

- Churchill, R. V., *Operational Mathematics*. 3rd ed., New York, NY: McGraw-Hill, 1972.
- Clark, R. N., *Introduction to Automatic Control Systems*. New York, NY: John Wiley, 1962.
- Clegg, J. C., "A nonlinear integrator for servomechanisms," *Trans. AIEE*, Pt. II, Vol. 77, pp. 41–42, 1958.
- Cohen, G. H. and G.A. Coon, "Theoretical Consideration of Retarded Control," *Trans. ASME*, 75, pp. 827–834, 1953.
- de Roover, D., A. Emami-Naeini, and J. L. Ebert, "Model-based control of fast-ramp RTP systems," *Sixth International Conference on Advanced Thermal Processing of Semiconductors*, pp. 177–186, Kyoto, Japan, September 1998.
- de Roover, D., L. Porter, A. Emami-Naeini, J. A. Marohn, S. Kuehn, S. Garner, and D. Smith, "An all-digital cantilever controller for MRFM and scanned probe microscopy using a combined DSP/FPGA design," *Am. Lab.*, Vol. 40, No. 8, pp. 12–17, 2008.
- de Vries, G., T. Hillen, M. Lewis, J. Muller, and B. Schonfisch, *A Course in Mathematical Biology*. SIAM, 2006.
- Dorato, P., *Analytic Feedback System Design: An Interpolation Approach*. Pacific Grove, CA: Brooks/Cole, 2000.
- Doyle, J. C., "Guaranteed margins for LQG regulators," *IEEE Trans. Autom. Control*, Vol. AC-23, pp. 756–757, 1978.
- Doyle, J. C. and G. Stein, "Robustness with observers," *IEEE Trans. Autom. Control*, Vol. AC-24, pp. 607–611, August 1979.
- Doyle, J. C. and G. Stein, "Multivariable feedback design: Concepts for a classical/ modern synthesis," *IEEE Trans. Autom. Control*, Vol. AC-26, No. 1, pp. 4–16, February 1981.
- Doyle, J. C., B. A. Francis, and A. Tannenbaum, *Feedback Control Theory*. New York, NY: Macmillan, 1992.
- Ebert, J. L., A. Emami-Naeini, and R. L. Kosut, "Thermal Modeling and control of rapid thermal processing systems," *Proceeding 34th IEEE Conference Decision and Control*, pp. 1304–1309, December 1995b.
- Ebert, J. L., A. Emami-Naeini, H. Aling, and R. L. Kosut, "Thermal modeling of rapid thermal processing systems," *Third International Rapid Thermal Processing Conference*, pp. 343–355, Amsterdam, Netherlands, August 1995a.
- Elgerd, O. I., *Electric Energy Systems Theory*. New York, NY: McGraw-Hill, 1982.
- Elgerd, O. I. and W. C. Stephens, "Effect of closed-loop transfer function pole and zero locations on the transient response of linear control systems," *Trans. Am. Inst. Electr. Eng. Part 1*, Vol. 42, pp. 121–127, 1959.

- Emami-Naeini, A., "The shapes of Nyquist plots: Connections with classical plane curves," *IEEE Control Systems Magazine*, pp. 102–115, October 2009.
- Emami-Naeini, A. and G. F. Franklin, "Zero assignment in the multi-variable robust servomechanism," *Proc. IEEE Conf. Dec. Control*, Vol. 21, pp. 891–893, December, 1982.
- Emami-Naeini, A., and P. Van Dooren, "Computation of zeros of linear multivariable systems," *Automatica*, Vol. 18, No. 4, pp. 415–430, 1982.
- Emami-Naeini, A., and P. Van Dooren, "On computation of transmission zeros and transfer functions," *Proc. IEEE Conf. Dec. Control*, pp. 51–55, December 1982.
- Emami-Naeini, A., J. L. Ebert, D. de Roover, R. L. Kosut, M. Dettori, L. Porter, and S. Ghosal, "Modeling and control of distributed thermal systems," *Proc. IEEE Trans. Control Systems Technol.*, Vol. 11, No. 5, pp. 668–683, September 2003.
- Etkin, B. and L. D. Reid, *Dynamics of Flight: Stability and Control*. 3rd ed., New York, NY: John Wiley, 1996.
- Evans, G. W., "Bringing root locus to the classroom," *IEEE Control Systems Magazine*, Vol. 24, pp. 74–81, 2004.
- Francis, B. A. and W. M. Wonham, "The internal model principle for linear multivariable regulators," *J. Appl. Maths. Optimization*, pp.170–194, 1975.
- Franklin, G. F., J. D. Powell, M. Workman, *Digital Control of Dynamic Systems*. 3rd ed., Half Moon Bay, CA: Ellis-Kagle Press, 1998.
- Freudenberg, J. S. and D. P. Looze, "Right half plane zeros and design tradeoffs in feedback systems," *IEEE Trans. Autom. Control*, Vol. AC-30, pp. 555–561, June 1985.
- Fuller, A. T., "The Early development of control theory," *J. Dyn. Syst. Meas. Control*, Vol. 98, pp. 109–118 and 224–235, 1976.
- Gardner, M. F. and J. L. Barnes, *Transients in Linear Systems*. New York, NY: John Wiley, 1942.
- Greenwood, D. T., *Principles of Dynamics*, 2nd ed, Englewood Cliffs, NJ: Prentice-Hall, 1988.
- Gunckel, T. L., III and G. F. Franklin, "A general solution for linear sampled data control," *J. Basic Eng.*, Vol. 85-D, pp. 197–201, 1963.
- Gyugyi, P., Y. Cho, G. F. Franklin, and T. Kailath, "Control of rapid thermal processing: A system theoretic approach," *Proceedings of IFAC World Congress*, 1993.
- Hanselman, D. C. and B. C. Littlefield, *Mastering MATLAB*. Upper Saddle River, NJ: Pearson, 2012.

- Hast, M., K. J. Åström, B. Bernhardsson, and S. Boyd, "PID Design by Convex-Concave Optimization," *Proc. European Control Conference*, pp. 4460–4465, July 2013.
- Heffley, R. K. and W. F. Jewell, *Aircraft Handling Qualities*, Technical Report 1004–1, System Technology, Inc., Hawthorne, CA, May 1972.
- Higham, D. J. and N. J. Higham, *MATLAB Guide*. 2nd ed., Philadelphia, PA: SIAM, 2005.
- Ho, M.-T., A. Datta, and S. P. Bhattacharyya, "An elementary derivation of the Routh- Hurwitz criterion," *IEEE Trans. Autom. Control*, Vol. 43, No. 3, pp. 405–409, 1998.
- Horowitz, I. M. and M. Sidi, *Quantitative Feedback Theory (QFT)*, QFT Publications, 4470 Grinnell Ave., Boulder, CO 80303, 1992.
- Huang, J-J. and D. B. DeBra, "Automatic tuning of Smith-predictor design using optimal parameter mismatch," *Proc. IEEE Conf. Dec. Contr.*, pp. 3307–3312, December 2000.
- Hubbard, M., Jr. and J. D. Powell, "Closed-loop control of internal combustion engine exhaust emissions," SUDAAR No. 473, Department of Aero/Astro, Stanford University, Stanford, CA, February 1974.
- James, H. M., N. B. Nichols, and R. S. Phillips, *Theory of Servomechanisms*. Radiation Lab. Series, 25. New York, NY: McGraw-Hill, 1947.
- Johnson, R. C., Jr., A. S. Foss, G. F. Franklin, R. V. Monopoli, and G. Stein, "Toward development of a practical benchmark example for adaptive control," *IEEE Contr. Syst. Mag.*, Vol. 1, No. 4, pp. 25–28, December 1981.
- Joseph, P. D. and J. T. Tou., "On linear control theory," *AIEE Transactions*, Vol. 80, pp. 193–196, 1961.
- Kailath, T., *Linear Systems*. Upper Saddle River, NJ: Prentice Hall, 1980.
- Kalman, R. E., "A new approach to linear filtering and prediction problems," *J. Basic Eng.*, Vol. 85, pp. 34–45, 1960a.
- Kalman, R. E., "Lyapunov functions for the problem of lur'e in automatic control," *Proc. Nat. Acad. Sci.*, Vol. 49, pp. 201–205, 1963.
- Kalman, R. E. and J. E. Bertram, "Control system analysis and design via the second method of Lyapunov. II. Discrete Systems," *J. Basic Eng.*, Vol. 82, pp. 394–400, 1960.
- Kalman, R. E., Y. C. Ho, and K. S. Narendra, "Controllability of linear dynamical systems," *Contrib. Diff. Eq.*, Vol. 1. New York, NY: John Wiley, 1962.
- Khalil, H. K., *Nonlinear Systems*. 3rd ed., Upper Saddle River, NJ: Prentice Hall, 2002.

- Kharitonov, V. L., "Asymptotic stability of an equilibrium position of a family of systems of linear differential equations," *Differential'nye Uravneniya*, Vol. 14, pp. 1483–1485, 1978.
- Kochenburger, R. J., "A frequency response method for analyzing and synthesizing contactor servomechanisms," *Trans. Am. Inst. Electr. Eng.*, Vol. 69, pp. 270–283, 1950.
- Kuo, B. C., ed., *Incremental Motion Control, Vol. 2: Step Motors and Control Systems*. Champaign, IL: SRL Publishing, 1980.
- Kuo, B. C., ed., *Proceedings of the Symposium Incremental Motion Control Systems and Devices, Part. 1: Step Motors and Controls*. Champaign-Urbana, IL: University of Illinois, 1972.
- Lanchester, F. W., *Aerodonetics*. London, UK: Archibald Constable, 1908.
- LaSalle, L. P. and S. Lefschetz, *Stability by Lyapunov's Direct Method*. New York, NY: Academic Press, 1961.
- Luyben, W. L. and M. L. Luyben, *Essentials of Process Control*, McGraw-Hill, New York, NY, 1997.
- Lyapunov, A. M., "Problème général de la stabilité du mouvement," *Ann. Fac. Sci. Univ. Toulouse Sci. Math. Sci. Phys.*, Vol. 9, pp. 203–474, 1907; original paper published in 1892 in *Commun. Soc. Math. Kharkow*, 1892; reprinted as Vol. 17 in *Annals of Math Studies*. Princeton, NJ: Princeton University Press, 1949.
- Ljung, L., *System Identification: Theory for the User*. 2nd ed., Upper Saddle River, NJ: Prentice Hall, 1999.
- Luenberger, D. G., "Observing the state of a linear system," *IEEE Trans. Mil. Electron.*, Vol. MIL-8, pp. 74–80, 1964.
- Mahon, B., *The Man who Changed Everything: The Life of James Clerk Maxwell*. UK: Wiley, 2003.
- Marsden, J. E. and M. J. Hoffman, *Basic Complex Analysis*. 3rd ed., Freeman, 1999.
- Mason, S. J., "Feedback theory: Some properties of signal flow graphs," *Proc. IRE*, Vol. 41, pp. 1144–1156, 1953.
- Mason, S. J., "Feedback theory: Further properties of signal flow graphs," *Proc. IRE*, Vol. 44, pp. 920–926, 1956.
- Maxwell, J. C., "On governors," *Proc. R. Soc. Lond.*, Vol. 16, pp. 270–283, 1868.
- Mayr, O., *The Origins of Feedback Control*. Cambridge, MA: MIT Press, 1970.
- McRuer, D. T., I. Askenas, and D. Graham, *Aircraft Dynamics and Automatic Control*. Princeton, NJ: Princeton University Press, 1973.

- Mello, B. A., L. Shaw, and Y. Tu, "Effects of receptor interaction in bacterial chemotaxis," *Biophys. J.*, Vol. 87, pp. 1578–1595, September 2004.
- Minimis, G. S. and C. C. Paige, "An algorithm for pole assignment of time invariant systems," *Int. J. Control.*, Vol. 35, No. 2, pp. 341–354, 1982.
- Moler, C. B., "Nineteen dubious ways to compute the exponential of a matrix, twenty-five years later," *SIAM Rev.*, Vol. 45, No. 1, pp. 3–49, 2003.
- Moler, C. B., *Numerical Computing with MATLAB*. Philadelphia, PA: SIAM, 2004.
- Norman, S. A., "Wafer temperature control in rapid thermal processing," Ph.D. Dissertation, Stanford University, Stanford, CA, 1992.
- Nyquist, H., "Regeneration theory," *Bell Systems Technical J.*, Vol. 11, pp. 126–147, 1932.
- Parks, P., "Lyapunov redesign of model reference adaptive control systems," *IEEE Trans. Autom. Control*, AC-11, No. 3, 1966.
- Perkins, W. R., P. V. Kokotovic, T. Boureret, and J. L. Schiano, "Sensitivity function methods in control system education," *IFAC Conference on Control Education*, June 1991.
- Ragazzini, J. R. and G. F. Franklin, *Sampled-Data Control Systems*. New York, NY: McGraw-Hill, 1958.
- Ragazzini, J. R., R. H. Randall, and F. A. Russell, "Analysis of problems in dynamics by electronic circuits," *Proc. IRE*, Vol. 35, No. 5, pp. 442–452, May 1947.
- Reliance Motion Control Corp., *DC Motor Speed Controls Servo Systems*. 5th ed., Eden Prairie, MN: Reliance Motion Control Corp., 1980.
- Routh, E. J., *Dynamics of a System of Rigid Bodies*. London, UK: MacMillan, 1905.
- Saberi, A., B. M. Chen, and P. Sannuti, *Loop Transfer Recovery: Analysis and Design*. New York: Springer-Verlag, 1993.
- Safonov, M. G. and G. Wyetzner, "Computer-aided stability analysis renders Popov criterion obsolete," *IEEE Trans. Autom. Control*, Vol. AC-32, pp. 1128–1131, 1987.
- Sandberg, I. W., "A frequency domain condition for stability of feedback systems containing a single time varying nonlinear element," *Bell Systems Technical J.*, Vol. 43, pp. 1581–1599, 1964.
- Sastry, S. S., *Nonlinear Systems; Analysis, Stability, and Control*. New York, NY: Springer-Verlag, 1999.
- Schmitz, E., "Robotic arm control," Ph.D. Dissertation, Stanford University, Stanford, CA, 1985.

- Sedra, A. S. and K. C. Smith, *Microelectronics Circuits*. 3rd ed., New York, NY: Oxford University Press, 1991.
- Simon, H. A., "Dynamic programming under uncertainty with a quadratic function," *Econometrica*, Vol. 24, pp. 74–81, 1956.
- Sinha, N. K. and B. Kuszta, *Modeling and Identification of Dynamic Systems*. New York, NY: Van Nostrand, 1983.
- Smith, O. J. M., *Feedback Control Systems*. New York, NY: McGraw-Hill, 1958.
- Sobel, D., *Galileo's Daughter*. New York, NY: Penguin Books, 2000.
- Stein, G. and M. Athans, "The LQG/LTR procedure for multivariable feedback control design," *IEEE Trans. Autom. Control*, Vol. AC-32, pp. 105–114, February 1987.
- Strang, G., *Linear Algebra and Its Applications*. 4th ed., Pacific Grove, CA: Cengage Learning, 2006.
- Swift, J., *On Poetry: A Rhapsody*, 1733, J. Bartlett, ed., *Familiar Quotations*. 15th ed., Boston, MA: Little Brown, 1980.
- Sze, S. M., ed. *VLSI Technology*. 2nd ed., New York, NY: McGraw-Hill, 1988.
- Taubman, P., *Secret Empire: Eisenhower, the CIA, and the Hidden Story of America's Space Espionage*. New York, NY: Simon and Schuster, 2003.
- Thomson, W. T. and M. D. Dahleh, *Theory of Vibration with Applications*. 5th ed., Upper Saddle River, NJ: Prentice Hall, 1998.
- Tischler, M. B., *Aircraft and Rotorcraft System Identification*. 2nd ed., Reston, VA: AIAA Education Series, 2012.
- Trankle, T. L., "Development of WMEC Tampa maneuvering model from sea trial data," Report MA-RD-760-87201. Palo Alto, CA: Systems Control Technology, March 1987.
- Trankle, T. L. and A. E. Bryson, Jr., "Control Logic to Track The Outputs of a Command Generator or Randomly Forced Target," *Journal of Guidance and Control*, Vol. 1, No. 2, pp. 130–135, 1978.
- Truxal, J. G., *Control System Synthesis*. New York, NY: McGraw-Hill, 1955.
- Ulsoy, A. G., H. Peng, and M. Cakmakci, *Automotive Control Systems*. New York, NY: Cambridge University Press, 2012.
- van der Linden, G., J. L. Ebert, A. Emami-Naeini, and R. L. Kosut "RTP robust control design: Part II: controller synthesis," *Fourth International Rapid Thermal Processing Conference*, pp. 263–271, September 1996.
- Van der Pol, B. and H. Bremmer, *Operational Calculus*. New York, NY: Cambridge University Press, 1955.

- Van Dooren, P., A. Emami-Naeini, and L. Silverman, "Stable Extraction of the Kronecker Structure of Pencils," *Proc. IEEE Conf. Dec. Control*, San Diego, CA, pp. 521–524, December 1978.
- Vidyasagar, M., *Nonlinear Systems Analysis*. 2nd ed., Upper Saddle River, NJ: Prentice Hall, 1993.
- Wiener, N., "Generalized harmonic analysis," *Acta Math.*, Vol. 55, pp. 117, 1930.
- Woodson, H. H. and J. R. Melcher, *Electromechanical Dynamics, Part I: Discrete Systems*. New York, NY: John Wiley, 1968.
- Workman, M. L., "Adaptive proximate time-optimal servomechanisms," Ph.D. Dissertation, Stanford University, Stanford, CA, 1987.
- Yakubovich, V. A., "Solution of certain matrix inequalities in the stability theory of nonlinear control systems," *Dokl. Akad. Nauk. SSSR*, Vol. 143, pp. 620–623, 1962.
- Yang, L. and P. A. Iglesias, "Feedback induced biphasic response in the chemotaxis pathway of Dictyostelium," in *American Control Conf.* (Portland, OR), pp. 4393–4398, June 2005.
- Yi, T.-M., Y. Huang, M. I. Simon, and J. C. Doyle, "Robust perfect adaptation in bacterial chemotaxis through integral feedback control," *PNAS*, Vol. 97, No. 9, pp. 4649–4653, April 2000.
- Zames, G., "On the input-output stability of time-varying nonlinear feedback systems—Part I: Conditions derived using concepts of loop gain, conicity and positivity," *IEEE Trans. Autom. Control*, Vol. AC-11, pp. 465–476, 1966.
- Zames, G., "On the input-output stability of time-varying nonlinear feedback systems—Part II: Conditions involving circles in the frequency plane and sector nonlinearities," *IEEE Trans. Autom. Control*, Vol. AC-11, pp. 228–238, 1966.
- Ziegler, J. G. and N. B. Nichols, "Optimum settings for automatic controllers," *Trans. ASME*, Vol. 64, pp. 759–768, 1942.
- Ziegler, J. G. and N. B. Nichols, "Process lags in automatic control circuits," *Trans. ASME*, Vol. 65, No. 5, pp. 433–444, July 1943.

# Index

## A

Abscissa of convergence, 865  
Ackermann's formula  
in estimator form, 539  
pole placement, 514  
undamped oscillator,  
514–515  
AC motor actuators, 80  
Activity, *E. coli*, 834–843  
Actuators, 26, 755, 760, 790  
AC motor, 80–81  
DC motor, 78  
rapid thermal processing  
(RTP) system, 819–820  
Actuator saturation, feedback  
system with, 701  
Adams prize, 37  
Adaptation, biological, 839–841  
Adaptive control, 728–731, 738  
Additional poles effect of, 164,  
172–174  
Agilent Technologies, 358n1  
Aircraft control, 316, 778  
design procedure, 782  
lateral, 781  
longitudinal, 790  
nonlinear equations, 778  
Aircraft coordinates, 778  
Aircraft response, 170  
Airy, G. B., 36, 248  
Aizerman's conjecture, 733  
Aliasing, 645, 661  
Alternating current (AC)  
induction motor, 80–81  
Altimeter, 471, 790, 795  
Altitude-hold autopilot,  
789–795  
Amplitude ratio, 123–124,  
126–127  
Amplitude scaling, 130, 184  
Amplitude stabilization, 434  
Analog computer components,  
489  
Analog implementation, 312  
Analog prefilters, 637, 661

Analog realization, 312  
Analog-to-digital (A/D)  
converters, 637, 660  
Analysis tools, 637, 667–668  
Analytic continuation, 866  
Angular velocity, 82  
Anti-alias prefilters, 661–662  
Anti-windup compensation for  
PI controller, 703–706  
Apollo, 607, 675, 844  
Arbitrary zero assignment, 564  
Argument principle, 379–380  
application of, 380–383  
Armature voltage, 79–82  
Arrival angles, rule for, 282  
Artificial intelligence (AI), 28  
Assigned zeros, 563  
Åström, Karl, 239n6, 675  
Asymptotes  
Angle of, 279, 280  
center of, 279, 281  
for negative locus, 323  
Asymtotically stable Lyapunov,  
723  
Asynchronous sampling, 666  
Athans, M., 593, 607  
Attitude hold, 792  
Attractant, biological,  
837–839  
Augmented state equations with  
integral control, 611  
Automatic control, 23  
Automatic landing and collision  
avoidance systems, 24  
Automobile suspension, 51  
Automotive engine, control of  
fuel-air ratio in, 795–803  
Automotive fuel/air ratio,  
control of, 795–803  
Autonomous estimator, 561  
example, 563, 565  
Autopilot design, via root locus,  
316–323  
via state-space, 777–795  
Auxiliary variable, 511

## B

Back emf voltage, 79–80  
Bacteria, 834–837  
Bacterial chemotaxis, 837  
Ball levitator, 689  
Band center, 154n10  
Band reject filter, 764  
Bandwidth, 71, 360  
Bang-bang control, 721–723  
Barkai, N., 837  
Barometric altimeter, 790  
Battin, Dick, 675, 844  
Bell, Alexander Graham, 363n3  
Bell Laboratories, 363  
Bellman, R., 39  
Berg, H., 835  
Bertram, J. E., 686, 728, 737  
BIBO stability, 174  
Bilateral Laplace transforms,  
866n1  
Bilinear approximation, 648  
Binary fission, 835  
Biological systems, 834,  
843–845  
Black, H. S., 37, 249, 450  
Block diagram, 26–29, 145–148  
Blocking zeros, 580  
Bode, H.W., 37–39, 123, 249,  
362, 450  
Bode plots, 124, 354–359  
for nonminimum phase, 374  
plotting techniques, 362–373  
Bode's gain-phase relationship,  
402–407  
Boeing 769, lateral and  
longitudinal control of a,  
777–795  
altitude-hold autopilot,  
789–795  
equations of motion, 777–778  
linearized longitudinal motion  
equations, 780  
stability augmentation, 778  
yaw damper, 782–789

- Bounded input-bounded output(BIBO) stability, 174–175
- Boyd, S. P., 597
- Brahe, Tycho, 96
- Breakaway points, 275, 292–293
- Break-in point, 275
- Break point, 275
- Bremmer, H, 128
- Brennan, Richard P., 95
- Bridged tee circuit, 73
- Bristol company, The, 248–249
- Bryson, A. E., 530, 585, 607, 710, 778
- Bryson's rule, 530
- Butterworth configuration, 594
- C**
- Campbell, G. A., 128
- Cancellations, transfer function, 139
- Canonical forms, 491–493
- Control, 491
- Modal, 493
- Observer, 497
- Capacitor, 175
- Carburetor, 795, 797, 844
- Cascaded tanks, 629
- Case studies
- automotive fuel/air ratio, control of, 795–803
  - Boeing 769, control of a, 777–795
  - E. coli* chemotaxis, 833–843
  - Quadrotor drone, 803–819
  - RTP systems in semiconductor wafer manufacturing, 819–833
  - Satellite attitude control, 759–777
- Catalytic converter, 796
- Cauchy's Principle of the Argument, 379n8
- Centrifugal governor. *See* Fly-ball governor
- Centrifugal-pendulum governor, 37
- Characteristic equation, 505
- Cheap control, 532–533
- Chemotaxis dynamics, 833–843
- Chemotaxis model, 837–839
- Circle criterion, 731–737
- Circuit with a current source, equations for a, 73–74
- Classical control, 39
- Clegg integrator, 746
- Closed-loop control, 23, 41
- Closed-loop cruise control, 31
- Closed-loop estimator, 769
- Closed-loop frequency-response, 407–408
- Closed loop stability, frequency response determination, 376
- Closed-loop system with sensor dynamics, 221
- Closed-loop transfer function, 182, 223, 376
- Closed-loop zero of the system, 183, 521, 564
- Collocated actuator, 58, 772
- Collocated sensor, 58, 772
- Command tracking, 32
- Communication satellite, 680
- Companion form matrix, 513
- Compensated open-loop transfer function, 405
- Compensation design using frequency response, 409–443
- design considerations, 433–435
- amplitude or gain stabilization, 434
  - Bode plot, 442
  - complementary sensitivity function, 439
  - performance frequency, 437
  - phase stabilization, 435
  - stability robustness, 436, 440, 441–443
- in terms of the sensitivity function, 435–437, 440–443
- uncertainty in a plant model, 440–441
- vector margin (VM), 442
- water bed effect, 442
- lag compensation, 420–422
- for DC motor, 424–426
  - for temperature control system, 422–423
- lead compensation, 410–412
- for DC motor, 412–416
- for temperature control system, 416–418
- for a type 23 servomechanism system, 419–420
- lead-lag compensator, 427
- PD compensation, 409–410
- PID compensation, 426
- proportional-integral (PI) compensation, 420
  - for spacecraft attitude control, 427–433
- state-space control design, 508
- Complementary sensitivity function, 215, 583, 593
- Complete transient response, 127
- Complex margin, 394
- Complex mechanical systems, 68
- Complex zeros, 169–170
- Bode plot of, 372–373
- Computed torque, 684, 687, 693
- Computer, digital control, 662–663
- Computer-aided Bode plot for complex poles and zeros, 373
- Computer-aided control design software, 41
- Computer aids, 41
- Conditionally stable compensator design, 552–554
- Conditionally stable systems, 400, 697, 713–715
- Constant closed loop magnitude, contours of, 446
- Continuation locus, 283
- Continuity relation, 88
- Contour evaluation, 379
- Control canonical form, 491
- Control, basic equations of advantage of feedback, 215
- closed-loop system, 210
- derivative control (D), 229
- feedforward control by plant model inversion, 244–246
- fundamental relationship of feedback systems, 215

- Control (*continued*)  
 historical perspectives, 247–249  
 integral control (I), 226–229  
 open-loop system, 210  
 proportional control (P), 224–226  
 proportional plus integral (PI) control, 229–230  
 proportional plus integral plus derivative (PID) control, 233–235  
 regulation, 213  
 sensitivity, 214–216  
 stability, 211–212  
 steady-state feedback gain, 214  
 tracking, 212–213  
 Ziegler–Nichols tuning of PID controller, 238–243
- Control characteristic equation, 510
- Controllability, 496
- Controller equations, 561
- Control responses of analog and digital implementations, 653, 656
- Control theory and practice, 247
- Convolution, 117–118, 131–132, 872–873  
 integral, 117–118  
 response by, 113–118
- Copernicus, Nicholas, 96
- Corner frequencies, 411
- Cosine signal derivative, 871
- Cost function, 533, 756
- Cover-up method of determining coefficients, 133
- Cramer's rule, 54
- Crossover frequency, 395  
 cross over at -23, 441
- Cruise control model, 48–51
- Cruise control step response, 484–485
- Cruise control transfer function using Matlab, 140
- D**
- D/A converters, 639
- Dakota autopilot, 316–323
- Damped natural frequency, 154
- Damping ratio, 154, 171
- Damping response in digital *versus* continuous design, 672–674
- DC gain of a system, 647
- DC gain of transfer function, 646
- DC servo system, compensator design for, 552–559  
 full-order compensator design for, 552–554  
 in observer canonical form, 552  
 redesign of, 556–558  
 with reduced-order estimator, 555–556
- second-order pole locations, 556–557
- using SRL technique, 556–558
- Decay ratio, 239–240
- Decibel, 363
- Delayed sinusoidal signal, 869–870
- Demethylation, 839–840
- Departure angles, root locus design for, 293
- Derivative, discrete control laws, 669
- Discrete-time domain, 636
- Diophantine equation, 599
- Derivative control (D), 229  
 Discrete, 669–670
- Derivative feedback, 229
- Derivative gain, 229
- Describing functions, 706–716  
 conditionally stable system, 713–715  
 definition, 707  
 for hysteresis nonlinearity, 711–712  
 for a relay nonlinearity, 709  
 for saturation nonlinearity, 708–709  
 sizing the actuator, 706  
 stability analysis using, 712–716
- Design criterion for space craft attitude control, 404–407
- Design synthesis, 161
- Desired gain, graphical calculation of, 286
- Desoer, C. A., 607
- Detroit Edison Company, 248
- Differentiation, 131, 871
- Digital autopilot, 675, 844
- Digital control, 636–676
- Digital-to-analog (D/A) converter, 639, 660–661
- Digitization, 637–639  
 analog-to-digital (A/D) converter, 637
- delay due to hold operation, 639
- difference equations, 637
- digital-to-analog (D/A) converter, 639
- discrete equivalents, 639
- free running, 638
- interrupt, 638
- sampled data system, 638
- Diophantine equation, 599
- Dirac, Paul, 116
- Direct current (DC) motor, 78
- actuators, 78  
 gain of a system, 135–136  
 modeling, 79–82  
 position control, 222–223  
 reference input with, 520–521  
 shaft's rotational velocity, 79  
 sketch of, 79  
 transfer function, 80–81, 141–142  
 with unity feedback, 222
- Direct design with rational transfer functions, 598–601
- Direct transfer function formulation, 598
- Direct transmission term, 483
- Discrete control laws, 669
- Discrete controller, 647, 650, 666
- Discrete design, 639  
 analysis tools, 667  
 damping and step response in digital *versus* continuous design, 672–674  
 discrete root locus, 668  
 exact discrete equivalent, 667  
 example, 670–672  
 feedback properties, 668–669
- Discrete equivalents, 639, 647
- Matched Pole-Zero, 653, 657
- Tustin's (bilinear) method, 647
- ZOH method, 651

- Discrete root locus, 668  
 Discrete signals, 637  
 Discrete systems  
   design by discrete  
 equivalents(emulation), 647  
 applicability limits, 659  
 bilinear approximation,  
   648  
   comparison of digital  
 approximation  
 methods, 658–659  
   matched pole-zero (MPZ)  
 method, 653–657  
   modified matched  
 pole-zero(MMPZ)  
 method, 657  
   Tustin's method, 647–651  
   zero-order hold (ZOH)  
 method, 651–653  
 hardware characteristics  
   analog-to-digital (A/D)  
 converters, 660  
   anti-alias prefilters,  
   661–662  
   computer, 663–664  
   digital-to-analog  
 converters, 660–661  
 historical perspective, 674–675  
 long division, for inversion,  
   641–643  
 relationship between  $s$  and  $z$ ,  
   643–645  
 sample-rate selection  
   anti-alias prefilter, effect of,  
   665–666  
   asynchronous sampling,  
   666  
   disturbance rejection, 665  
   tracking effectiveness, 665  
 $z$ -transform, 640–642  
 $z$ -transform inversion,  
   641–643  
 Discrete transfer function, 641  
 Distinct real roots, 133–134  
 Distributed parameter systems,  
   68–70  
 Disturbance error transfer  
   function, 223  
 Disturbance input, 227  
 Disturbance rejection, 32  
   sinusoidal, 576–582  
 Disturbance-to-error transfer  
   function, 222  
 Disturbance to the process, 25  
 Divide and conquer state space  
   design, 482  
 Dominant second order poles,  
   522–524  
 Double-integrator plant, 56  
 Double pendulum, 100  
 Double precision, 663  
 Doyle, J. C., 592–593  
 Drebbel, Cornelis, 34  
 Drebbel's incubator, 34  
 Drones, xiii, 58, 100, 312, 350,  
   470, 803–819, 863–864  
   Hexacopter, 102–103  
 Duality of estimation and  
   control, 539  
 Duality relationships, 539–540  
 Duffing's equation, 750  
 Dutch roll, 783  
 Dutch roll yaw damper, 473  
 Dynamic equations, 47  
 Dynamic response  
   amplitude and time scaling,  
   184  
   effects of zeros and additional  
 poles, 164–173  
   historical perspective, 184–185  
   pole locations, effect of,  
   150–158  
   stability, 174–184  
   state equations, 482–488  
   time-domain specifications,  
   159–163  
 Dynamic system with  
   saturation, 495
- E**
- E. coli*, 834  
*E. coli* genome, 835  
*E. coli* motion, 840  
 Effect of zero using Matlab,  
   150, 164, 168  
 Eigenvalues, 499, 502  
 Eigenvector, 499  
 Eigenvector/eigenvalue  
   problem, 499  
 Eigenvectors, 499  
 Einstein, Albert, 97  
 Electric circuits, models of,  
   71–76  
 Electric power line conductor,  
   206  
 Electromagnet, 77  
 Electromechanical systems,  
   dynamic models of, 78–82  
 Electromechanical systems,  
   models of  
   gears, 82–83  
   loudspeakers, 76–78  
   motors, 78–82  
 Electronic feedback amplifier,  
   37  
 Emulation design, 647  
   Bilinear, Tustins, 648  
   MPZ, 653, 657  
   EPROM, 663  
   ZOH, 651  
 Equations for a circuit with a  
   current source, 73–74  
 Equations of motion for rigid  
   bodies, 70–71  
 Equilibrium, 681, 683  
 Equivalent gain analysis  
   using frequency response,  
   706–712  
   using root locus, 694–700  
 Errors  
   constants, 217, 220  
   in equations for systems, 53  
   as a function of system type,  
   219  
   in output speed, 30  
 Error space, 573  
*Escherichia coli* chemotaxis, 837  
   chemotaxis signal pathway,  
   838  
   exact adaptation, 839  
   importance of, 837–838  
   ligands, 837  
   model, 840–843  
 Estimator design, 534–546  
 Estimator equations, 535, 541,  
   571  
 Estimator error characteristic  
   equation, 535  
 Estimator errors  
   closed-loop matrix for the  
 third-order case, 538  
   equation, 544, 561–562

- Estimator mode controllability, 568  
 Estimator/observer, 508  
 Estimator pole selection, 544–546  
 Estimator SRL equation, 545  
 Euler's relation, 122  
 Evans, W. R., 38, 270, 331  
 Evans form of characteristic equation, 272  
 Evans method, 331  
 Exact adaptation of activity, 839  
 Exact discrete equivalent, 651, 667  
 Excitation-Inhibition Model, 860–861  
 Expensive control, 531–532  
 Experimental models, 184  
 Exponentially decaying sinusoid, 870  
 Exponential order, Laplace transforms, 866  
 Extra pole, effect of, 172
- F**
- Factored zero-pole form, 138  
 Faraday, Michael, 96–97  
 Fast poles, 153  
 Feedback, first analysis of, 28–32  
 Feedback control, 24  
 Feedback law with integral control, 572  
 Feedback loop, 451, 512, 538, 650  
 Feedback output error to state estimate equation, 535  
 Feedback scheme for autopilot design, 317  
 Feedback structure, 209–210, 220  
 Feedback system for testing stability, 179  
 Feedback system fundamentals, 32–33  
 Feedforward, 24  
 Feedforward control by plant for DC motor, 244–246  
 model inversion, 244–246  
 Fibonacci numbers, 678  
 Final value theorem, 134–136, 171, 228, 878–879  
 for discrete systems, 645–647  
 incorrect use of, 135  
 Finite zeros, 139, 161, 173  
 First order system  
     impulse response, 151  
     SRL for, 526  
     step response, 151–152  
 First-order system response, 151  
     step response, 162  
 First order term, 365  
 Fixed point arithmetic, 664  
 Flagellum, 835, 838  
 Flexible robot arm, 70  
 Flexible satellite, 57  
 Fluid flow models, 83–95  
 Fluid flow rate, control of, 33  
 Fly-ball governor, 35  
     action of, 35–36  
     operating parts of a, 36  
 Fly-by-wire, 844  
 Folding, 645  
     and  $s$ -plane, 645  
 Forced differential equations  
     solution, 137  
 Force equilibrium, 88  
 Fourier, 112, 125, 185  
 Fourth-order partial differential equation, 68  
 Fourth order system in modal canonical form, 494  
 Foxboro Company, 248  
 Franklin, G. F., 607, 636, 644  
 Fraser, Don, 675, 844  
 Free-body diagram for cruise control, 49  
     satellite control, 58  
 Free running, 638  
 Frequency response, 354–451  
     Bode plot techniques, 362–373  
         advantages, 363  
         for complex poles and zeros, 371–372  
         composite curve, 367  
         computer-aided, 373  
         peak amplitude, 367  
         for real poles and zeros, 369–370  
     Bode's gain-phase relationship, 402–407  
     break points, 365  
     of a capacitor, 357  
 closed-loop  
     frequency-response, 407–408  
 compensation, 408–443  
 equivalent gain analysis using, 706–716  
 experimental, 358  
 frequency-response plot, 356  
 historical perspective, 450–451  
 of lag-lead compensation, 567  
 of lead compensator, 357–359  
 LTR design, 592  
 magnitude, 356, 366  
 neutral stability, 376–378  
 nonminimum phase, 374  
     steady-state errors, 374  
     velocity-error coefficient, 375  
 Nyquist stability criterion, 379–393  
 open-loop  
     frequency-response, 395  
 partial-fraction expansion, 355  
 phase, 356, 366  
 plot vs. time, 356  
 presentation  
     inverse Nyquist diagram, 450  
     Nichols chart, 445–450  
 resonant peak *versus* phase margin, 398  
 spacecraft attitude-control problem, 404–407  
 stability margins, 393–402  
     from Nichols chart for complex system, 448–450  
 stability specification, 449  
 time delay, 443–445  
 Frequency shift, 782  
 Fuel-air ratio control, 795, 847  
 Fuel injection, 797  
 Fuller, 35, 36  
 Full-order estimator, 534–540
- G**
- Gain margin (GM), 394  
 Gain phase relationship, 402

Gain stabilization, 310  
 Galilei, Galileo, 96  
 Gears, 82–83  
 Golden Nugget airlines, 349,  
 473  
 Gyroscope, 782

## H

Halley, Edmond, 95  
 Hanging crane, 65–68  
 Hardware characteristics of  
   discrete systems  
   analog-to-digital (A/D)  
     converters, 660  
   anti-alias prefilters, 661–662  
   computer, 662–663  
     central processor  
       unit(CPU), 662  
     DSP chips, 663  
     programmable read-only  
       memory (EPROM) or  
       flash memory, 663  
     random-access  
       memory(RAM), 663  
     read-only memory (ROM),  
       662–663  
   digital-to-analog converters,  
     660–661  
 Heat and fluid-flow models  
   heat flow, 84–88  
   incompressible fluid flow,  
     88–95  
 Heat exchanger  
   closed-loop Simulink  
     diagram, 604–605  
   control effort for, 606  
   design with pure time delay,  
     602–605  
   root locus for a, 606  
   tuning of, 241–243  
 Heaviside, Oliver, 184  
 operational calculus for  
   solving differential  
     equations, 184  
 Helicopter near hover, 340,  
 626  
 Hessenberg matrix, 618  
 Hexacopter, 102–103  
 High frequency plant  
   uncertainty, 434

Homogeneous differential  
   equation, 136–137  
 Hot air balloon, 851–853  
 Huygens, Christiaan, 36  
 Hydraulic actuators, 92–95  
   equations of motion, 92–95  
   linearization and  
     simplification equations,  
       94–95  
 Hydraulic piston, 89–90  
 Hysteresis nonlinearity,  
 715–716

## I

Ideal op-amp, 74  
 Impulse, 116, 154  
 Impulse response, 154–155  
 Impulse signal, 116  
 Incompressible fluid flow,  
 88–95  
 Inertial acceleration, 48  
 Inertial reference frame, 48  
 Initial value theorem, 877–878  
 Inner-loop design, 791  
 Input filter, 28  
 Instrument Landing  
   System(ILS), 32  
 Integral control (I), 226–229  
 Discrete, 669  
 Integral feedback, 226–229  
 Integrator, 75–76  
 Integrator anti windup circuit,  
 701–706  
   feedback system, 701–702  
   for a PI controller, 703–706  
   purpose of, 702  
 Internal model principle, 577  
 Internal stability, 176  
 Interrupt, 638  
 Inverse Laplace transform, 121,  
 126, 168  
   by partial-fraction expansion,  
     132–134, 874–877  
 Inverse nonlinearity, 687, 693  
 Inverse Nyquist diagram, 450  
 Inverse transform, 125  
 Inverted pendulum, 67

## J

James, H. M., 674

## K

Kalman, R. E., 39  
 Kalman Filter (LQF), 607  
 Kendall, David, 248  
 Kepler, Johannes, 96  
 Keynes, John Maynard, 96  
 Khalil, H., 707  
 Kharitonov Theorem, 183–184  
 Kirchhoff's current law (KCL),  
 72–73  
 Kirchhoff's voltage law (KVL),  
 72, 122  
 Kuo, B., 81

## L

Lag compensation, 301,  
 307–309, 569  
 Lamp nonlinearity, 831  
 Laplace, Pierre-Simon, 184–185  
 Laplace transform, 48, 118,  
 355, 567, 642–643  
   convolution, 131–132,  
     872–873  
   of cosine signal, 871  
   delayed sinusoidal signal, 869  
   derivative of a signal, 871  
   final value theorem, 134–136  
   of the impulse response, 119  
   of the input, 121  
   of integral of a time function,  
     131, 871  
   inverse, 125, 126  
   key property of, 125  
 $\mathcal{L}$ -, 128, 866  
   multiplication by time, 132  
   one-sided (or unilateral), 128  
   principle of superposition,  
     130, 867  
   procedure for determining, 125  
   properties of, 130–132,  
     867–875  
   ramp response of a first-order  
     system, 873  
   shift in frequency, 131, 869  
   of a signal  $f(t)$ , 124  
   of sinusoid function, 129–130  
   to solve differential equations,  
     136–138  
   of step and ramp functions,  
     129  
   table of, 867

- Laplace transform (*continued*)  
 time delay, 130, 868  
 time product, 132, 872  
 of sinusoidal signal,  
   874–875  
 time scaling, 131, 868–869  
 two-sided, 128  
 of unit-impulse function, 129  
 of  $y(t)$  and  $u(t)$ , 124
- Law of generators, 78
- Law of motors, 76
- Lead compensation, 301–307,  
 410–420  
 circuit of, 312
- Lead–lag compensator, 427
- Lead ratio, 412
- Least common multiple, 590
- Ligands, 837
- Limit cycle, 699
- Linear analysis methods, 63
- Linear closed-loop RTP  
 response for robust servo  
 mechanism controller, 829
- Linearization, 687, 755  
 by inverse nonlinearities, 693  
 of motion in a ball levitator,  
   689–691  
 by nonlinear feedback,  
   692–693  
 of nonlinear pendulum,  
   688–689, 693  
 of rapid thermal  
 processing(RTP) system,  
   693–694  
 by small-signal analysis,  
   687–688  
 of water tank revisited,  
   691–692
- Linear models of aircraft  
 motion, 783, 790
- Linear Quadratic  
 Gaussian(LQG) problem,  
   607
- Linear quadratic regulator  
 (LQR)  
 design, 524, 530–533  
 limiting behavior of regulator  
 poles, 531–533  
 robustness properties, 533
- Linear system analysis, 139–145  
 cruise control transfer  
 function, 140
- DC motor transfer function,  
 141–142  
 satellite transfer function,  
 143–145
- Linear time-invariant  
 systems(LTIs), 112, 116,  
 125, 127  
 stability of, 175–176
- Liquid-level control, 33
- Loop gain, 32
- Loop transfer recovery (LTR),  
 592–598  
 frequency response plots for,  
   596  
 for nonminimum-phase  
 systems, 594  
 plant inversion, 594  
 for satellite system, 595–598
- Simulink block diagram for,  
 597  
 use of, 593
- Loudspeakers, 76–77  
 with circuits, 78  
 equations of motion, 77–78  
 geometry for a, 77
- LTR, 592–594
- Luenberger, D. G., 607
- Lumped parameter model, 70
- Lyapunov, A. M., 37–38, 685,  
 737
- Lyapunov function, 686
- Lyapunov stability analysis,  
 723–731
- M**
- Magnetic ball levitator, 689
- Magnetic levitation, 343,  
 689–691
- Magnitude  
 frequency response, 123, 356
- Magnitude condition, 285
- Magnitude plot, 124  
 gain and phase margin,  
   394–395  
 transfer function classes, 364
- M and N circles, 446
- Manual control, 23
- Mason's rule, 150, 512
- Matched pole-zero (MPZ)  
 method, 653–657
- Mathematical model, 29, 46
- of dynamic response of a  
 system, 33
- Matlab, xiii, xiv, 41, 123  
 aircraft response using, 170  
 computing roots, 180  
 dynamics of a system, 62–63  
 impulse response by, 158  
 linear system analysis,  
   139–145  
 cruise control transfer  
 function, 140  
 DC motor transfer  
 function, 141–142  
 satellite transfer function,  
   143–145
- pidTuner, 241
- sisotool, 294–295  
 transformations using,  
   142–143
- Matlab commands, 897–902  
 a\b, 600–601  
 acker, 514, 540  
 axis, 389, 392  
 bode, 123–124, 417, 596  
 canon, 502  
 eig, 499  
 ezplot, 182  
 feedback, 150, 318  
 impulse, 154, 537, 543  
 initial, 537, 543  
 inv, 501–502  
 linmod, 688  
 linmod2, 688  
 loglog, 124, 358  
 logspace, 417  
 lqe, 596  
 lqr, 530, 596  
 lsim, 143  
 margin, 596  
 max, 443  
 nichols, 447  
 nyquist, 385, 388, 392  
 ones, 143  
 parallel, 150  
 pidTuner, 241  
 place, 517, 540  
 plot, 63, 143  
 poly, 138  
 pzmap, 152  
 residue, 134  
 rlocfind, 464  
 rlocus, 284, 289–293

- roots, 182, 507  
 semilogx, 124, 358, 373, 417  
 series, 150  
 sisotool, 294–295  
 sqrt, 578  
 ss, 502, 507  
 ssdata, 502  
 ss2tf, 504, 507  
 ss2zp, 490  
 step, 50, 62  
 tf, 141, 143, 154  
 tf2ss, 492  
 tf2zp, 490  
 tzero, 507
- Matlab's algorithm, 241  
 Matlab's PID Tuner App, 241  
 Matrix fraction descriptions (MFDs), 607  
 Maxwell, James Clerk, 36–37, 97, 248  
 Mayr, O., 33–34  
 Mechanical systems  
     combined rotation and translation, 65–68  
     rotational motion, 54–65  
         flexible satellite attitude control, 57–58  
         quadrotor drone, 58–61  
         satellite attitude control, 54–57  
         simple pendulum, 61–66  
     translational motion, 47–54  
         cruise-control model, 48–51  
         quarter-car model, 51–54
- Méchanique céleste* (Celestial Mechanics), 184  
 Mello, B. A., 839  
 Memoryless nonlinearity, 694  
 Method of computed torque, 687  
 Microphone, 107  
 Minimum phase systems and Bode plot, 374  
 MIT rule, 728  
 Modal canonical form, 493–497  
 Model, 29  
 Model-following design, 585  
 Modern control, 39  
 Modes of the system, 139
- Modified matched pole-zero(MMPZ) method, 657  
 Moler, Cleve, 333  
 Monic polynomial, 272, 599  
 Motors, 76–82  
     AC, 80  
     DC, 78–80
- N**
- Napoleon, 184  
 Natural frequency of system, 504  
 Natural mode of system, 504  
 N circles, 446  
 Natural response of the system, 151  
 Negative feedback, 146  
 Negative root locus, 277, 323–326  
 Neutrally stable, 176, 240  
 Newton, Isaac, 95–96  
 Newton's laws of motion, 70  
     free-body diagram, 49  
     history, 95  
     rotational motion, 54  
     third law, 60  
     translational motion, 47  
 Nichols, N. B., 248, 447, 674  
 Nichols plot, 398, 445–450  
 Node analysis, 72  
 Non-causal system, 118  
 Noncollocated system, 297  
 Nonlinear radiation heat transfer, 824  
 Nonlinear aircraft equations of motion, 778–779  
 Nonlinear automobile exhaust sensor, 797  
 Nonlinear systems  
     changing overshoot and saturation nonlinearity, 695–696  
     circle criterion, 731–737  
     describing functions, 706–716  
     historical perspective, 737–738  
     hysteresis nonlinearity, 715–716  
     integrator anti windup circuit, 701–706
- Lyapunov stability analysis, 723–731  
 need to study, 685  
 nonlinear characteristics, 687  
 nonlinear elements, 695  
 Nonminimum-phase zero, 167  
 Nonminimum-phase compensator, 555  
 Nonminimum phase systems Bode plot, 375  
     LTR, 593  
 Notch compensation, 301, 310–312, 700  
 Notch filter, 764–770  
     pole-zero pattern, 766  
 Nyquist, H., 38, 451  
 Nyquist frequency, 645  
 Nyquist rate, 661  
 Nyquist's frequency-response stability test, 174  
 Nyquist–Shannon sampling theorem, 661  
 Nyquist stability criterion, 379–393  
 Nyquist Plot  
     for an open-loop unstable system, 389–392  
     hysteresis nonlinearity, 711  
     for LQR design, 528  
     for a system with multiple crossover frequencies, 400–402  
     for a second-order system, 383–386  
     for a third-order system, 386–389
- O**
- Observability, 539  
 Observability matrix, 539  
 Observer canonical form, 497–498, 538  
 One-sided (or unilateral) Laplace transform, 128  
 Op-amp integrator, 76  
 Op-amp summer, 75  
 Open-loop control system, 23, 30  
 Operational amplifier, 74  
 Optimal control, 522, 524  
 Optimal design, 756

Ordinary differential equations(ODEs), 39, 150  
 Oscillatory time response, 157–158  
 Output matrix, 483  
 Overshoot, 159–161  
 versus damping ratio for the second-order system, 161

## P

Padé approximant, 331, 603  
 Papermaking machine, 43  
 Parseval's theorem, 873  
 Partial-fraction expansion, 132–134, 176, 355  
 using cover-up method, 133  
 Peak amplitude, 367  
 Peak time, 159–160  
 Pendulum, 61–66  
 control law, 510–511  
 moment of inertia, 61  
 reduced-order estimator for, 542–544  
 Simulink numerical simulation, 64  
 transfer function, 62  
 Phase  
 condition, 277  
 Frequency response, 123  
 margin (PM), 394, 398  
 Plot, 124  
 stabilization, 310, 434  
 Phillips, R. S., 674  
*Philosophia Naturalis Principia Mathematica*, 95–96  
 Phugoid mode, 791  
 PI control, 232–233  
 PID, 38, 233, 426  
 tuning, 241  
 Piper Dakota, 316–323, 507  
 Plant, 27  
 Plant inversion, 594  
 Plant uncertainty, 434  
 Poincaré, 737  
 Pole assignment, 552–554, 557, 599  
 Pole locations for a system, 150–158  
 Poles of a system, 132, 138–139  
 Pole-zero patterns on dynamic response, 173–174

Pontryagin, L. S., 39  
 Position error constant, 218, 374  
 Positive feedback, 146  
 Positive root locus, 277–287  
 Power db, 363  
 Principle of superposition, 113, 130  
 Process noise, 545  
 Process reaction curve, 238  
 Proportional control (P), 224–226  
 Proportional feedback, 224  
 Proportional gain, 224  
 Proportional-integral-derivative(PID) control, 38, 233–238, 426, 762–770  
 for a DC motor position control, 235–236  
 of motor speed, 235–236  
 Ziegler–Nichols tuning of, 238–244  
 Proportional-integral (PI) control, 181, 229–233  
 thermal system, 230–233  
 Prototype testing, 757  
 Proximate Time Optimal Servo(PTOS), 722–723  
 Pure time delay, 602–606  
 Pyrometers, 821

## Q

Q parametrization, 607  
 Quadcopter, 58–61, 100  
 Quadrotor Drone, xiii  
 actuators, 805  
 linear model, 805–809  
 optimal design, 815–819  
 PID controller, single axis, 810  
 Problems, 100, 350, 470, 863–864  
 process understanding, 804  
 root locus design, 312–316  
 rotational motion, 58–61  
 sensor selection, 804–805  
 state-space model, 815  
 24-D motion, horizontal plane, 813–815  
 Quality factor, 458  
 Quarter-car model, 51–54  
 Quarter decay ratio, 239–242

## R

Ragazzini, J. R., 674  
 Ramp function, 171, 216–217  
 Rapid thermal processing ( RTP) system  
 actuators, 824  
 block diagram of, 823  
 closed-loop system equations, 827–828  
 demands on an, 819–820  
 design of, 822–823  
 design with nonlinearities, 829–831  
 feedback gain matrix computed from Matlab, 827  
 generic, 822  
 laboratory model, 823  
 lamp geometries of, 822  
 lamp nonlinearity, 829–830  
 linear closed-loop RTP response for PI controller, 826  
 linear model, 824–825  
 optimal design, 826  
 performance specifications, 823–824  
 sensors, 824  
 Simulink block diagram, 828–829  
 temperature control, 832  
 temperature non uniformity, 826–827  
 temperature trajectory, 821, 829  
 Reduced-order estimator, 540–544  
 Reference input, 25  
 with full-state feedback, 518–522  
 control equation, 518  
 direct current (DC) motor, 520–522  
 gain calculation, 518  
 general structure, 561–570  
 Regulators, 23  
 Relay nonlinearity, 709  
 Reset control, 701  
 Reset windup, 701  
 Resonant frequency, 446  
 Ring-laser gyroscope, 782  
 Rise time, 159–160  
 Robot, 102

- Robustness, 32  
of integral control, 228  
of system type, 220
- Robust tracking, 571–592
- Robustness constraints, 441–443
- Roll mode, 783
- Room temperature control system, component block diagram of a, 26
- Root locus, 39, 270, 762, 774, 776  
analog and digital implementations, 312  
analysis and design of system with limit cycle using, 698–701  
arrival angles, rule for, 282  
asymptote angles, 279–280  
asymptotes, 279–280  
basic feedback system, 271–276  
for combined controller and estimator, 550  
compensation design, 301–312  
complex multiple roots, 299–300  
continuation locus, 283  
departure angles, rule for, 282  
design examples, 312–323  
equivalent gain analysis using, 694–705  
Evans, 272  
guidelines for determining, 276–287  
historical perspective, 39, 331–333  
magnitude condition, 285–286  
negative or  $0^\circ$ , 277, 323–326  
for noncollocated flexibility, 297–299  
parameter selection, 285–287  
phase condition, 277  
positive or  $180^\circ$ , 277–287  
for satellite control with collocated flexibility, 295–297  
stability of conditionally stable system, 696–697  
time delays, 331  
using lag compensation, 307–309  
using lead compensation, 302–307  
using notch compensation, 310–312  
using two parameters in succession, 326–328
- Root-locus form, 273
- Root-mean-square (RMS) value of the control, 597
- Rosenbrock, H. H., 607
- Rotational motion, 54
- Routh, E. J., 37, 451, 727
- Routh method, 177–184, 727
- RTP linear model, 824–825
- Rudder, 778
- Run-to-run control, 859
- S**
- Saberi, A., 593
- Safonov, M., 607
- Sample and Hold devices, 661
- Sampled data system, 638
- Sample period, 637
- Sample rate, 637
- Sample rate selection, 639
- Sastry, S. S., 728
- Satellite attitude control, 54–57, 236–238  
design of, 759–776  
historical perspective, 843–844  
loop transfer recovery (LTR), 595–597
- matched pole-zero (MPZ) method, 653–657
- root locus, 288–297  
with collocated flexibility, 295–297  
PD control, 288–291
- state-space control design, 549–552  
in state-variable form, 483–484
- symmetric root locus(SRL) design, 526–528
- Saturation nonlinearity, 695–696
- Scaling, 184
- Schmitt trigger circuit, 710–711
- Schmitz, E., 70
- Segway, 68
- Sensitivity function, 215
- time response to parameter changes, 247
- Sensor noise, 545
- Sensors  
collocated, 772  
rapid thermal processing ( RTP ) system, 824  
selection and placement, 27, 754
- Servomechanisms, 38
- Servo systems, 23
- Setpoint, 25
- Settling time, 159, 161–163
- Shanghai maglev train, 691–692
- Short-period modes, 791
- Sign errors, 53
- Simple compensation  
PID/lead-lag design, 755
- Simple feedback system, 25–28
- Simulink, xiv, 41, 56
- Simulink diagram  
for the anti windup, 704–705  
block diagram, 64–65  
heat exchanger, 605–606  
for nonlinear closed-loop RTP system, 830–831  
for RTP closed-loop control, 828, 830  
simulating *E. coli* chemotaxis, 841
- Simulink nonlinear simulation, 64–66, 704, 801, 830
- Simulink simulations, 579, 597
- Single-Input-Single-Output (SISO) systems, 482
- Sinusoid transform, 129–130
- Sisotool, 294–295
- Smith compensator, 602
- Space station digital controller, direct discrete design of, 670–672
- Speed control, system type for, 219
- Spiral mode, 783
- Spirule, 331
- s-plane, 152–158, 162–163
- $1/s^2$  plant, 56
- S-shape of the step response curve, 238
- Stability, 32, 37, 151, 155, 174–184, 211–212

- Stability (*continued*)  
 analysis and design based on,  
 37  
 bang-bang control,  
 721–723  
 Maxwell's and Routh's  
 stability problem, 38  
 phase plane, 717–720  
 analysis using describing  
 functions, 712–716  
 BIBO stability, 174–175  
 Lyapunov stability analysis,  
 723–731  
 Lyapunov redesign of  
 adaptive control,  
 728–731  
 Lyapunov's position  
 feedback system,  
 727–728  
 for second-order system,  
 726–727  
 necessary condition for,  
 176–177  
 Routh, 177–184  
*Versus* parameter range,  
 180–181  
 Stability margins, 393–402  
 of a conditionally stable  
 system, 400  
 Star tracker, 760  
 State of the system, 483  
 State-space control design  
 advantages of, 480–482  
 analog-computer  
 implementation, 489–490  
 block diagrams, 488–490  
 control canonical form,  
 491–502  
 in modal canonical form,  
 493  
 normal modes of the  
 system, 493  
 compensator design  
 for DC servo system,  
 552–554  
 frequency-response plots,  
 551  
 poles of combined control  
 law and estimator,  
 547–548
- reduced-order  
 compensator transfer  
 function, 549  
 regulator, 547  
 for satellite altitude  
 control, 549–552  
 transfer function, 548–549  
 direct design with rational  
 transfer functions, 598–602  
 Diophantine equation, 599  
 general controller in  
 polynomial form, 598  
 monic polynomials, 599  
 pole placements, 599–600  
 polynomial transfer  
 function model,  
 600–601  
 discrete models, 674  
 equations in state equations,  
 491–508  
 characteristic equation,  
 505  
 controllability matrix, 496  
 dynamic response from,  
 503–508  
 in modal canonical form,  
 493–497  
 observer canonical form,  
 497–498  
 of quadrotor, 815  
 state transformations, 495  
 transformation of thermal  
 system from control to  
 modal form, 500–501  
 estimator design approach  
 duality of estimation and  
 control, 539–540  
 full-order estimators,  
 534–536  
 left companion matrix, 538  
 observer canonical form,  
 538–539  
 reduced-order estimators,  
 540–544  
 selection of estimator pole  
 locations, 544–546  
 for simple pendulum,  
 436–437  
 SRL estimator design for a  
 simple pendulum, 546  
 extended estimator, 589–592
- full-state feedback,  
 control-law design for,  
 508–522  
 Ackermann's formula, 514  
 characteristic equation of  
 closed-loop system,  
 509–510  
 companion form matrix,  
 513  
 control canonical form,  
 511–512  
 control law, 508–514,  
 516–517  
 estimator/observer, 508  
 observer canonical form  
 with a zero, 516–517  
 reference input with,  
 518–521  
 historical perspective, 607–608  
 integral control, 571–572  
 of a motor speed system,  
 572–573  
 using error-space system,  
 583–585  
 model-following design,  
 585–589  
 for disk drive, 587–589  
 normal form, 481  
 phase plane, 481  
 pole-placement design  
 approach  
 comments on, 533–534  
 dominant second-order  
 poles, 522–524  
 linear quadratic  
 regulator(LQR)  
 design, 524, 530–531  
 symmetric root locus(SRL)  
 design, 524–533  
 reference input with estimator  
 general structure, 561–565  
 reduced-order estimator,  
 566  
 selecting gain, 570  
 robust tracking, 571–582  
 in state-variable form, 482  
 bridged tee circuit,  
 485–486  
 cruise control step  
 response, 484–485  
 DC motor, 487

- loudspeaker with circuit, 487  
 satellite attitude control model, 483–484  
 for time-delayed system, 602–605  
 State-variable approach to control theory, 37, 39  
 Steady-state error, 216  
     to polynomial inputs, 216–223  
 Steady-state tracking and disturbance rejection, 222–223  
     of motor speed, 591–592  
 Steady-state tracking error, 217–227  
     Steady-state error, 216–223  
 Step-response transform, 156  
 Step response with Matlab, 50–51  
 Successive loop closure, 326  
 Summer, 29  
 Summer circuit, 75  
 Superposition, 113  
 Sylvester equation, 586  
 Sylvester matrix, 600  
 Symbols for linear circuit elements, 71–72  
 Symmetric root locus (SRL)  
     closed-loop step response, 767  
     design, 524–533, 556, 756  
     for an inverted pendulum, 528–530  
     frequency response, 772  
     of lateral dynamics, 788  
     for the satellite system, 526–528  
     of satellite system, 771  
     for servo speed control, 526  
 SRL estimator design for a simple pendulum, 546  
 System error, 28  
 System identification, 46  
 System impulse response, 155  
 System modeling diagrams. *See*  
     Block diagram  
 System stability, 174  
 System type for regulation and disturbance rejection, 222–223
- System type for tracking, 217–221  
 Systems biology, 834
- T**
- Table leveller, 108  
 Tachometer feedback, 220–221  
 Taylor, George, 248  
 Temperature control, 26  
 Tesla, N., 80  
 Thermal control system, 85–86  
 Thermostat, 25, 27–28  
 Time constant, 151  
 Time-domain specifications  
     overshoot, 160–161  
     peak time, 160–161  
     rise time, 159–163  
     settling time, 159, 161–163  
 Time-delay, 443  
     design for, 602  
     magnitude and phase, 444  
     stability effect, 444  
 Time invariance, 113–117  
 Time-invariant systems, 116  
     output for a general input, 116  
 Time sequences associated with *z*-plane, 646  
 Tischler, M. B., 402  
 Torque-speed curves for a servomotor, 81  
 Torricelli, 737  
 Tracking, 23  
 Trankle, T., 348  
 Transfer function, 50,  
     53–54  
     for an RC circuit, 122–123  
     from block diagram, 147–148  
     Bode form, 364  
     of the closed-loop system, 182, 223, 376, 569  
     complex zeros, 169–170  
     DC gain of the system, 136  
     direct current (DC) motor, 78–80  
     frequency response and, 118–128  
     gears, 82–83  
     poles from state equations, 505
- of a simple system using Matlab, 149–150  
 thermal system, 503–504  
 Transfer function poles, 505  
 Transfer function zeros, 506  
 Transient response, 125–126  
     complex zeros, effect of, 170  
     settling time, 161–163  
     zero, effect of, 168  
 Transportation lag, 602  
 Transpose of a vector, 483  
 Truxal's formula, 223, 564–565  
 Type *k* system, definition, 220  
 Tungsten halogen lamp, 822  
 Tustin's method, 647–651  
 Two-mass system, suspension model, 51–54  
 Two-sided Laplace transform, 128
- U**
- Ultimate gain, 240  
 Ultimate period, 240  
 Ultimate sensitivity method, 240  
 Ultra-large-scale integrated(ULSI) circuit, 819  
 Uncontrollable systems, 515  
 Undamped natural frequency, 154  
 Uncontrollability of estimator modes, 568  
 Unit-impulse function, 129  
 Unit-step function, 117  
 Unity feedback system, 146  
 Unmanned Aerial Vehicles (UAVs), 803  
 Unstable system, 174  
 Upper companion form, 513  
 USCG Cutter Tampa, 348
- V**
- Van der Pol's equation, 749  
 Vector margin, 394, 399  
 Vector transpose, 483  
 Velocity error constant, 218  
 Vibration isolation, 861  
 Vidyasagar, M., 728  
 Voice coil, 76–77

**W**

- Washout, 784  
 Water tank height, equations for, 89  
     linearization of, 91–92  
 Watt, James, 35  
 Watt's flyball governor, 35  
 Widnall, Bill, 675  
 Winnie Mae, 843  
 Woodson, H. H., 681  
 Wright brothers, 843

**Y**

- Yakubovich, 733  
 Yaw damper, 782–789  
 Young's modulus, 69

**Z**

- Zadeh, L., 607  
 Zames, G., 607  
 Zero-order hold (ZOH), 639  
     approximation method, 651–653

- Zeros of a system, 132, 138–139  
     effects of, 164–173  
 Zero assignment, 561  
 Zero degree locus, 277, 323–326  
 Ziegler–Nichols tuning of PID controller, 238–244  
 Zirconia sensor, 797  
 $z$ -plane, 644  
 ZOH transfer function, 659, 667  
 $z$ -Transform, 640

*This page intentionally left blank*

# Appendix WA

## A Review of Complex Variables

This appendix is a brief summary of some results on complex variables theory, with emphasis on the facts needed in control theory. For a comprehensive study of basic complex variables theory, see standard textbooks such as Brown and Churchill (1996) or Marsden and Hoffman (1998).

### WA.1 Definition of a Complex Number

The complex numbers are distinguished from purely real numbers in that they also contain the **imaginary operator**, which we shall denote as  $j$ . By definition,

$$j^2 = -1 \quad \text{or} \quad j = \sqrt{-1}. \quad (\text{WA.1})$$

A **complex number** may be defined as

$$A = \sigma + j\omega, \quad (\text{WA.2})$$

where  $\sigma$  is the real part and  $\omega$  is the imaginary part, denoted, respectively, as

$$\sigma = \text{Re}(A), \quad \omega = \text{Im}(A). \quad (\text{WA.3})$$

Note the imaginary part of  $A$  is itself a real number.

Graphically, we may represent the complex number  $A$  in two ways. In the Cartesian coordinate system (see Fig. WA.1a),  $A$  is represented by a single point in the complex plane. In the polar coordinate system,  $A$  is represented by a vector with length  $r$  and an angle  $\theta$ ; the angle is measured in radians counter-clockwise from the positive real axis (see Fig. WA.1b). In polar form, the complex number  $A$  is denoted by

$$A = |A| \cdot \angle \arg A = r \cdot \angle \theta = re^{j\theta}, \quad 0 \leq \theta \leq 2\pi, \quad (\text{WA.4})$$

where  $r$ —called the **magnitude**, **modulus**, or **absolute value** of  $A$ —is the length of the vector representing  $A$ , namely,

$$r = |A| = \sqrt{\sigma^2 + \omega^2}, \quad (\text{WA.5})$$

and where  $\theta$  is given by

$$\tan \theta = \frac{\omega}{\sigma} \quad (\text{WA.6})$$

or

$$\theta = \arg(A) = \tan^{-1}\left(\frac{\omega}{\sigma}\right). \quad (\text{WA.7})$$

## 2 Appendix WA A Review of Complex Variables

**Figure WA.1**

The complex number  $A$  represented in  
 (a) Cartesian and  
 (b) polar coordinates

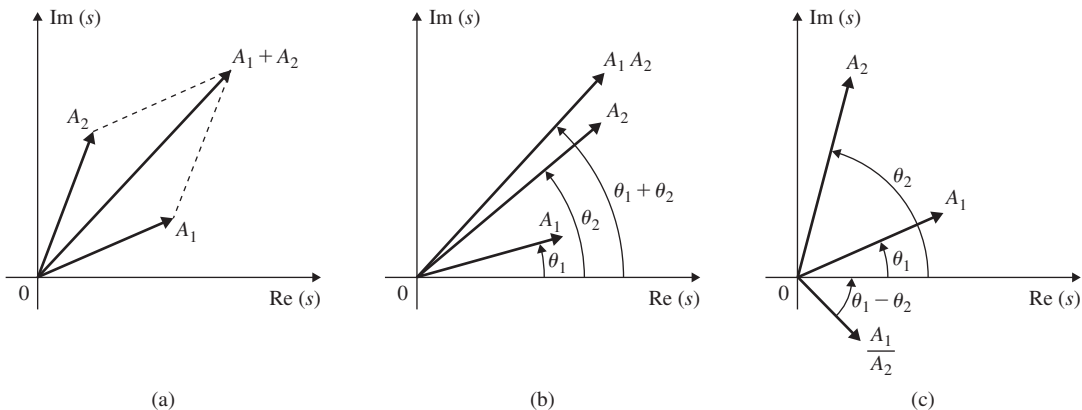
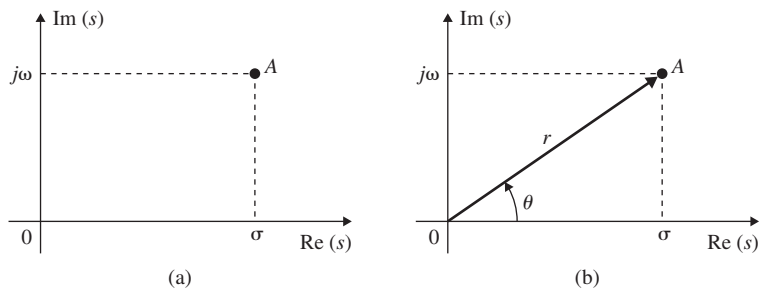


**Figure WA.2**

Arithmetic of complex numbers: (a) addition; (b) multiplication; (c) division

Care must be taken to compute the correct value of the angle, depending on the sign of the real and imaginary parts (that is, one must find the quadrant in which the complex number lies).

The **conjugate** of  $A$  is defined as

$$A^* = \sigma - j\omega. \quad (\text{WA.8})$$

Therefore,

$$(A^*)^* = A, \quad (\text{WA.9})$$

$$(A_1 \pm A_2)^* = A_1^* \pm A_2^*, \quad (\text{WA.10})$$

$$\left(\frac{A_1}{A_2}\right)^* = \frac{A_1^*}{A_2^*}, \quad (\text{WA.11})$$

$$(A_1 A_2)^* = A_1^* A_2^*, \quad (\text{WA.12})$$

$$\operatorname{Re}(A) = \frac{A + A^*}{2}, \quad \operatorname{Im}(A) = \frac{A - A^*}{2j}, \quad (\text{WA.13})$$

$$AA^* = (|A|)^2. \quad (\text{WA.14})$$

## WA.2 Algebraic Manipulations

### WA.2.1 Complex Addition

If we let

$$A_1 = \sigma_1 + j\omega_1 \quad \text{and} \quad A_2 = \sigma_2 + j\omega_2, \quad (\text{WA.15})$$

then

$$A_1 + A_2 = (\sigma_1 + j\omega_1) + (\sigma_2 + j\omega_2) = (\sigma_1 + \sigma_2) + j(\omega_1 + \omega_2). \quad (\text{WA.16})$$

Because each complex number is represented by a vector extending from the origin, we can add or subtract complex numbers graphically. The sum is obtained by adding the two vectors. This we do by constructing a parallelogram and finding its diagonal, as shown in Fig. WA.2a. Alternatively, we could start at the tail of one vector, draw a vector parallel to the other vector, then connect the origin to the new arrowhead.

Complex subtraction is very similar to complex addition.

### WA.2.2 Complex Multiplication

For two complex numbers defined according to Eq. (WA.15),

$$\begin{aligned} A_1 A_2 &= (\sigma_1 + j\omega_1)(\sigma_2 + j\omega_2) \\ &= (\sigma_1\sigma_2 - \omega_1\omega_2) + j(\omega_1\sigma_2 + \sigma_1\omega_2). \end{aligned} \quad (\text{WA.17})$$

The product of two complex numbers may be obtained graphically using polar representations, as shown in Fig. WA.2b.

### WA.2.3 Complex Division

The division of two complex numbers is carried out by **rationalization**. This means that both the numerator and denominator in the ratio are multiplied by the conjugate of the denominator:

$$\begin{aligned} \frac{A_1}{A_2} &= \frac{A_1 A_2^*}{A_2 A_2^*} \\ &= \frac{(\sigma_1\sigma_2 + \omega_1\omega_2) + j(\omega_1\sigma_2 - \sigma_1\omega_2)}{\sigma_2^2 + \omega_2^2}. \end{aligned} \quad (\text{WA.18})$$

From Eq. (WA.4), it follows that

$$A^{-1} = \frac{1}{r} e^{-j\theta}, \quad r \neq 0. \quad (\text{WA.19})$$

Also, if  $A_1 = r_1 e^{j\theta_1}$  and  $A_2 = r_2 e^{j\theta_2}$ , then

$$A_1 A_2 = r_1 r_2 e^{j(\theta_1 + \theta_2)}, \quad (\text{WA.20})$$

where  $|A_1 A_2| = r_1 r_2$  and  $\arg(A_1 A_2) = \theta_1 + \theta_2$ , and

$$\frac{A_1}{A_2} = \frac{r_1}{r_2} e^{j(\theta_1 - \theta_2)}, \quad r_2 \neq 0, \quad (\text{WA.21})$$

## 4 Appendix WA A Review of Complex Variables

where  $\left| \frac{A_1}{A_2} \right| = \frac{r_1}{r_2}$  and  $\arg\left(\frac{A_1}{A_2}\right) = \theta_1 - \theta_2$ . The division of complex numbers may be carried out graphically in polar coordinates as shown in Fig. WA.2c.

### EXAMPLE WA.1

#### *Frequency Response of First-Order System*

Find the magnitude and phase of the transfer function  $G(s) = \frac{1}{s+1}$ , where  $s = j\omega$ .

**Solution.** Substituting  $s = j\omega$  and rationalizing, we obtain

$$\begin{aligned} G(j\omega) &= \frac{1}{\sigma + 1 + j\omega} \frac{\sigma + 1 - j\omega}{\sigma + 1 - j\omega} \\ &= \frac{\sigma + 1 - j\omega}{(\sigma + 1)^2 + \omega^2}. \end{aligned}$$

Therefore, the magnitude and phase are

$$\begin{aligned} |G(j\omega)| &= \frac{\sqrt{(\sigma + 1)^2 + \omega^2}}{(\sigma + 1)^2 + \omega^2} = \frac{1}{\sqrt{(\sigma + 1)^2 + \omega^2}}, \\ \arg(G(j\omega)) &= \tan^{-1}\left(\frac{\text{Im}(G(j\omega))}{\text{Re}(G(j\omega))}\right) = \tan^{-1}\left(\frac{-\omega}{\sigma + 1}\right). \end{aligned}$$


---

### WA.3 Graphical Evaluation of Magnitude and Phase

Consider the transfer function

$$G(s) = \frac{\prod_{i=1}^m (s + z_i)}{\prod_{i=1}^n (s + p_i)}. \quad (\text{WA.22})$$

The value of the transfer function for sinusoidal inputs is found by replacing  $s$  with  $j\omega$ . The gain and phase are given by  $G(j\omega)$  and may be determined analytically or by a graphical procedure. Consider the pole-zero configuration for such a  $G(s)$  and a point  $s_0 = j\omega_0$  on the imaginary axis, as shown in Fig. WA.3. Also consider the vectors drawn from the poles and the zero to  $s_0$ . The magnitude of the transfer function evaluated at  $s_0 = j\omega_0$  is simply the ratio of the distance from the zero to the product of all the distances from the poles:

$$|G(j\omega_0)| = \frac{r_1}{r_2 r_3 r_4}. \quad (\text{WA.23})$$

The phase is given by the sum of the angles from the zero, minus the sum of the angles from the poles:

$$\arg G(j\omega_0) = \angle G(j\omega_0) = \theta_1 - (\theta_2 + \theta_3 + \theta_4). \quad (\text{WA.24})$$

This may be explained as follows: The term  $s + z_1$  is a vector addition of its two components. We may determine this equivalently as  $s - (-z_1)$ , which amounts to translation of the vector  $s + z_1$  starting at  $-z_1$ , as

**Figure WA.3**

Graphical determination of magnitude and phase

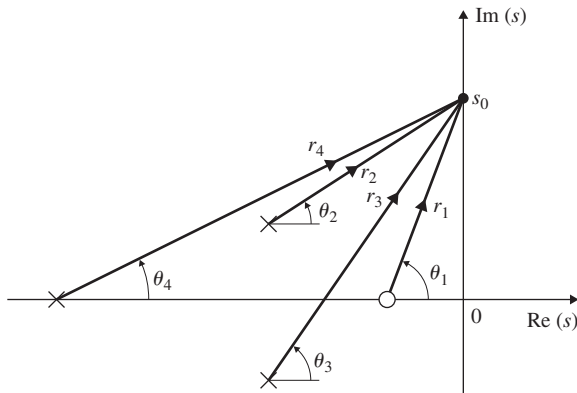
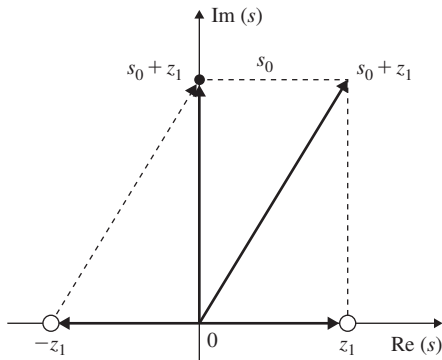
**Figure WA.4**

Illustration of graphical computation of  $s + z_1$



shown in Fig. WA.4. This means that a vector drawn from the zero location to  $s_0$  is equivalent to  $s + z_1$ . The same reasoning applies to the poles. We reflect  $p_1$ ,  $p_2$ , and  $p_3$  about the origin to obtain the pole locations. Then the vectors drawn from  $-p_1$ ,  $-p_2$ , and  $-p_3$  to  $s_0$  are the same as the vectors in the denominator represented in polar coordinates. Note that this method may also be used to evaluate  $s_0$  at places in the complex plane besides the imaginary axis.

## WA.4 Differentiation and Integration

The usual rules apply to complex differentiation. Let  $G(s)$  be differentiable with respect to  $s$ . Then the derivative at  $s_0$  is defined as

$$G'(s_0) = \lim_{s \rightarrow s_0} \frac{G(s) - G(s_0)}{s - s_0}, \quad (\text{WA.25})$$

provided that the limit exists. For conditions on the existence of the derivative, see Brown and Churchill (1996).

The standard rules also apply to integration, except that the constant of integration  $c$  is a complex constant:

$$\int G(s) ds = \int \operatorname{Re}[G(s)] ds + j \int \operatorname{Im}[G(s)] ds + c. \quad (\text{WA.26})$$

## WA.5 Euler's Relations

Let us now derive an important relationship involving the complex exponential. If we define

$$A = \cos \theta + j \sin \theta, \quad (\text{WA.27})$$

where  $\theta$  is in radians, then

$$\begin{aligned} \frac{dA}{d\theta} &= -\sin \theta + j \cos \theta = j^2 \sin \theta + j \cos \theta \\ &= j(\cos \theta + j \sin \theta) = jA. \end{aligned} \quad (\text{WA.28})$$

We collect the terms involving  $A$  to obtain

$$\frac{dA}{A} = jd\theta. \quad (\text{WA.29})$$

Integrating both sides of Eq. (WA.29) yields

$$\ln A = j\theta + c, \quad (\text{WA.30})$$

where  $c$  is a constant of integration. If we let  $\theta = 0$  in Eq. (WA.30), we find that  $c = 0$  or

$$A = e^{j\theta} = \cos \theta + j \sin \theta. \quad (\text{WA.31})$$

Similarly,

$$A^* = e^{-j\theta} = \cos \theta - j \sin \theta. \quad (\text{WA.32})$$

From Eqs. (WA.31) and (WA.32), it follows that

$$\cos \theta = \frac{e^{j\theta} + e^{-j\theta}}{2}, \quad (\text{WA.33})$$

$$\sin \theta = \frac{e^{j\theta} - e^{-j\theta}}{2j}. \quad (\text{WA.34})$$

## WA.6 Analytic Functions

Let us assume  $G$  is a complex-valued function defined in the complex plane. Let  $s_0$  be in the domain of  $G$ , which is assumed to be finite within some disk centered at  $s_0$ . Thus,  $G(s)$  is defined not only at  $s_0$  but also at all points in the disk centered at  $s_0$ . The function  $G$  is said to be **analytic** if its derivative exists at  $s_0$  and at each point in the neighborhood of  $s_0$ .

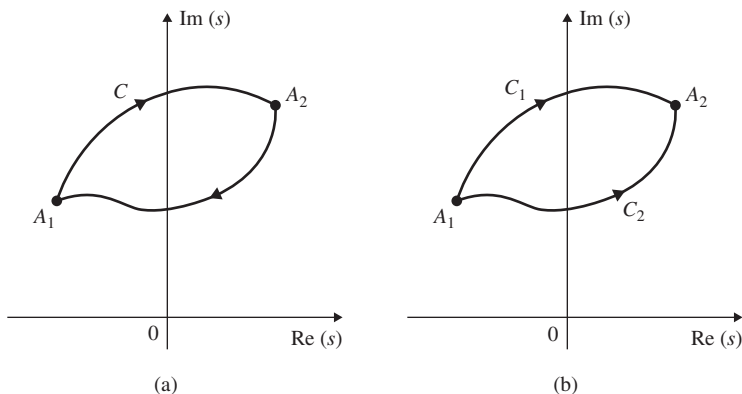
## WA.7 Cauchy's Theorem

A **contour** is a piecewise-smooth arc that consists of a number of smooth arcs joined together. A **simple closed contour** is a contour that does not intersect itself and ends on itself. Let  $C$  be a closed contour as shown in Fig. WA.5a, and let  $G$  be analytic inside and on  $C$ . Cauchy's theorem states that

$$\oint_C G(s)ds = 0. \quad (\text{WA.35})$$

**Figure WA.5**

Contours in the  $s$ -plane:  
 (a) a closed contour;  
 (b) two different paths between  $A_1$  and  $A_2$



There is a corollary to this theorem: Let  $C_1$  and  $C_2$  be two paths connecting the points  $A_1$  and  $A_2$  as in Fig. WA.5b. Then,

$$\int_{C_1} G(s) ds = \int_{C_2} G(s) ds. \quad (\text{WA.36})$$

## WA.8 Singularities and Residues

If a function  $G(s)$  is not analytic at  $s_0$ , but is analytic at some point in every neighborhood of  $s_0$ , it is said to be a **singularity**. A singular point is said to be an **isolated singularity** if  $G(s)$  is analytic everywhere else in the neighborhood of  $s_0$  except at  $s_0$ . Let  $G(s)$  be a **rational function** (that is, a ratio of polynomials). If the numerator and denominator are both analytic, then  $G(s)$  will be analytic except at the locations of the poles (that is, at the roots of the denominator). All singularities of rational algebraic functions are pole locations.

Let  $G(s)$  be analytic except at  $s_0$ . Then we may write  $G(s)$  in its Laurent series expansion form:

$$G(s) = \frac{A_{-n}}{(s - s_0)^n} + \dots + \frac{A_{-1}}{(s - s_0)} + B_0 + B_1(s - s_0) + \dots \quad (\text{WA.37})$$

The coefficient  $A_{-1}$  is called the **residue** of  $G(s)$  at  $s_0$ , and may be evaluated as

$$A_{-1} = \text{Res}[G(s); s_0] = \frac{1}{2\pi j} \oint_C G(s) ds, \quad (\text{WA.38})$$

where  $C$  denotes a closed arc within an analytic region centered at  $s_0$  that contains no other singularity, as shown in Fig. WA.6. When  $s_0$  is not repeated with  $n = 1$ , we have

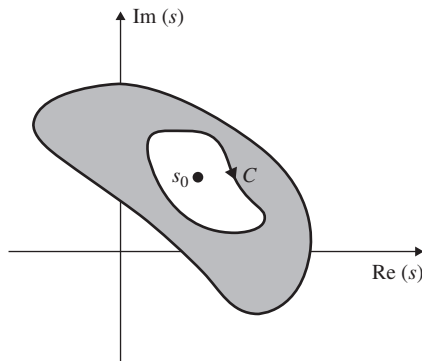
$$A_{-1} = \text{Res}[G(s); s_0] = (s - s_0)G(s)|_{s=s_0}. \quad (\text{WA.39})$$

This is the familiar cover-up method of computing residues.

## 8 Appendix WA A Review of Complex Variables

**Figure WA.6**

Contour around an isolated singularity



### WA.9 Residue Theorem

If the contour  $C$  contains  $l$  singularities, then Eq. (WA.39) may be generalized to yield **Cauchy's residue theorem**:

$$\frac{1}{2\pi j} \oint G(s) ds = \sum_{i=1}^l \text{Res}[G(s); s_i]. \quad (\text{WA.40})$$

### WA.10 The Argument Principle

Before stating the argument principle, we need a preliminary result from which the principle follows readily.

#### Number of Poles and Zeros

Let  $G(s)$  be an analytic function inside and on a closed contour  $C$ , except for a finite number of poles inside  $C$ . Then, for  $C$  described in the positive sense (clockwise direction),

$$\frac{1}{2\pi j} \oint \frac{G'(s)}{G(s)} ds = N - P, \quad (\text{WA.41})$$

or

$$\frac{1}{2\pi j} \oint d(\ln G) = N - P, \quad (\text{WA.42})$$

where  $N$  and  $P$  are the total number of zeros and poles of  $G$  inside  $C$ , respectively. A pole or zero of multiplicity  $k$  is counted  $k$  times.

**Proof** Let  $s_0$  be a zero of  $G$  with multiplicity  $k$ . Then, in some neighborhood of that point, we may write  $G(s)$  as

$$G(s) = (s - s_0)^k f(s), \quad (\text{WA.43})$$

where  $f(s)$  is analytic and  $f(s_0) \neq 0$ . If we differentiate Eq. (WA.43), we obtain

$$G'(s) = k(s - s_0)^{k-1}f(s) + (s - s_0)^kf'(s). \quad (\text{WA.44})$$

Equation (WA.44) may be rewritten as

$$\frac{G'(s)}{G(s)} = \frac{k}{s - s_0} + \frac{f'(s)}{f(s)}. \quad (\text{WA.45})$$

Therefore,  $G'(s)/G(s)$  has a pole at  $s = s_0$  with residue  $K$ . This analysis may be repeated for every zero. Hence, the sum of the residues of  $G'(s)/G(s)$  is the number of zeros of  $G(s)$  inside  $C$ . If  $s_0$  is a pole with multiplicity  $l$ , we may write

$$h(s) = (s - s_0)^l G(s), \quad (\text{WA.46})$$

where  $h(s)$  is analytic and  $h(s_0) \neq 0$ . Then Eq. (WA.46) may be rewritten as

$$G(s) = \frac{h(s)}{(s - s_0)^l}. \quad (\text{WA.47})$$

Differentiating Eq. (WA.47), we obtain

$$G'(s) = \frac{h'(s)}{(s - s_0)^l} - \frac{l h(s)}{(s - s_0)^{l+1}}, \quad (\text{WA.48})$$

so

$$\frac{G'(s)}{G(s)} = \frac{-l}{s - s_0} + \frac{h'(s)}{h(s)}. \quad (\text{WA.49})$$

This analysis may be repeated for every pole. The result is that the sum of the residues of  $G'(s)/G(s)$  at all the poles of  $G(s)$  is  $-P$ .

## The Argument Principle

Using Eq. (WA.38), we get

$$\frac{1}{2\pi j} \oint_C d[\ln G(s)] = N - P, \quad (\text{WA.50})$$

where  $d[\ln G(s)]$  was substituted for  $G'(s)/G(s)$ . If we write  $G(s)$  in polar form, then

$$\begin{aligned} \oint_\Gamma d[\ln G(s)] &= \oint_\Gamma d\{\ln |G(s)| + j \arg[\ln G(s)]\} \\ &= \ln |G(s)| \Big|_{s=s_1}^{s=s_2} + j \arg G(s) \Big|_{s=s_1}^{s=s_2}. \end{aligned} \quad (\text{WA.51})$$

Because  $\Gamma$  is a closed contour, the first term is zero, but the second term is  $2\pi$  times the net encirclements of the origin:

$$\frac{1}{2\pi j} \oint_\Gamma d[\ln G(s)] = N - P. \quad (\text{WA.52})$$

Intuitively, the argument principle may be stated as follows: We let  $G(s)$  be a rational function that is analytic except possibly at a finite number of points. We select an arbitrary contour in the  $s$ -plane so  $G(s)$

is analytic at every point on the contour (the contour does not pass through any of the singularities). The corresponding mapping into the  $G(s)$ -plane may encircle the origin. The number of times it does so is determined by the difference between the number of zeros and the number of poles of  $G(s)$  encircled by the  $s$ -plane contour. The direction of this encirclement is determined by which is greater,  $N$  (clockwise) or  $P$  (counter-clockwise). For example, if the contour encircles a single zero, the mapping will encircle the origin once in the clockwise direction. Similarly, if the contour encloses only a single pole, the mapping will encircle the origin, this time in the counter-clockwise direction. If the contour encircles no singularities, or if the contour encloses an equal number of poles and zeros, there will be no encirclement of the origin. A contour evaluation of  $G(s)$  will encircle the origin if there is a nonzero net difference between the encircled singularities. The mapping is **conformal** as well, which means that the magnitude and sense of the angles between smooth arcs is preserved. Chapter 6 provides a more detailed intuitive treatment of the argument principle and its application to feedback control in the form of the Nyquist stability theorem.

## WA.11 Bilinear Transformation

A bilinear transformation is of the form

$$w = \frac{as + b}{cs + d}, \quad (\text{WA.53})$$

where  $a, b, c, d$  are complex constants, and it is assumed  $ad - bc \neq 0$ . The bilinear transformation always transforms circles in the  $w$ -plane into circles in the  $s$ -plane. This can be shown in several ways. If we solve for  $s$ , we obtain

$$s = \frac{-dw + b}{cw - a}. \quad (\text{WA.54})$$

The equation for a circle in the  $w$ -plane is of the form

$$\frac{|w - \sigma|}{|w - \rho|} = R. \quad (\text{WA.55})$$

If we substitute for  $w$  in terms of  $s$  in Eq. (WA.53), we get

$$\frac{|s - \sigma'|}{|s - \rho'|} = R', \quad (\text{WA.56})$$

where

$$\sigma' = \frac{\sigma d - b}{a - \sigma c}, \quad \rho' = \frac{\rho d - b}{a - \rho c}, \quad R' = \left| \frac{a - \rho c}{a - \sigma c} \right| R, \quad (\text{WA.57})$$

which is the equation for a circle in the  $s$ -plane. For alternative proofs, the reader is referred to Brown and Churchill (1996) and Marsden and Hoffman (1998).

# Appendix WB

## Summary of Matrix Theory

In the text, we assume you are already somewhat familiar with matrix theory and with the solution of linear systems of equations. However, for the purposes of review we present here a brief summary of matrix theory with an emphasis on the results needed in control theory. For further study, see Strang (2006) and Gantmacher (1959).

### WB.1 Matrix Definitions

An array of numbers arranged in rows and columns is referred to as a **matrix**. If  $\mathbf{A}$  is a matrix with  $m$  rows and  $n$  columns, an  $m \times n$  (read “ $m$  by  $n$ ”) matrix, it is denoted as

$$\mathbf{A} = \begin{bmatrix} a_{11} & a_{12} & \cdots & a_{1n} \\ a_{21} & a_{22} & \cdots & a_{2n} \\ \vdots & \vdots & & \vdots \\ a_{m1} & a_{m2} & \cdots & a_{mn} \end{bmatrix}, \quad (\text{WB.1})$$

where the entries  $a_{ij}$  are its elements. If  $m = n$ , then the matrix is **square**; otherwise it is **rectangular**. Sometimes a matrix is simply denoted by  $\mathbf{A} = [a_{ij}]$ . If  $m = 1$  or  $n = 1$ , then the matrix reduces to a **row vector** or a **column vector**, respectively. A **submatrix** of  $\mathbf{A}$  is the matrix with certain rows and columns removed.

### WB.2 Elementary Operations on Matrices

If  $\mathbf{A}$  and  $\mathbf{B}$  are matrices of the same dimension, then their sum is defined by

$$\mathbf{C} = \mathbf{A} + \mathbf{B}, \quad (\text{WB.2})$$

where

$$c_{ij} = a_{ij} + b_{ij}. \quad (\text{WB.3})$$

That is, the addition is done element by element. It is easy to verify the following properties of matrices:

$$\mathbf{A} + \mathbf{B} = \mathbf{B} + \mathbf{A}, \quad (\text{WB.4})$$

$$(\mathbf{A} + \mathbf{B}) + \mathbf{C} = \mathbf{A} + (\mathbf{B} + \mathbf{C}). \quad (\text{WB.5})$$

Two matrices can be multiplied if they are compatible. Let  $\mathbf{A} = m \times n$  and  $\mathbf{B} = n \times p$ . Then the  $m \times p$  matrix

$$\mathbf{C} = \mathbf{AB}, \quad (\text{WB.6})$$

Commutative law for  
addition

Associative law for  
addition

## 12 Appendix WB Summary of Matrix Theory

is the product of the two matrices, where

$$c_{ij} = \sum_{k=1}^n a_{ik} b_{kj}. \quad (\text{WB.7})$$

Associative law for multiplication

Matrix multiplication satisfies the associative law

$$\mathbf{A}(\mathbf{BC}) = (\mathbf{AB})\mathbf{C}, \quad (\text{WB.8})$$

but not the commutative law; that is, in general,

$$\mathbf{AB} \neq \mathbf{BA}. \quad (\text{WB.9})$$

### WB.3 Trace

The **trace** of a square matrix is the sum of its diagonal elements:

$$\text{trace } \mathbf{A} = \sum_{i=1}^n a_{ii}. \quad (\text{WB.10})$$

### WB.4 Transpose

The  $n \times m$  matrix obtained by interchanging the rows and columns of  $\mathbf{A}$  is called the **transpose of matrix A**:

$$\mathbf{A}^T = \begin{bmatrix} a_{11} & a_{21} & \dots & a_{m1} \\ a_{12} & a_{22} & \dots & a_{m2} \\ \vdots & \vdots & & \vdots \\ a_{1n} & a_{2n} & \dots & a_{mn} \end{bmatrix}.$$

A matrix is said to be **symmetric** if

$$\mathbf{A}^T = \mathbf{A}. \quad (\text{WB.11})$$

Transposition

It is easy to show that

$$(\mathbf{AB})^T = \mathbf{B}^T \mathbf{A}^T, \quad (\text{WB.12})$$

$$(\mathbf{ABC})^T = \mathbf{C}^T \mathbf{B}^T \mathbf{A}^T, \quad (\text{WB.13})$$

$$(\mathbf{A} + \mathbf{B})^T = \mathbf{A}^T + \mathbf{B}^T. \quad (\text{WB.14})$$

### WB.5 Determinant and Matrix Inverse

The **determinant** of a square matrix is defined by Laplace's expansion

$$\det \mathbf{A} = \sum_{j=1}^n a_{ij} \gamma_{ij} \quad \text{for any } i = 1, 2, \dots, n, \quad (\text{WB.15})$$

where  $\gamma_{ij}$  is called the **cofactor** and

$$\gamma_{ij} = (-1)^{i+j} \det M_{ij}, \quad (\text{WB.16})$$

where the scalar  $\det M_{ij}$  is called a **minor**.  $M_{ij}$  is the same as the matrix  $\mathbf{A}$  except that its  $i$ th row and  $j$ th column have been removed. Note  $M_{ij}$  is always an  $(n - 1) \times (n - 1)$  matrix, and the minors and cofactors are identical except possibly for a sign.

The **adjugate** of a matrix is the transpose of the matrix of its cofactors:

$$\text{adj } \mathbf{A} = [\gamma_{ij}]^T. \quad (\text{WB.17})$$

It can be shown that

$$\mathbf{A} \text{adj } \mathbf{A} = (\det \mathbf{A}) \mathbf{I}, \quad (\text{WB.18})$$

where  $\mathbf{I}$  is called the **identity matrix**:

$$\mathbf{I} = \begin{bmatrix} 1 & 0 & \dots & \dots & 0 \\ 0 & 1 & 0 & \dots & 0 \\ \vdots & \vdots & \ddots & & \vdots \\ 0 & \dots & \dots & 0 & 1 \end{bmatrix},$$

that is,  $\mathbf{I}$  has ones along the diagonal and zeros elsewhere. If  $\det \mathbf{A} \neq 0$ , then the **inverse** of a matrix  $\mathbf{A}$  is defined by

$$\mathbf{A}^{-1} = \frac{\text{adj } \mathbf{A}}{\det \mathbf{A}}, \quad (\text{WB.19})$$

and has the property

$$\mathbf{A}\mathbf{A}^{-1} = \mathbf{A}^{-1}\mathbf{A} = \mathbf{I}. \quad (\text{WB.20})$$

Note a matrix has an inverse—that is, it is **nonsingular**—if its determinant is nonzero.

The inverse of the product of two matrices is the product of the inverse of the matrices in reverse order:

$$(\mathbf{AB})^{-1} = \mathbf{B}^{-1}\mathbf{A}^{-1} \quad (\text{WB.21})$$

### Inversion

and

$$(\mathbf{ABC})^{-1} = \mathbf{C}^{-1}\mathbf{B}^{-1}\mathbf{A}^{-1}. \quad (\text{WB.22})$$

## WB.6 Properties of the Determinant

When dealing with determinants of matrices, the following elementary (row or column) operations are useful:

1. If any row (or column) of  $\mathbf{A}$  is multiplied by a scalar  $\alpha$ , the resulting matrix  $\bar{\mathbf{A}}$  has the determinant

$$\det \bar{\mathbf{A}} = \alpha \det \mathbf{A}. \quad (\text{WB.23})$$

Hence

$$\det(\alpha \mathbf{A}) = \alpha^n \det \mathbf{A}. \quad (\text{WB.24})$$

2. If any two rows (or columns) of  $\mathbf{A}$  are interchanged to obtain  $\bar{\mathbf{A}}$ , then

$$\det \bar{\mathbf{A}} = -\det \mathbf{A}. \quad (\text{WB.25})$$

## 14 Appendix WB Summary of Matrix Theory

3. If a multiple of a row (or column) of  $\mathbf{A}$  is added to another to obtain  $\bar{\mathbf{A}}$ , then

$$\det \bar{\mathbf{A}} = \det \mathbf{A}. \quad (\text{WB.26})$$

4. It is also easy to show that

$$\det \mathbf{A} = \det \mathbf{A}^T \quad (\text{WB.27})$$

and

$$\det \mathbf{AB} = \det \mathbf{A} \det \mathbf{B}. \quad (\text{WB.28})$$

Applying Eq. (WB.28) to Eq. (WB.20), we have

$$\det \mathbf{A} \det \mathbf{A}^{-1} = 1. \quad (\text{WB.29})$$

If  $\mathbf{A}$  and  $\mathbf{B}$  are square matrices, then the determinant of the block triangular matrix is the product of the determinants of the diagonal blocks:

$$\det \begin{bmatrix} \mathbf{A} & \mathbf{C} \\ \mathbf{0} & \mathbf{B} \end{bmatrix} = \det \mathbf{A} \det \mathbf{B}. \quad (\text{WB.30})$$

If  $\mathbf{A}$  is nonsingular, then

$$\det \begin{bmatrix} \mathbf{A} & \mathbf{B} \\ \mathbf{C} & \mathbf{D} \end{bmatrix} = \det \mathbf{A} \det(\mathbf{D} - \mathbf{CA}^{-1}\mathbf{B}). \quad (\text{WB.31})$$

Using this identity, we can write the transfer function of a scalar system in a compact form:

$$G(s) = \mathbf{C}(s\mathbf{I} - \mathbf{A})^{-1}\mathbf{B} + \mathbf{D} = \frac{\det \begin{bmatrix} s\mathbf{I} - \mathbf{A} & \mathbf{B} \\ -\mathbf{C} & \mathbf{D} \end{bmatrix}}{\det(s\mathbf{I} - \mathbf{A})}. \quad (\text{WB.32})$$

## WB.7 Inverse of Block Triangular Matrices

If  $\mathbf{A}$  and  $\mathbf{B}$  are square invertible matrices, then

$$\begin{bmatrix} \mathbf{A} & \mathbf{C} \\ \mathbf{0} & \mathbf{B} \end{bmatrix}^{-1} = \begin{bmatrix} \mathbf{A}^{-1} & -\mathbf{A}^{-1}\mathbf{CB}^{-1} \\ \mathbf{0} & \mathbf{B}^{-1} \end{bmatrix}. \quad (\text{WB.33})$$

## WB.8 Special Matrices

### Diagonal matrix

Some matrices have special structures and are given names. We have already defined the identity matrix, which has a special form. A **diagonal matrix** has (possibly) nonzero elements along the main diagonal and zeros elsewhere:

$$\mathbf{A} = \begin{bmatrix} a_{11} & & \mathbf{0} & & & \\ & a_{22} & & & & \\ & & a_{33} & & & \\ & & & \ddots & & \\ & & & & \mathbf{0} & \\ & & & & & a_{nn} \end{bmatrix}. \quad (\text{WB.34})$$

### Upper triangular matrix

A matrix is said to be **(upper) triangular** if all the elements below the main diagonal are zeros:

$$\mathbf{A} = \begin{bmatrix} a_{11} & a_{12} & \cdots & a_{1n} \\ 0 & a_{22} & & \\ \vdots & 0 & & \vdots \\ 0 & \vdots & \ddots & \ddots \\ 0 & 0 & \cdots & 0 & a_{nn} \end{bmatrix}. \quad (\text{WB.35})$$

The determinant of a diagonal or triangular matrix is simply the product of its diagonal elements.

A matrix is said to be in the **(upper) companion form** if it has the structure

$$\mathbf{A}_c = \begin{bmatrix} -a_1 & -a_2 & \cdots & -a_n \\ 1 & 0 & \cdots & 0 \\ 0 & 1 & 0 & \cdots & 0 \\ \vdots & & \ddots & & \vdots \\ 0 & \cdots & \cdots & 1 & 0 \end{bmatrix}. \quad (\text{WB.36})$$

Note all the information is contained in the first row. Variants of this form are the lower, left, or right companion matrices. A **Vandermonde matrix** has the following structure:

$$\mathbf{A} = \begin{bmatrix} 1 & a_1 & a_1^2 & \cdots & a_1^{n-1} \\ 1 & a_2 & a_2^2 & \cdots & a_2^{n-1} \\ \vdots & \vdots & \vdots & & \vdots \\ 1 & a_n & a_n^2 & \cdots & a_n^{n-1} \end{bmatrix}. \quad (\text{WB.37})$$

## WB.9 Rank

The **rank** of a matrix is the number of its linearly independent rows or columns. If the rank of  $\mathbf{A}$  is  $r$ , then all  $(r+1) \times (r+1)$  submatrices of  $\mathbf{A}$  are singular, and there is at least one  $r \times r$  submatrix that is nonsingular. It is also true that

$$\text{row rank of } \mathbf{A} = \text{column rank of } \mathbf{A}. \quad (\text{WB.38})$$

## WB.10 Characteristic Polynomial

The **characteristic polynomial** of a matrix  $\mathbf{A}$  is defined by

$$\begin{aligned} a(s) &\triangleq \det(s\mathbf{I} - \mathbf{A}) \\ &= s^n + a_1 s^{n-1} + \cdots + a_{n-1} s + a_n, \end{aligned} \quad (\text{WB.39})$$

where the roots of the polynomial are referred to as **eigenvalues** of  $\mathbf{A}$ . We can write

$$a(s) = (s - \lambda_1)(s - \lambda_2) \cdots (s - \lambda_n), \quad (\text{WB.40})$$

where  $\{\lambda_i\}$  are the eigenvalues of  $\mathbf{A}$ . The characteristic polynomial of a companion matrix [for example, Eq. (WB.36)] is

$$\begin{aligned} a(s) &= \det(s\mathbf{I} - \mathbf{A}_c) \\ &= s^n + a_1 s^{n-1} + \cdots + a_{n-1} s + a_n. \end{aligned} \quad (\text{WB.41})$$

## WB.11 Cayley–Hamilton Theorem

The Cayley–Hamilton theorem states that every square matrix  $\mathbf{A}$  satisfies its characteristic polynomial. This means if  $\mathbf{A}$  is an  $n \times n$  matrix with characteristic equation  $a(s)$ , then

$$a(\mathbf{A}) \triangleq \mathbf{A}^n + a_1 \mathbf{A}^{n-1} + \cdots + a_{n-1} \mathbf{A} + a_n \mathbf{I} = 0. \quad (\text{WB.42})$$

## WB.12 Eigenvalues and Eigenvectors

Any scalar  $\lambda$  and nonzero vector  $\mathbf{v}$  that satisfy

$$\mathbf{A}\mathbf{v} = \lambda\mathbf{v}, \quad (\text{WB.43})$$

are referred to as the eigenvalue and the associated (**right**) **eigenvector** of the matrix  $\mathbf{A}$  [because  $\mathbf{v}$  appears to the right of  $\mathbf{A}$  in Eq. (WB.43)]. By rearranging terms in Eq. (WB.43), we get

$$(\lambda\mathbf{I} - \mathbf{A})\mathbf{v} = 0. \quad (\text{WB.44})$$

Because  $\mathbf{v}$  is nonzero,

$$\det(\lambda\mathbf{I} - \mathbf{A}) = 0, \quad (\text{WB.45})$$

so  $\lambda$  is an eigenvalue of the matrix  $\mathbf{A}$  as defined in Eq. (WB.43). The normalization of the eigenvectors is arbitrary; that is, if  $\mathbf{v}$  is an eigenvector, so is  $\alpha\mathbf{v}$ . The eigenvectors are usually normalized to have unit length; that is,  $\|\mathbf{v}\|^2 = \mathbf{v}^T \mathbf{v} = 1$ .

If  $\mathbf{w}^T$  is a nonzero row vector such that

$$\mathbf{w}^T \mathbf{A} = \lambda \mathbf{w}^T, \quad (\text{WB.46})$$

then  $\mathbf{w}$  is called a **left eigenvector** of  $\mathbf{A}$  [because  $\mathbf{w}^T$  appears to the left of  $\mathbf{A}$  in Eq. (WB.46)]. Note we can write

$$\mathbf{A}^T \mathbf{w} = \lambda \mathbf{w}, \quad (\text{WB.47})$$

so  $\mathbf{w}$  is simply a right eigenvector of  $\mathbf{A}^T$ .

## WB.13 Similarity Transformations

Consider the arbitrary nonsingular matrix  $\mathbf{T}$  such that

$$\bar{\mathbf{A}} = \mathbf{T}^{-1} \mathbf{A} \mathbf{T}. \quad (\text{WB.48})$$

The matrix operation shown in Eq. (WB.48) is referred to as a **similarity transformation**. If  $\mathbf{A}$  has a full set of eigenvectors, then we can choose  $\mathbf{T}$  to be the set of eigenvectors, and  $\bar{\mathbf{A}}$  will be diagonal.

Consider the set of equations in state-variable form:

$$\dot{\mathbf{x}} = \mathbf{Ax} + \mathbf{Bu}. \quad (\text{WB.49})$$

If we let

$$\mathbf{T}\xi = \mathbf{x}, \quad (\text{WB.50})$$

then Eq. (WB.49) becomes

$$\mathbf{T}\dot{\xi} = \mathbf{AT}\xi + \mathbf{Bu}, \quad (\text{WB.51})$$

and premultiplying both sides by  $\mathbf{T}^{-1}$ , we get

$$\begin{aligned} \dot{\xi} &= \mathbf{T}^{-1}\mathbf{AT}\xi + \mathbf{T}^{-1}\mathbf{Bu} \\ &= \bar{\mathbf{A}}\xi + \bar{\mathbf{B}}u, \end{aligned} \quad (\text{WB.52})$$

where

$$\begin{aligned} \bar{\mathbf{A}} &= \mathbf{T}^{-1}\mathbf{AT}, \\ \bar{\mathbf{B}} &= \mathbf{T}^{-1}\mathbf{B}. \end{aligned} \quad (\text{WB.53})$$

The characteristic polynomial of  $\bar{\mathbf{A}}$  is

$$\begin{aligned} \det(s\mathbf{I} - \bar{\mathbf{A}}) &= \det(s\mathbf{I} - \mathbf{T}^{-1}\mathbf{AT}) \\ &= \det(s\mathbf{T}^{-1}\mathbf{T} - \mathbf{T}^{-1}\mathbf{AT}) \\ &= \det[\mathbf{T}^{-1}(s\mathbf{I} - \mathbf{A})\mathbf{T}] \\ &= \det \mathbf{T}^{-1} \det(s\mathbf{I} - \mathbf{A}) \det \mathbf{T}. \end{aligned} \quad (\text{WB.54})$$

Using Eq. (WB.29), Eq. (WB.54) becomes

$$\det(s\mathbf{I} - \bar{\mathbf{A}}) = \det(s\mathbf{I} - \mathbf{A}). \quad (\text{WB.55})$$

From Eq. (WB.55), we can see that  $\bar{\mathbf{A}}$  and  $\mathbf{A}$  both have the same characteristic polynomial, giving us the important result that a similarity transformation does not change the eigenvalues of a matrix. From Eq. (WB.50), a new state made up of a linear combination of the old state has the same eigenvalues as the old set.

## WB.14 Matrix Exponential

Let  $\mathbf{A}$  be a square matrix. The **matrix exponential** of  $\mathbf{A}$  is defined as the series

$$e^{\mathbf{At}} = \mathbf{I} + \mathbf{At} + \frac{1}{2!}\mathbf{A}^2t^2 + \frac{\mathbf{A}^3t^3}{3!} + \dots \quad (\text{WB.56})$$

It can be shown that the series converges. If  $\mathbf{A}$  is an  $n \times n$  matrix, then  $e^{\mathbf{At}}$  is also an  $n \times n$  matrix and can be differentiated:

$$\frac{d}{dt}e^{\mathbf{At}} = \mathbf{A}e^{\mathbf{At}}. \quad (\text{WB.57})$$

Other properties of the matrix exponential are

$$e^{\mathbf{A}t_1}e^{\mathbf{A}t_2} = e^{\mathbf{A}(t_1+t_2)} \quad (\text{WB.58})$$

and, in general,

$$e^{\mathbf{A}}e^{\mathbf{B}} \neq e^{\mathbf{B}}e^{\mathbf{A}}. \quad (\text{WB.59})$$

(In the exceptional case where  $\mathbf{A}$  and  $\mathbf{B}$  commute—that is,  $\mathbf{AB} = \mathbf{BA}$ —then  $e^{\mathbf{A}}e^{\mathbf{B}} = e^{\mathbf{B}}e^{\mathbf{A}}$ .)

## WB.15 Fundamental Subspaces

The **range space** of  $\mathbf{A}$ , denoted by  $\mathcal{R}(\mathbf{A})$  and also called the **column space** of  $\mathbf{A}$ , is defined by the set of vectors

$$\mathbf{x} = \mathbf{Ay}, \quad (\text{WB.60})$$

for some vector  $\mathbf{y}$ . The **null space** of  $\mathbf{A}$ , denoted by  $\mathcal{N}(\mathbf{A})$ , is defined by the set of vectors  $\mathbf{x}$  such that

$$\mathbf{Ax} = \mathbf{0}. \quad (\text{WB.61})$$

If  $x \in \mathcal{N}(\mathbf{A})$  and  $y \in \mathcal{R}(\mathbf{A}^T)$ , then  $\mathbf{y}^T \mathbf{x} = 0$ ; that is, every vector in the null space of  $\mathbf{A}$  is **orthogonal** to every vector in the range space of  $\mathbf{A}^T$ .

## WB.16 Singular-Value Decomposition

The **singular-value decomposition (SVD)** is one of the most useful tools in linear algebra and has been widely used in control theory during the last few decades. Let  $\mathbf{A}$  be an  $m \times n$  matrix. Then there always exist matrices  $\mathbf{U}$ ,  $\mathbf{S}$ , and  $\mathbf{V}$  such that

$$\mathbf{A} = \mathbf{USV}^T. \quad (\text{WB.62})$$

Here  $\mathbf{U}$  and  $\mathbf{V}$  are **orthogonal matrices**; that is,

$$\mathbf{UU}^T = \mathbf{I}, \mathbf{VV}^T = \mathbf{I}. \quad (\text{WB.63})$$

$\mathbf{S}$  is a **quasidiagonal matrix** with singular values as its diagonal elements; that is,

$$\mathbf{S} = \begin{bmatrix} \Sigma & 0 \\ 0 & 0 \end{bmatrix}, \quad (\text{WB.64})$$

where  $\Sigma$  is a diagonal matrix of nonzero singular values in descending order:

$$\sigma_1 \geq \sigma_2 \geq \dots \geq \sigma_r > 0. \quad (\text{WB.65})$$

The unique diagonal elements of  $\mathbf{S}$  are called the **singular values**. The maximum singular value is denoted by  $\bar{\sigma}(\mathbf{A})$ , and the minimum singular value is denoted by  $\underline{\sigma}(\mathbf{A})$ . The rank of the matrix is the same as the number of nonzero singular values. The columns of  $\mathbf{U}$  and  $\mathbf{V}$ ,

$$\begin{aligned} \mathbf{U} &= [ u_1 \quad u_2 \quad \dots \quad u_m ], \\ \mathbf{V} &= [ v_1 \quad v_2 \quad \dots \quad v_n ], \end{aligned} \quad (\text{WB.66})$$

are called the left and right **singular vectors**, respectively. SVD provides complete information about the fundamental subspaces associated with a matrix:

$$\begin{aligned}\mathcal{N}(\mathbf{A}) &= \text{span} [ v_{r+1} \quad v_{r+2} \quad \dots \quad v_n ], \\ \mathcal{R}(\mathbf{A}) &= \text{span} [ u_1 \quad u_2 \quad \dots \quad u_r ], \\ \mathcal{R}(\mathbf{A}^T) &= \text{span} [ v_1 \quad v_2 \quad \dots \quad v_r ], \\ \mathcal{N}(\mathbf{A}^T) &= \text{span} [ u_{r+1} \quad u_{r+2} \quad \dots \quad u_m ].\end{aligned}\quad (\text{WB.67})$$

Here  $\mathcal{N}$  denotes the null space and  $\mathcal{R}$ , the range space, respectively.

The **norm** of the matrix  $\mathbf{A}$ , denoted by  $\|\mathbf{A}\|_2$ , is given by

$$\|\mathbf{A}\|_2 = \bar{\sigma}(\mathbf{A}). \quad (\text{WB.68})$$

If  $\mathbf{A}$  is a function of  $\omega$ , then the infinity norm of  $\mathbf{A}$ ,  $\|\mathbf{A}\|_\infty$ , is given by

$$\|\mathbf{A}(j\omega)\|_\infty = \max_{\omega} \bar{\sigma}(\mathbf{A}). \quad (\text{WB.69})$$

## WB.17 Positive Definite Matrices

A matrix  $\mathbf{A}$  is said to be **positive semidefinite** if

$$\mathbf{x}^T \mathbf{A} \mathbf{x} \geq 0 \quad \text{for all } \mathbf{x}. \quad (\text{WB.70})$$

The matrix is said to be **positive definite** if equality holds in Eq. (WB.70) only for  $\mathbf{x} = 0$ . A symmetric matrix is positive definite if and only if all of its eigenvalues are positive. It is positive semidefinite if and only if all of its eigenvalues are nonnegative.

An alternate method for determining positive definiteness is to test the minors of the matrix. A matrix is positive definite if all the leading principal minors are positive, and positive semidefinite if they are all nonnegative.

## WB.18 Matrix Identity

If  $\mathbf{A}$  is an  $n \times m$  matrix and  $\mathbf{B}$  is an  $m \times n$  matrix, then

$$\det[\mathbf{I}_n - \mathbf{AB}] = \det[\mathbf{I}_m - \mathbf{BA}],$$

where  $\mathbf{I}_n$  and  $\mathbf{I}_m$  are identity matrices of size  $n$  and  $m$ , respectively.

## WB.19 Cramer's Rule

Consider the solution to a linear system of equations:

$$\left[ \begin{array}{cccc} a_{11} & a_{12} & \cdots & a_{1n} \\ a_{21} & a_{22} & \cdots & a_{2n} \\ \vdots & \vdots & & \vdots \\ a_{n1} & a_{n2} & \cdots & a_{nn} \end{array} \right] \left[ \begin{array}{c} x_1 \\ x_2 \\ \vdots \\ x_n \end{array} \right] = \left[ \begin{array}{c} b_1 \\ b_2 \\ \vdots \\ b_n \end{array} \right], \quad (\text{WB.71})$$

## 20 Appendix WB Summary of Matrix Theory

or

$$Ax = b, \quad (\text{WB.72})$$

where  $A$  is a nonsingular square  $n \times n$  matrix,  $x$  is an  $n \times 1$  vector of the unknowns, and  $b$  is also an  $n \times 1$  vector. The solution can be expressed in terms of the ratio of the two determinants

$$x_i = \frac{\det(A_i)}{\det(A)}, \quad i = 1, 2, \dots, n \quad (\text{WB.73})$$

where  $A_i$  is the matrix  $A$  with its  $i$ th column replaced by  $b$ .

# Appendix WC

## Controllability and Observability

Controllability and observability are important structural properties of dynamic systems. First identified and studied by Kalman (1960) and later by Kalman et al. (1961), these properties have continued to be examined during the last five decades. We will discuss only a few of the known results for linear constant systems with one input and one output. In the text, we discuss these concepts in connection with control law and estimator designs. For example, in Section 7.4, we suggest that, if the square matrix given by

$$\mathcal{C} = [\mathbf{B} \ \mathbf{AB} \ \mathbf{A}^2\mathbf{B} \ \dots \ \mathbf{A}^{n-1}\mathbf{B}], \quad (\text{WC.1})$$

is nonsingular, by transformation of the state we can convert the given description into control-canonical form. We can then construct a control law that will give the closed-loop system an arbitrary characteristic equation.

### WC.1 Controllability

We begin our formal discussion of controllability with the first of four definitions.

**Definition WC.1** *The system  $(\mathbf{A}, \mathbf{B})$  is **controllable** if, for any given  $n$ -th-order polynomial  $\alpha_c(s)$ , there exists a (unique) control law  $u = -\mathbf{Kx}$  such that the characteristic polynomial of  $\mathbf{A} - \mathbf{BK}$  is  $\alpha_c(s)$ .*

From the results of Ackermann's formula (see Appendix WD), we have the following mathematical test for controllability:  $(\mathbf{A}, \mathbf{B})$  is a controllable pair if and only if the rank of  $\mathcal{C}$  is  $n$ . Definition WC.1 based on pole placement is a frequency-domain concept. Controllability can be equivalently defined in the time domain.

**Definition WC.2** *The system  $(\mathbf{A}, \mathbf{B})$  is **controllable** if there exists a (piecewise continuous) control signal  $u(t)$  that will take the state of the system from any initial state  $\mathbf{x}_0$  to any desired final state  $\mathbf{x}_f$  in a finite time interval.*

We will now show that the system is controllable by this definition if and only if  $\mathcal{C}$  is full rank. We first assume that the system is controllable but

$$\text{rank}[\mathbf{B} \ \mathbf{AB} \ \mathbf{A}^2\mathbf{B} \ \dots \ \mathbf{A}^{n-1}\mathbf{B}] < n. \quad (\text{WC.2})$$

We can then find a vector  $\mathbf{v}$  such that

$$\mathbf{v}[\mathbf{B} \mathbf{A} \mathbf{B} \mathbf{A}^2 \mathbf{B} \dots \mathbf{A}^{n-1} \mathbf{B}] = 0 \quad (\text{WC.3})$$

or

$$\mathbf{v}\mathbf{B} = \mathbf{v}\mathbf{AB} = \mathbf{v}\mathbf{A}^2\mathbf{B} = \dots = \mathbf{v}\mathbf{A}^{n-1}\mathbf{B} = 0. \quad (\text{WC.4})$$

The Cayley-Hamilton theorem states that  $\mathbf{A}$  satisfies its own characteristic equation, namely,

$$-\mathbf{A}^n = a_1\mathbf{A}^{n-1} + a_2\mathbf{A}^{n-2} + \dots + a_n\mathbf{I}. \quad (\text{WC.5})$$

Therefore,

$$-\mathbf{v}\mathbf{A}^n\mathbf{B} = a_1\mathbf{v}\mathbf{A}^{n-1}\mathbf{B} + a_2\mathbf{v}\mathbf{A}^{n-2}\mathbf{B} + \dots + a_n\mathbf{v}\mathbf{B} = 0. \quad (\text{WC.6})$$

By induction,  $\mathbf{v}\mathbf{A}^{n+k}\mathbf{B} = 0$  for  $k = 0, 1, 2, \dots$ , or  $\mathbf{v}\mathbf{A}^m\mathbf{B} = 0$  for  $m = 0, 1, 2, \dots$ , and thus

$$\mathbf{v}e^{\mathbf{At}}\mathbf{B} = \mathbf{v}\left(\mathbf{I} + \mathbf{At} + \frac{1}{2!}\mathbf{A}^2t^2 + \dots\right)\mathbf{B} = 0, \quad (\text{WC.7})$$

for all  $t$ . However, the zero initial-condition response ( $\mathbf{x}_0 = \mathbf{0}$ ) is

$$\begin{aligned} \mathbf{x}(t) &= \int_0^t e^{\mathbf{A}(t-\tau)}\mathbf{B}u(\tau) d\tau \\ &= e^{\mathbf{At}} \int_0^t e^{-\mathbf{A}\tau}\mathbf{B}u(\tau) d\tau. \end{aligned} \quad (\text{WC.8})$$

Using Eq. (WC.7), Eq. (WC.8) becomes

$$\mathbf{v}\mathbf{x}(t) = \int_0^t \mathbf{v}e^{\mathbf{A}(t-\tau)}\mathbf{B}u(\tau) d\tau = 0, \quad (\text{WC.9})$$

for all  $u(t)$  and  $t > 0$ . This implies that all points reachable from the origin are orthogonal to  $\mathbf{v}$ . This restricts the reachable space, and therefore contradicts the second definition of controllability. Thus if  $\mathcal{C}$  is singular,  $(\mathbf{A}, \mathbf{B})$  is not controllable by Definition WC.2.

Next, we assume  $\mathcal{C}$  is full rank but  $(\mathbf{A}, \mathbf{B})$  is uncontrollable by Definition WC.2. This means that there exists a nonzero vector  $\mathbf{v}$  such that

$$\mathbf{v} \int_0^{t_f} e^{\mathbf{A}^{(t_f-\tau)}}\mathbf{B}u(\tau) d\tau = 0, \quad (\text{WC.10})$$

because the whole state-space is not reachable. But Eq. (WC.10) implies that

$$\mathbf{v}e^{\mathbf{A}^{(t_f-\tau)}}\mathbf{B} = 0, \quad 0 \leq \tau \leq t_f. \quad (\text{WC.11})$$

If we set  $\tau = t_f$ , we see  $\mathbf{v}\mathbf{B} = 0$ . Also, differentiating Eq. (WC.11) and letting  $\tau = t_f$  gives  $\mathbf{v}\mathbf{AB} = 0$ . Continuing this process, we find

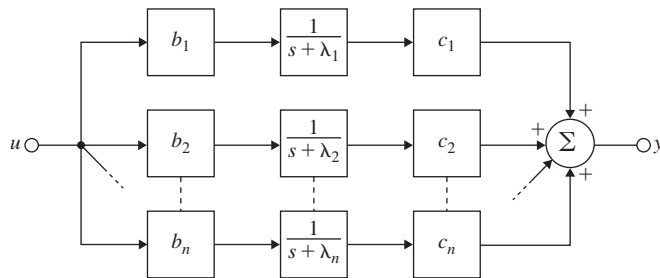
$$\mathbf{v}\mathbf{B} = \mathbf{v}\mathbf{AB} = \mathbf{v}\mathbf{A}^2\mathbf{B} = \dots = \mathbf{v}\mathbf{A}^{n-1}\mathbf{B} = 0, \quad (\text{WC.12})$$

which contradicts the assumption that  $\mathcal{C}$  is full rank.

We have now shown the system is controllable by Definition WC.2 if and only if the rank of  $\mathcal{C}$  is  $n$ , which is exactly the same condition we found for pole assignment.

**Figure WC.1**

Block diagram of a system with a diagonal matrix



Our final definition comes closest to the structural character of controllability.

**Definition WC.3** *The system  $(A, B)$  is controllable if every mode of  $A$  is connected to the control input.*

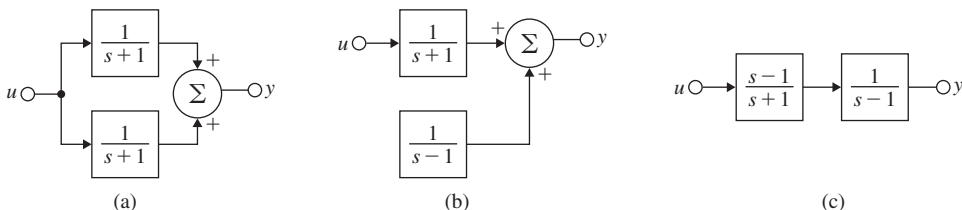
Because of the generality of the modal structure of systems, we will treat only the case of systems for which  $A$  can be transformed to diagonal form. (The double-integration plant does *not* qualify.) Suppose we have a diagonal matrix  $A_d$  and its corresponding input matrix  $B_d$  with elements  $b_i$ . The structure of such a system is shown in Fig. (WC.1). By definition, for a controllable system, the input must be connected to each mode so the  $b_i$  are all nonzero. However, this is not enough if the poles ( $\lambda_i$ ) are not distinct. Suppose, for instance, that  $\lambda_1 = \lambda_2$ . The first two state equations are then

$$\begin{aligned}\dot{x}_{1d} &= \lambda_1 x_{1d} + b_{1d}, \\ \dot{x}_{2d} &= \lambda_1 x_{2d} + b_{2d}.\end{aligned}\quad (\text{WC.13})$$

If we define a new state,  $\xi = b_2 x_{1d} - b_1 x_{2d}$ , the equation for  $\xi$  is

$$\dot{\xi} = b_2 \dot{x}_{1d} - b_1 \dot{x}_{2d} = b_2 \lambda_1 x_{1d} + b_2 b_{1d} - b_1 \lambda_1 x_{2d} - b_1 b_{2d} = \lambda_1 \xi,\quad (\text{WC.14})$$

which does not include the control  $u$ ; hence,  $\xi$  is not controllable. The point is that if any two poles are equal *in a diagonal  $A_d$  system with only one input*, we effectively have a hidden mode that is not connected to the control, and the system is not controllable (see Fig. WC.2a). This is because the two state variables move together exactly, so we cannot

**Figure WC.2**

Examples of uncontrollable systems

independently control  $x_{1d}$  and  $x_{2d}$ . Therefore, even in such a simple case, we have two conditions for controllability:

1. All eigenvalues of  $\mathbf{A}_d$  are distinct.
2. No element of  $\mathbf{B}_d$  is zero.

Now let us consider the controllability matrix of this diagonal system. By direct computation,

$$\begin{aligned} \mathcal{C} &= \begin{bmatrix} b_1 & b_1\lambda_1 & \dots & b_1\lambda_1^{n-1} \\ b_2 & b_2\lambda_2 & \dots & \vdots \\ \vdots & \vdots & \dots & \vdots \\ b_n & b_n\lambda_n & \dots & b_n\lambda_n^{n-1} \end{bmatrix} \\ &= \begin{bmatrix} b_1 & & \mathbf{0} \\ & b_2 & \\ & \ddots & \\ \mathbf{0} & & b_n \end{bmatrix} \begin{bmatrix} 1 & \lambda_1 & \lambda_1^2 & \dots & \lambda_1^{n-1} \\ 1 & \lambda_2 & \lambda_2^2 & \dots & \vdots \\ \vdots & \vdots & \vdots & \dots & \vdots \\ 1 & \lambda_n & \lambda_n^2 & \dots & \lambda_n^{n-1} \end{bmatrix}. \quad (\text{WC.15}) \end{aligned}$$

Note that the controllability matrix  $\mathcal{C}$  is the product of two matrices and is nonsingular if and only if both of these matrices are invertible. The first matrix has a determinant that is the product of  $b_i$ , and the second matrix (called a Vandermonde matrix) is nonsingular if and only if the  $\lambda_i$  are distinct. Thus, Definition WC.3 is equivalent to having a nonsingular  $\mathcal{C}$  also.

Important to the subject of controllability is the **Popov–Hautus–Rosenbrock (PHR) test** (see Rosenbrock, 1970, and Kailath, 1980), which is an alternate way to test the rank (or determinant) of  $\mathcal{C}$ . The system  $(\mathbf{A}, \mathbf{B})$  is controllable if the system of equations

$$\mathbf{v}^T [s\mathbf{I} - \mathbf{A} \quad \mathbf{B}] = \mathbf{0}^T, \quad (\text{WC.16})$$

has only the trivial solution  $\mathbf{v}^T = \mathbf{0}^T$ —that is, if the **matrix pencil**

$$\text{rank } [s\mathbf{I} - \mathbf{A} \quad \mathbf{B}] = n, \quad (\text{WC.17})$$

is full rank for all  $s$ , or if there is no nonzero  $\mathbf{v}^T$  such that<sup>1</sup>

$$\mathbf{v}^T \mathbf{A} = s\mathbf{v}^T, \quad (\text{WC.18})$$

$$\mathbf{v}^T \mathbf{B} = 0. \quad (\text{WC.19})$$

This test is equivalent to the rank-of- $\mathcal{C}$  test. It is easy to show that, if such a vector  $\mathbf{v}$  exists,  $\mathcal{C}$  is singular. For if a nonzero  $\mathbf{v}$  exists such that  $\mathbf{v}^T \mathbf{B} = 0$ , then by Eqs. (WC.18) and (WC.19), we have

$$\mathbf{v}^T \mathbf{AB} = s\mathbf{v}^T \mathbf{B} = 0. \quad (\text{WC.20})$$

Then, multiplying by  $\mathbf{AB}$ , we find that

$$\mathbf{v}^T \mathbf{A}^2 \mathbf{B} = s\mathbf{v}^T \mathbf{AB} = 0, \quad (\text{WC.21})$$

---

<sup>1</sup> $\mathbf{v}^T$  is a left eigenvector of  $\mathbf{A}$ .

and so on. Thus we determine that  $\mathbf{v}^T \mathcal{C} = \mathbf{0}^T$  has a nontrivial solution, that  $\mathcal{C}$  is singular, and that the system is not controllable. To show that a nontrivial  $\mathbf{v}^T$  exists if  $\mathcal{C}$  is singular requires more development, which we will not give here (see Kailath, 1980).

We have given two pictures of uncontrollability. Either a mode is physically disconnected from the input (see Fig. WC.2b), or else two parallel subsystems have identical characteristic roots (see Fig. WC.2a). The control engineer should be aware of the existence of a third simple situation, as illustrated in Fig. WC.2c, namely, a **pole-zero cancellation**. Here the problem is the mode at  $s = 1$  appears to be connected to the input, but is masked by the zero at  $s = 1$  in the preceding subsystem; the result is an uncontrollable system. This can be confirmed in several ways. First let us look at the controllability matrix. The system matrices are

$$\mathbf{A} = \begin{bmatrix} -1 & 0 \\ 1 & 1 \end{bmatrix}, \quad \mathbf{B} = \begin{bmatrix} -2 \\ 1 \end{bmatrix},$$

so the controllability matrix is

$$\mathcal{C} = [\mathbf{B} \quad \mathbf{AB}] = \begin{bmatrix} -2 & 2 \\ 1 & -1 \end{bmatrix}, \quad (\text{WC.22})$$

which is clearly singular. The controllability matrix may be computed using the `ctrb` command in Matlab: `[cc]=ctrb(A,B)`. If we compute the transfer function from  $u$  to  $x_2$ , we find

$$\mathbf{H}(s) = \frac{s-1}{s+1} \left( \frac{1}{s-1} \right) = \frac{1}{s+1}. \quad (\text{WC.23})$$

Because the natural mode at  $s = 1$  disappears from the input-output description, it is not connected to the input. Finally, if we consider the **PHR test**,

$$[s\mathbf{I} - \mathbf{A} \quad \mathbf{B}] = \begin{bmatrix} s+1 & 0 & -2 \\ -1 & s-1 & 1 \end{bmatrix}, \quad (\text{WC.24})$$

and let  $s = 1$ , then we must test the rank of

$$\begin{bmatrix} 2 & 0 & -2 \\ -1 & 0 & 1 \end{bmatrix},$$

which is clearly less than 2. This result means, again, that the system is uncontrollable.

**Definition WC.4** *The asymptotically stable system  $(\mathbf{A}, \mathbf{B})$  is **controllable** if the controllability Gramian, the square symmetric matrix  $\mathcal{C}_g$ , given by the solution to the Lyapunov equation*

$$\mathbf{AC}_g + \mathcal{C}_g \mathbf{A}^T + \mathbf{BB}^T = \mathbf{0}, \quad (\text{WC.25})$$

*is nonsingular. The controllability **Gramian** is also the solution to the following integral equation:*

$$\mathcal{C}_g = \int_0^\infty e^{\tau \mathbf{A}} \mathbf{BB}^T e^{\tau \mathbf{A}^T} d\tau. \quad (\text{WC.26})$$

*One physical interpretation of the controllability Gramian is that, if the input to the system is white Gaussian noise,  $C_g$  is the covariance of the state. The controllability Gramian (for an asymptotically stable system) can be computed with the following command in Matlab:  $[cg] = \text{gram}(A, B)$ .*

In conclusion, the four definitions for controllability—pole assignment (Definition WC.1), state reachability (Definition WC.2), mode coupling to the input (Definition WC.3), and controllability Gramian (Definition WC.4)—are equivalent. The tests for any of these four properties are found in terms of the rank of the controllability, controllability Gramian matrices, or the rank of the **matrix pencil**  $[sI - A \ B]$ . If  $C$  is nonsingular, we can assign the closed-loop poles arbitrarily by state feedback, we can move the state to any point in the state space in a finite time, and every mode is connected to the control input.<sup>2</sup>

## WC.2 Observability

So far, we have discussed only controllability. The concept of observability is parallel to that of controllability, and all of the results we have discussed thus far may be transformed to statements about observability by invoking the property of duality, as discussed in Section 7.7.2. The observability definitions are analogous to those for controllability.

*Definition WC.1:* The system  $(A, C)$  is **observable** if, for any  $n$ th-order polynomial  $\alpha_e(s)$ , there exists an estimator gain  $L$  such that the characteristic equation of the state estimator error is  $\alpha_e(s)$ .

*Definition WC.2:* The system  $(A, C)$  is **observable** if, for any  $x(0)$ , there is a finite time  $\tau$  such that  $x(0)$  can be determined (uniquely) from  $u(t)$  and  $y(t)$  for  $0 \leq t \leq \tau$ .

*Definition WC.3:* The system  $(A, C)$  is **observable** if every dynamic mode in  $A$  is connected to the output through  $C$ .

*Definition WC.4:* The asymptotically stable system  $(A, C)$  is **observable** if the observability Gramian is nonsingular.

As we saw in the discussion for controllability, mathematical tests can be developed for observability. The system is observable if the observability matrix

$$\mathcal{O} = \begin{bmatrix} C \\ CA \\ \vdots \\ CA^{n-1} \end{bmatrix}, \quad (\text{WC.27})$$

is nonsingular. If we take the transpose of  $\mathcal{O}$ , and let  $C^T = B$  and  $A^T = A$ , then we find the controllability matrix of  $(A, B)$ , which is another manifestation of duality. The observability matrix  $\mathcal{O}$  may be

---

<sup>2</sup>We have shown the latter for diagonal  $A$  only, but the result is true in general.

computed using the `obsv` command in Matlab: `[oo]=obsv(A,C)`. The system ( $\mathbf{A}$ ,  $\mathbf{C}$ ) is observable if the following **matrix pencil** is full rank for all  $s$ :

$$\text{rank} \begin{bmatrix} s\mathbf{I} - \mathbf{A} \\ \mathbf{C} \end{bmatrix} = n. \quad (\text{WC.28})$$

The observability Gramian  $\mathcal{O}_g$ , which is a symmetric matrix, and the solution to the integral equation

$$\mathcal{O}_g = \int_0^{\infty} e^{\tau \mathbf{A}^T} \mathbf{C}^T \mathbf{C} e^{\tau \mathbf{A}} d\tau, \quad (\text{WC.29})$$

as well as the Lyapunov equation

$$\mathbf{A}^T \mathcal{O}_g + \mathcal{O}_g \mathbf{A} + \mathbf{C}^T \mathbf{C} = \mathbf{0}, \quad (\text{WC.30})$$

also can be computed (for an asymptotically stable system) using the `gram` command in Matlab: `[og]=gram(A',C')`. The observability Gramian has an interpretation as the “information matrix” in the context of estimation.

# Appendix WD

## Ackermann's Formula for Pole Placement

Given the plant and state-variable equation

$$\dot{\mathbf{x}} = \mathbf{A}\mathbf{x} + \mathbf{B}u, \quad (\text{WD.1})$$

our objective is to find a state-feedback control law

$$u = -\mathbf{K}\mathbf{x}, \quad (\text{WD.2})$$

such that the closed-loop characteristic polynomial is

$$\alpha_c(s) = \det(s\mathbf{I} - \mathbf{A} + \mathbf{B}\mathbf{K}). \quad (\text{WD.3})$$

First we have to select  $\alpha_c(s)$ , which determines where the poles are to be shifted; then we have to find  $\mathbf{K}$  such that Eq. (WD.3) will be satisfied. Our technique is based on transforming the plant equation into control canonical form.

We begin by considering the effect of an arbitrary nonsingular transformation of the state, as

$$\mathbf{x} = \mathbf{T}\bar{\mathbf{x}}, \quad (\text{WD.4})$$

where  $\bar{\mathbf{x}}$  is the new transformed state. The state equations in the new coordinates, from Eq. (WD.4), are

$$\dot{\mathbf{x}} = \mathbf{T}\dot{\bar{\mathbf{x}}} = \mathbf{A}\mathbf{x} + \mathbf{B}u = \mathbf{A}\mathbf{T}\bar{\mathbf{x}} + \mathbf{B}u, \quad (\text{WD.5})$$

$$\dot{\bar{\mathbf{x}}} = \mathbf{T}^{-1}\mathbf{A}\mathbf{T}\bar{\mathbf{x}} + \mathbf{T}^{-1}\mathbf{B}u = \bar{\mathbf{A}}\bar{\mathbf{x}} + \bar{\mathbf{B}}u. \quad (\text{WD.6})$$

Now the controllability matrix for the original state,

$$\mathcal{C}_x = [ \mathbf{B} \quad \mathbf{AB} \quad \mathbf{A}^2\mathbf{B} \quad \dots \quad \mathbf{A}^{n-1}\mathbf{B} ], \quad (\text{WD.7})$$

provides a useful transformation matrix. We can also define the controllability matrix for the transformed state:

$$\mathcal{C}_{\bar{x}} = [ \bar{\mathbf{B}} \quad \bar{\mathbf{A}}\bar{\mathbf{B}} \quad \bar{\mathbf{A}}^2\bar{\mathbf{B}} \quad \dots \quad \bar{\mathbf{A}}^{n-1}\bar{\mathbf{B}} ]. \quad (\text{WD.8})$$

The two controllability matrices are related by

$$\mathcal{C}_{\bar{x}} = [ \mathbf{T}^{-1}\mathbf{B} \quad \mathbf{T}^{-1}\mathbf{AT}\mathbf{T}^{-1}\mathbf{B} \quad \dots ] = \mathbf{T}^{-1}\mathcal{C}_x \quad (\text{WD.9})$$

and the transformation matrix

$$\mathbf{T} = \mathcal{C}_x \mathcal{C}_{\bar{x}}^{-1}. \quad (\text{WD.10})$$

From Eqs. (WD.9) and (WD.10), we can draw some important conclusions. From Eq. (WD.9), we see if  $\mathcal{C}_x$  is nonsingular, then for any nonsingular  $\mathbf{T}$ ,  $\mathcal{C}_{\bar{x}}$  is also nonsingular. This means that a similarity

transformation of the state does not change the controllability properties of a system. We can look at this in another way. Suppose we would like to find a transformation to take the system  $(\mathbf{A}, \mathbf{B})$  into control canonical form. As we shall shortly see,  $\mathcal{C}_{\bar{x}}$  in that case is *always* nonsingular. From Eq. (WD.9), we see a nonsingular  $\mathbf{T}$  will always exist if and only if  $\mathcal{C}_x$  is nonsingular. We derive the following theorem.

**Theorem WD.1** *We can always transform  $(\mathbf{A}, \mathbf{B})$  into control canonical form if and only if the system is controllable.*

Let us take a closer look at the control canonical form and treat the third-order case, although the results are true for any  $n$ th-order case:

$$\bar{\mathbf{A}} = \mathbf{A}_c = \begin{bmatrix} -a_1 & -a_2 & -a_3 \\ 1 & 0 & 0 \\ 0 & 1 & 0 \end{bmatrix}, \quad \bar{\mathbf{B}} = \mathbf{B}_c = \begin{bmatrix} 1 \\ 0 \\ 0 \end{bmatrix}. \quad (\text{WD.11})$$

The controllability matrix, by direct computation, is

$$\mathcal{C}_{\bar{x}} = \mathcal{C}_c = \begin{bmatrix} 1 & -a_1 & a_1^2 - a_2 \\ 0 & 1 & -a_1 \\ 0 & 0 & 1 \end{bmatrix}. \quad (\text{WD.12})$$

Because this matrix is upper triangular with ones along the diagonal, it is always invertible. Also note the last row of  $\mathcal{C}_{\bar{x}}$  is the unit vector with all zeros, except for the last element, which is unity. We shall use this fact in the following.

As we pointed out in Section 7.5, the design of a control law for the state  $\bar{x}$  is trivial if the state equations happen to be in control canonical form. The characteristic equation is

$$s^3 + a_1 s^2 + a_2 s + a_3 = 0, \quad (\text{WD.13})$$

and the characteristic equation for the closed-loop system comes from

$$\mathbf{A}_{cl} = \mathbf{A}_c - \mathbf{B}_c \mathbf{K}_c \quad (\text{WD.14})$$

and has the coefficients shown:

$$s^3 + (a_1 + K_{c1})s^2 + (a_2 + K_{c2})s + (a_3 + K_{c3}) = 0. \quad (\text{WD.15})$$

To obtain the desired closed-loop pole locations, we must make the coefficients of  $s$  in Eq. (WD.15) match those in

$$\alpha_c(s) = s^3 + \alpha_1 s^2 + \alpha_2 s + \alpha_3, \quad (\text{WD.16})$$

so

$$a_1 + K_{c1} = \alpha_1, \quad a_2 + K_{c2} = \alpha_2, \quad a_3 + K_{c3} = \alpha_3, \quad (\text{WD.17})$$

or in vector form,

$$\mathbf{a} + \mathbf{K}_c = \boldsymbol{\alpha}, \quad (\text{WD.18})$$

where  $\mathbf{a}$  and  $\boldsymbol{\alpha}$  are row vectors containing the coefficients of the characteristic polynomials of the open-loop and closed-loop systems, respectively.

We now need to find a relationship between these polynomial coefficients and the matrix  $\mathbf{A}$ . The requirement is achieved by the Cayley–Hamilton theorem, which states that a matrix satisfies its own characteristic polynomial. For  $\mathbf{A}_c$ , this means that

$$\mathbf{A}_c^n + a_1 \mathbf{A}_c^{n-1} + a_2 \mathbf{A}_c^{n-2} + \cdots + a_n \mathbf{I} = \mathbf{0}. \quad (\text{WD.19})$$

Now suppose we form the polynomial  $\alpha_c(\mathbf{A})$ , which is the *closed-loop* characteristic polynomial with the matrix  $\mathbf{A}$  substituted for the complex variable  $s$ :

$$\alpha_c(\mathbf{A}_c) = \mathbf{A}_c^n + \alpha_1 \mathbf{A}_c^{n-1} + \alpha_2 \mathbf{A}_c^{n-2} + \cdots + \alpha_n \mathbf{I}. \quad (\text{WD.20})$$

If we solve Eq. (WD.19) for  $\mathbf{A}_c^n$  and substitute into Eq. (WD.20), we find that

$$\alpha_c(\mathbf{A}_c) = (-a_1 + \alpha_1) \mathbf{A}_c^{n-1} + (-a_2 + \alpha_2) \mathbf{A}_c^{n-2} + \cdots + (-a_n + \alpha_n) \mathbf{I}. \quad (\text{WD.21})$$

But, because  $\mathbf{A}_c$  has such a special structure, we observe that if we multiply it by the transpose of the  $n$ th unit vector,  $\mathbf{e}_n^T = [ 0 \ \cdots \ 0 \ 1 ]$ , we get

$$\mathbf{e}_n^T \mathbf{A}_c = [ 0 \ \cdots \ 0 \ 1 \ 0 ] = \mathbf{e}_{n-1}^T, \quad (\text{WD.22})$$

as we can see from Eq. (WD.11). If we multiply this vector again by  $\mathbf{A}_c$ , getting

$$\begin{aligned} (\mathbf{e}_n^T \mathbf{A}_c) \mathbf{A}_c &= [ 0 \ \cdots \ 0 \ 1 \ 0 ] \mathbf{A}_c \\ &= [ 0 \ \cdots \ 0 \ 1 \ 0 \ 0 ] = \mathbf{e}_{n-2}^T, \end{aligned} \quad (\text{WD.23})$$

and continue the process, successive unit vectors are generated until

$$\mathbf{e}_n^T \mathbf{A}_c^{n-1} = [ 1 \ 0 \ \cdots \ 0 ] = \mathbf{e}_1^T. \quad (\text{WD.24})$$

Therefore, if we multiply Eq. (WD.21) by  $\mathbf{e}_n^T$ , we find that

$$\begin{aligned} \mathbf{e}_n^T \alpha_c(\mathbf{A}_c) &= (-a_1 + \alpha_1) \mathbf{e}_1^T + (-a_2 + \alpha_2) \mathbf{e}_2^T + \cdots + (-a_n + \alpha_n) \mathbf{e}_n^T \\ &= [ K_{c1} \ K_{c2} \ \cdots \ K_{cn} ] = \mathbf{K}_c, \end{aligned} \quad (\text{WD.25})$$

where we use Eq. (WD.18), which relates  $\mathbf{K}_c$  to  $\mathbf{a}$  and  $\boldsymbol{\alpha}$ .

We now have a compact expression for the gains of the system in control canonical form as represented in Eq. (WD.25). However, we still need the expression for  $\mathbf{K}$ , which is the gain on the original state. If  $u = -\mathbf{K}_c \bar{\mathbf{x}}$ , then  $u = -\mathbf{K}_c \mathbf{T}^{-1} \mathbf{x}$ , so

$$\begin{aligned} \mathbf{K} &= \mathbf{K}_c \mathbf{T}^{-1} = \mathbf{e}_n^T \alpha_c(\mathbf{A}_c) \mathbf{T}^{-1} \\ &= \mathbf{e}_n^T \alpha_c(\mathbf{T}^{-1} \mathbf{A} \mathbf{T}) \mathbf{T}^{-1} \\ &= \mathbf{e}_n^T \mathbf{T}^{-1} \alpha_c(\mathbf{A}). \end{aligned} \quad (\text{WD.26})$$

In the last step of Eq. (WD.26), we used the fact that  $(\mathbf{T}^{-1} \mathbf{A} \mathbf{T})^k = \mathbf{T}^{-1} \mathbf{A}^k \mathbf{T}$  and that  $\alpha_c$  is a polynomial, that is, a sum of the powers of  $\mathbf{A}_c$ . From Eq. (WD.9), we see that

$$\mathbf{T}^{-1} = \mathcal{C}_c \mathcal{C}_x^{-1}. \quad (\text{WD.27})$$

## Ackermann's formula

With this substitution, Eq. (WD.26) becomes

$$\mathbf{K} = \mathbf{e}_n^T \mathcal{C}_c \mathcal{C}_{\mathbf{x}}^{-1} \alpha_c(\mathbf{A}). \quad (\text{WD.28})$$

Now, we use the observation made earlier for Eq. (WD.12) that the last row of  $\mathcal{C}_c$ , which is  $\mathbf{e}_n^T \mathcal{C}_c$ , is again  $\mathbf{e}_n^T$ . We finally obtain Ackermann's formula:

$$\mathbf{K} = \mathbf{e}_n^T \mathcal{C}_{\mathbf{x}}^{-1} \alpha_c(\mathbf{A}). \quad (\text{WD.29})$$

We note again that forming the explicit inverse of  $\mathcal{C}_{\mathbf{x}}$  is not advisable for numerical accuracy. Thus we need to solve  $\mathbf{b}^T$  such that

$$\mathbf{e}_n^T \mathcal{C}_{\mathbf{x}}^{-1} = \mathbf{b}^T. \quad (\text{WD.30})$$

We solve the linear set of equations

$$\mathbf{b}^T \mathcal{C}_{\mathbf{x}} = \mathbf{e}_n^T, \quad (\text{WD.31})$$

then compute

$$\mathbf{K} = \mathbf{b}^T \alpha_c(\mathbf{A}). \quad (\text{WD.32})$$

Ackermann's formula, Eq. (WD.29), even though elegant, is not recommended for systems with a large number of state variables. Even if it is used, Eqs. (WD.31) and (WD.32) are recommended for better numerical accuracy.

## Appendix W2.1.4

# Complex Mechanical Systems

In some cases, mechanical systems contain both translational and rotational portions. The procedure is the same as that described in Section 2.1: sketch the free-body diagrams, define coordinates and positive directions, determine all forces and moments acting, and apply Eqs. (2.1) and/or (2.10).

### EXAMPLE W2.1

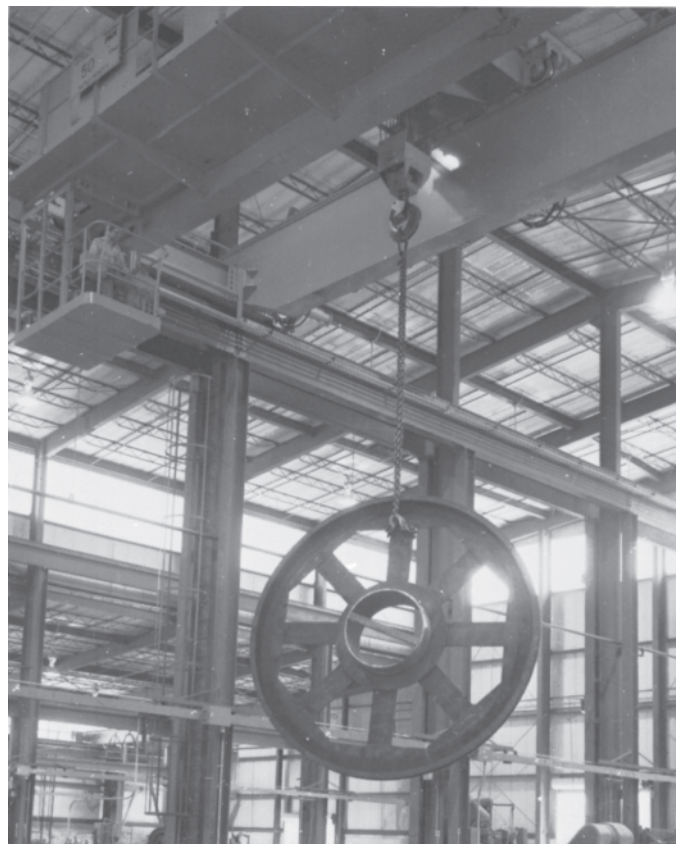
#### *Rotational and Translational Motion: Hanging Crane*

Write the equations of motion for the hanging crane pictured in Fig. W2.1 and shown schematically in Fig. W2.2. Linearize the equations

**Figure W2.1**

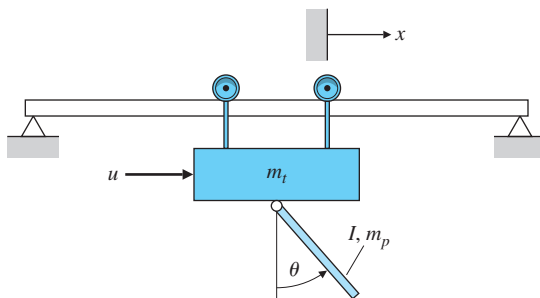
Crane with a hanging load

*Source: Photo courtesy of Harnischfeger Corporation, Milwaukee, Wisconsin*

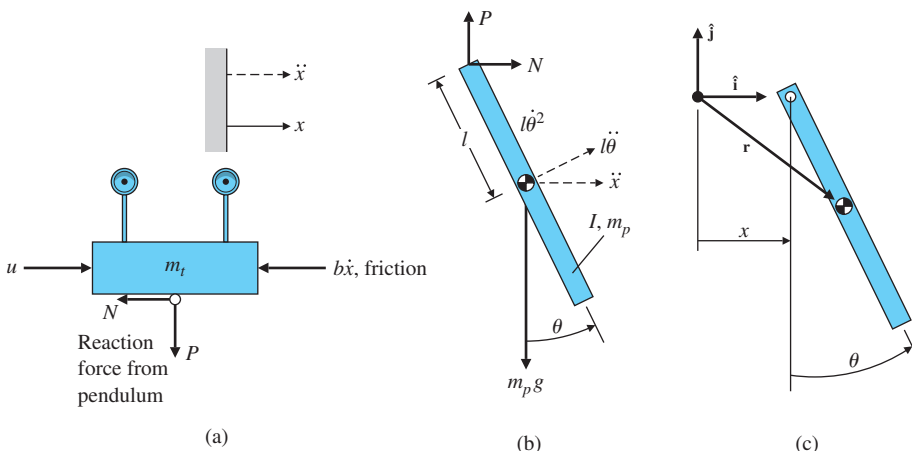
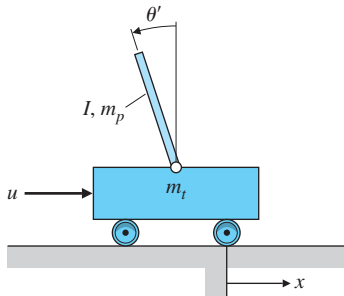


**Figure W2.2**

Schematic of the crane with hanging load

**Figure W2.3**

Inverted pendulum

**Figure W2.4**

Hanging crane: (a) free-body diagram of the trolley; (b) free-body diagram of the pendulum; (c) position vector of the pendulum

about  $\theta = 0$ , which would typically be valid for the hanging crane. Also linearize the equations for  $\theta = \pi$ , which represents the situation for the inverted pendulum shown in Fig. W2.3.

**Solution.** A schematic diagram of the hanging crane is shown in Fig. W2.2, while the free-body diagrams are shown in Fig. W2.4. In the case of the pendulum, the forces are shown with bold lines, while

the components of the inertial acceleration of its center of mass are shown with dashed lines. Because the pivot point of the pendulum is *not* fixed with respect to an inertial reference, the rotation of the pendulum and the motion of its mass center must be considered. The inertial acceleration needs to be determined because the vector  $\mathbf{a}$  in Eq. (2.1) is given with respect to an inertial reference. The inertial acceleration of the pendulum's mass center is the vector sum of the three dashed arrows shown in Fig. W2.4b. The derivation of the components of an object's acceleration is called **kinematics** and is usually studied as a prelude to the application of Newton's laws. The results of a kinematic study are shown in Fig. W2.4b. The component of acceleration along the pendulum is  $l\dot{\theta}^2$  and is called the centripetal acceleration. It is present for any object whose velocity is changing direction. The  $\ddot{x}$ -component of acceleration is a consequence of the pendulum pivot point accelerating at the trolley's acceleration and will always have the same direction and magnitude as those of the trolley's. The  $l\ddot{\theta}$  component is a result of angular acceleration of the pendulum and is always perpendicular to the pendulum.

These results can be confirmed by expressing the center of mass of the pendulum as a vector from an inertial reference, then differentiating that vector twice to obtain an inertial acceleration. Figure W2.4c shows  $\hat{\mathbf{i}}$  and  $\hat{\mathbf{j}}$  axes that are inertially fixed and a vector  $\mathbf{r}$  describing the position of the pendulum center of mass. The vector can be expressed as

$$\mathbf{r} = x\hat{\mathbf{i}} + l(\hat{\mathbf{i}} \sin \theta - \hat{\mathbf{j}} \cos \theta).$$

The first derivative of  $\mathbf{r}$  is

$$\dot{\mathbf{r}} = \dot{x}\hat{\mathbf{i}} + l\dot{\theta}(\hat{\mathbf{i}} \cos \theta + \hat{\mathbf{j}} \sin \theta).$$

Likewise, the second derivative of  $\mathbf{r}$  is

$$\ddot{\mathbf{r}} = \ddot{x}\hat{\mathbf{i}} + l\ddot{\theta}(\hat{\mathbf{i}} \cos \theta + \hat{\mathbf{j}} \sin \theta) - l\dot{\theta}^2(\hat{\mathbf{i}} \sin \theta - \hat{\mathbf{j}} \cos \theta).$$

Note the equation for  $\ddot{\mathbf{r}}$  confirms the acceleration components shown in Fig. W2.4b. The  $l\dot{\theta}^2$  term is aligned along the pendulum pointing toward the axis of rotation, and the  $l\ddot{\theta}$  term is aligned perpendicular to the pendulum pointing in the direction of a positive rotation.

Having all the forces and accelerations for the two bodies, we now proceed to apply Eq. (2.1). In the case of the trolley, Fig. W2.4a, we see that it is constrained by the tracks to move only in the  $x$ -direction; therefore, application of Eq. (2.11) in this direction yields

$$m_t \ddot{x} + b\dot{x} = u - N, \quad (\text{W2.1})$$

where  $N$  is an unknown reaction force applied by the pendulum. Conceptually, Eq. (2.1) can be applied to the pendulum of Fig. W2.4b in the vertical and horizontal directions, and Eq. (2.10) can be applied for rotational motion to yield three equations in the three unknowns:  $N$ ,  $P$ , and  $\theta$ . These three equations then can be manipulated to eliminate the reaction forces  $N$  and  $P$  so a single equation results describing the motion of the pendulum—that is, a single equation in  $\theta$ . For example,

application of Eq. (2.1) for pendulum motion in the  $x$ -direction yields

$$N = m_p \ddot{x} + m_p l \ddot{\theta} \cos \theta - m_p l \dot{\theta}^2 \sin \theta. \quad (\text{W2.2})$$

However, considerable algebra will be avoided if Eq. (2.1) is applied perpendicular to the pendulum to yield

$$P \sin \theta + N \cos \theta - m_p g \sin \theta = m_p l \ddot{\theta} + m_p \ddot{x} \cos \theta. \quad (\text{W2.3})$$

Application of Eq. (2.10) for the rotational pendulum motion, for which the moments are summed about the center of mass, yields

$$-Pl \sin \theta - Nl \cos \theta = I \ddot{\theta}, \quad (\text{W2.4})$$

where  $I$  is the moment of inertia about the pendulum's mass center. The reaction forces  $N$  and  $P$  can now be eliminated by combining Eqs. (W2.3) and (W2.4). This yields the equation

$$(I + m_p l^2) \ddot{\theta} + m_p g l \sin \theta = -m_p l \ddot{x} \cos \theta. \quad (\text{W2.5})$$

It is identical to a pendulum equation of motion, except that it contains a forcing function that is proportional to the trolley's acceleration.

An equation describing the trolley motion was found in Eq. (W2.1), but it contains the unknown reaction force  $N$ . By combining Eqs. (W2.2) and (W2.1),  $N$  can be eliminated to yield

$$(m_t + m_p) \ddot{x} + b \dot{x} + m_p l \ddot{\theta} \cos \theta - m_p l \dot{\theta}^2 \sin \theta = u. \quad (\text{W2.6})$$

Equations (W2.5) and (W2.6) are the nonlinear differential equations that describe the motion of the crane with its hanging load. For an accurate calculation of the motion of the system, these nonlinear equations need to be solved.

To linearize the equations for small motions about  $\theta = 0$ , let  $\cos \theta \cong 1$ ,  $\sin \theta \cong \theta$ , and  $\dot{\theta}^2 \cong 0$ ; thus, the equations are approximated by

$$\begin{aligned} (I + m_p l^2) \ddot{\theta} + m_p g l \theta &= -m_p l \ddot{x}, \\ (m_t + m_p) \ddot{x} + b \dot{x} + m_p l \ddot{\theta} &= u. \end{aligned} \quad (\text{W2.7})$$

Neglecting the friction term  $b$  leads to the transfer function from the control input  $u$  to the hanging crane angle  $\theta$ :

$$\frac{\Theta(s)}{U(s)} = \frac{-m_p l}{((I + m_p l^2)(m_t + m_p) - m_p^2 l^2)s^2 + m_p g l(m_t + m_p)}. \quad (\text{W2.8})$$

### Inverted pendulum equations

For the inverted pendulum in Fig. W2.3, where  $\theta \cong \pi$ , assume  $\theta = \pi + \theta'$ , where  $\theta'$  represents motion from the vertical *upward* direction. In this case,  $\cos \theta \cong -1$ ,  $\sin \theta \cong -\theta'$  in Eqs. (W2.5) and (W2.6), and Eqs. (W2.7) become<sup>1</sup>

$$(I + m_p l^2) \ddot{\theta}' - m_p g l \theta' = m_p l \ddot{x}, \\ (m_t + m_p) \ddot{x} + b \dot{x} - m_p l \ddot{\theta}' = u. \quad (\text{W2.9})$$

As noted in Example 2.2, a stable system will always have the same signs on each variable, which is the case for the stable hanging crane modeled by Eqs. (W2.7). However, the signs on  $\theta$  and  $\ddot{\theta}$  in the top Eq. (W2.9) are opposite, thus indicating instability, which is the characteristic of an inverted pendulum.

The transfer function, again without friction, is

$$\frac{\Theta'(s)}{U(s)} = \frac{m_p l}{((I + m_p l^2) - m_p^2 l^2)s^2 - m_p g l(m_t + m_p)}. \quad (\text{W2.10})$$

## W2.1 Additional Problems for Translational and Rotational Systems

Assume the driving force on the hanging crane of Fig. W2.2 is provided by a motor mounted on the cab with one of the support wheels connected directly to the motor's armature shaft. The motor constants are  $K_e$  and  $K_t$ , and the circuit driving the motor has a resistance  $R_a$  and negligible inductance. The wheel has a radius  $r$ . Write the equations of motion relating the applied motor voltage to the cab position and load angle.

**Solution.** The dynamics of the hanging crane are given by Eqs. (W2.5) and (W2.6),

$$(I + m_p l^2) \ddot{\theta} + m_p g l \sin \theta = -m_p l \ddot{x} \cos \theta, \\ (m_t + m_p) \ddot{x} + b \dot{x} + m_p l \ddot{\theta} \cos \theta - m_p l \dot{\theta}^2 \sin \theta = u,$$

where  $x$  is the position of the cab,  $\theta$  is the angle of the load, and  $u$  is the applied force that will be produced by the motor. Our task here is to find the force applied by the motor. Normally, the rotational dynamics of a motor is

$$J_1 \ddot{\theta}_m + b_1 \dot{\theta}_m = T_m = K_t i_a,$$

where the current is found from the motor circuit, which reduces to

$$R_a i_a = V_a - K_e \dot{\theta}_m,$$

<sup>1</sup>The inverted pendulum is often described with the angle of the pendulum being positive for *clockwise* motion. If defined that way, then reverse the sign on all terms in Eq. (W2.9) in  $\theta'$  or  $\dot{\theta}'$ .

for the case where the inductance is negligible. However, since the motor is geared directly to the cab,  $\theta_m$  and  $x$  are related kinematically by

$$x = r\theta_m,$$

and we can neglect any extra inertia or damping from the motor itself, compared to the inertia and damping of the large cab. Therefore, we can rewrite the two motor equations in terms of the force applied by the motor on the cab

$$\begin{aligned} u &= T_m/r = K_t i_a/r, \\ i_a &= (V_a - K_e \dot{\theta}_m)/R_a, \end{aligned}$$

where

$$\dot{\theta}_m = \dot{x}/r.$$

These equations, along with

$$(I + m_p l^2) \ddot{\theta} + m_p g l \sin \theta = -m_p l \ddot{x} \cos \theta,$$

$$(m_t + m_p) \ddot{x} + b \dot{x} + m_p l \ddot{\theta} \cos \theta - m_p l \dot{\theta}^2 \sin \theta = u,$$

constitute the required relations.

# Appendix W3.2.3

## △ W3.2.3 Mason's Rule and the Signal-Flow Graph

A compact alternative notation to the block diagram is given by the **signal-flow graph** introduced by S. J. Mason (1953, 1956). As with the block diagram, the signal-flow graph offers a visual tool for representing the causal relationships between the components of the system. The method consists of characterizing the system by a network of directed branches and associated gains (transfer functions) connected at nodes. Several block diagrams and their corresponding signal-flow graphs are shown in Fig. W3.1. The two ways of depicting a system are equivalent, and you can use either diagram to apply Mason's rule (to be defined shortly).

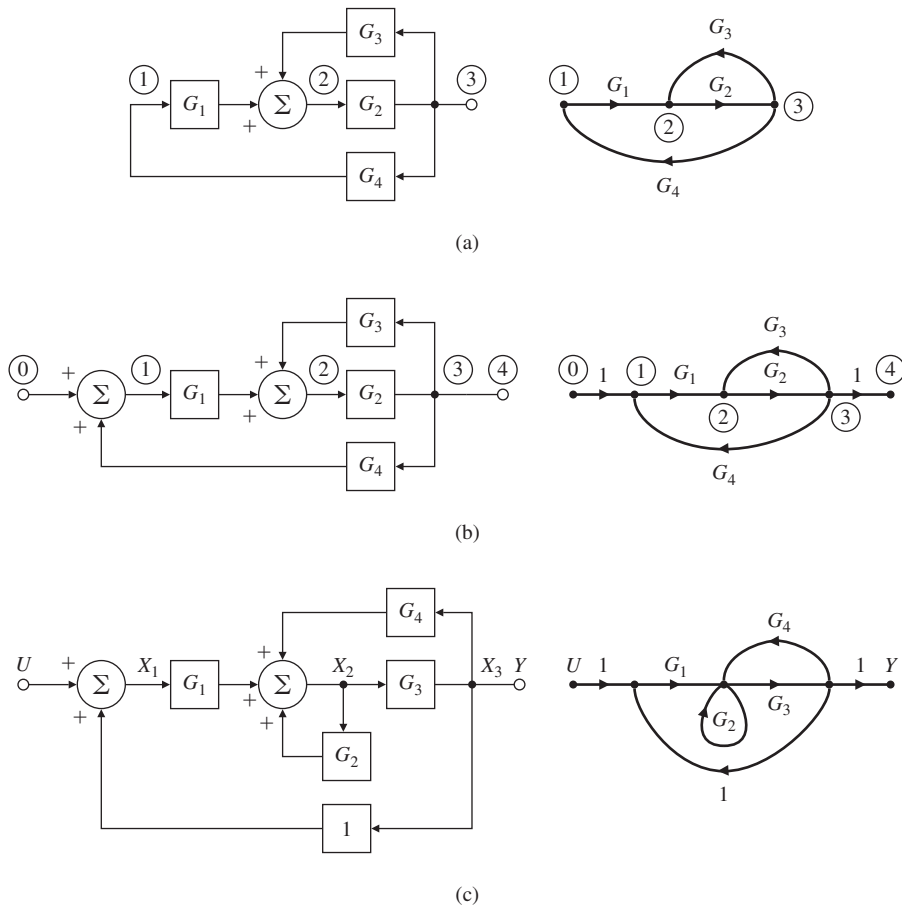
### Signal-flow graph

In a signal-flow graph, the internal signals in the diagram, such as the common input to several blocks or the output of a summing junction, are called **nodes**. The system input point and the system output point are also nodes; the input node has outgoing branches only, and the output node has incoming branches only. Mason defined a **path** through a block diagram as a sequence of connected blocks, the route passing from one node to another *in the direction of signal flow of the blocks* without including any block more than once. A **forward path** is a path from the input to output such that no node is included more than once. If the nodes are numbered in a convenient order, a forward path can be identified by the numbers that are included. Any closed path that returns to its starting node without passing through any node more than once is a **loop**, and a path that leads from a given variable back to the same variable is a **loop path**. The **path gain** is the product of component gains (transfer functions) making up the path. Similarly, the **loop gain** is the path gain associated with a loop—that is, the product of gains in a loop. If two paths have a common component, they are said to touch. Notice particularly in this connection that the input and the output of a summing junction are not the same and that the summing junction is a one-way device from its inputs to its output.

Mason's rule relates the graph to the algebra of the simultaneous equations it represents.<sup>1</sup> Consider Fig. W3.1c, where the signal at each node has been given a name and the gains are marked. Then the block diagram (or the signal-flow graph) represents the system of equations:

---

<sup>1</sup>The derivation is based on Cramer's rule for solving linear equations by determinants and is described in Mason's papers.

**Figure W3.1**

Block diagrams and corresponding signal-flow graphs

$$X_1(s) = X_3(s) + U(s),$$

$$X_2(s) = G_1(s)X_1(s) + G_2(s)X_2(s) + G_4(s)X_3(s),$$

$$Y(s) = 1X_3(s).$$

#### Mason's rule

Mason's rule states that the input–output transfer function associated with a signal-flow graph is given by

$$G(s) = \frac{Y(s)}{U(s)} = \frac{1}{\Delta} \sum_i G_i \Delta_i,$$

where

$G_i$  = path gain of the  $i$ th forward path,

$\Delta$  = the system determinant

$= 1 - \sum (\text{all individual loop gains}) + \sum (\text{gain products of all possible two loops that do not touch}) - \sum (\text{gain products of all possible three loops that do not touch}) + \dots,$

$\Delta_i = i\text{th forward path determinant}$

$= \text{value of } \Delta \text{ for that part of the block diagram that does not touch the } i\text{th forward path.}$

We will now illustrate the use of Mason's rule with some examples.

## EXAMPLE W3.1

### Mason's Rule in a Simple System

Find the transfer function for the block diagram in Fig. W3.2.

**Solution.** From the block diagram shown in Fig. W3.2, we have

*Forward Path*

$$1236 \quad G_1 = 1 \left( \frac{1}{s} \right) (b_1)(1)$$

$$12346 \quad G_2 = 1 \left( \frac{1}{s} \right) \left( \frac{1}{s} \right) (b_2)(1)$$

$$123456 \quad G_3 = 1 \left( \frac{1}{s} \right) \left( \frac{1}{s} \right) \left( \frac{1}{s} \right) (b_3)(1)$$

*Loop Path Gain*

$$232 \quad l_1 = -a_1/s$$

$$2342 \quad l_2 = -a_2/s^2$$

$$23452 \quad l_3 = -a_3/s^3$$

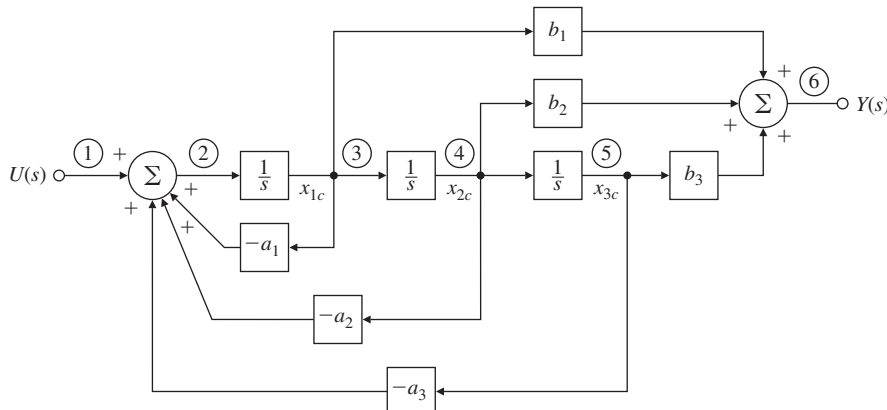


Figure W3.2

Block diagram for Example W3.1

and the determinants are

$$\Delta = 1 - \left( -\frac{a_1}{s} - \frac{a_2}{s^2} - \frac{a_3}{s^3} \right) + 0,$$

$$\Delta_1 = 1 - 0,$$

$$\Delta_2 = 1 - 0,$$

$$\Delta_3 = 1 - 0.$$

Applying Mason's rule, we find the transfer function to be

$$\begin{aligned} G(s) &= \frac{Y(s)}{U(s)} = \frac{(b_1/s) + (b_2/s^2) + (b_3/s^3)}{1 + (a_1/s) + (a_2/s^2) + (a_3/s^3)} \\ &= \frac{b_1 s^2 + b_2 s + b_3}{s^3 + a_1 s^2 + a_2 s + a_3}. \end{aligned}$$

Mason's rule is particularly useful for more complex systems where there are several loops, some of which do not sum into the same point.

## EXAMPLE W3.2

### *Mason's Rule in a Complex System*

Find the transfer function for the system shown in Fig. W3.3.

**Solution.** From the block diagram, we find that

#### Forward Path

$$\begin{aligned} 12456 & \quad G_1 = H_1 H_2 H_3 \\ 1236 & \quad G_2 = H_4 \end{aligned}$$

#### Loop Path Gain

$$\begin{aligned} 242 & \quad l_1 = H_1 H_5 \text{ (does not touch } l_3) \\ 454 & \quad l_2 = H_2 H_6 \\ 565 & \quad l_3 = H_3 H_7 \text{ (does not touch } l_1) \\ 236542 & \quad l_4 = H_4 H_7 H_6 H_5 \end{aligned}$$

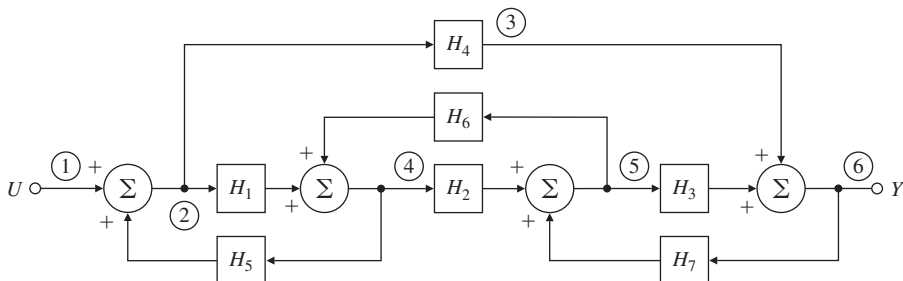


**Figure W3.3**

Block diagram for Example W3.2

and the determinants are

$$\Delta = 1 - (H_1 H_5 + H_2 H_6 + H_3 H_7 + H_4 H_7 H_6 H_5) + (H_1 H_5 H_3 H_7),$$

$$\Delta_1 = 1 - 0,$$

$$\Delta_2 = 1 - H_2 H_6.$$

Therefore,

$$G(s) = \frac{Y(s)}{U(s)} = \frac{H_1 H_2 H_3 + H_4 - H_4 H_2 H_6}{1 - H_1 H_5 - H_2 H_6 - H_3 H_7 - H_4 H_7 H_6 H_5 + H_1 H_5 H_3 H_7}.$$


---

Mason's rule is useful for solving relatively complicated block diagrams by hand. It yields the solution in the sense that it provides an explicit input–output relationship for the system represented by the diagram. The advantage compared with path-by-path block-diagram reduction is that it is systematic and algorithmic rather than problem dependent. Matlab and other control systems computer-aided software allow you to specify a system in terms of individual blocks in an overall system, and the software algorithms perform the required block-diagram reduction; therefore, Mason's rule is less important today than in the past. However, there are some derivations that rely on the concepts embodied by the rule, so it still has a role in the control designer's toolbox.

## △Appendix W.3.6.3.1 Routh Special Cases

If only the first element in one of the rows is zero, then we can consider a modified equation with one of the coefficients perturbed by  $\epsilon > 0$  and applying the test by taking the limit as  $\epsilon \rightarrow 0$ .

### EXAMPLE W3.3

#### Routh's Test for Special Case I

Consider the polynomial

$$a(s) = s^5 + 3s^4 + 2s^3 + 6s^2 + 6s + 9.$$

Determine whether any of the roots are in the RHP.

**Solution.** In this example, let the coefficient of  $s^3$  be  $2 + \epsilon$ . The test follows from there. The Routh array is

$s^5:$	1	2	6
$s^4:$	3	6	9
$s^3:$	$\epsilon$	3	0
$s^2:$	$\frac{6\epsilon - 9}{\epsilon}$	9	0
$s^1:$	$3 - \frac{3\epsilon^2}{2\epsilon - 3}$	0	0
$s^0:$	9	0.	

There are two sign changes in the first column of the array, which means there are two poles not in the LHP.<sup>1</sup>

### Special case II

Another special<sup>2</sup> case occurs when an entire row of the Routh array is zero. This indicates that there are complex conjugate pairs of roots that are mirror images of each other with respect to the imaginary axis. To apply Routh's test correctly, we follow the ensuing procedure. If the  $i$ th row is zero, we form an auxiliary equation from the previous (nonzero) row:

$$a_1(s) = \beta_1 s^{i+1} + \beta_2 s^{i-1} + \beta_3 s^{i-3} + \dots \quad (\text{W3.1})$$

Here  $\{\beta_i\}$  are the coefficients of the  $(i + 1)$ th row in the array. We then replace the  $i$ th row by the coefficients of the *derivative* of the auxiliary polynomial and complete the array. However, the roots of the auxiliary polynomial in Eq. (W3.1) are also roots of the characteristic equation, and these must be tested separately.

<sup>1</sup>The actual roots computed with Matlab are at  $-2.9043, 0.6567 \pm 1.2881j, -0.7046 \pm 0.9929j$ .

<sup>2</sup>Special case II.

**EXAMPLE W3.4***Routh Test for Special Case II*

For the polynomial

$$a(s) = s^5 + 5s^4 + 11s^3 + 23s^2 + 28s + 12,$$

determine whether there are any roots on the  $j\omega$  axis or in the RHP.

**Solution.** The Routh array is

$s^5$ :	1	11	28	
$s^4$ :	5	23	12	
$s^3$ :	6.4	25.6	0	
$s^2$ :	3	12		
$s$ :	0	0		$\leftarrow a_1(s) = 3s^2 + 12$
New $s$ :	6	0		$\leftarrow \frac{da_1(s)}{ds} = 6s$
$s^0$ :	12.			

There are no sign changes in the first column. Hence all the roots have negative real parts except for a pair on the imaginary axis. We may deduce this as follows: When we replace the zero in the first column by  $\epsilon > 0$ , there are no sign changes. If we let  $\epsilon < 0$ , then there are two sign changes. Thus, if  $\epsilon = 0$ , there are two poles on the imaginary axis, which are the roots of

$$a_1(s) = 3s^2 + 12 = 0,$$

or

$$s = \pm j2.$$

This agrees with the fact that the actual roots are at  $-3$ ,  $\pm 2j$ ,  $-1$ , and  $-1$ , as computed using the `roots` command in Matlab.

---

# Appendix W3.7

## System Identification

### W3.7.1 A Perspective on System Identification

In order to design controls for a dynamic system, it is necessary to have a model that will adequately describe the system's dynamics. The information available to the designer for this purpose is typically of three kinds.

1. **Physical model:** First, there is the knowledge of physics, chemistry, biology, and the other sciences which have over the years developed equations of motion to explain the dynamic response of rigid and flexible bodies, electric circuits and motors, fluids, chemical reactions, and many other constituents of systems to be controlled. The model based on this knowledge is referred to as a "physical" model. There are many advantages to this approach, including ease of controller development and testing. One disadvantage of this approach is that a fairly high-fidelity physical model must be developed.

2. **Black box model:** It is often the case that for extremely complex physical phenomena the laws of science are not adequate to give a satisfactory description of the dynamic plant that we wish to control. Examples include the force on a moving airplane caused by a control surface mounted on a wing, and the heat of combustion of a fossil fuel of uncertain composition. In these circumstances, the designer turns to data taken from experiments directly conducted to excite the plant and measure its response. The second approach uses an empirical or heuristic model referred to as the "black box" model. In this approach, the control engineer injects open-loop commands into the system and records the sensor response. The process of constructing models from experimental data is called **system identification**. Standard system identification techniques (for example, linear least-squares) are used to identify a dynamic input/output model. The advantage of this technique is that the control engineer does not need to have a deep understanding of how the system physically behaves, but instead can design a controller solely based on the derived model. There are several major disadvantages to this approach. First, the control engineer must have access to working hardware. Another serious disadvantage of this approach is that it does not provide insight or physical understanding of how specific hardware modifications will affect the control—usually hardware modifications require the control engineer to repeat the full cycle of system identification, control design, and validation. The advantage of this approach is that we use logic and data to model

inputs and outputs, and the detailed knowledge of the physics is not required.

3. **Grey box model:** The third approach is the use of the combination of physical and empirical models referred to as “grey box” modeling.

In identifying models for control, our motivation is very different from that of modeling as practiced in the sciences. In science, one seeks to develop models of nature as it is; in control, one seeks to develop models of the plant dynamics that will be adequate for the design of a controller that will cause the actual dynamics to be stable and to give good performance. The initial design of a control system typically considers a small signal analysis and is based on models that are linear and time-invariant (LTI). This is referred to as a “control relevant” model. Having accepted that the model is to be linear, we still must choose between several alternative descriptions of linear systems. If we examine the design methods described in the earlier chapters, we find that the required plant models may be grouped in two categories: parametric and nonparametric. For design via root locus or pole assignment, we require a parametric description such as a transfer function or a state-variable description from which we can obtain the poles and zeros of the plant. These equivalent models are completely described by the numbers that specify the coefficients of the polynomials, the elements of the state-description matrices, or the numbers that specify the poles and zeros. In either case, we call these numbers the *parameters* of the model, and the category of such models is a **parametric description** of the plant model.

In contrast to parametric models, the frequency-response methods of Nyquist, Bode, and Nichols require the curves of amplitude and phase of the transfer function  $G(j\omega) = Y(j\omega)/U(j\omega)$  as functions of  $\omega$ . Clearly, if we happen to have a parametric description of the system, we can compute the transfer function and the corresponding frequency response. However, if we are given the frequency response or its inverse transform, the impulse response, without parameters (perhaps obtained from experimental data), we have all we need to design a lead, lag, notch, or other compensation to achieve a desired bandwidth, phase margin, or other frequency response performance objective without ever knowing what the parameters are. We call the functional curves of  $G(j\omega)$  a **nonparametric** model because, in principle, there is no finite set of numbers that describes it exactly.

Because of the large data records necessary to obtain effective models and the complexity of many of the algorithms used, the use of computer aids is essential in identification. Developments such as Matlab’s System Identification Toolbox are enormous aids to the practical use of the system identification techniques. For detailed discussion on system identification, the reader is referred to Franklin, Powell, and Workman (1998).

#### Parametric model

#### Nonparametric model

### W3.7.2 Obtaining Models from Experimental Data

There are several reasons for using experimental data to obtain a model of the dynamic system to be controlled. In the first place, the best theoretical model built from equations of motion is still only an approximation of reality. Sometimes, as in the case of a very rigid spacecraft, the theoretical model is extremely good. Other times, as with many chemical processes such as papermaking or metalworking, the theoretical model is very approximate. In every case, before the final control design is done, it is important and prudent to verify the theoretical model with experimental data. Second, in situations for which the theoretical model is especially complicated or the physics of the process is poorly understood, the only reliable information on which to base the control design is the experimental data. Finally, the system is sometimes subject to online changes that occur when the environment of the system changes. Examples include when an aircraft changes altitude or speed, a paper machine is given a different composition of fiber, or a nonlinear system moves to a new operating point. On these occasions, we need to “retune” the controller by changing the control parameters. This requires a model for the new conditions, and experimental data are often the most effective, if not the only, information available for the new model.

#### Our sources of experimental data

There are four kinds of experimental data for generating a model:

1. **Transient response**, such as comes from an impulse or a step;
2. **Frequency-response data**, which result from exciting the system with sinusoidal inputs at many frequencies;
3. **Stochastic steady-state information**, as might come from flying an aircraft through turbulent weather or from some other natural source of randomness; and
4. **Pseudorandom-noise data**, as may be generated in a digital computer.

Each class of experimental data has its properties, advantages, and disadvantages.

#### Transient response

Transient-response data are quick and relatively easy to obtain. They are also often representative of the natural signals to which the system is subjected. Thus, a model derived from such data can be reliable for designing the control system. On the other hand, in order for the signal-to-noise ratio to be sufficiently high, the transient response must be highly noticeable. Consequently, the method is rarely suitable for normal operations, so the data must be collected as part of special tests. A second disadvantage is the data do not come in a form suitable for standard control systems designs, and some parts of the model, such as poles and zeros, must be computed from the

data.<sup>1</sup> This computation can be simple in special cases or complex in the general case.

#### Frequency response

Frequency-response data (see Chapter 6) are simple to obtain, but substantially more time consuming than transient-response information. This is especially so if the time constants of the process are large, as often occurs in chemical processing industries. As with the transient-response data, it is important to have a good signal-to-noise ratio, so obtaining frequency-response data can be very expensive. On the other hand, as we will see in Chapter 6, frequency-response data are exactly in the right form for frequency-response design methods; so once the data have been obtained, the control design can proceed immediately.

#### Stochastic steady-state

Normal operating records from a natural stochastic environment at first appear to be an attractive basis for modeling systems, since such records are by definition nondisruptive and inexpensive to obtain. Unfortunately, the quality of such data is inconsistent, tending to be worse just when the control is best, because then the upsets are minimal and the signals are smooth. At such times, some or even most of the system dynamics are hardly excited. Because they contribute little to the system output, they will not be found in the model constructed to explain the signals. The result is a model that represents only part of the system and is sometimes unsuitable for control. In some instances, as occurs when trying to model the dynamics of the electroencephalogram (brain waves) of a sleeping or anesthetized person to locate the frequency and intensity of alpha waves, normal records are the only possibility. Usually they are the last choice for control purposes.

#### Pseudorandom noise (PRBS)

Finally, the pseudorandom signals that can be constructed using digital logic have much appeal. Especially interesting for model making is the pseudorandom binary signal (PRBS). The PRBS takes on the value  $+A$  or  $-A$  according to the output (1 or 0) of a feedback shift register. The feedback to the register is a binary sum of various states of the register that have been selected to make the output period (which must repeat itself in finite time) as long as possible. For example, with a register of 20 bits,  $2^{20} - 1$  (over a million) steps are produced before the pattern repeats. Analysis beyond the scope of this text has revealed that the resulting signal is almost like a broadband random signal. Yet this signal is entirely under the control of the engineer who can set the level ( $A$ ) and the length (bits in the register) of the signal. The data obtained from tests with a PRBS must be analyzed by computer and both special-purpose hardware and programs for general-purpose computers have been developed to perform this analysis.

---

<sup>1</sup>Ziegler and Nichols (1943), building on the earlier work of Callender et al. (1936), use the step response directly in designing the controls for certain classes of processes. See Chapter 4 for details.

### W3.7.3 Models from Transient-Response Data

To obtain a model from transient data, we assume a step response is available. If the transient is a simple combination of elementary transients, then a reasonable low-order model can be estimated using hand calculations. For example, consider the step response shown in Fig. W3.4. The response is monotonic and smooth. If we assume it is given by a sum of exponentials, we can write

$$y(t) = y(\infty) + Ae^{-\alpha t} + Be^{-\beta t} + Ce^{-\gamma t} + \dots \quad (\text{W3.2})$$

Subtracting off the final value and assuming that  $-\alpha$  is the slowest pole, we write

$$\begin{aligned} y - y(\infty) &\cong Ae^{-\alpha t}, \\ \log_{10}[y - y(\infty)] &\cong \log_{10} A - \alpha t \log_{10} e, \\ &\cong \log_{10} A - 0.4343\alpha t. \end{aligned} \quad (\text{W3.3})$$

This is the equation of a line whose slope determines  $\alpha$  and intercept determines  $A$ . If we fit a line to the plot of  $\log_{10}[y - y(\infty)]$  (or  $\log_{10}[y(\infty) - y]$  if  $A$  is negative), then we can estimate  $A$  and  $\alpha$ . Once these are estimated, we plot  $y - [y(\infty) + Ae^{-\alpha t}]$ , which as a curve approximates  $Be^{-\beta t}$  and on the log plot is equivalent to  $\log_{10} B - 0.4345\beta t$ . We repeat the process, each time removing the slowest remaining term, until the data stop is accurate. Then we plot the final model step response and compare it with data so we can assess the quality of the computed model. It is possible to get a good fit to the step response and yet be far off from the true time constants (poles) of the system. However, the method gives a good approximation for control of processes whose step responses look like Fig. W3.4.

#### EXAMPLE W3.5

#### *Determining the Model from Time-Response Data*

Find the transfer function that generates the data given in Table W3.1 and plotted in Fig. W3.5.

**Solution.** Table W3.1 shows, and Fig. W3.5 implies, that the final value of the data is  $y(\infty) = 1$ . We know that  $A$  is negative because  $y(\infty)$  is greater than  $y(t)$ . Therefore, the first step in the process is to plot  $\log_{10}[y(\infty) - y]$ , which is shown in Fig. W3.6. From the line (fitted by eye), the values are

**Figure W3.4**

A step response characteristic of many chemical processes

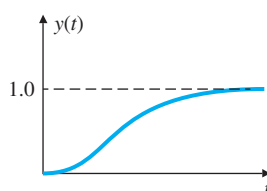


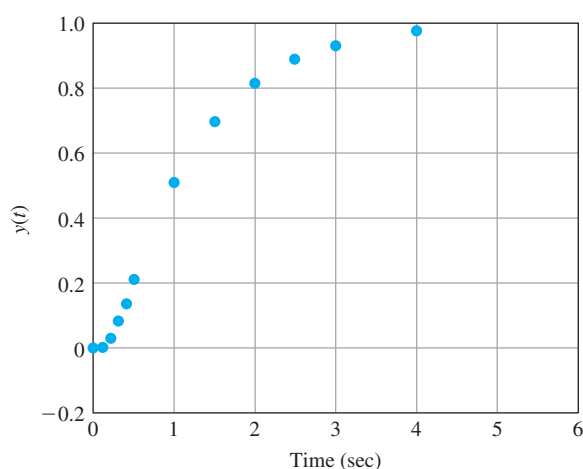
**TABLE W3.1**

Step Response Data			
<i>t</i>	<i>y(t)</i>	<i>t</i>	<i>y(t)</i>
0.1	0.000	1.0	0.510
0.1	0.005	1.5	0.700
0.2	0.034	2.0	0.817
0.3	0.085	2.5	0.890
0.4	0.140	3.0	0.932
0.5	0.215	4.0	0.975
		$\infty$	1.000

Based on Sinha, N. K. and B. Kusztza,  
Modeling and Identification of Dynamic  
Systems. New York: Van Nostrand, 1983.

**Figure W3.5**

Step response data in  
Table W3.1



$$\log_{10} |A| = 0.125,$$

$$0.4343\alpha = \frac{1.602 - 1.167}{\Delta t} = \frac{0.435}{1} \Rightarrow \alpha \cong 1.$$

Thus

$$A = -1.33,$$

$$\alpha = 1.0.$$

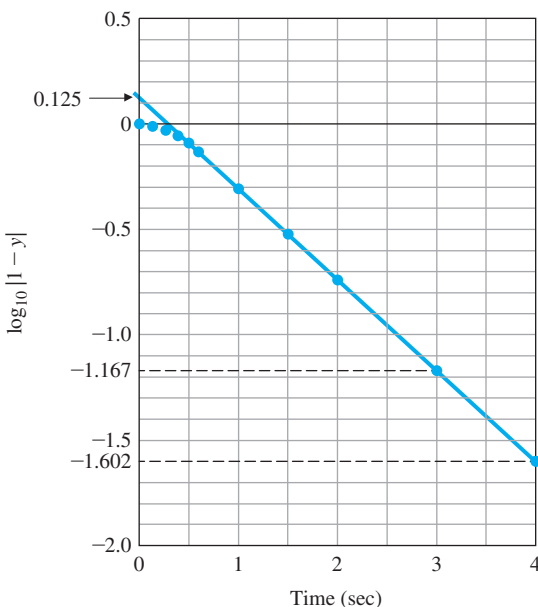
If we now subtract  $1 + Ae^{\alpha t}$  from the data and plot the log of the result, we find the plot of Fig. W3.7. Here we estimate

$$\log_{10} B = -0.48,$$

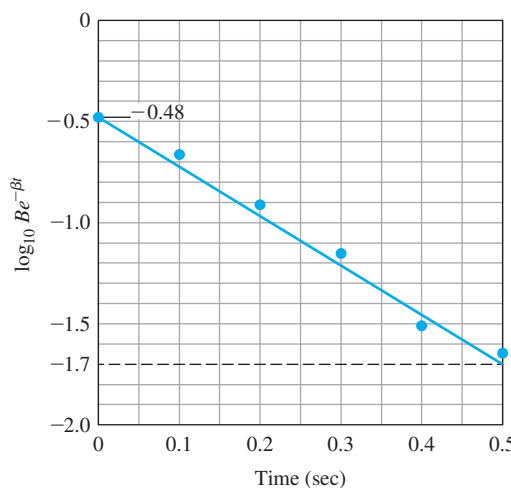
$$0.4343\beta = \frac{-0.48 - (-1.7)}{0.5} = 2.5,$$

**Figure W3.6**

$\log_{10}[y(\infty) - y]$   
versus  $t$

**Figure W3.7**

$\log_{10}[y - (1 + Ae^{-\alpha t})]$   
versus  $t$



$$\beta \approx 5.8,$$

$$B = 0.33.$$

Combining these results, we arrive at the  $y$  estimate

$$\hat{y}(t) \approx 1 - 1.33e^{-t} + 0.33e^{-5.8t}. \quad (\text{W3.4})$$

Equation (W3.4) is plotted as the colored line in Fig. W3.8 and shows a reasonable fit to the data, although some error is noticeable near  $t = 0$ .

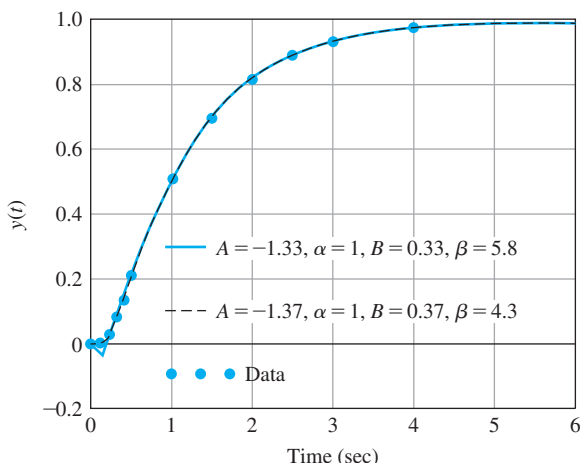
From  $\hat{y}(t)$ , we compute

$$\hat{Y}(s) = \frac{1}{s} - \frac{1.33}{s+1} + \frac{0.33}{s+5.8}$$

## 52 Appendix W3.7 System Identification

**Figure W3.8**

Model fits to the experimental data



$$\begin{aligned}
 &= \frac{(s+1)(s+5.8) - 1.33s(s+5.8) + 0.33s(s+1)}{s(s+1)(s+5.8)} \\
 &= \frac{-0.58s + 5.8}{s(s+1)(s+5.8)}.
 \end{aligned}$$

The resulting transfer function is

$$G(s) = \frac{-0.58(s-10)}{(s+1)(s+5.8)}.$$

Notice this method has given us a system with a zero in the RHP, even though the data showed no values of  $y$  that were negative. Very small differences in the estimated value for  $A$ , all of which approximately fit the data, can cause values of  $\beta$  to range from 4 to 6. This illustrates the sensitivity of pole locations to the quality of the data and emphasizes the need for a good signal-to-noise ratio.

By using a computer to perform the plotting, we are better able to iterate the four parameters to achieve the best overall fit. The data presentation in Figs. W3.6 and W3.7 can be obtained directly by using a semilog plot. This eliminates having to calculate  $\log_{10}$  and the exponential expression to find the values of the parameters. The equations of the lines to be fit to the data are  $y(t) = Ae^{\alpha t}$  and  $y(t) = Be^{\beta t}$ , which are straight lines on a semilog plot. The parameters  $A$  and  $\alpha$ , or  $B$  and  $\beta$ , are iteratively selected so the straight line comes as close as possible to passing through the data. This process produces the improved fit shown by the dashed black line in Fig. W3.8. The revised parameters,  $A = -1.37$ ,  $B = 0.37$ , and  $\beta = 4.3$  result in the transfer function

$$G(s) = \frac{-0.22s + 4.3}{(s+1)(s+4.3)}.$$

The RHP zero is still present, but it is now located at  $s \cong +20$  and has no noticeable effect on the time response.

This set of data was fitted quite well by a second-order model. In many cases, a higher-order model is required to explain the data and the modes may not be as well separated.

### Least-squares system identification

If the transient response has oscillatory modes, then these can sometimes be estimated by comparing them with the standard plots of Fig. 3.18. The period will give the frequency  $\omega_d$ , and the decay from one period to the next will afford an estimate of the damping ratio. If the response has a mixture of modes not well separated in frequency, then more sophisticated methods need to be used. One such is **least-squares system identification**, in which a numerical optimization routine selects the best combination of system parameters so as to minimize the fit error. The fit error is defined to be a scalar **cost function**

$$J = \sum_i (y_{data} - y_{model})^2, \quad i = 1, 2, 3, \dots, \text{for each data point,}$$

so fit errors at all data points are taken into account in determining the best value for the system parameters.

#### W3.7.3.1 Models from Other Data

As mentioned early in Section 3.1.2, we can also generate a model using frequency-response data, which are obtained by exciting the system with a set of sinusoids and plotting  $G(j\omega)$ . In Chapter 6, we show how such plots can be used directly for design. Alternatively, we can use the frequency response to estimate the poles and zeros of a transfer function using straight-line asymptotes on a logarithmic plot.

The construction of dynamic models from normal stochastic operating records or from the response to a PRBS can be based either on the concept of cross-correlation or on the least-squares fit of a discrete equivalent model, both topics in the field of **system identification**. They require substantial presentation and background that are beyond the scope of this text. An introduction to system identification can be found in Chapter 8 of Franklin et al. (1998), and a comprehensive treatment is given in Ljung (1999). Based largely on the work of Professor Ljung, the Matlab Toolbox on Identification provides substantial software to perform system identification and to verify the quality of the proposed models.

#### W3.7.4 Obtaining a Pole-Zero Model from Frequency-Response Data

As we pointed out earlier, it is relatively easy to obtain the frequency-response of a system experimentally. Sometimes it is desirable to obtain an approximate model, in terms of a transfer function, directly from the frequency response. The derivation of such a model can be done

to various degrees of accuracy. The method described in this section is usually adequate and is widely used in practice.

There are two ways to obtain a model from frequency-response data. In the first case, we can introduce a sinusoidal input, measure the gain (logarithm of the amplitude ratio of output to input) and the phase difference between output and input, and accept the curves plotted from this data as the model. Using the methods given in previous sections, we can derive the design directly from this information. In the second case, we wish to use the frequency data to verify a mathematical model obtained by other means. To do so, we need to extract an approximate transfer function from the plots, again by fitting straight lines to the data, estimating break points (that is, finding the poles and zeros), and using Fig. 6.3 to estimate the damping ratios of complex factors from the frequency overshoot. The next example illustrates the second case.

## EXAMPLE W3.6

### *Transfer Function from Measured Frequency Response*

Determine a transfer function from the frequency response plotted in Fig. W3.9, where frequency  $f$  is plotted in hertz.

**Solution.** Drawing an asymptote to the final slope of  $-2$  (or  $-40$  db per decade), we assume a break point at the frequency where the phase is  $-90^\circ$ . This occurs at  $f_1 \cong 1.66$  Hz ( $\omega_1 = 2\pi f_1 = 10.4$  rad/sec). We need to know the damping ratio in order to subtract out this second-order pole. For this, the phase curve may be of more help. Since the phase around the break-point frequency is symmetric, we draw a line at the slope of the phase curve at  $f_1$  to find that the phase asymptote intersects the  $0^\circ$  line at  $f_0 \cong 0.71$  Hz (or  $4.46$  rad/sec). This corresponds to  $f_1/f_0 \cong 2.34$ , which in time corresponds to  $\zeta \cong 0.5$ , as seen on the normalized response curves in Fig. 6.3b. The magnitude curve with the second-order factor taken out shows an asymptotic amplitude gain of about  $6.0$  db, or a factor of  $10^{6.0/20} = 2.0$ . As this is a gain rise, it occurs because of a lead compensation of the form

$$\frac{s/a + 1}{s/b + 1},$$

where  $b/a = 2.0$ . If we remove the second-order terms in the phase curve, we obtain a phase curve with a maximum phase of about  $20^\circ$ , which also corresponds to a frequency separation of about  $2$ . To locate the center of the lead compensation, we must estimate the point of maximum phase based on the lead term alone, which occurs at the geometric mean of the two break-point frequencies. The lead center seems to occur at  $f_2 \cong 0.3$  Hz (or  $\omega_2 = 1.88$  rad/sec).

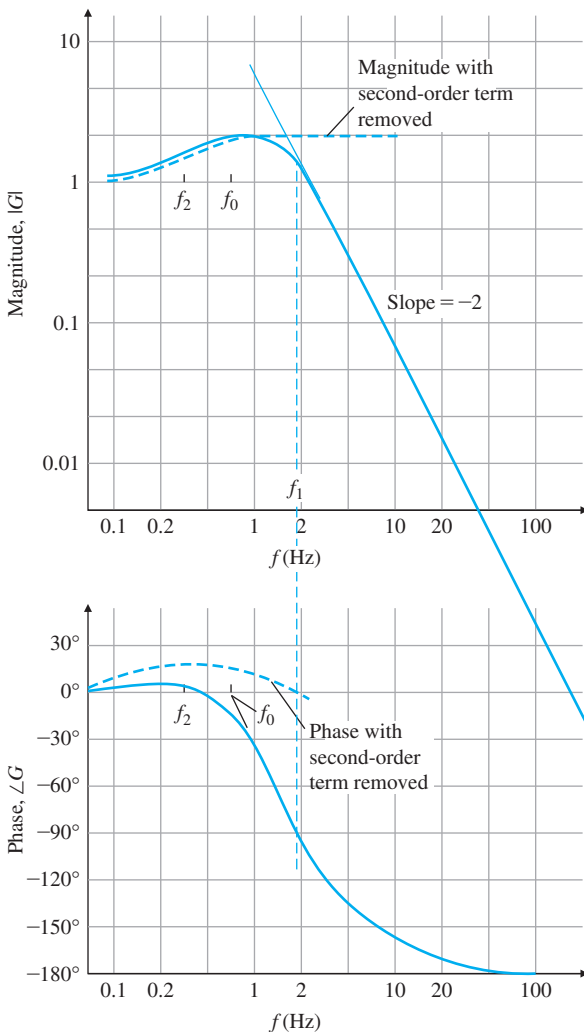
Thus, we have the relations

$$ab(1.88)^2 = 3.55,$$

$$\frac{b}{a} = 2,$$

**Figure W3.9**

Experimental frequency response



from which we can solve

$$2a^2 = 3.55,$$

$$a = 1.33,$$

$$b = 2.66.$$

**Model from measured response**

Our final model is given by

$$\hat{G}(s) = \frac{(s/1.33) + 1}{[(s/2.66) + 1][(s/10.4)^2 + (s/10.4) + 1]}. \quad (\text{W3.5})$$

The actual data were plotted from

$$G(s) = \frac{(s/2) + 1}{[(s/4) + 1][(s/10)^2 + (s/10) + 1]}.$$

As can be seen, we found the second-order term quite easily, but the location of the lead compensation is off in center frequency by a factor of  $4/2.66 \cong 1.5$ . However, the subtraction of the second-order term from the composite curve was not done with great accuracy, rather, by reading the curves. Again, as with the transient response, we conclude that by a bit of approximate plotting we can obtain a crude model (usually within a factor of 1.4 ( $\pm 3$  db) in amplitude and  $\pm 10^\circ$  in phase) that can be used for control design.

---

Refinements on these techniques with computer aids are rather obvious, and an interactive program for removing standard first- and second-order terms and accurately plotting the residual function would greatly improve the speed and accuracy of the process. It is also common to have computer tools that can find the parameters of an assumed model structure by minimizing the sum of squares of the difference between the model's frequency response and the experimental frequency response.

#### Further Reading for System Identification:

- [1] L. Ljung, *Perspectives on System Identification*, *Annual Reviews in Control*, 34, pp. 1–12, Elsevier, 2010.
- [2] L. Ljung, *System Identification: Theory for the User*, 2nd Ed., Prentice-Hall, 1999.
- [3] G. F. Franklin, J. D. Powell, M. L. Workman, *Digital Control of Dynamic Systems*, 3rd Ed. Ellis-Kagle Press, 1998.
- [4] M. B. Tischler and R. K. Remple, *Aircraft and Rotorcraft System Identification: Engineering Methods with Flight-Test Examples*, AIAA, 2006.
- [5] R. Pintelon and J. Schoukens, *System Identification: A Frequency Domain Approach*, 2nd ed., Wiley-IEEE Press, 2012.
- [6] System Identification Toolbox, The Mathworks.

# Appendix W3.8

## Amplitude and Time Scaling

The magnitude of the values of the variables in a problem is often very different, sometimes so much so that numerical difficulties arise. This was a serious problem years ago when equations were solved using analog computers, and it was routine to *scale* the variables so all had similar magnitudes. Today's widespread use of digital computers for solving differential equations has largely eliminated the need to scale a problem unless the number of variables is very large, because computers are now capable of accurately handling numbers with wide variations in magnitude. Nevertheless, it is wise to understand the principle of scaling for the few cases in which extreme variations in magnitude exist, and scaling is necessary or the computer word size is limited.

### W3.8.1 Amplitude Scaling

There are two types of scaling that are sometimes carried out: amplitude scaling and time scaling, as we have already seen in Section 3.1.4. **Amplitude scaling** is usually performed unwittingly by simply picking units that make sense for the problem at hand. For the ball levitator, expressing the motion in millimeters and the current in millamps would keep the numbers within a range that is easy to work with. Equations of motion are sometimes developed in the standard SI units such as meters, kilograms, and amperes, but when computing the motion of a rocket going into orbit, using kilometers makes more sense. The equations of motion are usually solved using computer-aided design software, which is often capable of working in any units. For higher-order systems, it becomes important to scale the problem so that system variables have similar numerical variations. A method for accomplishing the best scaling for a complex system is first to estimate the maximum values for each system variable, then to scale the system so that each variable varies between  $-1$  and  $1$ .

In general, we can perform amplitude scaling by defining the scaled variables for each state element. If

$$x' = S_x x, \quad (\text{W3.6})$$

then

$$\dot{x}' = S_x \dot{x} \quad \text{and} \quad \ddot{x}' = S_x \ddot{x}. \quad (\text{W3.7})$$

We then pick  $S_x$  to result in the appropriate scale change, substitute Eqs. (W3.6) and (W3.7) into the equations of motion, and recompute the coefficients.

## EXAMPLE W3.7

### Scaling for the Ball Levitator

The linearized equation of motion for the ball levitator (see Example 9.2, Chapter 9) is

$$\delta\ddot{x} = 1667\delta x + 47.6\delta i, \quad (\text{W3.8})$$

where  $\delta x$  is in units of meters and  $\delta i$  is in units of amperes. Scale the variables for the ball levitator to result in units of millimeters and millamps instead of meters and amps.

**Solution.** Referring to Eq. (W3.6), we define

$$\delta x' = S_x \delta x \quad \text{and} \quad \delta i' = S_i \delta i,$$

such that both  $S_x$  and  $S_i$  have a value of 1000 in order to convert  $\delta x$  and  $\delta i$  in meters and amps to  $\delta x'$  and  $\delta i'$  in millimeters and millamps. Substituting these relations into Eq. (W3.8) and taking note of Eq. (W3.7) yields

$$\delta\ddot{x}' = 1667\delta x' + 47.6 \frac{S_x}{S_i} \delta i'.$$

In this case,  $S_x = S_i$ , so Eq. (W3.8) remains unchanged. Had we scaled the two quantities by different amounts, there would have been a change in the last coefficient in the equation.

---

### W3.8.2 Time Scaling

The unit of time when using SI units or English units is seconds. Computer-aided design software is *usually* able to compute results accurately no matter how fast or slow the particular problem at hand. However, if a dynamic system responds in a few microseconds, or if there are characteristic frequencies in the system on the order of several megahertz, the problem may become ill-conditioned, so that the numerical routines produce errors. This can be particularly troublesome for high-order systems. The same holds true for an extremely slow system. It is therefore useful to know how to change the units of time should you encounter an ill-conditioned problem.

We define the new scaled time to be

$$\tau = \omega_o t, \quad (\text{W3.9})$$

such that, if  $t$  is measured in seconds and  $\omega_o = 1000$ , then  $\tau$  will be measured in milliseconds. The effect of the **time scaling** is to change the differentiation so

$$\dot{x} = \frac{dx}{dt} = \frac{dx}{d(\tau/\omega_o)} = \omega_o \frac{dx}{d\tau}, \quad (\text{W3.10})$$

and

$$\ddot{x} = \frac{d^2x}{dt^2} = \omega_o^2 \frac{d^2x}{d\tau^2}. \quad (\text{W3.11})$$

## EXAMPLE W3.8

### Time Scaling an Oscillator

The equation for an oscillator was derived in Example 2.6. For a case with a very fast natural frequency  $\omega_n = 15,000$  rad/sec (about 2 kHz), Eq. (2.23) can be rewritten as

$$\ddot{\theta} + 15,000^2 \cdot \theta = 10^6 \cdot T_c.$$

Determine the time-scaled equation so that the unit of time is milliseconds.

**Solution.** The value of  $\omega_o$  in Eq. (W3.9) is 1000. Equation (W3.11) shows that

$$\frac{d^2\theta}{d\tau^2} = 10^{-6} \cdot \ddot{\theta},$$

and the time-scaled equation becomes

$$\frac{d^2\theta}{d\tau^2} + 15^2 \cdot \theta = T_c.$$

In practice, we would then solve the equation

$$\ddot{\theta} + 15^2 \cdot \theta = T_c \quad (\text{W3.12})$$

and label the plots in milliseconds instead of seconds.

### W3.8.3 Time and Amplitude Scaling in State-Space

We have already discussed time and amplitude scaling in Chapter 3. We now extend the ideas to the state-variable form. Time scaling with  $\tau = \omega_o t$  replaces Eq. (7.3) with

$$\frac{d\mathbf{x}}{d\tau} = \frac{1}{\omega_o} \mathbf{A}\mathbf{x} + \frac{1}{\omega_o} \mathbf{B}u = \hat{\mathbf{A}}\mathbf{x} + \hat{\mathbf{B}}u. \quad (\text{W3.13})$$

Amplitude scaling of the state corresponds to replacing  $\mathbf{x}$  with  $\mathbf{z} = \mathbf{D}_x^{-1}\mathbf{x}$ , where  $\mathbf{D}_x$  is a diagonal matrix of scale factors. Input scaling corresponds to replacing  $u$  with  $v = \mathbf{D}_u^{-1}u$ . With these substitutions,

$$\mathbf{D}_x \dot{\mathbf{z}} = \frac{1}{\omega_o} \mathbf{A} \mathbf{D}_x \mathbf{z} + \frac{1}{\omega_o} \mathbf{B} \mathbf{D}_u v. \quad (\text{W3.14})$$

Then

$$\dot{\mathbf{z}} = \frac{1}{\omega_o} \mathbf{D}_x^{-1} \mathbf{A} \mathbf{D}_x \mathbf{z} + \frac{1}{\omega_o} \mathbf{D}_x^{-1} \mathbf{B} \mathbf{D}_u v = \hat{\mathbf{A}}\mathbf{z} + \hat{\mathbf{B}}v. \quad (\text{W3.15})$$

Equation (W3.15) compactly expresses the time- and amplitude-scaling operations. Regrettably, it does not relieve the engineer of the responsibility of actually thinking of good scale factors so scaled equations are in good shape.

**EXAMPLE W3.9***Time Scaling an Oscillator*

The equation for an oscillator was derived in Example 2.6. For a case with a very fast natural frequency  $\omega_n = 15,000$  rad/sec (about 2 kHz), Eq. (2.23) can be rewritten as

$$\ddot{\theta} + 15,000^2 \cdot \theta = 10^6 \cdot T_c.$$

Determine the time-scaled equation so the unit of time is milliseconds.

**Solution.** In state-variable form with a state vector  $\mathbf{x} = [\theta \ \dot{\theta}]^T$ , the unscaled matrices are

$$\mathbf{A} = \begin{bmatrix} 0 & 1 \\ -15,000^2 & 0 \end{bmatrix} \quad \text{and} \quad \mathbf{B} = \begin{bmatrix} 0 \\ 10^6 \end{bmatrix}.$$

Applying Eq. (W3.13) results in

$$\hat{\mathbf{A}} = \begin{bmatrix} 0 & \frac{1}{1000} \\ -\frac{15,000^2}{1000} & 0 \end{bmatrix} \quad \text{and} \quad \hat{\mathbf{B}} = \begin{bmatrix} 0 \\ 10^3 \end{bmatrix},$$

which yields state-variable equations that are scaled.

---

## Appendix W4.1.4.1

# The Filtered Case

Thus far, the analysis has been based on the simplest open- and closed-loop structures. A more general case includes a dynamic filter on the input and also dynamics in the sensor. The filtered open-loop structure is shown in Fig. W4.1 having the transfer function  $T_{ol} = GD_{ol}F$ . In this case, the open-loop controller transfer function has been simply replaced by  $D_{ol}F$ , and the discussion given for the unfiltered open-loop case is easily applied to this change.

For the filtered feedback case shown in Fig. W4.2, the changes are more significant. In that case, the transform of the system output is given by

$$Y = \frac{GD_{cl}F}{1 + GD_{cl}H} R + \frac{G}{1 + GD_{cl}H} W - \frac{HGD_{cl}}{1 + GD_{cl}H} V. \quad (\text{W4.1})$$

As is evident from this equation, the sensor dynamics,  $H$ , is part of the loop transfer function and enters into the question of stability with  $D_{cl}H$  replacing the  $D_{cl}$  of the unity feedback case. In fact, if  $F = H$ , then with respect to stability, tracking, and regulation, the filtered case is identical to the unity case with  $D_{cl}H$  replacing  $D_{cl}$ . On the other hand, the filter transfer function  $F$  can play the role of the open-loop controller except that here the filter  $F$  would be called on to modify the

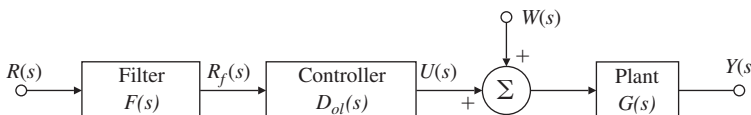


**Figure W4.1**

Filtered open-loop system

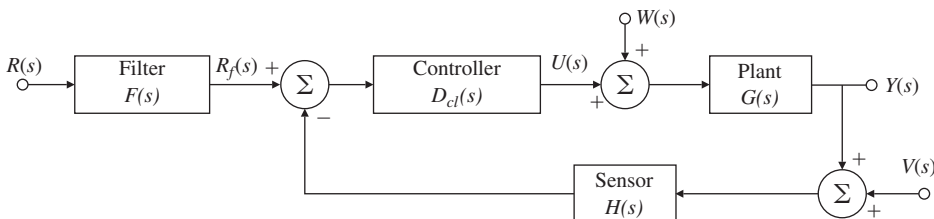


**Figure W4.2**

Filtered closed-loop.  $R$  = reference,  $U$  = control,  $Y$  = output,  $V$  = sensor noise

entire loop transfer function,  $\frac{GD_{cl}}{1+GD_{cl}H}$ , rather than simply  $GD_{ol}$ . Therefore, the filtered closed-loop structure can realize the best properties of both the open-loop and the unity feedback closed-loop cases. The controller,  $D_{cl}$ , can be designed to effectively regulate the system for the disturbance  $W$  and the sensor noise  $V$ , while the filter  $F$  is designed to improve the tracking accuracy. If the sensor dynamics  $H$  are accessible to the designer, this term also can be designed to improve the response to the sensor noise. The remaining issue is sensitivity.

Using the formula given in Eq. (4.18), with changes in the parameter of interest, we can compute

$$\mathcal{S}_F^{T_{cl}} = 1.0, \quad (\text{W4.2})$$

$$\mathcal{S}_G^{T_{cl}} = \frac{1}{1 + GD_{cl}H}, \quad (\text{W4.3})$$

$$\mathcal{S}_H^{T_{cl}} = -\frac{GD_{cl}H}{1 + GD_{cl}H}. \quad (\text{W4.4})$$

Of these, the most interesting is the last. Notice with respect to  $H$ , the sensitivity approaches unity as the loop gain grows. Therefore it is particularly important that the transfer function of the sensor be not only low in noise but also very stable in gain. Money spent on the sensor is money well spent!

## EXAMPLE W4.1

If  $S$  is the sensitivity of the filtered feedback system to changes in the plant transfer function, and  $T$  is the transfer function from reference to output, compute the sum of  $S + T$ . Show that  $S + T = 1$  if  $F = H$ .

- (a) Compute the sensitivity of the filtered feedback system shown in Fig. W4.2 with respect to changes in the plant transfer function,  $G$ .
- (b) Compute the sensitivity of the filtered feedback system shown in Fig. W4.2 with respect to changes in the controller transfer function,  $D_{cl}$ .
- (c) Compute the sensitivity of the filtered feedback system shown in Fig. W4.2 with respect to changes in the filter transfer function,  $F$ .
- (d) Compute the sensitivity of the filtered feedback system shown in Fig. W4.2 with respect to changes in the sensor transfer function,  $H$ . If  $S$  is the sensitivity of the filtered feedback system to changes in the plant transfer function and  $T$  is the transfer function from reference to output, compute the sum of  $S + T$ . Show that  $S + T = 1$  if  $F = H$ .

**Solution.** To answer the first question, we need the answer to part (a), so let's start there.

- (a) Applying the formula for sensitivity of  $T$  to changes in  $G$ :

$$\begin{aligned} T &= \frac{FD_{cl}G}{1 + D_{cl}GH}, \\ S &= G \frac{1 + D_{cl}GH}{FD_{cl}G} \frac{(1 + D_{cl}GH)FD_{cl} - FD_{cl}G(D_{cl}H)}{(1 + D_{cl}GH)^2} \\ &= \frac{1}{1 + D_{cl}GH}. \end{aligned}$$

Now

$$\begin{aligned} S + T &= \frac{1}{1 + D_{cl}GH} + \frac{FD_{cl}G}{1 + D_{cl}GH} \\ &= \frac{1 + FD_{cl}G}{1 + D_{cl}GH} \\ &= 1 \quad \text{if } F = H. \end{aligned} \tag{W4.5}$$

- (b) Applying the formula for sensitivity of  $T$  to changes in  $D_{cl}$ :

$$\begin{aligned} S_T^D &= D_{cl} \frac{1 + D_{cl}GH}{FD_{cl}G} \frac{(1 + D_{cl}GH)FG - FD_{cl}G(GH)}{(1 + D_{cl}GH)^2} \\ &= \frac{1}{1 + D_{cl}GH}. \end{aligned}$$

This is not surprising as  $D_{cl}$  and  $G$  are in series.

- (c) Applying the formula for sensitivity of  $T$  to changes in  $F$ :

$$\begin{aligned} S_T^F &= F \frac{1 + D_{cl}GH}{FD_{cl}G} \frac{(1 + D_{cl}GH)(D_{cl}G)}{(1 + D_{cl}GH)^2} \\ &\quad \frac{1 + D_{cl}GH}{1 + D_{cl}GH} \\ &= 1. \end{aligned}$$

In this case, the  $F$  term is in the open loop, so it has a sensitivity of unity.

- (d) Applying the formula for sensitivity of  $T$  to changes in  $H$ ,

$$\begin{aligned} S_T^H &= H \frac{1 + D_{cl}GH}{FD_{cl}G} \frac{(1 + D_{cl}GH)0 - FD_{cl}G(D_{cl}G)}{(1 + D_{cl}GH)^2} \\ &= -\frac{D_{cl}GH}{(1 + D_{cl}GH)}. \end{aligned}$$


---

## Appendix W4.2.2.1

# Truxal's Formula for the Error Constants

Truxal (1955) derived a formula for the velocity constant of a Type 1 system in terms of the closed-loop poles and zeros, which is a formula that connects the steady-state error to the system's dynamic response. Since control design often requires a trade-off between these two characteristics, Truxal's formula can be useful to know. Its derivation is quite direct. Suppose the closed-loop transfer function  $\mathcal{T}(s)$  of a Type 1 system is

$$\mathcal{T}(s) = K \frac{(s - z_1)(s - z_2) \cdots (s - z_m)}{(s - p_1)(s - p_2) \cdots (s - p_n)}. \quad (\text{W4.6})$$

Since the steady-state error in response to a step input in a Type 1 system is zero, the DC gain is unity; thus,

$$\mathcal{T}(0) = 1. \quad (\text{W4.7})$$

The system error is given by

$$E(s) \triangleq R(s) - Y(s) = R(s) \left[ 1 - \frac{Y(s)}{R(s)} \right] = R(s)[1 - \mathcal{T}(s)]. \quad (\text{W4.8})$$

The system error due to a unit ramp input is given by

$$E(s) = \frac{1 - \mathcal{T}(s)}{s^2}. \quad (\text{W4.9})$$

Using the Final Value Theorem, we get

$$e_{ss} = \lim_{s \rightarrow 0} \frac{1 - \mathcal{T}(s)}{s}. \quad (\text{W4.10})$$

Using L'Hôpital's rule, we rewrite Eq. (W4.10) as

$$e_{ss} = - \lim_{s \rightarrow 0} \frac{d\mathcal{T}}{ds}, \quad (\text{W4.11})$$

or

$$e_{ss} = - \lim_{s \rightarrow 0} \frac{d\mathcal{T}}{ds} = \frac{1}{K_v}. \quad (\text{W4.12})$$

Equation (W4.12) implies that  $1/K_v$  is related to the slope of the transfer function at the origin, which is a result shown in Section 6.1.2. Using Eq. (W4.7), we can rewrite Eq. (W4.12) as

$$e_{ss} = - \lim_{s \rightarrow 0} \frac{d\mathcal{T}}{ds} \frac{1}{\mathcal{T}}, \quad (\text{W4.13})$$

or

$$e_{ss} = - \lim_{s \rightarrow 0} \frac{d}{ds} [\ln \mathcal{T}(s)]. \quad (\text{W4.14})$$

Substituting Eq. (W4.6) into Eq. (W4.14), we get

$$e_{ss} = -\lim_{s \rightarrow 0} \frac{d}{ds} \left\{ \ln \left[ K \frac{\prod_{i=1}^m (s - z_i)}{\prod_{i=1}^n (s - p_i)} \right] \right\}, \quad (\text{W4.15})$$

$$= -\lim_{s \rightarrow 0} \frac{d}{ds} \left[ \ln K + \sum_{i=1}^m \ln(s - z_i) - \sum_{i=1}^n \ln(s - p_i) \right], \quad (\text{W4.16})$$

or

$$\frac{1}{K_v} = -\left. \frac{d \ln T}{ds} \right|_{s=0} = \sum_{i=1}^n -\frac{1}{p_i} + \sum_{i=1}^m \frac{1}{z_i}. \quad (\text{W4.17})$$

We observe from Eq. (W4.17) that  $K_v$  increases as the closed-loop poles move away from the origin. Similar relationships exist for other error coefficients, and these are explored in the problems.

## EXAMPLE W4.2

### Truxal's formula

A third-order Type 1 system has closed-loop poles at  $-2 \pm 2j$  and  $-0.1$ . The system has only one closed-loop zero. Where should the zero be if a  $K_v = 10 \text{ sec}^{-1}$  is desired?

**Solution.** From Truxal's formula, we have

$$\frac{1}{K_v} = -\frac{1}{-2+2j} - \frac{1}{-2-2j} - \frac{1}{-0.1} + \frac{1}{z},$$

or

$$0.1 = 0.5 + 10 + \frac{1}{z},$$

$$\begin{aligned} \frac{1}{z} &= 0.1 - 0.5 - 10 \\ &= -10.4. \end{aligned}$$

Therefore, the closed-loop zero should be at  $z = 1 / -10.4 = -0.096$ .

---

# Appendix W4.5

## Introduction to Digital Control

As a result of the revolution in the cost-effectiveness of digital computers, there has been an increasing use of digital logic in embedded applications such as controllers in feedback systems. A digital controller gives the designer much more flexibility to make modifications to the control law after the hardware design is fixed, because the formula for calculating the control signal is in the software rather than the hardware. In many instances, this means that the hardware and software designs can proceed almost independently, saving a great deal of time. Also, it is relatively easy to include binary logic and nonlinear operations as part of the function of a digital controller as compared to an analog controller. Special processors designed for real-time signal processing and known as digital signal processors (DSPs) are particularly well suited for use as real-time controllers. Chapter 8 includes a more extensive introduction to the math and concepts associated with the analysis and design of digital controllers and digital control systems. However, in order to be able to compare the analog designs of the next three chapters with reasonable digital equivalents, we give here a brief introduction to the most simple techniques for digital designs.

A digital controller differs from an analog controller in that the signals must be **sAMPLED** and **qUANTIZED**.<sup>1</sup> A signal to be used in digital logic needs to be sampled first and then the samples need to be converted by an analog-to-digital converter or A/D<sup>2</sup> into a quantized digital number. Once the digital computer has calculated the proper next control signal value, this value needs to be converted back into a voltage and held constant or otherwise extrapolated by a digital-to-analog converter or D/A<sup>3</sup> in order to be applied to the actuator of the process. The control signal is not changed until the next sampling period. As a result of sampling, there are strict limits on the speed and bandwidth of a digital controller. Discrete design methods that tend to minimize these limitations are described in Chapter 8. A reasonable rule of thumb for selecting the sampling period is that, during the rise-time of the

---

<sup>1</sup>A controller that operates on signals that are sampled but *not* quantized is called **discrete**, while one that operates on signals that are both sampled and quantized is called **digital**.

<sup>2</sup>Pronounced “A to D.”

<sup>3</sup>Often spelled DAC and pronounced as one word to rhyme with quack.

response to a step, the input to the discrete controller should be sampled approximately six times. By adjusting the controller for the effects of sampling, the sample period can be as large as two to three times per rise time. This corresponds to a sampling frequency that is 10 to 20 times the system's closed-loop bandwidth. The quantization of the controller signals introduces an equivalent extra noise into the system; to keep this interference at an acceptable level, the A/D converter usually has an accuracy of 10 to 12 bits, although inexpensive systems have been designed with only 8 bits. For a first analysis, the effects of the quantization are usually ignored, as they will be in this introduction. A simplified block diagram of a system with a digital controller is shown in Fig. W4.3.

For this introduction to digital control, we will describe a simplified technique for finding a discrete (sampled but not quantized) equivalent to a given continuous controller. The method depends on the sampling period,  $T_s$ , being short enough that the reconstructed control signal is close to the signal that the original analog controller would have produced. We also assume the numbers used in the digital logic have enough accurate bits so the quantization implied in the A/D and D/A processes can be ignored. While there are good analysis tools to determine how well these requirements are met, here we will test our results by simulation, following the well-known advice that “the proof of the pudding is in the eating.”

Finding a discrete equivalent to a given analog controller is equivalent to finding a recurrence equation for the samples of the control, which will approximate the differential equation of the controller. The assumption is we have the transfer function of an analog controller and wish to replace it with a discrete controller that will accept samples of the controller input  $e(kT_s)$  from a sampler and, using past values of the control signal  $u(kT_s)$  and present and past samples of the input  $e(kT_s)$ , will compute the next control signal to be sent to the actuator. As an example, consider a PID controller with the transfer function

$$U(s) = (k_P + \frac{k_I}{s} + k_D s) E(s), \quad (\text{W4.18})$$

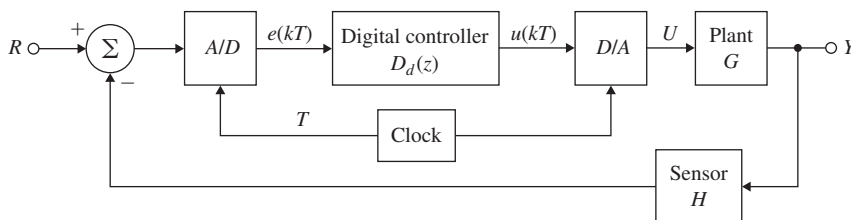


**Figure W4.3**

Block diagram of a digital controller

which is equivalent to the three terms of the time-domain expression

$$u(t) = k_p e(t) + k_I \int_0^t e(\tau) d\tau + k_D \dot{e}(t), \quad (\text{W4.19})$$

$$= u_P + u_I + u_D. \quad (\text{W4.20})$$

Based on these terms and the fact the system is linear, the next control sample can be computed term-by-term. The proportional term is immediate:

$$u_P(kT_s + T_s) = k_p e(kT_s + T_s). \quad (\text{W4.21})$$

The integral term can be computed by breaking the integral into two parts and approximating the second part, which is the integral over one sample period, as follows.

$$u_I(kT_s + T_s) = k_I \int_0^{kT_s + T_s} e(\tau) d\tau, \quad (\text{W4.22})$$

$$= k_I \int_0^{kT_s} e(\tau) d\tau + k_I \int_{kT_s}^{kT_s + T_s} e(\tau) d\tau, \quad (\text{W4.23})$$

$$= u_I(kT_s) + \{\text{area under } e(\tau) \text{ over one period}\}, \quad (\text{W4.24})$$

$$\cong u_I(kT_s) + k_I \frac{T_s}{2} \{e(kT_s + T_s) + e(kT_s)\}. \quad (\text{W4.25})$$

In Eq. (W4.25), the area in question has been approximated by that of the trapezoid formed by the base  $T_s$  and vertices  $e(kT_s + T_s)$  and  $e(kT_s)$ , as shown by the dashed line in Fig. W4.4.

The area also can be approximated by the rectangle of amplitude  $e(kT_s)$  and width  $T_s$  shown by the solid blue in Fig. W4.4 to give  $u_I(kT_s + T_s) = u_I(kT_s) + k_I T_s e(kT_s)$ . These and other possibilities are considered in Chapter 8.

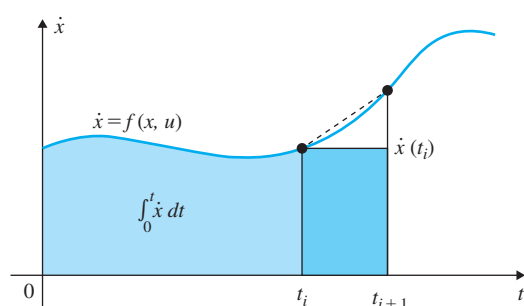
In the derivative term, the roles of  $u$  and  $e$  are reversed from integration and the consistent approximation can be written down at once from Eqs. (W4.25) and (W4.19) as

$$\frac{T_s}{2} \{u_D(kT_s + T_s) + u_D(kT_s)\} = k_D \{e(kT_s + T_s) - e(kT_s)\}. \quad (\text{W4.26})$$

As with linear analog transfer functions, these relations are greatly simplified and generalized by the use of transform ideas. At this time, the

**Figure W4.4**

Graphical interpretation of numerical integration



discrete transform will be introduced simply as a prediction operator  $z$  much as if we described the Laplace transform variable,  $s$ , as a differential operator.<sup>4</sup> Here we define the operator  $z$  as the forward shift operator in the sense that if  $U(z)$  is the transform of  $u(kT_s)$  then  $zU(z)$  will be the transform of  $u(kT_s + T_s)$ . With this definition, the integral term can be written as

$$zU_I(z) = U_I(z) + k_I \frac{T_s}{2} [zE(z) + E(z)], \quad (\text{W4.27})$$

$$U_I(z) = k_I \frac{T_s}{2} \frac{z+1}{z-1} E(z), \quad (\text{W4.28})$$

and from Eq. (W4.26), the derivative term becomes the inverse as

$$U_D(z) = k_D \frac{2}{T_s} \frac{z-1}{z+1} E(z). \quad (\text{W4.29})$$

The complete discrete PID controller is thus described by

$$U(z) = \left( k_P + k_I \frac{T_s}{2} \frac{z+1}{z-1} + k_D \frac{2}{T_s} \frac{z-1}{z+1} \right) E(z). \quad (\text{W4.30})$$

Comparing the two discrete equivalents of integration and differentiation with the corresponding analog terms, it is seen that the effect of the discrete approximation in the  $z$  domain is as if everywhere in the analog transfer function the operator  $s$  has been replaced by the composite operator  $\frac{2}{T_s} \frac{z-1}{z+1}$ . This is the trapezoid rule<sup>5</sup> of discrete equivalents and is usually referred to as Tustin's Method.

The discrete equivalent to  $D_c(s)$  is

$$D_d(z) = D_c \left( \frac{2}{T_s} \frac{z-1}{z+1} \right). \quad (\text{W4.31})$$

Trapezoid rule or Tustin's Method

## EXAMPLE W4.3

### *Discrete Equivalent*

Find the discrete equivalent to the analog controller having transfer function

$$D_c(s) = \frac{U(s)}{E(s)} = \frac{11s+1}{3s+1}, \quad (\text{W4.32})$$

using the sample period  $T_s = 1$ .

**Solution.** The discrete operator is  $\frac{2(z-1)}{z+1}$  and thus the discrete transfer function is

$$D_d(z) = \frac{U(z)}{E(z)} = D_c(s)|_{s=\frac{2}{T_s}} \frac{z-1}{z+1}, \quad (\text{W4.33})$$

$$= \frac{11 \left[ \frac{2(z-1)}{z+1} \right] + 1}{3 \left[ \frac{2(z-1)}{z+1} \right] + 1}. \quad (\text{W4.34})$$

---

<sup>4</sup>This is defined as the  $z$ -transform in Chapter 8.

<sup>5</sup>The formula is called Tustin's method after the English engineer who used the technique to study the responses of nonlinear circuits.

Clearing fractions, the discrete transfer function is

$$D_d(z) = \frac{U(z)}{E(z)} = \frac{23z - 21}{7z - 5}. \quad (\text{W4.35})$$

Converting the discrete transfer function to a discrete difference equation using the definition of  $z$  as the forward shift operator is done as follows. First we cross-multiply in Eq. (W4.35) to obtain

$$(7z - 5)U(z) = (23z - 21)E(z), \quad (\text{W4.36})$$

and interpreting  $z$  as a shift operator, this is equivalent to the difference equation<sup>6</sup>

$$7u(k+1) - 5u(k) = 23e(k+1) - 21e(k), \quad (\text{W4.37})$$

where we have replaced  $kT_s + T_s$  with  $k + 1$  to simplify the notation. To compute the next control at time  $kT_s + T_s$ , therefore, we solve the difference equation

$$u(k+1) = \frac{5}{7}u(k) + \frac{23}{7}e(k+1) - \frac{21}{7}e(k). \quad (\text{W4.38})$$


---

Now let's apply these results to a control problem. Fortunately, Matlab provides us with the Simulink capability to simulate both continuous and discrete systems allowing us to compare the responses of the systems with continuous and discrete controllers.

## EXAMPLE W4.4

### *Equivalent Discrete Controller for Speed Control*

A motor speed control is found to have the plant transfer function

$$\frac{Y}{U} = \frac{45}{(s+9)(s+5)}. \quad (\text{W4.39})$$

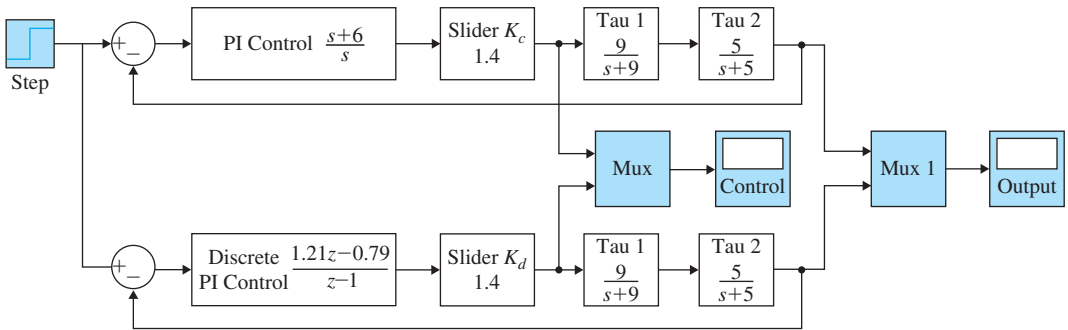
A PI controller designed for this system has the transfer function

$$D_c(s) = \frac{U}{E} = 1.4 \frac{s+6}{s}. \quad (\text{W4.40})$$

The closed-loop system has a rise time of about 0.2 sec, and an overshoot of about 20%. Design a discrete equivalent to this controller and compare the step responses and control signals of the two systems: (a) Compare the responses if the sample period is 0.07, which is about three samples per rise time. (b) Compare the responses with a sample period of  $T_s = 0.035$  sec, which corresponds to about six samples per rise time.

---

<sup>6</sup>The process is entirely similar to that used in Chapter 3 to find the ordinary differential equation to which a rational Laplace transform corresponds.

**Figure W4.5**

Simulink block diagram to compare continuous and discrete controllers

*Source: Reprinted with permission of The MathWorks, Inc.*

**Solution.** (a) Using the substitution given by Eq. (W4.31), the discrete equivalent for  $T_s = 0.07$  sec is given by replacing  $s$  by  $s \leftarrow \frac{2}{0.07} \frac{z-1}{z+1}$  in  $D_c(s)$  as

$$D_d(z) = 1.4 \frac{\frac{2}{0.07} \frac{z-1}{z+1} + 6}{\frac{2}{0.07} \frac{z-1}{z+1}}, \quad (\text{W4.41})$$

$$= 1.4 \frac{2(z-1) + 6 * 0.07(z+1)}{2(z-1)}, \quad (\text{W4.42})$$

$$= 1.4 \frac{1.21z - 0.79}{(z-1)}. \quad (\text{W4.43})$$

Based on this expression, the equation for the control is (the sample period is suppressed)

$$u(k+1) = u(k) + 1.4 * [1.21e(k+1) - 0.79e(k)]. \quad (\text{W4.44})$$

(b) For  $T_s = 0.035$  sec, the discrete transfer function is

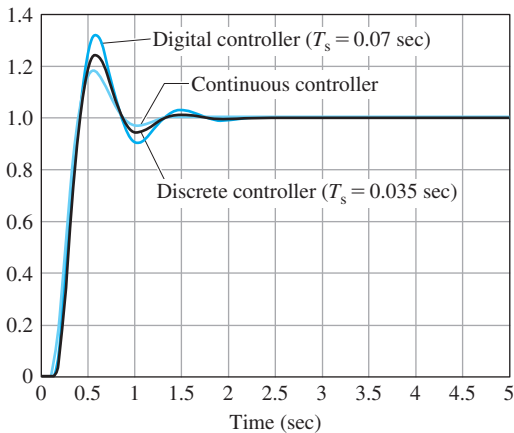
$$D_d(z) = 1.4 \frac{1.105z - 0.895}{z - 1}, \quad (\text{W4.45})$$

for which the difference equation is

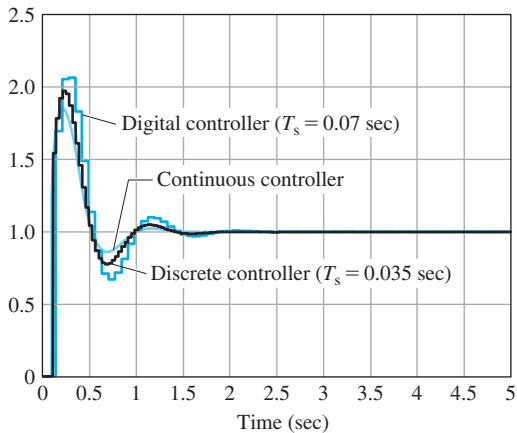
$$u(k+1) = u(k) + 1.4[1.105 e(k+1) - 0.895 e(k)].$$

A Simulink block diagram for simulating the two systems is given in Fig. W4.5, and plots of the step responses are given in Fig. W4.6a. The respective control signals are plotted in Fig. W4.6b. Notice the discrete controller for  $T_s = 0.07$  sec results in a substantial increase in the overshoot in the step response, while with  $T_s = 0.035$  sec, the digital controller matches the performance of the analog controller fairly well.

For controllers with many poles and zeros, making the continuous-to-discrete substitution called for in Eq. (W4.31) can be very tedious.



(a)



(b)

**Figure W4.6**

Comparison plots of a speed control system with continuous and discrete controllers: (a) output responses and (b) control signals

Fortunately, Matlab provides a command that does all the work. If one has a continuous transfer function given by  $D_c(s) = \frac{\text{numD}}{\text{denD}}$  represented in Matlab as  $\text{sysDc} = \text{tf}(\text{numD}, \text{denD})$ , then the discrete equivalent with sampling period  $T_s$  is given by

$$\text{sysDd} = \text{c2d}(\text{sysDc}, T_s, 't'). \quad (\text{W4.46})$$

In this expression, of course, the polynomials are represented in Matlab form. The last parameter in the `c2d` function given by 't' calls for the conversion to be done using Tustin's method. The alternatives can be found by asking Matlab for help `c2d`. For example, to compute the polynomials for  $T_s = 0.07$  sec for Example W4.4, the commands would be

```
numD = [1 6];
denD = [1 0];
sysDc = tf(numD, denD)
sysDd = c2d(sysDc, 0.07, 't')
```

# Appendix W4.6

## Sensitivity of Time Response to Parameter Change

We have considered the effects of errors on the steady-state gain of a dynamic system and showed how feedback control can reduce these errors. Since many control specifications are in terms of the step response, the sensitivity of the time response to parameter changes is sometimes very useful to explore. For example, by looking at the sensitivity plot, we can tell if increasing a particular parameter will increase or decrease the overshoot of the response.<sup>1</sup> The following analysis is also a good exercise in small-signal linearization.

To consider the sensitivity of the output  $y(t, \theta)$  of a system having a parameter of interest,  $\theta$ , we compute the effect of a perturbation in the parameter,  $\delta\theta$ , on the nominal response by using the Taylor's series expansion

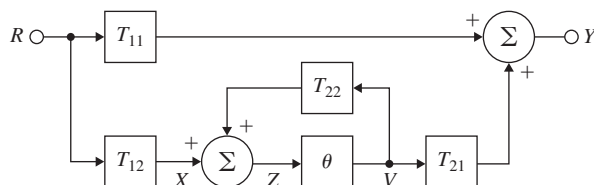
$$y(t, \theta + \delta\theta) = y(t, \theta) + \frac{\partial y}{\partial \theta} \delta\theta + \dots \quad (\text{W4.47})$$

The first-order approximation of the parameter perturbation effect is the term

$$\delta y(t) = \frac{\partial y}{\partial \theta} \delta\theta. \quad (\text{W4.48})$$

This function can be generated from the system itself as shown by Perkins et al., 1991. We assume the response depends linearly on the parameter, and therefore that the overall transfer function  $T(s, \theta)$  is composed of component transfer functions that can be defined to bring out the dependence on the parameter explicitly. A block diagram of the transfer function in terms of the components  $T_{ij}(s)$  can be expressed as shown in Fig. W4.7, where we have labeled the parameter as  $\theta$  and its

**Figure W4.7**  
Block diagram showing the dependence of output  $Y$  on parameter  $\theta$



<sup>1</sup>As we see in Chapter 5, the development of the Matlab root locus interface `rltool` gives the designer a computer aid to this result.

input signal as  $Z$ . In terms of this block diagram, the equations relating  $Y$  and  $Z$  to the reference input can be written immediately.

$$Y = T_{11}R + T_{21}\theta Z, \quad (\text{W4.49})$$

$$Z = T_{12}R + T_{22}\theta Z. \quad (\text{W4.50})$$

The perturbed equations are

$$Y + \delta Y = T_{11}R + T_{21}(\theta + \delta\theta)(Z + \delta Z), \quad (\text{W4.51})$$

$$Z + \delta Z = T_{12}R + T_{22}(\theta + \delta\theta)(Z + \delta Z). \quad (\text{W4.52})$$

Multiplying these out and ignoring the small term  $\delta\theta\delta Z$ , the expressions for the perturbations in  $Y$  and  $Z$  are given by

$$\delta Y = T_{21}(Z\delta\theta + \theta\delta Z), \quad (\text{W4.53})$$

$$\delta Z = T_{22}(Z\delta\theta + \theta\delta Z). \quad (\text{W4.54})$$

The solutions to these equations can be best presented as a block diagram, shown in Fig. W4.8a. The output of this figure is  $\frac{\partial y}{\partial \theta} \delta\theta$ ,

and we notice the input  $Z$  is multiplied by a gain of  $\delta\theta$ . Therefore, if we drop the block  $\delta\theta$ , the output will be simply  $\frac{\partial y}{\partial \theta}$  as shown in Fig. W4.8b.

Finally, to compute the sensitivity as the variation to a percent change  $\frac{\partial y(t, \theta)}{\partial \theta}$

in the parameter, which is  $\frac{\partial y}{\partial \ln \theta} = \frac{\frac{\partial \theta}{\partial \ln \theta}}{\frac{\partial y}{\partial \theta}} = \theta \frac{\partial y}{\partial \theta}$ , we need only shift

the input  $Z$  from the output side of the  $\theta$  block to its input, as shown in Fig. W4.8c. We are now in a position to give the final block diagram of the system as it is to be implemented, as shown in Fig. W4.9.

In this figure, it is clear that, to compute the sensitivity of the output to a parameter, one needs to simulate two copies of the system. The input to the first system is the reference input of interest, and the input to the second system is at the input to the parameter of interest of the variable  $Z$  taken from the input to the parameter in the original system. The transfer function from the reference input to the output sensitivity is readily computed to be

$$\frac{T_{12}\theta T_{21}}{(1 - \theta T_{22})^2}. \quad (\text{W4.55})$$

From this function, it is clear that:

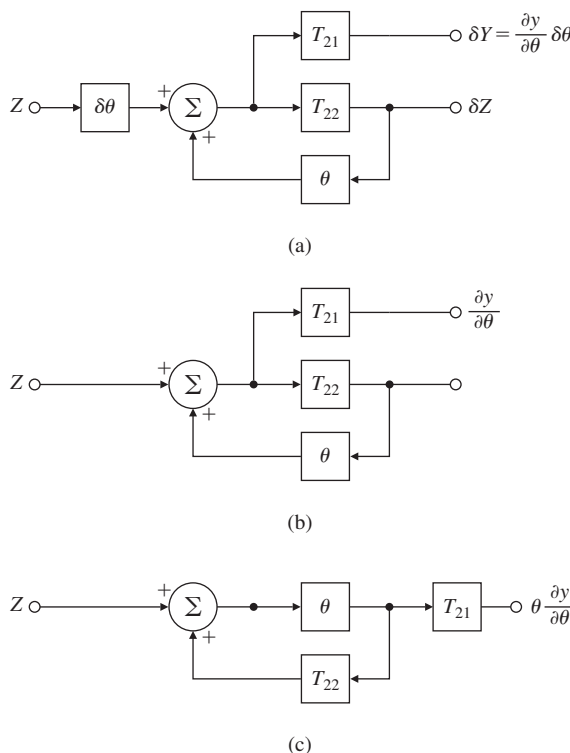
### Response sensitivity

To keep the sensitivity of the output signal to a parameter change low, it is important to have feedback with high gain around the parameter in question.

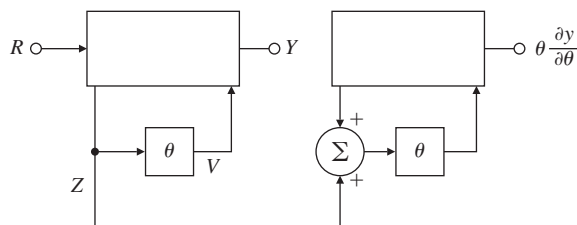
**Figure W4.8**

Block diagrams showing the generation of (a)  $\delta Y$  and  $\delta Z$ ; (b)  $\frac{\partial y}{\partial \theta}$ ; and (c)  $\theta \frac{\partial y}{\partial \theta}$

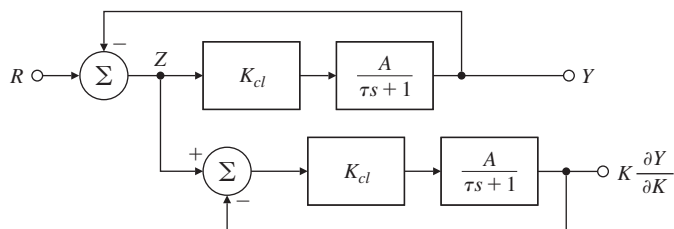
$$\theta \frac{\partial y}{\partial \theta}$$

**Figure W4.9**

Block diagram showing the computation of  $\theta \frac{\partial y}{\partial \theta}$  from the original transfer function

**Figure W4.10**

Block diagram showing the computation of the sensitivity of the output of the speed control example

**EXAMPLE W4.5**

### Time-Domain Sensitivity

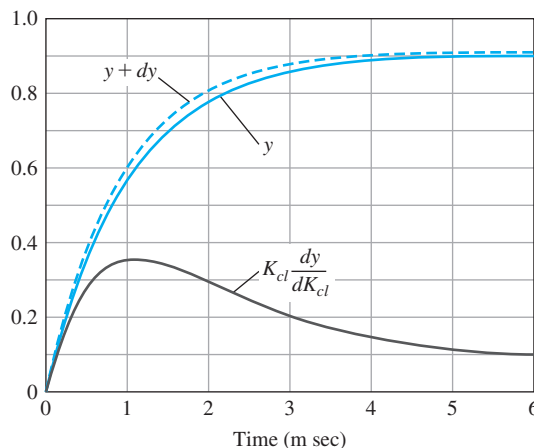
Compute the sensitivity of the output of the speed control example shown in the upper portion of Fig. W4.10 with respect to the control gain,  $K_{cl}$ . Take the nominal values to be  $K_{cl} = 9$ ,  $\tau = 0.01$  sec, and  $A = 1$  rad/volt-sec.

**Solution.** The required block diagram for the computation is given in Fig. W4.10 based on Fig. W4.9. In Matlab, we will construct the several transfer functions with  $T_{ij} = \frac{n_{ij}}{d_{ij}}$  and implement Eq. (W4.55). For comparison, we compute the nominal response from Fig. W4.7 and add 10% of the sensitivity to the nominal response. The instructions to do the computation in Matlab are

```
% script to compute sensitivity for Fig. W4.10
% First input the data for the component transfer functions Tij
% and the nominal parameter, Kcl for this problem
Kcl=9; tau=0.01;
n11=0; d11=1;
n12=1; d12=1;
n22=[0 -1]; d22= [tau 1];
n21=1; d21=[tau 1];
% Now compute the numerator and denominator polynomials of the
% transfer functions
% using the convolution function conv to multiply the polynomials
% and put them into system transfer function forms with the Matlab
% function tf.
% The over-all transfer function is
% Y/R =n11/d11 + (n12*n21*d22)/(d12*d21*[d22-Kcl*n22]) = sysy
% The transfer function from the reference input to the sensitivity is
% Kcl*(dy/dKcl)/R = sysdy
% Now define the numerators and denominators of several intermediate
% transfer functions
n1=Kcl*conv(n21,n12);
d1=conv(d21,d12);
n2=d22;
d2=[d22-Kcl*n22];
ny=conv(n1,n2);
dy=conv(d1,d2);
% Now put these together to form two intermediate transfer functions
sysy1 = tf(ny,dy);
sysy2 = tf(n11,d11);
% Now construct the final transfer functions
% The overall transfer function Y/R
sysy=sysy1+sysy2;
% The sensitivity transfer function
ndy=conv(ny,n2);
ddy=conv(dy,d2);
sysdy=tf(ndy,ddy);
% Now use these to compute the step responses and
% plot the output, the sensitivity and a perturbed response
[y,t]=step(sysy);
[yd,t]=step(sysdy);
plot(t,[y yd y+.1*yd]);
```

**Figure W4.11**

Plots of the output, the sensitivity, and the result of a 10% change in the parameter value for the speed control example



These instructions are constructed to compute the sensitivity for any system, given the several transfer functions. The script input is for the specific example. Plots of the output, its sensitivity, and the result of a 10% change in the parameter value are given in Fig. W4.11.

---

## Appendix W5.4.4

# Analog and Digital Implementations

Lead compensation can be physically realized in many ways. In analog electronics, a common method is to use an operational amplifier, an example of which is shown in Fig. W5.1. The transfer function of the circuit in Fig. W5.1 is readily found by the methods of Chapter 2 to be

$$D_{lead}(s) = -a \frac{s + z}{s + p}, \quad (\text{W5.1})$$

where

$$\begin{aligned} a &= \frac{p}{z}, \text{ if } R_f = R_1 + R_2, \\ z &= \frac{1}{R_1 C}, \\ p &= \frac{R_1 + R_2}{R_2} \cdot \frac{1}{R_1 C}. \end{aligned}$$

If a design for  $D_c(s)$  is complete and a digital implementation is desired, then the technique of Appendix W4.5 can be used by first selecting a sampling period  $T_s$  and then making substitution of  $\frac{2}{T_s} \frac{z-1}{z+1}$  for  $s$ .

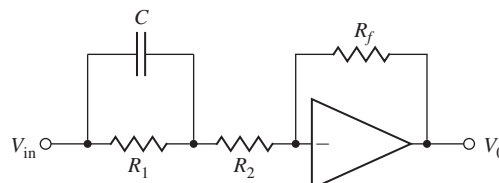
For example, consider the lead compensation  $D_c(s) = \frac{s+2}{s+13}$ . Then, since the rise time is about 0.3, a sampling period of six samples per rise time results in the selection of  $T_s = 0.05$  sec. With the substitution of  $\frac{2}{0.05} \frac{z-1}{z+1}$  for  $s$  into this transfer function, the discrete transfer function is

$$\begin{aligned} \frac{U(z)}{E(z)} &= \frac{40 \frac{z-1}{z+1} + 2}{40 \frac{z-1}{z+1} + 13} \\ &= \frac{1.55z - 1.4}{1.96z - 1}. \end{aligned} \quad (\text{W5.2})$$

Clearing fractions and using the fact that operating on the time functions  $zu(kT_s) = u(kT_s + T_s)$ , we see that Eq. (W5.2) is equivalent to the formula for the controller given by

**Figure W5.1**

Possible circuit of a lead compensation



$$u(kT_s + T_s) = \frac{1}{1.96}u(kT_s) + \frac{1.55}{1.96}e(kT_s + T_s) - \frac{1.4}{1.96}e(kT_s). \quad (\text{W5.3})$$

The Matlab commands to generate the discrete equivalent controller are

```
sysC=tf([1 2],[1 13]);
sysD=c2D(sysC,0.05,'tustin')
```

Fig. W5.2 shows the Simulink diagram for implementing the digital controller. The result of the simulation is contained in Fig. W5.3, which shows the comparison of analog and digital control outputs, and Fig. W5.4, which shows the analog and digital control outputs.

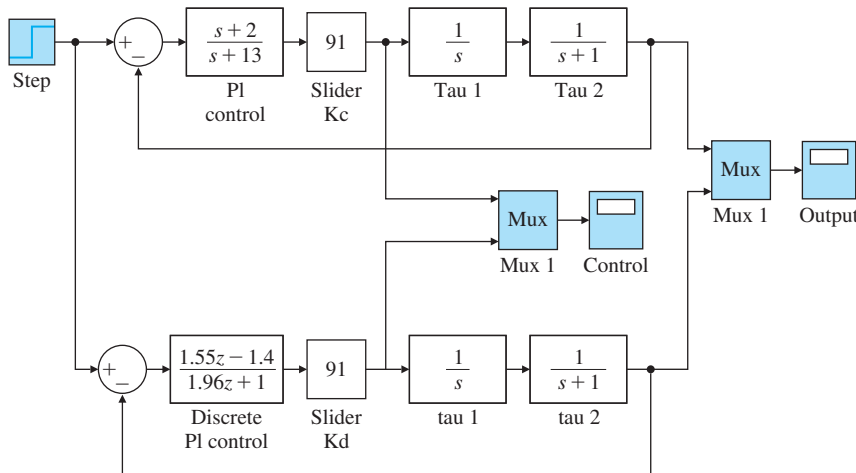


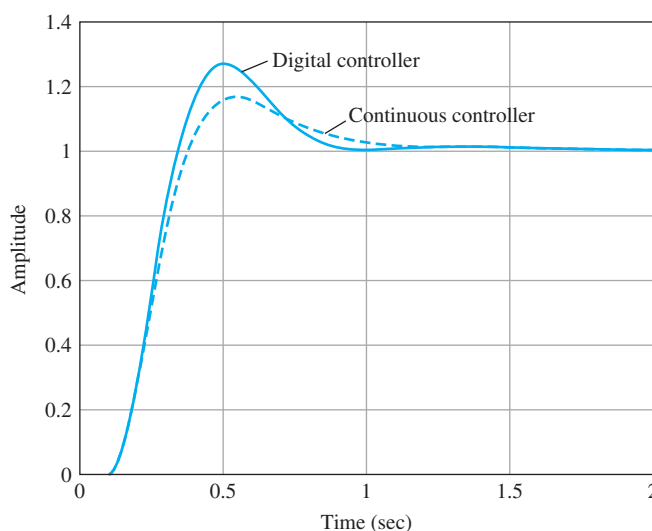
**Figure W5.2**

Simulink diagram for comparison of analog and digital control

Source: Reprinted with permission of The MathWorks, Inc.

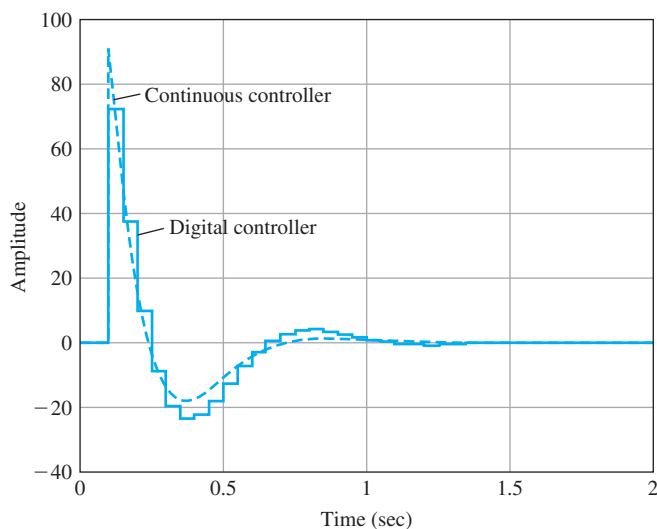
**Figure W5.3**

Comparison of analog and digital control output responses

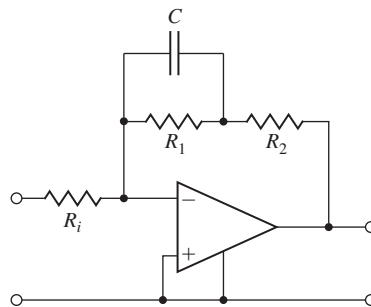


**Figure W5.4**

Comparison of analog and digital control time histories

**Figure W5.5**

Possible circuit of lag compensation



As with lead compensation, lag or notch compensation can be implemented using a digital computer and following the same procedure. However, they too can be implemented using analog electronics, and a circuit diagram of a lag network is given in Fig. W5.5. The transfer function of this circuit can be shown to be

$$D_c(s) = -a \frac{s + z}{s + p},$$

where

$$a = \frac{R_2}{R_i},$$

$$z = \frac{R_1 + R_2}{R_1 R_2 C},$$

$$p = \frac{1}{R_1 C}.$$

Usually  $R_i = R_2$ , so the high-frequency gain is unity, or  $a = 1$ , and the low-frequency increase in gain to enhance  $K_v$  or other error constant is set by  $k = a_p^z = \frac{R_1 + R_2}{R_2}$ .

## Appendix W5.6.3

# Root Locus with Time Delay

Time delays always reduce the stability of a system

An example of a root locus with time delay

Time delays often arise in control systems, both from delays in the process itself and from delays in the processing of sensed signals. Chemical plants often have processes with a time delay representing the time material takes to be transported via pipes or other conveyer. In measuring the attitude of a spacecraft en route to Mars, there is a significant time delay for the sensed quantity to arrive back on Earth due to the speed of light. There is also a small time delay in any digital control system due to the cycle time of the computer and the fact that data is processed at discrete intervals. Time delay *always* reduces the stability of a system; therefore, it is important to be able to analyze its effect. In this section, we will discuss how to use the root locus for such analysis. Although an exact method of analyzing time delay is available in the frequency-response methods described in Chapter 6, knowing several different ways to analyze a design provides the control designer with more flexibility and an ability to check the candidate solutions.

Consider the problem of designing a control system for the temperature of the heat exchanger described in Chapter 2. The transfer function between the control  $A_s$  and the measured output temperature  $T_m$  is described by two first-order terms plus a time delay  $T_d$  of 5 sec. The time delay results because the temperature sensor is physically located downstream from the exchanger, so there is a delay in its reading. The transfer function is

$$G(s) = \frac{e^{-5s}}{(10s + 1)(60s + 1)}, \quad (\text{W5.4})$$

where the  $e^{-5s}$  term arises from the time delay.<sup>1</sup>

The corresponding root-locus equations with respect to proportional gain  $K$  are

$$\begin{aligned} 1 + KG(s) &= 0, \\ 1 + K \frac{e^{-5s}}{(10s + 1)(60s + 1)} &= 0, \\ 600s^2 + 70s + 1 + Ke^{-5s} &= 0. \end{aligned} \quad (\text{W5.5})$$

How would we plot the root locus corresponding to Eq. (W5.5)? Since it is not a polynomial, we cannot proceed with the methods used in previous examples. So we reduce the given problem to one we have previously

<sup>1</sup>Time delay is often referred to as “transportation lag” in the process industries.

**Padé approximant**

solved by approximating the nonrational function  $e^{-5s}$  with a rational function. Since we are concerned with control systems, and hence typically with low frequencies, we want an approximation that will be good for small  $s$ .<sup>2</sup> The most common means for finding such an approximation is attributed to H. Padé. It consists of matching the series expansion of the transcendental function  $e^{-5s}$  with the series expansion of a rational function whose numerator is a polynomial of degree  $p$  and whose denominator is a polynomial of degree  $q$ . The result is called a  $(p, q)$  Padé approximant<sup>3</sup> to  $e^{-5s}$ . We will initially compute the approximants to  $e^{-s}$ , and in the final result, we will substitute  $T_{ds}$  for  $s$  to allow for any desired delay.

The resulting  $(1, 1)$  Padé approximant ( $p = q = 1$ ) is

$$e^{-T_{ds}} \approx \frac{1 - (T_{ds}/2)}{1 + (T_{ds}/2)}. \quad (\text{W5.6})$$

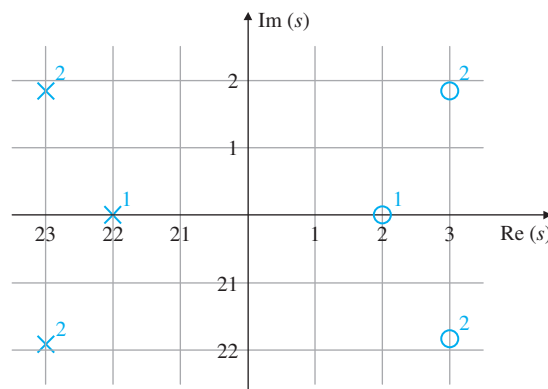
If we assume  $p = q = 2$ , we have five parameters and a better match is possible. In this case, we have the  $(2, 2)$  approximant, which has the transfer function

$$e^{-T_{ds}} \approx \frac{1 - T_{ds}/2 + (T_{ds})^2/12}{1 + T_{ds}/2 + (T_{ds})^2/12}. \quad (\text{W5.7})$$

The comparison of these approximants can be seen from their pole–zero configurations as plotted in Fig. W5.6. The locations of the poles are in the LHP and the zeros are in the RHP at the reflections of the poles.

**Figure W5.6**

Poles and zeros of the Padé approximants to  $e^{-s}$ , with superscripts identifying the corresponding approximants; for example,  $x^1$  represents the  $(1,1)$  approximant



<sup>2</sup>The nonrational function  $e^{-5s}$  is analytic for all finite values of  $s$  and so may be approximated by a rational function. If nonanalytic functions such as  $\sqrt{s}$  were involved, great caution would be needed in selecting an approximation that is valid near  $s = 0$ .

<sup>3</sup>The  $(p, p)$  Padé approximant for a delay of  $T$  sec is most commonly used and is computed by the Matlab command `[num,den] = pade(T, P)`.

In some cases, a very crude approximation is acceptable. For small delays, the  $(0, 1)$  approximant can be used, which is simply a first-order lag given by

$$e^{-T_d s} \cong \frac{1}{1 + T_d s}. \quad (\text{W5.8})$$

### Contrasting methods of approximating delay

To illustrate the effect of a delay and the accuracy of the different approximations, root loci for the heat exchanger are drawn in Fig. W5.7 for four cases. Notice for low gains and up to the point where the loci cross the imaginary axis, the approximate curves are very close to exact. However, the  $(2, 2)$  Padé curve follows the exact curve much further than does the first-order lag, and its increased accuracy would be useful if the delay were larger. All analyses of the delay show its destabilizing effect and how it limits the achievable response time of the system.

While the Padé approximation leads to a rational transfer function, in theory, it is not necessary for plotting a root locus. A direct application of the phase condition can be used to plot portions of an exact locus of a system with time delay. The phase-angle condition does not change if the transfer function of the process is nonrational, so we still must search for values of  $s$  for which the phase is  $180^\circ + 360^\circ l$ . If we write the transfer function as

$$G(s) = e^{-T_d s} \bar{G}(s),$$

the phase of  $G(s)$  is the phase of  $\bar{G}(s)$  minus  $T_d \omega$  for  $s = \sigma + j\omega$ . Thus we can formulate a root-locus problem as searching for locations where the phase of  $\bar{G}(s)$  is  $180^\circ + T_d \omega + 360^\circ(l-1)$ . To plot such a locus, we would fix  $\omega$  and search along a horizontal line in the  $s$ -plane until we found a point on the locus, then raise the value of  $\omega$ , change the target angle, and repeat. Similarly, the departure angles are modified by  $T_d \omega$ , where  $\omega$  is the imaginary part of the pole from which the departure is being

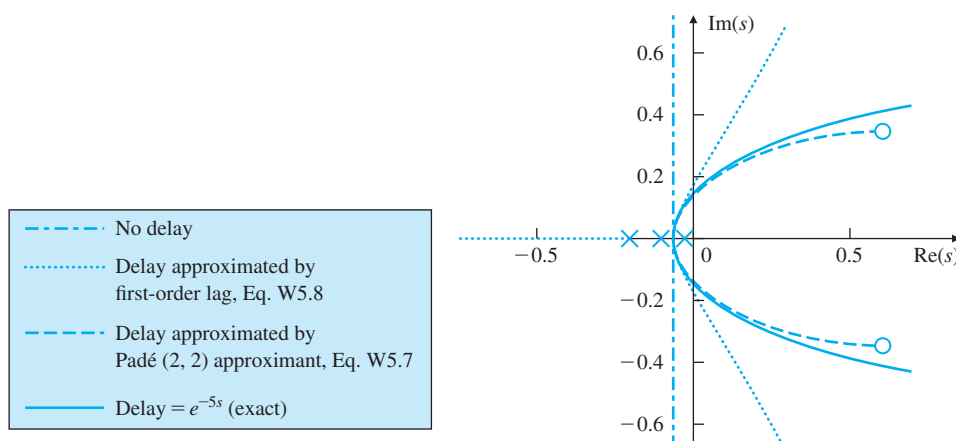


**Figure W5.7**

Root loci for the heat exchanger with and without time delay

## **84** Appendix W5.6.3 Root Locus with Time Delay

computed. Matlab does not provide a program to plot the root locus of systems with delay, so we must be satisfied here with Padé approximants. Since it is possible to plot the frequency response (or Bode plot) of delay exactly and easily, if the designer feels that the Padé approximant is not satisfactory, the expedient approach is to use the frequency-response design methods described in Chapter 6.

# Appendix W6.7.2

## Digital Implementation of Example 6.15

### EXAMPLE W6.1

#### *Lead Compensation for a DC Motor*

As an example of designing a lead compensator, let us repeat the design of compensation for the DC motor with the transfer function

$$G(s) = \frac{1}{s(s+1)},$$

that was carried out in Section 5.4.1. This also represents the model of a satellite-tracking antenna (see Fig. 3.60). This time we wish to obtain a steady-state error of less than 0.1 for a unit-ramp input. Furthermore, we desire an overshoot of  $M_p < 25\%$ .

1. Determine the lead compensation satisfying the specifications.
2. Determine the digital version of the compensation with  $T_s = 0.05$  sec.
3. Compare the step and ramp responses of both implementations.

#### Solution.

1. The steady-state error is given by

$$e_{ss} = \lim_{s \rightarrow 0} s \left[ \frac{D_c}{1 + KD_c(s)G(s)} \right] R(s), \quad (\text{W6.1})$$

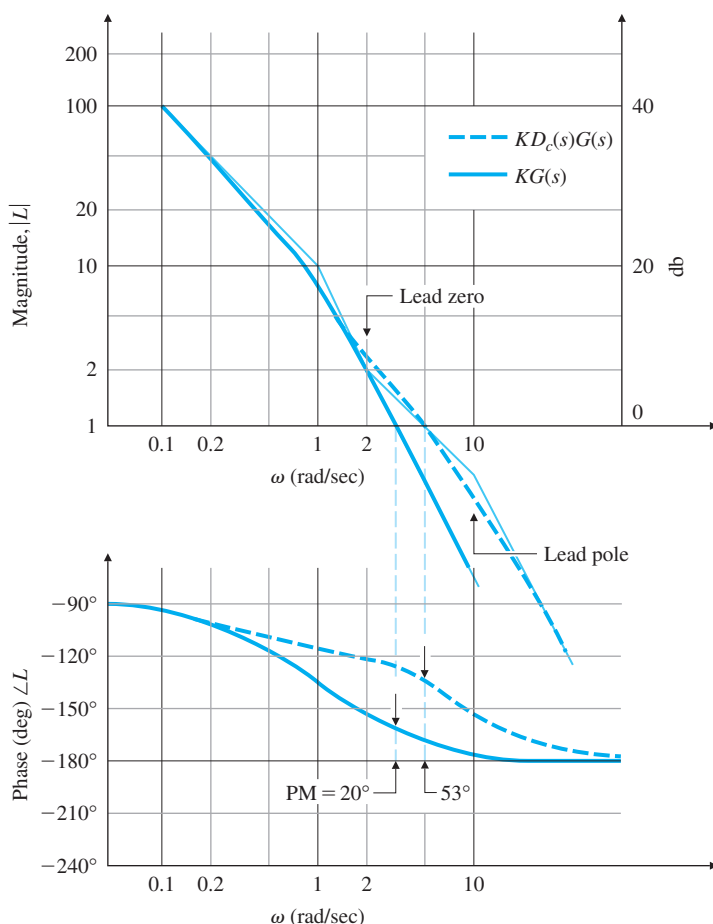
where  $R(s) = 1/s^2$  for a unit ramp, so Eq. (W6.1) reduces to

$$e_{ss} = \lim_{s \rightarrow 0} \left\{ \frac{1}{s + KD_c(s)[1/(s+1)]} \right\} = \frac{1}{KD_c(0)}.$$

Therefore, we find that  $KD_c(0)$ , which is the steady-state gain of the compensation, cannot be less than 10 ( $K_v \geq 10$ ) if it is to meet the error criterion, so we pick  $K = 10$ . To relate the overshoot requirement to PM, Fig. 6.37 shows that a PM of  $45^\circ$  should suffice. The frequency response of  $KG(s)$  in Fig. W6.1 shows that the PM =  $20^\circ$  if no phase lead is added by compensation. If it were possible to simply add phase without affecting the magnitude, we would need an additional phase of only  $25^\circ$  at the  $KG(s)$  crossover frequency of  $\omega = 3$  rad/sec. However, maintaining the same low-frequency gain and adding a compensator zero would

**Figure W6.1**

Frequency response for lead-compensation design



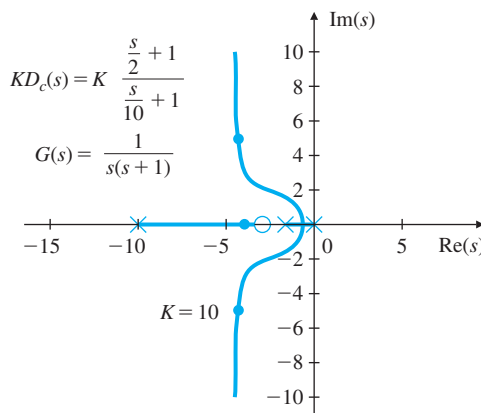
increase the crossover frequency; hence, more than a  $25^\circ$  phase contribution will be required from the lead compensation. To be safe, we will design the lead compensator so that it supplies a maximum phase lead of  $40^\circ$ . Fig. 6.53 shows  $1/\alpha = 5$  will accomplish that goal. We will derive the greatest benefit from the compensation if the maximum phase lead from the compensator occurs at the crossover frequency. With some trial and error, we determine that placing the zero at  $\omega = 2$  rad/sec and the pole at  $\omega = 10$  rad/sec causes the maximum phase lead to be at the crossover frequency. The compensation, therefore, is

$$KD_c(s) = 10 \frac{s/2 + 1}{s/10 + 1}.$$

The frequency-response characteristics of  $L(s) = KD_c(s)G(s)$  in Fig. W6.1 can be seen to yield a PM of  $53^\circ$ , which satisfies the design goals.

**Figure W6.2**

Root locus for lead-compensation design



The root locus for this design, originally given as Fig. 5.24, is repeated here as Fig. W6.2, with the root locations marked for  $K = 10$ . The locus is not needed for the frequency-response design procedure; it is presented here only for comparison with the root locus design method presented in Chapter 5. The entire process can be expedited by the use of Matlab's sisotool design tool, which simultaneously provides the root locus and the Bode plot through an interactive GUI interface. For this example, the Matlab statements

```
G=tf(1,[1 1 0]);
Dc=tf(10*[1/2 1],[1/10 1]);
sisotool(G,Dc)
```

will provide the plots as shown in Fig. W6.3. It also can be used to generate the Nyquist and time-response plots if desired.

2. To find the discrete equivalent of  $D_c(s)$ , we use the trapezoidal rule given by Eq. (W4.31). That is,

$$D_d(z) = \frac{\frac{2}{T_s} \frac{z-1}{z+1}/2 + 1}{\frac{2}{T_s} \frac{z-1}{z+1}/10 + 1}, \quad (\text{W6.2})$$

which, with  $T_s = 0.05$  sec, reduces to

$$D_d(z) = \frac{4.2z - 3.8}{z - 0.6}. \quad (\text{W6.3})$$

This same result can be obtained by the Matlab statements

```
sysDc = tf([0.5 1],[0.1 1]);
sysDd = c2d(sysDc, 0.05, 'tustin').
```

Because

$$\frac{U(z)}{E(z)} = KD_d(z), \quad (\text{W6.4})$$

the discrete control equation that results is

$$u(k+1) = 0.6u(k) + 10(4.2e(k+1) - 3.8e(k)). \quad (\text{W6.5})$$

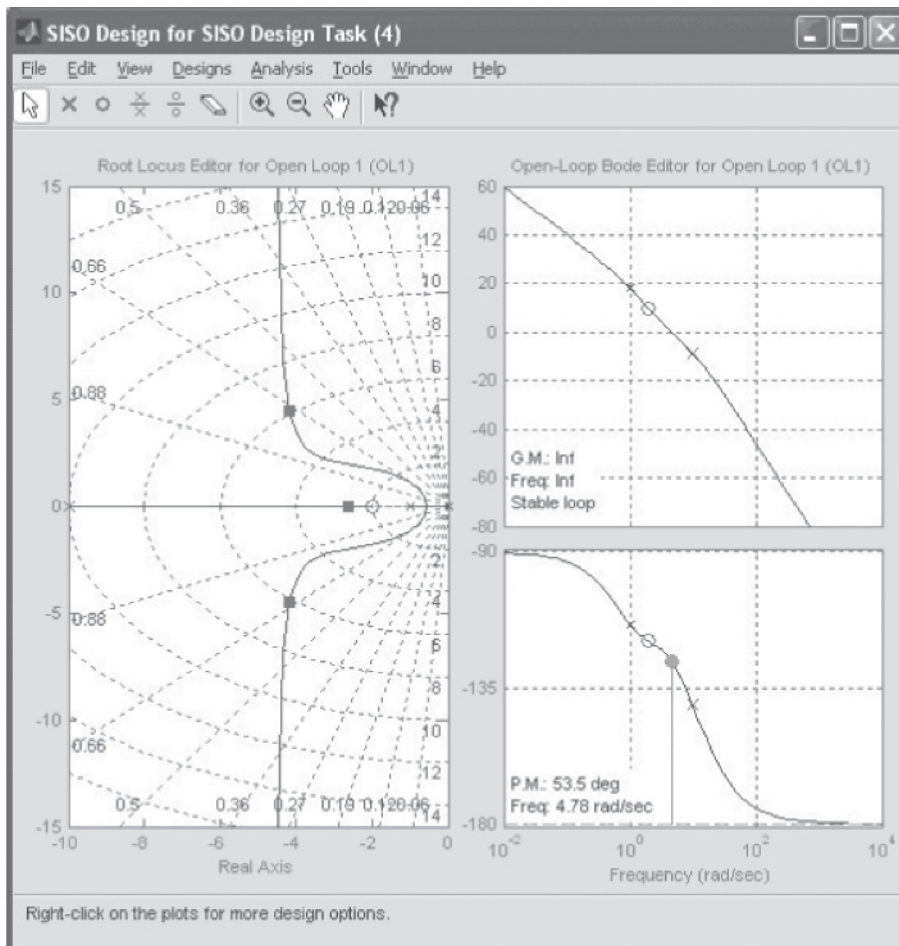


**Figure W6.3**

SISOTOOL graphical interface for Example W6.1

Source: Reprinted with permission of The MathWorks, Inc.

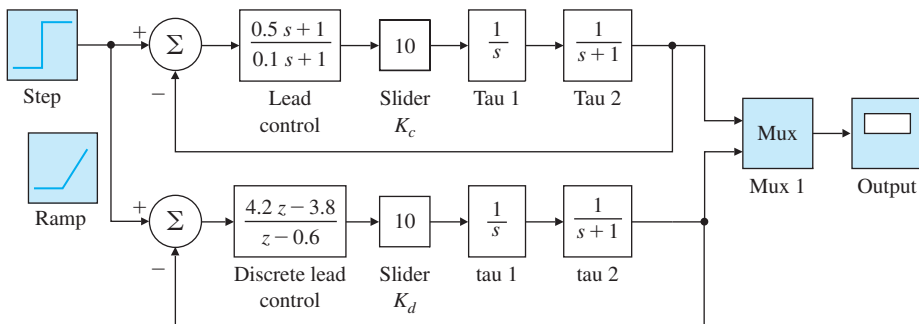


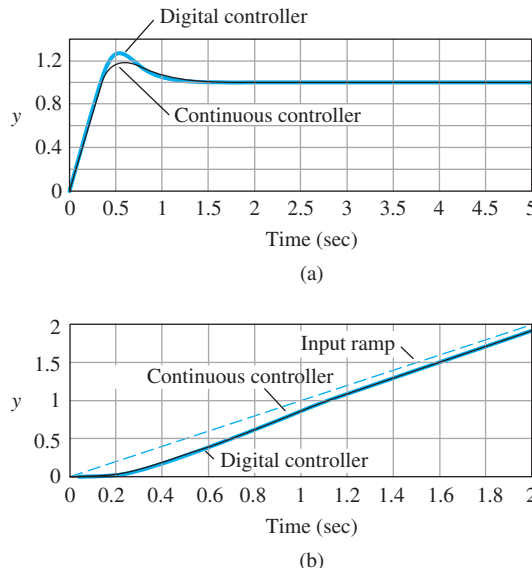
**Figure W6.4**

Simulink block diagram for transient response of lead-compensation design

Source: Reprinted with permission of The MathWorks, Inc.

**Figure W6.5**

Lead-compensation design: (a) step response; (b) ramp response



3. The Simulink block diagram of the continuous and discrete versions of  $D_c(s)$  controlling the DC motor is shown in Fig. W6.4. The step responses of the two controllers are plotted together in Fig. W6.5a and are reasonably close to one another; however, the discrete controller does exhibit slightly increased overshoot, as is often the case. Both overshoots are less than 25%, and thus meet the specifications. The ramp responses of the two controllers, shown in Fig. W6.5b, are essentially identical, and both meet the 0.1 specified error.

# Appendix W6.8.1

## Time Delay via the Nyquist Diagram

### EXAMPLE W6.2

#### Nyquist Plot for a System with Time Delay

Consider the system with

$$KG(s) = \frac{Ke^{-T_d s}}{s},$$

where  $T_d = 1$  sec. Determine the range of  $K$  for which the system is stable.

**Solution.** Because the Bode plotting rules do not apply for the phase of a time-delay term, we will use an analytical approach to determine the key features of the frequency response plot. As just discussed, the magnitude of the frequency response of the delay term is unity, and its phase is  $-\omega$  radians. The magnitude of the frequency response of the pure integrator is  $1/\omega$  with a constant phase of  $-\pi/2$ . Therefore,

$$\begin{aligned} G(j\omega) &= \frac{1}{\omega} e^{-j(\omega + \pi/2)} \\ &= \frac{1}{\omega} (-\sin \omega - j \cos \omega). \end{aligned} \quad (\text{W6.6})$$

Using Eq. (W6.6) and substituting in different values of  $\omega$ , we can generate the Nyquist plot, which is the spiral shown in Fig. W6.6.

Let us examine the shape of the spiral in more detail. We pick a Nyquist path with a small detour to the right of the origin. The effect of the pole at the origin is the large arc at infinity with a  $180^\circ$  sweep, as shown in Fig. W6.6. From Eq. (W6.6), for small values of  $\omega > 0$ , the real part of the frequency response is close to  $-1$  because  $\sin \omega \cong \omega$  and  $\text{Re}[G(j\omega)] \cong -1$ . Similarly, for small values of  $\omega > 0$ ,  $\cos \omega \cong 1$  and  $\text{Im}[G(j\omega)] \cong -1/\omega$ —that is, very large negative values, as shown in Fig. W6.6. To obtain the crossover points on the real axis, we set the imaginary part equal to zero:

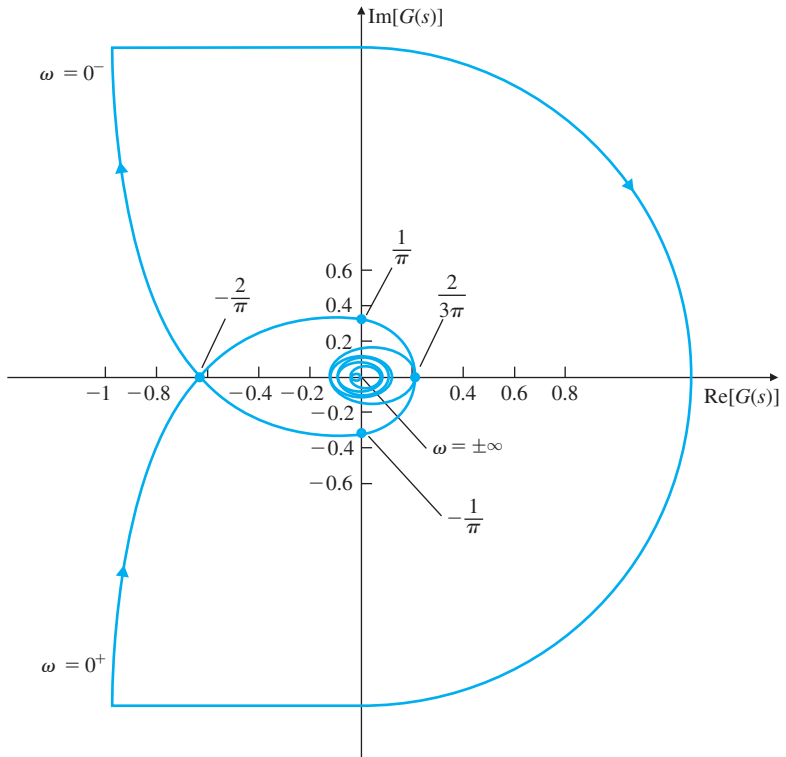
$$\frac{\cos \omega}{\omega} = 0. \quad (\text{W6.7})$$

The solution is then

$$\omega_0 = \frac{(2n+1)\pi}{2}, \quad n = 0, 1, 2, \dots \quad (\text{W6.8})$$

**Figure W6.6**

Nyquist plot for Example W6.2



After substituting Eq. (W6.8) back into Eq. (W6.6), we find that

$$G(j\omega_0) = \frac{(-1)^n}{(2n+1)} \left( \frac{2}{\pi} \right), \quad n = 0, 1, 2, \dots$$

So the first crossover of the negative real axis is at  $-2/\pi$ , corresponding to  $n = 0$ . The first crossover of the positive real axis occurs for  $n = 1$  and is located at  $2/3\pi$ . As we can infer from Fig. W6.6, there are an infinite number of other crossings of the real axis. Finally, for  $\omega = \infty$ , the Nyquist plot converges to the origin. Note that the Nyquist plot for  $\omega < 0$  is the mirror image of the one for  $\omega > 0$ .

The number of poles in the RHP is zero ( $P = 0$ ), so for closed-loop stability, we need  $Z = N = 0$ . Therefore, the Nyquist plot cannot be allowed to encircle the  $-1/K$  point. It will not do so as long as

$$-\frac{1}{K} < -\frac{2}{\pi}, \quad (\text{W6.9})$$

which means that, for stability, we must have  $0 < K < \pi/2$ .

## Appendix W6.9.2

# The Inverse Nyquist Diagram

The **inverse Nyquist plot** is simply the reciprocal of the Nyquist plot described in Section 6.3 and used in Section 6.4 for the definition and discussion of stability margins. It is obtained most easily by computing the inverse of the magnitude from the Bode plot and plotting that quantity at an angle in the complex plane, as indicated by the phase from the Bode plot. It can be used to find the PM and GM in the same way that the Nyquist plot was used. When  $|G(j\omega)| = 1$ ,  $|G^{-1}(j\omega)| = 1$  also, so the definition of PM is identical on the two plots. However, when the phase is  $-180^\circ$  or  $+180^\circ$ , the value of  $|G^{-1}(j\omega)|$  is the GM directly; no calculation of an inverse is required, as was the case for the Nyquist plot.

The inverse Nyquist plot for the system in Fig. 6.24 (see Example 6.9) is shown in Fig. W6.7 for the case where  $K = 1$  and the system is stable. Note  $GM = 2$  and  $PM \cong 20^\circ$ . As an example of a more complex case, Fig. W6.8 shows an inverse Nyquist plot for the sixth-order case whose Nyquist plot was shown in Fig. 6.41, and whose Nichols chart was shown in Fig. 6.83. Note here  $GM = 1.2$  and  $PM \cong 35^\circ$ . Had the two crossings of the unit circle not occurred at the same point, the crossing with the smallest PM would have been the appropriate one to use.

**Figure W6.7**

Inverse Nyquist plot for Example 6.9

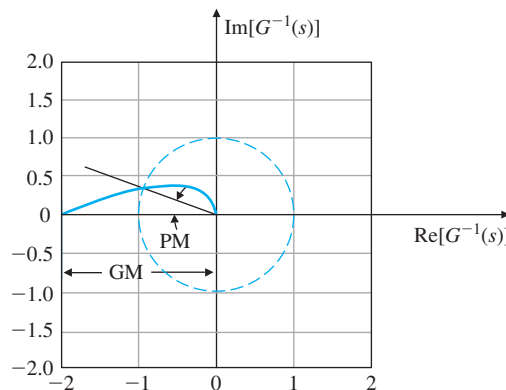
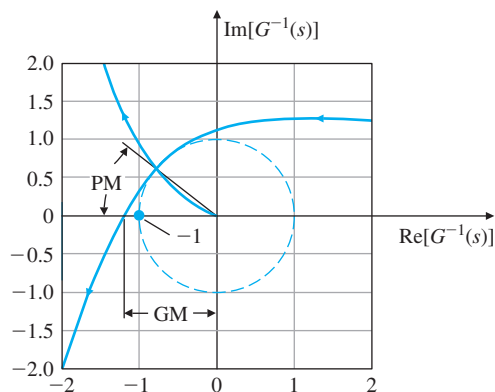


**Figure W6.8**

Inverse Nyquist plot of the system whose Nyquist plot is in Fig. 6.41



# Appendix W7.8

## Digital Implementation of Example 7.31

### EXAMPLE W7.1

#### *Redesign of the DC Servo Compensator*

For Example 7.31, derive an equivalent discrete controller with a sampling period of  $T_s = 0.1$  sec (10 times the fastest pole), and compare the continuous and digital control outputs and control efforts. Verify the design by plotting the step response and commenting on the comparison of the continuous and discrete responses.

**Solution.** The discrete equivalent for the controller is obtained from Matlab with the c2d command, as in

```
nc=94.5*conv([1 7.98],[1 2.52]); % form controller numerator
dc=conv([1 8.56 59.5348],[1 10.6]); % form controller denominator
sysDc=tf(nc,dc); % form controller system description
ts=0.1;% sampling time of 0.1 sec
sysDd=c2d(sysDc,ts,'zoh'); % convert controller to discrete time
```

#### Discrete controller

The resulting controller has the discrete transfer function

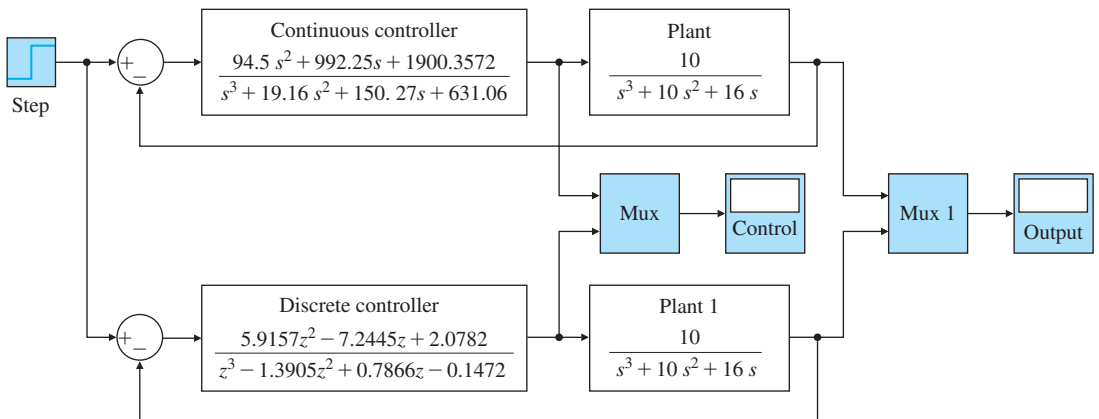
$$D_d(z) = \frac{5.9157(z + 0.766)(z + 0.4586)}{(z - 0.522 \pm 0.3903j)(z + 0.3465)}.$$

The equation for the control law (with the sample period suppressed for clarity) is

$$\begin{aligned} u(k+1) = & 1.3905u(k) - 0.7866u(k-1) + 0.1472u(k-2) \\ & + e(k) - 7.2445e(k-2) + 2.0782e(k-2). \end{aligned}$$

#### Simulink simulation

A Simulink diagram for simulating both the continuous and discrete systems is shown in Fig. W7.1. A comparison of the continuous and discrete step responses and control signals is shown in Fig. W7.2. Better agreement between the two responses can be obtained if the sampling period is reduced.

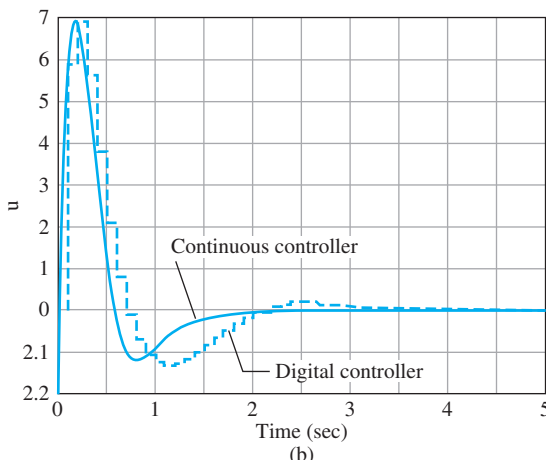
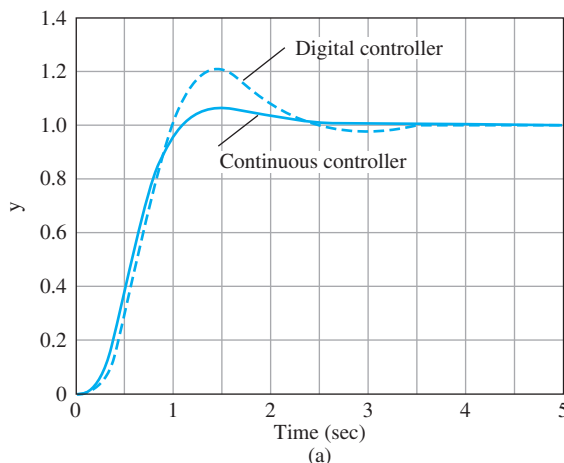
**Figure W7.1**

Simulink block diagram to compare continuous and discrete controllers

*Source: Reprinted with permission of The MathWorks, Inc.*

**Figure W7.2**

Comparison of step responses and control signals for continuous and discrete controllers: (a) step responses; (b) control signals



# Appendix W7.9

## Digital Implementation of Example 7.33

### EXAMPLE W7.2

#### *Servomechanism*

For Example 7.33, derive an equivalent discrete controller with a sampling period of  $T_s = 0.1$  sec ( $20 \times \omega_n = 20 \times 0.05 = 0.1$  sec), and compare the continuous and digital control outputs, as well as the control efforts. Verify the design by plotting the step response and commenting on the comparison of the continuous and discrete responses.

Matlab c2d

**Solution.** The discrete equivalent for the controller is obtained from Matlab by using the c2d command, as in

```
nc=conv([1 1],[8.32 0.8]); % controller numerator
dc=conv([1 4.08],[1 0.0196]); % controller denominator
sysDc=tf(nc,dc); % form controller system description
ts=0.1; % sampling time of 0.1 sec
sysDd=c2d(sysDc,ts,'zoh'); % convert to discrete time controller
```

The discrete controller has the discrete transfer function

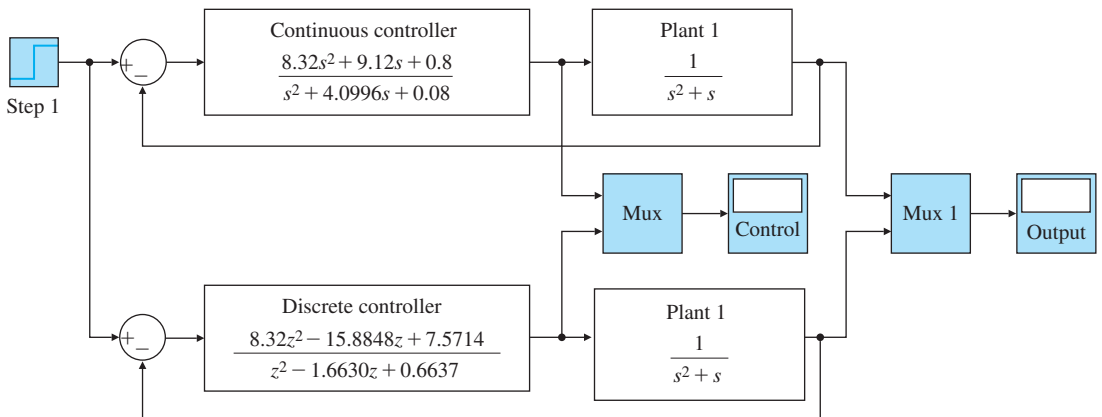
$$D_d(z) = \frac{8.32z^2 - 15.8855z + 7.5721}{z^2 - 1.6630z + 0.6637} = \frac{8.32(z - 0.9903)(z - 0.9191)}{(z - 0.998)(z - 0.6665)}.$$

The equation for the control law (with sample period suppressed for clarity) is

$$\begin{aligned} u(k+1) = & 1.6630u(k) + 0.6637u(k-1) + 8.32e(k+1) \\ & - 15.8855e(k) + 7.5721e(k-1). \end{aligned}$$

Simulink simulation

A Simulink diagram for simulating both the continuous and discrete systems is shown in Fig. W7.3. A comparison of the continuous and discrete step responses and control signals is shown in Fig. W7.4. Better agreement between the two responses was achieved because the sample rate was 20 times the bandwidth for this example.

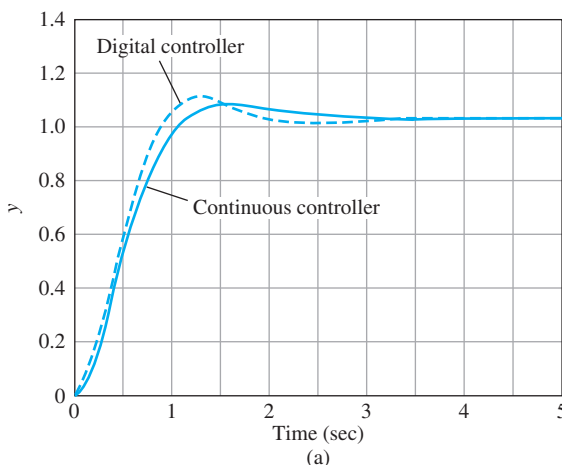
**Figure W7.3**

Simulink block diagram to compare continuous and discrete controllers

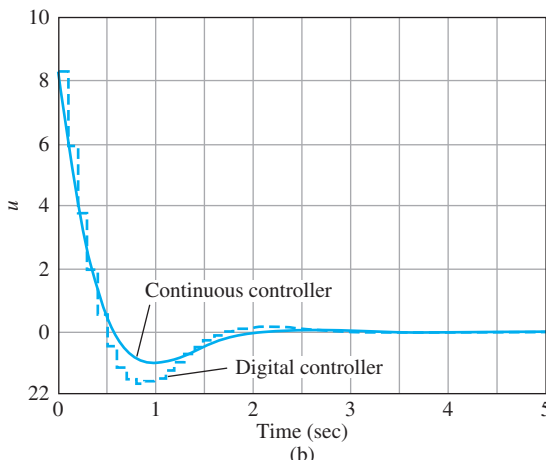
*Source: Reprinted with permission of The MathWorks, Inc.*

**Figure W7.4**

Comparison of step responses and control signals for continuous and discrete controllers: (a) step responses; (b) control signals



(a)



(b)

# Appendix W7.14

## Solution of State Equations

In this section, we consider the solution of state variable equations. This material is not necessary to understand the design of pole placement but will give a deeper insight into the method of state variables. It is instructive to consider first the unforced, or *homogenous*, system, which has the form

$$\dot{\mathbf{x}} = \mathbf{A}(t)\mathbf{x}, \quad \mathbf{x}(0) = \mathbf{x}_0. \quad (\text{W7.1})$$

If the elements of  $\mathbf{A}(t)$  are continuous functions of time, then the above equation has a *unique* solution for any initial state vector  $\mathbf{x}_0$ . There is a useful representation for the solution of this equation in terms of a matrix, called the *transition matrix*. Let  $\phi_i(t, t_0)$  be the solution to the special initial condition

$$\mathbf{x}(0) = \mathbf{e}_i = \begin{bmatrix} 0 \\ 0 \\ 1 \\ 0 \\ \vdots \\ 0 \end{bmatrix}. \quad \leftarrow i\text{th row} \quad (\text{W7.2})$$

If  $\mathbf{x}(t_0)$  is the actual initial condition at  $t_0$ , then we can express it in the decomposed form

$$\mathbf{x}(t_0) = \mathbf{x}_{01}\mathbf{e}_1 + \mathbf{x}_{02}\mathbf{e}_2 + \cdots + \mathbf{x}_{0n}\mathbf{e}_n. \quad (\text{W7.3})$$

Because Eq. (W7.1) is linear, the state  $\mathbf{x}(t)$  also can be expressed as a sum of the solutions to the special initial condition  $\phi_i$ , as

$$\mathbf{x}(t) = \mathbf{x}_{01}\phi_1(t, t_0) + \mathbf{x}_{02}\phi_2(t, t_0) + \cdots + \mathbf{x}_{0n}\phi_n(t, t_0), \quad (\text{W7.4})$$

or in matrix notation, as

$$\mathbf{x}(t) = [\phi_1(t, t_0), \phi_2(t, t_0), \dots, \phi_n(t, t_0)] \begin{bmatrix} \mathbf{x}_{01} \\ \mathbf{x}_{02} \\ \vdots \\ \mathbf{x}_{0n} \end{bmatrix}. \quad (\text{W7.5})$$

So we can define the *transition matrix*<sup>1</sup> to be

$$\Phi(t, t_0) = [\phi_1(t, t_0), \phi_2(t, t_0), \dots, \phi_n(t, t_0)], \quad (\text{W7.6})$$

---

<sup>1</sup>This is also referred to as the *fundamental matrix* of the differential equation.

and write the solution as

$$\mathbf{x}(t) = \Phi(t, t_0)\mathbf{x}(t_0), \quad (\text{W7.7})$$

where as the name implies, the transition matrix provides the transition between the state at time  $t_0$  to the state at time  $t$ . Furthermore, from Eq. (W7.7), we have

$$\frac{d}{dt}[\mathbf{x}(t)] = \frac{d}{dt}[\Phi(t, t_0)]\mathbf{x}(t_0), \quad (\text{W7.8})$$

and from Eqs. (W7.1) and (W7.8), we have

$$\frac{d}{dt}\mathbf{x}(t) = \mathbf{A}\mathbf{x}(t) = \mathbf{A}\Phi(t, t_0)\mathbf{x}(t_0). \quad (\text{W7.9})$$

Therefore

$$\frac{d}{dt}[\Phi(t, t_0)] = \mathbf{A}\Phi(t, t_0), \quad (\text{W7.10})$$

and also

$$\Phi(t, t) = \mathbf{I}. \quad (\text{W7.11})$$

The transition matrix can be shown to have many interesting properties. Among them are the following:

$$1. \Phi(t_2, t_0) = \Phi(t_2, t_1)\Phi(t_1, t_0); \quad (\text{W7.12})$$

$$2. \Phi^{-1}(t, \tau) = \Phi(\tau, t); \quad (\text{W7.13})$$

$$3. \frac{d}{dt}\Phi(t, \tau) = -\Phi(t, \tau)\mathbf{A}(\tau); \quad (\text{W7.14})$$

$$4. \det \Phi(t, t_0) = e^{\int_{t_0}^t \text{trace A}(\tau)d\tau}. \quad (\text{W7.15})$$

The second property implies that  $\Phi(t, \tau)$  is always invertible. What this means is that the solution is always unique so, given a particular value of state at time  $\tau$ , we can not only compute the future states from  $\Phi(t, \tau)$  but also past values  $\Phi^{-1}(t, \tau)$ .

For the inhomogenous case, with a forcing function input  $u(t)$ , the equation is

$$\dot{\mathbf{x}}(t) = \mathbf{A}(t)\mathbf{x}(t) + \mathbf{B}(t)u(t), \quad (\text{W7.16})$$

and the solution is

$$\mathbf{x}(t) = \Phi(t, t_0)\mathbf{x}_0 + \int_{t_0}^t \Phi(t, \tau)\mathbf{B}(\tau)u(\tau)d\tau. \quad (\text{W7.17})$$

We can verify this by substituting the supposed solution, Eq. (W7.17), into the differential equation, Eq. (W7.16), as

$$\frac{d}{dt}\mathbf{x}(t) = \frac{d}{dt}\Phi(t, t_0)\mathbf{x}_0 + \frac{d}{dt} \int_{t_0}^t \Phi(t, \tau)\mathbf{B}(\tau)u(\tau)d\tau. \quad (\text{W7.18})$$

The second term from calculus (using the Leibnitz formula) is

$$\frac{d}{dt} \int_{t_0}^t \Phi(t, \tau) \mathbf{B}(\tau) u(\tau) d\tau = \int_{t_0}^t \mathbf{A}(t) \Phi(t, \tau) \mathbf{B}(\tau) u(\tau) d\tau + \Phi(t, t) \mathbf{B}(t) u(t). \quad (\text{W7.19})$$

Using the basic relations, we have

$$\begin{aligned} \frac{d}{dt} \mathbf{x}(t) &= \mathbf{A}(t) \Phi(t, t_0) \mathbf{x}_0 + \mathbf{A}(t) \int_{t_0}^t \Phi(t, \tau) \mathbf{B}(\tau) u(\tau) d\tau \\ &\quad + \mathbf{B}(t) u(t), \end{aligned} \quad (\text{W7.20})$$

$$= \mathbf{A}(t) \mathbf{x}(t) + \mathbf{B}(t) u(t), \quad (\text{W7.21})$$

which shows that the proposed solution satisfies the system equation.  
For the time-invariant case

$$\Phi(t, t_0) = e^{\mathbf{A}(t-t_0)} = \Phi(t - t_0), \quad (\text{W7.22})$$

where

$$e^{\mathbf{A}t} = \left( \mathbf{I} + \mathbf{A}t + \frac{\mathbf{A}^2 t^2}{2!} + \dots \right) = \sum_{k=0}^{\infty} \frac{\mathbf{A}^k t^k}{k!}, \quad (\text{W7.23})$$

is an invertible  $n \times n$  exponential matrix, and by letting  $t = 0$ , we see that

$$e^0 = \mathbf{I}. \quad (\text{W7.24})$$

The state solution is now

$$\mathbf{x}(t) = e^{\mathbf{A}(t-t_0)} \mathbf{x}_0 + \int_{t_0}^t e^{\mathbf{A}(t-\tau)} \mathbf{B} u(\tau) d\tau, \quad (\text{W7.25})$$

and

$$y(t) = \mathbf{C} \mathbf{x}(t) = \mathbf{C} e^{\mathbf{A}(t-t_0)} \mathbf{x}_0 + \mathbf{C} \int_{t_0}^t e^{\mathbf{A}(t-\tau)} \mathbf{B} u(\tau) d\tau + D u(t). \quad (\text{W7.26})$$

Suppose  $\mathbf{x}(t_0) = \mathbf{x}_0 \equiv \mathbf{0}$ , then the output is given by the convolution integral

$$y(t) = \int_{t_0}^t \mathbf{h}(t - \tau) \mathbf{B} u(\tau) d\tau, \quad (\text{W7.27})$$

where  $h(t)$  is the *impulse response*. In terms of the state variables matrices,

$$h(t) = \mathbf{C} e^{\mathbf{A}t} \mathbf{B} + D \delta(t). \quad (\text{W7.28})$$

While there is no uniformly best way to compute the transition matrix, there are several methods that can be used to compute accurate approximations to it (See Moler, 2003; Franklin, Powell, and Workman,

1998). Three of these methods are matrix exponential series, inverse Laplace transform, and diagonalization of the system matrix. In the first technique, we use Eq. (W7.23):

$$e^{\mathbf{A}t} \triangleq \mathbf{I} + \mathbf{A}t + \frac{\mathbf{A}^2 t^2}{2!} + \frac{\mathbf{A}^3 t^3}{3!} + \dots, \quad (\text{W7.29})$$

and the series should be computed in a reliable fashion. For the second method, we notice if we define

$$\Phi(s) = (s\mathbf{I} - \mathbf{A})^{-1}, \quad (\text{W7.30})$$

then we can compute  $\Phi(s)$  from the  $\mathbf{A}$  matrix and matrix algebra. Given this matrix, we can use the inverse Laplace Transform to compute

$$\Phi(t) = \mathcal{L}^{-1}\{\Phi(s)\}, \quad (\text{W7.31})$$

$$= \mathcal{L}^{-1}\{(s\mathbf{I} - \mathbf{A})^{-1}\}. \quad (\text{W7.32})$$

The last method we mentioned operates on the system matrix. If the system matrix can be diagonalized, that is, if we can find a transformation matrix  $\mathbf{T}$  so that

$$\Lambda = \mathbf{T}^{-1} \mathbf{A} \mathbf{T}, \quad (\text{W7.33})$$

where  $\mathbf{A}$  is reduced to the similar but diagonal matrix

$$\Lambda = \text{diag}\{\lambda_1, \lambda_2, \dots, \lambda_n\}, \quad (\text{W7.34})$$

then from the series, Eq. (W7.23), we need only compute scalar exponentials, since

$$e^{\mathbf{A}t} = \mathbf{T}^{-1} \text{diag}\{e^{\lambda_1 t}, e^{\lambda_2 t}, \dots, e^{\lambda_n t}\} \mathbf{T}. \quad (\text{W7.35})$$

# Appendix W8.7

## Discrete State-Space Design Methods

We have seen in previous chapters that a linear, constant-coefficient continuous system can be represented by a set of first-order matrix differential equations of the form

$$\dot{\mathbf{x}} = \mathbf{A}\mathbf{x} + \mathbf{B}u, \quad (\text{W8.1})$$

where  $u$  is the control input to the system. The output equation can be expressed as

$$y = \mathbf{C}\mathbf{x} + \mathbf{D}u. \quad (\text{W8.2})$$

The solution to these equations (see Franklin et al., 1998) is

$$\mathbf{x}(t) = e^{\mathbf{A}(t-t_0)}\mathbf{x}(t_0) + \int_{t_0}^t e^{\mathbf{A}(t-\tau)}\mathbf{B}u(\tau) d\tau. \quad (\text{W8.3})$$

It is possible to use Eq. (W8.3) to obtain a discrete state-space representation of the system. Because the solution over one sample period results in a difference equation, we can alter the notation a bit (letting  $t = kT + T$  and  $t_0 = kT$ ) to arrive at a particularly useful version of Eq. (W8.3):

$$\mathbf{x}(kT + T) = e^{\mathbf{A}T}\mathbf{x}(kT) + \int_{kT}^{kT+T} e^{\mathbf{A}(kT+\tau-kT)}\mathbf{B}u(\tau) d\tau. \quad (\text{W8.4})$$

This result is not dependent on the type of hold, because  $u$  is specified in terms of its continuous time history  $u(\tau)$  over the sample interval. To find the discrete model of a continuous system where the input  $u(t)$  is the output of a ZOH, we let  $u(\tau)$  be a constant throughout the sample interval—that is,

$$u(\tau) = u(kT), kT \leq \tau < kT + T.$$

To facilitate the solution of Eq. (W8.4) for a ZOH, we let

$$\eta = kT + T - \tau,$$

which converts Eq. (W8.4) to

$$\mathbf{x}(kT + T) = e^{\mathbf{A}T}\mathbf{x}(kT) + \left( \int_0^T e^{\mathbf{A}\eta} d\eta \right) \mathbf{B}u(kT).$$

If we let

$$\Phi = e^{\mathbf{A}T}$$

and

$$\Gamma = \left( \int_0^T e^{\mathbf{A}\eta} d\eta \right) \mathbf{B}, \quad (\text{W8.5})$$

**Difference equations in standard form**

Eqs. (W8.4) and (W8.2) reduce to difference equations in standard form:

$$\mathbf{x}(k+1) = \Phi \mathbf{x}(k) + \Gamma u(k), \quad (\text{W8.6})$$

$$y(k) = \mathbf{C} \mathbf{x}(k) + D u(k). \quad (\text{W8.7})$$

Here  $\mathbf{x}(k+1)$  is a shorthand notation for  $\mathbf{x}(kT + T)$ ,  $\mathbf{x}(k)$  for  $\mathbf{x}(kT)$ , and  $u(k)$  for  $u(kT)$ . The series expansion

$$\Phi = e^{\mathbf{A}T} = \mathbf{I} + \mathbf{A}T + \frac{\mathbf{A}^2 T^2}{2!} + \frac{\mathbf{A}^3 T^3}{3!} + \dots$$

also can be written as

$$\Phi = \mathbf{I} + \mathbf{A}T\Psi, \quad (\text{W8.8})$$

where

$$\Psi = \mathbf{I} + \frac{\mathbf{A}T}{2!} + \frac{\mathbf{A}^2 T^2}{3!} + \dots.$$

The  $\Gamma$  integral in Eq. (W8.5) can be evaluated term by term to give

$$\begin{aligned} \Gamma &= \sum_{k=0}^{\infty} \frac{\mathbf{A}^k T^{k+1}}{(k+1)!} \mathbf{B} \\ &= \sum_{k=0}^{\infty} \frac{\mathbf{A}^k T^k}{(k+1)!} T \mathbf{B} \\ &= \Psi T \mathbf{B}. \end{aligned} \quad (\text{W8.9})$$

We evaluate  $\Psi$  by a series in the form

$$\Psi \cong \mathbf{I} + \frac{\mathbf{A}T}{2} \left\{ \mathbf{I} + \frac{\mathbf{A}T}{3} \left[ \mathbf{I} + \dots + \frac{\mathbf{A}T}{N-1} \left( \mathbf{I} + \frac{\mathbf{A}T}{N} \right) \right] \right\},$$

which has better numerical properties than the direct series. We then find  $\Gamma$  from Eq. (W8.9) and  $\Phi$  from Eq. (W8.8). For a discussion of various methods of numerical determination of  $\Phi$  and  $\Gamma$ , see Franklin et al. (1998) and Moler and van Loan (1978, 2003). The evaluation of the  $\Phi$  and  $\Gamma$  matrices in practice is carried out by the `c2d` function in Matlab.

To compare this method of representing the plant with the discrete transfer function, we can take the  $z$ -transform of Eqs. (W8.6) and (W8.7) with  $D = 0$  to obtain

$$(z\mathbf{I} - \Phi)\mathbf{X}(z) = \Gamma U(z), \quad (\text{W8.10})$$

$$Y(z) = \mathbf{C}\mathbf{X}(z). \quad (\text{W8.11})$$

Therefore,

$$\frac{Y(z)}{U(z)} = G(z) = \mathbf{C}(z\mathbf{I} - \Phi)^{-1}\Gamma. \quad (\text{W8.12})$$

**Matlab c2d**

**EXAMPLE W8.1***Discrete State-Space Representation of  $1/s^2$  Plant*

Use the relation in this section to verify that the discrete model of the  $1/s^2$  plant preceded by a ZOH is that given in the solution to Example 8.4.

**Solution.** The  $\Phi$  and  $\Gamma$  matrices can be calculated using Eqs. (W8.8) and (W8.9). Example 7.1 (with  $I = 1$ ) showed that the values for  $\mathbf{A}$  and  $\mathbf{B}$  are

$$\mathbf{A} = \begin{bmatrix} 0 & 1 \\ 0 & 0 \end{bmatrix}, \mathbf{B} = \begin{bmatrix} 0 \\ 1 \end{bmatrix}.$$

Because  $\mathbf{A}^2 = \mathbf{0}$  in this case, we have

$$\begin{aligned} \Phi &= \mathbf{I} + \mathbf{A}T + \frac{\mathbf{A}^2T^2}{2!} + \dots \\ &= \begin{bmatrix} 1 & 0 \\ 0 & 1 \end{bmatrix} + \begin{bmatrix} 0 & 1 \\ 0 & 0 \end{bmatrix}T = \begin{bmatrix} 1 & T \\ 0 & 1 \end{bmatrix}, \\ \Gamma &= \left( \mathbf{I} + \mathbf{A} \frac{T}{2!} \right) T \mathbf{B} \\ &= \left( \begin{bmatrix} T & 0 \\ 0 & T \end{bmatrix} + \begin{bmatrix} 0 & 1 \\ 0 & 0 \end{bmatrix} \frac{T^2}{2} \right) \begin{bmatrix} 0 \\ 1 \end{bmatrix} = \begin{bmatrix} T^2/2 \\ T \end{bmatrix}. \end{aligned}$$

Hence, using Eq. (W8.12), we obtain

$$\begin{aligned} G(z) &= \frac{Y(z)}{U(z)} = [1 \ 0] \left( z \begin{bmatrix} 1 & 0 \\ 0 & 1 \end{bmatrix} - \begin{bmatrix} 1 & T \\ 0 & 1 \end{bmatrix} \right)^{-1} \begin{bmatrix} T^2/2 \\ T \end{bmatrix} \\ &= \frac{T^2}{2} \begin{bmatrix} z+1 \\ (z-1)^2 \end{bmatrix}. \end{aligned} \quad (\text{W8.13})$$

This is the same result we obtained using Eq. (8.41) and the  $z$ -transform tables in Example 8.5.

Note to compute  $Y/U$ , we find the denominator of Eq. (W8.13) is  $\det(z\mathbf{I} - \Phi)$ , which was created by the matrix inverse in Eq. (W8.12). This determinant is the characteristic polynomial of the transfer function, and the zeros of the determinant are the poles of the plant. We have two poles at  $z = 1$  in this case, corresponding to two integrations in this plant's equations of motion.

We can further explore the question of poles and zeros and the state-space description by considering again the transform formulas [Eqs. (W8.10) and (W8.11)]. One way to interpret transfer-function poles from the perspective of the corresponding difference equation is that a pole is a value of  $z$  such that the equation has a nontrivial solution when the forcing input is zero. From Eq. (W8.10), this interpretation implies that the linear equations

$$(z\mathbf{I} - \Phi)\mathbf{X}(z) = \mathbf{0},$$

have a nontrivial solution. From matrix algebra the well-known requirement for a nontrivial solution is that  $\det(z\mathbf{I} - \Phi) = 0$ . Using the system in Example W8.1, we get

$$\begin{aligned}\det(z\mathbf{I} - \Phi) &= \det\left(\begin{bmatrix} z & 0 \\ 0 & z \end{bmatrix} - \begin{bmatrix} 1 & T \\ 0 & 1 \end{bmatrix}\right) \\ &= \det\begin{bmatrix} z-1 & -T \\ 0 & z-1 \end{bmatrix} \\ &= (z-1)^2 = 0,\end{aligned}$$

which is the characteristic equation, as we have seen. In Matlab, the poles of the system are found by  $P = \text{eig}(\Phi)$ .

Along the same line of reasoning, a system zero is a value of  $z$  such that the system output is zero even with a nonzero state-and-input combination. Thus, if we are able to find a nontrivial solution for  $\mathbf{X}(z_0)$  and  $\mathbf{U}(z_0)$  such that  $\mathbf{Y}(z_0)$  is identically zero, then  $z_0$  is a zero of the system. In combining Eqs. (W8.10) and (W8.11), we must satisfy the requirement that

$$\begin{bmatrix} z\mathbf{I} - \Phi & -\Gamma \\ \mathbf{C} & 0 \end{bmatrix} \begin{bmatrix} \mathbf{X}(z) \\ \mathbf{U}(z) \end{bmatrix} = \mathbf{0}.$$

Once more the condition for the existence of nontrivial solutions is that the determinant of the square coefficient system matrix be zero. For Example W8.1, the calculation is

$$\begin{aligned}\det \begin{bmatrix} z-1 & -T & -T^2/2 \\ 0 & z-1 & -T \\ 1 & 0 & 0 \end{bmatrix} &= \det \begin{bmatrix} -T & -T^2/2 \\ z-1 & -T \end{bmatrix} \\ &= T^2 + \frac{T^2}{2}(z-1) \\ &= \frac{T^2}{2}z + \frac{T^2}{2} \\ &= \frac{T^2}{2}(z+1).\end{aligned}$$

Thus we have a single zero at  $z = -1$ , as we have seen from the transfer function. In Matlab, the zeros are found by  $Z = \text{tzero}(\Phi, \Gamma, \mathbf{C}, \mathbf{D})$ .

Much of the algebra for discrete state-space control design is the same as for the continuous-time case discussed in Chapter 7. The poles of a discrete system can be moved to desirable locations by linear state-variable feedback

$$u = -\mathbf{Kx},$$

such that

$$\det(z\mathbf{I} - \Phi + \mathbf{\Gamma K}) = \alpha_c(z), \quad (\text{W8.14})$$

provided that the system is controllable. The system is controllable if the controllability matrix

$$\mathcal{C} = [\Gamma \quad \Phi\Gamma \quad \Phi^2\Gamma \quad \dots \quad \Phi^{n-1}\Gamma]$$

is full rank.

A discrete full-order estimator has the form

$$\bar{x}(k+1) = \Phi\bar{x}(k) + \Gamma u(k) + L[y(k) - C\bar{x}(k)],$$

where  $\bar{x}$  is the state estimate. The error equation,

$$\tilde{x}(k+1) = (\Phi - LC)\tilde{x}(k),$$

can be given arbitrary dynamics  $\alpha_e(z)$ , provided the system is observable, which requires that the observability matrix

$$\mathcal{O} = \begin{bmatrix} C \\ C\Phi \\ C\Phi^2 \\ \vdots \\ C\Phi^{n-1} \end{bmatrix}$$

be full rank.

As was true for the continuous-time case, if the open-loop transfer function is

$$G(z) = \frac{Y(z)}{U(z)} = \frac{b(z)}{a(z)},$$

then a state-space compensator can be designed such that

$$\frac{Y(z)}{R(z)} = \frac{K_s \gamma(z) b(z)}{\alpha_c(z) \alpha_e(z)},$$

where  $r$  is the reference input. The polynomials  $\alpha_c(z)$  and  $\alpha_e(z)$  are selected by the designer using exactly the same methods discussed in Chapter 7 for continuous systems.  $\alpha_c(z)$  results in a control gain  $K$  such that  $\det(zI - \Phi + \Gamma K) = \alpha_c(z)$ , and  $\alpha_e(z)$  results in an estimator gain  $L$  such that  $\det(zI - \Phi + LC) = \alpha_e(z)$ . If the estimator is structured according to Fig. 7.48a, the system zeros  $\gamma(z)$  will be identical to the estimator poles  $\alpha_e(z)$ , thus removing the estimator response from the closed-loop system response. However, if desired, we can arbitrarily select the polynomial  $\gamma(z)$  by providing suitable feed-forward from the reference input. Refer to Franklin et al. (1998) for details.

## EXAMPLE W8.2

### *State-Space Design of a Digital Controller*

Design a digital controller for a  $1/s^2$  plant to meet the specifications given in Example 8.2. Use state-space design methods, including the use of an estimator, and structure the reference input in two ways: (a) Use the error command shown in Fig. 7.47b, and (b) use the state command shown in Fig. 7.15 and Fig. 7.47a.

**Solution.** We find the state-space model of the  $1/s^2$  plant preceded by a ZOH using the Matlab statements

```
sysSSc = ss([0 1; 0 0], [0; 1], [1 0], 0);
T = 1;
sysSSd = c2d(sysSSc, T);
[Phi, Gam, C] = ssdata(sysSSd);
```

Using discrete analysis for Example 8.4, we find that the desired  $z$ -plane roots are at  $z = 0.78 \pm 0.18j$ . Solving the discrete pole-placement problem involves placing the eigenvalues of  $\Phi - \Gamma K$ , as indicated by Eq. (W8.14). Likewise, the solution of the continuous pole-placement problem involves placing the eigenvalues of  $A - BK$ , as indicated by Eq. (7.69). Because these two tasks are identical, we use the same function in Matlab for the continuous and discrete cases. Therefore, the control feedback matrix  $K$  is found by

```
pc = [0.78 + 0.18*j; 0.78 - 0.18*j];
K = acker(Phi, Gam, pc);
```

which yields

$$K = [0.0808 \ 0.3996].$$

To ensure the estimator roots are substantially faster than the control roots (so the estimator roots will have little effect on the output), we choose them to be at  $z = 0.2 \pm 0.2j$ . Therefore, the estimator feedback matrix  $L$  is found by

```
pe = [0.2 + 0.2*j; 0.2 - 0.2*j];
L = acker(Phi, C, pe);
```

which yields

$$L = \begin{bmatrix} 1.6 \\ 0.68 \end{bmatrix}.$$

The equations of the compensation for  $r = 0$  (regulation to  $x^T = [0 \ 0]$ ) are then

$$\bar{x}(k+1) = \Phi \bar{x}(k) + \Gamma u(k) + L[y(k) - C \bar{x}(k)], \quad (\text{W8.15})$$

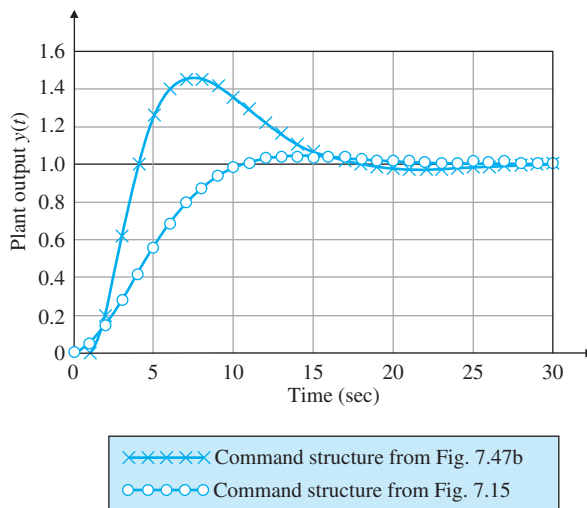
$$u(k) = -K \bar{x}(k). \quad (\text{W8.16})$$

- For the error command structure where the compensator is placed in the feedforward path, as shown in Fig. 7.47b in the book,  $y(k)$  from Eq. (W8.15) is replaced with  $y(k) - r$ , so the state description of the plant plus the estimator (a fourth-order system whose state vector is  $[x \ \bar{x}]^T$ ) is

```
A = [Phi - Gam*K; L*C Phi - Gam*K - L*C];
B = [0; 0; -L];
C = [1 0 0 0];
D = 0;
step(A,B,C,D).
```

**Figure W8.1**

Step response of  
Example W8.2



The resulting step response in Fig. W8.1 shows a response similar to that of the step responses in Fig. 8.21 in the text.

- For the state command structure described in Section 7.9 in the text, we wish to command the position element of the state vector so

$$\mathbf{N}_x = \begin{bmatrix} 1 \\ 0 \end{bmatrix},$$

and the  $1/s^2$  plant requires no steady control input for a constant output  $y$ . Therefore  $N_u = 0$ . To analyze a system with this command structure, we need to modify matrix  $\mathbf{B}$  from the preceding Matlab statement to properly introduce the reference input  $r$  according to Fig. 7.15. The Matlab statement

$$\mathbf{B} = [\mathbf{G}\mathbf{m}^*\mathbf{N}_x; \mathbf{G}\mathbf{m}^*\mathbf{N}_x];$$

channels  $r$  into both the plant and estimator equally, thus not exciting the estimator dynamics. The resulting step response in Fig. W8.1 shows a substantial reduction in the overshoot with this structure. In fact, the overshoot is now about 5%, which is expected for a second-order system with  $\zeta \cong 0.7$ . The previous designs all had considerably greater overshoot because of the effect of the extra zero and pole.

## SUMMARY OF STATE-SPACE DESIGN

- The continuous state-space form of a differential equation,

$$\dot{\mathbf{x}} = \mathbf{A}\mathbf{x} + \mathbf{B}u,$$

$$y = \mathbf{C}\mathbf{x} + \mathbf{D}u,$$

has a discrete counterpart in the difference equations

$$\mathbf{x}(k+1) = \Phi \mathbf{x}(k) + \Gamma u(k),$$

$$y(k) = \mathbf{C}x(k) + Du(k),$$

where

$$\Phi = e^{\mathbf{A}T}$$

$$\Gamma = \left( \int_0^T e^{\mathbf{A}\eta} d\eta \right) \mathbf{B}.$$

These matrices can be computed in Matlab by [Phi, Gam] = c2d(A,B,C,D) and used in state-space **discrete design** methods.

- The pole placement and estimation ideas are identical in the continuous and discrete domains.

## PROBLEMS

- W8.1** In Problem 8.11, we dealt with an experiment in magnetic levitation described by Eq. (8.54) that reduces to

$$\ddot{x} = 1000x + 20i.$$

Let the sampling time be 0.01 sec.

- (a) Use pole placement to design a controller for the magnetic levitator so that the closed-loop system meets the following specifications: settling time,  $t_s \leq 0.25$  sec, and overshoot to an initial offset in  $x$  that is less than 20%.
- (b) Plot the step response of  $x$ ,  $\tilde{x}$ , and  $i$  to an initial displacement in  $x$ .
- (c) Plot the root locus for changes in the plant gain, and mark the pole locations of your design.
- (d) Introduce a command reference input  $r$  (as discussed in Section 7.9) that does not excite the estimate of  $x$ . Measure or compute the frequency response from  $r$  to the system error  $r - x$  and give the highest frequency for which the error amplitude is less than 20% of the command amplitude.

- W8.2** *Servomechanism for Antenna Elevation Control:* Suppose it is desired to control the elevation of an antenna designed to track a satellite. A photo of such a system is shown in Fig. W8.2, and a schematic diagram is depicted in Fig. W8.3. The antenna and drive parts have a moment of inertia  $J$  and damping  $B$ , arising to some extent from bearing and aerodynamic friction, but mostly from the back emf of the DC drive motor. The equation of motion is

$$J\ddot{\theta} + B\dot{\theta} = T_c + T_d,$$

where

$$T_c = \text{net torque from the drive motor}, \quad (\text{W8.17})$$

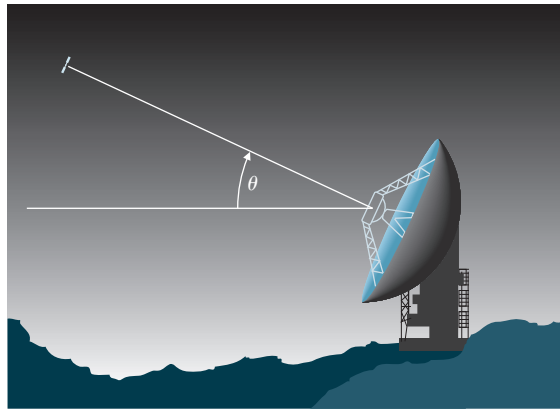
$$T_d = \text{disturbance torque due to wind}. \quad (\text{W8.18})$$

**Figure W8.2**

Satellite-tracking  
antenna (*Courtesy  
Space Systems/Loral*)

**Figure W8.3**

Schematic diagram of  
satellite-tracking  
antenna



If we define

$$\frac{B}{J} = a, \quad u = \frac{T_c}{B}, \quad \text{and} \quad w_d = \frac{T_d}{B},$$

the equation simplifies to

$$\frac{1}{a} \ddot{\theta} + \dot{\theta} = u + w_d.$$

After using the Laplace transformation, we obtain

$$\theta(s) = \frac{1}{s(s/a + 1)} [u(s) + w_d(s)],$$

or with no disturbance,

$$\frac{\theta(s)}{u(s)} = \frac{1}{s(s/a + 1)} = G_2(s).$$

With  $u(k)$  applied through a ZOH, the transfer function for an equivalent discrete-time system is

$$G_2(z) = \frac{\theta(z)}{u(z)} = K \frac{z + b}{(z - 1)(z - e^{-aT})},$$

where

$$K = \frac{aT - 1 + e^{-aT}}{a}, \quad b = \frac{1 - e^{-aT} - aTe^{-aT}}{aT - 1 + e^{-aT}}.$$

- (a) Let  $a = 0.1$  and  $x_1 = \dot{\theta}$ , and write the continuous-time state equations for the system.
- (b) Let  $T = 1$  sec, and find a state feedback gain  $\mathbf{K}$  for the equivalent discrete-time system that yields closed-loop poles corresponding to the following points in the s-plane:  $s = -1/2 \pm j\sqrt{\frac{3}{2}}$ . Plot the step response of the resulting design.
- (c) Design an estimator: Select  $\mathbf{L}$  so  $\alpha_e(z) = z^2$ .
- (d) Using the values for  $\mathbf{K}$  and  $\mathbf{L}$  computed in parts (b) and (c) as the gains for a combined estimator/controller, introduce a reference input that will leave the state estimate undisturbed. Plot the response of the closed-loop system due to a step change in the reference input. Also plot the system response to a step wind-gust disturbance.
- (e) Plot the root locus of the closed-loop system with respect to the plant gain, and mark the locations of the closed-loop poles.

**W8.3 Tank Fluid Temperature Control:** The temperature of a tank of fluid with a constant inflow and outflow rate is to be controlled by adjusting the temperature of the incoming fluid. The temperature of the incoming fluid is controlled by a mixing valve that adjusts the relative amounts of hot and cold supplies of the fluid (see Fig. W8.4). The distance between the valve and the point of discharge into the tank creates a time delay between the application of a temperature change at the mixing valve and the discharge of the flow with the changed temperature into the tank. The differential equation governing the tank temperature is

$$\dot{T}_e = \frac{1}{cM} (q_{\text{in}} - q_{\text{out}}),$$

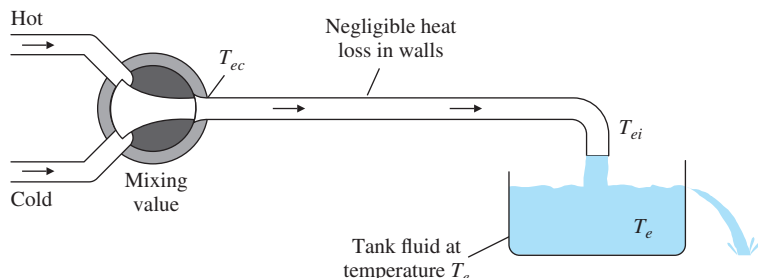
where

$T_e$  = tank temperature,

$c$  = specific heat of the fluid,

**Figure W8.4**

Tank temperature control



$M$  = fluid mass contained in the tank,

$$q_{\text{in}} = c\dot{m}_{\text{in}}T_{ei},$$

$$q_{\text{out}} = c\dot{m}_{\text{out}}T_e,$$

$\dot{m}$  = mass flow rate ( $\dot{m}_{\text{in}} = \dot{m}_{\text{out}}$ ),

$T_{ei}$  = temperature of fluid entering tank.

However, the temperature at the input to the tank at time  $t$  is equal to the control temperature  $\tau_d$  seconds in the past. This relationship may be expressed as

$$T_{ei}(t) = T_{ec}(t - \tau_d),$$

where

$\tau_d$  = delay time,

$T_{ec}$  = temperature of fluid immediately after the control valve and directly controllable by the valve.

Combining constants, we obtain

$$\dot{T}_e(t) + aT_e(t) = aT_{ec}(t - \tau_d),$$

where

$$a = \frac{\dot{m}}{M}.$$

The transfer function of the system is thus

$$\frac{T_e(s)}{T_{ec}(s)} = \frac{e^{-\tau_d s}}{s/a + 1} = G_3(s).$$

To form a discrete transfer function equivalent to  $G_3$  preceded by a ZOH, we must compute

$$G_3(z) = \mathcal{Z} \left\{ \left( \frac{1 - e^{-sT}}{s} \right) \left( \frac{e^{-\tau_d s}}{s/a + 1} \right) \right\}.$$

We assume for some integer  $l$ ,  $\tau_d = lT - mT$ , where  $0 \leq m < 1$ . Then

$$\begin{aligned} G_3(z) &= \mathcal{Z} \left\{ \left( \frac{1 - e^{-sT}}{s} \right) \left( \frac{e^{-lsT} e^{msT}}{s/a + 1} \right) \right\} \\ &= (1 - z^{-1})z^{-l} \mathcal{Z} \left\{ \frac{e^{msT}}{s(s/a + 1)} \right\} \\ &= (1 - z^{-1})z^{-l} \mathcal{Z} \left\{ \frac{e^{msT}}{s} - \frac{e^{msT}}{s + a} \right\} \\ &= \frac{z - 1}{z} \left( \frac{1}{z^l} \right) \mathcal{Z} \{ 1(t + mT) - e^{-a(t+mT)} 1(t + mT) \} \\ &= \frac{z - 1}{z} \left( \frac{1}{z^l} \right) \left( \frac{z}{z - 1} - \frac{e^{-amT} z}{z - e^{-aT}} \right) \\ &= \frac{1}{z^l} \left[ \frac{(1 - e^{-amT})z + e^{-amT} - e^{-aT}}{z - e^{-aT}} \right] \end{aligned}$$

$$= \left( \frac{1 - e^{-amT}}{z^l} \right) \left( \frac{z + \alpha}{z - e^{-aT}} \right),$$

and

$$\alpha = \frac{e^{-amT} - e^{-aT}}{1 - e^{-amT}}.$$

The zero location  $-\alpha$  varies from  $\alpha = \infty$  at  $m = 0$  to  $\alpha = 0$  as  $m \rightarrow 1$ . Note also  $G_3(1) = 1.0$  for all  $a, m$ , and  $l$ . For the specific values  $\tau_d = 1.5$ ,  $T = 1$ ,  $a = 1$ ,  $l = 2$ , and  $m = \frac{1}{2}$ , the transfer function reduces to

$$G_3(z) = 0.3935 \frac{z + 0.6065}{z^2(z - 0.3679)}.$$

- (a) Write the discrete-time system equations in state-space form.
- (b) Design a state feedback gain that yields  $\alpha_c(z) = z^3$ .
- (c) Design a state estimator with  $\alpha_e(z) = z^3$ .
- (d) Plot the root locus of the system with respect to the plant gain.
- (e) Plot the step response of the system.

**W8.4** Consider the linear equation  $\mathbf{Ax} = \mathbf{b}$ , where  $\mathbf{A}$  is an  $n \times n$  matrix. When  $\mathbf{b}$  is given, one way of solving for  $\mathbf{x}$  is to use the discrete-time recursion

$$\mathbf{x}(k+1) = (\mathbf{I} + c\mathbf{A})\mathbf{x}(k) - c\mathbf{b},$$

where  $c$  is a scalar to be chosen.

- (a) Show that the solution of  $\mathbf{Ax} = \mathbf{b}$  is the equilibrium point  $\mathbf{x}^*$  of the discrete-time system. An equilibrium point  $\mathbf{x}^*$  of a discrete-time system  $\mathbf{x}(k+1) = \mathbf{f}(\mathbf{x}(k))$  satisfies the relation  $\mathbf{x}^* = \mathbf{f}(\mathbf{x}^*)$ .
- (b) Consider the error  $\mathbf{e}(k) = \mathbf{x}(k) - \mathbf{x}^*$ . Write the linear equation that relates the error  $\mathbf{e}(k+1)$  to  $\mathbf{e}(k)$ .
- (c) Suppose  $|1 + c\lambda_i(\mathbf{A})| < 1$ ,  $i = 1, \dots, n$ , where  $\lambda_i(\mathbf{A})$  denotes the  $i$ th eigenvalue of  $\mathbf{A}$ . Show that, starting from any initial guess  $\mathbf{x}_0$ , the algorithm converges to  $\mathbf{x}^*$ . [Hint: For any matrix  $\mathbf{B}$ ,  $\lambda_i(\mathbf{I} + \mathbf{B}) = 1 + \lambda_i(\mathbf{B})$ .]

**W8.5** The open-loop plant of a unity feedback system has the transfer function

$$G(s) = \frac{1}{s(s+2)}.$$

Determine the transfer function of the equivalent digital plant using a sampling period of  $T = 1$  sec, and design a proportional controller for the discrete-time system that yields dominant closed-loop poles with a damping ratio  $\zeta$  of 0.7.

**W8.6** Write a computer program to compute  $\Phi$  and  $\Gamma$  from  $\mathbf{A}$ ,  $\mathbf{B}$ , and the sample period  $T$ . It is okay to use Matlab, but don't use c2d. Write code in Matlab to compute the discrete matrices using the relations developed in this chapter. Use your program to compute  $\Phi$  and  $\Gamma$  when

(a)

$$\mathbf{A} = \begin{bmatrix} -1 & 0 \\ 0 & -2 \end{bmatrix}, \quad \mathbf{B} = \begin{bmatrix} 1 \\ 1 \end{bmatrix}, \quad T = 0.2 \text{ sec},$$

(b)

$$\mathbf{A} = \begin{bmatrix} -3 & -2 \\ 1 & 0 \end{bmatrix}, \quad \mathbf{B} = \begin{bmatrix} 1 \\ 0 \end{bmatrix}, \quad T = 0.2 \text{ sec}.$$

**W8.7** Consider the following discrete-time system in state-space form:

$$\begin{bmatrix} x_1(k+1) \\ x_2(k+1) \end{bmatrix} = \begin{bmatrix} 0 & 1 \\ 0 & -1 \end{bmatrix} \begin{bmatrix} x_1(k) \\ x_2(k) \end{bmatrix} + \begin{bmatrix} 0 \\ 10 \end{bmatrix} u(k).$$

Use state feedback to relocate all of the system's poles to 0.5.

**W8.8** Let

$$\Phi = \begin{bmatrix} 1 & T \\ 0 & 1 \end{bmatrix} \quad \text{and} \quad \Gamma = \begin{bmatrix} T^2/2 \\ T \end{bmatrix}.$$

- (a) Find a transformation matrix  $\mathbf{T}$  so, if  $\mathbf{x} = \mathbf{T}\mathbf{w}$ , the state equations for  $\mathbf{w}$  will be in control canonical form.
- (b) Compute the gain  $\mathbf{K}_w$  so, if  $u = -\mathbf{K}_w\mathbf{w}$ , the characteristic equation will be  $\alpha_c(z) = z^2 - 1.6z + 0.7$ .
- (c) Use  $\mathbf{T}$  from part (a) to compute  $\mathbf{K}_x$ , which is the feedback gain required by the state equations in  $\mathbf{x}$  to achieve the desired characteristic polynomial.

**W8.9** Consider a system whose plant transfer function is  $1/s^2$  and has a piecewise constant input of the form

$$u(t) = u(kT), \quad kT \leq t < (k+1)T.$$

- (a) Show, if we restrict attention to the time instants  $kT$ ,  $k = 0, 1, 2, \dots$ , the resulting sampled-data system can be described by the equations

$$\begin{bmatrix} x_1(k+1) \\ x_2(k+1) \end{bmatrix} = \begin{bmatrix} 1 & 0 \\ T & 1 \end{bmatrix} \begin{bmatrix} x_1(k) \\ x_2(k) \end{bmatrix} + \begin{bmatrix} T \\ T^2/2 \end{bmatrix} u(k).$$

$$y(k) = [0 \ 1][x_1(k) \ x_2(k)]^T.$$

- (b) Design a second-order estimator that will always drive the error in the estimate of the initial state vector to zero in time  $2T$  or less.
- (c) Is it possible to estimate the initial state exactly with a first-order estimator? Justify your answer.

**W8.10** In this problem, you will show how to compute  $\Phi$  by changing states so that the system matrix is diagonal.

- (a) Using an infinite series expansion, compute  $e^{AT}$  for

$$\mathbf{A} = \begin{bmatrix} -1 & 0 \\ 0 & -2 \end{bmatrix}.$$

- (b) Show if  $\bar{\mathbf{A}} = \mathbf{T}\mathbf{A}\mathbf{T}^{-1}$  for some nonsingular transformation matrix  $\mathbf{T}$ , then

$$e^{\bar{\mathbf{A}}T} = \mathbf{T}e^{\mathbf{A}T}\mathbf{T}^{-1}.$$

- (c) Show if

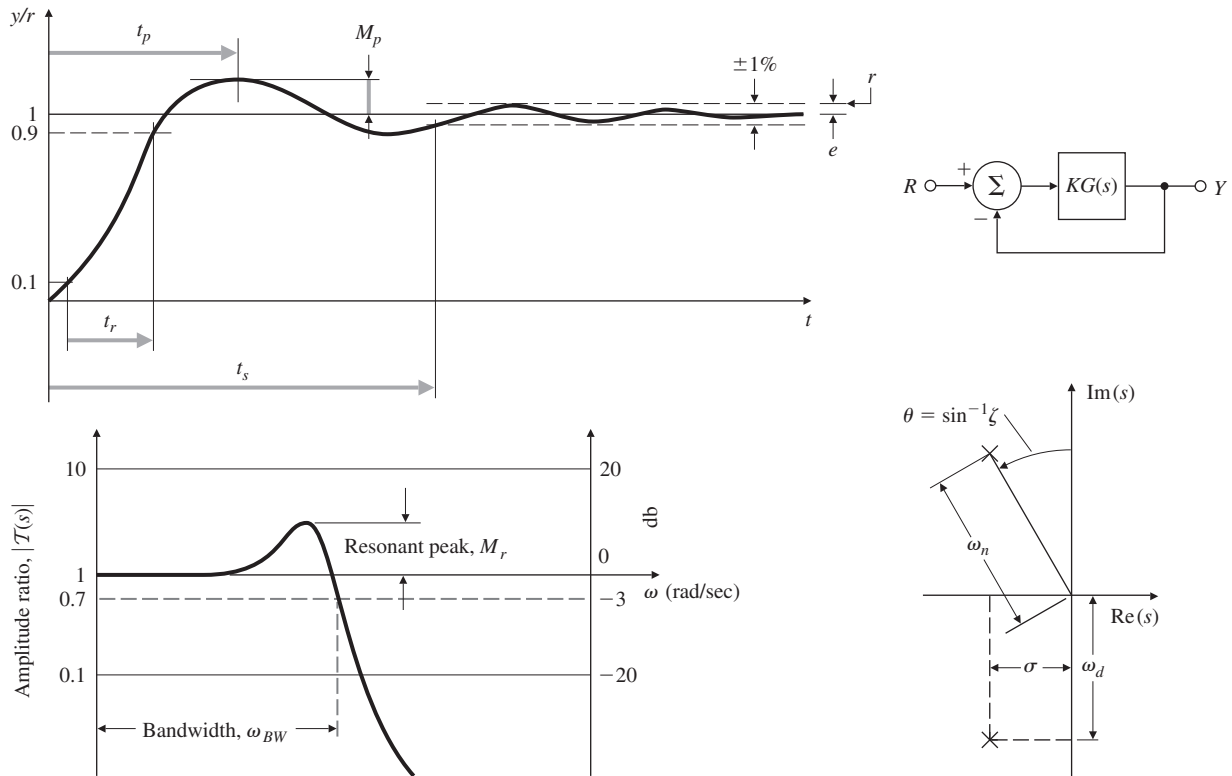
$$\bar{\mathbf{A}} = \begin{bmatrix} -3 & 1 \\ -2 & 0 \end{bmatrix},$$

there exists a  $\mathbf{T}$  such that  $\mathbf{T}\mathbf{A}\mathbf{T}^{-1} = \bar{\mathbf{A}}$ . (*Hint:* Write  $\mathbf{T}\mathbf{A} = \bar{\mathbf{A}}\mathbf{T}$ , assume four unknowns for the elements of  $\mathbf{T}$ , and solve. Next show that the columns of  $\mathbf{T}$  are the eigenvectors of  $\bar{\mathbf{A}}$ .)

- (d) Compute  $e^{\bar{\mathbf{A}}T}$ .

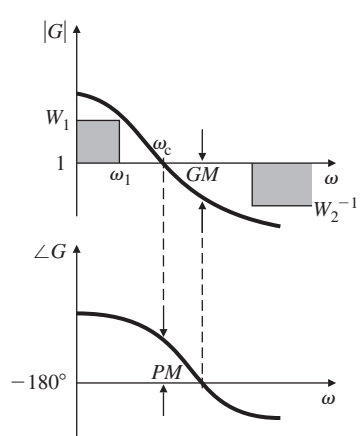
## Design Aids

### Closed Loop

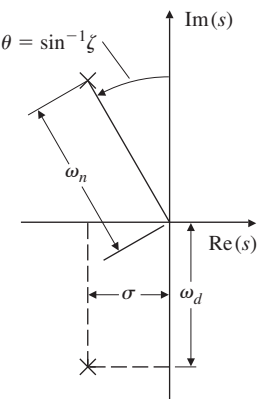


### Open Loop

### Design Relations



$$\begin{aligned}
 t_s &= \frac{4.6}{\sigma} & t_r &= \frac{1.8}{\omega_n} \\
 \sigma &= \zeta \omega_n & \omega_d &= \omega_n \sqrt{1 - \zeta^2} \\
 e_{ss} &= \frac{1}{1 + K_0}, \quad K_0 = |G(j\omega)|_{\omega=0} \\
 |E| &< \frac{1}{1 + W_1}, \quad \omega < \omega_1 \\
 \omega_{BW} &= \omega_c \quad \text{for } PM = 90^\circ \\
 \omega_{BW} &= 2\omega_c \quad \text{for } PM = 45^\circ \\
 M_r &\cong \frac{1}{2 \sin(PM/2)} \\
 M_p &= 5\%, \quad \zeta = 0.7 \\
 M_p &= 15\%, \quad \zeta = 0.5 \\
 M_p &= 35\%, \quad \zeta = 0.3 \\
 \zeta &\cong \frac{PM}{100} \quad \text{for } PM < 70^\circ
 \end{aligned}$$





# GLOBAL EDITION

This is a special edition of an established title widely used by colleges and universities throughout the world. Pearson published this exclusive edition for the benefit of students outside the United States and Canada. If you purchased this book within the United States or Canada, you should be aware that it has been imported without the approval of the Publisher or Author.

## Features

- **New!** Examples and problems on drones and control
- **New!** Section on anti-windup for integral control
- **New!** Example on thermal system control
- **Over 60 problems new or revised** from the 7th edition
- **Emphasis on design throughout the text** to develop confidence in solving design problems
- **Continued emphasis on mastering underlying techniques** coupled with computer-based methods for detailed calculations
- **Pedagogical features to help students manage information** including
  - *Chapter openers* that provide perspective and overview
  - *Margin notes* that point to important definitions, equations, and concepts
  - *Review questions* that guide in self-study



Pearson

ISBN-10	1-292-27452-2
ISBN-13	978-1-292-27452-2
9 000 0 >	
9 781292 274522	